Substituent Effects in Oxygenated Monocyclic Aromatic Hydrocarbons:
Ab Initio Based Group Additivity

Substituenteffecten in zuurstofbevattende monocyclische aromatische koolwaterstoffen:
ab initio gebaseerde groepsadditiviteit

Alper Ince

Promotoren: prof. dr. M.-F. Reyniers, prof. dr. ir. G. B. Marin
Proefschrift ingediend tot het behalen van de graad van
Doctor in de ingenieurswetenschappen: chemische technologie

UNIVERSITEIT
GENT

Vakgroep Materialen, Textiel en Chemische Proceskunde
Voorzitter: prof. dr. P. Kiekens
Faculteit Ingenieurswetenschappen en Architectuur
Academiejaar 2016 - 2017

ISBN 978-94-6355-023-9
NUR 952
Wettelijk depot: D/2017/10.500/58

EXAMENCOMMISSIE

Prof. dr. Daniël De Zutter [chairman]
Vakgroep Informatietechnologie
Faculteit Ingenieurswetenschappen en Architectuur
Universteit Gent

Prof. dr. ir. Guy B. Marin [promotor]
Vakgroep Materialen, Textiel en Chemische Proceskunde
Laboratorium voor Chemische Technologie
Faculteit Ingenieurswetenschappen en Architectuur
Universteit Gent

Prof. dr. Marie-Françoise Reyniers [promotor]
Vakgroep Materialen, Textiel en Chemische Proceskunde
Laboratorium voor Chemische Technologie
Faculteit Ingenieurswetenschappen en Architectuur
Universteit Gent

Prof. dr. ir. Nikolaos G. Papayannakos
Department of Chemical Engineering and Technology
School of Chemical Engineering
National Technical University of Athens

Prof. dr. ir. Pierre-Alexandre Glaude
Laboratoire Réactions et Génie des Procédés
National Polytechnic Institute of Lorraine

Prof. dr. Toon Verstraelen
Vakgroep Fysica en Sterrenkunde
Centrum voor Moleculaire Modellering
Faculteit Wetenschappen
Universteit Gent

Prof. dr. ir. Maarten K. Sabbe
Vakgroep Materialen, Textiel en Chemische Proceskunde
Laboratorium voor Chemische Technologie
Faculteit Ingenieurswetenschappen en Architectuur
Universteit Gent

Dr. ir. Hans-Heinrich Carstensen
Vakgroep Materialen, Textiel en Chemische Proceskunde
Laboratorium voor Chemische Technologie
Faculteit Ingenieurswetenschappen en Architectuur
Universteit Gent

Acknowledgements

Production of the scientific work and its narration in the form of a Ph.D. dissertation has been an overwhelming experience for me in many ways. So many nice people have been there to witness and support me in this period and I would like to show my thankfulness to them through a few words.

First and foremost, I would like to express my sincere gratitude to my advisors, Professors Guy B. Marin and Marie-Françoise Reyniers for giving me the opportunity to do Ph.D. research in the Laboratory for Chemical Technology. I appreciate the time I spent working with them, at both a professional and personal level. I would like to thank them very much for encouraging me and inspiring me throughout this experience.

Besides my advisors, I would like to thank the members of the Doctoral Examination Board for accepting to review this Ph.D. thesis. Their insightful comments, questions and suggestions led to significant improvements in the quality of the final manuscript.

I am very grateful to have senior scientist Dr. Hans-Heinrich Carstensen as a coach during this Ph.D. work. In this period, he has shown continuous support for this Ph.D. dissertation and related research. His guidance and immense knowledge contributed a lot to this study, during the time of both the research and the writing of this thesis. I believe that without his contributions, the presented research would not have the quality it currently possesses. Having him as an office mate has been extremely fortunate for me in terms of both personal and professional development.

I would like to particularly thank Prof. Dr. Ir. Maarten Sabbe, firstly because he has been a very good friend and an outstanding scientist. He has been one of the most important people in my support system during my Ph.D. period. With his ideas, I had the chance to overcome the problems I had, particularly regarding bash/awk scripting and fixing the large number of problems that arose regarding the application of codes that were previously written in LCT to the species of interest in this Ph.D. work. Moreover, his experience in developing group additive parameters for kinetics have particularly been very helpful in improving the quality of the work.

I appreciate the assistance and friendship of all my colleagues and administrative staff at LCT, which proved to be more than valuable. Their presence has been very supportive for me during these years of struggle. Their friendship rendered my stay in the beautiful city of Ghent more meaningful. Among all these valueable people, a special thanks goes to Aditya Dharanipragada Naga Venkata Ranga, Roxanne Hubesch, Chanakya Ranga and Stavros Theofanidis, for the long conversations about all the uncertainities in life (and the Ph.D.) and their unconditional friendship. Additionally, I would like to thank “that guy” (Jeroen Poissonnier), Jose Guillermo Rivera de la Cruz, Kaustav Niyogi, Nils De Rybel, Daria Otyuskaya, Tapas Rajkhowa and

Luis Lozano Guerra who have been there with their ideas and support at different stages of this Ph.D. work.

I owe my deepest gratitude to Prof. Dr. Deniz Üner for being there for me and showing me the right way at confusing crossroads of life. I managed to reach this crucial milestone in my life thanks to her presence and support that has been continuing for more than a decade.

I am also indebted to Prof. Dr. Şakir Erkoç for motivating me to enter the field of Computational Chemistry. I had the chance to learn the foundations of atomic physics and electronic structure methods from him and this knowledge has a significant share in bringing me to the point of completion of this thesis.

As well as the people from Ghent, I got long distance support from my friends from my pre-Ghent life like Ramazan Oğuz Canıaz who has always been there with me to remind me the things that we have achieved before and what potentials we do possess whenever I seem to be blinded with the surrounding difficulties and forget this. Another such friend is Salar Habibpur Sedani who has welcomed me in Ankara whenever I needed to go back there in the recent years. His friendship has always been so valuable for me and he never ceased to show his supportive approach at times of need.

I would like to thank my family for their encouragement and support. I am forever indebted to them for giving me the opportunities and experiences that have made me who I am. They selflessly encouraged me to explore new directions in life and seek my own path.

Living in the city of Ghent gave me the chance to meet wonderful people outside the laboratory as well. The first one of them is Hazal Ceylan who has been with me from the early years of this Ph.D. journey. With her, we stayed together like brother and sister against all the odds in

a foreign country we did not know much about where nobody knew about us and we knew about nobody in the beginning. Then, we started to discover what is going on around us and now, we consider Ghent as our home. I have had numerous thunderstorms during this Ph.D. thesis since the very early days and during our long phone conversations, she has been insisting me to not to abandon the boat no matter what and how difficult it gets.

I would like to thank my friend Abdurrahman Gökkaya for being probably the funniest person around during these years. His high energy and sense of humour was extremely crucial in getting through the darkest days. With him, we have been through so much and regardless of how difficult things have become, he was present with something funny to change the mood and bring positivity.

I would like to thank Wesley Van de Sijpe who has been there to cheer me up with his jokes even at the darkest times, along with his mature approach to life. Even after my long absences due to the hard work needed for the thesis, we were coming back like we spent all our days together. I also cannot forget the events and the dinners we attended with Jelle Behaegel, particularly in the first years of my stay in Ghent. His friendship has always been so valuable for me.

The years that I spent for the preparation of this Ph.D. dissertation has been life changing for me not only because of the scientific and personal experience that I have gained but also in Ghent, I met my best friend, my love, my fiancée and my wife-to-be Markéta Štěpánová during this period. I cannot imagine how difficult it would be trying to accomplish completing this Ph.D. dissertation without her presence, considering how arduous it has been despite all the support and help I got from her. From the first day that I met her to this very day, she was the number one person who had the most significant contribution to the maintenance of my

physical and psychological well-being when I lost myself trying to complex technical problems. Whenever things went wrong and depressive with research, we would go out on a late night walk regardless of how rainy Belgian weather was on that particularly night and this walk would magically bring a resolution no matter how difficult the problem was. After all these years, every time I look at her, I see how lucky I have been in every way and how the difficulties and misfortunes can bring the best gifts of life. Markéta, I dedicate this Ph.D. thesis to you.

Alper Ince

Ghent, Belgium, 2017

The research leading to these results has received funding from the European Research Council under the European Union's Seventh Framework Programme (FP7/2007-2013)/ERC grant MADPII agreement n° 290793. The SBO project "Bioleum" (IWT-SBO 130039) supported by the Institute for Promotion of Innovation through Science and Technology in Flanders (IWT) is acknowledged. This work was carried out using the STEVIN Supercomputer Infrastructure at Ghent University, funded by Ghent University, the Flemish Supercomputer Center (VSC), the Hercules Foundation and the Flemish Government – department EWI

Contents

List of Figures

List of Tables

Notation

Roman Symbols

A	pre-exponential factor	$m^3\ kmol^{-1}\ s^{-1}$ or s^{-1}
$\tilde{A}$	single-event pre-exponential factor	$m^3\ kmol^{-1}\ s^{-1}$ or s^{-1}
$\tilde{A}_{ref}$	single-event pre-exponential factor of the reference reaction	$m^3\ kmol^{-1}\ s^{-1}$ or s^{-1}
C_p	standard heat capacity	$J\ mol^{-1}\ K^{-1}$
E	energy	$kJ\ mol^{-1}$
$\Delta E(0\ K)$	activation barrier at 0 K including ZPVE	$kJ\ mol^{-1}$
ΔE_0	electronic activation barrier (excluding ZPVE)	$kJ\ mol^{-1}$
E_a	activation energy	$kJ\ mol^{-1}$
$E_{a,ref}$	activation energy of reference reaction	$kJ\ mol^{-1}$
E_{el}	electronic energy	$kJ\ mol^{-1}$
E_E	contribution of electronic energy	$kJ\ mol^{-1}$
E_R	contribution of rotational modes to total energy	$kJ\ mol^{-1}$
E_T	contribution of translational modes to total energy	$kJ\ mol^{-1}$
E_V	contribution of vibrational modes to total energy	$kJ\ mol^{-1}$
$E^{XC}[\rho]$	exchange-correlation functional	-

F	significance of regression	-
G	Gibbs free energy	kJ mol^{-1}
$\Delta^{\ddagger}G$	Gibbs activation energy	kJ mol^{-1}
$\Delta_r G°$	standard reaction Gibbs energy	kJ mol^{-1}
$\overline{GAV/NNI}$	estimation vector of GAVs and NNIs	-
$\overline{\Delta GAV^{\circ}/\Delta NNI^{\circ}}$	estimation vector of ΔGAV° and ΔNNI°	-
$\widehat{H}$	Hamiltonian operator	-
h	Planck constant	6.62 10^{-34} J s
$\Delta H^{\ddagger}$	activation enthalpy	kJ mol^{-1}
$\Delta_f H°$	standard enthalpy of formation	kJ mol^{-1}
$\Delta_f H^{\circ}_{gas,exp}$	experimental gas phase standard enthalpy of formation	kJ mol^{-1}
$\hat{J}_i$	direct term (a part of Fock operator)	-
k	reaction rate coefficient	m^3 mol^{-1} s^{-1}
$\tilde{k}$	single event rate coefficient	m^3 mol^{-1} s^{-1}
k_{GA}	Group additively calculated reaction rate coefficient	m^3 mol^{-1} s^{-1}
K	equilibrium coefficient	m^3 mol^{-1}
$\widehat{K}$	kinetic energy term (a part of Hamiltonian operator)	-
$\widehat{K}_i$	exchange term (a part of Fock operator)	-
k_B	Boltzmann constant	1.38 10^{-23} J K^{-1}
N	Number of pair natural orbitals (in extrapolation to CBS)	-
N_A	Avogadro constant	6.02 10^{23} molecules mol^{-1}
Δn	change in number of moles in a reaction	mol
n_e	number of single events	-
n_{opt}	number of optical isomers	-
q	molecular partition function	-
q^E	contribution of electronic degeneracy to q	-
q^R	contribution of rotational modes to q	-
q^T	contribution of translational modes to q	-

q^V	contribution of vibrational modes to q	-
$q^{\ddagger}$	molecular partition function of the transition state	-
Q	canonical partition function	-
R	universal gas constant	8.314 J mol^{-1} K^{-1}
r_j	the residual	-
$S°$	standard entropy	J mol^{-1} K^{-1}
$\Delta S^{\ddagger}$	activation entropy	J mol^{-1} K^{-1}
S°_{int}	intrinsic entropy	J mol^{-1} K^{-1}
T	temperature	K
U	Internal energy	kJ mol^{-1}
V	volume	m^3
V^{mol}	mole volume at standard pressure	m^3
$\hat{V}$	potential energy term (a part of Hamiltonian operator)	-
$\hat{V}_{ee}$	electronic correlation term	-
$\hat{V}_{nn}$	nucleus-nucleus interaction term	-
$\hat{V}_{ne}$	nucleus-electron interaction term	-
X_{ij}	occurrence matrix	-
$\bar{y}$	vector that contains the *ab initio* calculated property	-
y_i	*ab initio* calculated property	
$\hat{y}_i$	GA calculated property	

Greek Symbols

β	the matrix of parameter values	-
κ	tunneling coefficient	-
κ_{TCF}	tunneling coefficient obtained from tunneling correction function	
ν	frequency	cm^{-1} or s^{-1}
ρ	factor of deviation between rate coefficients	-
$<\rho>$	geometric mean factor of deviation	-
σ	global symmetry number	-

σ_{ext}	external symmetry number	-
σ_{int}	internal symmetry number	-
ψ	wavefunction	-

Sub- and superscripts

‡	transition state
•	radical
eq	equilibrium
exp	experimental
ext	external
int	internal
m-	*meta*
o-	*ortho*
opt	optical isomers
p-	*para*
ref	reference
tot	Total

Acronyms

1D-HR	uncoupled (one-dimensional) Hindered Rotation
AI	*ab initio*
BAC	bond additive corrections
BDE	bond dissociation energy
BR	benzylic radical
BTX	benzene, toluene and xylenes
CBS	complete basis set
CI	configuration interaction
CPU	central processing unit
CTST	canonical transition state theory
DFT	density functional theory

F	significance
GA	group additivity
GAV	group additive value
HAR	hydrogen abstraction reaction
HBI	hydrogen bond increment
HF	Hartree Fock
HLC	high level correction
HR	Hindered Rotation treatment of rotation about forming/breaking bond in transition state and product radical
LCT	Laboratory for Chemical Technology
MAD	mean absolute deviation
MAH	monocyclic aromatic hydrocarbon
MAR	monocyclic aromatic radical
MAX	maximum deviation
MD	mean deviation
MP	Moller-Plesset methods
NAO	natural atomic orbital
NBO	natural bond orbital
NHO	natural hybrid orbital
NPA	natural population analysis
NNI	non-nearest neighbor interaction
PAH	polycyclic aromatic hydrocarbon
PES	potential energy surface
RMS	root mean square deviation
RRHO	rigid rotor harmonic oscillator
SF	Scaling factor
SOC	spin orbit correction
SPC	single point calculation
SSQ	the objective function
TD	toluene derivative
TS	transition state
TST	transition state theory
VTST	variational transition state theory

ZPVE	zero-point vibrational energy

Samenvatting

Dit doctoraatsproefschrift draagt voornamelijk bij tot de uitbreiding van de groepsadditieve (GA) methode van Benson voor de berekening van de thermochemische eigenschappen van een breed bereik aan meervoudig gesubstitueerde monocyclische aromatische koolwaterstoffen, wat moleculen zijn die veel voorkomen in lignocellulose, een belangrijke component in biomassa. De groepsadditieve waarden (group additive values, GAVs) zijn afgeleid van accurate kwantumchemische berekeningen voor een beperkt aantal goedgekozen moleculen, en in dit doctoraat wordt aangetoond dat deze aanpak chemische accuratesse bereikt. Daarom zijn de GAVs afgeleid in dit werk bruikbaar in de ontwikkeling van kinetische modellen, wat één van de belangrijkste activiteiten is in het onderzoeksveld van de thermochemische omzetting van lignocellulose-gebaseerde biomassa.

Een van de kerndoelstellingen van chemische technologie is het ontwikkelen van nieuwe technologieën en het verbeteren van de efficiëntie van bestaande technologieën. Twee processen op basis van thermochemische omzetting worden intensief bestudeerd op het

Laboratorium voor Chemische Technologie (LCT) van de Universiteit Gent: het stoomkraken van voornamelijk koolwaterstofvoedingen om lichte olefinen en BTX-aromaten (Benzeen, Tolueen en Xyleen) te verkrijgen, en snelle pyrolyse van lignocellulose om deze om te zetten in bio-olie. Het eerste proces kan gezien de reeds zeer verregaande optimalisatie als matuur beschouwd worden, en er resten enkel nog kleine verbeteringen op het gebied van mogelijke voedingen, selectiviteit, energiegebruik, effectieve productietijd en operationele kost. Deze kleine verbeteringen kunnen gezien de grote schaal van het proces echter aanleiding geven tot grote economische meeropbrengsten. Het tweede proces, de thermochemische omzetting van lignocellulose, heeft echter nog volop ruimte voor verbetering. Beide processen hebben gemeen dat een grondig en gedetailleerd begrip van de onderliggende chemie een cruciale rol speelt in de procesoptimalisatie. Bovendien geldt voor beide processen dat aromaten een belangrijke rol spelen in de chemie. De lignine in lignocellulose bestaat uit eenheden fenylpropanoaat, waarbij bijkomende zuurstofbevattende functionele groepen gesubstitueerd zijn op de aromatische ring en zijketens. Een gedetailleerd kinetisch model moet daarom de chemie van aromatische moleculen correct beschrijven. Deze chemie ontbreekt momenteel grotendeels, ten dele omdat voor veel aromatische moleculen geen thermochemische data beschikbaar zijn. Het onderhavige doctoraatsproefschrift komt tegemoet aan deze nood aan meer en betere thermochemische data voor aromaten.

Het is praktisch niet haalbaar om voor alle moleculen die aanwezig zijn in gedetailleerde kinetische modellen de thermochemische data experimenteel te bepalen of via accurate *ab initio* methoden te berekenen. Niettemin is deze data vereist, in het bijzonder bij de automatische generering van kinetische modellen, zoals met bijvoorbeeld LCT-software als Genesys. Hier kan Benson-groepsadditiviteit de nood lenigen. Het toepassen van een

groepsadditieve methode vereist echter de beschikbaarheid van alle groepsadditieve waarden en correcties voor niet-gebonden interacties voor alle moleculaire fragmenten en interacties die kunnen voorkomen in de kinetische modellen. De bepaling van de nodige groepsadditieve waarden, evenals de identificatie en bepaling van de benodigde correcties voor niet-gebonden interacties, gebeurt op basis van regressie aan thermodynamische data voor een grote verzameling moleculen en radicalen, verkregen op basis van accurate *ab initio* berekeningen. Een gelijkaardige aanpak wordt gebruikt voor snelheidscoëfficiënten.

Hoewel commerciële *ab initio* programma's zoals *Gaussian 09* gebruiksvriendelijke implementaties van accurate post-Hartree-Fock methoden bevatten, zoals de composietmethoden CBS-QB3 en G4, is het aan de gebruiker om de betrouwbaarheid van de resultaten te garanderen. Uitgebreide vergelijking met experimentele data toont aan dat correcties voor spin-orbitaalkoppeling (voor CBS-QB3) en bindingsadditieve correcties (voor CBS-QB3 en G4) nodig zijn om te corrigeren voor systematische afwijkingen. Voorts dienen de berekeningen uitgevoerd te worden op het laagste-energie conformeer, dat evenwel vaak moeilijk te bepalen is. De geconvergeerde golffunctie moet de elektronische grondtoestand beschrijven, wat echter niet altijd het geval is waardoor de berekeningen die hierin in gebreke blijven geïdentificeerd en bijgestuurd moeten worden. De interne-rotorbehandeling leidt gemakkelijk tot kleine fouten, met name als de verkeerde vibratiemodes vervangen worden. Uit deze moeilijkheden wordt duidelijk dat vele factoren de kwaliteit van de *ab initio* referentiedatabank bepalen. Naast het van nabij opvolgen van de vermelde problemen wordt de referentiedatabank ook bewust groot gehouden, waarbij elke groepsadditieve parameter in tenminste 3 moleculen voorkomt. Dit laat niet enkel toe om moleculen te identificeren waar een of andere fout in de *ab initio* berekening plaatsvond, maar ook om de consistentie van de

finale data te verbeteren. Ten slotte werden ook de resultaten verkregen met de methoden G4 en CBS-QB3 vergeleken. Voor de meeste moleculen hebben beide methoden een gelijkaardige accuratesse, maar CBS-QB3 heeft problemen om fenylradicalen correct te beschrijven. Daarom is G4 de voorkeursmethode voor species die een fenylradicaal als kern hebben. Deze methode is echter veeleisender qua rekentijd en kan enkel op kleinere moleculen toegepast worden. Daarom moest een balans gevonden worden tussen accuratesse en rekentijd en werden de berekeningen voor twee hoofdstukken, i.e. hoofdstukken 5 en 6, op het CBS-QB3 niveau uitgevoerd.

Vooreerst is de methodologie toegepast op monocyclische aromatische koolwaterstoffen, waarbij het effect van zes substituenten op de thermodynamische eigenschappen systematisch nagegaan wordt, met name de substituenten hydroxy- (-OH), methoxy- (-OCH_3), formyl- (-CHO), vinyl- (-$CH{=}CH_2$), methyl- (-CH_3) en ethyl- (-CH_2CH_3). Dit doctoraatsproefschrift toont aan dat de interacties tussen de substituentgroepen op meervoudig gesubstitueerde benzenen een grote bijdrage hebben tot de thermodynamische eigenschappen voor dit type moleculen. Niet-gebonden interacties (non-nearest neighbor interactions, NNIs) zijn gedefinieerd in het kader van Bensons groepsadditieve methode, en aangezien deze interacties een grote invloed hebben op de thermodynamische eigenschappen kan chemische accuratesse niet bereikt worden zonder correcties voor deze NNIs. Natuurlijke bindende-orbitaalanalyse (natural bond orbital analysis, NBO) toont aan dat de geïntroduceerde NNIs fysisch zinvol zijn. Nog belangrijker is evenwel dat de correcties voor de interacties additief zijn en dat groepsadditiviteit voor sterk gesubstitueerde benzenen accurate thermochemische data oplevert.

Na het aantonen van de haalbaarheid van Bensons groepsadditieve methode voor moleculen, is dezelfde aanpak ook toegepast op de overeenkomstige radicalen in hoofdstuk 4. Ook hier levert groepsadditiviteit accurate data, maar er zijn een groot aantal NNIs vereist om te corrigeren voor interacties tussen de substituenten. Deze NNI-correcties kunnen zeer groot worden, zo bedraagt één van de correcties voor de standaardvormingsenthalpie zelfs meer dan 35 kJ mol^{-1}. De combinatie van de groepsadditieve data voor gesubstitueerde aromaten met deze voor hun overeenkomstige radicalen laat toe op een snelle en betrouwbare wijze bindingsdissociatie-energieën te berekenen, wat zeer interessant is voor bijvoorbeeld de identificatie van de zwakste binding in monocyclische aromatische koolwaterstoffen.

Nadere beschouwing van de NNI-correcties leert dat de correcties voor *ortho*-substitutie duidelijk domineren, gevolgd door deze voor *para*-substituent-interacties. Er zijn slechts een beperkt aantal significante *meta*-interacties geïdentificeerd, en deze behelzen bovendien louter interacties met zuurstofbevattende groepen. Deze vaststelling kan van pas komen bij het bestuderen van moleculen met substituenten die niet besproken worden in dit doctoraat.

Terwijl hoofdstukken 3 en 4 focussen op de thermodynamische eigenschappen van gesubstitueerde aromatische moleculen met kleine alkylsubstituenten, is hoofdstuk 5 gewijd aan de thermodynamische eigenschappen van tolueenderivaten waarin één of twee waterstofatomen van de methylgroep van tolueen vervangen zijn door een grotere, doorgaans onverzadigde alkylgroep. Ook de overeenkomstige benzylradicalen zijn behandeld in dit hoofdstuk. De resultaten bevestigen de conclusies van hoofdstukken 3 en 4, met name dat eens passende en fysisch zinvolle NNIs geïntroduceerd zijn de groepsadditief voorspelde thermodynamische data zeer betrouwbaar zijn. Ook hier zijn meer NNIs nodig voor radicalen

dan voor de overeenkomstige moleculen, en hebben in het bijzonder substituenten in *ortho*-positie van de gesubstitueerde alkylgroep een grote bijdrage.

Ten slotte worden kinetische groepsadditieve waarden ΔGAV^o gerapporteerd voor waterstofabstracties door een waterstofatoom van tolueenderivaten die al dan niet gesubstitueerd zijn met de 6 substituentgroepen -OH, $-OCH_3$, -CHO, $-CH{=}CH_2$, $-CH_3$ en $-CH_2CH_3$. Het beschouwde temperatuurbereik loopt van 300 tot 2000 K. Een totaal van 8 ΔGAV^os en 3 $\Delta NNI°$s is nodig om de Arrheniusparameters van de voorwaartse reacties te beschrijven, terwijl er 8 ΔGAV^os en 14 $\Delta NNI°$s nodig zijn voor de terugwaartse reacties. De bijdrage van kwantummechanische tunneleffecten tot de snelheidscoëfficiënten, iets wat groepsadditiviteit niet kan beschrijven, is in rekening gebracht door een afzonderlijke functie die corrigeert voor tunneling. Opnieuw kon aangetoond worden, maar nu voor reactiekinetiek, dat groepsadditieve berekeningen behoorlijk accuraat zijn. Voor de voorwaartse reactie is de meetkundig gemiddelde afwijkingsfactor tussen groepsadditieve en *ab initio* snelheidscoëfficiënten een factor 2.2 bij 330 K, 1.6 bij 600 K en minder dan 1.5 bij hogere temperaturen. Voor de terugwaartse reactie geldt een gelijkaardige accuratesse.

De groepsadditieve parameters bepaald in dit werk zijn consistent met de groepsadditieve modellen die reeds eerder ontwikkeld werden aan het LCT. De combinatie van alle beschikbare groepsadditieve waarden laat toe om thermodynamische eigenschappen te berekenen voor moleculen uit een groot aantal verbindingsklassen, waaronder nu ook monocyclische aromatische koolwaterstoffen. De kinetische ΔGAV^os bepaald in dit werk zijn slechts een eerste stap in de ontwikkeling van een kinetische databank voor reacties van monocyclische aromatische koolwaterstoffen. Niettemin bieden de ontwikkelde modellen een goed startpunt voor abstractiereacties met andere abstraherende radicalen, omdat de voornaamste reactanten

en producten dezelfde zijn en geometrieën van de transitietoestanden eenvoudig aangepast kunnen worden. Daarom biedt dit doctoraatsproefschrift een aanzienlijke stap voorwaarts in de ontwikkeling van betrouwbare kinetische modellen voor gasfasereacties waarbij aromaten betrokken zijn.

Summary

The main contribution of this Ph.D. dissertation is the extension of Benson's group additivity (GA) method to the calculation of thermochemical properties of a broad range of (poly)substituted monocyclic aromatic hydrocarbons, a class of compounds that is relevant for the conversion of lignocellulosic biomass. The group additive values (GAVs) are derived from high-level quantum chemical calculations for a limited set of well-chosen molecules and it is demonstrated that the approach used in this Ph.D. work is capable of achieving chemical accuracy, hence these GAVs are suitable for use in kinetic model development which is one of the main research activities in the area of thermochemical conversion of lignocellulosic biomass.

A core objective of chemical engineering is to develop new technologies and to improve the efficiency of existing ones. Two thermochemical conversion processes that are studied intensively at the Laboratory for Chemical Technology (LCT) of Ghent University are steam-cracking of mainly hydrocarbon feedstock to produce light olefins and BTX aromatics

(Benzene, Toluene and Xylene), and fast pyrolysis of lignocellulosic biomass to convert it mainly into a liquid called bio-oil. The first process belongs to the group of highly matured technologies, meaning that it is already well optimized and only gradual improvements in the areas of feedstock tolerance, selectivity control, energy efficiency, on-line time improvement and operation cost reduction can be expected. However, those small improvements translate into substantial economic benefits. On the other hand, the thermochemical conversion of lignocellulosic biomass is a technology, which still has plenty of room for improvement. Both examples have in common that a thorough and detailed understanding of the chemistry will play a crucial role in further process optimization. Another commonality is that aromatic molecules play an important role in the processes. The lignin component of lignocellulosic biomass consists of phenyl propanoic units with additional oxygenated functional groups attached to the aromatic ring and side chain. Any detailed kinetic model therefore must include proper chemistry for aromatic molecules. Currently this chemistry is lacking, partly because thermochemical information for many aromatic molecules are unavailable. The current thesis addresses this need.

It is practically not possible to either experimentally determine thermodynamic properties for every species found in detailed kinetic models or to calculate them with a high-level *ab initio* method. Nevertheless, this data is needed in particular if kinetic models are generated automatically, e.g. with software such as the Genesys code of LCT. Benson's group additivity approach caters for this need. However, application of Benson's method requires that group additivity parameters and non-nearest neighbor interaction terms for all moieties in the species that might appear as a part of the kinetic model are available. Identification and quantification of the appropriate non-nearest neighbor interactions together with the determination of the

necessary group additive values is done by assembling thermodynamic properties for a sufficiently large set of well-chosen molecules and radicals using high level *ab initio* calculations and employing these reference data combined with regression methods to optimize the GA parameters. A similar strategy is used for rate coefficients.

Even though commercial *ab initio* software such as the Gaussian 09 software suite contains user friendly implementations of high level post-Hartree Fock methods including the CBS-QB3 and G4 compound methods, it is up to the user to ensure that the results are reliable. Extensive comparisons with experimental data show that spin orbit (for CBS-QB3) and bond additivity corrections (for CBS-QB3 and G4) are needed to account for systematic deviations. Furthermore, the calculations should be performed for the lowest energy conformer, which is often difficult to determine. The converged wave function must describe the ground state, which is not always the case and failed calculations must be identified. The internal rotor treatment leads easily to small errors if incorrect vibrational modes are replaced. In summary, many factors determine the quality of the *ab initio* reference data base. Besides monitoring closely all possible problems mentioned above, the large reference data set is used to ensure that each GA parameter is present in at least three species. This redundancy helps not only to pinpoint cases where a mistake is made in the identification of the lowest energy conformer and/or an error in the calculations occurred but also to improve the consistency of the final data set. Last but not least, the results obtained with the G4 and CBS-QB3 methods were compared. For most cases, both methods give similar accuracies but CBS-QB3 has problems to handle phenyl radicals properly. Thus, the G4 method is the preferred method for species containing the phenyl radical moiety. However, it is more CPU time demanding and can only be applied to rather small species. Therefore, a trade off had to be made between accuracy and

computational cost and, hence, the calculations for **Chapters 5** and **6** were performed at the CBS-QB3 level of theory.

First, the established methodology is applied to closed shell monocyclic aromatic hydrocarbons and the impact of six substituents (hydroxy (-OH), methoxy (OCH_3), formyl (-CHO), vinyl (-CH=CH_2), methyl (CH_3) and ethyl (CH_2CH_3)) on the thermodynamic properties is systematically studied. This Ph.D. thesis demonstrates that the interactions between the substituent groups of multiply substituted benzenes contribute to a large extend to the thermodynamic properties of this type of molecules. Within the framework of Benson's GA method, non-nearest neighbor interaction corrections (NNIs) are defined to describe these interactions and since these interactions have a significant impact on the thermodynamics, chemical accuracy cannot be achieved without the application of NNI corrections. Natural bond orbital (NBO) analysis is employed to demonstrate that the identified NNIs are physically meaningful. Most importantly, though, the interactions are additive and GA calculations for highly (penta)substituted benzenes yield accurate data.

After having established the applicability of Benson's group additivity method for closed-shell molecules, the same approach is used for the corresponding radicals in **Chapter 4**. Again, very good accuracy of the GA calculations is observed, however a larger number of NNIs is required to correct for substituent interactions and some corrections are quite large, e.g. one interaction reduces the enthalpy of formation by more than 35 kJ mol^{-1}. The combination of GA data for closed shell substituted aromatic molecules and their corresponding radicals allows a fast and reliable calculation of bond dissociation energies, which is helpful for fast identification of the weakest bond in monocyclic aromatic hydrocarbons, e.g. lignin oligomers.

Inspection of the NNIs defined at this stage shows that those for *ortho* substitution clearly dominate, followed by those for *para* substituent interactions. Only very few significant *meta* interactions are identified and those exclusively involve oxygen-containing groups. This observation may be helpful if molecules are studied that contain substituent groups not covered in this thesis.

While **Chapters 3** and **4** focus on thermodynamics for substituted aromatic molecules with small alkyl side chains, **Chapter 5** is dedicated to the thermodynamics of toluene derivatives in which one or two hydrogen atoms of the -CH_3 group of toluene is/are replaced with larger mainly unsaturated alkyl groups. Also, included in this part are the corresponding benzylic radicals. The results essentially confirm the conclusions from **Chapters 3** and **4**, in the sense that once suitable and physically plausible NNIs are identified and assigned, GA predictions are very reliable. As before, more NNIs are needed for the radicals than for closed shell molecules and in particular substituents in *ortho* position to the extended alkyl group create significant interactions.

Finally, kinetic GA parameters (ΔGAV^os) are reported for H atom abstraction reactions by a hydrogen atom from unsubstituted and substituted toluene derivatives with the six substituent groups: -OH, -OCH_3, -CHO, -$CH{=}CH_2$, -CH_3, CH_2CH_3. The temperature range considered is 300 K to 2000 K. A set of 8 $\Delta GAV°$s and 3 $\Delta NNI°$s is needed to describe the Arrhenius parameters of the forward reactions while 8 $\Delta GAV°$s and 14 $\Delta NNI°$s are required for the reverse reaction. Quantum tunneling effects, which cannot be described by group additivity, are taken into consideration separately through a tunneling correction function. It is again shown, but this time for kinetics, that GA calculations are quite accurate. In the forward direction, the geometric mean factor of deviations between GA and *ab initio* results is 2.2 at

300 K, 1.6 at 600 K and less than 1.5 at higher temperatures. For the reverse direction, a similar accuracy is found.

The sets of GA parameters determined in this work are consistent with the GA values that were previously developed at LCT. All available sets combined allow thermodynamic property calculations for a large number of molecule families, which now include many monocyclic aromatic hydrocarbons. The kinetic ΔGAV°s reported here are just a first step to develop a kinetic database for reactions of monocyclic aromatic hydrocarbons. Nevertheless, the calculations present a good starting point for abstraction reactions with different abstracting radicals because the main reactants and products are the same and the transition state geometries can easily be adapted. Therefore, this thesis work presents a significant step forward towards reliable kinetic models for gas phase reactions involving aromatic species.

Chapter 1

Introduction

1.1 Aromatic Compounds

Among the various classes of chemical compounds that find application in the modern industry, aromatic molecules stand out owing to their use as starting materials or intermediate species in the mass production of a myriad of products in a wide range of fields like energy, medicine, transport, telecommunications, fashion and sports [1]. In spite of the fact that the aromatic molecules are named as such due to their olfactory character, in chemical terms, the word “aromatic” refers to a molecule that exhibits a chemical property termed as “aromaticity”, as described for benzene by August Kekulé, a former professor of Ghent University, for the first time in 1865 [2]. Aromaticity can be defined as the electron delocalization that is encountered in unsaturated cyclic compounds, which provides enhanced thermodynamic stability with respect to the other possible geometric or connective arrangements with the same

set of atoms. The term “aromatic” is generally used in an informal fashion to describe benzene derivatives since most common aromatics are derivatives of benzene and besides, this term was historically defined to refer to this class of compounds. However, it is known today that many non-benzene aromatics also exist, e.g. the nucleobases that possess two rings in DNA and RNA like adenine or guanine.

As a subdomain of the field of aromatic chemistry, the radical chemistry of monocyclic aromatic hydrocarbons (MAHs) is encountered in diverse areas. One example is the occurrence of monocyclic aromatic radicals (MARs) (phenyl (C_6H_5•) and benzyl ($C_6H_5CH_2$•)) as important intermediate species in the molecular growth chemistry that yields polycyclic aromatic hydrocarbons (PAHs) [3,4], coke [5] and soot [6]. In the last decades, phenol (C_6H_5OH) and phenolic compounds have been a center of attention in the biochemistry research due to their antioxidant activities in biological systems [7-9], meaning that they have an inhibiting effect on the oxidation of organic matter by transferring a hydrogen atom from an OH group to the chain-carrying radicals [8]. Also in radical initiated polymer chemistry, MARs take part as crucial intermediates [10,11]. The toluene derivatives and their corresponding radicals, i.e. the benzylic radicals are involved in the upgrading of heavy oils to valuable transportation fuels [12]. In addition to all of these applications, the gas phase chemistry of MAHs and MARs are relevant to some of the critical environmental issues of 21st century such as the depletion of the ozone layer in earth’s atmosphere and mitigation of the impact caused by the emissions of NO_X gases, which are known to contribute to the acid rains and to the formation of smog over populated areas [13-15]. Another important field of application is the steam cracking process in the petrochemicals industry, where saturated hydrocarbons are cracked to yield “pyrolysis gas”, which contains monocyclic aromatic

compounds that are known as BTX (benzene, toluene and xylenes) [16,17]. Here, the term "pyrolysis" refers to the gas phase thermochemical decomposition at high temperatures in the absence of oxygen. Pyrolysis is also utilized for the carbon black production and the thermochemical conversion of biomass [18-20]. In this Ph.D. dissertation, the focus on the gas phase chemistry of aromatics is mainly motivated by its application in the pyrolysis of lignin, a component of ligno-cellulosic biomass, as described below in detail.

1.2 Lignin pyrolysis

Contrary to the depleting fossil fuel sources, plant based biomass, i.e. ligno-cellulosic biomass attracts attention as a renewable alternative since the ligno-cellulosic biomass is the most abundant raw material on earth [21]. The use of ligno-cellulosic biomass as a source of fuel is also regarded as an environmentally friendlier alternative inasmuch as it is expected to alleviate the adverse impact of mankind on the environment like the global warming and the consequent climate change [22]. Furthermore, the processing of this biomaterial yields a wide variety of valuable commodity or specialty chemicals that serve as a valuable feed for several industrial processes.

Regarding the process technologies that are utilized for the thermochemical conversion of ligno-cellulosic biomass, several options are available, which can generally be categorized as enzymatic, catalytic and thermal processes [22,23]. According to this classification, the above-mentioned pyrolysis of biomass falls in the category of thermal processes. Current interests concerning thermochemical conversion of biomass leads to the need for a better understanding of the pyrolysis of its components cellulose, hemicellulose, and lignin. Given the relatively low O/C ratio compared to other biomass components and the richness in aromatic units,

pyrolysis of the lignin fraction has recently received special attention [24]. In this process, first, the lignin feedstock is heated and in a subsequent step, the resulting vapors are condensed to yield a liquid product that is known as “bio-oil” or “pyrolysis-oil” [24]. In the 80s, it was discovered that carrying out these two steps in a rapid manner (fast pyrolysis) maximizes the product yield of the bio-oil [24], which renders fast pyrolysis of lignin a plausible conversion route to liquid fuels and commodity chemicals.

On account of the reasons mentioned above, feasible mass production of bio-oils and chemicals via lignin pyrolysis has become one of the objectives of contemporary chemical engineering research. This ultimate objective inherently dictates the necessity of process optimization. The incentive for the process optimization is strong, in particular, for the larger scale processes, because an improvement of 0.1% in the product yield can lead to increases in annual profits by several hundred thousands of euros. The state-of–the-art approach in the optimization of industrial chemical processes employs detailed thermochemical and kinetic information regarding all the species and reactions involved in the process, i.e. microkinetic modeling. Recently, microkinetic modeling has been used in the optimization of several industrial processes such as steam cracking of hydrocarbons [25], combustion [26,27], and the formation of polycyclic aromatic hydrocarbons [28-30]. Nevertheless, the last decade has witnessed the transformation of kinetic micromodeling from the manual assembly of reaction networks to one in which software packages [31-36] are utilized to automatically generate comprehensive reaction mechanisms based on user-defined reaction rules. These software packages are responsible for bookkeeping of all the participating species that form and deplete upon reactions, including reactive intermediates. Analogous to manual kinetic model construction, these software packages require the availability of reliable thermochemical data for all the

species next to 'on-the-fly' calculation of the reaction rate coefficients of all the reactions that take part in the mechanism to be generated. Nonetheless, the large lacunas in the existing thermochemical and kinetic databases limit the predictive capability of these packages and the use of first-principle calculations to fill these gaps is still ongoing [37-39].

One of the major obstacles in the development of gas phase kinetic models for lignin pyrolysis is the absence of thermochemical and kinetic data concerning the reactions that involve substituted monocyclic aromatic molecules and radicals since these types of species make up the majority not only of the product slate and but also of the three main building blocks of lignin [40]. Collection of such data through experimental means is cumbersome since the number of occurring intermediate radical species are highly reactive in nature and, hence, short-lived. By the same token, it is not feasible to obtain data for a broad range of reaction conditions due to financial and instrumental limitations. In the last two decades, application of *ab initio* calculations to the field of kinetic studies has become a popular practice by virtue of the significant improvements in computational power and the advent of new quantum chemical methods that are capable of delivering accurate results and enabling the study of various reaction pathways in detail. Notwithstanding these advantages, utilization of *ab initio* calculations to obtain the necessary data for all the possible reactions in a free-radical process is nowhere close to an attainable approach since providing the necessary kinetic data for a vast range of reactions is computationally too demanding. This is particularly valid for the reactions that involve relatively large species, e.g. substituted aromatics, as the computational cost increases rapidly with increasing size of the molecule. As a result, several thermochemical property estimation methods [41-44] and rate coefficient estimation methods [45-49] based on first principles calculations for a limited number of well-chosen species and reactions are

developed. These models can easily be implemented in reaction network generation software packages and are capable of predicting thermochemical and kinetic data for a broad range of molecules and reactions. Hence, the availability of these models eliminates the need to obtain experimental or *ab initio* data for each one of the numerous species and reactions in a kinetic network.

1.3 Group Additivity Modeling

1.3.1 Thermodynamics

One of the most widely used approaches in thermodynamic property estimation is the Group Additivity (GA) method developed by Benson and coworkers [50-52]. The essence of Benson's method is that any thermochemical property of a molecule can be calculated from contributions ("group additive values (GAVs)") of smaller units, called groups. Benson defines a group as "a polyvalent atom in a molecule together with all its ligands" [52]. Even though GAVs are capable of accounting for the major part of a thermodynamic property, inclusion of contributions from interactions that extend beyond the range of a group is essential to achieve the level of accuracy needed for kinetic modeling. These so-called "non-nearest neighbor interactions" are incorporated into the group additivity method as correction terms (NNIs). The thermodynamic property "y" thus is calculated as

$$y = \sum_{1}^{i} n_i GAV_i + \sum_{1}^{j} n_j NNI_j \qquad (1\text{-}1)$$

The GAV_i refer to different groups which occur n_i times in the molecule and NNI_j is the j^{th} correction term which occurs n_j times in the molecule. For the calculation of thermodynamic properties of a molecule via Benson's Group Additivity method, the contributions from all the

groups and non-nearest neighbor interactions present in the molecule must be known. Therefore, an ongoing effort is to expand the available GAV/NNI databases towards previously ignored classes of compounds and to improve the accuracy of existing entries.

Group values for Benson's GA method were initially derived entirely from experimental data [52-56], but in the last decade several studies used computational means to define these parameters [57-64]. It has been shown that GA methods are able to calculate standard enthalpies of formation with "chemical accuracy," meaning with a standard deviation of not more than 4 kJ mol^{-1} [58-61]. This accuracy is comparable to that of high level *ab initio* methods, which require substantial computational time and effort. Benson's method has been successfully applied to standard enthalpies of formation of gas phase molecules [25,51,54,58,60,61] and also to entropies and heat capacities [42,50-52,59-61].

To ensure that the values obtained via GA are reliable, the GAV and NNI definitions have to be internally consistent. This means that (1) the GAV parameters are assigned in a systematic way resolving all linear dependencies [42], (2) the set of NNIs are comprehensive and well defined, and (3) all parameters are determined from reference data of equal quality. Marin and coworkers [58-61] have started to create such an internally consistent GAV/NNI database based on *ab initio* results at the CBS-QB3 level of theory. The earlier studies from this group provided GAV and NNI definitions that allow calculation of thermodynamic properties for aliphatic hydrocarbons like alkanes, alkenes, alkynes, and few cyclic hydrocarbons and their corresponding radicals [58,59], oxygenates such as alcohols, esters, ethers, ketones, carboxylic acids, ketenes and their corresponding radicals [61], and organic sulfur compounds [60].

For monocyclic aromatic compounds, with few exceptions, reliable experimental data are not available in literature. Moreover, among the several studies from Marin and coworkers that

provided GAVs and NNIs for the group additive parameter database, only Sabbe et al. reported GAVs for a very limited number of unsubstituted monocyclic aromatic hydrocarbons (MAHs) and monocyclic aromatic radicals (MARs) [58,59]. For the substituted counterparts of these species, no GAVs and NNIs have been reported before. The substituent effects in the substituted aromatic species cannot be taken into account by GAVs as these effects are beyond the range of a Benson "group". Hence, for a proper definition of these MAHs and MARs, the necessary NNIs have to be defined for these effects. Unfortunately, in the literature, only two NNIs of this nature are reported [50-52] for the MAHs and no NNIs are reported for MARs. Given the plethora of industrial processes in which (un)substituted monocyclic aromatic species play a fundamental role (e.g. lignin pyrolysis), development of the GA parameters that enables the calculation of the thermochemical properties of these species is certainly necessary to fill an important gap in the modern chemical engineering applications of gas phase chemistry.

1.3.2 Kinetics

Benson's group additivity method for thermodynamics was extended to the domain of kinetics by Saeys et al. [49,65] for the calculation of activation energies and further refined by Sabbe et al. [66,67] to include pre-exponential factors. This new approach in kinetic data estimation, coined as the "group contribution method", is adopted to develop predictive parameters based on a training set of *ab initio* kinetic data. Once these parameters are determined, they can be used to obtain the Arrhenius parameters that are necessary for the calculation of the reaction rate coefficients for all the reactions within the same family. In the group contribution method, Benson's GA is reformulated for the differences between reactants and the transition states in terms of enthalpy and entropy, which leads to direct group additivity for the activation energy

(E_a) and pre-exponential factor (A) [68]. Furthermore, in order to eliminate the temperature dependence of these parameters as much as possible, they are developed with respect to the Arrhenius parameters of a reference reaction, which is generally chosen as the simplest reaction that represents a particular family of reactions.

In the last decade, Marin and coworkers have successfully employed the group contribution method to develop a database of parameters that yield accurate Arrhenius parameters and reaction rate coefficients for a wide range of reaction families: hydrogen abstractions [67-70] and additions [66,71] between hydrocarbons, 1,2-hydrogen shifts and cyclization reactions for silicon-containing compounds [72-74], for α-hydrogen abstractions from thiols, sulfides, thiocarbonyl, and other sulfur compounds [75,76], for α-hydrogen abstractions from oxygenate compounds by carbon centered radicals and hydrogen abstraction reactions between oxygenates [68,77].

Concerning the reactions, in which aromatic species play an important role, the lack of availability of kinetic data is a major issue. This is particularly the case in the application of lignin pyrolysis, as a significant portion of the kinetic network of this process is comprised of reactions such as hydrogen abstractions from MAHs [78-80], additions to unsaturated bonds [79,80], intramolecular hydrogen transfers [80,81], CO elimination from (un)substituted phenoxies [80,82] and rearrangement of (un)substituted anisyls [80]. Given that the substituted MAHs and MARs that appear in these reactions may come with a wide variety of type, number and position of substituents, expanding the existing predictive kinetic parameter database in the direction of these reaction families can be considered as a rational next step in terms of the desideratum of the aforementioned chemical engineering applications, particularly the lignin pyrolysis.

1.4 Outline and objectives

The main objective of this research is to expand the above-mentioned thermodynamic and kinetic parameter databases to predictive parameters for the thermodynamics and the kinetics of unsubstituted and substituted monocyclic aromatic compounds. This Ph.D. dissertation consists of a compilation of two academic papers published within this research and the other two manuscripts that are planned to be submitted for publication in the near future.

The majority of the work in this present thesis is devoted to thermodynamics whereas only the last one focuses on kinetics. This is particularly so as this research aims to lay the groundwork for all the future systematic studies with the target of modeling the effects of substituents on the thermodynamics and kinetics involving aromatics. To this end, construction of a solid foundation with regard to the thermodynamics of a wide range of substituted MAHs and MARs is one of the most plausible starting points. Besides, as mentioned above, there is a vast number of reaction families in which substituted aromatic species take part and hence, development of predictive parameters for the kinetics of all of these reaction families goes beyond the frame of one Ph.D. study.

The general strategy for the development of the GA models presented in this thesis can be outlined as follows:

(1) A training set consisting of a limited number of molecules/reactions is constructed for the determination of thermochemical/kinetic data of the molecules/radicals or reactions from high level *ab initio* calculations.
(2) Group additive parameters are defined based on the chemical structure of the species.
(3) Substituent effects are identified.

(4) GA parameters, i.e. GAV and NNI for thermodynamics or ΔGAV° and ΔNNI° for kinetics, are simultaneously optimized.

(5) A validation set consisting of a limited number of well-chosen species/reactions that do not belong to the training set and for which thermochemistry/kinetics are available from high-level *ab initio* calculations is defined.

(6) The performance of the GA parameters is tested on the validation set.

(7) The training set and the validation set are combined to form a final set and the final values of the GA parameters, GAV and NNI, are reoptimized based on this set.

In **Chapter 2**, the methodology followed throughout this research is explained in detail. This chapter starts with a very brief explanation of the theory related to *ab initio* calculations. This is followed by a detailed explanation on the further processing of the data from the standard *ab initio* calculations to obtain the thermochemistry/kinetics for the species/reactions in the training and validation sets. Then, the details of the method of Benson's GA and the group contribution method of Saeys et al. [49,65] and Sabbe et al. [66,67] are discussed. Afterwards, the linear regression procedure that is used in the optimization of the predictive parameters based on the *ab initio* datasets is briefly described.

The first objective of this Ph.D. dissertation is to develop a set of GAV/NNI parameters that describes the thermochemistry of the unsubstituted, mono and multiply substituted MAHs. This is discussed in **Chapter 3**. Since this extension to the database is mainly motivated by the interest in modeling pyrolysis products of lignin, the following six substituent groups are considered: hydroxy (-OH), methoxy ($-OCH_3$), formyl (-CH=O), vinyl ($-CH=CH_2$), methyl ($-CH_3$) and ethyl ($-C_2H_5$). **Figure 1-1** illustrates the MAHs of interest where "X" and "Y" represent the first and the second substituent on the phenyl ring, respectively. The reference

dataset in this study is comprised of all the *ortho* (*o*-), *meta* (*m*-) and *para* (*p*-) combinations of the X and Y groups to ensure that all the substituent effects are covered.

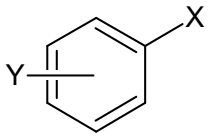

X, Y = -H, -OH, -OCH_3, -CHO,
-$CH{=}CH_2$, -CH_3, -C_2H_5

Figure 1-1 The unsubstituted and substituted monocyclic aromatic hydrocarbons of interest in the first part of the research (See **Chapter 3**).

The second objective in this research is to provide a set of GAV/NNI parameters that enables the group additive calculation of the thermochemical data for unsubstituted and substituted MARs. This is presented in **Chapter 4**. This chapter provides a continuation of the study in **Chapter 3**, where this objective is attained. The reference dataset in this chapter encompasses unsubstituted and substituted phenyl (C_6H_5•), phenoxy (C_6H_5O•), anisyl ($C_6H_5OCH_2$•), benzoyl (C_6H_5C•(=O)), β-styryl ($C_6H_5CH{=}CH$•) and benzylic radicals (benzyl ($C_6H_5CH_2$•) and 1-phenylethyl (C_6H_5CH•CH_3)) with the same six substituent groups (Y) as in **Chapter 3**.

It is known that the lignin structure consists of phenyl propanoid units [24,83] and some of the lignin pyrolysis products such as eugenol (2-methoxy-4-prop-2-enylphenol) [83] contain C_3 alkyl groups. The GA parameters developed in **Chapters 3** and **4** are not sufficient to allow thermodynamic calculations for species with such long unsaturated alkyl chains. The work in **Chapter 5** is mainly motivated by this need and the set of GA parameters obtained in **Chapters 3** and **4** is extended to alkyl substituents larger than the ones considered before (methyl and ethyl). In **Chapter 5**, two distinct sets of GAVs/NNIs are developed for substituted aromatic hydrocarbons and their corresponding radicals with a single alkyl side chain, which are toluene derivatives and benzylic radicals, respectively. **Figure 1-2** illustrates the dataset of interest where R represents the alkyl groups and Z represents the substituent groups.

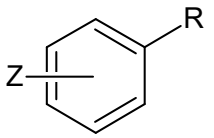

R = -$CH(CH_3)_2$, -$CH_2CH{=}CH_2$, -$CH(CH_3)CH{=}CH_2$, -$CH(CH{=}CH_2)_2$, -$CH_2C_6H_5$, -$CH(CH_3)C_6H_5$
Z = -OH, -OCH_3, -CHO, -$CH{=}CH_2$, -CH_3, -C_2H_5

Figure 1-2 The unsubstituted and substituted aromatics with alkyl chains of interest in the third part of the research (See **Chapter 5**).

Chapter 6 consists of the sole kinetic study in this Ph.D. dissertation where the first step into the research of kinetics for gas phase radical chemistry of aromatics is presented. In this chapter, predictive parameters are developed through the group contribution method that can be used for the calculation of accurate Arrhenius parameters and the reaction rate coefficients for the hydrogen abstraction reactions (HARs) from α-carbons of toluene derivatives by a hydrogen atom. The set of reactions within the framework of this study is outlined in **Figure 1-3** where R and Z denote the alkyl chains and the substituent groups on the phenyl rings, respectively. In all of these reactions, the reactants are comprised of a toluene derivative and a hydrogen atom while the products are a benzylic radical and a H_2 molecule.

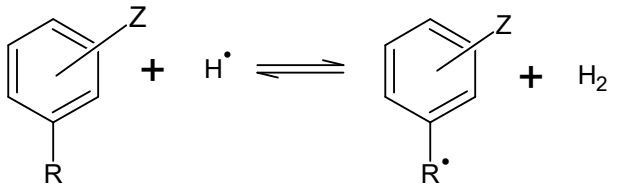

R = -CH_3, -C_2H_5, -$CH(CH_3)_2$, -$CH_2CH{=}CH_2$, -$CH(CH_3)CH{=}CH_2$, -$CH(CH{=}CH_2)_2$, -$CH_2C_6H_5$, -$CH(CH_3)C_6H_5$
Z = -OH, -OCH_3, -CHO, -$CH{=}CH_2$, -CH_3, -C_2H_5

Figure 1-3 The hydrogen abstraction reactions from the α-carbons of unsubstituted and substituted toluene derivatives by hydrogen atom. (See **Chapter 6**)

The conclusions from this Ph.D. work and the prospects for the future studies are conferred in the final chapter of this thesis (**Chapter 7**).

1.5 References

[1] Aromatics Improving the Quality of Your Life. Petrochemicals Europe website http://www.petrochemistry.eu/ftp/pressroom/APAEN.pdf. Updated January 24, 2017. Accessed January 25, 2017

[2] Kekulé A. Sur la constitution des substances aromatiques. *Bulletin de la Société Chimique de Paris*. 1865;3(2):98-110.

[3] Shukla B, Susa A, Miyoshi A, Koshi M. Role of Phenyl Radicals in the Growth of Polycyclic Aromatic Hydrocarbons. *The Journal of Physical Chemistry A.* 2008;112(11):2362-2369.

[4] Zhang F, Jones B, Maksyutenko P, Kaiser RI, Chin C, Kislov VV, Mebel AM. Formation of the Phenyl Radical [C6H5(X2A1)] under Single Collision Conditions: A Crossed Molecular Beam and ab Initio Study. *Journal of the American Chemical Society.* 2010;132(8):2672-2683.

[5] Albright LF, Marek JC. Mechanistic model for formation of coke in pyrolysis units producing ethylene. *Industrial & Engineering Chemistry Research.* 1988;27(5):755-759.

[6] Appel J, Bockhorn H, Frenklach M. Kinetic modeling of soot formation with detailed chemistry and physics: laminar premixed flames of C2 hydrocarbons. *Combustion and Flame.* 2000;121(1–2):122-136.

[7] Da Silva G, Chen CC, Bozzelli JW. Bond dissociation energy of the phenol O-H bond from ab initio calculations. *Chemical Physics Letters.* 2006;424(1-3):42-45.

[8] Foti MC. Antioxidant properties of phenols. *Journal of Pharmacy and Pharmacology.* 2007;59(12):1673-1685.

[9] Miranda MS, Esteves da Silva JCG, Liebman JF. Gas-phase thermochemical properties of some tri-substituted phenols: A density functional theory study. *The Journal of Chemical Thermodynamics.* 2015;80(0):65-72.

[10] Priddy DB. Recent Advances In Styrene Polymerization. *Polymer Synthesis.* 1994;111:67-114.

[11] Allushi A, Jockusch S, Yilmaz G, Yagci Y. Photoinitiated Metal-Free Controlled/Living Radical Polymerization Using Polynuclear Aromatic Hydrocarbons. *Macromolecules.* 2016;49(20):7785-7792.

[12] Hamelinck CN, Faaij APC, den Uil H, Boerrigter H. Production of FT transportation fuels from biomass; technical options, process analysis and optimisation, and development potential. *Energy.* 2004;29(11):1743-1771.

[13] Atkinson R, Carter WPL. Kinetics and mechanisms of the gas-phase reactions of ozone with organic compounds under atmospheric conditions. *Chemical Reviews.* 1984;84(5):437-470.

[14] Atkinson R, Arey J. Atmospheric chemistry of gas-phase polycyclic aromatic hydrocarbons: formation of atmospheric mutagens. *Environmental Health Perspectives.* 1994;102(Suppl 4):117-126.

[15] Atkinson R. Atmospheric chemistry of VOCs and NOx. *Atmospheric Environment.* 2000;34(12–14):2063-2101.

[16] Wiseman P. Ethylene by naphtha cracking. Free radicals in action. *Journal of Chemical Education.* 1977;54(3):154.

[17] Ren T, Patel M, Blok K. Olefins from conventional and heavy feedstocks: Energy use in steam cracking and alternative processes. *Energy.* 2006;31(4):425-451.

[18] Studebaker ML. The Chemistry of Carbon Black and Reinforcement. *Rubber Chemistry and Technology.* 1957;30(5):1400-1483.

[19] Boehm HP. Some aspects of the surface chemistry of carbon blacks and other carbons. *Carbon.* 1994;32(5):759-769.

[20] Kozlov A, Svishchev D, Donskoy I, Shamansky V. Impact of gas-phase chemistry on the composition of biomass pyrolysis products. *Journal of Thermal Analysis and Calorimetry.* 2015;122(3):1089-1098.

[21] Isikgor FH, Becer CR. Lignocellulosic biomass: a sustainable platform for the production of bio-based chemicals and polymers. *Polymer Chemistry.* 2015;6(25):4497-4559.

[22] Paraskevas P. *Sustainable conversion of biomass oxygenates: ab initio based model simulation*. Ghent, Belgium ; Athens, Greece: Ghent University. Faculty of

Engineering and Architecture ; National Technical University of Athens. School of Chemical Engineering, 2015.

[23] Stevens C, Brown RC. *Thermochemical processing of biomass: conversion into fuels, chemicals and power*: John Wiley & Sons; 2011.

[24] Mohan D, Pittman CU, Steele PH. Pyrolysis of Wood/Biomass for Bio-oil: A Critical Review. *Energy & Fuels.* 2006;20(3):848-889.

[25] Sabbe MK, Van Geem KM, Reyniers MF, Marin GB. First Principle-Based Simulation of Ethane Steam Cracking. *AIChE Journal.* 2011;57(2):482-496.

[26] Tran LS, Sirjean B, Glaude P-A, Fournet R, Battin-Leclerc F. Progress in detailed kinetic modeling of the combustion of oxygenated components of biofuels. *Energy.* 2012;43(1):4-18.

[27] Ranzi E. A wide-range kinetic modeling study of oxidation and combustion of transportation fuels and surrogate mixtures. *Energy & Fuels.* 2006;20(3):1024-1032.

[28] Richter H, Risoul V, Lafleur AL, Plummer EF, Howard JB, Peters WA. Chemical characterization and bioactivity of polycyclic aromatic hydrocarbons from non-oxidative thermal treatment of pyrene-contaminated soil at 250-1,000 degrees C. *Environmental Health Perspectives.* 2000;108(8):709-717.

[29] Norinaga K, Deutschmann O, Saegusa N, Hayashi J-I. Analysis of pyrolysis products from light hydrocarbons and kinetic modeling for growth of polycyclic aromatic hydrocarbons with detailed chemistry. *Journal of Analytical and Applied Pyrolysis.* 2009;86(1):148-160.

[30] Saggese C, Sánchez NE, Frassoldati A, Cuoci A, Faravelli T, Alzueta MU, Ranzi E. Kinetic Modeling Study of Polycyclic Aromatic Hydrocarbons and Soot Formation in Acetylene Pyrolysis. *Energy & Fuels.* 2014;28(2):1489-1501.

[31] Rangarajan S, Bhan A, Daoutidis P. Rule-Based Generation of Thermochemical Routes to Biomass Conversion. *Industrial & Engineering Chemistry Research.* 2010;49(21):10459-10470.

[32] Vandewiele NM, Van Geem KM, Reyniers M-F, Marin GB. Genesys: Kinetic model construction using chemo-informatics. *Chemical Engineering Journal.* 2012;207:526-538.

[33] Ratkiewicz A, Truong TN. A canonical form of the complex reaction mechanism. *Energy.* 2012;43(1):64-72.

[34] Karaba A, Zamostny P, Lederer J, Belohlav Z. Generalized Model of Hydrocarbons Pyrolysis Using Automated Reactions Network Generation. *Industrial & Engineering Chemistry Research.* 2013;52(44):15407-15416.

[35] Kim Y, Kim WY. Universal Structure Conversion Method for Organic Molecules: From Atomic Connectivity to Three-Dimensional Geometry. *Bulletin of the Korean Chemical Society.* 2015;36(7):1769-1777.

[36] Green WH, Allen JW, Buesser BA, Ashcraft RW, Beran GJ, Class CA, Gao C, Goldsmith CF, Harper MR, Jalan A. RMG–reaction mechanism generator v4. 0.12013.

[37] Broadbelt LJ, Stark SM, Klein MT. Computer Generated Pyrolysis Modeling: On-the-Fly Generation of Species, Reactions, and Rates. *Industrial & Engineering Chemistry Research.* 1994;33(4):790-799.

[38] Broadbelt LJ, Stark SM, Klein MT. Computer generated reaction networks: on-the-fly calculation of species properties using computational quantum chemistry. *Chemical Engineering Science.* 1994;49(24):4991-5010.

[39] Magoon GR, Green WH. Design and implementation of a next-generation software interface for on-the-fly quantum and force field calculations in automated reaction mechanism generation. *Computers & Chemical Engineering.* 2013;52:35-45.

[40] Jiang G, Nowakowski DJ, Bridgwater AV. Effect of the Temperature on the Composition of Lignin Pyrolysis Products. *Energy & Fuels.* 2010;24(8):4470-4475.

[41] Constantinou L, Gani R. New group contribution method for estimating properties of pure compounds. *AIChE Journal.* 1994;40(10):1697-1710.

[42] Benson SW. *Thermochemical kinetics; methods for the estimation of thermochemical data and rate parameters*. New York: Wiley; 1968.

[43] Laidler KJ. A system of molecular thermochemistry for organic gases and liquids. *Canadian Journal of Chemistry.* 1956;34(5):626-648.

[44] Leal JP. Additive Methods for Prediction of Thermochemical Properties. The Laidler Method Revisited. 1. Hydrocarbons. *Journal of Physical and Chemical Reference Data.* 2006;35(1):55-76.

[45] Evans MG, Polanyi M. Further considerations on the thermodynamics of chemical equilibria and reaction rates. *Transactions of the Faraday Society.* 1936;32(0):1333-1360.

[46] Evans MG, Polanyi M. Inertia and driving force of chemical reactions. *Transactions of the Faraday Society.* 1938;34(0):11-24.

[47] Denisov ET. New empirical models of radical abstraction reactions. *Russian Chemical Reviews.* 1997;66(10):859.

[48] Blowers P, Masel R. Engineering approximations for activation energies in hydrogen transfer reactions. *AIChE Journal.* 2000;46(10):2041-2052.

[49] Saeys M, Reyniers M-F, Marin G, Van Speybroeck V, Waroquier M. Ab initio group contribution method for activation energies for radical additions. *AIChE Journal.* 2004;50(2):426-444.

[50] Benson SW, Buss JH. Additivity Rules for the Estimation of Molecular Properties - Thermodynamic Properties. *Journal of Chemical Physics.* 1958;29(3):546-572.

[51] Benson SW, Cruickshank FR, Golden DM, Haugen G, O'Neal HE, Rodgers AS, Shaw R, Walsh R. Additivity rules for the estimation of thermochemical properties. *Chemical Reviews.* 1969;69(3):279-324.

[52] Benson SW. *Thermochemical kinetics : methods for the estimation of thermochemical data and rate parameters*. 2d ed. New York: Wiley; 1976.

[53] Cohen N. Thermochemistry of Alkyl Free-Radicals. *Journal of Physical Chemistry.* 1992;96(22):9052-9058.

[54] Cohen N. Revised Group Additivity Values for Enthalpies of Formation (at 298 K) of Carbon–Hydrogen and Carbon–Hydrogen–Oxygen Compounds. *Journal of Physical and Chemical Reference Data.* 1996;25(6):1411.

[55] Holmes JL, Aubry C. Group additivity values for estimating the enthalpy of formation of organic compounds: an update and reappraisal. 1. C, H, and O. *The Journal of Physical Chemistry A.* 2011;115(38):10576-10586.

[56] Holmes JL, Aubry C. Group Additivity Values for Estimating the Enthalpy of Formation of Organic Compounds: An Update and Reappraisal. 2. C, H, N, O, S, and Halogens. *The Journal of Physical Chemistry A.* 2012;116(26):7196-7209.

[57] Marsi I, Viskolcz B, Seres L. Application of the Group Additivity Method to Alkyl Radicals: An ab Initio Study. *The Journal of Physical Chemistry A.* 2000;104(19):4497-4504.

[58] Sabbe MK, Saeys M, Reyniers M-F, Marin GB, Van Speybroeck V, Waroquier M. Group Additive Values for the Gas Phase Standard Enthalpy of Formation of Hydrocarbons and Hydrocarbon Radicals. *The Journal of Physical Chemistry A.* 2005;109(33):7466-7480.

[59] Sabbe MK, De Vleeschouwer F, Reyniers M-F, Waroquier M, Marin GB. First Principles Based Group Additive Values for the Gas Phase Standard Entropy and Heat Capacity of Hydrocarbons and Hydrocarbon Radicals. *The Journal of Physical Chemistry A.* 2008;112(47):12235-12251.

[60] Vandeputte AG, Sabbe MK, Reyniers M-F, Marin GB. Modeling the gas-phase thermochemistry of organosulfur compounds. *Chemistry – A European Journal.* 2011;17(27):7656-7673.

[61] Paraskevas PD, Sabbe MK, Reyniers M-F, Papayannakos N, Marin GB. Group Additive Values for the Gas-Phase Standard Enthalpy of Formation, Entropy and Heat Capacity of Oxygenates. *Chemistry – A European Journal.* 2013;19(48):16431-16452.

[62] Sumathi R, Green W. Missing Thermochemical Groups for Large Unsaturated Hydrocarbons: Contrasting Predictions of G2 and CBS-Q. *The Journal of Physical Chemistry A.* 2002;106(46):11141-11149.

[63] Sun H, Bozzelli JW. Structures, Intramolecular Rotation Barriers, and Thermochemical Properties: Ethanol, α-Monoethanols, Dichloroethanols, and Corresponding Radicals Derived from H Atom Loss. *The Journal of Physical Chemistry A.* 2001;105(41):9543-9552.

[64] Sun H, Bozzelli JW. Structures, Rotational Barriers, Thermochemical Properties, and Additivity Groups for 2-Propanol, 2-Chloro-2-propanol and the Corresponding Alkoxy and Hydroxyalkyl Radicals. *The Journal of Physical Chemistry A.* 2002;106(15):3947-3956.

[65] Saeys M, Reyniers M-F, Marin G, Van Speybroeck V, Waroquier M. Ab Initio Calculations for Hydrocarbons: Enthalpy of Formation, Transition State Geometry,

and Activation Energy for Radical Reactions. *The Journal of Physical Chemistry. A.* 2003;107(43):9147-9159.

[66] Sabbe M, Reyniers M-F, Van Speybroeck V, Waroquier M, Marin G. Carbon-Centered Radical Addition and β-Scission Reactions: Modeling of Activation Energies and Pre-exponential Factors. *ChemPhysChem.* 2008;9(1):124-140.

[67] Sabbe MK, Vandeputte AG, Reyniers M-F, Waroquier M, Marin GB. Modeling the influence of resonance stabilization on the kinetics of hydrogen abstractions. *Physical Chemistry Chemical Physics.* 2010;12(6):1278-1298.

[68] Paraskevas PD, Sabbe MK, Reyniers M-F, Papayannakos N, Marin GB. Kinetic modeling of alpha-hydrogen abstractions from unsaturated and saturated oxygenate compounds by carbon-centered radicals. *ChemPhysChem.* 2014;15(9):1849-1866.

[69] Vandeputte AG, Sabbe MK, Reyniers M-F, Van Speybroeck V, Waroquier M, Marin GB. Theoretical Study of the Thermodynamics and Kinetics of Hydrogen Abstractions from Hydrocarbons. *The Journal of Physical Chemistry A.* 2007;111(46):11771-11786.

[70] Paraskevas PD, Sabbe MK, Reyniers M-F, Papayannakos NG, Marin GB. Kinetic Modeling of α-Hydrogen Abstractions from Unsaturated and Saturated Oxygenate Compounds by Hydrogen Atoms. *The Journal of Physical Chemistry A.* 2014;118(40):9296-9309.

[71] Sabbe M, Vandeputte A, Reyniers M-F, Van Speybroeck V, Waroquier M, Marin G. Ab Initio Thermochemistry and Kinetics for Carbon-Centered Radical Addition and β-Scission Reactions. *The Journal of Physical Chemistry A.* 2007;111(34):8416-8428.

[72] Adamczyk AJ, Reyniers MF, Marin GB, Broadbelt LJ. Kinetics of substituted silylene addition and elimination in silicon nanocluster growth captured by group additivity. *ChemPhysChem.* 2010;11(9):1978-1994.

[73] Adamczyk AJ, Reyniers M-F, Marin GB, Broadbelt LJ. Kinetic correlations for H 2 addition and elimination reaction mechanisms during silicon hydride pyrolysis. *Physical Chemistry Chemical Physics.* 2010;12(39):12676-12696.

[74] Adamczyk AJ, Reyniers M-F, Marin GB, Broadbelt LJ. Hydrogenated amorphous silicon nanostructures: novel structure–reactivity relationships for cyclization and ring opening in the gas phase. *Theoretical Chemistry Accounts.* 2011;128(1):91-113.

[75] Vandeputte AG, Sabbe MK, Reyniers M-F, Marin GB. Kinetics of α hydrogen abstractions from thiols, sulfides and thiocarbonyl compounds. *Physical Chemistry Chemical Physics.* 2012;14(37):12773-12793.

[76] Vandeputte AG, Reyniers MF, Marin GB. Kinetic modeling of hydrogen abstractions involving sulfur radicals. *ChemPhysChem.* 2013;14(16):3751-3771.

[77] Paraskevas PD, Sabbe MK, Reyniers M-F, Papayannakos NG, Marin GB. Group Additive Kinetics for Hydrogen Transfer Between Oxygenates. *The Journal of Physical Chemistry A.* 2015;119(27):6961-6980.

[78] Beste A, Buchanan AC. Substituent Effects on the Reaction Rates of Hydrogen Abstraction in the Pyrolysis of Phenethyl Phenyl Ethers. *Energy & Fuels.* 2010;24(5):2857-2867.

[79] Kawamoto H. Lignin pyrolysis reactions. *Journal of Wood Science.* 2017:1-16.

[80] Robichaud DJ, Scheer AM, Mukarakate C, Ormond TK, Buckingham GT, Ellison GB, Nimlos MR. Unimolecular thermal decomposition of dimethoxybenzenes. *The Journal of Chemical Physics.* 2014;140(23):234302.

[81] Suryan MM, Kafafi SA, Stein SE. The thermal decomposition of hydroxy- and methoxy-substituted anisoles. *Journal of the American Chemical Society.* 1989;111(4):1423-1429.

[82] Carstensen H-H, Dean AM. A quantitative kinetic analysis of CO elimination from phenoxy radicals. *International Journal of Chemical Kinetics.* 2012;44(1):75-89.

[83] Kibet J, Khachatryan L, Dellinger B. Molecular Products and Radicals from Pyrolysis of Lignin. *Environmental Science & Technology.* 2012;46(23):12994-13001.

Chapter 2

Methodology

The advent of computers and the consequent rise in the computational power have irreversibly transformed all the modern natural and applied sciences to the point where computational methods stand alongside theoretical and experimental methods in value. Chemistry and its applications in chemical engineering had their fair share of this revolution through modern simulation techniques such as molecular dynamics, Monte Carlo, computational fluid dynamics and *ab initio* methods. All the thermochemical and kinetic data presented in this Ph.D. dissertation is obtained through *ab initio* calculations, as discussed in detail below.

2.1 Ab initio Calculations

The term "*Ab initio*" is originally a Latin word which signifies "from the beginning". The *ab initio* calculations are also referred to as "first principles calculations" since these methods generate results based on the fundamental laws of nature. As the state of art *ab initio* calculations are carried out at the level of electrons in contemporary science, the term "*ab initio* calculations" is utilized to refer to the electronic structure calculations that are based on the quantum mechanics which describes the framework of the physical laws of nature that operate at that level.

At the heart of quantum mechanics lies the Schrödinger equation by which the properties of all electronic systems are described. A wealth of information in relation to the chemistry of a species can be obtained by solving the time-independent Schrödinger equation (Eq. (2-1)).

$$\hat{H}\psi = E\psi \tag{2-1}$$

In this equation, $\hat{H}$ represents the total Hamiltonian operator acting on the many-body wavefunction ψ whereas E is the energy eigenvalue of the state ψ. Here, $\hat{H}$ is composed of a kinetic energy term ($\hat{K}$) and a potential energy term ($\hat{V}$). The latter consists of the sum of three potential energy terms due to nucleus-nucleus interactions ($\hat{V}_{nn}$), nucleus-electron interactions ($\hat{V}_{ne}$) and electron-electron interactions ($\hat{V}_{ee}$), as given in Eq. (2-2). The $\hat{V}_{ee}$ term corresponds to the electronic correlation which refers to the fact that the motion of an electron is influenced by the presence of all the other electrons in the system due to the Coulomb repulsion between each pair of electrons.

$$\hat{H} = \hat{K} + \hat{V} = \hat{K} + \hat{V}_{nn} + \hat{V}_{ne} + \hat{V}_{ee} \tag{2-2}$$

The exact solution of the non-relativistic Schrödinger equation can be obtained by analytic techniques only for the hydrogen atom and hydrogenic systems such as the particle in a box and the harmonic oscillator [1]. For larger systems, the solution of the Schrödinger equation becomes a N-body problem which can only be realized numerically through some approximations. Depending on the size of the system, solutions of such complex equations can have enormous computational cost. With the aim of bringing cost-effective but yet acceptably accurate solutions to the time-independent Schrödinger equation in larger systems, a wide array of electronic structure methods, i.e. levels of theory, that employ a variety of approximations in defining $\hat{H}$ and ψ, are devised. One level of theory is distinguished from another by the level of complexity it brings in its treatment of electron correlation ($\hat{V}_{ee}$) and its description of the wavefunction (ψ). For instance, in some methods, linear combination of a set of one-electron functions (or orbitals), i.e. the basis sets, are used to construct molecular orbitals for the description of ψ to simplify the solution of the Schrödinger equation. As a general rule, the accuracy of a quantum chemical calculation increases if a larger number of basis functions are used which comes along with a rising computational cost. To describe the electronic structure of a N-body system appropriately, both of the above-mentioned factors (the electronic correlation and the basis sets) should be handled through a combination of sufficiently high level of theory with a sufficiently large basis set. The quantum chemical calculation methods can be classified into two broad groups as wavefunction based methods and density based methods (DFT).

The Hartree-Fock (HF) method is the simplest approach that falls under the category of wavefunction based methods. In this method, the wavefunction (ψ) is approximated by a single Slater determinant consisting of one spin orbital per electron, meaning that the motion of

electrons does not depend explicitly on the instantaneous motions of the other electrons. Based on this assumption, the system of equations is solved by an iterative algorithm to obtain the wavefunction that is assumed to correspond to the ground state wavefunction, i.e. the wavefunction that yields the lowest eigenvalue (energy). This method employs the Fock operator (Eq. (2-3)) on ψ to obtain the solutions for the Schrödinger equation (Eq. (2-4)). For each *i* in Eq. (2-4), there is an equivalent equation defining a system of Schrödinger-like, one-particle equations.

$$\hat{F} = \hat{h}_1 + \sum_i (\hat{J}_i - \hat{K}_i) \tag{2-3}$$

$$\hat{F}\phi_i = \epsilon_i \phi_i \tag{2-4}$$

In Eq. (2-3), $\hat{h}_1$ represents the Hamiltonian that is dependent only on one generalized coordinate which includes both spatial and spin degrees of freedom of one electron, $\hat{J}_i$ is the direct term which corresponds to the classical Coulomb interaction between electrons and $\hat{K}_i$ is the exchange term which introduces the non-classical antisymmetry effects into the Fock operator. The electronic exchange is a consequence of the Pauli exclusion principle, which states that the total wavefunction for the system must be antisymmetric under particle exchange [2].

The HF approximation can also be interpreted as taking the presence of other electrons into account in a mean-field theory context, meaning that every electron is assumed to feel the average field effect of the other electrons. However, this assumption leads to a significant discrepancy between the true total energy and the HF energy of a system. This discrepancy is known as the electron correlation energy. Although the major weakness of the Hartree-Fock method is its neglect of correlation energy which leads to remarkable deviations from

experimental data [2], it has proven useful as a starting point for relatively more complex theoretical methods where the correlation energy is taken into account. The two examples for such more complex wavefunction based methods (i.e. the post-Hartree-Fock methods) are the configuration interaction (CI) methods [3] and the many body perturbation theory (abbreviated as MP2, MP3, MP4 where the numbers 2, 3, 4 represent the order of the correction to the energy that the method provides) [4]. The MP methods are designed to improve the results of the Hartree-Fock method through incorporating the electronic correlation effects as perturbations to the Fock operator.

The other family of electronic structure techniques include methods that are based on Density Functional Theory (DFT) which considers the Schrödinger equation in terms of electronic density rather than the wavefunction. In the DFT methods, the properties of a many electron system can be determined using functionals, i.e. functions of a function, of the electronic density ($n(\vec{r})$).

An important approach in DFT formalism is the description of the electronic density through Kohn-Sham orbitals (Eq. (2-5)) [5,6] which assumes a system of fictitious system of "non-interacting electrons".

$$n(\vec{r}) = \sum_{n}^{N_e} |\phi_n(\vec{r})|^2 \tag{2-5}$$

The Kohn-Sham formalism simplifies the description of the total energy based on the electronic density ($\phi_n(\vec{r})$), as given below (Eq. (2-6)).

$$E[\rho] = -\frac{1}{2}\sum_{n}^{N_e}\int \phi_n^*(\vec{r})\nabla^2(\vec{r})\phi_n(\vec{r})d\vec{r} - \int n(\vec{r})V_{ne}(\vec{r})d\vec{r} + \frac{1}{2}\int\int d\vec{r}d\vec{r}'\frac{n(\vec{r})n(\vec{r}')}{|\vec{r}-\vec{r}'|} + E^{XC}[\rho] \quad (2\text{-}6)$$

In the expression above, N_e is the total number of electrons, V_{ne} is the potential representing nucleus electron interaction. Here, the first term is the kinetic energy of the non-interacting electrons, the second term represents the attractive interactions between the nuclei and the electrons, whereas the third term describes the classical Coulomb repulsion between the electrons. The last term of the equation ($E^{XC}[\rho]$) is the exchange-correlation functional, which incorporates the effects of exchange and correlation to the calculation of the total energy of the system. It should also be kept in mind that this term also encompasses the kinetic energy that is not considered as a part of the first term due to the Kohn-Sham approach, i.e. the difference between the true kinetic energy and the kinetic energy of the non-interacting electrons.

The main problem of the DFT formalism is the proper definition of the exchange and correlation functional ($E^{XC}[\rho]$ term) and the differences between various DFT methods lie in the manner of how this term is approximated. Some examples of widely used DFT methods are B3LYP [7], BMK [8] and the more modern Minnesota density functionals such as the MO6 family [9-11], which were shown to have improved performance compared to the B3LYP functional [9,12,13].

Some of the contemporary quantum chemical methods employ a combination of the results from a set of different wavefunction based methods and DFT methods to attain high accuracy. These levels of theory are known as the composite methods which can be exemplified by the widely used complete basis set (CBS) methods of Petersson and co-workers [14,15], the Gaussian methods by Curtiss et al. [16-21] and the Weizmann methods of Martin et al.

[8,22,23]. In this Ph.D. study, two of these composite methods; the CBS-QB3 method of Montgomery et al. [14] and the G4 method of Curtiss et al. [21] are utilized to obtain the thermochemical and the kinetic datasets that are necessary for the development of group additive models of interest.

The CBS-QB3 composite method [14] is composed of five steps. A CBS-QB3 calculation starts with geometry optimization at the B3LYP level with a 6-311G(2d,d,p) basis set (i.e. CBSB7). This is followed by a frequency calculation at the same level of theory and basis set. The following three steps are single point calculations (SPCs) at the CCSD(T)/6-31+G(d'), the MP4(SDQ)/6-31+G(d(f),p) (i.e. CBSB4) and the MP2/CBSB3 level. The results that are obtained from these three different levels of theory are extrapolated to the complete basis set (CBS) limit. To extrapolate to the CBS limit, the CBS-QB3 level of theory utilizes N^{-1} asymptotic convergence of second-order MP pair energies that are calculated from pair natural orbital expansions [14]. CBS extrapolation brings the advantage that smaller basis sets can be used at second-order MP and as a result, computational costs are decreased which renders it possible to apply CBS-QB3 on a wider range of systems. CBS-QB3 calculates the total energy by starting with the energy calculated from the MP2/CBSB3 calculation and adding (i) zero point vibrational energy, (ii) the contribution of energy from CBS extrapolation, (iii) the difference of electronic energies between MP4(SDQ) and MP2 calculations (iv) the difference of electronic energies between CCSD(T) and MP4(SDQ) calculations (v) an empirical correction term and a (vi) spin contamination correction term to the MP2 energy. Here, the spin contamination correction step is also empirical in nature. This step is designed to alleviate the issue of spin contamination in CBS-QB3 energies via a correction that is proportional to the $<S^2>$.

The G4 method [21] consists of six steps. The first two steps include geometry optimization and frequency analysis which are carried out at the level of B3LYP level with the 6-31G(2df,p) basis set. The rest of the steps are devoted to energy calculations. At the third step, the Hartree-Fock energy limit E(HF/ limit) is calculated [21]. In the following step, a series of SPCs is carried out, starting with the calculation of energy at the MP4 level with the basis set 6-31G(d). The energy obtained from this calculation is modified by corrections from a set of additional calculations. As Curtiss et al. explained [21], these calculations provide corrections for the diffuse functions (MP4/6-31+G(d)), higher polarization functions (MP4/6-31G(2df,p)), correlation effects beyond the fourth order perturbation theory (CCSD(T)/6-31G(d)), a correction for larger basis set effects and for the non-additivity caused by the assumption of separate basis set extensions for diffuse functions and higher polarization functions. At the fifth step, the spin-orbit corrections (SOCs) are calculated and the contributions of this correction and all the corrections from the previous steps are added to the E(MP4/6-31G(d)) to obtain energies. In the sixth and last step, high level corrections (HLCs) are calculated and added to the combined energy from the previous step to yield final G4 energies [21].

As discussed above, G4 differs from CBS-QB3 in the details of the geometry optimization and the frequency analysis step as well as in the way the final energy is approximated by a series of single point energy calculations. There is also an evident difference in the manner of how the electronic energies are calculated. Detailed explanation of these composite methods can be found in the original literature [14,21].

In the literature, the use of the CBS-QB3 level of theory is prevalent. In numerous studies, CBS-QB3 has been shown to produce accurate enthalpies of formation [24-26], entropies and heat capacities [25-27] and rate coefficients [28-35]. In addition to this, it is the level of theory

employed by Marin and coworkers in the prior studies to develop the thermodynamic [24-27] and kinetic databases [29-35] that are later used for the development of predictive models for thermodynamic and kinetic parameters used in kinetic model construction. For this reason, one could expect CBS-QB3 to be the preferred level of theory in the first two studies presented in this Ph.D. dissertation (**Chapter 3** and **4**) where the objective is to extend the GAV/NNI database of Marin and coworkers to monocyclic aromatic hydrocarbons and their corresponding radicals. Nevertheless, it has been noted that the CBS-QB3 calculated bond dissociation energies (BDEs) for some bonds in aromatic species like the C_6H_5—H bond in benzene, the C_6H_5—OH bond in phenol, and the C_6H_5—CHO bond in benzaldehyde deviate by more than 10 kJ mol^{-1} [36,37] from well-established experimental values. This casts doubts on the ability of the CBS-QB3 method to accurately describe the thermochemistry of aromatic molecules, particularly the radicals. In **Chapter 3**, it is discussed that G4 level of theory yields values that are in excellent agreement with the experimental data for the BDEs mentioned above. Nonetheless, this improvement comes with the cost of significantly higher CPU time demands, which limits the applicability of G4 calculations to smaller molecules. Consequently, in the third and fourth studies presented in this thesis (**Chapters 5** and **6**) where the focus is on the thermochemistry and kinetics of relatively larger aromatic molecules (toluene derivatives and benzylic radicals), CBS-QB3 is preferred over G4 because it is computationally too demanding for the majority of the molecules and the reactions studied. To ensure reliability of the reported CBS-QB3 data, validation using experimental data from the literature is provided in each of these two studies.

All electronic structure calculations in this Ph.D. thesis are performed with the Gaussian 09 software packages [38]. These calculations yield three crucial pieces of information that are important for the calculation of thermochemical properties, which are:

(i) Electronic energies at 0 K

(ii) The optimized geometries

(iii) Vibrational frequencies

In the following sections, a detailed explanation on the calculation of thermochemical properties based on these three pieces of *ab initio* based information is provided.

The self-consistent field (SCF) calculations yield a result when the calculation converges to a point, nevertheless, there is no guarantee of whether this stationary point is a local minimum or a saddle point, i.e. a maximum in one or more directions [39]. In the case of convergence at a saddle point instead of a local minimum, electronic energies that are higher than that of the ground state wavefunction are observed. With regard to the *ab initio* calculations involving monocyclic aromatic radicals (**Chapter 4**), a difficulty encountered with the default implementation of the G4 method is that in some instances abnormally high electronic energies are calculated. This led to the suspicion that the default guess of the initial wavefunction to solve the SCF problem does not always lead to the electronic ground state. To resolve this issue, a wavefunction stability test [39-41] is performed prior to each G4 calculation and the stabilized wavefunction is used as initial guess in the G4 method. This is realized by probing the second derivatives of the energy with respect to the orbital variations. This test also relaxes different constraints on the wavefunction, such as allowing the orbitals to become complex or reducing the symmetry of the orbitals. If the test indicates that a wavefunction is unstable, then, the wavefunction is displaced along the problematic eigenvector and optimized to give an

initial guess for a lower energy wavefunction. The wavefunction stability test is introduced as an initial step to the Gaussian 09 input file with the "Stable=Opt" keyword [38]. The stability test leads to remarkable improvements in the accuracy of some of the G4 energies, e.g. by more than 10 kJ mol^{-1} for some substituted benzoyl radicals. Using the stability test as pre-step provided the consistency in the data set that is needed to derive group additivity values. This practice is also followed for the CBS-QB3 calculations of benzylic radicals in **Chapter 5** and transition state structures in **Chapter 6**.

An another issue that is frequently encountered in unrestricted Hartree-Fock calculations for open-shell systems is the contamination of the wavefunctions by higher spin multiplicity states. In **Chapter 4**, high $<S^2>$ values are noted for several monocyclic aromatic radicals under investigation which is shown to lead to higher G4 electronic energies [42-46]. Extensive experimental validation (via available data from the literature) is provided for the G4 based bond dissociation energies (BDEs) to indicate that the final set of G4/BAC enthalpies of formation is reliable despite this spin contamination.

2.2 Thermochemistry

2.2.1 Statistical Mechanics

In the present Ph.D. work, the above-discussed *ab initio* methods are utilized to obtain thermochemical data for three thermochemical properties, i.e., the standard enthalpies of formation ($\Delta_f H^\circ$) and entropies (S°) at 298 K and heat capacities (C_p) in a wide range of temperatures (300 K, 400 K, 500 K, 600 K, 800 K, 1000 K and 1500 K). This is in line with the earlier studies [24-27] that contributed to the GAV/NNI database of Marin and coworkers. In these prior works, an in-house software was employed to calculate the thermochemical data

based on the output from *ab initio* calculations and in this Ph.D. dissertation, the same methodology is employed with some minor changes in implementation. A brief description of the theory behind this code can be found below.

The *ab initio* calculations yield crucial information for only one specific atom/molecule/radical or transition state structure. Evidently, chemical applications at the macroscale are much larger than this molecular scale. Given that one mole of atom/molecule contains Avogadro number of particles (N_A=6.02 10^{23}), at first sight, it might seem impossible to obtain any macroscopic property based on quantum chemical calculations as with the available computational technology, it is not possible for any supercomputer to solve a system of differential equations of anywhere close to that size. Furthermore, in *ab initio* calculations, the electronic energies are calculated at 0 K, i.e. the absolute zero, at which none of the relevant applications can take place. At this point, statistical mechanics (or statistical thermodynamics) comes into play and establishes the link between

(i) microscopic and macroscopic thermodynamic properties

(ii) 0 K and any temperature of interest

rendering the results from *ab initio* calculations practical for obtaining the desired thermochemical data [47]. Statistical mechanics achieves this through the concept of "ensemble" which represents an imaginary collection of smaller identical microscopic systems that replicate the properties of the system at the macroscopic scale [48,49]. One example of ensemble is the microcanonical ensemble where the microsystem is designed as an isolated system in which there is no transfer of mass or energy through the boundaries of the system. This ensemble is also known as the NVE-ensemble meaning that the total number of particles (N) and energy (E) in these systems are held constant within a fixed volume (V). However,

experiments in real life applications cannot be carried out under the condition of constant total energy and thus, a more practical ensemble that is capable of describing the properties of systems in real life should be employed. The canonical ensemble or the NVT-ensemble, which replicates the thermodynamic properties of a system that is in thermal contact with a thermal reservoir, i.e. a system where temperature is constant and energy is allowed to fluctuate, serves this purpose better. In this ensemble, energy transfer is permitted through the boundaries of this microsystem, however the boundaries are impermeable for the particles. Apart from these two, there are also other ensembles like the grand canonical ensemble, isobaric-isothermal ensemble and isoenthalpic-isobaric ensemble. Corresponding to the type of the selected ensemble, there is a partition function that represents the average number of states accessible at given conditions such as temperature, pressure etc... In this study, the canonical partition function, Q, is introduced for a canonical ensemble of constant volume, V, number of particles, N and temperature, T. The ideal gas assumption is utilized for this ensemble which converts the problem to a problem of determining molecular partition functions, q [49].

2.2.2 Molecular Partition Functions

The total energy of a molecule is the sum of contributions from its translational (E_T), rotational (E_R) and vibrational (E_V) modes and its electronic energy (E_E):

$$E = E_T + E_R + E_V + E_E \tag{2-7}$$

The separation of energy components given in Eq. (2-7) is an approximate approach because of the coupling between different modes, however it is satisfactorily accurate in most cases [49]. Provided that the energy can be calculated as the sum of independent contributions, the partition function factorizes into a product of these contributions (Eq. (2-8)).

$$q = q^T q^R q^V q^E \tag{2-8}$$

Translational motion is the motion of the center of mass of a molecule from one position to another. The partition function (q^T) corresponding to this motion is given below:

$$q^T = \frac{V}{\Lambda^3}, \Lambda = \frac{h}{(2\pi m k_B T)^{1/2}} \tag{2-9}$$

In this equation, V is the volume of the container carrying the molecule and Λ is the thermal wavelength which is the average de Broglie wavelength of the particles in an ideal gas at the specified temperature. h abbreviates the Planck constant, m is the mass of the particle, k_B corresponds to the Boltzmann constant and T is the temperature. For the calculation of the partition functions in this thesis, the ideal gas assumption is taken as the equation of state and the volume is described as $V = k_B T/P$ where P is the pressure taken as atmospheric pressure (1 atm = 101325 Nm^{-2}). For this component of q, no information is needed from the *ab initio* calculations.

The rotational motion in a molecule refers to the motion of that molecule about an axis. The form of the rotational partition function (q^R) is dependent on the optimized geometry of the molecule from the *ab initio* calculations, the temperature (T) and the external symmetry number of the molecule (σ_{ext}).

For linear molecules, q^R can be approximated as follows

$$q^R \approx \frac{k_B T}{B} \tag{2-10}$$

The linear molecules have one rotational constant (B). If this linear molecule has a symmetric geometry, σ_{ext} should be included in Eq. (2-10) as follows:

$$q^R \approx \frac{k_B T}{B\sigma_{\text{ext}}} \tag{2-11}$$

In the case of non-linear molecules, three rotational constants are necessary to describe the rotation of the molecule (*A*, *B*, *C*), as given in Eq. (2-12):

$$q^R \approx \frac{\sqrt{\pi}(k_B T)^{3/2}}{\sqrt{ABC}\sigma_{\text{ext}}} \tag{2-12}$$

It is possible to write q^R in different ways and in this study, the form of q^R is described in terms of characteristic rotational temperature (Θ_R) to simplify the expression of q^R. Θ_R is obtained as given in Eq. (2-13):

$$\Theta_R = \frac{B}{k_B} = \frac{\hbar^2}{2k_B I} \tag{2-13}$$

In Eq. (2-13), *I* represents the moment of inertia that is calculated from the optimized geometry. In linear molecules, there is only one *I* whereas for the nonlinear molecules, three moments of inertia are needed for the calculation of the rotational partition function.

The three different cases in Eqs (2-10), (2-11) and (2-12) are all defined in terms of Θ_R as follows:

Linear, asymmetric molecule: $$q^R \approx \frac{T}{\Theta_R} \tag{2-14}$$

Linear, symmetric molecule: $$q^R \approx \frac{T}{\Theta_R \sigma_{\text{ext}}} \tag{2-15}$$

Nonlinear molecule: $$q^R \approx \frac{\sqrt{\pi}}{\sigma_{\text{ext}}} \sqrt{\frac{T^3}{\Theta_{R,A}\Theta_{R,B}\Theta_{R,C}}} \tag{2-16}$$

It should be noted that for the nonlinear molecules, the partition function consists of three characteristic rotational temperatures ($\Theta_{R,A}\Theta_{R,B}\Theta_{R,C}$) that reflect the rotational constants *A*, *B* and *C* in Eq. (2-12), i.e. the three moments of inertia.

If two or more different measurable states of a quantum system are at the same electronic energy level, that level is referred to as degenerate. The degeneracy, i.e. the number of degenerate energy states (g) contribute to the molecular partition function through the electronic component which is calculated as follows:

$$q^E = \sum_{i=1}^{\infty} g_i e^{-\frac{\varepsilon_i}{kT}} \tag{2-17}$$

In this equation, g_i corresponds to the degeneracy of the i^{th} level and ε_i is its energy. Except for radicals, for which g_i is equal to 2 corresponding to the two orientations of the spin of the unpaired electron, q^E is 1 since the electronic energy separations from the ground state are usually very large.

The vibrational partition function (q^V) fundamentally needs the frequencies of the vibrational modes of motion (ν). q^V is a product of the contributions from all the modes of motion as given below is eq (2-18). While calculating q^V, the rigid rotor and harmonic oscillator (RRHO) approximation is applied except for those modes that resemble internal rotations. The harmonic oscillator frequencies are scaled by a recommended scaling factor (SF) of 0.99 for CBS-QB3 [14] and 0.9854 for G4 calculations [21].

$$q^V = \prod_{i}^{n} \frac{1}{1 - \exp\left(-\left(\frac{SF\ h\ \nu_i}{k_B T}\right)\right)} \tag{2-18}$$

i=1,2,3,....n where *n* is the total number of normal modes.

The RRHO approximation yields poor results for the majority of the internal rotations around single bonds since the one dimensional harmonic oscillator potential well can be very different from the potential curve of a rotation around a single bond. The poor treatment of internal rotors leads to a significant loss of accuracy in the thermochemistry, particularly for the entropy data [27]. To handle this problem, primarily, the rotations around all the single bonds are analyzed with the one-dimensional hindered rotor approach of Waroquier and coworkers [50-52]. Then, the hindrance potentials of the internal rotations are determined with relaxed potential energy surface scans at the B3LYP/6-31G(d) level and expanded as truncated Fourier series using the first six sine and cosine terms to calculate the contributions of internal rotations to the partition function and thermodynamic properties. In the earlier studies [25-27], harmonic oscillator frequencies associated with the internal rotors were obtained from the rotation profile. However, it was noted that, for some of the aromatic species under investigation, the frequencies that are calculated from the rotation profile did not match the corresponding internal rotations which led to remarkable errors, particularly in entropies. Therefore, these harmonic oscillator frequencies are visually identified through animation and then removed manually. This is realized through dividing the total partition function (q) by the contributions of vibrational partition functions corresponding to these harmonic oscillator frequencies (q_{1D-HO}) and multiplying this expression with one dimensional hindered rotor partition function (q_{1D-HR}), i.e. multiplying the total partition function with the expression given below (Eq. (2-19)).

$$\frac{q_{1D-HR}}{q_{1D-HO}} \tag{2-19}$$

Only internal rotors with total barriers below 50 kJ mol^{-1} are evaluated separately, all other modes are treated as harmonic oscillators. Internal rotations with very low barriers (less than

1 kJ mol^{-1}) are classified as free rotors. The reduced moment of inertia describing the rotation of the two molecule fragments around the axis that decouples internal from external rotation is calculated with the procedure described by Vansteenkiste et al. [50].

All reported thermochemical data in this Ph.D. dissertation are based on the lowest energy conformers of molecules at the CBS-QB3 and/or G4 level of theory. The hindrance potentials of the internal rotors are utilized to identify local minima on the potential energy surface, which are then evaluated at the G4 level in order to identify the lowest energy conformer. It should be kept in mind that this approach is a compromise between accuracy and effort since it does not necessarily guarantee that the global minimum is found if internal rotors are coupled. In this study, though, coupling is limited and thus the lowest energy configurations are located. Except for the manual selection of harmonic oscillator frequencies pertaining to the internal rotations, the used methodology is in line with previous studies by Marin and coworkers [24-27].

2.2.3 Calculation of Thermochemical Properties

The enthalpy of a molecule is calculated by adding the electronic energy at 0 K and the thermal contributions based on statistical thermodynamics, which account for the temperature-dependent occupation of translational, rotational and ro-vibrational energy levels, as given in Eq. (2-20) below.

$$H = E_{electronic} + ZPVE + H_{translation} + H_{external\,rotation} + H_{rovibrational} \qquad (2\text{-}20)$$

All the three pieces of information that are accessible from the output of *ab initio* calculations are employed to calculate enthalpies through Eq. (2-20). The first term on the right hand side, namely the electronic energy at 0 K ($E_{electronic}$) is among these three pieces, as mentioned in

Section 2.1. For the calculation of the second term, i.e. the zero-point vibrational energy ($ZPVE$), the vibrational frequencies that are calculated at the frequency analysis step of the *ab initio* calculations are used. The following three terms on the right hand side ($H_{translation}$, $H_{external\ rotation}$, $H_{rovibrational}$) can be calculated based on the three components of the molecular partition function, q^T, q^R, q^V, respectively, employing the two relations in Eqs (2-21) and (2-22) below. It has been mentioned before in Section 2.2 that for the calculation of q^T, no information is used from the *ab initio* calculations. Nonetheless, to calculate the q^R component of a molecule one needs the principle moments of inertia that can be calculated from the geometry of the optimized structure and vibrational frequencies can be employed to obtain the q^V component. Therefore, it can be concluded that the performance of an *ab initio* calculation is a function of its accuracy in determining electronic energies, optimized geometries and the vibrational frequencies.

$$U = k_B T^2 \left(\frac{\partial\, lnq}{\partial T}\right)_V \tag{2-21}$$

$$H = U + pV \tag{2-22}$$

The calculation of standard enthalpies of formation, which is the enthalpy relative to the composing elements in their standard state, always requires experimental information, as, for example, the enthalpy of carbon in its graphitic standard state cannot be determined accurately using *ab initio* methods. In the atomization energy method, the standard enthalpy of formation is obtained from the *ab initio* calculated enthalpy of atomization at 298 K and the experimental standard enthalpies of formation of atoms in the gas phase (gas, exp) at the same temperature, as given in Eq. (2-23):

$$\Delta_f H°\left(C_m H_n O_p; 298\ K\right) = m\Delta_f H^{\circ}{}_{gas,exp}(C) + n\Delta_f H^{\circ}{}_{gas,exp}(H) + p\,\Delta_f H^{\circ}{}_{gas,exp}(O) - [mH^{\circ}{}_{AI}(C) + nH^{\circ}{}_{AI}(H) + pH^{\circ}{}_{AI}(O) - H^{\circ}{}_{AI}(C_m H_n O_p)] \quad (2\text{-}23)$$

where $\Delta_f H^{\circ}_{gas,exp}$(C) = 716.68 kJ mol^{-1}, $\Delta_f H^{\circ}_{gas,exp}$(H) = 218.0 kJ mol^{-1} and $\Delta_f H^{\circ}_{gas,exp}$(O) = 249.18 kJ mol^{-1} at 298 K [37].

The last four terms of Eq. (2-23) represent the *ab initio* (AI) calculated atomization enthalpy for $C_m H_n O_p$ at 298 K, that is, the reaction enthalpy of the reaction below at 298K (Eq. (2-24)).

$$C_m H_n O_p \rightarrow mC + nH + pO \quad (2\text{-}24)$$

Two different types of corrections have been applied to the atomization energies. First, spin-orbit (SO) corrections of 0.35 kJ mol^{-1} per carbon atom and 0.93 kJ mol^{-1} per oxygen atom [17] have been applied to the results from the CBS-QB3 calculations only since SO corrections are part of the G4 methodology [21]. Second, "Bond Additive Corrections" (BACs) [53] are applied to eliminate the remaining systematic errors of *ab initio* calculations (Eq. (2-25)).

$$\Delta_f H^{\circ}(BAC) = \Delta_f H^{\circ}(CBSQB3\ or\ G4) + \sum_{ij} N_{ij} BAC_{ij} \quad (2\text{-}25)$$

where i and j run over the two different atom types and N_{ij} is the number of bonds between atoms of type i and j. As the CBS-QB3 and G4 methods suffer from different systematic bond-related errors, BAC values were developed for each methods.

Another popular practice in correcting for the systematic errors caused by the incomplete description of the electron correlation energy is to use reaction schemes such as isodesmic schemes [54]. In these schemes, hypothetical reactions that conserve the number of bonds of each order between each pair of atom types are constructed, involving species with a well-known enthalpy of formation. Nevertheless, it is not feasible to construct such a reaction for

every of the hundreds of compounds that need to be calculated in this work. Moreover, in the earlier studies that contributed to the Benson's GA parameters [24-26], BACs have been used to minimize systematic deviations on standard enthalpies of formation. Therefore, the atomization enthalpy method has been applied in combination with BACs.

The BACs that are defined to correct the systematic errors in the CBS-QB3 based enthalpy data ($\Delta_f H°$) are used in accordance with the earlier studies [24-26], however, as will be discussed later in **Chapter 3**, the agreement for the aromatic compounds considered in this work is not satisfactory. Thus, additional BAC values are defined to achieve optimal agreement between calculated and experimental enthalpies of formation. In particular, with the introduction of a differentiation between bonds of non-aromatic carbon atoms and aromatic carbon atoms, significant improvements are achieved in the BAC-corrected enthalpies of formation. BACs are defined for a total number of 9 types of bonds which are C-C, C-H, C=C, C-O, O-H, C=O, C_b-H, C_b-C_b, and C_b-O. The details of the derivation of these BACs are given in **Chapter 3**. In the same chapter, BACs have also been defined to correct for the systematic deviations in G4 calculations since G4 is used for the first time in the development of Benson's GA parameters for the database of Marin and coworkers. In **Chapter 4**, the same set of G4 BACs are applied to obtain the enthalpies of monocyclic aromatic radicals and in **Chapter 5**, the set of CBS-QB3 BACs are used to correct the enthalpies of toluene derivatives and benzylic radicals.

The task of assigning BAC corrections is straightforward for the closed-shell systems and the majority of the radicals however it can be ambiguous for the resonantly stabilized radicals because the corresponding Lewis structures often consist of different bond types. Since the only radical classes of interest within the framework of this thesis include aromatic radicals,

BAC corrections are based on Lewis structures that preserve the phenyl ring. These structures are expected to provide a plausible description of the electron configuration for the radical, for instance, in a phenoxy radical the largest spin density resides on the oxygen atom.

To calculate the entropy (S°) of a molecule, the optimized geometry and the vibrational frequencies of the molecule should be known, as given in Eq. (2-26).

$$S^{\circ} = k_B T \left(\frac{\partial \, ln \, q}{\partial T}\right)_V + k_B ln \, q \tag{2-26}$$

The calculation of entropy through the statistical mechanical methods does not take symmetry or contributions from steric centers into account. Therefore, the initial entropies need to be corrected for such contributions if the total entropy of a molecule is needed. Conversely, GAV and NNI parameters in Benson's GA method [55-58] are "symmetry-free" because they relate to moieties of a molecule and not to the entire molecule. Since the goal of the current study is to determine such GAVs and NNIs, the symmetry-independent "intrinsic" entropies ${S_{int}}^{\circ}$ are used:

$${S_{int}}^{\circ} = S^{\circ} + R \, ln \left(\frac{\sigma}{n_{opt}}\right) \tag{2-27}$$

where σ is the global symmetry number and n_{opt} is the number of optical isomers. The global symmetry number σ is the product of external symmetry number σ_{ext} and the internal symmetry numbers σ_{int}:

$$\sigma = \sigma_{ext} \prod_k \sigma_{int,k} \tag{2-28}$$

Using partition functions, the molar heat capacities (C_p) can be calculated by Eq. (2-29).

$$C_p = k_B + 2k_B T \frac{\partial \ln q}{\partial T} + k_B T^2 \frac{\partial^2 \ln q}{\partial T^2} \quad (2\text{-}29)$$

It is possible to calculate the Gibbs free energy of a species if its enthalpy and entropy is known:

$$G = H - TS \quad (2\text{-}30)$$

This parameter is important as it determines the equilibrium coefficient (K) of a reaction, as shown by Eq. (2-31):

$$K = exp\left(-\frac{\Delta_r G^\circ}{RT}\right) \quad (2\text{-}31)$$

Thermodynamics can explain whether a process or a reaction can occur via Gibbs free energy. However, thermodynamics alone cannot yield more information about the reactions as it focuses on the systems that are at equilibrium whereas a reacting system advances from a state of non-equilibrium to equilibrium or from one equilibrium point to another.

2.3 Kinetics

The study of chemical reactions and their rates are the focal point of research in the field of chemical kinetics. In the kinetics literature, several theories (canonical, variational, microcanonical) that link *ab initio* calculated data and the reaction rate coefficients are available. Among these theories, the canonical transition state theory (CTST) is selected for the calculations of the reaction rate coefficients, in line with the methodology used in earlier similar studies [29-35]. The TST assumes that the reactive system advances from reactants to products over the potential energy surface (PES) with respect to coordinates of atomic positions. Depending on the number of these coordinates, the shape of the PES can be a curve, a surface or a hypersurface. Despite its simplicity, TST is expected to yield sufficiently

accurate results since the class of reactions that are presented in this Ph.D. dissertation do not have limitations such as transition state structures with flat saddle points which require a more complex treatment like variational transition state (V-TST).

$$k(T) = \kappa\, n_e \tilde{k}(T) = \kappa n_e \tilde{A} exp(\frac{-E_a}{RT}) \tag{2-32}$$

In the relation above, κ is the tunneling coefficient, n_e is the number of single events, $\tilde{k}(T)$ the single event rate coefficient expression, $\tilde{A}$ is the single event pre-exponential factor and E_a is the activation energy. The number of single events are calculated by Eq. (2-33).

$$n_e = \frac{n_{opt,\ddagger}}{n_A n_B} \frac{\sigma_A \sigma_B}{\sigma_\ddagger} \tag{2-33}$$

The number of single events, n_e, i.e. the reaction path degeneracy accounts for the number of optical isomers (n_{opt}) and the global symmetry number (σ).

This expression can also be defined in terms of Gibbs free energy of activation ($\Delta G^\ddagger$) which is the standard Gibbs energy difference between the transition state of a reaction and the ground state of the reactants [59]:

$$k(T) = \kappa n_e \left(\frac{k_B T}{h}\right) {V_{mol}}^{\Delta n^\ddagger} exp(\frac{-\Delta G^\ddagger}{RT}) \tag{2-34}$$

In this relation, $\Delta n^\ddagger$ reflects the change in the number of moles and takes the values of 0 and 1 for unimolecular and bimolecular reactions, respectively. The V_{mol} represents the molar volume at standard pressure, and k_B and h are the Boltzmann and the Planck's constants, respectively. Eq. (2-34) provides a clear demonstration of how the TST theory establishes a link between the thermodynamics of reactants and the transition state and the kinetics of the reaction. Eq. (2-30) can be employed to write Eq. (2-35) in terms of activation enthalpies ($\Delta H^\ddagger$) and entropies as follows ($\Delta S^\ddagger$):

$$k(T) = \kappa\, n_e \left(\frac{k_B T}{h}\right) {V_{mol}}^{\Delta n} exp(\frac{\Delta S^{\ddagger}}{R}) exp(\frac{-\Delta H^{\ddagger}}{RT}) \quad (2\text{-}35)$$

A comparison between Eq. (2-32) and Eq. (2-35) points out that at a constant temperature, $\tilde{A}$ depends only on one variable, the entropy difference between transition state and reactant, $\Delta S^{\ddagger}$, i.e. the activation entropy, and analogously, the activation energy (E_a) is directly related to the enthalpy difference between transition state and reactant, $\Delta H^{\ddagger}$ (i.e. the activation enthalpy).

It is also possible to write this relation in terms of partition functions:

$$k(T) = \kappa n_e \left(\frac{k_B T}{h}\right) \frac{q^{\ddagger}}{q^R} exp(\frac{-\Delta E_{el}}{RT}) \quad (2\text{-}36)$$

In the prior studies, an in-house software that is developed to automatically calculate reaction rate coefficients via Eq. (2-36) is used [28-35]. Provided that the present thesis aims to extend the kinetic parameter database that were developed in these earlier works, the same methodology is followed in this thesis to preserve internal consistency of the database.

The ΔE_{el} term in Eq. (2-36) is calculated as the difference between the electronic energies of the reactant and the transition state at 0 K which are obtained at the CBS-QB3 level of theory. All final results from these *ab initio* calculations are based on the lowest energy conformer. For the calculation of the pre-exponential factor ($\tilde{A}$), the ratio of the partition functions for the transition state ($q^{\ddagger}$) and reactant (q^R) is needed. This ratio ($\frac{q^{\ddagger}}{q^R}$) also implies that the contributions from conserved modes, i.e. the non-reacting parts of the molecule, cancel out. This provides the justification to treat conserved modes as harmonic oscillators, which leads to substantial savings in CPU time. As discussed in earlier sections, the optimized geometries and the vibrational frequencies from *ab initio* results are used to obtain the molecular partition functions for the transition state ($q^{\ddagger}$) and reactant (q^R).

It is well-known that the phenomenon of quantum tunneling through the activation energy barrier contributes significantly to rate coefficients at low temperatures. This explains the reactive behavior of the molecules that are capable of undergoing reactions for which they are devoid of sufficient energy. Tunneling effects are particularly relevant at lower temperatures especially if light particles are involved in a reaction, such as the transferring hydrogen atom in the hydrogen abstraction reactions of interest in **Chapter 6**. For the calculation of tunneling coefficients, Vandeputte et al. evaluated three different zero curvature methods [45] and demonstrated that the tunneling method of Eckart [60] outperforms the other two, particularly at temperatures lower than 500 K. Besides, the performance of this method is well established in the literature [30,34,45]. Consequently, the one dimensional (1D) zero curvature Eckart method is utilized to obtain the tunneling coefficient (κ). κ provides a measure of the ratio of the number of particles that are capable of tunneling through the energy barrier to the number of particles that are only able to surmount the barrier.

Once the *ab initio* reaction rate coefficients are obtained, the *ab initio* Arrhenius parameters (E_a and $\tilde{A}$) are calculated based on the linear least-squares regression of the *ab initio* rate coefficients to the Arrhenius equation in the temperature range T −100 K to T+100 K with k sampled at intervals of 50 K, where T is the temperature of interest.

$$\ln k = \ln A - \frac{E_a}{RT} \tag{2-37}$$

2.4 Group Additivity Methods

2.4.1 Thermochemistry

In **Chapter 1**, the Benson's group additivity method (GA) was briefly introduced. In this section, some further details are provided concerning the definition of the group additive values (GAVs) for the various classes of aromatic species of interest in this Ph.D. study.

The GA method is based on the premise that any thermochemical property of a molecule can be calculated from contributions pertaining to the groups ("group additive values (GAVs)"). In line with the definition of the term "group", a group is denoted as $X-(A)_i(B)_j(C)_k(D)_l$ where the central atom X is surrounded by *i* number of ligand A, *j* number of ligands B, *k* number of ligand C and *l* number of ligand D and the central atom of the group, X, is separated from the ligands A, B, C and D with a "-". In this notation, different types of carbon atoms are distinguished: C stands for a single-, C_d for a double- and C_b for a carbon atom in a benzene ring and C° stands for a carbon radical. An exceptional case to the rules of Benson's group definition is encountered in the carbonylic C=O group which is considered as the central atom of the group and abbreviated as "CO" even though it is not an atom but rather a polyatomic group.

To exemplify the partitioning of a molecule according to Benson's GA method, a double substituted molecule, *p*-dihydroxybenzene (*p*-hydroxyphenol or hydroquinone) is given in **Figure 2-1**.

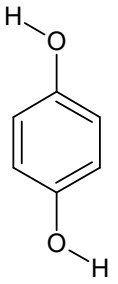

Figure 2-1 The structure of *p*-hydroxyphenoxy radical

For this molecule, the following Benson groups can be identified: C_b–(H), C_b–(O) and O–(C_b)(H), as given in Eq. (2-38). In the group notation, π-bonded ligands are omitted since these are implicitly included in the notation of the central atom, e.g. the C_b–(H) group always implies two C_b ligand bonds to the central atom. The substituent interaction between the two -OH groups that are in *para* position with respect to each other are captured with the NNI correction which is the last term on the right hand side in Eq. (2-38). With the identified groups, the standard enthalpy of formation can be found as:

$$\Delta_f H^\circ = 4\ GAV\ [C_b - (H)] + 2\ GAV\ [C_b - (O)] + 2\ GAV\ [O - (C_b)(H)] + NNI\ [p - OH + OH] \quad (2\text{-}38)$$

In **Chapters 3-5**, the GAV and the NNI values are determined by optimizing the agreement between the thermodynamic data calculated by the GA and the *ab initio* methods via least-squares linear regression.

To describe the thermochemical properties of monocyclic aromatic hydrocarbons (MAHs) that are relevant to lignin pyrolysis (benzene and (-un)substituted phenol, anisole, benzaldehyde, styrene, toluene and ethylbenzene) through Benson's GA method, a total of 14 GAVs are required. Among these, there are 3, namely C-(O)$(H)_3$, C-(C)$(H)_3$ and C_d-$(H)_2$, that describe the non-aromatic moieties in these molecules. These are taken from earlier studies [24,26,27] to ensure internal consistency with previous work. As a result of linear dependencies, four

additional GAVs cannot be determined independently from the remaining GAVs: O-(C_b)(H), CO-(C_b)(H), C_d-(C_b)(H) and C-(C_b)$(H)_3$. The O-(C_b)(H) group always appears together with a C_b-(O) group, a CO-(C_b)(H) group can only exist if also a C_b-(CO) group is present, the C_d-(C_b)(H) is always accompanied by a C_b-(C_d) group and the C-(C_b)$(H)_3$ requires the presence of the C_b-(C) group. The values for these four GAVs are set equal to the structurally similar GAVs O-(C_d)-(H), CO-(C_d)(H), C_d-(C_d)(H) and C-(C_d)$(H)_3$, respectively, as determined in the earlier studies by Sabbe et al. [24,27] and Paraskevas et al. [26]. These four GAVs and the aforementioned three non-aromatic GAVs are adopted and not subjected to optimization whereas the other 7 GAVs (C_b-(H), C_b-(C), C_b-(O), C_b-(CO), C_b-(C_d), O-(C_b)(C) and C-(C_b)$(C)_2$(H)) are optimized based on the thermochemical data. The optimized values for these 7 GAVs are available in **Chapter 3**.

For the corresponding monocyclic aromatic radicals (MARs) of the aforementioned MAHs, a total of 24 Group Additive Values (GAVs) need to be defined. In **Chapter 4**, these values are defined for a set of MARs that include phenyls, phenoxies, anisyls, benzoyls, styryls and benzyls. Among these groups, 7 GAVs have been defined in earlier studies [24,26,27] and 11 of them have been taken from the GAVs that are developed for the MAHs in **Chapter 3**. The parameters for these 18 GAVs are adopted and only 6 GAVs are obtained via optimization ($\dot{C}_b$, C_b-($\dot{O}$), O-($\dot{C}$)(C_b), C_b-($C\dot{O}$), $\dot{C}$-(C_b)$(H)_2$, $\dot{C}$-(C_b)(C)(H)), again, to ensure internal consistency with previously developed GAV/NNI databases.

As a general principle, two different types of GAVs are necessary for the description of the radicals in terms of Benson's GA parameters which are the GAVs for radical-centered groups and radical adjacent groups. In earlier studies, Sabbe et al. [24,27] demonstrated that for hydrocarbon radicals, the GAVs that describe a radical adjacent group can be substituted by

the similar non-radical groups without significant loss of accuracy. Therefore, only GAVs for the radical centered groups were developed. Paraskevas et al. [26] pointed out that the same substitution approach does not work for the oxygenated aliphatic radicals, mainly as oxygen (•O) and carbonyl (•C=O) moieties are not considered as center atoms of groups and thus, their contributions to thermodynamic properties have to be incorporated into adjacent groups. In the study presented in **Chapter 4**, the GAV definitions take these earlier observations into account. The defined GAVs are discussed in-depth in the following paragraph.

Only two new GAVs are needed to represent the carbon-centered radical groups for the benzyl radical which are $\dot{C}$-(C_b)($H)_2$ and $\dot{C}$-(C_b)(C)(H). Here, the radical-adjacent groups C_b-($\dot{C}$) and C-($\dot{C}$)$(H)_3$ found in benzyl and 1-phenylethyl radicals are substituted by the non-radical C_b-(C) and C-(C)$(H)_3$ groups. Only one radical-specific GAV, $\dot{C}_b$, is needed for phenyl and substituted phenyls. In spite of the fact that this GAV has already been defined by Sabbe et al. [24,27] based on CBS-QB3 calculations, in **Chapter 3**, it is pointed out that the CBS-QB3 calculations overestimates the $\Delta_f H^\circ$ of phenyl radical, which leads to a biased value of the GAV for the $\dot{C}_b$ group [24,27]. Therefore, this GAV is redefined in **Chapter 4** based on the G4/BAC dataset consisting of 25 phenylic MARs. For β-styryl radicals, no new GAVs are needed, since the $\dot{C}_d$-(H) GAV has already been defined by Sabbe et al. [24,27]. For the description of the phenoxylic and benzoylic MARs, two new GAVs are required which are the radical-adjacent groups C_b-($\dot{O}$) and C_b-($\dot{C}$O), respectively. To define anisylic radicals, $\dot{C}$-(O)$(H)_2$ and O-($\dot{C}$)(C_b) groups are necessary where the value for the former is taken from Paraskevas et al. [26] and the other one is obtained from the optimization. The optimized values concerning the 6 new GAVs that are defined for the description of MARs are tabulated in **Chapter 4**.

As discussed before in the Introduction, **Chapter 5** extends the application of Benson's GA method to the toluene derivatives that are larger than toluene and ethylbenzene and the corresponding benzylic radicals. To describe the thermochemistry of the aromatic species of interest in this chapter, a total of 27 GAVs are necessary. 4 of these parameters are available from the prior studies by Sabbe et al. [24,27] whereas 11 of them are taken from the earlier two chapters (**Chapters 3** and **4**). Thus, a total of 12 new GAVs are defined; one for each of the six different classes of substituted toluene derivatives and six different classes of corresponding benzylic radicals.

2.4.2 Kinetics

In **Chapters 3-5**, the applicability of Benson's GA method is extended to the domain of unsubstituted and substituted benzenes and their corresponding radicals and in **Chapter 6**, this experience is employed to explore the kinetics of hydrogen abstraction reactions (HARs) from the α-carbons of toluene derivatives by a hydrogen atom. A Benson-inspired approach, the group contribution method of Saeys et al. [61,62] and Sabbe et al. [29], is employed to develop predictive kinetic parameters with the aim of obtaining accurate reaction rate coefficients for a wide range of reactions in this class. This method is Benson-inspired in the sense that it stems from the idea of applying GAVs to describe the transition state structure of a reaction within the framework of TST. Nevertheless, instead of directly attempting to calculate the GAVs for the transition state structures, the focus of this method is on defining predictive parameters that can be used to obtain the differences of enthalpies and entropies between the transition state and the reactant in an accurate fashion, which in turn correspond to the two Arrhenius parameters of that reaction: the activation energies (E_a) and the pre-exponential factors (A), respectively. To eliminate temperature dependence from the predictive parameters, the

differences are considered as perturbations, ΔGAV°s, to the temperature-dependent Arrhenius parameters of a reference reaction. In the group contribution method, the parameters are called "ΔGAV°s" in lieu of GAVs as "Δ" refers to the difference between the thermodynamic properties of the transition state structure and the reactant and "°" corresponds to the fact that all of these parameters are defined with respect to the Arrhenius parameters of a reference reaction. The approach of the group contribution method in defining ΔGAV°s for transition state structures of these reactions is described in-depth in the paragraphs below.

A schematic representation of the transition-state structures for the HARs covered in this thesis is shown in **Figure 2-2**. In the figure, migration of the hydrogen atom from the carbon centered group (C_2) towards the abstracting hydrogen atom (H_1) is depicted.

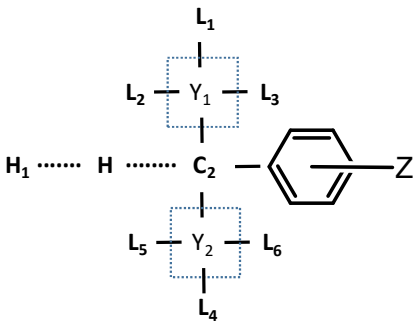

Figure 2-2 Scheme representing the transition state structure of the abstraction of a hydrogen atom that is bonded to the carbon atom C_2 by a hydrogen atom H_1. Z represents the substituent group on phenyl ring.

In **Figure 2-2**, the C_2 (the reacting carbon) centered reacting group (C_2-(H)(H_1)) corresponds to the major contributions to the Arrhenius parameters arising from the interaction between the abstracting hydrogen and the α-carbon from which hydrogen is abstracted, and this group is referred to as the primary contribution, i.e. the primary ΔGAV°. Contributions due to the presence of Y_1 and Y_2 groups, that are, the groups adjacent to the α-carbon atom from which a hydrogen atom migrates, are referred to as secondary ΔGAV°s. The interactions between the

primary group and the groups that reside further away from these groups are coined as "non-nearest neighbor interactions (ΔNNI°s)". The ΔNNI°s are crucial for the purposes of this work as these parameters reflect the effect of substitution on the reaction kinetics.

As given in Eq. (2-39), the activation energy of the reference reaction and the sum of the above-discussed contributions yields E_a of the HAR that is depicted in **Figure 2-2**.

$$E_a(T) = E_{a,ref}(T) + \Delta GAV^{\circ}_{E_a}(C_2) + \sum_{i=1}^{2} \Delta GAV^{\circ}_{E_a}(Y_i) + \sum_{l} \Delta NNI^{\circ}_{l} \quad (2\text{-}39)$$

The first term on the right hand side ($E_{a,ref}(T)$) represents E_a of the reference reaction. In this work, the selected reference reaction is the HAR from toluene by hydrogen atom as it is the simplest reaction within the family of reactions under investigation. The following two terms include primary and secondary ΔGAV° contributions to the activation energy and the last term, the ΔNNI°s, which, in the context of this study, represent the effect of the interactions between the extended side chain and the substituent group (Z) on the activation energy.

Saeys et al. have previously shown that for most radical reactions involving hydrocarbons the major contribution to the Arrhenius parameters is from the primary ΔGAV° contributions for the activation energies and the higher order contributions are negligible [61]. Similarly, Sabbe et al. also neglected secondary and tertiary ΔGAV° contributions for the estimation of pre-exponential factors for hydrocarbon chemistry [30]. Nevertheless, in the later works of Vandeputte et al. [31] and Paraskevas et al. [34], secondary ΔGAV° contributions were taken into account since in these works, it is shown that the sulfur or oxygen centered secondary groups affect the reaction kinetics profoundly depending on the type of secondary groups and thus, the ΔGAV° contributions due to these secondary groups could not be neglected. Besides, secondary groups distinguish between different types of compounds, e.g. oxygenates like

ethers, esters, acids, peroxides etc. which cannot be done using only primary groups. Since all the secondary groups of the reactions presented in this study are carbon-centered groups, only primary ΔGAV° contributions $\Delta GAV^{\circ}_{E_a}(C_2)$ are considered simplifying Eq. (2-39) to Eq. (2-40):

$$E_a(T) = E_{a,ref}(T) + \Delta GAV^{\circ}_{E_a}(C_2) + \sum_i \Delta NNI_i^{\circ} \quad (2\text{-}40)$$

Within the framework of Benson's GA method, the number of single events, n_e, is excluded from the GA modeling of entropies and eventually, group additive parameters are developed for intrinsic entropies [55,57]. This is also reflected here in the calculation of pre-exponential factors, where only the logarithm of the single-event pre-exponential factors ($log\tilde{A}$) are modeled excluding the number of single events (n_e), as given in Eq. (2-41) [29].

$$log\tilde{A} = logA - logn_e \quad (2\text{-}41)$$

Similar to activation energies (E_a), the logarithm of the single event pre-exponential factor ($log\tilde{A}$) of a target reaction can be obtained via Eq. (2-42).

$$log\tilde{A}(T) = log\tilde{A}_{ref}(T) + \Delta GAV^{\circ}_{log\tilde{A}}(C_2) + \sum_i \Delta NNI_i^{\circ} + logn_e \quad (2\text{-}42)$$

The first term on the right-hand side ($log\tilde{A}_{ref}$) is the logarithm of the single-event pre-exponential factor of the reference reaction. $\Delta GAV^{\circ}_{log\tilde{A}}(C_2)$ is the primary contribution and the $\sum_i \Delta NNI_i^{\circ}$ term represents the sum of the contributions from non-nearest neighbor interactions. The last term on the right-hand side ($logn_e$) is the logarithm of the number of single events. The tunneling contributions are excluded from the group additivity modeling of the pre-exponential factors, considering that the pre-exponential factors are based on the additivity of the entropies (of the reactant and the transition state structure) and tunneling is a non-classical

(quantum) effect that is not additive, but dependent on the potential energy surface for the reaction. Moreover, accurate calculation of tunneling contributions requires knowledge of the energy profile along the energy path and the imaginary frequency in the transition state. As both of these two properties are not accessible for the user who would be interested in calculating reaction rate coefficients at lower temperatures, a tunneling correction function, which enables the users to calculate tunneling coefficients with the GA-based information that is accessible for the user, is proposed in this work.

Inasmuch as tunneling effects are dominant at lower temperatures, the tunneling correction function is not needed to calculate reaction rate coefficients at temperatures higher than 1000 K where the tunneling correction factor can be taken as 1.

2.4.3 Linear Regression Procedure

In each of the four studies presented in this thesis (**Chapters 3-6**), the optimal values for the thermochemical or kinetic GA parameters are determined through simultaneously optimizing the agreement between the GA-based and the *ab initio* based reference datasets via unweighted least-squares linear regression analysis.

As mentioned in the earlier sections, a thermochemical/kinetic property (y) of a species/reaction is calculated through additivity of the values of GA parameters based on how many times they occur in that species/reaction. This leads to the following equation:

$$\sum_{i=1}^{m} X_i \beta_i = \hat{y} \tag{2-43}$$

where X_i is the number of occurence of the parameter i and β_i is the value of the i^{th} parameter among a total number of m parameters.

For each species/reaction j, $\sum_{i=1}^{m} X_{ij}\beta_i$ is equal to $\hat{y}_j$, which is the group additively calculated thermochemical/kinetic data for j whereas y_j represents the *ab initio* based thermochemical/kinetic data for j. Once Eq. (2-43) is written for all the n number of species/reactions, an overdetermined system of linear equations is obtained by Eq. (2-44):

$$\sum_{i=1}^{m} X_{ij}\beta_i = \hat{y}_j \qquad (j=1,2,\ldots\ldots n) \tag{2-44}$$

Here, X_{ij} is the occurrence matrix which carries the information on how many times each of the parameters occur in each of the species/reactions and it has the dimensions of m x n.

The difference between y_j and $\hat{y}_j$ is the "residual" which can be considered as a measure of the extent of the error in the group additively calculated data. The residual (r_j) is defined as follows:

$$r_j = y_j - \sum_{i=1}^{m} X_{ij}\beta_i \qquad (j=1,2,\ldots\ldots n) \tag{2-45}$$

In this linear regression analysis, the objective function SSQ, i.e. the square of the residual is minimized with respect to the GA-based parameters ($\bar{\beta}$):

$$SSQ = \sum_{j}^{n} (y_j - \hat{y}_j)^2 = \sum_{j}^{n} {r_j}^2 \tag{2-46}$$

$$\frac{\partial SSQ}{\partial \beta} = 0 \tag{2-47}$$

This minimization yields the following equation:

$$(X^T X)\bar{\beta} = X^T \bar{y} \tag{2-48}$$

The expression in Eq. (2-48) can be rearranged to the following equation that yields $\bar{\beta}$, the vector that contains the values of the GA parameters:

$$\bar{\beta} = (X^T X)^{-1} X^T \bar{y} \quad (2\text{-}49)$$

Since the occurrence matrix X and the $\bar{y}$ vector which contains the *ab initio* calculated thermochemical and/or kinetic data are available, $\bar{\beta}$ can easily be calculated from Eq. (2-49).

All the final values of the thermochemical and kinetic parameters in this Ph.D. dissertation are reported together with their 97.5% confidence intervals. An in-depth description of the calculation of confidence intervals can be found in Appendix C.

A statistical analysis is performed to assess the reliability of the linear regression and the quality of the optimization procedure upon each application. The quality of the fits is expressed in terms of the significance (F) of the regression, the mean absolute deviation (MAD), root-mean square deviation (RMS) and maximum deviation (MAX) between *ab initio* data and the data obtained via group additivity. The reported significance F of the regression is calculated with the following equation:

$$F = \frac{(\sum_{i=1}^{n} \hat{y}^2)/m}{(\sum_{i=1}^{n} (\hat{y}_i - y_i)^2)/(n-m)} \quad (2\text{-}50)$$

In Eq. (2-50), n is the number of species/reactions and m is the total number of GA-based parameters that took place in the linear regression procedure.

2.5 Natural Bond Orbitals

In **Chapter 3**, the underlying origins of the physical interactions contributing to the overall substituent effects that are encountered in the substituted MAHs are investigated via the Natural Bond Orbital (NBO) method of Weinhold and coworkers [63].

The NBO method is one of the many available analysis techniques bringing chemical insights based on the electronic wavefunction that is obtained from the solution of Schrodinger's equation in such a fashion that it can be interpreted in terms of the familiar language of localized Lewis-like chemical bond [64]. This method is employed through the NBO analysis 6.0 program [65] which transforms the many-body molecular wavefunction obtained from the Gaussian calculations into localized one electron orbitals that are termed as "Natural Atomic Orbitals (NAOs)."

To realize this, the program primarily obtains the "natural orbitals (NOs)" that correspond to the eigenorbitals $\{\theta_i\}$ of first-order reduced density matrix operator,$\Gamma^{(1)}$:

$$\Gamma^{(1)}\theta_i = q\theta_i \ (= 1,2,3 \ldots) \tag{2-51}$$

with the eigenvalues that correspond to the occupancies, q_i.

$$q_i = < \theta_i | \ \Gamma^{(1)} | \theta_i > \tag{2-52}$$

It should be kept in mind that the values for q_i are limited by Pauli's exclusion principle ($0 \ \leq q_i \leq 2$). The θ_is that maximize the orbital occupancies (q_i) are chosen to represent the molecular wavefunction in the most compact possible form [63].

Then, based on the NAOs, the program delivers a deep insight on the detailed chemical information concerning the populations of core, valence and higher energy Rydberg orbitals of every single atom as a part of Natural Population Analysis (NPA). In the framework of the NBO method, optimized linear combinations of NAOs form natural hybrid orbitals (NHOs) and the combination of these NHOs leads to bonding and antibonding NBOs, which are localized orbitals that describe the Lewis like molecular bonding pattern of electron pairs. From the idealized Lewis picture point of view, all filled NBOs are expected to have an occupancy of 2 and any departure from this ideal localized picture is interpreted as an

indication of delocalization. In this sense, NBOs can be referred to as 'chemist's basis set' since they render any aspect of the wavefunction to be expressed in terms of Lewis versus non-Lewis type contributions which establishes a bridge between the results of modern ab initio calculations and elementary valency and bonding concepts [63].

As a part of the NBO analysis, the second order perturbation theory analysis demonstrates the extent of stabilization due to the charge transfers from bonding orbitals to antibonding orbitals, i.e. transfer from a Lewis type donor orbital to a non-Lewis type acceptor orbital. The second order perturbation theory analysis is useful as it gives detailed insight into the contribution of hydrogen bonds and the mesomeric effects to the overall substituent interaction.

All the NBO calculations in this Ph.D. dissertation are carried out with results from single point energy calculations at the CCSD(T)/6-31G(d') level at the B3LYP//CBSB7 optimized geometry.

2.6 References

[1] Leach AR. *Molecular Modelling: Principles and Applications:* Prentice Hall; 2001.

[2] Springborg M. *Methods of Electronic-Structure Calculations: From Molecules to Solids:* Wiley; 2000.

[3] Szabo A, Ostlund NS. *Modern Quantum Chemistry: Introduction to Advanced Electronic Structure Theory:* Dover Publications; 2012.

[4] Møller C, Plesset MS. Note on an Approximation Treatment for Many-Electron Systems. *Physical Review.* 1934;46(7):618-622.

[5] Kohn W, Sham LJ. Self-Consistent Equations Including Exchange and Correlation Effects. *Physical Review.* 1965;140(4A):A1133-A1138.

[6] Hohenberg P, Kohn W. Inhomogeneous Electron Gas. *Physical Review.* 1964;136(3B):B864-B871.

[7] Becke AD. A new mixing of Hartree–Fock and local density-functional theories. *The Journal of Chemical Physics.* 1993;98(2):1372-1377.

[8] Boese AD, Martin JML. Development of density functionals for thermochemical kinetics. *The Journal of Chemical Physics.* 2004;121(8):3405-3416.

[9] Zhao Y, Truhlar DG. Density Functional for Spectroscopy: No Long-Range Self-Interaction Error, Good Performance for Rydberg and Charge-Transfer States, and Better Performance on Average than B3LYP for Ground States. *The Journal of Physical Chemistry A.* 2006;110(49):13126-13130.

[10] Zhao Y, Truhlar DG. A new local density functional for main-group thermochemistry, transition metal bonding, thermochemical kinetics, and noncovalent interactions. *The Journal of Chemical Physics.* 2006;125(19):194101.

[11] Zhao Y, Truhlar DG. The M06 suite of density functionals for main group thermochemistry, thermochemical kinetics, noncovalent interactions, excited states, and transition elements: two new functionals and systematic testing of four M06-class functionals and 12 other functionals. *Theoretical Chemistry Accounts.* 2008;120(1):215-241.

[12] Zhao Y, Truhlar DG. A Density Functional That Accounts for Medium-Range Correlation Energies in Organic Chemistry. *Organic Letters.* 2006;8(25):5753-5755.

[13] Rokob TA, Hamza A, Pápai I. Computing Reliable Energetics for Conjugate Addition Reactions. *Organic Letters.* 2007;9(21):4279-4282.

[14] Montgomery Jr JA, Frisch MJ, Ochterski JW, Petersson GA. A complete basis set model chemistry. VI. Use of density functional geometries and frequencies. *The Journal of Chemical Physics.* 1999;110(6):2822-2827.

[15] Montgomery JA, Frisch MJ, Ochterski JW, Petersson GA. A complete basis set model chemistry. VII. Use of the minimum population localization method. *The Journal of Chemical Physics.* 2000;112(15):6532.

[16] Curtiss LA, Raghavachari K, Trucks GW, Pople JA. Gaussian-2 theory for molecular energies of first- and second-row compounds. *The Journal of Chemical Physics.* 1991;94(11):7221-7230.

[17] Curtiss LA, Raghavachari K, Redfern PC, Pople JA. Assessment of Gaussian-2 and density functional theories for the computation of enthalpies of formation. *The Journal of Chemical Physics.* 1997;106(3):1063-1079.

[18] Curtiss LA, Raghavachari K, Redfern PC, Rassolov V, Pople JA. Gaussian-3 (G3) theory for molecules containing first and second-row atoms. *The Journal of Chemical Physics.* 1998;109(18):7764-7776.

[19] Baboul AG, Curtiss LA, Redfern PC, Raghavachari K. Gaussian-3 theory using density functional geometries and zero-point energies. *The Journal of Chemical Physics.* 1999;110(16):7650-7657.

[20] Curtiss LA, Redfern PC, Raghavachari K, Pople JA. Gaussian-3X (G3X) theory using coupled cluster and Brueckner energies. *Chemical Physics Letters.* 2002;359(5):390-396.

[21] Curtiss LA, Redfern PC, Raghavachari K. Gaussian-4 theory. *The Journal of Chemical Physics.* 2007;126(8):084108.

[22] Martin JM, de Oliveira G. Towards standard methods for benchmark quality ab initio thermochemistry—W1 and W2 theory. *The Journal of Chemical Physics.* 1999;111(5):1843-1856.

[23] Karton A, Rabinovich E, Martin JM, Ruscic B. W4 theory for computational thermochemistry: In pursuit of confident sub-kJ/mol predictions. *The Journal of Chemical Physics.* 2006;125(14):144108.

[24] Sabbe MK, Saeys M, Reyniers M-F, Marin GB, Van Speybroeck V, Waroquier M. Group Additive Values for the Gas Phase Standard Enthalpy of Formation of Hydrocarbons and Hydrocarbon Radicals. *The Journal of Physical Chemistry A.* 2005;109(33):7466-7480.

[25] Vandeputte AG, Sabbe MK, Reyniers MF, Marin GB. Modeling the gas-phase thermochemistry of organosulfur compounds. *Chemistry – A European Journal.* 2011;17(27):7656-7673.

[26] Paraskevas PD, Sabbe MK, Reyniers M-F, Papayannakos N, Marin GB. Group Additive Values for the Gas-Phase Standard Enthalpy of Formation, Entropy and Heat Capacity of Oxygenates. *Chemistry – A European Journal.* 2013;19(48):16431-16452.

[27] Sabbe MK, De Vleeschouwer F, Reyniers M-F, Waroquier M, Marin GB. First Principles Based Group Additive Values for the Gas Phase Standard Entropy and Heat Capacity of Hydrocarbons and Hydrocarbon Radicals. *The Journal of Physical Chemistry A.* 2008;112(47):12235-12251.

[28] Sabbe M, Vandeputte A, Reyniers M-F, Van Speybroeck V, Waroquier M, Marin G. Ab Initio Thermochemistry and Kinetics for Carbon-Centered Radical Addition and β-Scission Reactions. *The Journal of Physical Chemistry A.* 2007;111(34):8416-8428.

[29] Sabbe M, Reyniers M-F, Van Speybroeck V, Waroquier M, Marin G. Carbon-Centered Radical Addition and β-Scission Reactions: Modeling of Activation Energies and Pre-exponential Factors. *ChemPhysChem.* 2008;9(1):124-140.

[30] Sabbe MK, Vandeputte AG, Reyniers M-F, Waroquier M, Marin GB. Modeling the influence of resonance stabilization on the kinetics of hydrogen abstractions. *Physical Chemistry Chemical Physics.* 2010;12(6):1278-1298.

[31] Vandeputte AG, Sabbe MK, Reyniers M-F, Marin GB. Kinetics of α hydrogen abstractions from thiols, sulfides and thiocarbonyl compounds. *Physical Chemistry Chemical Physics.* 2012;14(37):12773-12793.

[32] Vandeputte AG, Reyniers MF, Marin GB. Kinetics of homolytic substitutions by hydrogen atoms at thiols and sulfides. *ChemPhysChem.* 2013;14(8):1703-1722.

[33] Vandeputte AG, Reyniers M-F, Marin GB. Kinetic modeling of hydrogen abstractions involving sulfur radicals. *ChemPhysChem.* 2013;14(16):3751-3771.

[34] Paraskevas PD, Sabbe MK, Reyniers M-F, Papayannakos NG, Marin GB. Kinetic Modeling of α-Hydrogen Abstractions from Unsaturated and Saturated Oxygenate Compounds by Hydrogen Atoms. *The Journal of Physical Chemistry A.* 2014;118(40):9296-9309.

[35] Paraskevas PD, Sabbe MK, Reyniers M-F, Papayannakos N, Marin GB. Kinetic modeling of alpha-hydrogen abstractions from unsaturated and saturated oxygenate compounds by carbon-centered radicals. *ChemPhysChem.* 2014;15(9):1849-1866.

[36] Blanksby SJ, Ellison GB. Bond dissociation energies of organic molecules. *Accounts of Chemical Research.* 2003;36(4):255-263.

[37] Luo Y-R. *Handbook of Bond Dissociation Energies in Organic Compounds.* Hoboken: CRC Press; 2002.

[38] Frisch MJ, Trucks GW, Schlegel HB, Scuseria GE, Robb MA, Cheeseman JR, Scalmani G, Barone V, Mennucci B, Petersson GA, Nakatsuji H, Caricato M, Li X, Hratchian HP, Izmaylov AF, Bloino J, Zheng G, Sonnenberg JL, Hada M, Ehara M, Toyota K, Fukuda R, Hasegawa J, Ishida M, Nakajima T, Honda Y, Kitao O, Nakai H, Vreven T, Montgomery Jr. JA, Peralta JE, Ogliaro F, Bearpark MJ, Heyd J, Brothers EN, Kudin KN, Staroverov VN, Kobayashi R, Normand J, Raghavachari K, Rendell AP, Burant JC, Iyengar SS, Tomasi J, Cossi M, Rega N, Millam NJ, Klene M, Knox JE, Cross JB, Bakken V, Adamo C, Jaramillo J, Gomperts R, Stratmann RE, Yazyev O, Austin AJ, Cammi R, Pomelli C, Ochterski JW, Martin RL, Morokuma K, Zakrzewski VG, Voth GA, Salvador P, Dannenberg JJ, Dapprich S, Daniels AD, Farkas Ö, Foresman JB, Ortiz JV, Cioslowski J, Fox DJ. *Gaussian 09, Version D.01.* Wallingford, CT, USA: Gaussian, Inc.; 2009.

[39] Schlegel HB, McDouall JJW. *Computational Advances in Organic Chemistry: Molecular Structure and Reactivity:* Springer Netherlands; 167-185, 1991.

[40] Seeger R, Pople JA. Self-consistent molecular orbital methods. XVIII. Constraints and stability in Hartree–Fock theory. *The Journal of Chemical Physics.* 1977;66(7):3045-3050.

[41] Bauernschmitt R, Ahlrichs R. Stability analysis for solutions of the closed shell Kohn–Sham equation. *The Journal of Chemical Physics.* 1996;104(22):9047-9052.

[42] Baker J, Scheiner A, Andzelm J. Spin contamination in density functional theory. *Chemical Physics Letters.* 1993;216(3):380-388.

[43] Cioslowski J, Liu GH, Martinov M, Piskorz P, Moncrieff D. Energetics and site specificity of the homolytic C-H bond cleavage in benzenoid hydrocarbons: An ab initio electronic structure study. *Journal of the American Chemical Society.* 1996;118(22):5261-5264.

[44] Menon AS, Radom L. Consequences of Spin Contamination in Unrestricted Calculations on Open-Shell Species: Effect of Hartree−Fock and Møller−Plesset Contributions in Hybrid and Double-Hybrid Density Functional Theory Approaches. *The Journal of Physical Chemistry A.* 2008;112(50):13225-13230.

[45] Vandeputte AG, Sabbe MK, Reyniers M-F, Van Speybroeck V, Waroquier M, Marin GB. Theoretical Study of the Thermodynamics and Kinetics of Hydrogen Abstractions from Hydrocarbons. *The Journal of Physical Chemistry A.* 2007;111(46):11771-11786.

[46] Blanquart G. Effects of spin contamination on estimating bond dissociation energies of polycyclic aromatic hydrocarbons. *International Journal of Quantum Chemistry.* 2015;115(12):796-801.

[47] Tuckerman M. *Statistical Mechanics: Theory and Molecular Simulation:* Oxford University Press; 2010.

[48] Laurendeau NM. *Statistical Thermodynamics: Fundamentals and Applications:* Cambridge University Press; 2005.

[49] Atkins PW. *Physical chemistry.* 5th ed: W.H. Freeman & Co (Sd); 1994.

[50] Vansteenkiste P, Van Speybroeck V, Marin GB, Waroquier M. Ab initio calculation of entropy and heat capacity of gas-phase n-alkanes using internal rotations. *The Journal of Physical Chemistry A.* 2003;107(17):3139-3145.

[51] Van Speybroeck V, Vansteenkiste P, Neck DV, Waroquier M. Why does the uncoupled hindered rotor model work well for the thermodynamics of n-alkanes? *Chemical Physics Letters.* 2005;402(4-6):479-484.

[52] Vansteenkiste P, Van Neck D, Van Speybroeck V, Waroquier M. An extended hindered-rotor model with incorporation of Coriolis and vibrational-rotational coupling

for calculating partition functions and derived quantities. *The Journal of Chemical Physics.* 2006;124(4):044314.

[53] Petersson GA, Malick D, Wilson W, Ochterski J, Montgomery JA, Frisch MJ. Calibration and comparison of the Gaussian-2, complete basis set, and density functional methods for computational thermochemistry. *The Journal of Chemical Physics.* 1998;109(24):10570.

[54] Hehre WJ, Ditchfield R, Radom L, Pople JA. Molecular orbital theory of the electronic structure of organic compounds. V. Molecular theory of bond separation. *Journal of the American Chemical Society.* 1970;92(16):4796-4801.

[55] Benson SW, Buss JH. Additivity Rules for the Estimation of Molecular Properties - Thermodynamic Properties. *Journal of Chemical Physics.* 1958;29(3):546-572.

[56] Benson SW. *Thermochemical kinetics; Methods for the Estimation of Thermochemical Data and Rate Parameters.* New York: Wiley; 1968.

[57] Benson SW, Cruickshank FR, Golden DM, Haugen G, O'Neal HE, Rodgers AS, Shaw R, Walsh R. Additivity rules for the estimation of thermochemical properties. *Chemical Reviews.* 1969;69(3):279-324.

[58] Benson SW. *Thermochemical Kinetics : Methods for the Estimation of Thermochemical Data and Rate Parameters.* 2d ed. New York: Wiley; 1976.

[59] IUPAC. *Compendium of Chemical Terminology,* 2nd ed. (the "Gold Book"). Compiled by A. D. McNaught and A. Wilkinson. Blackwell Scientific Publications, Oxford (1997).

[60] Eckart C. The Penetration of a Potential Barrier by Electrons. *Physical Review.* 1930;35(11):1303-1309.

[61] Saeys M, Reyniers M-F, Marin G, Van Speybroeck V, Waroquier M. Ab initio group contribution method for activation energies for radical additions. *AIChE Journal.* 2004;50(2):426-444.

[62] Saeys M, Reyniers M-F, Van Speybroeck V, Waroquier M, Marin GB. Ab initio group contribution method for activation energies of hydrogen abstraction reactions. *ChemPhysChem.* 2006;7(1):188-199.

[63] Weinhold F, Landis CR. Natural Bond Orbitals and Extensions of Localized Bonding Concepts. *Chemistry Education Research and Practice.* 2001;2:91-104.

[64] Glendening ED, Landis CR, Weinhold F. Natural bond orbital methods. *WIRES Computational Molecular Science*. 2012; 2: 1–42.

[65] Glendening ED, Badenhoop JK, Reed AE, Carpenter JE, Bohmann JA, Morales CM, Landis CR, Weinhold F. NBO 6.0: *Natural Bond Orbital Analysis Program.* Theoretical Chemistry Institute. 6 ed. University of Wisconsin, Madison 2013.

Chapter 3 Thermodynamics of oxygenated monocyclic aromatic hydrocarbons

This chapter includes the following paper:

Ince A, Carstensen H-H, Reyniers M-F, Marin GB. First-principles based group additivity values for thermochemical properties of substituted aromatic compounds. *AIChE Journal.* 2015;61(11):3858-3870.

3.1 Abstract

A set of 7 Benson group additive values (GAV) together with 15 correction terms for non-nearest neighbor interactions (NNI) is developed to calculate the gas phase standard enthalpies of formation, entropies and heat capacities of monocyclic aromatic compounds containing methyl, ethyl, vinyl, formyl, hydroxyl and methoxy substituents. These GAVs are obtained through least squares regression of a database of thermodynamic properties of 143 molecules, calculated at the post-Hartree–Fock G4 composite method. Out of the 15 NNIs, which account for several well-known substituent effects in aromatic molecules, 13 have been determined for the first time. All but two group additively calculated standard enthalpies of formation agree within 4 kJ mol^{-1}. The entropies and the heat capacities generally deviate less than 4 J mol^{-1} K^{-1} from the *ab initio* results. Natural bond orbital analysis is utilized to identify the underlying causes of the observed NNIs.

3.2 Introduction

The thermodynamic properties of molecules such as their standard enthalpy of formation ($\Delta_f H^\circ$), entropy (S°) and heat capacity (C_p) play a pivotal role in the construction of fundamental kinetic models, which become increasingly more important in the optimization of industrial processes [1-4]. In recent years, such reaction networks have been used in various areas such as steam cracking of hydrocarbons [4], combustion processes [5,6] and the formation of polycyclic aromatic hydrocarbons [7-9]. Current interests in the thermochemical conversion of biomass to liquid fuels or commodity chemicals leads to the need for kinetic models that describe the pyrolysis of its components cellulose, hemicellulose and lignin. The decomposition of lignin yields mainly substituted monocyclic aromatic compounds with

substituent groups such as hydroxy (-OH), methoxy (-OCH_3), formyl (-CHO), vinyl (-$CH{=}CH_2$) and alkyl (-R) [10-12]. With few exceptions, reliable experimental thermochemical data for these species are not available. Furthermore, it is not feasible to use highly accurate first-principle calculations for each molecule encountered in such conversion processes because of the high demands in computing time and hardware resources. Therefore, to be able to construct a reliable kinetic model for lignin pyrolysis or other conversion processes that involve substituted monocyclic aromatic hydrocarbons, alternative methods play an important role.

A popular approach to describe thermodynamic properties of gas phase species is the group additivity (GA) method developed by Benson and coworkers [13-16]. Benson's basic idea is to divide molecules into smaller units, called groups, and use an additive scheme to obtain thermochemical data based on contributions from these groups, which are known as "group additive values (GAVs)". According to Benson, a group is defined as "a polyvalent atom in a molecule together with all its ligands" [16]. Although GAVs account for the major part of a thermodynamic property, precise calculations require that additional contributions from interactions that extend beyond the range of a group have to be included as well. These so-called non-nearest neighbor interactions (NNIs) are incorporated into the GA method as correction terms. The thermodynamic property "y" thus is calculated as

$$y = \sum_{1}^{i} n_i \, GAV_i + \sum_{1}^{j} n_j NNI_j \qquad (3\text{-}1)$$

The GAV_i refer to different groups which occur n_i times in the molecule, and NNI_j is the j^{th} correction term which occurs n_j times in the molecule. To use this method, all required GAVs

and NNI correction terms must be known, and ongoing efforts aim to expand the GAV/NNI database and to improve the accuracy of existing entries.

Group values for Benson's GA method were initially derived entirely from experimental data [15,17-20], but in the last decade several studies used computational means to define these parameters [21-28]. It has been shown that GA methods are able to calculate standard enthalpies of formation with “chemical accuracy”, meaning with a standard deviation of not more than 4 kJ mol^{-1} [22-25]. This accuracy is comparable to that of high level *ab initio* methods, which require substantially more time and effort. Benson’s method has been successfully applied to standard enthalpies of formation of gas phase molecules [4,15,17,22,24,25], and also to entropies and heat capacities [13-16,23-25].

To ensure that the values obtained via GA are reliable, the GAV and NNI definitions have to be internally consistent. This means that (1) the GAV parameters are assigned in a systematic way resolving all linear dependencies [14], (2) the set of NNIs are comprehensive and well defined and (3) all parameters are determined from reference data of equal quality. Marin and coworkers [22-25] have started to create such an internally consistent GAV/NNI database based on *ab initio* results at the CBS-QB3 level of theory. Currently this database contains GAV and NNI definitions that allow calculation of thermodynamic properties for aliphatic hydrocarbons like alkanes, alkenes, alkynes and few cyclic hydrocarbons and their corresponding radicals [22,23], oxygenates such as alcohols, esters, ethers, ketones, carboxylic acids, ketenes and their corresponding radicals [25] and organic sulfur compounds [24]. The purpose of this study is to extend the GAV and NNI database to substituted monocyclic aromatic hydrocarbons (MAHs). As this extension is motivated by the interest in modeling pyrolysis products of lignin, the following substituent groups are considered: hydroxy (-OH),

methoxy (-OCH_3), formyl (-CHO), vinyl (-$CH{=}CH_2$) and methyl (-CH_3) and ethyl (-CH_2CH_3). The following approach is adapted: (1) A database of accurate gas phase standard enthalpies of formation ($\Delta_f H°$), entropies ($S°$) and heat capacities ($C_p(T)$) for a set of 133 molecules is constructed using high level electronic structure calculations. (2) The necessary GAVs are identified and preliminary values are assigned based on the data for mono-substituted benzenes. (3) Deficiencies in the group additively calculated data are used to identify those non-nearest-neighbor interactions (NNIs) that contribute significantly to the thermodynamic properties. (4) Natural Bond Orbital (NBO) analyses is carried out to support the NNI selections. (5) All unknown GAV and NNI parameters are finally simultaneously optimized to best reproduce the thermodynamic data of the entire reference data set.

3.3 Methodology

3.3.1 Electronic Structure Calculations

The Gaussian 09 software package [29] has been used to perform all electronic structure calculations. Thermodynamic properties are calculated at the CBS-QB3 [30] and G4 [31] levels of theory. The CBS-QB3 composite method is widely used and has been shown to produce accurate enthalpies of formation [22,24,25] and rate coefficients [32-35]. It was the method of choice for deriving GAV and NNI parameters in the previous studies by Sabbe et al. [22], Vandeputte et al. [24] and Paraskevas et al. [25] and it would be the preferred method to extend the GAV database for aromatic species. However, CBS-QB3 calculated bond dissociation energies for the C-H bond in benzene (483.0 kJ mol^{-1}), the C-O bond in phenol (480.7 kJ mol^{-1}) and the aryl-CHO bond in benzaldehyde (428.2 kJ mol^{-1}) deviate more than 10 kJ mol^{-1} from well-established experimental values (472.2 ± 2.2 kJ mol^{-1} [36], 465.7 ± 4.2

kJ mol^{-1} [36] and 415.5 ± 3.8 kJ mol^{-1} [37], respectively). This casts doubts on the ability of the CBS-QB3 method to accurately describe aromatic molecules. For this reason, calculations were also performed at the G4 level of theory. G4 is also a composite method but differs from CBS-QB3 calculations in the details of the geometry optimization and the frequency analysis step as well as in the way the final energy is approximated by a series of single point energy calculations. The extrapolation methods to the basis set limit and the applied corrections to the final energy are also different. Details can be found in the original literature [30,31]. In the context of this study it is worth noting that the G4 method yields extrapolated final electronic energies that are more accurate than the CBS-QB3 energies, however, at the cost of significantly higher CPU time demands, which effectively limits the applicability of G4 calculations to smaller molecules. With respect to the bond dissociation energies mentioned above, G4 yields those values to be 471.1 kJ mol^{-1}, 465.1 kJ mol^{-1} and 414.2 kJ mol^{-1}, respectively, in excellent agreement with the experimental data.

3.3.2 Hindered Rotor Treatment

In order to take thermochemical effects due to rotation of single bonds into consideration, the one-dimensional hindered rotor (1D-HR) approach of Van Speybroeck and coworkers [38-40] is applied. It is well known that such a treatment significantly improves the calculated thermochemical properties [39], in particular the entropy results. To calculate the contributions of internal rotations to the partition function and thermodynamic properties, the hindrance potentials for rotation are determined with relaxed potential energy surface scans at the B3LYP/6-31G(d) level and expanded to a truncated Fourier series using the first six sine and cosine terms. The internal rotations were identified via visual inspection of the animated vibrations. Only internal rotors with total barriers below 50 kJ mol^{-1} are evaluated separately,

all other modes are treated as a harmonic oscillators. Internal rotations with very low barriers (less than 1 kJ mol^{-1}) are considered free rotors. The reduced moment of inertia describing the rotation of the two molecule fragments around the axis which decouples internal from external rotation are calculated with the procedure described by Van Speybroeck et al. [39].

All thermochemical data calculated in this study are based on the lowest energy conformer of each molecule. The hindrance potentials of the internal rotors are used to identify low-energy conformers, which are then evaluated at the CBS-QB3 and G4 levels, respectively, to identify the lowest energy conformers. Note that this approach does not necessarily guarantee that the global minimum is found if internal rotors are coupled. The above described methodology is in line with the previous studies of Marin and coworkers [22,24,25].

3.3.3 Standard Enthalpy of Formation

The calculation of standard enthalpies of formation, which is the enthalpy relative to the composing elements in their standard state, always requires experimental information, as, for example, the enthalpy of carbon in its graphitic standard state cannot be determined accurately using *ab initio* methods. In the atomization energy method, the standard enthalpy of formation is obtained from the *ab initio* (AI) calculated enthalpy of atomization at 298 K and the experimental standard enthalpies of formation of atoms in the gas phase (gas,exp) at the same temperature, as given in Eq. (3-2):

$$\Delta_f H°\left(C_m H_n O_p; 298\ K\right) = m\Delta_f H^\circ{}_{gas,exp}(C) + n\Delta_f H^\circ{}_{gas,exp}(H) + p\,\Delta_f H^\circ{}_{gas,exp}(O) - \left[mH^\circ{}_{AI}(C) + nH^\circ{}_{AI}(H) + pH^\circ{}_{AI}(O) - H^\circ{}_{AI}(C_m H_n O_p)\right] \quad (3\text{-}2)$$

where $\Delta_f H^\circ_{gas,exp}$(C) = 716.68 kJ mol^{-1}, $\Delta_f H^\circ_{gas,exp}$(H) = 218.0 kJ mol^{-1} and $\Delta_f H^\circ_{gas,exp}$(O) = 249.18 kJ mol^{-1} at 298 K [36].

The last four terms of Eq. (3-2). yield the *ab initio* (AI) calculated atomization enthalpies for $C_mH_nO_p$ at 298 K, that is, the reaction enthalpy of Eq. (3-3) at 298 K.

$$C_mH_nO_p \rightarrow mC + nH + pO \tag{3-3}$$

Two different types of corrections have been applied to the atomization energies. First, spin-orbit (SO) corrections of 0.35 kJ mol^{-1} per carbon atom and 0.93 kJ mol^{-1} per oxygen atom [41] have been applied to the results from the CBS-QB3 calculations only since SO corrections are part of the G4 methodology [31]. Second, "Bond Additive Corrections" (BACs) [42] are applied to eliminate the remaining systematic errors of *ab initio* calculations

$$\Delta_f H^\circ(BAC) = \Delta_f H^\circ(CBS-QB3 \text{ or } G4) + \sum_{ij} N_{ij} BAC_{ij} \tag{3-4}$$

where i and j run over the two different atom types and N_{ij} is the number of bonds between atoms of type i and j. As the CBS-QB3 and G4 methods suffer from different systematic bond-related errors, BAC values were developed separately for both methods.

In this study, BACs are used in accordance with the earlier studies [22,25], however, since this work focuses on aromatic molecules, additional BAC values are defined to achieve optimal agreement between calculated and experimental enthalpies of formation. For this purpose, a training set of 77 molecules for which reliable experimental data is available, has been assembled. This training set, listed in **Table A-1** of Appendix A, contains 32 aliphatic hydrocarbons, 29 linear oxygenated hydrocarbons and 16 MAHs. The data for nonaromatic molecules were taken from the work of Paraskevas et al. [25]. The rather small number of aromatic molecules present in this set can be explained with the scarcity of reliable experimental data for this class of molecules. The thermodynamic data for the aromatic molecules were retrieved from the "Thermochemical Database" of the NIST Webbook [43].

Several criteria were used to select the data. First, entries reporting $\Delta_f H°$ values that were directly reported in the original study are preferred over those that have been deduced from published solid or liquid phase data. If the NIST Database contains several values for a given molecule, the entries with stated error margins are given priority. If several data with reported error bars exist, only those that overlapped with each other within the stated error margins were considered. Eventually, the average of the remaining data points was taken. Anisole (methoxybenzene) is the only molecule included in the training set that does not match the reliability criteria since there was no alternative methoxy (-OCH_3) substituted monoaromatic hydrocarbon available to be included in the BAC training set. For anisole, the average of the two available data points was taken even though they deviate by 8.8 kJ mol^{-1} despite the fact that the reported error margins suggest accuracies of 1.2 kJ mol^{-1} [44] and 0.92 kJ mol^{-1} [45], respectively.

Also provided in **Table A-1** of Appendix A are the deviations between CBS-QB3 (with SO corrections) and G4 calculated enthalpies of formation from the experimental data. It is evident, that in particular the CBS-QB3 results deviate substantially from the experimental values with the trend that the CBS-QB3 enthalpies are consistently higher than the measured ones. This is reflected in a mean deviation (MD) of 7.5 kJ mol^{-1} for the entire training set. The results from G4 calculations are generally closer to the experimental values (MD = 3.1 kJ mol^{-1}), but G4 also tends to overestimate the enthalpies of formation.

To correct the theoretically calculated enthalpies of formation, a distinction between nine different bonds is made, which are C-C, C-H, C=C, C-O, O-H, C=O, C_b-H, C_b-C_b, and C_b-O. By differentiating between bonds of nonaromatic carbon atoms and those formed by an

aromatic carbon atom, significant improvements of the corrected enthalpies of formation are achieved.

Out of the nine BACs for the bonds discussed above, six correction parameters have already been determined at the CBS-QB3 level of theory by Paraskevas et al. [25]. Those were kept constant and only the remaining three parameters were optimized via unweighted linear regression. Since no previously defined BACs for G4 calculations were available, all nine parameters were subjected to the least squares fitting procedure. The BAC values for both levels of theory are reported in **Table 3-1.** The differences between bond additivity corrected enthalpies of formation and the experimental data are provided in **Table A-1** of Appendix A together with the statistics. The mean deviations (MD) between BAC-corrected and experimental $\Delta_f H°$ data at 298 K are reduced to 0.0001 for both levels of theory and the mean absolute deviations (MAD) are 1.4 kJ mol^{-1} (for both methods). These values are significantly improved compared to those of the uncorrected data (8.2 kJ mol^{-1} and 3.3 kJ mol^{-1}, respectively). The maximum absolute deviations (MAX) are also clearly improved from 20.5 kJ mol^{-1} to 6.2 kJ mol^{-1} and 9.5 kJ mol^{-1} to 5.2 kJ mol^{-1}, respectively. The performance of BAC corrected CBS-QB3 and G4 calculations is further assessed using a test set of 14 MAHs. This test set contains MAHs for which the available experimental data do not fully meet the aforementioned criteria of reliability and thus they were not included in the training set. Given the higher uncertainty on the experimental values, the derived BACs are not expected to be as successful in improving the agreement between experimental and calculated enthalpies of formation as for the training set. Nevertheless, BACs should lower the MAD for $\Delta_f H°$ significantly at both levels of theory. **Table A-1** of Appendix A lists the test set molecules together with the experimental $\Delta_f H°$ values. Also provided are the deviations of the theoretical

enthalpies of formation (either CBS-QB3 or G4) from the experimental values prior to and after BAC are applied. As expected, the use of BAC clearly improves the agreement for this data set as well. For CBS-QB3, the MAD is reduced from 13.6 kJ mol^{-1} to 3.0 kJ mol^{-1} whereas at the G4 level a reduction of the MAD from 5.9 kJ mol^{-1} to 3.4 kJ mol^{-1} is observed.

Table 3-1 BAC values for CBS-QB3 and G4 data.

BACs [kJ mol^{-1}]									
	C-H	**C-C**	**C=C**	**C-O**	**O-H**	**C=O**	**C_b-C_b**	**C_b-H**	**C_b-O**
CBS-QB3[a]	-0.19	-2.07	-3.45	1.58	-1.77	3.11	**0.73**	**-2.51**	**-0.98**
G4	**-0.02**	**-1.09**	**0.00**	**-0.61**	**-1.44**	**0.50**	**2.04**	**-2.64**	**-4.77**

[a]The non-aromatic BAC values for CBS-QB3 are taken from Paraskevas et al. [25].
The boldfaced values are derived in this study.

A closer look at some data of the test set reveals that the experimental enthalpies of formation for *m*- and *p*-hydroxy phenol are not obtained accurately even when BACs are applied, while the $\Delta_f H°$ value for *o*-hydroxy phenol (catechol), which surprisingly is higher than those for the *m*- and *p*- isomers despite the fact that a hydrogen bond can be formed, is well reproduced. As it is not obvious, why the calculations at both levels of theory would fail just for these two molecules, one might question the reliability of the experimental data. Certainly, a validation of these measurements would be helpful.

Another observation to be noted is that the bond additive correction values for G4 are very high for all three bonds that involve an aromatic carbon and that the C_b-C_b and C_b-H BACs have similar magnitudes but opposite signs. Such large corrections appear to be in contrast to the good performance of G4 prior to the use of BAC. The C_b-H and C_b-C_b values are strongly correlated because for the current data set, every C_b-H bond requires the presence of a C_b-C_b, and at the same time, a large fraction of C_b atoms exist as C_b-(H) groups. The large BAC value found for G4 to correct errors in C_b-O bonds is expected to have a high uncertainty, because

only a very limited number of enthalpies of formation were available to obtain this parameter and some stated inaccuracies are rather high (e.g. anisole, as discussed before).

As discussed in earlier sections, some CBS-QB3 calculated bond dissociation energies deviate from established experimental values, while the corresponding G4 results agree well with the measurements. Given that rather high BAC values for the G4 method were found, it is important to verify that the bond dissociation energies still agree with experiment. For the C-H bond in benzene, the C-O bond in phenol and the Aryl-CHO bond in benzaldehyde, the $G4^{BAC}$ bond dissociation enthalpies are 474.7 kJ mol^{-1} (vs. 472.2 kJ mol^{-1}), 469.9 kJ mol^{-1} (vs. 465.7 kJ mol^{-1}) and 415.3 kJ mol^{-1} (vs. 415.5 kJ mol^{-1}), respectively. BAC-corrected CBS-QB3 values (485.4, 481.7 and 428.1 kJ mol^{-1}) still differ considerably more from the experimental values.

The similarly good performances of the CBS-QB3/BAC and G4/BAC calculation methods with respect to the enthalpies of formation of closed-shell aromatic molecules in the training and test sets (see Appendix A **Table A-1**) indicate that the poor bond dissociation enthalpy data obtained with CBS-QB3 are related to a problem with the enthalpy of formation for the phenyl radical.

3.3.4 Standard Intrinsic Entropies

The entropy for a molecule calculated via statistical methods does not take symmetry or contributions from steric centers into account. Therefore, the initial entropies need to be corrected for such contributions if the total entropy of a molecule is needed. Conversely, GAV and NNI parameters in Benson's GA method [14] are "symmetry-free", because they relate to moieties of a molecule and not to the entire molecule. Since the goal of the current study is to

determine such GAVs and NNIs, the symmetry-independent "intrinsic" entropies S_{int}° are used:

$$S_{int}^{\circ} = S^{\circ} + R\, ln\, (\frac{\sigma}{n_{opt}}) \tag{3-5}$$

where σ is the global symmetry number and n_{opt} is the number of optical isomers. The global symmetry number σ is the product of external symmetry number σ_{ext} and the internal symmetry numbers σ_{int}

$$\sigma = \sigma_{ext} \prod_{k} \sigma_{int,k} \tag{3-6}$$

3.3.5 Derivation of GAV & NNI values

The GAV and the NNI values are determined by optimizing the agreement between group additively calculated data and a large set of thermodynamic values for molecules that contain these groups. The latter data is obtained via electronic structure calculations according to the methodology discussed in the previous paragraphs. The following overall strategy has been followed:

(1) BAC corrected CBS-QB3 and G4 results are shown to compare equally well to experimental data. In anticipation of follow-up studies on radicals, the G4 method was chosen as reference for GAV development.

(2) Preliminary GAVs are assigned using results for benzene and the six monosubstituted benzenes. The initial assignment of GAVs is needed to aid the identification of NNIs in the following step.

(3) Application of the preliminary GAVs to all 63 double substituted benzenes reveals the need of NNIs and allows identification of those.

(4) The GAVs and NNIs are simultaneously optimized using the full set of training molecules (133).

(5) A test set consisting of 10 smaller MAH and 15 large MAHs is assembled to validate the transferability of the GAV/NNI data.

(6) Finally, the 10 G4 calculated entries of the test set are added to the training set and a final optimization yields the best set of GAV/NNIs.

Only the final GAV and NNI parameters are reported in the manuscript whereas preliminary and intermediate values of GAVs and NNIs are documented in the Appendix A.

Parameter optimization relied on the unweighted least-squares procedure. In this linear regression analysis, the following objective function is minimized:

$$SSQ = \sum_{i}^{n} (y_i - \hat{y}_i)^2 \tag{3-7}$$

In Eq. (3-7), y_i is the *ab initio* calculated enthalpy of formation ($\Delta_f H°$), entropy ($S°$) or heat capacity (C_p(T)) of the molecule *i* and $\hat{y}_i$ is the calculated thermochemical value via GA. This results in the equation

$$\overline{GAV/NNI} = (X^T X)^{-1} X^T \bar{y} \tag{3-8}$$

In Eq. (3-8), $\overline{GAV/NNI}$ is the calculated vector of the GAVs and NNIs parameters and X is the occurrence matrix where in each row, there is a molecule and in each column, there is either a GAV or NNI. The elements of this matrix X_{ij} specify the number of occurrences of group *j* in molecule *i*. Here, $\bar{y}$ is the vector which contains the *ab initio* thermodynamic property of

interest. If a group always appears in connection with another group, they are linearly dependent and the values of both groups cannot be determined independently. To eliminate such linear dependencies, several GAV values have to be assigned arbitrarily. In this study, this assignment is based on structurally similar groups, as will be discussed later in more detail.

Seven GAVs found in the molecules of the database have already been defined in an earlier study by Marin and coworkers [22,23,25]. These values were adopted and not subjected to the optimization procedure.

A statistical analysis is performed to assess the reliability of the linear regression step and the quality of the optimization procedure. The quality of the fits is expressed in terms of the significance (F) of the regression, the MAD, root-mean square (RMS) deviation, and maximum deviation (MAX) between *ab initio* data and data obtained via GA. The reported significance F of the regression is calculated with the following equation

$$F = \frac{\sum_{i=1}^{n} \frac{\hat{y}^2}{p}}{\sum_{i=1}^{n} \frac{(\hat{y}_i - y_i)^2}{n-p}} \tag{3-9}$$

n is the number of molecules and p is the total number of GAV and NNIs.

The NBO method of Weinhold and coworkers has been employed to interpret the underlying physical origin of the NNIs [46]. The NBO analysis 6.0 program [47] transforms the many electron molecular wavefunction obtained from the Gaussian calculation into localized orbitals that are termed as “Natural Atomic Orbitals (NAOs)”. The program delivers populations of core, valence and higher energy Rydberg orbitals of every single atom as a part of Natural Population Analysis. Optimized linear combinations of NAOs form natural hybrid orbitals (NHOs). Combination of NHOs leads to bonding and antibonding NBOs, which are localized

orbitals that describe the Lewis-like molecular bonding pattern of electron pairs. From the idealized Lewis picture point of view, all filled NBOs are expected to have an occupancy of 2 and any departure from this idealized localized picture is interpreted as the presence of delocalization. The NBO calculations are carried out with results from single point energy calculation at the CCSD(T)/6-31G(d') level at the B3LYP//CBSB7 optimized geometry.

3.4 Results and Discussion

CBS-QB3/BAC and G4/BAC calculations have been performed to construct databases of accurate gas phase standard enthalpies of formation ($\Delta_f H°$), entropies ($S°$) and heat capacities ($C_p(T)$, with T = 300 K, 400 K, 500 K, 600 K, 800 K, 1000 K and 1500 K) for 133 MAHs. The sets include benzene, six single substituted benzenes, all possible 63 double substituted benzenes and 63 triple substituted benzenes.

A comparison of the BAC-corrected standard enthalpies of formation obtained at both levels of theory reveals that both datasets agree well with each other. The MAD is 1.19 kJ mol^{-1} and only a few molecules out of 133 $\Delta_f H^\circ$ values deviate more than 4 kJ mol^{-1}. MAD for intrinsic entropies (S°_{int}) is 0.63 J mol^{-1} K^{-1} and that for the heat capacities (C_p) at 300 K is 0.4 J mol^{-1} K^{-1}. Histograms showing the distribution of these deviations are presented in **Figure A-2** and **Figure A-3** of Appendix A for standard enthalpies of formation and entropies, respectively. Based on the good agreement, either database is suitable to determine the GA parameters (GAV, NNI) for the MAHs of interest. Since the G4 method is more reliable for radicals from MAHs than CBS-QB3, the G4 database will be utilized as reference thermochemical database in this study.

3.4.1 Assignment of initial GAVs

In total 14 GAVs are required for the GA calculation of the thermodynamic properties of the 133 MAHs of the reference dataset. Among these, there are 3, namely C-(O)(H)$_3$, C-(C)(H)$_3$ and C$_d$-(H)$_2$, that describe nonaromatic moieties. These are taken from earlier studies [22,23,25] to ensure internal consistency with previous work. Due to linear dependencies, four additional GAVs cannot be determined independently from the remaining GAVs: O-(C$_b$)(H), CO-(C$_b$)(H), C$_d$-(C$_b$)(H) and C-(C$_b$)(H)$_3$. The O-(C$_b$)(H) always appears together with a C$_b$-(O) group, a CO-(C$_b$)(H) group can only exist if also a C$_b$-(CO) group is present, the C$_d$-(C$_b$)(H) is always accompanied by a C$_b$-(C$_d$) group and the C-(C$_b$)(H)$_3$ requires the presence of the C$_b$-(C) group. The values for these four GAVs are set equal to the structurally similar GAVs O-(C$_d$)(H), CO-(C$_d$)(H), C$_d$-(C$_d$)(H) and C-(C$_d$)(H)$_3$, respectively, as determined in the earlier studies by Sabbe et al. [22] and Paraskevas et al. [25]. All predefined GAVs are listed in **Table 3-2**. Once the linear dependencies in the occurrence matrix X are eliminated, the thermodynamic data of benzene and the six monosubstituted benzenes are used to provide initial assignments of the remaining independent GAVs. **Table A-4** in Appendix A lists these initial GAVs for standard enthalpies of formation ($\Delta_f H°$), entropies ($S°$) and heat capacities (C_p).

Table 3-2 GAVs taken from earlier studies by Marin and coworkers [22,23,25].

Fixed GAVs	GAV taken from	$\Delta_f H^\circ$ [kJ mol^{-1}]	S° [J mol^{-1} K^{-1}]	C_p [J mol^{-1} K^{-1}]						
				300 K	400 K	500 K	600 K	800 K	1000 K	1500 K
O-(C$_b$)(H)	O-(C$_d$)(H)[25]	-188.1	106.3	24.6	30.3	32.5	33.2	33.3	33.6	35.0
CO-(C$_b$)(H)	CO-(C$_d$)(H)[25]	-128.3	129.3	27.3	34.0	39.4	43.7	50.2	54.2	60.8
C$_d$-(C$_b$)(H)	C$_b$-(C$_d$)(H)[22,23]	30.4	25.7	18.1	24.1	29.1	32.7	37.1	40.0	43.1
C-(C$_b$)(H)$_3$	C-(C$_d$)(H)$_3$[22,23]	-42.9	127.2	25.0	31.8	38.2	43.9	53.2	60.5	72.3
C-(O)(H)$_3$	Ref.[25]	-42.9	127.1	25.3	32.1	38.4	44.1	53.4	60.6	72.5
C$_d$-(H)$_2$	Ref.[22,23]	25.1	115.8	20.6	25.8	30.8	34.9	41.4	46.4	54.6
C-(C)(H)$_3$	Ref.[22,23]	-42.9	127.1	25.3	32.1	38.4	44.1	53.4	60.6	72.5

The preliminary GAVs have been used to obtain the standard enthalpies of formation ($\Delta_f H^\circ$) and entropies (S°) of all 63 double substituted benzenes in the reference database. **Table A-5** in Appendix A lists those double substituted MAHs for which significant deviations between the reference data and the GAV-estimates can be found. Some deviations exceed 20 kJ mol^{-1} for the standard enthalpy of formation ($\Delta_f H^\circ$) and a large entropy difference of 23.1 J mol^{-1} K^{-1} is seen in one case. This clearly shows that NNI need to be accounted for to obtain reliable data from GA calculations. It is noticed that the largest deviations are found for substituents in *ortho* position, but several *para* substituted MAHs also display large deviations between the reference and group additively obtained data using the preliminary GAVs only. The observed differences in Appendix A **Table A-5** are used in the next section to identify suitable NNIs and to explain the physical origin of these interactions.

3.4.2 Identification of NNIs

Since the database of molecules includes all possible 63 double substituted MAHs that can be obtained with hydroxy (-OH), methoxy (-OCH_3), formyl (-CHO), vinyl (-$CH{=}CH_2$), methyl (-CH_3) and ethyl (-CH_2CH_3) groups, all the possible binary interactions between these substituents are captured. The differences between *ab initio* and group additively obtained data for double substituted MAHs (see Appendix A **Table A-5**) have been used to identify the most important non-nearest neighboring interactions (NNIs). In **Table 3-3**, these NNIs are listed together with (a) the molecules in which they occur, and (b) the possible origin of these interactions. Initial NNI values for $\Delta_f H°, S^\circ$ and C_p(300 K) are given in **Table A-6** of Appendix A.

Table 3-3 NNIs that are identified from the differences given in **Table A-5** in the Appendix A.

NNIs	Interacting Substituents	Molecules used in Identifying NNIs	Contributions to NNI
NNI1	*o*-OH+ CHO	29	HB[a], Mesomeric, Inductive
NNI2	*o*-CHO+ CHO	14	HB, Mesomeric, Inductive
NNI3	*o*-MeO+MeO	11	Anomeric, Mesomeric, Inductive
NNI4	*o*-CH=CH_2+ CHO	53	Steric, Inductive
NNI5	*o*-CH=CH_2+ CH=CH_2	17	Steric, Inductive
NNI6	*p*-OH/MeO+ OH/MeO	10,13,28	Mesomeric, Inductive
NNI7	*p*-CHO+ CHO	16	Mesomeric, Inductive
NNI8	*o*-Me/Et+ CHO	56,59	Steric, Mesomeric, Inductive
NNI9	*o*-CH=CH_2+ Me/Et	62,65	Steric
NNI10	*m*-CHO+ CHO	15	Inductive
NNI11	*p*-CHO+ OH/MeO	31,43	Mesomeric, Inductive
NNI12	*o*-MeO+ CHO	41	HB, Mesomeric, Inductive
NNI13	*o*-Me/Et+ Me/Et	20,23,68	Steric
NNI14	*o*-OH+ OH/MeO	8,26	HB, Mesomeric, Inductive
NNI15	*o*-CH=CH_2+ OH/MeO	32,44	Steric, Inductive

The full list of molecules and their molecule numbers are given in **Figure A-1** of Appendix A.
[a]HB: Hydrogen Bond

The general types of interactions between substituents of benzene are well established. The interactions given in **Table A-6** of Appendix A include hydrogen bonds (HBs), mesomeric, inductive, steric and anomeric effects. Some of these interactions may occur alone, others occur always in combinations. The use of NBO analysis, which reveals information about charge transfers between different NBOs, is useful to develop an understanding of the intramolecular interactions.

Among the 15 NNIs identified, 4 NNIs contain significant contributions from HB to the overall intramolecular interaction. They are listed in **Table A-7** of Appendix A together with the stabilization energies ($E(2)_{HB}$) due to charge transfer between the donor lone pair NBO of an

oxygen atom and the acceptor O-H or C-H Bond NBOs calculated by Second-Order Perturbation Theory Analysis as described in **Ref.** [46]. **Table A-7** of Appendix A demonstrates that stronger HBs correlate with shorter HB distances and also shows that hydrogen bond formation appears to be the major contributor to **NNI1**, while it plays a minor role in the overall destabilizing **NNI2** and **NNI12**.

Mesomeric effects are investigated via the charge distributions obtained from the NBO analysis. The natural charges on five arene carbons of benzene and the *ortho*, *meta* and *para* positions in single substituted MAHs are given in **Table A-8** of Appendix A. Also provided is the sum of these charges, which can be considered as a qualitative measure of the amount of charge transfer via resonance. Note, that the ring carbon which is substituted, is not included, because its charge results not only from resonance but also from inductive charge transfer. In benzene, the natural charge is equally distributed among all six carbons and the negative value of -0.235, which is counterbalanced by the positive charges on the hydrogens, indicates that aryl carbon atoms are more electronegative than hydrogen. An alkyl substituent ($-CH_3$/$-CH_2CH_3$) does not significantly alter the natural charge distribution or the total charge. The slight increase of the natural charges on the *ortho* and *para* carbon atoms indicates a very weak electron donating effect. In styrene (C_6H_5-$CH{=}CH_2$), the total charge of the five unsubstituted carbon atoms is only slightly lower than in benzene indicating a small electron withdrawing effect of the $-CH{=}CH_2$ group. Hydroxy (-OH) and methoxy ($-OCH_3$) substituents increase the electron density on the ring carbons in *ortho* and *para* position. At the same time, the electron density on the ring carbons in *meta* position is reduced. The total charge is increased, which is consistent with the +M effect assigned to these substituents. In benzaldehyde (C_6H_5-CHO), a reverse trend is noticeable: the presence of the formyl (-CHO)

group withdraws electrons from the ring carbons in *ortho* and *para* position, while a small charge increase is observed in the *meta* position. The total charge of the five unsubstituted carbon atoms is lower than in benzene due to the dominant -M effect.

The above discussion is qualitatively supported by results from second-order perturbation theory analysis. A strong mesomeric charge transfer (+M effect) from the lone pair NBO on oxygen atom (donor) to the closest π-bond NBO on the arene ring (acceptor) is found in anisole and phenol. The mesomeric effect in benzaldehyde is in the opposite direction (-M): charge is transferred from one of the π-bond NBOs on the arene ring to the π-bond NBO of the double bond of the -CHO group. In styrene, charge transfer is observed in two directions: from arene ring to the vinyl (-CH=CH_2) group and from the vinyl group to the arene ring. Both transfers effectively cancel out.

In double substituted MAHs, the total mesomeric effect is not simply the sum of the contributions of the individual substituents, but the mesomeric effect of one substituent impacts that of the second and vice versa. For example, the mesomeric interaction is stabilizing if a substituent with a +M effect is in *o*- or *p*- position relative to a substituent that has a -M effect. In this case, the -M substituent withdraws electrons from the same carbon atoms that gain electron density from the +M substituent. Double substituted MAHs with substituents that produce the same type of mesomeric effect (+M or -M) are destabilized if these substituents are in *o*- or *p*- position to each other. **Table A-9** of Appendix A presents all NNIs, which contain significant contributions from mesomeric effects.

Eleven out of 15 NNIs are needed to correct for substituent interactions in *ortho* position. This indicates the important role of steric or short distance interactions on the thermodynamic

properties. Three NNIs describe interactions of substituents in *p*- position and one in *meta* position. In all four cases, mesomeric effects dominate.

NNI1 accounts for the interaction of a OH group with a CHO group located in *o*- position. The main contribution arises from a very strong hydrogen bond between these groups. The stabilization energy is obtained by second-order perturbation theory analysis to be -23.5 kJ mol^{-1} (see **Table A-7** of Appendix A) and the short distance of 175 pm (1.75 *Å*) supports this high value. The +M character of CHO and the -M effect of the OH lead to additional stabilization. The presence of these two stabilizing interactions explain the high preliminary value of -28.7 kJ mol^{-1} (see **Table A-6** of Appendix A). The strong hydrogen bond between the OH and the CHO groups restricts the movement of both groups, which is reflected in a reduction of the entropy.

The strong electron withdrawing -M and -I effect of formyl groups are the reason why two formyl groups in *ortho* position destabilize the molecule. A weak hydrogen bond (calculated stabilization of -6.4 kJ mol^{-1}) only partially compensates the destabilizing resonance interaction. Therefore, **NNI2** leads to a large positive enthalpy correction.

NNI3 describes the repulsion between the lone pairs on the oxygen atoms of two OCH_3 groups in *o*- position relative to each other, for example, anomeric effect. The generalized anomeric effect refers to the conformational preference of a gauche structure over an antistructure for molecules with a C-X-C-Y moiety where X and Y are heteroatoms having nonbonding electron pairs (oxygen in this case) [48]. Further destabilization results from the combination of +M and -I effects of both groups, hence **NNI3** significantly increases the enthalpy of formation. In triple substituted benzenes, **NNI3** should be used to account for the anomeric effect in the cases

where a OH group and a OCH_3 are relative to each other in *o*- position and they do not form a hydrogen bond, i.e. lone pairs of the oxygen atoms on OH and OCH_3 groups repel each other.

A $-CH=CH_2$ group in *ortho* position to any other group leads to destabilization. Steric repulsion moves the $-CH=CH_2$ group out of plane and hence reduces the resonance between the aromatic ring and the vinyl group. In **NNI4** and **NNI5**, the neighboring groups are -CHO and $-CH=CH_2$, which both withdraw electrons from the ring via induction and resonance. This leads to additional destabilization.

NNI6 describes the interaction between an OH group with an OCH_3 group in *para* position. Both groups supply via resonance electron density the arene ring, which leads to destabilization as discussed earlier. The electron withdrawing -I effect reduces this destabilization but the mesomeric effects dominates and the overall result is destabilization.

NNI7 is the interaction of two CHO groups in *para* position. The combination of strong mesomeric and inductive effects leads to a notable destabilization.

Steric repulsion is the most crucial interaction in **NNI8** which describes the interaction of an alkyl group in *ortho* position to a formyl group. This leads to a positive $\Delta_f H^\circ$ correction term. As the internal rotation of the alkyl group is hindered, the entropy is reduced.

NNI9 corrects for the interaction between $-CH=CH_2$ and alkyl groups ($-CH_3$ or $-CH_2CH_3$) in *o*- position. Steric interaction is the only significant factor. The $\Delta_f H^\circ$ correction given for this term is smaller than those for other NNIs (**NNI4** and **NNI5**) that describe *ortho* vinyl interactions, because no other destabilizing factors are present.

NNI10 brings a correction term for the case where two CHO substituents are in *meta* position relative to each other. A CHO substituent withdraws electrons from the phenyl ring via

σ-system regardless of the second substituent group or the position of this second group. As both CHO groups withdraw electrons from the system, electron density is decreased in the ring, which leads to a destabilization. If two CHO groups reside at *o*- or *p*- position relative to each other as in **NNI2** and **NNI7** respectively, -M effect exists and combination of two electron withdrawing effects lead to a stronger destabilization. This is the reason why the enthalpy correction value in **NNI7** is larger than in **NNI10**.

In **NNI11**, a CHO group is in *p*- position to either a OH or a OCH_3 group. The combination of +M effect (CHO) with -M effect (OH or OCH_3) in *p*- position strongly stabilizes the molecule.

NNI12 describes the interaction between a CHO and OCH_3 group as in *o*-formylanisole. The combination of the weak hydrogen bond (-3.6 kJ mol^{-1}) and the stabilizing mesomeric effect should lead to an overall stabilization. However, the opposite is found, caused by a steric repulsion of both groups. In the most stable conformation, the OCH_3 group is directed away from the CHO group. The lone pair electrons of the methoxy group interfere with the π electrons of the carbonyl group.

NNI13 corrects for the steric repulsion between two alkyl groups in *o*- position. Restrictions of the internal rotations cause a reduction of the entropy.

NNI14 applies to OH groups that are in *ortho* position to an OH o OR substituent. According to the NBO analysis, the hydrogen bond provides stabilization of -8.9 kJ mol^{-1} (see **Table A-7** in Appendix A). The required correction value for the standard enthalpy of formation of **NNI14** is lower, though (see **Table A-6** of Appendix A). This is reasonable because apart from the hydrogen bond, destabilizing +M and -I interactions also play a role. **NNI14** reduces the entropy (S°), because the hydrogen bond decreases the flexibility.

If styrene is substituted in *o*- position by -OH or -OCH_3, which are +M groups, several effects occur simultaneously. Steric repulsion increases the enthalpy but the +M/-I combination provides stabilization. In total, a small destabilization results.

3.4.3 Simultaneous determination and Validation of GAVs and NNIs

In earlier sections, preliminary values were assigned to the GAVs and these GAVs were used to reproduce the thermochemical data of double substituted benzenes. The deviations between the calculations with these preliminary GAVs and the reference data were used to identify 15 NNIs. Then, physical interpretations of these interactions were provided with the help of NBO calculations. In this section, these GAV and NNI parameters are optimized simultaneously via least squares fitting using the information of the entire training set. These GAVs and NNIs are given in Appendix A **Table A-10** and **Table A-11,** respectively. Performance of the GAV/NNI parameter set is assessed through a statistical analysis. The results of this analysis are reported in Appendix A **Table A-12**. The MAD for the GA calculation of the standard enthalpies of formation of the entire reference data set of 133 molecules is 0.95 kJ mol^{-1}, and those for group additively calculated entropy and heat capacity data at all temperatures are 1.60 J mol^{-1} K^{-1} and < 1.56 J mol^{-1} K^{-1}, respectively. The improvement upon the inclusion of non-nearest neighbor NNIs is significant for all three thermodynamic properties. Introduction of NNIs lower the MAD for $\Delta_f H^\circ$ from 5.70 to 0.95 kJ mol^{-1}, and similar improvement can also be noted in the group additively calculated data for entropies (from 3.9 to 1.6 J mol^{-1} K^{-1}) and heat capacities (from 4.0[1] to 1.6 J mol^{-1} K^{-1}).

To test the transferability of the GAVs and NNIs, thermodynamic properties of a test set consisting of 9 triple substituted, 13 quadruple-substituted and 3 quintuple substituted MAHs are obtained using the GAVs and NNIs reported in **Table A-10** and **Table A-11** of

Appendix A. Due to the higher computational cost for the G4 method, *ab initio* data for 12 quadruple-substituted and 3 quintuple substituted MAHs could only be obtained with the CBS-QB3/BAC method whereas for the other 10 molecules, *ab initio* data is obtained with the G4/BAC method. As it has been shown that CBS-QB3 and G4 perform with similar accuracy for closed shell MAHs, reproducing CBS-QB3 *ab initio* data with GAVs obtained from G4 database is considered as an appropriate practice.

Differences between the *ab initio* and the GA based data are provided in **Table 3-4** and the actual *ab initio* values for $\Delta_f H^\circ$, S° and $C_p{}^\circ$ are collected in **Table A-13** of Appendix A. The statistics of the test set in **Table 3-4** demonstrates the good performance of the GAV/NNI set developed in this study. The MAD values of 1.8 kJ mol^{-1} ($\Delta_f H^\circ$) and 3.0 J mol^{-1} K^{-1} and 2.4 J mol^{-1} K^{-1} for S° and C_p(300 K) respectively, prove that the group values are transferable and that even highly substituted benzenes with strongly interacting substituents are obtained by GA with high accuracy. Since only 2 of the 15 NNIs have been reported in the literature before, data obtained with the GAVs and available NNIs in the literature is insufficient in reproducing thermochemical data for the multiple substituted benzenes. In this manner, the reported set of GAVs/NNIs enables the application of the method of Benson's GA to obtain thermochemical data for multiple substituted benzenes even for the quadruple and quintuple substituted benzenes that possess substituent groups of interest.

Table 3-4 Molecules in the test set, the differences between *ab initio* calculated data[a] and data obtained using the GAV and NNIs for standard enthalpy of formation ($\Delta_f H^\circ$), entropies (S°) at 298 K and heat capacities (C_p) at 300 K given in **Table A-10** and **Table A-11** of Appendix A and the statistics for the test set.

Test Set[a]	$\Delta_f H^\circ$ [kJ mol^{-1}]	S° [J mol^{-1} K^{-1}]	C_p **(300 K)** [J mol^{-1} K^{-1}]
1,3-divinyl-4-formylbenzene	**-0.1**	**0.9**	**0.4**
1,4-divinyl-2-formylbenzene	**-0.3**	**3.1**	**3.0**
1,3-dimethyl-2-hydroxybenzene	**-1.9**	**-3.5**	**-1.7**
1,3-dimethyl-5-hydroxybenzene	**-0.4**	**0.4**	**1.4**
1,4-dimethyl-2-hydroxybenzene	**-0.2**	**-1.4**	**1.8**
1,2-diethyl-3-hydroxybenzene	**-0.6**	**-6.2**	**1.8**
1,3-diethyl-6-hydroxybenzene	**0.5**	**-2.6**	**1.5**
1,4-diethyl-2-hydroxybenzene	**-0.9**	**-1.4**	**1.1**
1-ethyl-2-hydroxy-3-formylbenzene	**-2.4**	**-1.2**	**3.0**
1,3,5-trimethyl-2-hydroxybenzene	**0.7**	**-4.1**	**0.4**
1,2,3,4-Tetramethylbenzene	1.0	0.7	-4.9
1,2,3,4-Tetrahydroxybenzene	-6.5	3.6	-0.3
1,2-dihydroxy-4,5-diformylbenzene	0.7	1.6	5.4
1-methyl-2-hydroxy-3-methoxy-5-vinylbenzene	-1.2	-1.3	-0.7
1-methyl-3,4,5-trivinylbenzene	-3.2	-7.3	-2.1
1-hydroxy-2-vinyl-4,5-diformylbenzene	-1.9	-2.1	-4.8
1-vinyl-2,4-dimethyl-3-ethylbenzene	4.0	1.4	-6.8
1,3-dimethoxy-2-hydroxy-5-methylbenzene	1.8	3.1	-1.4
1,3,4-trihydroxy-2-methoxybenzene	2.0	-1.7	-1.9
1,3-vinyl-2-hydroxy-4-methylbenzene	-1.8	-5.0	-3.4
1-hydroxy-2-formyl-4-methyl-5-vinylbenzene	1.5	0.7	0.5
1,2-dihydroxy-3-methoxy-5-ethylbenzene	-1.1	7.2	-4.0
1,2-dihydroxy-3-methoxy-5,6-dimethylbenzene	-0.5	-3.2	-5.7
1-hydroxy-2,3-diformyl-4-methyl-6-vinylbenzene	-2.0	-7.1	-2.4
1,2,3,4,5-Pentahydroxybenzene	-8.7	4.4	0.1
Statistics for the Test Set			
SD	2.5	3.6	2.9
MAD	1.8	3.0	2.4
MAX	8.7	7.3	6.8

[a]Ten Molecules for which data is collected at G4 are given in boldface.

Table 3-5 GAVs for standard enthalpy of formation ($\Delta_f H^\circ$) and entropy (S°) at 298 K, and heat capacity (C_p) at various temperatures for MAHs derived from reference database, given with 97.5% confidence intervals.

GAVs	$\Delta_f H^\circ$	S°	C_p [J mol^{-1} K^{-1}]						
	[kJ mol^{-1}]	[J mol^{-1} K^{-1}]	300 K	400 K	500 K	600 K	800 K	1000 K	1500 K
C_b-(H)	13.7 ± 0.16	48.6 ± 0.28	13.3 ± 0.26	18.4	22.7	26.2	31.3	34.8	40.1
C_b-(O)	24.0 ± 0.41	-30.0 ± 0.70	12.1 ± 0.66	12.6	15.0	17.4	21.3	23.5	26.0
O-(C_b)(C)	-124.1 ±0.51	21.6 ± 0.88	20.3 ± 0.82	24.2	25.1	24.8	23.7	23.1	22.0
C_b-(CO)	21.5 ± 0.73	-33.5 ± 1.25	16.4 ± 1.16	17.8	19.7	21.6	24.5	26.6	27.4
C_b-(C_d)	24.3 ± 0.54	-35.0 ± 0.92	12.4 ± 0.86	14.8	16.4	18.0	20.9	22.6	25.6
C_b-(C)	23.5 ± 0.40	-33.6 ± 0.68	10.8 ± 0.63	13.8	16.5	18.7	21.9	23.8	26.2
C-(C_b)(C)$(H)_2$	-20.6 ± 0.45	38.6 ± 0.76	24.9 ± 0.71	30.7	36.0	40.4	47.3	52.3	60.0

Table 3-6 Corrections for NNIs derived based on full G4 molecule set for the standard enthalpies of formation ($\Delta_f H^\circ$) and entropies (S°) at 298 K and heat capacities (C_p) at various temperatures for MAHs.[a]

NNI	Interaction[b]	$\Delta_f H^\circ$	S°	C_p [J mol^{-1} K^{-1}]						
		[kJ mol^{-1}]	[J mol^{-1} K^{-1}]	300 K	400 K	500 K	600 K	800 K	1000 K	1500 K
NNI1	*o*-OH + CHO	-27.4 ± 1.52	-21.3 ± 2.60	-10.4 ± 2.43	-9.0	-7.4	-6.0	-3.4	-1.4	1.8
NNI2	*o*-CHO + CHO	21.1 ± 1.37	6.4 ± 2.35	1.7 ± 2.19	1.7	1.6	1.4	0.4	-0.8	-2.5
NNI3	Anomeric Effect	14.7 ± 1.25	7.8 ± 2.14	0.0 ± 2.00	-3.4	-4.7	-5.0	-4.4	-3.7	-2.2
NNI4	*o*-CH=CH_2 + CHO	11.9 ± 1.77	-2.6 ± 3.03	1.3 ± 2.82	1.6	2.1	2.5	2.4	1.8	0.3
NNI5	*o*-CH=CH_2+ CH=CH_2	8.1 ± 1.13	-2.3 ± 1.93	4.6 ± 1.80	3.2	2.1	1.3	0.2	-0.2	-0.5
NNI6	*p*-OH/MeO+ OH/MeO	7.3 ± 1.24	4.0 ± 2.12	1.7 ± 1.98	0.4	-0.8	-1.7	-2.3	-2.3	-1.7
NNI7	*p*-CHO+ CHO	9.9 ± 1.99	-0.8 ± 3.40	1.8 ± 3.17	1.4	1.0	0.7	0.1	-0.3	-0.9
NNI8	*o*-Me/Et+ CHO	8.1 ± 1.48	-2.4 ± 2.53	4.0 ±2.36	3.0	2.0	1.1	0.0	-0.6	-0.9
NNI9	*o*-CH=CH_2+ Me/Et	4.6 ± 1.29	-5.7 ± 2.21	5.7 ± 2.06	5.6	4.9	4.2	2.9	2.1	1.0
NNI10	*m*-CHO+ CHO	4.8 ± 1.13	0.1 ± 1.94	1.7 ± 1.80	1.0	0.5	0.1	-0.4	-0.7	-0.8
NNI11	*p*-CHO+ OH/MeO	-4.6 ± 1.30	-0.8 ± 2.23	-1.6 ± 2.08	-1.0	-0.3	0.2	0.9	1.2	1.5
NNI12	*o*-MeO+ CHO	7.9 ± 1.73	-1.7 ± 2.95	-2.6 ± 2.75	0.3	2.6	3.9	4.1	3.3	1.3
NNI13	*o*-Me/Et+ Me/Et	4.2 ± 0.86	-6.6 ± 1.47	3.3 ± 1.37	2.9	2.6	2.5	2.3	2.0	1.5
NNI14	*o*-OH+ OH/MeO	-3.0 ± 0.78	-5.6 ± 1.34	-2.7 ± 1.25	-1.5	0.2	2.0	4.2	4.8	3.7
NNI15	*o*-CH=CH_2+ OH/MeO	2.6 ± 1.20	-3.3 ± 2.04	2.5 ± 1.91	2.7	2.6	2.5	2.1	1.8	1.2

[a] 97.5 % confidence intervals for $\Delta_f H^\circ$ (298 K), S° (298 K) and C_p (300 K) are provided.

[b] Substituent groups are given as OH: hydroxy (-OH), MeO: methoxy (-OCH_3), Formyl: -CHO, Vinyl: -CH=CH_2, Me: methyl (-CH_3), Et: ethyl (-CH_2CH_3).

As a final step, the aforementioned 10 molecules in the test set for which *ab initio* data are collected at the G4 level is added into the training set of 133 molecules. Then, GAV and NNI parameters are optimized through a final linear regression analysis based on this reference

dataset of 143 molecules. The final GAV and NNI parameters together with their 97.5% confidence intervals are reported in **Table 3-5** (GAVs) and **Table 3-6** (NNIs). Only the confidence intervals for heat capacities (C_p) at 300 K are provided – those for the other C_p data have similar or lower values.

GAVs for singly substituted MAHs have been derived before by Benson et al. [15], Cohen [17], Holmes and Aubry [19], and Sabbe et al. [22]. The present GAVs for enthalpy of formation are compared in **Table 3-7** to those previously derived values. At a first glance, it seems that there are large deviations between the current data and those reported by Benson, Cohen and Holmes e. g. for the O-(C_b)(C) group. However, this can be explained by the fact that Benson and Cohen use a different way to eliminate linear dependencies than Holmes, Sabbe and this study. This illustrates the importance to use only internally consistent GAVs to obtain thermodynamic properties. This also shows that direct comparison of GAVs is not feasible. To allow a fair comparison, **Table 3-7** also list the sum of GAV values for pairs of linear dependent groups. From **Table 3-7**, it can be seen that the sum of linear dependent GAVs C_b-(O) and O-(C_b)(H) obtained by Cohen, Holmes and the GAVs reported in this study agree well. In earlier sections, it has been mentioned that the experimental heat of formation for anisole (methoxybenzene) is not well established. This uncertainty is reflected in the sum of the linear GAVs C_b-(O) and O-(C_b)(C). The value reported by Cohen for this pair is significantly higher than the other data, because his GAV was derived from the highest experimental enthalpy of formation for anisole (Fenwick et al. [44]). The assignments by Benson and Cohen and this study for GAV of the linear dependent pair C_b-(CO)+CO-(C_b)(H) match very well, whereas the value reported by Holmes is slightly lower. Good agreement is also noted for the pairs of linear dependent GAVs that include the C_b-(C) group. Overall, the

final GAV assignments derived in this work are very consistent with previous studies despite the fact that a significantly larger data set was used and that the GAVs were derived via full optimization together with the NNIs. This means that the selection of NNIs did not cause any notable interference with the GAVs.

Table 3-7 GAVs and pairs of linearly dependent GAVs for the standard enthalpies of formation ($\Delta_f H^\circ$) reported in the literature and obtained in this work.

GAVs	Literature				This Work
	Benson [15]	Cohen [18]	Holmes [19]	Sabbe/Paraskevas [22,35]	
$\Delta_f H^\circ$ [kJ mol^{-1}]					
C_b-(H)	13.8	13.8	13.8	13.8	13.7
C_b-(O)	-3.8	-3.8	25.0	-	24.0
O-(C_b)(C)	-96.2	-90.4	-124.0	-	-124.1
C_b-(CO)	15.5	15.5	18.0	-	21.5
C_b-(C_d)	23.8	24.3	27.0	24.0	24.3
C_b-(C)	23.1	23.0	23.0	24.4	23.5
C-(C_b)(C)$(H)_2$	-20.3	-19.2	-20.0	-21.2	-20.6
O-(C_b)(H)	-158.6	-161.1	-190.0	-	-188.1[a]
C-(O)$(H)_3$	-42.2	-42.9	-42.0	-42.9	-42.9[b]
CO-(C_b)(H)	-121.8	-122	-122.0	-	-128.3[a]
C_d-(C_b)(H)	28.4	26.5	28.0	30.4	30.4[b]
C_d-$(H)_2$	26.2	26.4	26.2	25.1	25.1[b]
C-(C_b)$(H)_3$	-42.7	-42.0	-42.0	-42.9	-42.9[b]
C-(C)$(H)_3$	-42.7	-42.0	-42.0	-42.9	-42.9[b]
Pairs of Linear Dependent GAVs					
C_b-(O) + O-(C_b)(H)	-162.4	-164.9	-165.0	-	-164.1
C_b-(O) + O-(C_b)(C)	-100.0	-94.2	-99.0	-	-100.1
C_b-(CO) + CO-(C_b)(H)	-106.3	-106.5	-104.0	-	-106.8
C_b-(C_d) + C_d-(C_b)(H)	52.1	50.8	55.0	54.4	54.7
C_b-(C) + C-(C_b)$(H)_3$	-19.6	-19.0	-19.0	-19.9	-19.4
C_b-(C) + C-(C_b)(C)$(H)_2$	2.8	3.8	3.0	1.8	2.9

[a]Values of these GAVs are set equal to the values of structurally GAVs reported in the previous studies of Sabbe and coworkers [22,25] in order to eliminate linear dependencies.
[b]Values of these GAVs are taken from the previous studies of Sabbe and coworkers [22,25] in order to eliminate linear dependencies.

Holmes and Aubry [19] investigated cis and trans 1-hydroxypropenal at the CBS-QB3 level of theory and explained the observed stability difference with intramolecular interactions that are

very similar to **NNI1**. The authors report a CBS-QB3 $\Delta_f H^\circ$ value of -241 kJ mol^{-1} for the trans isomer and a value of -276 kJ mol^{-1} for the cis isomer of 1-hydroxypropenal. They mention the fact that GA data for $\Delta_f H^\circ$ of the trans isomer agrees well (-246 ± 4 kJ mol^{-1}) with the reported CBS-QB3 data, but to obtain the enthalpy of formation of the more stable cis isomer accurately, an additional correction of -30 kJ mol^{-1} is needed. This value is in good agreement with the **NNI1** derived in this work. To correct for the interaction between two -OCH_3 groups, Cohen has suggested a $\Delta_f H^\circ$ correction of 12.6 kJ mol^{-1} which is comparable to **NNI3** (14.7 kJ mol^{-1}) reported in the present study. The derived $\Delta_f H^\circ$ correction for **NNI6** is found to be 4.1 kJ mol^{-1} for the interaction of two alkyl groups in *o*- position to each other which is expected to be a similar interaction to the steric repulsion between two alkyl groups in cis alkenes. In the work of Sabbe et al. [22], a NNI of 5.9 kJ mol^{-1} is assigned for the latter interaction, while a value of 4.6 kJ mol^{-1} was obtained by Cohen [18], and Benson [16] reports 4.2 kJ mol^{-1}.In this study, the **NNI6** correction term for S° is derived as -6.2 J mol^{-1} K^{-1} which is close to the "*ortho*" corrections derived earlier: -5.7 J mol^{-1} K^{-1} by Sabbe et al. [24], -6.7 J mol^{-1} K^{-1} by Benson [15] and Cohen [18]. All these comparisons demonstrate that the derived NNIs are plausible.

A statistical analysis is performed in order to assess the performance of the final GA parameters. The results are reported in **Table 3-8**. The MAD between the GA and *ab initio* calculated data of the standard enthalpies of formation of the entire reference data set of 143 molecules is 0.93 kJ mol^{-1}, and those for the entropy and heat capacity data at all temperatures are 1.66 J mol^{-1} K^{-1} and < 1.56 J mol^{-1} K^{-1}, respectively. Next-nearest neighbor interactions (NNIs) are found to be crucial as the drastic decrease of the MAD values shows. For example, the MAD for $\Delta_f H^\circ$ decreases from 5.70 kJ mol^{-1} to 0.95 kJ mol^{-1} after NNI corrections are introduced.

Table 3-8 statistics for the linear regression analysis of the GAVs and NNIs for the standard enthalpies of formation ($\Delta_f H^\circ$) and entropies (S°) at 298 K and heat capacities (C_p) at various temperatures for MAHs.[a]

	$\Delta_f H^\circ$	S°	C_p [J mol^{-1} K^{-1}]						
	[kJ mol^{-1}]	[J mol^{-1} K^{-1}]	300 K	400 K	500 K	600 K	800 K	1000 K	1500 K
F	33916	19264	13165	29262	53571	79914	122625	160869	345956
MAD	0.93	1.66	1.56	1.32	1.15	1.06	0.97	0.93	0.72
RMS	1.24	2.12	1.97	1.68	1.48	1.37	1.30	1.25	0.96
MAX	4.42	7.03	5.65	4.54	4.65	4.48	4.00	4.05	3.73

[a]**F:** Significance; **MAD:** mean average deviation; **RMS:** root mean square; **MAX:** maximum deviation.

All individual deviations between *ab initio* and group additively calculated thermodynamic data are provided in **Table A-14** of Appendix A. The distribution of the difference between the reference and the GA calculated enthalpies of formation is shown in **Figure A-4** of Appendix A. Almost all of the 143 enthalpies of formation obtained by GA are within 4 kJ mol^{-1}. Marginally higher deviations are seen for just two molecules: 4.1 kJ mol^{-1} for 1-hydroxy-2-methoxy-4-formylbenzene (**molecule 99**) and 4.4 kJ mol^{-1} for 1-formyl-3-methoxy-4-ethylbenzene (**molecule 124**). In **Figure A-5** and **Figure A-6** of Appendix A, similar histograms are presented for the difference distributions of the entropies (S°) and heat capacities ($C_p{}^\circ$) at 300 K. Again, the agreement is very good and most data differ by less than 4 J mol^{-1} K^{-1}.

3.4.4 Application of GAVs and NNIs

To demonstrate the use of the GAVs (see **Table 3-4**) and the NNIs (see **Table 3-5**) reported are in this study, an example calculation is done to obtain $\Delta_f H^\circ$ and S° of 1,2-dihydroxy-3-methoxy-5,6-dimethylbenzene. The structure of this molecule is given in **Figure 3-1.**

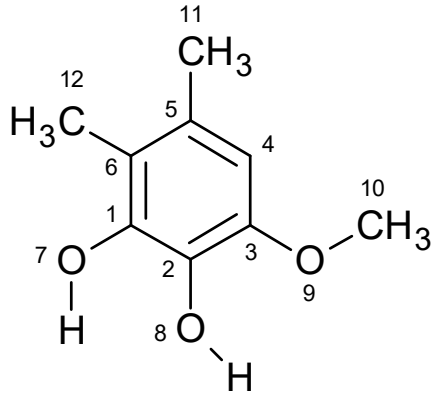

Figure 3-1 Structure of 1,2-dihydroxy-3-methoxy-5,6-dimethylbenzene given with numbers of the atom centers of the groups.

The 12 GAVs and 3 NNIs required for the GA calculation of standard enthalpy of formation ($\Delta_f H^\circ$) and entropy (S°) of this quintuple substituted MAH are shown in **Table 3-9**. **NNI 13** is used to correct for the interaction between two methyl groups in *o*- position to each other; **NNI14** is used twice to take two other *o*- interactions into account: the interaction between two OH groups and the interaction a OH and a OCH_3 group. No NNIs have been defined for other less significant interactions in this molecule which are also indicated in **Table 3-9**. The difference between CBS-QB3 values and GA calculated data for $\Delta_f H^\circ$ and S° are -0.4 and -2.7 J mol^{-1} K^{-1} which shows that the neglected interactions do not lead to a significant loss of accuracy in the group additively calculated data and the present GAVs/NNIs are successful in describing thermochemical data for this quintuple substituted benzene.

Table 3-9 Application of GAVs/NNIs for the calculation of standard enthalpy of formation ($\Delta_f H^\circ$) and entropy (S°) of 1,2-dihydroxy-3-methoxy-5,6-dimethylbenzene (see **Figure 3-1**). Intrinsic entropy calculation ($S_{int}{}^\circ$) and comparison of the CBS-QB3 results with GA calculated values are also provided.

Application of Group Additive Method							
GAVs				**NNIs**			
Center #	**GAVs**	$\Delta_f H^\circ$ **[kJ mol^{-1}]**	S° **[J mol^{-1} K^{-1}]**	**NNI**	**Interaction**	$\Delta_f H^\circ$ **[kJ mol^{-1}]**	S° **[J mol^{-1} K^{-1}]**
1	C_b-(O)	24.0	-30.0	**Interactions of Substituent OH (Atom 7)**			
2	C_b-(O)	24.0	-30.0	NNI14	*o*-OH+OH	-3.0	-5.6
3	C_b-(O)	24.0	-30.0	-	*m*-OH+OCH_3	0	0
4	C_b-(H)	13.7	48.6	-	*o*-OH+Me	0	0
5	C_b-(C)	23.5	-33.6	-	*m*-OH+Me	0	0
6	C_b-(C)	23.5	-33.6	**Interactions of Substituent OH (Atom 8)**			
7	O-(C_b)(H)	-188.1	106.3	NNI14	*o*-OH+OCH_3	-3.0	-5.6
8	O-(C_b)(H)	-188.1	106.3	**Interactions of Substituent OCH_3 (Atoms 9 and 10)**			
9	O-(C_b)(C)	-124.1	21.6	-	*m*- OCH_3+Me	0	0
10	C-(O)$(H)_3$	-42.9	127.1	-	*p*- OCH_3+Me	0	0
11	C-(C_b)$(H)_3$	-42.9	127.2	**Interactions of Substituent Me (Atom 11)**			
12	C-(C_b)$(H)_3$	-42.9	127.2	NNI13	*o*-Me+Me	+4.2	-6.6
$\sum GAVs$		-496.3	507.2	$\sum NNIs$		-1.8	-17.8
$\sum GAVs + NNIs$		-506.5	489.4				
Standard Intrinsic Entropy Calculation				**Comparison of CBS-QB3 vs. GAVs/NNIs**			
σ_{int}	3*3*3=27 (Atoms 10, 11, 12)	σ/n_{opt}	27			$\Delta_f H^\circ$ **[kJ mol^{-1}]**	S° **[J mol^{-1} K^{-1}]**
σ_{ext}	1	S°(CBS-QB3)	478.9 [J mol^{-1} K^{-1}]	CBS-QB3		-498.5	486.7
σ	27	$S_{int}{}^\circ$(CBS-QB3)	486.7 [J mol^{-1} K^{-1}]	$\sum GAVs + NNIs$		-498.1	489.4
n_{opt}	1			$(CBS-QB3) - \sum GAVs + NNIs$		-0.4	-2.7

3.5 Conclusions

A set of seven GAV and 15 NNI has been derived to obtain the thermodynamic properties of MAHs with six substituents: hydroxy (-OH), methoxy (-OCH_3), formyl (-CHO), vinyl (-CH=CH_2) and the alkyl groups methyl (-CH_3) and ethyl (-CH_2CH_3). The GAV and NNI parameters were determined from a set of 143 molecules (reference data), whose

thermodynamic values were calculated with bond additivity corrected (BAC) G4 theory. The BAC values were obtained as part of this study from a set of 77 molecules, for which accurate experimental data exist. Parallel computations with the CBS-QB3 method yielded similar results, which indicates that the CBS-QB3 method is reliable for closed-shell molecules and observed problems with bond dissociation energies are caused by problems to describe the phenyl radical accurately.

NNIs were found to be crucial to achieve accurate GA calculations. NBO calculations were employed to ensure that the defined NNIs are meaningful and to provide insight into the type of interactions that cause either stabilization or destabilization. Values obtained with the optimized GAV and NNI parameters agree very well with the reference data set. The MAD are 0.93 kJ mol^{-1} for $\Delta_f H^\circ$, 1.66 J mol^{-1} K^{-1} for $S^\circ$and less than 1.56 J mol^{-1} K^{-1} for C_p values at all studied temperatures. All GA based enthalpies are within 5 kJ mol^{-1} for the *ab initio* values and only for two molecules, the deviation exceeds 4 kJ mol^{-1}. Similarly, the entropies are for almost all molecules reproduced to within 4 J mol^{-1} K^{-1}, which demonstrated the high accuracy obtained with the GAV/NNI set calculated in this study. Further validation using nine triple-substituted, thirteen quadruple-substituted and one quintuple-substituted benzene underscores the predictive capability. Combined with previously published GAV for hydrocarbon and oxygenated hydrocarbon species, an internally consistent set of GA parameters is now available for closed-shell monocyclic aromatic molecules. Future work will extend this towards radicals.

3.6 Acknowledgments

The research leading to these results has received funding from the European Research Council under the European Union's Seventh Framework Programme (FP7/2007-2013)/ERC grant agreement n° 290793. This work was carried out using the STEVIN Supercomputer Infrastructure at Ghent University, funded by Ghent University, the Flemish Supercomputer Center (VSC), the Hercules Foundation and the Flemish Government – department EWI.

3.7 References

[1] Clymans PJ, Froment GF. Computer-Generation of Reaction Paths and Rate-Equations in the Thermal-Cracking of Normal and Branched Paraffins. *Computers & Chemical Engineering.* 1984;8(2):137-142.

[2] Hillewaert LP, Dierickx JL, Froment GF. Computer-Generation of Reaction Schemes and Rate-Equations for Thermal-Cracking. *AIChE Journal.* 1988;34(1):17-24.

[3] Green WH, Barton PI, Bhattacharjee B, Matheu DM, Schwer DA, Song J, Sumathi R, Carstensen H-H, Dean AM, Grenda JM. Computer construction of detailed chemical kinetic models for gas-phase reactors. *Industrial & Engineering Chemistry Research.* 2001;40(23):5362-5370.

[4] Sabbe MK, Van Geem KM, Reyniers M-F, Marin GB. First Principle-Based Simulation of Ethane Steam Cracking. *AIChE Journal.* 2011;57(2):482-496.

[5] Ranzi E. A wide-range kinetic modeling study of oxidation and combustion of transportation fuels and surrogate mixtures. *Energy & Fuels.* 2006;20(3):1024-1032.

[6] Tran LS, Sirjean B, Glaude P-A, Fournet R, Battin-Leclerc F. Progress in detailed kinetic modeling of the combustion of oxygenated components of biofuels. *Energy.* 2012;43(1):4-18.

[7] Richter H, Risoul V, Lafleur AL, Plummer EF, Howard JB, Peters WA. Chemical characterization and bioactivity of polycyclic aromatic hydrocarbons from non-oxidative thermal treatment of pyrene-contaminated soil at 250-1,000 degrees C. *Environmental Health Perspectives.* 2000;108(8):709-717.

[8] Norinaga K, Deutschmann O, Saegusa N, Hayashi J-I. Analysis of pyrolysis products from light hydrocarbons and kinetic modeling for growth of polycyclic aromatic hydrocarbons with detailed chemistry. *Journal of Analytical and Applied Pyrolysis.* 2009;86(1):148-160.

[9] Saggese C, Sánchez NE, Frassoldati A, Cuoci A, Faravelli T, Alzueta MU, Ranzi E. Kinetic Modeling Study of Polycyclic Aromatic Hydrocarbons and Soot Formation in Acetylene Pyrolysis. *Energy & Fuels.* 2014;28(2):1489-1501.

[10] Evans RJ, Milne TA. Molecular characterization of the pyrolysis of biomass. *Energy & Fuels.* 1987;1(2):15.

[11] Patwardhan PR, Brown RC, Shanks BH. Understanding the fast pyrolysis of lignin. *ChemSusChem.* 2011;4(11):1629-1636.

[12] Sangha AK, Petridis L, Smith JC, Ziebell A, Parks JM. Molecular simulation as a tool for studying lignin. *Environmental Progress & Sustainable Energy.* 2012;31(1):47-54.

[13] Benson SW, Buss JH. Additivity Rules for the Estimation of Molecular Properties - Thermodynamic Properties. *The Journal of Chemical Physics.* 1958;29(3):546-572.

[14] Benson SW. *Thermochemical kinetics; methods for the estimation of thermochemical data and rate parameters*. New York: Wiley; 1968.

[15] Benson SW, Cruickshank FR, Golden DM, Haugen G, O'Neal HE, Rodgers AS, Shaw R, Walsh R. Additivity rules for the estimation of thermochemical properties. *Chemical Reviews.* 1969;69(3):279-324.

[16] Benson SW. *Thermochemical kinetics : methods for the estimation of thermochemical data and rate parameters (2nd edition)*. New York: Wiley; 1976.

[17] Cohen N. Thermochemistry of Alkyl Free-Radicals. *Journal of Physical Chemistry.* 1992;96(22):9052-9058.

[18] Cohen N. Revised Group Additivity Values for Enthalpies of Formation (at 298 K) of Carbon–Hydrogen and Carbon–Hydrogen–Oxygen Compounds. *Journal of Physical and Chemical Reference Data.* 1996;25(6):1411.

[19] Holmes JL, Aubry C. Group additivity values for estimating the enthalpy of formation of organic compounds: an update and reappraisal. 1. C, H, and O. *The Journal of Physical Chemistry A.* 2011;115(38):10576-10586.

[20] Holmes JL, Aubry C. Group Additivity Values for Estimating the Enthalpy of Formation of Organic Compounds: An Update and Reappraisal. 2. C, H, N, O, S, and Halogens. *The Journal of Physical Chemistry A.* 2012;116(26):7196-7209.

[21] Marsi I, Viskolcz B, Seres L. Application of the Group Additivity Method to Alkyl Radicals: An ab Initio Study. *The Journal of Physical Chemistry A.* 2000;104(19):4497-4504.

[22] Sabbe MK, Saeys M, Reyniers M-F, Marin GB, Van Speybroeck V, Waroquier M. Group Additive Values for the Gas Phase Standard Enthalpy of Formation of Hydrocarbons and Hydrocarbon Radicals. *The Journal of Physical Chemistry A.* 2005;109(33):7466-7480.

[23] Sabbe MK, De Vleeschouwer F, Reyniers M-F, Waroquier M, Marin GB. First Principles Based Group Additive Values for the Gas Phase Standard Entropy and Heat Capacity of Hydrocarbons and Hydrocarbon Radicals. *The Journal of Physical Chemistry A.* 2008;112(47):12235-12251.

[24] Vandeputte AG, Sabbe MK, Reyniers M-F, Marin GB. Modeling the gas-phase thermochemistry of organosulfur compounds. *Chemistry – A European Journal.* 2011;17(27):7656-7673.

[25] Paraskevas PD, Sabbe MK, Reyniers M-F, Papayannakos N, Marin GB. Group Additive Values for the Gas-Phase Standard Enthalpy of Formation, Entropy and Heat Capacity of Oxygenates. *Chemistry – A European Journal.* 2013;19(48):16431-16452.

[26] Sumathi R, Green W. Missing Thermochemical Groups for Large Unsaturated Hydrocarbons: Contrasting Predictions of G2 and CBS-Q. *The Journal of Physical Chemistry A.* 2002;106(46):11141-11149.

[27] Sun H, Bozzelli JW. Structures, Intramolecular Rotation Barriers, and Thermochemical Properties: Ethanol, α-Monoethanols, Dichloroethanols, and Corresponding Radicals Derived from H Atom Loss. *The Journal of Physical Chemistry A.* 2001;105(41):9543-9552.

[28] Sun H, Bozzelli JW. Structures, Rotational Barriers, Thermochemical Properties, and Additivity Groups for 2-Propanol, 2-Chloro-2-propanol and the Corresponding Alkoxy and Hydroxyalkyl Radicals. *The Journal of Physical Chemistry A.* 2002;106(15):3947-3956.

[29] Frisch MJ, Trucks GW, Schlegel HB, Scuseria GE, Robb MA, Cheeseman JR, Scalmani G, Barone V, Mennucci B, Petersson GA, Nakatsuji H, Caricato M, Li X, Hratchian HP, Izmaylov AF, Bloino J, Zheng G, Sonnenberg JL, Hada M, Ehara M, Toyota K, Fukuda R, Hasegawa J, Ishida M, Nakajima T, Honda Y, Kitao O, Nakai H, Vreven T, Montgomery Jr. JA, Peralta JE, Ogliaro F, Bearpark MJ, Heyd J, Brothers EN, Kudin KN, Staroverov VN, Kobayashi R, Normand J, Raghavachari K, Rendell AP, Burant JC, Iyengar SS, Tomasi J, Cossi M, Rega N, Millam NJ, Klene M, Knox JE, Cross JB, Bakken V, Adamo C, Jaramillo J, Gomperts R, Stratmann RE, Yazyev O, Austin AJ, Cammi R, Pomelli C, Ochterski JW, Martin RL, Morokuma K, Zakrzewski VG, Voth GA, Salvador P, Dannenberg JJ, Dapprich S, Daniels AD,

Farkas Ö, Foresman JB, Ortiz JV, Cioslowski J, Fox DJ. Gaussian 09, Version D.01. Wallingford, CT, USA: Gaussian, Inc.; 2009.

[30] Montgomery Jr JA, Frisch MJ, Ochterski JW, Petersson GA. A complete basis set model chemistry. VI. Use of density functional geometries and frequencies. *The Journal of Chemical Physics.* 1999;110(6):2822-2827.

[31] Curtiss LA, Redfern PC, Raghavachari K. Gaussian-4 theory. *The Journal of Chemical Physics.* 2007;126(8):084108.

[32] Paraskevas PD, Sabbe MK, Reyniers M-F, Papayannakos N, Marin GB. Kinetic modeling of alpha-hydrogen abstractions from unsaturated and saturated oxygenate compounds by carbon-centered radicals. *ChemPhysChem.* 2014;15(9):1849-1866.

[33] Paraskevas PD, Sabbe MK, Reyniers M-F, Papayannakos NG, Marin GB. Kinetic Modeling of α-Hydrogen Abstractions from Unsaturated and Saturated Oxygenate Compounds by Hydrogen Atoms. *The Journal of Physical Chemistry A.* 2014;118(40):9296-9309.

[34] Sabbe M, Vandeputte A, Reyniers M-F, Van Speybroeck V, Waroquier M, Marin G. Ab Initio Thermochemistry and Kinetics for Carbon-Centered Radical Addition and β-Scission Reactions. *The Journal of Physical Chemistry A.* 2007;111(34):8416-8428.

[35] Sabbe M, Reyniers M-F, Van Speybroeck V, Waroquier M, Marin G. Carbon-Centered Radical Addition and β-Scission Reactions: Modeling of Activation Energies and Pre-exponential Factors. *ChemPhysChem.* 2008;9(1):124-140.

[36] Luo Y. *Bond Dissociation Energies In CRC Handbook of Chemistry and Physics*; Lide, DR, Ed: CRC Press/Taylor and Francis: Boca Raton, FL; 2008.

[37] Blanksby SJ, Ellison GB. Bond Dissociation Energies of Organic Molecules. *Accounts of Chemical Research.* 2003;36(4):255-263.

[38] Vansteenkiste P, Van Speybroeck V, Marin GB, Waroquier M. Ab initio calculation of entropy and heat capacity of gas-phase n-alkanes using internal rotations. *The Journal of Physical Chemistry A.* 2003;107(17):3139-3145.

[39] Van Speybroeck V, Vansteenkiste P, Neck DV, Waroquier M. Why does the uncoupled hindered rotor model work well for the thermodynamics of n-alkanes? *Chemical Physics Letters.* 2005;402(4-6):479-484.

[40] Vansteenkiste P, Van Neck D, Van Speybroeck V, Waroquier M. An extended hindered-rotor model with incorporation of Coriolis and vibrational-rotational coupling for calculating partition functions and derived quantities. *The Journal of Chemical Physics.* 2006;124(4):044314.

[41] Curtiss LA, Raghavachari K, Redfern PC, Pople JA. Assessment of Gaussian-2 and density functional theories for the computation of enthalpies of formation. *The Journal of Chemical Physics.* 1997;106(3):1063-1079.

[42] Petersson GA, Malick D, Wilson W, Ochterski J, Montgomery JA, Frisch MJ. Calibration and comparison of the Gaussian-2, complete basis set, and density functional methods for computational thermochemistry. *The Journal of Chemical Physics.* 1998;109(24):10570.

[43] Burgess DR. *"Thermochemical Data" in NIST Chemistry WebBook, NIST Standard Reference Database Number 69*. Gaithersburg MD, 20899: National Institute of Standards and Technology; 2005.

[44] Fenwick J, Harrop D, Head A. Thermodynamic properties of organic oxygen compounds 41. Enthalpies of formation of eight ethers. *The Journal of Chemical Thermodynamics.* 1975;7(10):943-954.

[45] Lebedeva ND, Katin YA. Heats of combustion of certain monosubstituted benzenes. *Russian Journal of Physical Chemistry.* 1972;46:1.

[46] Weinhold F, Landis CR. Natural Bond Orbitals and Extensions of Localized Bonding Concepts. *Chemistry Education Research and Practice.* 2001;2:91-104.

[47] Glendening ED, Landis CR, Weinhold F. NBO 6.0: Natural bond orbital analysis program [computer program]. Version 6. University of Wisconsin, Madison; 2013.

[48] IUPAC. Compendium of Chemical Terminology, 2nd ed. (the "Gold Book"). Compiled by A. D. McNaught and A. Wilkinson. Blackwell Scientific Publications, Oxford (1997). XML on-line corrected version: http://goldbook.iupac.org (2006-) created by M. Nic, J. Jirat, B. Kosata; updates compiled by A. Jenkins. ISBN 0-9678550-9-8. doi:10.1351/goldbook.; Blackwell Scientific Publications Oxford, 1997.

Chapter 4

Thermodynamics of oxygenated monocyclic aromatic radicals

This chapter includes the following paper:

Ince A, Carstensen H-H, Sabbe MK, Reyniers M-F, Marin GB. Group additive modeling of substituent effects in monocyclic aromatic hydrocarbon radicals. *AIChE Journal.* 2017;63(6):2089-2106.

4.1 Abstract

The thermodynamic properties of the unsubstituted and substituted phenyl, phenoxy, anisyl, benzoyl, styryl and benzyl radicals with six substituents (hydroxy, methoxy, formyl, vinyl, methyl and ethyl) are calculated with the bond additivity corrected (BAC) post-Hartree–Fock G4 method. Bond dissociation energies of monocyclic aromatic hydrocarbons are calculated and used to identify substituent interactions in these radicals. Benson's Group Additivity (GA) scheme is extended to aromatic radicals by defining 6 GAV and 29 NNI parameters through least squares regression to a database of thermodynamic properties of 369 radicals. Comparison between G4/BAC and GA calculated thermodynamic values shows that the standard enthalpies of formation generally agree within 4 kJ mol^{-1}, whereas the entropies and the heat capacities deviate less than 4 J mol^{-1} K^{-1}.

4.2 Introduction

Radical chemistry plays an important role in various areas of life such as pyrolysis (steam cracking, thermochemical conversion of biomass, carbon black production) [1-4], corrosion (rusting) [5], radical-initiated polymer chemistry [6], oxidation (internal combustion engines, metabolism) [7,8] and environment (NO_x and ozone formation) [9-11] to name a few. Among the radicals involved, monocyclic aromatic radicals present an important sub-family. For example, phenyl (C_6H_5•) and benzyl ($C_6H_5CH_2$•) radicals are important intermediates in molecular growth chemistry forming polycyclic aromatic hydrocarbons (PAHs) [12,13], coke [14] and soot [15]. Phenoxy (C_6H_5O•) radicals are crucial for the coal processing [16], antioxidants [17,18] and lignin chemistry [19,20].

One area of great interest in chemical engineering is the conversion of lignocellulosic biomass to liquid fuels, energy, and chemicals. Given the relatively low O/C ratio compared to other biomass components and the richness in aromatic units, the lignin fraction has recently received special attention as a source for highly valuable products [21]. One conversion strategy for biomass is the thermochemical route, in which fast pyrolysis is used to yield mainly a liquid product (bio oil), which is then upgraded in subsequent steps to the desired products. Since pyrolysis chemistry is generally dominated by radical mechanisms it is expected that monocyclic aromatic hydrocarbon (MAH) radicals (MARs) play a pivotal role in this process.

To support the optimization of thermochemical conversion of biomass, kinetic models are needed that are able to optimize process conditions and minimize costly and time-consuming experiments. Kinetic models have been used successfully in the past for that purpose [22-25]. One obstacle in developing such models for biomass is that reliable thermochemical data for a large number of intermediates and products including those related to lignin are unknown [26-29]. Therefore, a recent study employed electronic structure methods to generate a large set of thermochemical data for single, double and various triple substituted MAHs [30]. A similar comprehensive thermochemical data set for MARs is still unavailable. The aim of the current work is to address this shortcoming.

In recent years, kinetic modeling has changed from being a manual reaction network assembling task performed by experienced kineticists to one in which software packages [31-35] are used to generate comprehensive reaction mechanisms automatically based on user-defined reaction rules. Such software packages need to keep track of the formation and consumption of all participating species, including reactive intermediates. Assignment of thermochemical properties for all these species is one of the current limitations of automated

network generating tools because of the aforementioned gaps in thermochemical databases and because the use of 'on-the-fly' first-principle calculations for each molecule or radical encountered is still in its infancy stage [36-38]. Therefore, estimation methods for thermochemical properties of a large variety of molecule classes are of crucial importance.

One popular approach to estimate thermodynamic properties of gas-phase species is the Group Additivity (GA) method developed by Benson and coworkers [39-42]. The essence of Benson's method is that any thermochemical property of a molecule can be calculated from contributions ("group additive values [GAVs]") of smaller units, called groups. Benson defines a group as "a polyvalent atom in a molecule together with all its ligands" [42]. Even though GAVs are able to account for the major part of a thermodynamic property, inclusion of the contributions from interactions that extend beyond the range of a group is essential to achieve the level of accuracy needed for kinetic modeling. These so-called "non-nearest neighbor interactions" are incorporated into the group additivity method as correction terms (NNIs). The thermodynamic property "y" thus is calculated as

$$y = \sum_{1}^{i} n_i \, GAV_i + \sum_{1}^{j} n_j \, NNI_j \qquad (4\text{-}1)$$

The GAV_i refer to different groups which occur n_i times in the molecule and NNI_j is the j^{th} correction term which occurs n_j times in the molecule. For the calculation of thermodynamic properties of a molecule via Benson's Group Additivity, the contributions from all present groups and NNI must be known. Therefore, an ongoing effort is to expand the available GAV/NNI database toward previously ignored molecule classes and to improve the accuracy of existing entries.

In order to ensure reliable GA results, the GAV and NNI parameters need to be internally consistent. This implies that (1) GAVs are defined and parameters are assigned in a systematic way resolving all linear dependencies, (2) the set of NNIs are comprehensive and well-defined and (3) all parameters are determined from reference data of equal quality. Marin and coworkers [30,43-46] have begun to create such an internally consistent GAV/NNI database based on *ab initio* results at either the CBS-QB3 or the G4 level of theory. Currently this database contains GAV and NNI values that allow calculation of thermodynamic properties for aliphatic hydrocarbons and their corresponding radicals [43,44], oxygenated hydrocarbons including radicals [46], organic sulfur compounds [45] and MAHs [30]. The purpose of this study is to extend the GAV and NNI database to those substituted MARs, which are expected to play a significant role in lignin pyrolysis.

An alternative approach to determine thermochemical properties of free radicals is to use so-called hydrogen bond increments (HBI) [43,44,46,47]. A HBI describes the change of a thermochemical property caused by the loss of a hydrogen atom. Hence, the thermodynamic property, *y*, of a radical X derived from the parent XH by removing the hydrogen is calculated as

$$y(X) = y\,(XH) + HBI\,(X) \tag{4-2}$$

The thermodynamic property for the corresponding parent molecules may be obtained by any means including Benson's GA method. In contrast to the GA method, the HBI(X) parameters are not restricted to groups but may describe larger moieties, for example, resonance stabilized subgroups, which are difficult to describe by GAV and NNI contributions. Sabbe et al. [43,44] showed that the HBI method performs better than GA for such radicals. One drawback of HBIs is that HBIs are not additive, meaning that only one HBI can be applied per radical. For

complex substitution patterns this means that each combination of substituents requires its own HBI. This lack of transferability prevents accurate description of unknown higher substituted MARs. As will be shown later, NNIs for radical groups are transferable and results for single and double-substituted radicals can be translated straightforwardly to multiple-substituted MARs. Therefore, this study does not develop HBI parameters but solely focuses on GAVs and NNIs.

The article is organized as follows: first, a database of accurate gas-phase standard enthalpies of formation ($\Delta_f H°$), entropies ($S°$) and heat capacities ($C_p(T)$) is constructed for a set of 369 MARs. This set is divided into two parts: a training set to determine new GAV and NNI parameters, and a test set used to demonstrate transferability. To identify which NNIs are necessary, bond dissociation energies (BDEs) for all radical classes considered in this work are calculated and analyzed. Once preliminary GAV/NNI values are available and transferability of these new GA parameters is established, all available thermodynamic data are combined to determine the final GAV and NNI values via a least squares procedure. Finally, an example is discussed to demonstrate the use and performance of these new GA values.

4.3 Methodology

4.3.1 Electronic Structure Calculations

The Gaussian 09 software package [48] has been used to perform all electronic structure calculations and the G4 [49] level of theory was selected to calculate the thermodynamic properties of all MARs (see Appendix B **Figure B-1 - Figure B-14** for a full list of these MARs). The primary results from these calculations are electronic 0 K energies, geometries

and harmonic oscillator frequencies. This information is used to calculate standard enthalpy of formations ($\Delta_f H°$), entropies ($S°$) at 298 K as well as heat capacities (C_p) at various temperatures via statistical mechanics. Prior to their use, harmonic oscillator frequencies are scaled by the default factor of 0.9854 [49] and the rigid rotor and harmonic oscillator (RRHO) approximation is applied [48] except for those modes that resemble internal rotations [50]. The latter are analyzed with the one-dimensional hindered rotor approach of Waroquier and coworkers [51-53]. To calculate the contributions of internal rotations to the partition function and thermodynamic properties, their hindrance potentials are determined with relaxed potential energy surface scans at the B3LYP/6-31G(d) level and expanded as truncated Fourier series using the first six sine and cosine terms. Harmonic oscillator frequencies associated with the internal rotors are identified via animation and then removed. Only internal rotors with total barriers below 50 kJ mol^{-1} are evaluated separately, all other modes are treated as harmonic oscillators. Internal rotations with very low barriers (less than 1 kJ mol^{-1}) are classified as free rotors. The reduced moment of inertia describing the rotation of the two molecule fragments around the axis that decouples internal from external rotation is calculated with the procedure described by Vansteenkiste et al [51].

All reported thermochemical data are based on the lowest energy conformer found for a molecule at the G4 level of theory. The hindrance potentials of the internal rotors are utilized to identify local minima on the potential energy surface, which are then evaluated at the G4 level in order to identify the lowest energy conformer. Note that this approach is a compromise between accuracy and effort as it does not necessarily guarantee that the global minimum is found if internal rotors are coupled. In this study,though, coupling is limited and thus the lowest

energy configurations have been located. The used methodology is in line with previous studies by Marin and coworkers [44-46].

4.3.2 Standard Enthalpy of Formations

The electronic energies obtained from the G4 method are converted to standard enthalpies of formation $\Delta_f H°$ with the atomization energy method as shown in Eq. (4-3):

$$\Delta_f H°\left(C_m H_n O_p; 298\ K\right) = m\Delta_f H^{\circ}_{gas,exp}(C) + n\Delta_f H^{\circ}_{gas,exp}(H) + p\,\Delta_f H^{\circ}_{gas,exp}(O) - [mH^{\circ}_{AI}(C) + nH^{\circ}_{AI}(H) + pH^{\circ}_{AI}(O) - H^{\circ}_{AI}(C_m H_n O_p)] \quad (4\text{-}3)$$

where $\Delta_f H^{\circ}_{gas,exp}$(C) = 716.68 kJ mol^{-1}, $\Delta_f H^{\circ}_{gas,exp}$(H) = 218.0 kJ mol^{-1} and $\Delta_f H^{\circ}_{gas,exp}$(O) = 249.18 kJ mol^{-1} at 298 K [54].

The first three terms of the right-hand side are the experimental standard enthalpies of formation of the atoms in the gas phase (gas,exp) at 298 K and the expression in brackets is the *ab initio* calculated atomization enthalpy for $C_mH_nO_p$, that is, the reaction enthalpy for the reaction at 298 K given in Eq. (4-4):

$$C_m H_n O_p \rightarrow mC + nH + pO \quad (4\text{-}4)$$

Note that spin-orbit corrections are part of the G4 methodology [49] and do not have to be applied separately. However, additional systematic errors are encountered in electronic structure calculations and these can largely be eliminated via “Bond Additive Corrections” (BACs) [55] as given in Eq. (4-5).

$$\Delta_f H^{\circ}(G4/BAC) = \Delta_f H^{\circ}(G4) + \sum_{ij} N_{ij} BAC_{ij} \quad (4\text{-}5)$$

in which *i* and *j* run over all atom types and N_{ij} is the number of bonds between atoms of type *i* and *j*. The required BACs for the G4 level of theory are taken from an earlier study [30].

Assigning BAC corrections for resonantly stabilized radicals can be ambiguous since the corresponding Lewis structures often contain different bond types. As this manuscript focuses on aromatic radicals, BAC corrections are based on Lewis structures that preserve the phenyl ring. The latter structures are expected to provide a reasonable description of the electron configuration of the radical, for example, in a phenoxy radical the largest spin density is on the oxygen atom.

A difficulty encountered in this study while using the default implementation of the G4 method is that in some instances abnormally high electronic energies are calculated. This lead to the suspicion that the default guess of the initial wavefunction to solve the self-consistent field problem does not always lead to the electronic ground state. To resolve this issue, a wavefunction stability test [48,56,57] was performed prior to each G4 calculation and the stabilized wavefunction is used as initial guess in the G4 method. Particularly the energies of some *para*-substituted benzoyl radicals improved by more than 10 kJ mol^{-1}. Using the stability test as pre-step provided the consistency in the data set that is needed to derive group additivity values.

One of the issues frequently encountered in unrestricted Hartree-Fock calculations for open-shell systems is the contamination of the wavefunctions by higher spin multiplicity states. This leads to electronic energies that are unrealistically low [58-62]. High $<\hat{S}^2>$ values are noted for several MARs under investigation, particularly for some substituted benzoyl radicals. Extensive validation against reported experimental data indicates that the final set of G4/BAC enthalpies of formation is reliable despite these spin contaminations. The use of a large training set introduces a high degree of redundancy and allows the identification of outliers. Such outliers were initially observed for (substituted) *o*-vinylbenzoyl radicals. Slight modifications

of the starting geometry resulted in drastic differences in energies and only the internally consistent low-energy values are used. The alternative – to invoke multi-reference wavefunction calculations – was not followed because such a method would drastically differ from previous GAV/NNI studies and lead to inconsistencies within the overall GA database.

4.3.3 Standard Intrinsic Entropies

The entropy for a radical calculated via statistical methods as described above does not take symmetry or contributions from stereoisomeric centers into account. Hence, the initial entropy needs to be corrected for such contributions if the total entropy of a molecule is needed. On the other hand, GAV and NNI parameters in Benson's group additivity method [42] are "symmetry-free", because they relate to moieties of a molecule and not to the entire molecule. Since the goal of this study is to determine such GAVs and NNIs, the symmetry-independent "intrinsic" entropies S_{int}° are used:

$$S_{int}^{\circ} = S^{\circ} + R\ ln\ (\frac{\sigma}{n_{opt}}) \tag{4-6}$$

σ is the global symmetry number and n_{opt} is the number of optical isomers. The global symmetry number σ is the product of external symmetry number σ_{ext} and the internal symmetry numbers σ_{int}:

$$\sigma = \sigma_{ext} \prod_{k} \sigma_{int,k} \tag{4-7}$$

4.3.4 BDE Analysis

The bond dissociation energy (BDE) of a X-Y bond in a molecule XY is defined as the difference between the sum of $\Delta_f H^\circ$ of the $X^\bullet$ and $Y^\bullet$ radicals, and the $\Delta_f H^\circ$ of the XY parent molecule (Eq. (4-8)).

$$BDE_{X-Y} = \Delta_f H^\circ(X^\bullet) + \Delta_f H^\circ(Y^\bullet) - \Delta_f H^\circ(XY) \tag{4-8}$$

BDEs are helpful in estimating the activation energies of reaction families, for which the activation energies correlate with the BDEs via Evans-Polanyi relationships. Within this study, BDEs are used for two purposes. First, if experimental BDE data exist these are used to validate the accuracy of the current calculations. Second, BDEs provide a means to identify NNIs in MARs. To illustrate the use of BDEs to identify NNIs, consider the difference in BDE between a substituted and an unsubstituted MAH (ΔBDE):

$$\begin{aligned}\Delta BDE = BDE_{Y_Z-X} - BDE_{Y_H-X} = \left(\Delta_f H^\circ(Y_Z^\bullet) - \Delta_f H^\circ(Y_H^\bullet)\right) \\ -\left(\Delta_f H^\circ(Y_Z X) - \Delta_f H^\circ(Y_H X)\right)\end{aligned} \tag{4-9}$$

Here, BDE_{Y_Z-X} denotes the BDE of a Z substituted MAH Y_Z-X and BDE_{Y_H-X} describes the BDE of the corresponding un-substituted aromatic species. $Y_Z^\bullet$ and $Y_H^\bullet$ symbolize the Z-substituted and un-substituted fragments, respectively. Note that the same X fragment is formed in the substituted and unsubstituted cases and hence its contribution cancels out in Eq. (4-9). If the enthalpies of formation of the parent molecules $Y_Z X$ and $Y_H X$ are known, the change in heat of formation upon substitution of the radical ($Y^\bullet$) can be determined:

$$\left(\Delta_f H^\circ(Y_Z^\bullet) - \Delta_f H^\circ(Y_H^\bullet)\right) = \Delta BDE - \left(\Delta_f H^\circ(Y_Z X) - \Delta_f H^\circ(Y_H X)\right) \tag{4-10}$$

To apply Eq. (4-10) to identify NNIs for radicals in Benson's GA scheme, the $\Delta_f H^\circ$ in Eq. (4-10) are written in terms of GA parameters using Benson's nomenclature [42] distinguishing different types of carbon atoms, namely a single bonded carbon (C), a double bonded carbon (C_d) and a carbon in an aromatic ring (C_b) are abbreviated differently. For instance, the group additive value, $GAV_{C_b-(H)}$, refers to the group in which an aryl carbon (C_b) is the center atom, which is bonded to a hydrogen atom. The difference in BDE of the phenylic C—H bond upon substitution by Z, i.e. reaction (i) to (ii)

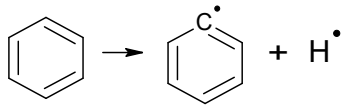

(i)

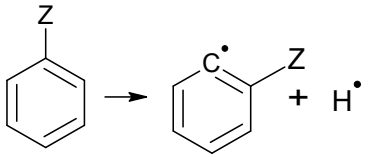

(ii)

can be obtained as follows:

$$\Delta_f H^\circ(\mathrm{C_6H_5—H}) = 6\,GAV_{C_b-(H)},$$

$$\Delta_f H^\circ(\mathrm{C_6H_5^\bullet}) = 5\,GAV_{C_b-(H)} + GAV_{C_b^\bullet},$$

$$\Delta_f H^\circ(\mathrm{Z-C_6H_4—H}) = 5\,GAV_{C_b-(H)} + GAV_{C_b-(Z)} + GAV_{Z-(C_b)} + NNI_{Parent}, \quad (4\text{-}11)$$

$$\Delta_f H^\circ(\mathrm{Z-C_6H_4^\bullet}) = 4\,GAV_{C_b-(H)} + GAV_{C_b^\bullet} + GAV_{C_b-(Z)} + GAV_{Z-(C_b)} + NNI_{Radical}.$$

and substitution into Eq. (4-10) then yields:

$$\Delta BDE = NNI_{Radical} - NNI_{Parent} \quad (4\text{-}12)$$

This demonstrates that the change in BDE upon the introduction of a substituent group Z is only a function of the difference between substituent effects in the radical and the

corresponding parent molecule. Equation (4-12) lays the foundation for $NNI_{Radical}$ identification in this study as the ΔBDEs are calculated with the G4/BAC methodology and the NNI_{Parent} terms are already known from the study of Ince et al. [30].

From Eq. (4-12), one can distinguish three cases:

$$\Delta BDE > 0 \;\rightarrow\; NNI_{Radical} > NNI_{Parent},$$
$$\Delta BDE = 0 \;\rightarrow\; NNI_{Radical} = NNI_{Parent}, \qquad (4\text{-}13)$$
$$\Delta BDE < 0 \;\rightarrow\; NNI_{Radical} < NNI_{Parent}.$$

The above derivation assumes that the ΔBDE values calculated by group additivity are identical to those calculated by G4/BAC. Since there is no 100% agreement between G4/BAC and GA data, $NNI_{Radical}$ values derived from Eq. (4-12) are only approximations. Nevertheless, they provide good initial guesses for the NNIs of interest.

In some cases, scission of bonds that belong to different MAHs may yield the same radicals. For instance, compare reactions (ii) and (iii) where $Z\text{–}C_6H_4^{\bullet}$ radical is obtained from two different parent molecules e.g. $Z - C_6H_4 — H$ and $Z - C_6H_4 — Y$. Since both reactions yield the same radical, the magnitude of the substituent effects in $Z\text{–}C_6H_4^{\bullet}$ which are calculated from the BDE analyses (Eq. (4-12)) of these two reactions are expected to be very similar and, hence, this is used to support identification of NNIs. This practice is followed for all cases in which different reactions lead to the same $NNI_{Radical}$. For each substituent effect appearing in multiple reactions, the individual values are averaged and this average is reported as the preliminary NNI correction term.

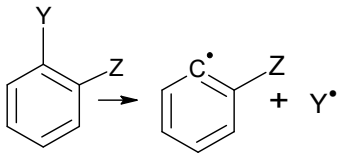

(iii)

4.3.5 Derivation of GAV and NNI values

I. Linear Regression Procedure

The GAV and the NNI values are determined through simultaneously optimizing the agreement between group additively calculated and *ab initio* thermodynamic data for MAH radicals via unweighted least-squares analysis. In this linear regression analysis, the following objective function is minimized:

$$SSQ = \sum_{i}^{n} (y_i - \hat{y}_i)^2 \tag{4-14}$$

In Eq. (4-14), y_i is the *ab initio* calculated enthalpy of formation ($\Delta_f H°$), entropy ($S°$) or heat capacity (C_p(T)) of the radical i and $\hat{y}_i$ is the calculated thermochemical value via group additivity. This results in the equation:

$$\overline{GAV/NNI} = (X^T X)^{-1} X^T \bar{y} \tag{4-15}$$

In Eq. (4-15), $\overline{GAV/NNI}$ is the calculated vector of the group additive values and NNI parameters and X is the occurrence matrix in which each row represents a radical and each column refers to a GAV or NNI. The elements of this matrix X_{ij} specify the number of occurrences of group j in radical i. Here, $\bar{y}$ is the vector of all y_i.

A statistical analysis is performed to assess the reliability of the linear regression step and the quality of the optimization procedure. The quality of the fits is expressed in terms of the

significance (F) of the regression, the mean absolute deviation (MAD), root-mean square deviation (RMS) and maximum deviation (MAX) between *ab initio* data and the data obtained via group additivity. The reported significance F of the regression is calculated with the following equation:

$$F = \frac{(\sum_{i=1}^{n} \hat{y}^2)/p}{(\sum_{i=1}^{n} (\hat{y}_i - y_i)^2)/(n-p)} \quad (4\text{-}16)$$

In Eq. (4-16), n is the number of molecules and p is the number of parameters. More details regarding the linear regression procedure and the statistical analysis are provided in Appendix B.

II. Definition of the GAVs for MARs

A total of 24 GAVs are required to describe all the MARs (See Appendix B) studied in this work. Among these, 18 GAVs have already been defined in earlier studies. They are given in **Table 4-1** [30,43,44,46]. These 18 GAVs can be divided into 14 GAVs which describe non-radical groups, and 4 GAVs which relate to radical moieties. The parameters for these 18 GAVs are adopted and not subjected to optimization. This was done to ensure internal consistency with previously developed GAV/NNI databases.

Generally, the GA description of radicals requires two types of radical-specific GAVs: GAVs for radical-centered and radical adjacent groups. For hydrocarbon radicals, Sabbe et al. [43,44] showed that GAVs describing a radical adjacent group can be substituted by the analogous non-radical groups without significant loss of accuracy. Hence only GAVs for the radical centered groups were developed. Investigating radicals of oxygenates, Paraskevas et al. [46] noticed that the same replacement strategy does not work for these radicals, mainly because oxygen (•O) and carbonyl (•C=O) moieties are not considered as center atoms of groups and

hence their contributions to thermodynamic properties have to be incorporated into adjacent groups. The GAV definitions in the present study take the discussed previous observations into account. For benzyl radical, only two new GAVs are needed to represent the carbon-centered radical groups, Ċ-(C_b)(H)$_2$ and Ċ-(C_b)(C)(H). The radical-adjacent groups C_b-(Ċ) and C-(Ċ)(H)$_3$ found in benzyl and 1-phenylethyl radicals are replaced by the nonradical C_b-(C) and C-(C)(H)$_3$ GAVs.

Table 4-1 GAVs taken from earlier studies [30,43,44,46].

Predefined GAVs	Source	$\Delta_f H^\circ$	S°	C_p [J mol^{-1} K^{-1}]						
		[kJ mol^{-1}]	[J mol^{-1} K^{-1}]	300 K	400 K	500 K	600 K	800 K	1000 K	1500 K
C_b-(H)	Ref. [30]	13.7	48.6	13.3	18.4	22.7	26.2	31.3	34.8	40.1
C_b-(O)	Ref. [30]	24.0	-30.0	12.1	12.6	15.0	17.4	21.3	23.5	26.0
C_b-(C)	Ref. [30]	23.5	-33.6	10.8	13.8	16.5	18.7	21.9	23.8	26.2
C_b-(CO)	Ref. [30]	21.5	-33.7	16.4	17.8	19.7	21.6	24.4	26.6	27.4
C_b-(C_d)	Ref. [30]	24.3	-35.0	12.4	14.8	16.4	18.0	20.9	22.6	25.6
O-(C_b)(C)	Ref. [30]	-124.1	21.6	20.3	24.2	25.1	24.8	23.7	23.1	22.0
C-(O)(H)$_3$	Ref. [46]	-42.9	127.1	25.3	32.1	38.4	44.1	53.4	60.6	72.5
O-(C_b)(H)	Ref. [46]	-188.1	106.3	24.6	30.3	32.5	33.2	33.3	33.6	35.0
CO-(C_b)(H)	Ref. [46]	-128.3	129.3	27.3	34.0	39.4	43.7	50.2	54.2	60.8
C-(C_b)(H)$_3$	Ref. [43,44]	-42.9	127.2	25.0	31.8	38.2	43.9	53.2	60.5	72.3
C_d-(C_b)(H)	Ref. [43,44]	30.4	25.7	18.1	24.1	29.1	32.7	37.1	40.0	43.1
C_d-(H)$_2$	Ref. [43,44]	25.1	115.8	20.6	25.8	30.8	34.9	41.4	46.4	54.6
C-(C_b)(C)(H)$_2$	Ref. [30]	-20.6	38.6	24.9	30.7	36.0	40.4	47.3	52.3	60.0
C-(C)(H)$_3$	Ref. [43,44]	-42.9	127.2	25.3	32.1	38.4	44.1	53.4	60.6	72.5
Ċ-(O)(H)$_2$	Ref. [46]	147.2	126.2	27.5	33.1	37.8	41.4	46.7	50.4	56.2
Ċ$_d$-(H)	Ref. [43,44]	275.8	121.4	20.6	23.6	25.7	27.4	30.1	32.3	35.6
C_b-(Ċ)	Same as C_b-(C)[a] [30,43,44]	23.5	-33.6	10.8	13.8	16.5	18.7	21.9	23.8	26.2
C-(Ċ)(H)$_3$	Same as C-(C)(H)$_3$ [43,44]	-42.9	127.2	25.3	32.1	38.4	44.1	53.4	60.6	72.5

[a]The newer values from Ref. [30] are used for C_b-(C).

For phenyl and substituted phenyls, only the radical-specific GAV, Ċ$_b$, is needed. Although this GAV has already been defined by Sabbe et al. [43,44] based on CBS-QB3 calculations, Ince et al. [30] showed that the CBS-QB3 method overestimates the $\Delta_f H°$ of phenyl radical, which leads to a biased value of the GAV for the Ċ$_b$ group [43]. Therefore, in this study this

GAV is redefined with the G4/BAC dataset that encompasses 25 phenylic MARs. For β-styryl radicals, no new GAVs are needed, because the $\dot{C}_d$-(H) GAV has already been defined by Sabbe et al. [43,44].

Two new GAVs are needed for phenoxylic and benzoylic MARs: the radical-adjacent groups C_b-($\dot{O}$) and C_b-($\dot{C}O$). For the radical moiety in anisylic radicals, the O-($\dot{C}$)(C_b) is missing and needs to be defined and the value for the $\dot{C}$-(O)$(H)_2$ group is taken from Paraskevas et al. [46].

4.4 Results and Discussion

G4/BAC calculations have been performed to construct a database of accurate gas-phase standard enthalpies of formation ($\Delta_f H°$), entropies ($S°$) and heat capacities ($C_p(T)$, at T = 300, 400, 500, 600, 800, 1000 and 1500 K) for 369 MARs. This database is divided into a training set (316 MARs) and a test set (53 MARs). The training set is used to assign initial GAV and NNI values via linear regression and the test set serves to prove the transferability of these GAV/NNI parameters, meaning their applicability to larger MARs or MARs not present in the training set. Afterwards, both sets are combined and final values for the GAV/NNI parameters are determined via regression.

This complete MAR database, which is provided in the Appendix B, can be grouped into six subsets reflecting the radical classes considered. These subsets distinguish between unsubstituted and substituted phenyl (C_6H_5•), phenoxy (C_6H_5O•), anisyl ($C_6H_5OCH_2$•), benzoyl (C_6H_5CO•(=O)), β-styryl (C_6H_5CH=CH•) and benzylic radicals (benzyl ($C_6H_5CH_2$•) and 1-phenylethyl (C_6H_5CH•CH_3)). Besides phenyl and 25 single substituted MARs, the database contains 128 double substituted MARs, which include all *ortho* (*o*-), *meta* (*m*-) and *para* (*p*-) combinations of hydroxy (-OH), methoxy (-OCH_3), formyl (-CHO), vinyl

(-CH=CH_2), and alkyl (-CH_3 and –C_2H_5) substituent groups, and additionally 212 triple and 3 quadruple substituted MARs. The *o*-formyl substituted benzoyl radical is removed from the set of molecules described above as the geometry optimization yields a bicyclic radical, which does not fit to the category of radicals of interest in this article. This radical is discussed later in more detail. Furthermore, all α-styryl radicals are excluded since they rearrange without barrier to species that are no longer aromatic. See Appendix B **Figure B-14** for a list of these radicals, which are not used for GA parameter development.

BDEs of 323 bonds found in MAHs have been calculated. Besides benzene, these bonds occur in 69 single substituted and double substituted MAHs (*ortho*, *meta* and *para*), in which the substituent groups are -OH, -OCH_3, -CHO, -CH=CH_2, -CH_3 and -CH_2CH_3. The $\Delta_f H^\circ$ data for the MAHs are taken from Ince et al. [30] while the $\Delta_f H^\circ$ data for the MARs and the small radical fragments are from the current study. The datasets for the $\Delta_f H^\circ$ of the MAHs, MARs, the small radical fragments and the BDEs which are calculated from these are provided in the Appendix B (**Table B-1 - Table B-5**).

4.4.1 Performance of G4/BAC Method

To assess the accuracy of the data obtained by the G4/BAC method, literature-reported $\Delta_f H^\circ$ of MARs and BDEs leading to these MARs can be compared. This is done in **Table 4-2** using selected published data for simple MAHs. A more extensive comparison presented in the Appendix B (See Appendix B **Figure B-15** and **Figure B-16**) shows that the G4/BAC calculated BDE energies are in the center of the range of experimental literature data, hence the G4/BAC method reproduces the general trends. The entries in **Table 4-2** are discussed in detail in the following paragraphs, along with some *ab initio* values from the literature.

Table 4-2 An overview of the bonds in benzene and single substituted benzenes for which the BDEs analyses are performed.[a]

	Bond	$BDE_{G4/BAC}$	BDE_{exp}	Prototypical Reaction
Phenyl 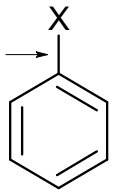	C_b—H	473.7	474.1 ± 8.9 [63,64] 472.8 ± 3.4 [63,65] 472.2 ± 2.2 [66,67]	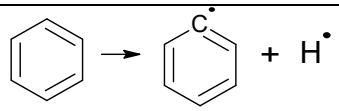
	C_b—OH	469.0	470.3±2.5 [68]	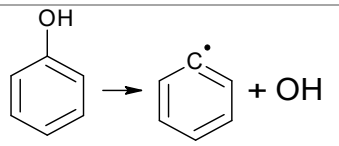
	C_b—OCH_3	428.6	422.4±4.2 [68]	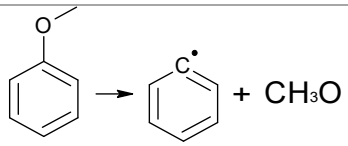
	C_b—CHO	415.3	415.5±3.8 [68]	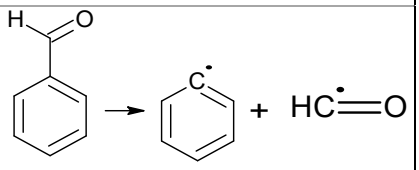
	C_b—$CH{=}CH_2$	484.4	485.3±4.2 [68]	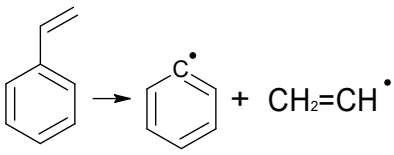
	C_b—CH_3	433.3	433.0±2.5 [68]	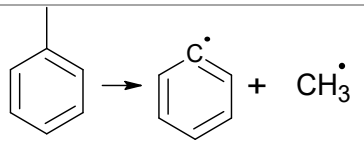
	C_b—CH_2CH_3	427.6	427.6±2.9 [68]	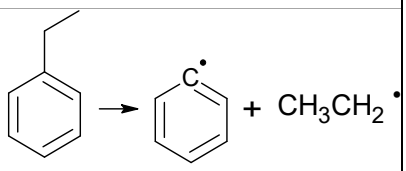

Phenoxy 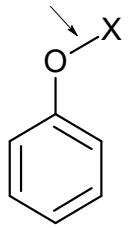	O—H	368.1	368.1±2.6 [69] 368.2±6.3 [54] 365.3±3.2 [70]	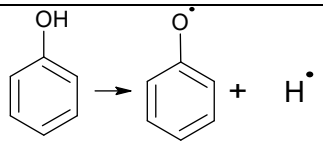
	O—CH_3	273.1	272.1 [54,71] 272.8 [54,72] 273.1 [54,73]	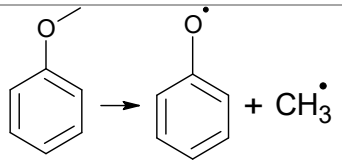
Anisyl 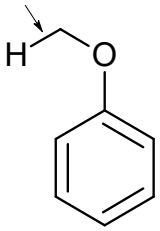	C—H	402.1	-	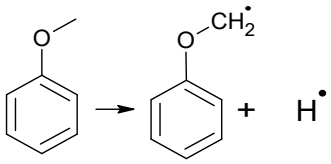
Benzoyl 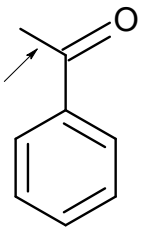	(C=O)—H	373.6	372 [54,74]	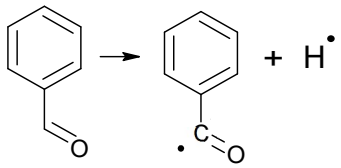
β-Styryl 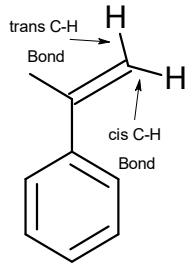	C—H(Cis)	465.7	-	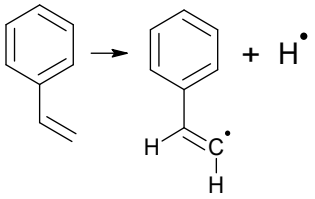
	C—H(Trans)	470.2	-	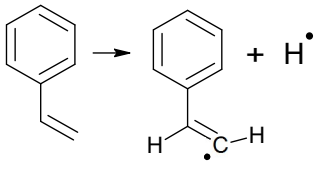

Benzyl 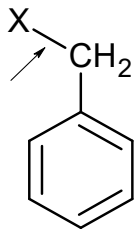	C—H	377	375.3±2.5 [68,75]	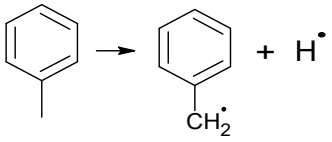
	C_α—C_β	324	319.7±7.1 [76]	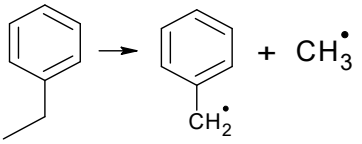
Ethyl Benzene 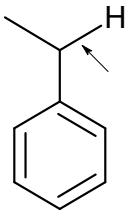	C_α—H	364.6	364.1 [77]	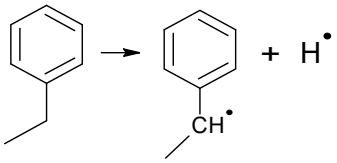

[a]All BDEs are given in kJ mol^{-1}.

The BDE of the C—H bond in benzene, 474.1 ± 8.9 kJ mol^{-1}, is obtained with the $\Delta_f H^\circ$ for benzene (82.9 ± 0.9 kJ mol^{-1}) [63] recommended by Roux et al. and the $\Delta_f H^\circ$ for phenyl radical (339. ± 8. kJ mol^{-1}) [64] suggested by Tsang et al. If the $\Delta_f H^\circ$ value of phenyl from recent photoionization measurements by Stevens et al. (337.7 ± 2.5 kJ mol^{-1}) [65] is used instead, the BDE value amounts to 472.8 ± 3.4 kJ mol^{-1}. Ervin and Deturi calculated a value of 472.2 ± 2.2 kJ mol^{-1} based on the electron affinity of the phenyl radical from the photoelectron spectroscopy data reported by Gunion et al. [66,67]. Van Speybroeck et al. studied the BDE utilizing B3P86/6-311G** and calculated it as 472.5 kJ mol^{-1}. The G4/BAC calculated BDE of 473.7 kJ mol^{-1} obtained in this study is in good agreement with all values mentioned above. The agreement between the G4/BAC method and the experimental data is similarly good for the BDEs of all C_6H_5—X bonds except the C_6H_5—OCH_3 bond in anisole. The large deviation (6.2 kJ mol^{-1}) in the latter case is mainly caused by the ambiguity of the $\Delta_f H^\circ$ value for anisole.

The NIST Webbook [78] contains four entries which differ by 8.8 kJ mol^{-1} for this molecule and only two of them (-67.8 kJ mol^{-1} [79] and -76.9 kJ mol^{-1} [80]) have reported uncertainties. Ince et al. developed BACs considering the average of these two values, which therefore is highly uncertain. This explains the discrepancy with literature BDEs for anisole.

The $\Delta_f H°$ values of 54. ± 6. kJ mol^{-1} by Tsang et al. [64] and 55.5 ± 2.4 kJ mol^{-1} by Simoes et al. [69] for phenoxy radical agree well with the GA/BAC result of 54.1 kJ mol^{-1}. For the C_6H_5O—H bond, three experimental BDE values are available in the literature, which are 368.1 ± 2.6 kJ mol^{-1} [69], 368.2 ± 6.3 kJ mol^{-1} [54] and 365.3 ± 3.2 kJ mol^{-1} [70]. These reported values are close to the G4-calculated value of 368.1 kJ mol^{-1}. Similarly, the reported BDE values for the C_6H_5O—CH_3 bond in anisole, 272.1 kJ mol^{-1} [71], 272.8 kJ mol^{-1} [72] and 273.1 kJ mol^{-1} [73], compare favorably with the value of 273.1 kJ mol^{-1} obtained in this study.

The standard enthalpy of formation of benzoyl radical measured with photoacoustic calorimetry by Simoes and Griller is 116.1 ± 11 kJ mol^{-1} [81] and this value is in good agreement with the G4/BAC result of 118.2 kJ mol^{-1}. For the BDE, Lund et al. [74] reported a value of 372 kJ mol^{-1} which is again close to the G4/BAC value (373.6 kJ mol^{-1}). For the $C_6H_5CH_2$—H bond in toluene, Ellison et al. [75] reported a value of 375.7 ± 2.5 kJ mol^{-1} deduced from ion flow tube experiments, which matches within the error margins the G4/BAC result of 377.0 kJ mol^{-1}. Van Speybroeck [82] performed *ab initio* calculations utilizing B3P86/6-311G** method and their result (376.1 kJ mol^{-1}) lies in-between the experimental and G4/BAC values. All comparisons above show that the chosen methodology yields reliable enthalpies of formation for the MARs of interest.

4.4.2 BDE Analysis of MAHs

The objective of the following BDE analysis is to identify NNIs by comparing the BDE in the un-substituted MAH with that found upon addition of a substituent group Z, $\Delta BDE=BDE_Z-BDE_H$. Taking into account the known substituent effects in the parent molecules [30], non-nearest neighbor effects involving the radical site can be obtained (Eq. (4-13)). Therefore, ΔBDEs for various bonds are presented in **Figure 4-1** in the form of bar diagrams.

Table 4-3 lists the identified substituent interactions and the preliminary values assigned for these NNIs based on the BDE analysis. In the Methodology section, it was pointed out that the $NNI_{Radical}$ values obtained via Eq. (4-13) are only initial estimates. The column "Substituent Effects In Radical" of **Table 4-3** lists those initial guesses for individual radicals and in "Preliminary $NNI_{radical}$ Values" the averaged substituent effects are used as initial guess for the corresponding NNI. In the following subsections, some ΔBDEs shown in **Figure 4-1** and the identified NNIs in **Table 4-3** are discussed in detail.

Two more NNI parameters are needed to describe the interactions in MARs: One NNI is required to describe the entropy changes caused by steric interactions between the alkyl and benzyl groups in *o*-CH_3 and *o*-CH_2CH_3 substituted benzyls. The second NNI describes the difference between trans and cis *β*-styryl radicals. Since these two NNIs (NNI24 and NNI29) are not obtained from the BDE analysis, they are not included in **Table 4-3**.

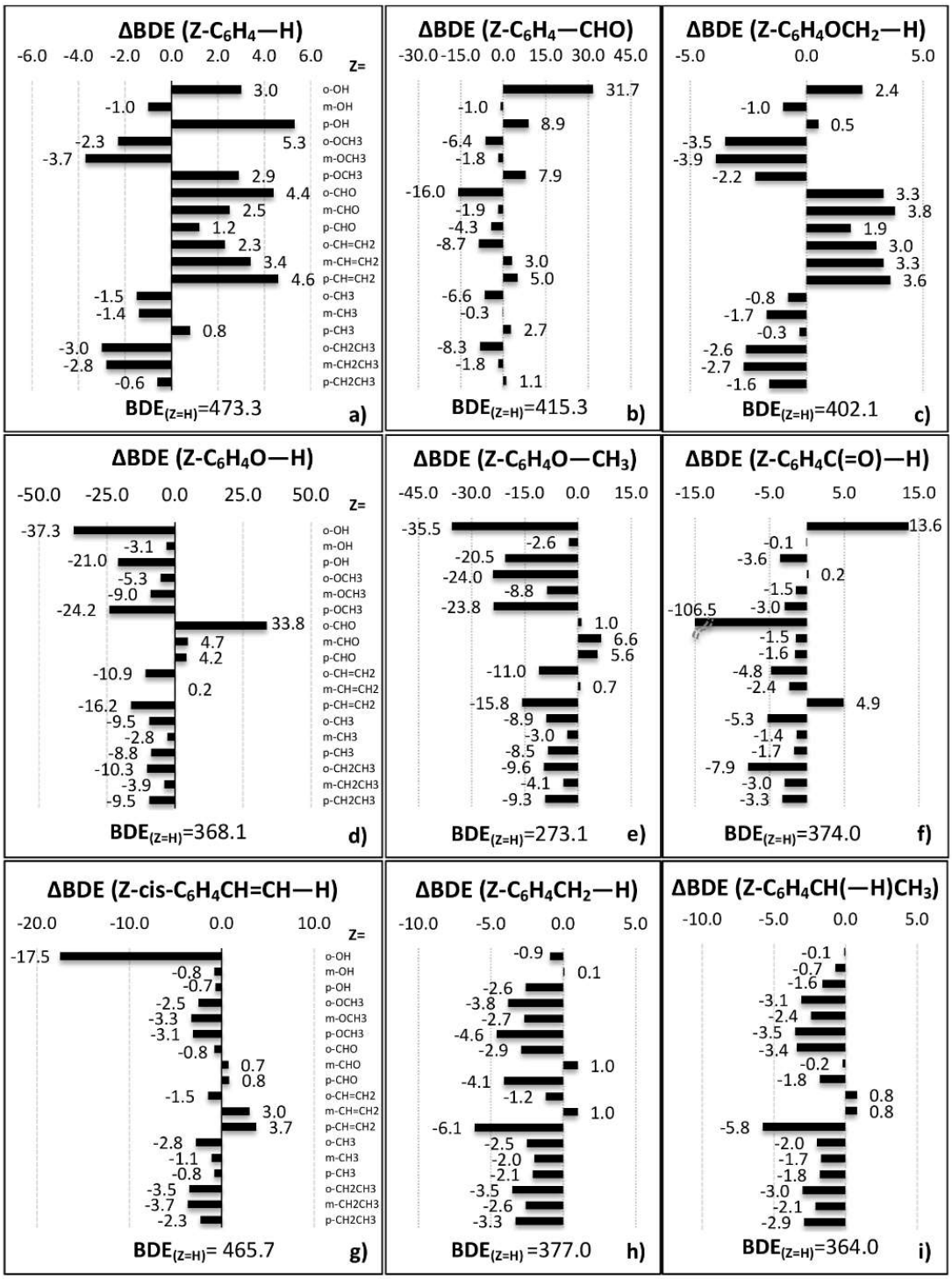

Figure 4-1 ΔBDEs (= BDE_Z – BDE_H) for **(a)** Z-C_6H_4—H, **(b)** Z-C_6H_4—CHO, **(c)** Z-$C_6H_4OCH_2$—H, **(d)** Z-C_6H_4O—H, **(e)** Z-C_6H_4O—CH_3, **(f)** Z-C_6H_5CO—H, **(g)** Z-cis-C_6H_4CH=CH—H, **(h)** Z-$C_6H_4CH_2$—H and **(i)** Z-C_6H_4CH(—H)CH_3 for various Z groups. Below each plot, the BDEs for the bonds in unsubstituted MAHs ($BDE_{(Z=H)}$) are given. See text for the details regarding the definition of ΔBDEs. Note that the scale of the x-axis differs for the different cases. All units are kJ mol^{-1}.

Table 4-3 An overview of the results of the BDE analysis: analyzed bonds, identified substituent interactions and the preliminary values assigned for these NNIs.[a]

#[b]	Bond	Interaction[c]	ΔBDE[d]	NNI_{Parent}[e]	Substituent Effects In Radicals[f]	Preliminary $NNI_{radical}$ values
Anisyl (Z-$C_6H_4OCH_2$•[g])						
1	*p*-OH-$C_6H_4OCH_2$—H	*p*-OH/OCH_3—$C_6H_4OCH_2$•	0.5	7.3	7.8	6.5
	p-OCH_3-$C_6H_4OCH_2$—H		-2.2	7.3	5.1	
2	*o*-OCH_3-$C_6H_4OCH_2$—H	*o*-OCH_3—$C_6H_4OCH_2$•	-3.5	14.7	11.2	11.2
3	*o*-CHO-$C_6H_4OCH_2$—H	*o*-CHO—$C_6H_4OCH_2$•	3.3	7.9	11.2	11.2
Phenoxy (Z-C_6H_4O•[g])						
4	*o*-OH-C_6H_4O—H	*o*-OH—C_6H_4O•	-37.3	-3.0	-40.3	-39.4
	o-OH-C_6H_4O—CH_3		-35.5	-3.0	-38.5	
5	*o*-OCH_3-C_6H_4O—H	*o*-OCH_3—C_6H_4O•	-5.3	-3.0	-8.3	-8.8
	o-OCH_3-C_6H_4O—CH_3		-24.0	14.7	-9.3	
6	*m*-OCH_3-C_6H_4O—H	*m*-OCH_3—C_6H_4O•	-9.0	0.0	-9.0	-8.9
	m-OCH_3-C_6H_4O—CH_3		-8.8	0.0	-8.8	
7	*p*-OH-C_6H_4O—H	*p*-OH/OCH_3—C_6H_4O•	-21.0	7.3	-13.7	-15.1
	p-OH-C_6H_4O—CH_3		-20.5	7.3	-13.2	
	p-OCH_3-C_6H_4O—H		-24.2	7.3	-16.9	
	p-OCH_3-C_6H_4O—CH_3		-23.8	7.3	-16.5	
8	*o*-CHO-C_6H_4O—H	*o*-CHO—C_6H_4O•	33.8	-27.4	6.4	7.7
	o-CHO-C_6H_4O—CH_3		1.0	7.9	8.9	
9	*m*-CHO-C_6H_4O—H	*m*-CHO—C_6H_4O•	4.7	0.0	4.7	5.6
	m-CHO-C_6H_4O—CH_3		6.6	0.0	6.6	
10	*o*-CH=CH_2-C_6H_4O—H	*o*-CH=CH_2—C_6H_4O•	-10.9	2.6	-8.3	-8.3
	o-CH=CH_2-C_6H_4O—CH_3		-11.0	2.6	-8.4	
11	*p*-CH=CH_2-C_6H_4O—H	*p*-CH=CH_2—C_6H_4O•	-16.2	0.0	-16.2	-16.0
	p-CH=CH_2-C_6H_4O—CH_3		-15.8	0.0	-15.8	
12	*o*-CH_3-C_6H_4O—H	*o*-CH_3/CH_2CH_3—C_6H_4O•	-9.5	0.0	-9.5	-9.6
	o-CH_3-C_6H_4O—CH_3		-8.9	0.0	-8.9	
	o-CH_2CH_3-C_6H_4O—H		-10.3	0.0	-10.3	
	o-CH_2CH_3-C_6H_4O—CH_3		-9.6	0.0	-9.6	
13	*p*-CH_3-C_6H_4O—H	*p*-CH_3/CH_2CH_3—C_6H_4O•	-8.8	0.0	-8.8	-9.0
	p-CH_3-C_6H_4O—CH_3		-8.5	0.0	-8.5	
	p-CH_2CH_3-C_6H_4O—H		-9.5	0.0	-9.5	
	p-CH_2CH_3-C_6H_4O—CH_3		-9.3	0.0	-9.3	

Benzoyl (Z-C_6H_4C•=O[g])						
14	*o-OH-C_6H_4C(=O)—H*	*o*-OH—C_6H_4C•=O	13.6	-27.4	-13.8	-13.8
15	*p-OH-C_6H_4C(=O)—H*	*p*-OH/OCH_3—C_6H_4C•=O	-3.6	-4.6	-8.2	-7.9
	p-OCH_3-C_6H_4(C=O)—H		-3.0	-4.6	-7.6	
16	*o-OCH_3-C_6H_4(C=O)—H*	*o*-OCH_3—C_6H_4C•=O	0.2	7.9	8.1	8.1
17	*m-CHO-C_6H_4(C=O)—H*	*m*-CHO—C_6H_4C•=O	-1.5	4.8	3.3	3.3
18	*p-CHO-C_6H_4(C=O)—H*	*p*-CHO—C_6H_4C•=O	-1.6	9.9	8.3	8.3
19	*o-CH=CH_2-C_6H_4(C=O)—H*	*o*-CH=CH_2—C_6H_4C•=O	-4.8	11.9	7.1	7.1
Styryl (Z-C_6H_4CH=CH•[g])						
20	*o-OH-C_6H_4CH=CH—H (cis C-H bond)*	*o*-OH—trans-C_6H_4CH=CH•	-17.5	2.6	-14.9	-14.9
21	*o-CHO-C_6H_4CH=CH—H (cis C-H bond)*	*o*-CHO—trans/cis-C_6H_4CH=CH•	-0.8	11.9	11.1	12.7
	o-CHO-C_6H_4CH=CH—H (trans C-H bond)		2.3	11.9	14.2	
22	*o-CH=CH_2-C_6H_4CH=CH—H (cis C-H bond)*	*o*-CH=CH_2—trans/cis-C_6H_4CH=CH•	-1.5	8.1	6.6	6.6
	o-CH=CH_2-C_6H_4CH=CH—H (trans C-H bond)		-1.4	8.1	6.7	
23	*o-CH_3-C_6H_4CH=CH—H (cis C-H bond)*	*o*-CH_3/CH_2CH_3—trans/cis-C_6H_4CH=CH•	-2.8	4.6	1.8	2.6
	o-CH_3-C_6H_4CH=CH—H (trans C-H bond)		-1.2	4.6	3.4	
Benzyl (Z-$C_6H_4CH_2$•[g])/1-Phenylethyl (Z-C_6H_4C•HCH_3[g])						
25	*p-CH=CH_2-$C_6H_4CH_2$—H*	*p*-CH=CH_2—$C_6H_4CH_2$•/C_6H_4C•HCH_3	-6.1	0.0	-6.1	-6.0
	p-CH=CH_2-C_6H_4C(—H)HCH_3		-5.8	0.0	-5.8	
	p-CH=CH_2-$C_6H_4CH_2$—CH_3		-6.1	0.0	-6.1	
26	*o-CH=CH_2-$C_6H_4CH_2$—H*	*o*-CH=CH_2—$C_6H_4CH_2$•/C_6H_4C•HCH_3	-1.2	4.6	3.4	4.2
	o-CH=CH_2-C_6H_4C(—H)HCH_3		0.8	4.6	5.4	
	o-CH=CH_2-$C_6H_4CH_2$—CH_3		-0.9	4.6	3.7	
27	*p-CHO-$C_6H_4CH_2$—H*	*p*-CHO—$C_6H_4CH_2$•/C_6H_4C•HCH_3	-4.1	0.0	-4.1	-3.4
	p-CHO-C_6H_4C(—H)HCH_3		-1.8	0.0	-1.8	
	p-CHO-$C_6H_4CH_2$—CH_3		-4.3	0.0	-4.3	
28	*o-CHO-$C_6H_4CH_2$—H*	*o*-CHO—$C_6H_4CH_2$•/C_6H_4C•HCH_3	-2.9	8.1	5.2	5.4
	o-CHO-C_6H_4C(—H)HCH_3		-3.4	8.1	5.7	
	o-CHO-$C_6H_4CH_2$—CH_3		-3.1	8.1	5.4	

[a] All units are kJ mol^{-1}.

[b] Twenty-seven NNIs identified from BDE analysis. Refer to text for the two missing NNIs in this list (**NNI24** and **NNI29**).

[c] The interaction for which the NNI parameter is derived. For instance, in **NNI4**, *o*-OH-C_6H_4O• refers to the interaction between the phenoxy radical site (C_6H_4O•) and a OH group in *ortho* position.

[d] ΔBDE denotes the difference between the bond dissociation energy of a substituted MAH and that of its unsubstituted counterpart (see Eq. (4-9)).

[e] The NNIs (substituent effects) in the parent MAHs are taken from Ref. [30].

[f]This value is obtained through Eq. (4-12) ($NNI_{Radical} = \Delta BDE - NNI_{Parent}$).
[g]Z is one of the following six substituent groups: -OH, $-OCH_3$, -CHO, $-CH{=}CH_2$, $-CH_3$, $-C_2H_5$ in *ortho*, *meta*, or *para* position to the radical substituent.

I. Phenyl Radicals

In **Figure 4-1 (a)** and **(b)** ΔBDE results are plotted for C_b—H and C_b—CHO bond scissions leading to phenyl radicals. **Table 4-2** shows that these bonds are strong and require 473.7 kJ mol^{-1} and 415.3 kJ mol^{-1}, respectively, for cleavage. Upon substitution, the BDE for the C_b—H bond changes slightly. The largest increase is 5.3 kJ mol^{-1} and the largest reduction amounts to -3.7 kJ mol^{-1}. According to Eq. (4-12), these changes are related to interactions between the Z-groups and the phenylic radical site. Given that these radicals are highly unstable, they are likely to be of minor importance in many reaction systems, and an introduction of NNIs to capture these small effects seems not warranted.

The BDE differences for the C_b—CHO bond cleavage shown in **Figure 4-1 (b)** are more difficult to explain because interactions between the –CHO group and the Z group may exist in the parent MAHs. Since these interactions disappear upon removal of CHO, any significant absolute ΔBDE value mainly points to a substituent effect in the parent molecule. The most notable of these deviations is the Z = *o*-OH case. The parent MAH (*o*-hydroxybenzaldehyde) is strongly stabilized by H bond formation and resonance effects [30]. All the other large deviations in **Figure 4-1 (b)** can be explained in a similar fashion.

Phenyl radicals can also be formed by removing any other of the five X substituents considered in this work (X = -OH, $-OCH_3$, $-CH{=}CH_2$, $-CH_3$ and $-CH_2CH_3$). ΔBDE plots for those are provided in Appendix B **Figure B-17**. Analyses of these cases lead to similar conclusions as discussed above.

Since in general the BDE changes upon substitution are relatively small, no NNIs are defined for substituted phenyl radicals.

II. Anisyl Radicals

The scission of the $C_6H_5OCH_2$—H bond in anisole is the prototypical anisyl radical forming reaction (see **Table 4-2**). The bond is clearly stronger than the phenoxy—CH_3 bond (discussed in the following section) but weaker than aryl—H bonds. The impact of substitution on the BDE is shown in **Figure 4-1 (c)** in terms of ΔBDE values. It can be seen that all ΔBDE values are within ± 4 kJ mol^{-1}. Since most parent molecules are free of substituent interactions, this means that anisyl radicals experience generally only minor NNIs. Among the few exceptions are Z = *p*-OH/OCH_3, Z = *o*-OCH_3 and Z = *o*-CHO substituents. These substituents cause non-negligible interactions in the MAHs and similar effects are observed in the radicals (**Table 4-3**). For instance, for Z = *o*-OCH_3, electron pair repulsion (anomeric effect) causes destabilization in the parent molecule as well as in the radical. For the Z = *o*-CHO case, in the parent molecule *o*-formylanisole, the inductive electron withdrawing effect (-I effect) of OCH_3 and CHO groups leads to an effective destabilization. The same effects also destabilize the corresponding *o*-formylanisyl radical leading to a very small change in ΔBDE values. As shown in **Table 4-2**, the ΔBDE of the C—H bonds obtained for the Z = *p*-OH and Z = OCH_3 cases are very small and the destabilizing substituent effects encountered in the parent molecules (*p*-hydroxyanisole and *p*-methoxyanisole) [30] are also reflected in the corresponding anisyl radicals implying that the substituent effects in the radicals are similar to that of the closed shell molecules.

III. Phenoxy Radicals

In **Figure 4-1 (d)** and **(e)**, the largest absolute ΔBDE values are noted for Z = *o*-OH (-37.3 kJ mol^{-1} and -35.5 kJ mol^{-1}, respectively). The substituent effect in the parent molecules is minor (-3.0 kJ mol^{-1}) [30], which means that a strong stabilizing interaction exists in the radical. The preliminary value of this NNI amounts to -39.4 kJ mol^{-1}. It describes the interaction between the phenoxy radical site (O•) and the *o*-OH substituent. This strong stabilization can be rationalized by resonance between the π-electron donating (+M effect) *o*-OH group and the electron accepting (-M effect) phenoxy radical. In addition, a H-bond is formed that is stronger than that in the parent molecules. This strong H-bond is discussed in several earlier studies in literature [71,83,84]. The resonance stabilization is also expected to be present in *p*-hydroxy phenoxy and *p*-methoxy phenoxy radicals and indeed, highly negative ΔBDE are calculated (-21.0 kJ mol^{-1} and -20.5 kJ mol^{-1} for O—H bonds in *p*-hydroxy or *p*-methoxy phenol and the O—CH_3 bonds in *p*-hydroxy or *p*-methoxy anisole, respectively). Taking into account NNI interactions in the parents, the preliminary NNIs for Z = *p*-OH and *p*-OCH_3 are calculated as -15.1 kJ mol^{-1}. From the difference in the preliminary NNIs for *o*- and *p*-hydroxy phenoxy radicals (See **Table 4-3**), it can be concluded that the H bond in the radical provides a stabilization of some 25 kJ mol^{-1}. Resonance effects are not at play for Z = *m*-OH and thus the ΔBDE value is close to zero. No NNI is needed for Z = *m*-OH.

The ΔBDE values for Z = *o*-OCH_3 substituted phenoxy radical formation either from *o*-hydroxyanisole or *o*-methoxyanisole differ according to **Figure 4-1 (d)** and **(e)** by 18.7 kJ mol^{-1}. As the same radicals are formed, this difference is caused by substituent interactions in the parent molecules. Through the BDE analysis, a value of -8.8 kJ mol^{-1} is found for the interaction between the phenoxy radical group and OCH_3 in *ortho* position. This stabilization

can be explained with a mesomeric effect between the π-electron donating (+M effect) OCH_3 group and the electron accepting (-M effect) phenoxy radical site. This resonance stabilization also occurs for Z = *p*-OCH_3, however in this case a stabilization of -15.1 kJ mol^{-1} is found. Therefore, in *ortho* position a second counteracting effect must be present, which is steric repulsion. For Z = *m*-OCH_3 substituted phenol and anisole, no significant substituent effect was reported [30]. However, ΔBDE values of approximately -8.9 kJ mol^{-1} are calculated, which point to a substituent effect in the *m*-methoxyphenoxy radical.

The very low pressure pyrolysis (VLPP) experiments by Suryan et al. [71] point out that the BDE of the O—C bonds in the methoxy groups of the *o*-OCH_3 and *p*-OCH_3 substituted anisoles are significantly lower than that of the same bond in anisole whereas for the Z = *m*-OCH_3 case, the ΔBDE of this bond has a less negative value. Considering the known substituent effects in the parent molecules [30], it can be inferred that the aforementioned observations on the radical stability of methoxyphenoxy radicals are in line with the conclusions of this work. The DFT calculations by Beste and Buchanan [85], Klein and Lukes [86] and Chandra and Uchimaru [87] also agree qualitatively with these findings.

Figure 4-1 (d) and **(e)** show that the ΔBDE values for *o*-hydroxy benzaldehyde and *ortho* methoxy benzaldehyde differ significantly (33.8 kJ mol^{-1} and 1.0 kJ mol^{-1}, respectively). This again is mainly caused by interactions in the parent molecules: *o*-hydroxy benzaldehyde is stabilized by a H bond, which is not present in the *o*-methoxy benzaldehyde molecule. After taking the NNIs in the parent molecules into account, a destabilization of 7.7 kJ mol^{-1} is found for *o*-formylphenoxy radical. It can be explained with two additive effects: destabilizing mesomeric effect between the π-electron donating (-M effect) *o*-CHO group and the electron accepting (-M effect) phenoxy radical, and steric repulsion. For Z = *m*-CHO substituted phenol

and anisole, positive ΔBDE values are found which average to 5.6 kJ mol^{-1}. Since the parent molecules have no known NNIs, this ΔBDE value can be equated to destabilizing substituent effects in the *m*-formylphenoxy radical (see **Table 4-3**). Although the ΔBDE values in **Figure 4-1 (d)** and **(e)** for *p*-CHO substituted phenols and anisoles are similar to that of the corresponding *m*-CHO substituted MAHs, there is no entry in **Table 4-3** for the NNIs of the *p*-formyl substituted phenoxy radical. This is caused by the stabilizing substituent effect of -4.6 kJ mol^{-1} in the parent molecules (*p*-formylphenol and *p*-formylanisole) [30] being solely responsible for these ΔBDE values while the substituent effects in the *p*-formyl substituted phenoxy radical are insignificant.

All non-nearest neighbor effects discussed so far for phenoxy radicals are related to oxygenated substituents. **Table 4-3** reveals that pure hydrocarbon substituent groups have stabilizing effects. This is particularly true for vinyl and alkyl substituents in *ortho* and *para* position. For Z = *o*-$CH{=}CH_2$ a stabilization of -8.3 kJ mol^{-1} is found upon the BDE analysis. For Z = *p*-$CH{=}CH_2$ the stabilization is with -16.0 kJ mol^{-1} almost twice as large and caused by resonance stabilization. An additional destabilizing effect, steric repulsion, is active in *ortho*-vinyl phenoxy radical [30]. Alkyl groups in *ortho* or *para* positions are found to stabilize phenoxy radicals by approximately 6-8 kJ mol^{-1}. Similar to alkyl radicals, which become more stable with increased alkyl substitution, a similar hyperconjugative stabilization can be assumed for alkyl substituents attached to those aryl carbon atoms that carry a partial spin.

IV. Benzoyl Radicals

$C_6H_5C(=O)$—H bond scission in benzaldehyde yields the benzoyl radical. The heat of reaction for this reaction is 374 kJ mol^{-1} (See **Table 4-2**), hence the BDE is similar to that of the phenolic

O—H bond. ΔBDE values for substituted benzoyl radical forming reactions are given in **Figure 4-1 (f)**.

The radical formed through $C_6H_5C(=O)$—H scission may exist in two substantially different geometries: (1) in the aromatic benzoyl form with a sp^2 carbonyl carbon configuration, or (2) as a ketene cyclohexadienyl structure with the typical linear C=C=O arrangement. Bennett et al. [88] measured the electronic spin resonance (ESR) spectrum for the benzoyl radical and showed that the angle between the C=O and the C-C bonds is close to that of a sp^2 hybridized carbon. This agrees with the geometry for benzoyl radical obtained in the current study. The ΔBDE value for *o*-formylbenzaldehyde (Z = *o*-CHO) shown in **Figure 4-1 (f)** differs obviously from all other data (ΔBDE = -106.5 kJ mol^{-1}**).** This is explained with the fact that the initial *o*-formyl benzoyl radical is not stable but undergoes ring closure to form the 1(3H)-Isobenzofuranonyl radical (See **Scheme 4-1**). Mendenhall et al. [89] observed the same rearrangement. Given the unusual structure of this radical it is excluded from the thermochemical dataset used to develop the group additivity parameters.

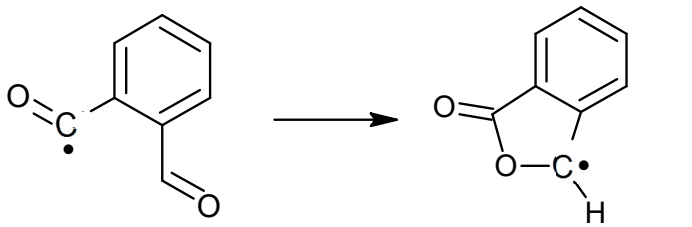

a) o-formyl benzoyl **b)** 1(3H)-Isobenzofuranoyl

Scheme 4-1 a) *o*-formyl benzoyl radical and **b)** the stable 1(3H)-Isobenzofuranonyl radical

In most cases investigated, the BDE of the $C_6H_5C(=O)$—H bond decreases upon substitution, since the ΔBDEs values are negative for all but three cases (see **Figure 4-1 (f)**). The BDE analyses show that six important substituent interactions exist. These are listed in **Table 4-3**.

While most absolute ΔBDE values are small, of the large values, the Z = *o*-OH case stands out. In this case, the formyl bond appears stronger than usual. For the *o*-hydroxy benzaldehyde parent molecule, a strong stabilizing interaction (-27.4 kJ mol^{-1}) between the hydroxyl and formyl group was observed [30]. Were this stabilization completely missing in the radical, the ΔBDE would have been 27.4 kJ mol^{-1}, but the observed value is only 13.6 kJ mol^{-1}. Thus, a stabilizing interaction (-13.8 kJ mol^{-1}) must exist in the radical: resonance between the electron donating OH (+M effect) and the electron withdrawing (-M effect) benzoyl group on one hand and formation of a hydrogen bond on the other. The mesomeric effects are also active for Z = *p*-OH and Z = *p*-OCH_3 and hence these radicals are also stabilized, however by a lower amount.

The ΔBDE value for *o*-OCH_3 substitution of the benzoyl radical is almost zero, however, since a destabilizing substituent effect of 7.9 kJ mol^{-1} is seen in the parent molecule, a NNI of similar value is identified for the *o*-methoxybenzoyl radical (See **Table 4-3**).

Similar NNIs in parents and radicals are also found for Z = *m*-CHO and Z = *p*-CHO. The substituent effect in *m*-formylbenzaldehyde is explained by Ince et al. [30] with inductive electron withdrawing effects (-I effect) of both substituents. This destabilizing effect is somewhat smaller in the radical than in the parent as **Table 4-3** shows. In *p*-formylbenzaldehyde, the electron withdrawing mesomeric effect (–M effect) of both formyl groups destabilize the molecule by 9.9 kJ mol^{-1}. Since the ΔBDE for Z = *p*-CHO is 1.6 kJ mol^{-1}, the substituent effect in *p*-formylbenzoyl is found to be 8.3 kJ mol^{-1}.

In *ortho*-vinyl benzaldehyde strong destabilization (11.9 kJ mol^{-1}) was observed due to steric interactions and a resulting out-of-plane configuration of the vinyl group [30]. The ΔBDE value of -4.8 kJ mol^{-1} for the Z = *o*-$CH{=}CH_2$ substituted benzoyl radical shows that this

interaction is also present in the radical, albeit in a reduced way, and a NNI to account for this needs to be defined.

Relatively large ΔBDE values are found for Z = *o*-CH_3 and Z = *o*-CH_2CH_3. These ΔBDE values can be traced back to steric interactions between the alkyl and formyl groups in the parent molecules [30]. In the corresponding radicals no significant steric repulsion is observed and thus no NNIs are needed.

V. Styryl Radicals

The vinyl group (-$CH=CH_2$) in styrene (vinylbenzene) contains three hydrogen atoms which give rise to three different MARs. The prototypical reactions that yield these three radicals are given in Appendix B **Figure B-23**. The optimized geometries of the G4 calculations show that trans-*β*-styryl and cis-*β*-styryl radicals prefer structures, which preserve the aromatic phenyl ring. However, unsubstituted and substituted *α*-styryl radicals were found to prefer allenic structures (ethenylidenecyclohexadienyl) without any exceptions. The expected *α*-styryl ($C_5H_5C•=CH_2$) and the observed structures of these radicals are provided in Appendix B **Figure B-23**. ESR spectroscopy studies by Bennett et al. [90] and Bonazzola et al. [91] support the preference of the allenic conformation. The thermochemical data and related BDE for these radicals are also provided in Appendix B **Table B-2** and **Table B-5**, respectively. Since the thermochemistry of nonaromatic radicals is beyond the scope of this work, only the BDEs for *β*-styryl radicals are discussed.

In **Figure 4-1 (g)**, the ΔBDEs are given for the scission of the cis-*β*-C—H bonds in substituted styrenes leading to formation of trans-*β*-styryl radicals. The features in **Figure 4-1 (g)** are generally similar to that of the trans-β-C—H bonds except for the Z = *o*-OH case discussed below, hence the ΔBDEs for the trans-*β*-C—H bonds are only provided in Appendix B

Figure B-24. These bonds are strong, comparable to the aryl-C—H bonds discussed previously (see **Table 4-2**). The entries in **Table 4-2** also make clear that the two vinylic C—H bonds are not equal. Note that breaking the trans-*β*-C—H bond in styrene leads to the cis-*β*-styryl radical and vice versa. The formation of trans-*β*-styryl radicals (the phenyl group of the C_6H_5CH= moiety and the C—H bond of the =CH• moiety point in opposite directions) is found to be on average 4.5 kJ mol^{-1} lower in energy than the formation of the cis-*β*-styryl radical. A NNI is needed to account for this difference.

The largest ΔBDE value is calculated for Z = *o*-OH in trans-*β*-styryl radical (**Figure 4-1 (g)**). The parent molecule *o*-hydroxystyrene is slightly destabilized, by 2.6 kJ mol^{-1}, according to Ince et al. [30]. Therefore, a strong stabilizing interaction of -14.9 kJ mol^{-1} must be present in *o*-hydroxy-trans-*β*-styryl. This strong interaction involving the hydrogen of -OH group and the carbon radical site is shown in a threedimensional molecular orbital representation (**Figure B-25**) in the Appendix B. This interaction might be identified as a weak 3-center 3-electron bond (O—H—C•). For geometric reasons such a 3-center 3-electron bond is not possible in cis-*β*-styryl radical, which explains the significant differences in BDE for the two C—-H bonds in *o*-hydroxy styrene (the ΔBDE for *o*-OH substituted cis-*β*-styryl is 0.7 kJ mol^{-1}, see Appendix B **Figure B-24**).

The destabilizing substituent interactions in *o*-formyl, *o*-vinyl and *o*-alkyl (methyl and ethyl) substituted styrenes are explained with repulsive steric effects [30]. It can be noted from **Table 4-3** that the ΔBDE values for the *β*-C—H bonds in these molecules are small. Therefore the substituent effects in the corresponding *β*-styryl radicals must be close to those of the parents. For all these radicals, the destabilizing interactions are related to steric effects. These three NNIs are applied regardless of whether it is a trans- or cis-styryl radical.

VI. Benzyl and 1-Phenylethyl Radicals

Table 4-2 lists two prototypical reactions that yield benzyl radical: the scission of the C_α—H bond of the methyl group in toluene and the C_α—C_β bond scission of the ethyl group in ethylbenzene. Secondary benzyl radicals (1-phenylethyl) are formed by scission of the C_α—H bond in ethylbenzene. The BDE analyses of these three bonds and the substituent effects in the resulting substituted benzyl and 1-phenylethyl radicals are discussed in this section.

The BDE of the C—H bond in toluene is with 377 kJ mol^{-1} only about 10 kJ mol^{-1} higher than the BDE for the O—H bond in phenol (See **Table 4-2**) whereas the BDE of the C_α—H bond in ethylbenzene (364 kJ mol^{-1}) is similar to that in phenol. The approximately 10 kJ mol^{-1} change in bond strength is expected for the formation of a primary versus a secondary radical. The BDE of the C_α—C_β bond in ethylbenzene is much lower (324.7 kJ mol^{-1}) than the C_α—H bonds in toluene and ethylbenzene. The ΔBDE values for the C_α—H bonds in substituted toluenes and ethyl benzenes are shown **Figure 4-1 (h)** and **(i)**,respectively whereas the ΔBDE values for the C_α—C_β bonds in substituted ethylbenzenes are provided in the Appendix B **Figure B-26**. For these three bonds, it is found that the absolute values of most ΔBDEs are small and that most values are negative, indicating the tendency that substitution stabilizes benzyl and 1-phenylethyl radicals. Comparison between **Figure 4-1 (h)** and **(i)** shows that the ΔBDEs of these bonds generally follow very similar trends. Since the substituent effects in the parent molecules are similar [30], the same must be true for the radicals. Consequently, any NNI developed for substituted benzyl radicals is also applicable to substituted 1-phenylethyl radicals and hence, they are grouped together in **Table 4-3**. As mentioned above, the initial approximate values for the substitutent effects in substituted benzyl radicals can be calculated based on either the C_α—H bonds in substituted toluenes or the C_α—C_β bond in substituted

ethylbenzenes. In the following, the discussion will mainly focus on C_α—H bonds in substituted toluenes, nonetheless it should be kept in mind that it is possible to obtain the same initial approximates from the BDE analysis of C_α—C_β bonds in substituted ethyl benzenes (See **Table 4-3**).

The largest absolute ΔBDE value is calculated for Z = *p*-CH=CH_2 in both toluene and ethylbenzene. Since no substituent interaction is found in these parent molecules [30], a radical specific substituent interaction must exist which is stabilizing by roughly -6.0 kJ mol^{-1}. It is easily explained by resonance between the CH_2•/C•HCH_3 radical sites (+M effect) and the substituent -CH=CH_2 group (-M effect). The mesomeric effect is not operative when the -CH=CH_2 group is in *ortho* position as steric repulsion pushes the vinyl group out of the plane of the phenyl ring and thereby prevents resonance. Using ΔBDE of -1.2 kJ mol^{-1} for Z = *o*-CH=CH_2 and the known substituent effect in the parent molecules (4.6 kJ mol^{-1}), one calculates the overall NNI in *o*-vinyl benzyl radical as 3.4 kJ mol^{-1}. In addition to the C_α—H bond in toluene, the BDE analyses of two more bonds are also considered (C_α—H and C_α—C_β bonds of *o*-vinylethylbenzene, See **Table 4-3**) to obtain the average approximate value of 4.2 kJ mol^{-1} for this NNI.

Based on the discussion of vinyl substituted benzyl and 1-phenylethyl radicals, one would expect similar interactions in formyl substituted benzyl radicals. This is indeed the case. Analysis of the C—H bond in *p*-CHO substituted toluene yields the value of -4.1 kJ mol^{-1} for the substituent effect in *p*-formylbenzyl radical. Taking the other two similar bonds into consideration (See **Table 4-3**), the preliminary NNI value for this interaction is calculated as -3.4 kJ mol^{-1} since the parent molecules have no substituent interactions (see **Table 4-3**). The mesomeric interaction between the CH_2•/C•HCH_3 radical sites (+M effect) and the

substituent -CHO group (-M effect) leads to this stabilization. For Z = *o*-CHO, steric hindrances exist in the substituted toluene and ethylbenzene (8.1 kJ mol^{-1}) and this repulsive effect causes the destabilization that is observed for the corresponding radicals. The magnitude of this destabilization, that is, the preliminary NNI value of this interactionis determined as 5.4 kJ mol^{-1}.

A rather large ΔBDE value is also found for the C_{α}—H bond in *p*-OCH_3 substituted toluene (-4.6 kJ mol^{-1}). No NNI is present in the parent *p*-methoxy toluene, which implies that a sizable stabilizing effect should be present in the radical. However, no NNI entry is listed in **Table 4-3** for this interaction**.** This can be explained in the following way: the deviation between the GA and the G4/BAC results for the parent molecule (*p*-methoxy toluene) is approximately 2.3 kJ mol^{-1}, hence a small substituent effect exists even though no NNI was derived [30]. If this substituent effect is taken into account, the BDE analysis yields a value of -2.3 kJ mol^{-1} for the substituent interaction in the corresponding radical which is also considered as too small to warrant a NNI correction term. This assessment is confirmed by the full optimization of all GAV/NNI parameters as will be discussed later.

Several previous studies addressed the change of BDEs of the C_{α}—H bond in toluene upon the presence of *para* substituents [92-96]. It was found that the benzyl radical is stabilized upon introduction of a substituent group, irrespective of whether the Z group is an electron donor or acceptor. The present findings confirm these conclusions since all *para*-Z-$C_6H_4CH_2$—H bonds are weaker than that in toluene.

4.4.3 Development of GAV and NNI parameters for Monocyclic Aromatic Radicals

The six GAVs needed for the GA calculation of the MARs studied in this work have been described in the Methodology section. The discussion of BDEs in the previous paragraphs indicated that significant NNIs exist in MARs, which must be accounted for. In Appendix B **Table B-6**, all NNIs defined in this study are listed and the types of interactions associated with the NNIs are briefly explained. Among these 29 NNIs, 28 provide, among others, corrections for the enthalpy of formation, while the remaining NNI is mainly defined to improve the entropy and heat capacity calculations in *o*-methyl benzyl and *o*-ethyl benzyl radicals. The initial estimates for the NNIs are deduced from the stability analyses of the radicals (BDE analyses) as described in the paragraphs above (See **Table 4-3**).

The optimal values for the GAV/NNI parameters are determined in three steps. First, the differences between G4/BAC and GA calculated thermochemical properties for a training set of 316 MARs (See Appendix B **Table B-1**) are minimized through the simultaneous linear regression of all new GAVs and NNIs. Second, transferability of these parameters is tested with a set of 53 MARs, which contains radicals not used in the regression (See Appendix B **Table B-11**). Third, the two data sets are combined and the final GAV/NNI parameters are determined by regression against this combined set.

I. Determination of Preliminary GAV/NNI Values

The training set encompasses single and double substituted MARs, along with a large number of triple substituted MARs. The latter are needed to improve the statistical significance of the regression results by making sure that each NNI appears in at least three radicals. In triple substituted MARs two of the three substituent groups have non-radical character. Their

interaction is taken into account by applying the corresponding NNIs for the closed-shell molecules as reported in the study of Ince et al. [30]. (See Appendix B **Table B-7** for a full list of these NNIs).

The preliminary GAVs and NNIs obtained from simultaneous linear regression analysis applied to the training set are given in Appendix B **Table B-8** and **Table B-9**, and the statistics of the linear regression can be found in Appendix B **Table B-10**. The deviations between G4/BAC and GA results are within 4 kJ mol^{-1} for $\Delta_f H^\circ$ for 286 radicals out of the 316 MARs in the training set. For S° at 298 K and heat capacities (C_p) at 300 K, the data for 11 and 12 MARs, respectively, deviate by more than 4 J mol^{-1} K^{-1}. Despite the large size of the training set, the MAD values are low for all three thermochemical properties. This indicates that the identified set of NNIs is capable of describing all important substituent interactions in the MARs.

II. Validation of the GAV/NNI Parameters

The set of preliminary GAV/NNI parameters obtained through the above-described training set are tested against thermodynamic properties of 53 radicals that are not a part of the training set. A list of the MARs in the validation set is available in Appendix B **Figure B-8** – **Figure B-13** and their thermochemical data calculated at the level of G4/BAC can be found in Appendix B **Table B-11**. The test molecules contain exclusively highly (triple and quadruple) substituted MARs, because all single and double substituted species have been used to identify and define the preliminary GAV/NNI values. Thus, this validation test mainly probes the applicability of additive NNI corrections towards multiple substituted aromatic radicals. For example, in 2,3,4-trihydroxyphenoxy radical, three hydroxyl groups in *o*-, *m*-, and *p*- position to the phenoxy group may interact with the radical site. In addition, the interactions among

these hydroxyl groups need to be accounted for. Application of all appropriate NNI corrections lead to GA calculated heat of formation that differs by only 3.3 kJ mol^{-1} from the G4/BAC $\Delta_f H^\circ$ value.

Comparisons between the GA calculations and the G4/BAC test set before and after the application of NNIs are available in Appendix B **Table B-12** for $\Delta_f H^\circ$ and S° at 298 K and C_p at 300 K. The predicted 53 $\Delta_f H^\circ$ values using the preliminary GAV/NNI parameters agree satisfactory with the G4/BAC data as the MAD of 2.7 kJ mol^{-1} and the MAX value of 7.4 kJ mol^{-1} show. Among these 53 MARs, 8 deviate by more than 4 kJ mol^{-1} and the MAX value is slightly higher than that of the training set (6.66 kJ mol^{-1}). In these multiple substituted MARs, the small errors in the predictions of individual substituent effects add up and lead to relatively higher deviations, nonetheless, given the complexity of the substituted MARs, they can be considered as satisfactory. Besides, in the following section, it is shown that these deviations decrease upon the final optimization of the GAV/NNI parameters. The statistics reported in Appendix B **Table B-12** also indicate that these parameters are similarly successful in reducing the deviations between G4/BAC and GA calculated entropies and heat capacities (C_p) for the MARs in the validation set.

Based on the comparisons with the validation set it can be concluded that the GAV/NNI set developed in this work can successfully be used for highly substituted MARs.

III. Final Set of GAV/NNI Parameters

As described above, the training and validation sets are combined, to the final set of 369 MARs. With this data set the optimal group additive parameters are determined via the linear regression procedure. The final GAV and NNI values together with their 97.5% confidence

intervals are given in **Table 4-4** and **Table 4-5**, respectively. Only the confidence intervals for heat capacities (C_p) at 300 K are provided – those for the other C_p data have similar or lower value (see Appendix B **Table B-13** and **Table B-14** for the confidence intervals for GAVs and NNIs of heat capacities at higher temperatures, respectively). These confidence intervals represent uncertainties due to statistical errors. Several sources of uncertainty exist, for example the uncertainties due to the spread of the available experimental data used to derive BAC values by Ince et al. [30], errors related with the use of temperature independent frequency scaling factors within the harmonic oscillator rigid rotor approximation or errors originating from the methodology followed during the hindered rotor treatment. Since quantification of these errors is beyond the scope of this work, only statistical uncertainties are reported. In **Table 4-5**, along with the regression results, the numbers of occurrences of the NNIs are provided. Every NNI parameter is derived from at least three different MARs to ensure statistical significance.

Table 4-4 GAVs for standard enthalpy of formation ($\Delta_f H^\circ$) and entropy (S°) at 298 K, and heat capacity (C_p) at various temperatures for the MARs of the final database.[a]

GAVs	$\Delta_f H^\circ$	S°	C_p [J mol^{-1} K^{-1}]						
	[kJ mol^{-1}]	[J mol^{-1} K^{-1}]	300 K	400 K	500 K	600 K	800 K	1000 K	1500 K
Ċ$_b$	270.6 ± 1.0	52.7 ± 0.9	12.0 ± 0.8	14.6	16.5	17.8	19.5	20.6	21.7
C$_b$-(Ȯ)	-16.5 ± 1.4	73.3 ± 1.2	28.0 ± 1.0	32.8	36.4	38.9	42.2	44.2	45.7
O-(Ċ)(C$_b$)	-130.1 ± 1.1	28.3 ± 0.9	15.5 ± 0.8	19.8	21.1	21.4	21.0	20.9	20.4
C$_b$-(CȮ)	48.3 ± 1.3	102.5 ± 1.1	43.0 ± 0.9	48.9	53.6	57.0	61.4	63.9	65.9
Ċ-(C$_b$)(H)$_2$	113.0 ± 0.9	111.7 ± 0.8	27.2 ± 0.7	33.6	38.7	42.5	48.0	52.1	58.5
Ċ-(C$_b$)(C)(H)	124.8 ± 1.2	32.4 ± 1.1	21.7 ± 0.9	26.0	30.1	33.0	37.0	40.1	44.0

[a]The standard deviations are for 97.5% confidence intervals.

Table 4-5 NNI values[a] derived from the full G4/BAC radical set for standard enthalpies of formation ($\Delta_f H^\circ$) and standard entropies (S°) at 298 K and heat capacities (C_p) at various temperatures.

NNI #	Description of Interaction[b]	$\Delta_f H^\circ$	S°	C_p[J mol^{-1} K^{-1}]							#[c]
		[kJ mol^{-1}]	[J mol^{-1} K^{-1}]	300 K	400 K	500 K	600 K	800 K	1000 K	1500 K	
NNI1	*p*-OH/OCH_3-$C_6H_4OCH_2$•	6.0 ± 2.3	3.8 ± 2.0	0.4 ± 1.7	-0.8	-1.8	-2.4	-2.7	-2.5	-1.4	6
NNI2	*o*-OCH_3-$C_6H_4OCH_2$•	7.0 ± 2.8	-4.8 ± 2.4	2.2 ± 2.0	5.0	6.0	5.8	4.2	2.6	0.5	4
NNI3	*o*-CHO-$C_6H_4OCH_2$•	11.5 ± 2.2	1.2 ± 1.9	3.9 ± 1.6	0.9	-0.9	-1.5	-1.4	-1.2	-0.6	7
NNI4	*o*-OH-C_6H_4O•	-37.1 ± 1.5	-10.6 ± 1.3	-8.6 ± 1.1	-7.7	-6.6	-5.3	-3.1	-1.3	1.6	18
NNI5	*o*-OCH_3-C_6H_4O•	-6.4 ± 1.5	0.4 ± 1.3	-2.5 ± 1.1	-2.6	-2.2	-1.4	-0.3	0.2	0.5	17
NNI6	*m*-OCH_3-C_6H_4O•	-6.9 ± 2.2	-4.2 ± 1.9	0.9 ± 1.6	3.2	4.1	4.3	3.4	2.3	0.9	7
NNI7	*p*-OH/OCH_3-C_6H_4O•	-15.8 ± 1.7	-2.8 ± 1.5	-2.8 ± 1.3	-2.5	-1.9	-1.2	-0.1	0.7	1.6	12
NNI8	*o*-CHO-C_6H_4O•	5.7 ± 1.4	-0.4 ± 1.3	-0.9 ± 1.1	-0.1	0.8	1.7	2.9	2.9	1.7	21
NNI9	*m*-CHO-C_6H_4O•	4.7 ± 1.9	3.6 ± 1.6	1.6 ± 1.4	1.6	1.6	1.6	1.2	0.9	0.5	10
NNI10	*o*-$CH=CH_2$-C_6H_4O•	-6.4 ± 2.2	-3.7 ± 1.9	0 ± 1.6	0.0	0.1	0.4	1.0	1.3	1.5	7
NNI11	*p*-$CH=CH_2$-C_6H_4O•	-12.9 ± 3.2	-3 ± 2.7	0.3 ± 2.3	0.2	0.2	0.5	0.9	1.2	1.1	3
NNI12	*o*-CH_3/CH_2CH_3-C_6H_4O•	-8.6 ± 1.5	1.1 ± 1.3	-0.6 ± 1.1	-0.5	-0.4	-0.2	-0.2	-0.1	-0.2	13
NNI13	*p*-CH_3/CH_2CH_3-C_6H_4O•	-5.8 ± 2.3	0.3 ± 2.0	-0.7 ± 1.7	-0.5	-0.4	-0.4	-0.3	-0.2	-0.2	6
NNI14	*o*-OH-C_6H_4C•=O	-16.8 ± 1.8	-19.1 ± 1.6	-6.4 ± 1.3	-4.5	-2.9	-1.0	2.3	4.7	6.9	12
NNI15	*p*-OH/OCH_3-C_6H_4C•=O	-8.6 ± 1.9	-3.7 ± 1.6	-3.3 ± 1.3	-2.7	-2.0	-1.0	0.2	0.8	1.5	11
NNI16	*o*-OCH_3-C_6H_4C•=O	7.4 ± 2.3	2.4 ± 1.9	2.5 ± 1.6	1.4	0.4	0.0	-0.6	-0.8	-0.7	7
NNI17	*m*-CHO-C_6H_4C•=O	4.6 ± 2.3	3.4 ± 2.0	0.3 ± 1.7	0.7	0.7	0.5	0.0	-0.3	0.1	6
NNI18	*p*-CHO-C_6H_4C•=O	5.4 ± 3.3	13.6 ± 2.8	-1 ± 2.3	-2.4	-3.5	-4.1	-4.5	-4.3	-3.2	3
NNI19	*o*-$CH=CH_2$-C_6H_4C•=O	4 ± 2.4	-5.8 ± 2.1	3.2 ± 1.7	3.5	3.2	2.6	1.5	0.6	0.1	6
NNI20	*o*-OH-trans/cis-$C_6H_4CH=CH$•	-14.2 ± 1.8	-17.6 ± 1.6	-5.5 ± 1.3	-2.9	0.6	4.6	10.1	12.0	9.4	11
NNI21	*o*-CHO-trans/cis-$C_6H_4CH=CH$•	14.6 ± 1.6	-5.4 ± 1.4	2.2 ± 1.2	3.4	3.6	3.3	2.4	1.8	1.0	11
NNI22	*o*-$CH=CH_2$-trans/cis-$C_6H_4CH=CH$•	7.6 ± 1.6	-5.5 ± 1.4	2 ± 1.8	2.5	2.2	1.8	1.1	0.7	0.3	11
NNI23	*o*-CH_3/CH_2CH_3-trans/cis-$C_6H_4CH=CH$•	4.2 ± 1.3	-3.8 ± 1.1	2.9 ± 0.9	2.7	2.1	1.5	0.6	0.3	-0.1	19
NNI24	$C_6H_4CH=CH$•Cis Correction	-4.2 ± 1.0	-3.6 ± 0.8	1.4 ± 0.7	1.6	2.2	2.4	2.4	2.2	1.7	45
NNI25	*p*-$CH=CH_2$-$C_6H_4CH_2$•/C_6H_4C•HCH_3	-5.8 ± 2.1	-3.7 ± 1.8	0.9 ± 1.5	1.1	1.2	1.4	1.6	1.6	1.3	7
NNI26	*o*-$CH=CH_2$-$C_6H_4CH_2$•/C_6H_4C•HCH_3	6.7 ± 2.1	-0.5 ± 1.8	1.8 ± 1.5	1.2	0.6	0.1	-0.5	-0.7	-0.7	7
NNI27	*p*-CHO-$C_6H_4CH_2$•/C_6H_4C•HCH_3	-5.2 ± 2.2	0.6 ± 1.9	-1.2 ± 1.6	-0.9	-0.6	-0.4	-0.3	-0.1	0.3	6

NNI28	*o*-CHO-$C_6H_4CH_2$•/C_6H_4C•HCH_3	5.5 ± 1.7	1.9 ± 1.5	1.8 ± 1.3	2.1	1.8	1.2	0.4	-0.2	-0.5	8
NNI29	*o*-CH_3/CH_2CH_3-$C_6H_4CH_2$•/C_6H_4C•HCH_3	2.7 ± 1.4	-3.6 ± 1.2	3.4 ± 1.0	2.6	1.8	1.2	0.5	0.3	0.0	20

[a]97.5% confidence intervals for $\Delta_f H^\circ$ (298 K), S° (98 K), and C_p (300 K) are provided.
[b]Interaction between a nonradical Z group and the radical substituent on a phenyl fragment, for example, *o*-OH—C_6H_4O• corresponds to the substituent interaction between the OH group and the O• group.
[c]The number of radicals in which the NNI appears.

The deviations between G4/BAC and GA calculated $\Delta_f H^\circ$, S° at 298 K and C_p at various temperatures for all MARs of the full database are reported in **Table B-15** of Appendix B. In **Table 4-6**, the statistics for the final optimization of the GAV/NNI parameter set are given. The MAD between the GA and G4/BAC calculated $\Delta_f H^\circ$values is 1.99 kJ mol^{-1} and the maximum deviation is 6.30 kJ mol^{-1}. For the majority of the MARs (327 MARs out of 369), the deviations are smaller than 4 kJ mol^{-1}. The deviations are approximately normal distributed (Appendix B **Figure B-29**) which indicates that there is no obvious bias in the GA calculations towards certain substituent combinations. The agreements between GA and G4/BAC calculated $S^\circ$and C_p values, respectively, are also very good. The MAD values for these two thermochemical properties are 1.75 J mol^{-1} K^{-1} and < 1.33 J mol^{-1} K^{-1} (for all temperatures), respectively. For only 17 out of 369 species the entropy and the $C_{p(300\,K)}$ values deviate by more than 4 J mol^{-1} K^{-1}. Histograms showing the distributions of the S° and C_p differences are provided in Appendix B **Figure B-30** and **Figure B-31**, respectively. Again, these distributions are Gaussian-like shaped.

Table 4-6 Statistics for the linear regression analysis of the final set of GAVs and NNIs for the standard enthalpies of formation ($\Delta_f H^\circ$) and entropies (S°) at 298 K and heat capacities (C_p) at various temperatures.[a]

	$\Delta_f H^\circ$	S°	C_p [J mol^{-1} K^{-1}]						
	[kJ mol^{-1}]	[J mol^{-1} K^{-1}]	300 K	400 K	500 K	600 K	800 K	1000 K	1500 K
MAD	1.99	1.75	1.32	1.16	1.10	1.11	1.13	1.03	0.79
RMS	2.48	2.13	1.78	1.60	1.52	1.52	1.57	1.44	1.12
MAX	6.30	6.18	5.99	5.54	4.94	5.18	5.88	5.52	5.13
F	15778	10025	1743	3059	4222	4934	5667	7543	14067

[a]**F:** Significance; **MAD:** mean average deviation; **RMS:** root mean square; **MAX:** maximum deviation.

The statistical results indicate that the GA method provides reliable thermochemical data for multiple substituted monocyclic aromatic radicals within or close to "chemical accuracy", and that a rather small number of NNIs is required to achieve this level of accuracy.

IV. Application of GAV/NNI Parameters

To demonstrate the use of the GAVs (see **Table 4-4**) and the NNIs (see **Table 4-5**) reported in this study, the calculation of $\Delta_f H^\circ$ and S° for 2-hydroxy-4-methoxy-6-formylphenoxy radical is presented in the following. The structure of this radical is shown in **Scheme 4-2**. 10 GAVs and 3 NNIs are required to describe this radical. All the necessary information for the GA calculation of this MAR can be found in **Table 4-7**. The group assignments follow the numbering in **Scheme 4-2**. Only one radical-specific GAV is needed, which is the radial-adjacent C_b-(Ȯ) group typical for phenoxy radicals. All other 9 GAVs are nonradical aromatic groups which are taken from Ince et al. [30]. The summation of the GAVs for $\Delta_f H^\circ$ and S° yields the values of -403.0 kJ mol^{-1} and 461.3 J mol^{-1} K^{-1}, respectively. Considering that the G4/BAC values for $\Delta_f H^\circ$ and $S_{int}{}^\circ$ are -453.2 kJ mol^{-1} and 447.5 J mol^{-1} K^{-1}, respectively, there are significant differences (50.2 kJ mol^{-1} and 13.8 J mol^{-1} K^{-1}, respectively) between the results from the GA calculations and G4/BAC method.

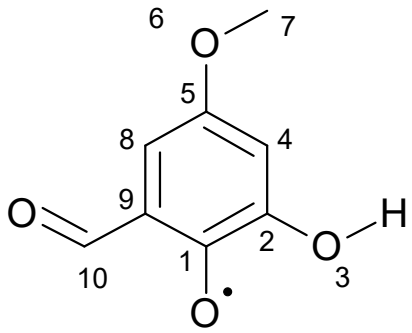

Scheme 4-2 2-hydroxy-4-methoxy-6-formylphenoxy.

Table 4-7 Application of GAVs/NNIs for the estimation of standard snthalpy of formation ($\Delta_f H^\circ$) and entropy (S°) of 2-Hydroxy-4-Methoxy-6-Formylphenoxy radical (see **Scheme 4-2**).[a]

GAVs				**NNIs**			
Center #	**GAVs**	$\Delta_f H^\circ$ [kJ mol^{-1}]	S_{int}° [J mol^{-1} K^{-1}]	**NNI**	**Interaction**	$\Delta_f H^\circ$ [kJ mol^{-1}]	S_{int}° [J mol^{-1} K^{-1}]
				Between Radical Group and Substituent (See **Table 4-6**)			
1	C_b-(Ȯ)	-16.5	73.3	**Interaction of O• and OH**			
2	C_b-(O)	24.0	-30.0	NNI4	*o*-O•+OH	-37.1	-10.6
3	O-(C_b)(H)	-188.1	106.3	**Interaction of O• and OCH_3**			
4	C_b-(H)	13.7	48.6	NNI7	*p*-O•+OCH_3	-15.8	-2.8
5	C_b-(O)	24.0	-30.0	**Interaction of O• and CHO**			
6	O-(C_b)(C)	-124.1	21.6	NNI8	*o*-O•+CHO	5.7	-0.4
7	C-(O)(H)$_3$	-42.9	127.1	**Interactions Between Substituents**[b]			
8	C_b-(H)	13.7	48.6	*m*-OH+OCH_3		-	-
9	C_b-(CO)	21.5	-33.5	*m*-OH+CHO		-	-
10	CO-(C_b)(H)	-128.3	129.3	*m*-OCH_3+CHO		-	-
$\sum GAVs$		-403.0	461.3	$\sum NNIs$		-47.2	-13.8
$\sum GAVs + NNIs$		-450.2	447.5				
Entropy Calculation				**Comparison of G4/BAC vs. GAVs/NNIs**			
σ_{int}	3 (Atom #7)	σ/n_{opt}	3			$\Delta_f H^\circ$ [kJ mol^{-1}]	S_{int}° [J mol^{-1} K^{-1}]
σ_{ext}	1	S° (G4/BAC)	440.3 J mol^{-1} K^{-1}	**G4/BAC**		-453.2	449.4
σ[c]	3	S_{int}° (G4/BAC)	449.4 J mol^{-1} K^{-1}	$\sum GAVs + NNIs$		-450.2	447.5
n_{opt}	1			(G4/BAC) - $\sum GAVs + NNIs$		-3.0	1.9

[a]Intrinsic entropy calculation (S_{int}°) and comparison of the G4/BAC results with GA calculated values are also provided.
[b]Ince et al. [30] did not define any NNI correction for the three nonradical substituent interactions in this radical.
[c]σ represents the total symmetry number which is necessary for the calculation of intrinsic entropies (see Eq. (4-6))

This points to significant substituent interactions exist in the 2-hydroxy-4-methoxy-6-formylphenoxy radical. The sum of all applicable NNIs amounts to corrections of -47.2 kJ mol^{-1} for the enthalpy and -13.8 J mol^{-1} K^{-1} for the entropy. All NNIs of this example are related to interactions between the radical site and the three non-radical substituent groups, while no NNI exist among the non-radical groups themselves. The appropriate NNIs are **NNI4**, **NNI7** and **NNI8** to account for the interactions of the oxygen radical moiety (O•) with *o*-OH, *p*-OCH_3 and *o*-CHO groups, respectively.

By adding the NNI contributions to the sum of GAVs, the final values for $\Delta_f H^\circ$ and S° are obtained as -450.2 kJ mol^{-1} and 447.5 J mol^{-1} K^{-1}, respectively. They are in good agreement with the G4/BAC data. The deviations are -3.0 kJ mol^{-1} and 1.9 J mol^{-1} K^{-1} for $\Delta_f H^\circ$ and S°, respectively, for this quadruple substituted MAR.

4.5 Summary and Conclusions

The thermodynamic properties of 369 MAH radicals (phenyl, phenoxy, anisyl, benzoyl, styryl, and benzyl) with six different substituents (-OH, -OCH_3, -CHO, -$CH{=}CH_2$, -CH_3 and -CH_2CH_3) have been calculated with the bond additivity corrected G4 level of theory. The obtained heats of formation are combined with the previously calculated values for multiply substituted MAHs to calculate BDEs. Deviations in the BDEs forming substituted MARs from that for the un-substituted radical are used to identify NNIs within the MAH radicals.

To extend the application of Benson's Group Additivity (GA) method to the monocyclic aromatic radicals, 6 new GAVs and 29 NNIs are determined. The thermodynamic data obtained with the optimized GAV and NNI parameters agree very well with the reference data set. The MAD are 1.99 kJ mol^{-1} for $\Delta_f H^\circ$, 1.75 J mol^{-1} K^{-1} for S° at 298 K and less than 1.32 J

mol^{-1} K^{-1} for C_p values at all studied temperatures. Group additivity-based enthalpies are mostly within 4 kJ mol^{-1} for the *ab initio* values. Similarly, the entropies and the heat capacities for the majority of the radicals are reproduced to within 4 J mol^{-1} K^{-1}, which demonstrates the high accuracy obtained with the GAV/NNI set calculated in this study. Further validation using triple-substituted and quadruple-substituted monocyclic aromatic radicals underscore the predictive capability. Combined with previously published set of GAVs for the MAHs, an internally consistent set of group additivity parameters is now available for MAH radicals. Furthermore, being consistent with and complementary to other GAV sets developed in this laboratory for a variety of functionalized hydrocarbons, this data will help to extend the capability to create fundamentally based reliable kinetic models using state-of-the-art automated reaction mechanism generating tools.

4.6 Acknowledgments

The research leading to these results has received funding from the European Research Council under the European Union's Seventh Framework Programme (FP7/2007-2013)/ERC grant MADPII agreement n° 290793. The SBO project "Bioleum" (IWT-SBO 130039) supported by the Institute for Promotion of Innovation through Science and Technology in Flanders (IWT) is acknowledged. This work was carried out using the STEVIN Supercomputer Infrastructure at Ghent University, funded by Ghent University, the Flemish Supercomputer Center (VSC), the Hercules Foundation and the Flemish Government – department EWI.

4.7 References

[1] Wiseman P. Ethylene by naphtha cracking. Free radicals in action. *Journal of Chemical Education.* 1977;54(3):154.

[2] Studebaker ML. The Chemistry of Carbon Black and Reinforcement. *Rubber Chemistry and Technology.* 1957;30(5):1400-1483.

[3] Boehm HP. Some aspects of the surface chemistry of carbon blacks and other carbons. *Carbon.* 1994;32(5):759-769.

[4] Kozlov A, Svishchev D, Donskoy I, Shamansky V. Impact of gas-phase chemistry on the composition of biomass pyrolysis products. *Journal of Thermal Analysis and Calorimetry.* 2015;122(3):1089-1098.

[5] Nakamura K, Yamada Y, Takada Y, Mokudai T, Ikai H, Inagaki R, Kanno T, Sasaki K, Kohno M, Niwano Y. Corrosive effect of disinfection solution containing hydroxyl radicals generated by photolysis of H_2O_2 on dental metals. *Dental Materials Journal.* 2012;31(6):941-946.

[6] Priddy DB. Recent Advances In Styrene Polymerization. *Polymer Synthesis.* 1994;111:67-114.

[7] Wallington TJ, Kaiser EW, Farrell JT. Automotive fuels and internal combustion engines: a chemical perspective. *Chemical Society Reviews.* 2006;35(4):335-347.

[8] Cook NC, Samman S. Flavonoids—Chemistry, metabolism, cardioprotective effects, and dietary sources. *The Journal of Nutritional Biochemistry.* 1996;7(2):66-76.

[9] Freeman B. Free radical chemistry of nitric oxide : Looking at the dark side. *Chest.* 1994;105:79S-84S.

[10] Atkinson R, Carter WPL. Kinetics and mechanisms of the gas-phase reactions of ozone with organic compounds under atmospheric conditions. *Chemical Reviews.* 1984;84(5):437-470.

[11] Monks PS. Gas-phase radical chemistry in the troposphere. *Chemical Society Reviews.* 2005;34(5):376-395.

[12] Shukla B, Susa A, Miyoshi A, Koshi M. Role of Phenyl Radicals in the Growth of Polycyclic Aromatic Hydrocarbons. *The Journal of Physical Chemistry A.* 2008;112(11):2362-2369.

[13] Zhang F, Jones B, Maksyutenko P, Kaiser RI, Chin C, Kislov VV, Mebel AM. Formation of the Phenyl Radical [C6H5(X2A1)] under Single Collision Conditions: A Crossed Molecular Beam and ab Initio Study. *Journal of the American Chemical Society.* 2010;132(8):2672-2683.

[14] Albright LF, Marek JC. Mechanistic model for formation of coke in pyrolysis units producing ethylene. *Industrial & Engineering Chemistry Research.* 1988;27(5):755-759.

[15] Appel J, Bockhorn H, Frenklach M. Kinetic modeling of soot formation with detailed chemistry and physics: laminar premixed flames of C2 hydrocarbons. *Combustion and Flame.* 2000;121(1–2):122-136.

[16] Li L, Fan H, Hu H. A theoretical study on bond dissociation enthalpies of coal based model compounds. *Fuel.* 2015;153(0):70-77.

[17] Da Silva G, Chen CC, Bozzelli JW. Bond dissociation energy of the phenol O-H bond from ab initio calculations. *Chemical Physics Letters.* 2006;424(1-3):42-45.

[18] Miranda MS, Esteves da Silva JCG, Liebman JF. Gas-phase thermochemical properties of some tri-substituted phenols: A density functional theory study. *The Journal of Chemical Thermodynamics.* 2015;80(0):65-72.

[19] Britt PF, Buchanan AC, Cooney MJ, Martineau DR. Flash Vacuum Pyrolysis of Methoxy-Substituted Lignin Model Compounds. *The Journal of Organic Chemistry.* 2000;65(5):1376-1389.

[20] Jarvis MW, Daily JW, Carstensen H-H, Dean AM, Sharma S, Dayton DC, Robichaud DJ, Nimlos MR. Direct Detection of Products from the Pyrolysis of 2-Phenethyl Phenyl Ether. *The Journal of Physical Chemistry A.* 2011;115(4):428-438.

[21] Mohan D, Pittman CU, Steele PH. Pyrolysis of Wood/Biomass for Bio-oil: A Critical Review. *Energy & Fuels.* 2006;20(3):848-889.

[22] Ranzi E. A wide-range kinetic modeling study of oxidation and combustion of transportation fuels and surrogate mixtures. *Energy & Fuels.* 2006;20(3):1024-1032.

[23] Norinaga K, Deutschmann O, Saegusa N, Hayashi J-I. Analysis of pyrolysis products from light hydrocarbons and kinetic modeling for growth of polycyclic aromatic hydrocarbons with detailed chemistry. *Journal of Analytical and Applied Pyrolysis.* 2009;86(1):148-160.

[24] Sabbe MK, Van Geem KM, Reyniers M-F, Marin GB. First Principle-Based Simulation of Ethane Steam Cracking. *AIChE Journal.* 2011;57(2):482-496.

[25] Saggese C, Sánchez NE, Frassoldati A, Cuoci A, Faravelli T, Alzueta MU, Ranzi E. Kinetic Modeling Study of Polycyclic Aromatic Hydrocarbons and Soot Formation in Acetylene Pyrolysis. *Energy & Fuels.* 2014;28(2):1489-1501.

[26] Kibet J, Khachatryan L, Dellinger B. Molecular Products and Radicals from Pyrolysis of Lignin. *Environmental Science & Technology.* 2012;46(23):12994-13001.

[27] Hu J, Shen D, Xiao R, Wu S, Zhang H. Free-Radical Analysis on Thermochemical Transformation of Lignin to Phenolic Compounds. *Energy & Fuels.* 2013;27(1):285-293.

[28] Bährle C, Custodis V, Jeschke G, van Bokhoven JA, Vogel F. In situ Observation of Radicals and Molecular Products During Lignin Pyrolysis. *ChemSusChem.* 2014;7(7):2022-2029.

[29] Bai X, Kim KH, Brown RC, Dalluge E, Hutchinson C, Lee YJ, Dalluge D. Formation of phenolic oligomers during fast pyrolysis of lignin. *Fuel.* 2014;128(0):170-179.

[30] Ince A, Carstensen H-H, Reyniers M-F, Marin GB. First-principles based group additivity values for thermochemical properties of substituted aromatic compounds. *AIChE Journal.* 2015;61(11):3858-3870.

[31] Rangarajan S, Bhan A, Daoutidis P. Rule-Based Generation of Thermochemical Routes to Biomass Conversion. *Industrial & Engineering Chemistry Research.* 2010;49(21):10459-10470.

[32] Vandewiele NM, Van Geem KM, Reyniers M-F, Marin GB. Genesys: Kinetic model construction using chemo-informatics. *Chemical Engineering Journal.* 2012;207:526-538.

[33] Ratkiewicz A, Truong TN. A canonical form of the complex reaction mechanism. *Energy.* 2012;43(1):64-72.

[34] Karaba A, Zamostny P, Lederer J, Belohlav Z. Generalized Model of Hydrocarbons Pyrolysis Using Automated Reactions Network Generation. *Industrial & Engineering Chemistry Research.* 2013;52(44):15407-15416.

[35] Kim Y, Kim WY. Universal Structure Conversion Method for Organic Molecules: From Atomic Connectivity to Three-Dimensional Geometry. *Bulletin of the Korean Chemical Society.* 2015;36(7):1769-1777.

[36] Broadbelt LJ, Stark SM, Klein MT. Computer Generated Pyrolysis Modeling: On-the-Fly Generation of Species, Reactions, and Rates. *Industrial & Engineering Chemistry Research.* 1994;33(4):790-799.

[37] Broadbelt LJ, Stark SM, Klein MT. Computer generated reaction networks: on-the-fly calculation of species properties using computational quantum chemistry. *Chemical Engineering Science.* 1994;49(24):4991-5010.

[38] Magoon GR, Green WH. Design and implementation of a next-generation software interface for on-the-fly quantum and force field calculations in automated reaction mechanism generation. *Computers & Chemical Engineering.* 2013;52:35-45.

[39] Benson SW, Buss JH. Additivity Rules for the Estimation of Molecular Properties - Thermodynamic Properties. *Journal of Chemical Physics.* 1958;29(3):546-572.

[40] Benson SW. *Thermochemical kinetics; methods for the estimation of thermochemical data and rate parameters*. New York: Wiley; 1968.

[41] Benson SW, Cruickshank FR, Golden DM, Haugen G, O'Neal HE, Rodgers AS, Shaw R, Walsh R. Additivity rules for the estimation of thermochemical properties. *Chemical Reviews.* 1969;69(3):279-324.

[42] Benson SW. *Thermochemical kinetics : methods for the estimation of thermochemical data and rate parameters*. 2d ed. New York: Wiley; 1976.

[43] Sabbe MK, Saeys M, Reyniers M-F, Marin GB, Van Speybroeck V, Waroquier M. Group Additive Values for the Gas Phase Standard Enthalpy of Formation of Hydrocarbons and Hydrocarbon Radicals. *The Journal of Physical Chemistry A.* 2005;109(33):7466-7480.

[44] Sabbe MK, De Vleeschouwer F, Reyniers M-F, Waroquier M, Marin GB. First Principles Based Group Additive Values for the Gas Phase Standard Entropy and Heat Capacity of Hydrocarbons and Hydrocarbon Radicals. *The Journal of Physical Chemistry A.* 2008;112(47):12235-12251.

[45] Vandeputte AG, Sabbe MK, Reyniers MF, Marin GB. Modeling the gas-phase thermochemistry of organosulfur compounds. *Chemistry – A European Journal.* 2011;17(27):7656-7673.

[46] Paraskevas PD, Sabbe MK, Reyniers M-F, Papayannakos N, Marin GB. Group Additive Values for the Gas-Phase Standard Enthalpy of Formation, Entropy and Heat Capacity of Oxygenates. *Chemistry – A European Journal.* 2013;19(48):16431-16452.

[47] Lay T, Bozzelli J, Dean A, Ritter E. Hydrogen Atom Bond Increments for Calculation of Thermodynamic Properties of Hydrocarbon Radical Species. *Journal of Physical Chemistry.* 1995;99(39):14514-14527.

[48] Frisch MJ, Trucks GW, Schlegel HB, Scuseria GE, Robb MA, Cheeseman JR, Scalmani G, Barone V, Mennucci B, Petersson GA, Nakatsuji H, Caricato M, Li X, Hratchian HP, Izmaylov AF, Bloino J, Zheng G, Sonnenberg JL, Hada M, Ehara M, Toyota K, Fukuda R, Hasegawa J, Ishida M, Nakajima T, Honda Y, Kitao O, Nakai H, Vreven T, Montgomery Jr. JA, Peralta JE, Ogliaro F, Bearpark MJ, Heyd J, Brothers EN, Kudin KN, Staroverov VN, Kobayashi R, Normand J, Raghavachari K, Rendell AP, Burant JC, Iyengar SS, Tomasi J, Cossi M, Rega N, Millam NJ, Klene M, Knox JE, Cross JB, Bakken V, Adamo C, Jaramillo J, Gomperts R, Stratmann RE, Yazyev O, Austin AJ, Cammi R, Pomelli C, Ochterski JW, Martin RL, Morokuma K, Zakrzewski VG, Voth GA, Salvador P, Dannenberg JJ, Dapprich S, Daniels AD, Farkas Ö, Foresman JB, Ortiz JV, Cioslowski J, Fox DJ. Gaussian 09, Version D.01. Wallingford, CT, USA: Gaussian, Inc.; 2009.

[49] Curtiss LA, Redfern PC, Raghavachari K. Gaussian-4 theory. *The Journal of Chemical Physics.* 2007;126(8):084108.

[50] Ayala PY, Schlegel HB. Identification and treatment of internal rotation in normal mode vibrational analysis. *The Journal of Chemical Physics.* 1998;108(6):2314-2325.

[51] Vansteenkiste P, Van Speybroeck V, Marin GB, Waroquier M. Ab initio calculation of entropy and heat capacity of gas-phase n-alkanes using internal rotations. *The Journal of Physical Chemistry A.* 2003;107(17):3139-3145.

[52] Van Speybroeck V, Vansteenkiste P, Neck DV, Waroquier M. Why does the uncoupled hindered rotor model work well for the thermodynamics of n-alkanes? *Chemical Physics Letters.* 2005;402(4-6):479-484.

[53] Vansteenkiste P, Van Neck D, Van Speybroeck V, Waroquier M. An extended hindered-rotor model with incorporation of Coriolis and vibrational-rotational coupling for calculating partition functions and derived quantities. *The Journal of Chemical Physics.* 2006;124(4):044314.

[54] Luo Y-R. *Handbook of Bond Dissociation Energies in Organic Compounds*. Hoboken: CRC Press; 2002.

[55] Petersson GA, Malick D, Wilson W, Ochterski J, Montgomery JA, Frisch MJ. Calibration and comparison of the Gaussian-2, complete basis set, and density functional methods for computational thermochemistry. *The Journal of Chemical Physics.* 1998;109(24):10570.

[56] Seeger R, Pople JA. Self-consistent molecular orbital methods. XVIII. Constraints and stability in Hartree–Fock theory. *The Journal of Chemical Physics.* 1977;66(7):3045-3050.

[57] Bauernschmitt R, Ahlrichs R. Stability analysis for solutions of the closed shell Kohn–Sham equation. *The Journal of Chemical Physics.* 1996;104(22):9047-9052.

[58] Cioslowski J, Liu GH, Martinov M, Piskorz P, Moncrieff D. Energetics and site specificity of the homolytic C-H bond cleavage in benzenoid hydrocarbons: An ab initio electronic structure study. *Journal of the American Chemical Society.* 1996;118(22):5261-5264.

[59] Vandeputte AG, Sabbe MK, Reyniers M-F, Van Speybroeck V, Waroquier M, Marin GB. Theoretical Study of the Thermodynamics and Kinetics of Hydrogen Abstractions from Hydrocarbons. *The Journal of Physical Chemistry A.* 2007;111(46):11771-11786.

[60] Menon AS, Radom L. Consequences of Spin Contamination in Unrestricted Calculations on Open-Shell Species: Effect of Hartree−Fock and Møller−Plesset Contributions in Hybrid and Double-Hybrid Density Functional Theory Approaches. *The Journal of Physical Chemistry A.* 2008;112(50):13225-13230.

[61] Blanquart G. Effects of spin contamination on estimating bond dissociation energies of polycyclic aromatic hydrocarbons. *International Journal of Quantum Chemistry.* 2015;115(12):796-801.

[62] Baker J, Scheiner A, Andzelm J. Spin contamination in density functional theory. *Chemical Physics Letters.* 1993;216(3):380-388.

[63] Roux MV, Temprado M, Chickos JS, Nagano Y. Critically Evaluated Thermochemical Properties of Polycyclic Aromatic Hydrocarbons. *Journal of Physical and Chemical Reference Data.* 2008;37(4):1855.

[64] Tsang W. Heats of formation of organic free radicals by kinetic methods. *Energetics of organic free radicals*: Springer; 1996:22-58.

[65] Stevens WR, Ruscic B, Baer T. Heats of Formation of C6H5•, C6H5+, and C6H5NO by Threshold Photoelectron Photoion Coincidence and Active Thermochemical Tables Analysis. *The Journal of Physical Chemistry A.* 2010;114(50):13134-13145.

[66] Ervin KM, DeTuri VF. Anchoring the Gas-Phase Acidity Scale†. *The Journal of Physical Chemistry A.* 2002;106(42):9947-9956.

[67] Gunion RF, Gilles MK, Polak ML, Lineberger W. Ultraviolet photoelectron spectroscopy of the phenide, benzyl and phenoxide anions, with ab initio calculations. *International Journal of Mass Spectrometry and Ion Processes.* 1992;117:601-620.

[68] Blanksby SJ, Ellison GB. Bond Dissociation Energies of Organic Molecules. *Accounts of Chemical Research.* 2003;36(4):255-263.

[69] Simões RG, Agapito F, Diogo HP, Da Piedade MEM. Enthalpy of Formation of Anisole: Implications for the Controversy on the O–H Bond Dissociation Enthalpy in Phenol. *The Journal of Physical Chemistry A.* 2014;118(46):11026-11032.

[70] Scheer AM, Mukarakate C, Robichaud DJ, Nimlos MR, Carstensen H-H, Ellison GB. Unimolecular thermal decomposition of phenol and d(5)-phenol: Direct observation of cyclopentadiene formation via cyclohexadienone. *Journal of Chemical Physics.* 2012;136(4).

[71] Suryan MM, Kafafi SA, Stein SE. The thermal decomposition of hydroxy- and methoxy-substituted anisoles. *Journal of the American Chemical Society.* 1989;111(4):1423-1429.

[72] Arends IWCE, Louw R, Mulder P. Kinetic study of the thermolysis of anisole in a hydrogen atmosphere. *The Journal of Physical Chemistry.* 1993;97(30):7914-7925.

[73] Pratt DA, de Heer MI, Mulder P, Ingold KU. Oxygen−Carbon Bond Dissociation Enthalpies of Benzyl Phenyl Ethers and Anisoles. An Example of Temperature Dependent Substituent Effects. *Journal of the American Chemical Society.* 2001;123(23):5518-5526.

[74] Lund H, Daasbjerg K, Ochiallini D, Pedersen S. Potentials and reactions of some electrogenerated radicals. *Russian Journal of Electrochemistry.* 1995;31(9):865-872.

[75] Ellison GB, Davico GE, Bierbaum VM, DePuy CH. Thermochemistry of the benzyl and allyl radicals and ions. *International Journal of Mass Spectrometry and Ion Processes.* 1996;156(1–2):109-131.

[76] Pedley JB. *Thermochemical data of organic compounds*. 2nd ed. London : Chapman and Hall; 1986.

[77] Denisov ET, Denisova T. *Handbook of antioxidants: bond dissociation energies, rate constants, activation energies, and enthalpies of reactions.* Vol 100: CRC press; 1999.

[78] Burgess DR. *"Thermochemical Data" in NIST Chemistry WebBook, NIST Standard Reference Database Number 69*. Gaithersburg MD, 20899: National Institute of Standards and Technology; 2005.

[79] Fenwick J, Harrop D, Head A. Thermodynamic properties of organic oxygen compounds 41. Enthalpies of formation of eight ethers. *The Journal of Chemical Thermodynamics.* 1975;7(10):943-954.

[80] Lebedeva ND, Katin YA. Heats of combustion of certain monosubstituted benzenes. *Russian Journal of Physical Chemistry.* 1972;46:1.

[81] Simões JAM, Griller D. Enthalpy of formation of the benzoyl radical by photoacoustic calorimetry. *Chemical Physics Letters.* 1989;158(1–2):175-177.

[82] Van Speybroeck V, Marin GB, Waroquier M. Hydrocarbon Bond Dissociation Enthalpies: From Substituted Aromatics to Large Polyaromatics. *ChemPhysChem.* 2006;7(10):2205-2214.

[83] Lucarini M, Pedrielli P, Pedulli GF, Cabiddu S, Fattuoni C. Bond Dissociation Energies of O−H Bonds in Substituted Phenols from Equilibration Studies. *The Journal of Organic Chemistry.* 1996;61(26):9259-9263.

[84] Wright JS, Johnson ER, DiLabio GA. Predicting the activity of phenolic antioxidants: theoretical method, analysis of substituent effects, and application to major families of antioxidants. *Journal of the American Chemical Society.* 2001;123(6):1173-1183.

[85] Beste A, Buchanan AC. Computational Study of Bond Dissociation Enthalpies for Lignin Model Compounds. Substituent Effects in Phenethyl Phenyl Ethers. *The Journal of Organic Chemistry.* 2009;74(7):2837-2841.

[86] Klein E, Lukes V. Study of gas-phase O-H bond dissociation enthalpies and ionization potentials of substituted phenols - Applicability of ab initio and DFT/B3LYP methods. *Chemical Physics.* 2006;330(3):515-525.

[87] Chandra A, Uchimaru T. The O-H Bond Dissociation Energies of Substituted Phenols and Proton Affinities of Substituted Phenoxide Ions: A DFT Study. *International Journal of Molecular Sciences.* 2002;3(4):407.

[88] Bennett JE, Mile B. ESR studies of the acetyl and benzoyl radicals. *Transactions of the Faraday Society.* 1971;67(0):1587-1597.

[89] Mendenhall GD, Protasiewicz JD, Brown CE, Ingold KU, Lusztyk J. 5-Endo Closure of the 2-Formylbenzoyl Radical. *Journal of the American Chemical Society.* 1994;116(5):1718-1724.

[90] Bennett J, Howard J. ESR spectrum of the α-styryl radical. *Chemical Physics Letters.* 1971;9(5):460-462.

[91] Bonazzola L, Fenistein S, Marx R. Electronic structure of α-substituted vinyl radicals. *Molecular Physics.* 1971;22(4):689-695.

[92] Wu Y-D, Lai DKW. A Density Functional Study of Substituent Effects on the O−H and O−CH3 Bond Dissociation Energies in Phenol and Anisole. *The Journal of Organic Chemistry.* 1996;61(22):7904-7910.

[93] Bean GP. An AM1 study of the effect of substituents on the bond dissociation energies of anilines, phenols, and α-substituted toluenes. *Tetrahedron.* 2002;58(50):9941-9948.

[94] Bordwell F, Zhang S, Zhang X-M, Liu W-Z. Homolytic bond dissociation enthalpies of the acidic HA bonds caused by proximate substituents in sets of methyl ketones, carboxylic esters, and carboxamides related to changes in ground state energies. *Journal of the American Chemical Society.* 1995;117(27):7092-7096.

[95] Viehe HG, Janousek Z, Merényi R. *Substituent effects in radical chemistry*: Springer; 1986.

[96] Jiang X, Ji G. A self-consistent and cross-checked scale of spin-delocalization substituent constants, the .sigma.JJ.bul. scale. *The Journal of Organic Chemistry.* 1992;57(22):6051-6056.

Chapter 5

Thermodynamics of Toluene Derivatives and Benzylic Radicals

This chapter is planned to be submitted as a manuscript for publication with the following title:

Modeling of Thermodynamics of Toluene Derivatives and Benzylic Radicals Via Group Additivity

Authors: Alper Ince, Hans-Heinrich Carstensen, Maarten Sabbe, Marie-Françoise Reyniers and Guy B. Marin

5.1 Abstract

The thermodynamic properties of unsubstituted, mono-, di- and trisubstituted toluene derivatives and benzylic radicals with hydroxy, methoxy, formyl, vinyl, methyl and ethyl substituents are calculated with the bond additivity corrected (BAC) post-Hartree-Fock CBS-QB3 method. Benson's Group Additivity scheme is extended to toluene derivatives by determining 6 group additive value (GAV) and 5 non-nearest neighbor interaction (NNI) parameters through least squares regression to a database of thermodynamic properties of 168 compounds and to benzylic radicals by defining 6 GAV and 14 NNI parameters based on a set of 168 radicals via the same methodology as for the toluene derivatives. Comparison between CBS-QB3/BAC and GA calculated thermodynamic values shows that the standard enthalpies of formation generally agree within 4 kJ mol^{-1}, whereas the entropies and the heat capacities generally deviate less than 4 J mol^{-1} K^{-1}.

5.2 Introduction

For more than a decade, a consistent database of Group Additivity (GA) parameters to calculate thermodynamic properties of molecules relevant for the thermochemistry of H/C, H/C/S and H/C/O compounds via Benson's group additivity method is being developed at Laboratory for Chemical Technology (LCT) [1-4]. In **Chapters 3** and **4**, this database was successfully extended towards substituted monocyclic aromatic hydrocarbons and their corresponding radicals. In these chapters, it was shown that the influence of six lignin-relevant substituents, namely hydroxy (-OH), methoxy (-OCH_3), formyl (-CHO), vinyl (-$CH{=}CH_2$), methyl (-CH_3) and ethyl (-CH_2CH_3) on the enthalpy of formation ($\Delta_f H^\circ$), the entropy ($S°$) and heat capacities

(C_p) at different temperatures can accurately be calculated with a small number of physically meaningful correction factors, called non-nearest neighbor interactions or NNI. With the applicability of GA for aromatic hydrocarbons being established, the next step forward is to extend the research towards larger alkyl substituents. For example, lignin, the second largest component found in ligno-cellulosic biomass, consists of phenyl propanoid units and lignin pyrolysis products such as eugenol (2-methoxy-4-prop-2-enylphenol) [5] which contain C_3 alkyl groups. The GA parameters (GAVs) developed in earlier work are not sufficient to allow thermodynamic calculations for aromatic species with long unsaturated alkyl chains. Apart from lignin pyrolysis, aromatic species with extended hydrocarbon side chains are also important for several other industrial processes such as steam cracking of crude oils [6] and upgrading of heavy oils to transportation fuels [7]. Therefore, there is a need to apply GA to such molecules and, consequently, the aim of the present study is to develop GAVs and NNIs for substituted aromatic hydrocarbons and radicals with a single alkyl side chain. To keep the number of calculations manageable, six extended alkyl side chains are considered (see **Figure 5-1**), which correspond to the molecule classes of (1) isopropylbenzenes (2-phenylpropanes), (2) allylbenzenes (3-phenylpropenes), (3) α-methyl allylbenzenes (3-phenylbutenes), (4) α-vinyl allylbenzenes (3-phenyl-1,4-pentadiene), (5) diphenylmethanes (1-phenylmethylbenzene), and (6) 1,1-diphenylethanes (1-phenylethylbenzene) as well as their benzylic radicals. All molecules considered are toluene or benzyl derivatives. The selection of these target species has several reasons. First, while the chosen alkyl groups are bulkier than the toluenes and ethylbenzenes considered in the previous two chapters, they can directly be compared to these simpler toluene derivatives. Second, except for isopropyl benzenes, all classes contain unsaturated side chains which, due to their stiffness and π-electron systems, are

expected to be challenging for the GA method. Third, these species are important for future kinetic studies on H abstraction reactions from toluene derivatives and for the development of detailed kinetic mechanisms for lignin model compounds or for coke formation (e.g. the kinetic study that will be presented in **Chapter 6**).

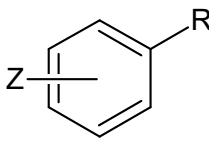

R = -$CH(CH_3)_2$, -$CH_2CH{=}CH_2$, -$CH(CH_3)CH{=}CH_2$, -$CH(CH{=}CH_2)_2$, -$CH_2C_6H_5$, -$CH(CH_3)C_6H_5$
Z = -OH, -OCH_3, -CHO, -$CH{=}CH_2$, -CH_3, -C_2H_5

Figure 5-1 The unsubstituted and substituted toluene derivatives with alkyl chains (**R**) and substituent groups (**Z**) of interest.

Due to the nature of the GA method, the development of new parameters faces several challenges which can be summarized by the need to keep the datasets internally consistent. Even though Benson's definition of a group as "a polyvalent atom in a molecule together with all its ligands" makes it generally easy to divide any molecule into well-defined groups, the contributions of these groups to the thermodynamic properties of a molecule are not uniquely defined in cases of linear dependencies (e. g. in case two groups always appear simultaneously such as the C_b-(C) and C-(C_b)$(H)_3$ groups in (-un)substituted toluenes). Therefore, some values should be assigned arbitrarily and GA calculations are only reliable if these linear dependencies are resolved in a consistent way. A second challenge is the choice of reference data needed to calibrate GA parameters. Here, it is important to ensure that all reference datasets are reliable and of similar quality. Finally, the introduction and definition of NNIs for non-nearest neighbor effects is not straightforward as no rules are available to identify NNIs. In recent work presented in **Chapter 3 and 4**, three factors have been taken into consideration in the identification of NNIs: (1) target accuracies have been established, amounting to 4 kJ mol^{-1} for the enthalpy of formation and 4 J mol^{-1} s^{-1} for entropy and C_p data and NNIs are defined if

these thresholds are severely missed, (2) systematic deviations of GA calculations are used to identify NNIs, (3) all NNI definitions are analyzed for their physical meaning that justifies the need for these correction parameters.

Taking the aforementioned challenges into account, the current work adopts the following approach to establish GAV and NNI parameters for toluene derivatives and for their benzylic radicals: (i) a database of accurate gas phase standard enthalpies of formation ($\Delta_f H°$), entropies ($S°$) and heat capacities ($C_p(T)$) for a set of 114 species (training set) is constructed using high level electronic structure calculations, (ii) the necessary GAVs are identified and these GAVs are applied to calculate thermodynamic properties of singly-substituted species, (iii) deficiencies in the group additively calculated results are used to identify those non-nearest-neighbor interactions (NNIs) that contribute significantly to the thermodynamic properties, (iv) the performance of this set of GAV and NNI parameters are tested with 54 species (validation set) not included in the training set, (v) the optimal new GAV and NNI parameters are regressed in a final step against the combined training and validation set.

5.3 Methodology

The calculation method has been thoroughly explained in the earlier chapters (**Chapters 3** and **4**) and with one exception, this study employs the theory as explained before. Therefore, only a brief description is provided here.

5.3.1 Thermodynamic data

All electronic structure calculations are performed with the Gaussian software packages [8]. In contrast to **Chapters 3** and **4** where the G4 level of theory [9] is used, energy calculations

are done with the CBS-QB3 [10] composite method. The reason is that using the G4 method for all molecules present in the data set is computationally too demanding. The reliability of the CBS-QB3 method for the species of interest will be discussed in the results section. CBS-QB3 calculations yield electronic energies at 0 K, optimized geometries and harmonic oscillator frequencies. This data is converted to standard enthalpy of formations ($\Delta_f H°$), entropies ($S°$) at 298 K and heat capacities (C_p) at various temperatures through statistical mechanical methods. Harmonic oscillator frequencies are scaled by the default factor of 0.99 [10] prior to their use and modes that resemble internal rotations are treated separately with the one dimensional hindered rotor (1D-HR) approach of Waroquier and coworkers [11-13]. The 1D-HR treatment significantly improves the calculated thermochemical properties [13], especially the entropies of molecules with multiple internal rotors. The hindrance potentials of internal rotations are determined with relaxed potential energy surface scans at the B3LYP/6-31G(d) level. Hindrance energies are obtained by changing the corresponding dihedral angle in steps of 10 degrees until full rotation is reached. These are expanded to a truncated Fourier series using the first six sine and cosine terms. The vibrational frequencies corresponding to these rotations are identified through visual inspection of the animated vibrations and their contributions to the partition function are replaced by the partition function of the hindered rotor. Only internal rotors with total barriers below 50 kJ mol^{-1} are evaluated separately, all other modes are treated as a harmonic oscillator. Internal rotations with very low barriers (less than 1 kJ mol^{-1}) are considered as free rotors. The reduced moment of inertia describing the rotation of the two molecule fragments around the axis which decouples internal from external rotation are calculated with the procedure described by Van Speybroeck et al. [12]. All thermochemical data calculated in the present study are based on the lowest energy conformer

of each molecule. The hindrance potentials of the internal rotors are used to determine low-energy structures, which are then evaluated at the CBS-QB3 level to identify the lowest energy conformer.

Standard enthalpies of formation $\Delta_f H°$ are obtained from spin-orbit (SO) corrected CBS-QB3 with the atomization energy method that is described in earlier chapters. These enthalpies are further improved with "Bond Additive Corrections" (BACs) [14]. The required BACs are taken from the earlier study in **Chapter 3 (Table 3-1)** and Paraskevas et al. [4].

In the benzylic radicals from unsubstituted and substituted allylbenzene (3-phenyl-1-propen-3-yl), α-methyl allylbenzene (3-phenyl-1-buten-3-yl) and α-vinyl allylbenzene (3-phenyl-1,4-pentadien-3-yl), classes, resonance stabilization plays a significant role. As the focus of this study is solely on benzylic radicals, BAC corrections are based on Lewis structures that preserve the phenyl ring. The latter structures are expected to provide a reasonable description of the electron configuration of the radical, e. g. in a benzyl radical the largest spin density is on the carbon atom that is bonded to the ring.

The standard entropy of a molecule (S°), which is calculated from the partition functions, contains contributions from molecular symmetry and possibly entropy of mixing if racemic mixtures of molecules are considered. In order to apply Benson's Group Additivity method [15], "symmetry-free" intrinsic entropy (S_{int}°) values are needed. These are obtained as follows:

$$S_{int}^{\circ} = S^{\circ} + R\, ln\, (\frac{\sigma}{n_{opt}}) \qquad (5\text{-}1)$$

In Eq. (5-1), σ represents the global symmetry number whereas n_{opt} is the number of optical isomers. The global symmetry number σ is the product of external symmetry number σ_{ext} and the internal symmetry numbers σ_{int}:

$$\sigma = \sigma_{ext} \prod_{k} \sigma_{int,k} \quad (5\text{-}2)$$

5.3.2 Derivation of GAV and NNI values

The GAV and the NNI values are determined through simultaneously optimizing the agreement between group additively calculated data and *ab initio* thermodynamic data for the aromatic species via unweighted least-squares analysis. In this linear regression analysis, the following objective function is minimized:

$$SSQ = \sum_{i}^{n} (y_i - \hat{y}_i)^2 \quad (5\text{-}3)$$

In Eq. (5-3), y_i is the *ab initio* calculated enthalpy of formation ($\Delta_f H°$), entropy ($S°$) or heat capacity (C_p(T)) of the radical i and $\hat{y}_i$ is the calculated thermochemical value via group additivity. This results in the equation:

$$\overline{GAV/NNI} = (X^T X)^{-1} X^T \bar{y} \quad (5\text{-}4)$$

In Eq. (5-4), $\overline{GAV/NNI}$ is the calculated vector of the group additive values and non-nearest neighbor interaction parameters and X is the occurrence matrix in which each row represents a molecule/radical and each column refers to a GAV or NNI. The elements of this matrix X_{ij} specify the number of occurrences of group *j* in molecule/radical *i*. Here, $\bar{y}$ is the vector of all y_i.

A statistical analysis is performed to assess the reliability of the linear regression step and the quality of the optimization procedure. The quality of the fits is expressed in terms of the significance (F) of the regression, the mean absolute deviation (MAD), root-mean square deviation (RMS) and maximum deviation (MAX) between *ab initio* data and the data obtained

via group additivity. The reported significance F of the regression is calculated with the following equation:

$$F = \frac{(\sum_{i=1}^{n} \hat{y}^2)/p}{(\sum_{i=1}^{n} (\hat{y}_i - y_i)^2)/(n-p)} \quad (5\text{-}5)$$

In Eq. (5-5), *n* is the number of molecules and *p* is the number of parameters.

5.4 GAV and NNI values from previous studies

In Benson's method, different types of carbon atoms are distinguished in terms of notation and the same notation is also adopted in this study. Benson's groups are indicated as X-(A)(B)(C)(D) where the central atom of the group, X, is separated from the ligands A, B, C and D with a "-". Groups that contain sp^3 type carbon atoms are denoted as 'C' whereas 'C_d', 'C_b' and '$\dot{C}$' represent double bonded carbon atoms, unfused aromatic carbon atoms and carbon atoms with a radical center, respectively. For example, a group with a double bonded carbon central atom, which has one carbon and one hydrogen atom as ligands is denoted as C_d-(C)(H).

To describe all species in the present study (See **Figures C-1** to **C-24** of Appendix C), in total 27 group additive values (GAVs) are required. Among these, 15 GAVs have already been defined in earlier studies, six are characteristic for the toluene derivatives studied and the remaining six GAVs are used to describe the corresponding benzylic radicals. The 15 known GAVs are listed in **Table 5-1**. The parameters for these GAVs are adopted from previous work (Ref. [1,2,4] and **Chapter 3**) and not subjected to optimization to ensure internal consistency with the previously developed GAV/NNI databases.

Table 5-1 GAVs taken from earlier studies [1,2,4].

Predefined GAVs	Source	$\Delta_f H^\circ$	S°	C_p [J mol^{-1} K^{-1}]						
		[kJ mol^{-1}]	[J mol^{-1} K^{-1}]	300 K	400 K	500 K	600 K	800 K	1000 K	1500 K
C_b-(H)	**Table 3-5**	13.7	48.6	13.3	18.4	22.7	26.2	31.3	34.8	40.1
C_b-(O)	**Table 3-5**	24.0	-30.0	12.1	12.6	15.0	17.4	21.3	23.5	26.0
C_b-(C)[a]	**Table 3-5**	23.5	-33.6	10.8	13.8	16.5	18.7	21.9	23.8	26.2
C_b-(CO)	**Table 3-5**	21.5	-33.7	16.4	17.8	19.7	21.6	24.4	26.6	27.4
C_b-(C_d)(H)	**Table 3-5**	24.3	-35.0	12.4	14.8	16.4	18.0	20.9	22.6	25.6
O-(C_b)(C)	**Table 3-5**	-124.1	21.6	20.3	24.2	25.1	24.8	23.7	23.1	22.0
C-(O)$(H)_3$	Ref. [4]	-42.9	127.1	25.3	32.1	38.4	44.1	53.4	60.6	72.5
O-(C_b)(H)	**Table 3-2**	-188.1	106.3	24.6	30.3	32.5	33.2	33.3	33.6	35.0
CO-(C_b)(H)	**Table 3-2**	-128.3	129.3	27.3	34.0	39.4	43.7	50.2	54.2	60.8
C_d-(C)(H)	Ref. [1,2]	37.1	32.9	18.4	21.7	25.0	28.0	32.7	36.1	41.2
C_d-(C_b)(H)	**Table 3-2**	30.4	25.7	18.1	24.1	29.1	32.7	37.1	40.0	43.1
C-(C_b)$(H)_3$	Ref. [1,2]	-42.9	127.2	25.0	31.8	38.2	43.9	53.2	60.5	72.3
C_d-$(H)_2$	Ref. [1,2]	25.1	115.8	20.6	25.8	30.8	34.9	41.4	46.4	54.6
C-(C_b)(C)$(H)_2$	**Table 3-5**	-20.6	38.6	24.9	30.7	36.0	40.4	47.3	52.3	60.0
C-(C)$(H)_3$	Ref. [1,2]	-42.9	127.2	25.3	32.1	38.4	44.1	53.4	60.6	72.5

[a] For the C_b-(C) group, instead of the older value from Sabbe et al. [1,2], the newer value from **Chapter 3** (**Table 3-5**) is used.

Generally, the GA description of radicals such as the benzylic radicals considered in this work requires two types of radical-specific GAVs: GAVs for radical-centered and radical adjacent groups. For hydrocarbon radicals, Sabbe et al. [1,2] showed that GAVs describing a radical adjacent group can be substituted by the analogous non-radical groups without significant loss of accuracy. Here, the same strategy is followed: only the six GAVs that are needed to describe the different radical centered groups in the investigated benzylic radicals are determined. This approach is applicable to the present set of benzylic radicals since these radicals do not possess any oxygen atom in the proximity of the radical center (i.e. oxygens appear in Z groups only) and thus, they can be considered as similar to the hydrocarbon radicals even though they possess oxygen atoms.

5.5 Results and Discussion

The objective of this study is to develop GAV and NNI parameters needed to calculate thermodynamic data for unsubstituted (C_6H_5R) or substituted ($Z_nC_6H_{5-n}R$) alkyl benzenes with extended alkyl groups R. As shown in **Figure 5-1**, six different alkyl groups (R) are considered and the substituent groups (Z) are chosen from the set Z = -OH, -OCH_3, -CHO, -$CH{=}CH_2$, -CH_3, -C_2H_5. To assign initial values to the newly defined GAVs and NNIs, a training set containing unsubstituted and single substituted alkyl benzenes with Z at the *ortho (o-)*, *meta (m-)* or *para (p-)* position relative to the alkyl group R is created. Each alkyl R leads to 19 entries and the training set molecules consists in total of 114 closed-shell molecules. Similarly, six different benzylic radicals R• exist and the corresponding training set has again 114 entries.

CBS-QB3/BAC calculations have been performed to assign accurate gas phase standard enthalpies of formation ($\Delta_f H°$), entropies ($S°$) and heat capacities ($C_p(T)$, at T = 300 K, 400 K, 500 K, 600 K, 800 K, 1000 K and 1500 K) to all molecules and radicals. The thermochemical data (See **Table C-1** and **Table C-2** of Appendix C for molecules and **Table C-3 a**nd **Table C-4** of Appendix C for radicals), are grouped by molecule class: isopropylbenzenes (Propan-2-yl)benzenes), allylbenzenes (3-phenylpropenes), α-methyl allylbenzenes (3-phenylbutenes), α-vinyl allylbenzenes (3-phenyl-1,4-pentadienes), diphenylmethanes (1-phenylmethylbenzenes) and 1,1-diphenylethanes (1-phenylethylbenzenes).

Although previous works of Sabbe et al. [1,2], Vandeputte et al. [3] and Paraskevas et al. [4] provide evidence for good accuracy of the CBS-QB3/BAC method, it is prudent to demonstrate this again for the types of molecules under investigation using the small number of entries in the NIST Thermochemical Database as experimental reference data [16].

Prosen et al. conducted static bomb calorimetry experiments to determine the $\Delta_f H°$ of isopropylbenzene [17] and they reported a value of 3.9 ± 1.1 kJ mol^{-1} which agrees well with the CBS-QB3/BAC value of 3.4 kJ mol^{-1}. The latter value is also close to the CBS-QB3/BAC data reported by Sabbe et al. (3.0 kJ mol^{-1}) [1], and the small difference mainly originates from the redefinition of BACs in **Chapter 3**. Nesternova et al. [18] found a heat of formation of -175.3 kJ mol^{-1} for hydroxy substituted isopropylbenzenes, regardless of the relative position of the -OH substituent, based on chemical equilibria experiments and concluded that no notable substituent effect on the overall $\Delta_f H°$ exists. This value and observation agrees well with the CBS-QB3/BAC results of -177.7 kJ mol^{-1}, -176.3 kJ mol^{-1} and -174.9 kJ mol^{-1} for *ortho*, *meta* and *para* hydroxy isopropylbenzene, respectively. For the gas phase $\Delta_f H°$ of diphenylmethane, Roux and Temprado [19] recommend a value of 163.7 ± 2.3 kJ mol^{-1} from corrections of liquid and solid phase heats of formation. This value agrees well with the CBS-QB3/BAC result of 162.0 kJ mol^{-1} in the present study.

Regarding monocyclic aromatic radicals (MARs), it was pointed out in **Chapters 3** and **4** that in general accurate thermodynamic data (enthalpies) can be obtained with the CBS-QB3 method although G4 was the preferred level of theory for the calculations. However, one exception is the $\Delta_f H°$ of the phenyl radical for which CBS-QB3/BAC yields a value of 355.6 mol^{-1}, which is remarkably higher than the experimental values reported by Tsang [20] (339.0 ± 8 kJ mol^{-1}) and by Stevens et al. (337.7 ± 2.5 kJ mol^{-1}) [21]. Recently, this problem has also been noted by Somers et al [22]. However, to study the relatively larger aromatics of interest within the framework of this study, G4 is computationally too costly to be applicable and therefore, CBS-QB3/BAC was selected as the method of choice. Comparison of BDEs for toluene and ethylbenzene shows that CBS-QB3/BAC results are in good agreement with either

experimental or G4/BAC calculated values. For example, for the C-H bond in toluene, CBS-QB3/BAC yields a BDE of 380.5 kJ mol^{-1}, the G4/BAC value is 377.0 kJ mol^{-1}. These values are close to the experimental value of 375.3±2.5 kJ mol^{-1} reported by Ellison et al. [23]. Similarly, for ethylbenzene (C_α-H bond), the CBS-QB3/BAC value is 367.5 kJ mol^{-1}, which is close to the G4 value of 364.7 kJ mol^{-1} and these values are in close proximity to the most recent experimental value of 364.1 kJ mol^{-1} by Denisov et al. [24].

GAV and NNI definitions and assignments for closed shell toluene derivatives and open-shell benzylic radicals will be discussed separately in the following paragraphs.

5.5.1 Group Additive Parameters for Toluene Derivatives

I. Preliminary GAVs and NNIs

All molecules of interest in this section belong to the class of toluene derivatives, which necessarily contain C_b-(H) and C_b-(C) groups next to those that describe the substituents. These two GAVs have been defined in previous studies and they are listed in **Table 5-1**. **Table 5-1** also contains all the required non-aromatic GAVs taken from earlier studies [1,2], e.g. C-(C)$(H)_3$, C_d-(C)(H) and C_d-$(H)_2$. The C-(C)$(H)_3$ group is needed for isopropylbenzene, whereas the groups C_d-(C)(H) and C_d-$(H)_2$ are found in allylbenzenes, α-methyl allylbenzenes and α-vinyl allylbenzenes. All these GAVs are kept at their reported values and are not subjected to optimization.

Each of the six toluene derivative classes contains one class specific GAV. Sabbe et al. previously reported GAVs for the C-(C_b)$(C)_2$(H), C-(C_b)(C_d)$(H)_2$ and C-(C_b)(C_d)(C)(H) groups, derived from isopropylbenzene, allylbenzene and α-methyl allylbenzene, respectively [1,2]. Unfortunately, the use of these pre-defined GAVs does not lead to an optimal

reproduction of the CBS-QB3/BAC data calculated in the current work. Since the current dataset is significantly larger compared to the one used by Sabbe et al., e.g. 30 molecules contain the C-(C_b)(C)$_2$(H) group, it was decided to re-optimize these values. The three remaining molecule classes – α-vinyl allylbenzene, diphenylmethane and 1,1-diphenylethane – contain the C-(C_b)(C_d)$_2$(H), C-(C_b)$_2$(H)$_2$ and C-(C_b)$_2$(C)(H) GAVs, which are currently not yet available in the GAV database. Therefore, GAV parameters for six molecular (non-radical) groups will be derived in this section.

While GAVs are sufficient to describe unsubstituted toluene derivatives, they fail to properly predict thermodynamic properties of some single-substituted toluene derivatives. This points to the presence of non-nearest neighbor interactions (NNIs) among the substituents. To account for these additional interactions, NNI correction terms need to be developed. The necessary NNIs are identified through deviations between *ab initio* calculated thermodynamic properties (See **Table C-1** of Appendix C) and GA calculations that use only GAVs. Preliminary values of GAVs are determined from a training set consisting of unsubstituted and single-substituted toluenes (see **Table C-5** of Appendix C). In some of the singly-substituted toluenes, significant deviations are encountered (see **Table C-6** of Appendix C for the deviations). These deviations provide initial guesses for the NNIs which are identified from them.

For the description of the substituent effects in isopropylbenzenes, the three NNIs that were previously defined in **Table 3-6** for toluenes/ethylbenzenes are used with alteration. Such a practice is followed since these NNIs are capable of correcting for the deficiencies between the *ab initio* and GA based thermochemical data sufficiently, as shown in **Table C-7** of Appendix C for four different *o*- substitutions (*o*-CHO, *o*-CH=CH_2, *o*-CH_3 and *o*-CH_2CH_3). Among the substituted isopropylbenzenes, only in these four cases, significant deficiencies are

encountered and accordingly, NNI corrections are defined for those. Moreover, the physical interpretation of the effects upon substitution by these four groups are similar for all of the three substituted alkylbenzenes (toluenes, ethylbenzenes and isopropylbenzenes) bringing further justification to this approach. To describe the substituent effects for the other five compound classes of interest, just five new NNIs had to be defined. These NNIs are named as "**NNITD** (NNI of toluene derivatives)" to distinguish them from those discussed later for benzylic radicals (**NNIBR**) and they will be discussed in-depth in the following paragraphs. In **Table 5-2**, the previously defined three NNIs (NNI*s) can be found along with the preliminary values for the newly defined NNIs.

After assigning initial values to the six new GAVs and five new NNIs using unsubstituted and singly-substituted toluenes, the values were refined through linear regression. The obtained values are documented in **Table C-9** and **Table C-10** of Appendix C, respectively. The deviations between GA and *ab initio* calculated thermodynamic properties before and after the inclusion of NNIs are reported in **Table C-11** of Appendix C to demonstrate the importance of non-nearest neighbor interactions. According to the results presented in this table, the mean absolute deviation (MAD) between the two datasets drop from 1.8 kJ mol^{-1} to 1.1 kJ mol^{-1} for the standard enthalpies of formation, from 4.5 J mol^{-1} K^{-1} to 1.7 J mol^{-1} K^{-1} for the entropies at 298 K, and from 2.4 J mol^{-1} K^{-1} to 1.2 J mol^{-1} K^{-1} for heat capacities at 300 K upon inclusion of NNIs. Introduction of NNIs also reduces the maximum absolute deviation (MAX) values significantly from 9.7 kJ mol^{-1} to 4.4 kJ mol^{-1} for $\Delta_f H°$, from 22.7 J mol^{-1} K^{-1} to 5.2 J mol^{-1} K^{-1} for $S°$, and from 9.5 J mol^{-1} K^{-1} to 5.0 J mol^{-1} K^{-1} for the heat capacities at 300 K.

Table 5-2 Non-nearest neighbor interactions (NNIs) in toluene derivatives (NNITDs) that are identified from the differences given in **Table C-6** of Appendix C.

NNI #	Toluene Derivatives $C_6H_5CH(X_1)(X_2)$	Substituent Group	Physical interpretation of the overall interaction	Preliminary $\Delta_f H^\circ$ value for the NNI[a] [kJ mol^{-1}]	Preliminary ΔS° value for the NNI[a] [J mol^{-1} K^{-1}]
NNI*1[b]	X_1 = -H X_2 = -H/-CH_3 (**NNI 8** in **Table 3-6**)	*o*-CHO	* SE[c] * Restriction of rotation: decrease in entropy	8.1[e]	-2.4[e]
	Applicable to X_1 = -CH_3 X_2 = -CH_3				
NNI*2[b]	X_1 = -H X_2 = -H/-CH_3 (**NNI 9** in **Table 3-6**)	*o*-CH=CH_2	* SE[c] * Restriction of rotation: decrease in entropy	4.6[e]	-5.7[e]
	Applicable to X_1 = -CH_3 X_2 = -CH_3				
NNI*3[b]	X_1 = -H X_2 = -H/-CH_3 (**NNI 13** in **Table 3-6**)	*o*-CH_3	* SE[c] * Restriction of rotation: decrease in entropy	4.2[e]	-6.6[e]
	Applicable to X_1 = -CH_3 X_2 = -CH_3	*o*-CH_2CH_3			
NNITD1	X_1 = -H X_2 = -CH=CH_2	*o*-OH	* HB[d] * Restriction of rotation: decrease in entropy	-9.4	-26.9
NNITD2	X_1 = -CH_3 X_2 = -CH=CH_2	*o*-OH	* Restriction of rotation: decrease in entropy	-1.8	-8.9
	X_1 = -H X_2 = -C_6H_5				
	X_1 = -CH_3 X_2 = -C_6H_5				
NNITD3	X_1 = -CH=CH_2 X_2 = -CH=CH_2	*o*-OH	* Stabilizing HB[d] vs. SE[c] * Restriction of rotation: decrease in entropy	-3.6	-16.4
NNITD4	X_1 = -H X_2 = -CH=CH_2	*o*-OCH_3	* Restriction of rotation: decrease in entropy	-0.1	-10.1
	X_1 = -CH_3 X_2 = -CH=CH_2				
	X_1 = -CH=CH_2 X_2 = -CH=CH_2				
	X_1 = -H X_2 = -C_6H_5				
	X_1 = -CH_3				

	X_2 = -C_6H_5				
NNITD5	X_1 = -H X_2 = -CH=CH_2	*o*-CHO	* SE[c] * Restriction of rotation: decrease in entropy	3.6	-10.5
	X_1 = -CH_3 X_2 = -CH=CH_2	*o*-CH=CH_2			
	X_1 = -CH=CH_2 X_2 = -CH=CH_2	*o*-CH_3			
	X_1 = -H X_2 = -C_6H_5	*o*-CH_2CH_3			
	X_1 = -CH_3 X_2 = -C_6H_5				

[a] These preliminary values are obtained from the simultaneous linear regression of **GAVs** and **NNIs** based on the training set.
[b] **NNI*1, NNI*2, NNI*3:** The three NNI*s for *o*-CHO, *o*-CH=CH_2 and *o*-CH_3/CH_2CH_3 substituted toluenes/ethylbenzenes, respectively are taken from **Chapter 3**. These parameters can effectively reproduce their isopropyl counterparts and no new NNIs (**NNITD**s) are defined in this study to capture these interactions (see text).
[c] **SE:** Steric effect.
[d] **HB:** Hydrogen Bond.
[e] The $\Delta_f H^\circ$ and ΔS° values for the NNIs are taken from **Chapter 3**.

The preliminary NNI values obtained for $\Delta_f H^\circ$ and S° as discussed above are included in **Table 5-2.** In this table, note that (a) only substituents in *ortho* position are found to cause significant non-nearest neighbor interactions, (b) except for **NNITD1** all enthalpy corrections are rather small and (c) all NNI corrections lead to significant losses in entropy. The last effect is not surprising because the methyl rotor in toluene is a free rotor and any interaction can introduce hindrances to this rotational mode. Also included in **Table 5-2** are brief descriptions of the physical effects that lead to the observed interactions. These will now be discussed in more detail.

The first three NNITDs account for interactions of an OH group in *o*- position to the alkyl group. In *o*-OH substituted allylbenzene (molecule **TDT2/2,** see **Figure C-25** of Appendix C), a hydrogen bond is formed between the allyl group (-$CH_2CH=CH_2$) and the -OH group. This causes a strong stabilizing effect of -9.4 kJ mol^{-1} (**NNITD1** in **Table 5-2**), but also a sharp decrease of the entropy (-26.9 J mol^{-1} K^{-1}). This interaction is shown in a three-dimensional molecular orbital representation (**Figure C-26** of Appendix C). **NNITD2** corrects interactions

of the *o*-OH group with three other toluene derivative classes: α-methyl allylbenzenes, diphenylmethanes and diphenylethanes. Although these molecules are quite different, similar interactions by *o*-OH are observed. In these molecules, unlike for the **NNITD1** case, the H atom of the OH group points away from the alkyl group as can be seen in **Figure C-27, C-28** and **C-29** of Appendix C (molecules **TDT3/2, TDT5/2, TDT6/2**). It is also noted that the lowest energy conformer structures of these molecules are roughly 5.5 kJ mol^{-1} lower in energy than the structures where the H atom of the OH group points towards the alkylchain. Here, the OH substituent has only a minor NNI impact on the enthalpy, which is consistent with the obtained optimized structures for the lowest energy conformer. Nevertheless, *o*-OH substitution reduces the entropy by approximately -8.9 J mol^{-1} K^{-1} and **NNITD2** takes this into account. **NNITD3** is defined to describe an interaction that is very similar to **NNITD1** which accounts for the substituent interaction in *o*-OH substituted vinylbenzene. In this molecule, a hydrogen bond is formed between the *o*-OH group and one of the vinyl groups in α-vinyl allylbenzene (molecule **TDT4/2,** see **Figure C-30** of Appendix C). However, the distance between the π system of the C=C bond and the OH group in *ortho* position are larger than in *o*-OH substituted allylbenzene which is explained with the presence of the second vinyl group that exerts a repulsive steric effect. This can also be seen by comparing the dihedral angles that are given in **Figure C-25** and **C-30** for *o*-OH substituted allylbenzene and α-vinyl allylbenzene, respectively. Therefore, the observed stabilization of -3.6 kJ mol^{-1} is much lower than seen in allylbenzene. In **NNITD3**, the entropy reduction is relatively smaller than in **NNITD1** since restriction to rotation is smaller in *o*-OH substituted α-vinyl allylbenzene than the *o*-OH substituted allylbenzene, leading to a smaller correction value for **NNITD3**. This

substituent interaction is presented in a three-dimensional molecular orbital representation (**Figure C-31** of Appendix C).

None of the *o*- methoxy substituted toluene derivatives investigated in this work exhibits a significant non-nearest neighbor effect on the enthalpy, whereas due to the restriction of internal rotations (particularly the rotations around the C_b-C bond on the extended side chains and the C_b-O bond on the methoxy group) the entropies decrease by -10.1 J mol^{-1} K^{-1}. **NNITD4** accounts for this entropy effect and it can be used in all the classes of *o*-OCH_3 substituted toluene derivatives apart from isopropylbenzene. **NNITD4** is very similar to **NNITD2**, not only in the sense that it is a correction defined mostly for entropy decrease and it does not have any significant effect on enthalpy, but also because the –OCH_3 group points away from the extended side chain in *o*- position, behaving like the –OH group in **NNITD2**. The last NNI parameter, **NNITD5**, corrects for the repulsive steric effects between the extended side chains and four different substituent groups (-CHO, -$CH{=}CH_2$, -CH_3 and -CH_2CH_3) in *o*- position with respect to these chains. Similar to all the other four **NNITD**s, the presence of these groups in *o*- position causes a notable decrease in entropy.

II. Validation set

The transferability of the GAV/NNI parameters developed from the training set (See **Table C-9** and **Table C-10** of Appendix C) is tested with a validation set consisting of 54 double-substituted toluene derivatives (see **Table C-2** of Appendix C). The toluene derivatives are chosen such that the performance of each GAV and NNI is tested at least twice.

In double-substituted toluene derivatives, in addition to the substituent interactions between the extended alkyl chain and the substituent group, substituent interactions exist between the two substituent groups as well. As the NNIs that describe the significant interactions between

two different substituents (*a*-X+Y where *a*- reflects the relative positioning of the two substituents) are previously defined in **Chapter 3**, they are used here to calculate the thermochemical properties of the molecules in the validation set (See **Table C-8** of Appendix C for a full list of such parameters used in this work).

The deviations along with the statistics between the *ab initio* and the GA-calculated value before and after the introduction of NNITDs are provided in **Table C-12** of Appendix C for all molecules of the validation set. The deviations emphasize the earlier observation that NNIs are of the utmost importance for the performance of GA calculations. MAX values for the training set before the application of NNITDs are very high: 9.8 kJ mol^{-1} for $\Delta_f H^\circ$ and 33.8 J mol^{-1} K^{-1} and 12.1 J mol^{-1} K^{-1} for S° and C_p(300 K), respectively. The inclusion of NNITDs within the GA calculations decrease the MAX values substantially: 5.7 kJ mol^{-1} for $\Delta_f H^\circ$ and 5.9 J mol^{-1} K^{-1} and 5.7 J mol^{-1} K^{-1} for S° and C_p(300 K), respectively. Similarly, the MAD values drop from 3.5 kJ mol^{-1} to 2.0 kJ mol^{-1} for $\Delta_f H^\circ$ and from 9.5 J mol^{-1} K^{-1} to 2.1 J mol^{-1} K^{-1} and from 4.9 J mol^{-1} K^{-1} to 1.9 J mol^{-1} K^{-1} for S° and C_p(300 K), respectively.

The results demonstrate the transferability of the new GA parameters because the present GAV/NNITD parameters are capable of reproducing the *ab initio* based thermochemical data of a set of double-substituted toluene derivatives with good accuracy.

III. Final set

Finally, the training set and the validation set are combined to the final set of 168 toluene derivatives. After these sets are combined, the GAV/NNI parameter set is reoptimized via the linear regression procedure to obtain the GAV and NNI data that best predict a large spectrum of multiply substituted toluene derivatives. The final GAV and NNI values together with their

97.5% confidence intervals are given in **Table 5-3** and **Table 5-4**, respectively. In **Table 5-4**, along with the regression results, the numbers of occurrences of the NNIs are provided. Every NNI parameter is derived from at least three different toluene derivatives to ensure good statistical significance.

Table 5-3 Final set of GAVs with 97.5% confidence intervals for toluene derivatives.

GAVs	$\Delta_f H^\circ$ [kJ mol^{-1}]	S° [J mol^{-1} K^{-1}]	C_p [J mol^{-1} K^{-1}]						
			300 K	400 K	500 K	600 K	800 K	1000 K	1500 K
C-(C_b)(C)$_2$(H)	-4.0 ± 0.67	-51.0 ± 0.83	23.6 ± 0.71	29.8 ± 0.66	34.4 ± 0.6	37.7 ± 0.56	42.1 ± 0.52	44.8 ± 0.51	47.9 ± 0.49
C-(C_b)(C_d)(H)$_2$	-19.3 ± 0.83	39.4 ± 1.03	23.8 ± 0.87	30.6 ± 0.82	36.0 ± 0.74	40.4 ± 0.69	46.9 ± 0.64	51.7 ± 0.64	58.3 ± 0.61
C-(C_b)(C_d)(C)(H)	-3.2 ± 0.74	-61.1 ± 0.92	24.3 ± 0.79	31.4 ± 0.74	35.8 ± 0.67	38.9 ± 0.62	42.6 ± 0.58	44.7 ± 0.57	46.4 ± 0.55
C-(C_b)(C_d)$_2$(H)	-1.0 ± 0.81	-58.5 ± 1.00	30.3 ± 0.85	36.0 ± 0.8	39.1 ± 0.72	40.7 ± 0.68	42.7 ± 0.63	44.0 ± 0.62	45.0 ± 0.59
C-(C_b)$_2$(H)$_2$	-23.4 ± 0.75	43.2 ± 0.93	21.8 ± 0.79	27.9 ± 0.74	33.4 ± 0.67	37.6 ± 0.63	44.0 ± 0.58	48.8 ± 0.58	54.6 ± 0.55
C-(C_b)$_2$(C)(H)	-6.0 ± 0.78	-57.3 ± 0.96	24.5 ± 0.82	30.3 ± 0.77	34.1 ± 0.69	36.5 ± 0.65	39.1 ± 0.60	41.0 ± 0.60	41.6 ± 0.57

Table 5-4 Final set of NNITDs with 97.5% confidence intervals for toluene derivatives.

#NNIs	$\Delta_f H^\circ$ [kJ mol^{-1}]	S° [J mol^{-1} K^{-1}]	C_p [J mol^{-1} K^{-1}]							#[a]
			300 K	400 K	500 K	600 K	800 K	1000 K	1500 K	
NNITD1	-7.2 ± 1.78	-26.0 ± 2.20	8.0 ± 1.88	8.8 ± 1.76	9.7 ± 1.59	10.0 ± 1.49	10.4 ± 1.38	9.0 ± 1.37	4.9 ± 1.31	4
NNITD2	-2.3 ± 1.17	-9.2 ± 1.45	6.7 ± 1.24	6.1 ± 1.16	5.3 ± 1.05	4.9 ± 0.98	4.7 ± 0.91	4.4 ± 0.90	4.0 ± 0.86	13
NNITD3	-3.8 ± 2.26	-17.5 ± 2.80	-3.2 ± 2.39	10.5 ± 2.24	15.0 ± 2.02	15.9 ± 1.89	17.1 ± 1.76	17.3 ± 1.74	12.6 ± 1.66	3
NNITD4	1.0 ± 1.19	-9.6 ± 1.47	2.6 ± 1.25	3.5 ± 1.18	4.0 ± 1.06	4.9 ± 0.99	4.8 ± 0.92	4.5 ± 0.91	4.0 ± 0.87	11
NNITD5	3.6 ± 0.73	-9.9 ± 0.91	6.6 ± 0.77	6.0 ± 0.73	5.6 ± 0.65	5.0 ± 0.61	4.0 ± 0.57	3.4 ± 0.56	2.3 ± 0.54	39

[a] The number of radicals in which the NNI appears.

The deviations between the *ab initio* and GA calculated $\Delta_f H^\circ$, S° at 298 K and C_p at various temperatures for all the toluene derivatives of the full database are reported in **Table C-13** of Appendix C. In **Table 5-5**, the statistics for the final optimization of the GAV/NNI parameters are given. The MAD between the GA and *ab initio* calculated $\Delta_f H^\circ$values is 1.33 kJ mol^{-1} and the MAX is 5.30 kJ mol^{-1}. For the majority of the toluene derivatives (all but 5 molecules), the

deviations are smaller than 4 kJ mol^{-1}. The deviations have an approximate normal distribution (**Figure C-32** of Appendix C) indicating that there is no obvious bias in the GA calculations towards certain substituent combinations. The agreement between GA and *ab initio* calculated S° and C_p values is acceptable as well. The MAD values for these two thermochemical properties are 1.82 J mol^{-1} K^{-1} and < 1.42 J mol^{-1} K^{-1} (for all temperatures), respectively. For only 10 species the entropy values deviate by more than 4 J mol^{-1} K^{-1} whereas for the C_p(300 K) values, only 7 species deviate by more than 4 J mol^{-1} K^{-1}. Histograms showing the distributions of the S° and C_p differences are provided in **Figure C-33** and **Figure C-34** of Appendix C, respectively. Again, these distributions have a Gaussian-like shape.

Table 5-5 Statistics for the linear regression analysis of the GAVs and NNIs for the standard enthalpies of formation ($\Delta_f H^\circ$) and entropies (S°) at 298 K and heat capacities (C_p) at various temperatures for toluene derivatives.[a]

	$\Delta_f H^\circ$	S°	C_p [J mol^{-1} K^{-1}]						
	[kJ mol^{-1}]	[J mol^{-1} K^{-1}]	300 K	400 K	500 K	600 K	800 K	1000 K	1500 K
MAD	1.33	1.82	1.42	1.33	1.24	1.15	1.13	1.12	1.05
RMS	1.77	2.19	1.87	1.75	1.58	1.48	1.38	1.36	1.30
MAX	5.30	5.15	5.15	4.74	4.60	4.71	3.76	3.68	3.30
F	721	8907	3053	5286	8309	11101	15447	17793	21670

[a] **F:** Significance; **MAD:** mean average deviation; **RMS:** root mean square; **MAX:** maximum deviation.

The statistical results demonstrate that the set of GA parameters (6 GAVs and 5 NNITDs) presented in this study are capable of providing reliable thermochemical data for the full set of 168 unsubstituted and substituted toluene derivatives.

5.5.2 Group Additive Parameters for Benzylic Radicals

I. Preliminary GAVs and NNIs

The strategy used to develop GA parameters for the toluene derivatives is also applied to calculate thermodynamic properties of the corresponding benzylic radicals. Among the

required radical specific GAVs, the C_b-(Ċ) is common to all benzylic radicals. Following the practice of Sabbe et al. [1,2], this radical adjacent group is substituted by the analogous non-radical group, C_b-(C). Furthermore, three non-aromatic groups, C-(Ċ)$(H)_3$, C_d-(Ċ)(H) and C_d-$(H)_2$, are taken from the earlier studies [1,2]. The C-(Ċ)$(H)_3$ and C_d-(Ċ)(H) groups are radical adjacent groups, thus they are substituted by C-(C)$(H)_3$ and C_d-(C)(H), respectively, and the C_d-$(H)_2$ is known. The values for these GAVs are provided in **Table 5-1**. Besides these known GAVs, each studied benzylic radical class requires one extra radical centered GAV that is specific to that class; pertaining to six different GAVs (Ċ-$(C_b)(C)_2(H)$, Ċ-$(C_b)(C_d)(H)_2$, Ċ-$(C_b)(C_d)(C)(H)$, Ċ-$(C_b)(C_d)_2(H)$, Ċ-$(C_b)_2(H)_2$ and Ċ-$(C_b)_2(C)(H)$) for each of the six benzylic radical classes considered in this study. Sabbe et al. reported values for three of them: Ċ-$(C_b)(C)_2(H)$, Ċ-$(C_b)(C_d)(H)_2$ and Ċ-$(C_b)(C_d)(C)(H)$ [1,2] that describe benzylic radicals, which are derivable from isopropylbenzene (2-phenyl-2-propyl), allylbenzene (3-phenyl-1-propen-3-yl) and α-methyl allylbenzene (3-phenyl-1-buten-3-yl) molecules, respectively [1,2]. The parameters for these GAVs are rederived in the present study even though they have been assigned previously. The main justification for this is that the GA calculations improve clearly with new assignments. Furthermore, the original GAV values were derived from just one or two benzylic radicals [1,2], whereas in the present study, these three GAVs appear in substantially more radicals, e.g. a set of 30 benzylic radicals contain the Ċ-$(C_b)(C)_2(H)$ group.

To apply the GA method to the remaining three radical classes α-vinyl allylbenzene (3-phenyl-1,4-pentadien-3-yl), diphenylmethane (diphenylmethyl) and 1,1-diphenylethane (1,1-diphenylethyl) GAVs for the Ċ-$(C_b)(C_d)_2(H)$, Ċ-$(C_b)_2(H)_2$ and Ċ-$(C_b)_2(C)(H)$ groups are needed, respectively. These GAVs have not been studied before. For the description of the six

substituents (-OH,-OCH_3,-CHO,-$CH=CH_2$,-CH_3,-CH_2CH_3) on the phenyl ring, 10 GAVs are used, which are taken from **Chapter 3** and listed in **Table 5-1**.

In summary, all but six GAVs needed for the radicals studied in this work are available from the literature and the parameters for the remaining six GAVs will be derived from the *ab initio* data calculated here. While GAVs are sufficient to predict the thermochemical properties of the unsubstituted benzylic radicals, it is expected that, similar to the toluenes, non-nearest neighbor interactions have to be taken into account for substituted benzylic radicals. In **Chapter 4**, it was shown that substitution on the phenyl ring can have remarkable effects on the thermodynamic properties of substituted benzyl and 1-phenylethyl radicals. Deviations between *ab initio* and solely GAV based calculated thermodynamic values found for the training set of 114 radicals are again used to identify these substituent effects and to assign initial values to the NNIs. The structures of all radicals of the training set are provided in **Figures C-13** to **C-18** of Appendix C and the corresponding thermochemical data is available in **Table C-3**.

Once all NNIs are identified, their values together with the new GAVs are optimized through the least squares regression procedure. These preliminary GAVs and the differences between the GA and *ab initio* datasets after the inclusion of preliminary GAV parameters can be found in **Table C-14** and **Table C-15** of Appendix C, respectively.

In the previous chapter, it was also shown that the NNIs for substituted benzyl radicals are applicable to substituted 1-phenylethyl radicals as well. Here, the applicability of these parameters to the larger 2-phenyl-2-propyl radical, i.e. the benzylic radical derived from isopropylbenzene, is tested. All NNIs involving radical moieties from earlier work are reproduced in **Table C-16** of Appendix C. In **Table C-17**, these NNIs are compared to non-

nearest neighbor $\Delta_f H°$ and $S°$ effects (CBS-QB3/BAC – GAV) in substituted 2-phenyl-2-propyls. It can be noted that *para* substituted 2-phenyl-2-propyl radicals can be described with the same NNIs that work for benzyl and 1-phenylethyl. In **Chapter 4**, the interactions in the simpler alkylphenyls were explained with the interplay of the mesomeric effects between the $CH_2^{\bullet}$/$C^{\bullet}HCH_3$ radical sites (+M effect) and the substituent -CHO and -CH=CH_2 groups (-M effect). The same explanation holds for the *p*-substituted 2-phenyl-2-propyls since the optimized structure of these radicals are similarly planar (See **Figure C-35** and **C-36**). In the case of *o*-substituents, the previously developed NNIs are systematically smaller than the substituent effects found for *o*-substituted 2-phenyl-2-propyl radicals (See **Table C-17**). This leads to the conclusion that the application of those NNIs should be limited to benzyls/1-phenylethyls and for 2-phenyl-2-propyls, new NNIs should be defined to describe the overall substituent interaction. A deeper understanding of the substituent effects can be gained by comparing the optimized structures of *o*-substituted benzyl and 1-phenylethyl with those of the corresponding 2-phenyl-2-propyls (See **Figures C-37 - C-42**). For instance, in *o*-OH and *o*-OCH_3 substituted benzyl and 1-phenylethyl radicals, no significant substituent effect is noted because the $CH_2^{\bullet}$ and $C^{\bullet}HCH_3$ moieties are arranged such that they hardly interact with the OH and OCH_3 substituents through steric repulsion. Such an arrangement is not possible for the $C^{\bullet}(CH_3)_2$ group. Instead, one of its methyl groups sterically interacts with the *o*-OH/OCH_3 groups, leading to destabilization but little loss of entropy. In **Chapter 4**, separate NNIs were defined for *o*-CHO, *o*-CH=CH_2 and *o*-CH_3/CH_2CH_3 substituted benzyls/1-phenylethyls, which was explained with steric effects of different magnitudes. In 2-phenyl-2-propyls, the presence of a second methyl group bonded to the radical carbon atom leads again to much stronger steric effects and destabilization. Again, the impact on entropies is rather small. In conclusion, a total

number of 4 new NNIs have to be defined to describe the substituent effects in the *o*-substituted 2-phenyl-2-propyls (one for *o*-OH/OCH_3, one for *o*-CHO, one for *o*-$CH{=}CH_2$ and one for *o*-CH_3/CH_2CH_3) whereas no new NNI is necessary for the *p*-substituted members. The substituent interactions in the substituted 2-phenyl-2-propyls and the NNIs that are defined to correct for these effects are discussed in the following paragraphs in detail.

For the remaining benzylic radicals studied, substituent effects of similar nature encountered in different classes are combined to a common NNI, ensuring that the thermochemical data for all benzylic radicals of interest can be accurately calculated with the smallest number of parameters. This way, a total of 14 new NNIs, including the four discussed above, are sufficient to describe all NNI effects. These NNIs are listed in **Table 5-6**. The NNIs are labeled "**NNIBR**" to indicate that these NNIs are developed for benzylic radicals. A detailed discussion of the origin of the identified substituent interactions will be given below.

Table 5-6 Non-nearest neighbor interactions (NNIs) in benzylic radicals (NNIBRs) that are identified from the differences given in **Table C-15** of Appendix C.

NNI #	Benzylic Radicals $C_6H_5C{\bullet}(X_1)(X_2)$	Substituent Group	Physical interpretation of the overall interaction	Preliminary $\Delta_f H^\circ$ value for the NNI[a] [kJ mol^{-1}]	Preliminary ΔS° value for the NNI[a] [J mol^{-1} K^{-1}]
NNIBR1	X_1 = -CH_3 X_2 = -CH_3	*o*-OH *o*-OCH_3	* SE[b]	11.7	-0.2
NNIBR2	X_1 = -CH_3 X_2 = -CH_3	*o*-CHO	* SE[b]	21.6	-0.2
NNIBR3	X_1 = -CH_3 X_2 = -CH_3	*o*-$CH{=}CH_2$	* SE[b]	20.2	-0.5
NNIBR4	X_1 = -CH_3 X_2 = -CH_3	*o*-CH_3 *o*-CH_2CH_3	* SE[b]	26.0	-3.1
NNI1**[d]	X_1 = -H X_2 = -H/-CH_3 (**NNI 27** in **Table 4-5**)	*p*-CHO	* Mesomeric Stabilization: Interaction of **+M**	-5.2[e]	0.6[e]

	Applicable to X_1 = -CH_3 X_2 = -CH_3 and X_1 = -H X_2 = -CH=CH_2		**effect** of radical moiety and **-M effect** of CHO and CH=CH_2 groups.		
NNI2**[d]	X_1 = -H X_2 = -H/-CH_3 (**NNI 27** in **Table 4-5**)	*p*-CH=CH_2	* Mesomeric Stabilization: Interaction of **+M effect** of radical moiety and **-M effect** of CHO and CH=CH_2 groups.	-5.8[e]	-3.7[e]
	Applicable to X_1 = -CH_3 X_2 = -CH_3 and X_1 = -H X_2 = -CH=CH_2				
NNIBR5	X_1 = -H X_2 = -CH=CH_2	*o*-OCH_3 *o*-CHO *o*-CH=CH_2 *o*-CH_3 *o*-CH_2CH_3	* SE[b] * Decrease of entropy due to restriction of rotation	5.9	-7.6
NNIBR6	X_1 = -CH_3 X_2 = -CH=CH_2	*o*-OH	* Competition of SE[b] vs. HB[c]. * Decrease of entropy due to restriction of rotation	2.1	-5.7
NNIBR7	X_1 = -CH_3 X_2 = -CH=CH_2	*o*-OCH_3 *o*-CHO *o*-CH=CH_2 *o*-CH_3 *o*-CH_2CH_3	* SE[b] * Decrease of entropy due to restriction of rotation	14.6	-5.0
NNIBR8	X_1 = -CH_3 X_2 = -CH=CH_2	*p*-CHO	* Mesomeric Stabilization: Interaction of **+M effect** of radical moiety and **-M effect** of CHO and CH=CH_2 groups.	-4.8	-0.1
	X_1 = -H X_2 = -C_6H_5				
	X_1 = -CH_3 X_2 = -C_6H_5				
	X_1 = -CH_3 X_2 = -CH=CH_2	*p*-CH=CH_2			
	X_1 = -H X_2 = -C_6H_5				
	X_1 = -CH_3 X_2 = -C_6H_5				
NNIBR9	X_1 = -CH=CH_2 X_2 = -CH=CH_2	*o*-OH	* HB[b] * Decrease of entropy due to restriction of rotation	-14.3	-14.6

NNIBR10	X_1 = -CH=CH_2 X_2 = -CH=CH_2	*o*-OCH_3	* Decrease of entropy due to restriction of rotation	1.6	-5.5
NNIBR11	X_1 = -CH=CH_2 X_2 = -CH=CH_2	*o*-CHO *o*-CH=CH_2 *o*-CH_3 *o*-CH_2CH_3	* HB[b] * Decrease of entropy due to restriction of rotation	-5.9	-20.3
NNIBR12	X_1 = -H X_2 = -C_6H_5 X_1 = -CH_3 X_2 = -C_6H_5	*o*-OH	* HB[b] * Decrease of entropy due to restriction of rotation	-5.8	-4.0
NNIBR13	X_1 = -H X_2 = -C_6H_5 X_1 = -CH_3 X_2 = -C_6H_5	*o*-OCH_3	* Weak SE[c] * Decrease of entropy due to restriction of rotation	3.3	-10.9
NNIBR14	X_1 = -H X_2 = -C_6H_5 X_1 = -CH_3 X_2 = -C_6H_5	*o*-CHO *o*-CH=CH_2 *o*-CH_3 *o*-CH_2CH_3 *o*-CHO *o*-CH=CH_2 *o*-CH_3 *o*-CH_2CH_3	* SE[c] * Decrease of entropy due to restriction of rotation	6.8	-3.6

[a] The values are obtained from the simultaneous linear regression of **GAVs** and **NNIs** from **Table C-18** and **Table C-19** of Appendix C.
[b] **HB:** Hydrogen Bond.
[c] **SE:** Steric effect.
[d] **NNI**1, NNI**2:** These two NNI**s were defined in **Chapter 4** for different *p*-substituted benzyls/1-phenylethyls. These parameters can effectively reproduce their 2-phenyl-2-propyl counterparts and no new NNIs (**NNIBR**s) are defined in this study to capture these interactions.
[e] The $\Delta_f H^\circ$ and S° values for the NNIs that are taken from **Chapter 4**.

The first four of these NNIBRs (**NNIBR1** to **NNIBR4**) account for the substituent interactions in *o*-substituted 2-phenyl-2-propyls. These parameters describe the interactions in *o*-OH/OCH_3, *o*-CHO, *o*-CH=CH_2 and *o*-CH_3/CH_2CH_3 substituted 2-phenyl-2-propyls, respectively, all of which are provided in **Table 5-6**. As described above, these NNIs take into account the substituent effects caused by the repulsive steric effects of different magnitudes between the extended side chains (R groups) and the substituent groups (Z groups).

Two distinct NNIs were defined to describe the substituent interactions in *p*-CHO and *p*-$CH=CH_2$ substituted benzyl/1-phenylethyl radicals in **Chapter 4**. The comparison of these NNIs with the deviations between the thermochemical data obtained via CBS-QB3/BAC calculations and the preliminary GAVs in **Table C-17** of Appendix C demonstrate that these previously defined NNI parameters can describe the substituent effects in *p*-CHO and *p*-$CH=CH_2$ substituted 2-phenyl-2-propyls. Thus, no new NNIs are needed for them. In **Table 5-6**, these two NNIs are abbreviated as **NNI**1** and **NNI**2** to differentiate them from the NNIs that are defined for the first time in this study for the benzylic radicals (**NNIBRs**). The interplay of the mesomeric effects between the radical site (+M effect) and the substituent -CHO and -$CH=CH_2$ groups (-M effect) lead to stabilization in these two radicals (See **Figure C-35** and **C-36** of Appendix C for optimized geometries of these radicals).

Interestingly, the applicability of **NNI**1** and **NNI**2** extends beyond the above discussed alkylphenyls to their similarly substituted 3-phenyl-1-propen-3-yl counterparts (See **Figure C-43** and **C-44** of Appendix C). The reason for this transferability is that the structures of all these radicals are planar and hence, the electronic charge transfer between two moieties that reside in *p*-position with respect to each other is possible through the π-system.

In *o*-OCH_3, *o*-CHO, *o*-$CH=CH_2$, *o*-CH_3 and *o*-CH_2CH_3 substituted 3-phenyl-1-propen-3-yl radicals, the interactions between the extended alkyl chain and the substituent groups lead to destabilization due to the steric repulsion. Since the magnitude of the overall substituent effects caused by these groups are similar, these interactions are grouped under the umbrella of one parameter, **NNIBR5**.

Although the only difference between the *o*-OH substituted 3-phenyl-1-propen-3-yl and 3-phenyl-1-buten-3-yl is the presence of one methyl group bonded to the α-carbon instead of a

hydrogen atom, the structures of the radicals and the consequent intramolecular interactions within these structures are very different (See the comparison of the optimized structures of the *o*-OH substituted 3-phenyl-1-propen-3-yl and 3-phenyl-1-buten-3-yl radicals in **Figure C-45** in the of Appendix C). The *o*-OH substituted 3-phenyl-1-propen-3-yl radical has a planar structure whereas the extended side chain in 3-phenyl-1-buten-3-yl is not in the same plane as the phenyl ring. This is caused by a repulsive steric interaction between the extra methyl group and the aromatic ring. The steric interaction is partially compensated by a stabilizing hydrogen bond but the resulting overall substituent effect is still slightly destabilizing. **NNIBR6** accounts for this substituent effect. The steric interaction has also an effect on internal rotors, which explains why **NNIBR6** decreases the entropy significantly. Similar to 3-phenyl-1-propen-3-yl, all the steric repulsive substituent effects caused by the *o*-substitution of the five remaining substituents groups (-OCH_3, -CHO, -$CH{=}CH_2$, -CH_3 and -CH_2CH_3) in 3-phenyl-1-buten-3-yl can be combined to one NNI, **NNIBR7**. It is easily notable that the magnitude of the steric effect in **NNIBR7** is much stronger than the substituent effect in **NNIBR5** due to the presence of the methyl group at the α-carbon.

The stabilizing mesomeric effects in *p*-CHO/$CH{=}CH_2$ substituted alkylphenyls and 3-phenyl-1-propen-3-yls have been mentioned above. Similar effects are noted in *p*-substituted 3-phenyl-1-buten-3-yl, diphenylmethyl and 1-diphenylethyl radicals, albeit to a lesser extent, because the extended side chains in these radicals are not in plane with the phenyl group. The presence of either a methyl group or phenyl group (or both) at the α-carbon of the benzylic radical rotates the extended side chain out of plane (within a range from 15° to 45°) and thereby changes the efficiency of the mesomeric interaction with the *p*-CHO/$CH{=}CH_2$ groups (See the

structures of these radicals in **Figure C-46** to **C-51** of Appendix C). Consequently, **NNI******1** or **NNI******2** are not applicable to these cases. Instead **NNIBR8** accounts for these interactions.

The angle between the phenyl ring and the π-system of the extended side chain (-C$^{\bullet}$(CH=CH$_2$)$_2$) in unsubstituted and *o*-substituted 3-phenyl-1,4-pentadien-3-yl radicals varies within the range 60° to 90° (See **Figures C-52** to **C-58** of Appendix C). Such non-planar structures allow unusual hydrogen bonds to be found while they at the same time render mesomeric effects impossible. As a result of this, no NNIs need to be defined for *p*-CHO/CH=CH$_2$ substitution (See **Figures C-59** and **C-60** of Appendix C). The *o*-OH substituted 3-phenyl-1,4-pentadien-3-yl is stabilized by a strong hydrogen bond (O-H---C•) and **NNIBR9** corrects for this effect. **NNIBR10** is defined to describe the notable entropy decrease caused by *o*-OCH$_3$ substitution due to a restriction of the internal rotations.

In the 3-phenyl-1,4-pentadien-3-yl radicals, *ortho* substitution by -CHO, -CH=CH$_2$, -CH$_3$ and -CH$_2$CH$_3$ groups cause stabilization. This is explained with the hydrogen bond-like interaction (C-H---C•), meaning a stabilizing interaction of a C-H moiety of the substituent with the radical site. Such special effects are possible due to the specific structure of this radical in which the extended side chain is almost perpendicular to the phenyl ring. This interaction is represented by the parameter **NNIBR11**. Besides their stabilizing effects on enthalpy, the substitution of -CHO, -CH=CH$_2$, -CH$_3$ and -CH$_2$CH$_3$ groups on 3-phenyl-1,4-pentadien-3-yl radical lead to significant decreases in the entropy of 3-phenyl-1,4-pentadien-3-yl radicals (-20.3 J mol^{-1} K^{-1}) as these *o*-substitutions prevent rotation of several bonds within the radical.

Diphenylmethyl radical and 1,1-diphenylethyl differ by an extra methyl group in the latter radical attached to the radical center. One might expect this additional methyl group to have a big impact on the substituent effect as seen for the 3-phenyl-1-propen-3-yl and 3-phenyl-1-

buten-3-yl radical pairs. However, this is not the case because diphenylmethyl is already non-planar and the additional methyl group thus cannot change the structure notably. As a result, each of the three separate NNIs (**NNIBR12**, **NNIBR13** and **NNIBR14**) which reflect the *o*-substituent effects caused by the six different groups of interest on diphenylmethyls also apply for 1,1-diphenylethyls. **NNIBR12** corrects for the *o*-OH substitution (See **Figures C-61** and **C-62** of Appendix C), where a hydrogen bond causes stabilization of the radical and simultaneously restricts internal rotations, thus decreasing entropy. **NNIBR13** and **NNIBR14** are two correction parameters defined to describe interactions caused by all other five *o*-substituted groups (See **Figures C-63** to **C-72** of Appendix C). The former applies to *o*-OCH_3 substituted diphenylic radicals and the latter to *o*-CHO, *o*-$CH{=}CH_2$, *o*-CH_3 and *o*-CH_2CH_3. **NNIBR13** and **NNIBR14** originate from similar physical effects, nevertheless two NNIs are defined to improve the accuracy of the GA calculations.

With all required NNIs being defined and initialized, improved GAV and NNI parameters are obtained by regressing those against the training set. The results are presented in **Table C-18** and **Table C-19** of Appendix C, respectively. The deviations between the GA and *ab initio* based data before and after the inclusion of the newly defined NNIs are reported in **Table C-20** of Appendix C, along with the statistics regarding the regression. It can be noted from the statistics that the MAD between the two datasets drops from 4.0 kJ mol^{-1} to 1.2 kJ mol^{-1} for standard enthalpies of formation and from 3.3 J mol^{-1} K^{-1} to 1.6 J mol^{-1} K^{-1} in entropies at 298 K, and from 2.4 J mol^{-1} K^{-1} to 1.3 J mol^{-1} K^{-1} for heat capacities at 300 K upon inclusion of NNIs as a part of the GA calculations. The MAX values drop from 26.6 kJ mol^{-1} to 5.1 kJ mol^{-1} for the $\Delta_f H°$ and from 22.7 J mol^{-1} K^{-1} to 4.4 J mol^{-1} K^{-1} for the $S°$ values, whereas it decreases from 17.0 J mol^{-1} K^{-1} to 5.3 J mol^{-1} K^{-1} for the heat capacities at 300 K.

II. Validation set

The set of preliminary GAV/NNI parameters are tested against thermodynamic properties of 54 doubly-substituted benzylic radicals that are not a part of the training set. The radicals of the validation set are shown in **Figures C-19 – C-24** of Appendix C and their corresponding thermochemical data can be found in **Table C-4** of Appendix C.

Analogous to doubly-substituted toluene derivatives, several doubly-substituted benzylic radicals from the validation set contain non-nearest neighbor interactions between the two substituent groups. To take the interactions between the two substituents into account, the NNIs that were derived in **Chapters 3** are used. The values of these NNIs are listed in **Table C-8** of Appendix C. For example, in 3-methyl-4-vinyl-1,1-diphenylethyl radical (See **Figure 5-2 (a)**), an interaction between the radical bearing extended side chain and the vinyl group in *p*-position exists. This interaction is captured by **NNIBR7** (See **Table C-19** of Appendix C), as discussed in-depth above. In addition to this interaction, the repulsive destabilization between -CH=CH_2 and -CH_3 groups needs to be taken into account which is realized through a NNI that is previously defined in **Chapter 3** (**NNI9** in **Table 3-6**). Application of all appropriate NNI corrections lead to the GA calculated standard enthalpy of formation that differs by only 1.6 kJ mol^{-1} from the *ab initio* $\Delta_f H^\circ$ value.

In a few cases among the doubly-substituted benzylic radicals, the interaction between the extended benzylic radical moiety (R group) and one of the substituents (one of the two Z groups) interferes with the substituent effects among the two substituent groups. This leads to an unavoidable decrease in accuracy of the GA calculations. For instance, in the doubly-substituted 2-phenyl-2-propyl radical with two CHO groups in 2,5 positions, i.e. 1,4-diformyl-2-(prop-2-yl) benzene (See **Figure 5-2 (b)**), accounting for the interaction between the two

formyl groups in *para* position (9.9 kJ mol^{-1}; see **Table C-8**) and for the C$^{\bullet}$(CH3)$_2$ and the *o*-CHO group (21.6 kJ mol^{-1}; see **Table C-19**) results in a deviation between GA and *ab initio* data in the validation set (5.7 kJ mol^{-1}).

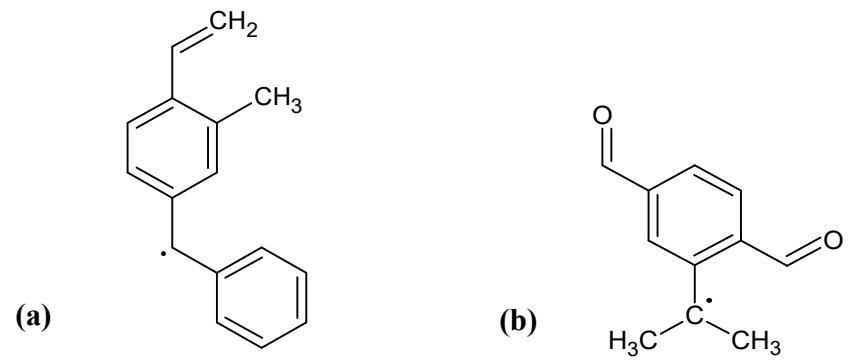

Figure 5-2 The structures of **(a)** 3-methyl-4-vinyl-1,1-diphenylethyl and **(b)** 1,4-diformyl-2-(prop-2-yl)-benzene radicals.

This large deviation is mainly due to the steric repulsion between the C$^{\bullet}$(CH$_3$)$_2$ and the *o*-CHO group which causes the *o*-CHO group to move out of the plane of the phenyl ring (see the optimized geometry of this molecule in **Figure C-73** of Appendix C, molecule **BRV1/3**) resulting in weakening the mesomeric interactions with the *p*–CHO group as compared to the *p*-diformylbenzene. Therefore, utilizing the NNI correction for the interaction between the two CHO groups leads to lower accuracy than the accuracy that would be obtained if this NNI would not be considered (-4.2 kJ mol^{-1}).

Comparisons between the GA calculations and the *ab initio* data for the validation set before and after the application of NNIs are available in **Table C-21** of Appendix C for $\Delta_f H^\circ$ and S° at 298K and C_p at 300 K. The 54 $\Delta_f H^\circ$ values using the GAV/NNI parameters agree satisfactorily with the CBS-QB3/BAC data as the MAD of 2.4 kJ mol^{-1} and the MAX value of 5.7 kJ mol^{-1} show. Among these 54 benzylic radicals, 6 deviate by more than 4 kJ mol^{-1} and the MAX value is slightly higher than that of the training set (5.0 kJ mol^{-1}). In doubly-

substituted benzylic radicals, small errors in the predictions of individual substituent effects add up and lead to relatively larger deviations. Nonetheless, given the complexity of the substituted MARs, the accuracy can be considered as satisfactory. Besides, in the following section, it is shown that these deviations become smaller upon the final optimization of the GAV/NNI parameters. The statistics reported in **Table C-21** also indicate that these parameters are similarly successful in reducing the deviations between the CBS-QB3/BAC and GA calculated entropies (S°) and heat capacities (C_p) for the MARs in the validation set.

Given the good agreement between the CBS-QB3/BAC and GA calculated thermochemical data for the validation set, it can be expected that the GAV/NNI set developed in this work can successfully be applied to higher substituted MARs.

III. Final set

The development of the GA parameters is finalized by combining the training and validation sets to a final set of 168 benzylic radicals. This set is used to optimize the GAV/NNI parameters through a linear regression analysis. The final GAV and NNI parameters together with their 97.5% confidence intervals are reported in **Table 5-7** (GAVs) and **Table 5-8** (NNIs).

Table 5-7 GAVs for standard enthalpy of formation ($\Delta_f H^\circ$) and entropy (S°) at 298 K, and heat capacity (C_p) at various temperatures for benzylic radicals derived from reference database, given with 97.5% confidence intervals.

GAVs	$\Delta_f H^\circ$	S°	C_p [J mol^{-1} K^{-1}]						
	[kJ mol^{-1}]	[J mol^{-1} K^{-1}]	300 K	400 K	500 K	600 K	800 K	1000 K	1500 K
Ċ-(C$_b$)(C)$_2$	139.9 ± 1.06	-38.8 ± 0.98	14.2 ± 1.05	18.6 ± 0.90	21.4 ± 0.79	23.5 ± 0.74	26.4 ± 0.72	28.1 ± 0.69	28.7 ± 0.59
Ċ-(C$_b$)(C$_d$)(H)	91.4 ± 1.02	20.1 ± 0.95	22.4 ± 1.02	29.9 ± 0.88	34.6 ± 0.76	37.9 ± 0.72	42.2 ± 0.70	44.8 ± 0.67	47.0 ± 0.57
Ċ-(C$_b$)(C$_d$)(C)	106.7 ± 1.12	-51.5 ± 1.03	18.9 ± 1.11	25.5 ± 0.95	28.5 ± 0.83	29.9 ± 0.79	30.5 ± 0.76	30.2 ± 0.73	27.3 ± 0.62
Ċ-(C$_b$)(C$_d$)$_2$	79.2 ± 1.17	-67.4 ± 1.09	22.7 ± 1.16	28.6 ± 1.02	32.0 ± 0.87	34.0 ± 0.83	35.8 ± 0.80	36.3 ± 0.77	34.2 ± 0.65

Ċ-(C$_b$)$_2$(H)	120.2 ± 1.01	26.1 ± 0.94	27.7 ± 1.01	34.4 ± 0.86	38.8 ± 0.75	41.6 ± 0.71	44.7 ± 0.69	45.9 ± 0.66	44.4 ± 0.56
Ċ-(C$_b$)$_2$(C)	132.0 ± 1.01	-51.5 ± 0.94	28.0 ± 1.00	30.5 ± 0.87	32.0 ± 0.75	32.4 ± 0.71	31.6 ± 0.69	30.8 ± 0.66	26.8 ± 0.57

Table 5-8 Corrections for non-nearest neighbor interactions in benzylic radicals (NNIBRs) derived based on full CBS-QB3 molecule set for the standard enthalpies of formation ($\Delta_f H^\circ$) and entropies (S°) at 298 K and heat capacities (C_p) of benzylic radicals at various temperatures, given with 97.5% confidence intervals.

NNIs	$\Delta_f H^\circ$	S°	C_p [J mol^{-1} K^{-1}]						
	[kJ mol^{-1}]	[J mol^{-1} K^{-1}]	300 K	400 K	500 K	600 K	800 K	1000 K	1500 K
NNIBR1	12.8 ± 2.36	-0.2 ± 2.19	0.9 ± 2.34	-1.0 ± 2.02	-1.3 ± 1.76	-1.2 ± 1.67	-1.0 ± 1.61	-1.1 ± 1.55	-1.6 ± 1.32
NNIBR2	20.3 ± 2.66	-2.8 ± 2.46	8.7 ± 2.63	6.4 ± 2.27	4.3 ± 1.98	2.5 ± 1.87	-0.3 ± 1.82	-2.2 ± 1.74	-4.1 ± 1.49
NNIBR3	18.9 ± 2.66	-2.6 ± 2.46	14.7 ± 2.63	12.6 ± 2.27	10.3 ± 1.98	8.2 ± 1.87	4.9 ± 1.82	2.5 ± 1.74	-0.6 ± 1.49
NNIBR4	26.2 ± 2.36	-3.3 ± 2.19	5.2 ± 2.34	4.1 ± 2.02	3.1 ± 1.76	2.2 ± 1.67	0.8 ± 1.61	-0.3 ± 1.55	-2 ± 1.32
NNIBR5	5.2 ± 1.81	-8.4 ± 1.68	4.4 ± 1.80	4.2 ± 1.55	4.9 ± 1.35	4.9 ± 1.28	3.5 ± 1.24	3.0 ± 1.19	1.5 ± 1.01
NNIBR6	3.2 ± 2.18	-4.5 ± 2.02	5.3 ± 2.16	3.7 ± 1.87	2.4 ± 1.62	1.6 ± 1.54	0.4 ± 1.49	0.3 ± 1.43	0.5 ± 1.22
NNIBR7	14.2 ± 1.68	-5.5 ± 1.55	5.2 ± 1.66	3.0 ± 1.43	1.7 ± 1.25	0.7 ± 1.18	-0.4 ± 1.15	-1.0 ± 1.10	-0.8 ± 0.94
NNIBR8	-5.6 ± 1.19	-0.3 ± 1.10	1.1 ± 1.18	0.6 ± 1.02	0.5 ± 0.88	0.4 ± 0.84	0.5 ± 0.81	0.5 ± 0.78	0.2 ± 0.66
NNIBR9	-11.5 ± 2.71	-12.9 ± 2.51	3.4 ± 2.68	0.1 ± 2.31	1.9 ± 2.01	2.9 ± 1.91	2.7 ± 1.85	2.5 ± 1.77	-1.1 ± 1.51
NNIBR10	0.4 ± 2.71	-6.9 ± 2.51	5.3 ± 2.68	1.3 ± 2.31	1.1 ± 2.01	0.6 ± 1.91	0.1 ± 1.85	0.6 ± 1.77	1.9 ± 1.51
NNIBR11	-6.2 ± 1.9	-20.6 ± 1.76	-2.7 ± 1.88	0.3 ± 1.62	1.5 ± 1.41	1.8 ± 1.34	1.5 ± 1.30	1.6 ± 1.24	3.7 ± 1.06
NNIBR12	-5.2 ± 1.78	-3.0 ± 1.65	2.3 ± 1.77	2.3 ± 1.53	2.8 ± 1.33	3.1 ± 1.26	3.5 ± 1.22	3.4 ± 1.17	1.9 ± 1.00
NNIBR13	2.7 ± 2.25	-9.8 ± 2.09	6.4 ± 2.23	5.9 ± 1.93	5.9 ± 1.68	5.5 ± 1.59	4.3 ± 1.54	3.0 ± 1.48	1.1 ± 1.26
NNIBR14	6.7 ± 1.36	-3.7 ± 1.26	6.0 ± 1.35	5.0 ± 1.16	4.1 ± 1.01	3.5 ± 0.96	3.1 ± 0.93	2.4 ± 0.89	0.9 ± 0.76

A statistical analysis is performed in order to assess the performance of the reported parameters. The results of this analysis are reported in **Table 5-9**. The MAD for the prediction of the standard enthalpies of formation of the entire reference data set of benzylic radicals is 1.59 kJ mol^{-1}, and those for the entropy and heat capacity predictions at all temperatures are 1.52 J mol^{-1} K^{-1} and < 1.54 J mol^{-1} K^{-1}, respectively. Inclusion of corrections for next-nearest neighbor interactions (NNIs) is found to be crucial as the drastic decrease of the MAD values

shows. For example, the MAD for $\Delta_f H^\circ$ decreases from 4.89 kJ mol^{-1} to 1.59 kJ mol^{-1} after NNI corrections are introduced.

Table 5-9 Statistics for the linear regression analysis of the GAVs and NNIs for the standard enthalpies of formation *($\Delta_f H^\circ$)* and entropies *(S°)* at 298 K and heat capacities *(C_p)* at various temperatures for benzylic radicals.[a]

	$\Delta_f H^\circ$	S°	C_p [J mol^{-1} K^{-1}]						
	[kJ mol^{-1}]	[J mol^{-1} K^{-1}]	300 K	400 K	500 K	600 K	800 K	1000 K	1500 K
MAD	1.59	1.52	1.54	1.29	1.08	1.00	0.99	0.94	0.83
RMS	1.98	1.84	1.97	1.70	1.48	1.40	1.36	1.30	1.11
MAX	5.96	4.42	5.71	5.30	5.65	5.29	4.56	4.26	3.36
F	29626	6563	1552	3082	5135	6537	7999	9260	12371

[a] **F:** Significance; **MAD:** mean average deviation; **RMS:** root mean square; **MAX**: maximum deviation.

All individual deviations between GA and *ab initio* based thermodynamic data are provided in **Table C-21**. The distribution of the difference between reference and GA predicted enthalpies of formation is shown in **Figure C-74**. Almost all 168 enthalpies of formation are predicted within 4 kJ mol^{-1}. In **Figure C-75** and **Figure C-76**, similar histograms are presented for the difference distributions of the entropies (S°) and heat capacities (C_p) at 300 K. Again, the agreement is very good and most data differ by less than 4 J mol^{-1} K^{-1}.

5.5.3 Comparison of the final GAVs with the literature values

GAVs have been derived before by Cohen [25], Holmes and Aubry [26] and Sabbe et al. [1] for some of the toluene derivatives classes considered here. In **Table 5-10**, the GAVs that are reported in this study are compared with the GAVs from the literature for several groups in the toluene derivatives and the benzylic radicals. There is very good agreement between values reported in the literature and the present study for the C-(C$_b$)(C)$_2$(H) group in isopropylbenzenes as all of the values are within 0.7 kJ mol^{-1}. The new enthalpy value for the C-(C$_b$)(C$_d$)(H)$_2$ group agrees within 0.5 kJ mol^{-1} with the GAV parameter reported by Sabbe et

al. [1] (-19.8 kJ mol^{-1}), however both values are in conflict with that reported by Cohen. An explanation of this discrepancy could be that Cohen used solid phase standard enthalpy of formation data to derive this GAV. Cohen mentions this GAV as one of the "questionable" values since it is derived from the only one experimental data available in Cohen's database for allylbenzene. Sabbe et al. [1] also reported a GAV for the C-(C_b)(C_d)(C)(H) group, which agrees well with the present value. The GAV that is derived for the C-(C_b)$_2$(H)$_2$ group falls between the values reported by Cohen [25] and Holmes and Aubry [26] (within roughly 3 kJ mol^{-1} of both), which underscores the agreement between the present value and the values from these studies. For the C-(C_b)$_2$(C)(H) group, Cohen reported the value of -4.6 kJ mol^{-1}, which is in agreement with the value of -6.0 kJ mol^{-1} of the present work.

Table 5-10 Comparison of the GAVs for the standard enthalpies of formation ($\Delta_f H^\circ$) reported in the literature and obtained in this work.

GAVs for $\Delta_f H°$ [kJ mol^{-1}]				
Groups	**Literature**			**This Work**
	Cohen [25]	**Holmes [26]**	**Sabbe [1]**	
C-(C_b)(C)$_2$(H)	-4.6	-4.0	-4.7	-4.0 ± 0.67
C-(C_b)(C_d)(H)$_2$	-10.5	-18.0	-19.8	-19.3 ± 0.83
C-(C_b)(C_d)(C)(H)	-	-	-3.8	-3.2 ± 0.74
C-(C_b)$_2$(H)$_2$	-26.4	-20.0	-	-23.4 ± 0.75
C-(C_b)$_2$(C)(H)	-4.6	-	-	-6.0 ± 0.78
Ċ-(C_b)(C)$_2$	-	-	142.6	140.9 ± 1.06
Ċ-(C_b)(C_d)(H)	-	-	123.6	91.8 ± 1.02
Ċ-(C_b)(C_d)(C)	-	-	98.1	107.6 ± 1.12

Only Sabbe et al. [1] reported GAVs ($\Delta_f H^\circ$) for some benzylic radical groups. The values for the Ċ-(C_b)(C)$_2$ group from Sabbe et al. and this study agree well. However, **Table 5-10** demonstrates a remarkable discrepancy between the GAVs for the Ċ-(C_b)(C_d)(H) and Ċ-(C_b)(C_d)(C) groups. The *ab initio* $\Delta_f H°$ values for the benzylic radicals in both studies are very similar, which should lead to similar GAVs. However, in the previous study of Sabbe et al. an

error was made in the derivation of these two GAVs, and they should be replaced with the ones reported in the present study.

5.6 Conclusions

A set of predictive group additive parameters has been derived to obtain the thermodynamic properties of substituted toluene derivatives (6 GAVs and 5 NNIs) and the corresponding benzylic radicals (6 GAVs and 14 NNIs). Six different classes of substituted toluene derivatives and benzylic radicals have been considered with all the possible *o*-, *m*- and *p*-substituent combinations of these groups: hydroxy (-OH), methoxy (-OCH_3), formyl (-CHO), vinyl (-$CH{=}CH_2$), methyl (-CH_3) and ethyl (-CH_2CH_3). The parameters were determined from two sets of 168 toluene derivatives and 168 benzylic radicals, whose thermodynamic values were calculated with bond additivity corrected (BAC) CBS-QB3 theory.

NNIs were found to be crucial to achieve accurate GA calculations for both toluene derivatives and the benzylic radicals. Thermodynamic properties for the toluene derivatives obtained with the new GAV and NNI parameters agree very well with the *ab initio* reference data set. The MADs are 1.33 kJ mol^{-1} for $\Delta_f H^\circ$, 1.82 J mol^{-1} K^{-1} for $S^\circ$and less than 1.42 J mol^{-1} K^{-1} for C_p values at all studied temperatures. Similar accuracy is noted for in the substituted benzylic radicals as well. The MADs are 1.59 kJ mol^{-1} for $\Delta_f H^\circ$, 1.52 J mol^{-1} K^{-1} for $S^\circ$and less than 1.54 J mol^{-1} K^{-1} for C_p values at all studied temperatures. All GA based toluene derivative enthalpies are within 5.3 kJ mol^{-1} of the *ab initio* values and the deviation exceeds 4 kJ mol^{-1} for a very small number of molecules. Similar accuracy is obtained for the benzylic radicals: the highest deviation between group additively and *ab initio* calculated $\Delta_f H^\circ$ data within the entire set of benzylic radicals is 5.7 kJ mol^{-1}. Similarly, the entropies and the heat capacities

for the majority of the radicals are reproduced to within 4 J mol^{-1} K^{-1}, which underlines the good accuracy obtainable with the GAV/NNI set calculated in this study.

Combined with previously published set of GAVs for the monocyclic aromatic hydrocarbons and monocyclic aromatic radicals, the parameters presented in this work extend the applicability of Benson's group additivity method to a wider range of substituted monocyclic aromatic compounds and radicals.

5.7 Acknowledgments

The research leading to these results has received funding from the European Research Council under the European Union's Seventh Framework Programme (FP7/2007-2013)/ERC grant MADPII agreement n° 290793. The SBO project "Bioleum" (IWT-SBO 130039) supported by the Institute for Promotion of Innovation through Science and Technology in Flanders (IWT) is acknowledged. This work was carried out using the STEVIN Supercomputer Infrastructure at Ghent University, funded by Ghent University, the Flemish Supercomputer Center (VSC), the Hercules Foundation and the Flemish Government – department EWI.

5.8 References

[1] Sabbe MK, Saeys M, Reyniers M-F, Marin GB, Van Speybroeck V, Waroquier M. Group Additive Values for the Gas Phase Standard Enthalpy of Formation of Hydrocarbons and Hydrocarbon Radicals. *The Journal of Physical Chemistry A*. 2005;109(33):7466-7480.

[2] Sabbe MK, De Vleeschouwer F, Reyniers M-F, Waroquier M, Marin GB. First Principles Based Group Additive Values for the Gas Phase Standard Entropy and Heat Capacity of Hydrocarbons and Hydrocarbon Radicals. *The Journal of Physical Chemistry A.* 2008;112(47):12235-12251.

[3] Vandeputte AG, Sabbe MK, Reyniers MF, Marin GB. Modeling the gas-phase thermochemistry of organosulfur compounds. *Chemistry – A European Journal.* 2011;17(27):7656-7673.

[4] Paraskevas PD, Sabbe MK, Reyniers M-F, Papayannakos N, Marin GB. Group Additive Values for the Gas-Phase Standard Enthalpy of Formation, Entropy and Heat Capacity of Oxygenates. *Chemistry – A European Journal.* 2013;19(48):16431-16452.

[5] Kibet J, Khachatryan L, Dellinger B. Molecular Products and Radicals from Pyrolysis of Lignin. *Environmental Science & Technology.* 2012;46(23):12994-13001.

[6] Van Geem KM, Hudebine D, Reyniers MF, Wahl F, Verstraete JJ, Marin GB. Molecular reconstruction of naphtha steam cracking feedstocks based on commercial indices. *Computers & Chemical Engineering*. 2007;31(9):1020-1034.

[7] Hamelinck CN, Faaij APC, den Uil H, Boerrigter H. Production of FT transportation fuels from biomass; technical options, process analysis and optimisation, and development potential. *Energy*. 2004;29(11):1743-1771.

[8] Frisch MJ, Trucks GW, Schlegel HB, Scuseria GE, Robb MA, Cheeseman JR, Scalmani G, Barone V, Mennucci B, Petersson GA, Nakatsuji H, Caricato M, Li X, Hratchian HP, Izmaylov AF, Bloino J, Zheng G, Sonnenberg JL, Hada M, Ehara M, Toyota K, Fukuda R, Hasegawa J, Ishida M, Nakajima T, Honda Y, Kitao O, Nakai H, Vreven T, Montgomery Jr. JA, Peralta JE, Ogliaro F, Bearpark MJ, Heyd J, Brothers EN, Kudin KN, Staroverov VN, Kobayashi R, Normand J, Raghavachari K, Rendell AP, Burant JC, Iyengar SS, Tomasi J, Cossi M, Rega N, Millam NJ, Klene M, Knox

JE, Cross JB, Bakken V, Adamo C, Jaramillo J, Gomperts R, Stratmann RE, Yazyev O, Austin AJ, Cammi R, Pomelli C, Ochterski JW, Martin RL, Morokuma K, Zakrzewski VG, Voth GA, Salvador P, Dannenberg JJ, Dapprich S, Daniels AD, Farkas Ö, Foresman JB, Ortiz JV, Cioslowski J, Fox DJ. Gaussian 09, Version D.01. Wallingford, CT, USA: Gaussian, Inc.; 2009.

[9] Curtiss LA, Redfern PC, Raghavachari K. Gaussian-4 theory. *The Journal of Chemical Physics.* 2007;126(8):084108.

[10] Montgomery Jr JA, Frisch MJ, Ochterski JW, Petersson GA. A complete basis set model chemistry. VI. Use of density functional geometries and frequencies. *The Journal of Chemical Physics.* 1999;110(6):2822-2827.

[11] Vansteenkiste P, Van Speybroeck V, Marin GB, Waroquier M. Ab initio calculation of entropy and heat capacity of gas-phase n-alkanes using internal rotations. *The Journal of Physical Chemistry A.* 2003;107(17):3139-3145.

[12] Van Speybroeck V, Vansteenkiste P, Neck DV, Waroquier M. Why does the uncoupled hindered rotor model work well for the thermodynamics of n-alkanes? *Chemical Physics Letters.* 2005;402(4-6):479-484.

[13] Vansteenkiste P, Van Neck D, Van Speybroeck V, Waroquier M. An extended hindered-rotor model with incorporation of Coriolis and vibrational-rotational coupling for calculating partition functions and derived quantities. *The Journal of Chemical Physics.* 2006;124(4):044314.

[14] Petersson GA, Malick D, Wilson W, Ochterski J, Montgomery JA, Frisch MJ. Calibration and comparison of the Gaussian-2, complete basis set, and density functional methods for computational thermochemistry. *The Journal of Chemical Physics.* 1998;109(24):10570.

[15] Benson SW. *Thermochemical Kinetics: Methods for the Estimation of Thermochemical Data and Rate Parameters*. 2d ed. New York: Wiley; 1976.

[16] NIST Chemical Kinetics Database. National Institute of Standards and Technology; 2015. http://kinetics.nist.gov/. Accessed 15 September 2016.

[17] Prosen E, Rossini F. Heats of combustion and formation of the paraffin hydrocarbons at 25 C. *Journal of Research of the National Bureau of Standards.* 1945:263-267.

[18] Nesterova TN, Pimerzin AA, Rozhnov AM, Karlina TN. Equilibria for the isomerization of (secondary-alkyl)phenols and cyclohexylphenols. *The Journal of Chemical Thermodynamics.* 1989;21(4):385-395.

[19] Roux MV, Temprado M, Chickos JS, Nagano Y. Critically Evaluated Thermochemical Properties of Polycyclic Aromatic Hydrocarbons. *Journal of Physical and Chemical Reference Data.* 2008;37(4):1855.

[20] Tsang W. Heats of Formation of Organic Free Radicals by Kinetic Methods. In: Martinho Simões J, Greenberg A, Liebman J, eds. *Energetics of Organic Free Radicals.* Vol 4: Springer Netherlands; 1996:22-58.

[21] Stevens WR, Ruscic B, Baer T. Heats of Formation of C6H5•, C6H5+, and C6H5NO by Threshold Photoelectron Photoion Coincidence and Active Thermochemical Tables Analysis. *The Journal of Physical Chemistry A.* 2010;114(50):13134-13145.

[22] Somers KP, Simmie JM. Benchmarking Compound Methods (CBS-QB3, CBS-APNO, G3, G4, W1BD) against the Active Thermochemical Tables: Formation Enthalpies of Radicals. *The Journal of Physical Chemistry A.* 2015;119(33):8922-8933.

[23] Blanksby SJ, Ellison GB. Bond Dissociation Energies of Organic Molecules. *Accounts of Chemical Research.* 2003;36(4):255-263.

[24] Denisov ET, Denisova T. *Handbook of Antioxidants: Bond Dissociation Energies, Rate Constants, Activation Energies, and Enthalpies of Reactions.* Vol 100: CRC press; 1999.

[25] Cohen N. Revised Group Additivity Values for Enthalpies of Formation (at 298 K) of Carbon–Hydrogen and Carbon–Hydrogen–Oxygen Compounds. *Journal of Physical and Chemical Reference Data.* 1996;25(6):1411.

[26] Holmes JL, Aubry C. Group additivity values for estimating the enthalpy of formation of organic compounds: an update and reappraisal. 1. C, H, and O. *The Journal of Physical Chemistry A.* 2011;115(38):10576-10586.

Chapter 6

Kinetics of Benzylic Hydrogen Abstractions from Toluene Derivatives by Hydrogen Atoms

This chapter is planned to be submitted as a manuscript for publication with the following title:

Group Additive Kinetic Modeling of Benzylic Hydrogen Abstractions from Toluene Derivatives by Hydrogen Atoms

Authors: Alper Ince, Hans-Heinrich Carstensen, Maarten Sabbe, Marie-Françoise Reyniers and Guy B. Marin .

6.1 Abstract

The Arrhenius parameters and rate coefficients of the hydrogen abstraction reactions by a hydrogen atom from unsubstituted and substituted toluene derivatives with six substituents (hydroxy, methoxy, formyl, vinyl, methyl and ethyl) are calculated at the post Hartree-Fock CBS-QB3 level of theory at temperatures from 300 K to 2000 K. A Group Additivity (GA) model is constructed to describe the Arrhenius parameters of these reactions by defining 8 group additive values (ΔGAV°s) and 3 non-nearest neighbor interactions (ΔNNI°s) for the reactions in the forward direction, and 8 ΔGAV°s and 14 ΔNNI°s for the reactions in the reverse direction through least squares regression to a database of Arrhenius parameters based on a set of 211 reactions. Quantum tunneling effects are taken into consideration separately through an empirical equation. The GA model and the proposed tunneling correction function are used in tandem to reproduce CBS-QB3 rate coefficients. In the forward direction, the mean factor of deviations between GA and *ab initio* calculated rate coefficients is 2.2 at 300 K, 1.6 at 600 K and less than 1.5 at higher temperatures. The accuracy of the proposed model is similar in the reverse direction.

6.2 Introduction

Numerous technologically important processes such as steam cracking that converts fossil fuels to commodity chemicals, or combustion in boilers and internal combustion engines are based on gas-phase chemistry at high temperatures. The crucial role of hydrogen abstraction reactions (HARs) has been thoroughly investigated for conventional fuels. The transition to green, sustainable resources such as lignocellulosic biomass causes a change of the feedstock chemical composition from mainly hydrocarbons to heavily oxygenated compounds. Hence,

new reaction families should be introduced that account for reactivity differences caused by the presence of oxygen in the molecules.

Hydrogen abstraction reactions of toluene derivatives are of importance for at least two reasons. First, toluene and substituted toluene derivatives are formed in high yields in pyrolysis reactions. Therefore, their subsequent chemistry has a significant impact on the yields of desired (BTX base chemicals) or undesired (deposits) products. Second, the building blocks of lignin, the second largest component found in biomass, are phenyl propane derivatives which in turn can be considered as toluene derivatives. Any lignin model will include a sub-mechanism for toluene derivatives.

While past kinetic models were mainly developed manually, the ever-increasing size of such models demands the use of computer tools to create, extend and maintain today's models. Obviously, automated mechanism generating tools only produce useful models if they have access to reliable thermodynamic information for species and kinetic parameters for all reactions encountered. Fast methods are needed to calculate such properties simply based on the structure of the molecule or reaction family of interest. The group additivity (GA) approach by Benson is an elegant example of such methods. Previous studies at the Laboratory for Chemical Technology (LCT) of Ghent University have shown that Benson's group additivity method enables accurate calculations of thermodynamic properties for open-chain hydrocarbons [1,2], oxygenates [3], and sulfur compounds [4], as well as reliable rate coefficient calculations for H abstraction reactions and radical addition reactions for reactions involving above listed molecule classes [5-16]. In **Chapters 3-5**, the GAV (group additive value) database was extended to substituted monocyclic aromatic species. The aim of this chapter is to build on these earlier studies and to provide group additivity parameters for the

calculation of rate coefficients for H abstractions from substituted toluenes. More specifically, the focus of this study is on exploring reactivity changes in the H abstraction reaction by H atoms caused (a) by substituent groups attached to the aromatic ring and (b) by replacing one or both hydrogens of the simple CH_2 benzyl radical site with larger hydrocarbon groups. The entire set of reactions considered is illustrated in **Figure 6-1**.

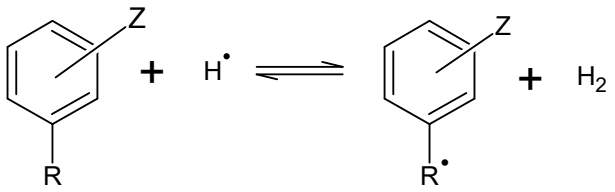

R = -CH_3, -C_2H_5, -$CH(CH_3)_2$, -$CH_2CH{=}CH_2$, -$CH(CH_3)CH{=}CH_2$, -$CH(CH{=}CH_2)_2$, -$CH_2C_6H_5$, -$CH(CH_3)C_6H_5$
Z = -OH, -OCH_3, -CHO, -$CH{=}CH_2$, -CH_3, -C_2H_5

Figure 6-1 The hydrogen abstraction reactions of interest in the present study. R represents the extended alkyl side chain and Z represents the substituent group.

A methodology to utilize Benson's group additivity concept for rate coefficients was introduced by Saeys et al. and further elaborated by Sabbe et al. [5,6,9]. This method, known as the group contribution method, is based on the idea that the rate coefficient for any reaction belonging to the same reaction family is given by the rate coefficient of a representative (reference) reaction and additive corrections to the pre-exponential (log(A)) term and activation energy (E_a), in a similar fashion to the structural method of Willems and Froment [17,18]. The corrections are needed to account for changes to the reactive center and its surrounding environment. A and E_a are directly related to entropy and enthalpy differences, respectively, between transition state and reactant(s) and the additivity assumption for these properties is well established. Since this concept has been used in the past to calculate rate coefficients for H atom abstraction [6,8,10-15] as well as for bond scission reactions [5,7,9,16],

the objective of the current study is to extend the existing database in a consistent way to the aromatic reactants shown in **Figure 6-1**.

After a thorough discussion of the applied methodology in the following section, the remainder of this chapter describes how this concept (i.e. the group contribution method) is used for the reactions shown in **Figure 6-1**. First, rate coefficients for reactions forming large training and validation sets are calculated theoretically using reliable electronic structure methods. Second, deviations between the pre-selected reference reaction and reactions of the training set are used to identify group additivity parameters describing these differences in terms of corrections to the pre-exponential factor and the barrier heights of the reference reaction. Third, the identified group additivity values are tested against reactions in the validation set. Fourth, both reaction sets are combined and used to regress the best group additivity parameters for the entire set of reactions. Finally, a tunneling correction model is introduced to account for quantum mechanical tunneling contributions.

6.3 Methodology

6.3.1 The group contribution method: a group additivity method for rate coefficients

The reaction family (hydrogen abstraction reactions (HARs) from substituted toluenes) studied in the current work is schematically described in **Figure 6-2**. In each of the reactions that belong to this family, a H atom abstracts a H atom attached to the alpha carbon which is the carbon C_2 in alpha (α) position to the phenyl group. This α-carbon has two additional ligands labeled as Y_1 and Y_2 which are varied, as shown in **Figure 6-1**. Similarly, the substituents Z are varied in terms of group (see **Figure 6-1**) and position relative to the bond to C_2. Obviously,

the simplest member of this reaction family is H abstraction from toluene itself and this reaction serves as the reference reaction.

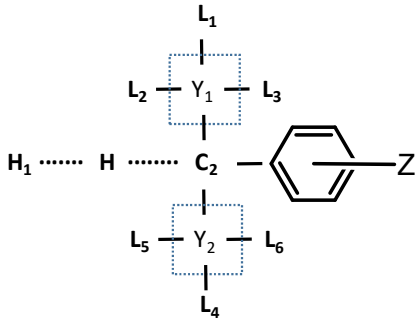

Figure 6-2 Scheme that represents the transition state of the abstraction of a hydrogen atom that is bonded to the carbon atom C_2 by a hydrogen atom ($H^{\bullet}$). Z represents the substituent group on phenyl ring.

If only a limited temperature range is considered, then the reaction rate coefficient might be represented accurately with the Arrhenius equation.

$$k(T) = \kappa n_e \tilde{k}(T) = \kappa n_e \tilde{A} exp(\frac{-E_a}{RT}) \tag{6-1}$$

In Eq. (6-1), n_e is the number of single events, $\tilde{k}(T)$ the single event rate coefficient expression, $\tilde{A}$ the single event pre-exponential factor and E_a is the activation energy.

The rate coefficient can be calculated through *ab initio* methods with transition state theory, either formulated in terms of thermodynamic properties or partition functions:

$$\begin{aligned} k(T) &= \kappa n_e \left(\frac{k_B * T}{h}\right) {V_{mol}}^{\Delta n^{\ddagger}} \exp\left(\frac{-\Delta G^{\ddagger}}{RT}\right) \\ &= \kappa n_e \left(\frac{k_B T}{h}\right) {V_{mol}}^{\Delta n} exp(\frac{\Delta S^{\ddagger}}{R}) exp(\frac{-\Delta H^{\ddagger}}{RT}) \end{aligned} \tag{6-2}$$

$$k(T) = \kappa n_e \left(\frac{k_B T}{h}\right) \frac{q^{\ddagger}}{q^R} exp(\frac{-\Delta E_{el}}{RT}) \tag{6-3}$$

V^{mol} is the molar volume at standard pressure (1 bar) and Δn reflects the change in the number of moles through reaction and takes the values of 1 and 0 for bimolecular and unimolecular reactions, respectively.

A comparison between Eq. (6-1) and Eq. (6-2) shows that $\tilde{A}$ depends only on one variable, the entropy difference between transition state and reactant, $\Delta S^{\ddagger}$, and similarly, the activation energy is directly related to the enthalpy difference between transition state and reactant, $\Delta H^{\ddagger}$.

From equation Eq. (6-3) it becomes clear that only the ratio of the partition functions for the transition state ($q^{\ddagger}$) and reactant (q^{R}) is needed, which means that the contributions from conserved modes, i.e. the non-reacting parts of the molecule, cancel out. This provides the justification to treat conserved modes as harmonic oscillators, which leads to substantial savings in CPU time.

By relating the rate coefficients of the members of a given reaction family to that of the reference reaction, group additivity parameters can be defined that are rather independent of temperature, as the latter effect is largely captured by the rate coefficient of the reference reaction. This leads to the following equations [5,6,9] (Eq. (6-4) and Eq. (6-5)):

$$k_{GA} = \exp(\log(\tilde{A}))\exp(\frac{-\mathrm{E}_a}{RT}) \tag{6-4}$$

where the Arrhenius parameters are given below as

$$\begin{aligned} E_a(T) &= E_{a,ref}(T) + \Delta GAV^{\circ}_{E_a}(C_2) + \sum_i \Delta NNI_i^{\circ}\, log\tilde{A}(T) \\ &= log\tilde{A}_{ref}(T) + \Delta GAV^{\circ}_{log\tilde{A}}(C_2) + \sum_i \Delta NNI_i^{\circ} \end{aligned} \tag{6-5}$$

The ΔGAV^0 parameters represent the difference of E_a or $\log(\tilde{A})$ between the reaction of interest and the reference reaction. While the transition state of any reaction is the same for the forward and reverse direction, the ΔGAV^0 parameters for both directions differ and need to be determined separately. While the ΔGAV^0 parameters describe the direct impact of substituents on the reacting carbon atom, additional non-nearest neighbor interactions such as steric repulsion or electronic effects for distant moieties of the reacting molecule exist which cannot be incorporated in ΔGAV^0 terms. To account for such contributions, ΔNNI^0s but must be defined and assigned with proper correction values. Identification of ΔNNI^0s is not straightforward not unambiguous. Nevertheless, these correction terms significantly expand the applicability of the GA method. The aim of this study is to determine a set of ΔGAV^0 and ΔNNI^0 for the target reactions.

6.3.2 Ab initio rate coefficients

The rate coefficients are calculated at the composite CBS-QB3 level of theory [19] as implemented in the Gaussian 09 software package (Revision D.01) [20]. The CBS-QB3 level of theory has been used successfully in prior GA kinetic studies, which also showed that CBS-QB3 based rate coefficients generally agree well with published rate coefficients. Previous work includes hydrogen abstractions from hydrocarbons [6,8,10], oxygenates [13-15], organosulfur compounds [11,12], and radical addition reactions to hydrocarbons [5,7,9] and oxygenates [16]. Selecting the same CBS-QB3 method in the current study thus ensured that the results are consistent with the older data.

All results are based on the lowest energy conformer. The CBS-QB3 data contains all information needed to apply Eq. (6-2). Partition functions (q) are calculated at the level of

B3LYP with CBSB7 basis set (6-311G(2d,d,p)) using a default scaling factor of 0.99. As mentioned above, it is assumed that the internal rotational modes of the non-reacting part of the molecule are conserved, hence, they cancel out and do not need to be treated in an elaborate way. Paraskevas et al. demonstrated the applicability of this assumption on a similar family of reactions, i.e. HARs from oxygenated aliphatic compounds by hydrogen atoms [14]. The methyl rotations in toluene and *m*- and *p*- substituted toluenes are free rotors whereas hydrogen abstraction from these methyl groups render the corresponding rotations in the transition state structures as hindered rotors. Therefore, these are non-conserved modes which should be treated separately.

It is well-known that quantum mechanical tunneling contributes significantly to rate coefficients are low temperature. Therefore, TST rate coefficients are generally multiplied with a tunneling correction factor κ to take such contributions into account. Group additivity cannot predict such contributions. Therefore, the databases used to determine ΔGAV^0 and ΔNNI^0 parameters contain rate coefficients without tunneling corrections. The incorporation of the contributions from quantum effects into the group additive reaction rate coefficients is discussed in the later sections of the methodology part.

The temperature dependent *ab initio* reaction rate coefficients, which were calculated in steps of 50 K, are converted to Arrhenius parameters (E_a and log A) through linear regression. For each temperature T, the results for the temperature range T −100 K to T+100 K are used.

6.3.3 Assignment of ΔGAV^0 and ΔNNI^0 values

The required ΔGAV^0s are determined by the structure of the toluene derivatives. Benson defines a group as “a polyvalent atom with all of its ligands” and denotes it as X-

$(A)_i(B)_j(C)_k(D)_l$ where X is the central atom surrounded by i A atoms, j B atoms, k C atoms, and l D atoms [21]. To improve accuracy, Benson distinguishes between different carbon types: single-bonded sp^3 carbon atom (C), double-bonded sp^2 carbon atom (C_d) and benzene-type carbon (C_b). Using these carbon species, the eight toluene derivatives (different R in **Figure 6-1**) lead to the following ΔGAV^0s: $\Delta GAV^0(C\text{-}(C_b)(H)_2)$, $\Delta GAV^0(C\text{-}(C_b)(C)(H))$, $\Delta GAV^0(C\text{-}(C_b)(C)_2)$, $\Delta GAV^0(C\text{-}(C_b)(C_d)(H))$, $\Delta GAV^0(C\text{-}(C_b)(C_d)(C))$, $\Delta GAV^0(C\text{-}(C_b)(C_d)_2)$, $\Delta GAV^0(C\text{-}(C_b)_2(H))$ and $\Delta GAV^0(C\text{-}(C_b)_2(C))$. The simplest prototype reactions resembling these ΔGAV^0s are used to assign values for these groups. ΔNNI^0s are assigned based on the need to improve rate coefficients that otherwise deviate too much from the *ab initio* data.

Once all ΔGAV^0s and ΔNNI^0s are identified, the agreement between group additively and *ab initio* calculated Arrhenius parameters is improved through linear regression. To do so, typically an unweighted least-squares analysis

$$SSQ = \sum_i^n (y_i - \hat{y}_i)^2 \tag{6-6}$$

is employed. In Eq. (6-6), y_i is the *ab initio* calculated Arrhenius parameter, i.e. activation energy barrier (E_a) or logarithm of intrinsic pre-exponential factor ($log\tilde{A}$), of the reaction i and $\hat{y}_i$ is the calculated Arrhenius parameter value via group additivity. This results in the equation:

$$\overline{\Delta GAV°/\Delta NNI°} = (X^T X)^{-1} X^T \bar{y} \tag{6-7}$$

In Eq. (6-7), $\overline{\Delta GAV°/\Delta NNI°}$ is the calculated vector of the group additive parameters and X is the occurrence matrix in which each row represents a reaction and each column refers to a $\Delta GAV°$ or $\Delta NNI°$. The elements of this matrix X_{ij} specify the number of occurrences of group j in radical i. Here, $\bar{y}$ is the vector of all y_i.

A statistical analysis is performed to assess the reliability of the linear regression step and the quality of the optimization procedure. The quality of the fits is expressed in terms of the significance (F) of the regression, the mean absolute deviation (MAD), root-mean square deviation (RMS) and maximum deviation (MAX) between *ab initio* data and the data obtained via group additivity. The reported significance F of the regression is calculated with the following equation:

$$F = \frac{(\sum_{i=1}^{n} \hat{y}^2)/p}{(\sum_{i=1}^{n} (\hat{y}_i - y_i)^2)/(n-p)} \tag{6-8}$$

In Eq. (6-8), n is the number of reactions and p is the total number of ΔGAV° and ΔNNI° parameters.

6.3.4 Tunneling model

As mentioned above, reaction rate coefficients that are calculated through group contribution method exclude quantum tunneling effects. Such a practice is followed since the calculation of tunneling coefficients require knowledge that cannot be obtained based on the geometries of the participating species. The fundamental piece of information that is necessary is the imaginary frequency of the transition state which is not an accessible information for the users. To incorporate the tunneling corrections that are calculated by asymmetric one-dimensional Eckart potentials [22] into GA calculations, a correction function is developed, which only depends on information available by GA. This function is discussed in detail in the results section.

6.3.5 Comparison between GA and ab initio rate coefficients

The ultimate objective of this study is to enable calculation of accurate reaction rate coefficients for a broad range of reactions belonging to the same reaction family. This is done through:

$$k = \kappa_{TCF}\, n_e k_{GA} \tag{6-9}$$

In Eq. (6-9), κ_{TCF} is the tunneling coefficient calculated with the tunneling correction function and n_e is the number of single events. The rate coefficient obtained with Eq. (6-9) can be compared to the *ab initio* result to assess the accuracy of the GA method. A good measure for such a comparison is the "factor of deviation" (ρ), as given in Eq. (6-10).

$$\begin{aligned} k_{AI} > k_{GA}, \rho &= \frac{k_{AI}}{k_{GA}} \\ k_{GA} > k_{AI}, \rho &= \frac{k_{GA}}{k_{AI}} \end{aligned} \tag{6-10}$$

By definition, the factor ρ always has a value equal to or higher than 1 and a low value for ρ for a reaction indicates good agreement between *ab initio* and GA-based reaction rate coefficients, i.e. better performance of GA parameters in reproducing *ab initio* reaction rate coefficients. Moreover, it permits calculation of geometric mean factor of deviation of the rate coefficients ($<\rho>$) of a set of reactions.

6.4 Results and Discussion

6.4.1 Ab initio rate coefficients and Arrhenius parameters

The transition state theory calculations have been carried out to populate the training set needed to derive the desired group additivity parameters. Each of the eight different alkyl groups R shown in **Figure 6-1** yields 19 reactants, which consist of the HARs from one unsubstituted

(no Z) and 18 single substituted toluene derivatives (6 different substituents, three different positions (*ortho* (*o*-), *meta* (*m*-) and *para* (*p*-))). Combined, this leads to a training set of 152 reactions. The list of these reactions is given in **Figure D-1 - Figure D-8** of Appendix D. Arrhenius parameters for these reactions were determined at 300 K, 600 K, 1000 K, 1500 K and 2000 K and the data for the forward and reverse direction are documented, respectively, in **Table D-1, Table D-2, Table D-3, Table D-4** and **Table D-5** of Appendix D. These tables contain also the Eckart tunneling correction factors. The internal (σ_{int}) and external symmetry (σ_{ext}) and the number of optical isomers (n_{opt}) of reactants, products and transition states for these reactions are given in **Table D-6** of Appendix D.

There is only very limited experimental data available e.g. in the NIST Chemical Kinetics Database [23] to validate the current calculation results. A recent study by Oehlschlager et al. [24] reports the rate coefficient for α-HAR from toluene by a hydrogen atom for the temperature range of 700 K to 1800 K. At 1000 K, the CBS-QB3 calculated rate coefficient (5.8 10^5 m^3 mol^{-1} s^{-1}) agrees within a factor of 1.3 with the value by Oehlschlager et al. (7.4 10^5 m^3 mol^{-1} s^{-1}) [24]. Ellis et al. [25] reported a rate coefficient for the same reaction applicable to temperatures ranging from 500 K to 1500 K. At 500 K, the experimental rate coefficient (5.9 10^3 m^3 mol^{-1} s^{-1}) is higher than the that of the CBS-QB3 (4.6 10^3 m^3 mol^{-1} s^{-1}) by a factor of 1.3, whereas at 1000 K, the experimental reaction rate coefficient is 1.1 10^6 m^3 mol^{-1} s^{-1}, a factor of 1.5 higher than the CBS-QB3 based rate coefficient (7.4 10^5 m^3 mol^{-1} s^{-1}). In order to achieve this level of agreement, the methyl rotor in toluene had to be treated as a free rotor and not as harmonic oscillator as mentioned in the methodology section.

Ellis et al. [25] also reported a rate coefficient for α-HAR from ethylbenzene by hydrogen atom for the same temperature range. This reaction rate coefficient yields a value of 2.2 10^6 m^3 mol^{-1}

s^{-1} at 1000 K which is a factor of 2.9 higher than the CBS-QB3 data for this reaction (7.6 10^5 m^3 mol^{-1} s^{-1}). This discrepancy is of same magnitude as for toluene. One reason why the CBS-QB3 calculated rate coefficient is lower is that the methyl rotor in the transition state is treated as a harmonic oscillator, assuming that the rotation is already completely disabled in the transition state. A hindered rotor treatment would have increased the pre-exponential factor and thus the rate coefficient. Nevertheless, both comparisons show that the *ab initio* calculated results are close to the experimental data.

6.4.2 Development of the group additive model

I. Assigning group additive parameters

The H abstraction from toluene by a hydrogen atom is chosen as reference reaction and, hence H abstraction from H_2 by the benzyl radical serves as the reference reaction for all the reverse reactions (See **Figure 6-3**). The activation energies (E_a) and the logarithms of single event pre-exponential factors ($\log\tilde{A}$) of this reaction are given at 300 K, 600 K, 1000 K, 1500 K and 2000 K in both forward and reverse directions in **Table 6-1**.

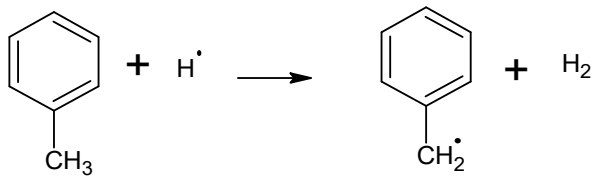

Figure 6-3 The reference reaction.

Table 6-1 The activation energies (E_a) and the logarithms of single event pre-exponential factors ($\log\tilde{A}$) of the reference reaction are given for a wide range of temperatures from 300 K to 2000 K in both forward and reverse directions.

T	Forward		Reverse	
	$E_{a,f}$[a]	$\log\tilde{A}_f$[b]	$E_{a,r}$[c]	$\log\tilde{A}_r$[d]
300 K	35.8	9.615	96.2	8.990
600 K	41.2	10.263	98.5	9.252
1000 K	49.8	10.837	105.8	9.734
1500 K	59.4	11.247	116.6	10.191
2000 K	67.8	11.502	127.2	10.510

[a] **$E_{a,f}$:** Activation energy of the forward reaction, given in kJ mol^{-1}.
[b] **$\log\tilde{A}_f$:** Logarithm of the pre-exponential factor of the forward reaction, given in m^3 mol^{-1} s^{-1}.
[c] **$E_{a,r}$:** Activation energy of the reverse reaction, given in kJ mol^{-1}.
[d] **$\log\tilde{A}_r$:** Logarithm of the pre-exponential factor of the reverse reaction, given in m^3 mol^{-1} s^{-1}.

Given the selection of the reference reaction, the ΔGAV° values can be initialized using the rate coefficients for the unsubstituted (no Z groups) alkyl benzenes. Obviously, the initial $\Delta GAV^{\circ}_{E_a}$(C-(C_b)(H_2)) and $\Delta GA^{\circ}_{\log\tilde{A}}$ (C-(C_b)(H_2)) values must be close to zero and the values for the other seven ΔGAV° pairs reflect the differences in log $\tilde{A}$ and E_a between the corresponding Arrhenius parameters and those of the reference reaction. An alternative way for initialization is to use the entire training set of 152 reactions to determine the optimized ΔGAV° values through linear regression with the assumption that no non-nearest neighbor effects exist. Following this strategy, the initial values given in **Table D-7** of Appendix D are obtained.

Deviations of GA calculated rate coefficients using the initial set of eight ΔGAV° values from the *ab initio* based rate coefficients indicate the existence of non-nearest neighbor effects. These deviations are given in **Table D-8** and **Table D-9** of Appendix D for the forward and reverse directions, respectively. Using these tables, 3 ΔNNI°s are identified for the HARs in the forward direction and 14 ΔNNI°s are identified for the HARs in the reverse direction. These

ΔNNI°s are listed in **Table 6-2**. Since ΔNNI° cannot unambiguously be identified but result from the interpretation of deficiencies of GA predictions, it is important to justify the selection of ΔNNI°s made. One criterion for selection is that the newly introduced ΔNNI°s clearly improve the geometric mean factor (<ρ>) and the maximum factor of deviation (ρ_{max}) between the CBS-QB3 and GA based rate coefficients. Another factor is the plausibility of the ΔNNI°s, meaning that one can identify a physical reason for them. Therefore, **Table 6-2** contains a brief justification of each ΔNNI°. A more detailed discussion of the origin of the ΔNNI°s can be found below. Since these ΔNNI°s are actually sets of two values, one for E_a and the second for log$\tilde{A}$, the deviations between *ab initio* and GA rate coefficients need to be examined at different temperatures. As a general trend, the impact of the deviations in activation energies (E_a) on the rate coefficient decreases with increasing temperature while the log$\tilde{A}$ term affects the rate coefficients more as the temperature increases. These two effects come to balance at the isokinetic temperature where rate coefficients pertaining to the HARs from unsubstituted and substituted toluene derivatives are the same, meaning that substitution has no effect on the reaction rate coefficients. In some cases, the isokinetic temperature is within the calculated temperature range (300 K-2000 K) while in some other cases, substitution leads to an increase or decrease in rate coefficients throughout the whole range of temperatures under investigation. Consequently, the ΔNNI° identification made use of the entire range of temperatures studied.

Once all required ΔNNI°s are introduced, the ΔGAV° and ΔNNI° parameters can be optimized through linear regression. The updated values are provided in **Table D-10** and **Table D-11**, respectively. The deviations between the *ab initio* and the GA-based values for the E_a and log$\tilde{A}$

of the reactions in the training set in the forward and reverse directions are available in **Table D-12** and **Table D-13**, respectively.

Table 6-2 ΔNNI°s for the forward reactions (**ΔNNI$_f$°**s) and the reverse reactions (**ΔNNI$_r$°**s), the reactant of the HARs for which these parameters are defined, physical interpretation of the parameters and the preliminary activation energy values for these ΔNNI°s.

ΔNNI° #	**Singly substituted toluene derivative or benzylic radical class (ZC_6H_4R)[a]**	**Substituent group (Z)**	**Physical interpretation of the overall interaction**	**E_a [b] [kJ mol^{-1}]**	**log$\widetilde{A}$ [c] [m^3 mol^{-1} s^{-1}]**
Forward Reactions (ΔNNI$_f$°s)					
ΔNNI$_f$°1	$C_6H_4CH(CH_3)_2$	*o*-CHO	* Stronger destabilization due to SE[d] in the TS[e] than in the reactant.	6.8	-0.207
		o-$CH=CH_2$			
		o-CH_3			
		o-CH_2CH_3			
ΔNNI$_f$°2	$C_6H_4CH(CH=CH_2)_2$	*o*-CH_3	* Stronger steric destabilization due to SE in the TS than in the reactant.	6.7	-0.127
		o-CH_2CH_3			
ΔNNI$_f$°3	$C_6H_4CH_2C_6H_5$ $C_6H_4CH(CH_3)C_6H_5$	*o*-OH	* HB[f] in the TS is stronger than in the reactant.	-5.5	-0.347
Reverse Reactions (ΔNNI$_r$°s)					
ΔNNI$_r$°1	$C_6H_4C\bullet(CH_3)_2$	*o*-OH	* Destabilization caused by SE is stronger in the reactant than in the TS.	-10.4	-0.018
		o-OCH_3			
ΔNNI$_r$°2	$C_6H_4C\bullet(CH_3)_2$	*o*-CHO	* Destabilization caused by SE is stronger in the reactant than in the TS.	-5.0	0.573
		o-$CH=CH_2$			
ΔNNI$_r$°3	$C_6H_4C\bullet(CH_3)_2$	*o*-CH_3	* Destabilization caused by SE is stronger in the reactant than in the TS.	-10.2	0.424
		o-CH_2CH_3			
ΔNNI$_r$°4	$C_6H_4C\bullet HCH=CH_2$	*o*-OH	* There is HB in the TS whereas in the reactant radical, -OH group points away from $-CH_2CH=CH_2$ group.	-6.0	-0.354
ΔNNI$_r$°5	$C_6H_4CH_2\bullet$	*p*-CHO	* Mesomeric stabilization of the radical: **M+** effect of the extended side chain interacts with the **M-** effect of the -CHO and $-CH=CH_2$ substituent groups.	7.9	0.110
	$C_6H_4CH\bullet CH_3$				
	$C_6H_4C\bullet(CH_3)_2$	*p*-$CH=CH_2$			
	$C_6H_4C\bullet HCH=CH_2$				
ΔNNI$_r$°6	$C_6H_4C\bullet(CH_3)CH=CH_2$	*o*-OCH_3	* Destabilization caused by SE is stronger in the radical than in the TS.	-7.4	0.136
		o-CHO			
		o-$CH=CH_2$			
		o-CH_3			
		o-CH_2CH_3			

ΔNNI$_r$°7	$C_6H_4C•(CH=CH_2)_2$	*o*-OH	* HB in the reactant is stronger than that of the TS.	3.8	-0.361
ΔNNI$_r$°8	$C_6H_4C•(CH=CH_2)_2$	*o*-OCH_3	* Significant entropy decrease in the radical upon restriction of rotation, which is absent in the TS.	3.1	-1.043
ΔNNI$_r$°9	$C_6H_4C•(CH=CH_2)_2$	*o*-CHO	* Combination of the stabilization of the reactant due to HB and the destabilization of the TS caused by SE.	6.7	-1.076
ΔNNI$_r$°10	$C_6H_4C•(CH=CH_2)_2$	*o*-$CH=CH_2$ *o*-CH_3 *o*-CH_2CH_3	* Combination of the stabilization of the reactant due to HB and the destabilization of the TS caused by SE.	12.9	-1.010
ΔNNI$_r$°11	$C_6H_4C•HC_6H_5$ $C_6H_4C•(CH_3)C_6H_5$	*o*-OH	* HB in the TS is stronger than that of the reactant.	-3.4	-0.588
ΔNNI$_r$°12	$C_6H_4C•HC_6H_5$ $C_6H_4C•(CH_3)C_6H_5$	*o*-OCH_3	* Destabilization of the radical caused by SE.	-6.5	-0.580
ΔNNI$_r$°13	$C_6H_4C•HC_6H_5$ $C_6H_4C•(CH_3)C_6H_5$	*o*-CHO *o*-$CH=CH_2$ *o*-CH_3 *o*-CH_2CH_3	* Steric destabilization in the radical is slightly stronger than that of the TS. * Significant entropy decrease in the radical upon restriction of rotation, which is absent in the TS.	-2.2	-0.595
ΔNNI$_r$°14	$C_6H_4C•(CH_3)CH=CH_2$ $C_6H_4C•HC_6H_5$ $C_6H_4C•(CH_3)C_6H_5$	*p*-CHO *p*-$CH=CH_2$	* Mesomeric stabilization of the radical: **M+** effect of the extended side chain interacts with the **M-** effect of the -CHO and -$CH=CH_2$ substituent groups.	6.3	0.125

[a] The list of **R** (extended side chain) and **Z** (substituent) groups are given in **Figure 6-1**.
[b] The values of activation energies (E_as) are obtained from the simultaneous linear regression of **ΔGAV°s** and **ΔNNI°s** based on the training set, which are taken from **Table D-10** and **Table D-11** of Appendix D.
[c] The values of **ΔGAV°s** and **ΔNNI°s** for the logarithm of the single event pre-exponential factors ($\log\tilde{A}$s).
[d] **SE:** Steric effect.
[e] **TS:** Transition state.
[f] **HB:** Hydrogen bond.

The ΔNNI°s that are introduced to correct for the substituent effects, the differences in the forward reactions are labeled $\Delta NNI_f°$s to distinguish these parameters from the ΔNNI°s needed for the reverse reactions, i.e. the $\Delta NNI_r°$s. In **Table 6-2**, 3 $\Delta NNI_f°$s and 14 $\Delta NNI_r°$s are reported. The larger number of required ΔNNI° for the reverse direction seems plausible

because substituent effects are expected to play a larger role in benzyl radicals than in the closed shell toluene derivatives. This expectation is in agreement with the observations on thermodynamics for toluene derivatives and benzylic radicals that are discussed in **Chapters 3-5**. **Table 6-2** shows that all $\Delta NNI_f°$s apply to *o*- substituted reactants (i.e. toluene derivatives) whereas $\Delta NNI_r°$s are needed for *o*- and *p*- substituted abstracting benzylic radicals. This again is consistent with the thermodynamic data discussed in **Chapters 3-5**.

II. Discussion of the ΔNNI°s

II.1 ΔNNI$_f$°s for the forward direction

$\Delta NNI_f°1$ corrects the Arrhenius parameters for HARs from -CHO, -CH=CH_2, -CH_3 or -CH_2CH_3 *o*- substituted isopropylbenzenes ($C_6H_5CH(CH_3)_2$). The optimized structures of the species involved in these reactions are available in **Figures D-9** – **D-12** of Appendix D. In these reactions, the bulky substituents create repulsive steric effects in the reactant as well as in the transition state (TS). Since the destabilization is stronger in the TS, the activation energy increases, as given in **Table 6-2**, by 6.8 kJ mol^{-1}.

$\Delta NNI_f°2$ corrects for substituent effects observed in the HARs from *o*-CH_3 and *o*-CH_2CH_3 substituted α-vinylallylbenzenes (See **Figures D-13** and **D-14**). Similar to **$\Delta NNI_f°1$**, steric effects are present in both the reactants and TS structures of these HARs and the relatively larger steric repulsion noted in the TS amounts to 6.7 kJ mol^{-1}.

The TS structures of the HARs from *o*-OH substituted diphenylmethane and 1,1-diphenylmethane are characterized by stabilizing interaction of the polar OH group and the second aromatic ring (see **Figures D-15** and **D-16**). Such a stabilization is not seen in the reactant molecules as the OH groups point away from the extended side chains. The structural

differences noted between the TS structures and the reactants cause a significant decrease in the E_a of the HARs of -5.5 kJ mol^{-1}.

Concerning the log$\tilde{A}$s, all three ΔNNI_f°s discussed above reduce the pre-exponential part of the rate coefficients (see **Table D-11** of Appendix D), indicating a loss of activation entropy relative to the reference reaction. This is expected because the stronger steric or hydrogen bond effects in the TS structures increase their stiffness.

Because the first two ΔNNI_f° corrections increase the E_a value and reduce log$\tilde{A}$ they lead to smaller reaction rate coefficients. In **ΔNNI_f°3**, the E_a and log$\tilde{A}$ values are both negative, meaning that the two parameters impact the rate coefficient in opposite directions. In HARs from both *o*-OH substituted diphenylmethane and diphenylethane, this ΔNNI_f° correction accelerates the reaction due to the reduced barrier at all the temperatures of interest. However, with increasing temperatures, the differences between the rate coefficients of the HARs from these two molecules and their unsubstituted counterparts decrease as the decreases in pre-exponential factors caused by substituent effects leads to smaller increases in the rate coefficients.

II.2 ΔNNI_r°s for the reverse direction

The first three ΔNNI_r°s in **Table 6-2** address non-next neighbor effects in HARs from H_2 by singly substituted 2-phenyl-2-propyl radicals. These substituent effects are caused by steric repulsions in the 2-phenyl-2-propyl radicals and to a lesser degree in the TS structures. Since the radicals are more destabilized than the TS, the E_a of the reaction decreases. Among the three correction parameters, **ΔNNI_r°1** is used if the Z groups are *o*-OH or *o*-OCH_3, whereas **ΔNNI_r°2** and **ΔNNI_r°3** are defined to describe Z = *o*-CHO/$CH{=}CH_2$ and Z = *o*-CH_3/CH_2CH_3 cases, respectively. In terms of magnitude, **ΔNNI_r°2** is smaller (−5.0 kJ mol^{-1}) than the other

two correction parameters, which both correct the barrier by approximately −10.0 kJ mol^{-1}, as seen in **Table 6-2**.

In the optimized geometries of *o*-OH or *o*-OCH_3 substituted 2-phenyl-2-propyls (See **Figure D-17** and **D-18**), one of the methyl groups that are bonded to the α-carbon bearing the radical center are very close to the oxygen atom whereas this interaction is relatively weaker in the TS structures as the methyl is further away from the oxygen in the TS than in the optimized geometry of the radical. This geometric feature of the substituent also causes the presence of -OH or -OCH_3 groups in *o*- position to the extended side chain (-$CH(CH_3)_2$) to have a negligibly small impact on the entropies of both the reactant and the TS structure, leading to almost zero values for the **$\Delta NNI_r°1$** parameter for pre-exponential factors. The fact that the **$\Delta NNI_r°1$** parameter is negative for the E_a and almost zero for $\log\tilde{A}$ implies that this parameter corrects for an increase in the reaction rate coefficients as compared to the reference reaction.

Regarding the HARs from H_2 by *o*-CHO and *o*-$CH=CH_2$ substituted 2-phenyl-2-propyls (See **Figures D-9** and **D-10** of Appendix D), the steric repulsion in the radicals is stronger than in the o-OH/OCH_3 substituted case and it forces the substituent groups (-CHO and -$CH=CH_2$) out of the plane of the phenyl ring which explains why the magnitude of the E_a correction for **$\Delta NNI_r°2$** is smaller than that of **$\Delta NNI_r°1$.** The geometries of these radicals indicate a very strong restriction of rotation around the bonds upon the presence of the Z groups, an effect that is absent in the TS structure. This clarifies the reason behind the highly positive values of **$\Delta NNI_r°2$** for $\log\tilde{A}$. For **$\Delta NNI_r°2$**, the correction parameter for E_a is negative and that of the $\log\tilde{A}$ is positive, leading to an increase in the reaction rate coefficients.

The strong steric effects encountered in *o*-CH_3/CH_2CH_3 substituted 2-phenyl-2-propyls are caused by the alkyl groups directly facing each other in these radicals (See **Figures D-11** and

D-12 of Appendix D). Since the TS structure of the HAR in **ΔNNI$_r$°3** is devoid of such a strong effect, the magnitude of the activation energy correction is -10.2 kJ mol^{-1}. The value of **ΔNNI$_r$°3** correction for log$\tilde{A}$ is highly positive, analogous to that of the **ΔNNI$_r$°2**, due to the similar reasons explained above for **ΔNNI$_r$°2**. Therefore, the group additively calculated reaction rate coefficients increase upon applying **ΔNNI$_r$°3** parameters to incorporate relevant substituent effects into the Arrhenius parameters.

ΔNNI$_r$°4 accounts for a stabilizing hydrogen bond formed between the -OH group and the π-system of the extended side chain in the TS structure (see **Figure D-19** of Appendix D). The stiffness created by the hydrogen bond explains the log$\tilde{A}$ reduction.

Four of the eight benzylic radical classes of interest, namely the alkylphenyls (benzyls, 1-phenylethyls, 2-phenyl-2-propyls) and the 3-phenyl-1-propen-3-yls, are resonantly stabilized and *p*-CHO and *p*-CH=CH$_2$ substitution on these radicals increase the mesomeric stabilization (+M effect by the extended side chains and -M effect by the substituents), as explained before in **Chapter 4** and **Chapter 5**. In the TS of the H abstraction reaction from H$_2$ by these radicals (**Figures D-20 - D-27** of Appendix D), the radical site is already in the process of forming a new bond to the migrating H atom. Therefore, the mesomeric effects noted in the radicals cannot be encountered in the TS which explains the positive correction of 7.9 kJ mol^{-1} for the E$_a$, listed as **ΔNNI$_r$°5** in **Table 6-2**. The pre-exponential factors remain largely unchanged due to the long distance between R and Z groups.

The effect of steric interactions encountered in five different *o*- substituted (*o*-OCH$_3$, *o*-CHO, *o*-CH=CH$_2$, *o*-CH$_3$ and *o*-CH$_2$CH$_3$) 3-phenyl-1-buten-3-yl radicals, see **Figures D-28 - D-32** of Appendix D, on the HAR kinetics are accounted for with **ΔNNI$_r$°6**. Since the destabilizing repulsive interactions are stronger in the benzylic radicals than in the corresponding TS

structures, the activation energies decrease by 7.4 kJ mol^{-1}. The steric repulsion also has an influence on the pre-exponential factor. Since the benzylic carbon transitions from sp^2 to sp^3, the TS can respond to the substituents in a more flexible manner than the radical. Therefore, the activation entropy and thus log$\tilde{A}$ increase.

In Phenyl-C•R_2 radicals with small R groups, the C•R_2 is in plane with the phenyl group. This is no longer the case for the more voluminous R group in 3-phenyl-1,4-pentadien-3-yl radical. Instead, this radical is best viewed as a linear pentadienyl chain substituted with a phenyl group at C_3. The non-planar arrangement reduces the mesomeric stabilization of the radical site by the phenyl group significantly and the amount of remaining stabilization strongly depends on the degree of non-planarity (See **Figures D-33** – **D-38** of Appendix D). This structural difference and the related structure of the TS for H abstraction from H_2 by 3-phenyl-1,4-pentadien-3-yl is incorporated in the corresponding ΔGAV°. Additional effects by *ortho* (*o*-) substituents are accounted for by 4 **ΔNNI$_r$°**s (**ΔNNI$_r$°**s **7-10** in **Table 6-2**). All four corrections cause an increase in activation energy, which can be explained with a stronger repulsive *o*-interaction in the TS compared to the reacting radical. Oxygen containing substituent groups lead to smaller corrections than pure hydrocarbon substituents, which points to electronic interactions between the oxygen electron pairs and the π-bonds of the radical chain. This destabilization is stronger in the reacting radical than in the transition state and counterbalances the bulkiness effect.

The increase in activation energy due to steric repulsion is in line with a large decrease of the pre-exponential factor, because the internal modes of the TS are more restricted by *o*- groups than those of the radical. The log$\tilde{A}$ correction for **ΔNNI$_r$°7** is notably smaller than those of the other three **ΔNNI$_r$°**s. This can be explained by a hydrogen bond formed between the OH

substituent and one π-bond of the pentadienyl moiety. This hydrogen bond reduces the entropy of the reacting radical and counter-balances the *o*- effect on the entropy of the transition state. The next three ΔNNI°s in **Table 6-2**, namely Δ**NNI$_r$°**s **11-13**, are defined for HARs from H_2 by *o*- substituted diphenylmethyl and 1,1-diphenylethyl radicals (See **Figures D-39** – **D-50** of Appendix D). These HARs are similar to those of 3-phenyl-1,4-pentadien-3-yls in the sense that the radical experiences less mesomeric stabilization because the bulky groups attached to the radical bearing carbon prevent proper planar alignments of the π-systems. This makes the rate coefficients of these reactions again very sensitive to *o*- substituents. Δ**NNI$_r$°11** is special because it corrects for the impact of a hydrogen bond formed by an *o*-OH group with the π-system of a phenyl ring. The hydrogen bond is stronger in the TS than in the reactant, hence E_a decreases by -3.4 kJ mol^{-1} and the log$\tilde{A}$ is also reduced. Δ**NNI$_r$°12** and Δ**NNI$_r$°13** account for steric repulsive effects. Both lead to reduced activation energies because the destabilizing effects are stronger in the radical than in the TS, in which the radical center changes already to a sp^3 hybridization and hence contributes less to resonance. The activation energy decrease by -6.5 kJ mol^{-1} for *o*-OCH_3 substitution (Δ**NNI$_r$°12**) but only by -2.2 kJ mol^{-1} for -CHO, -$CH{=}CH_2$, -CH_3, and -CH_2CH_3 substituents. The unique larger E_a reduction by the -OCH_3 group might be caused by interactions of the lone-pair electrons with the π–system (anomeric effect). All discussed interactions restrict internal rotations or low-frequency oscillations. Since those modes contribute more in the TS than in the reactants, the overall effect is a reduction of log$\tilde{A}$. Δ**NNI$_r$°14** describes the substituent effects on the HARs from H_2 by *p*-CHO and *p*-$CH{=}CH_2$ substituted 3-phenyl-1-buten-3-yls, diphenylmethyls and 1,1-diphenylethyl radicals. A correction is needed for these reactions because there are stabilizing mesomeric interactions in the radical whereas there are no such interactions in the TS, leading to an increase in the

activation energies. In a similar fashion to $\Delta\mathbf{NNI_r°5}$, the interplay of the mesomeric effects between the radical bearing extended side chains (+M effect) and the substituents (-M effect) stabilize *p*-CHO and *p*-CH=CH_2 substituted 3-phenyl-1-buten-3-yls, diphenylmethyls and 1,1-diphenylethyls by 6.3 kJ mol^{-1}. Provided that these substitutions do not have any remarkable effect on the entropies, and thus the $\log\tilde{A}$, it can be concluded that these substituents decrease the reaction rate coefficients of the corresponding HARs.

The deviations between the values obtained from *ab initio* and GA calculations for the forward and reverse directions are available in **Table D-12** and **Table D-13** of Appendix D, respectively. Furthermore, in order to assess the performance of the ΔGAV°/ΔNNI° parameter set reported in this work, the rate coefficients calculated with these parameters are compared to the *ab initio* based rate coefficients through the factor of deviations (ρ). ρ values for all the HARs in the training set are reported in **Table D-14** of Appendix D at all the five temperatures studied. It should be kept in mind that the *ab initio* rate coefficients discussed here do not include tunneling effects since the contribution due to these effects will be modeled separately in the following section via a tunneling model. In **Table D-15** of Appendix D, the performance of the GA parameters is demonstrated, through a comparison of Arrhenius parameters and the reaction rate coefficients.

The mean absolute deviation (MAD) of the activation energies between the CBS-QB3 and GA based data for the HARs in the forward and the reverse directions is less than 1.7 kJ mol^{-1} and 1.5 kJ mol^{-1}, respectively, at all the temperatures of interest. All the E_as agree within 4.7 kJ mol^{-1} for both forward and reverse directions at 300 K, where the activation energy has the most prominent effect on the reaction rate coefficients among the temperatures studied. It can be noted from **Table D-15** of Appendix D that at higher temperatures, the maximum deviations

in the activation energies are much less the same in both directions. Concerning the pre-exponential factors, the MAD in the $\log\tilde{A}$ is 0.106 and 0.143 in forward and reverse directions, respectively, at 300 K. In the forward direction, the MAD values that represent the deviations in $\log\tilde{A}$ parameters gradually increase from 0.106 to 0.135 from 300 K to 2000 K, whereas in the reverse direction, the MADs are similar for all the five temperatures. At all the five different temperatures, the maximum absolute deviations (MAX) are within 0.514 in both directions. These MAD and MAX values demonstrate that the present set of ΔGAV°/ΔNNI° parameters is capable of reproducing the Arrhenius parameters of the HARs in the training set.

The geometric mean factor of deviations (<ρ>) between the reaction rate coefficients calculated by CBS-QB3 and the ΔGAV°/ΔNNI° parameters is less than 2 for both forward and reverse directions. The performance of the parameters in obtaining satisfactory agreement for the reaction rate coefficients improves with increasing temperature. At 300 K, the maximum factor of deviations (ρ_{max}) are 7.0 and 7.2 for forward and reverse directions, respectively. At 600 K, ρ_{max} is 3.3 in the forward direction and 4.0 in the reverse. At 1000 K, 1500 K and 2000 K, all the ρ values are lower than 3.4 in both directions. In conclusion, the parameters reported in this study have a satisfactory performance in reproducing CBS-QB3 based reaction rate coefficients.

The CBS-QB3 rate coefficients do not include quantum tunneling effects and these effects are calculated separately with Eckart potentials. Similarly, the GA parameters that are developed using the CBS-QB3 dataset excludes these effects. In the following section, a tunneling correction function is proposed to model the tunneling effects. The final values for the reaction rate coefficients are obtained by using the GA parameters and then, employing the tunneling correction function to correct for the tunneling effects.

III. Tunneling correction function

The extent of quantum tunneling cannot modeled by group additivity. According to the simplest model, quantum tunneling (κ) is a function of the imaginary frequency of the transition state ($lm(v^{\ddagger})$) and the temperature (T) [26].

$$\kappa(T) = 1 + \frac{1}{24}\left(\frac{hlm(v^{\ddagger})}{k_B T}\right)^2 \tag{6-11}$$

Since the imaginary frequency is not available to users or automated mechanism generating tools, tunneling corrections must be incorporated via an equation that only contains available information which is E_a and $log\tilde{A}$.

Sabbe et al. [10] and Paraskevas et al. [13] proposed the use of different polynomial tunneling correction functions, which were capable of describing their datasets well. In the present study, the tunneling correction factor κ is approximated as

$$\kappa(T) = 1 + 125\left(\frac{E_{a,exo}}{T}\right)^2 \tag{6-12}$$

It reflects the observation that the *ab initio* calculated κ_{Eckart} correction factors [22] correlate reasonably well with $E_{a,exo}$, the activation energy for the direction of the exothermic reaction which is always the reaction in the forward direction for the HARs under investigation. A graphical comparison of the Eckart tunneling coefficients and the coefficients obtained from Eq. (6-12) at 300 K is available in **Figure D-51** of Appendix D. The tunneling factor converges to 1 at high temperatures similar to the original Wigner model (Eq. (6-11)).

Eq. (6-12) reproduces the κ_{Eckart} factors with an average factor of 1.2 at 300 K and for the majority of the HARs within the training set the factor is 1.5 or less at this temperature. With

increasing temperature the agreement improves and the mean factor of deviation is only 1.1 at both 600 K and 1000 K, while at higher temperatures, tunneling contributions can be neglected.

6.4.3 Transferability of the new group additivity parameters

The performance of the simultaneously optimized ΔGAV°s and ΔNNI°s and the tunneling correction function (Eq. (6-12)) is tested with a set of 59 reactions not included in the training set. This validation set includes HARs that only probe the effects of substitution on the phenyl ring, i.e. the reactants of the HARs in the validation set include doubly-substituted toluene derivatives which possess two Z groups on the phenyl ring whereas no substitution on R groups is considered. The aim of the validation set is to test transferability of the new ΔGAV°s and ΔNNI°s to the HARs involving multiply-substituted HARs. See **Figures D-52** – **D-59** of Appendix D for a list of these reactions.

The Arrhenius parameters ($\mathbf{E_a}$ and $\mathbf{log}\widetilde{\boldsymbol{A}}$), Eckart tunneling correction factors (κ_{eckart}) and the reaction rate coefficients for all HARs in the validation set are reported in **Table D-17 - Table D-21** of Appendix D for both the forward and the reverse directions at temperatures of 300 K, 600 K, 1000 K, 1500 K and 2000 K. Information needed to calculate the number of single events is provided in **Table D-22**. The Eckart tunneling coefficients of these HARs are compared in **Table D-23** at 300 K, 600 K and 1000 K with those obtained with Eq. (6-12). The deviations between *ab initio* and GA calculated Arrhenius parameters are tabulated in **Table D-24** and **Table D-25** of Appendix D, in the forward and reverse directions, respectively. Factors of deviation (ρ) between the *ab initio* and GA rate coefficients are reported in **Table D-26**. The statistics reflecting the performance of the GA model and the tunneling model proposed in this manuscript in reproducing the *ab initio* data is illustrated in **Table D-27**.

The tunneling correction factor reproduces the Eckart tunneling coefficients accurately within a factor of 1.2 at 300 K, in agreement with the observed factor of deviation of 1.2 on the training set. Within the validation set, the maximum factor of deviation is 1.8 at this temperature. Furthermore, at 600 K and 1000 K, all the deviations are within 1.2 and 1.1, respectively. This illustrates that the tunneling model equation (Eq. (6-12)), used along with the GA-based activation energies in the exothermic direction is sufficiently successful in reproducing the Eckart tunneling coefficients.

Table D-27 also indicates that the Arrhenius parameters are reproduced by the GA parameters to a satisfactory extent. The MADs between the activation energies ($\mathbf{E_a}$) calculated by the GA parameters and the CBS-QB3 values is 2.5 kJ mol^{-1} at all the five temperatures of interest in the forward direction whereas in reverse direction, they vary from 2.5 kJ mol^{-1} to 2.7 kJ mol^{-1} depending on the temperature. Regarding log$\tilde{A}$s, at 300 K, the MAD is 0.200 and at higher temperatures, MADs gradually increase to a value of 0.213 at 2000 K, whereas in the reverse direction, the MADs are approximately 0.300 at all the temperatures of interest. Given the good agreement between the CBS-QB3 and GA calculated Arrhenius parameters for the validation set, it can be concluded that the ΔGAV°/ΔNNI° set developed in this work is transferable to obtain the rate coefficients of HARs from multiply substituted toluene derivatives by hydrogen atoms.

The purpose of the developed GA parameters and the tunneling correction function is to obtain rate coefficients that are close to accurate CBS-QB3-calculated rate coefficients. A measure of success in this endeavor is the factor of deviation (ρ) between the rate coefficients calculated by these two methods, as described before in the methodology section. These ρ values are relatively high at 300 K and decline with increasing temperatures. At 300 K, the $<\rho>$ is 2.5 in

the forward and 2.1 in the reverse direction and ρ_{max} is 7.8 and 10.3 in the forward and reverse directions, respectively. At higher temperatures, $<\rho>$ values are equal to or less than 1.7 in the forward and 1.6 in the reverse directions. At 600 K, ρ values are below 3.5 and at 1000 K they do not exceed 2.8 in the forward direction. In the reverse direction, the ρ_{max} values are higher, e.g. 5.1 at 600 K, 3.7 at 1000 K and 3.4 at 1500 K. Although these maximum values are higher than desired they are nevertheless accurate enough for e.g. automated mechanism generation applications. In the following, the outliers will be discussed in more detail.

Among the HARs in the validation set, the largest deviations in the activation energies are noted in the HAR from 2-$CH=CH_2$-5-OH-$C_6H_3CH(CH=CH_2)_2$ in both directions (See reaction **V-610** in **Figure D-57**). This demonstrates that the CBS-QB3 energy of the transition state structure of this reaction is somewhat higher than expected based on the GA predictions. Moreover, there are significant deviations between the $\log\tilde{A}$ values calculated by CBS-QB3 and GA in both directions. Nevertheless, the discrepancies in E_a and $\log\tilde{A}$ is not reflected in terms of ρ as the deviations in both Arrhenius parameters have positive values, which act in opposite directions regarding the agreement in rate coefficients, i.e. $\log\tilde{A}$ deviations cause positive errors in reaction rate coefficients whereas deviations in E_a cause negative errors which cancel each other to a degree. In consideration of the deviations in ρ, the largest values are encountered in cases where the two Arrhenius parameters have significant deviations with opposite signs. For instance, at 300 K, the largest ρ (10.3) is noted in the HAR from 2,5-$(OH)_2$-$C_6H_3CH(CH_3)CH=CH_2$ in the reverse direction (See reaction **V-503** in **Figure D-56**). It can be noted from **Table D-24** that the deviation in E_a is positive (4.4 kJ mol^{-1}), whereas the deviation in $\log\tilde{A}$ is negative (-0.334 m^3 mol^{-1} s^{-1}). Provided that the deviations in the Arrhenius parameters of this HAR are similar at higher temperatures, it is not surprising to see that this

reaction ranks as the second highest deviating HAR in terms of ρ (4.9 at 600 K, 3.6 at 1000 K, 3.3 at 1500 K and 3.1 at 2000 K). If the deviation of the pre-exponential factor of a HAR is not significant, significant deviations in activation energies can be enough to cause high ρ at lower temperatures, e.g. the largest ρ value (7.8) is encountered in the HAR from 2-CH_3-4-$CH{=}CH_2$-$C_6H_3CH(CH_3)CH{=}CH_2$ by hydrogen atom in the forward direction at 300 K (See reaction **V-505** in **Figure D-56**). Since the effect of E_a deviations on rate coefficients decrease upon increasing temperatures, ρ values are much lower at higher temperatures. For this reaction, ρ is 2.85 at 600 K and less than 2 at 1000 K, 1500 K and 2000 K. There are also examples within the validation set for the opposite case, where the large deviations in pre-exponential factors lead to large ρ values at high temperatures. One of these examples is the HAR from 2,6-$(CHO)_2$-$C_6H_3CH_2CH_3$ in the reverse direction (See reaction **V-205** in **Figure D-53**), for which the highest ρ values are noted at 1500 K (3.3) and 2000 K (3.4).

The low mean factors of deviation ($<\rho>$) between the reaction rate coefficients calculated by CBS-QB3 and the GA parameters demonstrate the transferability of the set of ΔGAV°s and ΔNNI°s to HARs from α-carbons of eight different doubly substituted toluene classes by hydrogen atom under investigation. Given the satisfactory agreement in terms of the Arrhenius parameters and the tunneling coefficients, it can be concluded that the present group additivity model and the tunneling model have the capability to yield accurate reaction rate coefficients at all the five temperatures of interest for these reactions.

6.4.4 Final optimization of the GA parameters

Finally, all the HARs within the training and validation sets are combined and the set of group additive parameters are re-optimized to yield the ΔGAV°s and the ΔNNI°s that successfully describe the full set of 211 HARs reported in this study. The final values of the ΔGAV°s and

the ΔNNI°s that are obtained upon the re-optimization of parameters can be found in **Table 6-3** and **Table 6-4**, respectively.

Provided that each ΔGAV° represents HARs from one of the eight classes of toluene derivatives, they are present at least 20 times in the combined set of reactions and the regressed data have high statistical significance. ΔNNI° corrections apply generally only to few reactions. The selection of reactions in this study was done in such a way that each ΔNNI° is represented in the final set at least three times. Therefore, along with the final values of each ΔNNI°, **Table 6-4** also reports the number of HARs from which each ΔNNI° is derived.

Table 6-3 ΔGAV°s (ΔGAV°$_f$s and ΔGAV°$_r$s) obtained upon the optimization based on the final set for the forward and reverse directions.

$\Delta GAV°_f$	**Forward direction**									
	$E_{a,f}$[a]					**$logA_f$[b]**				
	300 K	**600 K**	**1000 K**	**1500 K**	**2000 K**	**300 K**	**600 K**	**1000 K**	**1500 K**	**2000 K**
C_2-(C_b)(H)$_2$	-1.1 ± 0.93	-0.8 ± 0.93	-0.8 ± 0.93	-1.0 ± 0.95	-0.8 ± 0.94	0.005 ± 0.06	-0.035 ± 0.07	-0.041 ± 0.07	0.017 ± 0.07	-0.034 ± 0.19
C_2-(C_b)(C)(H)	-6.4 ± 0.85	-8.1 ± 0.85	-10.3 ± 0.85	-12 ± 0.86	-13.1 ± 0.85	0.138 ± 0.06	-0.173 ± 0.06	-0.203 ± 0.06	-0.402 ± 0.06	-0.435 ± 0.16
C_2-(C_b)(C)$_2$	-12.4 ± 0.97	-14.0 ± 0.97	-16.3 ± 0.97	-18.1 ± 0.99	-19.2 ± 0.98	0.159 ± 0.07	-0.038 ± 0.07	-0.193 ± 0.07	-0.272 ± 0.07	-0.305 ± 0.18
C_2-(C_b)(C_d)(H)	-11.3 ± 0.91	-12.8 ± 0.91	-15.1 ± 0.91	-17 ± 0.93	-18.1 ± 0.92	0.376 ± 0.06	0.188 ± 0.07	0.029 ± 0.07	-0.050 ± 0.07	-0.085 ± 0.18
C_2-(C_b)(C_d)(C)	-16.7 ± 0.91	-18.3 ± 0.91	-20.8 ± 0.91	-22.8 ± 0.93	-24 ± 0.92	0.328 ± 0.06	0.135 ± 0.07	-0.042 ± 0.07	-0.126 ± 0.07	-0.165 ± 0.18
C_2-(C_b)(C_d)$_2$	-18.6 ± 0.93	-20.4 ± 0.93	-22.9 ± 0.93	-24.8 ± 0.95	-26.0 ± 0.94	0.296 ± 0.06	0.089 ± 0.07	-0.086 ± 0.07	-0.171 ± 0.07	-0.209 ± 0.18
C_2-(C_b)$_2$(H)	-4.6 ± 0.97	-6.2 ± 0.97	-8.5 ± 0.97	-10.3 ± 0.98	-11.4 ± 0.97	-0.081 ± 0.07	-0.277 ± 0.07	-0.431 ± 0.07	-0.509 ± 0.07	-0.543 ± 0.18
C_2-(C_b)$_2$(C)	-8.7 ± 0.97	-10.3 ± 0.97	-12.7 ± 0.97	-14.7 ± 0.98	-15.8 ± 0.97	-0.009 ± 0.07	-0.208 ± 0.07	-0.373 ± 0.07	-0.457 ± 0.07	-0.493 ± 0.18
$\Delta GAV°_r$	**Reverse direction**									
	$E_{a,r}$[c]					**$logA_r$[d]**				
	300 K	**600 K**	**1000 K**	**1500 K**	**2000 K**	**300 K**	**600 K**	**1000 K**	**1500 K**	**2000 K**
C_2-(C_b)(H)$_2$	0.5 ± 1.00	0.6 ± 1.01	0.6 ± 1.00	0.9 ± 1.01	1.0 ± 1.01	0.061 ± 0.09	0.044 ± 0.09	0.058 ± 0.09	0.068 ± 0.09	0.065 ± 0.19
C_2-(C_b)(C)(H)	3.9 ± 0.91	3.4 ± 0.92	3.0 ± 0.91	3.3 ± 0.92	4.3 ± 0.93	-0.701 ± 0.08	-0.768 ± 0.09	-0.794 ± 0.08	-0.783 ± 0.08	-0.745 ± 0.13
C_2-(C_b)(C)$_2$	0.8 ± 1.23	0.5 ± 1.25	0.2 ± 1.24	0.6 ± 1.25	1.5 ± 1.26	-1.573 ± 0.11	-1.628 ± 0.12	-1.649 ± 0.11	-1.636 ± 0.11	-1.608 ± 0.20
C_2-(C_b)(C_d)(H)	37.9 ± 1.03	37.6 ± 1.04	37.2 ± 1.03	37.6 ± 1.04	38.6 ± 1.05	0.038 ± 0.10	0.006 ± 0.10	-0.018 ± 0.10	-0.003 ± 0.10	0.027 ± 0.16

C_2-(C_b)(C_d)(C)	30.9 ± 1.25	30.7 ± 1.27	30.4 ± 1.25	30.7 ± 1.26	31.7 ± 1.27	-0.767 ± 0.12	-0.791 ± 0.12	-0.815 ± 0.12	-0.803 ± 0.12	-0.769 ± 0.2
C_2-(C_b)(C_d)$_2$	57.8 ± 1.32	57.9 ± 1.34	57.6 ± 1.32	57.9 ± 1.34	58.9 ± 1.35	0.261 ± 0.12	0.266 ± 0.12	0.245 ± 0.12	0.259 ± 0.12	0.287 ± 0.22
C_2-(C_b)$_2$(H)	20.2 ± 1.20	20.0 ± 1.22	19.9 ± 1.21	20.5 ± 1.22	21.6 ± 1.23	0.33 ± 0.11	0.322 ± 0.11	0.314 ± 0.11	0.335 ± 0.11	0.375 ± 0.18
C_2-(C_b)$_2$(C)	15.2 ± 1.18	14.9 ± 1.19	14.7 ± 1.18	15.1 ± 1.19	16.1 ± 1.20	-0.457 ± 0.11	-0.48 ± 0.11	-0.498 ± 0.11	-0.484 ± 0.11	-0.450 ± 0.18

[a] **$E_{a,r}$:** Activation energy of the forward reaction, given in kJ mol^{-1}.
[b] **logA_r:** Logarithm of the pre-exponential factor of the forward reaction, given in m^3 mol^{-1} s^{-1}.
[c] **$E_{a,r}$:** Activation energy of the reverse reaction, given in kJ mol^{-1}.
[d] **logA_r:** Logarithm of the pre-exponential factor of the reverse reaction, given in m^3 mol^{-1} s^{-1}.

Table 6-4 ΔNNI°s obtained upon the optimization based on the final set for the forward and reverse directions.

$\Delta NNI_f°$	**Forward direction**									
	$E_{a,f}$[a]					**logA_f[b]**				**#[e]**
	300 K	**600 K**	**1000 K**	**1500 K**	**2000 K**	**300 K**	**600 K**	**1000 K**	**1500 K**	**2000 K**	
ΔNNIf°1	6.8 ± 1.81	6.8 ± 1.80	6.6 ± 1.81	6.7 ± 1.83	6.8 ± 1.82	-0.209 ± 0.13	-0.221 ± 0.13	-0.199 ± 0.13	-0.185 ± 0.14	-0.178 ± 0.27	9
ΔNNIf°2	7.1 ± 2.25	7.0 ± 2.24	7.0 ± 2.25	6.9 ± 2.28	6.9 ± 2.26	-0.017 ± 0.16	-0.022 ± 0.17	-0.017 ± 0.17	-0.019 ± 0.17	-0.018 ± 0.34	5
ΔNNIf°3	-3.8 ± 2.01	-4.0 ± 2.01	-4.0 ± 2.01	-4.0 ± 2.03	-4.1 ± 2.02	-0.291 ± 0.14	-0.314 ± 0.15	-0.317 ± 0.15	-0.317 ± 0.15	-0.316 ± 0.31	6
$\Delta NNI_r°$	**Reverse direction**									
	$E_{a,r}$[c]					**logA_r[d]**				**#[e]**
	300 K	**600 K**	**1000 K**	**1500 K**	**2000 K**	**300 K**	**600 K**	**1000 K**	**1500 K**	**2000 K**	
ΔNNIr°1	-10.2 ± 1.92	-10.2 ± 1.95	-10.2 ± 1.93	-10.2 ± 1.94	-10.1 ± 1.96	0.129 ± 0.18	0.129 ± 0.18	0.134 ± 0.18	0.136 ± 0.18	0.135 ± 0.36	6
ΔNNIr°2	-3.8 ± 2.31	-3.7 ± 2.33	-3.5 ± 2.31	-3.5 ± 2.33	-3.4 ± 2.35	0.714 ± 0.22	0.714 ± 0.21	0.727 ± 0.21	0.738 ± 0.21	0.717 ± 0.45	6
ΔNNIr°3	-10.0 ± 2.68	-9.3 ± 2.72	-9.7 ± 2.69	-9.2 ± 2.71	-8.9 ± 2.73	0.397 ± 0.25	0.397 ± 0.25	0.409 ± 0.25	0.412 ± 0.25	0.411 ± 0.51	4
ΔNNIr°4	-8.1 ± 2.94	-8.8 ± 2.98	-8.1 ± 2.95	-7.6 ± 2.98	-7.5 ± 3.00	-0.433 ± 0.27	-0.433 ± 0.28	-0.428 ± 0.27	-0.422 ± 0.27	-0.419 ± 0.54	4
ΔNNIr°5	8.3 ± 1.26	8.5 ± 1.28	8.5 ± 1.27	8.4 ± 1.28	8.4 ± 1.29	0.062 ± 0.12	0.062 ± 0.12	0.061 ± 0.12	0.062 ± 0.12	0.059 ± 0.23	18
ΔNNIr°6	-5.7 ± 1.95	-5.6 ± 1.97	-5.7 ± 1.95	-6.0 ± 1.97	-6.4 ± 1.98	0.273 ± 0.18	0.273 ± 0.18	0.261 ± 0.18	0.259 ± 0.18	0.224 ± 0.41	10
ΔNNIr°7	5.8 ± 3.05	5.7 ± 3.09	5.5 ± 3.06	5.4 ± 3.09	5.3 ± 3.11	-0.315 ± 0.28	-0.315 ± 0.29	-0.328 ± 0.28	-0.338 ± 0.28	-0.342 ± 0.57	3
ΔNNIr°8	3.2 ± 3.05	2.7 ± 3.09	-0.5 ± 3.06	1.0 ± 3.09	1.0 ± 3.11	-0.882 ± 0.28	-0.882 ± 0.29	-0.877 ± 0.28	-0.872 ± 0.28	-0.87 ± 0.56	3
ΔNNIr°9	6.4 ± 3.05	5.4 ± 3.09	6.4 ± 3.06	5.5 ± 3.09	5.5 ± 3.11	-1.186 ± 0.28	-1.186 ± 0.29	-1.211 ± 0.28	-1.225 ± 0.28	-1.23 ± 0.57	3
ΔNNIr°10	11.5 ± 2.23	11.2 ± 2.26	11.1 ± 2.24	10.9 ± 2.26	10.7 ± 2.28	-1.129 ± 0.21	-1.129 ± 0.21	-1.138 ± 0.21	-1.142 ± 0.21	-1.143 ± 0.42	7
ΔNNIr°11	-2.9 ± 2.17	-2.9 ± 2.2	-2.9 ± 2.17	-2.9 ± 2.19	-2.9 ± 2.21	-0.592 ± 0.21	-0.592 ± 0.22	-0.588 ± 0.21	-0.587 ± 0.20	-0.586 ± 0.41	6
ΔNNIr°12	-7.9 ± 2.57	-7.9 ± 2.61	-7.8 ± 2.58	-7.7 ± 2.61	-7.8 ± 2.62	-0.597 ± 0.24	-0.597 ± 0.24	-0.591 ± 0.24	-0.586 ± 0.24	-0.591 ± 0.48	4
ΔNNIr°13	-1.6 ± 1.73	-1.6 ± 1.76	-1.5 ± 1.74	-1.5 ± 1.75	-1.5 ± 1.77	-0.532 ± 0.16	-0.532 ± 0.16	-0.529 ± 0.16	-0.527 ± 0.16	-0.532 ± 0.33	11

$\Delta NNI_r°14$	6.1 ± 1.66	6.4 ± 1.68	6.5 ± 1.66	6.4 ± 1.68	6.1 ± 1.69	0.152 ± 0.15	0.151 ± 0.16	0.143 ± 0.15	0.148 ± 0.15	0.113 ± 0.34	10

[a] **$E_{a,r}$:** Activation energy of the forward reaction, given in kJ mol^{-1}.

[b] **$logA_r$:** Logarithm of the pre-exponential factor of the forward reaction, given in m^3 mol^{-1} s^{-1}.

[c] **$E_{a,r}$:** Activation energy of the reverse reaction, given in kJ mol^{-1}.

[d] **$logA_r$:** Logarithm of the pre-exponential factor of the reverse reaction, given in m^3 mol^{-1} s^{-1}.

[e] **#:** The number of HARs from which each ΔNNI° is derived.

A statistical analysis is performed to assess the performance of the set of ΔGAV°/ΔNNI° parameters. The results of this analysis are reported in **Table 6-5**. The deviations observed between the Arrhenius parameters in the forward and the reverse directions are given in **Table D-28** and **Table D-29** of Appendix D, respectively. The MADs of the E_as for in the forward and the reverse directions are 1.8 kJ mol^{-1} and the MADs of the log$\tilde{A}$s are slightly lower for the forward direction than for the reverse directions at all temperatures. *Ab initio* and GA calculated activation energies deviate no more than 6.7 kJ mol^{-1} for both directions.

Table 6-5 Statistics for the linear regression analysis of the final set of ΔGAV°s and ΔNNI°s for the activation energies (E_a) and the logarithm of the pre-exponential factors (log$\tilde{A}$), given along with the geometric mean (<ρ>) and the maximum (ρ_{max}) factor of deviations between the *ab initio* reaction rate coefficients and reaction rate coefficients obtained from the group additivity model and the tunneling model at 300 K, 600 K, 1000 K, 1500 K and 2000 K.

		Forward					**Reverse**				
		300 K	**600 K**	**1000 K**	**1500 K**	**2000 K**	**300 K**	**600 K**	**1000 K**	**1500 K**	**2000 K**
E_a[a]	**F**[d]	463	593	805	974	1116	1518	1464	1473	1470	1513
	MAD[e]	1.8	1.8	1.8	1.8	1.8	1.8	1.8	1.8	1.8	1.8
	RMS[f]	2.2	2.2	2.2	2.3	2.2	2.3	2.3	2.3	2.3	2.3
	MAX[g]	6.6	6.5	6.5	6.6	6.7	6.6	6.7	6.6	6.7	6.7
log$\tilde{A}$ [b]	**F**	38	22	44	70	81	99	106	113	111	105
	MAD	0.114	0.128	0.121	0.130	0.131	0.170	0.170	0.169	0.168	0.167
	RMS	0.154	0.169	0.164	0.169	0.171	0.210	0.211	0.209	0.208	0.209
	MAX	0.453	0.482	0.475	0.468	0.485	0.560	0.551	0.540	0.534	0.531
k[c]	**<ρ>** [h]	2.2	1.6	1.4	1.4	1.4	2.0	1.5	1.4	1.4	1.4
	ρ_{max} [i]	9.5	3.9	3.4	3.3	3.2	8.4	4.3	3.0	3.0	2.9

[a] **E_a:** Statistics for the activation energy, given in kJ mol^{-1}.

[b] **log$\tilde{A}$:** Statistics for the logarithm of the pre-exponential factor, given in m^3 mol^{-1} s^{-1}.

[c] **k:** Statistics for the performance of the predictive GA parameters in obtaining accurate reaction rate coefficients. This is given in terms of factor of deviation (**ρ**), a unitless value, as described in the methodology section of the manuscript.

[d] **F:** Significance

[e] **MAD:** Mean absolute deviation of the activation energies between the CBS-QB3 based E_as and the E_as calculated by reported GA parameters, given in kJ mol^{-1}.
[f] **RMS:** Root mean square.
[g] **MAX:** Maximum absolute deviation between the CBS-QB3 based E_as and the E_as calculated by reported GA parameters among the training set of activation energies, given in m^3 mol^{-1} s^{-1}.
[h] **$<\rho>$:** The geometric mean of the factor of deviations between the reaction rate coefficients calculated by CBS-QB3 and the GA parameters.
[i] **ρ_{max}:** The maximum factor of deviations between the reaction rate coefficients calculated by CBS-QB3 and the GA parameters.

Table 6-5 shows that the mean factor of deviation ($<\rho>$) values are similar in both directions and among the five temperatures of interest, the worst agreement is attained at 300 K; a factor of 2.2 for the forward direction and 2.0 for the reverse direction. A full list of the factors of deviations can be found in **Table D-30** of Appendix D for the entire set of reactions. At higher temperatures, the agreement improves remarkably in both directions. At 600 K, all the deviations are within factors of 3.9 and 4.3 for the forward and reverse directions, respectively and for temperatures above 1000 K the values reduce to 3.4 and 3.0, respectively. Among the final set of 211 HARs, the GA calculated rate coefficients for 29 reactions deviate by more than a factor of 4 from the *ab initio* data at 300 K for the forward direction, while this number is 30 for the reverse direction. At 600 K, only for 1 reaction the factor of deviation is larger than 4 for both the forward and reverse directions. In summary, the predictive capability of the final set of GA parameters together with the tunneling function yield accurate reaction rate coefficients for the family of HARs discussed in this manuscript.

In the earlier studies, Sabbe [7] and Paraskevas [13] mentioned the existence of an issue in preserving thermodynamic consistency if the reactions in both directions are separately calculated from the set of GA parameters. This problem is resolved through obtaining the rate coefficients for the reverse reactions using the reaction equilibria. This practice can also be followed in the present study, as discussed and exemplified in-depth in the following paragraphs.

6.4.5 Thermodynamic consistency and application of the GA parameters

The fact that the GA based reaction rate coefficients are calculated separately for the forward and the reverse directions may lead to thermodynamic inconsistencies. These inconsistencies mainly originate from the methodology employed to calculate the *ab initio* reaction rate coefficients from which the GA parameters are obtained, because thermodynamic properties are generally calculated by treating internal modes that resemble internal rotations as 1-D hindered rotors, while transition state calculations skip these treatments for the majority of the conserved modes (except HARs from toluene and substituted toluenes). This leads to the question of how to apply GA for kinetics. One option is to use the GA method to calculate forward and reverse rate coefficients independently and accept inconsistencies with thermodynamic properties. Alternatively, the kinetic GA parameters can be used for the forward rate coefficient and the reaction rate coefficient for the reverse direction is determined from microscopic reversibility [7,13]. The latter requires the equilibrium coefficient which can be calculated via GA as long as all GAV/NNI data are available. For reactions considered in the current study, GAV and NNI parameters to calculate thermodynamic properties of the reactants and products are available from **Chapter 3, 4** and **5**.

The use of the ΔGAV°/ΔNNI° parameters developed in this work is illustrated with the example reaction given in **Figure 6-4**, which shows the HAR from the benzylic position of 2-hydroxy-4-methyl-1,1-diphenylethane. In this example, the reaction rate coefficient of the forward reaction will be calculated at 300 K. Then, the rate coefficient of the HAR in the reverse direction will be calculated from reaction equilibrium coefficient. All the information needed for these calculations are found in **Table 6-6**.

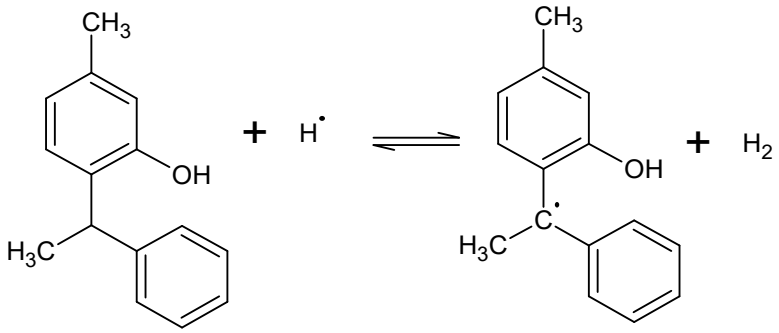

Figure 6-4 Hydrogen abstraction reaction (HAR) from the benzylic position of 2-hydroxy-4-methyl-1,1-diphenylethane by hydrogen atom.

The set of GA parameters yields 23.3 kJ mol^{-1} and 9.315 for activation energy (E_a) and the logarithm of the single-event pre-exponential factors ($\log\tilde{A}$), respectively, and the tunneling correction factor is 1.7 (calculated using Eq. (6-12), See **Table D-23**). The factor of deviation between the group additively calculated reaction rate coefficient ($\mathbf{k_{f(\Delta GAV°)}}$=290.6 m^3 mol^{-1} s^{-1}) and the *ab initio* reaction rate coefficient ($\mathbf{k_{f(ab\ initio)}}$=296.8 m^3 mol^{-1} s^{-1}) is 1.02 which reflects a perfect agreement between two methods. In **Table 6-6**, the reaction rate coefficients for the HAR in the reverse direction calculated by CBS-QB3 ($\mathbf{k_{r(ab\ initio)}}$) is compared with the set of ΔGAV°/ΔNNI° parameters ($\mathbf{k_{r(\Delta GAV°)}}$) and the reaction equilibria ($\mathbf{k_{r(Keq)}}$). This comparison demonstrates that the $\mathbf{k_{r(Keq)}}$ agrees satisfactorily with both $\mathbf{k_{r(ab\ initio)}}$ and $\mathbf{k_{r(\Delta GAV°)}}$.

6.4.6 Applicability of ΔGAV°s and ΔNNI°s for various extended side chains

One of the main objectives of the present study was to create a set of parameters, with which reaction rate coefficients of HARs from multiply substituted toluene derivatives can be calculated without the necessity of any experimental and/or *ab initio* data, regardless of the location of the substitution on the phenyl ring. In line with this objective, the GA parameters were tested on a validation set that only consists of HARs from multiply substituted toluene

derivatives by hydrogen atoms, in other words, in the validation set, the transferability of GA parameters to the HARs that involve variations in substituent Z groups were probed (See Z groups in **Figure 6-1**). Nonetheless, in toluene derivatives, substitution is not just possible on the phenyl ring but also on the extended side chains (R groups in **Figure 6-1**). Even though the present set of ΔGAV°s and ΔNNI°s does not focus on obtaining reaction rate coefficients for the HARs from such toluene derivatives, the obtained GA parameters could allow to calculate the kinetic data for such reactions.

Table 6-6 The group additive calculation for the HAR from 2-hydroxy-4-methyl-1,1-diphenylethane by hydrogen atom in the forward direction.

Calculation of Arrhenius Parameters of the HAR in the Forward Direction				
E_a	$E_{a,ref}$		35.8	23.4 kJ mol^{-1}
	ΔGAV°	C_2-(C_b)$_2$(C)	-8.7 (**Table 6-3**)	
	ΔNNI°	Δ*NNI*$_f$°3	-3.7 (**Table 6-4**)	
$Log\tilde{A}$	$Log\tilde{A}_{ref}$		9.615	9.315 m^3 mol^{-1} s^{-1}
	ΔGAV°	C_2-(C_b)$_2$(C)	-0.009 (**Table 6-3**)	
	ΔNNI°	Δ*NNI*$_f$°3	-0.291 (**Table 6-4**)	

Calculation of Reaction Rate Coefficients				
Forward Direction				
n_e	1	$k_{f(\Delta GAV°)}$[b]	**Performance of GA Method in obtaining k_f**	
T	300 K	290.6 m^3 mol^{-1} s^{-1}	$k_{f(\Delta GAV°)}$	290.6
κ_{TCF}[a]	1.7 (**Eq. 6-12**)		$k_{f(ab\ initio)}$[c]	296.8
			ρ[d]	1.89

Reverse Direction								
Group Additive Calculation for Reactants and Products			**Reaction Thermodynamics**		**Using Keq to calculate k_r**		**Performance of K_{eq} in obtaining k_r**	
Species	$\Delta_fH°$	$\Delta S°$	$\Delta_rG°$[i]		k_r		$k_{r(Keq)}$[k]	4.6E-14
Reactant 1[e]	-77.9	552.1	$\Delta_rH°$	-82.0	$\Delta_rG°/RT$	-36.4	$k_{r(\Delta GAV°)}$[l]	3.9E-14
Reactant 2[f]	217	114.7	$\Delta_rS°$	28.2	K_{eq}[j]	6.4E+15	$k_{r(ab\ initio)}$[m]	2.3E-14
Product 1[g]	57.1	564.4	$\Delta_rG°$	-90.5	k_f	296.8	$k_{r(\Delta GAV°)}/k_{r(Keq)}$	1.18
Product 2[h]	0	130.6			$k_{r(Keq)}$	4.6E-14	$k_{r(ab\ initio)}/k_{r(Keq)}$	2.04

[a] κ_{TCF}: Tunneling coefficient that is obtained from the tunneling correction function (Eq. (6-12)).
[b] $k_{f(\Delta GAV°)}$: Group additively calculated reaction rate coefficient.
[c] $k_{f(ab\ initio)}$: Reaction rate coefficient obtained from *ab initio* calculations.
[d] ρ: The factor of deviation, $\rho = k_{f(CBS\text{-}QB3)}/k_{f(\Delta GAV°)}$

[c] **Reactant 1:** 2-hydroxy-4-methyl-1,1-diphenylethane (See **Figure 6-4**).
[f] **Reactant 2:** Hydrogen atom (See **Figure 6-4**).
[g] **Product 1:** The benzylic radical from 2-hydroxy-4-methyl-1,1-diphenylethane (See **Figure 6-4**).
[h] **Product 2:** H_2 molecule (See **Figure 6-4**).
[i] $\Delta_r G^\circ$: The standard Gibbs energy of reaction, $\Delta_r G^\circ = \Delta_r H^\circ - T\Delta_r S^\circ$.
[j] $\mathbf{K_{eq}}$: The reaction equilibria coefficient, $K_{eq}=\exp(-\Delta_r G^\circ/RT)$.
[k] $\mathbf{k_{r(Keq)}}$: The reaction rate coefficient of the HAR in the reverse direction that is calculated using K_{eq}.
[l] $\mathbf{k_{r(\Delta GAV°)}}$: The reaction rate coefficient of the HAR in the reverse direction that is calculated using the set of ΔGAV°/ΔNNI° parameters.
[m] $\mathbf{k_{r(ab\ initio)}}$: The *ab initio* reaction rate coefficient of the HAR in the reverse direction

In this section, the extent of transferability of the presented set of ΔGAV°s (**Table 6-3**) to the HARs of this type are tested on a set of 16 reactions. The list of these reactions can be found in **Figure D-60** of Appendix D. The first four reactions that belong to this set include HARs with variations on R= $-CH_2CH_3$ which resembles n-alkane chain. In these four reactions, the transferability is probed with extensions to propyl and butyl. Apart from these four, this set also includes 3 variations on R= $-CH(CH_3)_2$ (substituted isopropylbenzenes), 3 variations on R= $-CH_2CH{=}CH_2$ (substituted allylbenzenes), 3 variations on R= $-CHCH_3CH{=}CH_2$ (substituted α-methylallylbenzenes), 2 variations on R= $CH(CH{=}CH_2)_2$ (substituted α-vinylallylbenzenes) and 1 variation on R= $-CHCH_3C_6H_5$ (substituted diphenylethane). One of the reactions that belong to this set are illustrated with the example reaction given in **Figure 6-5**, which shows the HAR from 2,3-dimethyl-4-phenylpent-2-ene (Reaction **S-113** in **Figure D-60**).

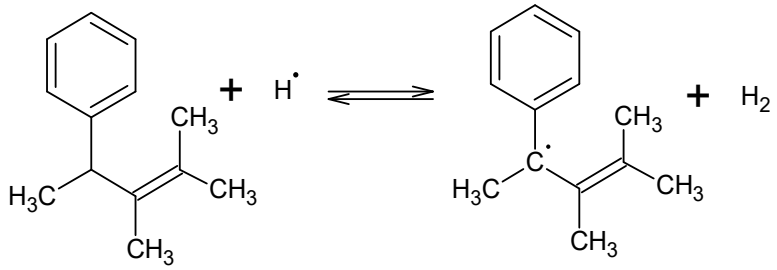

Figure 6-5 Hydrogen abstraction reaction (HAR) from the benzylic position of 2,3-dimethyl-4-phenylpent-2-ene by hydrogen atom.

Generally, the ΔGAV°s are expected to reproduce the *ab initio* reaction rate coefficients accurately for the HARs in which substitution on the extended side chain (**R**) of the reactant has similar thermodynamic effects on the transition state structure since the substituent effects cancel out and hence, no ΔNNI° parameter is necessary to correct for the differences. However, in some other reactions, there are significant differences between the reactants and the transition state structures in terms of the magnitude of substituent effects and the ΔNNI°s that are reported in this study do not capture the effects due to such substituent interactions. Consequently, the GA-based reaction rate coefficients are expected to deviate from the *ab initio* data for such reactions. In **Chapters 3-5**, it has been shown that substitutions on phenyl ring have the tendency to affect radicals (the reactants in the reverse direction) more than closed shell structures (the reactants in the forward direction). Based on the fact that the number of presently reported ΔNNI°s in the forward direction (3) is less than the number of ΔNNI°s reported in the reverse direction (14), it can be argued that it is far more likely to observe failure in the predictions concerning the reverse direction than the forward.

The Arrhenius parameters, Eckart tunneling correction factors and rate coefficients of the 16 reactions in the above-discussed set are given in **Table D-31 - Table D-35** at 300 K, 600 K, 1000 K, 1500 K and 2000 K, respectively. In **Table D-36**, the number of single events for both the reactions in the forward and the reverse directions are provided, along with the internal and external symmetry numbers and the number of optical isomers of all the species involved in these reactions. The deviations between the Arrhenius parameters obtained from *ab initio* calculations and the GA parameters are reported in **Table D-37** and **Table D-38** for the forward and reverse directions, respectively and the factors of deviation (ρ) are provided in **Table D-39**. The statistics that reflect the performance of the ΔGAV°s (See **Table D-40** of Appendix

D) demonstrate that the mean factors of deviation (<ρ>) between the CBS-QB3 and the GA-based reaction rate coefficients are 2.9, 2.1 and 1.8 for the HARs in the forward direction at 300 K, 600 K and 1000 K, respectively. Nevertheless, for the HARs in the reverse direction, half of the ρ values are higher than 10 at 300 K and a remarkable number of them deviate by a factor of more than 100. This indicates that, in general, the ΔGAV°s can be employed to reproduce rate coefficients for the HARs in the forward direction whereas they seem to fail to do so for a significant portion of the HARs in the reverse direction, especially at 300 K. It is advisable to obtain reaction rate coefficients for the reverse direction through reaction equilibria, as mentioned before for resolving the issue regarding thermodynamic stability. In the following paragraphs, the extent of transferability of the reported ΔGAV°s (**Table 6-3**) to various extended side chains are discussed in-depth.

Among the factor of deviations for the 16 reactions in the forward direction, only for one reaction, the ρ values at all the temperatures of interest are too high to be considered as satisfactory. This is the HAR from 2,3-dimethyl-4-phenylpent-2-ene (see **Figure 6-5**) by hydrogen atom. The reactant of this HAR is a triple substituted α-methylallylbenzene, where all the substituents are methyl groups. One of these methyl groups reside on the double bonded β carbon, whereas the other two are on the γ carbon that is located on the other side of the double bond. Evidently, these methyl groups lead to a double cis interaction in the reactant, as discussed before by Sabbe et al.[1,2]. In the transition state structure of this HAR, the overall thermodynamic effect caused by the presence of these substituents is different than in the reactant due to the differences in geometries leading to large deviations in the log$\tilde{A}$ values and thus, causing factors of deviation (ρ) to be quite high (e.g. 31.3 at 300 K, 14.7 at 600 K and 10.9 at 1000 K). In the HAR from α-methylallylbenzene by hydrogen atom, the dihedral angle

between the two substituents on the α-carbon is approximately zero in both the reactant and the transition state structure (See **Figure D-61** of Appendix D for the optimized geometries and dihedral angles) whereas in the HAR from 2,3-dimethyl-4-phenylpent-2-ene, this dihedral angle is 111.9° in the reactant and 83.3° in the transition state. This difference in the geometries, i.e. the dihedral angles explain difference of magnitudes in the substituent effects on the stiffness of species which is reflected in the varying $\log\tilde{A}$ values. Unfortunately, no ΔNNI° is defined in the earlier studies and in **Table 6-4** that can correct for this substituent effect. Consequently, this HAR is excluded from the statistics reported in **Table D-40**. For the remaining HARs in this set, the reaction rate coefficients are reproduced to a satisfactory extent, as the $<\rho>$ values show for all the temperatures of interest except 300 K ($<\rho>$ values are 2.9, 2.2, 1.8,1.5 and 1.5 at 300 K, 600 K, 1000 K, 1500 K and 2000 K, respectively). Based on these results, the ΔGAV°s that are defined to describe the HARs in the forward direction are recommended for application on the HARs of this nature at all the temperatures except at 300 K. However, caution should be exercised in the application of these parameters for HARs from toluene derivatives with highly substituted extended side chains in the sense that the accuracy of the calculated reaction rate coefficients may decrease with increasing substitution, as in the case discussed above (HAR from 2,3-dimethyl-4-phenylpent-2-ene).

Table D-39 shows that the deviations among the HARs of interest in the reverse direction tend to decrease upon increasing temperatures and for some of them, the agreement is satisfactory. In this set, the **C_2-(C_b)(H)$_2$** and **C_2-(C_b)$_2$(H)** groups are not probed because there are no possible variations on R for the relevant HARs. ρ values are within 4.3 for all the four reactions on which the **C_2-(C_b)(C)(H)** group is applicable at all the temperatures of interest. This points out that this ΔGAV° can safely be used for the GA calculation of rate coefficients for the HARs

in the reverse direction involving linear (unbranched) alkylphenyl radicals such as n-propylbenzyl or n-butylbenzyl. **C_2-(C_b)$_2$(C)** is another ΔGAV° that performs successfully in reproducing the CBS-QB3 rate coefficients: for the reverse direction of the HAR from diphenylpropane by hydrogen atom, the ρ values are 4.3, 2.5, 2.2, 2.1 and 2.2 at 300 K, 600 K, 1000 K, 1500 K and 2000 K, respectively. Considering that the ρ values for the HARs, for which the **C_2-(C_b)(C_d)(C)** groups can be employed, are within 4 at 600 K, 1000 K, 1500 K and 2000 K, this ΔGAV° also seems to be successful in reproducing the reaction rate coefficients at all the temperatures except 300 K for which significantly high deviations are observed. Regarding the HARs, with which the other three ΔGAV°s that are probed (**C_2-(C_b)(C)$_2$, C_2-(C_b)(C_d)(H)** and **C_2-(C_b)(C_d)$_2$**), significantly large deviations are encountered. The general conclusion drawn for the forward direction in the paragraphs above that high degree of substitution decreases the extent of agreement also holds for the HARs in the reverse direction. For instance, the radical reactants of the two HARs consisting of double methyl substitution on β-carbons have extreme deviations, e.g. the deviation of 33434 encountered in the HAR from H_2 by 1,2,2-trimethyl-1-phenylpropyl radical (see reaction **S-107** in **Figure D-60**) at 300 K. Despite the fact that the ΔGAV°s in the reverse direction can be useful in reproducing some of the CBS-QB3 reaction rate coefficients, it seems difficult to draw a well-defined line between the cases for which these parameters can efficiently work and the ones for which they cannot. As a result of this, in order to obtain reaction rate coefficients for such HARs via ΔGAV°s while staying on the safe side, it is recommended to employ reaction equilibria and the thermochemical GA parameters reported in **Chapter 3**, **4** and **5** as mentioned earlier in this section.

6.5 Conclusions

The rate coefficients for 211 hydrogen abstraction reactions (HARs) from the benzylic position of toluene derivatives by hydrogen atom have been calculated with the CBS-QB3 level of theory and Eckart tunneling corrections. Six substituents (-OH, -OCH_3, -CHO, -$CH{=}CH_2$, -CH_3 and -CH_2CH_3) to the aromatic ring have been considered and the alkyl group has been varied to include toluenes, ethylbenzenes, isopropylbenzenes, allylbenzenes (2-phenylpropenes), α-methyl allylbenzenes (3-phenylbutenes), α-vinyl allylbenzenes (3-phenyl-1,4-pentadienes), diphenylmethanes and 1,1-diphenylethanes. The extensive data set is used to derive 8 ΔGAV° and 3 ΔNNI° group additivity (GA) parameters to calculate the single event pre-exponential factors and the activation energies ($\tilde{A}$, E_a) for this reaction family in the temperature range of 300 K to 2000 K in the forward direction. To accurately describe the reverse direction, H atom abstraction from molecular hydrogen by benzylic radicals, requires a set of 8 ΔGAV°s and 14 ΔNNI°s. The need for a higher number of ΔNNI°s for the reverse reactions stems from the fact that the thermodynamic properties of benzylic radicals are more strongly affected by substitution effects than those for toluene derivatives. This is in line with the observations from **Chapters 3-5**. Tunneling contributions calculated with asymmetric Eckart potentials have been expressed as a correction function which depends solely on E_a. The final rate coefficient for any reaction of this reaction family is calculated as product of the GA single event rate coefficient, the tunneling correction factor and the number of events.

At 1000 K, the mean absolute deviations between the activation energies and the logarithms of single event pre-exponential factors calculated from *ab initio* and GA calculations amount to 1.8 kJ mol^{-1} and 0.121 $m^3\ mol^{-1}\ s^{-1}$ in the forward direction, respectively. The geometric mean

factor of deviations (<ρ>) for the rate coefficients is 1.4 at temperatures above 1000 K meaning that *ab initio* and GA calculated rate coefficients differ on average by 40%. A similar accuracy is observed for the reverse reaction. This shows that the GA parameters developed in the present work can be used reliably to obtain reaction rate coefficients for hydrogen abstraction reactions from a wide range of ring-substituted toluene derivatives.

The transferability towards modified alkyl side chains have also been tested and the results show that the GA parameters for the forward direction are transferable. Since thermodynamic properties of benzylic radicals are very sensitive to small structural changes, the transferability of GA parameters for the reverse reactions is limited to those cases in which the changes to the alkyl group do not create additional steric interactions. Therefore, it is recommended to apply the developed GA parameters to the forward reaction and to use the thermodynamic equilibrium constant to calculate the rate coefficient for the reverse reaction. The required GA parameters to calculate the equilibrium coefficient are reported in **Chapter 3-5**.

6.6 Acknowledgments

The research leading to these results has received funding from the European Research Council under the European Union's Seventh Framework Programme (FP7/2007-2013)/ERC grant MADPII agreement n° 290793. The SBO project "Bioleum" (IWT-SBO 130039) supported by the Institute for Promotion of Innovation through Science and Technology in Flanders (IWT) is acknowledged. This work was carried out using the STEVIN Supercomputer Infrastructure at Ghent University, funded by Ghent University, the Flemish Supercomputer Center (VSC), the Hercules Foundation and the Flemish Government – department EWI.

6.7 References

[1] Sabbe MK, Saeys M, Reyniers M-F, Marin GB, Van Speybroeck V, Waroquier M. Group Additive Values for the Gas Phase Standard Enthalpy of Formation of Hydrocarbons and Hydrocarbon Radicals. *The Journal of Physical Chemistry A.* 2005;109(33):7466-7480.

[2] Sabbe MK, De Vleeschouwer F, Reyniers M-F, Waroquier M, Marin GB. First Principles Based Group Additive Values for the Gas Phase Standard Entropy and Heat Capacity of Hydrocarbons and Hydrocarbon Radicals. *The Journal of Physical Chemistry A.* 2008;112(47):12235-12251.

[3] Paraskevas PD, Sabbe MK, Reyniers M-F, Papayannakos N, Marin GB. Group Additive Values for the Gas-Phase Standard Enthalpy of Formation, Entropy and Heat Capacity of Oxygenates. *Chemistry – A European Journal.* 2013;19(48):16431-16452.

[4] Vandeputte AG, Sabbe MK, Reyniers MF, Marin GB. Modeling the gas-phase thermochemistry of organosulfur compounds. *Chemistry – A European Journal.* 2011;17(27):7656-7673.

[5] Saeys M, Reyniers M-F, Marin G, Van Speybroeck V, Waroquier M. Ab initio group contribution method for activation energies for radical additions. *AIChE Journal.* 2004;50(2):426-444.

[6] Saeys M, Reyniers MF, Van Speybroeck V, Waroquier M, Marin GB. Ab initio group contribution method for activation energies of hydrogen abstraction reactions. *ChemPhysChem.* 2006;7(1):188-199.

[7] Sabbe M, Vandeputte A, Reyniers M-F, Van Speybroeck V, Waroquier M, Marin G. Ab Initio Thermochemistry and Kinetics for Carbon-Centered Radical Addition and β-Scission Reactions. *The Journal of Physical Chemistry A.* 2007;111(34):8416-8428.

[8] Vandeputte AG, Sabbe MK, Reyniers M-F, Van Speybroeck V, Waroquier M, Marin GB. Theoretical Study of the Thermodynamics and Kinetics of Hydrogen Abstractions from Hydrocarbons. *The Journal of Physical Chemistry A.* 2007;111(46):11771-11786.

[9] [9] Sabbe M, Reyniers M-F, Van Speybroeck V, Waroquier M, Marin G. Carbon-Centered Radical Addition and β-Scission Reactions: Modeling of Activation Energies and Pre-exponential Factors. *ChemPhysChem.* 2008;9(1):124-140.

[10] Sabbe MK, Vandeputte AG, Reyniers M-F, Waroquier M, Marin GB. Modeling the influence of resonance stabilization on the kinetics of hydrogen abstractions. *Physical Chemistry Chemical Physics.* 2010;12(6):1278-1298.

[11] Vandeputte AG, Sabbe MK, Reyniers M-F, Marin GB. Kinetics of α hydrogen abstractions from thiols, sulfides and thiocarbonyl compounds. *Physical Chemistry Chemical Physics.* 2012;14(37):12773-12793.

[12] Vandeputte AG, Reyniers M-F, Marin GB. Kinetic Modeling of Hydrogen Abstractions Involving Sulfur Radicals. *ChemPhysChem.* 2013;14(16):3751-3771.

[13] Paraskevas PD, Sabbe MK, Reyniers MF, Papayannakos N, Marin GB. Kinetic modeling of alpha-hydrogen abstractions from unsaturated and saturated oxygenate compounds by carbon-centered radicals. *ChemPhysChem.* 2014;15(9):1849-1866.

[14] Paraskevas PD, Sabbe MK, Reyniers M-F, Papayannakos NG, Marin GB. Kinetic Modeling of α-Hydrogen Abstractions from Unsaturated and Saturated Oxygenate Compounds by Hydrogen Atoms. *The Journal of Physical Chemistry A.* 2014;118(40):9296-9309.

[15] Paraskevas PD, Sabbe MK, Reyniers M-F, Papayannakos NG, Marin GB. Group Additive Kinetics for Hydrogen Transfer Between Oxygenates. *The Journal of Physical Chemistry A.* 2015;119(27):6961-6980.

[16] [16] Paraskevas PD, Sabbe MK, Reyniers M-F, Marin GB, Papayannakos NG. Group additive kinetic modeling for carbon-centered radical addition to oxygenates and β-scission of oxygenates. *AIChE Journal.* 2016;62(3):802-814.

[17] Willems PA and Froment GF. *Industrial and Engineering Chemistry Research*. 1988; 27: 1959–1966.

[18] Willems PA and Froment GF. *Industrial and Engineering Chemistry Research*. 1988; 27:1966–1971.

[19] Montgomery JA, Frisch MJ, Ochterski JW, Petersson GA. A complete basis set model chemistry. VI. Use of density functional geometries and frequencies. *Journal of Chemical Physics.* Feb 8 1999;110(6):2822-2827.

[20] Frisch MJ, Trucks GW, Schlegel HB, Scuseria GE, Robb MA, Cheeseman JR, Scalmani G, Barone V, Mennucci B, Petersson GA, Nakatsuji H, Caricato M, Li X, Hratchian HP, Izmaylov AF, Bloino J, Zheng G, Sonnenberg JL, Hada M, Ehara M,

Toyota K, Fukuda R, Hasegawa J, Ishida M, Nakajima T, Honda Y, Kitao O, Nakai H, Vreven T, Montgomery Jr. JA, Peralta JE, Ogliaro F, Bearpark MJ, Heyd J, Brothers EN, Kudin KN, Staroverov VN, Kobayashi R, Normand J, Raghavachari K, Rendell AP, Burant JC, Iyengar SS, Tomasi J, Cossi M, Rega N, Millam NJ, Klene M, Knox JE, Cross JB, Bakken V, Adamo C, Jaramillo J, Gomperts R, Stratmann RE, Yazyev O, Austin AJ, Cammi R, Pomelli C, Ochterski JW, Martin RL, Morokuma K, Zakrzewski VG, Voth GA, Salvador P, Dannenberg JJ, Dapprich S, Daniels AD, Farkas Ö, Foresman JB, Ortiz JV, Cioslowski J, Fox DJ. Gaussian 09, Version D.01. Wallingford, CT, USA: Gaussian, Inc.; 2009.

[21] Benson SW. *Thermochemical kinetics : methods for the estimation of thermochemical data and rate parameters*. 2d ed. New York: Wiley; 1976.

[22] Eckart C. The Penetration of a Potential Barrier by Electrons. *Physical Review.* 1930;35(11):1303-1309.

[23] NIST Chemical Kinetics Database. National Institute of Standards and Technology; 2015. http://kinetics.nist.gov/. Accessed 15 September 2016.

[24] Oehlschlaeger MA, Davidson DF, Hanson RK. Experimental Investigation of Toluene + H → Benzyl + H2 at High Temperatures. *The Journal of Physical Chemistry A.* 2006;110(32):9867-9873.

[25] Ellis C, Scott MS, Walker RW. Addition of toluene and ethylbenzene to mixtures of H2 and O2 at 772 K: Part 2: formation of products and determination of kinetic data for H+ additive and for other elementary reactions involved. *Combustion and Flame.* 2003;132(3):291-304.

[26] Hirschfelder J, Wigner E. Some Quantum-Mechanical Considerations in the Theory of Reactions Involving an Activation Energy. *The Journal of Chemical Physics.* 1939;7(8):616-628.

Chapter 7

Conclusions and Perspectives

In this Ph.D. dissertation, Benson's group additive (GA) parameters [1-4] were reported to describe the thermochemistry of a wide range of unsubstituted and substituted monocyclic aromatic molecule/radical classes based on datasets that were formed through quantum chemical calculations. Then, a first step was taken in the direction of kinetics encompassing these aromatic species with a study that involves GA based parameter development for the hydrogen abstraction reactions (HARs) from the benzylic position of toluene derivatives by a hydrogen atom. These parameters enable reliable prediction of thermochemical and kinetic data for any molecule or reaction that belongs to the studied molecule/reaction families.

The Laboratory for Chemical Technology (LCT) of Ghent University has effectively been following this strategy to systematically investigate the gas phase thermodynamics and kinetics of diverse molecule classes such as hydrocarbons [5-10], organosulfur compounds [11-14] and

oxygenates [15-20] with the aim of developing a database of GA parameters. The parameters that were reported in the present Ph.D. work provide an extension of this parameter database to monocyclic aromatic compounds.

In **Chapters 3-5**, *ab initio* based thermochemical data was reported for 863 monocyclic aromatic species (molecules and radicals) consisting of unsubstituted and substituted benzenes, phenols, anisoles, benzaldehydes, styrenes, toluenes, ethylbenzenes, isopropylbenzenes, allylbenzenes, α-methylallylbenzenes, α-vinylallylbenzenes, diphenylmethanes and diphenylethanes, i.e. monocyclic aromatics considering six different substituent groups (hydroxy (-OH), methoxy (OCH_3), formyl (-C=O), vinyl (-CH=CH_2) and the alkyl groups methyl (-CH_3) and ethyl (-CH_2CH_3)) and a wide range of radicals that can be derived from these species. This extensive dataset was utilized to develop 25 group additive values (GAVs) and 63 non-nearest neighbor interaction (NNI) correction parameters. With these GA parameters, the majority of the *ab initio* standard enthalpy of formations ($\Delta_f H°$) and entropies ($S°$) at 298 K can be reproduced within chemical accuracy which is taken to be 4 kJ mol^{-1} for the $\Delta_f H°$ and 4 J mol^{-1} K^{-1} for S° for most of the training and test species. Moreover, the heat capacities (C_p) can be reproduced at the temperature range of 300 K-1500 K within 4 J mol^{-1} K^{-1} for the same set. This holds even for highly substituted molecules such as the quintuply-substituted monocyclic aromatic molecule 1,2-dihydroxy-3-methoxy-5,6-dimethylbenzene which demonstrates that the GA contributions and NNI corrections are indeed additive.

Inclusion of the NNI corrections proved to be extremely crucial in obtaining the good agreement between group additively and the *ab initio* calculated thermochemical properties. In **Chapters 3-5**, the physical interactions which cause the overall substituent effects described by the 63 NNIs are discussed in-depth. While forming the reference datasets, all possible

combinations of single and double *ortho (o-)*, *meta (m-)* and *para (p-)* substitutions on the phenyl ring with the above-mentioned six substituents of interest were considered to ensure that all possible substituent interactions are covered as part of this study. To the best of our knowledge, such a systematic investigation of substituent effects in the gas phase chemistry of monocyclic aromatic compounds is unprecedented.

Another motivation to focus on the physical interpretation of the NNI parameters was to scrutinize the accuracy of the reference data based on chemical knowledge. This practice was considered as crucial since it was noted that obtaining high quality *ab initio* data is difficult and the initially obtained values are likely to be inaccurate due to several reasons, such as difficulties in correctly identifying the lowest energy conformer, identifying the appropriate frequency to remove while replacing the harmonic oscillator partition function that corresponds to an internal rotation with the hindered rotor partition function or failures in hindered rotor calculations in highly coupled systems. In other words, critical evaluation of datasets based on the analysis of the optimized geometry or on natural bond orbital analysis (as in **Chapter 3**) were utilized as a guide to pinpoint problematic or suspicious data points. The ambiguities in the reference dataset led to the need to perform additional calculations to resolve such issues to attain as high quality data as possible. Moreover, the datasets were expanded in such a manner that every NNI parameter was estimated based on at least three different compounds. This practice ensures high statistical significance of the parameters and thus confidence that the corrections are meaningful and justified. The focus on highly accurate and redundant *ab initio* data and the physical explanation of the NNIs are mutually dependent since high quality data allow identification of physical interactions and the corresponding

NNIs. Also, the apparent need for NNIs that are difficult to justify provide the means to detect insufficiencies in the *ab initio* data.

Out of the 63 NNIs defined in this study, only four were defined to correct for non-nearest neighbor interactions between *meta* substituents. Furthermore, it was noted that only oxygenated substituents in *meta* position seem to interact; these interactions are present in *m*-diformylbenzene, *m*-OCH_3 and *m*-CHO substituted phenoxies and *m*-CHO substituted benzoyl. Substitutions in *para* position lead more frequently to interactions and 12 such NNIs have been identified. For such long-range interactions to occur, both substituents must be able to interact through the π-system of the phenyl ring. As all three oxygenated substituent groups investigated (-OH, -OCH_3 and -CHO) impose strong +M or -M effects, closed-shell aromatic species with oxygenated groups in *para* position will always require NNI corrections. On the other hand, in styrene and the toluene derivatives, *para* substitution does not lead to such interactions because resonance requires both substituents to participate. Phenoxy and benzoyl radicals are affected from *para* substitution more than their parent molecules and in all the eight different classes of benzylic radicals considered, substitution of only -CHO and -$CH{=}CH_2$ groups have a remarkable influence at *para* position. The majority of the NNI parameters were dedicated to describe the effects upon *ortho* substitution which is not surprising because it becomes more probable to have significant substituent effects as the proximity between two substituents increase. Several physical effects such as steric repulsion, hydrogen bonding and anomeric repulsion are only possible between two substituent groups in *ortho* position because in other positions, the distance between the substituents are too large for these effects to take place.

As briefly mentioned above, one of the most fundamental conclusions from this Ph.D. thesis is the recognition of the difficulty to obtain highly accurate *ab initio* data. Gaussian is a user-friendly program with which CBS-QB3 and G4 calculations can be realized by just selecting the necessary keywords and options and then, this software yields some values; however, these values may not necessarily be accurate. In this work, three extra precautions were used to improve the reliability of the reported results. First of them was the focus on the meticulous search for lowest energy conformers which had a profound impact on the quality of the $\Delta_f H°$ data. For this purpose, first, the hindrance potentials of the internal rotors which were calculated at the low DFT (B3LYP) level of theory were used to identify low-energy conformers. Then, each one of these conformers was evaluated at the higher CBS-QB3 or G4 level. This two-step approach showed that the lowest energy conformer search by only using the lower energy points of the hindrance potentials could lead to structures that do not reflect the lowest energy conformer at higher levels and inclusion of the second step improved the results for such cases. The second precaution is to include a wavefunction stability test [21-23] as a pre-step before CBS-QB3 and G4 calculations for radicals and transition state structures. The need for this precaution originated from a severe problem that was noted in the default guess of the initial wavefunction while solving the self-consistent field problem as this guess did not always lead to the electronic ground state. The stabilized wavefunction from this test was employed as initial guess in the subsequent CBS-QB3 or G4 calculations. As discussed before in **Chapter 4**, this test led to improvements of more than 10 kJ mol^{-1} for *para* substituted benzoyl radicals. The third of these precautions is the systematic but manual identification of the frequencies which correspond to the internal rotations and the removal of their contribution from the harmonic oscillator partition function. In the earlier studies by

Sabbe et al. [9] and Paraskevas et al. [15], harmonic oscillator frequencies associated with the internal rotors were obtained from the rotation profile. This approach led to significant errors for the species that are presented in this Ph.D. dissertation because a notable part of the frequencies obtained from the rotation profile significantly differ from the value of the frequencies that corresponds to the internal rotations. Therefore, instead of obtaining the frequencies pertaining to the internal rotations from the rotation profile as in the earlier studies [9,15], these frequencies are identified manually through visual inspection which resulted in remarkable improvements in the quality of the $S°$ and C_p data.

In the only kinetics study of this Ph.D. work that is presented in **Chapter 6**, the GA-based parameters were developed based on a set of 211 hydrogen abstraction reactions (HARs) from the benzylic position of toluene derivatives by a hydrogen atom using the CBS-QB3 level of theory and Eckart tunneling corrections. These reactions include HARs from the eight toluene derivative classes for which thermochemical GA parameters have been reported in **Chapters 3-5**. Substituent effects upon substitution by six substituent groups (-OH, -OCH_3, -CHO, -$CH{=}CH_2$, -CH_3, -CH_2CH_3) were investigated and analogous to the thermochemical studies, the effects imposed due to *ortho*, *meta* and *para* substitutions with these six groups were included to probe all the possible substituent effects on the kinetics. To describe the reaction rate coefficients of the HARs in the forward direction, 8 ΔGAV°s and 3 ΔNNI°s were defined whereas 8 ΔGAV°s and 14 ΔNNI°s were reported for the reverse direction. For the particular set of reactions under investigation, the reported set of ΔGAV°/ΔNNI° parameters lead to accurate results for the *ab initio* reaction rate coefficients with high accuracy.

The number of ΔNNI°s that were defined for the reverse direction are higher than that of the forward. This is mainly because the thermochemistry of the reactants of the HARs in the

reverse direction, i.e. the benzylic radicals are affected by substitution to a much stronger extent than the toluene derivatives. Hence, particularly due to the resonance effects in these radicals it is harder to reproduce accurate rate coefficients for the HARs in the reverse direction using the set of ΔGAV°s/ΔNNI°s directly. An alternative way to obtain reaction rate coefficients for these HARs is through the reaction equilibria (as described before in **Chapter 6**) employing ΔGAV°s and ΔNNI°s to calculate rate coefficients for the forward direction and the GAVs/NNIs for the thermochemistry of the reactants and products.

Among all the ΔNNI°s that were reported for the HARs in both directions, *meta* substitutions and all the *para* substitutions except the ones by -CHO and -CH=CH_2 groups have no effect on the kinetics of HARs from toluene derivatives. Thus, in both directions, most of these ΔNNI°s correspond to the effects of *ortho* substitutions. This conclusion can be a helpful starting point for future kinetic studies regarding the GA parameter development for the HARs from toluene derivatives, e.g. by carbon or oxygen centered radicals. Indeed all the HARs from reactants with the above-mentioned substitutions can be excluded safely from the reference dataset, leading to a remarkable reduction in the effort required to develop the set of GA parameters for those HAR families.

Even though this thesis only investigates a specific HAR family which might at a first glance seem as a small contribution towards development of a kinetic database for substituted aromatics, there are several important conclusions from this work that can serve as a guide for future studies. First, the reactant and the product data are common to all such HARs and are available from this Ph.D. work, therefore only transition state structures remain to be calculated in further studies. Second, initial guesses of the transition state structures for relevant abstraction reactions can be easily obtained by taking the transition states for the HARs by a

hydrogen atom studied in this Ph.D. dissertation and adding the necessary groups to their reactive moiety which avoids laborious transition state searches. Third, it is expected that similar ΔNNI°s should be found for other HARs, e.g. those by CH_3. Hence, the tedious identification of ΔNNI°s can be replaced by verifying that (at least most of) the identified interactions are also present for other abstracting radicals. Hence, one merely must refit the parameters. Fourth, additional ΔNNI°s are easily predictable based on the structure of the radical and the physical understanding obtained in this Ph.D. work. Fifth, the training set can be substantially reduced because it has been shown in **Chapter 6** that the ΔNNI°s are only needed for *o*- substituents in the forward direction.

The current study was conducted as part of a project aiming at the development of kinetic models for biomass fast pyrolysis with special focus on lignin. Lignin, an important component of ligno-cellulosic biomass such as wood or grass, is a polymer of mainly three monomers [24-27]. Depending on the plant type, the contributions of the G (guaiacylpropane), S (syringylpropane), and H (*p*-hydroxyphenylpropane) subunits vary significantly and any kinetic model needs to be able to account for such variations. Taking the lignin structure illustrated in **Figure 7-1** as example, it is clear that the reported GA parameters are essential to calculate its thermochemical properties. Furthermore, since the GAVs for the corresponding radicals are known as well, it is a straightforward exercise to determine the most vulnerable bonds and thus to predict where the thermal decomposition of lignin will likely begin, should bond scission indeed be the initiation step. But one can go even further and use GAVs to investigate how structural changes will affect the reactivity (e.g. bond dissociation energies). A simple example is given in **Figure 7-2**, which shows that *p*-vinylphenol substructures as found in mono-lignols are much easier to oxidize (lower BDE) than phenols without this *p*-

vinyl structure. Such information is valuable in the context of genetically engineering new plants with superior commercialization potential.

Evidently these lignin structures are too large to be studied at high levels of theory with the state-of-art computational resources, hence GA calculations will likely present the most accurate thermodynamic data available today. In addition, GA calculations are fast and easy to calculate and thus allow for quick and convenient evaluation of the thermal stability of lignin molecules or their fragments. One obvious application is the assessment of bond stabilities as the weakest bonds contribute generally to the initial thermal decomposition. The results presented in **Chapters 3** and **4** make it possible to address the question whether radical formation will presumably start with CH_3–O bond scission of the G or S units or alternatively with cleavage of the 8-O-4 (β-O-4) ether bond.

A related question is the formation of the lignin polymer, which is assumed to involve the corresponding phenoxy radicals. Obviously, very stable phenolic bonds are difficult to break in plant cells and one wonders if the unsaturated character of the three monolignols (*p*-vinylphenol, *p*-vinylguaiacol and *p*-vinylsyringol) supports the phenoxy radical formation. The GA values derived in the current work can answer this question (See **Figure 7-2**).

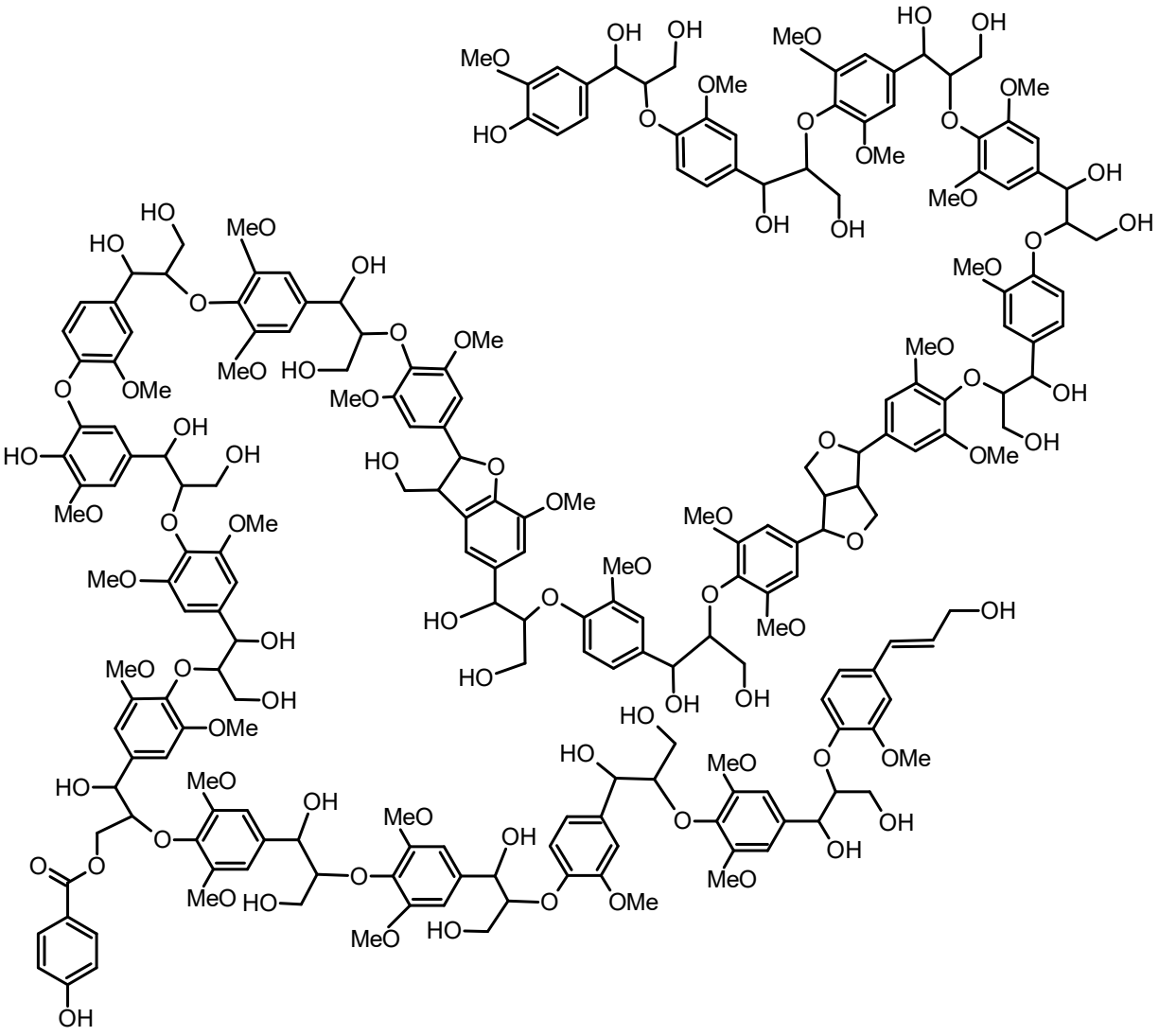

Figure 7-1 A representative lignin structure [28].

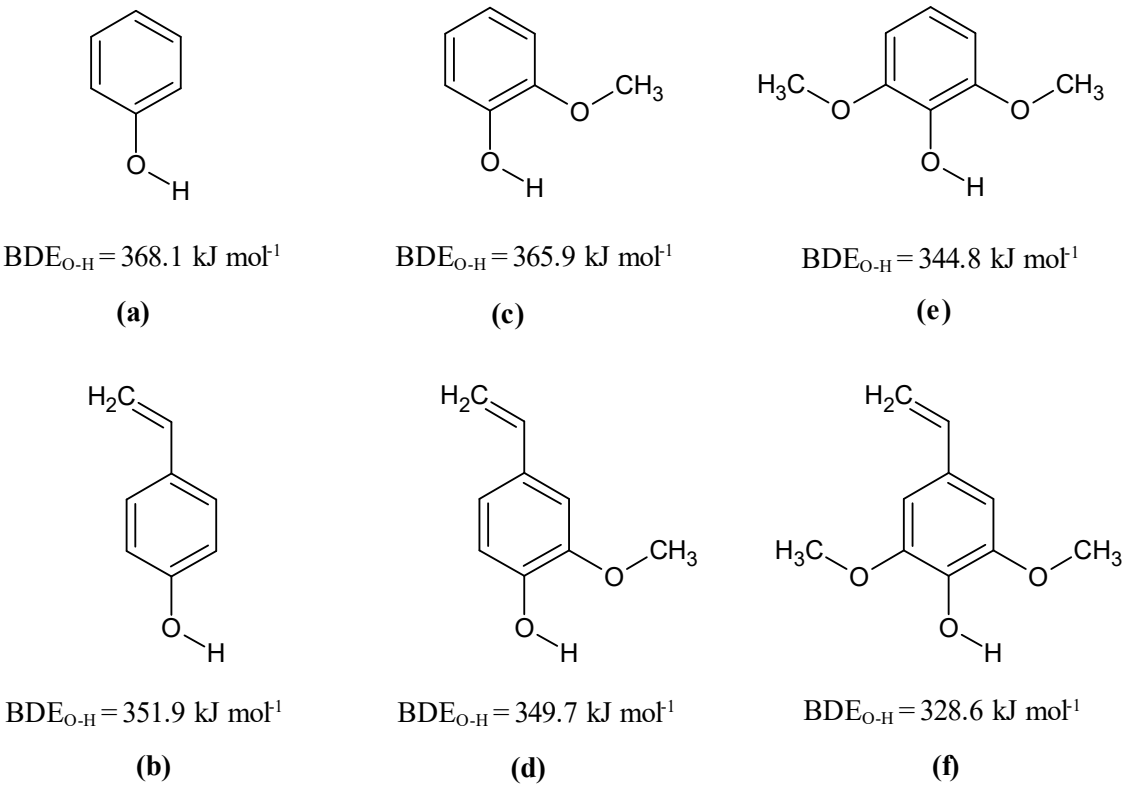

Figure 7-2 The structures of **(a)** phenol, **(b)** *p*-vinylphenol, **(c)** guaiacol (*o*-methoxyphenol), **(d)** *p*-vinylguaiacol (2-methoxy-4-vinylphenol), **(e)** syringol (2,6-dimethoxyphenol), **(f)** *p*-vinylsyringol **(**2,6-dimethoxy-4-vinylphenol) and the bond dissociation energies of the O-H bond (BDE_{O-H}) in all these six structures.

The results from this Ph.D. are not only applicable to lignin pyrolysis but also for a wide range of other industrial applications. One example is the steam cracking process in the petrochemicals industry, in which a hydrocarbon feedstock is cracked to yield "pyrolysis gas" with the objective to produce BTX (benzene, toluene and xylenes) next to light olefins (ethylene, propylene and butenes) and other products [28,29]. Another example is often the undesired molecular growth chemistry leading to polycyclic aromatic hydrocarbons (PAHs) [30,31], coke [32] and soot [33]. Process control over these processes requires detailed kinetic models and the current Ph.D. dissertation provides some of the input data needed to address the chemistry of the aromatic species present in those models. State-of-the-art tools to generate

those models are automatic mechanism generators such as the software "Genesys" developed at LCT [34]. Reliable models can only be generated automatically if thermodynamic and kinetic information for all important reaction steps are available in the appropriate databases and if this data is internally consistent. The GAV and ΔGAV° data presented in this thesis fill some of the gaps although much more is left to be done.

This Ph.D. thesis presents the first systematic group additive study at LCT dealing with aromatic molecules in-depth. Even though many GAVs and ΔGAV°s have been developed within the framework of this study, there is an immense work left to be done. Below, some potential extensions to the presented work and some recommendations for future studies can be found.

(I) GA based parameter development can be continued in the direction of various molecule or reaction families.

   (a) Focusing on lignin, additional GAVs are needed to fully describe the chemistry of its various structural subunits. Some GAVs are missing for the propanoid side chain and for ring structures found in lignin linkages and so are the NNIs accounting for hydrogen bonds between the hydroxyl groups of the propanoid chain and the methoxy substituents on the aromatic ring.

   (b) Numerous reaction families convert aromatic molecules to non-aromatic hydrocarbons. GA parameters are needed for the thermochemistry of cyclic hydrocarbons for several applications, e.g. for the calculation of lignin relevant moieties (See **Figure 7-1**).

   (c) The current research is restricted to single ring hydrocarbon aromatics. Similar data for polycyclic aromatic molecules are needed for molecular weight

growth models. GAVs for heteroatom aromatic molecules are required to address the formation of furans in biomass pyrolysis.

(d) Up to now, ΔGAV° parameters are available for just one hydrogen atom abstraction reaction (HAR) family. ΔGAV°s for many more families are needed to develop complete kinetic models. Some are:

- HARs from toluene derivatives by methyl and carbon-centered radicals.
- HARs from toluene derivatives by oxygen centered radicals.
- HARs from oxygenated monocyclic aromatic hydrocarbons (MAHs) by hydrogen atom or carbon-centered or oxygen-centered radicals.
- HARs from oxygenated MAHs by phenoxy radical.

(II) The changes that needed to be implemented in the methodology to determine GAVs for the class of compounds studied in this Ph.D. thesis (using physical explanation of interactions to test reliability of *ab initio* data, detailed lowest energy conformer search, wavefunction stability test for radicals and transition state structures and manual removal of harmonic oscillator frequencies) lead to significant improvements in the accuracy of the reported thermochemical/kinetic data and, hence, the updated methodology developed in this work should be used as a standard approach in future *ab initio* calculations and group additivity development. Moreover, the present approach can also be employed to double check the reliability of some of the data published in the earlier studies.

(III) Despite the long list of recommendations given above concerning the GA development for a wide range of possible reaction families, this should not lead to digression from the main source of motivation which is the optimization of industrial processes. Therefore,

the selection of the reaction families for GA development should be carried out by taking the requirements of the intended application into consideration, i.e. the extensions should be in the direction of the missing thermochemical and kinetic data in the kinetic network of the industrial application under investigation. In line with this purpose, a kinetic model can be constructed first and then, the decision of which reaction families should be selected for GA development should be made based on the missing thermochemical/kinetic data in this model as GA development is a strenuous task and the award should be worth the effort.

Although there is still a long way to go, a solid foundation is provided with the work that is presented in this Ph.D. dissertation. The good accuracy achieved with the GAV/NNI sets provides the incentive to advance in this direction.

References

[1] Benson SW, Buss JH. Additivity Rules for the Estimation of Molecular Properties - Thermodynamic Properties. *Journal of Chemical Physics.* 1958;29(3):546-572.

[2] Benson SW. *Thermochemical kinetics; methods for the estimation of thermochemical data and rate parameters*. New York: Wiley; 1968.

[3] Benson SW, Cruickshank FR, Golden DM, Haugen G, O'Neal HE, Rodgers AS, Shaw R, Walsh R. Additivity rules for the estimation of thermochemical properties. *Chemical Reviews.* 1969;69(3):279-324.

[4] Benson SW. *Thermochemical kinetics : methods for the estimation of thermochemical data and rate parameters*. 2d ed. New York: Wiley; 1976.

[5] Sabbe MK, Saeys M, Reyniers M-F, Marin GB, Van Speybroeck V, Waroquier M. Group Additive Values for the Gas Phase Standard Enthalpy of Formation of Hydrocarbons and Hydrocarbon Radicals. *The Journal of Physical Chemistry A.* 2005;109(33):7466-7480.

[6] Sabbe M, Vandeputte A, Reyniers M-F, Van Speybroeck V, Waroquier M, Marin G. Ab Initio Thermochemistry and Kinetics for Carbon-Centered Radical Addition and β-Scission Reactions. *The Journal of Physical Chemistry A.* 2007;111(34):8416-8428.

[7] Vandeputte AG, Sabbe MK, Reyniers M-F, Van Speybroeck V, Waroquier M, Marin GB. Theoretical Study of the Thermodynamics and Kinetics of Hydrogen Abstractions from Hydrocarbons. *The Journal of Physical Chemistry A.* 2007;111(46):11771-11786.

[8] Sabbe M, Reyniers M-F, Van Speybroeck V, Waroquier M, Marin G. Carbon-Centered Radical Addition and β-Scission Reactions: Modeling of Activation Energies and Pre-exponential Factors. *ChemPhysChem.* 2008;9(1):124-140.

[9] Sabbe MK, De Vleeschouwer F, Reyniers M-F, Waroquier M, Marin GB. First Principles Based Group Additive Values for the Gas Phase Standard Entropy and Heat Capacity of Hydrocarbons and Hydrocarbon Radicals. *The Journal of Physical Chemistry A.* 2008;112(47):12235-12251.

[10] Sabbe MK, Vandeputte AG, Reyniers M-F, Waroquier M, Marin GB. Modeling the influence of resonance stabilization on the kinetics of hydrogen abstractions. *Physical Chemistry Chemical Physics.* 2010;12(6):1278-1298.

[11] Vandeputte AG, Sabbe MK, Reyniers M-F, Marin GB. Modeling the gas-phase thermochemistry of organosulfur compounds. *Chemistry – A European Journal.* 2011;17(27):7656-7673.

[12] Vandeputte AG, Sabbe MK, Reyniers M-F, Marin GB. Kinetics of α hydrogen abstractions from thiols, sulfides and thiocarbonyl compounds. *Physical Chemistry Chemical Physics.* 2012;14(37):12773-12793.

[13] Vandeputte AG, Reyniers M-F, Marin GB. Kinetic modeling of hydrogen abstractions involving sulfur radicals. *ChemPhysChem.* 2013;14(16):3751-3771.

[14] Vandeputte AG, Reyniers M-F, Marin GB. Kinetics of homolytic substitutions by hydrogen atoms at thiols and sulfides. *ChemPhysChem.* 2013;14(8):1703-1722.

[15] Paraskevas PD, Sabbe MK, Reyniers M-F, Papayannakos N, Marin GB. Group Additive Values for the Gas-Phase Standard Enthalpy of Formation, Entropy and Heat Capacity of Oxygenates. *Chemistry – A European Journal.* 2013;19(48):16431-16452.

[16] Paraskevas PD, Sabbe MK, Reyniers M-F, Papayannakos N, Marin GB. Kinetic modeling of alpha-hydrogen abstractions from unsaturated and saturated oxygenate compounds by carbon-centered radicals. *ChemPhysChem.* 2014;15(9):1849-1866.

[17] Paraskevas PD, Sabbe MK, Reyniers M-F, Papayannakos NG, Marin GB. Kinetic Modeling of α-Hydrogen Abstractions from Unsaturated and Saturated Oxygenate Compounds by Hydrogen Atoms. *The Journal of Physical Chemistry A.* 2014;118(40):9296-9309.

[18] Paraskevas P. *Sustainable conversion of biomass oxygenates: ab initio based model simulation*. Ghent, Belgium ; Athens, Greece: Ghent University. Faculty of Engineering and Architecture ; National Technical University of Athens. School of Chemical Engineering, 2015.

[19] Paraskevas PD, Sabbe MK, Reyniers M-F, Papayannakos NG, Marin GB. Group Additive Kinetics for Hydrogen Transfer Between Oxygenates. *The Journal of Physical Chemistry A.* 2015;119(27):6961-6980.

[20] Paraskevas PD, Sabbe MK, Reyniers M-F, Marin GB, Papayannakos NG. Group additive kinetic modeling for carbon-centered radical addition to oxygenates and β-scission of oxygenates. *AIChE Journal.* 2016;62(3):802-814.

[21] Seeger R, Pople JA. Self-consistent molecular orbital methods. XVIII. Constraints and stability in Hartree–Fock theory. *The Journal of Chemical Physics.* 1977;66(7):3045-3050.

[22] Frisch MJ, Trucks GW, Schlegel HB, Scuseria GE, Robb MA, Cheeseman JR, Scalmani G, Barone V, Mennucci B, Petersson GA, Nakatsuji H, Caricato M, Li X, Hratchian HP, Izmaylov AF, Bloino J, Zheng G, Sonnenberg JL, Hada M, Ehara M, Toyota K, Fukuda R, Hasegawa J, Ishida M, Nakajima T, Honda Y, Kitao O, Nakai H, Vreven T, Montgomery Jr. JA, Peralta JE, Ogliaro F, Bearpark MJ, Heyd J, Brothers EN, Kudin KN, Staroverov VN, Kobayashi R, Normand J, Raghavachari K, Rendell AP, Burant JC, Iyengar SS, Tomasi J, Cossi M, Rega N, Millam NJ, Klene M, Knox JE, Cross JB, Bakken V, Adamo C, Jaramillo J, Gomperts R, Stratmann RE, Yazyev O, Austin AJ, Cammi R, Pomelli C, Ochterski JW, Martin RL, Morokuma K, Zakrzewski VG, Voth GA, Salvador P, Dannenberg JJ, Dapprich S, Daniels AD, Farkas Ö, Foresman JB, Ortiz JV, Cioslowski J, Fox DJ. Gaussian 09, Version D.01. Wallingford, CT, USA: Gaussian, Inc.; 2009.

[23] Bauernschmitt R, Ahlrichs R. Stability analysis for solutions of the closed shell Kohn–Sham equation. *The Journal of Chemical Physics.* 1996;104(22):9047-9052.

[24] Collard F-X and Blin J. A review on pyrolysis of biomass constituents: Mechanisms and composition of the products obtained from the conversion of cellulose, hemicelluloses and lignins. *Renewable and Sustainable Energy Reviews.* 2014;38:594–608.

[25] Hosoya T, Kawamoto H, Saka S. Role of methoxyl group in char formation from lignin-related compounds. *Journal of Analytical and Applied Pyrolysis.* 2009; 84: 79-83.

[26] Shen DK, Gua S, Luo KH, Wangb SR, Fang MX. The pyrolytic degradation of wood-derived lignin from pulping process. *Bioresource Technology.* 2010;101: 6136–6146.

[27] Custodis VBF, Hemberger P, Ma Z, van Bokhoven JA. Mechanism of Fast Pyrolysis of Lignin: Studying Model Compounds. *The Journal of Physical Chemistry B*. 2014; 118: 8524−8531.

[28] Vanholme R, Demedts B, Morreel K, Ralph J and Boerjan W. Lignin Biosynthesis and Structure. *Plant Physiology*. 2013: 54:519-546.

[29] Wiseman P. Ethylene by naphtha cracking. Free radicals in action. *Journal of Chemical Education.* 1977;54(3):154.

[30] Ren T, Patel M, Blok K. Olefins from conventional and heavy feedstocks: Energy use in steam cracking and alternative processes. *Energy.* 2006;31(4):425-451.

[31] Shukla B, Susa A, Miyoshi A, Koshi M. Role of Phenyl Radicals in the Growth of Polycyclic Aromatic Hydrocarbons. *The Journal of Physical Chemistry A.* 2008;112(11):2362-2369.

[32] Zhang F, Jones B, Maksyutenko P, Kaiser RI, Chin C, Kislov VV, Mebel AM. Formation of the Phenyl Radical [C6H5(X2A1)] under Single Collision Conditions: A Crossed Molecular Beam and ab Initio Study. *Journal of the American Chemical Society.* 2010;132(8):2672-2683.

[33] Albright LF, Marek JC. Mechanistic model for formation of coke in pyrolysis units producing ethylene. *Industrial & Engineering Chemistry Research.* 1988;27(5):755-759.

[34] Appel J, Bockhorn H, Frenklach M. Kinetic modeling of soot formation with detailed chemistry and physics: laminar premixed flames of C2 hydrocarbons. *Combustion and Flame.* 2000;121(1–2):122-136.

[35] Vandewiele NM, Van Geem KM, Reyniers MF, Marin GB. Genesys: Kinetic model construction using chemo-informatics. *Chemical Engineering Journal*. 2012;207:526-538.

Appendix A

Supporting Information for Chapter 3

Contents

A.1 List of Molecules

The 143 monoaromatic hydrocarbons (MAHs) used in the CBS-QB3 and G4 molecule sets from which GAVs and NNIs are derived are given in **Figure A-1**. The abbreviations given in this part are also used in the rest of the Supporting Material.

All the molecules in this database are substituted benzenes. Benzene and six single substituted benzenes are given with their full names. However, in the names of multiple substituted benzenes, the substituent groups hydroxy (-OH), methoxy (-OCH_3), formyl (-C=O), vinyl (-$CH=CH_2$), methyl (-CH_3) and ethyl (-CH_2CH_3) are denoted as OH, MeO, For, Vin, Me and Et respectively. "D" represents double substitution and "T" represents triple substitution with the same substituent. In double substituted benzenes, the abbreviations with uppercase letters *o*-, *m*- and *p*- refer to two substituents being in *ortho*, *meta* and *para* position to each other.

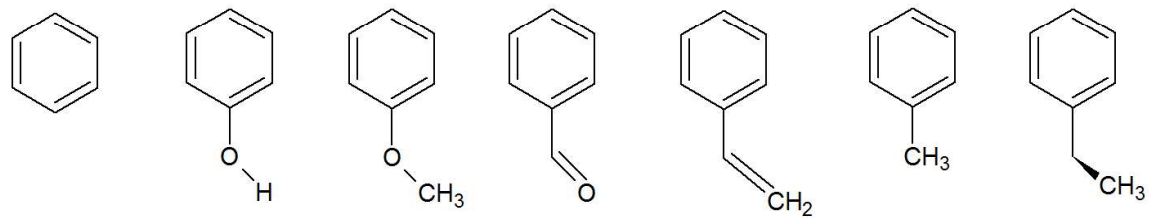

1-Benzene **2**-Phenol **3**-Anisole **4**-Benzaldehyde **5**-Styrene **6**-Toluene **7**-Ethyl Benzene

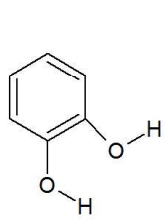

8-o-DOH

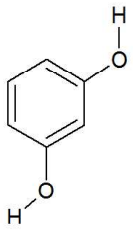

9-m-DOH

10-p-DOH

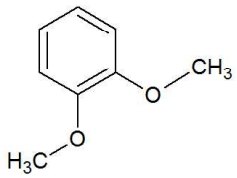

11-o-DMeO

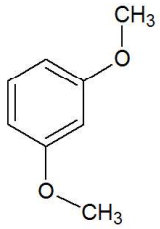

12-m-DMeO

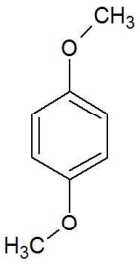

13-p-DMeO

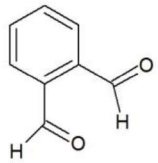

14-o-DFor

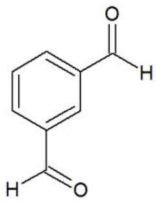

15-m-DFor

16-p-DFor

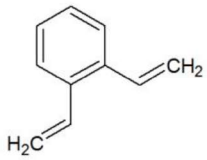

17-o-DVin

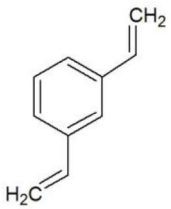

18-m-DVin

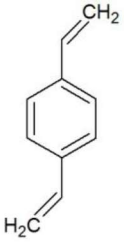

19-p-DVin

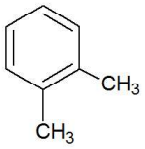

20-o-DMe

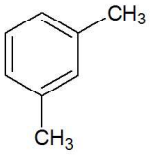

21-m-DMe

22-p-DMe

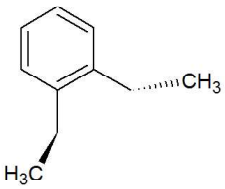

23-o-DEt

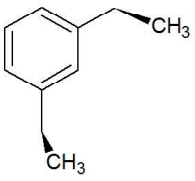

24-m-DEt

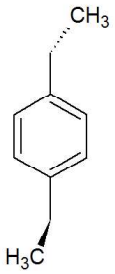

25-p-Det

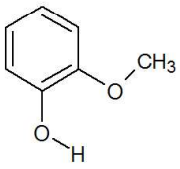

26-o-OHMeO

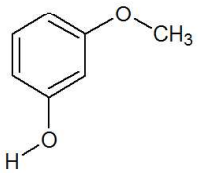

27-m-OHMeO

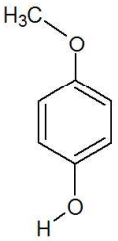

28-p-OHMeO

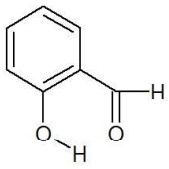

29-o-OHFor

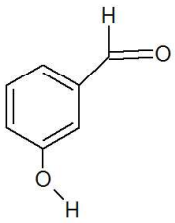

30-m-OHFor

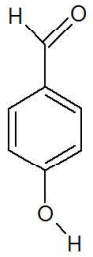

31-p-OHFor

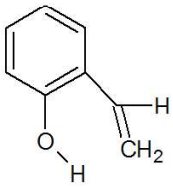

32-o-OHVin

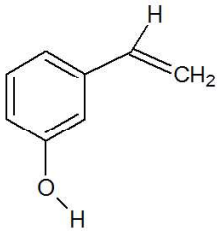

33-m-OHVin

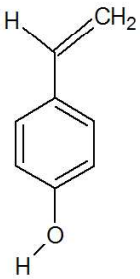

34-p-OHVin

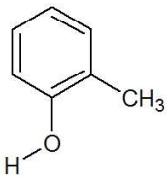

35-o-OHMe

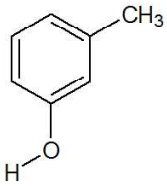

36-m-OHMe

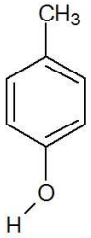

37-p-OHMe

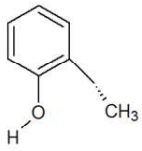

38-o-OHEt

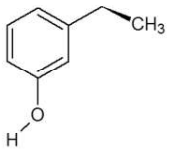

39-m-OHEt

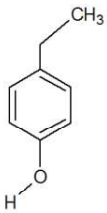

40-p-OHEt

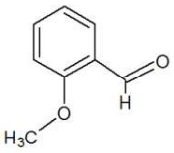

41-o-MeOFor

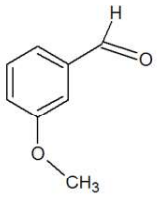

42-m-MeOFor

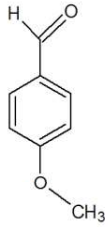

43-p-MeOFor

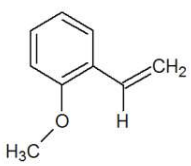

44-o-MeOVin

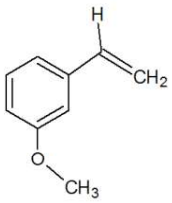

45-m-MeOVin

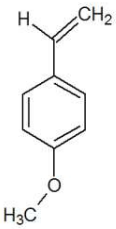

46-p-MeOVin

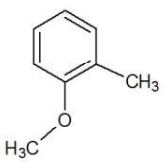

47-o-MeOMe

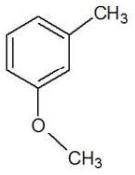

48-m-MeOMe

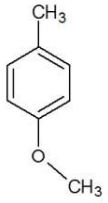

49-p-MeOMe

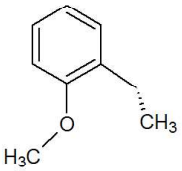

50-o-MeOEt

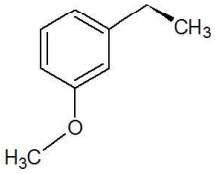

51-m-MeOEt

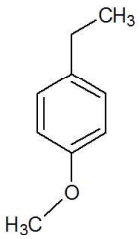

52-p-MeOEt

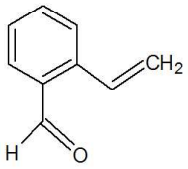

53-o-ForVin

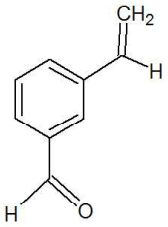

54-m-ForVin

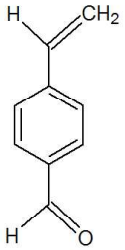

55-p-ForVin

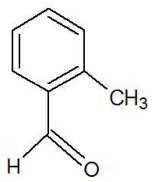

56-o-ForMe

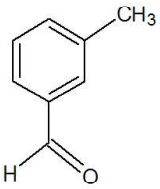

57-m-ForMe

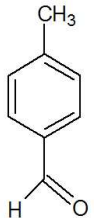

58-p-ForMe

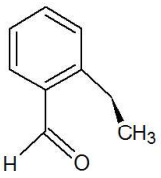

59-o-ForEt

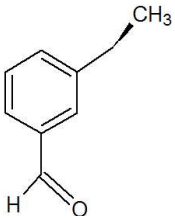

60-m-ForEt

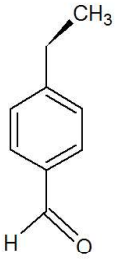

61-p-ForEt

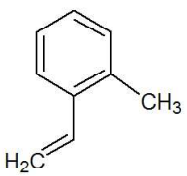

62-o-VinMe

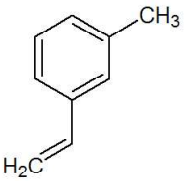

63-m-VinMe

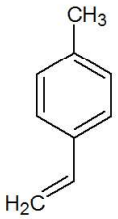

64-p-VinMe

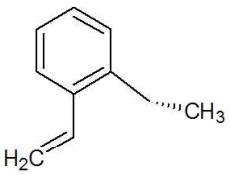

65-o-VinEt

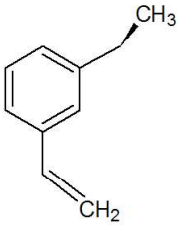

66-m-VinEt

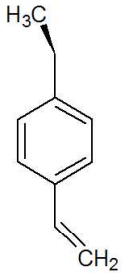

67-p-VinEt

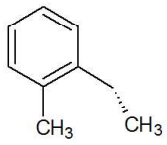

68-o-MeEt

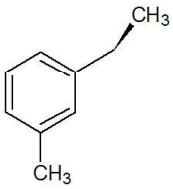

69-m-MeEt

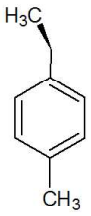

70-p-MeEt

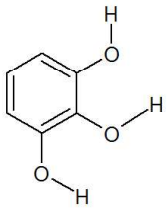

71-1,2,3-TOH

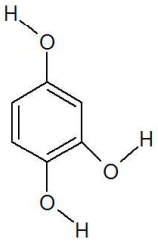

72-1,2,4-TOH

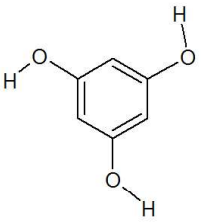

73-1,3,5-TOH

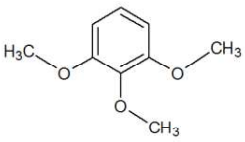

74-1,2,3-TMeO

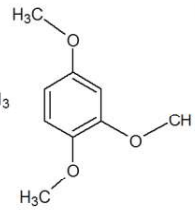

75-1,2,4-TMeO

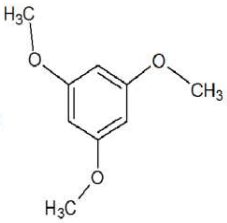

76-1,3,5-TMeO

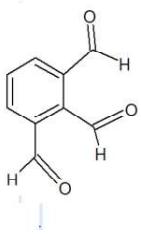

77-1,2,3-TFor

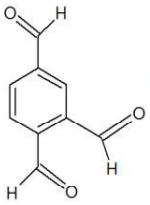

78-1,2,4-TFor

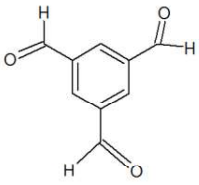

79-1,3,5-TFor

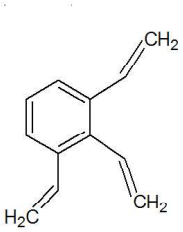

80-1,2,3-TVin

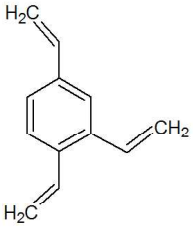

81-1,2,4-TVin

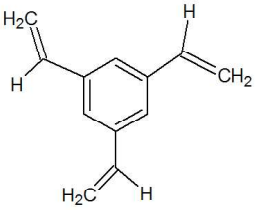

82-1,3,5-TVin

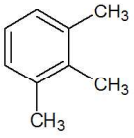

83-1,2,3-TMe

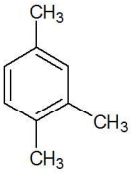

84-1,2,4-TMe

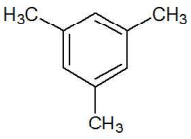

85-1,3,5-TMe

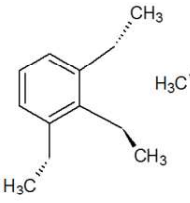

86-1,2,3-TEt

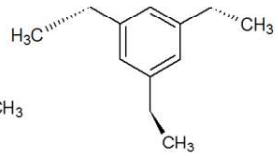

87-1,3,5-TEt

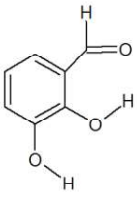

88-1,2-OH-3-For

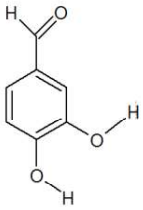

89-1,2-OH-4-For

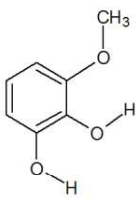

90-1,2-OH-3-MeO

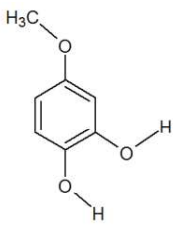

91-1,2-OH-4-MeO

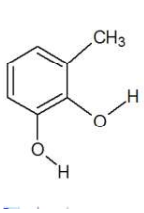

92-1,2-OH-3-Me

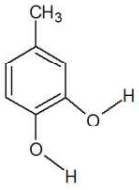

93-1,2-OH-4-Me

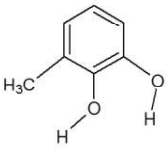

94-1,2-OH-6-Me

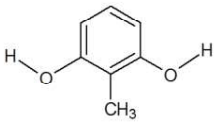

95-1,3-OH-2-Me

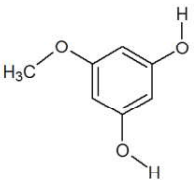

96-1,3-OH-5-MeO

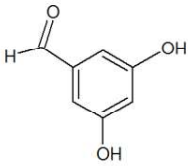

97-1,3-OH-5-For

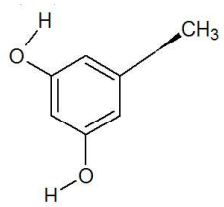

98-1,3-OH-5-Et

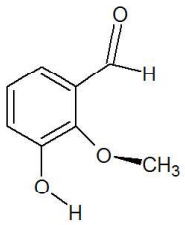

99-1-OH-2-MeO-3-For

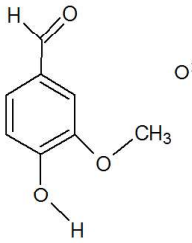

100-1-OH-2-MeO-4-For

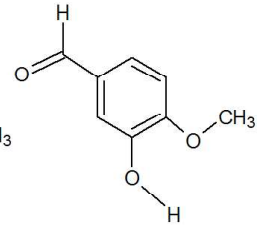

101-1-OH-2-MeO-5-For

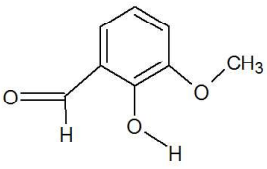

102-1-OH-2-MeO-6-For

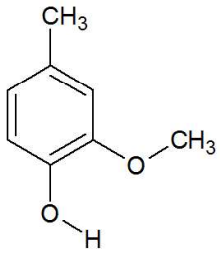

103-1-OH-2-MeO-4-Me

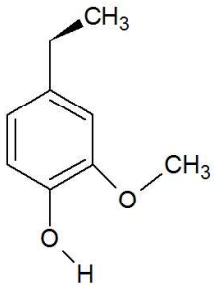

104-1-OH-2-MeO-4-Me

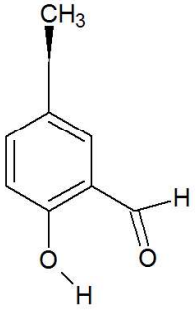

105-1-OH-2-For-4-Et

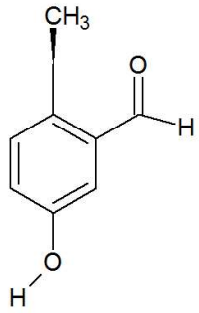

106-1-OH-3-For-4-Et

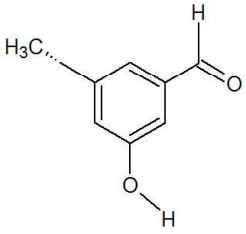

107-1-OH-3-For-5-Et

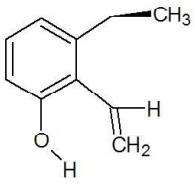

108-1-OH-2-Vin-3-Et

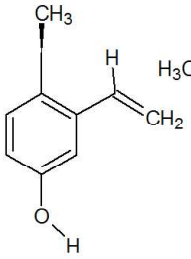

109-1-OH-3-Vin-4-Et

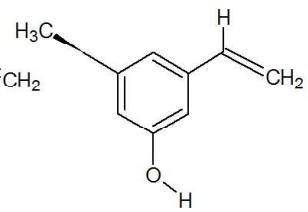

110-1-OH-3-Vin-5-Et

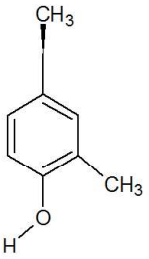

111-1-OH-2-Me-4-Et

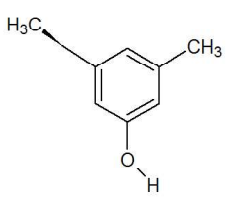

112-1-OH-3-Me-5-Et

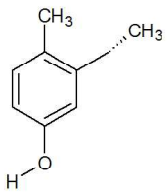

113-1-OH-3-Et-4-Me

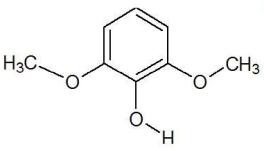

114-1,3-MeO-2-OH

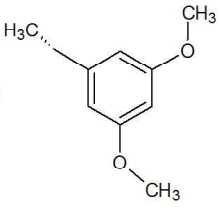

115-1,3-MeO-5-Et

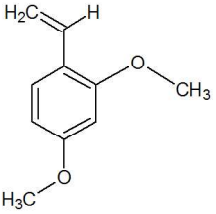

116-1,3-MeO-4-Vin

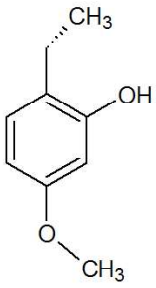

117-1-MeO-3-OH-4-Et

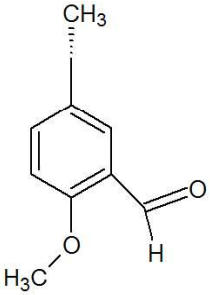

118-1-MeO-2-For-4-Et

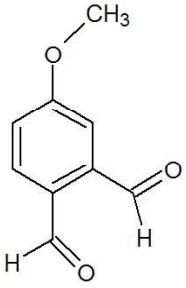

119-1,2-For-4-MeO

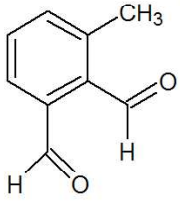

120-1,2-For-3-Me

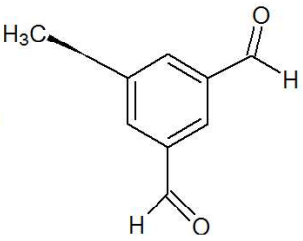

121-1,3-For-5-Et

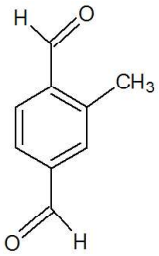

122-1,4-For-3-Me

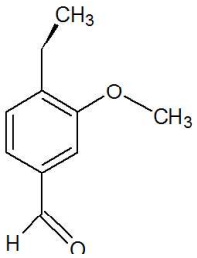

123-1-For-3-MeO-4-Et

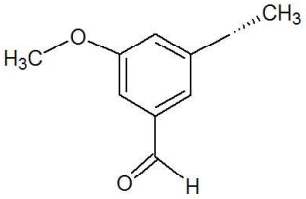

124-1-For-3-Et-5-MeO

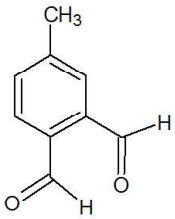

125-1,2-For-4-Me

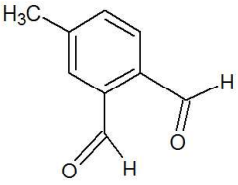

126-1,2-For-5-Me

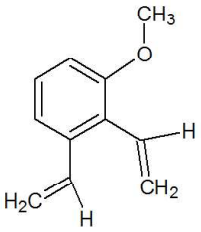

127-1,2-Vin-3-MeO

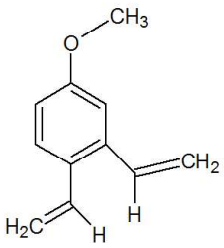

128-1,2-Vin-4-MeO

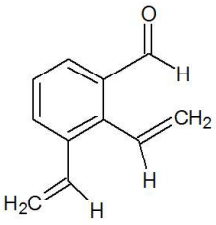

129-1,2-Vin-3-For

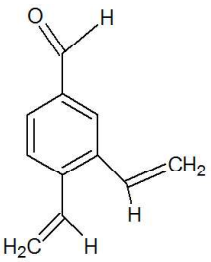

130-1,2-Vin-4-For

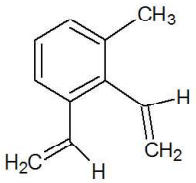

131-1,2-Vin-3-Me

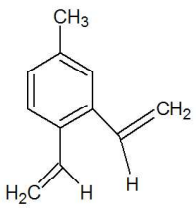

132-1,2-Vin-4-Me

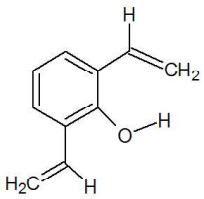

133-1,3-Vin-2-OH

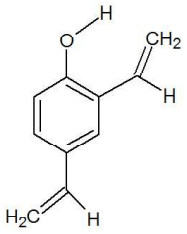

134-1,3-Vin-4-OH

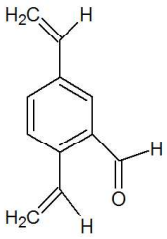

135-1,4-Vin-2-For

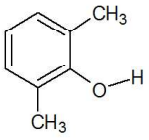

136-1,3-Me-2-OH

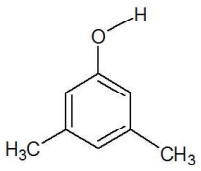

137-1,3-Me-5-OH

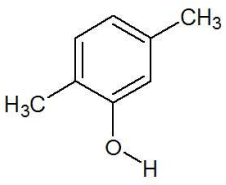

138-1,4-Me-2-OH

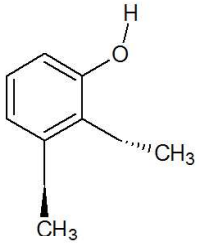

139-1,2-Et-3-OH

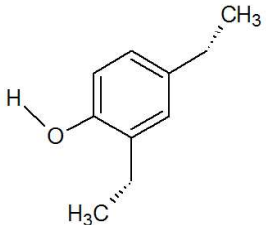

140-1,3-Et-6-OH

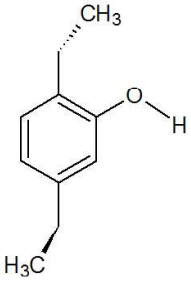

141-1,4-Et-2-OH

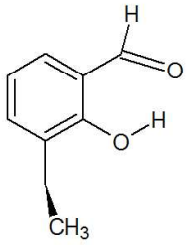

142-1-Et-2-OH-3-For

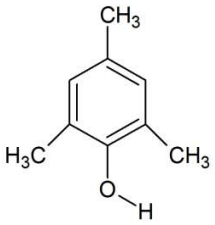

143-1,3,5-Me-2-OH

Figure A-1 The list of monocyclic aromatic molecules considered throughout **Chapter 3** and abbreviations used to describe these molecules and their geometries.

A.2 Development of Bond Additive Corrections (BACs)

In **Table A-1**, training set of molecules used in the development of Bond Additive Correction (BAC) parameters is given.

Table A-1 Set of molecules used to calibrate and validate the Bond Additive Correction (BAC) values at 298K for the CBS-QB3 and G4 levels of theory. "CBS-QB3" refers to uncorrected (except for spin-orbit corrections) results, "CBS-QB3/BAC" are the results after bond additivity corrections have been applied. The same distinction hold for "G4" and "G4/BAC".

Training set for BACs	$\Delta_f H°$ [kJ mol^{-1}]				
	Experiment	**CBS-QB3 - Experiment**	**CBS-QB3/BAC - Experiment**	**G4 - Experiment**	**G4/BAC - Experiment**
Non-aromatic Molecules [1]					
Ethane	-84.2	3.1	-0.1	1.9	0.7
Propane	-104.7	5.1	-0.6	2.6	0.3
n-Butane	-126.4	8.8	0.7	4.8	1.4
Isobutane	-135.0	8.2	0.1	4.2	0.7
n-Pentane	-146.8	11.4	0.9	5.9	1.3
Neopentane	-168.7	10.2	-0.4	3.7	-0.9
n-hexane	-167.2	13.8	0.8	6.7	1.0
2-Methyl-pentane	-174.3	9.9	-3.1	5.5	-0.2
2,3-dimethylbutane	-177.8	12.3	-0.7	4.8	-0.9
Heptane	-187.8	16.7	1.2	7.6	0.8
2,2,3-Trimethyl-butane	-204.8	12.2	-3.3	2.6	-4.2
Octane	-208.4	19.2	1.3	7.1	-0.9
Ethene	52.3	4.3	0.1	0.3	0.2
Allene	190.4	5.8	-1.9	-0.5	-0.6
Propene	20.1	6.7	0.0	1.5	0.3
1-Butene	-0.6	10.3	1.2	3.6	1.3
cis-2-Butene	-7.7	10.5	1.4	-0.8	-3.1
trans-2-Butene	-10.8	8.8	-0.3	2.4	0.1
Isobutene	-16.7	8.8	-0.3	1.9	-0.4
1,3-Butadiene	111.0	10.1	0.0	1.6	0.4
1,2-Butadiene	163.9	7.1	-3.0	-0.4	-1.6
cis-2-Pentene	-28.0	10.8	-0.8	5.8	2.3
trans-2-Pentene	-33.1	13.9	2.3	5.8	2.3
1,3-Pentadiene	76.2	14.2	1.6	4.3	2.0
1,4-Pentadiene	106.3	14.3	1.7	3.6	1.3
3-Methyl-1-butene	-27.4	11.1	-0.5	2.9	-0.6
2-Methyl-2-butene	-41.5	11.1	-0.5	3.2	-0.3
2-Methyl-1,3-butadiene	75.7	12.3	-0.3	2.6	0.3
3-Methyl-1,2-butadiene	129.1	10.3	-2.3	1.2	-1.1
1,5-hexadiene	85.0	15.7	0.7	2.7	-0.7
2,3-Dimethyl-2-Butene	-70.3	17.5	3.5	8.5	3.9
3,3-Dimethyl-1-Butene	-59.8	12.2	-1.8	2.9	-1.7
Methoxy-methane	-184.1	-2.6	-0.5	0.9	-0.4

Methoxy-ethane	-216.4	-1.6	-2.0	0.9	-1.5
Ethoxy-ethane	-252.5	3.1	0.2	4.8	1.2
1-Ethoxy-propane	-272.2	3.8	-1.5	4.7	0.0
1-Propoxy-propane	-296.0	8.6	0.8	8.5	2.7
Methanol	-201.3	-1.1	-1.9	1.5	-0.6
Ethanol	-235.1	2.1	-1.1	1.9	-1.4
1-Propanol	-256.3	5.7	0.0	3.3	-1.1
2-Propanone	-217.4	2.9	0.7	1.7	-0.1
2-Butanone	-238.5	4.6	0.0	3.0	0.0
2-Pentanone	-259.1	7.5	0.4	4.4	0.4
3-Pentanone	-257.3	4.2	-2.9	1.9	-2.2
2,3-Butanedione	-326.8	-0.7	-1.8	-0.4	-2.8
Ethanal	-170.7	5.5	5.6	5.4	4.7
Propanal	-190.4	6.7	4.4	6.0	4.2
Ethanedial	-212.0	-4.1	-0.7	-3.0	-3.2
2-oxo-propanal	-271.0	-1.6	-0.4	-1.1	-2.4
Methyl methanoate	-358.8	-4.9	0.4	-0.6	-1.5
Methyl ethanoate	-410.0	-4.6	-1.5	-0.8	-2.7
Ethyl methanoate	-398.0	3.1	6.2	7.1	5.2
Ethyl ethanoate	-445.2	-0.4	0.2	2.9	-0.1
Ethyl propanoate	-465.1	0.8	-1.1	6.1	1.9
Ethyl butanoate	-485.0	2.1	-2.2	3.3	-2.0
Diethyl carbonate	-640.2	-3.4	0.0	3.8	-0.5
Methanoic acid	-378.7	-2.5	0.1	1.1	-0.5
Ethanoic acid	-432.4	-0.3	0.0	3.0	0.3
Propanoic acid	-455.4	4.1	2.0	6.8	3.0
Ketene	-48.0	1.7	1.0	0.1	0.1
Ethenol	-126.5	5.3	1.1	0.7	-1.4
	Statistics				
Mean Deviation (MD)		1.5	0.1	3.1	0.0
Mean Absolute Deviation (MAD)		3.4	1.3	3.3	1.4
Maximum Absolute Deviation (MAX)		8.6	6.2	9.5	5.2
Aromatic Molecules[a]					
Benzene	82.9 [2,3]	9.8	-0.8	2.7	-0.9
Phenol	-96.4 [4,5]	11.8	0.8	7.6	0.4
Anisole	-72.6 [6,7]	5.2	-2.9	4.8	-1.6
Benzaldehyde	-37.0 [8,7,9]	7.5	0.2	1.2	-0.4
Toluene	50.1 [2,3]	10.2	-0.6	1.3	-0.9
EthylBenzene	29.8 [2]	12.5	-0.7	1.7	-1.6
α-Methyl Styrene	118.3 [10]	10.6	-0.3	0.4	-0.2
Acetophenone	-86.7 [11]	10.4	-0.5	-0.7	-1.3
Benzophenone	49.0 [12]	10.8	-0.1	0.6	0.0
BiPhenyl	181.4 [3,13-15]	10.1	-0.9	4.5	-1.2
o-Methyl Toluene	19.0 [2]	15.3	4.3	9.5	3.8
m-Methyl Toluene	17.2 [16]	9.8	-1.2	4.3	-1.4
p-Methyl Toluene	17.9 [16]	13.5	-3.2	0.3	-3.0
o-Methyl Phenol	-128.5 [4,5]	13.1	-2.5	-0.7	-0.6
m-Methyl Phenol	-133.0 [4,5]	12.3	5.0	5.6	4.0
p-Methyl Phenol	-125.4 [4,5]	20.5	3.2	6.5	2.8

	Statistics				
Mean Deviation (MD)		11.5	0.0	3.1	0.0
Mean Absolute Deviation (MAD)		11.5	1.7	3.3	1.5
Maximum Absolute Deviation (MAX)		20.5	6.2	9.5	4.0
Test Set for BACs	$\Delta_f H°$ **[kJ mol^{-1}]**				
	Experiment	**CBS-QB3 - Experiment**	**CBS-QB3/BAC - Experiment**	**G4 - Experiment**	**G4/BAC - Experiment**
Propyl Benzene	7.8 [2]	15.1	-0.6	2.7	-1.7
Isopropyl Benzene	3.9 [2]	14.0	-1.7	0.7	-3.7
n-Butyl Benzene	-13.8 [16]	18.6	0.3	4.6	-0.9
t-Butyl Benzene	-22.7 [16]	14.7	-3.4	-0.1	-5.6
Styrene	146.9 [17]	14.6	0.3	3.1	1.0
o-Ethyl Toluene	1.2 [18]	11.6	-1.8	-0.4	-2.2
m-Ethyl Toluene	-1.9 [18]	12.0	-1.4	-0.8	-2.6
p-Ethyl Toluene	-3.3 [18]	13.5	0.1	1.2	-0.6
o-Hydroxy Phenol	-274.8 [19]	7.9	-3.3	9.8	-1.0
m-Hydroxy Phenol	-284.7 [19]	20.8	9.6	21.6	10.8
p-Hydroxy Phenol	-277.0 [19]	19.7	8.5	21.7	10.9
o-Hydroxy Benzaldehyde	-245.6 [20]	15.2	7.7	8.7	3.5
m-Hydroxy Benzaldehyde	-213.7 [20]	5.1	-2.4	3.5	-1.7
p-Hydroxy Benzaldehyde	-217.8 [20]	7.1	-0.4	4.0	-1.2
	Statistics				
Mean Deviation (MD)		13.6	0.8	5.7	0.4
Mean Absolute Deviation (MAD)		13.6	3.0	5.9	3.4
Maximum Absolute Deviation (MAX)		20.8	9.6	21.7	10.9

[a]Experimental data taken from the NIST database based on selection criteria described in the text. If several references are given for a single molecule the average value has been used.

A.3 Thermochemical Database for determination of GAV and NNI

All the thermochemical data obtained for the CBS-QB3 and G4 datasets are given in **Table A-2** and **Table A-3**, respectively. In these two tables, raw standard enthalpy of formation data ($\Delta_f H^\circ$), BAC-corrected standard enthalpy of formation values ($\Delta_f H^\circ + BAC$), molecular entropy data (S°) intrinsic entropy values ($S^\circ{}_{int}$) are given at 298 K whereas C_p values are given at 300 K, 400 K, 500 K, 600 K, 800 K, 1000 K and 1500 K. $\Delta_f H^\circ$values are given in kJ mol^{-1} whereas $S^\circ{}_{int}$ and C_p values are given in J mol^{-1} K^{-1}. Total symmetry number (σ_{sym}) and number of optical isomers (n_{opt}) which are important in calculation of intrinsic entropy values from molecular entropy data are also provided. The numbering of the molecules is consistent with the list of molecules given in **Figure A-1**.

Histograms showing the distribution of the deviations between BAC-corrected CBS-QB3 and G4 standard enthalpy of formations and intrinsic entropies are given in **Figure A-2** and **Figure A-3** respectively.

Table A-2 Thermochemical database obtained at the level of CBS-QB3.

#	Training set for GAV and NNI	$\Delta_f H^\circ$	$\Delta_f H^\circ + BAC$	S°	$S^\circ{}_{int}$	σ_{totsym}	n_{opt}	C_p						
		298 K		298 K				300 K	400 K	500 K	600 K	800 K	1000 K	1500 K
1	Benzene	92.7	82.1	268.6	289.3	12	1	81.7	111.7	137.4	158.1	188.5	209.6	240.7
2	Phenol (Hydroxybenzene)	-84.6	-95.6	313.7	319.5	2	1	102.8	134.8	161.1	181.8	211.4	231.7	261.7
3	Anisole (Methoxybenzene)	-64.0	-72.1	346.8	361.7	6	1	123.9	161.0	192.2	217.3	254.8	281.1	320.5
4	Benzaldehyde (Formylbenzene)	-29.5	-36.8	332.2	337.9	2	1	110.0	143.6	172.5	196.0	230.7	254.5	288.1
5	Styrene (Vinylbenzene)	161.8	147.6	342.1	347.9	2	1	118.9	157.9	191.0	217.7	256.8	284.0	324.1
6	Toluene (Methylbenzene)	60.3	49.5	320.2	335.1	6	1	103.3	138.4	169.1	194.4	232.3	259.2	299.3
7	EthylBenzene	42.3	29.1	360.0	374.9	6	1	128.0	168.8	204.6	234.2	278.9	310.8	358.8
8	*o*-dihydroxybenzene	-266.9	-278.1	337.9	343.6	2	1	123.2	157.6	185.9	208.0	238.4	257.8	285.2
9	*m*-dihydroxybenzene	-263.9	-275.1	343.4	349.2	2	1	124.4	158.2	185.1	205.9	234.9	254.3	283.0
10	*p*-dihydroxybenzene	-257.3	-268.5	341.0	352.5	4	1	125.4	157.9	183.6	203.6	232.2	251.8	281.3
11	*o*-dimethoxybenzene	-207.0	-212.6	414.1	438.1	18	1	174.4	211.4	244.9	273.5	318.1	350.3	399.2
12	*m*-dimethoxybenzene	-221.1	-226.7	410.4	434.5	18	1	169.2	212.1	248.3	277.6	321.7	353.1	400.5
13	*p*-dimethoxybenzene	-217.0	-222.6	410.5	440.3	36	1	168.3	209.4	244.6	273.8	318.5	350.7	399.4
14	*o*-diformylbenzene	-133.8	-137.8	388.8	394.6	2	1	142.9	179.7	211.8	238.3	277.0	302.2	335.5
15	*m*-diformylbenzene	-147.8	-151.8	379.1	384.8	2	1	141.4	177.7	209.1	235.1	273.6	299.8	335.5

16	*p*-diformylbenzene	-147.9	-151.9	375.0	386.5	4	1	138.8	176.0	208.0	234.4	273.3	299.5	335.2
17	*o*-divinylbenzene	238.4	220.6	402.3	408.0	2	1	160.3	205.7	244.5	276.1	323.1	356.2	406.0
18	*m*-divinylbenzene	230.5	212.7	401.4	407.2	2	1	156.3	204.1	244.6	277.2	325.0	358.3	407.5
19	*p*-divinylbenzene	230.1	212.3	393.9	405.5	4	1	156.5	204.3	244.8	277.6	325.6	358.8	407.9
20	*o*-dimethylbenzene	29.6	18.7	351.4	375.4	18	1	130.3	168.8	203.4	232.6	277.3	309.5	358.1
21	*m*-dimethylbenzene	28.3	17.4	356.7	380.7	18	1	124.9	165.1	200.8	230.6	276.2	308.8	357.8
22	*p*-dimethylbenzene	28.0	17.1	351.1	380.9	36	1	125.0	165.1	200.7	230.6	276.1	308.8	357.8
23	*o*-diethylbenzene	-3.5	-19.3	428.8	452.9	18	1	177.1	227.8	273.7	312.4	371.9	414.7	478.9
24	*m*-diethylbenzene	-8.0	-23.8	441.5	459.7	9	1	174.5	225.9	271.8	310.3	369.4	412.0	476.6
25	*p*-diethylbenzene	-8.2	-24.0	431.0	460.7	36	1	174.2	225.6	271.6	310.1	369.3	412.0	476.9
26	*o*-methoxyphenol	-247.8	-256.1	374.6	383.7	3	1	143.6	182.2	215.6	243.0	283.0	309.6	346.9
27	*m*-methoxyphenol	-241.7	-250.0	381.0	390.1	3	1	147.2	185.5	217.0	242.0	278.3	303.7	341.7
28	*p*-methoxyphenol	-236.8	-245.1	386.8	395.9	3	1	146.8	183.7	214.2	238.9	275.5	301.4	340.4
29	*o*-formylphenol	-234.6	-242.1	345.3	345.3	1	1	123.9	160.2	190.7	215.3	251.3	275.9	311.3
30	*m*-formylphenol	-208.6	-216.1	363.9	363.9	1	1	136.4	170.4	198.9	221.8	255.1	277.6	309.7
31	*p*-formylphenol	-211.0	-218.5	362.0	362.0	1	1	130.0	165.7	195.5	219.3	253.5	276.6	309.6
32	*o*-vinylphenol	-13.0	-27.5	374.1	374.1	1	1	146.1	184.7	216.5	241.8	279.0	305.0	344.2
33	*m*-vinylphenol	-15.6	-30.1	378.1	378.1	1	1	140.4	181.1	214.8	241.4	279.8	306.0	345.1
34	*p*-vinylphenol	-15.1	-29.6	377.5	377.5	1	1	140.1	181.0	214.8	241.6	280.1	306.4	345.4
35	*o*-methylphenol	-118.4	-129.4	353.9	363.1	3	1	127.6	163.3	193.8	218.6	255.4	281.2	320.1
36	*m*-methylphenol	-117.7	-128.7	356.1	365.2	3	1	124.5	161.6	192.9	218.1	255.3	281.3	320.2
37	*p*-methylphenol	-115.6	-126.6	350.6	365.5	6	1	124.6	161.4	192.6	217.8	255.0	281.0	320.1
38	*o*-ethylphenol	-136.7	-150.2	391.1	400.2	3	1	153.0	194.6	230.3	259.4	302.9	333.7	380.1
39	*m*-ethylphenol	-135.7	-149.2	395.8	405.0	3	1	149.0	191.7	228.2	257.8	301.8	332.9	379.7
40	*p*-ethylphenol	-134.0	-147.5	396.0	405.2	3	1	149.2	191.8	228.1	257.7	301.7	332.7	379.6
41	*o*-formylanisole	-182.9	-187.7	398.2	407.4	3	1	155.1	198.0	234.1	262.9	304.4	332.1	371.0
42	*m*-formylanisole	-189.5	-194.3	398.0	407.1	3	1	157.8	197.2	230.8	258.2	299.0	327.4	368.7
43	*p*-formylanisole	-191.2	-196.0	402.5	411.6	3	1	151.4	192.4	227.5	256.1	298.1	327.2	369.0
44	*o*-vinylanisole	6.7	-5.0	407.1	416.2	3	1	163.9	209.2	247.5	278.6	324.9	357.4	405.6
45	*m*-vinylanisole	4.7	-7.0	411.8	421.0	3	1	161.7	207.4	245.9	277.0	323.1	355.5	403.9
46	*p*-vinylanisole	5.2	-6.5	411.3	420.4	3	1	161.5	207.4	246.1	277.4	323.6	356.0	404.3
47	*o*-methylanisole	-98.4	-106.7	381.7	400.0	9	1	148.2	190.8	227.7	257.8	302.8	334.4	381.4
48	*m*-methylanisole	-96.4	-104.7	388.7	406.9	9	1	145.6	187.7	223.9	253.7	298.6	330.7	379.1
49	*p*-methylanisole	-95.0	-103.3	389.7	407.9	9	1	146.5	188.3	224.2	253.8	298.6	330.7	379.0
50	*o*-ethylanisole	-116.8	-127.5	422.2	440.5	9	1	172.6	220.8	262.9	297.6	349.9	386.9	441.8
51	*m*-ethylanisole	-114.8	-125.5	428.0	446.3	9	1	170.1	217.9	259.2	293.3	345.1	382.3	438.5
52	*p*-ethylanisole	-113.4	-124.1	429.2	447.5	9	1	170.6	218.1	259.2	293.2	345.0	382.2	438.5
53	*o*-vinylbenzaldehyde	49.2	38.3	394.1	394.1	1	1	148.8	191.7	228.7	258.7	302.5	331.7	372.8
54	*m*-vinylbenzaldehyde	39.3	28.4	396.8	396.8	1	1	147.3	189.8	226.1	255.6	299.0	328.8	371.5
55	*p*-vinylbenzaldehyde	39.1	28.2	399.6	399.6	1	1	147.1	189.7	226.0	255.5	299.0	328.9	371.7
56	*o*-methylbenzaldehyde	-57.2	-64.7	372.1	381.3	3	1	138.6	175.4	207.9	235.1	276.2	305.1	346.8
57	*m*-methylbenzaldehyde	-63.1	-70.6	374.4	383.5	3	1	131.7	170.3	204.2	232.3	274.5	304.0	346.7
58	*p*-methylbenzaldehyde	-63.6	-71.1	377.9	387.0	3	1	131.5	170.2	204.1	232.2	274.5	304.0	346.8
59	*o*-ethylbenzaldehyde	-75.6	-85.5	411.6	420.8	3	1	163.1	206.1	243.9	275.5	323.6	357.5	407.0
60	*m*-ethylbenzaldehyde	-81.5	-91.4	415.2	424.3	3	1	156.1	200.4	239.5	271.9	321.0	355.6	406.0
61	*p*-ethylbenzaldehyde	-81.8	-91.7	411.8	420.9	3	1	156.0	200.4	239.4	271.8	320.9	355.6	406.2
62	*o*-methylstyrene	134.0	119.6	380.3	389.5	3	1	146.0	188.6	225.4	255.6	301.2	333.6	382.4
63	*m*-methylstyrene	129.4	115.0	384.5	393.6	3	1	140.6	184.6	222.7	253.9	300.7	333.6	382.7
64	*p*-methylstyrene	129.6	115.2	384.2	393.3	3	1	140.6	184.6	222.7	254.0	300.7	333.7	382.8
65	*o*-ethylstyrene	116.1	99.3	417.9	427.1	3	1	170.3	220.2	262.8	297.5	349.7	387.0	443.0
66	*m*-ethylstyrene	110.9	94.1	424.9	434.0	3	1	165.6	215.1	258.3	293.8	347.3	385.2	442.1
67	*p*-ethylstyrene	111.1	94.3	424.7	433.9	3	1	165.3	214.9	258.2	293.8	347.3	385.3	442.2
68	*o*-ethyltoluene	12.8	-0.6	397.4	415.6	9	1	151.7	197.1	237.7	271.8	324.1	361.7	418.2
69	*m*-ethyltoluene	10.1	-3.3	402.0	420.2	9	1	149.7	195.5	236.3	270.4	322.8	360.4	417.3
70	*p*-ethyltoluene	10.2	-3.2	402.3	420.6	9	1	149.5	195.3	236.1	270.3	322.7	360.4	417.3
71	1,2,3-Trihydroxybenzene	-448.4	-459.8	359.5	365.3	2	1	147.0	183.6	212.9	235.6	266.0	284.6	309.5
72	1,2,4-Trihydroxybenzene	-437.8	-449.2	371.4	371.4	1	1	152.3	186.7	213.4	233.7	261.1	278.8	304.9
73	1,3,5-Trihydroxybenzene	-439.6	-451.0	365.2	374.4	3	1	152.7	185.9	212.1	232.0	259.3	277.3	304.3
74	1,2,3-Trimethoxybenzene	-351.7	-354.8	485.6	518.7	54	1	211.2	255.2	295.0	329.0	381.8	420.2	478.1
75	1,2,4-Trimethoxybenzene	-359.9	-363.0	484.6	512.0	27	1	219.0	262.2	300.2	332.8	384.0	421.5	478.8
76	1,3,5-Trimethoxybenzene	-380.1	-383.2	462.6	499.2	81	1	218.7	267.2	307.4	340.1	389.8	425.7	480.8

77	1,2,3-Triformylbenzene	-238.3	-238.9	436.2	441.9	2	1	174.9	215.1	249.3	277.0	316.7	342.7	377.9
78	1,2,4-Triformylbenzene	-248.8	-249.4	436.0	436.0	1	1	174.8	214.3	249.0	277.9	320.2	347.5	382.6
79	1,3,5-Triformylbenzene	-263.8	-264.4	419.4	434.3	6	1	176.9	214.8	248.1	276.0	317.7	345.8	383.1
80	1,2,3-Trivinylbenzene	314.9	293.4	455.9	461.7	2	1	201.2	255.9	302.4	340.0	395.3	433.9	491.3
81	1,2,4-Trivinylbenzene	306.6	285.1	464.8	464.8	1	1	197.9	252.3	298.5	336.1	391.8	431.0	489.6
82	1,3,5-Trivinylbenzene	300.5	279.0	465.7	465.7	1	1	193.8	250.3	298.1	336.5	393.0	432.3	490.6
83	1,2,3-Trimethylbenzene	1.4	-9.7	387.3	420.5	54	1	149.2	193.9	234.1	268.1	320.7	358.8	416.5
84	1,2,4-Trimethylbenzene	-1.9	-13.0	394.1	421.5	27	1	151.8	195.3	234.9	268.7	321.1	359.1	416.7
85	1,3,5-Trimethylbenzene	-3.7	-14.8	383.9	426.2	162	1	146.7	191.8	232.5	266.9	320.0	358.4	416.3
86	1,2,3-Triethylbenzene	-48.1	-66.6	495.3	522.8	27	1	233.4	293.7	348.7	395.6	468.7	521.6	601.0
87	1,3,5-Triethylbenzene	-58.5	-77.0	505.6	544.5	108	1	221.0	283.0	339.0	386.4	459.8	513.3	595.0
88	1,2-dihydroxy-3-formylbenzene	-419.5	-427.3	367.5	367.5	1	1	143.6	182.5	215.3	241.8	279.8	304.2	336.9
89	1,2-dihydroxy -4-formylbenzene	-396.4	-404.2	383.3	383.3	1	1	152.1	190.6	222.7	248.0	283.2	305.4	335.1
90	1,2-dihydroxy-3-methoxybenzene	-429.2	-437.8	398.0	407.2	3	1	164.3	205.4	240.5	269.0	309.5	335.4	370.4
91	1,2-dihydroxy-4-methoxybenzene	-417.5	-426.1	406.2	415.4	3	1	172.7	211.9	243.7	268.8	304.4	328.4	364.0
92	1,2-dihydroxy-3-methylbenzene	-300.7	-311.9	376.2	385.3	3	1	149.2	187.1	219.3	245.4	283.0	308.0	344.0
93	1,2-dihydroxy-4-methylbenzene	-297.9	-309.1	377.3	386.5	3	1	148.3	187.6	220.2	246.1	283.1	307.7	343.6
94	1,2-dihydroxy-6-methylbenzene	-302.2	-313.4	375.6	384.7	3	1	148.3	187.2	219.9	246.3	283.9	308.8	344.5
95	1,3-dihydroxy-2-methylbenzene	-297.4	-308.6	374.3	395.0	12	1	145.7	184.0	215.5	240.6	277.0	302.3	340.4
96	1,3-dihydroxy-5-methoxybenzene	-419.7	-428.3	402.5	417.4	6	1	173.8	212.2	243.3	267.6	302.6	326.7	363.1
97	1,3-dihydroxy-5-formylbenzene	-385.4	-393.2	391.2	391.2	1	1	159.1	195.5	224.6	247.3	279.4	300.7	331.0
98	1,3-dihydroxy-5-ethylbenzene	-313.2	-326.9	418.6	433.5	6	1	172.3	216.0	252.7	282.1	325.3	355.4	400.8
99	1-hydroxy-2-methoxy-3-formylbenzene	-358.2	-363.2	427.6	436.8	3	1	171.5	215.5	252.8	282.4	324.3	351.9	390.7
100	1-hydroxy-2-methoxy-4-formylbenzene	-378.6	-383.6	418.8	427.9	3	1	174.4	216.5	252.7	282.5	326.8	356.6	397.1
101	1-hydroxy-2-methoxy-5-formylbenzene	-373.7	-378.7	423.6	432.8	3	1	173.3	216.8	253.9	283.8	326.7	354.9	394.0
102	1-hydroxy-2-methoxy-6-formylbenzene	-367.5	-372.5	419.6	428.8	3	1	173.7	216.5	253.3	283.6	328.4	358.2	397.5
103	1-hydroxy-2-methoxy-4-methylbenzene	-278.9	-287.4	409.5	427.7	9	1	165.4	209.0	247.4	279.4	326.9	359.2	405.4
104	1-hydroxy-2-methoxy-4-ethylbenzene	-297.2	-308.2	452.2	470.5	9	1	190.7	239.4	282.6	318.8	373.1	410.5	464.5
105	1-hydroxy-2-formyl-4-ethylbenzene	-284.8	-295.0	421.3	430.4	3	1	170.1	217.0	257.7	291.2	341.6	377.0	429.2
106	1-hydroxy-3-formyl-4-ethylbenzene	-252.8	-263.0	441.9	451.1	3	1	185.0	229.6	267.9	299.3	346.5	379.6	427.9
107	1-hydroxy-3-formyl-5-ethylbenzene	-260.3	-270.5	443.2	452.3	3	1	181.7	226.6	265.4	297.4	345.2	378.6	427.4
108	1-hydroxy-2-vinyl-3-ethylbenzene	-61.5	-78.6	447.3	456.5	3	1	195.3	246.8	290.1	325.0	376.4	412.3	466.0
109	1-hydroxy-3-vinyl-4-ethylbenzene	-61.0	-78.1	446.3	455.5	3	1	192.0	243.7	286.9	321.6	373.0	409.3	464.1
110	1-hydroxy-3-vinyl-5-ethylbenzene	-66.9	-84.0	454.6	463.7	3	1	186.7	238.0	281.8	317.4	370.1	407.2	462.9
111	1-hydroxy-2-methyl-4-ethylbenzene	-168.1	-181.7	430.2	448.5	9	1	174.3	220.4	260.9	294.5	345.6	382.3	438.0
112	1-hydroxy-3-methyl-5-ethylbenzene	-168.2	-181.8	429.5	447.8	9	1	169.7	217.7	259.4	293.7	345.5	382.4	438.1
113	1-hydroxy-3-ethyl-4-methylbenzene	-163.7	-177.3	427.1	445.4	9	1	172.9	220.1	261.3	295.4	347.0	383.7	439.2
114	1,3-dimethoxy-2-hydroxybenzene	-391.7	-397.5	439.8	463.9	18	1	184.8	227.9	265.4	296.3	342.5	374.6	422.1
115	1,3-dimethoxy-5-ethylbenzene	-272.5	-280.7	485.8	519.0	54	1	215.6	269.0	315.2	353.4	411.8	454.1	518.3
116	1,3-dimethoxy-4-vinylbenzene	-151.3	-160.5	467.6	485.8	9	1	206.9	259.6	303.7	339.4	392.6	430.1	486.0
117	1-methoxy-3-hydroxy-4-ethylbenzene	-292.2	-303.2	452.6	470.9	9	1	193.9	243.0	284.5	318.3	369.0	405.1	459.9
118	1-methoxy-2-formyl-4-ethylbenzene	-233.9	-241.2	469.7	488.0	9	1	200.3	253.8	300.2	338.0	394.1	432.9	488.9
119	1,2-diformyl-4-methylbenzene	-298.6	-300.0	452.5	461.6	3	1	187.3	230.2	267.8	298.9	345.2	376.2	418.1
120	1,2-diformyl-3-methylbenzene	-156.2	-160.3	425.4	434.6	3	1	165.9	206.9	243.3	273.6	318.4	348.8	391.4
121	1,3-diformyl-5-ethylbenzene	-201.2	-207.7	458.7	467.8	3	1	187.2	234.3	276.0	311.0	363.9	400.9	453.3
122	1,4-diformyl-3-methylbenzene	-176.3	-180.4	420.2	429.3	3	1	167.6	207.9	243.6	273.6	318.8	350.0	393.7
123	1-formyl-3-methoxy-4-ethylbenzene	-245.3	-252.6	472.5	490.8	9	1	202.5	253.6	298.9	336.6	393.6	433.4	490.7
124	1-formyl-3-methoxy-5-ethylbenzene	-241.6	-248.9	474.0	492.2	9	1	203.2	253.5	297.4	333.8	389.1	428.4	486.4
125	1,2-diformyl-4-methylbenzene	-168.9	-173.0	428.8	438.0	3	1	164.6	206.1	243.2	274.3	320.8	352.0	394.3
126	1,2-diformyl-5-methylbenzene	-168.9	-173.0	429.9	439.1	3	1	164.9	206.2	243.0	273.8	319.8	350.8	393.4
127	1,2-divinyl-3-methoxybenzene	84.3	69.0	459.5	468.7	3	1	210.3	264.5	309.2	344.9	397.6	434.6	490.1
128	1,2-divinyl-4-methoxybenzene	81.0	65.7	468.5	477.6	3	1	202.6	255.3	299.8	335.9	389.9	428.2	486.0
129	1,2-divinyl-3-formylbenzene	127.1	112.7	448.5	448.5	1	1	191.7	241.1	283.5	317.9	368.6	403.5	454.0
130	1,2-divinyl-4-formylbenzene	115.2	100.8	454.0	454.0	1	1	189.3	238.0	279.9	314.2	365.5	401.3	453.5
131	1,2-divinyl-3-methylbenzene	211.4	193.4	433.5	442.6	3	1	191.5	241.7	284.6	319.7	372.4	409.9	466.6
132	1,2-divinyl-4-methylbenzene	205.8	187.8	443.5	452.6	3	1	181.8	232.5	276.3	312.5	367.0	405.9	464.6
133	1,3-divinyl-2-hydroxybenzene	56.0	37.9	430.5	430.5	1	1	186.0	232.7	271.4	302.4	348.0	379.9	427.9

Table A-3 Thermochemical database obtained at the level of G4.

#	Training set for GAV and NNI	$\Delta_f H°$	$\Delta_f H° + BAC$	$S°$	$S°_{int}$	$\sigma_{tot}{}^{sym}$	n_{opt}	C_p						
		298 K		298 K				300 K	400 K	500 K	600 K	800 K	1000 K	1500 K
1	Benzene	85.6	82.0	268.7	289.4	12	1	81.9	112.0	137.6	158.3	188.6	209.6	240.7
2	Phenol (Hydroxybenzene)	-88.8	-96.0	313.6	319.3	2	1	102.7	134.7	161.0	181.7	211.3	231.6	261.6
3	Anisole (Methoxybenzene)	-67.8	-74.2	346.5	361.4	6	1	123.7	160.8	192.0	217.2	254.6	280.9	320.4
4	Benzaldehyde (Formylbenzene)	-35.8	-37.4	332.3	338.1	2	1	110.0	143.7	172.5	196.0	230.6	254.4	288.0
5	Styrene (Vinylbenzene)	150.0	147.9	342.0	347.7	2	1	118.9	157.9	190.9	217.6	256.7	283.8	324.0
6	Toluene (Methylbenzene)	51.3	49.2	320.1	335.0	6	1	103.4	138.6	169.2	194.5	232.4	259.1	299.2
7	EthylBenzene	31.5	28.2	360.1	375.0	6	1	128.2	169.0	204.7	234.3	279.0	310.8	358.7
8	*o*-dihydroxybenzene	-265.0	-275.8	337.4	343.1	2	1	122.9	157.3	185.6	207.7	238.2	257.6	285.1
9	*m*-dihydroxybenzene	-263.1	-273.9	342.1	347.9	2	1	125.5	158.6	185.2	205.8	234.6	253.9	282.7
10	*p*-dihydroxybenzene	-255.3	-266.1	340.6	352.2	4	1	125.0	157.4	183.2	203.2	231.9	251.6	281.2
11	*o*-dimethoxybenzene	-206.1	-215.3	413.6	437.6	18	1	174.1	211.1	244.5	273.2	317.8	350.1	399.0
12	*m*-dimethoxybenzene	-221.8	-231.0	409.8	433.9	18	1	168.6	211.6	247.7	277.1	321.3	352.7	400.3
13	*p*-dimethoxybenzene	-214.2	-223.4	408.7	438.5	36	1	167.6	209.0	244.3	273.6	318.4	350.6	399.3
14	*o*-diformylbenzene	-136.8	-136.4	389.5	395.3	2	1	143.7	180.1	212.0	238.4	277.0	302.1	335.4
15	*m*-diformylbenzene	-152.8	-152.4	379.3	385.1	2	1	141.4	177.6	209.0	234.9	273.5	299.6	335.4
16	*p*-diformylbenzene	-151.7	-151.3	377.4	389.0	4	1	139.0	176.1	208.0	234.2	273.1	299.3	335.1
17	*o*-divinylbenzene	222.8	222.2	401.3	407.1	2	1	160.4	205.7	244.5	276.0	322.9	356.0	405.7
18	*m*-divinylbenzene	214.5	213.9	400.5	406.3	2	1	156.1	203.8	244.3	276.8	324.7	357.9	407.2
19	*p*-divinylbenzene	213.8	213.2	393.4	405.0	4	1	156.2	204.0	244.5	277.2	325.3	358.6	407.7
20	*o*-dimethylbenzene	19.4	18.8	351.3	375.3	18	1	130.3	168.9	203.5	232.6	277.4	309.5	358.1
21	*m*-dimethylbenzene	17.2	16.6	356.7	380.7	18	1	125.0	165.2	200.9	230.7	276.1	308.7	357.7
22	*p*-dimethylbenzene	17.8	17.2	351.1	380.9	36	1	125.0	165.1	200.8	230.6	276.1	308.7	357.7
23	*o*-diethylbenzene	-17.5	-20.4	428.8	452.8	18	1	177.3	228.0	274.0	312.6	371.9	414.6	478.8
24	*m*-diethylbenzene	-22.7	-25.6	441.8	460.1	9	1	174.6	226.1	272.0	310.4	369.4	411.9	476.4
25	*p*-diethylbenzene	-22.0	-24.9	431.0	460.8	36	1	174.3	225.8	271.8	310.3	369.3	411.9	476.7
26	*o*-methoxyphenol	-245.8	-255.8	374.1	383.3	3	1	143.3	181.9	215.3	242.7	282.7	309.4	346.8
27	*m*-methoxyphenol	-242.6	-252.6	380.5	389.7	3	1	146.7	184.9	216.5	241.5	278.0	303.4	341.5
28	*p*-methoxyphenol	-234.8	-244.8	386.4	395.5	3	1	146.1	183.0	213.6	238.3	275.1	301.1	340.3
29	*o*-formylphenol	-238.9	-244.1	344.9	344.9	1	1	123.6	159.8	190.4	215.0	251.1	275.7	311.2
30	*m*-formylphenol	-210.2	-215.4	363.8	363.8	1	1	136.1	170.1	198.6	221.6	254.9	277.4	309.5
31	*p*-formylphenol	-213.8	-219.0	365.0	365.0	1	1	129.8	165.5	195.4	219.4	253.9	277.1	309.9
32	*o*-vinylphenol	-22.1	-27.8	377.0	377.0	1	1	142.1	181.5	214.4	240.7	279.0	305.4	344.7
33	*m*-vinylphenol	-24.2	-29.9	377.6	377.6	1	1	139.9	180.6	214.3	241.0	279.4	305.8	344.9
34	*p*-vinylphenol	-24.0	-29.7	377.0	377.0	1	1	139.7	180.6	214.4	241.2	279.8	306.2	345.2
35	*o*-methylphenol	-124.0	-129.7	353.8	362.9	3	1	127.5	163.2	193.7	218.5	255.3	281.1	320.0
36	*m*-methylphenol	-123.5	-129.2	355.9	365.0	3	1	124.3	161.3	192.7	217.9	255.2	281.2	320.1
37	*p*-methylphenol	-121.1	-126.8	350.4	365.3	6	1	124.4	161.2	192.4	217.6	254.8	280.9	320.0
38	*o*-ethylphenol	-143.7	-150.5	391.4	400.5	3	1	153.0	194.6	230.3	259.4	302.9	333.6	380.0
39	*m*-ethylphenol	-143.4	-150.2	395.7	404.8	3	1	148.9	191.6	228.0	257.7	301.7	332.7	379.5
40	*p*-ethylphenol	-141.1	-147.9	395.9	405.0	3	1	149.1	191.7	228.0	257.6	301.5	332.6	379.5
41	*o*-formylanisole	-185.1	-189.5	398.2	407.3	3	1	154.7	197.4	233.5	262.4	303.9	331.7	370.9
42	*m*-formylanisole	-191.1	-195.5	397.9	407.0	3	1	157.5	196.8	230.4	257.9	298.7	327.2	368.5
43	*p*-formylanisole	-194.2	-198.6	402.2	411.4	3	1	151.2	192.1	227.2	255.8	297.9	326.9	368.8
44	*o*-vinylanisole	-1.0	-5.9	406.7	415.8	3	1	163.6	208.9	247.2	278.4	324.7	357.2	405.3
45	*m*-vinylanisole	-3.7	-8.6	412.8	421.9	3	1	161.6	207.2	245.6	276.7	322.8	355.2	403.7
46	*p*-vinylanisole	-3.4	-8.3	410.8	419.9	3	1	161.1	207.0	245.7	277.0	323.3	355.7	404.1
47	*o*-methylanisole	-103.6	-108.5	381.5	399.7	9	1	148.1	190.7	227.6	257.7	302.6	334.2	381.3
48	*m*-methylanisole	-102.3	-107.2	388.4	406.6	9	1	145.3	187.3	223.4	253.2	298.2	330.3	378.8
49	*p*-methylanisole	-100.4	-105.3	389.2	407.5	9	1	146.2	188.1	224.0	253.5	298.4	330.5	378.9
50	*o*-ethylanisole	-123.4	-129.4	421.9	440.1	9	1	172.5	220.8	262.8	297.5	349.7	386.7	441.6
51	*m*-ethylanisole	-122.2	-128.2	429.5	447.7	9	1	170.3	217.9	259.1	293.2	344.9	382.1	438.3
52	*p*-ethylanisole	-120.3	-126.3	427.3	445.6	9	1	170.1	217.7	258.9	293.0	344.7	381.9	438.3
53	*o*-vinylbenzaldehyde	39.6	39.5	394.3	394.3	1	1	149.0	191.7	228.6	258.7	302.3	331.6	372.6
54	*m*-vinylbenzaldehyde	29.0	28.9	396.5	396.5	1	1	147.2	189.7	225.9	255.4	298.8	328.6	371.3
55	*p*-vinylbenzaldehyde	28.2	28.1	399.5	399.5	1	1	147.4	189.7	225.9	255.4	298.9	328.7	371.6
56	*o*-methylbenzaldehyde	-65.0	-65.1	372.1	381.2	3	1	138.6	175.5	208.0	235.1	276.2	305.0	346.7

57	*m*-methylbenzaldehyde	-71.2	-71.3	374.6	383.7	3	1	131.7	170.3	204.2	232.2	274.4	303.9	346.5
58	*p*-methylbenzaldehyde	-72.0	-72.1	378.0	387.2	3	1	131.9	170.5	204.3	232.3	274.5	304.0	346.6
59	*o*-ethylbenzaldehyde	-84.6	-85.8	411.5	420.6	3	1	163.2	206.2	244.0	275.5	323.5	357.4	406.9
60	*m*-ethylbenzaldehyde	-90.9	-92.1	413.1	422.2	3	1	155.8	200.3	239.4	271.8	320.9	355.4	405.9
61	*p*-ethylbenzaldehyde	-91.6	-92.8	412.0	421.1	3	1	156.1	200.4	239.4	271.8	320.8	355.4	406.0
62	*o*-methylstyrene	120.8	120.2	380.5	389.7	3	1	146.0	188.6	225.4	255.6	301.1	333.5	382.3
63	*m*-methylstyrene	115.5	114.9	384.1	393.2	3	1	140.4	184.5	222.6	253.8	300.5	333.4	382.5
64	*p*-methylstyrene	115.5	114.9	384.0	393.1	3	1	140.6	184.6	222.6	253.9	300.6	333.5	382.6
65	*o*-ethylstyrene	100.7	98.9	416.6	425.7	3	1	170.1	220.1	262.7	297.5	349.6	386.8	442.8
66	*m*-ethylstyrene	95.6	93.8	424.7	433.8	3	1	165.5	215.0	258.2	293.7	347.1	385.0	441.9
67	*p*-ethylstyrene	95.7	93.9	424.5	433.7	3	1	165.3	214.9	258.1	293.7	347.1	385.1	442.0
68	*o*-ethyltoluene	0.8	-1.0	397.3	415.5	9	1	151.8	197.3	237.9	272.0	324.1	361.6	418.1
69	*m*-ethyltoluene	-2.7	-4.5	401.9	420.2	9	1	149.8	195.6	236.4	270.5	322.7	360.3	417.2
70	*p*-ethyltoluene	-2.1	-3.9	402.3	420.6	9	1	149.6	195.5	236.3	270.4	322.7	360.3	417.2
71	1,2,3-Trihydroxybenzene	-443.0	-457.3	358.9	364.7	2	1	146.4	183.1	212.5	235.2	265.7	284.4	309.4
72	1,2,4-Trihydroxybenzene	-432.9	-447.2	370.7	370.7	1	1	151.9	186.3	213.0	233.3	260.7	278.5	304.8
73	1,3,5-Trihydroxybenzene	-437.8	-452.1	364.7	373.8	3	1	151.9	185.1	211.3	231.3	258.8	277.0	304.2
74	1,2,3-Trimethoxybenzene	-346.1	-358.1	484.8	518.0	54	1	210.9	254.7	294.4	328.4	381.3	419.7	477.8
75	1,2,4-Trimethoxybenzene	-354.7	-366.7	483.8	511.2	27	1	218.3	261.5	299.5	332.1	383.5	421.1	478.6
76	1,3,5-Trimethoxybenzene	-377.0	-389.0	464.0	500.6	81	1	218.3	266.6	306.7	339.5	389.2	425.3	480.5
77	1,2,3-Triformylbenzene	-240.2	-237.7	440.1	445.9	2	1	173.8	214.0	248.4	276.2	316.1	342.3	377.7
78	1,2,4-Triformylbenzene	-250.8	-248.3	436.4	436.4	1	1	174.8	214.1	248.8	277.6	319.9	347.3	382.5
79	1,3,5-Triformylbenzene	-267.5	-265.0	419.8	434.7	6	1	176.8	214.6	247.8	275.7	317.4	345.5	382.9
80	1,2,3-Trivinylbenzene	294.9	295.8	455.0	460.8	2	1	201.2	255.6	302.0	339.5	394.6	433.2	490.7
81	1,2,4-Trivinylbenzene	286.5	287.4	463.8	463.8	1	1	197.4	251.8	298.1	335.6	391.4	430.6	489.3
82	1,3,5-Trivinylbenzene	279.2	280.1	465.1	465.1	1	1	193.3	249.7	297.5	335.9	392.5	431.8	490.3
83	1,2,3-Trimethylbenzene	-10.9	-10.0	385.9	419.1	54	1	149.3	194.0	234.2	268.2	320.8	358.8	416.4
84	1,2,4-Trimethylbenzene	-14.3	-13.4	393.9	421.3	27	1	151.8	195.4	235.0	268.7	321.1	359.0	416.5
85	1,3,5-Trimethylbenzene	-16.6	-15.7	384.5	426.8	162	1	146.7	191.9	232.5	266.9	319.9	358.2	416.2
86	1,2,3-Triethylbenzene	-65.8	-68.3	489.6	522.7	54	1	233.6	294.0	349.0	395.9	468.7	521.5	600.8
87	1,3,5-Triethylbenzene	-76.7	-79.2	505.7	544.6	108	1	221.1	283.1	339.1	386.5	459.7	513.1	594.7
88	1,2-dihydroxy-3-formylbenzene	-416.0	-424.7	367.2	367.2	1	1	143.2	181.9	214.6	241.1	279.1	303.6	336.6
89	1,2-dihydroxy -4-formylbenzene	-393.2	-401.9	386.3	386.3	1	1	154.9	192.8	224.3	249.4	284.4	306.5	335.8
90	1,2-dihydroxy-3-methoxybenzene	-423.6	-437.1	398.6	407.7	3	1	164.2	205.2	240.2	268.7	309.2	335.2	370.3
91	1,2-dihydroxy-4-methoxybenzene	-412.4	-425.9	405.4	414.5	3	1	172.0	211.2	243.1	268.2	304.0	328.1	363.8
92	1,2-dihydroxy-3-methylbenzene	-300.6	-309.9	375.7	384.8	3	1	148.9	186.8	219.1	245.2	282.8	307.8	343.9
93	1,2-dihydroxy-4-methylbenzene	-298.1	-307.4	377.0	386.1	3	1	147.9	187.2	219.8	245.8	282.9	307.5	343.5
94	1,2-dihydroxy-6-methylbenzene	-302.1	-311.4	375.1	384.3	3	1	148.0	186.9	219.7	246.1	283.7	308.6	344.3
95	1,3-dihydroxy-2-methylbenzene	-299.4	-308.7	374.0	394.7	12	1	145.5	183.8	215.3	240.3	276.7	302.1	340.3
96	1,3-dihydroxy-5-methoxybenzene	-417.5	-431.0	401.7	416.6	6	1	173.0	211.3	242.5	266.9	302.0	326.3	362.9
97	1,3-dihydroxy-5-formylbenzene	-384.3	-393.0	390.9	390.9	1	1	158.7	194.9	224.0	246.8	279.0	300.3	330.8
98	1,3-dihydroxy-5-ethylbenzene	-317.8	-328.2	418.2	433.1	6	1	171.8	215.5	252.2	281.7	324.9	355.1	400.6
99	1-hydroxy-2-methoxy-3-formylbenzene	-352.9	-360.8	427.1	436.2	3	1	171.1	215.1	252.4	282.0	323.9	351.6	390.6
100	1-hydroxy-2-methoxy-4-formylbenzene	-375.6	-383.5	418.2	427.3	3	1	173.7	215.9	252.2	282.2	326.7	356.6	397.1
101	1-hydroxy-2-methoxy-5-formylbenzene	-371.0	-378.9	423.3	432.4	3	1	172.8	216.2	253.3	283.3	326.3	354.6	393.8
102	1-hydroxy-2-methoxy-6-formylbenzene	-364.7	-372.6	420.8	430.0	3	1	173.6	216.2	253.0	283.3	328.2	358.0	397.4
103	1-hydroxy-2-methoxy-4-methylbenzene	-278.3	-286.8	409.0	427.2	9	1	165.0	208.6	247.0	279.1	326.6	359.0	405.2
104	1-hydroxy-2-methoxy-4-ethylbenzene	-298.1	-307.7	451.9	470.2	9	1	190.2	238.9	282.2	318.4	372.7	410.2	464.3
105	1-hydroxy-2-formyl-4-ethylbenzene	-289.7	-294.5	420.8	430.0	3	1	169.8	216.6	257.3	290.9	341.3	376.8	429.0
106	1-hydroxy-3-formyl-4-ethylbenzene	-255.9	-260.7	440.4	449.6	3	1	184.4	229.2	267.5	299.0	346.2	379.3	427.7
107	1-hydroxy-3-formyl-5-ethylbenzene	-265.5	-270.3	443.1	452.2	3	1	181.9	226.5	265.3	297.2	345.0	378.4	427.3
108	1-hydroxy-2-vinyl-3-ethylbenzene	-72.7	-78.0	447.5	456.6	3	1	195.4	246.8	290.1	325.0	376.3	412.1	465.8
109	1-hydroxy-3-vinyl-4-ethylbenzene	-72.2	-77.5	445.4	454.5	3	1	191.5	243.3	286.5	321.2	372.7	409.0	463.9
110	1-hydroxy-3-vinyl-5-ethylbenzene	-74.8	-80.1	453.8	462.9	3	1	186.8	237.9	281.6	317.1	369.8	407.0	462.8
111	1-hydroxy-2-methyl-4-ethylbenzene	-176.1	-181.4	429.9	448.2	9	1	174.1	220.2	260.7	294.4	345.5	382.1	437.9
112	1-hydroxy-3-methyl-5-ethylbenzene	-178.1	-183.4	433.1	451.4	9	1	171.2	218.6	260.0	294.1	345.7	382.4	438.1
113	1-hydroxy-3-ethyl-4-methylbenzene	-172.2	-177.5	426.7	445.0	9	1	172.7	219.9	261.1	295.2	346.8	383.6	439.0
114	1,3-dimethoxy-2-hydroxybenzene	-386.2	-399.0	440.7	464.7	18	1	183.6	226.9	264.6	295.7	342.0	374.2	421.9
115	1,3-dimethoxy-5-ethylbenzene	-276.1	-284.9	484.6	517.7	54	1	214.2	267.4	313.6	351.9	410.6	453.1	517.9
116	1,3-dimethoxy-4-vinylbenzene	-155.2	-162.9	467.0	485.3	9	1	206.2	258.9	303.0	338.8	392.0	429.6	485.7
117	1-methoxy-3-hydroxy-4-ethylbenzene	-295.2	-304.8	453.3	471.5	9	1	193.8	242.7	284.2	318.1	368.8	404.9	459.7

118	1-methoxy-2-formyl-4-ethylbenzene	-238.7	-242.7	471.3	489.6	9	1	200.5	253.8	300.1	337.9	393.9	432.7	488.7
119	1,2-diformyl-4-methylbenzene	-297.6	-300.0	452.5	461.6	3	1	186.9	229.7	267.3	298.5	344.8	375.9	417.9
120	1,2-diformyl-3-methylbenzene	-162.3	-160.4	424.0	433.1	3	1	165.5	206.0	241.8	271.4	315.5	345.9	389.4
121	1,3-diformyl-5-ethylbenzene	-209.4	-208.6	458.7	467.8	3	1	187.2	234.3	275.9	310.8	363.7	400.7	453.1
122	1,4-diformyl-3-methylbenzene	-181.8	-179.9	420.1	429.2	3	1	167.6	207.9	243.5	273.4	318.6	349.8	393.6
123	1-formyl-3-methoxy-4-ethylbenzene	-249.2	-253.2	472.3	490.6	9	1	202.4	253.4	298.6	336.4	393.4	433.2	490.5
124	1-formyl-3-methoxy-5-ethylbenzene	-246.0	-250.0	477.3	495.5	9	1	203.5	253.5	297.3	333.6	388.9	428.1	486.2
125	1,2-diformyl-4-methylbenzene	-173.8	-171.9	429.4	438.5	3	1	164.6	206.0	243.1	274.2	320.7	351.8	394.1
126	1,2-diformyl-5-methylbenzene	-173.8	-171.9	429.9	439.1	3	1	165.3	206.4	243.0	273.7	319.7	350.7	393.3
127	1,2-divinyl-3-methoxybenzene	72.9	69.5	458.8	467.9	3	1	209.7	263.8	308.5	344.3	397.2	434.2	489.7
128	1,2-divinyl-4-methoxybenzene	69.1	65.7	469.7	478.8	3	1	202.2	254.9	299.4	335.5	389.5	427.8	485.7
129	1,2-divinyl-3-formylbenzene	112.7	114.1	447.7	447.7	1	1	191.4	240.8	283.2	317.6	368.3	403.1	453.7
130	1,2-divinyl-4-formylbenzene	100.8	102.2	453.4	453.4	1	1	188.7	237.6	279.6	313.9	365.2	401.0	453.3
131	1,2-divinyl-3-methylbenzene	193.3	194.2	432.3	441.5	3	1	192.1	242.1	284.7	319.6	372.2	409.6	466.3
132	1,2-divinyl-4-methylbenzene	188.2	189.1	443.3	452.4	3	1	181.0	231.6	275.6	311.8	366.5	405.4	464.2
133	1,3-divinyl-2-hydroxybenzene	45.1	40.9	429.0	429.0	1	1	186.4	233.4	271.9	302.6	347.9	379.7	427.7

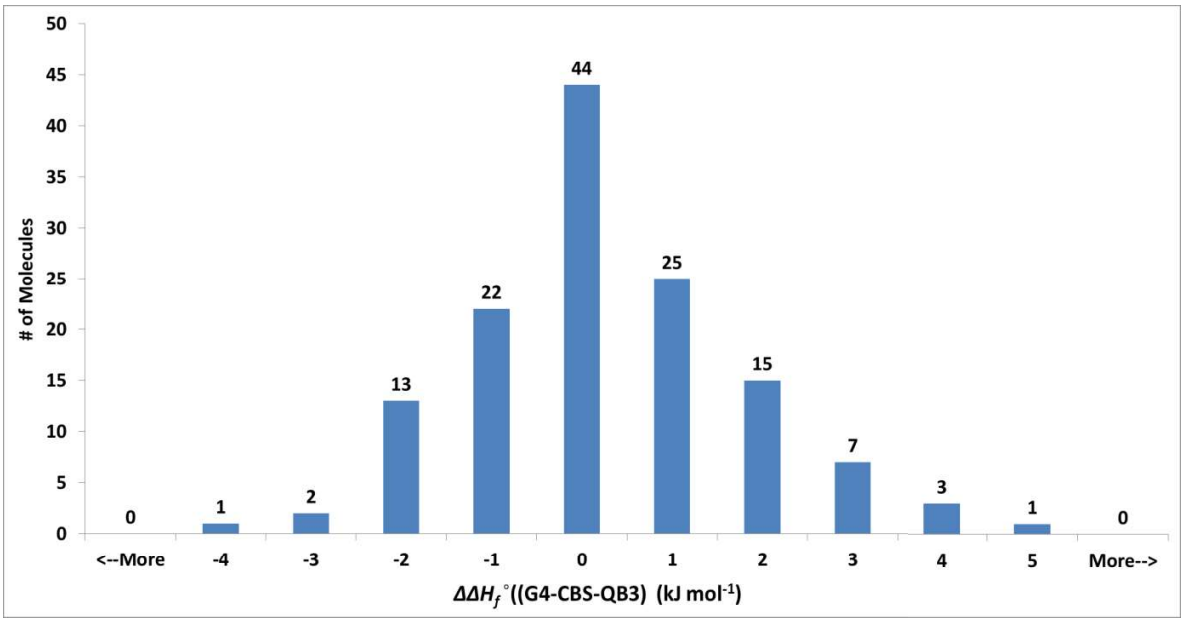

Figure A-2 Distribution of the differences between BAC-corrected CBS-QB3 and G4 standard enthalpies of formation, $\Delta\Delta_f H°$(G4-CBS-QB3).

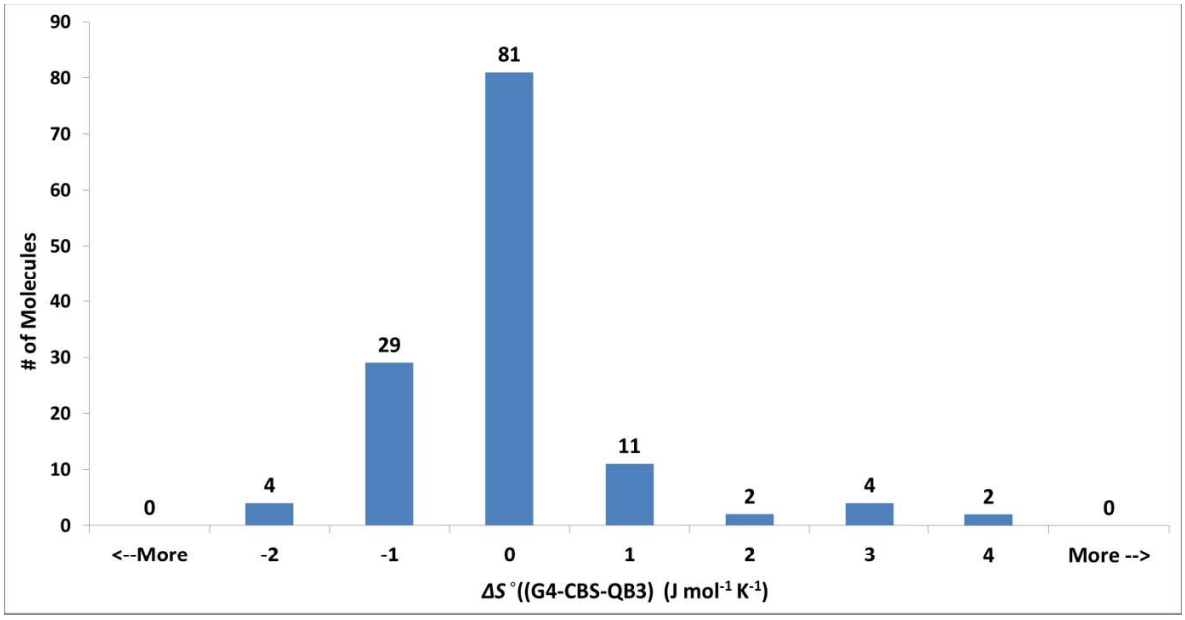

Figure A-3 Distribution of the differences between BAC-corrected CBS-QB3 and G4 entropies, ΔS°(G4-CBS-QB3).

A.4 Assignment of Preliminary GAVs and identification of NNIs

Preliminary GAV assignments based on benzene and six single substituted benzenes (phenol, anisole, benzaldehyde, styrene, toluene and ethyl benzene) are given in **Table A-4**. GA estimations for standard enthalpy of formations and entropies for some double substituted benzenes are given in **Table A-5**. The molecules given in **Table A-5** are double substituted benzenes for which significant deviations are noted between *ab initio* calculated and GAV predicted values using the preliminary GAVs only. NNI parameters identified from the differences given in **Table A-5** are given in **Table A-6**. **Table A-6** also lists the molecules from which initial NNI assignments are derived and the physical components of these NNIs.

Table A-4 Preliminary GAVs assignments.

GAVs	$\Delta_f H^\circ$ [kJ mol^{-1}]	S° [J mol^{-1} K^{-1}]	C_p [J mol^{-1} K^{-1}]						
			300 K	400 K	500 K	600 K	800 K	1000 K	1500 K
C_b-(H)	13.0	48.7	13.1	18.3	22.6	26.1	31.1	34.7	40.0
C_b-(O)	22.4	-32.3	11.0	11.9	14.8	17.8	22.5	25.0	27.3
O-(C_b)(C)	-118.8	24.9	21.4	24.4	24.7	24.0	22.4	21.6	20.8
C_b-(CO)	27.6	-33.2	16.8	18.3	20.3	22.2	24.8	26.6	26.9
C_b-(C_d)	27.8	-36.5	14.5	16.6	17.7	19.0	21.5	23.0	25.7
C_b-(C)	26.3	-34.7	11.9	14.7	17.3	19.5	22.6	24.4	26.4
C-(C_b)(C)$(H)_2$	-22.3	38.2	24.7	30.6	35.9	40.2	47.1	52.2	60.0

Table A-5 Comparison of *ab initio* standard enthalpy of formation ($\Delta_f H°$) and entropy (S°) reference data and predictions by preliminary GAVs for double substituted benzenes for which significant deviations are noted.

Mol #	Molecule Name	$\Delta_f H°$ [kJ mol^{-1}]			S° [J mol^{-1}K^{-1}]		
		Reference Data	Prediction with preliminary GAVs	Reference – GA predictions	Reference Data	Prediction with Preliminary GAVs	Reference – GA predictions
8	*o*-dihydroxybenzene	-275.8	-274.0	-1.8	343.1	349.3	-6.2
10	*p*-dihydroxybenzene	-266.1	-274.0	7.9	352.2	349.3	2.8
11	*o*-dimethoxybenzene	-215.3	-230.4	15.1	437.6	433.5	4.1
13	*p*-dimethoxybenzene	-223.4	-230.4	7.0	438.5	433.5	5.0
14	*o*-diformylbenzene	-136.4	-156.8	20.4	395.3	386.8	8.5
15	*m*-diformylbenzene	-152.4	-156.8	4.4	385.1	386.8	-1.7
16	*p*-diformylbenzene	-151.3	-156.8	5.5	389.0	386.8	2.2
17	*o*-divinylbenzene	222.2	213.8	8.4	406.1	407.1	-1.0
20	*o*-dimethylbenzene	18.8	16.4	2.4	375.3	380.7	-5.4
23	*o*-diethylbenzene	-20.4	-25.5	5.1	452.8	460.5	-7.7
26	*o*-methoxyphenol	-255.8	-252.2	-3.6	383.3	391.4	-8.2
28	*p*-methoxyphenol	-244.8	-252.2	7.4	395.5	391.4	4.1
29	*o*-formylphenol	-244.1	-215.4	-28.7	344.9	368.1	-23.1
31	*p*-formylphenol	-219.0	-215.4	-3.6	365.0	368.1	-3.1
32	*o*-vinylphenol	-27.8	-30.1	2.3	377.0	377.7	-0.7
41	*o*-formylanisole	-189.5	-193.6	4.1	407.3	410.1	-2.9
43	*p*-formylanisole	-198.6	-193.6	-5.0	411.4	410.1	1.2
44	*o*-vinylanisole	-5.9	-8.3	2.4	415.8	419.8	-4.0
53	*o*-vinylbenzaldehyde	39.5	28.5	11.0	394.3	396.4	-2.2
56	*o*-methylbenzaldehyde	-65.1	-70.2	5.1	381.2	383.7	-2.6
59	*o*-ethylbenzaldehyde	-85.8	-91.1	5.3	420.6	423.7	-3.0
62	*o*-methylstyrene	120.2	115.1	5.1	389.7	393.4	-3.7
65	*o*-ethylstyrene	98.9	94.1	4.8	425.7	433.3	-7.6
68	*o*-ethyltoluene	-1.0	-4.6	3.6	415.5	420.6	-5.1

Table A-6 Identified non-nearest neighbor interactions (NNIs) and their initial values identified from the differences given in **Table A-5** in the Supporting Information. The full list of molecules and their molecule numbers are given in **Figure A-1** of the Supporting Information.

NNI	Interacting substituents	$\Delta_f H^\circ$ [kJ mol^{-1}]	S° [J mol^{-1} K^{-1}]	C_p [J mol^{-1} K^{-1}]	Molecules used in identifying NNIs	Components of NNI
NNI1	*o*-OH+CHO	-28.7	-23.1	-4.3	29	HB[a], Mesomeric, Inductive
NNI2	*o*-CHO+CHO	20.4	8.5	0.7	14	HB, Mesomeric, Inductive
NNI3	*o*-OCH_3+OCH_3	15.1	4.1	1.0	11	Anomeric, Mesomeric, Inductive
NNI4	*o*-$CH=CH_2$+CHO	11.0	-2.2	-0.3	53	Steric, Inductive
NNI5	*o*-$CH=CH_2$+$CH=CH_2$	8.4	-1.0	-0.5	17	Steric, Inductive
NNI6	*p*-OH/OCH_3+OH/OCH_3	7.4	4.0	-0.7	10, 13, 28	Mesomeric, Inductive
NNI7	*p*-CHO+CHO	5.5	2.2	-2.5	16	Mesomeric, Inductive
NNI8	*o*-CH_3/CH_2CH_3+CHO	5.2	-2.8	-1.4	56, 59	Steric, Mesomeric, Inductive
NNI9	*o*-$CH=CH_2$+CH_3/CH_2CH_3	5.0	-5.7	0.1	62, 65	Steric
NNI10	*m*-CHO+CHO	4.4	-1.7	1.9	15	Inductive
NNI11	*p*-CHO+OH/OCH_3	-4.3	-1.0	2.0	31,43	Mesomeric, Inductive
NNI12	*o*-OCH_3+CHO	4.1	-2.9	-0.9	41	HB, Mesomeric, Inductive
NNI13	*o*-CH_3/CH_2CH_3+CH_3/CH_2CH_3	3.7	-6.1	-0.8	20, 23,68	Steric
NNI14	*o*-OH+OH/OCH_3	-2.7	-7.2	-0.7	8, 26	HB, Mesomeric, Inductive
NNI15	*o*-$CH=CH_2$+OH/OCH_3	2.4	-2.4	0.1	32, 44	Steric, Inductive

[a]HB: Hydrogen Bond

A.5 Physical interactions between substituents

In this section, results from NBO calculations and observations based on NBO results are given. These results and interpretations are crucial in understanding the physical interactions between substituents. **Table A-7** lists NNIs in which hydrogen bonds contribute to the overall interaction. In **Table A-8**, atomic charges calculated by NBO is given. In **Table A-9**, NNIs where mesomeric effects have a significant contribution to the resulting interaction are given.

Table A-7 NNIs in which hydrogen bonds (HB) contribute to the overall interaction.

NNI	Interaction	Hydrogen Bond (HB)	$d_{H..O}$ (pm)	Preliminary NNI	$E(2)_{HB}$[a]	Molecule[b]
NNI1	*o*-OH+ CHO	O-H...O=C	175	-28.7	-23.5	*o*-formylphenol
NNI2	*o*-CHO+ CHO	C-H...O=C	222	20.4	-6.4	*o*-diformylbenzene
NNI12	*o*-OCH_3+ CHO	C-H...O	240	4.1	-3.6	*o*-formylanisole
NNI14	*o*-OH+ OH/OCH_3	O-H...O	208	-2.7	-8.9	*o*-dihydroxybenzene

[a] Stabilization energy due to hydrogen bonding.
[b] The molecules used to calculate $E(2)_{HB}$.

Table A-8 Natural charges on carbons on the arene ring of benzene and single substituted benzenes.

Molecule	Average Charge on *o*- C atoms	Average Charge on *m*- C atoms	Charge on *p*- C atoms	Sum of charges on the 5 unsubstituted C atoms	Total charge – charge in benzene ring
C_6H_6	**Charge on C atoms in benzene is -0.235**			-1.175	0
C_6H_5-OH	-0.315	-0.194	-0.284	-1.304	+0.129
C_6H_5-OCH_3	-0.313	-0.198	-0.282	-1.303	+0.128
C_6H_5-CHO	-0.170	-0.251	-0.191	-1.032	-0.143
C_6H_5-$CH=CH_2$	-0.211	-0.228	-0.234	-1.113	-0.063
C_6H_5-CH_3	-0.238	-0.221	-0.250	-1.168	-0.007
C_6H_5-CH_2CH_3	-0.236	-0.222	-0.249	-1.165	-0.010

Table A-9 NNIs where mesomeric effects have a significant contribution to the resulting interaction.

NNI	Substitutents and position	Substituent 1	Substituent 2	Total effect of resonance
NNI1	OH, CHO (*ortho*)	+M effect	-M effect	Stabilizing
NNI2	CHO, CHO (*ortho*)	-M effect	-M effect	Destabilizing
NNI3	OCH_3, OCH_3 (*ortho*)	+M effect	+M effect	Destabilizing
NNI4	$CH=CH_2$, CHO (*ortho*)	Weak -M effect	-M effect	Destabilizing
NNI6	OH/OCH_3, OH/OCH_3 (*ortho*)	+M effect	+M effect	Destabilizing
NNI7	CHO, CHO (*ortho*)	-M effect	-M effect	Destabilizing
NNI11	CHO, OH/OCH_3 (*para*)	-M effect	+M effect	Stabilizing
NNI12	OCH_3, CHO (*ortho*)	+M effect	-M effect	Stabilizing
NNI14	OH+ OH/OCH_3 (*ortho*)	+M effect	+M effect	Destabilizing
NNI15	$CH=CH_2$,OH/OCH_3 (*ortho*)	Weak -M effect	+M effect	Destabilizing

A.6 Initial Simultaneous Optimization of GAVs and NNIs

GAVs and NNIs obtained from the initial simultaneous optimization of GAVs and NNIs are given in **Table A-10** and **Table A-11** respectively. Statistical analysis results are given for this linear regression in **Table A-12**.

Table A-10 GAV parameters obtained from simultaneous optimization of GAVs and NNIs.

GAVs	$\Delta_f H^\circ$	S°	C_p						
	[kJ mol^{-1}]	[J mol^{-1} K^{-1}]	300 K	400 K	500 K	600 K	800 K	1000 K	1500 K
C_b-(H)	13.7	48.5	13.3	18.4	22.7	26.2	31.3	34.9	40.1
C_b-(O)	24.0	-29.7	11.9	12.5	14.9	17.3	21.2	23.4	26.0
O-(C_b)(C)	-124.1	21.4	20.4	24.3	25.2	24.9	23.7	23.1	22.0
C_b-(CO)	21.5	-33.5	16.4	17.8	19.7	21.6	24.4	26.6	27.4
C_b-(C_d)	24.3	-35.0	12.4	14.8	16.3	17.9	20.8	22.5	25.6
C_b-(C)	23.6	-33.3	10.6	13.7	16.4	18.6	21.8	23.8	26.1
C-(C_b)(C)$(H)_2$	-20.6	38.6	24.9	30.7	35.9	40.4	47.3	52.3	60.1

Table A-11 Corrections for non-next neighbor interactions (NNIs) derived from simultaneous optimization of GAVs and NNIs based on G4 molecule set for the standard enthalpies of formation ($\Delta_f H^\circ$) and entropies (S°) at 298 K and heat capacities (C_p) at various temperatures for MAHs.[a]

NNI	Interaction	$\Delta_f H^\circ$	S°	C_p						
		[kJ mol^{-1}]	[J mol^{-1} K^{-1}]	300 K	400 K	500 K	600 K	800 K	1000 K	1500 K
NNI1	*o*-OH+CHO	-26.8	-21.2	-10.6	-9.2	-7.6	-6.1	-3.5	-1.5	1.8
NNI2	*o*-CHO+CHO	21.1	6.5	1.7	1.6	1.6	1.4	0.4	-0.8	-2.5
NNI3	Anomeric Effect	14.7	7.8	0.0	-3.4	-4.7	-5.0	-4.4	-3.7	-2.2
NNI4	*o*-$CH=CH_2$+CHO	12.1	-3.5	1.0	1.3	1.8	2.1	1.9	1.3	0.0
NNI5	*o*-$CH=CH_2$+$CH=CH_2$	8.0	-2.1	4.5	3.2	2.1	1.3	0.4	-0.1	-0.4
NNI6	*p*-OH/OCH_3+ OH/OCH_3	7.3	3.9	1.8	0.4	-0.8	-1.6	-2.3	-2.3	-1.7
NNI7	*p*-CHO+CHO	9.9	-0.7	1.7	1.3	0.9	0.6	0.1	-0.3	-0.9

NNI8	*o*-CH_3/CH_2CH_3+CHO	8.0	-2.6	4.1	3.1	2.0	1.1	0.0	-0.5	-0.9
NNI9	*o*-CH=CH_2+CH_3/CH_2CH_3	4.5	-5.9	5.8	5.7	5.0	4.2	3.0	2.2	1.1
NNI10	*m*-CHO+CHO	4.9	0.2	1.6	1.0	0.5	0.1	-0.4	-0.7	-0.8
NNI11	*p*-CHO+OH/OCH_3	-4.5	-0.7	-1.7	-1.1	-0.4	0.2	0.9	1.2	1.5
NNI12	*o*-OCH_3+CHO	7.9	-1.7	-2.6	0.3	2.7	3.9	4.2	3.3	1.3
NNI13	*o*-CH_3/CH_2CH_3+CH_3/CH_2CH_3	4.2	-6.6	3.5	2.9	2.5	2.3	2.1	1.9	1.4
NNI14	*o*-OH+OH/OCH_3	-3.1	-5.9	-2.5	-1.4	0.3	2.1	4.3	4.9	3.8
NNI15	*o*-CH=CH_2+OH/OCH_3	2.6	-3.4	2.9	3.0	2.8	2.6	2.2	1.9	1.2

Table A-12 Statistics for the simultaneous linear regression analysis of the GAVs and NNIs for the standard enthalpies of formation ($\Delta_f H^\circ$) and entropies (S°) at 298 K and heat capacities (C_p) at various temperatures for MAHs.[a]

	$\Delta_f H^\circ$	S°	C_p						
	[kJ mol^{-1}]	**[J mol^{-1} K^{-1}]**	**300 K**	**400 K**	**500 K**	**600 K**	**800 K**	**1000 K**	**1500 K**
F	30226	19383	11924	26272	48018	71884	110949	144609	306843
MAD	0.95	1.60	1.56	1.33	1.16	1.07	0.98	0.94	0.73
RMS	1.26	2.07	1.99	1.70	1.50	1.38	1.31	1.26	0.97
MAX	4.45	7.35	5.59	4.63	4.44	4.31	4.09	4.12	3.72
[a] F:Significance; **MAD:** mean average deviation ; **RMS:** root mean square ; **MAX:** maximum deviation.									

A.7 Test Set for GAV and NNI

Table A-13 lists 25 molecules in the test set. *Ab initio* data is collected at G4 for 10 of the 25 molecules in this test set, which are given in **boldface** in the table. For the other 15 molecules, the thermochemical data is collected at CBS-QB3. GA predictions are made with the GAVs and NNIs given in **Table A-10** and **Table A-11** respectively. GA estimates without NNI corrections (GAV) and with NNI corrections (GAV+NNI) are separately given in **Table A-13**.

Table A-13 *Ab initio* data and GA estimates for the molecules in the test set.

Test set for GAV and NNI	$\Delta_f H^\circ$ **[kJ mol^{-1}]**			S° **[J mol^{-1} K^{-1}]**			C_p **[300 K]**		
	Ab initio	**GAV**	**GAV+NNI**	***Ab initio***	**GAV**	**GAV+NNI**	***Ab initio***	**GAV**	**GAV+NNI**
1,3-divinyl-4-formylbenzene	**39.0**	**36.5**	**39.1**	**435.2**	**431.8**	**432.7**	**178.7**	**181.5**	**179.0**
1,4-divinyl-2-formylbenzene	**105.5**	**93.7**	**105.8**	**454.5**	**451.0**	**454.2**	**185.8**	**186.8**	**187.2**
1,3-dimethyl-2-hydroxybenzene	**-163.6**	**-161.7**	**-161.7**	**410.0**	**410.0**	**406.5**	**147.6**	**147.6**	**150.6**
1,3-dimethyl-5-hydroxybenzene	**-162.1**	**-161.7**	**-161.7**	**410.0**	**410.0**	**410.4**	**147.6**	**147.6**	**145.9**
1,4-dimethyl-2-hydroxybenzene	**-161.9**	**-161.7**	**-161.7**	**410.0**	**410.0**	**408.6**	**147.6**	**147.6**	**149.0**
1,2-diethyl-3-hydroxybenzene	**-199.4**	**-202.9**	**-198.8**	**487.3**	**480.7**	**474.4**	**197.5**	**201.0**	**202.8**
1,3-diethyl-6-hydroxybenzene	**-202.4**	**-202.9**	**-202.9**	**487.3**	**487.3**	**484.7**	**197.5**	**197.5**	**199.3**

1,4-diethyl-2-hydroxybenzene	**-203.8**	**-202.9**	**-202.9**	**487.3**	**487.3**	**485.9**	**197.5**	**197.5**	**199.0**
1-ethyl-2-hydroxy-3-formylbenzene	**-299.0**	**-269.8**	**-296.6**	**450.6**	**429.3**	**428.1**	**180.7**	**170.1**	**171.2**
1,3,5-trimethyl-2-hydroxybenzene	**-193.9**	**-194.7**	**-194.7**	**455.5**	**455.5**	**451.4**	**169.9**	**169.9**	**172.8**
1,2,3,4-Tetramethylbenzene	-36.5	-49.9	-37.4	453.7	472.8	453.0	174.5	168.9	179.4
1,2,3,4-Tetrahydroxybenzene	-637.3	-628.9	-630.8	393.2	403.3	389.5	166.6	172.8	167.0
1,2-dihydroxy-4,5-diformylbenzene	-504.8	-514.4	-505.4	442.6	441.9	441.1	188.2	187.0	182.9
1-methyl-2-hydroxy-3-methoxy-5-vinylbenzene	-223.5	-219.2	-222.3	485.6	492.9	487.0	204.2	207.4	204.9
1-methyl-3,4,5-trivinylbenzene	260.2	247.4	263.4	499.2	510.6	506.5	222.4	215.4	224.4
1-hydroxy-2-vinyl-4,5-diformylbenzene	-253.2	-270.6	-251.4	472.1	471.8	474.2	199.7	201.6	204.5
1-vinyl-2,4-dimethyl-3-ethylbenzene	45.5	28.6	41.4	506.3	524.0	505.0	215.3	209.3	222.1
1,3-dimethoxy-2-hydroxy-5-methylbenzene	-428.6	-442.0	-430.4	510.1	505.1	507.0	210.0	214.0	211.4
1,3,4-trihydroxy-2-methoxybenzene	-601.7	-607.9	-603.6	441.8	445.5	443.5	191.2	193.9	193.1
1,3-vinyl-2-hydroxy-4-methylbenzene	8.8	3.5	10.7	466.3	480.6	471.3	206.2	200.9	209.6
1-hydroxy-2-formyl-4-methyl-5-vinylbenzene	-203.8	-183.1	-205.3	443.6	469.9	442.9	189.2	193.5	188.7
1,2-dihydroxy-3-methoxy-5-ethylbenzene	-490.9	-483.7	-489.8	496.9	501.5	489.7	208.7	217.8	212.8
1,2-dihydroxy-3-methoxy-5,6-dimethylbenzene	-498.5	-496.1	-498.0	486.7	508.3	489.9	207.8	215.1	213.6
1-hydroxy-2,3-diformyl-4-methyl-6-vinylbenzene	-303.2	-303.6	-301.2	492.9	517.3	500.0	216.7	223.8	219.0
1,2,3,4,5-Pentahydroxybenzene	-813.0	-806.6	-804.3	420.0	431.3	415.6	189.5	196.0	189.4
*10 Molecules for which data is collected at G4 are given in boldface.									

A.8 Deviations between group additivity estimates and reference dataset

Deviations between group additivity estimates and reference dataset for enthalpy of formations ($\Delta_f H°$), entropies ($S°$) and heat capacities (C_p) are given in **Table A-14**. Numbering of the molecules is consistent with the list of molecules given in **Figure A-1**.

The distribution of the difference between reference and GA predicted enthalpies of formation is shown in **Figure A-4**. In **Figure A-5** and **Figure A-6**, similar histograms are presented for the difference distributions of the entropies (S°) and heat capacities (C_p) at 300 K.

Table A-14 Differences between group additivity estimates and *ab initio* calculated values for standard enthalpy of formation ($\Delta_f H°$), entropy ($S°$) and heat capacity (C_p) of the training set of MAHs. Standard enthalpies of formation ($\Delta_f H°$) are given in kJ mol^{-1}, whereas entropies ($S°$) and heat capacities (C_p) are in J mol^{-1} K^{-1}.

Group additivity predicted (GA) – *Ab initio* calculated values (AI)										
#	**Training and test set for GAVs/NNIs**	$\Delta_f H°$	$S°$	C_p						
		298 K	**298 K**	**300 K**	**400 K**	**500 K**	**600 K**	**800 K**	**1000 K**	**1500 K**
1	Benzene	-0.295	1.87	-2.288	-1.665	-1.229	-0.97	-0.666	-0.504	-0.287
2	Phenol (Hydroxybenzene)	-0.132	-0.373	0.316	0.242	0.169	0.126	0.042	-0.117	-0.166
3	Anisole (Methoxybenzene)	-0.898	0.146	0.144	-0.036	0.012	0.184	0.43	0.574	0.501
4	Benzaldehyde (Formylbenzene)	-1.138	0.958	0.017	0.011	0.16	0.285	0.527	0.487	0.459
5	Styrene (Vinylbenzene)	0.36	1.904	-1.466	-1.331	-1.116	-1.041	-0.848	-0.674	-0.424
6	Toluene (Methylbenzene)	-0.331	1.441	-1.165	-1.026	-0.861	-0.821	-0.709	-0.553	-0.42
7	EthylBenzene	-0.035	-0.06	-0.99	-0.616	-0.267	-0.089	0.058	0.145	0.131
8	*o*-dihydroxybenzene	-0.869	-1.942	0.864	0.676	0.496	0.486	0.632	0.921	0.98
9	*m*-dihydroxybenzene	0.031	-1.316	0.92	0.948	0.768	0.522	0.15	-0.031	-0.244
10	*p*-dihydroxybenzene	-0.105	-1.441	3.318	2.615	1.917	1.376	0.406	-0.211	-0.579
11	*o*-dimethoxybenzene	-1.503	1.816	-5.727	-3.029	-1.399	-0.643	-0.112	0.016	0.086
12	*m*-dimethoxybenzene	-0.901	-2.078	-0.524	-0.407	-0.047	0.339	0.826	1.152	1.089
13	*p*-dimethoxybenzene	-0.836	-2.503	2.374	2.66	2.503	2.093	1.281	0.772	0.254
14	*o*-diformylbenzene	-1.52	-2.731	-1.528	-1.234	-1.256	-1.557	-2.081	-2.009	-1.256
15	*m*-diformylbenzene	-1.647	1.931	0.665	0.586	0.552	0.599	0.556	0.55	0.389
16	*p*-diformylbenzene	2.173	-3.694	3.207	2.468	2.083	1.898	1.584	1.282	0.616
17	*o*-divinylbenzene	-1.611	-3.197	-0.521	1.079	1.851	2.229	2.335	2.071	1.396
18	*m*-divinylbenzene	1.016	1.638	-0.845	-0.997	-1.103	-1.012	-0.931	-0.745	-0.461
19	*p*-divinylbenzene	1.716	2.938	-0.945	-1.197	-1.303	-1.412	-1.531	-1.445	-0.961
20	*o*-dimethylbenzene	1.359	-0.216	-2.277	-1.369	-0.724	-0.243	0.228	0.492	0.493
21	*m*-dimethylbenzene	-0.567	0.912	-0.142	-0.386	-0.594	-0.671	-0.652	-0.703	-0.553
22	*p*-dimethylbenzene	-1.167	0.712	-0.142	-0.286	-0.494	-0.571	-0.652	-0.703	-0.553
23	*o*-diethylbenzene	-0.748	-0.716	0.671	1.149	0.964	0.82	0.461	0.188	-0.105
24	*m*-diethylbenzene	0.326	-1.489	0.206	0.332	0.494	0.692	0.782	0.894	0.85
25	*p*-diethylbenzene	-0.374	-2.189	0.506	0.632	0.694	0.792	0.882	0.894	0.55
26	*o*-methoxyphenol	0.065	0.477	1.292	1.899	1.638	1.045	-0.18	-0.888	-1.254
27	*m*-methoxyphenol	-0.335	-0.497	0.548	0.471	0.311	0.38	0.438	0.461	0.423
28	*p*-methoxyphenol	-0.47	-2.122	3.046	2.837	2.36	1.834	0.893	0.28	-0.213
29	*o*-formylphenol	0.379	0.257	-0.635	-0.508	-0.412	-0.231	-0.009	0.116	0.079
30	*m*-formylphenol	-0.875	2.916	-2.679	-1.782	-1.141	-0.819	-0.365	-0.126	-0.019
31	*p*-formylphenol	-1.808	0.553	2.132	1.942	1.844	1.721	1.598	1.453	1.069
32	*o*-vinylphenol	3.996	-3.774	3.361	3.652	3.336	2.796	1.725	1.028	0.255
33	*m*-vinylphenol	0.423	-0.339	0.937	0.575	0.282	0.055	-0.14	-0.288	-0.302
34	*p*-vinylphenol	0.223	0.261	1.137	0.575	0.182	-0.145	-0.54	-0.688	-0.602
35	*o*-methylphenol	0.732	1.198	-1.861	-1.019	-0.563	-0.325	-0.201	-0.167	-0.199
36	*m*-methylphenol	0.232	-0.902	1.339	0.881	0.437	0.275	-0.101	-0.267	-0.299
37	*p*-methylphenol	-2.168	-1.202	1.239	0.981	0.737	0.575	0.299	0.033	-0.199
38	*o*-ethylphenol	0.928	2.097	-2.387	-1.609	-1.069	-0.693	-0.434	-0.268	-0.147
39	*m*-ethylphenol	0.628	-2.203	1.713	1.391	1.231	1.007	0.766	0.632	0.353
40	*p*-ethylphenol	-1.672	-2.403	1.513	1.291	1.231	1.107	0.966	0.732	0.353
41	*o*-formylanisole	2.192	-0.043	-2.934	-2.852	-2.453	-2.092	-1.511	-1.112	-0.647
42	*m*-formylanisole	0.159	2.335	-3.251	-2.66	-2.098	-1.561	-0.477	0.065	0.448
43	*p*-formylanisole	-1.273	-3.227	1.56	1.164	0.887	0.88	1.286	1.644	1.636
44	*o*-vinylanisole	3.13	0.045	2.689	2.074	1.379	0.655	-0.287	-0.781	-0.879
45	*m*-vinylanisole	0.158	-2.02	0.066	-0.202	-0.175	-0.087	0.148	0.304	0.364

46	*p*-vinylanisole	-0.142	-0.02	0.566	-0.002	-0.275	-0.387	-0.352	-0.196	-0.036
47	*o*-methylanisole	0.566	7.017	-1.633	-2.697	-3.62	-3.966	-3.813	-3.275	-2.032
48	*m*-methylanisole	-0.734	0.117	1.167	0.703	0.58	0.534	0.587	0.625	0.468
49	*p*-methylanisole	-2.634	-0.783	0.267	-0.097	-0.02	0.234	0.387	0.425	0.368
50	*o*-ethylanisole	0.863	5.117	-1.059	-1.987	-2.726	-3.235	-3.546	-3.377	-2.28
51	*m*-ethylanisole	-0.337	-2.483	1.141	0.913	0.974	1.065	1.254	1.223	1.02
52	*p*-ethylanisole	-2.237	-0.383	1.341	1.113	1.174	1.265	1.454	1.423	1.02
53	*o*-vinylbenzaldehyde	0.539	0.222	0.111	-0.215	-0.493	-0.766	-0.967	-1.025	-0.728
54	*m*-vinylbenzaldehyde	-0.782	0.893	0.638	0.245	0.173	0.114	0.245	0.317	0.323
55	*p*-vinylbenzaldehyde	0.018	-2.107	0.438	0.245	0.173	0.114	0.145	0.217	0.023
56	*o*-methylbenzaldehyde	1.682	0.383	-2.052	-1.62	-1.442	-1.379	-1.333	-1.197	-0.727
57	*m*-methylbenzaldehyde	-0.073	0.529	0.94	0.65	0.428	0.434	0.484	0.438	0.326
58	*p*-methylbenzaldehyde	0.727	-2.97	0.74	0.45	0.328	0.334	0.384	0.338	0.226
59	*o*-ethylbenzaldehyde	1.778	-0.517	-1.678	-1.511	-1.348	-1.248	-1.267	-1.198	-0.876
60	*m*-ethylbenzaldehyde	0.123	0.529	1.814	1.46	1.322	1.366	1.351	1.336	0.978
61	*p*-ethylbenzaldehyde	0.823	1.629	1.514	1.36	1.322	1.366	1.451	1.336	0.878
62	*o*-methylstyrene	0.997	1.04	-1.32	-0.816	-0.494	-0.25	-0.026	-0.008	0
63	*m*-methylstyrene	0.625	1.575	-0.343	-0.692	-0.849	-0.892	-0.891	-0.824	-0.557
64	*p*-methylstyrene	0.625	1.675	-0.543	-0.792	-0.849	-0.992	-0.991	-0.924	-0.657
65	*o*-ethylstyrene	1.494	3.539	-0.446	-1.506	-1.7	-1.619	-1.159	-0.91	-0.448
66	*m*-ethylstyrene	0.921	-0.526	-0.469	-0.383	-0.355	-0.26	-0.125	-0.025	0.095
67	*p*-ethylstyrene	0.821	-0.426	-0.269	-0.282	-0.255	-0.26	-0.125	-0.125	-0.005
68	*o*-ethyltoluene	0.456	-1.916	1.197	1.04	0.97	0.889	0.895	0.79	0.544
69	*m*-ethyltoluene	-0.17	-0.089	0.032	0.023	0	0.06	0.115	0.096	-0.002
70	*p*-ethyltoluene	-0.77	-0.489	0.232	0.123	0.1	0.16	0.115	0.096	-0.002
71	1,2,3-Trihydroxybenzene	0.095	-1.311	-1.889	-2.089	-1.478	-0.653	0.623	1.159	1.325
72	1,2,4-Trihydroxybenzene	0.459	2.29	-2.835	-3.25	-2.957	-2.364	-0.904	-0.073	0.466
73	1,3,5-Trihydroxybenzene	0.493	0.441	-2.076	-0.945	-0.534	-0.482	-0.642	-0.744	-0.723
74	1,2,3-Trimethoxybenzene	-0.408	-0.715	2.002	0.678	-0.21	-0.67	-0.953	-0.942	-0.529
75	1,2,4-Trimethoxybenzene	0.759	2.667	-3.797	-2.533	-1.609	-1.234	-1.16	-1.086	-0.861
76	1,3,5-Trimethoxybenzene	0.296	1.499	-5.992	-4.977	-3.405	-2.007	0.022	0.93	1.378
77	1,2,3-Triformylbenzene	0.498	0.179	0.528	0.022	0.427	1.201	2.61	2.994	2.128
78	1,2,4-Triformylbenzene	-0.109	2.417	-0.437	-0.376	-0.634	-0.944	-1.425	-1.515	-1.099
79	1,3,5-Triformylbenzene	0.178	0.489	-1.042	-0.84	-0.755	-0.726	-0.679	-0.616	-0.499
80	1,2,3-Trivinylbenzene	-2.883	-2.598	1.123	1.389	0.918	0.4	0.018	-0.184	-0.083
81	1,2,4-Trivinylbenzene	-0.155	-1.563	0.3	1.213	1.663	1.858	1.752	1.501	0.96
82	1,3,5-Trivinylbenzene	1.472	1.172	-0.224	-0.663	-0.891	-0.884	-0.813	-0.615	-0.397
83	1,2,3-Trimethylbenzene	1.449	-5.372	4.511	3.487	3.013	2.834	2.765	2.637	2.005
84	1,2,4-Trimethylbenzene	0.724	-1.045	-1.154	-0.63	-0.257	0.006	0.285	0.442	0.46
85	1,3,5-Trimethylbenzene	-1.102	-0.017	0.781	0.153	-0.226	-0.522	-0.694	-0.752	-0.686
86	1,2,3-Triethylbenzene	-2.161	6.527	-4.867	-4.085	-3.505	-3.271	-3.035	-2.868	-2.241
87	1,3,5-Triethylbenzene	0.487	-2.319	1.303	1.381	1.456	1.473	1.605	1.543	0.968
88	1,2-hydroxy-3-formylbenzene	0.442	0.188	0.512	0.427	0.314	0.03	-0.519	-0.746	-0.675
89	1,2-hydroxy-4-formylbenzene	0.556	1.484	-2.221	-2.323	-2.129	-1.918	-1.412	-0.909	-0.186
90	1,2-hydroxy-3-methoxybenzene	0.929	-1.692	1.139	1.633	1.665	1.405	0.81	0.35	-0.108
91	1,2-hydroxy-4-methoxybenzene	0.193	1.109	-2.106	-2.328	-2.214	-1.705	-0.516	0.318	0.933
92	1,2-hydroxy-3-methylbenzene	0.395	1.529	-2.513	-1.584	-1.037	-0.664	-0.211	0.171	0.547
93	1,2-hydroxy-4-methylbenzene	-2.105	0.229	-1.513	-1.984	-1.737	-1.264	-0.311	0.471	0.947
94	1,2-hydroxy-6-methylbenzene	1.895	2.029	-1.613	-1.684	-1.637	-1.564	-1.111	-0.629	0.147
95	1,3-hydroxy-2-methylbenzene	1.995	-2.945	3.543	2.988	2.635	2.371	1.807	1.22	0.523
96	1,3-hydroxy-5-methoxybenzene	0.428	0.26	-2.348	-1.322	-0.891	-0.524	-0.154	-0.053	0.044
97	1,3-hydroxy-5-formylbenzene	-1.012	3.473	-1.876	-1.975	-1.743	-1.523	-1.057	-0.64	-0.298
98	1,3-hydroxy-5-ethylbenzene	0.891	-2.846	2.217	2.097	1.829	1.503	0.974	0.618	0.274
99	1-hydroxy-2-methoxy-3-formylbenzene	-4.145	-1.285	4.07	4.055	3.445	2.804	1.897	1.375	0.675
100	1-hydroxy-2-methoxy-4-formylbenzene	3.19	3.104	-0.193	0.399	0.814	0.84	-0.024	-1.018	-2.019

101	1-hydroxy-2-methoxy-5-formylbenzene	-1.41	-1.996	0.707	0.099	-0.286	-0.26	0.376	0.982	1.281
102	1-hydroxy-2-methoxy-6-formylbenzene	-3.177	1.566	1.396	0.975	0.228	-0.601	-2.487	-3.697	-3.807
103	1-hydroxy-2-methoxy-4-methylbenzene	-1.77	1.748	2.215	2.438	1.906	0.994	-0.323	-1.037	-1.286
104	1-hydroxy-2-methoxy-4-ethylbenzene	-1.474	-2.752	1.989	2.948	2.8	2.226	0.944	0.161	-0.335
105	1-hydroxy-2-formyl-4-ethylbenzene	-2.661	-1.172	0.762	0.741	0.749	0.75	0.914	0.865	0.698
106	1-hydroxy-3-formyl-4-ethylbenzene	-1.059	-1.86	0.526	0.096	-0.05	-0.252	-0.559	-0.712	-0.655
107	1-hydroxy-3-formyl-5-ethylbenzene	0.586	-1.814	-0.882	-0.133	0.221	0.462	0.659	0.723	0.599
108	1-hydroxy-2-vinyl-3-ethylbenzene	0.757	0.296	-2.342	-3.599	-4.302	-4.623	-4.451	-3.823	-2.427
109	1-hydroxy-3-vinyl-4-ethylbenzene	0.257	2.396	1.558	-0.099	-0.702	-0.823	-0.851	-0.723	-0.527
110	1-hydroxy-3-vinyl-5-ethylbenzene	-2.816	-1.969	1.634	1.324	1.044	0.836	0.583	0.361	0.216
111	1-hydroxy-2-methyl-4-ethylbenzene	-1.007	-0.432	-0.864	0.03	0.499	0.656	0.723	0.682	0.32
112	1-hydroxy-3-methyl-5-ethylbenzene	0.993	-3.632	2.036	1.63	1.199	0.956	0.523	0.382	0.12
113	1-hydroxy-3-ethyl-4-methylbenzene	-0.781	-3.759	3.701	3.047	2.568	2.185	1.603	1.177	0.665
114	1,3-methoxy-2-hydroxybenzene	1.56	-3.053	5.52	4.206	3.427	3.218	3.178	2.954	1.832
115	1,3-methoxy-5-ethylbenzene	-0.44	-2.207	1.473	1.842	2.115	2.42	2.65	2.601	1.908
116	1,3-methoxy-4-vinylbenzene	3.327	0.821	4.321	2.504	1.221	0.309	-0.491	-0.803	-0.79
117	1-methoxy-3-hydroxy-4-ethylbenzene	-1.574	1.374	1.045	0.72	0.672	0.661	0.762	0.81	0.641
118	1-methoxy-2-formyl-4-ethylbenzene	1.953	1.328	-1.137	-1.203	-0.992	-0.711	-0.387	-0.263	-0.028
119	1,2-formyl-4-methylbenzene	0.745	0.083	-1.985	-1.28	-1.129	-1.262	-1.823	-2.153	-1.78
120	1,2-formyl-3-methylbenzene	-2.401	1.994	3.204	3.035	2.841	2.879	3.158	3.107	2.257
121	1,3-formyl-5-ethylbenzene	1.114	-3.398	2.462	1.935	1.713	1.58	1.48	1.299	1.107
122	1,4-formyl-3-methylbenzene	-2.063	1.277	-2.77	-2.092	-1.449	-0.953	-0.159	0.233	0.483
123	1-formyl-3-methoxy-4-ethylbenzene	4.42	2.405	-0.554	-1.211	-2.237	-3.18	-4.053	-4.086	-3.134
124	1-formyl-3-methoxy-5-ethylbenzene	1.22	-2.495	-1.654	-1.311	-0.937	-0.38	0.447	1.014	1.166
125	1,2-formyl-4-methylbenzene	1.145	-0.76	0.195	0.106	-0.388	-1.008	-2.024	-2.259	-1.589
126	1,2-formyl-5-methylbenzene	1.145	-1.36	-0.505	-0.294	-0.288	-0.508	-1.024	-1.159	-0.789
127	1,2-vinyl-3-methoxybenzene	-0.041	2.244	-0.966	-2.616	-3.354	-3.575	-3.404	-2.835	-1.758
128	1,2-vinyl-4-methoxybenzene	-1.914	-4.621	1.91	2.308	2.592	2.784	2.831	2.649	1.885
129	1,2-vinyl-3-formylbenzene	-1.733	1.121	0.156	0.895	1.474	2.004	2.416	2.42	1.692
130	1,2-vinyl-4-formylbenzene	-1.754	-1.708	1.583	2.555	3.04	3.284	3.228	2.862	1.843
131	1,2-vinyl-3-methylbenzene	-0.774	3.539	-4.975	-4.105	-3.227	-2.58	-1.743	-1.163	-0.479
132	1,2-vinyl-4-methylbenzene	-1.347	-3.326	1.501	2.418	2.719	2.779	2.492	2.122	1.264
133	1,3-vinyl-2-hydroxybenzene	1.952	2.56	-3.118	-2.014	-0.751	0.125	0.743	0.758	0.418
134	1,3-vinyl-4-hydroxybenzene	-1.821	2.895	-0.441	-1.191	-1.605	-1.816	-1.723	-1.558	-1.039
135	1,4-vinyl-2-formylbenzene	1.194	-1.344	-0.268	-0.681	-0.98	-1.238	-1.449	-1.395	-0.965
136	1,3-methyl-2-hydroxybenzene	1.796	2.769	-2.338	-1.579	-0.995	-0.675	-0.444	-0.416	-0.431
137	1,3-methyl-5-hydroxybenzene	0.296	-1.131	2.362	1.521	0.905	0.425	-0.144	-0.316	-0.431
138	1,4-methyl-2-hydroxybenzene	0.096	0.669	-0.738	-0.279	-0.095	-0.075	-0.144	-0.316	-0.332
139	1,2-ethyl-3-hydroxybenzene	0.415	5.341	-1.425	-2.044	-2.538	-2.784	-2.931	-2.625	-1.584
140	1,3-ethyl-6-hydroxybenzene	-0.711	1.568	-1.09	-0.361	0.193	0.488	0.69	0.68	0.671
141	1,4-ethyl-2-hydroxybenzene	0.689	0.368	-0.79	-0.161	0.193	0.388	0.59	0.58	0.471
142	1-ethyl-2-hydroxy-3-formylbenzene	1.839	0.728	-0.638	-0.659	-0.651	-0.55	-0.386	-0.235	-0.102
143	1,3,5-methyl-2-hydroxybenzene	-0.639	3.04	-1.915	-1.44	-1.028	-0.826	-0.686	-0.666	-0.564

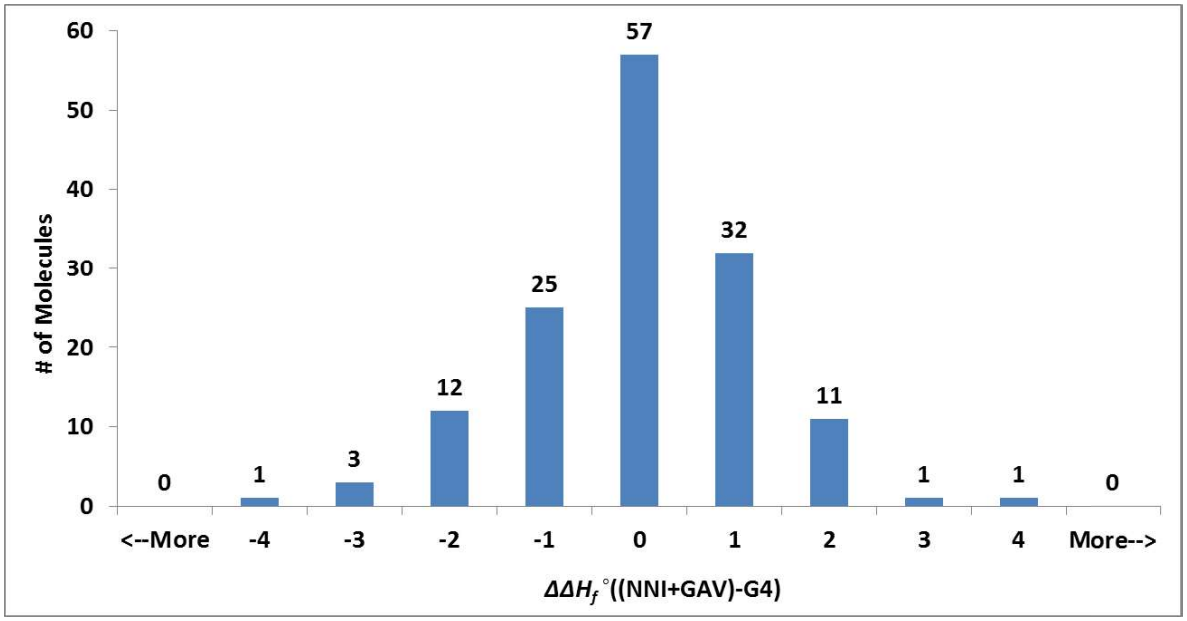

Figure A-4 Distribution of the differences between final GA estimates and G4 predictions for $\Delta_f H^\circ$ values of the molecules in the reference set, $\Delta\Delta_f H°$((NNI+GAV)-G4).

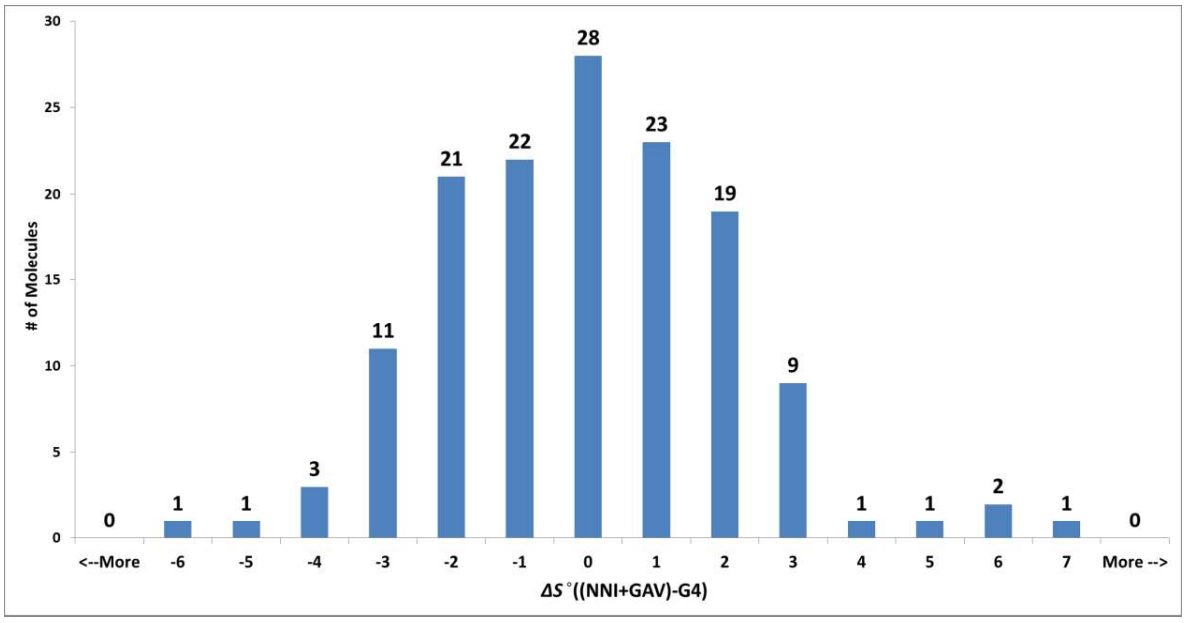

Figure A-5 Distribution of the differences between final GA estimates and G4 predictions for S° values of the molecules in the reference set, ΔS°((NNI+GAV)-G4).

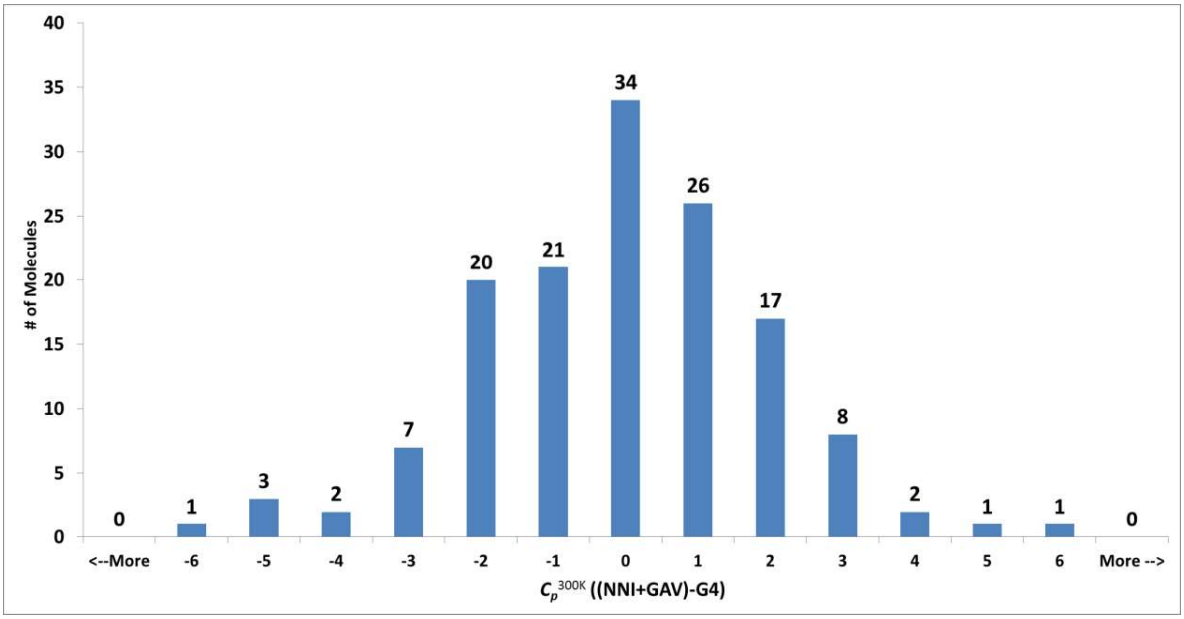

Figure A-6 Distribution of the differences between final GA estimates and G4 predictions for C_p values of the molecules in the reference set at 300 K, C_p^{300K} ((NNI+GAV)-G4).

A.9 Optimized Geometries

Optimized geometries for 133 MAHs used in the CBS-QB3 and G4 training sets are given in **Table A-15** and **Table A-16** respectively. The numbering and naming of the molecules is consistent with the list of molecules given in **Figure A-1**.

Benzene and six single substituted benzenes are given with their full names. However, in the names of multiple substituted benzenes, the substituent groups hydroxy (-OH), methoxy (-OCH_3), formyl (-C=O), vinyl (-CH=CH_2), methyl (-CH_3) and ethyl (-CH_2CH_3) are denoted as OH, MeO, For, Vin, Me and Et respectively. "D" represents double substitution and "T" represents triple substitution with the same substituent. In double substituted benzenes, the abbreviations with uppercase letters O-, M- and P- refer to two substituents being in *ortho*, *meta* and *para* position to each other.

Table A-15 Optimized geometries at the level of CBS-QB3.

1-Benzene

Standard orientation:

Center Number	Atomic Number	Atomic Type	Coordinates (Angstroms) X	Y	Z
1	6	0	0.000000	0.000000	1.393968
2	1	0	0.000000	0.000000	2.478342
3	6	0	0.000000	1.207192	0.696978
4	6	0	0.000000	1.207201	-0.696979
5	6	0	0.000000	0.000000	-1.393955
6	6	0	0.000000	-1.207201	-0.696979
7	6	0	0.000000	-1.207192	0.696978
8	1	0	0.000000	2.146352	1.239200
9	1	0	0.000000	2.146358	-1.239206
10	1	0	0.000000	0.000000	-2.478402
11	1	0	0.000000	-2.146358	-1.239206
12	1	0	0.000000	-2.146352	1.239200

2-Phenol

Standard orientation:

Center Number	Atomic Number	Atomic Type	Coordinates (Angstroms) X	Y	Z
1	6	0	-1.187021	-1.161773	0.000000
2	1	0	-2.126195	-1.704320	0.000000
3	6	0	0.021033	-1.854518	0.000000
4	6	0	1.218159	-1.138422	0.000000
5	6	0	1.215139	0.252081	0.000000
6	6	0	0.000000	0.940138	0.000000
7	6	0	-1.203255	0.231245	0.000000
8	1	0	0.030409	-2.937859	0.000000
9	1	0	2.165463	-1.666188	0.000000
10	1	0	2.137193	0.820457	0.000000
11	8	0	0.050459	2.306507	0.000000
12	1	0	-2.148135	0.767594	0.000000
13	1	0	-0.846735	2.655760	0.000000

3-Anisole

Standard orientation:

Center Number	Atomic Number	Atomic Type	Coordinates (Angstroms) X	Y	Z
1	6	0	0.472899	-1.838678	0.000000
2	1	0	1.199286	-2.644292	0.000000
3	6	0	-0.886241	-2.127783	0.000000
4	6	0	-1.805825	-1.075907	0.000000
5	6	0	-1.371098	0.241205	0.000000
6	6	0	0.000000	0.528220	0.000000
7	6	0	0.926746	-0.517830	0.000000
8	1	0	-1.228677	-3.155715	0.000000
9	1	0	-2.869962	-1.284721	0.000000
10	1	0	-2.069485	1.069368	0.000000
11	8	0	0.326367	1.853275	0.000000
12	1	0	1.990229	-0.320464	0.000000
13	6	0	1.699768	2.212120	0.000000
14	1	0	1.722965	3.300728	0.000000
15	1	0	2.213604	1.840406	0.893826
16	1	0	2.213604	1.840406	-0.893826

4-Benzaldehyde

Standard orientation:

Center Number	Atomic Number	Atomic Type	Coordinates (Angstroms) X	Y	Z
1	6	0	-0.742790	-1.723452	0.000000
2	1	0	-1.544437	-2.453750	0.000000
3	6	0	0.588429	-2.148677	0.000000
4	6	0	1.625249	-1.217129	0.000000
5	6	0	1.330221	0.142982	0.000000
6	6	0	0.000000	0.573935	0.000000
7	6	0	-1.037600	-0.367144	0.000000
8	1	0	0.816131	-3.208869	0.000000
9	1	0	2.656288	-1.551293	0.000000
10	1	0	2.130280	0.877050	0.000000
11	6	0	-0.304592	2.022999	0.000000
12	1	0	-2.060296	-0.008774	0.000000
13	8	0	-1.417901	2.495426	0.000000
14	1	0	0.591735	2.681144	0.000000

5-Styrene

Standard orientation:

Center Number	Atomic Number	Atomic Type	Coordinates (Angstroms) X	Y	Z
1	6	0	1.529939	-0.094056	0.015367
2	6	0	0.207228	0.342618	-0.221715
3	6	0	-0.822731	-0.624120	-0.299606
4	6	0	-0.517381	-1.971366	-0.105157
5	6	0	0.790525	-2.379005	0.148235
6	6	0	1.815651	-1.447112	0.198785
7	6	0	-0.081487	1.774457	-0.442146
8	6	0	0.409577	2.810394	0.250446
9	6	0	-2.266414	-0.225219	-0.530884
10	6	0	-2.966072	0.299285	0.735488
11	8	0	2.590554	0.761035	0.051995
12	1	0	-1.312935	-2.706777	-0.154253
13	1	0	1.012579	-3.430112	0.295334
14	1	0	2.844672	-1.737085	0.371626
15	1	0	-0.766903	1.998282	-1.256529
16	1	0	0.143092	3.828288	-0.008988
17	1	0	1.047959	2.681237	1.118495
18	1	0	2.289659	1.637802	-0.223085
19	1	0	-2.333438	0.532652	-1.318188
20	1	0	-2.809685	-1.097640	-0.904774
21	1	0	-4.007761	0.557235	0.524319
22	1	0	-2.956851	-0.457988	1.523642
23	1	0	-2.467836	1.190564	1.123557

6-Toluene

Standard orientation:

Center Number	Atomic Number	Atomic Type	Coordinates (Angstroms) X	Y	Z
1	6	0	0.193840	-1.200131	-0.008713
2	6	0	0.912338	0.000052	-0.011423
3	6	0	0.193779	1.200167	-0.008710
4	6	0	-1.199135	1.202924	0.002049
5	6	0	-1.901668	-0.000035	0.008339
6	6	0	-1.199048	-1.202971	0.002050
7	6	0	2.422451	0.000021	0.009198
8	1	0	2.828226	-0.882765	-0.490460
9	1	0	2.801687	-0.002903	1.037130
10	1	0	2.828189	0.885598	-0.485489
11	1	0	0.731767	2.143048	-0.017379
12	1	0	-1.735709	2.145482	0.001560
13	1	0	-2.985822	-0.000074	0.013706
14	1	0	-1.735572	-2.145558	0.001566
15	1	0	0.731884	-2.142985	-0.017383

7-EthylBenzene

Standard orientation:

Center Number	Atomic Number	Atomic Type	Coordinates (Angstroms) X	Y	Z
1	6	0	-0.271002	-1.200641	-0.183625
2	6	0	0.433467	-0.000375	-0.326698
3	6	0	-0.270397	1.200286	-0.184059
4	6	0	-1.635019	1.203655	0.095679
5	6	0	-2.322876	0.000408	0.237574
6	6	0	-1.635591	-1.203237	0.096098
7	6	0	1.923451	-0.000626	-0.591568
8	6	0	2.762357	0.000441	0.698285
9	1	0	2.185559	-0.878231	-1.191237
10	1	0	2.185369	0.875996	-1.192732
11	1	0	0.256158	2.142915	-0.298855
12	1	0	-2.162112	2.146018	0.197981
13	1	0	-3.385676	0.000538	0.451918
14	1	0	-2.163324	-2.145225	0.198662
15	1	0	0.255137	-2.143554	-0.298098
16	1	0	2.545568	0.883418	1.305422
17	1	0	2.545040	-0.881194	1.307190
18	1	0	3.831941	-0.000148	0.469636

8-O-DOH

Standard orientation:

Center Number	Atomic Number	Atomic Type	Coordinates (Angstroms) X	Y	Z
1	6	0	-1.909042	-0.659446	0.000000
2	6	0	-1.879883	0.731281	0.000000
3	6	0	-0.653511	1.399656	0.000000
4	6	0	0.529542	0.673874	0.000000

5	6	0	0.503904	-0.729631	0.000000
6	6	0	-0.719542	-1.388739	0.000000
7	8	0	1.665993	-1.440679	0.000000
8	1	0	-0.719495	-2.472073	0.000000
9	1	0	-2.857069	-1.184087	0.000000
10	1	0	-0.617828	2.485323	-0.000001
11	1	0	2.395799	-0.808184	0.000002
12	1	0	-2.801153	1.301116	0.000000
13	8	0	1.789849	1.231325	-0.000001
14	1	0	1.724203	2.190766	0.000007

9-M-DOH

Standard orientation:

Center Number	Atomic Number	Atomic Type	Coordinates (Angstroms) X	Y	Z
1	6	0	0.000000	0.000000	1.768752
2	1	0	0.000000	0.000000	2.852863
3	6	0	0.000000	1.211460	1.084555
4	6	0	0.000000	1.202605	-0.314181
5	6	0	0.000000	0.000000	-1.016796
6	6	0	0.000000	-1.202605	-0.314181
7	6	0	0.000000	-1.211460	1.084555
8	1	0	0.000000	2.151839	1.626375
9	8	0	0.000000	2.351347	-1.053013
10	1	0	0.000000	0.000000	-2.098696
11	8	0	0.000000	-2.351347	-1.053013
12	1	0	0.000000	-2.151839	1.626375
13	1	0	0.000000	-3.107634	-0.457465
14	1	0	0.000000	3.107634	-0.457465

10-P-DOH

Standard orientation:

Center Number	Atomic Number	Atomic Type	Coordinates (Angstroms) X	Y	Z
1	6	0	1.206566	0.695552	0.000000
2	1	0	2.151773	1.224691	0.000000
3	6	0	1.213525	-0.698400	0.000000
4	6	0	0.000099	-1.388347	0.000000
5	6	0	-1.206747	-0.695481	0.000000
6	6	0	-1.213755	0.698039	0.000000
7	6	0	0.000000	1.388247	0.000000
8	1	0	-2.151476	-1.225173	0.000000
9	8	0	-2.431515	1.329198	0.000000
10	1	0	0.006738	2.474488	0.000000
11	1	0	-2.291891	2.281128	0.000000
12	1	0	-0.007384	-2.474603	0.000000
13	8	0	2.431713	-1.328861	0.000000
14	1	0	2.292528	-2.280887	0.000000

11-O-DMeO

Standard orientation:

Center Number	Atomic Number	Atomic Type	Coordinates (Angstroms) X	Y	Z
1	6	0	2.381632	0.267786	0.000000
2	1	0	3.398658	0.642470	0.000000
3	6	0	2.132910	-1.093431	0.000000
4	6	0	0.813929	-1.563483	0.000000
5	6	0	-0.255023	-0.673995	0.000000
6	6	0	0.000000	0.720518	0.000000
7	6	0	1.314553	1.174257	0.000000
8	1	0	2.951392	-1.803566	0.000000
9	1	0	0.630557	-2.629537	0.000000
10	8	0	-1.569269	-1.029110	0.000000
11	8	0	-1.103407	1.517906	0.000000
12	1	0	1.520257	2.236182	0.000000
13	6	0	-0.912719	2.922967	0.000000
14	1	0	-1.911164	3.357347	0.000000
15	1	0	-0.373027	3.257532	0.893661
16	1	0	-0.373027	3.257532	-0.893661
17	6	0	-1.888726	-2.410610	0.000000
18	1	0	-2.976305	-2.462995	0.000000
19	1	0	-1.502630	-2.914691	-0.893673
20	1	0	-1.502630	-2.914691	0.893673

12-M-DMeO

Standard orientation:

Center	Atomic	Atomic	Coordinates (Angstroms)

Number	Number	Type	X	Y	Z
1	6	0	-0.545344	-2.021060	0.000000
2	1	0	-0.757395	-3.084499	0.000000
3	6	0	0.787835	-1.594929	0.000000
4	6	0	1.051018	-0.226095	0.000000
5	6	0	0.000000	0.703004	0.000000
6	6	0	-1.317116	0.255818	0.000000
7	6	0	-1.594933	-1.120435	0.000000
8	1	0	1.585865	-2.323654	0.000000
9	8	0	2.300097	0.324677	0.000000
10	1	0	0.258486	1.752269	0.000000
11	8	0	-2.404447	1.078097	0.000000
12	1	0	-2.627948	-1.443560	0.000000
13	6	0	-2.190978	2.482062	0.000000
14	1	0	-3.181879	2.933411	0.000000
15	1	0	-1.645661	2.805756	0.893611
16	1	0	-1.645661	2.805756	-0.893611
17	6	0	3.421604	-0.546153	0.000000
18	1	0	4.298968	0.098827	0.000000
19	1	0	3.438753	-1.179886	0.893740
20	1	0	3.438753	-1.179886	-0.893740

13-P-DMeO

Standard orientation:

Center Number	Atomic Number	Atomic Type	Coordinates (Angstroms) X	Y	Z
1	6	0	-1.208274	0.696533	0.000000
2	1	0	-2.131863	1.259952	0.000000
3	6	0	-1.215919	-0.702266	0.000000
4	6	0	-0.000133	-1.386476	0.000000
5	6	0	1.208290	-0.696889	0.000000
6	6	0	1.215859	0.701959	0.000000
7	6	0	0.000000	1.386209	0.000000
8	8	0	-2.344030	-1.478397	0.000000
9	1	0	2.131634	-1.260399	0.000000
10	8	0	2.343876	1.478330	0.000000
11	1	0	0.017640	2.469361	0.000000
12	6	0	3.604359	0.829486	0.000000
13	1	0	4.349577	1.623675	0.000000
14	1	0	3.740629	0.208900	0.893672
15	1	0	3.740629	0.208900	-0.893672
16	6	0	-3.604098	-0.828787	0.000000
17	1	0	-4.349735	-1.622582	0.000000
18	1	0	-3.740012	-0.208115	0.893669
19	1	0	-3.740012	-0.208115	-0.893669
20	1	0	-0.017758	-2.469656	0.000000

14-O-DFor

Standard orientation:

Center Number	Atomic Number	Atomic Type	Coordinates (Angstroms) X	Y	Z
1	6	0	2.393213	0.148331	0.000000
2	1	0	3.407051	0.532124	0.000000
3	6	0	2.165566	-1.226067	0.000000
4	6	0	0.859775	-1.704121	0.000000
5	6	0	-0.235053	-0.830853	0.000000
6	6	0	0.000000	0.565769	0.000000
7	6	0	1.317287	1.030024	0.000000
8	1	0	2.998390	-1.919531	0.000000
9	1	0	0.677694	-2.773940	0.000000
10	6	0	-1.573784	-1.480232	0.000000
11	6	0	-1.087223	1.600718	0.000000
12	1	0	1.471048	2.102269	0.000000
13	8	0	-0.841888	2.787103	0.000000
14	1	0	-2.118369	1.224342	0.000000
15	8	0	-2.653657	-0.936727	0.000000
16	1	0	-1.510147	-2.589684	0.000000

15-M-DFor

Standard orientation:

Center Number	Atomic Number	Atomic Type	Coordinates (Angstroms) X	Y	Z
1	6	0	-0.364094	-2.035840	0.000000
2	1	0	-0.506970	-3.110312	0.000000
3	6	0	0.917192	-1.502650	0.000000
4	6	0	1.103736	-0.110819	0.000000
5	6	0	0.000000	0.736292	0.000000
6	6	0	-1.293682	0.203533	0.000000
7	6	0	-1.468742	-1.182762	0.000000
8	1	0	1.794312	-2.139154	0.000000
9	6	0	2.475692	0.457146	0.000000
10	1	0	0.119504	1.815041	0.000000
11	6	0	-2.472163	1.104224	0.000000
12	1	0	-2.473926	-1.593194	0.000000

13	8	0	-2.410398	2.310915	0.000000
14	1	0	-3.453196	0.582440	0.000000
15	8	0	3.487564	-0.202983	0.000000
16	1	0	2.515311	1.566979	0.000000

16-P-DFor

Standard orientation:

Center Number	Atomic Number	Atomic Type	Coordinates (Angstroms) X	Y	Z
1	6	0	1.212187	-0.689889	0.000000
2	1	0	2.148800	-1.239244	0.000000
3	6	0	0.000002	-1.392097	0.000000
4	6	0	-1.214962	-0.696917	0.000000
5	6	0	-1.212235	0.689927	0.000000
6	6	0	0.000000	1.392093	0.000000
7	6	0	1.214994	0.696934	0.000000
8	6	0	0.007061	-2.877488	0.000000
9	1	0	-2.137695	-1.264560	0.000000
10	1	0	-2.148570	1.239094	0.000000
11	6	0	-0.007066	2.877461	0.000000
12	1	0	2.137732	1.264548	0.000000
13	8	0	0.985756	3.565617	0.000000
14	1	0	-1.019424	3.334902	0.000000
15	8	0	-0.985774	-3.565616	0.000000
16	1	0	1.019417	-3.334906	0.000000

17-O-DVin

Standard orientation:

Center Number	Atomic Number	Atomic Type	Coordinates (Angstroms) X	Y	Z
1	6	0	-0.691071	2.294826	0.089513
2	1	0	-1.233475	3.230362	0.167053
3	6	0	0.691294	2.294773	-0.089500
4	6	0	1.373128	1.088006	-0.177782
5	6	0	0.703115	-0.140905	-0.085624
6	6	0	-0.703134	-0.140860	0.085509
7	6	0	-1.373013	1.088125	0.177751
8	1	0	1.233789	3.230265	-0.166942
9	1	0	2.442550	1.088683	-0.353803
10	6	0	1.452745	-1.406581	-0.212210
11	6	0	-1.452782	-1.406501	0.211953
12	1	0	-2.442416	1.088934	0.353895
13	6	0	-2.705519	-1.613984	-0.200606
14	1	0	-0.925098	-2.229173	0.686179
15	1	0	-3.194044	-2.569219	-0.048454
16	1	0	-3.279405	-0.848570	-0.712178
17	6	0	2.705248	-1.614222	0.200941
18	1	0	0.925311	-2.229011	-0.687156
19	1	0	3.193886	-2.569385	0.048682
20	1	0	3.278836	-0.848949	0.713062

18-M-DVin

Standard orientation:

Center Number	Atomic Number	Atomic Type	Coordinates (Angstroms) X	Y	Z
1	6	0	-1.209443	1.219089	-0.008802
2	6	0	-0.000007	1.905432	-0.007644
3	6	0	1.209436	1.219101	-0.009086
4	6	0	1.228624	-0.183335	-0.012000
5	6	0	0.000006	-0.856671	-0.015980
6	6	0	-1.228618	-0.183346	-0.011755
7	6	0	2.470735	-0.973498	-0.011917
8	6	0	3.724662	-0.517798	0.037964
9	6	0	-2.470721	-0.973521	-0.011460
10	6	0	-3.724671	-0.517791	0.037571
11	1	0	-0.000012	2.989939	-0.008228
12	1	0	2.138218	1.776883	-0.012454
13	1	0	0.000011	-1.942764	-0.019911
14	1	0	-2.138232	1.776862	-0.011877
15	1	0	-2.320323	-2.050136	-0.053222
16	1	0	-4.564558	-1.201845	0.032228
17	1	0	-3.964244	0.538527	0.086456
18	1	0	2.320361	-2.050081	-0.054565
19	1	0	4.564558	-1.201838	0.032353
20	1	0	3.964205	0.538479	0.087881

19-P-DVin

Standard orientation:

Center	Atomic	Atomic	Coordinates (Angstroms)

Number	Number	Type	X	Y	Z
1	6	0	-0.691449	-0.993360	-0.000078
2	6	0	0.691455	-0.993357	-0.000156
3	6	0	1.422770	0.209359	-0.000112
4	6	0	0.694769	1.406455	-0.000023
5	6	0	-0.694770	1.406452	0.000066
6	6	0	-1.422768	0.209354	0.000040
7	6	0	2.890630	0.262625	-0.000164
8	6	0	3.744259	-0.765150	0.000272
9	6	0	-2.890627	0.262621	0.000118
10	6	0	-3.744267	-0.765146	-0.000009
11	1	0	1.215318	-1.942175	-0.000292
12	1	0	1.229440	2.350855	-0.000004
13	1	0	-1.229445	2.350850	0.000149
14	1	0	-1.215305	-1.942180	-0.000120
15	1	0	-3.304274	1.268830	0.000292
16	1	0	-4.814432	-0.597705	0.000068
17	1	0	-3.418889	-1.799350	-0.000197
18	1	0	3.304283	1.268832	-0.000574
19	1	0	4.814426	-0.597722	0.000180
20	1	0	3.418866	-1.799349	0.000763

20-O-DMe

Standard orientation:

Center Number	Atomic Number	Atomic Type	Coordinates (Angstroms) X	Y	Z
1	6	0	1.772795	1.479543	0.000058
2	1	0	1.586030	2.554839	0.000773
3	1	0	2.382750	1.246871	-0.879317
4	1	0	2.383360	1.245831	0.878714
5	6	0	0.477016	0.704861	0.000020
6	6	0	0.477019	-0.704863	0.000000
7	6	0	-0.745086	-1.381545	0.000048
8	6	0	-1.957241	-0.695184	0.000038
9	6	0	-1.957247	0.695178	-0.000043
10	6	0	-0.745091	1.381540	-0.000040
11	6	0	1.772811	-1.479531	-0.000064
12	1	0	-0.745082	-2.467068	0.000083
13	1	0	-2.892013	-1.244700	0.000097
14	1	0	-2.892019	1.244691	-0.000101
15	1	0	-0.745068	2.467064	-0.000116
16	1	0	1.586054	-2.554830	-0.001259
17	1	0	2.383543	-1.245441	-0.878504
18	1	0	2.382591	-1.247253	0.879536

21-M-DMe

Standard orientation:

Center Number	Atomic Number	Atomic Type	Coordinates (Angstroms) X	Y	Z
1	6	0	2.527294	-1.031028	0.008599
2	1	0	3.325333	-0.468055	-0.481054
3	1	0	2.435060	-1.995976	-0.495537
4	1	0	2.850175	-1.228976	1.036758
5	6	0	1.222994	-0.269509	-0.012948
6	6	0	0.000213	-0.947016	-0.000024
7	6	0	-1.222542	-0.270272	0.012929
8	6	0	-1.207647	1.127784	0.016512
9	6	0	-0.000424	1.820386	-0.000002
10	6	0	1.207433	1.128153	-0.016510
11	1	0	0.000465	-2.033792	-0.000051
12	6	0	-2.527128	-1.031305	-0.008580
13	1	0	-2.144928	1.674886	0.029915
14	1	0	-0.000604	2.905117	0.000007
15	1	0	2.144410	1.675724	-0.029877
16	1	0	-3.314883	-0.486366	0.517072
17	1	0	-2.871522	-1.192421	-1.036186
18	1	0	-2.424671	-2.013295	0.459095

22-P-DMe

Standard orientation:

Center Number	Atomic Number	Atomic Type	Coordinates (Angstroms) X	Y	Z
1	6	0	-0.696156	1.196074	-0.007848
2	6	0	-1.419453	0.000184	-0.013967
3	6	0	-0.695876	-1.195913	-0.007844
4	6	0	0.695993	-1.195856	0.007712
5	6	0	1.419450	0.000317	0.013876
6	6	0	0.696028	1.196130	0.007721
7	6	0	-2.929467	-0.000269	0.005185
8	6	0	2.929474	-0.000198	-0.004949
9	1	0	-3.311802	-0.012959	1.031984
10	1	0	-3.334526	-0.878237	-0.503822
11	1	0	-3.334675	0.889651	-0.482334

12	1	0	-1.228724	-2.141955	-0.013575
13	1	0	1.228904	-2.141870	0.013372
14	1	0	1.228826	2.142176	0.013388
15	1	0	-1.229022	2.142087	-0.013614
16	1	0	3.334458	0.894519	0.473846
17	1	0	3.334509	-0.873038	0.512892
18	1	0	3.312087	-0.023190	-1.031453

23-O-DEt

Standard orientation:

Center Number	Atomic Number	Atomic Type	Coordinates (Angstroms) X	Y	Z
1	6	0	1.237607	-1.283106	0.505094
2	1	0	1.237550	-2.292606	0.905527
3	6	0	2.449240	-0.647369	0.255384
4	6	0	2.449241	0.647368	-0.255384
5	6	0	1.237608	1.283106	-0.505094
6	6	0	0.010658	0.655735	-0.257556
7	6	0	0.010658	-0.655735	0.257556
8	1	0	3.383839	-1.158142	0.459102
9	1	0	3.383840	1.158141	-0.459102
10	1	0	1.237550	2.292606	-0.905527
11	6	0	-1.267930	1.431013	-0.513240
12	6	0	-1.267931	-1.431012	0.513240
13	1	0	-2.066751	0.760197	-0.838920
14	6	0	-1.742134	2.231745	0.713021
15	1	0	-1.097725	2.123471	-1.343557
16	1	0	-2.658628	2.785152	0.488732
17	1	0	-1.942943	1.575120	1.563737
18	1	0	-0.979991	2.950089	1.026094
19	6	0	-1.742134	-2.231745	-0.713021
20	1	0	-1.097725	-2.123471	1.343557
21	1	0	-2.066751	-0.760197	0.838920
22	1	0	-2.658629	-2.785152	-0.488732
23	1	0	-1.942944	-1.575120	-1.563737
24	1	0	-0.979992	-2.950089	-1.026094

24-M-DEt

Standard orientation:

Center Number	Atomic Number	Atomic Type	Coordinates (Angstroms) X	Y	Z
1	6	0	1.223165	0.137854	-0.336164
2	6	0	2.530461	-0.594020	-0.550794
3	6	0	1.207281	1.461275	0.115196
4	6	0	-0.000092	2.117552	0.338600
5	6	0	-1.207372	1.461121	0.115111
6	6	0	-1.223057	0.137720	-0.336313
7	6	0	0.000107	-0.502685	-0.556334
8	1	0	2.144915	1.982244	0.282350
9	1	0	-0.000169	3.147611	0.678699
10	1	0	-2.145064	1.981972	0.282274
11	6	0	-2.530198	-0.594415	-0.550977
12	1	0	0.000177	-1.527198	-0.920245
13	6	0	-3.024103	-1.323088	0.710999
14	1	0	-3.295168	0.116884	-0.878679
15	1	0	-2.411826	-1.319435	-1.362688
16	1	0	-3.969614	-1.839010	0.520657
17	1	0	-2.293939	-2.064960	1.045354
18	1	0	-3.180862	-0.619378	1.532866
19	6	0	3.023861	-1.323445	0.710939
20	1	0	2.412502	-1.318525	-1.363022
21	1	0	3.295485	0.117584	-0.877699
22	1	0	3.969753	-1.838774	0.520876
23	1	0	3.179658	-0.620293	1.533469
24	1	0	2.293836	-2.065943	1.044208

25-P-DEt

Standard orientation:

Center Number	Atomic Number	Atomic Type	Coordinates (Angstroms) X	Y	Z
1	6	0	0.676165	1.196843	0.165280
2	1	0	1.194653	2.142521	0.293039
3	6	0	1.378609	0.000014	0.336339
4	6	0	0.676165	-1.196821	0.165309
5	6	0	-0.676167	-1.196817	-0.165284
6	6	0	-1.378607	0.000015	-0.336341
7	6	0	-0.676167	1.196851	-0.165313
8	6	0	2.858055	0.000044	0.653505
9	1	0	1.194621	-2.142476	0.293096
10	1	0	-1.194636	-2.142471	-0.293039
11	6	0	-2.858058	-0.000015	-0.653504
12	1	0	-1.194625	2.142505	-0.293101
13	6	0	-3.743935	-0.000022	0.604465

14	1	0	-3.098587	0.876952	-1.263274
15	1	0	-3.098538	-0.877017	-1.263243
16	1	0	-4.804597	0.000121	0.337063
17	1	0	-3.549291	-0.882376	1.220036
18	1	0	-3.549083	0.882185	1.220178
19	1	0	3.098549	0.877093	1.263170
20	1	0	3.098567	-0.876876	1.263350
21	6	0	3.743937	-0.000070	-0.604460
22	1	0	4.804598	-0.000214	-0.337053
23	1	0	3.549071	-0.882321	-1.220104
24	1	0	3.549314	0.882239	-1.220101

26-O-OHMeO

Standard orientation:

Center Number	Atomic Number	Atomic Type	Coordinates (Angstroms) X	Y	Z
1	6	0	1.373579	0.237833	0.000000
2	1	0	2.056876	1.077237	0.000000
3	6	0	1.875683	-1.068058	0.000000
4	6	0	1.004399	-2.149951	0.000000
5	6	0	-0.376241	-1.941268	0.000000
6	6	0	-0.884138	-0.649979	0.000000
7	6	0	0.000000	0.446219	0.000000
8	1	0	2.947478	-1.226175	0.000000
9	1	0	1.391465	-3.162109	0.000000
10	1	0	-1.074945	-2.769234	0.000000
11	8	0	-2.229575	-0.441422	0.000000
12	8	0	-0.635350	1.665679	0.000000
13	1	0	-2.368873	0.514860	0.000000
14	6	0	0.160461	2.842342	0.000000
15	1	0	-0.536891	3.678492	0.000000
16	1	0	0.790916	2.895023	0.894134
17	1	0	0.790916	2.895023	-0.894134

27-M-OHMeO

Standard orientation:

Center Number	Atomic Number	Atomic Type	Coordinates (Angstroms) X	Y	Z
1	6	0	-0.829923	-0.350559	0.000000
2	8	0	-2.191085	-0.290447	0.000000
3	6	0	-0.278205	-1.640264	0.000000
4	6	0	1.098981	-1.789453	0.000000
5	6	0	1.947337	-0.680053	0.000000
6	6	0	1.387544	0.595209	0.000000
7	6	0	0.000000	0.769590	0.000000
8	1	0	-0.946079	-2.491868	0.000000
9	1	0	1.527471	-2.785382	0.000000
10	1	0	3.025212	-0.807302	0.000000
11	8	0	2.143808	1.734544	0.000000
12	1	0	-0.385546	1.779086	0.000000
13	1	0	3.075247	1.491779	0.000000
14	6	0	-2.814341	0.986099	0.000000
15	1	0	-3.885892	0.793088	0.000000
16	1	0	-2.550278	1.562205	0.893774
17	1	0	-2.550278	1.562205	-0.893774

28-P-OHMeO

Standard orientation:

Center Number	Atomic Number	Atomic Type	Coordinates (Angstroms) X	Y	Z
1	6	0	-1.295672	0.445505	0.000000
2	1	0	-2.132200	1.133940	0.000000
3	6	0	0.000000	0.969653	0.000000
4	6	0	1.088285	0.093525	0.000000
5	6	0	0.878756	-1.285176	0.000000
6	6	0	-0.411989	-1.804136	0.000000
7	6	0	-1.500767	-0.927476	0.000000
8	8	0	0.093244	2.335745	0.000000
9	1	0	2.103734	0.466215	0.000000
10	1	0	1.717999	-1.970036	0.000000
11	8	0	-0.554419	-3.168320	0.000000
12	1	0	-2.514270	-1.318589	0.000000
13	1	0	-1.491564	-3.386030	0.000000
14	6	0	1.385666	2.918460	0.000000
15	1	0	1.228067	3.996045	0.000000
16	1	0	1.955984	2.638467	0.893689
17	1	0	1.955984	2.638467	-0.893689

29-O-OHFor

Standard orientation:

Center Number	Atomic Number	Atomic Type	Coordinates (Angstroms) X	Y	Z
1	6	0	1.387903	0.873113	0.000000
2	1	0	1.744962	1.898380	0.000000
3	6	0	2.281603	-0.180762	0.000000
4	6	0	1.784725	-1.493157	0.000000
5	6	0	0.423241	-1.750380	0.000000
6	6	0	-0.489335	-0.687220	0.000000
7	6	0	0.000000	0.644646	0.000000
8	1	0	3.349247	-0.000629	0.000000
9	1	0	2.478420	-2.326769	0.000000
10	1	0	0.035969	-2.761741	0.000000
11	8	0	-1.799511	-0.960489	0.000000
12	6	0	-0.929509	1.762157	0.000000
13	1	0	-2.279976	-0.101640	0.000000
14	8	0	-2.151462	1.649497	0.000000
15	1	0	-0.472606	2.769960	0.000000

30-M-OHFor

Standard orientation:

Center Number	Atomic Number	Atomic Type	Coordinates (Angstroms) X	Y	Z
1	6	0	0.000000	0.805945	0.000000
2	6	0	0.897290	-0.267534	0.000000
3	6	0	0.427466	-1.582689	0.000000
4	6	0	-0.946034	-1.818830	0.000000
5	6	0	-1.842365	-0.757087	0.000000
6	6	0	-1.368502	0.561954	0.000000
7	6	0	2.354554	-0.003485	0.000000
8	8	0	2.856043	1.097252	0.000000
9	8	0	-2.300844	1.556176	0.000000
10	1	0	1.131130	-2.408023	0.000000
11	1	0	-1.324420	-2.834506	0.000000
12	1	0	-2.912700	-0.923574	0.000000
13	1	0	0.399164	1.815625	0.000000
14	1	0	-1.856121	2.410820	0.000000
15	1	0	2.986894	-0.917404	0.000000

31-P-OHFor

Standard orientation:

Center Number	Atomic Number	Atomic Type	Coordinates (Angstroms) X	Y	Z
1	6	0	-1.125080	0.195445	0.000000
2	1	0	-2.108295	0.652147	0.000000
3	6	0	0.000000	1.031141	0.000000
4	6	0	1.276325	0.455042	0.000000
5	6	0	1.437674	-0.921715	0.000000
6	6	0	0.306859	-1.744409	0.000000
7	6	0	-0.977307	-1.180848	0.000000
8	6	0	-0.157782	2.496487	0.000000
9	1	0	2.151613	1.097459	0.000000
10	1	0	2.418334	-1.380614	0.000000
11	8	0	0.513361	-3.087316	0.000000
12	1	0	-1.850499	-1.826907	0.000000
13	1	0	-0.334666	-3.544549	0.000000
14	8	0	-1.218514	3.081632	0.000000
15	1	0	0.800611	3.061081	0.000000

32-O-OHVin

Standard orientation:

Center Number	Atomic Number	Atomic Type	Coordinates (Angstroms) X	Y	Z
1	6	0	-0.672514	-1.470376	-0.055056
2	6	0	-2.009659	-1.117822	0.061130
3	6	0	-2.356178	0.232882	0.119081
4	6	0	-1.373279	1.210847	0.045292
5	6	0	-0.028211	0.852914	-0.059662
6	6	0	0.348872	-0.506913	-0.089869
7	8	0	0.873731	1.870932	-0.152451
8	6	0	1.748363	-0.952461	-0.186481
9	6	0	2.837843	-0.364848	0.326269
10	1	0	-2.774272	-1.884175	0.102035
11	1	0	-3.396135	0.526275	0.207517
12	1	0	-1.621431	2.265212	0.061324
13	1	0	-0.393631	-2.518067	-0.103278
14	1	0	1.887302	-1.889135	-0.722886
15	1	0	3.818324	-0.804652	0.188997
16	1	0	2.791778	0.526202	0.943196
17	1	0	1.726792	1.505539	-0.421522

33-M-OHVin

Standard orientation:

Center Number	Atomic Number	Atomic Type	Coordinates (Angstroms) X	Y	Z
1	6	0	-1.924454	0.668887	0.000040
2	6	0	-1.078546	1.769020	0.000038
3	6	0	0.305284	1.603983	-0.000004
4	6	0	0.869748	0.321683	-0.000038
5	6	0	0.009032	-0.787544	-0.000046
6	6	0	-1.371326	-0.616330	-0.000005
7	6	0	2.335478	0.190875	-0.000067
8	6	0	3.055907	-0.933274	0.000087
9	8	0	-2.243006	-1.668901	-0.000013
10	1	0	-1.502037	2.767104	0.000068
11	1	0	0.955299	2.471695	-0.000005
12	1	0	0.416909	-1.793791	-0.000101
13	1	0	-3.002013	0.776411	0.000068
14	1	0	-1.745311	-2.492980	-0.000044
15	1	0	2.869145	1.138515	-0.000221
16	1	0	4.138550	-0.899229	0.000046
17	1	0	2.606765	-1.920316	0.000269

34-P-OHVin

Standard orientation:

Center Number	Atomic Number	Atomic Type	Coordinates (Angstroms) X	Y	Z
1	6	0	1.267860	0.422454	0.000000
2	1	0	2.150033	1.054238	0.000000
3	6	0	0.000000	1.018952	0.000000
4	6	0	-1.115840	0.162396	0.000000
5	6	0	-0.973231	-1.214602	0.000000
6	6	0	0.303666	-1.786524	0.000000
7	6	0	1.426635	-0.959664	0.000000
8	6	0	-0.105219	2.484310	0.000000
9	1	0	-2.115656	0.580270	0.000000
10	1	0	-1.836436	-1.869085	0.000000
11	8	0	0.382816	-3.148959	0.000000
12	1	0	2.422434	-1.393693	0.000000
13	1	0	1.308585	-3.413263	0.000000
14	6	0	-1.215812	3.226906	0.000000
15	1	0	0.851489	3.002875	0.000000
16	1	0	-1.160253	4.308567	0.000000
17	1	0	-2.211078	2.796403	0.000000

35-O-OHMe

Standard orientation:

Center Number	Atomic Number	Atomic Type	Coordinates (Angstroms) X	Y	Z
1	8	0	-0.630816	2.074308	0.000000
2	1	0	0.031773	2.772523	0.000000
3	6	0	0.000000	0.857630	0.000000
4	6	0	-0.823089	-0.280549	0.000000
5	6	0	-0.202368	-1.528883	0.000000
6	6	0	1.186610	-1.661506	0.000000
7	6	0	1.982188	-0.521206	0.000000
8	6	0	1.388859	0.739629	0.000000
9	6	0	-2.320937	-0.123380	0.000000
10	1	0	-0.825613	-2.417502	0.000000
11	1	0	1.639005	-2.646140	0.000000
12	1	0	3.063055	-0.604581	0.000000
13	1	0	2.004914	1.634845	0.000000
14	1	0	-2.814590	-1.096782	0.000000
15	1	0	-2.659798	0.436385	0.876790
16	1	0	-2.659798	0.436385	-0.876790

36-M-OHMe

Standard orientation:

Center Number	Atomic Number	Atomic Type	Coordinates (Angstroms) X	Y	Z
1	8	0	-2.310372	-1.188444	0.001018
2	1	0	-3.107126	-0.648339	0.004897
3	6	0	-1.215127	-0.369322	0.000911
4	6	0	0.039257	-0.981051	-0.009837
5	6	0	1.204933	-0.215498	-0.012275
6	6	0	1.097901	1.181037	-0.008547
7	6	0	-0.153180	1.788847	0.002450
8	6	0	-1.316127	1.022525	0.007678
9	1	0	0.083391	-2.064393	-0.018685
10	6	0	2.557948	-0.886006	0.009711
11	1	0	1.995475	1.789645	-0.016323

12	1	0	-0.228988	2.870627	0.002883
13	1	0	-2.291608	1.500180	0.012448
14	1	0	3.313005	-0.273661	-0.488499
15	1	0	2.895926	-1.049919	1.038820
16	1	0	2.529276	-1.859782	-0.484233

37-P-OHMe

Standard orientation:

Center Number	Atomic Number	Atomic Type	Coordinates (Angstroms) X	Y	Z
1	6	0	-0.662266	-1.194082	-0.005945
2	6	0	-1.378766	0.010025	-0.006956
3	6	0	-0.645471	1.197040	-0.006101
4	6	0	0.748831	1.192433	-0.001050
5	6	0	1.440628	-0.017550	0.002220
6	6	0	0.725940	-1.217359	-0.001031
7	6	0	-2.889116	0.015746	0.008251
8	8	0	2.806878	-0.094239	0.005176
9	1	0	-3.299423	-0.680095	-0.729209
10	1	0	-3.284124	1.009159	-0.215134
11	1	0	-3.280559	-0.281709	0.987186
12	1	0	-1.167583	2.148498	-0.010766
13	1	0	1.295154	2.131655	-0.002703
14	1	0	1.273898	-2.151972	-0.002555
15	1	0	-1.202844	-2.135583	-0.010665
16	1	0	3.171781	0.796439	0.006116

38-O-OHEt

Standard orientation:

Center Number	Atomic Number	Atomic Type	Coordinates (Angstroms) X	Y	Z
1	6	0	-0.188440	0.897919	-0.105124
2	6	0	-1.545265	1.088784	0.153719
3	6	0	-2.401191	-0.006641	0.242754
4	6	0	-1.900403	-1.292647	0.071356
5	6	0	-0.541731	-1.468901	-0.189598
6	6	0	0.339978	-0.391593	-0.282902
7	6	0	1.814637	-0.588994	-0.548473
8	6	0	2.684358	-0.454904	0.713884
9	8	0	0.686618	1.950071	-0.200285
10	1	0	-1.930587	2.096517	0.284533
11	1	0	-3.454613	0.151504	0.444031
12	1	0	-2.558652	-2.150996	0.135730
13	1	0	-0.149252	-2.471256	-0.330412
14	1	0	1.962397	-1.579135	-0.990058
15	1	0	2.149177	0.143482	-1.288961
16	1	0	3.740175	-0.612479	0.475387
17	1	0	2.580551	0.540536	1.149970
18	1	0	2.393864	-1.190133	1.469268
19	1	0	0.202333	2.773246	-0.080904

39-M-OHEt

Standard orientation:

Center Number	Atomic Number	Atomic Type	Coordinates (Angstroms) X	Y	Z
1	6	0	-0.892351	1.800256	0.116164
2	1	0	-1.158587	2.842241	0.255512
3	6	0	-1.883405	0.825024	0.199069
4	6	0	-1.540259	-0.514787	0.012162
5	6	0	-0.216502	-0.868105	-0.253687
6	6	0	0.778082	0.106391	-0.335606
7	6	0	0.427402	1.449772	-0.148829
8	1	0	-2.913847	1.102103	0.402115
9	8	0	-2.458133	-1.526920	0.073380
10	1	0	0.017312	-1.916973	-0.399768
11	6	0	2.217615	-0.289814	-0.583296
12	1	0	1.189045	2.219070	-0.216953
13	6	0	2.995578	-0.560477	0.716263
14	1	0	2.245339	-1.184057	-1.213720
15	1	0	2.719370	0.504186	-1.145436
16	1	0	4.030209	-0.841974	0.500587
17	1	0	3.011147	0.326514	1.355110
18	1	0	2.534574	-1.371515	1.286066
19	1	0	-3.326455	-1.153797	0.256009

40-P-OHEt

Standard orientation:

Center Number	Atomic Number	Atomic Type	Coordinates (Angstroms) X	Y	Z

1	6	0	1.170435	-1.218122	-0.032980
2	1	0	1.711559	-2.153843	0.039998
3	6	0	1.877854	-0.020306	0.080682
4	6	0	1.196393	1.192677	-0.020533
5	6	0	-0.180816	1.200814	-0.231063
6	6	0	-0.908561	0.014167	-0.345035
7	6	0	-0.202753	-1.191056	-0.242728
8	8	0	3.228632	-0.098770	0.283654
9	1	0	1.740335	2.129927	0.059434
10	1	0	-0.694747	2.153603	-0.312594
11	6	0	-2.409862	0.028618	-0.534526
12	1	0	-0.738433	-2.130957	-0.334556
13	6	0	-3.189164	-0.012121	0.791403
14	1	0	-2.696737	0.925570	-1.093088
15	1	0	-2.706088	-0.825922	-1.151857
16	1	0	-4.268507	-0.002284	0.613384
17	1	0	-2.947598	-0.914318	1.359885
18	1	0	-2.940567	0.849093	1.417561
19	1	0	3.590577	0.791256	0.341276

41-O-MeOFor

Standard orientation:

Center Number	Atomic Number	Atomic Type	Coordinates (Angstroms) X	Y	Z
1	6	0	-0.746548	-0.254719	-0.000001
2	6	0	-1.581447	0.866762	-0.000003
3	6	0	-1.059446	2.152378	0.000000
4	6	0	0.324523	2.320803	0.000003
5	6	0	1.182720	1.223437	0.000002
6	6	0	0.654029	-0.071750	-0.000002
7	8	0	1.412783	-1.199446	-0.000008
8	6	0	2.830723	-1.079627	0.000002
9	6	0	-1.352706	-1.606774	0.000007
10	8	0	-2.549334	-1.805978	-0.000002
11	1	0	-2.650458	0.688360	-0.000002
12	1	0	-1.716658	3.013426	0.000000
13	1	0	0.749112	3.318711	0.000005
14	1	0	2.251802	1.384994	0.000000
15	1	0	3.211925	-2.099017	-0.000003
16	1	0	3.187071	-0.558915	-0.894808
17	1	0	3.187059	-0.558928	0.894824
18	1	0	-0.638525	-2.448290	0.000026

42-M-MeOFor

Standard orientation:

Center Number	Atomic Number	Atomic Type	Coordinates (Angstroms) X	Y	Z
1	6	0	-1.260493	0.100504	-0.000037
2	6	0	-0.001895	-0.518222	-0.000275
3	6	0	1.146911	0.266360	-0.000040
4	6	0	1.031085	1.667610	0.000073
5	6	0	-0.217357	2.270279	0.000080
6	6	0	-1.374405	1.489669	0.000179
7	8	0	2.417926	-0.216513	-0.000536
8	6	0	2.602952	-1.627862	0.000433
9	1	0	1.941427	2.255022	0.000008
10	6	0	-2.481923	-0.736939	-0.000133
11	8	0	-2.490383	-1.946874	0.000069
12	1	0	-0.288516	3.351822	0.000268
13	1	0	-2.355080	1.953214	0.000319
14	1	0	0.029268	-1.599379	-0.000616
15	1	0	3.680022	-1.784596	0.000272
16	1	0	2.168298	-2.087080	0.894580
17	1	0	2.167908	-2.088435	-0.892836
18	1	0	-3.432924	-0.161870	0.000054

43-P-MeOFor

Standard orientation:

Center Number	Atomic Number	Atomic Type	Coordinates (Angstroms) X	Y	Z
1	6	0	1.138566	-0.798239	0.000000
2	1	0	2.063262	-1.368033	0.000000
3	6	0	-0.082538	-1.473243	0.000000
4	6	0	-1.273795	-0.726766	0.000000
5	6	0	-1.236101	0.651435	0.000000
6	6	0	0.000000	1.323600	0.000000
7	6	0	1.193889	0.592508	0.000000
8	6	0	-0.117658	-2.946149	0.000000
9	1	0	-2.217144	-1.260020	0.000000
10	1	0	-2.141337	1.246214	0.000000
11	8	0	-0.072566	2.676815	0.000000

12	1	0	2.153226	1.091259	0.000000
13	6	0	1.134824	3.430791	0.000000
14	1	0	0.830209	4.475538	0.000000
15	1	0	1.732374	3.226995	0.894646
16	1	0	1.732374	3.226995	-0.894646
17	8	0	-1.125104	-3.618626	0.000000
18	1	0	0.885276	-3.428085	0.000000

44-O-MeOVin

Standard orientation:

Center Number	Atomic Number	Atomic Type	Coordinates (Angstroms) X	Y	Z
1	6	0	-1.383454	1.027455	0.049385
2	6	0	-0.737023	2.262393	0.049066
3	6	0	0.650382	2.328005	-0.019202
4	6	0	1.387616	1.150040	-0.084260
5	6	0	0.775598	-0.108052	-0.072998
6	6	0	-0.637747	-0.151823	-0.011355
7	6	0	1.541621	-1.362401	-0.139368
8	6	0	2.832281	-1.517503	0.167553
9	8	0	-1.195621	-1.397997	-0.007160
10	6	0	-2.609851	-1.517414	0.028123
11	1	0	-1.327231	3.170695	0.095176
12	1	0	1.154886	3.286867	-0.033571
13	1	0	2.467004	1.201612	-0.167664
14	1	0	-2.463113	0.993467	0.100653
15	1	0	-2.817448	-2.586124	0.010309
16	1	0	-3.026795	-1.084422	0.944089
17	1	0	-3.076087	-1.043717	-0.842956
18	1	0	0.974400	-2.230909	-0.455423
19	1	0	3.313504	-2.483370	0.070503
20	1	0	3.449313	-0.704322	0.534504

45-M-MeOVin

Standard orientation:

Center Number	Atomic Number	Atomic Type	Coordinates (Angstroms) X	Y	Z
1	6	0	-1.171578	1.620672	-0.000092
2	6	0	0.038303	2.294309	-0.000099
3	6	0	1.242840	1.590008	-0.000005
4	6	0	1.246366	0.191511	0.000120
5	6	0	0.015427	-0.490771	0.000168
6	6	0	-1.182781	0.217411	0.000017
7	6	0	2.538605	-0.512913	0.000182
8	6	0	2.753324	-1.830888	-0.000254
9	8	0	-2.420528	-0.356707	-0.000031
10	6	0	-2.512863	-1.773451	0.000029
11	1	0	0.046683	3.378529	-0.000143
12	1	0	2.185261	2.126173	-0.000087
13	1	0	0.008646	-1.571529	0.000437
14	1	0	-2.118923	2.145447	-0.000123
15	1	0	-3.577492	-2.001683	0.000036
16	1	0	-2.050761	-2.207336	-0.894011
17	1	0	-2.050707	-2.207271	0.894064
18	1	0	3.405596	0.143902	0.000601
19	1	0	3.760637	-2.229263	-0.000138
20	1	0	1.949425	-2.558635	-0.000780

46-P-MeOVin

Standard orientation:

Center Number	Atomic Number	Atomic Type	Coordinates (Angstroms) X	Y	Z
1	6	0	1.208492	0.651588	0.000000
2	1	0	2.135672	1.216140	0.000000
3	6	0	1.263989	-0.745878	0.000000
4	6	0	0.037764	-1.438651	0.000000
5	6	0	-1.168994	-0.766181	0.000000
6	6	0	-1.201235	0.636645	0.000000
7	6	0	0.000000	1.347221	0.000000
8	6	0	2.571039	-1.415907	0.000000
9	1	0	0.029697	-2.522311	0.000000
10	1	0	-2.111391	-1.300623	0.000000
11	8	0	-2.441154	1.200442	0.000000
12	1	0	0.010367	2.428810	0.000000
13	6	0	-2.540502	2.617329	0.000000
14	1	0	-3.605996	2.840982	0.000000
15	1	0	-2.079814	3.052360	0.893967
16	1	0	-2.079814	3.052360	-0.893967
17	6	0	2.819228	-2.728804	0.000000
18	1	0	3.422671	-0.738398	0.000000
19	1	0	3.836250	-3.101584	0.000000
20	1	0	2.032911	-3.475447	0.000000

47-O-MeOMe

Standard orientation:

Center Number	Atomic Number	Atomic Type	Coordinates (Angstroms) X	Y	Z
1	6	0	1.102216	-2.113959	0.000000
2	1	0	1.522410	-3.113147	0.000000
3	6	0	1.931354	-1.001057	0.000000
4	6	0	1.385547	0.284280	0.000000
5	6	0	0.000000	0.449256	0.000000
6	6	0	-0.858735	-0.668291	0.000000
7	6	0	-0.282836	-1.935245	0.000000
8	1	0	3.009088	-1.119926	0.000000
9	1	0	2.044580	1.142088	0.000000
10	8	0	-0.628148	1.664289	0.000000
11	6	0	-2.351352	-0.467900	0.000000
12	1	0	-0.935834	-2.802230	0.000000
13	1	0	-2.871299	-1.427590	0.000000
14	1	0	-2.674205	0.101643	0.876417
15	1	0	-2.674205	0.101643	-0.876417
16	6	0	0.165137	2.840849	0.000000
17	1	0	-0.536612	3.673586	0.000000
18	1	0	0.796636	2.901012	0.893628
19	1	0	0.796636	2.901012	-0.893628

48-M-MeOMe

Standard orientation:

Center Number	Atomic Number	Atomic Type	Coordinates (Angstroms) X	Y	Z
1	6	0	1.669409	1.103883	-0.000001
2	6	0	0.485609	1.826550	0.000000
3	6	0	-0.754749	1.182807	0.000001
4	6	0	-0.790158	-0.211911	0.000000
5	6	0	0.406434	-0.941376	-0.000002
6	6	0	1.639339	-0.299747	-0.000002
7	8	0	-1.931959	-0.960380	0.000000
8	6	0	-3.180834	-0.285818	0.000001
9	6	0	2.924197	-1.093339	0.000002
10	1	0	0.515617	2.910799	0.000001
11	1	0	-1.663508	1.769101	0.000001
12	1	0	0.339949	-2.023498	-0.000004
13	1	0	2.622187	1.622638	-0.000002
14	1	0	3.530944	-0.861388	0.880819
15	1	0	2.729727	-2.167367	-0.000055
16	1	0	3.531001	-0.861304	-0.880753
17	1	0	-3.940753	-1.065740	0.000001
18	1	0	-3.302487	0.336754	0.893716
19	1	0	-3.302488	0.336754	-0.893715

49-P-MeOMe

Standard orientation:

Center Number	Atomic Number	Atomic Type	Coordinates (Angstroms) X	Y	Z
1	6	0	-1.272300	1.183648	-0.000014
2	6	0	0.099169	1.376909	-0.000003
3	6	0	0.966080	0.276500	0.000003
4	6	0	0.431928	-1.011733	-0.000005
5	6	0	-0.955330	-1.184545	-0.000016
6	6	0	-1.832279	-0.103178	-0.000017
7	8	0	2.300013	0.570675	0.000010
8	6	0	3.226578	-0.503993	0.000006
9	6	0	-3.330014	-0.295633	0.000022
10	1	0	0.529149	2.371403	-0.000005
11	1	0	1.072824	-1.883215	-0.000009
12	1	0	-1.353581	-2.194320	-0.000027
13	1	0	-1.926058	2.050550	-0.000022
14	1	0	-3.792338	0.161859	-0.880595
15	1	0	-3.593560	-1.355402	-0.000470
16	1	0	-3.792180	0.160989	0.881177
17	1	0	4.214568	-0.046050	0.000011
18	1	0	3.119039	-1.129536	0.893710
19	1	0	3.119042	-1.129526	-0.893705

50-O-MeOEt

Standard orientation:

Center Number	Atomic Number	Atomic Type	Coordinates (Angstroms) X	Y	Z
1	6	0	-1.303237	1.141278	0.168279

2	1	0	-1.408375	2.208190	0.312286
3	6	0	-2.433066	0.324931	0.244777
4	6	0	-2.320248	-1.046064	0.059926
5	6	0	-1.065240	-1.597922	-0.203205
6	6	0	0.082814	-0.813650	-0.283376
7	6	0	-0.053509	0.576660	-0.091846
8	1	0	-3.398996	0.773674	0.448036
9	1	0	-3.195375	-1.682885	0.114892
10	1	0	-0.971822	-2.668778	-0.355572
11	6	0	1.439204	-1.424816	-0.551044
12	8	0	1.105281	1.300057	-0.183327
13	1	0	1.976573	-0.808063	-1.276880
14	6	0	2.302340	-1.572941	0.714130
15	1	0	1.295326	-2.407567	-1.010224
16	1	0	3.268547	-2.025963	0.473553
17	1	0	2.488638	-0.598743	1.170102
18	1	0	1.806152	-2.206302	1.454579
19	6	0	1.042706	2.710090	-0.035031
20	1	0	2.063764	3.068104	-0.158110
21	1	0	0.404926	3.167287	-0.799881
22	1	0	0.677801	2.995197	0.958175

51-M-MeOEt

Standard orientation:

Center Number	Atomic Number	Atomic Type	Coordinates (Angstroms) X	Y	Z
1	6	0	1.075742	1.450183	-0.128455
2	6	0	-0.186743	1.976871	0.108984
3	6	0	-1.315490	1.155927	0.145469
4	6	0	-1.160813	-0.216446	-0.062550
5	6	0	0.112688	-0.746285	-0.301775
6	6	0	1.237460	0.072449	-0.336453
7	8	0	-2.182643	-1.122047	-0.056657
8	6	0	-3.501747	-0.651078	0.173873
9	6	0	2.612588	-0.520288	-0.556301
10	6	0	3.326538	-0.880583	0.758109
11	1	0	-0.306136	3.043645	0.264661
12	1	0	-2.288848	1.590240	0.328486
13	1	0	0.195459	-1.815356	-0.464593
14	1	0	1.940294	2.104781	-0.159337
15	1	0	2.526875	-1.416664	-1.178339
16	1	0	3.227278	0.191199	-1.117169
17	1	0	4.316562	-1.302254	0.562192
18	1	0	3.452864	0.002376	1.390265
19	1	0	2.750391	-1.615509	1.326447
20	1	0	-4.142815	-1.530442	0.134643
21	1	0	-3.595363	-0.180042	1.159040
22	1	0	-3.816758	0.059892	-0.598451

52-P-MeOEt

Standard orientation:

Center Number	Atomic Number	Atomic Type	Coordinates (Angstroms) X	Y	Z
1	6	0	-0.583206	1.400793	-0.043343
2	1	0	-1.035972	2.380284	0.054071
3	6	0	-1.414836	0.275568	0.001190
4	6	0	-0.852625	-0.995194	-0.132024
5	6	0	0.527279	-1.124299	-0.304544
6	6	0	1.371670	-0.016125	-0.348397
7	6	0	0.784050	1.250231	-0.215248
8	8	0	-2.746740	0.525894	0.171252
9	1	0	-1.468983	-1.883981	-0.108894
10	1	0	0.947842	-2.119615	-0.411659
11	6	0	2.869508	-0.170978	-0.496589
12	1	0	1.410894	2.136020	-0.252718
13	6	0	3.610512	-0.218917	0.850912
14	1	0	3.086070	-1.085025	-1.058970
15	1	0	3.263408	0.658328	-1.093715
16	1	0	4.688940	-0.328015	0.702812
17	1	0	3.438344	0.695217	1.425573
18	1	0	3.264037	-1.060234	1.457245
19	6	0	-3.638674	-0.576719	0.221851
20	1	0	-4.631029	-0.151197	0.363155
21	1	0	-3.622538	-1.151956	-0.711075
22	1	0	-3.409159	-1.243133	1.061317

53-O-ForVin

Standard orientation:

Center Number	Atomic Number	Atomic Type	Coordinates (Angstroms) X	Y	Z
1	6	0	-0.811327	-1.470026	-0.133265
2	6	0	-2.150484	-1.107608	-0.044585
3	6	0	-2.511114	0.233939	0.069679
4	6	0	-1.512052	1.196123	0.086275

5	6	0	-0.156262	0.848465	0.002411
6	6	0	0.218094	-0.517746	-0.097116
7	6	0	0.795971	1.984682	0.034143
8	8	0	2.004415	1.938752	-0.020446
9	6	0	1.627427	-0.943047	-0.181136
10	6	0	2.091916	-2.125019	0.233405
11	1	0	-2.915818	-1.875178	-0.077122
12	1	0	-3.553683	0.521613	0.134524
13	1	0	-1.774521	2.246413	0.167280
14	1	0	-0.553008	-2.514439	-0.258843
15	1	0	2.321639	-0.212404	-0.573790
16	1	0	3.141891	-2.372625	0.132346
17	1	0	1.461793	-2.870690	0.706514
18	1	0	0.283376	2.968720	0.113790

54-M-ForVin

Standard orientation:

Center Number	Atomic Number	Atomic Type	Coordinates (Angstroms) X	Y	Z
1	6	0	-1.075329	1.619013	-0.000001
2	6	0	0.166028	2.248553	0.000004
3	6	0	1.327650	1.485003	0.000005
4	6	0	1.236328	0.088451	0.000001
5	6	0	-0.012123	-0.535079	-0.000004
6	6	0	-1.191193	0.217364	-0.000004
7	6	0	2.472906	-0.729482	0.000000
8	8	0	2.502109	-1.938237	-0.000003
9	6	0	-2.533896	-0.387648	-0.000008
10	6	0	-2.832615	-1.688359	0.000010
11	1	0	0.222792	3.330920	0.000006
12	1	0	2.302718	1.961702	0.000008
13	1	0	-0.032660	-1.618243	-0.000008
14	1	0	-1.978731	2.220296	-0.000002
15	1	0	-3.353189	0.327704	-0.000027
16	1	0	-3.863550	-2.020567	0.000005
17	1	0	-2.075459	-2.464223	0.000032
18	1	0	3.414673	-0.138589	0.000002

55-P-ForVin

Standard orientation:

Center Number	Atomic Number	Atomic Type	Coordinates (Angstroms) X	Y	Z
1	6	0	0.650897	1.413059	-0.000005
2	6	0	-0.738169	1.401600	0.000030
3	6	0	-1.432231	0.189694	0.000022
4	6	0	-0.710439	-1.013679	-0.000026
5	6	0	0.671384	-0.999980	-0.000066
6	6	0	1.383821	0.216062	-0.000053
7	6	0	-2.909996	0.179353	0.000078
8	8	0	-3.594677	-0.818780	-0.000018
9	6	0	2.851962	0.285010	-0.000066
10	6	0	3.710491	-0.738104	0.000099
11	1	0	-1.290297	2.336387	0.000058
12	1	0	-1.262999	-1.945801	-0.000034
13	1	0	1.209824	-1.939936	-0.000124
14	1	0	1.182910	2.358301	0.000004
15	1	0	3.258027	1.293751	-0.000191
16	1	0	4.779561	-0.564436	0.000099
17	1	0	3.391625	-1.774084	0.000277
18	1	0	-3.377555	1.187971	-0.000022

56-O-ForMe

Standard orientation:

Center Number	Atomic Number	Atomic Type	Coordinates (Angstroms) X	Y	Z
1	6	0	1.852561	-1.457674	0.000000
2	1	0	2.561830	-2.278313	0.000000
3	6	0	2.307626	-0.141808	0.000000
4	6	0	1.377028	0.888186	0.000000
5	6	0	0.000000	0.626423	0.000000
6	6	0	-0.469019	-0.709377	0.000000
7	6	0	0.485410	-1.729075	0.000000
8	1	0	3.369254	0.075034	0.000000
9	1	0	1.711132	1.921349	0.000000
10	6	0	-0.894212	1.804932	0.000000
11	6	0	-1.934680	-1.059186	0.000000
12	1	0	0.148329	-2.760238	0.000000
13	1	0	-2.064714	-2.143230	0.000000
14	1	0	-2.444297	-0.641185	0.870772
15	1	0	-2.444297	-0.641185	-0.870772
16	8	0	-2.105200	1.795139	0.000000
17	1	0	-0.343923	2.772126	0.000000

57-M-ForMe

Standard orientation:

Center Number	Atomic Number	Atomic Type	Coordinates (Angstroms) X	Y	Z
1	6	0	1.785887	-0.821456	0.000000
2	6	0	0.868670	-1.867704	0.000000
3	6	0	-0.496235	-1.592800	0.000000
4	6	0	-0.933214	-0.266703	0.000000
5	6	0	0.000000	0.778304	0.000000
6	6	0	1.366853	0.518803	0.000000
7	6	0	-2.383397	0.030300	0.000000
8	8	0	-2.863985	1.140547	0.000000
9	6	0	2.379834	1.638244	0.000000
10	1	0	1.219116	-2.893820	0.000000
11	1	0	-1.221895	-2.400138	0.000000
12	1	0	-0.374185	1.796243	0.000000
13	1	0	2.848517	-1.044598	0.000000
14	1	0	3.027081	1.585936	0.880897
15	1	0	3.027081	1.585936	-0.880897
16	1	0	1.891781	2.614223	0.000000
17	1	0	-3.036007	-0.870085	0.000000

58-P-ForMe

Standard orientation:

Center Number	Atomic Number	Atomic Type	Coordinates (Angstroms) X	Y	Z
1	6	0	1.270114	0.486234	0.000000
2	1	0	2.150581	1.122123	0.000000
3	6	0	0.000000	1.067169	0.000000
4	6	0	-1.131803	0.240079	0.000000
5	6	0	-0.986184	-1.136950	0.000000
6	6	0	0.287130	-1.730384	0.000000
7	6	0	1.410212	-0.898064	0.000000
8	6	0	-0.142830	2.538211	0.000000
9	1	0	-2.111178	0.704033	0.000000
10	1	0	-1.867598	-1.770484	0.000000
11	6	0	0.427913	-3.231777	0.000000
12	1	0	2.401202	-1.339505	0.000000
13	1	0	1.475892	-3.536279	0.000000
14	1	0	-0.051279	-3.671527	0.880228
15	1	0	-0.051279	-3.671527	-0.880228
16	8	0	-1.196875	3.132904	0.000000
17	1	0	0.821340	3.092828	0.000000

59-O-ForEt

Standard orientation:

Center Number	Atomic Number	Atomic Type	Coordinates (Angstroms) X	Y	Z
1	6	0	1.473649	1.264074	0.201851
2	1	0	1.620922	2.326301	0.371780
3	6	0	2.560828	0.402190	0.230158
4	6	0	2.348303	-0.954148	-0.002701
5	6	0	1.063266	-1.428575	-0.257046
6	6	0	-0.048635	-0.582224	-0.280888
7	6	0	0.173963	0.796103	-0.043087
8	1	0	3.557733	0.779590	0.424716
9	1	0	3.183734	-1.645587	0.007901
10	1	0	0.915805	-2.486905	-0.446386
11	6	0	-1.415959	-1.176924	-0.538061
12	6	0	-0.889923	1.826594	-0.050705
13	1	0	-2.002354	-0.507908	-1.167886
14	6	0	-2.204393	-1.453815	0.754640
15	1	0	-1.280741	-2.115589	-1.084442
16	1	0	-3.165658	-1.918380	0.519391
17	1	0	-1.654054	-2.127781	1.417083
18	1	0	-2.404740	-0.525632	1.291445
19	8	0	-2.080266	1.650641	-0.188699
20	1	0	-0.495121	2.857112	0.091025

60-M-ForEt

Standard orientation:

Center Number	Atomic Number	Atomic Type	Coordinates (Angstroms) X	Y	Z
1	6	0	-0.099089	2.176543	0.101068
2	1	0	-0.060072	3.252585	0.226535
3	6	0	-1.313374	1.503698	0.194414
4	6	0	-1.350514	0.117487	0.023136

5	6	0	-0.169781	-0.587157	-0.239494
6	6	0	1.053304	0.072295	-0.334056
7	6	0	1.068912	1.464715	-0.160511
8	1	0	-2.231401	2.047185	0.394835
9	6	0	-2.642204	-0.601239	0.115105
10	1	0	-0.235399	-1.661882	-0.372505
11	6	0	2.335494	-0.691948	-0.581155
12	1	0	2.011858	1.997291	-0.237933
13	6	0	3.036122	-1.119389	0.720306
14	1	0	2.116195	-1.579503	-1.182097
15	1	0	3.017899	-0.074242	-1.173746
16	1	0	3.957472	-1.666903	0.504194
17	1	0	3.293833	-0.250500	1.331934
18	1	0	2.389062	-1.766411	1.318187
19	8	0	-2.781981	-1.794963	-0.021181
20	1	0	-3.516822	0.052049	0.327169

61-P-ForEt

Standard orientation:

Center Number	Atomic Number	Atomic Type	Coordinates (Angstroms) X	Y	Z
1	6	0	-0.709655	1.362706	-0.025881
2	1	0	-1.182703	2.334213	0.082229
3	6	0	-1.494232	0.206614	0.007276
4	6	0	-0.880238	-1.043810	-0.139551
5	6	0	0.492112	-1.127262	-0.314243
6	6	0	1.289212	0.027800	-0.347042
7	6	0	0.666637	1.272564	-0.201662
8	6	0	-2.957878	0.308704	0.190853
9	1	0	-1.501847	-1.931301	-0.117283
10	1	0	0.960952	-2.098915	-0.433409
11	6	0	2.789514	-0.075156	-0.498528
12	1	0	1.267017	2.176038	-0.231890
13	6	0	3.513712	-0.238035	0.850150
14	1	0	3.031126	-0.926167	-1.142946
15	1	0	3.165700	0.818820	-1.005242
16	1	0	4.594542	-0.311323	0.703084
17	1	0	3.316988	0.614016	1.506004
18	1	0	3.179830	-1.140507	1.368634
19	8	0	-3.718881	-0.631162	0.230895
20	1	0	-3.335666	1.349679	0.295421

62-O-VinMe

Standard orientation:

Center Number	Atomic Number	Atomic Type	Coordinates (Angstroms) X	Y	Z
1	6	0	2.284049	-0.561591	0.072391
2	1	0	3.355830	-0.711226	0.139576
3	6	0	1.425365	-1.652189	-0.035517
4	6	0	0.055450	-1.440243	-0.127311
5	6	0	-0.489378	-0.147439	-0.104286
6	6	0	0.384128	0.959759	-0.006028
7	6	0	1.758870	0.727393	0.083711
8	1	0	1.820599	-2.661502	-0.060347
9	1	0	-0.609626	-2.288168	-0.244182
10	6	0	-1.948027	0.054098	-0.191963
11	6	0	-0.136867	2.378005	0.025914
12	1	0	2.429694	1.576452	0.167002
13	1	0	0.682938	3.086549	0.155698
14	1	0	-0.656022	2.641726	-0.901700
15	1	0	-0.845281	2.530471	0.845351
16	6	0	-2.887051	-0.795056	0.232898
17	1	0	-2.274788	0.990016	-0.636745
18	1	0	-3.940165	-0.570649	0.111223
19	1	0	-2.642413	-1.730090	0.725267

62-M-VinMe

Standard orientation:

Center Number	Atomic Number	Atomic Type	Coordinates (Angstroms) X	Y	Z
1	6	0	-1.659829	1.069010	-0.005745
2	6	0	-0.496171	1.839474	0.000470
3	6	0	0.751757	1.233671	0.001869
4	6	0	0.860080	-0.166671	-0.004220
5	6	0	-0.321640	-0.919714	-0.011045
6	6	0	-1.586477	-0.325007	-0.009130
7	6	0	2.150790	-0.874201	-0.007433
8	6	0	3.374023	-0.339077	0.012046
9	6	0	-2.835845	-1.173259	0.013176
10	1	0	-0.568696	2.921648	0.000291
11	1	0	1.643663	1.848786	0.002612
12	1	0	-0.248525	-2.003752	-0.019676

13	1	0	-2.629398	1.556331	-0.010372
14	1	0	-3.701764	-0.615886	-0.350344
15	1	0	-2.723195	-2.065987	-0.607163
16	1	0	-3.064234	-1.509905	1.030292
17	1	0	2.069684	-1.959006	-0.026727
18	1	0	4.255532	-0.968679	0.007530
19	1	0	3.546798	0.731095	0.033630

64-P-VinMe

Standard orientation:

Center Number	Atomic Number	Atomic Type	Coordinates (Angstroms) X	Y	Z
1	6	0	-0.958998	-1.176365	0.000000
2	1	0	-1.840413	-1.810642	0.000000
3	6	0	0.312776	-1.768064	0.000000
4	6	0	1.421647	-0.921322	0.000000
5	6	0	1.268380	0.462655	0.000000
6	6	0	0.000000	1.056628	0.000000
7	6	0	-1.114967	0.200937	0.000000
8	6	0	0.464811	-3.269284	0.000000
9	1	0	2.419767	-1.347492	0.000000
10	1	0	2.149138	1.097043	0.000000
11	6	0	-0.105906	2.523332	0.000000
12	1	0	-2.115701	0.617308	0.000000
13	6	0	-1.218602	3.262086	0.000000
14	1	0	0.850084	3.042973	0.000000
15	1	0	-1.166715	4.344069	0.000000
16	1	0	-2.212089	2.827676	0.000000
17	1	0	1.516297	-3.562792	0.000000
18	1	0	-0.007607	-3.715881	0.880657
19	1	0	-0.007607	-3.715881	-0.880657

65-O-VinEt

Standard orientation:

Center Number	Atomic Number	Atomic Type	Coordinates (Angstroms) X	Y	Z
1	6	0	-1.216056	1.304829	0.040843
2	1	0	-1.230844	2.388321	0.067184
3	6	0	-2.400582	0.600973	0.212655
4	6	0	-2.392198	-0.789283	0.131007
5	6	0	-1.196796	-1.452588	-0.125765
6	6	0	0.007509	-0.762485	-0.297331
7	6	0	0.001634	0.648789	-0.201448
8	1	0	-3.326858	1.134701	0.393570
9	1	0	-3.310682	-1.352323	0.253656
10	1	0	-1.192419	-2.535786	-0.197278
11	6	0	1.278426	-1.555188	-0.528503
12	6	0	1.241887	1.430652	-0.369408
13	1	0	1.876211	-1.096555	-1.322634
14	6	0	2.143759	-1.706025	0.734992
15	1	0	1.004793	-2.548855	-0.895098
16	1	0	3.040294	-2.295897	0.523842
17	1	0	2.459996	-0.732777	1.117467
18	1	0	1.585462	-2.209461	1.528667
19	6	0	1.505066	2.617419	0.183828
20	1	0	2.007284	0.985864	-0.999169
21	1	0	2.438622	3.130963	-0.013477
22	1	0	0.812258	3.109252	0.858044

66-M-VinEt

Standard orientation:

Center Number	Atomic Number	Atomic Type	Coordinates (Angstroms) X	Y	Z
1	6	0	-1.217570	1.569230	0.187504
2	6	0	0.024576	2.190103	0.098302
3	6	0	1.164807	1.437323	-0.160361
4	6	0	1.076822	0.049276	-0.333516
5	6	0	-0.175105	-0.555829	-0.243053
6	6	0	-1.340124	0.183098	0.018095
7	6	0	2.320969	-0.777771	-0.577401
8	6	0	3.015567	-1.214067	0.724220
9	6	0	-2.675029	-0.429379	0.116144
10	6	0	-2.992417	-1.721217	-0.000341
11	1	0	0.101865	3.264274	0.225900
12	1	0	2.130922	1.926401	-0.235528
13	1	0	-0.244280	-1.629193	-0.385797
14	1	0	-2.105277	2.160685	0.386271
15	1	0	-3.479902	0.277032	0.308152
16	1	0	-4.020161	-2.050727	0.092578
17	1	0	-2.254856	-2.493083	-0.189627
18	1	0	2.058375	-1.665164	-1.161830
19	1	0	3.025424	-0.201992	-1.186445

20	1	0	3.910182	-1.805846	0.510685
21	1	0	3.316654	-0.346735	1.317813
22	1	0	2.346082	-1.820260	1.340261

66-P-VinEt

Standard orientation:

Center Number	Atomic Number	Atomic Type	Coordinates (Angstroms) X	Y	Z
1	6	0	0.515237	-1.119210	-0.315966
2	1	0	0.971122	-2.097609	-0.433564
3	6	0	1.326937	0.023017	-0.345051
4	6	0	0.704738	1.265296	-0.200831
5	6	0	-0.672618	1.362289	-0.031117
6	6	0	-1.486576	0.221298	0.000631
7	6	0	-0.858731	-1.026176	-0.147214
8	6	0	2.827599	-0.090796	-0.490060
9	1	0	1.304555	2.169897	-0.226465
10	1	0	-1.130616	2.340707	0.074664
11	6	0	-2.937617	0.380907	0.179372
12	1	0	-1.450626	-1.934128	-0.135167
13	6	0	-3.864566	-0.579083	0.233386
14	1	0	-3.267600	1.413127	0.277088
15	1	0	-4.910724	-0.333711	0.370233
16	1	0	-3.624787	-1.632864	0.145024
17	6	0	3.550738	-0.253431	0.858913
18	1	0	3.066988	-0.944862	-1.131954
19	1	0	3.211615	0.798623	-0.999722
20	1	0	4.631971	-0.333905	0.715307
21	1	0	3.357340	0.601853	1.511770
22	1	0	3.209906	-1.151797	1.380409

68-O-MeEt

Standard orientation:

Center Number	Atomic Number	Atomic Type	Coordinates (Angstroms) X	Y	Z
1	6	0	-1.608602	1.016099	0.197174
2	1	0	-2.054433	1.990783	0.369175
3	6	0	-2.409846	-0.121192	0.248046
4	6	0	-1.841363	-1.370154	0.020925
5	6	0	-0.479525	-1.461694	-0.251769
6	6	0	0.338098	-0.328129	-0.300677
7	6	0	-0.238799	0.937799	-0.073388
8	1	0	-3.469407	-0.029576	0.459547
9	1	0	-2.451681	-2.265943	0.050877
10	1	0	-0.035931	-2.435730	-0.435853
11	6	0	1.820543	-0.498453	-0.564761
12	6	0	0.581856	2.206421	-0.132842
13	1	0	2.205475	0.353335	-1.132528
14	6	0	2.649212	-0.668097	0.721808
15	1	0	1.967601	-1.378867	-1.198091
16	1	0	3.711340	-0.788124	0.489718
17	1	0	2.544371	0.196515	1.382295
18	1	0	2.322201	-1.549198	1.280002
19	1	0	-0.033877	3.075851	0.104452
20	1	0	1.417601	2.189940	0.572577
21	1	0	1.007295	2.365419	-1.129269

69-M-MeEt

Standard orientation:

Center Number	Atomic Number	Atomic Type	Coordinates (Angstroms) X	Y	Z
1	6	0	-0.788795	1.865320	0.119034
2	1	0	-1.005581	2.918640	0.261111
3	6	0	0.513792	1.455822	-0.151935
4	6	0	0.806923	0.101072	-0.335900
5	6	0	-0.238332	-0.822882	-0.245563
6	6	0	-1.553342	-0.431515	0.021961
7	6	0	-1.815525	0.929152	0.207365
8	1	0	1.308905	2.191541	-0.222191
9	6	0	2.226908	-0.359733	-0.585107
10	1	0	-0.021801	-1.878156	-0.390831
11	6	0	-2.666964	-1.450562	0.076383
12	1	0	-2.828436	1.256489	0.419210
13	1	0	-3.468014	-1.129835	0.746520
14	1	0	-3.110369	-1.601933	-0.914073
15	1	0	-2.303882	-2.421071	0.422829
16	6	0	2.995784	-0.664308	0.712379
17	1	0	2.213561	-1.255232	-1.214761
18	1	0	2.763752	0.409291	-1.149856
19	1	0	4.016114	-0.993115	0.495075
20	1	0	3.053231	0.221766	1.350196
21	1	0	2.499828	-1.452577	1.285061

70-P-MeEt

Standard orientation:

Center Number	Atomic Number	Atomic Type	Coordinates (Angstroms) X	Y	Z
1	6	0	0.230497	1.196329	-0.238104
2	1	0	0.757483	2.142339	-0.320088
3	6	0	0.945877	0.000004	-0.346201
4	6	0	0.230497	-1.196324	-0.238109
5	6	0	-1.145831	-1.196506	-0.028869
6	6	0	-1.860878	0.000001	0.077825
7	6	0	-1.145833	1.196507	-0.028863
8	6	0	2.447551	0.000005	-0.531294
9	1	0	0.757486	-2.142332	-0.320097
10	1	0	-1.673366	-2.142227	0.050120
11	6	0	-3.358830	-0.000004	0.268939
12	1	0	-1.673370	2.142227	0.050130
13	1	0	-3.690697	0.884081	0.818591
14	1	0	-3.880299	-0.000168	-0.694777
15	1	0	-3.690655	-0.883936	0.818864
16	6	0	3.218860	-0.000008	0.800074
17	1	0	2.741095	-0.876961	-1.117406
18	1	0	2.741096	0.876980	-1.117390
19	1	0	4.299024	-0.000007	0.627540
20	1	0	2.970369	0.882263	1.396067
21	1	0	2.970368	-0.882287	1.396052

71-1,2,3-TOH

Standard orientation:

Center Number	Atomic Number	Atomic Type	Coordinates (Angstroms) X	Y	Z
1	6	0	1.173049	-1.427017	0.000000
2	1	0	2.104982	-1.982962	0.000000
3	6	0	-0.055095	-2.088650	0.000000
4	6	0	-1.251101	-1.377424	0.000000
5	6	0	-1.225135	0.016757	0.000000
6	6	0	0.000000	0.686904	0.000000
7	6	0	1.191815	-0.034901	0.000000
8	1	0	-0.076826	-3.171742	0.000000
9	1	0	-2.210568	-1.878750	0.000000
10	8	0	-2.388139	0.724691	0.000000
11	8	0	-0.026580	2.060400	0.000000
12	8	0	2.333274	0.736253	0.000000
13	1	0	-2.161207	1.663600	0.000000
14	1	0	0.884931	2.377151	0.000000
15	1	0	3.109049	0.167932	0.000000

72-1,2,4-TOH

Standard orientation:

Center Number	Atomic Number	Atomic Type	Coordinates (Angstroms) X	Y	Z
1	6	0	0.000000	1.032178	0.000000
2	8	0	-0.102119	2.403873	0.000000
3	6	0	1.205261	0.345506	0.000000
4	6	0	1.204360	-1.052109	0.000000
5	6	0	-0.003764	-1.744276	0.000000
6	6	0	-1.210546	-1.041223	0.000000
7	6	0	-1.224055	0.345431	0.000000
8	1	0	2.152749	0.873648	0.000000
9	8	0	2.426418	-1.673302	0.000000
10	1	0	-0.011656	-2.829596	0.000000
11	1	0	-2.158185	-1.565917	0.000000
12	8	0	-2.408619	1.027607	0.000000
13	1	0	-2.202163	1.970492	0.000000
14	1	0	0.774799	2.798899	0.000000
15	1	0	2.291471	-2.625997	0.000000

73-1,3,5-TOH

Standard orientation:

Center Number	Atomic Number	Atomic Type	Coordinates (Angstroms) X	Y	Z
1	6	0	-1.401069	0.063587	-0.000064
2	6	0	-0.635754	1.232253	-0.000093
3	6	0	0.755625	1.181590	0.000057
4	6	0	1.385033	-0.065533	-0.000011
5	6	0	0.645490	-1.245172	-0.000010
6	6	0	-0.749265	-1.166707	-0.000031
7	8	0	-1.319319	2.413533	0.000135

8	8	0	2.749863	-0.064237	-0.000072
9	8	0	-1.430587	-2.349318	-0.000090
10	1	0	1.360453	2.081035	-0.000099
11	1	0	1.122062	-2.218672	-0.000060
12	1	0	-2.482425	0.137642	-0.000007
13	1	0	-2.375861	-2.167070	0.000877
14	1	0	-0.688929	3.141112	-0.000473
15	1	0	3.064692	-0.973985	0.000900

74-1,2,3-TMeO

Standard orientation:

Center Number	Atomic Number	Atomic Type	Coordinates (Angstroms) X	Y	Z
1	6	0	-1.213613	-1.658570	0.149112
2	1	0	-2.141196	-2.205769	0.241918
3	6	0	-0.000002	-2.330140	0.255835
4	6	0	1.213610	-1.658569	0.149157
5	6	0	1.214128	-0.276602	-0.072550
6	6	0	0.000000	0.416440	-0.201860
7	6	0	-1.214131	-0.276599	-0.072567
8	1	0	-0.000005	-3.400665	0.426351
9	1	0	2.141191	-2.205769	0.241969
10	8	0	2.335009	0.490824	-0.180349
11	8	0	0.000005	1.754379	-0.494810
12	8	0	-2.335012	0.490833	-0.180306
13	6	0	3.598764	-0.152173	-0.113228
14	6	0	0.000005	2.615235	0.646020
15	6	0	-3.598763	-0.152171	-0.113233
16	1	0	4.338840	0.636084	-0.241932
17	1	0	3.754371	-0.638865	0.856435
18	1	0	3.716230	-0.891934	-0.912821
19	1	0	0.000117	3.634719	0.259943
20	1	0	-0.896390	2.458834	1.254982
21	1	0	0.896271	2.458683	1.255123
22	1	0	-4.338840	0.636094	-0.241877
23	1	0	-3.716228	-0.891873	-0.912882
24	1	0	-3.754371	-0.638938	0.856392

75-1,2,4-TMeO

Standard orientation:

Center Number	Atomic Number	Atomic Type	Coordinates (Angstroms) X	Y	Z
1	6	0	-1.208274	0.696533	0.000000
2	1	0	-2.131863	1.259952	0.000000
3	6	0	-1.215919	-0.702266	0.000000
4	6	0	-0.000133	-1.386476	0.000000
5	6	0	1.208290	-0.696889	0.000000
6	6	0	1.215859	0.701959	0.000000
7	6	0	0.000000	1.386209	0.000000
8	8	0	-2.344030	-1.478397	0.000000
9	1	0	2.131634	-1.260399	0.000000
10	8	0	2.343876	1.478330	0.000000
11	1	0	0.017640	2.469361	0.000000
12	6	0	3.604359	0.829486	0.000000
13	1	0	4.349577	1.623675	0.000000
14	1	0	3.740629	0.208900	0.893672
15	1	0	3.740629	0.208900	-0.893672
16	6	0	-3.604098	-0.828787	0.000000
17	1	0	-4.349735	-1.622582	0.000000
18	1	0	-3.740012	-0.208115	0.893669
19	1	0	-3.740012	-0.208115	-0.893669
20	1	0	-0.017758	-2.469656	0.000000

76-1,3,5-TMeO

Standard orientation:

Center Number	Atomic Number	Atomic Type	Coordinates (Angstroms) X	Y	Z
1	6	0	-0.545344	-2.021060	0.000000
2	1	0	-0.757395	-3.084499	0.000000
3	6	0	0.787835	-1.594929	0.000000
4	6	0	1.051018	-0.226095	0.000000
5	6	0	0.000000	0.703004	0.000000
6	6	0	-1.317116	0.255818	0.000000
7	6	0	-1.594933	-1.120435	0.000000
8	1	0	1.585865	-2.323654	0.000000
9	8	0	2.300097	0.324677	0.000000
10	1	0	0.258486	1.752269	0.000000
11	8	0	-2.404447	1.078097	0.000000
12	1	0	-2.627948	-1.443560	0.000000
13	6	0	-2.190978	2.482062	0.000000
14	1	0	-3.181879	2.933411	0.000000
15	1	0	-1.645661	2.805756	0.893611

16	1	0	-1.645661	2.805756	-0.893611
17	6	0	3.421604	-0.546153	0.000000
18	1	0	4.298968	0.098827	0.000000
19	1	0	3.438753	-1.179886	0.893740
20	1	0	3.438753	-1.179886	-0.893740

77-1,2,3-TFor

Standard orientation:

Center Number	Atomic Number	Atomic Type	Coordinates (Angstroms) X	Y	Z
1	6	0	-1.372241	1.536619	-0.044625
2	1	0	-2.406921	1.855499	-0.082804
3	6	0	-0.332984	2.453048	-0.077381
4	6	0	0.979304	1.994868	-0.017228
5	6	0	1.259002	0.628292	0.062809
6	6	0	0.201590	-0.312394	0.099130
7	6	0	-1.124077	0.159489	0.046652
8	1	0	-0.540069	3.514039	-0.150136
9	1	0	1.804021	2.699507	-0.050438
10	6	0	2.692573	0.241701	0.031001
11	6	0	0.489258	-1.783781	0.211538
12	6	0	-2.335302	-0.726996	0.139786
13	8	0	3.121808	-0.880246	-0.104258
14	1	0	3.385926	1.103256	0.129507
15	8	0	-0.191989	-2.628916	-0.321018
16	1	0	1.352893	-2.055467	0.835955
17	8	0	-3.451559	-0.301282	-0.049529
18	1	0	-2.164673	-1.778344	0.406260

78-1,2,4-TFor

Standard orientation:

Center Number	Atomic Number	Atomic Type	Coordinates (Angstroms) X	Y	Z
1	6	0	0.000000	0.890728	0.000000
2	6	0	-0.244284	2.373757	0.000000
3	6	0	-1.126793	0.066026	0.000000
4	6	0	-1.011215	-1.322425	0.000000
5	6	0	0.256733	-1.914245	0.000000
6	6	0	1.384173	-1.109040	0.000000
7	6	0	1.281042	0.290896	0.000000
8	1	0	-2.101163	0.543479	0.000000
9	6	0	-2.233005	-2.172667	0.000000
10	1	0	0.329950	-2.995148	0.000000
11	1	0	2.370039	-1.562211	0.000000
12	6	0	2.575984	1.030856	0.000000
13	8	0	2.728975	2.228955	0.000000
14	1	0	3.456976	0.355057	0.000000
15	8	0	-1.364924	2.831954	0.000000
16	1	0	0.644571	3.017057	0.000000
17	8	0	-2.214878	-3.379778	0.000000
18	1	0	-3.189575	-1.610594	0.000000

79-1,3,5-TFor

Standard orientation:

Center Number	Atomic Number	Atomic Type	Coordinates (Angstroms) X	Y	Z
1	6	0	0.000000	1.394034	0.000000
2	1	0	-0.027130	2.479618	0.000000
3	6	0	1.208469	0.705753	0.000000
4	6	0	1.207343	-0.697089	0.000000
5	6	0	0.007001	-1.399483	0.000000
6	6	0	-1.207331	-0.697065	0.000000
7	6	0	-1.215479	0.693658	0.000000
8	6	0	2.496068	1.448617	0.000000
9	1	0	2.160664	-1.216175	0.000000
10	6	0	0.006497	-2.885977	0.000000
11	1	0	-2.133554	-1.263087	0.000000
12	6	0	-2.502583	1.437391	0.000000
13	8	0	-2.587103	2.641882	0.000000
14	1	0	-3.408757	0.796755	0.000000
15	8	0	3.581475	0.919634	0.000000
16	1	0	2.394224	2.553700	0.000000
17	8	0	-0.994345	-3.561447	0.000000
18	1	0	1.014424	-3.350387	0.000000

80-1,2,3-TVin

Standard orientation:

Center Number	Atomic Number	Atomic Type	Coordinates (Angstroms) X	Y	Z

1	6	0	0.991883	-1.777331	0.038225
2	1	0	1.875365	-2.397133	0.132231
3	6	0	-0.249437	-2.368748	-0.144687
4	6	0	-1.389163	-1.576712	-0.209557
5	6	0	-1.302867	-0.185879	-0.087199
6	6	0	-0.033735	0.424980	0.077099
7	6	0	1.127213	-0.384724	0.143878
8	1	0	-0.330334	-3.446459	-0.231999
9	1	0	-2.357104	-2.032112	-0.381934
10	6	0	-2.526356	0.637508	-0.183989
11	6	0	0.023948	1.898300	0.206759
12	6	0	2.464772	0.189820	0.393024
13	6	0	-3.731949	0.289895	0.271835
14	1	0	-2.416777	1.602070	-0.671491
15	1	0	-4.589169	0.939701	0.140121
16	1	0	-3.902467	-0.642560	0.799566
17	6	0	0.883461	2.718495	-0.401821
18	1	0	-0.738778	2.338957	0.844249
19	1	0	0.835659	3.790241	-0.244565
20	1	0	1.646256	2.355447	-1.080685
21	6	0	3.619169	-0.298600	-0.066870
22	1	0	2.488418	1.084984	1.006737
23	1	0	4.564104	0.162571	0.195405
24	1	0	3.663191	-1.157728	-0.727815

81-1,2,4-TVin

Standard orientation:

Center Number	Atomic Number	Atomic Type	Coordinates (Angstroms) X	Y	Z
1	6	0	-1.115459	-0.610874	-0.077200
2	6	0	-2.547973	-0.943676	-0.170237
3	6	0	-0.681660	0.727039	0.075545
4	6	0	0.692779	0.989419	0.136385
5	6	0	1.660416	-0.014332	0.034581
6	6	0	1.211852	-1.336146	-0.127390
7	6	0	-0.140901	-1.618029	-0.182780
8	6	0	-1.651437	1.832132	0.216557
9	1	0	1.017995	2.011141	0.300010
10	6	0	3.081504	0.354151	0.108243
11	1	0	1.925002	-2.147081	-0.215814
12	1	0	-0.462004	-2.640629	-0.343594
13	6	0	-3.110822	-2.094158	0.209847
14	1	0	-3.189971	-0.174332	-0.589331
15	1	0	-4.173590	-2.264236	0.084797
16	1	0	-2.540151	-2.895188	0.667357
17	6	0	-1.476040	3.081279	-0.220416
18	1	0	-2.580866	1.590816	0.724401
19	1	0	-2.229231	3.842813	-0.055972
20	1	0	-0.587685	3.383072	-0.765065
21	6	0	4.138300	-0.455532	-0.000024
22	1	0	3.265046	1.414643	0.266723
23	1	0	5.146231	-0.065148	0.070500
24	1	0	4.045865	-1.523509	-0.162678

82-1,3,5-TVin

Standard orientation:

Center Number	Atomic Number	Atomic Type	Coordinates (Angstroms) X	Y	Z
1	6	0	-1.380732	-0.143992	0.000004
2	6	0	-0.833402	1.139428	0.000001
3	6	0	0.565691	1.267725	-0.000006
4	6	0	1.403516	0.152012	-0.000008
5	6	0	0.815078	-1.123789	-0.000005
6	6	0	-0.570065	-1.291490	0.000001
7	6	0	-1.742274	2.298209	0.000004
8	6	0	-1.413205	3.591925	0.000004
9	6	0	2.861478	0.359762	-0.000012
10	6	0	3.817312	-0.572101	0.000015
11	6	0	-1.119199	-2.657973	0.000002
12	6	0	-2.404159	-3.019739	-0.000004
13	1	0	1.015328	2.254201	-0.000009
14	1	0	1.444545	-2.006449	-0.000010
15	1	0	-2.459864	-0.247852	0.000010
16	1	0	-0.367759	-3.444475	0.000007
17	1	0	-2.685767	-4.065706	-0.000002
18	1	0	-3.217494	-2.302851	-0.000010
19	1	0	3.166821	1.403798	-0.000037
20	1	0	4.863934	-0.292938	0.000009
21	1	0	3.603199	-1.634924	0.000045
22	1	0	-2.799112	2.040643	0.000008
23	1	0	-2.178318	4.358706	0.000006
24	1	0	-0.385739	3.937987	0.000001

83-1,2,3-TMe

Standard orientation:

Center Number	Atomic Number	Atomic Type	Coordinates (Angstroms) X	Y	Z
1	6	0	1.212479	0.080801	-0.000012
2	6	0	0.013130	-0.660347	-0.000021
3	6	0	-1.222880	0.014709	-0.000009
4	6	0	-1.237819	1.413269	0.000000
5	6	0	-0.056803	2.144482	0.000004
6	6	0	1.161860	1.476148	0.000001
7	6	0	0.084625	-2.171100	0.000005
8	6	0	-2.540489	-0.730118	0.000004
9	6	0	2.551994	-0.617302	0.000003
10	1	0	0.622793	-2.543766	0.878244
11	1	0	0.623431	-2.543777	-0.877831
12	1	0	-0.900142	-2.634405	-0.000347
13	1	0	-2.191573	1.930852	0.000008
14	1	0	-0.085752	3.228525	0.000016
15	1	0	2.088863	2.040380	0.000013
16	1	0	-3.376144	-0.028096	0.000015
17	1	0	-2.648741	-1.370823	-0.880796
18	1	0	-2.648722	-1.370831	0.880799
19	1	0	3.368268	0.107031	0.000055
20	1	0	2.675547	-1.259205	0.878753
21	1	0	2.675598	-1.259137	-0.878789

84-1,2,4-TMe

Standard orientation:

Center Number	Atomic Number	Atomic Type	Coordinates (Angstroms) X	Y	Z
1	6	0	-0.699253	0.754943	-0.000569
2	6	0	-1.698629	1.886712	-0.000922
3	6	0	0.668258	1.030103	-0.005414
4	6	0	1.637781	0.021498	-0.006682
5	6	0	1.198356	-1.301059	-0.006306
6	6	0	-0.163754	-1.594553	-0.001471
7	6	0	-1.129000	-0.587892	0.002038
8	1	0	0.990053	2.068229	-0.009646
9	6	0	3.108387	0.364938	0.007989
10	1	0	1.921911	-2.110052	-0.010965
11	1	0	-0.483644	-2.632027	-0.002688
12	6	0	-2.597643	-0.936570	0.005189
13	1	0	-3.112049	-0.533529	-0.873871
14	1	0	-2.742357	-2.018450	0.007762
15	1	0	-3.109013	-0.529705	0.884228
16	1	0	-2.349035	1.851040	0.879551
17	1	0	-1.194968	2.854971	-0.004026
18	1	0	-2.352976	1.847339	-0.878314
19	1	0	3.722996	-0.512226	-0.205016
20	1	0	3.347095	1.131367	-0.734938
21	1	0	3.414975	0.754318	0.984817

85-1,3,5-TMe

Standard orientation:

Center Number	Atomic Number	Atomic Type	Coordinates (Angstroms) X	Y	Z
1	6	0	1.200688	-0.693218	0.000000
2	1	0	2.142896	-1.234356	0.000000
3	6	0	1.215979	0.708242	0.000000
4	6	0	0.000000	1.386409	0.000000
5	6	0	-1.221387	0.698991	0.000000
6	6	0	-1.200672	-0.693204	0.000000
7	6	0	0.005322	-1.407179	0.000000
8	6	0	2.528517	1.456059	0.000000
9	1	0	-0.002439	2.472911	0.000000
10	6	0	-2.525229	1.461706	0.000000
11	1	0	-2.140355	-1.238633	0.000000
12	6	0	-0.003256	-2.917780	0.000000
13	1	0	1.011015	-3.321857	0.000000
14	1	0	-0.520535	-3.311379	0.880691
15	1	0	-0.520535	-3.311379	-0.880691
16	1	0	2.371435	2.536507	0.000000
17	1	0	3.127989	1.204825	0.880693
18	1	0	3.127989	1.204825	-0.880693
19	1	0	-3.382350	0.785413	0.000000
20	1	0	-2.607438	2.106485	0.880690
21	1	0	-2.607438	2.106485	-0.880690

86-1,2,3-TEt

Standard orientation:

Center Number	Atomic Number	Atomic Type	Coordinates (Angstroms) X	Y	Z

1	6	0	-1.218387	0.433985	-0.211199
2	6	0	-2.569895	-0.245426	-0.075873
3	6	0	-1.198604	1.818836	-0.403004
4	6	0	-0.000210	2.514089	-0.499609
5	6	0	1.198283	1.819066	-0.402876
6	6	0	1.218263	0.434190	-0.211119
7	6	0	0.000012	-0.271823	-0.112210
8	1	0	-2.140128	2.353502	-0.483307
9	1	0	-0.000323	3.587167	-0.656647
10	1	0	2.139740	2.353871	-0.483019
11	6	0	2.569885	-0.245059	-0.075872
12	6	0	0.000176	-1.783634	0.049079
13	1	0	2.545128	-1.252431	-0.497508
14	6	0	3.068944	-0.310867	1.378886
15	1	0	3.298892	0.311901	-0.672542
16	1	0	4.050196	-0.791168	1.434970
17	1	0	3.157456	0.692357	1.803808
18	1	0	2.379602	-0.875155	2.012660
19	1	0	-0.868341	-2.097487	0.631632
20	1	0	0.868859	-2.097291	0.631485
21	6	0	0.000156	-2.534721	-1.295544
22	1	0	-0.000320	-3.617515	-1.139395
23	1	0	-0.879647	-2.278486	-1.891401
24	1	0	0.880449	-2.279235	-1.891015
25	1	0	-2.545103	-1.252885	-0.497260
26	1	0	-3.299032	0.311391	-0.672505
27	6	0	-3.068774	-0.311017	1.379036
28	1	0	-4.049739	-0.791867	1.435413
29	1	0	-2.378998	-0.874697	2.012871
30	1	0	-3.157783	0.692313	1.803590

87-1,3,5-TEt

Standard orientation:

Center Number	Atomic Number	Atomic Type	Coordinates (Angstroms) X	Y	Z
1	6	0	-0.621605	-1.219047	-0.360717
2	6	0	-1.267648	0.000836	-0.577592
3	6	0	-0.619871	1.219840	-0.360683
4	6	0	0.706421	1.200054	0.078689
5	6	0	1.384868	-0.001014	0.301586
6	6	0	0.704749	-1.201102	0.078679
7	6	0	-1.349679	2.530862	-0.560802
8	6	0	-2.067824	3.018423	0.709626
9	6	0	2.837387	-0.002020	0.727780
10	6	0	3.812847	-0.002041	-0.462102
11	6	0	-1.353108	-2.529124	-0.560858
12	6	0	-2.071892	-3.015810	0.709527
13	1	0	1.224055	2.141022	0.246513
14	1	0	1.221046	-2.142805	0.246476
15	1	0	-2.296216	0.001598	-0.929120
16	1	0	-2.084411	-2.416987	-1.367844
17	1	0	-0.643411	-3.295488	-0.888885
18	1	0	-2.588021	-3.963244	0.529273
19	1	0	-1.361887	-3.166264	1.527167
20	1	0	-2.812182	-2.284388	1.044574
21	1	0	-0.639021	3.296332	-0.888833
22	1	0	-2.081148	2.419651	-1.367759
23	1	0	-2.582796	3.966485	0.529385
24	1	0	-2.808985	2.287879	1.044661
25	1	0	-1.357605	3.167990	1.527241
26	1	0	3.032824	0.874756	1.353637
27	1	0	3.031829	-0.879554	1.352875
28	1	0	4.851099	-0.002758	-0.117791
29	1	0	3.662996	-0.883990	-1.090575
30	1	0	3.663957	0.880626	-1.089794

88-1,2-OH-3-For

Standard orientation:

Center Number	Atomic Number	Atomic Type	Coordinates (Angstroms) X	Y	Z
1	6	0	0.796288	-0.597464	0.000000
2	6	0	2.244063	-0.462997	0.000000
3	6	0	0.181005	-1.865623	0.000000
4	6	0	-1.196997	-1.965063	0.000000
5	6	0	-1.986445	-0.805463	0.000000
6	6	0	-1.402336	0.452354	0.000000
7	6	0	0.000000	0.562863	0.000000
8	1	0	0.804142	-2.753238	0.000000
9	1	0	-1.677989	-2.935284	0.000000
10	1	0	-3.068220	-0.867369	0.000000
11	8	0	-2.169534	1.572606	0.000000
12	8	0	0.506382	1.813777	0.000000
13	1	0	-1.574185	2.334642	0.000000
14	1	0	1.488634	1.729401	0.000000
15	8	0	2.837392	0.611969	0.000000

16	1	0	2.820225	-1.406597	0.000000

89-1,2-OH-4-For

Standard orientation:

Center Number	Atomic Number	Atomic Type	Coordinates (Angstroms) X	Y	Z
1	6	0	0.000000	0.982720	0.000000
2	1	0	-0.010682	2.068278	0.000000
3	6	0	1.240489	0.323052	0.000000
4	6	0	1.282508	-1.072886	0.000000
5	6	0	0.105956	-1.815324	0.000000
6	6	0	-1.122602	-1.162588	0.000000
7	6	0	-1.166231	0.248497	0.000000
8	6	0	2.485949	1.108500	0.000000
9	1	0	2.241261	-1.580529	0.000000
10	1	0	0.114803	-2.898170	0.000000
11	8	0	-2.271838	-1.876712	0.000000
12	8	0	-2.434842	0.776945	0.000000
13	1	0	-3.010769	-1.253103	0.000000
14	1	0	-2.393567	1.738385	0.000000
15	8	0	2.542754	2.319355	0.000000
16	1	0	3.413948	0.496610	0.000000

90-1,2-OH-3-MeO

Standard orientation:

Center Number	Atomic Number	Atomic Type	Coordinates (Angstroms) X	Y	Z
1	6	0	0.651128	-0.449618	0.000000
2	8	0	2.021684	-0.344822	0.000000
3	6	0	-0.088408	-1.630778	0.000000
4	6	0	-1.483730	-1.552953	0.000000
5	6	0	-2.137995	-0.326958	0.000000
6	6	0	-1.392353	0.852381	0.000000
7	6	0	0.000000	0.787407	0.000000
8	1	0	0.402607	-2.594089	0.000000
9	1	0	-2.064427	-2.467621	0.000000
10	1	0	-3.218462	-0.258320	0.000000
11	8	0	-2.020257	2.061392	0.000000
12	8	0	0.693751	1.972188	0.000000
13	1	0	-1.338713	2.745796	0.000000
14	1	0	1.635014	1.756245	0.000000
15	6	0	2.787793	-1.542299	0.000000
16	1	0	3.831494	-1.232202	0.000000
17	1	0	2.586223	-2.141486	0.894158
18	1	0	2.586223	-2.141486	-0.894158

91-1,2-OH-4-MeO

Standard orientation:

Center Number	Atomic Number	Atomic Type	Coordinates (Angstroms) X	Y	Z
1	6	0	0.000000	1.153133	0.000000
2	1	0	0.150036	2.227852	0.000000
3	6	0	1.123956	0.315712	0.000000
4	6	0	0.952433	-1.067282	0.000000
5	6	0	-0.339454	-1.605664	0.000000
6	6	0	-1.456086	-0.787263	0.000000
7	6	0	-1.270988	0.605423	0.000000
8	8	0	2.331716	0.959313	0.000000
9	1	0	1.800502	-1.737353	0.000000
10	1	0	-0.487816	-2.678744	0.000000
11	8	0	-2.713383	-1.323751	0.000000
12	8	0	-2.430081	1.347156	0.000000
13	1	0	-3.342374	-0.591749	0.000000
14	1	0	-2.218617	2.285385	0.000000
15	6	0	3.508729	0.167810	0.000000
16	1	0	4.341105	0.870022	0.000000
17	1	0	3.569804	-0.464181	0.893597
18	1	0	3.569804	-0.464181	-0.893597

92-1,2-OH-3-Me

Standard orientation:

Center Number	Atomic Number	Atomic Type	Coordinates (Angstroms) X	Y	Z
1	6	0	-1.184515	0.129072	-0.000036
2	6	0	-2.548376	-0.518118	0.000099
3	6	0	-1.026942	1.520181	-0.000031
4	6	0	0.239808	2.095164	-0.000029
5	6	0	1.378993	1.292969	0.000006

6	6	0	1.245183	-0.090457	0.000012
7	6	0	-0.034956	-0.661403	-0.000023
8	1	0	-1.910030	2.149415	-0.000049
9	1	0	0.344697	3.173709	-0.000043
10	1	0	2.375567	1.717249	0.000032
11	8	0	2.352203	-0.885155	0.000036
12	8	0	-0.049373	-2.042501	-0.000054
13	1	0	2.052302	-1.803136	0.000319
14	1	0	-0.954797	-2.365331	-0.000505
15	1	0	-2.705483	-1.145805	0.886070
16	1	0	-3.334771	0.237371	-0.000373
17	1	0	-2.705296	-1.146676	-0.885295

93-1,2-OH-4-Me

Standard orientation:

Center Number	Atomic Number	Atomic Type	Coordinates (Angstroms) X	Y	Z
1	6	0	-1.177498	0.313935	0.000000
2	1	0	-2.129756	0.839925	0.000000
3	6	0	-1.152304	-1.088164	0.000000
4	6	0	0.089696	-1.721615	0.000000
5	6	0	1.277891	-0.988570	0.000000
6	6	0	1.244977	0.398277	0.000000
7	6	0	0.000000	1.046022	0.000000
8	6	0	-2.441547	-1.874530	0.000000
9	1	0	0.137363	-2.805003	0.000000
10	1	0	2.242702	-1.481514	0.000000
11	8	0	2.402679	1.119013	0.000000
12	8	0	0.061342	2.422810	0.000000
13	1	0	2.164015	2.054618	0.000000
14	1	0	-0.827544	2.789938	0.000000
15	1	0	-2.245934	-2.948513	0.000000
16	1	0	-3.050157	-1.648082	0.881502
17	1	0	-3.050157	-1.648082	-0.881502

94-1,2-OH-6-Me

Standard orientation:

Center Number	Atomic Number	Atomic Type	Coordinates (Angstroms) X	Y	Z
1	6	0	-1.332919	1.315578	-0.000008
2	1	0	-2.316148	1.776762	-0.000020
3	6	0	-0.177509	2.096913	0.000001
4	6	0	1.073414	1.488339	0.000016
5	6	0	1.206455	0.095421	0.000015
6	6	0	0.043913	-0.678740	0.000014
7	6	0	-1.216579	-0.067910	-0.000002
8	6	0	2.549070	-0.586915	-0.000022
9	8	0	0.146465	-2.040976	0.000017
10	8	0	-2.283649	-0.941931	-0.000012
11	1	0	-0.749886	-2.400464	0.000005
12	1	0	-3.109389	-0.449150	-0.000011
13	1	0	-0.259444	3.177201	-0.000001
14	1	0	1.969878	2.098665	0.000027
15	1	0	2.664548	-1.230905	-0.876888
16	1	0	3.358027	0.145553	-0.000324
17	1	0	2.664808	-1.230507	0.877094

95-1,3-OH-2-Me

Standard orientation:

Center Number	Atomic Number	Atomic Type	Coordinates (Angstroms) X	Y	Z
1	6	0	-1.200776	1.419301	-0.000549
2	1	0	-2.143041	1.958505	0.002703
3	6	0	0.007644	2.106070	-0.001901
4	6	0	1.210973	1.410664	-0.000558
5	6	0	1.196303	0.013001	0.000820
6	6	0	-0.002149	-0.711797	-0.005252
7	6	0	-1.195347	0.021810	0.000818
8	1	0	0.011572	3.189886	-0.002274
9	1	0	2.156961	1.943326	0.002702
10	8	0	2.356613	-0.715113	0.007833
11	6	0	-0.010248	-2.217792	-0.007682
12	8	0	-2.359582	-0.699820	0.007772
13	1	0	-0.884417	-2.597216	-0.537469
14	1	0	0.893298	-2.607088	-0.476530
15	1	0	-0.049210	-2.615872	1.012556
16	1	0	-3.103597	-0.090192	-0.020161
17	1	0	3.103789	-0.109426	-0.020542

96-1,3-OH-5-MeO

Standard orientation:

Center Number	Atomic Number	Atomic Type	Coordinates (Angstroms) X	Y	Z
1	6	0	-1.455853	-0.914162	0.000000
2	8	0	-2.687188	-1.504482	0.000000
3	6	0	-1.294172	0.465521	0.000000
4	6	0	0.000000	1.003536	0.000000
5	6	0	1.118279	0.172478	0.000000
6	6	0	0.924539	-1.213612	0.000000
7	6	0	-0.349471	-1.769501	0.000000
8	1	0	-2.141786	1.141100	0.000000
9	8	0	0.061016	2.363849	0.000000
10	1	0	2.129651	0.550334	0.000000
11	8	0	2.052743	-1.983397	0.000000
12	1	0	-0.507106	-2.841909	0.000000
13	1	0	1.799327	-2.912075	0.000000
14	1	0	-3.363085	-0.819032	0.000000
15	6	0	1.339217	2.985276	0.000000
16	1	0	1.147002	4.056949	0.000000
17	1	0	1.914093	2.719828	0.893791
18	1	0	1.914093	2.719828	-0.893791

97-1,3-OH-5-For

Standard orientation:

Center Number	Atomic Number	Atomic Type	Coordinates (Angstroms) X	Y	Z
1	6	0	-1.010096	-1.121423	0.000000
2	8	0	-2.071958	-1.975513	0.000000
3	6	0	-1.149555	0.261243	0.000000
4	6	0	0.000000	1.058785	0.000000
5	6	0	1.272707	0.493340	0.000000
6	6	0	1.398597	-0.898750	0.000000
7	6	0	0.262868	-1.704559	0.000000
8	1	0	-2.122302	0.741006	0.000000
9	6	0	-0.134058	2.536164	0.000000
10	1	0	2.164042	1.109420	0.000000
11	8	0	2.660600	-1.412647	0.000000
12	1	0	0.339279	-2.786786	0.000000
13	1	0	2.616909	-2.374497	0.000000
14	1	0	-2.888657	-1.465097	0.000000
15	8	0	-1.186594	3.130871	0.000000
16	1	0	0.831559	3.085470	0.000000

98-1,3-OH-5-Et

Standard orientation:

Center Number	Atomic Number	Atomic Type	Coordinates (Angstroms) X	Y	Z
1	6	0	-1.107656	1.210661	0.012539
2	6	0	0.265362	1.195337	-0.229612
3	6	0	0.942886	-0.023478	-0.351857
4	6	0	0.234548	-1.217224	-0.231737
5	6	0	-1.141041	-1.191813	0.011367
6	6	0	-1.820192	0.017753	0.135272
7	6	0	2.440285	-0.042150	-0.571924
8	6	0	3.238398	-0.031207	0.743420
9	8	0	-1.778433	-2.395493	0.115950
10	8	0	-1.819839	2.370743	0.136120
11	1	0	0.729114	-2.176329	-0.328337
12	1	0	-2.888448	0.056438	0.319176
13	1	0	0.807868	2.131544	-0.329596
14	1	0	-1.221079	3.117418	0.033472
15	1	0	-2.715338	-2.243635	0.276655
16	1	0	2.709044	-0.931495	-1.149866
17	1	0	2.729587	0.822780	-1.177485
18	1	0	4.314183	-0.045886	0.546832
19	1	0	3.013001	0.862229	1.331742
20	1	0	2.992705	-0.902329	1.356048

99-1-OH-2-MeO-3-For

Standard orientation:

Center Number	Atomic Number	Atomic Type	Coordinates (Angstroms) X	Y	Z
1	6	0	-0.936591	-0.237862	-0.079675
2	6	0	-2.165326	0.572436	-0.242873
3	6	0	-1.038261	-1.614356	0.167328
4	6	0	0.106874	-2.389298	0.274101
5	6	0	1.369835	-1.815498	0.122234
6	6	0	1.486538	-0.450221	-0.120724
7	6	0	0.331582	0.340253	-0.204007
8	1	0	-2.029294	-2.042077	0.260183

9	1	0	0.026821	-3.454032	0.464179
10	1	0	2.273245	-2.411538	0.185465
11	8	0	2.710385	0.113228	-0.278584
12	8	0	0.518749	1.686667	-0.455875
13	1	0	2.556836	1.022338	-0.573225
14	6	0	0.521170	2.514201	0.714398
15	1	0	0.722417	3.531466	0.373407
16	1	0	-0.451089	2.483765	1.219039
17	1	0	1.299749	2.198911	1.419274
18	8	0	-3.286260	0.140928	-0.089615
19	1	0	-1.996608	1.626653	-0.540421

100-1-OH-2-MeO-4-For

Standard orientation:

Center Number	Atomic Number	Atomic Type	Coordinates (Angstroms) X	Y	Z
1	6	0	0.461425	0.653283	-0.000057
2	6	0	-0.862194	0.264325	0.000085
3	6	0	-1.199762	-1.111324	0.000101
4	6	0	-0.197513	-2.073630	-0.000087
5	6	0	1.137222	-1.678120	-0.000088
6	6	0	1.473813	-0.324342	-0.000062
7	8	0	-1.955492	1.089653	-0.000381
8	6	0	-1.735283	2.497803	0.000117
9	8	0	-2.499831	-1.482551	0.000338
10	6	0	2.885601	0.091648	-0.000084
11	8	0	3.272290	1.240955	0.000177
12	1	0	-0.483756	-3.118034	-0.000091
13	1	0	1.922425	-2.426831	-0.000159
14	1	0	0.760337	1.693391	-0.000199
15	1	0	-3.031079	-0.673487	-0.000958
16	1	0	-2.722587	2.955718	-0.000012
17	1	0	-1.186376	2.808453	0.894514
18	1	0	-1.185858	2.809110	-0.893731
19	1	0	3.611299	-0.750641	0.000016

101-1-OH-2-MeO-5-For

Standard orientation:

Center Number	Atomic Number	Atomic Type	Coordinates (Angstroms) X	Y	Z
1	1	0	2.139755	1.148007	0.000000
2	6	0	1.251634	0.528471	0.000000
3	6	0	0.000000	1.110986	0.000000
4	8	0	-0.132844	2.462562	0.000000
5	1	0	-1.078345	2.662085	0.000000
6	6	0	-1.152731	0.289363	0.000000
7	8	0	-2.322751	0.993892	0.000000
8	6	0	-3.555276	0.279403	0.000000
9	1	0	-3.648230	-0.343630	0.894994
10	1	0	-3.648230	-0.343630	-0.894994
11	1	0	-4.338758	1.034642	0.000000
12	6	0	1.375364	-0.869902	0.000000
13	6	0	2.712198	-1.495758	0.000000
14	6	0	0.236076	-1.673400	0.000000
15	1	0	0.336758	-2.753425	0.000000
16	6	0	-1.034076	-1.096314	0.000000
17	1	0	-1.914610	-1.724703	0.000000
18	8	0	3.762923	-0.894996	0.000000
19	1	0	2.693900	-2.608104	0.000000

102-1-OH-2-MeO-6-For

Standard orientation:

Center Number	Atomic Number	Atomic Type	Coordinates (Angstroms) X	Y	Z
1	6	0	2.476534	1.043078	0.000000
2	6	0	1.293888	0.153193	0.000000
3	6	0	0.000000	0.682122	0.000000
4	8	0	-0.203323	2.023308	0.000000
5	1	0	-1.159935	2.167523	0.000000
6	6	0	-1.112259	-0.186467	0.000000
7	8	0	-2.315595	0.473612	0.000000
8	6	0	-3.512456	-0.295925	0.000000
9	1	0	-3.577605	-0.923584	0.894774
10	1	0	-3.577605	-0.923584	-0.894774
11	1	0	-4.331101	0.421330	0.000000
12	6	0	1.466426	-1.242691	0.000000
13	6	0	0.374769	-2.087481	0.000000
14	1	0	0.510852	-3.162095	0.000000
15	6	0	-0.926494	-1.559558	0.000000
16	1	0	-1.777477	-2.228186	0.000000
17	1	0	2.480864	-1.621542	0.000000
18	8	0	3.620739	0.641456	0.000000

19	1	0	2.254988	2.125505	0.000000

103-1-OH-2-MeO-4-Me

Standard orientation:

Center Number	Atomic Number	Atomic Type	Coordinates (Angstroms) X	Y	Z
1	6	0	-0.580291	1.247975	0.000000
2	6	0	0.676155	1.830212	-0.000001
3	6	0	1.821773	1.029638	-0.000001
4	6	0	1.732082	-0.359184	0.000000
5	6	0	0.455322	-0.946532	0.000001
6	6	0	-0.685410	-0.156603	0.000001
7	8	0	-1.703224	2.020162	0.000000
8	8	0	-1.983507	-0.610582	0.000001
9	1	0	0.369264	-2.026452	0.000001
10	6	0	2.965444	-1.231144	0.000000
11	1	0	2.797089	1.503942	-0.000002
12	1	0	0.745282	2.911426	-0.000002
13	1	0	-2.459868	1.419195	0.000000
14	6	0	-2.211619	-2.012582	-0.000002
15	1	0	-3.292681	-2.142411	-0.000003
16	1	0	-1.789010	-2.483555	-0.894087
17	1	0	-1.789011	-2.483559	0.894081
18	1	0	2.998967	-1.879942	0.881430
19	1	0	2.998956	-1.879959	-0.881417
20	1	0	3.874125	-0.626004	-0.000011

104-1-OH-2-MeO-4-Et

Standard orientation:

Center Number	Atomic Number	Atomic Type	Coordinates (Angstroms) X	Y	Z
1	6	0	1.366429	-0.173482	-0.342629
2	6	0	0.282530	0.714779	-0.249411
3	6	0	-1.005329	0.239342	-0.040485
4	6	0	-1.242769	-1.142583	0.081094
5	6	0	-0.176180	-2.022841	-0.012461
6	6	0	1.116567	-1.539031	-0.223055
7	8	0	-2.143656	1.004619	0.061775
8	6	0	-2.023864	2.415859	-0.046209
9	8	0	-2.507999	-1.607026	0.281785
10	1	0	-0.373316	-3.084518	0.076319
11	1	0	1.938628	-2.242961	-0.298580
12	1	0	0.460461	1.778888	-0.347992
13	1	0	-3.090755	-0.836807	0.311660
14	1	0	-3.031386	2.813560	0.064684
15	1	0	-1.383908	2.821651	0.744729
16	1	0	-1.624038	2.706835	-1.023589
17	6	0	2.772399	0.354980	-0.530165
18	6	0	3.459275	0.740338	0.791499
19	1	0	3.375666	-0.402098	-1.040974
20	1	0	2.750344	1.227806	-1.191799
21	1	0	4.471175	1.116263	0.613532
22	1	0	2.896515	1.518413	1.314662
23	1	0	3.529495	-0.121948	1.459790

105-1-OH-2-For-4-Et

Standard orientation:

Center Number	Atomic Number	Atomic Type	Coordinates (Angstroms) X	Y	Z
1	6	0	-0.941044	-0.504920	-0.081564
2	6	0	0.392287	-0.911263	-0.274503
3	6	0	1.433911	-0.000092	-0.345205
4	6	0	1.105658	1.364340	-0.218805
5	6	0	-0.194534	1.801142	-0.028461
6	6	0	-1.241200	0.873795	0.045382
7	8	0	-2.491879	1.317616	0.228138
8	6	0	-2.007142	-1.490458	-0.017578
9	8	0	-3.193295	-1.221874	0.147942
10	1	0	0.595612	-1.974486	-0.373186
11	6	0	2.871042	-0.440552	-0.517934
12	1	0	1.899573	2.102814	-0.278385
13	1	0	-0.430036	2.854527	0.061403
14	1	0	-3.081704	0.530495	0.250154
15	1	0	-1.695711	-2.546609	-0.128841
16	6	0	3.646098	-0.517600	0.808591
17	1	0	2.892332	-1.419555	-1.006575
18	1	0	3.383431	0.251426	-1.194800
19	1	0	4.679964	-0.831280	0.639553
20	1	0	3.666238	0.453607	1.310506
21	1	0	3.181239	-1.233223	1.491990

106-1-OH-3-For-4-Et

Standard orientation:

Center Number	Atomic Number	Atomic Type	Coordinates (Angstroms) X	Y	Z
1	6	0	2.199587	0.046588	0.086023
2	6	0	1.224495	1.038372	0.088130
3	6	0	-0.127263	0.724781	-0.094418
4	6	0	-0.536279	-0.615310	-0.299204
5	6	0	0.466174	-1.586633	-0.306217
6	6	0	1.811038	-1.277038	-0.115354
7	6	0	-1.052096	1.884616	-0.074988
8	8	0	-2.259217	1.856364	-0.160519
9	8	0	3.496739	0.428126	0.276765
10	6	0	-1.976871	-1.039812	-0.488979
11	1	0	0.188833	-2.622851	-0.469893
12	1	0	2.555939	-2.067778	-0.129178
13	1	0	1.530343	2.068648	0.234773
14	1	0	4.065822	-0.347929	0.251423
15	1	0	-0.525365	2.858282	0.032379
16	6	0	-2.743483	-1.198627	0.835856
17	1	0	-2.501739	-0.314988	-1.111505
18	1	0	-1.980862	-1.995897	-1.022259
19	1	0	-3.763708	-1.543288	0.646025
20	1	0	-2.255239	-1.926253	1.490381
21	1	0	-2.806010	-0.245497	1.362785

107-1-OH-3-For-5-Et

Standard orientation:

Center Number	Atomic Number	Atomic Type	Coordinates (Angstroms) X	Y	Z
1	6	0	-0.949016	1.169973	-0.212504
2	6	0	0.356348	1.630388	0.003568
3	6	0	1.408596	0.727086	0.080806
4	6	0	1.146626	-0.639625	-0.060730
5	6	0	-0.154347	-1.094754	-0.275627
6	6	0	-1.219852	-0.189999	-0.352732
7	8	0	0.523497	2.978729	0.125597
8	6	0	2.262193	-1.610953	0.013234
9	8	0	3.421681	-1.318344	0.196665
10	6	0	-2.639887	-0.675490	-0.546332
11	6	0	-3.356248	-0.971883	0.782655
12	1	0	-0.336590	-2.159308	-0.388684
13	1	0	-1.745698	1.903351	-0.273235
14	1	0	2.432128	1.049514	0.243626
15	1	0	1.456623	3.171762	0.265324
16	1	0	1.957138	-2.671859	-0.115117
17	1	0	-3.207189	0.075810	-1.103964
18	1	0	-2.631018	-1.580088	-1.162304
19	1	0	-4.376881	-1.321088	0.604444
20	1	0	-2.828359	-1.742938	1.349979
21	1	0	-3.408063	-0.076700	1.407813

108-1-OH-2-Vin-3-Et

Standard orientation:

Center Number	Atomic Number	Atomic Type	Coordinates (Angstroms) X	Y	Z
1	6	0	0.274323	0.346746	-0.040662
2	6	0	-0.915499	-0.371430	-0.296870
3	6	0	-0.878649	-1.764542	-0.360723
4	6	0	0.311460	-2.457729	-0.151320
5	6	0	1.481724	-1.768901	0.129281
6	6	0	1.468372	-0.374898	0.180435
7	8	0	2.652048	0.234691	0.473105
8	6	0	0.262668	1.823834	0.032781
9	6	0	1.162020	2.657199	-0.505315
10	1	0	-1.789896	-2.309295	-0.583081
11	1	0	0.325659	-3.540639	-0.205014
12	1	0	2.418002	-2.281965	0.310948
13	6	0	-2.239025	0.339786	-0.502043
14	1	0	-0.565112	2.267301	0.580549
15	1	0	1.069114	3.730048	-0.383163
16	1	0	1.986937	2.306692	-1.117240
17	1	0	2.487365	1.177317	0.611061
18	1	0	-2.081057	1.300816	-0.998626
19	1	0	-2.852265	-0.257035	-1.183665
20	6	0	-3.019959	0.554743	0.807283
21	1	0	-3.972167	1.057046	0.614743
22	1	0	-3.232119	-0.400875	1.293286
23	1	0	-2.455463	1.164212	1.518285

109-1-OH-3-Vin-4-Et

Standard orientation:

Center Number	Atomic Number	Atomic Type	Coordinates (Angstroms) X	Y	Z
1	6	0	-1.148280	0.882780	-0.057541
2	6	0	-2.092861	-0.128462	0.078078
3	6	0	-1.688097	-1.462245	0.018160
4	6	0	-0.345392	-1.752317	-0.177943
5	6	0	0.627572	-0.755297	-0.313825
6	6	0	0.213139	0.592911	-0.240920
7	8	0	-3.425950	0.122370	0.253271
8	6	0	2.078995	-1.158985	-0.478876
9	6	0	2.897848	-1.064666	0.820419
10	6	0	1.184285	1.696209	-0.368869
11	6	0	1.071154	2.914677	0.166085
12	1	0	-0.037926	-2.791975	-0.230097
13	1	0	-1.472532	1.919172	-0.051469
14	1	0	-2.430402	-2.245377	0.111701
15	1	0	-3.568212	1.074257	0.270726
16	1	0	2.076447	1.479652	-0.949264
17	1	0	1.830826	3.669580	0.001623
18	1	0	0.234330	3.196972	0.795916
19	1	0	2.560723	-0.552655	-1.252943
20	1	0	2.110591	-2.189094	-0.846149
21	1	0	3.931719	-1.381069	0.653896
22	1	0	2.913778	-0.042105	1.205101
23	1	0	2.468086	-1.703948	1.596188

110-1-OH-3-Vin-5-Et

Standard orientation:

Center Number	Atomic Number	Atomic Type	Coordinates (Angstroms) X	Y	Z
1	6	0	0.262314	1.653611	0.002044
2	6	0	-1.027844	1.157030	-0.206769
3	6	0	-1.236645	-0.212088	-0.350890
4	6	0	-0.136718	-1.074455	-0.285207
5	6	0	1.161206	-0.593670	-0.075386
6	6	0	1.349363	0.789609	0.067942
7	6	0	2.272264	-1.557088	-0.018881
8	6	0	3.564115	-1.302305	0.202654
9	8	0	0.391184	3.008941	0.129728
10	6	0	-2.635281	-0.759733	-0.536950
11	1	0	-0.289623	-2.142552	-0.403948
12	1	0	2.344060	1.195375	0.223663
13	1	0	-1.851568	1.859980	-0.259209
14	1	0	1.319299	3.226966	0.263031
15	1	0	1.976527	-2.591757	-0.176824
16	1	0	4.293225	-2.103186	0.221358
17	1	0	3.945412	-0.301688	0.373898
18	6	0	-3.327429	-1.097226	0.795020
19	1	0	-3.240543	-0.030464	-1.084203
20	1	0	-2.591640	-1.659049	-1.159425
21	1	0	-4.333277	-1.490695	0.623178
22	1	0	-2.760102	-1.847267	1.352376
23	1	0	-3.413313	-0.209311	1.426821

111-1-OH-2-Me-4-Et

Standard orientation:

Center Number	Atomic Number	Atomic Type	Coordinates (Angstroms) X	Y	Z
1	6	0	0.656682	-1.416134	-0.213225
2	6	0	-0.703935	-1.631919	-0.004948
3	6	0	-1.579506	-0.552004	0.073005
4	6	0	-1.105823	0.762566	-0.059232
5	6	0	0.260377	0.942732	-0.266257
6	6	0	1.164325	-0.123786	-0.346306
7	8	0	-2.927409	-0.709176	0.273131
8	6	0	-2.067503	1.919149	0.018623
9	6	0	2.645727	0.123513	-0.533471
10	6	0	3.397517	0.338247	0.791564
11	1	0	-3.126559	-1.648049	0.344977
12	1	0	0.633151	1.957727	-0.374997
13	1	0	1.325522	-2.268587	-0.276734
14	1	0	-1.086777	-2.644456	0.092008
15	1	0	-1.545346	2.869442	-0.106430
16	1	0	-2.839517	1.844372	-0.753014
17	1	0	-2.589268	1.935227	0.980167
18	1	0	3.090176	-0.723748	-1.065847
19	1	0	2.790146	0.999600	-1.174462
20	1	0	4.462681	0.515044	0.615246
21	1	0	2.996487	1.198587	1.334249
22	1	0	3.301426	-0.535937	1.441263

112-1-OH-3-Me-5-Et

Standard orientation:

Center Number	Atomic Number	Atomic Type	Coordinates (Angstroms) X	Y	Z
1	6	0	0.965399	-0.012433	-0.352354
2	6	0	0.336552	1.223792	-0.227252
3	6	0	-1.037161	1.289954	0.013006
4	6	0	-1.787957	0.122094	0.128183
5	6	0	-1.172541	-1.128161	0.002913
6	6	0	0.200151	-1.180643	-0.236336
7	8	0	-1.593390	2.535083	0.122967
8	6	0	-1.994294	-2.390231	0.117251
9	6	0	2.461078	-0.092230	-0.570647
10	6	0	3.254780	-0.166544	0.745356
11	1	0	-2.538469	2.444028	0.281499
12	1	0	-2.858084	0.184133	0.311894
13	1	0	0.685226	-2.146327	-0.340061
14	1	0	0.893517	2.149632	-0.317295
15	1	0	-1.366678	-3.279970	0.041294
16	1	0	-2.523771	-2.433896	1.074014
17	1	0	-2.749020	-2.444911	-0.673809
18	1	0	2.691455	-0.971443	-1.180814
19	1	0	2.791679	0.780222	-1.142777
20	1	0	4.329533	-0.224617	0.550713
21	1	0	3.068594	0.715290	1.363960
22	1	0	2.967094	-1.046400	1.326936

113-1-OH-3-Et-4-Me

Standard orientation:

Center Number	Atomic Number	Atomic Type	Coordinates (Angstroms) X	Y	Z
1	6	0	1.886580	0.977267	0.231288
2	6	0	0.698182	1.702192	0.191892
3	6	0	-0.532093	1.097980	-0.072022
4	6	0	-0.555511	-0.293412	-0.306310
5	6	0	0.636206	-1.017257	-0.270958
6	6	0	1.854762	-0.395073	-0.002878
7	6	0	-1.787993	1.938762	-0.118011
8	8	0	2.975623	-1.180820	0.012197
9	1	0	-1.561894	2.980217	0.119013
10	1	0	-2.543174	1.595948	0.595622
11	1	0	-2.253620	1.921984	-1.109250
12	6	0	-1.850333	-1.037422	-0.563976
13	1	0	0.635852	-2.085856	-0.456774
14	1	0	2.827678	1.478655	0.438534
15	1	0	0.732728	2.772188	0.370452
16	1	0	3.741792	-0.630213	0.202512
17	6	0	-2.531186	-1.526897	0.727164
18	1	0	-2.545476	-0.403151	-1.121044
19	1	0	-1.642069	-1.900352	-1.203675
20	1	0	-3.460755	-2.057096	0.501126
21	1	0	-1.876162	-2.208520	1.275767
22	1	0	-2.771569	-0.694082	1.393005

114-1,3-MeO-2-OH

Standard orientation:

Center Number	Atomic Number	Atomic Type	Coordinates (Angstroms) X	Y	Z
1	6	0	-0.039290	2.103239	-0.000001
2	6	0	-1.237603	1.393605	0.000000
3	6	0	-1.225744	-0.005279	0.000000
4	6	0	0.000999	-0.684468	-0.000002
5	6	0	1.195007	0.047493	-0.000001
6	6	0	1.185888	1.441586	-0.000002
7	8	0	-2.331513	-0.800730	0.000001
8	6	0	-3.604848	-0.176125	0.000002
9	8	0	0.018894	-2.045171	-0.000002
10	8	0	2.317114	-0.749265	-0.000002
11	1	0	2.109466	2.003943	-0.000005
12	1	0	-0.061378	3.186391	-0.000002
13	1	0	-2.176091	1.930143	0.000001
14	1	0	-4.331700	-0.986856	0.000002
15	1	0	-3.752289	0.441103	0.893855
16	1	0	-3.752290	0.441104	-0.893851
17	1	0	0.949247	-2.306655	0.000000
18	6	0	3.591345	-0.121867	0.000004
19	1	0	4.323906	-0.927501	0.000016
20	1	0	3.730326	0.495272	-0.894131
21	1	0	3.730313	0.495284	0.894133

115-1,3-MeO-5-Et

Standard orientation:

Center Number	Atomic Number	Atomic Type	Coordinates (Angstroms) X	Y	Z
1	6	0	-0.216922	-1.458447	-0.275661
2	6	0	1.038279	-0.872832	-0.355383
3	6	0	1.167484	0.520927	-0.228358
4	6	0	0.033424	1.301768	-0.021266
5	6	0	-1.236900	0.713345	0.061843
6	6	0	-1.355529	-0.665531	-0.066194
7	8	0	0.042185	2.661113	0.110783
8	6	0	1.287019	3.339673	0.039674
9	8	0	-2.538884	-1.341178	-0.006145
10	6	0	-3.731381	-0.598011	0.198963
11	6	0	2.273593	-1.728914	-0.538824
12	1	0	2.149351	0.969588	-0.299996
13	1	0	-2.085698	1.362967	0.219152
14	1	0	-0.347175	-2.529397	-0.376421
15	1	0	-4.538589	-1.328737	0.212782
16	1	0	-3.711794	-0.062059	1.154525
17	1	0	-3.904158	0.117120	-0.613102
18	1	0	1.057678	4.396067	0.171355
19	1	0	1.968158	3.015824	0.834655
20	1	0	1.770462	3.193421	-0.932803
21	6	0	2.950612	-2.097948	0.792500
22	1	0	2.002099	-2.645004	-1.071816
23	1	0	2.991411	-1.199482	-1.174149
24	1	0	3.838479	-2.713591	0.621885
25	1	0	3.258975	-1.202234	1.338206
26	1	0	2.266320	-2.658153	1.434868

116-1,3-MeO-4-Vin

Standard orientation:

Center Number	Atomic Number	Atomic Type	Coordinates (Angstroms) X	Y	Z
1	6	0	-0.144880	-1.644417	-0.094945
2	1	0	-0.434111	-2.686365	-0.167808
3	6	0	-1.146354	-0.673597	-0.068802
4	6	0	-0.727357	0.680917	-0.018818
5	6	0	0.622215	1.011981	0.017225
6	6	0	1.595500	0.005740	0.001978
7	6	0	1.213068	-1.334477	-0.056711
8	6	0	-2.578423	-0.999249	-0.107261
9	8	0	-1.723116	1.612224	-0.000503
10	1	0	0.962508	2.036434	0.061547
11	8	0	2.884676	0.447491	0.040225
12	1	0	1.944127	-2.130071	-0.086126
13	6	0	3.929063	-0.515740	0.033899
14	1	0	4.857001	0.052256	0.076496
15	1	0	3.869618	-1.178065	0.904570
16	1	0	3.915078	-1.117383	-0.881624
17	6	0	-1.375050	2.988784	0.029453
18	1	0	-2.318205	3.532772	0.027762
19	1	0	-0.813840	3.240288	0.935917
20	1	0	-0.789649	3.274283	-0.851379
21	6	0	-3.136276	-2.180936	0.172980
22	1	0	-3.226748	-0.174419	-0.382338
23	1	0	-4.207739	-2.320655	0.094428
24	1	0	-2.559547	-3.040832	0.496799

117-1-MeO-3-OH-4-Et

Standard orientation:

Center Number	Atomic Number	Atomic Type	Coordinates (Angstroms) X	Y	Z
1	6	0	-0.892539	0.804076	-0.056410
2	6	0	-1.565142	-0.414488	0.007093
3	6	0	-0.845815	-1.612284	-0.087004
4	6	0	0.530549	-1.567558	-0.238917
5	6	0	1.241324	-0.362302	-0.301146
6	6	0	0.496592	0.820550	-0.206737
7	8	0	-2.915170	-0.538146	0.154390
8	6	0	-3.696174	0.643988	0.250050
9	8	0	1.076188	2.062067	-0.253752
10	1	0	-1.383938	-2.550390	-0.042002
11	1	0	1.081984	-2.499576	-0.315136
12	6	0	2.749215	-0.342931	-0.428334
13	1	0	-1.403744	1.754368	0.004428
14	1	0	2.015106	1.968432	-0.441174
15	1	0	-4.726929	0.311133	0.361466
16	1	0	-3.413342	1.243561	1.122567
17	1	0	-3.609870	1.257431	-0.653851
18	1	0	3.063609	0.406540	-1.169481
19	6	0	3.483458	-0.087101	0.901496
20	1	0	3.078155	-1.300207	-0.841798
21	1	0	4.567837	-0.079222	0.758379
22	1	0	3.193401	0.870684	1.342613

23	1	0	3.240778	-0.865834	1.628336

118-1-MeO-2-For-4-Et

Standard orientation:

Center Number	Atomic Number	Atomic Type	Coordinates (Angstroms) X	Y	Z
1	6	0	-0.506121	-1.604370	-0.128265
2	6	0	-1.241633	-0.421807	-0.009355
3	6	0	-0.568056	0.817041	-0.064533
4	6	0	0.819253	0.834435	-0.233549
5	6	0	1.568312	-0.333235	-0.351202
6	6	0	0.875313	-1.547580	-0.295973
7	8	0	-2.591429	-0.377419	0.154504
8	6	0	-3.318683	-1.598458	0.213274
9	6	0	-1.297524	2.101351	0.047056
10	8	0	-0.758794	3.187693	0.000694
11	6	0	3.073744	-0.293522	-0.496733
12	6	0	3.810497	-0.303631	0.853751
13	1	0	1.295180	1.808733	-0.275272
14	1	0	1.425215	-2.478978	-0.391654
15	1	0	-0.996302	-2.567789	-0.096915
16	1	0	-4.360766	-1.314487	0.347822
17	1	0	-3.215543	-2.169965	-0.715155
18	1	0	-2.998207	-2.213934	1.060448
19	1	0	-2.390203	2.016992	0.178856
20	1	0	3.403601	-1.149244	-1.094946
21	1	0	3.358264	0.603110	-1.055913
22	1	0	4.893970	-0.272691	0.708351
23	1	0	3.525091	0.559474	1.460888
24	1	0	3.570881	-1.204765	1.425070

119-1,2-For-4-MeO

Standard orientation:

Center Number	Atomic Number	Atomic Type	Coordinates (Angstroms) X	Y	Z
1	6	0	0.820918	-1.895442	0.000000
2	1	0	1.114067	-2.937761	0.000000
3	6	0	-0.546952	-1.581968	0.000000
4	6	0	-0.944178	-0.242846	0.000000
5	6	0	0.000000	0.783978	0.000000
6	6	0	1.380021	0.475899	0.000000
7	6	0	1.755531	-0.878404	0.000000
8	8	0	-1.394045	-2.634292	0.000000
9	1	0	-1.985656	0.048899	0.000000
10	6	0	-0.541867	2.184678	0.000000
11	6	0	2.485669	1.459227	0.000000
12	1	0	2.811390	-1.129069	0.000000
13	8	0	2.401238	2.667718	0.000000
14	1	0	3.486558	0.975201	0.000000
15	8	0	-1.732342	2.412114	0.000000
16	1	0	0.201974	2.991526	0.000000
17	6	0	-2.800447	-2.385170	0.000000
18	1	0	-3.270321	-3.366356	0.000000
19	1	0	-3.104495	-1.833234	0.894357
20	1	0	-3.104495	-1.833234	-0.894357

120-1,2-For-3-Me

Standard orientation:

Center Number	Atomic Number	Atomic Type	Coordinates (Angstroms) X	Y	Z
1	6	0	0.773965	1.939167	-0.000002
2	6	0	-0.519261	2.444733	0.000000
3	6	0	-1.592410	1.565822	0.000001
4	6	0	-1.416277	0.174742	0.000001
5	6	0	-0.099400	-0.341994	-0.000001
6	6	0	1.002021	0.560804	-0.000002
7	6	0	-2.652319	-0.690645	0.000002
8	6	0	0.145439	-1.817593	-0.000003
9	8	0	-0.735238	-2.653422	-0.000002
10	6	0	2.449510	0.193376	-0.000001
11	8	0	2.951067	-0.906262	0.000005
12	1	0	-0.689996	3.515042	0.000000
13	1	0	-2.603165	1.959168	0.000003
14	1	0	1.621803	2.615737	-0.000003
15	1	0	3.101802	1.092723	-0.000005
16	1	0	1.201686	-2.113827	-0.000004
17	1	0	-2.680419	-1.349666	0.869283
18	1	0	-3.545517	-0.062518	0.000006
19	1	0	-2.680425	-1.349662	-0.869282

121-1,3-For-5-Et

Standard orientation:

Center Number	Atomic Number	Atomic Type	Coordinates (Angstroms) X	Y	Z
1	6	0	1.273757	-0.812719	-0.058839
2	6	0	0.022009	-1.395243	-0.268010
3	6	0	-1.142784	-0.620755	-0.354092
4	6	0	-1.015301	0.760375	-0.225630
5	6	0	0.235059	1.361459	-0.014829
6	6	0	1.379377	0.575727	0.069357
7	6	0	-2.496625	-1.268076	-0.544984
8	6	0	-3.171387	-1.642637	0.786068
9	6	0	0.337471	2.836906	0.113287
10	8	0	-0.600682	3.596169	0.049276
11	6	0	2.484632	-1.665166	0.021226
12	8	0	3.604893	-1.249051	0.200993
13	1	0	-1.884436	1.406518	-0.291193
14	1	0	2.358055	1.016161	0.228836
15	1	0	-0.045299	-2.475313	-0.371592
16	1	0	2.292669	-2.753310	-0.098363
17	1	0	1.368799	3.214385	0.278275
18	1	0	-3.146243	-0.586209	-1.101405
19	1	0	-2.385545	-2.165796	-1.161183
20	1	0	-4.145190	-2.106489	0.609376
21	1	0	-2.558629	-2.347839	1.354044
22	1	0	-3.325124	-0.758282	1.409727

122-1,4-For-3-Me

Standard orientation:

Center Number	Atomic Number	Atomic Type	Coordinates (Angstroms) X	Y	Z
1	6	0	1.162589	-1.026490	0.000000
2	1	0	2.100890	-1.572934	0.000000
3	6	0	1.200499	0.377468	0.000000
4	6	0	0.000000	1.125993	0.000000
5	6	0	-1.198828	0.410682	0.000000
6	6	0	-1.230743	-0.986080	0.000000
7	6	0	-0.037509	-1.714555	0.000000
8	6	0	2.547062	0.999661	0.000000
9	6	0	-0.028216	2.632334	0.000000
10	1	0	-2.137677	0.957209	0.000000
11	6	0	-2.538127	-1.691253	0.000000
12	1	0	-0.079708	-2.796693	0.000000
13	8	0	-2.666147	-2.892481	0.000000
14	1	0	-3.425020	-1.022162	0.000000
15	8	0	2.789664	2.184838	0.000000
16	1	0	3.374741	0.257506	0.000000
17	1	0	-1.059157	2.991172	0.000000
18	1	0	0.488717	3.040246	0.871033
19	1	0	0.488717	3.040246	-0.871033

123-1-For-3-MeO-4-Et

Standard orientation:

Center Number	Atomic Number	Atomic Type	Coordinates (Angstroms) X	Y	Z
1	6	0	1.126150	-1.803850	-0.117633
2	6	0	1.723170	-0.552183	0.010758
3	6	0	0.937847	0.609234	-0.013260
4	6	0	-0.439254	0.510661	-0.162154
5	6	0	-1.061728	-0.754686	-0.294641
6	6	0	-0.256530	-1.890745	-0.270325
7	6	0	3.188144	-0.441722	0.170584
8	8	0	3.796345	0.598736	0.288001
9	8	0	-1.282015	1.582913	-0.196537
10	6	0	-0.723293	2.888103	-0.099334
11	6	0	-2.560719	-0.857100	-0.440827
12	1	0	-0.726650	-2.862758	-0.377671
13	1	0	1.736171	-2.700953	-0.101988
14	1	0	1.443321	1.560166	0.086931
15	1	0	-1.564988	3.575611	-0.160936
16	1	0	-0.205510	3.030943	0.854879
17	1	0	-0.029108	3.087069	-0.922426
18	1	0	3.723608	-1.415829	0.176984
19	6	0	-3.312100	-0.686513	0.892131
20	1	0	-2.905923	-0.093379	-1.142897
21	1	0	-2.805443	-1.830604	-0.875405
22	1	0	-4.391056	-0.774766	0.738373
23	1	0	-3.008950	-1.449820	1.613655
24	1	0	-3.110240	0.293922	1.326981

124-1-For-3-MeO-5-Et

Standard orientation:

Center Number	Atomic Number	Atomic Type	Coordinates (Angstroms) X	Y	Z
1	6	0	0.889709	1.168830	-0.257300
2	6	0	-0.486100	1.279890	-0.070530
3	6	0	-1.295973	0.139638	0.023753
4	6	0	-0.705116	-1.115071	-0.073520
5	6	0	0.683327	-1.220043	-0.262143
6	6	0	1.492531	-0.092579	-0.354550
7	6	0	-1.104823	2.621626	0.024771
8	8	0	-2.285902	2.829381	0.187173
9	8	0	-1.375037	-2.297294	-0.003614
10	6	0	-2.785681	-2.261189	0.181668
11	1	0	1.107220	-2.215410	-0.339035
12	6	0	2.990788	-0.227947	-0.518415
13	1	0	1.494399	2.067800	-0.333163
14	1	0	-2.358674	0.280204	0.165381
15	1	0	-3.107265	-3.300753	0.207988
16	1	0	-3.052447	-1.773614	1.125325
17	1	0	-3.284471	-1.746634	-0.646476
18	1	0	-0.387290	3.465719	-0.065407
19	6	0	3.739782	-0.248114	0.825298
20	1	0	3.213643	-1.145503	-1.071189
21	1	0	3.363502	0.601361	-1.127897
22	1	0	4.817583	-0.344233	0.668404
23	1	0	3.560203	0.670993	1.389298
24	1	0	3.410451	-1.086875	1.444101

125-1,2-For-4-Me

Standard orientation:

Center Number	Atomic Number	Atomic Type	Coordinates (Angstroms) X	Y	Z
1	6	0	1.152987	-1.710106	0.000000
2	1	0	1.589026	-2.704253	0.000000
3	6	0	1.992375	-0.589227	0.000000
4	6	0	1.390646	0.668994	0.000000
5	6	0	0.000000	0.835328	0.000000
6	6	0	-0.831307	-0.308504	0.000000
7	6	0	-0.227632	-1.569148	0.000000
8	6	0	3.491727	-0.745972	0.000000
9	6	0	-0.474244	2.245532	0.000000
10	6	0	-2.328489	-0.265438	0.000000
11	1	0	-0.877011	-2.436272	0.000000
12	8	0	-3.000370	-1.274586	0.000000
13	1	0	-2.787448	0.731880	0.000000
14	8	0	-1.618671	2.635617	0.000000
15	1	0	0.361665	2.977972	0.000000
16	1	0	2.018530	1.555197	0.000000
17	1	0	3.995890	0.221671	0.000000
18	1	0	3.827653	-1.301599	0.880578
19	1	0	3.827653	-1.301599	-0.880578

126-1,2-For-5-Me

Standard orientation:

Center Number	Atomic Number	Atomic Type	Coordinates (Angstroms) X	Y	Z
1	6	0	-2.000780	-0.095284	-0.000506
2	6	0	-3.447829	0.326435	0.000788
3	6	0	-1.633390	-1.443360	-0.000640
4	6	0	-0.292653	-1.811156	-0.000316
5	6	0	0.727608	-0.854432	0.000026
6	6	0	0.367269	0.516258	-0.000041
7	6	0	-0.981992	0.863009	-0.000329
8	6	0	2.114004	-1.385361	0.000251
9	6	0	1.360087	1.642048	-0.000025
10	1	0	-1.221441	1.920858	-0.000576
11	8	0	1.015150	2.803627	-0.000343
12	1	0	2.419677	1.354798	0.000301
13	8	0	3.144958	-0.752190	0.000538
14	1	0	2.145387	-2.496485	0.000173
15	1	0	-0.026379	-2.863363	-0.000502
16	1	0	-2.400845	-2.209863	-0.001127
17	1	0	-3.673541	0.950568	-0.868702
18	1	0	-4.116977	-0.535301	-0.017265
19	1	0	-3.680686	0.918354	0.890891

127-1,2-Vin-3-MeO

Standard orientation:

Center Number	Atomic Number	Atomic Type	Coordinates (Angstroms) X	Y	Z
1	6	0	0.288766	-2.336885	0.083026

2	6	0	1.411029	-1.508821	0.084460
3	6	0	1.242098	-0.130649	-0.022310
4	6	0	-0.048489	0.448243	-0.117871
5	6	0	-1.171549	-0.409751	-0.134384
6	6	0	-0.980703	-1.799027	-0.033947
7	6	0	-2.537621	0.113605	-0.330530
8	6	0	-3.654053	-0.414714	0.176736
9	6	0	-0.125049	1.917833	-0.200837
10	6	0	-1.045116	2.709653	0.356910
11	8	0	2.281426	0.755570	-0.023657
12	6	0	3.608652	0.256676	0.047881
13	1	0	-4.625361	0.008562	-0.050971
14	1	0	-3.638723	-1.269706	0.844189
15	1	0	-2.617000	1.002722	-0.948827
16	1	0	0.694969	2.383611	-0.738215
17	1	0	-0.992943	3.785624	0.234110
18	1	0	-1.854522	2.325400	0.965641
19	1	0	-1.841892	-2.452750	-0.090726
20	1	0	2.397742	-1.942900	0.166575
21	1	0	0.419199	-3.410886	0.154435
22	1	0	4.255717	1.131837	0.017033
23	1	0	3.782757	-0.287571	0.982613
24	1	0	3.840855	-0.395483	-0.801408

128-1,2-Vin-4-MeO

Standard orientation:

Center Number	Atomic Number	Atomic Type	Coordinates (Angstroms) X	Y	Z
1	1	0	-4.719657	-1.092178	0.136573
2	1	0	-3.344304	-2.188162	0.695408
3	6	0	-3.653398	-1.249552	0.247868
4	1	0	-3.166173	0.606919	-0.551085
5	6	0	-2.775799	-0.319663	-0.140027
6	6	0	-1.307652	-0.431134	-0.074351
7	6	0	-0.486833	0.710850	0.058556
8	6	0	-1.077430	2.056463	0.205928
9	1	0	-2.035241	2.102535	0.715783
10	6	0	-0.538910	3.198712	-0.227729
11	1	0	-1.031319	4.149086	-0.058701
12	1	0	0.396594	3.225444	-0.776450
13	6	0	0.910543	0.564050	0.092808
14	6	0	1.502848	-0.690862	-0.018381
15	1	0	-1.295840	-2.565996	-0.335932
16	6	0	-0.681680	-1.685244	-0.189544
17	6	0	0.692362	-1.824801	-0.160903
18	8	0	2.845780	-0.921468	0.008388
19	1	0	1.166169	-2.794224	-0.255008
20	1	0	1.516434	1.446156	0.245488
21	6	0	3.723229	0.187938	0.139211
22	1	0	4.729950	-0.226314	0.122094
23	1	0	3.607410	0.892083	-0.692338
24	1	0	3.566055	0.715850	1.086442

129-1,2-Vin-3-For

Standard orientation:

Center Number	Atomic Number	Atomic Type	Coordinates (Angstroms) X	Y	Z
1	6	0	0.136492	-2.349046	0.259953
2	1	0	0.186562	-3.422494	0.401829
3	6	0	-1.086933	-1.718779	0.107207
4	6	0	-1.154397	-0.330056	-0.066426
5	6	0	0.024795	0.447821	-0.059066
6	6	0	1.276637	-0.204913	0.069308
7	6	0	1.306199	-1.594149	0.235857
8	1	0	-2.016941	-2.274182	0.103379
9	6	0	-2.499445	0.243217	-0.353209
10	6	0	-0.002973	1.922897	-0.188688
11	6	0	2.532147	0.572875	0.085022
12	1	0	2.262608	-2.081958	0.384106
13	6	0	3.707098	0.156167	-0.391809
14	1	0	2.473081	1.565030	0.523067
15	1	0	4.590860	0.779443	-0.324515
16	1	0	3.826264	-0.808208	-0.874317
17	6	0	-0.754791	2.750591	0.538931
18	1	0	0.681720	2.348191	-0.918437
19	1	0	-0.712089	3.823478	0.390220
20	1	0	-1.420151	2.389874	1.316185
21	8	0	-3.533924	-0.371510	-0.209298
22	1	0	-2.509487	1.273148	-0.749617

130-1,2-Vin-4-For

Standard orientation:

Center	Atomic	Atomic	Coordinates (Angstroms)

Number	Number	Type	X	Y	Z
1	6	0	1.241557	-1.342968	-0.139363
2	1	0	1.987857	-2.123182	-0.229181
3	6	0	1.665499	-0.018248	0.028133
4	6	0	0.717114	0.996829	0.135324
5	6	0	-0.656249	0.731464	0.075234
6	6	0	-1.080023	-0.611446	-0.083796
7	6	0	-0.110302	-1.625401	-0.195374
8	6	0	3.106742	0.307892	0.100328
9	6	0	-1.633027	1.829288	0.223161
10	6	0	-2.513423	-0.943528	-0.176999
11	1	0	-0.437502	-2.644903	-0.361227
12	6	0	-3.072889	-2.088951	0.221219
13	1	0	-3.153980	-0.179091	-0.606458
14	1	0	-4.135714	-2.262295	0.101873
15	1	0	-2.499986	-2.881203	0.690818
16	6	0	-1.465312	3.078849	-0.214896
17	1	0	-2.557173	1.582192	0.737523
18	1	0	-2.220204	3.837381	-0.045473
19	1	0	-0.582098	3.384561	-0.765788
20	1	0	1.050961	2.016249	0.300681
21	8	0	4.002799	-0.500031	0.011524
22	1	0	3.327323	1.387851	0.247216

131-1,2-Vin-3-Me

Standard orientation:

Center Number	Atomic Number	Atomic Type	Coordinates (Angstroms) X	Y	Z
1	6	0	0.727094	-2.307997	0.105567
2	6	0	1.811044	-1.434243	0.111216
3	6	0	1.624685	-0.058846	-0.014206
4	6	0	0.312655	0.459605	-0.129351
5	6	0	-0.792143	-0.428602	-0.145185
6	6	0	-0.557660	-1.807684	-0.031643
7	6	0	-2.173949	0.050913	-0.346800
8	6	0	-3.276240	-0.514083	0.152250
9	6	0	0.151606	1.926154	-0.224840
10	6	0	-0.752747	2.676758	0.408700
11	6	0	2.827527	0.856437	0.008484
12	1	0	-4.258978	-0.120079	-0.078868
13	1	0	-3.238756	-1.371831	0.815344
14	1	0	-2.280538	0.940408	-0.960282
15	1	0	0.880229	2.436152	-0.850822
16	1	0	-0.772947	3.752668	0.275885
17	1	0	-1.484894	2.252066	1.085277
18	1	0	2.818356	-1.824806	0.210764
19	1	0	-1.398617	-2.488224	-0.088967
20	1	0	0.888954	-3.376961	0.188615
21	1	0	3.742406	0.284687	0.172434
22	1	0	2.943461	1.399532	-0.935706
23	1	0	2.750088	1.605928	0.801161

132-1,2-Vin-4-Me

Standard orientation:

Center Number	Atomic Number	Atomic Type	Coordinates (Angstroms) X	Y	Z
1	1	0	4.177435	-1.614332	-0.090221
2	1	0	2.678169	-2.500270	-0.702338
3	6	0	3.101777	-1.625232	-0.220939
4	1	0	2.845667	0.258310	0.625771
5	6	0	2.347788	-0.599181	0.181980
6	6	0	0.877814	-0.517751	0.086007
7	6	0	0.220161	0.724571	-0.071747
8	6	0	0.987418	1.977870	-0.215536
9	1	0	1.952648	1.893121	-0.706686
10	6	0	0.595657	3.184686	0.200380
11	1	0	1.211416	4.060899	0.034748
12	1	0	-0.339554	3.338400	0.728207
13	6	0	-1.181447	0.748223	-0.135575
14	6	0	-1.955227	-0.404604	-0.032729
15	6	0	-3.462269	-0.346115	-0.092745
16	1	0	0.584750	-2.628368	0.357030
17	6	0	0.093307	-1.676232	0.193084
18	6	0	-1.290753	-1.626185	0.133057
19	1	0	-1.864492	-2.543454	0.221681
20	1	0	-1.675121	1.699176	-0.304440
21	1	0	-3.905168	-0.592835	0.877950
22	1	0	-3.811613	0.649419	-0.373269
23	1	0	-3.859492	-1.060364	-0.819850

133-1,3-Vin-2-OH

Standard orientation:

Center Number	Atomic Number	Atomic Type	Coordinates (Angstroms) X	Y	Z
1	6	0	0.357808	2.261281	0.076720
2	1	0	0.562148	3.323721	0.134220
3	6	0	-0.947215	1.806845	-0.063323
4	6	0	-1.239754	0.436720	-0.098834
5	6	0	-0.164584	-0.476229	-0.057327
6	6	0	1.169071	-0.034969	0.064240
7	6	0	1.398447	1.343666	0.152957
8	1	0	-1.766815	2.515389	-0.119865
9	6	0	-2.646201	0.012823	-0.211602
10	8	0	-0.363986	-1.821662	-0.161178
11	6	0	2.255797	-1.026637	0.101593
12	1	0	2.413572	1.697696	0.288189
13	6	0	3.555071	-0.786294	-0.093628
14	1	0	1.940761	-2.046197	0.293354
15	1	0	4.281371	-1.587824	-0.032730
16	1	0	3.942441	0.198926	-0.329632
17	6	0	-3.225913	-1.072727	0.317920
18	1	0	-3.278416	0.696367	-0.774845
19	1	0	-4.281694	-1.263051	0.167256
20	1	0	-2.697378	-1.769665	0.959601
21	1	0	-1.279261	-1.978935	-0.428421

Table A-16 Optimized geometries at the level of G4.

1-Benzene

Standard orientation:

Center Number	Atomic Number	Atomic Type	Coordinates (Angstroms) X	Y	Z
1	6	0	0.000000	0.000000	1.393611
2	1	0	0.000000	0.000000	2.478748
3	6	0	0.000000	1.206884	0.696801
4	6	0	0.000000	1.206893	-0.696801
5	6	0	0.000000	0.000000	-1.393598
6	6	0	0.000000	-1.206893	-0.696801
7	6	0	0.000000	-1.206884	0.696801
8	1	0	0.000000	2.146700	1.239404
9	1	0	0.000000	2.146705	-1.239410
10	1	0	0.000000	0.000000	-2.478803
11	1	0	0.000000	-2.146705	-1.239410
12	1	0	0.000000	-2.146700	1.239404

2-Phenol

Standard orientation:

Center Number	Atomic Number	Atomic Type	Coordinates (Angstroms) X	Y	Z
1	6	0	-1.185904	-1.160917	0.000000
2	1	0	-2.125877	-1.703156	0.000000
3	6	0	0.021581	-1.853496	0.000000
4	6	0	1.218293	-1.137149	0.000000
5	6	0	1.215186	0.252730	0.000000
6	6	0	0.000000	0.940372	0.000000
7	6	0	-1.202650	0.231662	0.000000
8	1	0	0.031421	-2.937490	0.000000
9	1	0	2.166431	-1.665120	0.000000
10	1	0	2.137594	0.822023	0.000000
11	8	0	0.048597	2.303260	0.000000
12	1	0	-2.147480	0.769421	0.000000
13	1	0	-0.849904	2.649032	0.000000

3-Anisole

Standard orientation:

Center Number	Atomic Number	Atomic Type	Coordinates (Angstroms) X	Y	Z
1	6	0	0.474288	-1.835139	0.000000
2	1	0	1.202209	-2.640226	0.000000
3	6	0	-0.884408	-2.125385	0.000000
4	6	0	-1.804214	-1.074784	0.000000
5	6	0	-1.370257	0.242327	0.000000
6	6	0	0.000000	0.530079	0.000000
7	6	0	0.927303	-0.514677	0.000000
8	1	0	-1.226287	-3.154227	0.000000
9	1	0	-2.869159	-1.283753	0.000000
10	1	0	-2.069732	1.070543	0.000000
11	8	0	0.325032	1.852243	0.000000
12	1	0	1.990933	-0.315034	0.000000
13	6	0	1.694340	2.203493	0.000000
14	1	0	1.728616	3.294282	0.000000
15	1	0	2.210426	1.827493	0.893042
16	1	0	2.210426	1.827493	-0.893042

4-Benzaldehyde

Standard orientation:

Center Number	Atomic Number	Atomic Type	Coordinates (Angstroms) X	Y	Z
1	6	0	-0.743124	-1.722476	0.000000
2	1	0	-1.544589	-2.453591	0.000000
3	6	0	0.587931	-2.147305	0.000000
4	6	0	1.624767	-1.216305	0.000000
5	6	0	1.329458	0.143240	0.000000
6	6	0	0.000000	0.573398	0.000000
7	6	0	-1.038018	-0.366768	0.000000
8	1	0	0.815414	-3.208371	0.000000
9	1	0	2.656687	-1.550358	0.000000
10	1	0	2.128380	0.879708	0.000000
11	6	0	-0.303930	2.021247	0.000000
12	1	0	-2.060726	-0.006499	0.000000
13	8	0	-1.416786	2.494029	0.000000
14	1	0	0.596619	2.676689	0.000000

5-Styrene

Standard orientation:

Center Number	Atomic Number	Atomic Type	Coordinates (Angstroms) X	Y	Z
1	6	0	-1.360536	1.326059	-0.000013
2	1	0	-1.729458	2.346687	-0.000022
3	6	0	-2.260767	0.259867	0.000018
4	6	0	-1.776225	-1.044704	0.000025
5	6	0	-0.404662	-1.277922	0.000003
6	6	0	0.514253	-0.218768	-0.000023
7	6	0	0.007597	1.090907	-0.000033
8	1	0	-3.329257	0.447386	0.000034
9	1	0	-2.465449	-1.882834	0.000047
10	1	0	-0.031632	-2.298020	0.000009
11	6	0	1.950642	-0.526277	-0.000036
12	1	0	0.690848	1.933202	-0.000063
13	6	0	2.971767	0.333184	0.000054
14	1	0	2.179177	-1.591039	-0.000156
15	1	0	3.996920	-0.019040	0.000012
16	1	0	2.836431	1.409581	0.000166

6-Toluene

Standard orientation:

Center Number	Atomic Number	Atomic Type	Coordinates (Angstroms) X	Y	Z
1	6	0	1.198485	-1.202757	0.002093
2	1	0	1.734939	-2.146274	0.001133
3	6	0	1.900925	-0.000076	0.008243
4	6	0	1.198653	1.202665	0.002082
5	6	0	-0.193673	1.199829	-0.008558
6	6	0	-0.911369	0.000100	-0.010621
7	6	0	-0.193804	-1.199749	-0.008568
8	1	0	2.985809	-0.000151	0.013186
9	1	0	1.735209	2.146115	0.001111
10	1	0	-0.733383	2.142597	-0.017394
11	6	0	-2.420634	0.000029	0.008620
12	1	0	-0.733635	-2.142453	-0.017429
13	1	0	-2.827520	-0.884665	-0.489922
14	1	0	-2.805328	-0.001933	1.036223
15	1	0	-2.827590	0.886508	-0.486652

7-Ethyl Benzene

Standard orientation:

Center Number	Atomic Number	Atomic Type	Coordinates (Angstroms) X	Y	Z
1	6	0	-0.269959	-1.200094	-0.184120
2	6	0	0.433680	-0.000399	-0.326786
3	6	0	-0.269385	1.199820	-0.184515
4	6	0	-1.633310	1.203282	0.095573
5	6	0	-2.320917	0.000403	0.237440
6	6	0	-1.633860	-1.202998	0.095910
7	6	0	1.922215	-0.000524	-0.592745
8	6	0	2.757106	0.000409	0.699857
9	1	0	2.187307	-0.879477	-1.191733
10	1	0	2.187181	0.877593	-1.193052
11	1	0	0.258837	2.142361	-0.299463
12	1	0	-2.160397	2.146545	0.197907
13	1	0	-3.384399	0.000727	0.452141
14	1	0	-2.161314	-2.145972	0.198487
15	1	0	0.258004	-2.142885	-0.298736
16	1	0	2.536369	0.883983	1.307140
17	1	0	2.536465	-0.882414	1.308430
18	1	0	3.828528	0.000154	0.475187

8-O-DOH

Standard orientation:

Center Number	Atomic Number	Atomic Type	Coordinates (Angstroms) X	Y	Z
1	6	0	-1.907879	-0.658455	0.000000
2	6	0	-1.877643	0.731730	0.000000
3	6	0	-0.651110	1.398818	0.000000
4	6	0	0.531265	0.672945	0.000000
5	6	0	0.504034	-0.730200	0.000000
6	6	0	-0.719162	-1.388391	0.000000
7	8	0	1.663838	-1.440688	0.000000
8	1	0	-0.720727	-2.472533	0.000000
9	1	0	-2.856600	-1.183475	0.000000

10	1	0	-0.612843	2.485196	0.000000
11	1	0	2.392107	-0.806875	0.000000
12	1	0	-2.798730	1.303258	0.000000
13	8	0	1.786769	1.231367	0.000000
14	1	0	1.714917	2.190320	0.000000

9-M-DOH

Standard orientation:

Center Number	Atomic Number	Atomic Type	Coordinates (Angstroms) X	Y	Z
1	6	0	-1.227088	-1.087823	0.000000
2	6	0	-0.020984	-1.775366	0.000000
3	6	0	1.198530	-1.100979	0.000000
4	6	0	1.201358	0.294184	0.000000
5	6	0	0.000000	1.003116	0.000000
6	6	0	-1.208231	0.309652	0.000000
7	8	0	2.350987	1.027021	0.000000
8	8	0	-2.409265	0.952889	0.000000
9	1	0	-0.026744	-2.860454	0.000000
10	1	0	2.135830	-1.649413	0.000000
11	1	0	0.028911	2.088356	0.000000
12	1	0	-2.179222	-1.603552	0.000000
13	1	0	-2.256725	1.903515	0.000000
14	1	0	3.102671	0.425572	0.000000

10-P-DOH

Standard orientation:

Center Number	Atomic Number	Atomic Type	Coordinates (Angstroms) X	Y	Z
1	6	0	-0.695463	1.206427	0.000000
2	1	0	-1.247619	2.139095	0.000000
3	6	0	-1.399663	0.003821	0.000000
4	6	0	-0.695463	-1.200958	0.000000
5	6	0	0.695462	-1.206426	0.000000
6	6	0	1.399663	-0.003821	0.000000
7	6	0	0.695462	1.200959	0.000000
8	1	0	1.247617	-2.139093	0.000000
9	8	0	2.766462	-0.066064	0.000000
10	1	0	1.235614	2.144308	0.000000
11	1	0	3.119092	0.829272	0.000000
12	1	0	-1.235615	-2.144307	0.000000
13	8	0	-2.766462	0.066061	0.000000
14	1	0	-3.119089	-0.829275	0.000000

11-O-DMeO

Standard orientation:

Center Number	Atomic Number	Atomic Type	Coordinates (Angstroms) X	Y	Z
1	6	0	-2.128337	-1.095455	0.000000
2	1	0	-2.946212	-1.807469	0.000000
3	6	0	-2.378941	0.265299	0.000000
4	6	0	-1.313945	1.173036	0.000000
5	6	0	0.000000	0.720198	0.000000
6	6	0	0.256580	-0.672981	0.000000
7	6	0	-0.809821	-1.564216	0.000000
8	1	0	-3.396812	0.639227	0.000000
9	1	0	-1.519390	2.235691	0.000000
10	8	0	1.101964	1.516196	0.000000
11	8	0	1.569842	-1.024086	0.000000
12	1	0	-0.623262	-2.630359	0.000000
13	6	0	1.886168	-2.400542	0.000000
14	1	0	2.975831	-2.460969	0.000000
15	1	0	1.497194	-2.907782	0.892942
16	1	0	1.497194	-2.907782	-0.892942
17	6	0	0.906965	2.915017	0.000000
18	1	0	1.903535	3.359832	0.000000
19	1	0	0.362734	3.250300	-0.892937
20	1	0	0.362734	3.250300	0.892937

12-M-DMeO

Standard orientation:

Center Number	Atomic Number	Atomic Type	Coordinates (Angstroms) X	Y	Z
1	6	0	-0.542280	-2.018632	0.000000
2	1	0	-0.753496	-3.083177	0.000000
3	6	0	0.789483	-1.591673	0.000000
4	6	0	1.051183	-0.223037	0.000000
5	6	0	0.000000	0.704899	0.000000

6	6	0	-1.316424	0.256579	0.000000
7	6	0	-1.592500	-1.118959	0.000000
8	1	0	1.589653	-2.318831	0.000000
9	8	0	2.297596	0.326372	0.000000
10	1	0	0.255762	1.755436	0.000000
11	8	0	-2.402476	1.075939	0.000000
12	1	0	-2.625716	-1.443767	0.000000
13	6	0	-2.186671	2.473444	0.000000
14	1	0	-3.176124	2.933823	0.000000
15	1	0	-1.637255	2.798836	0.892826
16	1	0	-1.637255	2.798836	-0.892826
17	6	0	3.410048	-0.546221	0.000000
18	1	0	4.296190	0.090885	0.000000
19	1	0	3.425122	-1.184462	0.892910
20	1	0	3.425122	-1.184462	-0.892910

13-P-DMeO

Standard orientation:

Center Number	Atomic Number	Atomic Type	Coordinates (Angstroms) X	Y	Z
1	6	0	1.431821	-0.764490	0.000000
2	1	0	2.434763	-1.176087	0.000000
3	6	0	1.281330	0.629110	0.000000
4	6	0	0.000000	1.171386	0.000000
5	6	0	-1.122735	0.334116	0.000000
6	6	0	-0.968428	-1.048650	0.000000
7	6	0	0.324373	-1.590363	0.000000
8	8	0	2.439387	1.352624	0.000000
9	1	0	-2.106578	0.785258	0.000000
10	8	0	-1.992125	-1.952302	0.000000
11	1	0	0.432805	-2.669041	0.000000
12	6	0	-3.312648	-1.453339	0.000000
13	1	0	-3.969526	-2.325056	0.000000
14	1	0	-3.519545	-0.847831	0.892837
15	1	0	-3.519545	-0.847831	-0.892837
16	6	0	2.337664	2.760602	0.000000
17	1	0	3.360489	3.141664	0.000000
18	1	0	1.816269	3.131544	-0.892838
19	1	0	1.816269	3.131544	0.892838
20	1	0	-0.151756	2.243036	0.000000

14-O-DFor

Standard orientation:

Center Number	Atomic Number	Atomic Type	Coordinates (Angstroms) X	Y	Z
1	6	0	2.392134	0.144038	0.000000
2	1	0	3.407441	0.526212	0.000000
3	6	0	2.161961	-1.229796	0.000000
4	6	0	0.855512	-1.704922	0.000000
5	6	0	-0.237100	-0.830103	0.000000
6	6	0	0.000000	0.565390	0.000000
7	6	0	1.317886	1.027155	0.000000
8	1	0	2.993928	-1.925563	0.000000
9	1	0	0.669294	-2.774945	0.000000
10	6	0	-1.575509	-1.475824	0.000000
11	6	0	-1.082845	1.601972	0.000000
12	1	0	1.471398	2.100215	0.000000
13	8	0	-0.833907	2.787529	0.000000
14	1	0	-2.115137	1.224097	0.000000
15	8	0	-2.654709	-0.931339	0.000000
16	1	0	-1.510236	-2.587000	0.000000

15-M-DFor

Standard orientation:

Center Number	Atomic Number	Atomic Type	Coordinates (Angstroms) X	Y	Z
1	6	0	-1.310662	1.173779	-0.000072
2	6	0	-0.237642	2.053500	-0.000076
3	6	0	1.064986	1.553945	0.000016
4	6	0	1.296926	0.176589	0.000121
5	6	0	0.211646	-0.705807	0.000156
6	6	0	-1.088808	-0.212565	0.000042
7	6	0	2.684019	-0.344254	0.000119
8	8	0	2.974170	-1.517054	-0.000278
9	6	0	-2.238303	-1.149808	0.000035
10	8	0	-3.397271	-0.808678	-0.000048
11	1	0	-0.409514	3.124213	-0.000173
12	1	0	1.911374	2.235449	-0.000006
13	1	0	0.407634	-1.774009	0.000263
14	1	0	-2.335253	1.529261	-0.000173
15	1	0	-1.952660	-2.224774	0.000117
16	1	0	3.470259	0.443439	0.000536

16-P-DFor

Standard orientation:

Center Number	Atomic Number	Atomic Type	Coordinates (Angstroms) X	Y	Z
1	6	0	1.215061	-0.696352	0.000000
2	6	0	1.211984	0.689896	0.000000
3	6	0	0.000000	1.391189	0.000000
4	6	0	-1.215070	0.696388	0.000000
5	6	0	-1.211911	-0.689889	0.000000
6	6	0	0.000021	-1.391199	0.000000
7	6	0	0.007081	2.874893	0.000000
8	8	0	-0.985590	3.563244	0.000000
9	6	0	-0.007102	-2.874891	0.000000
10	8	0	0.985531	-3.563291	0.000000
11	1	0	2.147722	1.241760	0.000000
12	1	0	-2.137565	1.265689	0.000000
13	1	0	-2.147617	-1.241762	0.000000
14	1	0	2.137596	-1.265576	0.000000
15	1	0	-1.022832	-3.329023	0.000000
16	1	0	1.022783	3.329075	0.000000

17-O-DVin

Standard orientation:

Center Number	Atomic Number	Atomic Type	Coordinates (Angstroms) X	Y	Z
1	6	0	0.691258	2.292345	-0.084430
2	1	0	1.235046	3.228318	-0.157269
3	6	0	-0.692114	2.292102	0.084434
4	6	0	-1.373404	1.085382	0.167656
5	6	0	-0.703334	-0.143031	0.080781
6	6	0	0.703438	-0.142803	-0.080585
7	6	0	1.373004	1.085893	-0.167605
8	1	0	-1.236266	3.227876	0.157089
9	1	0	-2.445118	1.084227	0.334766
10	6	0	-1.452750	-1.406365	0.202205
11	6	0	1.453116	-1.405930	-0.201793
12	1	0	2.444671	1.085224	-0.335017
13	6	0	2.713432	-1.607714	0.188727
14	1	0	0.916575	-2.235640	-0.655085
15	1	0	3.201613	-2.564573	0.040980
16	1	0	3.298889	-0.835749	0.678022
17	6	0	-2.712683	-1.608529	-0.189280
18	1	0	-0.916478	-2.235646	0.656635
19	1	0	-3.200924	-2.565344	-0.041426
20	1	0	-3.297785	-0.836784	-0.679354

18-M-DVin

Standard orientation:

Center Number	Atomic Number	Atomic Type	Coordinates (Angstroms) X	Y	Z
1	6	0	-0.407196	-2.048797	0.000000
2	1	0	-0.569550	-3.121757	0.000000
3	6	0	-1.499747	-1.184538	0.000000
4	6	0	-1.315068	0.203302	0.000000
5	6	0	0.000000	0.689950	0.000000
6	6	0	1.109511	-0.159111	0.000000
7	6	0	0.885232	-1.547251	0.000000
8	1	0	-2.508502	-1.586314	0.000000
9	6	0	-2.495854	1.077923	0.000000
10	1	0	0.173078	1.761569	0.000000
11	6	0	2.453898	0.434873	0.000000
12	1	0	1.725191	-2.232759	0.000000
13	6	0	3.627545	-0.200141	0.000000
14	1	0	2.461348	1.523762	0.000000
15	1	0	4.560170	0.352288	0.000000
16	1	0	3.712893	-1.281603	0.000000
17	6	0	-2.526711	2.412077	0.000000
18	1	0	-3.445190	0.544562	0.000000
19	1	0	-3.469027	2.947780	0.000000
20	1	0	-1.630068	3.022748	0.000000

19-P-DVin

Standard orientation:

Center Number	Atomic Number	Atomic Type	Coordinates (Angstroms) X	Y	Z
1	6	0	0.691218	-0.993524	-0.000058
2	6	0	-0.691203	-0.993531	-0.000087

3	6	0	-1.422530	0.208366	-0.000050
4	6	0	-0.694235	1.404929	-0.000004
5	6	0	0.694231	1.404936	0.000028
6	6	0	1.422534	0.208379	0.000005
7	6	0	-2.887760	0.262164	-0.000063
8	6	0	-3.743958	-0.762705	0.000132
9	6	0	2.887765	0.262173	0.000038
10	6	0	3.743942	-0.762713	0.000031
11	1	0	-1.216454	-1.942517	-0.000161
12	1	0	-1.230096	2.349659	0.000015
13	1	0	1.230083	2.349671	0.000069
14	1	0	1.216483	-1.942503	-0.000094
15	1	0	3.297988	1.270947	0.000073
16	1	0	4.814751	-0.594689	0.000059
17	1	0	3.422601	-1.798854	-0.000001
18	1	0	-3.297970	1.270944	-0.000236
19	1	0	-4.814763	-0.594655	0.000098
20	1	0	-3.422647	-1.798854	0.000344

20-O-DMe

Standard orientation:

Center Number	Atomic Number	Atomic Type	Coordinates (Angstroms) X	Y	Z
1	6	0	-1.956868	0.694978	0.000017
2	1	0	-2.892098	1.245348	0.000041
3	6	0	-1.956847	-0.695054	0.000011
4	6	0	-0.744853	-1.381016	-0.000022
5	6	0	0.476042	-0.704384	-0.000037
6	6	0	0.476004	0.704398	-0.000033
7	6	0	-0.744907	1.380992	-0.000008
8	1	0	-2.891957	-1.245401	0.000027
9	1	0	-0.743193	-2.467359	-0.000030
10	6	0	1.772008	-1.477154	0.000002
11	6	0	1.771930	1.477220	-0.000001
12	1	0	-0.743281	2.467335	-0.000006
13	1	0	1.587657	2.554478	-0.000611
14	1	0	2.384648	1.243543	0.879109
15	1	0	2.385276	1.242602	-0.878412
16	1	0	2.385470	-1.242646	-0.878333
17	1	0	2.384656	-1.243363	0.879139
18	1	0	1.587772	-2.554421	-0.000502

21-M-DMe

Standard orientation:

Center Number	Atomic Number	Atomic Type	Coordinates (Angstroms) X	Y	Z
1	6	0	0.000233	1.819483	0.004449
2	1	0	0.000332	2.904987	0.003627
3	6	0	-1.207006	1.127281	-0.000511
4	6	0	-1.222177	-0.269804	-0.009376
5	6	0	-0.000117	-0.946678	-0.018112
6	6	0	1.221923	-0.270225	-0.009193
7	6	0	1.207122	1.127078	-0.000264
8	1	0	-2.145370	1.674178	-0.003899
9	6	0	-2.526373	-1.029948	0.009584
10	1	0	-0.000258	-2.034014	-0.035675
11	6	0	2.526277	-1.030114	0.009460
12	1	0	2.145656	1.673708	-0.003480
13	1	0	3.304477	-0.503402	-0.551186
14	1	0	2.897478	-1.157896	1.034031
15	1	0	2.413969	-2.029060	-0.421670
16	1	0	-2.419426	-2.020147	-0.442724
17	1	0	-2.885129	-1.178651	1.035783
18	1	0	-3.311026	-0.492144	-0.531027

22-P-DMe

Standard orientation:

Center Number	Atomic Number	Atomic Type	Coordinates (Angstroms) X	Y	Z
1	6	0	0.695696	1.195819	0.007657
2	1	0	1.229848	2.141964	0.012922
3	6	0	1.418357	0.000210	0.012994
4	6	0	0.695551	-1.195629	0.007666
5	6	0	-0.695563	-1.195623	-0.007675
6	6	0	-1.418357	0.000223	-0.012999
7	6	0	-0.695685	1.195825	-0.007666
8	6	0	2.927438	-0.000203	-0.004571
9	1	0	1.229736	-2.141776	0.012974
10	1	0	-1.229756	-2.141766	-0.012995
11	6	0	-2.927437	-0.000197	0.004588
12	1	0	-1.229832	2.141974	-0.012942
13	1	0	-3.333366	0.892388	-0.480667

14	1	0	-3.333313	-0.878191	-0.506830
15	1	0	-3.315680	-0.015672	1.030801
16	1	0	3.333305	-0.878433	0.506445
17	1	0	3.315700	-0.015186	-1.030783
18	1	0	3.333361	0.892156	0.481113

23-O-DEt

Standard orientation:

Center Number	Atomic Number	Atomic Type	Coordinates (Angstroms) X	Y	Z
1	6	0	1.236587	1.282653	-0.503874
2	1	0	1.234711	2.293434	-0.903323
3	6	0	2.448092	0.647509	-0.254523
4	6	0	2.448090	-0.647521	0.254520
5	6	0	1.236584	-1.282661	0.503872
6	6	0	0.010696	-0.655506	0.256662
7	6	0	0.010698	0.655502	-0.256662
8	1	0	3.383001	1.159284	-0.458071
9	1	0	3.382998	-1.159299	0.458066
10	1	0	1.234705	-2.293442	0.903322
11	6	0	-1.266918	-1.429779	0.514727
12	6	0	-1.266914	1.429780	-0.514723
13	1	0	-2.067548	-0.760137	0.843178
14	6	0	-1.741303	-2.226776	-0.714168
15	1	0	-1.095786	-2.126759	1.342966
16	1	0	-2.655773	-2.785698	-0.490454
17	1	0	-1.946596	-1.565973	-1.562396
18	1	0	-0.975043	-2.940422	-1.032789
19	6	0	-1.741280	2.226793	0.714168
20	1	0	-1.095785	2.126750	-1.342972
21	1	0	-2.067551	0.760141	-0.843158
22	1	0	-2.655748	2.785719	0.490459
23	1	0	-1.946569	1.565999	1.562404
24	1	0	-0.975012	2.940437	1.032775

24-M-DEt

Standard orientation:

Center Number	Atomic Number	Atomic Type	Coordinates (Angstroms) X	Y	Z
1	6	0	0.000010	-0.659390	-0.000039
2	6	0	1.178202	0.017270	0.325384
3	6	0	1.162419	1.414804	0.323735
4	6	0	-0.000041	2.108115	-0.000001
5	6	0	-1.162481	1.414776	-0.323744
6	6	0	-1.178212	0.017239	-0.325417
7	6	0	2.448851	-0.744032	0.631020
8	6	0	3.299855	-1.008622	-0.623424
9	6	0	-2.448848	-0.744092	-0.631032
10	6	0	-3.299781	-1.008642	0.623492
11	1	0	2.066401	1.961116	0.577777
12	1	0	-0.000045	3.193625	0.000002
13	1	0	-2.066486	1.961045	-0.577797
14	1	0	0.000029	-1.747446	-0.000078
15	1	0	-3.045696	-0.182200	-1.358819
16	1	0	-2.198424	-1.700498	-1.104435
17	1	0	-4.211627	-1.559343	0.370851
18	1	0	-2.739973	-1.595513	1.358665
19	1	0	-3.591245	-0.068961	1.103366
20	1	0	3.045640	-0.182117	1.358840
21	1	0	2.198414	-1.700428	1.104446
22	1	0	4.211677	-1.559326	-0.370695
23	1	0	2.740107	-1.595525	-1.358620
24	1	0	3.591390	-0.068982	-1.103338

25-P-DEt

Standard orientation:

Center Number	Atomic Number	Atomic Type	Coordinates (Angstroms) X	Y	Z
1	6	0	0.675644	1.196378	0.165874
2	1	0	1.195414	2.142142	0.293880
3	6	0	1.377376	-0.000079	0.336885
4	6	0	0.675543	-1.196342	0.165938
5	6	0	-0.675644	-1.196354	-0.165875
6	6	0	-1.377376	0.000105	-0.336885
7	6	0	-0.675543	1.196367	-0.165939
8	6	0	2.855430	0.000077	0.654941
9	1	0	1.195341	-2.142136	0.293986
10	1	0	-1.195414	-2.142117	-0.293881
11	6	0	-2.855430	-0.000054	-0.654940
12	1	0	-1.195341	2.142161	-0.293986
13	6	0	-3.737074	-0.000006	0.606218
14	1	0	-3.098907	0.878315	-1.264054

15	1	0	-3.098706	-0.878564	-1.263963
16	1	0	-4.799783	0.000015	0.343024
17	1	0	-3.538519	-0.883092	1.221876
18	1	0	-3.538667	0.883252	1.221804
19	1	0	3.098719	0.878624	1.263904
20	1	0	3.098893	-0.878255	1.264114
21	6	0	3.737075	-0.000070	-0.606217
22	1	0	4.799783	-0.000093	-0.343023
23	1	0	3.538652	-0.883365	-1.221746
24	1	0	3.538535	0.882979	-1.221933

26-O-OHMeO

Standard orientation:

Center Number	Atomic Number	Atomic Type	Coordinates (Angstroms) X	Y	Z
1	6	0	-0.015766	-1.391688	0.000007
2	1	0	0.685392	-2.216928	-0.000033
3	6	0	-1.391346	-1.645323	0.000000
4	6	0	-2.294987	-0.591177	0.000005
5	6	0	-1.837275	0.727644	0.000006
6	6	0	-0.475289	0.989331	-0.000009
7	6	0	0.440524	-0.080227	-0.000026
8	1	0	-1.742870	-2.670933	0.000009
9	1	0	-3.361760	-0.786046	0.000025
10	1	0	-2.524132	1.566448	0.000044
11	8	0	-0.022714	2.270832	0.000007
12	8	0	1.752892	0.317717	-0.000108
13	1	0	0.942444	2.227674	0.000248
14	6	0	2.753423	-0.681772	0.000059
15	1	0	3.711187	-0.158901	-0.001077
16	1	0	2.686918	-1.314419	0.894107
17	1	0	2.685701	-1.316023	-0.892762

27-M-OHMeO

Standard orientation:

Center Number	Atomic Number	Atomic Type	Coordinates (Angstroms) X	Y	Z
1	6	0	-0.832019	-0.347805	0.000000
2	8	0	-2.190355	-0.284675	0.000000
3	6	0	-0.283722	-1.637876	0.000000
4	6	0	1.093017	-1.790614	0.000000
5	6	0	1.943074	-0.684080	0.000000
6	6	0	1.386512	0.592336	0.000000
7	6	0	0.000000	0.770523	0.000000
8	1	0	-0.953747	-2.488663	0.000000
9	1	0	1.519275	-2.788494	0.000000
10	1	0	3.021499	-0.812194	0.000000
11	8	0	2.146138	1.725756	0.000000
12	1	0	-0.385317	1.780690	0.000000
13	1	0	3.075834	1.475988	0.000000
14	6	0	-2.802905	0.990192	0.000000
15	1	0	-3.879163	0.809814	0.000000
16	1	0	-2.534194	1.569076	0.892959
17	1	0	-2.534194	1.569076	-0.892959

28-P-OHMeO

Standard orientation:

Center Number	Atomic Number	Atomic Type	Coordinates (Angstroms) X	Y	Z
1	6	0	-1.519443	-0.912989	0.000000
2	6	0	-1.301088	0.454127	0.000000
3	6	0	0.000000	0.971470	0.000000
4	6	0	1.081002	0.091696	0.000000
5	6	0	0.857139	-1.287737	0.000000
6	6	0	-0.436384	-1.797039	0.000000
7	8	0	0.100329	2.333596	0.000000
8	6	0	1.393275	2.900124	0.000000
9	8	0	-0.712282	-3.136773	0.000000
10	1	0	-2.132199	1.150201	0.000000
11	1	0	2.099626	0.457098	0.000000
12	1	0	1.707341	-1.965232	0.000000
13	1	0	-2.525637	-1.316248	0.000000
14	1	0	0.116760	-3.625504	0.000000
15	1	0	1.253317	3.982615	0.000000
16	1	0	1.964708	2.612289	0.892942
17	1	0	1.964708	2.612289	-0.892942

29-O-OHFor

Standard orientation:

Center Number	Atomic Number	Atomic Type	Coordinates (Angstroms) X	Y	Z
1	6	0	1.385889	0.876174	0.000000
2	1	0	1.739226	1.903780	0.000000
3	6	0	2.281467	-0.175943	0.000000
4	6	0	1.786574	-1.488515	0.000000
5	6	0	0.425800	-1.749559	0.000000
6	6	0	-0.488002	-0.688285	0.000000
7	6	0	0.000000	0.644305	0.000000
8	1	0	3.349495	0.006060	0.000000
9	1	0	2.482588	-2.321474	0.000000
10	1	0	0.041020	-2.762644	0.000000
11	8	0	-1.795924	-0.955478	0.000000
12	6	0	-0.933875	1.755285	0.000000
13	1	0	-2.266733	-0.088735	0.000000
14	8	0	-2.155707	1.637496	0.000000
15	1	0	-0.479666	2.766102	0.000000

30-M-OHFor

Standard orientation:

Center Number	Atomic Number	Atomic Type	Coordinates (Angstroms) X	Y	Z
1	6	0	0.015155	-0.806469	0.000077
2	6	0	0.891064	0.284315	-0.000117
3	6	0	0.396131	1.589090	-0.000038
4	6	0	-0.981250	1.798989	0.000026
5	6	0	-1.856095	0.720225	-0.000027
6	6	0	-1.357390	-0.589394	0.000003
7	6	0	2.352106	0.050863	0.000064
8	8	0	2.876311	-1.039144	-0.000114
9	8	0	-2.267425	-1.600256	0.000002
10	1	0	1.085501	2.427413	-0.000067
11	1	0	-1.378985	2.808119	0.000062
12	1	0	-2.930417	0.865718	-0.000112
13	1	0	0.434408	-1.808577	0.000403
14	1	0	-1.803177	-2.444174	0.000005
15	1	0	2.963252	0.980983	0.000677

31-P-OHFor

Standard orientation:

Center Number	Atomic Number	Atomic Type	Coordinates (Angstroms) X	Y	Z
1	6	0	-1.124995	0.195221	0.000000
2	1	0	-2.107683	0.653665	0.000000
3	6	0	0.000000	1.030391	0.000000
4	6	0	1.275798	0.454285	0.000000
5	6	0	1.437116	-0.921724	0.000000
6	6	0	0.306117	-1.744077	0.000000
7	6	0	-0.977679	-1.180473	0.000000
8	6	0	-0.155893	2.494137	0.000000
9	1	0	2.150424	1.099037	0.000000
10	1	0	2.418169	-1.381734	0.000000
11	8	0	0.510208	-3.084090	0.000000
12	1	0	-1.850260	-1.828616	0.000000
13	1	0	-0.339469	-3.538221	0.000000
14	8	0	-1.215350	3.080940	0.000000
15	1	0	0.807171	3.054517	0.000000

32-O-OHVin

Standard orientation:

Center Number	Atomic Number	Atomic Type	Coordinates (Angstroms) X	Y	Z
1	6	0	-0.006326	-1.410467	-0.068262
2	6	0	1.357547	-1.667733	-0.020567
3	6	0	2.255756	-0.604044	0.037725
4	6	0	1.780649	0.702104	0.045587
5	6	0	0.409210	0.952671	0.000505
6	6	0	-0.519644	-0.106157	-0.051689
7	8	0	-0.082837	2.225864	0.013981
8	6	0	-1.956673	0.190715	-0.101305
9	6	0	-2.957258	-0.665112	0.120631
10	1	0	1.718757	-2.689820	-0.038262
11	1	0	3.324503	-0.786760	0.071089
12	1	0	2.473987	1.538542	0.089534
13	1	0	-0.701100	-2.240409	-0.138405
14	1	0	-2.200167	1.222498	-0.335048
15	1	0	-3.990335	-0.345334	0.044990
16	1	0	-2.795837	-1.703126	0.392824
17	1	0	0.653330	2.845642	0.025688

33-M-OHVin

Standard orientation:

Center Number	Atomic Number	Atomic Type	Coordinates (Angstroms) X	Y	Z
1	6	0	-1.924397	0.668298	0.000013
2	6	0	-1.077678	1.767851	0.000011
3	6	0	0.304922	1.601925	-0.000001
4	6	0	0.869131	0.319890	-0.000011
5	6	0	0.007910	-0.787832	-0.000013
6	6	0	-1.372168	-0.616527	0.000001
7	6	0	2.332432	0.190689	-0.000022
8	6	0	3.056804	-0.930225	0.000028
9	8	0	-2.240807	-1.667539	-0.000004
10	1	0	-1.500545	2.767154	0.000019
11	1	0	0.956831	2.469246	-0.000002
12	1	0	0.415818	-1.794949	-0.000031
13	1	0	-3.002564	0.777131	0.000022
14	1	0	-1.739686	-2.489689	-0.000032
15	1	0	2.862153	1.141765	-0.000073
16	1	0	4.140149	-0.894613	0.000012
17	1	0	2.612569	-1.920152	0.000088

34-P-OHVin

Standard orientation:

Center Number	Atomic Number	Atomic Type	Coordinates (Angstroms) X	Y	Z
1	6	0	1.266471	0.419589	0.000000
2	1	0	2.149584	1.051755	0.000000
3	6	0	0.000000	1.018080	0.000000
4	6	0	-1.116247	0.163291	0.000000
5	6	0	-0.975875	-1.213729	0.000000
6	6	0	0.299854	-1.786851	0.000000
7	6	0	1.423679	-0.961621	0.000000
8	6	0	-0.101140	2.480936	0.000000
9	1	0	-2.115855	0.584196	0.000000
10	1	0	-1.840890	-1.867108	0.000000
11	8	0	0.379478	-3.146171	0.000000
12	1	0	2.419111	-1.398340	0.000000
13	1	0	1.306275	-3.407436	0.000000
14	6	0	-1.206905	3.229533	0.000000
15	1	0	0.860087	2.993398	0.000000
16	1	0	-1.147469	4.311746	0.000000
17	1	0	-2.205688	2.805789	0.000000

35-O-OHMe

Standard orientation:

Center Number	Atomic Number	Atomic Type	Coordinates (Angstroms) X	Y	Z
1	8	0	-0.627802	2.072431	0.000000
2	1	0	0.037373	2.768242	0.000000
3	6	0	0.000000	0.858137	0.000000
4	6	0	-0.822860	-0.279251	0.000000
5	6	0	-0.202760	-1.527183	0.000000
6	6	0	1.185346	-1.660885	0.000000
7	6	0	1.981075	-0.520960	0.000000
8	6	0	1.388299	0.739502	0.000000
9	6	0	-2.320637	-0.124260	0.000000
10	1	0	-0.827851	-2.415558	0.000000
11	1	0	1.637140	-2.646508	0.000000
12	1	0	3.062758	-0.604019	0.000000
13	1	0	2.003375	1.636239	0.000000
14	1	0	-2.813550	-1.099619	0.000000
15	1	0	-2.663801	0.435583	0.876999
16	1	0	-2.663801	0.435583	-0.876999

36-M-OHMe

Standard orientation:

Center Number	Atomic Number	Atomic Type	Coordinates (Angstroms) X	Y	Z
1	8	0	-2.308707	-1.186808	0.000778
2	1	0	-3.103622	-0.643789	0.005726
3	6	0	-1.215319	-0.370608	0.000918
4	6	0	0.039304	-0.981615	-0.009284
5	6	0	1.203761	-0.215732	-0.010891
6	6	0	1.096510	1.180122	-0.007952
7	6	0	-0.154120	1.787145	0.002278
8	6	0	-1.316432	1.020488	0.007227
9	1	0	0.085790	-2.065554	-0.017415
10	6	0	2.557749	-0.883101	0.008724

11	1	0	1.995173	1.788470	-0.015436
12	1	0	-0.230556	2.869738	0.002299
13	1	0	-2.293350	1.496735	0.011368
14	1	0	3.291228	-0.313293	-0.569591
15	1	0	2.944471	-0.962388	1.032258
16	1	0	2.511799	-1.895645	-0.401549

37-P-OHMe

Standard orientation:

Center Number	Atomic Number	Atomic Type	Coordinates (Angstroms) X	Y	Z
1	6	0	0.643727	1.197010	-0.000039
2	6	0	1.377324	0.011084	-0.000042
3	6	0	0.662287	-1.193249	-0.000038
4	6	0	-0.725205	-1.217974	-0.000006
5	6	0	-1.440467	-0.018519	0.000015
6	6	0	-0.749927	1.191595	-0.000006
7	6	0	2.886772	0.016588	0.000051
8	8	0	-2.803314	-0.094319	0.000032
9	1	0	3.280035	1.036870	-0.001280
10	1	0	3.292308	-0.496158	-0.879902
11	1	0	3.292202	-0.493777	0.881450
12	1	0	1.204952	-2.134562	-0.000072
13	1	0	-1.272368	-2.153878	-0.000017
14	1	0	-1.298569	2.130244	-0.000020
15	1	0	1.166490	2.149040	-0.000069
16	1	0	-3.165608	0.797565	0.000036

38-O-OHEt

Standard orientation:

Center Number	Atomic Number	Atomic Type	Coordinates (Angstroms) X	Y	Z
1	6	0	-0.185641	0.896348	-0.105831
2	6	0	-1.541487	1.090890	0.152123
3	6	0	-2.399861	-0.001758	0.242599
4	6	0	-1.902480	-1.289050	0.072622
5	6	0	-0.544838	-1.468381	-0.187953
6	6	0	0.339356	-0.394190	-0.281562
7	6	0	1.812731	-0.595405	-0.547795
8	6	0	2.682027	-0.449456	0.713970
9	8	0	0.689049	1.944220	-0.203017
10	1	0	-1.922833	2.101111	0.281226
11	1	0	-3.453582	0.159898	0.443841
12	1	0	-2.562852	-2.146559	0.137609
13	1	0	-0.153534	-2.472279	-0.327869
14	1	0	1.960846	-1.591127	-0.979979
15	1	0	2.150251	0.130476	-1.295665
16	1	0	3.739237	-0.607742	0.477587
17	1	0	2.574930	0.550412	1.142499
18	1	0	2.391167	-1.179174	1.476414
19	1	0	0.205131	2.767243	-0.080571

39-M-OHEt

Standard orientation:

Center Number	Atomic Number	Atomic Type	Coordinates (Angstroms) X	Y	Z
1	6	0	-0.889266	1.798889	0.114768
2	1	0	-1.154204	2.842128	0.253752
3	6	0	-1.880920	0.825441	0.198513
4	6	0	-1.540075	-0.514707	0.012314
5	6	0	-0.217409	-0.869449	-0.254163
6	6	0	0.778009	0.103566	-0.336374
7	6	0	0.429524	1.446450	-0.150659
8	1	0	-2.911985	1.102528	0.402031
9	8	0	-2.458784	-1.521597	0.074787
10	1	0	0.017096	-1.919018	-0.399744
11	6	0	2.216193	-0.293964	-0.584451
12	1	0	1.193591	2.214323	-0.219274
13	6	0	2.991459	-0.556230	0.718673
14	1	0	2.245521	-1.193964	-1.208995
15	1	0	2.720464	0.497400	-1.150739
16	1	0	4.027768	-0.839119	0.507849
17	1	0	3.003965	0.336089	1.352471
18	1	0	2.527568	-1.364162	1.293168
19	1	0	-3.324604	-1.143404	0.259455

40-P-EtOH

Standard orientation:

Center	Atomic	Atomic	Coordinates (Angstroms)

Number	Number	Type	X	Y	Z
1	6	0	0.203741	-1.190259	-0.243501
2	6	0	-1.168947	-1.218731	-0.033119
3	6	0	-1.876642	-0.021499	0.080845
4	6	0	-1.195929	1.191688	-0.020156
5	6	0	0.180143	1.200457	-0.231173
6	6	0	0.908226	0.014577	-0.345308
7	8	0	-3.224154	-0.098299	0.283329
8	6	0	2.408175	0.030110	-0.535737
9	6	0	3.183261	-0.012596	0.792796
10	1	0	-1.709223	-2.155785	0.039689
11	1	0	-1.741992	2.128462	0.060299
12	1	0	0.694911	2.153793	-0.312518
13	1	0	0.741573	-2.129915	-0.335653
14	1	0	2.697297	0.929539	-1.091922
15	1	0	2.707766	-0.824699	-1.153592
16	1	0	4.264301	-0.002079	0.619078
17	1	0	2.930741	0.848210	1.420317
18	1	0	2.938550	-0.916811	1.359355
19	1	0	-3.582858	0.793203	0.340440

41-O-MeOFor

Standard orientation:

Center Number	Atomic Number	Atomic Type	Coordinates (Angstroms) X	Y	Z
1	6	0	-1.574923	0.874627	0.000122
2	1	0	-2.645397	0.700380	0.000193
3	6	0	-1.045732	2.156541	0.000022
4	6	0	0.339099	2.315645	-0.000071
5	6	0	1.190504	1.213666	-0.000107
6	6	0	0.654224	-0.077587	0.000071
7	6	0	-0.746934	-0.251921	0.000230
8	1	0	-1.697687	3.022432	0.000017
9	1	0	0.770664	3.311561	-0.000183
10	1	0	2.261291	1.367455	-0.000097
11	8	0	1.405167	-1.206620	-0.000102
12	6	0	-1.361375	-1.598006	0.000271
13	6	0	2.817292	-1.089987	-0.000034
14	1	0	3.178189	-0.566856	-0.893998
15	1	0	3.177874	-0.566971	0.894150
16	1	0	3.202602	-2.110428	-0.000077
17	8	0	-2.559001	-1.789769	-0.000419
18	1	0	-0.649795	-2.444334	0.001146

42-M-MeOFor

Standard orientation:

Center Number	Atomic Number	Atomic Type	Coordinates (Angstroms) X	Y	Z
1	6	0	1.258152	0.101351	0.000000
2	6	0	0.000999	-0.519500	0.000004
3	6	0	-1.148654	0.263286	0.000004
4	6	0	-1.034300	1.663909	0.000001
5	6	0	0.212806	2.268977	-0.000002
6	6	0	1.369871	1.490238	-0.000003
7	8	0	-2.416394	-0.220244	0.000005
8	6	0	-2.593312	-1.626606	-0.000006
9	1	0	-1.945991	2.250766	0.000002
10	6	0	2.480558	-0.731743	0.000000
11	8	0	2.492992	-1.941439	0.000000
12	1	0	0.282168	3.351462	-0.000005
13	1	0	2.351550	1.953440	-0.000006
14	1	0	-0.028047	-1.601118	0.000008
15	1	0	-3.671021	-1.795320	-0.000034
16	1	0	-2.153672	-2.087922	-0.892982
17	1	0	-2.153718	-2.087931	0.892988
18	1	0	3.429223	-0.149393	0.000000

43-P-MeOFor

Standard orientation:

Center Number	Atomic Number	Atomic Type	Coordinates (Angstroms) X	Y	Z
1	6	0	0.833401	1.040065	-0.000030
2	6	0	-0.536662	1.280478	-0.000018
3	6	0	-1.455446	0.230966	-0.000012
4	6	0	-0.979111	-1.091082	-0.000041
5	6	0	0.375538	-1.346389	-0.000012
6	6	0	1.294091	-0.281454	-0.000008
7	6	0	-2.900339	0.509863	0.000046
8	8	0	-3.771915	-0.331008	0.000040
9	8	0	2.598495	-0.638429	0.000018
10	6	0	3.583222	0.381765	0.000029

11	1	0	-0.899134	2.305036	-0.000021
12	1	0	-1.701896	-1.899433	-0.000102
13	1	0	0.765186	-2.357860	-0.000007
14	1	0	1.525698	1.871366	-0.000041
15	1	0	4.546499	-0.129848	0.000052
16	1	0	3.508463	1.012900	-0.893952
17	1	0	3.508428	1.012915	0.893997
18	1	0	-3.154040	1.595153	-0.000115

44-O-MeOVin

Standard orientation:

Center Number	Atomic Number	Atomic Type	Coordinates (Angstroms) X	Y	Z
1	6	0	-1.393003	1.013068	0.045414
2	6	0	-0.757845	2.253122	0.044060
3	6	0	0.628950	2.330883	-0.018314
4	6	0	1.375834	1.159769	-0.076935
5	6	0	0.775614	-0.103598	-0.064890
6	6	0	-0.636965	-0.159033	-0.008750
7	6	0	1.551161	-1.349573	-0.126806
8	6	0	2.849263	-1.492328	0.151274
9	8	0	-1.183946	-1.406612	-0.002007
10	6	0	-2.591795	-1.531462	0.023034
11	1	0	-1.357170	3.156658	0.085126
12	1	0	1.125853	3.294484	-0.032369
13	1	0	2.456104	1.219589	-0.154470
14	1	0	-2.473047	0.968087	0.092128
15	1	0	-2.800844	-2.602401	0.005364
16	1	0	-3.021158	-1.096428	0.934631
17	1	0	-3.057310	-1.058546	-0.851248
18	1	0	0.983131	-2.226886	-0.419222
19	1	0	3.336621	-2.456293	0.058104
20	1	0	3.472102	-0.670446	0.489487

45-M-MeOVin

Standard orientation:

Center Number	Atomic Number	Atomic Type	Coordinates (Angstroms) X	Y	Z
1	6	0	1.176223	1.616222	-0.000108
2	6	0	-0.032126	2.292483	-0.000127
3	6	0	-1.236824	1.590825	0.000021
4	6	0	-1.243562	0.192725	0.000173
5	6	0	-0.014459	-0.491414	0.000167
6	6	0	1.185002	0.213810	0.000006
7	6	0	-2.535735	-0.506615	0.000314
8	6	0	-2.758378	-1.822621	-0.000421
9	8	0	2.418676	-0.361950	-0.000243
10	6	0	2.501175	-1.773576	0.000186
11	1	0	-0.038458	3.377562	-0.000210
12	1	0	-2.179543	2.128137	0.000008
13	1	0	-0.009757	-1.572888	0.000603
14	1	0	2.125004	2.139992	-0.000161
15	1	0	3.565309	-2.015494	-0.000320
16	1	0	2.033828	-2.207359	0.893817
17	1	0	2.032743	-2.207995	-0.892569
18	1	0	-3.398968	0.156883	0.001043
19	1	0	-3.767873	-2.217450	-0.000221
20	1	0	-1.959586	-2.556833	-0.001321

46-P-MeOVin

Center Number	Atomic Number	Atomic Type	Coordinates (Angstroms) X	Y	Z
1	6	0	1.206270	0.649265	0.000000
2	1	0	2.135419	1.212009	0.000000
3	6	0	1.260465	-0.747903	0.000000
4	6	0	0.033770	-1.438226	0.000000
5	6	0	-1.171659	-0.764049	0.000000
6	6	0	-1.202004	0.638142	0.000000
7	6	0	0.000000	1.346720	0.000000
8	6	0	2.564896	-1.417107	0.000000
9	1	0	0.025053	-2.522825	0.000000
10	1	0	-2.115228	-1.297947	0.000000
11	8	0	-2.438051	1.203057	0.000000
12	1	0	0.011085	2.428871	0.000000
13	6	0	-2.527806	2.614892	0.000000
14	1	0	-3.592955	2.851645	0.000000
15	1	0	-2.061645	3.050377	0.893205
16	1	0	-2.061645	3.050377	-0.893205
17	6	0	2.816494	-2.728599	0.000000
18	1	0	3.414724	-0.735670	0.000000
19	1	0	3.834278	-3.101255	0.000000
20	1	0	2.032776	-3.478857	0.000000

47-O-MeOMe

Standard orientation:

Center Number	Atomic Number	Atomic Type	Coordinates (Angstroms) X	Y	Z
1	6	0	-2.283646	-0.676407	-0.000005
2	1	0	-3.345277	-0.897192	-0.000008
3	6	0	-1.349770	-1.702607	0.000010
4	6	0	0.015870	-1.413388	0.000002
5	6	0	0.442536	-0.085717	-0.000012
6	6	0	-0.489869	0.970241	0.000005
7	6	0	-1.842868	0.647938	-0.000010
8	1	0	-1.672088	-2.738727	0.000028
9	1	0	0.732968	-2.224002	0.000019
10	8	0	1.752012	0.297547	-0.000038
11	6	0	-0.007638	2.396806	0.000016
12	1	0	-2.568317	1.456463	-0.000024
13	1	0	-0.851027	3.091858	-0.000025
14	1	0	0.614414	2.607938	0.876691
15	1	0	0.614528	2.607921	-0.876584
16	6	0	2.746710	-0.706270	0.000016
17	1	0	3.705524	-0.184770	-0.000022
18	1	0	2.682610	-1.341670	0.892943
19	1	0	2.682619	-1.341761	-0.892849

48-M-MeOMe

Standard orientation:

Center Number	Atomic Number	Atomic Type	Coordinates (Angstroms) X	Y	Z
1	6	0	-1.054820	-1.836476	0.000000
2	1	0	-1.467326	-2.840363	0.000000
3	6	0	0.319114	-1.664465	0.000000
4	6	0	0.852878	-0.369358	0.000000
5	6	0	0.000000	0.733599	0.000000
6	6	0	-1.391199	0.557735	0.000000
7	6	0	-1.911689	-0.733608	0.000000
8	1	0	1.001324	-2.506582	0.000000
9	8	0	2.212938	-0.293688	0.000000
10	1	0	0.400404	1.740316	0.000000
11	6	0	-2.297562	1.765456	0.000000
12	1	0	-2.986775	-0.880819	0.000000
13	1	0	-3.350415	1.472166	0.000000
14	1	0	-2.125189	2.394704	0.880757
15	1	0	-2.125189	2.394704	-0.880757
16	6	0	2.813062	0.985862	0.000000
17	1	0	3.891188	0.816198	0.000000
18	1	0	2.539886	1.563358	-0.892886
19	1	0	2.539886	1.563358	0.892886

49-P-MeOMe

Standard orientation:

Center Number	Atomic Number	Atomic Type	Coordinates (Angstroms) X	Y	Z
1	6	0	1.091126	0.138544	0.000000
2	1	0	2.105504	0.516086	0.000000
3	6	0	0.000000	1.006595	0.000000
4	6	0	-1.296193	0.476654	0.000000
5	6	0	-1.488522	-0.894527	0.000000
6	6	0	-0.406420	-1.786463	0.000000
7	6	0	0.874318	-1.241484	0.000000
8	8	0	0.085898	2.366486	0.000000
9	1	0	-2.134496	1.164262	0.000000
10	1	0	-2.502474	-1.285069	0.000000
11	6	0	-0.632593	-3.278581	0.000000
12	1	0	1.735210	-1.904047	0.000000
13	1	0	0.315225	-3.823793	0.000000
14	1	0	-1.200693	-3.600464	0.880611
15	1	0	-1.200693	-3.600464	-0.880611
16	6	0	1.372473	2.950892	0.000000
17	1	0	1.216812	4.031140	0.000000
18	1	0	1.946644	2.670338	0.892889
19	1	0	1.946644	2.670338	-0.892889

50-O-MeOEt

Standard orientation:

Center Number	Atomic Number	Atomic Type	Coordinates (Angstroms) X	Y	Z
1	6	0	-1.303581	1.138132	0.167007

2	1	0	-1.408991	2.205741	0.309688
3	6	0	-2.431495	0.320080	0.244658
4	6	0	-2.316769	-1.050630	0.061161
5	6	0	-1.061485	-1.600005	-0.201650
6	6	0	0.084591	-0.814359	-0.282042
7	6	0	-0.053926	0.575112	-0.092606
8	1	0	-3.398570	0.768282	0.447967
9	1	0	-3.191126	-1.689600	0.116801
10	1	0	-0.964986	-2.671584	-0.353122
11	6	0	1.441752	-1.422017	-0.550477
12	8	0	1.101087	1.298413	-0.185846
13	1	0	1.977179	-0.809762	-1.283818
14	6	0	2.308538	-1.554183	0.714492
15	1	0	1.301167	-2.411107	-1.000132
16	1	0	3.277514	-2.004948	0.476344
17	1	0	2.489651	-0.573440	1.161767
18	1	0	1.816069	-2.183335	1.462875
19	6	0	1.031171	2.701882	-0.035991
20	1	0	2.050509	3.071902	-0.159795
21	1	0	0.386658	3.159774	-0.797517
22	1	0	0.663454	2.986704	0.958391

51-M-MeOEt

Standard orientation:

Center Number	Atomic Number	Atomic Type	Coordinates (Angstroms) X	Y	Z
1	6	0	1.235579	0.067196	-0.337650
2	6	0	1.075207	1.444274	-0.131885
3	6	0	-0.186126	1.972328	0.105368
4	6	0	-1.315356	1.153068	0.143530
5	6	0	-1.162274	-0.219147	-0.062592
6	6	0	0.110242	-0.749672	-0.301945
7	8	0	-2.183041	-1.121251	-0.054840
8	6	0	-3.493494	-0.644337	0.176216
9	6	0	2.609619	-0.526024	-0.557038
10	6	0	3.325915	-0.866243	0.761609
11	1	0	-0.304676	3.040238	0.259719
12	1	0	-2.289160	1.587693	0.326541
13	1	0	0.193500	-1.819749	-0.463127
14	1	0	1.941748	2.097404	-0.163830
15	1	0	2.524441	-1.432862	-1.166224
16	1	0	3.223840	0.179296	-1.128824
17	1	0	4.317854	-1.288597	0.571413
18	1	0	3.449529	0.027284	1.381678
19	1	0	2.750382	-1.594662	1.341458
20	1	0	-4.146168	-1.518373	0.140607
21	1	0	-3.584984	-0.167203	1.160754
22	1	0	-3.807852	0.070887	-0.595124

52-P-MeOEt

Standard orientation:

Center Number	Atomic Number	Atomic Type	Coordinates (Angstroms) X	Y	Z
1	6	0	-0.581634	1.399790	-0.046276
2	1	0	-1.032449	2.381240	0.048874
3	6	0	-1.414971	0.276565	0.001164
4	6	0	-0.855120	-0.995204	-0.128969
5	6	0	0.523576	-1.126308	-0.301809
6	6	0	1.369710	-0.020231	-0.348441
7	6	0	0.784775	1.246494	-0.218518
8	8	0	-2.743355	0.528179	0.170281
9	1	0	-1.474178	-1.882718	-0.103440
10	1	0	0.943646	-2.123053	-0.406445
11	6	0	2.866003	-0.177617	-0.497707
12	1	0	1.414384	2.131288	-0.258102
13	6	0	3.604463	-0.209895	0.851846
14	1	0	3.083460	-1.099796	-1.049035
15	1	0	3.262617	0.645777	-1.103753
16	1	0	4.684297	-0.320425	0.707922
17	1	0	3.429440	0.711917	1.415896
18	1	0	3.255427	-1.044832	1.467901
19	6	0	-3.628024	-0.572703	0.222365
20	1	0	-4.626469	-0.154939	0.362991
21	1	0	-3.609506	-1.153951	-0.708987
22	1	0	-3.396494	-1.241278	1.061999

53-O-ForVin

Standard orientation:

Center Number	Atomic Number	Atomic Type	Coordinates (Angstroms) X	Y	Z
1	6	0	-0.806981	-1.471033	-0.126820
2	6	0	-2.146725	-1.112223	-0.038620

3	6	0	-2.511194	0.228630	0.068664
4	6	0	-1.514489	1.192829	0.079508
5	6	0	-0.158832	0.847961	-0.001776
6	6	0	0.219677	-0.516652	-0.096133
7	6	0	0.790334	1.984301	0.029425
8	8	0	1.999479	1.939425	-0.006045
9	6	0	1.627872	-0.936931	-0.182951
10	6	0	2.097588	-2.118237	0.226019
11	1	0	-2.910179	-1.883003	-0.065852
12	1	0	-3.555143	0.514346	0.132108
13	1	0	-1.777449	2.244324	0.155180
14	1	0	-0.544001	-2.515794	-0.247471
15	1	0	2.315898	-0.201855	-0.580567
16	1	0	3.147890	-2.365963	0.120623
17	1	0	1.471578	-2.867970	0.699529
18	1	0	0.272080	2.968637	0.090923

54-M-ForVin

Standard orientation:

Center Number	Atomic Number	Atomic Type	Coordinates (Angstroms) X	Y	Z
1	6	0	-0.479963	-2.017187	0.000000
2	1	0	-0.657204	-3.087361	0.000000
3	6	0	-1.554382	-1.130376	0.000000
4	6	0	-1.314043	0.244125	0.000000
5	6	0	0.000000	0.722040	0.000000
6	6	0	1.089133	-0.151648	0.000000
7	6	0	0.821569	-1.534117	0.000000
8	1	0	-2.576179	-1.498874	0.000000
9	6	0	-2.451723	1.190844	0.000000
10	1	0	0.153077	1.796553	0.000000
11	6	0	2.449763	0.404031	0.000000
12	1	0	1.645167	-2.239783	0.000000
13	6	0	3.603083	-0.266722	0.000000
14	1	0	2.486577	1.491758	0.000000
15	1	0	4.551859	0.257270	0.000000
16	1	0	3.656694	-1.350287	0.000000
17	8	0	-2.348572	2.395421	0.000000
18	1	0	-3.452037	0.701421	0.000000

55-P-ForVin

Standard orientation:

Center Number	Atomic Number	Atomic Type	Coordinates (Angstroms) X	Y	Z
1	6	0	-1.383246	0.214623	0.000057
2	6	0	-0.670854	-1.000894	0.000197
3	6	0	0.710683	-1.014405	0.000243
4	6	0	1.431730	0.188996	0.000114
5	6	0	0.737654	1.400310	-0.000009
6	6	0	-0.650577	1.411303	-0.000025
7	6	0	2.908299	0.179860	0.000053
8	8	0	3.593832	-0.817116	-0.000354
9	6	0	-2.848897	0.284678	-0.000020
10	6	0	-3.710678	-0.735069	-0.000199
11	1	0	1.264854	-1.946501	0.000366
12	1	0	1.291453	2.335165	-0.000097
13	1	0	-1.184327	2.356667	-0.000133
14	1	0	-1.210953	-1.941018	0.000280
15	1	0	-3.250527	1.296387	0.000068
16	1	0	-4.780350	-0.559994	-0.000235
17	1	0	-3.396472	-1.773198	-0.000328
18	1	0	3.370986	1.193010	0.000441

56-O-ForMe

Standard orientation:

Center Number	Atomic Number	Atomic Type	Coordinates (Angstroms) X	Y	Z
1	6	0	1.854009	-1.454189	0.000000
2	1	0	2.564384	-2.274696	0.000000
3	6	0	2.307495	-0.138027	0.000000
4	6	0	1.375442	0.890271	0.000000
5	6	0	0.000000	0.626286	0.000000
6	6	0	-0.467562	-0.709122	0.000000
7	6	0	0.487446	-1.726987	0.000000
8	1	0	3.369484	0.080716	0.000000
9	1	0	1.706023	1.925448	0.000000
10	6	0	-0.896461	1.800821	0.000000
11	6	0	-1.932704	-1.058601	0.000000
12	1	0	0.150284	-2.759071	0.000000
13	1	0	-2.063931	-2.143965	0.000000
14	1	0	-2.444270	-0.639229	0.870716
15	1	0	-2.444270	-0.639229	-0.870716

16	8	0	-2.107261	1.787206	0.000000
17	1	0	-0.345623	2.769670	0.000000

57-M-ForMe

Standard orientation:

Center Number	Atomic Number	Atomic Type	Coordinates (Angstroms) X	Y	Z
1	6	0	1.784638	-0.820587	0.000000
2	6	0	0.868062	-1.866603	0.000000
3	6	0	-0.496333	-1.591409	0.000000
4	6	0	-0.932796	-0.266074	0.000000
5	6	0	0.000000	0.778881	0.000000
6	6	0	1.366093	0.519317	0.000000
7	6	0	-2.382165	0.029031	0.000000
8	8	0	-2.863679	1.138445	0.000000
9	6	0	2.379558	1.637396	0.000000
10	1	0	1.218477	-2.893265	0.000000
11	1	0	-1.224076	-2.397874	0.000000
12	1	0	-0.374794	1.797326	0.000000
13	1	0	2.848298	-1.042496	0.000000
14	1	0	3.029192	1.585059	0.880819
15	1	0	3.029192	1.585059	-0.880819
16	1	0	1.891991	2.615145	0.000000
17	1	0	-3.031187	-0.876219	0.000000

58-P-ForMe

Standard orientation:

Center Number	Atomic Number	Atomic Type	Coordinates (Angstroms) X	Y	Z
1	6	0	1.269406	0.486369	0.000000
2	1	0	2.149046	1.124495	0.000000
3	6	0	0.000000	1.066578	0.000000
4	6	0	-1.132110	0.240125	0.000000
5	6	0	-0.986200	-1.136172	0.000000
6	6	0	0.286960	-1.728746	0.000000
7	6	0	1.409848	-0.897403	0.000000
8	6	0	-0.142308	2.536306	0.000000
9	1	0	-2.111530	0.705661	0.000000
10	1	0	-1.866852	-1.772008	0.000000
11	6	0	0.427554	-3.229658	0.000000
12	1	0	2.401086	-1.340055	0.000000
13	1	0	1.476761	-3.534839	0.000000
14	1	0	-0.052784	-3.671560	0.880206
15	1	0	-0.052784	-3.671560	-0.880206
16	8	0	-1.195942	3.130956	0.000000
17	1	0	0.825691	3.087819	0.000000

59-O-ForEt

Standard orientation:

Center Number	Atomic Number	Atomic Type	Coordinates (Angstroms) X	Y	Z
1	6	0	1.471467	1.265017	0.199538
2	1	0	1.614426	2.329021	0.367661
3	6	0	2.560174	0.405670	0.229884
4	6	0	2.349576	-0.951223	-0.000294
5	6	0	1.065700	-1.427788	-0.254243
6	6	0	-0.047064	-0.584053	-0.279850
7	6	0	0.173765	0.794222	-0.044979
8	1	0	3.556939	0.785537	0.424344
9	1	0	3.186430	-1.642181	0.011666
10	1	0	0.918868	-2.487442	-0.441662
11	6	0	-1.412699	-1.179647	-0.538435
12	6	0	-0.891754	1.820369	-0.052971
13	1	0	-1.997291	-0.515583	-1.177380
14	6	0	-2.206074	-1.441860	0.754847
15	1	0	-1.276302	-2.125877	-1.074134
16	1	0	-3.164057	-1.916681	0.521744
17	1	0	-1.653748	-2.103432	1.430081
18	1	0	-2.413029	-0.505316	1.276905
19	8	0	-2.081786	1.640564	-0.187985
20	1	0	-0.496493	2.853205	0.083671

60-M-ForEt

Standard orientation:

Center Number	Atomic Number	Atomic Type	Coordinates (Angstroms) X	Y	Z
1	6	0	-0.092644	2.172197	0.097672
2	1	0	-0.049535	3.249038	0.221728

3	6	0	-1.308666	1.503791	0.192196
4	6	0	-1.351007	0.118155	0.022726
5	6	0	-0.173246	-0.590904	-0.239662
6	6	0	1.051656	0.063652	-0.334856
7	6	0	1.071869	1.455548	-0.163548
8	1	0	-2.226507	2.049204	0.392532
9	6	0	-2.644469	-0.593351	0.116887
10	1	0	-0.243272	-1.666221	-0.371415
11	6	0	2.331153	-0.703383	-0.581885
12	1	0	2.018094	1.983954	-0.242177
13	6	0	3.041717	-1.104850	0.722615
14	1	0	2.108069	-1.603872	-1.164347
15	1	0	3.009962	-0.095496	-1.191160
16	1	0	3.963571	-1.655265	0.510887
17	1	0	3.301319	-0.222433	1.316250
18	1	0	2.398262	-1.741324	1.337969
19	8	0	-2.790450	-1.786484	-0.016451
20	1	0	-3.514552	0.069160	0.328469

61-P-ForEt

Standard orientation:

Center Number	Atomic Number	Atomic Type	Coordinates (Angstroms) X	Y	Z
1	6	0	-0.708628	1.361636	-0.026250
2	1	0	-1.183865	2.332967	0.081690
3	6	0	-1.492903	0.206118	0.007377
4	6	0	-0.879397	-1.044270	-0.139160
5	6	0	0.492299	-1.127211	-0.314437
6	6	0	1.288698	0.027261	-0.347237
7	6	0	0.666723	1.271628	-0.202460
8	6	0	-2.954540	0.309019	0.190693
9	1	0	-1.502488	-1.931511	-0.116345
10	1	0	0.963081	-2.098865	-0.433423
11	6	0	2.787988	-0.075458	-0.499671
12	1	0	1.268662	2.174997	-0.232994
13	6	0	3.507708	-0.236826	0.851769
14	1	0	3.031925	-0.928869	-1.142441
15	1	0	3.166404	0.819329	-1.006242
16	1	0	4.590123	-0.310376	0.708958
17	1	0	3.306998	0.616799	1.506653
18	1	0	3.170352	-1.139731	1.370155
19	8	0	-3.716336	-0.629956	0.230697
20	1	0	-3.328195	1.353536	0.294673

62-O-VinMe

Standard orientation:

Center Number	Atomic Number	Atomic Type	Coordinates (Angstroms) X	Y	Z
1	6	0	-2.281054	-0.572218	-0.066690
2	1	0	-3.353155	-0.727177	-0.128171
3	6	0	-1.415815	-1.657950	0.033616
4	6	0	-0.047198	-1.438376	0.117942
5	6	0	0.490889	-0.143499	0.095164
6	6	0	-0.389474	0.957983	0.004923
7	6	0	-1.762476	0.718938	-0.077621
8	1	0	-1.804916	-2.670459	0.057285
9	1	0	0.624389	-2.283139	0.227944
10	6	0	1.945883	0.067107	0.174806
11	6	0	0.122275	2.379207	-0.024158
12	1	0	-2.437507	1.566377	-0.154261
13	1	0	-0.702265	3.083827	-0.158199
14	1	0	0.635910	2.648703	0.906715
15	1	0	0.836150	2.539302	-0.839207
16	6	0	2.892529	-0.790821	-0.212743
17	1	0	2.264356	1.023676	0.581920
18	1	0	3.944664	-0.554688	-0.099110
19	1	0	2.659009	-1.748652	-0.666344

63-M-VinMe

Standard orientation:

Center Number	Atomic Number	Atomic Type	Coordinates (Angstroms) X	Y	Z
1	6	0	-0.948401	1.851788	0.000029
2	1	0	-1.314744	2.873358	0.000052
3	6	0	0.421744	1.607129	0.000000
4	6	0	0.914831	0.296845	-0.000028
5	6	0	-0.013042	-0.757781	-0.000036
6	6	0	-1.385620	-0.531182	-0.000007
7	6	0	-1.846752	0.792584	0.000026
8	1	0	1.121187	2.437748	0.000002
9	6	0	2.368691	0.086099	-0.000050
10	1	0	0.344541	-1.782671	-0.000075

11	6	0	-2.365363	-1.679834	-0.000008
12	1	0	-2.915317	0.987447	0.000045
13	1	0	-3.016957	-1.647680	-0.880571
14	1	0	-1.850710	-2.644184	-0.000024
15	1	0	-3.016936	-1.647700	0.880572
16	6	0	3.029518	-1.073604	0.000064
17	1	0	2.951918	1.005802	-0.000165
18	1	0	4.113246	-1.097701	0.000031
19	1	0	2.530135	-2.036680	0.000198

64-P-VinMe

Standard orientation:

Center Number	Atomic Number	Atomic Type	Coordinates (Angstroms) X	Y	Z
1	6	0	-0.960160	-1.175335	0.000000
2	1	0	-1.841894	-1.810355	0.000000
3	6	0	0.310626	-1.767289	0.000000
4	6	0	1.419732	-0.921796	0.000000
5	6	0	1.267400	0.461349	0.000000
6	6	0	0.000000	1.056256	0.000000
7	6	0	-1.115138	0.201402	0.000000
8	6	0	0.461872	-3.267787	0.000000
9	1	0	2.417989	-1.349730	0.000000
10	1	0	2.148626	1.096562	0.000000
11	6	0	-0.103410	2.520382	0.000000
12	1	0	-2.115914	0.619907	0.000000
13	6	0	-1.212366	3.263590	0.000000
14	1	0	0.856321	3.035290	0.000000
15	1	0	-1.158353	4.346196	0.000000
16	1	0	-2.208887	2.834668	0.000000
17	1	0	1.514448	-3.562782	0.000000
18	1	0	-0.011838	-3.717192	0.880390
19	1	0	-0.011838	-3.717192	-0.880390

65-O-VinEt

Standard orientation:

Center Number	Atomic Number	Atomic Type	Coordinates (Angstroms) X	Y	Z
1	6	0	-1.197922	1.316281	0.040285
2	1	0	-1.194276	2.400747	0.065719
3	6	0	-2.393151	0.631248	0.211584
4	6	0	-2.405619	-0.758609	0.132055
5	6	0	-1.220017	-1.439653	-0.122210
6	6	0	-0.006390	-0.768490	-0.293043
7	6	0	0.009054	0.642152	-0.200191
8	1	0	-3.311593	1.179938	0.392045
9	1	0	-3.332984	-1.308439	0.254215
10	1	0	-1.230459	-2.523770	-0.191853
11	6	0	1.252884	-1.578405	-0.522751
12	6	0	1.259653	1.403016	-0.367078
13	1	0	1.844281	-1.148003	-1.339550
14	6	0	2.136000	-1.699551	0.731806
15	1	0	0.966010	-2.581285	-0.857035
16	1	0	3.025133	-2.303957	0.525422
17	1	0	2.465352	-0.715953	1.079063
18	1	0	1.584137	-2.173205	1.549797
19	6	0	1.537763	2.592188	0.172398
20	1	0	2.022294	0.936914	-0.986371
21	1	0	2.480397	3.090877	-0.023637
22	1	0	0.848176	3.105074	0.835055

66-M-VinEt

Standard orientation:

Center Number	Atomic Number	Atomic Type	Coordinates (Angstroms) X	Y	Z
1	6	0	-1.212970	1.568566	0.186265
2	6	0	0.029709	2.186288	0.093575
3	6	0	1.167137	1.430212	-0.165313
4	6	0	1.075660	0.042793	-0.334247
5	6	0	-0.176966	-0.558532	-0.240792
6	6	0	-1.339645	0.182979	0.020117
7	6	0	2.317052	-0.786662	-0.577710
8	6	0	3.018071	-1.203164	0.727114
9	6	0	-2.673877	-0.423856	0.121415
10	6	0	-3.000543	-1.712050	-0.002392
11	1	0	0.109614	3.261355	0.218666
12	1	0	2.135637	1.915950	-0.243081
13	1	0	-0.248858	-1.633196	-0.379202
14	1	0	-2.100311	2.162017	0.385410
15	1	0	-3.472897	0.288133	0.323030
16	1	0	-4.029817	-2.038033	0.094395
17	1	0	-2.270089	-2.488756	-0.202619

18	1	0	2.051377	-1.684221	-1.147583
19	1	0	3.019895	-0.219087	-1.198747
20	1	0	3.913339	-1.797691	0.518901
21	1	0	3.320104	-0.325195	1.306972
22	1	0	2.350233	-1.800730	1.355667

67-P-VinEt

Standard orientation:

Center Number	Atomic Number	Atomic Type	Coordinates (Angstroms) X	Y	Z
1	6	0	0.516408	-1.118701	-0.316585
2	1	0	0.974223	-2.097242	-0.434048
3	6	0	1.326817	0.023264	-0.345305
4	6	0	0.704288	1.264702	-0.200990
5	6	0	-0.672131	1.360741	-0.030986
6	6	0	-1.485489	0.219901	0.000530
7	6	0	-0.856978	-1.026722	-0.147408
8	6	0	2.826541	-0.089637	-0.490980
9	1	0	1.304817	2.169861	-0.226110
10	1	0	-1.132017	2.339224	0.075091
11	6	0	-2.933863	0.379866	0.178807
12	1	0	-1.449607	-1.935229	-0.135428
13	6	0	-3.863400	-0.576761	0.233366
14	1	0	-3.259690	1.414559	0.276076
15	1	0	-4.910045	-0.330159	0.370230
16	1	0	-3.628091	-1.632189	0.145641
17	6	0	3.544924	-0.253461	0.860361
18	1	0	3.068659	-0.944699	-1.132969
19	1	0	3.212854	0.801690	-0.998658
20	1	0	4.627780	-0.334057	0.721121
21	1	0	3.347876	0.602212	1.513975
22	1	0	3.200534	-1.153127	1.380221

68-O-MeEt

Standard orientation:

Center Number	Atomic Number	Atomic Type	Coordinates (Angstroms) X	Y	Z
1	6	0	-1.607673	1.015309	0.197187
2	1	0	-2.052914	1.991144	0.369296
3	6	0	-2.408344	-0.121925	0.247625
4	6	0	-1.839235	-1.370163	0.020291
5	6	0	-0.477780	-1.460409	-0.252602
6	6	0	0.338371	-0.327089	-0.300720
7	6	0	-0.238994	0.937446	-0.073775
8	1	0	-3.468565	-0.030495	0.459551
9	1	0	-2.448930	-2.267249	0.049906
10	1	0	-0.031705	-2.434177	-0.436936
11	6	0	1.819735	-0.495747	-0.565956
12	6	0	0.581487	2.205454	-0.131610
13	1	0	2.207597	0.359740	-1.128822
14	6	0	2.644331	-0.670465	0.722756
15	1	0	1.969664	-1.375229	-1.202386
16	1	0	3.707893	-0.792913	0.493786
17	1	0	2.538931	0.194037	1.385706
18	1	0	2.311749	-1.552561	1.278825
19	1	0	-0.033679	3.076327	0.108888
20	1	0	1.420921	2.188315	0.571789
21	1	0	1.007649	2.368594	-1.128772

69-M-MeEt

Standard orientation:

Center Number	Atomic Number	Atomic Type	Coordinates (Angstroms) X	Y	Z
1	6	0	-0.793495	1.863734	0.127757
2	1	0	-1.014496	2.916622	0.272403
3	6	0	0.512589	1.459032	-0.134058
4	6	0	0.808993	0.108700	-0.333673
5	6	0	-0.235734	-0.817507	-0.265925
6	6	0	-1.551424	-0.432582	-0.001037
7	6	0	-1.818683	0.925915	0.193490
8	1	0	1.307534	2.197076	-0.192652
9	6	0	2.229331	-0.346156	-0.584945
10	1	0	-0.017423	-1.870304	-0.430539
11	6	0	-2.656438	-1.457256	0.089239
12	1	0	-2.836669	1.249157	0.391057
13	1	0	-3.585262	-1.084720	-0.353961
14	1	0	-2.384665	-2.384934	-0.422189
15	1	0	-2.878078	-1.712380	1.133006
16	6	0	2.985894	-0.676370	0.713721
17	1	0	2.221897	-1.230991	-1.231976
18	1	0	2.772842	0.434556	-1.129534
19	1	0	4.009335	-1.001400	0.500422

20	1	0	3.036007	0.198328	1.369957
21	1	0	2.482780	-1.476063	1.266596

70-P-MeEt

Standard orientation:

Center Number	Atomic Number	Atomic Type	Coordinates (Angstroms) X	Y	Z
1	6	0	0.231118	1.196026	-0.239030
2	1	0	0.759582	2.142150	-0.320590
3	6	0	0.945905	0.000116	-0.346910
4	6	0	0.231212	-1.195871	-0.239197
5	6	0	-1.144198	-1.196196	-0.029431
6	6	0	-1.858664	-0.000030	0.076772
7	6	0	-1.144296	1.196209	-0.029268
8	6	0	2.446365	0.000180	-0.532194
9	1	0	0.759753	-2.141939	-0.320895
10	1	0	-1.673035	-2.142040	0.049854
11	6	0	-3.355475	-0.000112	0.269754
12	1	0	-1.673211	2.141997	0.050152
13	1	0	-3.688096	0.885774	0.818933
14	1	0	-3.882787	-0.001149	-0.692537
15	1	0	-3.687791	-0.885056	0.820643
16	6	0	3.212307	-0.000229	0.802465
17	1	0	2.743056	-0.878066	-1.117399
18	1	0	2.743044	0.878786	-1.116861
19	1	0	4.294266	-0.000179	0.635044
20	1	0	2.959786	0.882746	1.398219
21	1	0	2.959788	-0.883571	1.397677

71-1,2,3-TOH

Standard orientation:

Center Number	Atomic Number	Atomic Type	Coordinates (Angstroms) X	Y	Z
1	6	0	1.170730	-1.425683	0.000000
2	1	0	2.103804	-1.981058	0.000000
3	6	0	-0.056950	-2.086552	0.000000
4	6	0	-1.252361	-1.374900	0.000000
5	6	0	-1.224726	0.018457	0.000000
6	6	0	0.000000	0.688489	0.000000
7	6	0	1.191125	-0.034016	0.000000
8	1	0	-0.078831	-3.170468	0.000000
9	1	0	-2.212551	-1.876355	0.000000
10	8	0	-2.385572	0.726168	0.000000
11	8	0	-0.024245	2.059041	0.000000
12	8	0	2.332739	0.730218	0.000000
13	1	0	-2.154964	1.663958	0.000000
14	1	0	0.888658	2.370413	0.000000
15	1	0	3.103602	0.155321	0.000000

72-1,2,4-TOH

Standard orientation:

Center Number	Atomic Number	Atomic Type	Coordinates (Angstroms) X	Y	Z
1	6	0	-1.223657	0.346092	0.000000
2	6	0	0.000000	1.032803	0.000000
3	6	0	1.204605	0.345810	0.000000
4	6	0	1.202999	-1.051420	0.000000
5	6	0	-0.004657	-1.742901	0.000000
6	6	0	-1.210896	-1.039938	0.000000
7	8	0	-0.097651	2.401643	0.000000
8	8	0	2.421550	-1.673770	0.000000
9	8	0	-2.406333	1.027575	0.000000
10	1	0	2.152034	0.875441	0.000000
11	1	0	-0.011846	-2.828892	0.000000
12	1	0	-2.158651	-1.566003	0.000000
13	1	0	-2.195933	1.969152	0.000000
14	1	0	0.782236	2.789814	0.000000
15	1	0	2.281267	-2.625781	0.000000

73-1,3,5-TOH

Standard orientation:

Center Number	Atomic Number	Atomic Type	Coordinates (Angstroms) X	Y	Z
1	6	0	-1.010788	-0.948552	0.000000
2	6	0	0.317609	-1.365470	0.000000
3	6	0	1.326864	-0.401101	0.000000
4	6	0	1.023723	0.957782	0.000000
5	6	0	-0.316073	1.349645	0.000000

6	6	0	-1.341326	0.407676	0.000000
7	8	0	2.611188	-0.854941	0.000001
8	8	0	-0.565188	2.688821	0.000000
9	8	0	-2.046003	-1.833865	-0.000001
10	1	0	1.800098	1.715014	0.000000
11	1	0	-2.385298	0.701411	0.000001
12	1	0	0.585208	-2.416443	0.000000
13	1	0	-1.690697	-2.728621	0.000003
14	1	0	3.208379	-0.099829	-0.000002
15	1	0	-1.517728	2.828453	0.000002

74-1,2,3-TMeO

Standard orientation:

Center Number	Atomic Number	Atomic Type	Coordinates (Angstroms) X	Y	Z
1	6	0	-1.213834	-1.656302	0.147281
2	1	0	-2.142479	-2.202946	0.239071
3	6	0	-0.000107	-2.326866	0.254265
4	6	0	1.213667	-1.656384	0.147285
5	6	0	1.214176	-0.275730	-0.076242
6	6	0	-0.000015	0.416475	-0.200128
7	6	0	-1.214252	-0.275645	-0.076240
8	1	0	-0.000143	-3.397915	0.427061
9	1	0	2.142275	-2.203091	0.239076
10	8	0	2.332159	0.490689	-0.187722
11	8	0	0.000018	1.753557	-0.492868
12	8	0	-2.332183	0.490848	-0.187706
13	6	0	3.588875	-0.151417	-0.105021
14	6	0	0.000331	2.609225	0.644221
15	6	0	-3.588941	-0.151170	-0.104977
16	1	0	4.337685	0.632168	-0.232787
17	1	0	3.736548	-0.635209	0.869450
18	1	0	3.713925	-0.901383	-0.896600
19	1	0	0.000303	3.633022	0.263070
20	1	0	-0.895386	2.452606	1.257774
21	1	0	0.896307	2.452500	1.257366
22	1	0	-4.337700	0.632467	-0.232720
23	1	0	-3.714064	-0.901124	-0.896556
24	1	0	-3.736622	-0.634957	0.869495

75-1,2,4-TMeO

Standard orientation:

Center Number	Atomic Number	Atomic Type	Coordinates (Angstroms) X	Y	Z
1	6	0	1.113337	-0.602980	0.000000
2	6	0	0.683122	0.748517	-0.000001
3	6	0	-0.671186	1.039184	-0.000002
4	6	0	-1.625290	0.009049	-0.000002
5	6	0	-1.213213	-1.314406	-0.000001
6	6	0	0.159977	-1.606764	0.000000
7	8	0	1.673213	1.677174	-0.000001
8	6	0	1.302451	3.040801	0.000002
9	8	0	-2.925406	0.428420	-0.000004
10	6	0	-3.933538	-0.559930	0.000004
11	8	0	2.463424	-0.791263	0.000002
12	6	0	2.937499	-2.119690	0.000000
13	1	0	-1.031227	2.058791	-0.000003
14	1	0	-1.923955	-2.129371	-0.000001
15	1	0	0.467452	-2.644507	0.000001
16	1	0	4.027062	-2.054633	-0.000002
17	1	0	2.609951	-2.670094	0.892753
18	1	0	2.609948	-2.670093	-0.892754
19	1	0	2.234784	3.607883	0.000005
20	1	0	0.719706	3.302898	-0.892801
21	1	0	0.719703	3.302893	0.892806
22	1	0	-4.885795	-0.026317	0.000006
23	1	0	-3.878219	-1.197401	-0.892646
24	1	0	-3.878211	-1.197395	0.892658

76-1,3,5-TMeO

Standard orientation:

Center Number	Atomic Number	Atomic Type	Coordinates (Angstroms) X	Y	Z
1	6	0	-1.205384	0.719393	0.000003
2	6	0	-1.207115	-0.685243	-0.000009
3	6	0	-0.020268	-1.403651	-0.000013
4	6	0	1.197058	-0.702824	-0.000004
5	6	0	1.225784	0.684227	0.000007
6	6	0	0.010193	1.388047	0.000010
7	8	0	-2.443948	-1.253624	-0.000020
8	6	0	-2.529453	-2.665233	0.000022
9	8	0	2.307757	-1.489703	-0.000010

10	6	0	3.572899	-0.857745	0.000003
11	8	0	0.136256	2.743388	0.000024
12	6	0	-1.043664	3.522981	-0.000016
13	1	0	0.012704	-2.483401	-0.000028
14	1	0	2.144391	1.252658	0.000013
15	1	0	-2.156960	1.230708	0.000010
16	1	0	-0.719241	4.565034	-0.000029
17	1	0	-1.653555	3.334267	-0.892739
18	1	0	-1.653593	3.334304	0.892690
19	1	0	-3.594173	-2.905023	0.000048
20	1	0	-2.061265	-3.099290	-0.892689
21	1	0	-2.061229	-3.099238	0.892738
22	1	0	4.313069	-1.659789	-0.000001
23	1	0	3.714520	-0.235212	-0.892708
24	1	0	3.714510	-0.235229	0.892727

77-1,2,3-TFor

Standard orientation:

Center Number	Atomic Number	Atomic Type	Coordinates (Angstroms) X	Y	Z
1	6	0	-1.372462	1.537948	-0.044131
2	1	0	-2.408869	1.853937	-0.083473
3	6	0	-0.334190	2.455839	-0.078144
4	6	0	0.978627	1.999389	-0.016084
5	6	0	1.258178	0.633738	0.065089
6	6	0	0.203143	-0.306323	0.104373
7	6	0	-1.121874	0.161796	0.051586
8	1	0	-0.542322	3.517350	-0.152428
9	1	0	1.804668	2.703884	-0.049742
10	6	0	2.685332	0.235466	0.032413
11	6	0	0.487533	-1.775131	0.222215
12	6	0	-2.325712	-0.728235	0.153347
13	8	0	3.099331	-0.890340	-0.120543
14	1	0	3.388226	1.089166	0.148160
15	8	0	-0.179798	-2.619906	-0.328115
16	1	0	1.333192	-2.043577	0.875837
17	8	0	-3.441981	-0.319736	-0.069871
18	1	0	-2.146761	-1.767832	0.465886

78-1,2,4-TFor

Standard orientation:

Center Number	Atomic Number	Atomic Type	Coordinates (Angstroms) X	Y	Z
1	6	0	0.000000	0.891091	0.000000
2	6	0	-0.244283	2.371900	0.000000
3	6	0	-1.126184	0.066277	0.000000
4	6	0	-1.011084	-1.321821	0.000000
5	6	0	0.256874	-1.913587	0.000000
6	6	0	1.383828	-1.108212	0.000000
7	6	0	1.280457	0.290946	0.000000
8	1	0	-2.100974	0.544623	0.000000
9	6	0	-2.231354	-2.170900	0.000000
10	1	0	0.328617	-2.995310	0.000000
11	1	0	2.371428	-1.559865	0.000000
12	6	0	2.573713	1.030298	0.000000
13	8	0	2.728095	2.228144	0.000000
14	1	0	3.453750	0.350288	0.000000
15	8	0	-1.365152	2.829405	0.000000
16	1	0	0.648401	3.012643	0.000000
17	8	0	-2.213663	-3.378062	0.000000
18	1	0	-3.187257	-1.604229	0.000000

79-1,3,5-TFor

Standard orientation:

Center Number	Atomic Number	Atomic Type	Coordinates (Angstroms) X	Y	Z
1	6	0	-1.206675	-0.696697	0.000000
2	1	0	-2.133490	-1.263182	0.000000
3	6	0	-1.215445	0.693704	0.000000
4	6	0	0.000000	1.393344	0.000000
5	6	0	1.208506	0.705735	0.000000
6	6	0	1.206702	-0.696693	0.000000
7	6	0	0.006960	-1.399480	0.000000
8	6	0	-2.501402	1.436224	0.000000
9	1	0	-0.027170	2.479230	0.000000
10	6	0	2.494500	1.448189	0.000000
11	1	0	2.160692	-1.216110	0.000000
12	6	0	0.006879	-2.884411	0.000000
13	8	0	-0.993442	-3.560535	0.000000
14	1	0	1.018473	-3.345013	0.000000
15	8	0	-2.586807	2.640588	0.000000
16	1	0	-3.406078	0.790440	0.000000

17	8	0	3.580235	0.920021	0.000000
18	1	0	2.387528	2.554552	0.000000

80-1,2,3-TVin

Standard orientation:

Center Number	Atomic Number	Atomic Type	Coordinates (Angstroms) X	Y	Z
1	6	0	0.984193	-1.777969	0.040558
2	1	0	1.868042	-2.399073	0.132415
3	6	0	-0.259230	-2.366137	-0.135308
4	6	0	-1.395488	-1.569983	-0.198647
5	6	0	-1.304036	-0.179668	-0.082126
6	6	0	-0.032815	0.427048	0.075920
7	6	0	1.124583	-0.386322	0.141109
8	1	0	-0.344362	-3.444564	-0.218727
9	1	0	-2.367126	-2.021657	-0.365059
10	6	0	-2.523178	0.645758	-0.179011
11	6	0	0.029147	1.897886	0.199557
12	6	0	2.463455	0.182383	0.381313
13	6	0	-3.736470	0.294163	0.251450
14	1	0	-2.402965	1.619545	-0.646975
15	1	0	-4.591482	0.948061	0.120199
16	1	0	-3.919848	-0.648108	0.758138
17	6	0	0.909600	2.716465	-0.380725
18	1	0	-0.754090	2.342724	0.810062
19	1	0	0.858978	3.789359	-0.227605
20	1	0	1.695828	2.353702	-1.033307
21	6	0	3.614893	-0.314661	-0.075416
22	1	0	2.489830	1.084111	0.987001
23	1	0	4.564188	0.142865	0.180231
24	1	0	3.655078	-1.180735	-0.728416

81-1,2,4-TVin

Standard orientation:

Center Number	Atomic Number	Atomic Type	Coordinates (Angstroms) X	Y	Z
1	6	0	-1.118154	-0.608649	-0.072976
2	6	0	-2.549123	-0.938397	-0.161868
3	6	0	-0.680996	0.728719	0.071635
4	6	0	0.693314	0.987111	0.127664
5	6	0	1.658993	-0.018115	0.030323
6	6	0	1.206705	-1.339236	-0.123627
7	6	0	-0.146333	-1.617665	-0.174490
8	6	0	-1.645974	1.835303	0.208078
9	1	0	1.021459	2.010134	0.283597
10	6	0	3.078177	0.347894	0.099573
11	1	0	1.918880	-2.152527	-0.208579
12	1	0	-0.471522	-2.640970	-0.328332
13	6	0	-3.113564	-2.093766	0.199033
14	1	0	-3.191257	-0.158874	-0.563609
15	1	0	-4.177994	-2.260366	0.077583
16	1	0	-2.543943	-2.906818	0.637545
17	6	0	-1.459314	3.089614	-0.207741
18	1	0	-2.585537	1.589858	0.696554
19	1	0	-2.212098	3.853303	-0.047095
20	1	0	-0.560058	3.398061	-0.731462
21	6	0	4.135124	-0.462417	0.005969
22	1	0	3.259756	1.412046	0.242170
23	1	0	5.144369	-0.072521	0.071463
24	1	0	4.044812	-1.533696	-0.139278

82-1,3,5-TVin

Standard orientation:

Center Number	Atomic Number	Atomic Type	Coordinates (Angstroms) X	Y	Z
1	6	0	-0.782645	1.144974	-0.000203
2	6	0	-1.407984	-0.101987	-0.000362
3	6	0	-0.600310	-1.250381	-0.000441
4	6	0	0.792240	-1.168407	-0.000214
5	6	0	1.382976	0.105248	0.000020
6	6	0	0.615723	1.270256	0.000010
7	6	0	-2.877122	-0.157642	-0.000480
8	6	0	-3.654049	-1.242378	0.000930
9	6	0	1.575142	-2.412820	-0.000293
10	6	0	2.903049	-2.542975	0.000375
11	6	0	1.302017	2.570440	0.000184
12	6	0	0.750948	3.785588	0.000206
13	1	0	-1.061846	-2.232474	-0.000804
14	1	0	2.464271	0.196496	0.000111
15	1	0	-1.402337	2.035766	-0.000214
16	1	0	2.388635	2.501155	0.000305
17	1	0	1.367580	4.677043	0.000337

18	1	0	-0.321784	3.946926	0.000097
19	1	0	0.971929	-3.319282	-0.000940
20	1	0	3.366926	-3.522639	0.000242
21	1	0	3.578958	-1.694491	0.001105
22	1	0	-3.360355	0.818075	-0.001774
23	1	0	-4.734376	-1.153969	0.000669
24	1	0	-3.257520	-2.252103	0.002470

83-1,2,3-TMe

Standard orientation:

Center Number	Atomic Number	Atomic Type	Coordinates (Angstroms) X	Y	Z
1	6	0	1.211236	0.082781	0.000000
2	6	0	0.013831	-0.659202	-0.000001
3	6	0	-1.221994	0.013516	0.000000
4	6	0	-1.239043	1.411207	0.000000
5	6	0	-0.059506	2.144110	0.000000
6	6	0	1.159537	1.477200	0.000000
7	6	0	0.088387	-2.169166	0.000000
8	6	0	-2.537908	-0.732830	0.000000
9	6	0	2.550135	-0.614788	0.000001
10	1	0	0.629264	-2.542870	0.877971
11	1	0	0.629281	-2.542870	-0.877961
12	1	0	-0.896656	-2.635406	-0.000010
13	1	0	-2.194832	1.926716	0.000000
14	1	0	-0.089963	3.228809	0.000000
15	1	0	2.087320	2.041667	0.000000
16	1	0	-3.376486	-0.031889	0.000002
17	1	0	-2.647250	-1.376039	-0.880670
18	1	0	-2.647248	-1.376041	0.880670
19	1	0	3.368403	0.109545	0.000007
20	1	0	2.675055	-1.259301	0.878529
21	1	0	2.675061	-1.259291	-0.878534

84-1,2,4-TMe

Standard orientation:

Center Number	Atomic Number	Atomic Type	Coordinates (Angstroms) X	Y	Z
1	6	0	0.698816	0.754019	-0.000542
2	6	0	1.699720	1.883311	-0.001086
3	6	0	-0.667362	1.030125	-0.006139
4	6	0	-1.636916	0.022530	-0.007199
5	6	0	-1.198739	-1.299934	-0.007244
6	6	0	0.162522	-1.594101	-0.001533
7	6	0	1.127358	-0.588168	0.002489
8	1	0	-0.988816	2.069162	-0.011284
9	6	0	-3.106631	0.365700	0.008786
10	1	0	-1.924060	-2.108357	-0.012719
11	1	0	0.483312	-2.632152	-0.003271
12	6	0	2.595315	-0.935760	0.005804
13	1	0	3.109114	-0.526790	0.884343
14	1	0	2.742235	-2.018854	0.009036
15	1	0	3.112133	-0.531711	-0.873282
16	1	0	2.357536	1.842624	-0.877730
17	1	0	1.198350	2.854436	-0.005286
18	1	0	2.352259	1.847628	0.879719
19	1	0	-3.720850	-0.500986	-0.250787
20	1	0	-3.426622	0.710132	0.999946
21	1	0	-3.339090	1.168543	-0.698696

85-1,3,5-TMe

Standard orientation:

Center Number	Atomic Number	Atomic Type	Coordinates (Angstroms) X	Y	Z
1	6	0	-1.401270	-0.121423	-0.000006
2	6	0	-0.798143	1.132491	0.000016
3	6	0	0.595472	1.274261	0.000008
4	6	0	1.379819	0.124960	-0.000016
5	6	0	0.805813	-1.152828	-0.000035
6	6	0	-0.581686	-1.257427	-0.000040
7	6	0	1.221872	2.648041	0.000001
8	6	0	1.682338	-2.382197	0.000028
9	6	0	-2.904199	-0.265868	0.000013
10	1	0	-1.422145	2.022890	0.000024
11	1	0	2.462931	0.220158	-0.000033
12	1	0	-1.040840	-2.243006	-0.000079
13	1	0	-3.398965	0.708983	-0.000227
14	1	0	-3.252371	-0.818352	-0.880256
15	1	0	-3.252385	-0.817910	0.880556
16	1	0	2.313495	2.589056	0.000255
17	1	0	0.917879	3.225585	-0.880547
18	1	0	0.917475	3.225778	0.880282

19	1	0	1.085422	-3.298065	-0.000967
20	1	0	2.335466	-2.407107	-0.879818
21	1	0	2.333938	-2.408072	0.880989

86-1,2,3-TEt

Standard orientation:

Center Number	Atomic Number	Atomic Type	Coordinates (Angstroms) X	Y	Z
1	6	0	-1.217178	0.433732	-0.210850
2	6	0	-2.568750	-0.244604	-0.080212
3	6	0	-1.197626	1.817899	-0.401241
4	6	0	0.000055	2.513684	-0.496056
5	6	0	1.197705	1.817846	-0.401243
6	6	0	1.217189	0.433678	-0.210853
7	6	0	-0.000011	-0.271834	-0.113121
8	1	0	-2.140688	2.351681	-0.480295
9	1	0	0.000077	3.587652	-0.651702
10	1	0	2.140789	2.351581	-0.480295
11	6	0	2.568733	-0.244712	-0.080220
12	6	0	-0.000044	-1.782364	0.053672
13	1	0	2.546361	-1.253269	-0.502765
14	6	0	3.066999	-0.310652	1.375085
15	1	0	3.298738	0.314901	-0.675791
16	1	0	4.051742	-0.785938	1.431854
17	1	0	3.148435	0.693969	1.801739
18	1	0	2.378896	-0.880106	2.007972
19	1	0	-0.869903	-2.096351	0.636811
20	1	0	0.869817	-2.096394	0.636792
21	6	0	-0.000072	-2.535427	-1.290190
22	1	0	-0.000118	-3.619056	-1.132907
23	1	0	-0.881092	-2.279173	-1.886879
24	1	0	0.880972	-2.279248	-1.886868
25	1	0	-2.546429	-1.253137	-0.502817
26	1	0	-3.298753	0.315076	-0.675733
27	6	0	-3.066978	-0.310609	1.375103
28	1	0	-4.051725	-0.785877	1.431873
29	1	0	-2.378864	-0.880112	2.007944
30	1	0	-3.148385	0.693992	1.801812

87-1,3,5-TEt

Standard orientation:

Center Number	Atomic Number	Atomic Type	Coordinates (Angstroms) X	Y	Z
1	6	0	-0.623149	-1.217251	-0.361543
2	6	0	-1.265284	0.003368	-0.579508
3	6	0	-0.616024	1.220430	-0.361671
4	6	0	0.709066	1.197218	0.078527
5	6	0	1.384523	-0.004296	0.301829
6	6	0	0.702049	-1.201993	0.078613
7	6	0	-1.342346	2.531812	-0.561951
8	6	0	-2.059655	3.014579	0.711024
9	6	0	2.835447	-0.008549	0.729844
10	6	0	3.807606	-0.009433	-0.462885
11	6	0	-1.357255	-2.524654	-0.561830
12	6	0	-2.078584	-3.002147	0.710740
13	1	0	1.228997	2.137763	0.247142
14	1	0	1.216376	-2.145536	0.247327
15	1	0	-2.294527	0.006329	-0.931691
16	1	0	-2.089311	-2.413058	-1.370091
17	1	0	-0.649559	-3.296639	-0.885602
18	1	0	-2.599901	-3.948806	0.535478
19	1	0	-1.368008	-3.151062	1.529982
20	1	0	-2.815557	-2.263781	1.042474
21	1	0	-0.630594	3.299610	-0.886761
22	1	0	-2.075997	2.424295	-1.369316
23	1	0	-2.575291	3.964282	0.535349
24	1	0	-2.800728	2.280911	1.043894
25	1	0	-1.347435	3.159835	1.529501
26	1	0	3.034913	0.868757	1.356110
27	1	0	3.030302	-0.888556	1.353775
28	1	0	4.848041	-0.012440	-0.122079
29	1	0	3.652687	-0.891414	-1.092446
30	1	0	3.657230	0.875007	-1.090179

88-1,2-OH-3-For

Standard orientation:

Center Number	Atomic Number	Atomic Type	Coordinates (Angstroms) X	Y	Z
1	6	0	0.000000	0.563248	0.000000
2	6	0	0.794585	-0.598668	0.000000
3	6	0	0.178942	-1.865393	0.000000
4	6	0	-1.198659	-1.963380	0.000000

5	6	0	-1.986717	-0.802863	0.000000
6	6	0	-1.402054	0.454018	0.000000
7	6	0	2.239664	-0.461117	0.000000
8	8	0	2.831878	0.615082	0.000000
9	8	0	-2.165483	1.574380	0.000000
10	8	0	0.514007	1.806333	0.000000
11	1	0	0.802986	-2.753390	0.000000
12	1	0	-1.681157	-2.933733	0.000000
13	1	0	-3.069412	-0.864754	0.000000
14	1	0	-1.564593	2.331982	0.000000
15	1	0	1.497067	1.704181	0.000000
16	1	0	2.817334	-1.405715	0.000000

89-1,2-OH-4-For

Standard orientation:

Center Number	Atomic Number	Atomic Type	Coordinates (Angstroms) X	Y	Z
1	6	0	0.000000	0.982597	0.000000
2	1	0	-0.008705	2.068754	0.000000
3	6	0	1.239447	0.321420	0.000000
4	6	0	1.279203	-1.073860	0.000000
5	6	0	0.102426	-1.814765	0.000000
6	6	0	-1.124629	-1.160046	0.000000
7	6	0	-1.167466	0.250677	0.000000
8	6	0	2.485998	1.101805	0.000000
9	1	0	2.239016	-1.581306	0.000000
10	1	0	0.110402	-2.898399	0.000000
11	8	0	-2.273173	-1.871465	0.000000
12	8	0	-2.430639	0.782169	0.000000
13	1	0	-3.009019	-1.244576	0.000000
14	1	0	-2.381533	1.743123	0.000000
15	8	0	2.547425	2.312210	0.000000
16	1	0	3.411059	0.482130	0.000000

90-1,2-OH-3-MeO

Standard orientation:

Center Number	Atomic Number	Atomic Type	Coordinates (Angstroms) X	Y	Z
1	6	0	0.653581	-0.446422	0.000000
2	8	0	2.020766	-0.342011	0.000000
3	6	0	-0.083261	-1.628501	0.000000
4	6	0	-1.477872	-1.553519	0.000000
5	6	0	-2.134943	-0.329323	0.000000
6	6	0	-1.391940	0.850609	0.000000
7	6	0	0.000000	0.788971	0.000000
8	1	0	0.410961	-2.590804	0.000000
9	1	0	-2.056614	-2.470400	0.000000
10	1	0	-3.216214	-0.263797	0.000000
11	8	0	-2.021129	2.056699	0.000000
12	8	0	0.692178	1.971074	0.000000
13	1	0	-1.338771	2.739998	0.000000
14	1	0	1.632043	1.750961	0.000000
15	6	0	2.777908	-1.537529	0.000000
16	1	0	3.826750	-1.237020	0.000000
17	1	0	2.573246	-2.140377	0.893415
18	1	0	2.573246	-2.140377	-0.893415

91-1,2-OH-4-MeO

Standard orientation:

Center Number	Atomic Number	Atomic Type	Coordinates (Angstroms) X	Y	Z
1	6	0	0.000000	1.153172	0.000000
2	1	0	0.147874	2.228530	0.000000
3	6	0	1.124000	0.316477	0.000000
4	6	0	0.953307	-1.065781	0.000000
5	6	0	-0.337996	-1.604306	0.000000
6	6	0	-1.454633	-0.786697	0.000000
7	6	0	-1.270691	0.605719	0.000000
8	8	0	2.329092	0.958714	0.000000
9	1	0	1.802658	-1.735097	0.000000
10	1	0	-0.484600	-2.678444	0.000000
11	8	0	-2.709334	-1.322554	0.000000
12	8	0	-2.425181	1.347590	0.000000
13	1	0	-3.335931	-0.588750	0.000000
14	1	0	-2.208486	2.284566	0.000000
15	6	0	3.497557	0.165062	0.000000
16	1	0	4.338921	0.860308	0.000000
17	1	0	3.556841	-0.471494	0.892803
18	1	0	3.556841	-0.471494	-0.892803

92-1,2-OH-3-Me

Standard orientation:

Center Number	Atomic Number	Atomic Type	Coordinates (Angstroms) X	Y	Z
1	6	0	-1.182424	0.132155	-0.000001
2	6	0	-2.547943	-0.510449	-0.000006
3	6	0	-1.020797	1.521895	0.000002
4	6	0	0.246916	2.093173	0.000003
5	6	0	1.383338	1.287526	-0.000001
6	6	0	1.245044	-0.094885	-0.000001
7	6	0	-0.036176	-0.662426	0.000000
8	1	0	-1.903415	2.153184	0.000002
9	1	0	0.355032	3.172170	0.000005
10	1	0	2.381701	1.709556	-0.000002
11	8	0	2.347726	-0.891905	-0.000002
12	8	0	-0.058253	-2.038785	0.000008
13	1	0	2.041922	-1.807686	-0.000016
14	1	0	-0.967300	-2.350829	0.000001
15	1	0	-2.709137	-1.140687	0.885329
16	1	0	-3.333211	0.248605	-0.000018
17	1	0	-2.709127	-1.140721	-0.885314

93-1,2-OH-4-Me

Standard orientation:

Center Number	Atomic Number	Atomic Type	Coordinates (Angstroms) X	Y	Z
1	6	0	-1.175872	0.313912	0.000000
2	1	0	-2.128934	0.839355	0.000000
3	6	0	-1.150110	-1.087771	0.000000
4	6	0	0.091330	-1.720085	0.000000
5	6	0	1.279066	-0.986992	0.000000
6	6	0	1.245121	0.399191	0.000000
7	6	0	0.000000	1.046921	0.000000
8	6	0	-2.438022	-1.874750	0.000000
9	1	0	0.138999	-2.804304	0.000000
10	1	0	2.244031	-1.481306	0.000000
11	8	0	2.399921	1.119827	0.000000
12	8	0	0.057123	2.419815	0.000000
13	1	0	2.157483	2.054201	0.000000
14	1	0	-0.834346	2.780527	0.000000
15	1	0	-2.242052	-2.950149	0.000000
16	1	0	-3.050303	-1.649004	0.881037
17	1	0	-3.050303	-1.649004	-0.881037

94-1,2-OH-6-Me

Standard orientation:

Center Number	Atomic Number	Atomic Type	Coordinates (Angstroms) X	Y	Z
1	6	0	1.335866	1.310002	0.000002
2	1	0	2.321771	1.767194	0.000005
3	6	0	0.183333	2.094538	-0.000001
4	6	0	-1.068595	1.489331	-0.000004
5	6	0	-1.205239	0.097678	-0.000003
6	6	0	-0.045502	-0.679573	-0.000002
7	6	0	1.216579	-0.072834	0.000001
8	6	0	-2.550442	-0.579598	0.000006
9	8	0	-0.152050	-2.038907	-0.000006
10	8	0	2.280840	-0.943917	0.000003
11	1	0	0.743861	-2.398542	-0.000003
12	1	0	3.104165	-0.447261	0.000004
13	1	0	0.268547	3.175319	-0.000001
14	1	0	-1.964693	2.101627	-0.000007
15	1	0	-2.671118	-1.224805	0.877163
16	1	0	-3.357774	0.156698	-0.000049
17	1	0	-2.671080	-1.224902	-0.877084

95-1,3-OH-2-Me

Standard orientation:

Center Number	Atomic Number	Atomic Type	Coordinates (Angstroms) X	Y	Z
1	6	0	1.205295	1.413882	-0.001041
2	1	0	2.150798	1.948678	0.001637
3	6	0	-0.000161	2.104772	-0.003018
4	6	0	-1.205510	1.413699	-0.001042
5	6	0	-1.195262	0.016917	0.001790
6	6	0	0.000046	-0.712157	-0.003247
7	6	0	1.195243	0.017103	0.001791
8	1	0	-0.000244	3.189472	-0.004596
9	1	0	-2.151091	1.948357	0.001636

10	8	0	-2.355502	-0.705196	0.009207
11	6	0	0.000216	-2.218626	-0.009982
12	8	0	2.355564	-0.704874	0.009204
13	1	0	0.890098	-2.601911	-0.512867
14	1	0	0.001017	-2.625693	1.008836
15	1	0	-0.890266	-2.602124	-0.511620
16	1	0	-3.099077	-0.095082	-0.020918
17	1	0	3.099073	-0.094677	-0.020900

96-1,3-OH-5-MeO

Standard orientation:

Center Number	Atomic Number	Atomic Type	Coordinates (Angstroms) X	Y	Z
1	6	0	1.748652	0.434435	0.000003
2	6	0	1.444735	-0.929499	0.000002
3	6	0	0.126912	-1.368354	-0.000003
4	6	0	-0.909268	-0.426331	-0.000007
5	6	0	-0.632171	0.938812	-0.000006
6	6	0	0.704370	1.351534	-0.000001
7	8	0	2.498394	-1.793884	0.000006
8	8	0	-2.164760	-0.947832	-0.000015
9	6	0	-3.261202	-0.053338	0.000016
10	8	0	0.923953	2.696898	-0.000001
11	1	0	-0.122785	-2.423796	-0.000007
12	1	0	-1.405643	1.692817	-0.000012
13	1	0	2.786427	0.749587	0.000008
14	1	0	1.873213	2.857215	0.000005
15	1	0	2.160441	-2.695336	0.000006
16	1	0	-4.158584	-0.674293	0.000020
17	1	0	-3.262954	0.584381	0.892978
18	1	0	-3.262984	0.584408	-0.892928

97-1,3-OH-5-For

Standard orientation:

Center Number	Atomic Number	Atomic Type	Coordinates (Angstroms) X	Y	Z
1	6	0	0.262022	-1.703875	0.000000
2	6	0	1.398132	-0.898731	0.000000
3	6	0	1.272168	0.492499	0.000000
4	6	0	0.000000	1.058537	0.000000
5	6	0	-1.149088	0.261205	0.000000
6	6	0	-1.010394	-1.121414	0.000000
7	8	0	2.656479	-1.414470	0.000000
8	6	0	-0.131959	2.534274	0.000000
9	8	0	-1.183465	3.130959	0.000000
10	8	0	-2.071327	-1.972296	0.000000
11	1	0	2.162785	1.110903	0.000000
12	1	0	-2.122031	0.741670	0.000000
13	1	0	0.340217	-2.786769	0.000000
14	1	0	-2.885627	-1.457913	0.000000
15	1	0	2.608075	-2.376204	0.000000
16	1	0	0.837799	3.079799	0.000000

98-1,3-OH-5-Et

Standard orientation:

Center Number	Atomic Number	Atomic Type	Coordinates (Angstroms) X	Y	Z
1	6	0	-1.106284	1.210618	0.012475
2	6	0	0.265976	1.193776	-0.230908
3	6	0	0.942672	-0.023970	-0.353034
4	6	0	0.233623	-1.216882	-0.233108
5	6	0	-1.140964	-1.191086	0.011049
6	6	0	-1.819165	0.018622	0.135455
7	6	0	2.439452	-0.043777	-0.572963
8	6	0	3.231967	-0.033203	0.745899
9	8	0	-1.779146	-2.391195	0.116125
10	8	0	-1.814003	2.370070	0.136417
11	1	0	0.729339	-2.176278	-0.329435
12	1	0	-2.887947	0.056055	0.320456
13	1	0	0.809515	2.130305	-0.330043
14	1	0	-1.211283	3.113455	0.031709
15	1	0	-2.715173	-2.235011	0.278480
16	1	0	2.710714	-0.934819	-1.149988
17	1	0	2.732329	0.822650	-1.177309
18	1	0	4.309844	-0.048103	0.554771
19	1	0	3.002487	0.861309	1.333688
20	1	0	2.981696	-0.905152	1.358151

99-1-OH-2-MeO-3-For

Standard orientation:

Center Number	Atomic Number	Atomic Type	Coordinates (Angstroms) X	Y	Z
1	6	0	-0.936667	-0.237658	-0.079688
2	6	0	-2.165266	0.572841	-0.242838
3	6	0	-1.038608	-1.614129	0.167315
4	6	0	0.106373	-2.389289	0.274074
5	6	0	1.369444	-1.815729	0.122209
6	6	0	1.486421	-0.450473	-0.120737
7	6	0	0.331611	0.340221	-0.204037
8	1	0	-2.029732	-2.041639	0.260184
9	1	0	0.026122	-3.454009	0.464148
10	1	0	2.272738	-2.411944	0.185442
11	8	0	2.710388	0.112722	-0.278556
12	8	0	0.518952	1.686607	-0.455947
13	1	0	2.557045	1.021849	-0.573250
14	6	0	0.521965	2.514010	0.714416
15	1	0	0.722968	3.531311	0.373394
16	1	0	-0.450020	2.483451	1.219587
17	1	0	1.300954	2.198679	1.418829
18	8	0	-3.286254	0.141483	-0.089529
19	1	0	-1.996405	1.627041	-0.540356

100-1-OH-2-MeO-4-For

Standard orientation:

Center Number	Atomic Number	Atomic Type	Coordinates (Angstroms) X	Y	Z
1	1	0	2.141317	1.147513	0.000000
2	6	0	1.250999	0.530015	0.000000
3	6	0	0.000000	1.112665	0.000000
4	8	0	-0.134024	2.461847	0.000000
5	1	0	-1.080207	2.657437	0.000000
6	6	0	-1.152886	0.292018	0.000000
7	8	0	-2.320891	0.993194	0.000000
8	6	0	-3.543903	0.275267	0.000000
9	1	0	-3.635276	-0.352460	0.894301
10	1	0	-3.635276	-0.352460	-0.894301
11	1	0	-4.336806	1.024076	0.000000
12	6	0	1.373693	-0.868337	0.000000
13	6	0	2.707697	-1.495770	0.000000
14	6	0	0.234116	-1.670203	0.000000
15	1	0	0.336182	-2.750943	0.000000
16	6	0	-1.035282	-1.093396	0.000000
17	1	0	-1.917401	-1.720643	0.000000
18	8	0	3.759577	-0.897087	0.000000
19	1	0	2.683568	-2.609709	0.000000

101-1-OH-2-MeO-5-For

Standard orientation:

Center Number	Atomic Number	Atomic Type	Coordinates (Angstroms) X	Y	Z
1	1	0	2.141317	1.147513	0.000000
2	6	0	1.250999	0.530015	0.000000
3	6	0	0.000000	1.112665	0.000000
4	8	0	-0.134024	2.461847	0.000000
5	1	0	-1.080207	2.657437	0.000000
6	6	0	-1.152886	0.292018	0.000000
7	8	0	-2.320891	0.993194	0.000000
8	6	0	-3.543903	0.275267	0.000000
9	1	0	-3.635276	-0.352460	0.894301
10	1	0	-3.635276	-0.352460	-0.894301
11	1	0	-4.336806	1.024076	0.000000
12	6	0	1.373693	-0.868337	0.000000
13	6	0	2.707697	-1.495770	0.000000
14	6	0	0.234116	-1.670203	0.000000
15	1	0	0.336182	-2.750943	0.000000
16	6	0	-1.035282	-1.093396	0.000000
17	1	0	-1.917401	-1.720643	0.000000
18	8	0	3.759577	-0.897087	0.000000
19	1	0	2.683568	-2.609709	0.000000

102-1-OH-2-MeO-6-For

Standard orientation:

Center Number	Atomic Number	Atomic Type	Coordinates (Angstroms) X	Y	Z
1	6	0	2.476131	1.039867	0.000000
2	6	0	1.293043	0.153976	0.000000
3	6	0	0.000000	0.684030	0.000000
4	8	0	-0.203768	2.022460	0.000000
5	1	0	-1.160692	2.162810	0.000000
6	6	0	-1.113288	-0.182552	0.000000

7	8	0	-2.314054	0.474835	0.000000
8	6	0	-3.501364	-0.297235	0.000000
9	1	0	-3.564901	-0.929578	0.894046
10	1	0	-3.564901	-0.929578	-0.894046
11	1	0	-4.329074	0.413195	0.000000
12	6	0	1.462935	-1.241992	0.000000
13	6	0	0.370592	-2.085104	0.000000
14	1	0	0.504458	-3.160787	0.000000
15	6	0	-0.929345	-1.555329	0.000000
16	1	0	-1.782431	-2.222385	0.000000
17	1	0	2.478048	-1.621028	0.000000
18	8	0	3.619495	0.636354	0.000000
19	1	0	2.253887	2.124196	0.000000

103-1-OH,2-MeO,4-Me

Standard orientation:

Center Number	Atomic Number	Atomic Type	Coordinates (Angstroms) X	Y	Z
1	6	0	-0.949108	1.169355	-0.213258
2	6	0	0.354755	1.631464	0.003544
3	6	0	1.407126	0.728324	0.080767
4	6	0	1.146436	-0.638157	-0.061209
5	6	0	-0.153920	-1.093202	-0.276660
6	6	0	-1.219448	-0.190556	-0.353441
7	8	0	0.522141	2.976620	0.125742
8	6	0	2.259722	-1.609468	0.012886
9	8	0	3.419362	-1.318569	0.197129
10	6	0	-2.638476	-0.676485	-0.547254
11	6	0	-3.349881	-0.972166	0.784766
12	1	0	-0.334673	-2.158883	-0.389512
13	1	0	-1.748257	1.901377	-0.274039
14	1	0	2.431001	1.051267	0.244180
15	1	0	1.455886	3.166348	0.266454
16	1	0	1.948945	-2.670472	-0.116923
17	1	0	-3.209337	0.075035	-1.103768
18	1	0	-2.630743	-1.583318	-1.162398
19	1	0	-4.371720	-1.323387	0.611095
20	1	0	-2.816925	-1.742113	1.351512
21	1	0	-3.399425	-0.074907	1.409590

104-1-OH-2-MeO-4-Et

Standard orientation:

Center Number	Atomic Number	Atomic Type	Coordinates (Angstroms) X	Y	Z
1	6	0	-1.364534	-0.184361	-0.342133
2	6	0	-0.285989	0.709699	-0.251005
3	6	0	1.003718	0.242465	-0.041253
4	6	0	1.248056	-1.137991	0.082357
5	6	0	0.187057	-2.024308	-0.009453
6	6	0	-1.107518	-1.547441	-0.220774
7	8	0	2.133743	1.013590	0.059331
8	6	0	1.998501	2.416903	-0.049874
9	8	0	2.513935	-1.592751	0.283166
10	1	0	0.389195	-3.085690	0.080852
11	1	0	-1.927227	-2.255539	-0.294520
12	1	0	-0.470380	1.773271	-0.350969
13	1	0	3.088856	-0.816820	0.311327
14	1	0	3.001529	2.832299	0.060481
15	1	0	1.592400	2.705469	-1.027607
16	1	0	1.350571	2.819483	0.738962
17	6	0	-2.771994	0.337020	-0.530077
18	6	0	-3.444966	0.745677	0.791943
19	1	0	-2.758974	1.199614	-1.207600
20	1	0	-3.380214	-0.431320	-1.020671
21	1	0	-4.459768	1.119000	0.619062
22	1	0	-3.506523	-0.105797	1.476996
23	1	0	-2.874884	1.533334	1.295335

105-1-OH-2-For-4-Et

Standard orientation:

Center Number	Atomic Number	Atomic Type	Coordinates (Angstroms) X	Y	Z
1	6	0	-1.238153	0.874811	0.043001
2	6	0	-0.942445	-0.505559	-0.079997
3	6	0	0.387670	-0.918173	-0.271398
4	6	0	1.432654	-0.011952	-0.344150
5	6	0	1.109395	1.353465	-0.222151
6	6	0	-0.188084	1.797656	-0.033190
7	6	0	-2.014058	-1.481637	-0.012582
8	8	0	-3.198852	-1.204823	0.151853
9	6	0	2.867416	-0.456431	-0.516791

10	6	0	3.648840	-0.497770	0.807771
11	8	0	-2.486236	1.315986	0.223489
12	1	0	0.585957	-1.983614	-0.366704
13	1	0	1.908346	2.087825	-0.283757
14	1	0	-0.418221	2.853234	0.053495
15	1	0	-3.070083	0.521627	0.245943
16	1	0	-1.707806	-2.541342	-0.120379
17	1	0	2.886382	-1.449473	-0.979582
18	1	0	3.377913	0.218630	-1.214288
19	1	0	4.683538	-0.814272	0.642576
20	1	0	3.668584	0.487748	1.284186
21	1	0	3.186677	-1.196113	1.512687

106-1-OH-3-For-4-Et

Standard orientation:

Center Number	Atomic Number	Atomic Type	Coordinates (Angstroms) X	Y	Z
1	6	0	2.199950	0.050551	0.086303
2	6	0	1.222797	1.039880	0.086249
3	6	0	-0.127506	0.722765	-0.096184
4	6	0	-0.534269	-0.617465	-0.297606
5	6	0	0.469812	-1.586239	-0.302879
6	6	0	1.813193	-1.274011	-0.112288
7	6	0	-1.055009	1.878035	-0.077717
8	8	0	-2.262263	1.845468	-0.159510
9	8	0	3.494043	0.431128	0.275705
10	6	0	-1.972980	-1.043625	-0.489450
11	1	0	0.193486	-2.624002	-0.464651
12	1	0	2.561038	-2.063033	-0.124565
13	1	0	1.523893	2.072706	0.230893
14	1	0	4.060759	-0.346841	0.251666
15	1	0	-0.528131	2.854143	0.024438
16	6	0	-2.743712	-1.187114	0.835199
17	1	0	-2.496891	-0.324971	-1.122338
18	1	0	-1.975338	-2.007531	-1.011470
19	1	0	-3.761642	-1.542478	0.646616
20	1	0	-2.252077	-1.902405	1.502773
21	1	0	-2.812990	-0.225017	1.347311

107-1-OH-3-For-5-Et

Standard orientation:

Center Number	Atomic Number	Atomic Type	Coordinates (Angstroms) X	Y	Z
1	6	0	-0.949108	1.169355	-0.213258
2	6	0	0.354755	1.631464	0.003544
3	6	0	1.407126	0.728324	0.080767
4	6	0	1.146436	-0.638157	-0.061209
5	6	0	-0.153920	-1.093202	-0.276660
6	6	0	-1.219448	-0.190556	-0.353441
7	8	0	0.522141	2.976620	0.125742
8	6	0	2.259722	-1.609468	0.012886
9	8	0	3.419362	-1.318569	0.197129
10	6	0	-2.638476	-0.676485	-0.547254
11	6	0	-3.349881	-0.972166	0.784766
12	1	0	-0.334673	-2.158883	-0.389512
13	1	0	-1.748257	1.901377	-0.274039
14	1	0	2.431001	1.051267	0.244180
15	1	0	1.455886	3.166348	0.266454
16	1	0	1.948945	-2.670472	-0.116923
17	1	0	-3.209337	0.075035	-1.103768
18	1	0	-2.630743	-1.583318	-1.162398
19	1	0	-4.371720	-1.323387	0.611095
20	1	0	-2.816925	-1.742113	1.351512
21	1	0	-3.399425	-0.074907	1.409590

108-1-OH-2-Vin-3-Et

Standard orientation:

Center Number	Atomic Number	Atomic Type	Coordinates (Angstroms) X	Y	Z
1	6	0	0.276660	0.345345	-0.044716
2	6	0	-0.917644	-0.364148	-0.297357
3	6	0	-0.892701	-1.756794	-0.357968
4	6	0	0.291478	-2.458897	-0.148846
5	6	0	1.467351	-1.778773	0.128726
6	6	0	1.464943	-0.384981	0.177156
7	8	0	2.648736	0.215750	0.470640
8	6	0	0.276001	1.820016	0.026686
9	6	0	1.188119	2.650908	-0.493388
10	1	0	-1.810020	-2.293794	-0.577990
11	1	0	0.296700	-3.542830	-0.200102
12	1	0	2.400120	-2.299398	0.311265
13	6	0	-2.234771	0.356798	-0.504086

14	1	0	-0.558699	2.267142	0.563231
15	1	0	1.100705	3.724719	-0.369037
16	1	0	2.021777	2.300732	-1.094688
17	1	0	2.485877	1.160128	0.600889
18	1	0	-2.070208	1.320744	-0.995779
19	1	0	-2.853894	-0.233374	-1.188550
20	6	0	-3.013604	0.570961	0.806763
21	1	0	-3.965610	1.076980	0.617168
22	1	0	-3.226674	-0.386878	1.291199
23	1	0	-2.444951	1.177215	1.519466

109-1-OH-3-Vin-4-Et

Standard orientation:

Center Number	Atomic Number	Atomic Type	Coordinates (Angstroms) X	Y	Z
1	6	0	-1.140684	0.885779	-0.058005
2	6	0	-2.094819	-0.116413	0.078290
3	6	0	-1.701542	-1.453180	0.021509
4	6	0	-0.361015	-1.754366	-0.172857
5	6	0	0.619495	-0.767057	-0.309571
6	6	0	0.216960	0.584568	-0.240167
7	8	0	-3.421933	0.148089	0.251628
8	6	0	2.067215	-1.180984	-0.473545
9	6	0	2.894943	-1.044927	0.816617
10	6	0	1.197343	1.676751	-0.368090
11	6	0	1.092053	2.900501	0.155071
12	1	0	-0.061035	-2.797287	-0.222630
13	1	0	-1.455549	1.925910	-0.052899
14	1	0	-2.450233	-2.231123	0.115636
15	1	0	-3.551586	1.101964	0.266488
16	1	0	2.091889	1.445105	-0.940810
17	1	0	1.858922	3.649222	-0.008852
18	1	0	0.252467	3.197376	0.775469
19	1	0	2.547451	-0.602058	-1.271662
20	1	0	2.093932	-2.224296	-0.806720
21	1	0	3.927834	-1.370285	0.654900
22	1	0	2.914987	-0.007912	1.164595
23	1	0	2.466690	-1.655354	1.617937

110-1-OH-3-Vin-5-Et

Standard orientation:

Center Number	Atomic Number	Atomic Type	Coordinates (Angstroms) X	Y	Z
1	6	0	0.078728	1.553858	0.000091
2	6	0	-1.130426	0.848039	0.000173
3	6	0	-1.128963	-0.541887	0.000223
4	6	0	0.101488	-1.211359	0.000181
5	6	0	1.316876	-0.523377	0.000077
6	6	0	1.291788	0.880852	0.000036
7	6	0	2.566437	-1.296139	0.000001
8	6	0	3.817410	-0.831151	-0.000369
9	8	0	-0.005911	2.915891	0.000044
10	6	0	-2.408161	-1.360484	0.000421
11	1	0	0.113348	-2.297984	0.000209
12	1	0	2.218486	1.447494	-0.000022
13	1	0	-2.051127	1.417831	0.000217
14	1	0	0.883521	3.284499	0.000024
15	1	0	2.421844	-2.375203	0.000262
16	1	0	4.664507	-1.507475	-0.000390
17	1	0	4.052857	0.227993	-0.000682
18	6	0	-3.720239	-0.574535	-0.000674
19	1	0	-2.388341	-2.028471	-0.870931
20	1	0	-2.388970	-2.027053	0.872882
21	1	0	-4.572505	-1.260229	-0.001114
22	1	0	-3.808609	0.064490	0.883765
23	1	0	-3.807348	0.064080	-0.885535

111-1-OH-2-Me-4-Et

Standard orientation:

Center Number	Atomic Number	Atomic Type	Coordinates (Angstroms) X	Y	Z
1	6	0	0.656481	-1.415697	-0.213513
2	6	0	-0.703265	-1.631566	-0.004643
3	6	0	-1.578563	-0.552090	0.073155
4	6	0	-1.104911	0.761816	-0.059469
5	6	0	0.260335	0.941574	-0.267051
6	6	0	1.163865	-0.123964	-0.346733
7	8	0	-2.922929	-0.709867	0.273003
8	6	0	-2.065216	1.919376	0.018423
9	6	0	2.644039	0.123250	-0.534631
10	6	0	3.390880	0.339120	0.793126
11	1	0	-3.118997	-1.649522	0.344605

12	1	0	0.633849	1.957311	-0.375765
13	1	0	1.326554	-2.268295	-0.276766
14	1	0	-1.087426	-2.644315	0.092775
15	1	0	-1.541291	2.870204	-0.107598
16	1	0	-2.840094	1.847227	-0.752787
17	1	0	-2.588530	1.938644	0.980835
18	1	0	3.091777	-0.725327	-1.065163
19	1	0	2.790810	1.000882	-1.175494
20	1	0	4.457724	0.516775	0.621369
21	1	0	2.985551	1.200243	1.334241
22	1	0	3.291644	-0.535805	1.443739

112-1-OH-3-Me-5-Et

Standard orientation:

Center Number	Atomic Number	Atomic Type	Coordinates (Angstroms) X	Y	Z
1	6	0	0.202697	-1.177684	-0.239463
2	6	0	0.965662	-0.009266	-0.353094
3	6	0	0.334764	1.225394	-0.226787
4	6	0	-1.038550	1.289532	0.013425
5	6	0	-1.786290	0.120066	0.126616
6	6	0	-1.169420	-1.128195	0.000056
7	6	0	2.460633	-0.086508	-0.571490
8	6	0	3.248619	-0.166880	0.747763
9	8	0	-1.597511	2.529724	0.124583
10	6	0	-1.986859	-2.392053	0.117987
11	1	0	-2.542052	2.432610	0.283469
12	1	0	-2.857315	0.180127	0.309835
13	1	0	0.689821	-2.143088	-0.344559
14	1	0	0.892117	2.151997	-0.315849
15	1	0	-1.364167	-3.281091	-0.009673
16	1	0	-2.474346	-2.462279	1.097150
17	1	0	-2.780249	-2.427181	-0.637347
18	1	0	2.793866	0.790315	-1.138034
19	1	0	2.694724	-0.964159	-1.184951
20	1	0	4.325398	-0.224061	0.558487
21	1	0	3.058050	0.712913	1.370387
22	1	0	2.956699	-1.050327	1.324346

113-1-OH-3-Et-4-Me

Standard orientation:

Center Number	Atomic Number	Atomic Type	Coordinates (Angstroms) X	Y	Z
1	6	0	1.885518	0.976167	0.230991
2	6	0	0.697872	1.700698	0.191682
3	6	0	-0.531678	1.096914	-0.072974
4	6	0	-0.555617	-0.293222	-0.306747
5	6	0	0.635132	-1.017193	-0.272016
6	6	0	1.853728	-0.395910	-0.003349
7	6	0	-1.787162	1.936911	-0.116810
8	8	0	2.972709	-1.178201	0.012038
9	1	0	-1.561589	2.979845	0.121389
10	1	0	-2.544441	1.593446	0.596716
11	1	0	-2.256948	1.922232	-1.107861
12	6	0	-1.850352	-1.035423	-0.565158
13	1	0	0.632477	-2.086573	-0.458079
14	1	0	2.827898	1.476376	0.438683
15	1	0	0.731331	2.771619	0.370351
16	1	0	3.736403	-0.624810	0.204886
17	6	0	-2.525307	-1.526958	0.728503
18	1	0	-2.549374	-0.398995	-1.117570
19	1	0	-1.645349	-1.899018	-1.207496
20	1	0	-3.455974	-2.059006	0.506434
21	1	0	-1.865239	-2.207863	1.274792
22	1	0	-2.763673	-0.693548	1.396718

114-1,3-Met-2-OH

Standard orientation:

Center Number	Atomic Number	Atomic Type	Coordinates (Angstroms) X	Y	Z
1	6	0	-0.891885	0.803565	-0.057346
2	6	0	-1.566683	-0.413502	0.008338
3	6	0	-0.849910	-1.612133	-0.081680
4	6	0	0.526390	-1.570070	-0.232658
5	6	0	1.239102	-0.367827	-0.297200
6	6	0	0.496756	0.816996	-0.206630
7	8	0	-2.914196	-0.533709	0.154497
8	6	0	-3.685136	0.648199	0.246049
9	8	0	1.077369	2.053848	-0.258665
10	1	0	-1.389394	-2.550136	-0.034818
11	1	0	1.077214	-2.503772	-0.306151

12	6	0	2.745752	-0.351462	-0.429058
13	1	0	-1.403049	1.754644	0.001616
14	1	0	2.020460	1.953573	-0.419079
15	1	0	-4.722090	0.326867	0.358051
16	1	0	-3.399050	1.252884	1.116374
17	1	0	-3.594025	1.263213	-0.658625
18	1	0	3.061129	0.385567	-1.184152
19	6	0	3.481312	-0.072675	0.895916
20	1	0	3.074346	-1.317901	-0.825431
21	1	0	4.566519	-0.063237	0.751417
22	1	0	3.187934	0.891926	1.323597
23	1	0	3.240437	-0.841282	1.636160

115-1,3-MeO-5-Et

Standard orientation:

Center Number	Atomic Number	Atomic Type	Coordinates (Angstroms) X	Y	Z
1	6	0	-0.057759	1.321100	-0.031769
2	6	0	-1.189591	0.521441	-0.221399
3	6	0	-1.042171	-0.866040	-0.361796
4	6	0	0.228091	-1.440378	-0.314878
5	6	0	1.358581	-0.636975	-0.122601
6	6	0	1.218678	0.748617	0.017578
7	6	0	-2.266371	-1.745665	-0.523374
8	6	0	-2.839018	-2.224304	0.822880
9	8	0	2.563897	-1.282808	-0.098063
10	6	0	3.731309	-0.588098	0.294010
11	8	0	-0.087212	2.680133	0.110533
12	6	0	-1.343611	3.332445	0.071214
13	1	0	0.348072	-2.513427	-0.429816
14	1	0	2.072536	1.398404	0.156603
15	1	0	-2.181358	0.957252	-0.267337
16	1	0	-1.134505	4.395744	0.204918
17	1	0	-1.849590	3.182265	-0.891979
18	1	0	-2.004480	2.989789	0.878781
19	1	0	4.556763	-1.288730	0.150704
20	1	0	3.906264	0.302833	-0.323219
21	1	0	3.687416	-0.286341	1.349190
22	1	0	-3.043235	-1.195973	-1.069814
23	1	0	-2.011390	-2.618499	-1.136879
24	1	0	-3.720626	-2.857891	0.671315
25	1	0	-2.094559	-2.802990	1.380640
26	1	0	-3.133629	-1.373896	1.447946

116-1,3-MeO-4-Vin

Standard orientation:

Center Number	Atomic Number	Atomic Type	Coordinates (Angstroms) X	Y	Z
1	6	0	-0.146335	-1.641345	-0.084760
2	1	0	-0.437777	-2.683793	-0.151697
3	6	0	-1.147177	-0.669904	-0.059926
4	6	0	-0.725815	0.683172	-0.015179
5	6	0	0.623736	1.012412	0.016384
6	6	0	1.595492	0.005417	0.002030
7	6	0	1.211069	-1.334102	-0.050825
8	6	0	-2.577469	-0.993065	-0.096050
9	8	0	-1.717478	1.614721	0.003310
10	1	0	0.963878	2.037739	0.056070
11	8	0	2.882751	0.443565	0.035817
12	1	0	1.942085	-2.130499	-0.078054
13	6	0	3.917061	-0.521889	0.029501
14	1	0	4.853678	0.036795	0.068623
15	1	0	3.856315	-1.186132	0.900996
16	1	0	3.898059	-1.130072	-0.883883
17	6	0	-1.364530	2.983865	0.023834
18	1	0	-2.304343	3.538448	0.020607
19	1	0	-0.796704	3.241349	0.926905
20	1	0	-0.775996	3.263763	-0.859131
21	6	0	-3.139139	-2.179309	0.153025
22	1	0	-3.224667	-0.158353	-0.346280
23	1	0	-4.212184	-2.314081	0.078153
24	1	0	-2.565886	-3.052964	0.446458

117-1-MeO-3-OH-4-Et

Standard orientation:

Center Number	Atomic Number	Atomic Type	Coordinates (Angstroms) X	Y	Z
1	6	0	-0.891885	0.803565	-0.057346
2	6	0	-1.566683	-0.413502	0.008338
3	6	0	-0.849910	-1.612133	-0.081680
4	6	0	0.526390	-1.570070	-0.232658
5	6	0	1.239102	-0.367827	-0.297200

6	6	0	0.496756	0.816996	-0.206630
7	8	0	-2.914196	-0.533709	0.154497
8	6	0	-3.685136	0.648199	0.246049
9	8	0	1.077369	2.053848	-0.258665
10	1	0	-1.389394	-2.550136	-0.034818
11	1	0	1.077214	-2.503772	-0.306151
12	6	0	2.745752	-0.351462	-0.429058
13	1	0	-1.403049	1.754644	0.001616
14	1	0	2.020460	1.953573	-0.419079
15	1	0	-4.722090	0.326867	0.358051
16	1	0	-3.399050	1.252884	1.116374
17	1	0	-3.594025	1.263213	-0.658625
18	1	0	3.061129	0.385567	-1.184152
19	6	0	3.481312	-0.072675	0.895916
20	1	0	3.074346	-1.317901	-0.825431
21	1	0	4.566519	-0.063237	0.751417
22	1	0	3.187934	0.891926	1.323597
23	1	0	3.240437	-0.841282	1.636160

118-1-MeO-2-For-4-Et

Standard orientation:

Center Number	Atomic Number	Atomic Type	Coordinates (Angstroms) X	Y	Z
1	6	0	0.500631	-1.602509	-0.129756
2	6	0	1.240603	-0.423565	-0.009730
3	6	0	0.572379	0.817698	-0.063918
4	6	0	-0.814625	0.840514	-0.233389
5	6	0	-1.568252	-0.323133	-0.351671
6	6	0	-0.879705	-1.539405	-0.297758
7	8	0	2.587391	-0.386139	0.153799
8	6	0	3.301365	-1.608025	0.211356
9	6	0	1.305615	2.097603	0.049328
10	8	0	0.771561	3.185965	0.005044
11	6	0	-3.072446	-0.278761	-0.498029
12	6	0	-3.805851	-0.311278	0.854104
13	1	0	-1.286028	1.817861	-0.274322
14	1	0	-1.434447	-2.468936	-0.394445
15	1	0	0.987967	-2.568026	-0.099388
16	1	0	4.349495	-1.337818	0.346988
17	1	0	2.974829	-2.226143	1.056786
18	1	0	3.193145	-2.182183	-0.717145
19	1	0	2.399777	2.006328	0.180867
20	1	0	-3.357578	0.629088	-1.041201
21	1	0	-3.405522	-1.125227	-1.110050
22	1	0	-4.890733	-0.277808	0.712347
23	1	0	-3.563697	-1.222854	1.410150
24	1	0	-3.517103	0.542277	1.475445

119-1,2-For-4-MeO

Standard orientation:

Center Number	Atomic Number	Atomic Type	Coordinates (Angstroms) X	Y	Z
1	6	0	-0.967172	-1.824323	-0.000026
2	1	0	-1.597247	-2.706007	-0.000019
3	6	0	-1.577365	-0.561340	0.000011
4	6	0	-0.780272	0.585450	-0.000029
5	6	0	0.611001	0.490234	-0.000080
6	6	0	1.232612	-0.779338	-0.000083
7	6	0	0.410825	-1.917961	-0.000071
8	8	0	-2.925784	-0.557334	0.000065
9	1	0	-1.202743	1.581615	-0.000030
10	6	0	1.364507	1.787234	-0.000200
11	6	0	2.689626	-1.027840	-0.000017
12	1	0	0.876873	-2.899050	-0.000088
13	8	0	3.581139	-0.208052	0.000299
14	1	0	2.933445	-2.114425	-0.000257
15	8	0	0.797648	2.858331	0.000073
16	1	0	2.460631	1.706727	-0.000721
17	6	0	-3.602283	0.693341	0.000068
18	1	0	-4.666573	0.456318	0.000115
19	1	0	-3.358597	1.279297	0.893696
20	1	0	-3.358698	1.279230	-0.893628

120-1,2-For-3-Me

Standard orientation:

Center Number	Atomic Number	Atomic Type	Coordinates (Angstroms) X	Y	Z
1	6	0	-0.585810	-2.295447	-0.067544
2	1	0	-0.696952	-3.373397	-0.121071
3	6	0	-1.714434	-1.482345	-0.039006
4	6	0	-1.609930	-0.091642	0.026702
5	6	0	-0.321873	0.489359	0.056657

6	6	0	0.825431	-0.339353	0.045628
7	6	0	0.678287	-1.725275	-0.019968
8	1	0	-2.701361	-1.933255	-0.072784
9	6	0	-2.881811	0.730811	0.031972
10	6	0	-0.207287	1.969091	0.055225
11	6	0	2.230578	0.169483	0.178262
12	1	0	1.576841	-2.330891	-0.024251
13	8	0	3.189946	-0.530284	-0.057457
14	1	0	2.348349	1.203204	0.533778
15	8	0	0.784592	2.599940	-0.238596
16	1	0	-1.132719	2.505337	0.343935
17	1	0	-2.934664	1.418161	-0.818038
18	1	0	-3.752766	0.073672	-0.022701
19	1	0	-2.981945	1.331836	0.941978

121-1,3-For-5-Et

Standard orientation:

Center Number	Atomic Number	Atomic Type	Coordinates (Angstroms) X	Y	Z
1	6	0	-1.270083	-0.814352	-0.059604
2	6	0	-0.016895	-1.391960	-0.269241
3	6	0	1.145586	-0.615443	-0.354413
4	6	0	1.013623	0.764793	-0.226137
5	6	0	-0.237839	1.362525	-0.014764
6	6	0	-1.379366	0.573451	0.069474
7	6	0	2.499868	-1.259720	-0.545840
8	6	0	3.164913	-1.643592	0.787734
9	6	0	-0.344806	2.835986	0.114239
10	8	0	0.590488	3.598565	0.051119
11	6	0	-2.475989	-1.671148	0.019984
12	8	0	-3.597964	-1.260394	0.200208
13	1	0	1.881058	1.414540	-0.292013
14	1	0	-2.359754	1.011533	0.229606
15	1	0	0.052801	-2.472769	-0.373580
16	1	0	-2.274389	-2.759189	-0.101367
17	1	0	-1.380664	3.206309	0.279257
18	1	0	2.392968	-2.154743	-1.169127
19	1	0	3.153995	-0.572434	-1.092922
20	1	0	4.140699	-2.107332	0.615197
21	1	0	3.313329	-0.762045	1.419049
22	1	0	2.545687	-2.352476	1.346680

122-1,4-For-3-Me

Standard orientation:

Center Number	Atomic Number	Atomic Type	Coordinates (Angstroms) X	Y	Z
1	6	0	-0.136552	-1.545074	-0.000071
2	1	0	-0.443499	-2.587210	-0.000175
3	6	0	-1.129210	-0.552912	-0.000131
4	6	0	-0.774639	0.816056	-0.000177
5	6	0	0.586366	1.122085	-0.000225
6	6	0	1.570928	0.131565	0.000003
7	6	0	1.207432	-1.218289	0.000112
8	6	0	-2.533360	-1.026286	-0.000359
9	6	0	-1.792378	1.926143	-0.000100
10	1	0	0.892331	2.165431	-0.000456
11	6	0	3.002831	0.520226	0.000021
12	1	0	1.984663	-1.973368	0.000234
13	8	0	3.923103	-0.262307	0.000238
14	1	0	3.181029	1.618605	-0.000184
15	8	0	-3.524147	-0.332321	0.000686
16	1	0	-2.621217	-2.136220	-0.001763
17	1	0	-1.292819	2.898369	-0.004922
18	1	0	-2.453697	1.862313	-0.868353
19	1	0	-2.446937	1.868020	0.873779

123-1-For-3-MeO-4-Et

Standard orientation:

Center Number	Atomic Number	Atomic Type	Coordinates (Angstroms) X	Y	Z
1	6	0	0.252786	-1.890988	-0.268210
2	6	0	-1.128754	-1.800991	-0.115810
3	6	0	-1.722998	-0.548406	0.011033
4	6	0	-0.935631	0.611433	-0.014408
5	6	0	0.440776	0.509316	-0.162886
6	6	0	1.059736	-0.757003	-0.293097
7	6	0	-3.186514	-0.436817	0.170493
8	8	0	-3.794234	0.603587	0.287108
9	8	0	1.284763	1.576835	-0.199115
10	6	0	0.728412	2.876220	-0.100233
11	6	0	2.558129	-0.861865	-0.440273
12	6	0	3.308258	-0.677686	0.892012

13	1	0	0.722081	-2.864509	-0.374346
14	1	0	-1.742764	-2.696258	-0.099062
15	1	0	-1.439759	1.563725	0.084642
16	1	0	1.568176	3.569872	-0.162468
17	1	0	0.028833	3.077848	-0.920737
18	1	0	0.208501	3.020315	0.854908
19	1	0	-3.719440	-1.414462	0.177042
20	1	0	2.803325	-1.841067	-0.864987
21	1	0	2.905932	-0.104403	-1.150106
22	1	0	4.388454	-0.767104	0.740490
23	1	0	3.103673	0.307896	1.317321
24	1	0	3.003560	-1.434505	1.621642

124-1-For-3-MeO-5-Et

Standard orientation:

Center Number	Atomic Number	Atomic Type	Coordinates (Angstroms) X	Y	Z
1	6	0	1.491549	-0.096059	-0.355147
2	6	0	0.889910	1.164457	-0.258683
3	6	0	-0.485055	1.277594	-0.071567
4	6	0	-1.296177	0.138658	0.023570
5	6	0	-0.707046	-1.116637	-0.073277
6	6	0	0.680484	-1.221817	-0.262425
7	6	0	-1.099751	2.619556	0.023538
8	8	0	-2.279832	2.830763	0.186758
9	8	0	-1.376854	-2.295563	-0.002742
10	6	0	-2.781243	-2.252720	0.182525
11	6	0	2.988806	-0.233043	-0.519200
12	6	0	3.733547	-0.243741	0.827237
13	1	0	1.105272	-2.217822	-0.338916
14	1	0	1.495213	2.064000	-0.334541
15	1	0	-2.359032	0.280921	0.165773
16	1	0	-3.114227	-3.291218	0.210551
17	1	0	-3.048553	-1.760368	1.125806
18	1	0	-3.281247	-1.733448	-0.644508
19	1	0	-0.375515	3.460129	-0.068309
20	1	0	3.213665	-1.155806	-1.065196
21	1	0	3.363831	0.593748	-1.133139
22	1	0	4.813093	-0.339357	0.675019
23	1	0	3.549158	0.679831	1.384998
24	1	0	3.401678	-1.079698	1.450900

125-1,2-For-4-Me

Standard orientation:

Center Number	Atomic Number	Atomic Type	Coordinates (Angstroms) X	Y	Z
1	6	0	1.151552	-1.709782	0.000000
2	1	0	1.588737	-2.704168	0.000000
3	6	0	1.990889	-0.589444	0.000000
4	6	0	1.389640	0.668273	0.000000
5	6	0	0.000000	0.835503	0.000000
6	6	0	-0.831575	-0.307422	0.000000
7	6	0	-0.228517	-1.568114	0.000000
8	6	0	3.489758	-0.746189	0.000000
9	6	0	-0.473806	2.243917	0.000000
10	6	0	-2.326985	-0.264874	0.000000
11	1	0	-0.880381	-2.434337	0.000000
12	8	0	-2.998076	-1.274241	0.000000
13	1	0	-2.782764	0.735702	0.000000
14	8	0	-1.617683	2.634997	0.000000
15	1	0	0.366135	2.974554	0.000000
16	1	0	2.018051	1.555255	0.000000
17	1	0	3.994618	0.222716	0.000000
18	1	0	3.827970	-1.303488	0.880483
19	1	0	3.827970	-1.303488	-0.880483

126-1,2-For-5-Me

Standard orientation:

Center Number	Atomic Number	Atomic Type	Coordinates (Angstroms) X	Y	Z
1	6	0	-1.999326	-0.095632	-0.002113
2	6	0	-3.446388	0.324537	0.003437
3	6	0	-1.631744	-1.443132	-0.002872
4	6	0	-0.291396	-1.810252	-0.001366
5	6	0	0.728020	-0.853541	0.000186
6	6	0	0.367935	0.516479	-0.000173
7	6	0	-0.981231	0.862539	-0.001544
8	6	0	2.113046	-1.383462	0.001136
9	6	0	1.358476	1.641762	-0.000128
10	1	0	-1.220242	1.921224	-0.002779
11	8	0	1.012153	2.802788	-0.001470
12	1	0	2.418812	1.351017	0.001264

13	8	0	3.144307	-0.751256	0.002338
14	1	0	2.140793	-2.496471	0.000845
15	1	0	-0.022905	-2.862816	-0.002318
16	1	0	-2.400246	-2.209810	-0.005102
17	1	0	-3.661895	1.005165	-0.826818
18	1	0	-4.115056	-0.535740	-0.078291
19	1	0	-3.695293	0.859392	0.926862

127-1,2-Vin-3-MeO

Standard orientation:

Center Number	Atomic Number	Atomic Type	Coordinates (Angstroms) X	Y	Z
1	6	0	0.296931	-2.334425	0.077474
2	6	0	1.416458	-1.503692	0.081464
3	6	0	1.243336	-0.126186	-0.019592
4	6	0	-0.047924	0.449560	-0.112897
5	6	0	-1.167979	-0.411319	-0.132109
6	6	0	-0.973637	-1.799150	-0.036207
7	6	0	-2.533559	0.108104	-0.324080
8	6	0	-3.649046	-0.426433	0.177417
9	6	0	-0.127834	1.916815	-0.192493
10	6	0	-1.061454	2.709064	0.341154
11	8	0	2.278514	0.760329	-0.014959
12	6	0	3.599574	0.260818	0.045234
13	1	0	-4.623088	-0.005835	-0.046809
14	1	0	-3.633002	-1.287555	0.837862
15	1	0	-2.612613	1.002887	-0.935918
16	1	0	0.704430	2.383831	-0.711662
17	1	0	-1.008604	3.785802	0.219171
18	1	0	-1.887764	2.326682	0.928897
19	1	0	-1.835184	-2.453681	-0.093768
20	1	0	2.405448	-1.934363	0.161315
21	1	0	0.430438	-3.409067	0.145817
22	1	0	4.254199	1.133450	0.015045
23	1	0	3.781135	-0.292634	0.975436
24	1	0	3.827299	-0.391086	-0.807908

128-1,2-Vin-4-MeO

Standard orientation:

Center Number	Atomic Number	Atomic Type	Coordinates (Angstroms) X	Y	Z
1	1	0	-4.723699	-1.079671	0.124955
2	1	0	-3.355050	-2.191830	0.664407
3	6	0	-3.657335	-1.242293	0.234249
4	1	0	-3.159966	0.626459	-0.529440
5	6	0	-2.774663	-0.310101	-0.134409
6	6	0	-1.309286	-0.426027	-0.070253
7	6	0	-0.483814	0.712938	0.056296
8	6	0	-1.066880	2.059960	0.197276
9	1	0	-2.035645	2.108145	0.687442
10	6	0	-0.513201	3.201653	-0.217081
11	1	0	-1.002051	4.155580	-0.053443
12	1	0	0.434917	3.228080	-0.744893
13	6	0	0.911990	0.560371	0.089183
14	6	0	1.499878	-0.696542	-0.016881
15	1	0	-1.307780	-2.561121	-0.320718
16	6	0	-0.688352	-1.681986	-0.180135
17	6	0	0.684765	-1.827263	-0.153329
18	8	0	2.838985	-0.930737	0.008660
19	1	0	1.153962	-2.800255	-0.242420
20	1	0	1.521730	1.441506	0.236642
21	6	0	3.711823	0.175778	0.131601
22	1	0	4.723649	-0.232442	0.112903
23	1	0	3.591409	0.880984	-0.700854
24	1	0	3.557081	0.711534	1.077030

129-1,2-Vin-3-For

Standard orientation:

Center Number	Atomic Number	Atomic Type	Coordinates (Angstroms) X	Y	Z
1	6	0	0.148336	-2.348412	0.247748
2	1	0	0.204343	-3.423090	0.383839
3	6	0	-1.077840	-1.722643	0.100613
4	6	0	-1.151280	-0.333672	-0.065885
5	6	0	0.023672	0.448631	-0.059836
6	6	0	1.278097	-0.198596	0.063778
7	6	0	1.313637	-1.587756	0.224201
8	1	0	-2.007238	-2.280504	0.096970
9	6	0	-2.498553	0.232216	-0.346940
10	6	0	-0.010483	1.921152	-0.186977
11	6	0	2.527352	0.584486	0.080308
12	1	0	2.273884	-2.071605	0.366937

13	6	0	3.714185	0.166496	-0.363766
14	1	0	2.451908	1.587256	0.492949
15	1	0	4.593181	0.797690	-0.296859
16	1	0	3.852472	-0.809121	-0.819001
17	6	0	-0.783330	2.746751	0.520722
18	1	0	0.691615	2.349737	-0.899290
19	1	0	-0.743670	3.820621	0.373087
20	1	0	-1.467638	2.385115	1.281711
21	8	0	-3.530160	-0.383461	-0.188671
22	1	0	-2.510334	1.259684	-0.754772

130-1,2-Vin-4-For

Standard orientation:

Center Number	Atomic Number	Atomic Type	Coordinates (Angstroms) X	Y	Z
1	6	0	1.236863	-1.346681	-0.132025
2	1	0	1.982639	-2.128955	-0.216344
3	6	0	1.663834	-0.021978	0.026753
4	6	0	0.717647	0.994812	0.128134
5	6	0	-0.655631	0.733206	0.071108
6	6	0	-1.082216	-0.609330	-0.079777
7	6	0	-0.115344	-1.625572	-0.185329
8	6	0	3.103885	0.301910	0.095583
9	6	0	-1.628194	1.832296	0.212880
10	6	0	-2.514148	-0.938015	-0.170507
11	1	0	-0.447014	-2.645729	-0.343972
12	6	0	-3.075986	-2.087863	0.210113
13	1	0	-3.153951	-0.163793	-0.585299
14	1	0	-4.140286	-2.257990	0.092810
15	1	0	-2.504842	-2.891318	0.663878
16	6	0	-1.448033	3.087314	-0.202944
17	1	0	-2.563659	1.580482	0.705690
18	1	0	-2.202932	3.847977	-0.038826
19	1	0	-0.552276	3.399825	-0.730381
20	1	0	1.054764	2.015378	0.285525
21	8	0	3.998638	-0.507683	0.010884
22	1	0	3.322388	1.384975	0.235912

131-1,2-Vin-3-Me

Standard orientation:

Center Number	Atomic Number	Atomic Type	Coordinates (Angstroms) X	Y	Z
1	6	0	0.737020	-2.304870	0.099664
2	6	0	1.817016	-1.426893	0.107802
3	6	0	1.624844	-0.052757	-0.012153
4	6	0	0.311961	0.462020	-0.124174
5	6	0	-0.788430	-0.430150	-0.142886
6	6	0	-0.548925	-1.808022	-0.034626
7	6	0	-2.170348	0.042967	-0.339995
8	6	0	-3.270401	-0.529814	0.153806
9	6	0	0.148362	1.925811	-0.211858
10	6	0	-0.780746	2.673620	0.388342
11	6	0	2.824604	0.865940	0.012577
12	1	0	-4.256495	-0.140381	-0.073918
13	1	0	-3.230419	-1.393034	0.810538
14	1	0	-2.278405	0.937592	-0.947488
15	1	0	0.902435	2.440832	-0.804111
16	1	0	-0.795976	3.751056	0.261867
17	1	0	-1.541601	2.247927	1.032575
18	1	0	2.827209	-1.812956	0.204582
19	1	0	-1.389821	-2.489917	-0.092848
20	1	0	0.902889	-3.374186	0.179562
21	1	0	3.741091	0.298377	0.191504
22	1	0	2.950358	1.401012	-0.936832
23	1	0	2.738988	1.626574	0.795574

132-1,2-Vin-4-Me

Standard orientation:

Center Number	Atomic Number	Atomic Type	Coordinates (Angstroms) X	Y	Z
1	1	0	-4.185259	-1.599846	0.082708
2	1	0	-2.689969	-2.506269	0.670626
3	6	0	-3.108562	-1.617308	0.209570
4	1	0	-2.844274	0.282406	-0.598033
5	6	0	-2.349892	-0.587442	-0.172897
6	6	0	-0.881840	-0.512543	-0.080955
7	6	0	-0.217740	0.726845	0.067639
8	6	0	-0.976660	1.982890	0.205473
9	1	0	-1.952815	1.898687	0.676395
10	6	0	-0.570089	3.191481	-0.189246
11	1	0	-1.183215	4.071223	-0.028339
12	1	0	0.377358	3.347421	-0.695252

13	6	0	1.183395	0.742848	0.126493
14	6	0	1.950845	-0.413476	0.028725
15	6	0	3.457269	-0.363252	0.090670
16	1	0	-0.602026	-2.625705	-0.339754
17	6	0	-0.103553	-1.675003	-0.183304
18	6	0	1.280071	-1.632273	-0.128147
19	1	0	1.849957	-2.553186	-0.212663
20	1	0	1.682925	1.693344	0.286122
21	1	0	3.905447	-0.692615	-0.854131
22	1	0	3.815172	0.649529	0.293264
23	1	0	3.847247	-1.021587	0.874925

133-1,3-Vin-2-OH

Standard orientation:

Center Number	Atomic Number	Atomic Type	Coordinates (Angstroms) X	Y	Z
1	6	0	1.399337	1.341721	0.143910
2	6	0	0.360217	2.260398	0.072136
3	6	0	-0.945272	1.806650	-0.061136
4	6	0	-1.239421	0.437683	-0.093664
5	6	0	-0.165068	-0.476201	-0.057514
6	6	0	1.169232	-0.036667	0.057524
7	6	0	-2.644645	0.017451	-0.197255
8	6	0	-3.225841	-1.076486	0.312532
9	8	0	-0.368279	-1.816800	-0.165567
10	6	0	2.253559	-1.027641	0.090510
11	6	0	3.556631	-0.789017	-0.076189
12	1	0	0.566228	3.323392	0.126319
13	1	0	-1.766237	2.515355	-0.113817
14	1	0	2.416675	1.694750	0.271983
15	1	0	1.932172	-2.050316	0.258931
16	1	0	4.280970	-1.593615	-0.019557
17	1	0	3.954313	0.199240	-0.283047
18	1	0	-3.278989	0.715794	-0.742100
19	1	0	-4.283975	-1.260698	0.164906
20	1	0	-2.699440	-1.790232	0.938276
21	1	0	-1.287848	-1.966624	-0.422481

A.10 References

[1] Paraskevas PD, Sabbe MK, Reyniers M-F, Papayannakos N, Marin GB. Group additive values for the gas-phase standard enthalpy of formation, entropy and heat capacity of oxygenates. *Chemistry - A European Journal*. 2013; 19: 16431-16452.

[2] Prosen E, Gilmont R, Rossini F. Heats of combustion of benzene, toluene, ethyl-benzene, o-xylene, m-xylene, p-xylene, n-propylbenzene, and styrene. *Journal of Research of the National Bureau of Standards*. 1945; 34: 65-70.

[3] Roux MV, Temprado M, Chickos JS, Nagano Y. Critically Evaluated Thermochemical Properties of Polycyclic Aromatic Hydrocarbons. *Journal of Physical Chemistry Reference Data*. 2008; 37: 1855.

[4] Andon RJL, Biddiscombe DP, Cox JD, Handley R, Harrop D, Herington EFG, Martin JF. Thermodynamic properties of organic oxygen compounds. Part I. Preparation and physical properties of pure phenol, cresols, and xylenols. *Journal of The Chemical Society*. 1960; 5246.

[5] Cox JD. The heats of combustion of phenol and the three cresols. *Pure Applied Chemistry* 1961; 2: 125-128.

[6] Fenwick J, Harrop D, Head A. Thermodynamic properties of organic oxygen compounds 41. Enthalpies of formation of eight ethers. *The Journal of Chemical Thermodynamics.* 1975;7(10):943-954.

[7] Lebedeva ND, Katin YA. Standard enthalpy of formation of nitrobenzene. *Russian Journal of Physical Chemistry.* 1972; 46: 1.

[8] Ambrose D, Connett JE, Green JHS, Hales JH, Head AJ, Martin JF. *The Journal of Chemical Thermodynamics.* 1975; 7: 1143-1157.

[9] R. K. Solly, S. W. Benson. Thermochemistry of the reaction of benzaldehyde with iodine. The enthalpy of formation of benzaldehyde and benzoyl iodide. *The Journal of Chemical Thermodynamics.* 1971; 3: 203.

[10] Guthrie JP. Equilibrium constants for a series of simple aldol condensations, and linear free energy relations with other carbonyl addition reactions. *Canadian Journal of Chemistry.* 1978; 56: 962-973.

[11] Cox JD, Pilcher G. *Thermochemistry of Organic and Organometallic Compounds: Academic Press*: New York, 1970.

[12] Sabbah R, Laffitte M. Etude thermodynamique de la molecule de benzophenone. *Thermochimica Acta.* 1978; 23: 196-198.

[13] Chirico RD, Knipmeyer SE, Nguyen A, Steele WV. The thermodynamic properties of biphenyl. *The Journal of Chemical Thermodynamics.* 1989; 21: 1307-1331.

[14] Coleman DJ, Pilcher G. Heats of combustion of biphenyl, bibenzyl, naphthalene, anthracene, and phenanthrene. *Transactions of the Faraday Society.* 1966; 62: 821-827.

[15] Montgomery RL, Rossini FD, Mansson M. Enthalpies of combustion, vaporization, and formation of phenylbenzene, cyclohexylbenzene, and cyclohexylcyclohexane; enthalpy of hydrogenation of certain aromatic systems. *Journal of Chemical Engineering Data.* 1978; 23: 125-129.

[16] Prosen EJ, Johnson WH, Rossini FD. Heats of combustion and formation at 25°C of the alkylbenzenes through C10H14, and of the higher normal monoalkylbenzenes. *Journal of Research of the National Bureau of Standards.* 1946; 36: 455-461.

[17] Prosen EJ, Rossini FD. Heats of combustion and formation of the paraffin hydrocarbons at 25° C. *Journal of Research of the National Bureau of Standards.* 1945; 263-267.

[18] Johnson WH, Prosen EJ, Rossini FD. Heats of combustion and isomerization of the eight C9H12 alkylbenzenes. *Journal of Research of the National Bureau of Standards.* 1945; 35: 141-146.

[19] Sabbah R, Buluku ENLE. Thermodynamic study of three isomers of dihydroxybenzene. *Canadian Journal of Chemistry.* 1991; 69: 481-488.

[20] Ribeiro da Silva MAV, Goncalves MV, Monte MJS. Thermodynamic study on hydroxybenzaldehyde derivatives: 3- and 4-Hydroxybenzaldehyde isomers and 3,5-di-tert-butyl-2-hydroxybenzaldehyde. *The Journal of Chemical Thermodynamics.* 2010; 42: 472-477.

Appendix B

Supporting Information for Chapter 4

Contents

B.1 The Linear Regression Procedure and the Statistical Analysis

The Linear Regression and the calculation of $\overline{GAV/NNI}$ vector

As described in **Chapter 4**, a thermochemical property (y) of a radical is calculated through additivity of the values of GAV and NNI parameters based on how many times they occur in that radical. This leads to the following equation:

$$\sum_{i=1}^{n} X_i \beta_i = y \tag{B-1}$$

where X_i is the number of occurence of the parameter *i* in the radical and β_i is the value of the i^{th} parameter, which is calculated through the linear regression procedure. For each radical *j*, $\sum_{i=1}^{n} X_{ij}\beta_i$ is equal to $\hat{y}_j$, which is the group additively calculated thermochemical data of the radical whereas y_j represents the G4/BAC based thermochemical data for *j*.

Once Eq. (B-1) is written for all the *m* number of radicals, an overdetermined system of linear equations is obtained:

$$\sum_{j=1}^{m} X_{ij}\beta_i = y_j \qquad (i=1,2,\ldots\ldots n) \tag{B-2}$$

Here, X_{ij} is the occurrence matrix which carries the information on how many times each of the parameters occur in each of the radicals and it has the dimensions of m x n.

Least-squares linear regression is carried out to solve this system of equations and obtain β_i vector, which contains the GAV/NNI parameters.

The difference between y_j and $\hat{y}_j$ can be called as "residual", as given in Eq. (B-3).

$$r_j = y_j - \sum_{i=1}^{n} X_i \beta_i \tag{B-3}$$

and the sum of the square of these residuals (SSQ) are given in Eq. (B-4).

$$SSQ = \sum_{j=1}^{m} (y_j - \hat{y}_j)^2 \tag{B-4}$$

The objective function SSQ, i.e. the square root of the difference between *ab initio* data and the GA predictions with respect to the GAV/NNI parameters, β is minimized (argmin (SSQ)).

$$\frac{\partial SSQ}{\partial \beta} = 0 \tag{B-5}$$

This minimization yields the following equation:

$$(X^T X)\bar{\beta} = X^T \bar{y} \tag{B-6}$$

The expression in Eq. (B-6) can be rearranged to the following equation that yields $\bar{\beta}$, which is the $\overline{GAV/NNI}$ vector given in Eq. (4-15) of the text:

$$\overline{GAV/NNI} = (X^T X)^{-1} X^T \bar{y} \tag{B-7}$$

Since, the occurence matrix and the $\bar{y}$ vector, which contains the G4/BAC calculated thermochemical data are available, $\overline{GAV/NNI}$ vector can easily be calculated from Eq. (B-7) above. The $(X^T X)^{-1}$ matrix is separately calculated since it is needed for the calculation of confidence intervals, as explained below.

Calculation of Uncertainity of Parameters

First, mean squared errors (MSE) are calculated using SSQ and the degrees of freedom:

$$MSE = \frac{SSQ}{n_{molecules} - n_{parameters}} \quad \text{(B-8)}$$

MSE includes the variance of the residuals and the errors due to bias, i.e. systematic errors.

$$MSE = \sigma^2 + Bias^2 \quad \text{(B-9)}$$

These confidence intervals represent uncertainties only due to statistical errors. Several systematic sources of error exist, as explained in the text, they are not taken into consideration in this study and hence, the MSE is assumed to be equal to only σ^2.

Then, the variance-covarience matrix of parameters is calculated from the following equation:

$$\sum_{ij} Cov(X_i, X_j) = (X^T X)^{-1} * \sigma^2 \quad \text{(B-10)}$$

The diagonal of the covariance-variance matrix ($Cov(X_i, X_j)$) contains variances of the parameters, whereas the covariances of the parameters are obtained from the off-diagonals of this matrix.

The square root of the diagonal elements of the covariance-variance matrix, i.e. the standard deviations on the parameters, are used to calculate the confidence interval (CI_i) at 97.5% confidence level ($t_{97.5}$) of the i^{th} parameter.

$$CI_i = t_{97.5,i} * \sqrt{Cov(X_i, X_i)} \quad \text{(B-11)}$$

The final GAV and NNI parameters are reported with their uncertainities ($\beta_i \pm CI_i$) in **Table 4-4** and **Table 4-5**, respectively.

B.2 List of Radicals

In this section of the Supporting Information, all the 389 radicals that appear in various sections of the article are listed.

Out of 389 radicals that appear in the article, 369 of them are monocyclic aromatic radicals (MARs) which are used for the development of GAV/NNI parameters, whereas the other 20 radicals are excluded due to the reasons described in the manuscript. The MARs within the framework of this study include unsubstituted and substituted phenyls (C_6H_5•), phenoxies (C_6H_5O•), anisyls ($C_6H_5OCH_2$•), benzoyls (C_6H_5C•=O), *β*-trans-styrlys (t-C_6H_5CH=CH•), β-cis-styrlys (c-C_6H_5CH=CH•), benzyls ($C_6H_5CH_2$•) and *α*-methylbenzyls (C_6H_5CH•CH_3).

These radicals are listed in three different sets: training set (**T**), validation set (**V**) and special cases set (**S**). Training set (**T**) includes 316 MARs that are used in the simultaneous determination of the preliminary Group Additive Values (GAVs) and non-nearest neighbor interactions (NNIs). Validation set (**V**) is used in order to test the applicability of the obtained GAVs and NNIs for the radicals that are outside the training set and this set encompasses 53 MARs. As described in the article, the final determination of these parameters is realized through the optimization of GAVs/NNIs based on the final set of 369 MARs which is formed via combination of training and validation sets. Special cases set (**S**) includes the set of 20 radicals that are excluded from the Group Additivity parameter development sets due to the reasons described in the article.

Each of these radical classes are listed in different subsets and the numbering of the radicals are based on these subset definitions. The number that corresponds to the n^{th} radical in m^{th} subset in the training set is given as "**Tm/n**", e.g. 21st radical in phenyl subset (1st subset) in

the training set is numbered as **T1/21**. Six subsets exist in both training and test sets. These subsets are given in the following order: phenyl, phenoxy, anisyl, benzoyl, styryl and benzyl. Representations of the MARs in each of these subsets are given in the following subsections (**Figure B-1** - **Figure B-14**) above the numbers and the abbreviations of the names of the corresponding MARs. In the list of molecules of the training set (**T**), these abbreviations are explained in each subsection for each subset with one example. In the validation set (**V**), the abbreviation of the radical names and the numbering method is the same, except that the numbering starts with "**V**" instead of "**T**".

In the substituted MARs of interest, the substituent groups are hydroxy (-OH), methoxy (-OCH_3), formyl (-CHO), vinyl (-$CH{=}CH_2$), methyl (-CH_3) and ethyl (-CH_2CH_3).

B.2.1 Training Set

I. *Phenyl Subset*

In the phenyl subset, there are 23 MARs. This subset of MARs includes unsubstituted phenyl, 18 single substituted phenyls, 3 double substituted phenyls and 1 triple substituted phenyl. In the names given below, "C_6H_5•" refers to phenyl radical and single substituted phenyls are given as XC_6H_4• where X=-H,-OH,-OCH_3,-CHO, -$CH{=}CH_2$,-CH_3 or -CH_2CH_3. For instance, *ortho* hydroxy substituted phenyl (MAR no. **T1/2**) is abbreviated as *o*-OHC_6H_4•.

In double and triple substituted phenyls, the location of the radical site on the aryl ring is given as "C•", e.g. 1-C•-2-OH-3-OCH_3-5-CHO (MAR no. **T1/23**) represents 2-hydroxy-3-methoxy-5-formylphenyl.

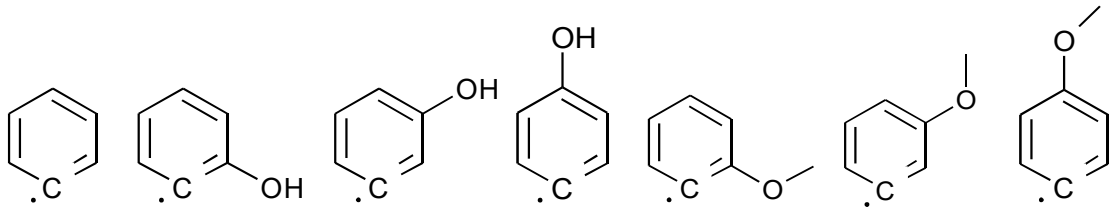

T1/1-C_6H_5• **T1/2**-o-OHC_6H_4• **T1/3**-m-OHC_6H_4• **T1/4**-p-OHC_6H_4• **T1/5**-o-$OCH_3C_6H_4$• **T1/6**-m-$OCH_3C_6H_4$• **T1/7**-p-$OCH_3C_6H_4$•

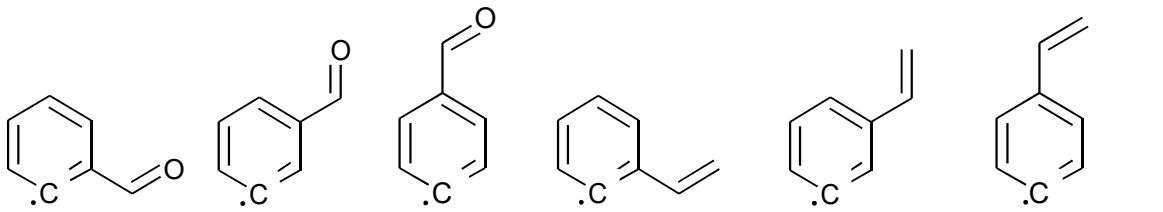

T1/8-o-$CHOC_6H_4$• **T1/9**-m-$CHOC_6H_4$• **T1/10**-p-$CHOC_6H_4$• **T1/11**-o-$CH{=}CH_2C_6H_4$• **T1/12**-m-$CH{=}CH_2C_6H_4$• **T1/13**-p-$CH{=}CH_2C_6H_4$•

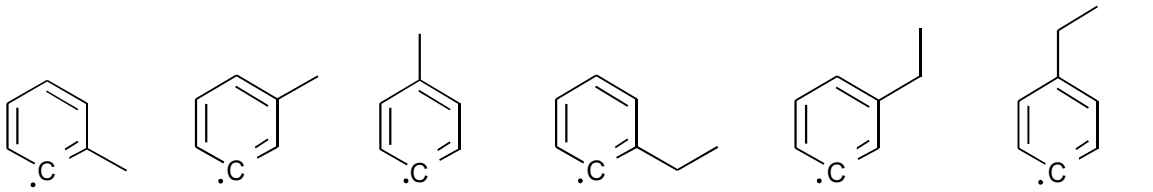

T1/14-o-$CH_3C_6H_4$• **T1/15**-m-$CH_3C_6H_4$• **T1/16**-p-$CH_3C_6H_4$• **T1/17**-o-$CH_2CH_3C_6H_4$• **T1/18**-m-$CH_2CH_3C_6H_4$• **T1/19**-p-$CH_2CH_3C_6H_4$•

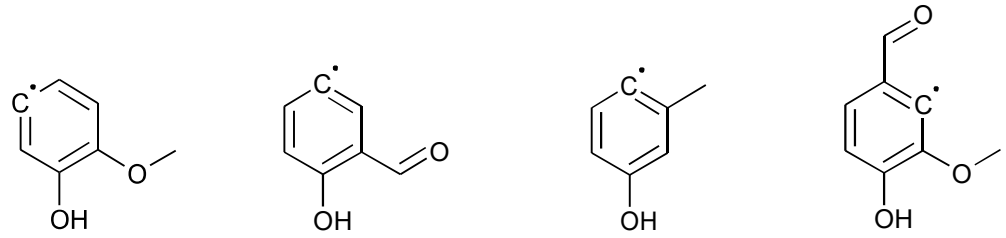

T1/20-1-C•-3-OH-4-OCH_3 **T1/21**-1-C•-3-OH-4-CHO **T1/22**-1-C•-2-CH_3-4-OH **T1/23**-1-C•-2-OCH_3-3-OH-6-CHO

Figure B-1 List of radicals in phenyl subset of the training set.

II. *Anisyl Subset*

There are 33 MARs in the "anisyl" subset of the training set of MARs which is composed of anisyl, 18 double substituted, 14 triple substituted anisyls. "$C_6H_5OCH_2$•" refers to anisyl radical and double substituted anisyls are given as $(X)C_6H_4OCH_2$• where X=-OH, -OCH_3,-CHO, -$CH{=}CH_2$,-CH_3 or -CH_2CH_3. For instance, *ortho* hydroxy substituted anisyl (MAR no. **T2/2**) is abbreviated as *o*-$OHC_6H_4OCH_2$•.

In triple substituted anisyls, "OCH_2•" is used to indicate radical substituent group. As an example; 2-hydroxy-5-vinylanisyl (MAR no. **T2/24**) is abbreviated as 1-OCH_2•-2-OH-5-$CH{=}CH_2$.

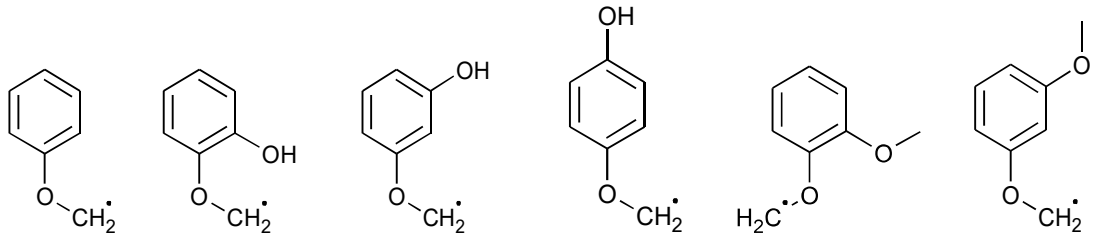

T2/1-$C_6H_5OCH_2$• **T2/2**-o-$(OH)C_6H_4OCH_2$• **T2/3**-m-$(OH)C_6H_4OCH_2$• **T2/4**-p-$(OH)C_6H_4OCH_2$• **T2/5**-o-$(OCH_3)C_6H_4OCH_2$• **T2/6**-m-$(OCH_3)C_6H_4OCH_2$•

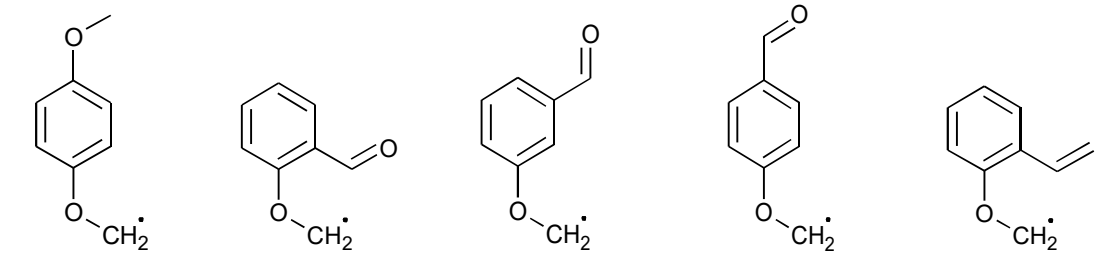

T2/7-p-$(OCH_3)C_6H_4OCH_2$• **T2/8**-o-$(CHO)C_6H_4OCH_2$• **T2/9**-m-$(CHO)C_6H_4OCH_2$• **T2/10**-p-$(CHO)C_6H_4OCH_2$• **T2/11**-o-$(CH{=}CH_2)C_6H_4OCH_2$•

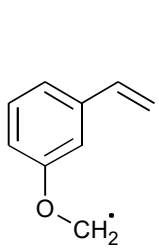

T2/12-m-(CH=CH$_2$)C$_6$H$_4$OCH$_2$• **T2/13**-p-(CH=CH$_2$)C$_6$H$_4$OCH$_2$• **T2/14**-o-(CH$_3$)C$_6$H$_4$OCH$_2$• **T2/15**-m-(CH$_3$)C$_6$H$_4$OCH$_2$• **T2/16**-p-(CH$_3$)C$_6$H$_4$OCH$_2$•

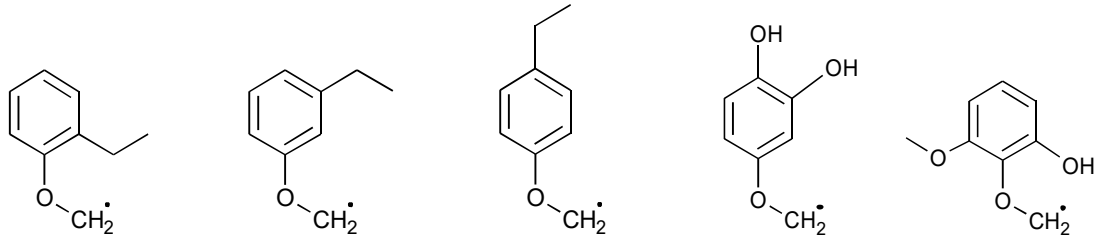

T2/17-o-(CH$_2$CH$_3$)C$_6$H$_4$OCH$_2$• **T2/18**-m-(CH$_2$CH$_3$)C$_6$H$_4$OCH$_2$• **T2/19**-p-(CH$_2$CH$_3$)C$_6$H$_4$OCH$_2$• **T2/20**-1-OCH$_2$•-3,4-OH **T2/21**-1-OCH$_2$•-2-OH-6-OCH$_3$

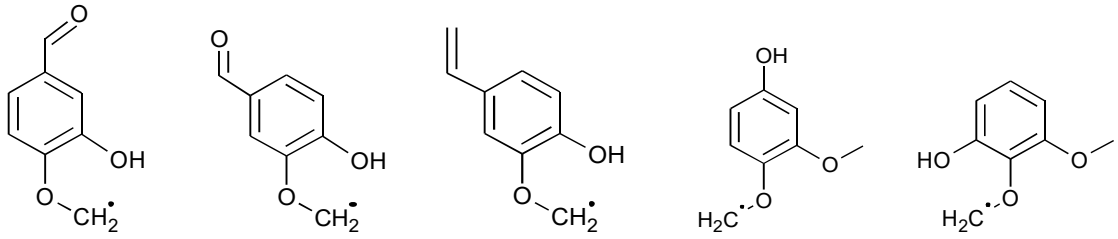

T2/22-1-OCH$_2$•-2-OH-4-CHO **T2/23**-1-OCH$_2$•-2-OH-5-CHO **T2/24**-1-OCH$_2$•-2-OH-5-CH=CH$_2$ **T2/25**-1-OCH$_2$•-2-OCH$_3$-4-OH **T2/26**-1-OCH$_2$•-2-OCH$_3$-6-OH

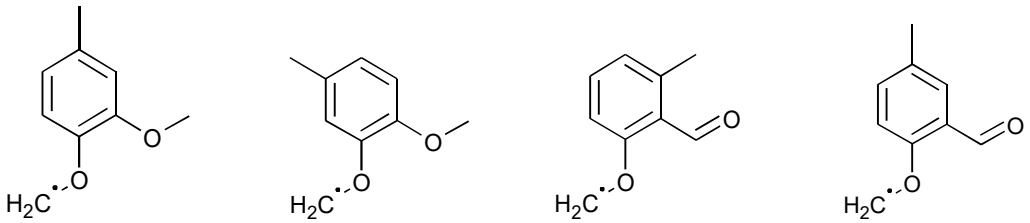

T2/27-1-OCH$_2$•-2-OCH$_3$-4-CH$_3$ **T2/28**-1-OCH$_2$•-2-OCH$_3$-5-CH$_3$ **T2/29**-1-OCH$_2$•-2-CHO-3-CH$_3$ **T2/30**-1-OCH$_2$•-2-CHO-4-CH$_3$

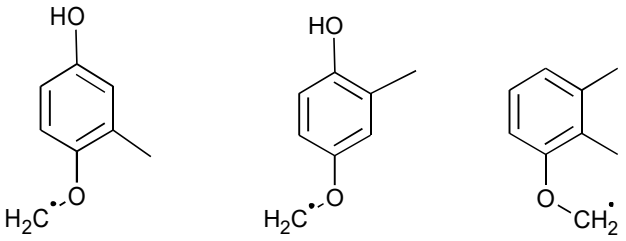

T2/31-1-OCH_2•-2-CH_3-4-OH **T2/32**-1-OCH_2•-3-CH_3-4-OH **T2/33**-1-OCH_2•-2,3-CH_3

Figure B-2 List of radicals in anisyl subset of the training set.

III. ***Phenoxy Subset***

There are 68 MARs in the "phenoxy" subset of the training set of MARs which is composed of phenoxy, 18 double, 47 triple and 2 quadruple phenoxies. "C_6H_5O•" refers to phenoxy radical and double substituted phenoxies are given as (X)C_6H_4O• where X=-OH,-OCH_3,-CHO, -CH=CH_2,-CH_3 or -CH_2CH_3. For instance, *ortho* hydroxy substituted phenoxy (MAR no. **T3/2**) is abbreviated as *o*-OHC_6H_4O•.

In multiple (triple and quadruple) substituted phenoxies, "O•" is used to indicate oxygen substituent with radical center. As an example; 2-formyl-4-methylphenoxy (MAR no. **T3/59**) is abbreviated as 1-O•-2-CHO-4-CH_3.

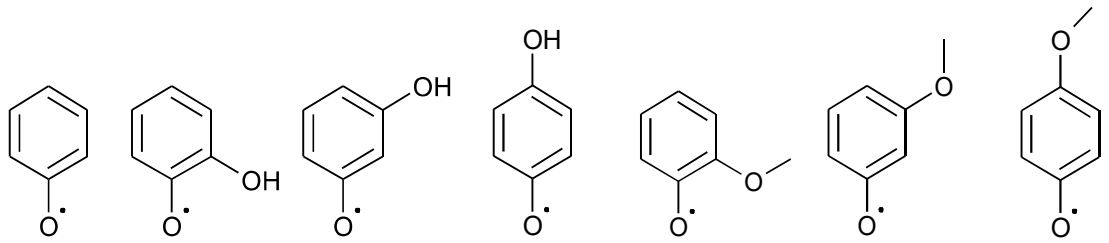

T3/1-C_6H_5O• **T3/2**-o-(OH)C_6H_4O• **T3/3**-m-(OH)C_6H_4O• **T3/4**-p-(OH)C_6H_4O• **T3/5**-o-(OCH_3)C6H4O• **T3/6**-m-(OCH_3)C6H4O• **T3/7**-p-(OCH_3)C_6H_4O•

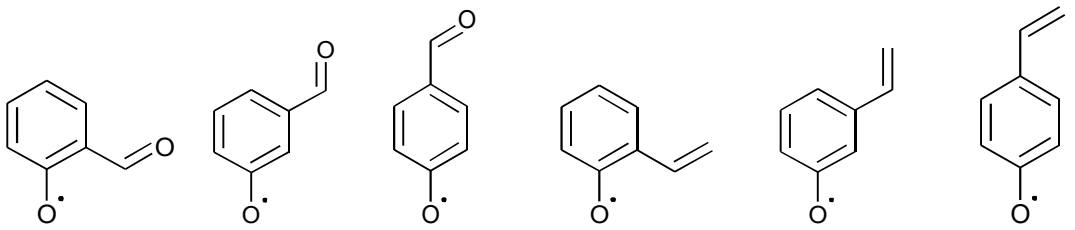

T3/8-o-(CHO)C_6H_4O• **T3/9**-m-(CHO)C_6H_4O• **T3/10**-p-(CHO)C_6H_4O• **T3/11**-o-($CH{=}CH_2$)C_6H_4O• **T3/12**-m-($CH{=}CH_2$)C_6H_4O• **T3/13**-p-($CH{=}CH_2$)C_6H_4O•

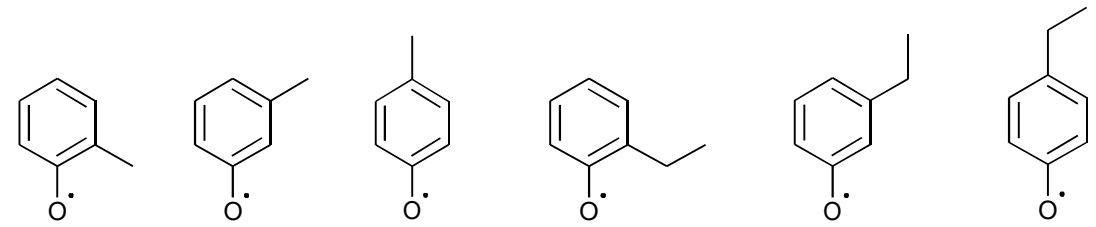

T3/14-o-(CH_3)C_6H_4O• **T3/15**-m-(CH_3)C_6H_4O• **T3/16**-p-(CH_3)C_6H_4O• **T3/17**-o-(CH_2CH_3)C_6H_4O• **T3/18**-m-(CH_2CH_3)C_6H_4O• **T3/19**-p-(CH_2CH_3)C_6H_4O•

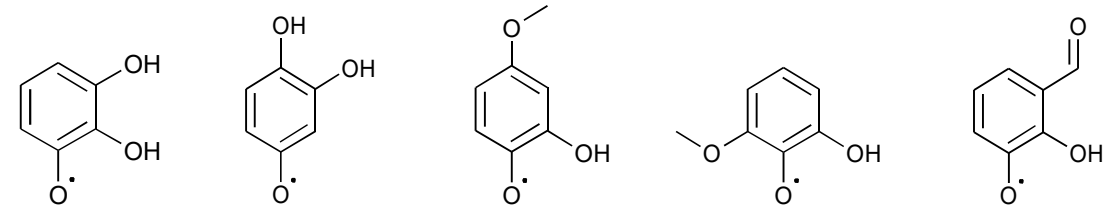

T3/20-1-O•-2,3-OH **T3/21**-1-O•-3,4-OH **T3/22**-1-O•-2-OH-4-OCH_3 **T3/23**-1-O•-2-OH-6-OCH_3 **T3/24**-1-O•-2-OH-3-CHO

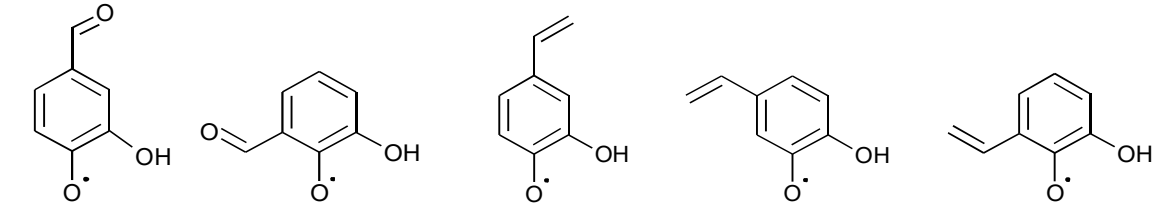

T3/25-1-O•-2-OH-4-CHO **T2/26**-1-O•-2-OH-6-CHO **T2/27**-1-O•-2-OH-4-$CH{=}CH_2$ **T2/28**-1-O•-2-OH-5-$CH{=}CH_2$ **T2/29**-1-O•-2-OH-6-$CH{=}CH_2$

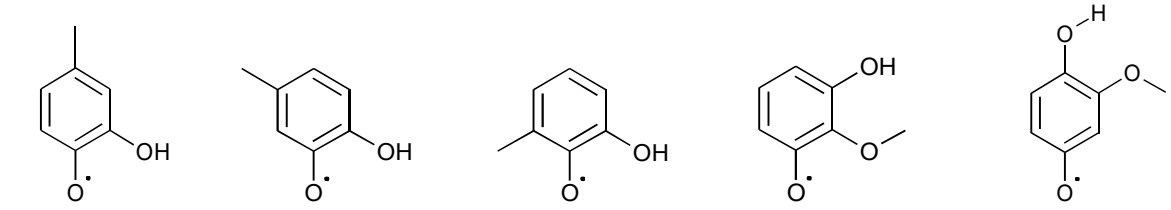

T2/30-1-O•-2-OH-4-CH_3 **T2/31**-1-O•-2-OH-5-CH_3 **T2/32**-1-O•-2-OH-6-CH_3 **T3/33**-1-O•-2-OCH_3-3-OH **T3/34**-1-O•-3-OCH_3-4-OH

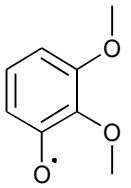

T3/35-1-O•-2,3-OCH_3

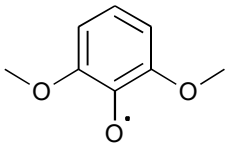

T3/36-1-O•-2,6-OCH_3

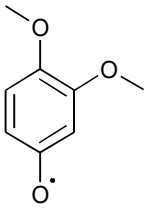

T3/37-1-O•-3,4-OCH_3

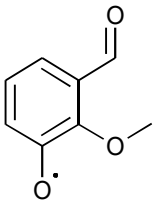

T3/38-1-O•-2-OCH_3-3-CHO

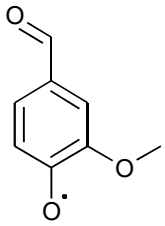

T3/39-1-O•-2-OCH_3-4-CHO

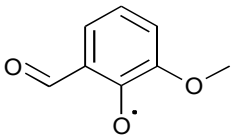

T3/40-1-O•-2-OCH_3-6-CHO

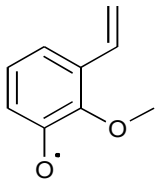

T3/41-1-O•-2-OCH_3-3-$CH=CH_2$

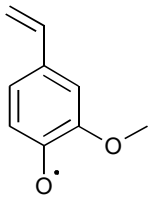

T3/42-1-O•-2-OCH_3-4-$CH=CH_2$

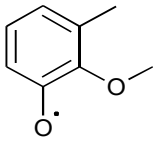

T3/43-1-O•-2-OCH_3-3-CH_3

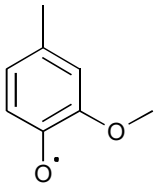

T3/44-1-O•-2-OCH_3-4-CH_3

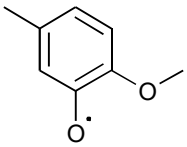

T3/45-1-O•-2-OCH_3-5-CH_3

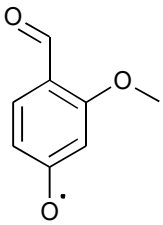

T3/46-1-O•-3-OCH_3-4-CHO

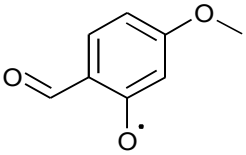

T3/47-1-O•-3-OCH_3-6-CHO

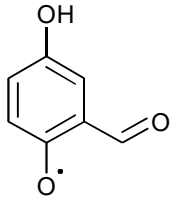

T3/48-1-O•-2-CHO-4-OH

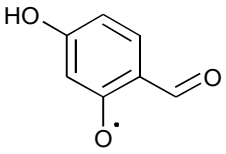

T3/49-1-O•-2-CHO-5-OH

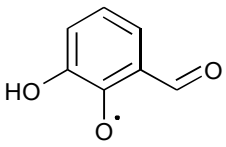

T3/50-1-O•-2-CHO-6-OH

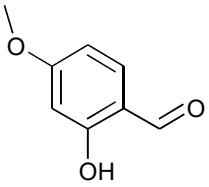

T3/51-1-O•-2-CHO-5-OCH_3

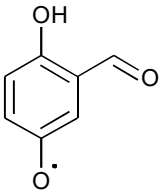

T3/52-1-O•-3-CHO-4-OH

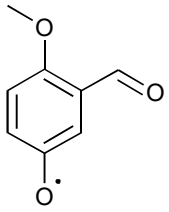

T3/53-1-O•-3-CHO-4-OCH_3

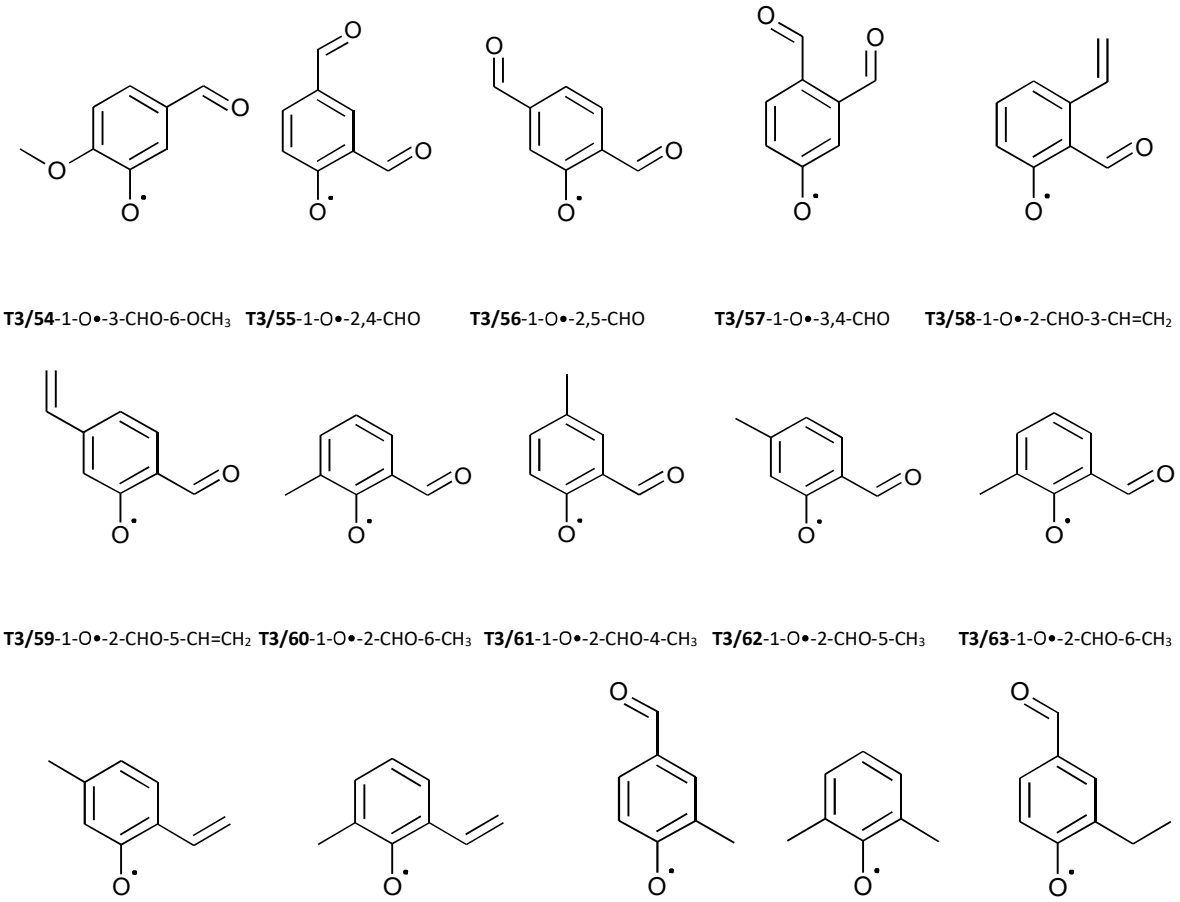

Figure B-3 List of radicals in phenoxy subset of the training set.

IV. ***Benzoyl Subset***

There are 42 MARs in the "benzoyl" subset of the training set of MARs which is composed of benzoyl, 18 double substituted and 23 triple substituted benzoyls. "$C_6H_5C\bullet=O$" refers to benzoyl radical and double substituted benzoyls are given as $(X)C_6H_4C\bullet=O$ where X=-OH, $-OCH_3$, -CHO, $-CH=CH_2$, $-CH_3$ or $-CH_2CH_3$. For instance, *ortho* hydroxy substituted benzoyl (MAR no. **T4/2**) is abbreviated as *o*-$OHC_6H_4C\bullet=O$.

In triple substituted benzoyls, "C•=O" is used to indicate radical substituent group. As an example; 3-hydroxy-4-vinylbenzoyl (MAR no. **T4/25**) is abbreviated as 1-C•=O-3-OH-4-$CH{=}CH_2$.

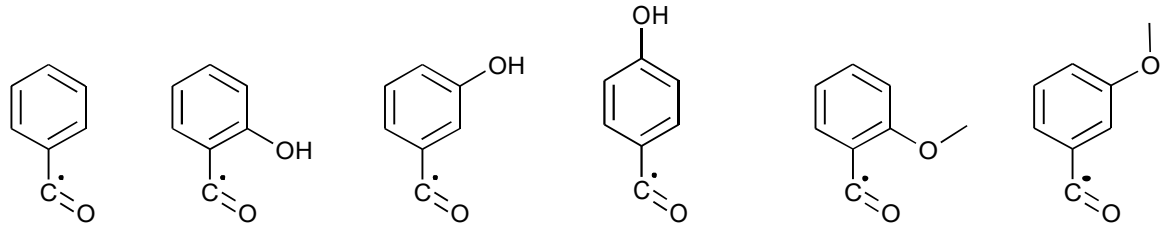

T4/1-$C_6H_5C{\bullet}{=}O$ **T4/2**-o-$(OH)C_6H_4C{\bullet}{=}O$ **T4/3**-m-$(OH)C_6H_4C{\bullet}{=}O$ **T4/4**-p-$(OH)C_6H_4C{\bullet}{=}O$ **T4/5**-o-$(OCH_3)C_6H_4C{\bullet}{=}O$ **T4/6**-m-$(OCH_3)C_6H_4C{\bullet}{=}O$

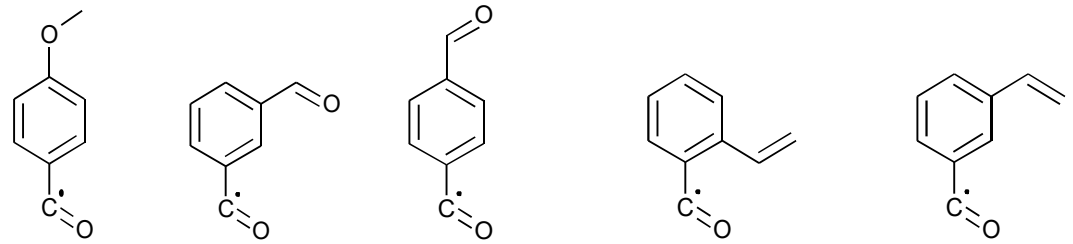

T4/7-p-$(OCH_3)C_6H_4C{\bullet}{=}O$ **T4/8**-m-$(CHO)C_6H_4C{\bullet}{=}O$ **T4/9**-p-$(CHO)C_6H_4C{\bullet}{=}O$ **T4/10**-o-$(CH{=}CH_2)C_6H_4C{\bullet}{=}O$ **T4/11**-m-$(CH{=}CH_2)C_6H_4C{\bullet}{=}O$

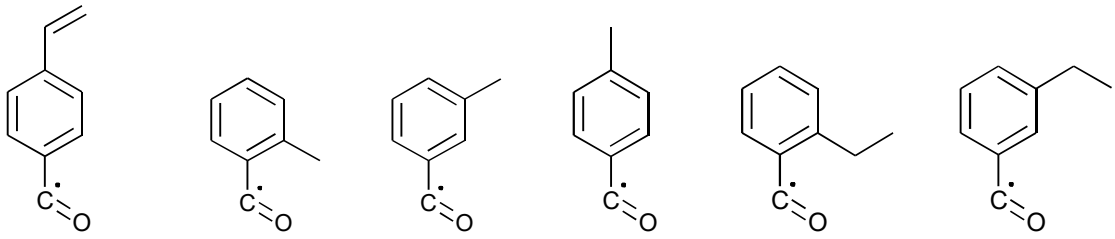

T4/12-p-$(CH{=}CH_2)C_6H_4C{\bullet}{=}O$ **T4/13**-o-$(CH_3)C_6H_4C{\bullet}{=}O$ **T4/14**-m-$(CH_3)C_6H_4C{\bullet}{=}O$ **T4/15**-p-$(CH_3)C_6H_4C{\bullet}{=}O$ **T4/16**-o-$(CH_2CH_3)C_6H_4C{\bullet}{=}O$ **T4/17**-m-$(CH_2CH_3)C_6H_4C{\bullet}{=}O$

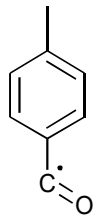

T4/18-p-$(CH_2CH_3)C_6H_4C\bullet=O$

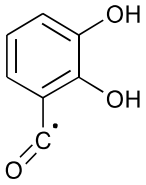

T4/19-1-C•=O-2,3-OH

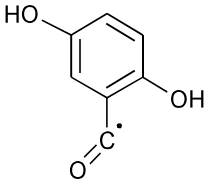

T4/20-1-C•=O-2,5-OH

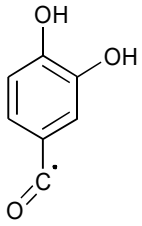

T4/21-1-C•=O-3,4-OH

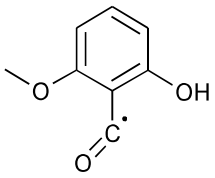

T4/22-1-C•=O-2-OH-6-OCH_3

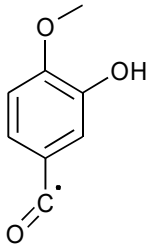

T4/23-1-C•=O-3-OH-4-OCH_3

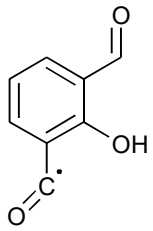

T4/24-1-C•=O-2-OH-3-CHO

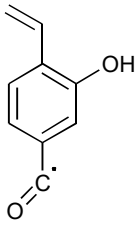

T4/25-1-C•=O-3-OH-4-$CH=CH_2$

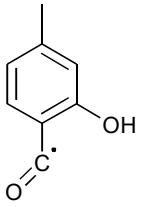

T4/26-1-C•=O-2-OH-4-CH_3

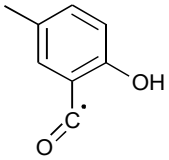

T4/27-1-C•=O-2-OH-5-CH_3

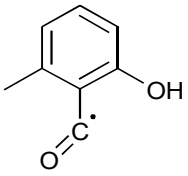

T4/28-1-C•=O-2-OH-6-CH_3

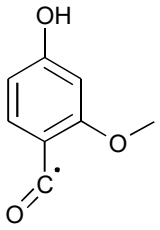

T4/29-1-C•=O-2-OCH_3-4-OH

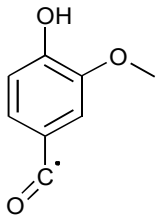

T4/30-1-C•=O-3-OCH_3-4-OH

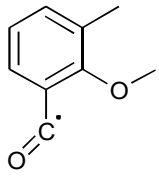

T4/31-1-C•=O-2-OCH_3-3-CH_3

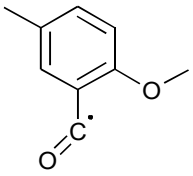

T4/32-1-C•=O-2-OCH_3-5-CH_3

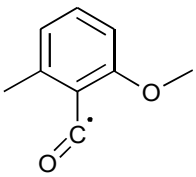

T4/33-1-C•=O-2-OCH_3-6-CH_3

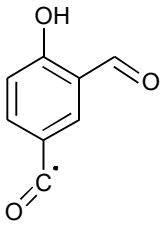

T4/34-1-C•=O-3-CHO-4-OH

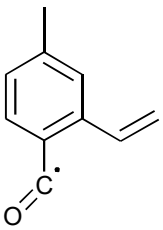

T4/35-1-C•=O-2-$CH=CH_2$-4-CH_3

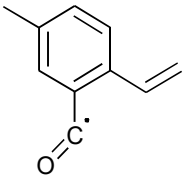

T4/36-1-C•=O-2-$CH=CH_2$-5-CH_3

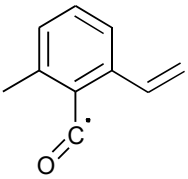

T4/37-1-C•=O-2-$CH=CH_2$-6-CH_3

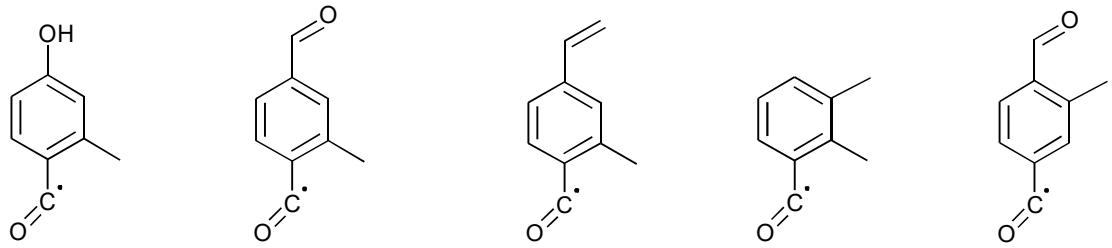

T4/38-1-C•=O-2-CH_3-4-OH **T4/39**-1-C•=O-2-CH_3-4-CHO **T4/40**-1-C•=O-2-CH_3-4-CH=CH_2 **T4/41**-1-C•=O-2,3-CH_3 **T4/42**-1-C•=O-3-CH_3-4-CHO

Figure B-4 List of radicals in benzoyl subset of the training set.

V. *β-Styryl Subset*

There are 80 styrlys in this subset of the training set of MARs which is composed of 38 unsubstituted and substituted trans-β-styryls and 42 unsubstituted and substituted cis-β-styryls. "t-$C_6H_5CH=CH•$" and "c-$C_6H_5CH=CH•$" refers to trans-β-styryl and cis-β-styryl radicals, respectively. The names of the double substituted radicals of trans-β-styryls and cis-β-styryls are given as (X)t-$C_6H_5CH=CH•$ and (X)c-$C_6H_5CH=CH•$, respectively where X= -OH, -OCH_3, -CHO, -$CH=CH_2$, -CH_3 or -CH_2CH_3. For instance, *ortho* hydroxy substituted trans-β-styryl (MAR no. **T5/2**) is abbreviated as *o*-(OH)t-$C_6H_4CH=CH•$.

In triple substituted styryls, "t-CH=CH•" and "c-CH=CH•" represents the trans and cis radical vinyl groups, respectively. As an example; 2-hydroxy-5-vinyl trans-β-styryl (MAR no. **T5/25**) is abbreviated as 1-(t-CH=CH•)-2-OH-5-$CH=CH_2$.

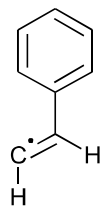

T5/1-t-$C_6H_5CH=CH•$

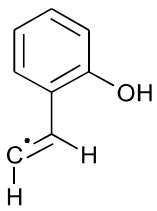

T5/2-o-(OH)t-$C_6H_4CH=CH•$

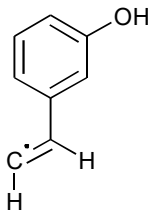

T5/3-m-(OH)t-$C_6H_4CH=CH•$

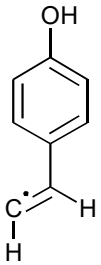

T5/4-p-(OH)t-$C_6H_4CH=CH•$

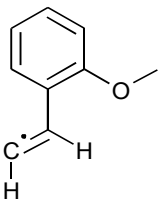

T5/5-o-(OCH_3)t-$C_6H_4CH=CH•$

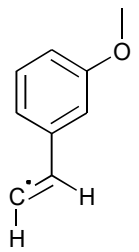

T5/6-m-(OCH_3)t-$C_6H_4CH=CH•$

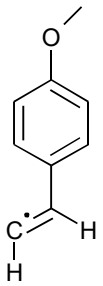

T5/7-p-(OCH_3)t-$C_6H_4CH=CH•$

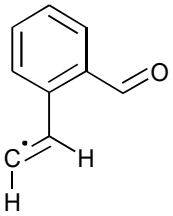

T5/8-o-(CHO)t-$C_6H_4CH=CH•$

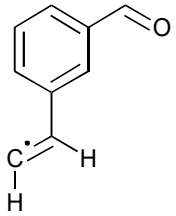

T5/9-m-(CHO)t-$C_6H_4CH=CH•$

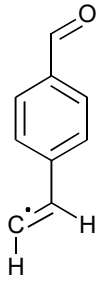

T5/10-p-(CHO)t-$C_6H_4CH{=}CH\bullet$

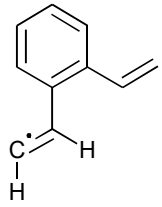

T5/11-o-$(CH{=}CH_2)$t-$C_6H_4CH{=}CH\bullet$

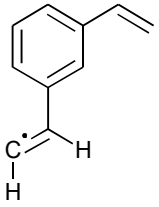

T5/12-m-$(CH{=}CH_2)$t-$C_6H_4CH{=}CH\bullet$

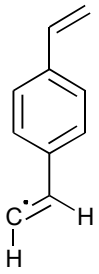

T5/13-p-$(CH{=}CH_2)$t-$C_6H_4CH{=}CH\bullet$

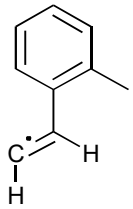

T5/14-o-(CH_3)t-$C_6H_4CH{=}CH\bullet$

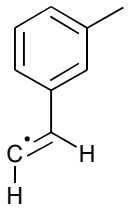

T5/15-m-(CH_3)t-$C_6H_4CH{=}CH\bullet$

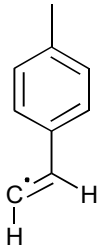

T5/16-p-(CH_3)t-$C_6H_4CH{=}CH\bullet$

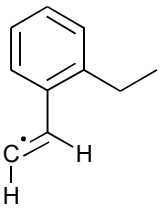

T5/17-o-$(CH_2CH_3)C_6H_4CH{=}CH\bullet$

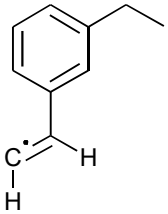

T5/18-m-$(CH_2CH_3)C_6H_4CH{=}CH\bullet$

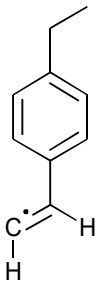

T5/19-p-$(CH_2CH_3)C_6H_4CH{=}CH\bullet$

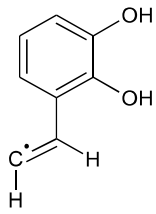

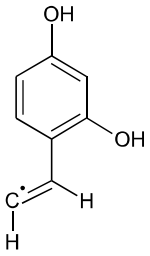

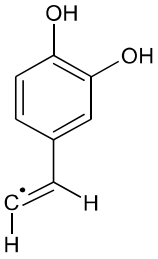

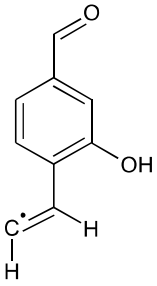

T5/20-1-(t-CH=CH•)-2,3-OH **T5/21**-1-(t-CH=CH•)-2,4-OH **T5/22**-1-(t-CH=CH•)-3,4-OH **T5/23**-1-(t-CH=CH•)-2-OH-4-CHO

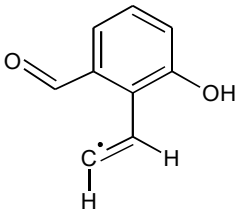

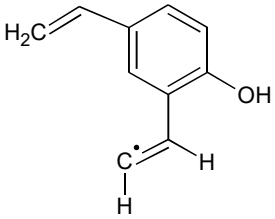

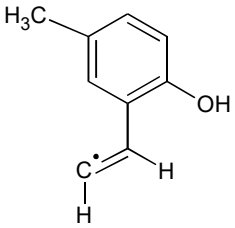

T5/24-1-(t-CH=CH•)-2-OH-6-CHO **T5/25**-1-(t-CH=CH•)-2-OH-5-CH=CH_2 **T5/26**-1-(t-CH=CH•)-2-OH-5-CH_3

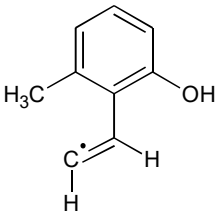

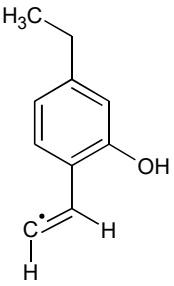

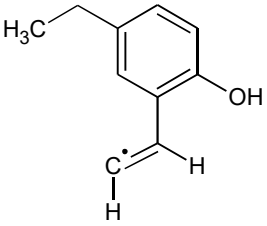

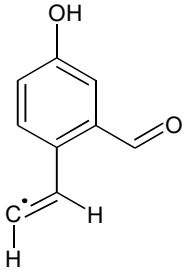

T5/27-1-(t-CH=CH•)-2-OH-6-CH_3 **T5/28**-1-(t-CH=CH•)-2-OH-4-CH_2CH_3 **T5/29**-1-(t-CH=CH•)-2-OH-5-CH_2CH_3 **T5/30**-1-(t-CH=CH•)-2-CHO-4-OH

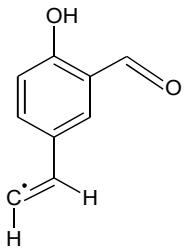

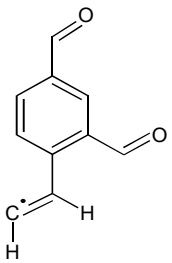

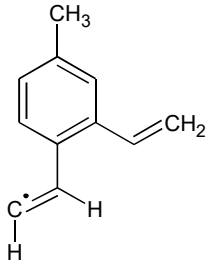

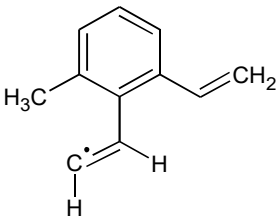

T5/31-1-(t-CH=CH•)-3-CHO-4-OH **T5/32**-1-(t-CH=CH•)-2,4-CHO **T5/33**-1-(t-CH=CH•)-2-CH=CH_2-4-CH_3 **T5/34**-1-(t-CH=CH•)-2-CH=CH_2-6-CH_3

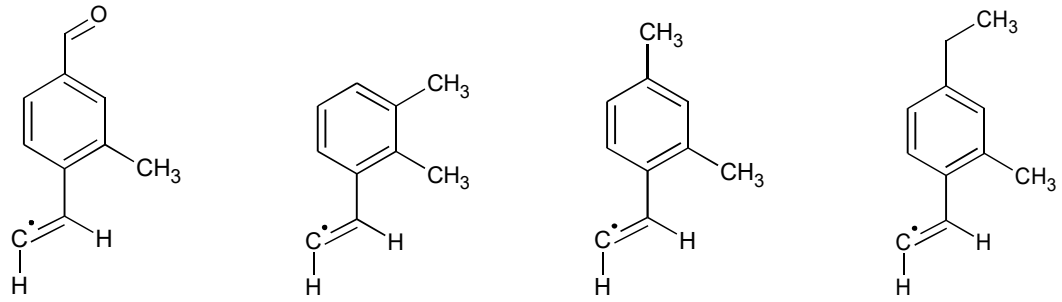

T5/35-1-(t-CH=CH•)-2-CH_3-4-CHO **T5/36**-1-(t-CH=CH•)-2,3-CH_3 **T5/37**-1-(t-CH=CH•)-2,4-CH_3 **T5/38**-1-(t-CH=CH•)-2-CH_3-4-CH_2CH_3

Figure B-5 Trans-β-styryl radicals in styryls subset of the training set.

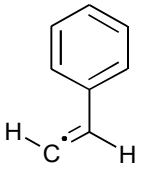

T5/39-c-$C_6H_5CH{=}CH\bullet$

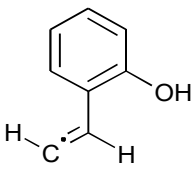

T5/40-o-(OH)c-$C_6H_4CH{=}CH\bullet$

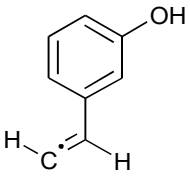

T5/41-m-(OH)c-$C_6H_4CH{=}CH\bullet$

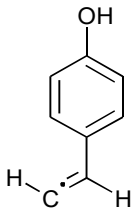

T5/42-p-(OH)c-$C_6H_4CH{=}CH\bullet$

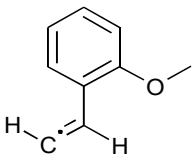

T5/43-o-(OCH_3)c-$C_6H_4CH{=}CH\bullet$

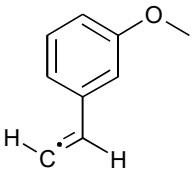

T5/44-m-(OCH_3)c-$C_6H_4CH{=}CH\bullet$

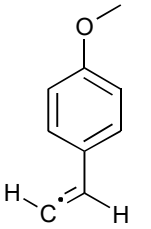

T5/45-p-(OCH_3)c-$C_6H_4CH{=}CH\bullet$

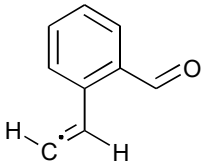

T5/46-o-(CHO)c-$C_6H_4CH{=}CH\bullet$

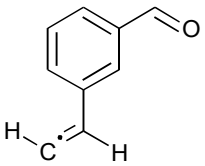

T5/47-m-(CHO)c-$C_6H_4CH{=}CH\bullet$

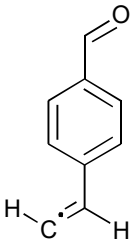

T5/48-p-(CHO)c-$C_6H_4CH{=}CH\bullet$

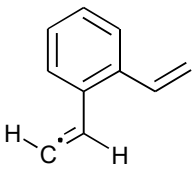

T5/49-o-$(CH{=}CH_2)$c-$C_6H_4CH{=}CH\bullet$

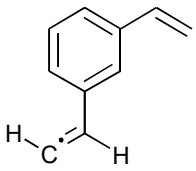

T5/50-m-$(CH{=}CH_2)$c-$C_6H_4CH{=}CH\bullet$

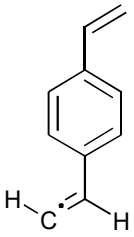

T5/51-p-$(CH{=}CH_2)$c-$C_6H_4CH{=}CH\bullet$

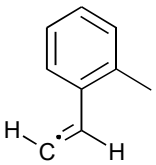

T5/52-o-(CH_3)c-$C_6H_4CH{=}CH\bullet$

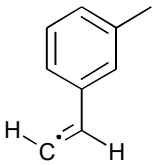

T5/53-m-(CH_3)c-$C_6H_4CH{=}CH\bullet$

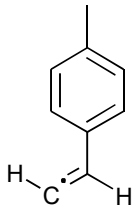

T5/54-p-(CH_3)c-$C_6H_4CH{=}CH\bullet$

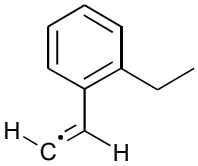

T5/55-o-$(CH_2CH_3)C_6H_4CH{=}CH\bullet$

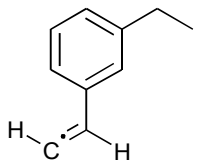

T5/56-m-$(CH_2CH_3)C_6H_4CH{=}CH\bullet$

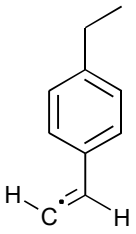

T5/57-p-$(CH_2CH_3)C_6H_4CH{=}CH\bullet$

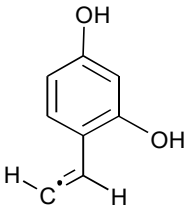

T5/58-1-(c-CH=CH•)-2,4-OH

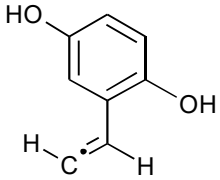

T5/59-1-(c-CH=CH•)-2,5-OH

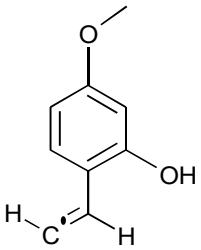

T5/60-1-(c-CH=CH•)-2-OH-4-OCH_3

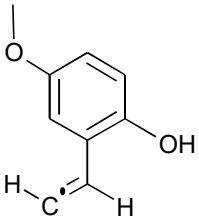

T5/61-1-(c-CH=CH•)-2-OH-5-OCH_3

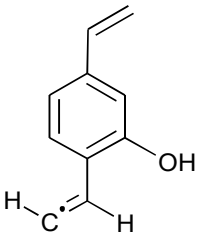

T5/62-1-(c-CH=CH•)-2-OH-4-$CH{=}CH_2$

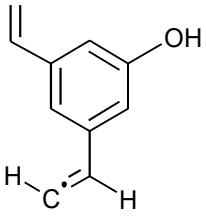

T5/63-1-(c-CH=CH•)-3-OH-5-$CH{=}CH_2$

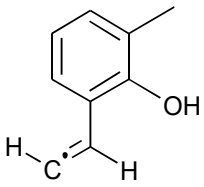

T5/64-1-(c-CH=CH•)-2-OH-3-CH_3

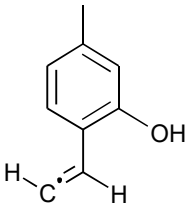

T5/65-1-(c-CH=CH•)-2-OH-4-CH_3

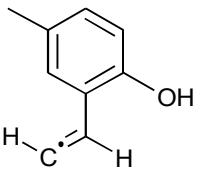

T5/66-1-(c-CH=CH•)-2-OH-5-CH_3

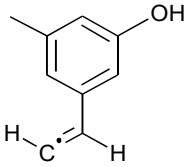

T5/67-1-(c-CH=CH•)-3-OH-5-CH_3

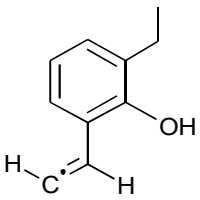

T5/68-1-(c-CH=CH•)-2-OH-3-CH_2CH_3

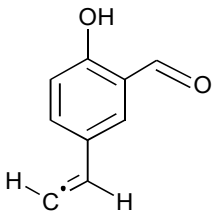

T5/69-1-(c-CH=CH•)-3-CHO-4-OH

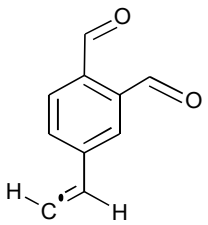

T5/70-1-(c-CH=CH•)-2,4-CHO

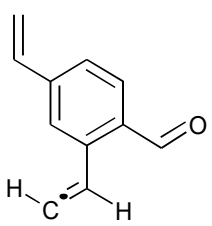

T5/71-1-(c-CH=CH•)-2-CHO-5-CH=CH$_2$

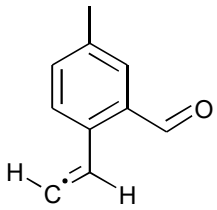

T5/72-1-(c-CH=CH•)-2-CHO-4-CH$_3$

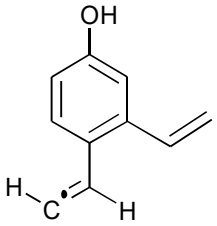

T5/73-1-(c-CH=CH•)-2-CH=CH$_2$-4-OH

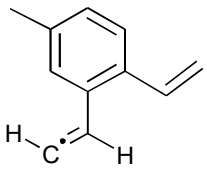

T5/74-1-(c-CH=CH•)-2-CH=CH$_2$-5-CH$_3$

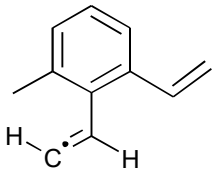

T5/75-1-(c-CH=CH•)-2-CH=CH$_2$-6-CH$_3$

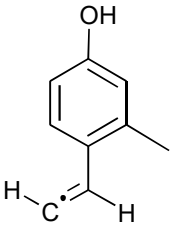

T5/76-1-(c-CH=CH•)-2-CH$_3$-4-OH

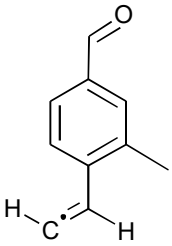

T5/77-1-(c-CH=CH•)-2-CH$_3$-4-CHO

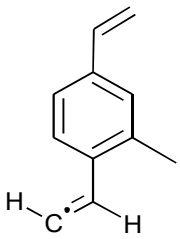

T5/78-1-(c-CH=CH•)-2-CH$_3$-4-CH=CH$_2$

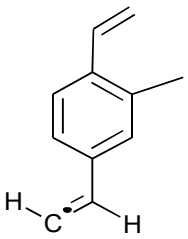

T5/79-1-(c-CH=CH•)-3-CH$_3$-4-CH=CH$_2$

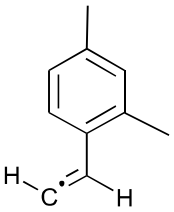

T5/80-1-(c-CH=CH•)-2,4-CH$_3$

Figure B-6 Cis-β-styryl radicals in styryls subset of the training set.

VI. ***Benzyl/1-Phenylethyl Subset***

There are 70 MARs in the "benzyl" subset of the training set of MARs which is composed of benzyl, α-methylbenzyl, 18 double substituted, 32 triple substituted benzyls and 18 double substituted α-methylbenzyls. "$C_6H_5CH_2$•" and "C_6H_5CH•CH_3" refers to benzyl and α-methylbenzyl radicals, respectively. Double substituted benzyls and α-methylbenzyls are given as $(X)C_6H_4CH_2$• and $(X)C_6H_4CH$•CH_3, respectively where X= -OH, -OCH_3, -CHO, -$CH{=}CH_2$, -CH_3 or -CH_2CH_3. For instance, *ortho* hydroxy substituted benzyl (MAR no. **6/2**) is abbreviated as *o*-$OHC_6H_4CH_2$•.

In triple substituted benzyls, "CH_2•" is used to indicate radical substituent group. As an example; 2,4-dihydroxybenzyl (MAR no. **6/21**) is abbreviated as 1-CH_2•-2,4-OH. There are no triple substituted α-methylbenzyls in the database.

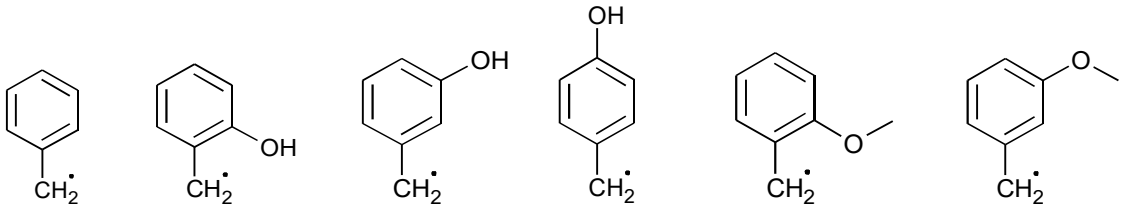

T6/1-$C_6H_5CH_2$• **T6/2**-o-$(OH)C_6H_4CH_2$• **T6/3**-m-$(OH)C_6H_4CH_2$• **T6/4**-p-$(OH)C_6H_4CH_2$• **T6/5**-o-$(OCH_3)C_6H_4CH_2$• **T6/6**-m-$(OCH_3)C_6H_4CH_2$•

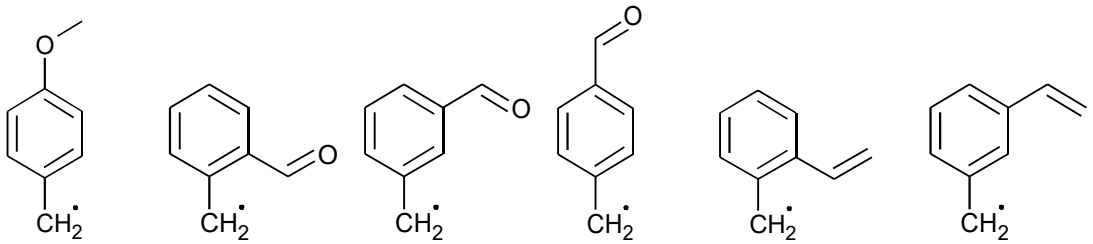

T6/7-p-$(OCH_3)C_6H_4CH_2$• **T6/8**-o-$(CHO)C_6H_4CH_2$• **T6/9**-m-$(CHO)C_6H_4CH_2$•**T6/10**-p-$(CHO)C_6H_4CH_2$• **T6/11**-o-$(CH{=}CH_2)C_6H_4CH_2$• **T6/12**-m-$(CH{=}CH_2)C_6H_4CH_2$•

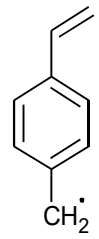

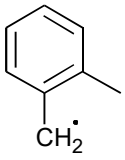

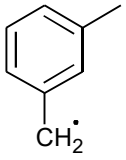

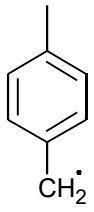

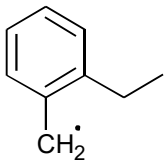

T6/13-(p-CH=CH$_2$)C$_6$H$_4$CH$_2$• **T6/14**-o-(CH$_3$)C$_6$H$_4$CH$_2$• **T6/15**-m-(CH$_3$)C$_6$H$_4$CH$_2$• **T6/16**-p-(CH$_3$)C$_6$H$_4$CH$_2$• **T6/17**-o-(CH$_2$CH$_3$)C$_6$H$_4$CH$_2$•

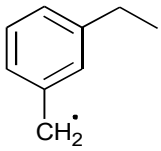

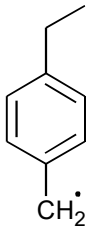

T6/18-m-(CH$_2$CH$_3$)C$_6$H$_4$CH$_2$• **T6/19**-p-(CH$_2$CH$_3$)C$_6$H$_4$CH$_2$•

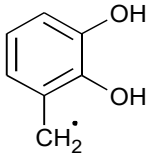

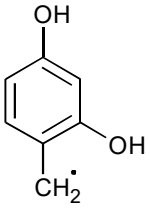

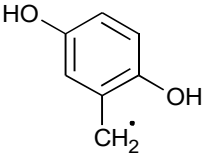

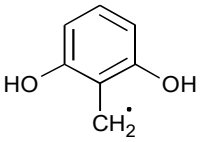

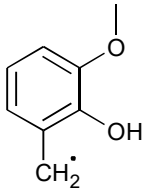

T6/20-1-CH$_2$•-2,3-OH **T6/21**-1-CH$_2$•-2,4-OH **T6/22**-1-CH$_2$•-2,5-OH **T6/23**-1-CH$_2$•-2,6-OH **T6/24**-1-CH$_2$•-2-OH-3-OCH$_3$

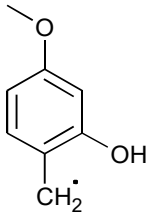

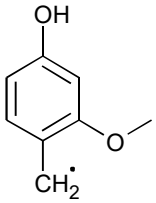

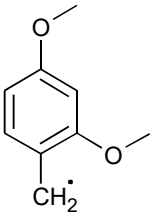

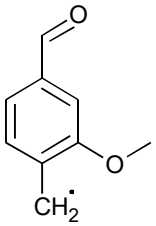

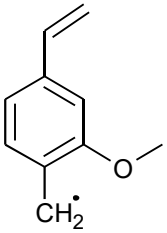

T6/25-1-CH$_2$•-2-OH-4-OCH$_3$ **T6/26**-1-CH$_2$•-2-OCH$_3$-4-OH **T6/27**-1-CH$_2$•-2,4-OCH$_3$ **T6/28**-1-CH$_2$•-2-OCH$_3$-4-CHO **T6/29**-1-CH$_2$•-2-OCH$_3$-4-CH=CH$_2$

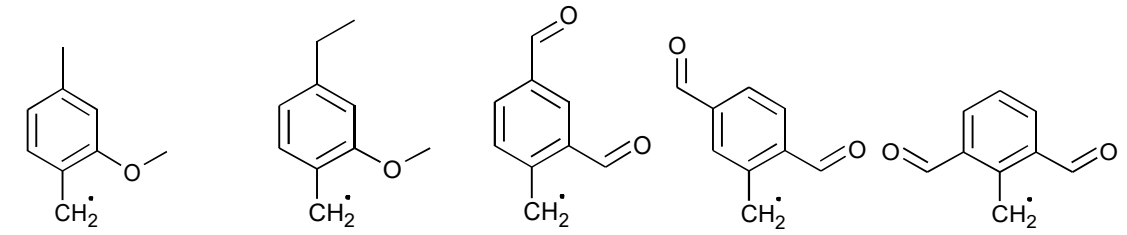

T6/30-1-CH_2•-2-OCH_3-4-CH_3 **T6/31**-1-CH_2•-2-OCH_3-4-CH_2CH_3 **T6/32**-1-CH_2•-2,4-CHO **T6/33**-1-CH_2•-2,5-CHO **T6/34**-1-CH_2•-2,6-CHO

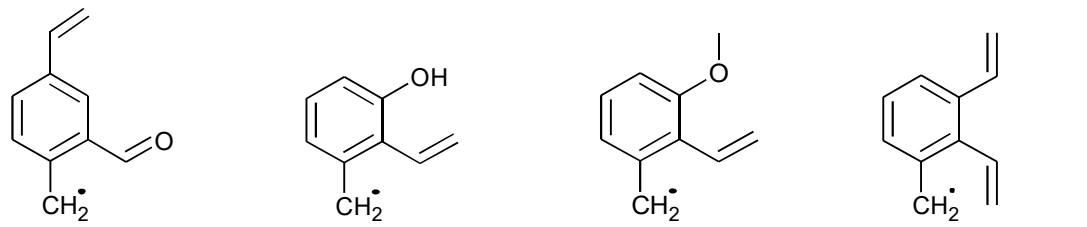

T6/35-1-CH_2•-2-CHO-4-$CH=CH_2$ **T6/36**-1-CH_2•-2-$CH=CH_2$-3-OH **T6/37**-1-CH_2•-2-$CH=CH_2$-3-OCH_3 **T6/38**-1-CH_2•-2,3-$CH=CH_2$

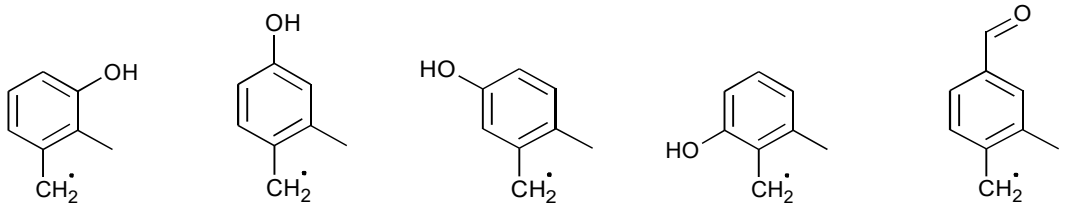

T6/39-1-CH_2•-2-CH_3-3-OH **T6/40**-1-CH_2•-2-CH_3-4-OH **T6/41**-1-CH_2•-2-CH_3-5-OH **T6/42**-1-CH_2•-2-CH_3-6-OH **T6/43**-1-CH_2•-2-CH_3-4-CHO

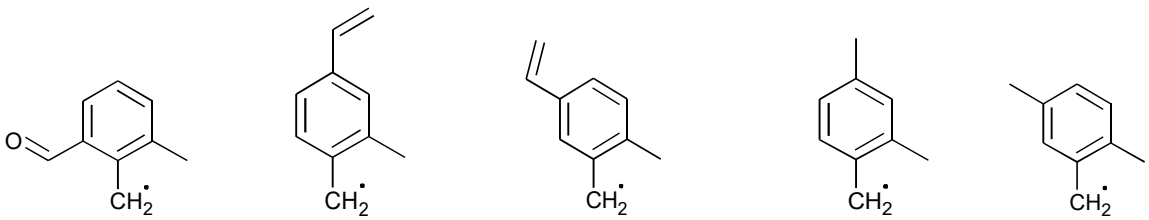

T6/44-1-CH_2•-2-CH_3-6-CHO **T6/45**-1-CH_2•-2-CH_3-4-$CH=CH_2$ **T6/46**-1-CH_2•-2-CH_3-5-$CH=CH_2$ **T6/47**-1-CH_2•-2,4-CH_3 **T6/48**-1-CH_2•-2,5-CH_3

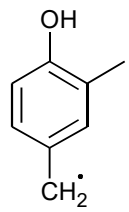

T6/49-1-CH_2•-3-CH_3-4-OH

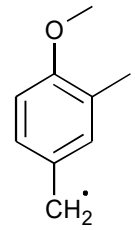

T6/50-1-CH_2•-3-CH_3-4-OCH_3

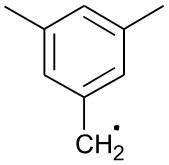

T6/51-1-CH_2•-3,5-CH_3

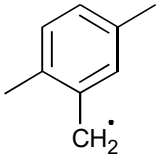

T6/52-1-CH_2•-3,6-CH_3

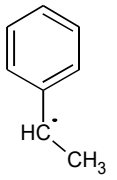

T6/53-C_6H_5CH•CH_3

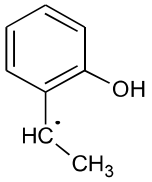

T6/54-o-(OH)C_6H_4CH•CH_3

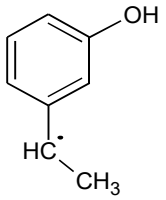

T6/55-m-(OH)C_6H_4CH•CH_3

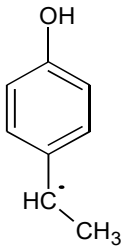

T6/56-p-(OH)C_6H_4CH•CH_3

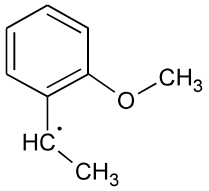

T6/57-o-(OCH_3)C_6H_4CH•C

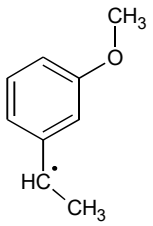

T6/58-m-(OCH_3)C_6H_4CH•CH_3

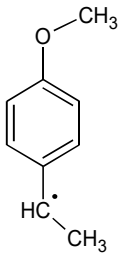

T6/59-p-(OCH_3)C_6H_4CH•CH_3

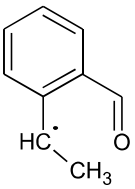

T6/60-o-(CHO)C_6H_4CH•CH_3

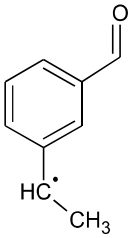

T6/61-m-(CHO)C_6H_4CH•CH_3

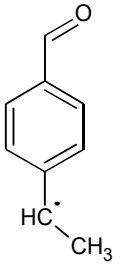

T6/62-p-(CHO)C_6H_4CH•CH_3

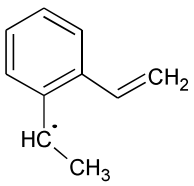

T6/63-o-($CH=CH_2$)C_6H_4CH•CH_3

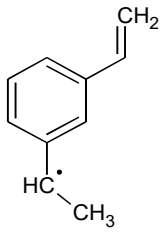

T6/64-m-($CH=CH_2$)C_6H_4CH•CH_3

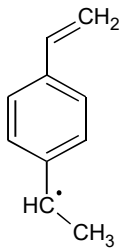

T6/65-p-($CH=CH_2$)C_6H_4CH•CH_3

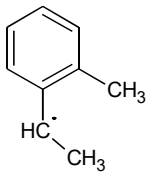

T6/66-o-(CH_3)C_6H_4CH•CH_3

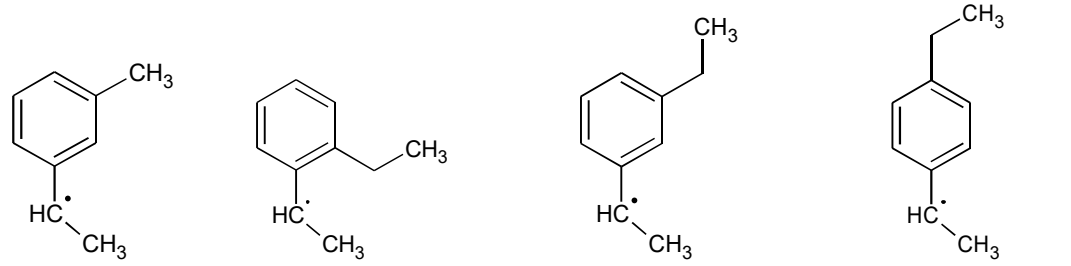

T6/67-m-$(CH_3)C_6H_4CH•CH_3$ **T6/68**-o-$(CH_2CH_3)C_6H_4CH•CH_3$ **T6/69**-m-$(CH_2CH_3)C_6H_4CH•CH_3$ **T6/70**-p-$(CH_2CH_3)C_6H_4CH•CH_3$

Figure B-7 List of radicals in benzyl subset of the training set.

B.2.2 Validation Set

Validation set encompases 53 MARs. This set of MARs include 2 phenyls (C_6H_5•), 12 phenoxies (C_6H_5O•), 5 anisyls ($C_6H_5OCH_2$•), 9 benzoyls (C_6H_5C•=O), 7 β-trans-styrlys (t-C_6H_5CH=CH•), 8 β-cis-styrlys (c-C_6H_5CH=CH•), 9 benzyls ($C_6H_5CH_2$•) and 1 α-methylbenzyl (C_6H_5CH•CH_3). Similar to the training set, these radicals are grouped into six subsets; namely phenyl, phenoxy, anisyl, benzoyl, styryl and benzyl subsets. In the following subsections, six subsets of the validation set is given.

Numbering of the MARs are exactly the same as in the training set, except that the notation starts with "**V**" instead of "**T**". As an example, the 3rd radical in the phenoxy subset of the training set (2-hydroxy-3-vinylphenoxy) is numbered as "**V2/3".**

I. ***Phenyl Subset***

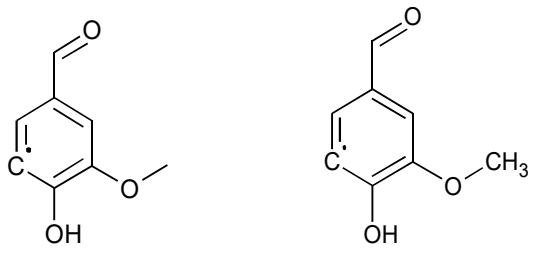

V1/1-1-C•-2-OH-3-CHO-5-OCH_3 **V1/2**-1-C•-2-CHO-5-OH-6-OCH_3

Figure B-8 List of radicals in phenyl subset of the test set.

II. ***Anisyl Subset***

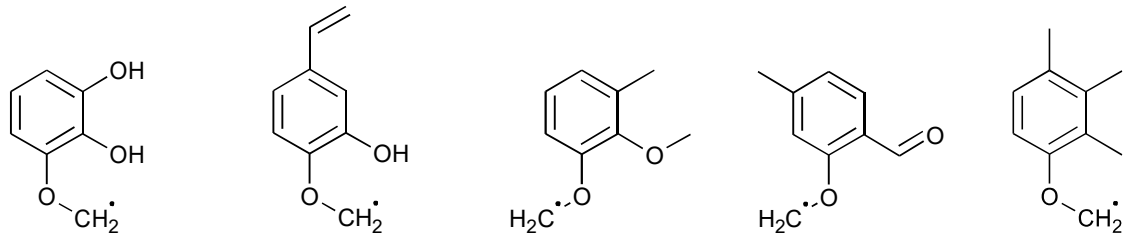

V2/1-1-OCH_2•-2,3-OH **V2/2**-1-OCH_2•-2-OH-4-$CH=CH_2$ **V2/3**-1-OCH_2•-2-OCH_3-3-CH_3 **V2/4**-1-OCH_2•-2-CHO-5-CH_3 **V2/5**-1-OCH_2•-2,3,4-CH_3

Figure B-9 List of radicals in anisyl subset of the test set.

III. ***Phenoxy Subset***

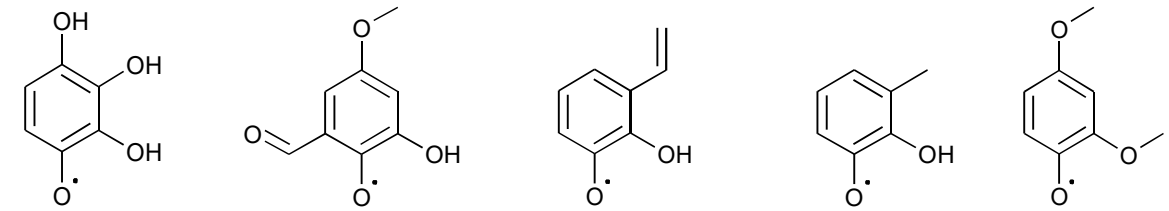

V3/1-1-O•-2,3,4-OH **V3/2**-1-O•-2-OH-4-OCH_3-6-CHO **V3/3**-1-O•-2-OH-3-$CH=CH_2$ **V3/4**-1-O•-2-OH-3-CH_3 **V3/5**-1-O•-2,4-OCH_3

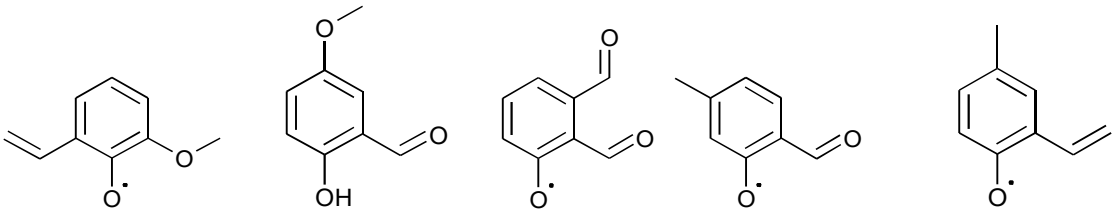

V3/6-1-O•-2-OCH_3-6-$CH=CH_2$ **V3/7**-1-O•-2-CHO-4-OCH_3 **V3/8**-1-O•-2,3-CHO **V3/9**-1-O•-2-CHO-5-CH_3 **V3/10**-1-O•-2-$CH=CH_2$-4-CH_3

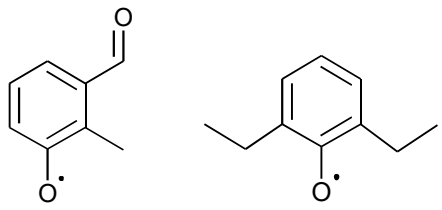

V3/11-1-O•-2-CH_3-3-CHO **V3/12**-1-O•-2,6-CH_2CH_3

Figure B-10 List of radicals in phenoxy subset of the test set.

IV. ***Benzoyl Subset***

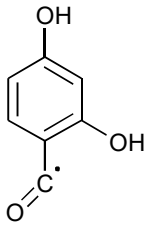

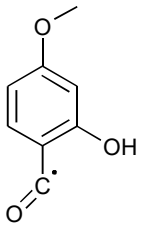

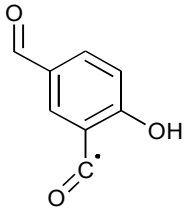

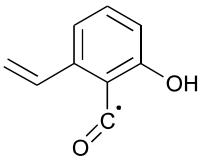

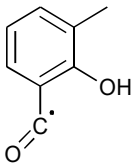

V4/1-1-C•=O-2,4-OH **V4/2**-1-C•=O-2-OH-4-OCH_3 **V4/3**-1-C•=O-2-OH-5-CHO **V4/4**-1-C•=O-2-OH-6-$CH=CH_2$ **V4/5**-1-C•=O-2-OH-3-CH_3

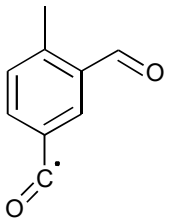

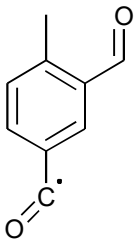

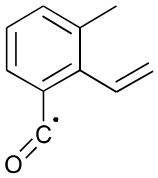

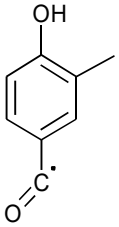

V4/6-1-C•=O-3-CHO-4-CH_3 **V4/7**-1-C•=O-3-CHO-4-CH_3 **V4/8**-1-C•=O-2-$CH=CH_2$-3-CH_3 **V4/9**-1-C•=O-3-CH_3-4-OH

Figure B-11 List of radicals in benzoyl subset of the test set.

V. *β-Styryl Subset*

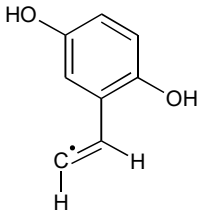

V5/1-1-(t-CH=CH•)-2,5-OH

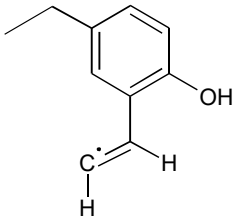

V5/2-1-(t-CH=CH•)-2-OH-5-CH_2CH_3

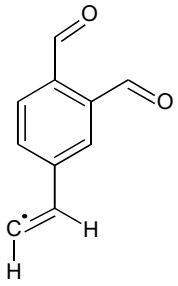

V5/3-1-(t-CH=CH•)-3,4-CHO

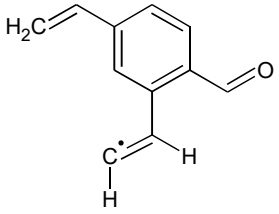

V5/4-1-(t-CH=CH•)-2-CHO-5-$CH=CH_2$

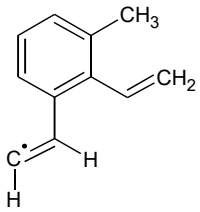

V5/5-1-(t-CH=CH•)-2-$CH=CH_2$-3-CH_3

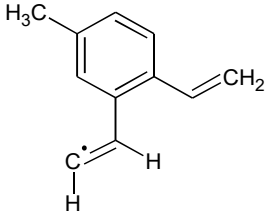

V5/6-1-(t-CH=CH•)-2-$CH=CH_2$-5-CH_3

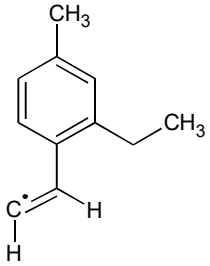

V5/7-1-(t-CH=CH•)-2-CH_2CH_3-4-CH_3

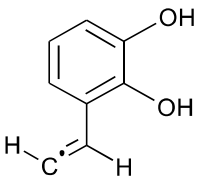

V5/8-1-(c-CH=CH•)-2,3-OH

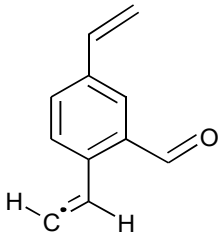

V5/9-1-(c-CH=CH•)-2-CHO-4-CH=CH

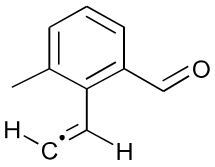

V5/10-1-(c-CH=CH•)-2-CHO-6-CH_3

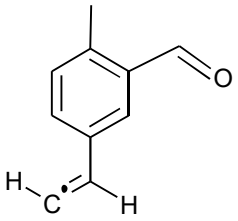

V5/11-1-(c-CH=CH•)-3-CHO-4-CH_3

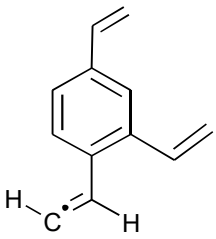

V5/12-1-(c-CH=CH•)-2,4-$CH=CH_2$

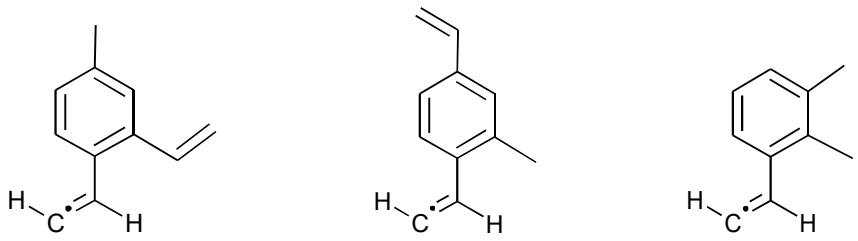

V5/13-1-(c-CH=CH•)-2-CH=CH_2-4-CH_3 **V5/14**-1-(c-CH=CH•)-2-CH_3-4-CH=CH_2 **V5/15**-1-(c-CH=CH•)-2,3-CH_3

Figure B-12 List of radicals in β-styryl subset of the test set.

VI. *Benzyl/1-Phenylethyl Subset*

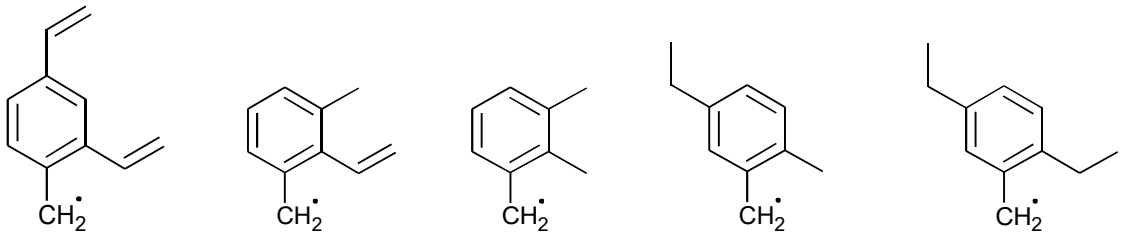

V6/1-1-CH_2•-2,4-$CH=CH_2$ **V6/2**-1-CH_2•-2-$CH=CH_2$-3-CH_3 **V6/3**-1-CH_2•-2,3-CH_3 **V6/4**-1-CH_2•-2-CH_3-5-CH_2CH_3 **V6/5**-1-CH_2•-2,5-CH_2CH_3

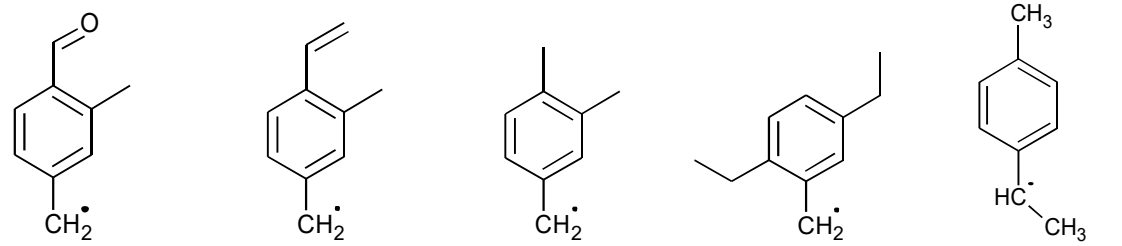

V6/6-1-CH_2•-3-CH_3-4-CHO **V6/7**-1-CH_2•-3-CH_3-4-$CH=CH_2$ **V6/8**-1-CH_2•-3,4-CH_3 **V6/9**-1-CH_2•-3,6-CH_2CH_3 **V6/10**-p-$(CH_3)C_6H_4CH$•CH_3

Figure B-13 List of radicals in benzyl subset of the test set.

B.2.3 Special Cases Set

In the special cases set, there are 20 radicals which are excluded from the training set.

α-styryls can be obtained via hydrogen abstraction from the α-carbon on the vinyl substituent and these radicals prefer an allenic conformation as shown in **Figure B-14** (no. **S1/1** to **S1/19**). "C•C_5H_5=CH_2" refers to α-styryl and double substituted α-styryls are given as (X)C•C_5H_5=CH_2, respectively where X=-OH,-OCH_3,-CHO, -CH=CH_2,-CH_3 or -CH_2CH_3. For instance, *ortho* hydroxy substituted α-styryl (**S1/2**) is abbreviated as *o*-(OH)C•C_5H_5=CH_2.

Similarly, the G4 based optimized structure of the o-formylbenzoyl radical (no. **S2/1**) is different than the expected structure where carbonyl group and the formyl group forms a five-membered ring.

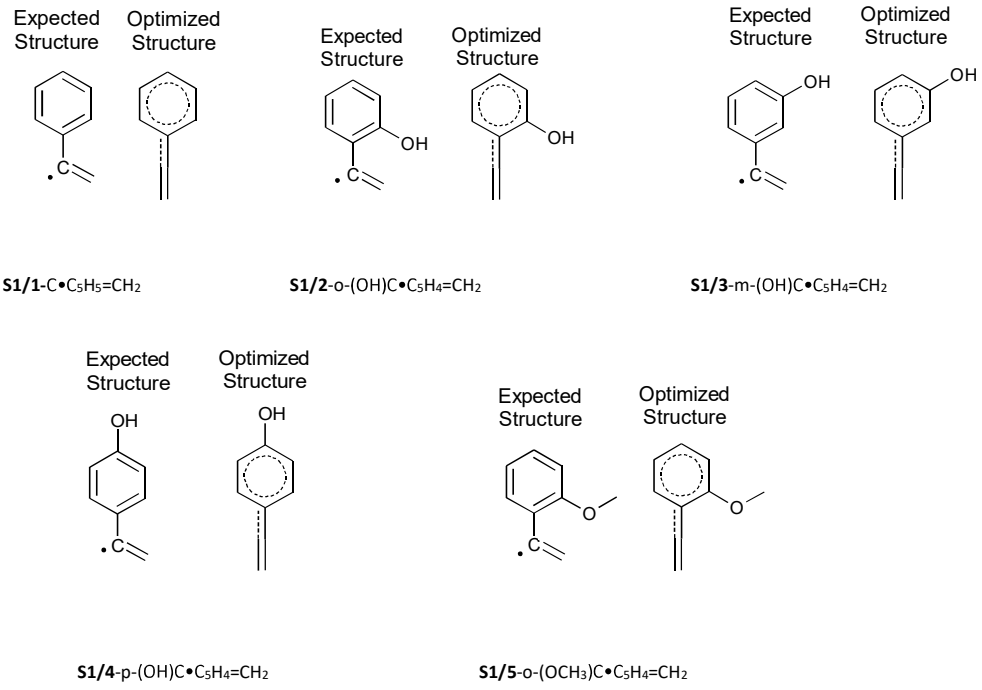

S1/1-C•C_5H_5=CH_2 **S1/2**-o-(OH)C•C_5H_4=CH_2 **S1/3**-m-(OH)C•C_5H_4=CH_2

S1/4-p-(OH)C•C_5H_4=CH_2 **S1/5**-o-(OCH_3)C•C_5H_4=CH_2

Expected Structure Optimized Structure

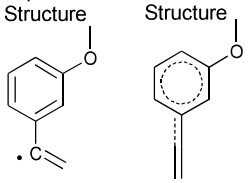

S1/6-m-$(OCH_3)C\bullet C_5H_4{=}CH_2$

Expected Structure Optimized Structure

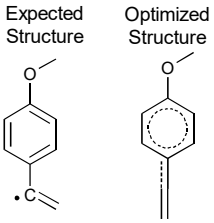

S1/7-p-$(OCH_3)C\bullet C_5H_4{=}CH_2$

Expected Structure Optimized Structure

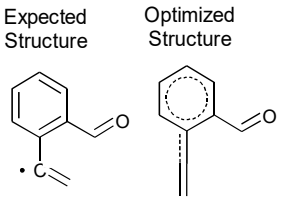

S1/8-o-$(CHO)C\bullet C_5H_4{=}CH_2$

Expected Structure Optimized Structure

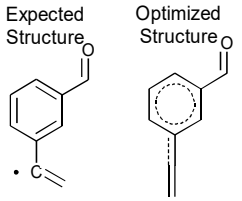

S1/9-m-$(CHO)C\bullet C_5H_4{=}CH_2$

Expected Structure Optimized Structure

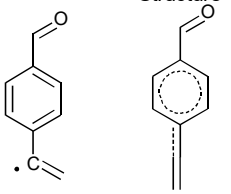

S1/10-p-$(CHO)C\bullet C_5H_4{=}CH_2$

Expected Structure Optimized Structure

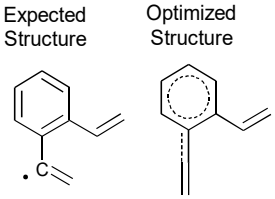

S1/11-o-$(CH{=}CH_2)C\bullet C_5H_4{=}CH_2$

Expected Structure Optimized Structure

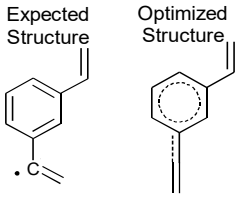

S1/12-m-$(CH{=}CH_2)C\bullet C_5H_4{=}CH_2$

Expected Structure Optimized Structure

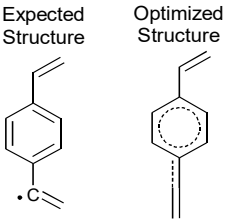

S1/13-p-$(CH{=}CH_2)C\bullet C_5H_4{=}CH_2$

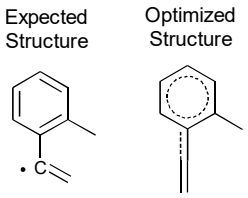

S1/14-o-$(CH_3)C\bullet C_5H_4=CH_2$

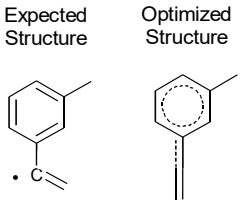

S1/15-m-$(CH_3)C\bullet C_5H_4=CH_2$

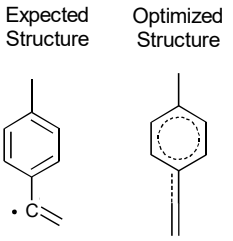

S1/16-p-$(CH_3)C\bullet C_5H_4=CH_2$

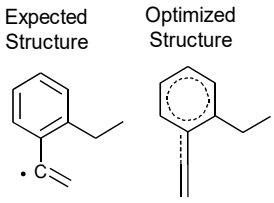

S1/17-o-$(CH_2CH_3)C\bullet C_5H_4=CH_2$

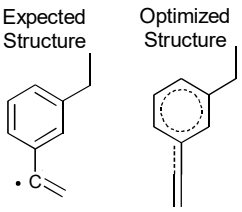

S1/18-m-$(CH_2CH_3)C\bullet C_5H_4=CH_2$

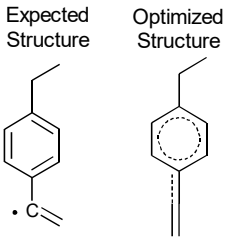

S1/19-p-$(CH_2CH_3)C\bullet C_5H_4=CH_2$

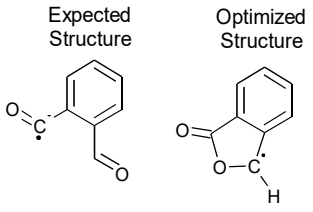

S2/1-1(3H)-Isobenzofuranonyl

Figure B-14 List of radicals in special cases set.

B.3 Thermochemical Database

B.3.1 Thermochemical Database Used in The Training Set

All the thermochemical data obtained used for the derivation of GAVs are NNIs are given in **Table B-1** respectively. In these two tables, raw standard enthalpy of formation data ($\Delta_f H^\circ$), BAC-corrected standard enthalpy of formation values ($\Delta_f H^\circ + BAC$), molecular entropy data (S°) intrinsic entropy values (S°_{int}) are given at 298 K whereas C_p values are given at 300 K, 400 K, 500 K, 600 K, 800 K, 1000 K and 1500 K. $\Delta_f H^\circ$values are given in kJ mol^{-1} and S°_{int} and C_p values in J mol^{-1} K^{-1}. Total symmetry number (σ_{sym}) and number of optical isomers (n_{opt}) which are important in calculation of intrinsic entropy values from molecular entropy data is also provided. The numbering of the molecules is consistent with the list of molecules given in **Figure B-1**.

Table B-1 Thermochemical database used as the training set for development of Group Additive Values (GAVs) and non-nearest neighbor interactions (NNIs). The units of standard enthalpy of formation ($\Delta_f H^\circ$) data is given in kJ mol^{-1} whereas the units of entropies (S°) and heat capacities (C_p) are given in J mol^{-1} K^{-1}.

#	Training set for GAV and NNI	$\Delta_f H^\circ$ (298 K)		S° (298 K)				C_p						
		$\Delta_f H^\circ_{G4}$	$\Delta_f H^\circ_{G4/BAC}$	S°	S°_{int}	$\sigma_{tot°sym}$	n_{opt}	300 K	400 K	500 K	600 K	800 K	1000 K	1500 K
Subset 1: Phenyl Subset														
T1/1	C_6H_5•	338.7	337.7	288.5	294.2	2	1	80.1	107.8	131.0	149.6	176.5	194.9	221.9
T1/2	*o*-OHC_6H_4•	167.3	162.7	319.9	319.9	1	1	104.0	134.0	157.7	176.0	201.4	218.5	243.5
T1/3	*m*-OHC_6H_4•	163.3	158.7	324.5	324.5	1	1	101.1	130.5	154.4	172.9	199.1	216.8	242.7
T1/4	*p*-OHC_6H_4•	169.6	165.0	319.1	324.8	2	1	101.2	130.4	154.0	172.4	198.7	216.4	242.4
T1/5	*o*-$MeOC_6H_4$•	183.0	179.2	355.1	364.2	3	1	123.2	158.6	188.2	211.7	245.4	268.5	302.7
T1/6	*m*-$MeOC_6H_4$•	181.6	177.8	357.5	366.6	3	1	122.4	156.7	185.4	208.4	242.4	266.2	301.5
T1/7	*p*-$MeOC_6H_4$•	188.2	184.4	352.5	367.4	6	1	122.3	156.3	184.7	207.7	241.8	265.7	301.3
T1/8	*o*-$CHOC_6H_4$•	221.7	222.7	340.3	340.3	1	1	112.0	143.1	169.0	189.9	220.3	240.8	269.4
T1/9	*m*-$CHOC_6H_4$•	219.8	220.8	343.1	343.1	1	1	108.5	139.6	166.0	187.4	218.7	239.8	269.2
T1/10	*p*-$CHOC_6H_4$•	218.5	219.5	337.2	342.9	2	1	108.3	139.5	165.9	187.3	218.5	239.7	269.3
T1/11	*o*-$CH{=}CH_2C_6H_4$•	405.4	405.9	351.6	351.6	1	1	120.2	155.6	185.8	210.1	245.6	269.9	305.6
T1/12	*m*-$CH{=}CH_2C_6H_4$•	406.5	407.0	352.9	352.9	1	1	117.2	153.7	184.3	208.9	244.6	269.1	305.1
T1/13	*p*-$CH{=}CH_2C_6H_4$•	407.7	408.2	347.1	352.9	2	1	117.1	153.5	184.1	208.7	244.4	269.0	305.0
T1/14	*o*-$CH_3C_6H_4$•	302.9	303.4	331.3	340.4	3	1	101.5	134.2	162.4	185.6	220.1	244.3	280.2
T1/15	*m*-$CH_3C_6H_4$•	303.0	303.5	330.8	340.0	3	1	101.6	134.3	162.6	185.8	220.3	244.5	280.3
T1/16	*p*-$CH_3C_6H_4$•	305.2	305.7	325.0	339.9	6	1	101.6	134.2	162.5	185.6	220.2	244.4	280.3
T1/17	*o*-$CH_2CH_3C_6H_4$•	281.6	281.0	366.2	381.1	6	1	124.7	163.6	197.3	225.0	266.5	295.8	339.7
T1/18	*m*-$CH_2CH_3C_6H_4$•	281.8	281.2	371.0	380.2	3	1	126.2	164.5	198.0	225.5	266.8	296.0	339.8
T1/19	*p*-$CH_2CH_3C_6H_4$•	284.0	283.4	364.7	379.6	6	1	126.6	164.8	198.2	225.6	266.9	296.1	339.9
T1/20	1-C•-3-OH-4-OCH_3	7.9	0.6	380.3	389.4	3	1	141.2	176.7	207.6	233.0	270.0	294.4	328.0

T1/21	1-C•-3-OH-4-CHO	22.0	19.5	350.2	350.2	1	1	121.9	155.6	185.5	208.0	241.6	265.7	302.4
T1/22	1-C•-2-CH_3-4-OH	132.8	129.7	361.8	371.0	3	1	122.7	156.8	185.5	208.5	242.3	265.8	300.8
T1/23	1-C•-2-OCH_3-3-OH-6-CHO	-120.6	-125.9	424.7	433.8	3	1	171.2	212.2	246.8	275.0	316.1	343.1	378.9
Subset 2: Anisyl Subset														
T2/1	$C_6H_5OCH_2$•	116.3	109.9	364.0	369.7	2	1	122.2	157.6	186.9	210.2	244.1	267.4	302.1
T2/2	*o*-$OHC_6H_4OCH_2$•	-59.3	-69.3	385.5	391.2	2	1	145.1	182.3	213.4	238.1	272.6	295.0	326.6
T2/3	*m*-$OHC_6H_4OCH_2$•	-59.5	-69.5	393.0	398.8	2	1	144.2	181.1	210.9	234.1	267.2	289.7	323.1
T2/4	*p*-$OHC_6H_4OCH_2$•	-50.2	-60.2	393.8	399.5	2	1	143.8	180.1	209.5	232.6	265.8	288.6	322.5
T2/5	*o*-$OCH_3C_6H_4OCH_2$•	-25.5	-34.7	425.4	440.3	6	1	174.5	212.0	243.5	269.7	309.5	338.1	381.4
T2/6	*m*-$OCH_3C_6H_4OCH_2$•	-41.6	-50.8	423.1	438.0	6	1	164.6	206.8	241.6	269.4	310.3	339.0	381.9
T2/7	*p*-$OCH_3C_6H_4OCH_2$•	-32.3	-41.5	427.7	442.6	6	1	165.1	206.2	240.4	268.1	309.2	338.1	381.5
T2/8	*o*-$CHOC_6H_4OCH_2$•	2.3	-2.1	404.8	410.6	2	1	155.9	197.3	230.6	256.4	292.7	316.9	351.2
T2/9	*m*-$CHOC_6H_4OCH_2$•	-3.2	-7.6	418.7	418.7	1	1	153.1	191.2	223.2	249.0	286.8	312.6	349.6
T2/10	*p*-$CHOC_6H_4OCH_2$•	-8.2	-12.6	402.7	417.6	6	1	150.9	189.8	222.5	248.7	286.9	312.9	350.1
T2/11	*o*-$CH=CH_2C_6H_4OCH_2$•	180.1	175.2	416.5	422.3	2	1	163.5	207.8	244.2	273.1	314.9	343.7	386.5
T2/12	*m*-$CH=CH_2C_6H_4OCH_2$•	177.7	172.8	422.0	427.8	2	1	159.9	203.9	240.4	269.6	312.2	341.7	385.4
T2/13	*p*-$CH=CH_2C_6H_4OCH_2$•	178.4	173.5	425.6	425.6	1	1	159.8	203.9	240.6	270.0	312.6	342.1	385.7
T2/14	*o*-$CH_3C_6H_4OCH_2$•	79.7	74.8	393.7	408.6	6	1	147.9	188.5	222.8	250.4	291.1	319.5	362.0
T2/15	*m*-$CH_3C_6H_4OCH_2$•	80.1	75.2	400.4	415.3	6	1	144.0	184.3	218.5	246.4	287.8	317.0	360.6
T2/16	*p*-$CH_3C_6H_4OCH_2$•	81.7	76.8	399.1	414.0	6	1	143.4	183.7	218.0	245.9	287.5	316.8	360.5
T2/17	*o*-$CH_2CH_3C_6H_4OCH_2$•	58.1	52.1	433.7	448.6	6	1	172.5	218.9	258.4	290.5	338.1	371.7	422.0
T2/18	*m*-$CH_2CH_3C_6H_4OCH_2$•	59.2	53.2	437.6	452.5	6	1	167.7	214.0	253.6	285.9	334.2	368.5	419.9
T2/19	*p*-$CH_2CH_3C_6H_4OCH_2$•	62.2	56.2	437.5	452.4	6	1	168.5	214.5	253.9	286.1	334.3	368.5	420.0
T2/20	1-OCH_2•-3,4-OH	-229.0	-242.5	418.0	423.8	2	1	163.6	201.8	233.3	258.1	292.6	314.8	346.4
T2/21	1-OCH_2•-2-OH-6-OCH_3	-202.8	-215.5	450.7	465.6	6	1	188.4	230.8	266.7	295.9	338.2	366.3	406.5
T2/22	1-OCH_2•-2-OH-4-CHO	-181.1	-189.0	435.8	441.5	2	1	174.5	216.4	250.9	278.0	315.8	340.2	373.9
T2/23	1-OCH_2•-2-OH-5-CHO	-184.9	-192.8	442.1	442.1	1	1	175.3	215.2	249.0	276.3	315.3	340.7	375.2
T2/24	1-OCH_2•-2-OH-5-$CH=CH_2$	1.1	-7.4	443.6	449.4	2	1	182.4	227.8	266.2	297.0	340.7	369.5	410.3
T2/25	1-OCH_2•-2-OCH_3-4-OH	-195.7	-208.4	454.1	469.0	6	1	196.9	236.0	267.7	293.4	332.2	359.9	402.2
T2/26	1-OCH_2•-2-OCH_3-6-OH	-202.8	-215.5	450.7	465.6	6	1	188.4	230.8	266.7	295.9	338.2	366.3	406.5
T2/27	1-OCH_2•-2-OCH_3-4-CH_3	-60.8	-68.5	460.7	484.7	18	1	195.7	238.2	274.9	305.8	353.4	387.8	440.0
T2/28	1-OCH_2•-2-OCH_3-5-CH_3	-60.4	-68.1	466.5	484.8	9	1	196.5	238.5	275.0	305.7	353.2	387.6	439.8
T2/29	1-OCH_2•-2-CHO-3-CH_3	-27.5	-30.4	437.8	452.7	6	1	178.9	224.5	263.1	294.1	338.6	368.4	410.5
T2/30	1-OCH_2•-2-CHO-4-CH_3	-31.7	-34.6	441.6	456.5	6	1	176.8	223.3	261.8	292.3	336.4	366.5	409.8
T2/31	1-OCH_2•-2-CH_3-4-OH	-87.7	-96.2	426.3	441.2	6	1	169.9	210.5	244.4	271.7	312.0	340.1	382.3
T2/32	1-OCH_2•-3-CH_3-4-OH	-87.3	-95.8	438.2	443.9	2	1	168.1	207.8	241.4	268.8	309.4	337.9	380.9
T2/33	1-OCH_2•-2,3-CH_3	48.7	45.3	431.0	449.3	9	1	169.9	215.3	254.3	286.3	334.5	368.9	420.5
Subset 3: Phenoxy Subset														
T3/1	C_6H_5O•	59.9	54.1	309.8	315.5	2	1	95.6	125.5	150.4	170.2	198.6	217.9	245.8
T3/2	*o*-OHC_6H_4O•	-153.6	-162.9	332.6	332.6	1	1	109.7	141.7	168.1	189.1	219.1	239.4	268.7
T3/3	*m*-OHC_6H_4O•	-117.5	-126.8	341.7	341.7	1	1	120.2	151.8	176.9	196.1	223.1	241.1	267.3
T3/4	*p*-OHC_6H_4O•	-127.6	-136.9	338.2	344.0	2	1	114.5	146.3	172.4	192.9	221.8	240.9	267.9
T3/5	*o*-$OCH_3C_6H_4O$•	-102.4	-110.9	376.0	385.1	3	1	136.7	173.1	204.0	229.1	265.7	290.7	326.9
T3/6	*m*-$OCH_3C_6H_4O$•	-102.9	-111.4	374.0	383.1	3	1	140.3	179.1	210.3	234.5	268.7	292.1	326.8
T3/7	*p*-$OCH_3C_6H_4O$•	-110.3	-118.8	376.7	385.9	3	1	135.4	172.4	203.7	229.0	265.7	290.7	326.7
T3/8	*o*-$CHOC_6H_4O$•	-56.4	-60.1	364.7	364.7	1	1	124.8	158.6	187.6	211.3	245.3	267.2	295.7
T3/9	*m*-$CHOC_6H_4O$•	-56.8	-60.5	368.1	368.1	1	1	128.2	160.6	187.9	209.9	241.9	263.5	293.3
T3/10	*p*-$CHOC_6H_4O$•	-60.9	-64.6	362.0	367.7	2	1	124.1	157.5	185.5	208.1	240.8	262.8	293.3
T3/11	*o*-$CH=CH_2C_6H_4O$•	115.7	111.4	370.2	370.2	1	1	132.6	171.3	203.7	229.8	267.8	293.6	330.8
T3/12	*m*-$CH=CH_2C_6H_4O$•	124.7	120.4	373.8	373.8	1	1	133.6	171.9	204.0	229.6	266.7	292.0	329.0
T3/13	*p*-$CH=CH_2C_6H_4O$•	108.5	104.2	370.2	370.2	1	1	132.9	171.6	204.0	230.1	267.9	293.7	330.7
T3/14	*o*-$CH_3C_6H_4O$•	15.2	10.9	351.2	360.3	3	1	117.4	152.2	182.0	206.3	242.3	267.4	304.2
T3/15	*m*-$CH_3C_6H_4O$•	22.4	18.1	351.9	361.0	3	1	117.6	152.4	182.2	206.5	242.5	267.5	304.3
T3/16	*p*-$CH_3C_6H_4O$•	18.8	14.5	352.5	361.6	3	1	116.9	151.9	181.8	206.1	242.2	267.4	304.3
T3/17	*o*-$CH_2CH_3C_6H_4O$•	-5.3	-10.7	389.3	398.4	3	1	141.9	182.8	218.1	246.9	289.8	319.8	364.2
T3/18	*m*-$CH_2CH_3C_6H_4O$•	1.4	-4.0	392.1	401.2	3	1	141.5	182.2	217.3	246.0	288.8	318.9	363.6
T3/19	*p*-$CH_2CH_3C_6H_4O$•	-1.9	-7.3	392.9	402.0	3	1	141.1	181.7	216.8	245.6	288.5	318.7	363.6
T3/20	1-O•-2,3-OH	-326.8	-339.7	357.1	357.1	1	1	131.5	167.0	195.6	217.4	246.9	265.5	291.8
T3/21	1-O•-3,4-OH	-312.1	-325.0	361.6	361.6	1	1	134.7	169.3	197.8	220.2	251.3	270.5	294.9
T3/22	1-O•-2-OH-4-OCH_3	-325.4	-337.5	391.6	400.8	3	1	153.4	191.8	224.0	249.9	287.4	313.0	349.9
T3/23	1-O•-2-OH-6-OCH_3	-307.6	-319.7	397.5	406.6	3	1	150.0	188.3	220.7	246.8	284.9	310.9	348.7
T3/24	1-O•-2-OH-3-CHO	-269.0	-276.3	381.0	381.0	1	1	140.4	177.1	207.3	231.2	265.0	287.1	317.3
T3/25	1-O•-2-OH-4-CHO	-274.5	-281.8	382.6	382.6	1	1	139.8	174.6	203.8	227.4	261.6	284.5	316.4
T3/26	1-O•-2-OH-6-CHO	-268.4	-275.7	381.2	381.2	1	1	139.2	175.6	206.3	230.9	265.7	288.1	318.0
T3/27	1-O•-2-OH-4-$CH=CH_2$	-102.1	-109.9	387.9	387.9	1	1	147.2	188.0	221.9	249.1	288.4	315.1	353.3
T3/28	1-O•-2-OH-5-$CH=CH_2$	-89.1	-96.9	389.4	389.4	1	1	148.6	188.6	222.0	248.8	287.5	313.9	352.2
T3/29	1-O•-2-OH-6-$CH=CH_2$	-95.0	-102.8	384.8	384.8	1	1	147.1	187.8	221.7	249.0	288.4	315.2	353.5

T3/30	1-O•-2-OH-4-CH_3	-194.8	-202.6	369.1	378.3	3	1	131.3	168.3	199.7	225.2	262.9	289.0	327.2
T3/31	1-O•-2-OH-5-CH_3	-191.3	-199.1	368.8	377.9	3	1	132.1	168.8	200.0	225.4	263.0	289.0	327.3
T3/32	1-O•-2-OH-6-CH_3	-197.4	-205.2	368.2	377.4	3	1	132.1	168.8	200.0	225.4	263.0	289.0	327.2
T3/33	1-O•-2-OCH_3-3-OH	-280.2	-292.3	399.7	408.8	3	1	153.2	191.7	225.0	252.3	291.8	317.7	352.9
T3/34	1-O•-3-OCH_3-4-OH	-298.9	-311.0	394.5	403.6	3	1	153.1	198.0	233.0	259.0	291.7	318.4	355.0
T3/35	1-O•-2,3-OCH_3	-271.2	-282.5	433.5	451.8	9	1	180.2	223.3	260.2	290.1	333.9	363.9	407.5
T3/36	1-O•-2,6-OCH_3	-269.1	-280.4	439.9	458.2	9	1	179.7	222.3	259.0	288.9	332.9	363.2	407.4
T3/37	1-O•-3,4-OCH_3	-262.1	-273.4	435.6	453.8	9	1	185.4	224.0	260.0	288.0	336.7	364.7	407.0
T3/38	1-O•-2-OCH_3-3-CHO	-216.8	-223.3	425.6	434.7	3	1	165.3	206.2	241.5	270.3	312.5	340.6	378.1
T3/39	1-O•-2-OCH_3-4-CHO	-225.4	-231.9	429.1	438.3	3	1	168.2	206.9	240.3	267.9	308.6	336.3	374.8
T3/40	1-O•-2-OCH_3-6-CHO	-218.5	-225.0	422.9	432.0	3	1	165.8	206.0	241.2	270.1	312.3	340.0	376.8
T3/41	1-O•-2-OCH_3-3-$CH{=}CH_2$	-35.4	-42.4	432.4	441.5	3	1	171.8	216.8	255.5	287.3	334.2	366.3	412.1
T3/42	1-O•-2-OCH_3-4-$CH{=}CH_2$	-49.6	-56.6	433.9	443.0	3	1	174.5	218.8	257.0	288.1	334.0	365.5	410.8
T3/43	1-O•-2-OCH_3-3-CH_3	-140.3	-147.3	413.7	431.9	9	1	158.2	198.7	234.5	264.5	310.2	342.3	388.2
T3/44	1-O•-2-OCH_3-4-CH_3	-142.7	-149.7	412.1	430.3	9	1	158.2	199.6	235.5	265.1	309.4	340.2	385.3
T3/45	1-O•-2-OCH_3-5-CH_3	-139.8	-146.8	411.4	429.7	9	1	159.1	200.3	236.1	265.7	309.8	340.6	385.5
T3/46	1-O•-3-OCH_3-4-CHO	-219.3	-225.8	416.3	425.4	3	1	165.3	208.3	245.1	274.7	316.4	343.2	378.6
T3/47	1-O•-3-OCH_3-6-CHO	-223.0	-229.5	416.4	425.6	3	1	168.3	211.0	246.6	275.1	315.7	342.2	377.7
T3/48	1-O•-2-CHO-4-OH	-247.5	-254.8	385.8	385.8	1	1	144.4	179.5	209.0	233.1	268.1	290.8	319.6
T3/49	1-O•-2-CHO-5-OH	-236.3	-243.6	387.6	387.6	1	1	148.0	183.5	212.9	236.4	269.7	290.8	318.0
T3/50	1-O•-2-CHO-6-OH	-268.5	-275.8	381.4	381.4	1	1	139.1	175.4	206.0	230.6	265.5	288.1	318.1
T3/51	1-O•-2-CHO-5-OCH_3	-222.9	-229.4	422.2	431.3	3	1	168.5	211.1	246.7	275.1	315.7	342.2	377.7
T3/52	1-O•-3-CHO-4-OH	-272.1	-279.4	370.8	370.8	1	1	136.3	172.2	202.0	225.9	260.4	283.6	316.2
T3/53	1-O•-3-CHO-4-OCH_3	-216.0	-222.5	428.7	437.8	3	1	170.4	210.5	245.2	273.6	314.3	340.6	375.9
T3/54	1-O•-3-CHO-6-OCH_3	-224.2	-230.7	425.0	434.1	3	1	170.4	209.2	242.3	269.5	309.8	337.1	375.2
T3/55	1-O•-2,4-CHO	-174.0	-175.7	411.8	411.8	1	1	155.8	192.3	224.1	250.2	288.2	312.6	343.1
T3/56	1-O•-2,5-CHO	-169.5	-171.2	415.2	415.2	1	1	157.1	193.6	225.3	251.3	288.8	312.7	342.8
T3/57	1-O•-3,4-CHO	-164.1	-165.8	412.7	418.5	2	1	161.7	199.6	231.0	256.0	291.1	313.2	341.5
T3/58	1-O•-2-CHO-3-$CH{=}CH_2$	19.1	16.9	417.8	417.8	1	1	160.3	203.8	241.1	271.5	315.3	343.6	380.6
T3/59	1-O•-2-CHO-5-$CH{=}CH_2$	7.7	5.5	420.6	420.6	1	1	162.5	204.7	241.0	270.5	313.3	341.5	379.2
T3/60	1-O•-2-CHO-3-CH_3	-87.8	-90.0	395.0	404.1	3	1	148.4	186.3	219.5	247.3	288.9	317.0	354.8
T3/61	1-O•-2-CHO-4-CH_3	-99.8	-102.0	399.5	408.6	3	1	145.7	184.5	218.6	246.8	288.7	316.7	354.5
T3/62	1-O•-2-CHO-5-CH_3	-95.6	-97.8	398.1	407.3	3	1	146.3	185.1	219.1	247.3	289.0	316.8	354.4
T3/63	1-O•-2-CHO-6-CH_3	-101.9	-104.1	400.1	409.2	3	1	146.5	185.2	219.2	247.4	288.9	316.6	354.1
T3/64	1-O•-2-CH=CH_2-5-CH_3	77.0	74.2	405.3	414.4	3	1	155.3	198.6	235.8	266.3	311.8	343.4	389.5
T3/65	1-O•-2-CH=CH_2-6-CH_3	72.2	69.4	409.6	418.7	3	1	155.8	198.9	236.2	266.7	312.1	343.6	389.5
T3/66	1-O•-2-CH_3-4-CHO	-107.2	-109.4	403.9	413.1	3	1	146.3	184.3	217.2	244.3	284.6	312.3	351.8
T3/67	1-O•-2,6-CH_3	-29.0	-31.8	386.4	404.7	9	1	139.7	179.1	213.8	242.6	286.1	316.9	362.7
T3/68	1-O•-2-CH_2CH_3-4-CHO	-127.9	-131.3	442.5	451.7	3	1	170.3	214.6	253.0	284.6	331.8	364.5	411.5
Subset 4: Benzoyl Subset														
T4/1	C_6H_5C•=O	119.8	118.2	340.0	345.7	2	1	109.5	140.9	167.0	187.8	217.5	237.5	266.1
T4/2	*o*-OHC_6H_5C•=O	-69.7	-74.8	355.3	355.3	1	1	130.0	164.9	193.6	216.5	249.4	270.5	297.0
T4/3	*m*-OHC_6H_5C•=O	-54.7	-59.8	373.9	373.9	1	1	132.7	165.1	191.5	212.0	240.8	259.9	287.2
T4/4	*p*-OHC_6H_5C•=O	-61.8	-66.9	371.5	371.5	1	1	128.7	162.2	189.7	211.3	241.7	261.5	288.9
T4/5	*o*-$OCH_3C_6H_5$ C•=O	-29.3	-33.7	411.3	420.4	3	1	156.0	191.7	221.8	246.2	282.5	307.8	345.1
T4/6	*m*-$OCH_3C_6H_5$ C•=O	-37.0	-41.4	407.3	416.4	3	1	154.9	192.4	223.6	248.6	284.9	309.8	346.3
T4/7	*p*-$OCH_3C_6H_5$ C•=O	-41.6	-46.0	406.0	415.1	3	1	149.9	188.6	221.4	247.7	285.7	311.2	347.7
T4/8	*m*-$CHOC_6H_5$ C•=O	1.3	1.8	398.8	398.8	1	1	139.3	173.6	202.6	225.9	259.8	282.3	313.4
T4/9	*p*-$CHOC_6H_5$ C•=O	2.3	2.8	406.6	406.6	1	1	139.8	172.6	200.6	223.5	257.3	280.2	311.9
T4/10	*o*-$CH{=}CH_2C_6H_5C$•=O	190.4	190.3	395.8	395.8	1	1	149.7	190.5	224.3	251.0	288.8	314.1	350.5
T4/11	*m*-$CH{=}CH_2C_6H_5C$•=O	182.2	182.1	404.6	404.6	1	1	146.7	186.8	220.3	247.0	285.5	311.6	349.3
T4/12	*p*-$CH{=}CH_2C_6H_5C$•=O	188.7	188.6	403.7	403.7	1	1	146.7	186.9	220.5	247.2	285.7	311.8	349.5
T4/13	*o*-$CH_3C_6H_5C$•=O	85.3	85.2	377.8	387.0	3	1	133.0	168.8	199.5	224.5	261.4	287.0	324.5
T4/14	*m*-$CH_3C_6H_5C$•=O	83.0	82.9	382.3	391.4	3	1	131.1	167.5	198.6	223.9	261.2	287.0	324.6
T4/15	*p*-$CH_3C_6H_5C$•=O	81.9	81.8	380.7	389.8	3	1	130.9	167.4	198.7	224.1	261.6	287.4	324.9
T4/16	*o*-$CH_2CH_3C_6H_5C$•=O	63.1	61.9	419.0	428.2	3	1	158.0	200.2	236.3	265.8	309.4	339.8	384.6
T4/17	*m*-$CH_2CH_3C_6H_5C$•=O	61.7	60.5	423.1	432.2	3	1	155.7	197.7	234.0	263.7	307.8	338.5	383.9
T4/18	*p*-$CH_2CH_3C_6H_5C$•=O	60.7	59.5	420.1	429.2	3	1	155.4	197.5	233.9	263.7	308.0	338.8	384.2
T4/19	1-C•=O -2,3-OH	-251.2	-259.9	376.0	376.0	1	1	146.5	184.0	214.4	238.1	271.0	291.5	318.2
T4/20	1-C•=O -2,5-OH	-235.4	-244.1	384.4	384.4	1	1	151.4	185.9	213.5	235.5	267.9	289.9	318.6
T4/21	1-C•=O -3,4-OH	-238.8	-247.5	390.1	390.1	1	1	151.4	187.4	216.7	239.5	270.6	289.6	314.1
T4/22	1-C•=O -3-OH-4-OCH_3	-219.8	-227.7	425.0	434.1	3	1	170.9	213.0	248.2	276.1	315.0	339.7	373.2
T4/23	1-C•=O -3-OH-6-OCH_3	-196.9	-204.8	441.4	450.5	3	1	180.9	215.9	245.1	268.9	304.1	328.7	365.4
T4/24	1-C•=O -2-OH-3-CHO	-188.7	-191.8	402.5	402.5	1	1	156.9	196.0	227.9	253.1	288.7	311.7	342.2
T4/25	1-C•=O -3-OH-4-$CH{=}CH_2$	9.4	5.8	429.5	429.5	1	1	167.8	209.0	243.2	270.1	308.4	334.0	370.7
T4/26	1-C•=O -2-OH-4-CH_3	-112.8	-116.4	388.1	397.2	3	1	145.1	183.9	216.7	243.4	282.9	310.2	350.2
T4/27	1-C•=O -2-OH-5-CH_3	-104.0	-107.6	391.8	400.9	3	1	151.4	191.1	224.7	252.3	293.0	319.9	355.5
T4/28	1-C•=O -2-OH-6-CH_3	-109.0	-112.6	391.5	400.6	3	1	149.1	187.7	220.1	246.4	285.3	312.3	351.2

T4/29	1-C•=O -2-OCH_3-4-OH	-213.4	-221.3	432.1	441.2	3	1	177.9	215.9	247.1	272.1	308.3	332.8	368.2
T4/30	1-C•=O -3-OCH_3-4-OH	-223.0	-230.9	424.0	433.1	3	1	170.7	210.8	244.9	272.8	313.4	340.1	375.6
T4/31	1-C•=O -2-OCH_3-3-CH_3	-59.7	-62.6	443.6	461.9	9	1	177.9	221.2	258.5	288.8	333.1	363.3	407.3
T4/32	1-C•=O -2-OCH_3-5-CH_3	-63.9	-66.8	448.0	466.3	9	1	177.0	217.7	252.8	281.9	326.0	357.1	403.6
T4/33	1-C•=O -2-OCH_3-6-CH_3	-62.0	-64.9	441.1	459.4	9	1	183.3	223.2	256.6	284.2	326.6	357.2	403.3
T4/34	1-C•=O -3-CHO-4-OH	-209.0	-212.1	401.5	401.5	1	1	151.5	188.5	219.6	244.7	281.5	306.4	342.2
T4/35	1-C•=O -2-CH=CH_2-4-CH_3	151.3	152.7	430.6	439.7	3	1	171.3	217.2	256.2	287.5	333.0	364.0	409.2
T4/36	1-C•=O -2-CH=CH_2-5-CH_3	147.6	149.0	431.5	440.7	3	1	171.9	217.6	256.4	287.5	332.7	363.7	409.0
T4/37	1-C•=O -2-CH=CH_2-6-CH_3	154.1	155.5	430.7	439.8	3	1	178.7	221.6	257.7	287.0	330.8	361.6	407.6
T4/38	1-C•=O -2-CH_3-4-OH	-100.8	-104.4	403.0	412.1	3	1	152.5	190.3	222.4	248.4	286.0	311.3	347.4
T4/39	1-C•=O -2-CH_3-4-CHO	-34.1	-32.2	443.7	452.8	3	1	159.7	197.9	231.2	259.0	300.6	329.4	370.2
T4/40	1-C•=O -2-CH_3-4-CH=CH_2	152.9	154.3	435.2	444.3	3	1	170.3	214.9	253.0	283.9	329.6	361.3	407.8
T4/41	1-C•=O -2,3-CH_3	-29.4	-27.5	433.8	442.9	3	1	165.5	202.4	234.7	261.7	302.2	330.3	370.3
T4/42	1-C•=O -3-CH_3-4-CHO	52.7	54.1	411.2	429.4	9	1	163.1	201.8	235.8	264.2	307.3	337.9	383.6
Subset 5: β-Styryl Subset														
T5/1	t-C_6H_5CH=CH•	397.8	395.7	344.8	350.6	2	1	119.7	156.7	187.4	211.8	247.1	271.2	306.4
T5/2	*o*-(OH)t-C_6H_5CH=CH•	208.2	202.5	361.9	361.9	1	1	138.6	179.1	213.4	241.4	281.2	305.8	336.7
T5/3	*m*-(OH)t-C_6H_5CH=CH•	222.8	217.1	379.3	379.3	1	1	142.3	180.5	211.5	235.7	270.2	293.4	327.4
T5/4	*p*-(OH)t-C_6H_5CH=CH•	223.1	217.4	379.6	379.6	1	1	140.5	179.3	210.8	235.3	270.0	293.4	327.5
T5/5	*o*-(OCH_3)t-C_6H_5CH=CH•	244.3	239.4	410.4	419.6	3	1	164.9	208.0	243.9	272.8	315.4	345.0	388.2
T5/6	*m*-(OCH_3)t-C_6H_5CH=CH•	240.8	235.9	414.4	423.5	3	1	164.2	207.2	242.9	271.6	313.6	342.9	386.3
T5/7	*p*-(OCH_3)t-C_6H_5CH=CH•	241.3	236.4	413.7	422.8	3	1	161.8	205.8	242.1	271.1	313.6	343.0	386.4
T5/8	*o*-(CHO)t-C_6H_5CH=CH•	286.6	286.5	393.0	393.0	1	1	152.3	194.3	228.7	255.9	294.7	320.4	356.0
T5/9	*m*-(CHO)t-C_6H_5CH=CH•	277.5	277.4	402.9	402.9	1	1	149.8	189.5	223.0	250.0	289.4	316.1	353.8
T5/10	*p*-(CHO)t-C_6H_5CH=CH•	276.8	276.7	401.6	401.6	1	1	148.2	188.5	222.4	249.6	289.3	316.1	354.0
T5/11	*o*-($CH=CH_2$)t-C_6H_5CH=CH•	469.1	468.5	408.0	408.0	1	1	159.8	204.7	242.5	272.7	316.4	346.2	390.0
T5/12	*m*-($CH=CH_2$)t-C_6H_5CH=CH•	465.3	464.7	408.8	408.8	1	1	156.9	202.7	240.7	271.1	315.1	345.3	389.6
T5/13	*p*-($CH=CH_2$)t-C_6H_5CH=CH•	465.3	464.7	407.3	407.3	1	1	156.9	202.7	240.9	271.3	315.6	345.8	390.1
T5/14	*o*-(CH_3)t-C_6H_5CH=CH•	365.8	365.2	386.7	395.8	3	1	150.3	189.6	223.5	251.2	292.5	321.7	365.2
T5/15	*m*-(CH_3)t-C_6H_5CH=CH•	362.2	361.6	387.0	396.1	3	1	141.3	183.4	219.0	248.0	290.9	320.7	364.9
T5/16	*p*-(CH_3)t-C_6H_5CH=CH•	362.5	361.9	386.3	395.5	3	1	141.3	183.3	219.0	248.0	290.9	320.8	364.9
T5/17	*o*-(CH_2CH_3)t-C_6H_5CH=CH•	345.0	343.3	423.4	432.5	3	1	172.2	218.4	258.1	290.5	339.1	373.5	425.0
T5/18	*m*-(CH_2CH_3)t-C_6H_5CH=CH•	339.7	338.0	428.2	437.3	3	1	165.3	212.9	253.9	287.3	337.2	372.2	424.2
T5/19	*p*-(CH_2CH_3)t-C_6H_5CH=CH•	341.4	339.7	430.5	439.7	3	1	166.2	213.8	254.6	287.9	337.5	372.4	424.4
T5/20	1-(t-CH=CH•)-2,3-OH	49.3	40.1	403.8	403.8	1	1	162.4	202.0	234.0	259.3	294.9	317.9	350.2
T5/21	1-(t-CH=CH•)-2,4-OH	30.4	21.2	389.7	389.7	1	1	159.3	200.8	235.3	263.2	303.2	328.4	359.4
T5/22	1-(t-CH=CH•)-3,4-OH	45.4	36.2	398.3	398.3	1	1	164.9	206.0	238.9	264.2	299.0	321.1	351.9
T5/23	1-(t-CH=CH•)-2-OH-4-CHO	89.9	86.3	409.1	409.1	1	1	167.4	211.5	249.2	280.0	323.6	350.5	383.5
T5/24	1-(t-CH=CH•)-2-OH-6-CHO	94.1	90.5	403.3	403.3	1	1	166.8	211.4	248.6	278.9	323.4	352.8	389.4
T5/25	1-(t-CH=CH•)-2-OH-5-CH=CH_2	276.2	272.0	419.9	419.9	1	1	175.9	224.9	266.7	300.7	349.3	380.3	420.3
T5/26	1-(t-CH=CH•)-2-OH-5-CH_3	176.1	171.9	398.6	407.8	3	1	160.3	205.6	244.9	277.5	324.8	355.2	395.0
T5/27	1-(t-CH=CH•)-2-OH-6-CH_3	178.1	173.9	395.0	404.1	3	1	164.0	208.6	247.2	279.0	325.1	355.1	394.9
T5/28	1-(t-CH=CH•)-2-OH-4-CH_2CH_3	150.7	145.4	439.9	449.1	3	1	184.7	235.7	280.1	317.0	371.3	407.0	454.8
T5/29	1-(t-CH=CH•)-2-OH-5-CH_2CH_3	154.8	149.5	438.0	447.1	3	1	185.0	236.0	280.6	317.5	371.5	406.9	454.4
T5/30	1-(t-CH=CH•)-2-CHO-4-OH	114.3	110.7	418.9	418.9	1	1	172.7	216.7	251.9	279.2	317.4	342.3	376.7
T5/31	1-(t-CH=CH•)-3-CHO-4-OH	73.3	69.7	408.6	408.6	1	1	162.9	205.4	240.8	269.1	310.7	339.5	381.8
T5/32	1-(t-CH=CH•)-2,4-CHO	168.1	170.1	442.3	442.3	1	1	181.2	226.6	264.0	293.8	336.7	365.1	403.4
T5/33	1-(t-CH=CH•)-2-CH=CH_2-4-CH_3	433.4	434.3	439.3	448.5	3	1	181.0	231.5	274.5	309.3	360.5	396.0	448.6
T5/34	1-(t-CH=CH•)-2-CH=CH_2-6-CH_3	437.2	438.1	441.4	450.6	3	1	182.3	231.8	273.7	307.8	358.8	394.7	448.0
T5/35	1-(t-CH=CH•)-2-CH_3-4-CHO	244.3	245.7	434.7	443.9	3	1	175.5	219.3	257.0	288.0	334.2	366.3	412.6
T5/36	1-(t-CH=CH•)-2,3-CH_3	337.6	338.5	414.7	433.0	9	1	169.7	214.6	253.7	286.0	335.1	370.1	422.9
T5/37	1-(t-CH=CH•)-2,4-CH_3	330.1	331.0	421.2	439.5	9	1	169.7	214.8	254.1	286.6	335.9	371.0	423.6
T5/38	1-(t-CH=CH•)-2-CH_3-4-CH_2CH_3	308.9	308.7	458.9	477.2	9	1	194.2	245.0	289.5	326.4	382.5	422.6	483.0
T5/39	c-C_6H_5CH=CH•	402.2	400.1	353.1	353.1	1	1	119.0	155.9	186.4	210.6	245.6	269.8	305.3
T5/40	*o*-(OH)c-C_6H_5CH=CH•	226.5	220.8	382.5	382.5	1	1	142.9	179.8	209.5	232.9	266.9	290.4	325.4
T5/41	*m*-(OH)c-C_6H_5CH=CH•	227.3	221.6	383.1	383.1	1	1	140.0	178.6	209.7	233.9	268.3	291.7	326.2
T5/42	*p*-(OH)c-C_6H_5CH=CH•	228.0	222.3	382.5	382.5	1	1	140.0	178.7	209.9	234.2	268.7	292.0	326.5
T5/43	*o*-(OCH_3)c-C_6H_5CH=CH•	245.2	240.3	418.6	427.7	3	1	159.7	203.9	240.9	270.6	313.8	343.6	387.2
T5/44	*m*-(OCH_3)c-C_6H_5CH=CH•	245.4	240.5	416.9	426.0	3	1	161.3	205.0	241.0	269.6	311.7	341.2	385.1
T5/45	*p*-(OCH_3)c-C_6H_5CH=CH•	246.2	241.3	416.4	425.5	3	1	161.3	205.1	241.2	270.0	312.2	341.6	385.4
T5/46	*o*-(CHO)c-C_6H_5CH=CH•	294.1	294.0	400.8	400.8	1	1	153.0	192.6	225.4	251.8	290.2	316.3	353.2
T5/47	*m*-(CHO)c-C_6H_5CH=CH•	281.7	281.6	407.0	407.0	1	1	146.8	187.1	220.6	247.3	285.8	312.0	349.8
T5/48	*p*-(CHO)c-C_6H_5CH=CH•	281.6	281.5	399.8	399.8	1	1	147.2	187.6	221.3	248.4	287.9	314.8	352.9
T5/49	*o*-($CH=CH_2$)c-C_6H_5CH=CH•	473.6	473.0	408.2	408.2	1	1	160.4	205.0	241.9	271.3	314.1	343.9	388.3
T5/50	*m*-($CH=CH_2$)c-C_6H_5CH=CH•	469.6	469.0	411.7	411.7	1	1	156.2	201.8	239.6	269.8	313.6	343.8	388.5
T5/51	*p*-($CH=CH_2$)c-C_6H_5CH=CH•	469.7	469.1	410.4	410.4	1	1	156.3	202.0	240.0	270.2	314.2	344.5	389.0
T5/52	*o*-(CH_3)c-C_6H_5CH=CH•	371.8	371.2	385.0	394.2	3	1	143.0	184.5	219.4	247.7	289.8	319.5	363.8
T5/53	*m*-(CH_3)c-C_6H_5CH=CH•	365.8	365.2	389.8	399.0	3	1	140.4	182.2	217.7	246.5	289.3	319.3	363.9

T5/54	*p*-(CH_3)c-C_6H_5CH=CH•	367.0	366.4	389.4	398.5	3	1	140.7	182.6	218.0	246.8	289.5	319.4	363.9
T5/55	*o*-(CH_2CH_3)c-C_6H_5CH=CH•	348.9	347.2	424.0	433.2	3	1	170.1	216.5	256.0	288.4	337.2	371.9	424.0
T5/56	*m*-(CH_2CH_3)c-C_6H_5CH=CH•	345.5	343.8	430.1	439.2	3	1	165.5	212.9	253.5	286.6	336.0	370.9	423.2
T5/57	*p*-(CH_2CH_3)c-C_6H_5CH=CH•	345.8	344.1	429.7	438.8	3	1	165.4	212.9	253.5	286.6	336.1	371.0	423.4
T5/58	1-(c-CH=CH•)-2,4-OH	50.1	40.9	407.8	407.8	1	1	166.6	205.1	235.2	258.5	291.4	313.8	347.2
T5/59	1-(c-CH=CH•)-2,5-OH	62.0	52.8	415.2	415.2	1	1	166.1	202.8	231.8	254.5	287.5	310.4	345.1
T5/60	1-(c-CH=CH•)-2-OH-4-OCH_3	67.7	59.2	440.1	449.3	3	1	187.8	231.5	266.6	294.4	335.0	363.3	406.0
T5/61	1-(c-CH=CH•)-2-OH-5-OCH_3	82.4	73.9	449.7	458.9	3	1	187.4	228.6	262.3	289.6	330.7	359.8	404.1
T5/62	1-(c-CH=CH•)-2-OH-4-CH=CH_2	293.5	289.3	439.1	439.1	1	1	180.5	226.1	263.2	292.5	335.3	364.8	408.9
T5/63	1-(c-CH=CH•)-3-OH-5-CH=CH_2	290.1	285.9	438.6	438.6	1	1	178.5	225.8	264.3	294.6	337.8	367.2	410.4
T5/64	1-(c-CH=CH•)-2-OH-3-CH_3	190.2	186.0	416.2	425.4	3	1	169.1	209.1	242.7	270.1	311.1	340.1	383.9
T5/65	1-(c-CH=CH•)-2-OH-4-CH_3	190.5	186.3	417.7	426.9	3	1	164.6	206.6	241.4	269.4	310.9	340.1	384.0
T5/66	1-(c-CH=CH•)-2-OH-5-CH_3	194.0	189.8	419.0	428.2	3	1	165.1	206.5	241.0	268.9	310.4	339.7	383.8
T5/67	1-(c-CH=CH•)-3-OH-5-CH_3	186.4	182.2	415.7	424.8	3	1	163.7	207.0	243.0	271.9	313.9	342.9	385.9
T5/68	1-(c-CH=CH•)-2-OH-3-CH_2CH_3	169.2	163.9	454.5	463.6	3	1	194.3	240.3	279.3	311.0	358.7	392.7	443.9
T5/69	1-(c-CH=CH•)-3-CHO-4-OH	78.4	74.8	407.9	407.9	1	1	161.7	204.2	239.4	267.5	308.2	335.9	375.9
T5/70	1-(c-CH=CH•)-2,4-CHO	176.1	178.1	445.7	445.7	1	1	181.6	224.7	260.7	289.8	332.5	361.2	400.7
T5/71	1-(c-CH=CH•)-2-CHO-5-CH=CH_2	359.2	360.6	457.1	457.1	1	1	189.6	238.1	278.4	310.8	358.1	390.3	436.5
T5/72	1-(c-CH=CH•)-2-CHO-4-CH_3	258.6	260.0	436.5	445.6	3	1	174.9	219.3	257.0	287.9	333.9	365.7	411.6
T5/73	1-(c-CH=CH•)-2-CH=CH_2-4-OH	299.1	294.9	436.1	436.1	1	1	180.2	226.6	264.5	294.3	337.0	366.2	409.5
T5/74	1-(c-CH=CH•)-2-CH=CH_2-5-CH_3	438.4	439.3	442.9	452.0	3	1	181.4	230.7	272.7	306.9	357.7	393.4	446.8
T5/75	1-(c-CH=CH•)-2-CH=CH_2-6-CH_3	441.7	442.6	439.5	448.6	3	1	191.1	238.6	278.6	311.1	359.9	394.7	447.2
T5/76	1-(c-CH=CH•)-2-CH_3-4-OH	196.2	192.0	413.6	422.7	3	1	163.9	207.3	243.0	271.5	313.0	341.9	385.0
T5/77	1-(c-CH=CH•)-2-CH_3-4-CHO	250.2	251.6	435.8	445.0	3	1	171.7	216.7	254.8	285.9	332.2	364.5	411.4
T5/78	1-(c-CH=CH•)-2-CH_3-4-CH=CH_2	438.8	439.7	442.7	451.9	3	1	180.9	230.4	272.6	306.9	357.9	393.7	447.2
T5/79	1-(c-CH=CH•)-3-CH_3-4-CH=CH_2	437.6	438.5	442.9	452.1	3	1	183.4	232.8	274.5	308.3	358.6	394.0	447.2
T5/80	1-(c-CH=CH•)-2,4-CH_3	336.2	337.1	420.6	438.9	9	1	164.7	211.2	251.1	284.0	333.7	369.1	422.4
Subset 6: Benzyl Subset														
T6/1	$C_6H_5CH_2$•	210.3	208.2	314.5	320.3	2	1	106.3	141.1	169.9	192.8	226.5	249.9	284.8
T6/2	*o*-(OH)$C_6H_5CH_2$•	34.1	28.4	349.1	349.1	1	1	128.9	164.4	193.3	216.0	248.7	271.4	305.4
T6/3	*m*-(OH)$C_6H_5CH_2$•	35.6	29.9	350.1	350.1	1	1	127.7	164.0	193.4	216.3	249.2	271.8	305.7
T6/4	*p*-(OH)$C_6H_5CH_2$•	35.3	29.6	344.7	350.4	2	1	127.0	163.5	193.0	216.1	249.2	272.0	305.8
T6/5	*o*-(OCH_3)$C_6H_5CH_2$•	51.6	46.7	377.1	386.3	3	1	148.1	191.2	226.8	255.0	296.1	324.6	366.8
T6/6	*m*-(OCH_3) $C_6H_5CH_2$•	54.0	49.1	384.4	393.5	3	1	150.2	191.1	225.0	252.3	292.7	321.4	364.6
T6/7	*p*-(OCH_3)$C_6H_5CH_2$•	54.0	49.1	383.9	393.0	3	1	148.1	189.7	224.2	251.8	292.6	321.4	364.7
T6/8	*o*-(CHO)$C_6H_5CH_2$•	91.1	91.0	367.4	367.4	1	1	137.5	176.1	207.9	233.2	270.4	295.9	332.6
T6/9	*m*-(CHO)$C_6H_5CH_2$•	88.8	88.7	368.4	368.4	1	1	134.8	173.0	204.9	230.7	268.6	294.7	332.1
T6/10	*p*-(CHO)$C_6H_5CH_2$•	82.9	82.8	365.5	371.3	2	1	133.9	172.2	204.2	230.1	268.2	294.5	332.4
T6/11	*o*-(CH=CH_2)$C_6H_5CH_2$•	278.6	278.0	377.6	377.6	1	1	145.5	188.6	224.2	252.6	294.3	323.6	367.6
T6/12	*m*-(CH=CH_2)$C_6H_5CH_2$•	275.5	274.9	378.6	378.6	1	1	143.9	187.3	223.4	252.3	294.6	324.1	368.1
T6/13	*p*-(CH=CH_2)$C_6H_5CH_2$•	268.4	267.8	375.9	375.9	1	1	143.3	187.0	223.5	252.7	295.6	325.3	369.1
T6/14	*o*-(CH_3)$C_6H_5CH_2$•	175.9	175.3	352.2	361.3	3	1	131.3	170.4	203.6	230.7	271.3	300.1	343.6
T6/15	*m*-(CH_3)$C_6H_5CH_2$•	174.2	173.6	356.7	365.9	3	1	127.9	167.7	201.5	229.1	270.3	299.4	343.3
T6/16	*p*-(CH_3)$C_6H_5CH_2$•	174.7	174.1	351.4	366.3	6	1	127.8	167.5	201.3	228.9	270.2	299.4	343.3
T6/17	*o*-(CH_2CH_3)$C_6H_5CH_2$•	156.3	154.6	391.0	400.1	3	1	154.6	199.9	238.7	270.4	318.4	352.5	404.0
T6/18	*m*-(CH_2CH_3)$C_6H_5CH_2$•	153.7	152.0	396.3	405.5	3	1	152.8	198.1	237.0	268.9	316.8	351.0	402.7
T6/19	*p*-(CH_2CH_3)$C_6H_5CH_2$•	153.6	151.9	397.0	406.1	3	1	152.4	197.8	236.8	268.7	316.7	351.0	402.8
T6/20	1-CH_2•-2,3-OH	-144.4	-153.6	371.0	371.0	1	1	148.6	187.5	218.8	243.2	277.2	299.1	330.0
T6/21	1-CH_2•-2,4-OH	-142.1	-151.3	373.2	379.0	2	1	147.3	185.3	215.3	238.5	271.2	293.3	326.1
T6/22	1-CH_2•-2,5-OH	-133.5	-142.7	380.7	380.7	1	1	151.7	187.5	215.9	238.1	269.9	291.9	325.4
T6/23	1-CH_2•-2,6-OH	-143.0	-152.2	372.2	377.9	2	1	148.6	185.7	215.2	238.0	270.4	292.6	325.9
T6/24	1-CH_2•-2-OH-3-OCH_3	-126.0	-134.5	404.8	413.9	3	1	166.3	208.8	245.3	275.3	319.5	349.3	391.2
T6/25	1-CH_2•-2-OH-4-OCH_3	-121.8	-130.3	411.8	420.9	3	1	171.0	213.0	247.3	274.6	314.6	342.7	385.1
T6/26	1-CH_2•-2-OCH_3-4-OH	-124.0	-132.5	406.9	416.0	3	1	170.5	214.7	250.8	279.0	319.5	347.1	388.1
T6/27	1-CH_2•-2,4-OCH_3	-105.5	-113.2	438.8	457.0	9	1	191.1	240.6	281.6	314.4	362.6	396.4	446.9
T6/28	1-CH_2•-2-OCH_3-4-CHO	-80.4	-83.3	427.0	436.2	3	1	176.3	222.0	261.1	292.9	339.5	371.2	416.2
T6/29	1-CH_2•-2-OCH_3-4-CH=CH_2	107.9	104.5	432.4	441.6	3	1	184.9	237.0	280.5	315.2	365.7	400.5	451.5
T6/30	1-CH_2•-2-OCH_3-4-CH_3	15.6	12.2	414.2	432.5	9	1	170.0	218.1	258.6	291.4	340.0	374.2	425.3
T6/31	1-CH_2•-2-OCH_3-4-CH_2CH_3	-5.1	-9.6	452.4	470.6	9	1	194.4	248.2	293.9	331.0	386.4	425.6	484.6
T6/32	1-CH_2•-2,4-CHO	-33.3	-31.4	419.5	419.5	1	1	165.4	207.5	242.5	270.8	312.3	340.6	380.1
T6/33	1-CH_2•-2,5-CHO	-26.7	-24.8	419.7	419.7	1	1	167.0	209.0	243.9	272.0	313.3	341.2	379.9
T6/34	1-CH_2•-2,6-CHO	-19.2	-17.3	420.9	420.9	1	1	170.0	210.2	244.0	271.6	312.5	340.3	378.9
T6/35	1-CH_2•-2-CHO-4-CH=CH_2	148.6	150.0	422.5	422.5	1	1	174.7	222.1	261.4	293.0	339.4	371.2	416.9
T6/36	1-CH_2•-2-CH=CH_2-3-OH	100.9	96.7	398.5	404.3	2	1	169.3	216.8	254.4	283.2	323.7	351.0	391.6
T6/37	1-CH_2•-2-CH=CH_2-3-OCH_3	131.9	128.5	436.2	445.4	3	1	188.0	236.7	277.5	310.6	360.0	395.0	447.5
T6/38	1-CH_2•-2,3-CH=CH_2	350.6	351.5	431.7	431.7	1	1	187.7	238.7	281.1	315.0	364.7	399.4	451.6
T6/39	1-CH_2•-2-CH_3-3-OH	3.3	-0.9	382.9	392.0	3	1	152.7	192.4	225.5	252.3	292.2	320.5	363.5
T6/40	1-CH_2•-2-CH_3-4-OH	-0.3	-4.5	381.8	390.9	3	1	152.2	193.1	226.9	254.1	294.2	322.3	364.7

T6/41	1-CH_2•-2-CH_3-5-OH	3.2	-1.0	382.4	391.5	3	1	152.9	193.3	226.8	253.8	293.7	321.8	364.3
T6/42	1-CH_2•-2-CH_3-6-OH	-0.6	-4.8	380.3	389.4	3	1	154.8	194.5	227.5	254.2	293.8	321.7	364.2
T6/43	1-CH_2•-2-CH_3-4-CHO	47.2	48.6	403.5	412.6	3	1	159.3	201.7	238.1	268.0	313.1	344.7	391.2
T6/44	1-CH_2•-2-CH_3-6-CHO	57.5	58.9	401.7	410.9	3	1	164.0	207.0	243.0	272.3	316.1	346.7	391.6
T6/45	1-CH_2•-2-CH_3-4-CH=CH_2	233.1	234.0	407.4	416.6	3	1	168.5	216.5	257.3	290.7	340.5	375.6	428.0
T6/46	1-CH_2•-2-CH_3-5-CH=CH_2	240.7	241.6	410.3	419.4	3	1	169.0	216.6	257.1	290.1	339.4	374.3	426.9
T6/47	1-CH_2•-2,4-CH_3	140.0	140.9	388.8	407.0	9	1	152.9	196.9	235.1	266.7	315.0	349.6	402.1
T6/48	1-CH_2•-2,5-CH_3	140.4	141.3	388.7	407.0	9	1	153.0	197.0	235.1	266.8	315.0	349.6	402.1
T6/49	1-CH_2•-3-CH_3-4-OH	-1.5	-5.7	384.2	393.4	3	1	152.1	192.3	225.9	253.1	293.3	321.6	364.3
T6/50	1-CH_2•-3-CH_3-4-OCH_3	16.7	13.3	416.1	434.4	9	1	172.7	219.6	259.8	292.4	340.9	374.8	425.6
T6/51	1-CH_2•-3,5-CH_3	138.3	139.2	387.4	411.4	18	1	149.6	194.4	233.2	265.3	314.1	349.0	401.8
T6/52	1-CH_2•-3,6-CH_3	140.7	141.6	388.7	407.0	9	1	152.9	196.9	235.1	266.8	315.0	349.6	402.1
T6/53	C_6H_5CH•CH_3	178.1	174.9	359.0	368.2	3	1	124.6	164.6	199.0	227.1	269.1	298.8	343.1
T6/54	*o*-(OH)C_6H_5CH•CH_3	2.8	-4.0	387.3	396.4	3	1	148.7	188.9	222.9	250.4	291.3	320.1	363.6
T6/55	*m*-(OH)C_6H_5CH•CH_3	2.5	-4.3	389.0	398.2	3	1	145.7	187.4	222.4	250.6	291.9	320.7	364.0
T6/56	*p*-(OH)C_6H_5CH•CH_3	3.9	-2.9	389.4	398.5	3	1	145.5	187.2	222.2	250.4	291.8	320.8	364.1
T6/57	*o*-(OCH_3)C_6H_5CH•CH_3	20.1	14.1	420.0	438.2	9	1	167.5	215.2	255.8	288.8	338.1	373.0	425.1
T6/58	*m*-(OCH_3)C_6H_5CH•CH_3	22.0	16.0	422.0	440.3	9	1	169.9	214.9	253.7	285.8	334.5	369.5	422.4
T6/59	*p*-(OCH_3)C_6H_5CH•CH_3	22.8	16.8	422.0	440.3	9	1	166.7	213.3	253.2	285.9	335.1	370.1	422.9
T6/60	*o*-(CHO)C_6H_5CH•CH_3	58.6	57.4	407.4	416.6	3	1	156.0	200.3	238.0	268.5	313.8	345.3	391.0
T6/61	*m*-(CHO)C_6H_5CH•CH_3	55.5	54.3	410.1	419.2	3	1	153.4	196.7	234.2	265.1	311.4	343.7	390.5
T6/62	*p*-(CHO)C_6H_5CH•CH_3	53.2	52.0	405.0	414.1	3	1	153.2	196.6	234.1	265.0	311.3	343.6	390.5
T6/63	*o*-(CH=CH_2)C_6H_5CH•CH_3	248.1	246.4	415.6	424.7	3	1	164.7	212.6	253.4	286.8	336.8	372.3	425.7
T6/64	*m*-(CH=CH_2)C_6H_5CH•CH_3	243.0	241.3	417.0	426.1	3	1	162.4	210.9	252.6	286.6	337.3	373.0	426.4
T6/65	*p*-(CH=CH_2)C_6H_5CH•CH_3	236.5	234.8	413.7	422.9	3	1	161.8	210.7	252.7	287.1	338.3	374.1	427.4
T6/66	*o*-(CH_3)C_6H_5CH•CH_3	145.4	143.7	390.0	408.3	9	1	150.4	194.7	233.4	265.5	314.3	349.2	402.0
T6/67	*m*-(CH_3)C_6H_5CH•CH_3	142.2	140.5	395.5	413.8	9	1	146.3	191.3	230.7	263.4	313.0	348.4	401.6
T6/68	*o*-(CH_2CH_3)C_6H_5CH•CH_3	126.1	123.2	428.5	446.8	9	1	173.9	224.2	268.4	305.1	361.2	401.5	462.3
T6/69	*m*-(CH_2CH_3)C_6H_5CH•CH_3	121.8	118.9	435.6	453.9	9	1	171.3	221.8	266.3	303.2	359.5	399.9	461.0
T6/70	*p*-(CH_2CH_3)C_6H_5CH•CH_3	121.7	118.8	436.0	454.3	9	1	170.9	221.5	266.0	303.1	359.5	399.9	461.1

B.3.2 Thermochemical Database of The Special Cases Set

Thermochemical database for the special cases set which include the molecules that are excluded from the training set for development of Group Additive Values (GAVs) and non-nearest neighbor interactions (NNIs) are given in **Table B-2**.

Table B-2 Thermochemical database for the special cases set. The units of standard enthalpy of formation ($\Delta_f H^\circ$) data is given in kJ mol^{-1} whereas the units of entropies (S°) and heat capacities (C_p) are given in J mol^{-1} K^{-1}.

Special Cases Set														
#	Radicals	$\Delta_f H^\circ$ (298 K)		S° (298 K)				C_p						
		$\Delta_f H^\circ_{G4}$	$\Delta_f H^\circ_{G4/BAC}$	S°	S°_{int}	$\sigma_{tot^\circ sym}$	n_{opt}	300 K	400 K	500 K	600 K	800 K	1000 K	1500 K
S1/1	C•C$_5$H$_5$=CH$_2$	363.1	357.4	345.9	351.7	2	1	122.4	158.4	188.2	212.2	247.5	272.1	308.5
S1/2	(*o*-OH)C•C$_5$H$_5$=CH$_2$	180.5	174.4	377.8	377.8	1	1	143.5	183.0	214.8	239.6	274.5	297.7	331.6
S1/3	(*m*-OH)C•C$_5$H$_5$=CH$_2$	188.6	182.5	381.8	381.8	1	1	143.9	181.4	211.7	235.7	270.2	294.0	329.3
S1/4	(*p*-OH)C•C$_5$H$_5$=CH$_2$	190.0	183.9	384.4	384.4	1	1	143.2	180.7	211.2	235.3	270.0	293.9	329.4
S1/5	(*o*-OCH$_3$)C•C$_5$H$_5$=CH$_2$	207.0	201.1	422.5	431.6	3	1	169.9	213.6	249.1	277.0	317.5	346.1	389.4
S1/6	(*m*-OCH$_3$)C•C$_5$H$_5$=CH$_2$	206.7	200.8	415.7	424.9	3	1	166.9	208.8	243.7	271.9	313.9	343.6	388.3
S1/7	(*p*-OCH$_3$)C•C$_5$H$_5$=CH$_2$	208.6	202.7	418.3	427.5	3	1	165.2	207.4	242.7	271.2	313.6	343.5	388.3
S1/8	(*o*-CHO)C•C$_5$H$_5$=CH$_2$	243.1	237.9	400.0	400.0	1	1	152.1	191.0	223.7	250.4	289.8	317.0	356.0
S1/9	(*m*-CHO)C•C$_5$H$_5$=CH$_2$	243.7	238.5	407.8	407.8	1	1	151.9	191.4	224.2	250.5	288.9	315.3	353.4
S1/10	(*p*-CHO)C•C$_5$H$_5$=CH$_2$	233.1	227.9	391.7	391.7	1	1	149.6	189.1	222.2	249.0	288.5	315.8	355.5
S1/11	(*o*-CH=CH$_2$)C•C$_5$H$_5$=CH$_2$	427.2	421.4	405.4	405.4	1	1	161.6	206.0	243.1	272.9	316.7	347.2	392.4
S1/12	(*m*-CH=CH$_2$)C•C$_5$H$_5$=CH$_2$	428.2	422.4	409.7	409.7	1	1	160.2	204.7	241.8	271.6	315.6	346.2	391.7
S1/13	(*p*-CH=CH$_2$)C•C$_5$H$_5$=CH$_2$	419.5	413.7	403.3	403.3	1	1	159.4	204.3	241.9	272.2	316.8	347.6	393.0
S1/14	(*o*-CH$_3$)C•C$_5$H$_5$=CH$_2$	324.8	319.0	382.0	391.1	3	1	145.5	186.0	220.6	248.9	291.6	321.8	367.1
S1/15	(*m*-CH$_3$)C•C$_5$H$_5$=CH$_2$	328.4	322.6	382.1	391.2	3	1	147.8	188.8	223.7	252.1	294.3	324.1	368.4
S1/16	(*p*-CH$_3$)C•C$_5$H$_5$=CH$_2$	327.8	322.0	388.9	398.0	3	1	143.8	184.7	219.6	248.2	291.1	321.6	367.0
S1/17	(*o*-CH$_2$CH$_3$)C•C$_5$H$_5$=CH$_2$	303.7	296.8	424.1	433.2	3	1	169.3	216.0	256.1	289.1	338.9	374.3	427.2
S1/18	(*m*-CH$_2$CH$_3$)C•C$_5$H$_5$=CH$_2$	306.4	299.5	428.1	437.2	3	1	168.9	215.4	255.4	288.2	337.8	373.2	426.3
S1/19	(*p*-CH$_2$CH$_3$)C•C$_5$H$_5$=CH$_2$	306.6	299.7	428.9	438.1	3	1	168.5	215.1	255.1	288.0	337.7	373.2	426.5
S2/1	1(3H)-Isobenzofuranonyl	-87.2	-88.5	353.7	353.7	1	1	128.4	167.2	198.8	223.7	259.1	282.5	315.5

B.4 Bond Dissociation Energies

In this section, the database of Bond Dissociation Energies (BDEs) and the standard enthalpy of formation ($\Delta_f H^\circ$) data used in the calculation of these BDEs are given. The calculation of the BDEs is carried out according to Eq. (4-5) described in the Methodology section of **Chapter 4**.

All the reported $\Delta_f H^\circ$data is calculated with the G4/BAC method described in the Methodology section of **Chapter 4**. The $\Delta_f H^\circ$data for the monocyclic aromatic radicals (MARs) are taken from **Table B-1** and **Table B-2**. The standard enthalpy of formation ($\Delta_f H^\circ$) data for the closed-shell monocyclic aromatic hydrocarbons (MAHs) used in the calculation of bond dissociation energies (BDEs) are given in **Table B-3**. This data is taken from the study that is presented in **Chapter 3**. The G4/BAC data for the small radicals are given in **Table B-4**.

With the aid of the information in **Table B-1**, **Table B-3** and **Table B-4**, the database of bond dissociation energies (BDEs) are constructed. This database includes BDE for 297 bonds in 70 MAHs and it is given in **Table B-5**. In this table, first, name of the molecule is given and then, the BDEs for all the bonds (available in the database) in that molecule is given one by one. In order to indicate the bond, "-" is used and besides, the smaller moiety of the molecule on one side of the bond is shown in bold. As an instance, C_6H_5-**OH** indicates the bond between ring carbon and the oxygen atom in phenol (C_6H_5OH). In double substituted MAHs, one of the substituents and its position with respect to the other substituent is given in square parenthesis "[ ]". The other substituent is the substituent which possess the bond of interest and the smaller moiety on the other side of this bond is given in bold. For example, [(*m*-OH)]C_6H_4O-**CH_3** represents the O-C bond in the methoxy group of the *m*-methoxyphenol (or *m*-hydroxymethoxybenzene).

The BDEs of the C_6H_5-X bonds (X=-CH=CH_2, -OCH_3, and –OH) are excluded from the discussion in the text as the trends in these BDEs can only be useful in explaining substituent interactions in MAHs which are already done in **Chapter 3**. In the text, X=-H, -CHO and -CH_3 cases are given as examples, and the information regarding the other excluded groups is given in In **Figure B-15**.

Table B-3 BAC-corrected $\Delta_f H^\circ$ data at the level for G4 for monocyclic aromatic hydrocarbons (MAHs) taken from **Chapter 3**.

Mol. #	Molecule Name	$\Delta_f H^\circ_{G4/BAC}$ [kJ mol^{-1}]
1	Benzene	82
2	Phenol (Hydroxybenzene)	-96
3	Anisole (Methoxybenzene)	-74.2
4	Benzaldehyde (Formylbenzene)	-37.4
5	Styrene (Vinylbenzene)	147.9
6	Toluene (Methylbenzene)	49.2
7	EthylBenzene	28.2
8	*o*-dihydroxybenzene	-275.8
9	*m*-dihydroxybenzene	-273.9
10	*p*-dihydroxybenzene	-266.1
11	*o*-dimethoxybenzene	-215.3
12	*m*-dimethoxybenzene	-231
13	*p*-dimethoxybenzene	-223.4
14	*o*-diformylbenzene	-136.4
15	*m*-diformylbenzene	-152.4
16	*p*-diformylbenzene	-151.3
17	*o*-divinylbenzene	222.2
18	*m*-divinylbenzene	213.9
19	*p*-divinylbenzene	213.2
20	*o*-dimethylbenzene	18.8
21	*m*-dimethylbenzene	16.6
22	*p*-dimethylbenzene	17.2
23	*o*-diethylbenzene	-20.4
24	*m*-diethylbenzene	-25.6
25	*p*-diethylbenzene	-24.9
26	*o*-methoxyphenol	-255.8
27	*m*-methoxyphenol	-252.6
28	*p*-methoxyphenol	-244.8
29	*o*-formylphenol	-244.1
30	*m*-formylphenol	-215.4
31	*p*-formylphenol	-219
32	*o*-vinylphenol	-27.8
33	*m*-vinylphenol	-29.9
34	*p*-vinylphenol	-29.7

35	*o*-methylphenol	-129.7
36	*m*-methylphenol	-129.2
37	*p*-methylphenol	-126.8
38	*o*-ethylphenol	-150.5
39	*m*-ethylphenol	-150.2
40	*p*-ethylphenol	-147.9
41	*o*-formylanisole	-189.5
42	*m*-formylanisole	-195.5
43	*p*-formylanisole	-198.6
44	*o*-vinylanisole	-5.9
45	*m*-vinylanisole	-8.6
46	*p*-vinylanisole	-8.3
47	*o*-methylanisole	-108.5
48	*m*-methylanisole	-107.2
49	*p*-methylanisole	-105.3
50	*o*-ethylanisole	-129.4
51	*m*-ethylanisole	-128.2
52	*p*-ethylanisole	-126.3
53	*o*-vinylbenzaldehyde	39.5
54	*m*-vinylbenzaldehyde	28.9
55	*p*-vinylbenzaldehyde	28.1
56	*o*-methylbenzaldehyde	-65.1
57	*m*-methylbenzaldehyde	-71.3
58	*p*-methylbenzaldehyde	-72.1
59	*o*-ethylbenzaldehyde	-85.8
60	*m*-ethylbenzaldehyde	-92.1
61	*p*-ethylbenzaldehyde	-92.8
62	*o*-methylstyrene	120.2
63	*m*-methylstyrene	114.9
64	*p*-methylstyrene	114.9
65	*o*-ethylstyrene	98.9
66	*m*-ethylstyrene	93.8
67	*p*-ethylstyrene	93.9
68	*o*-ethyltoluene	-1.0
69	*m*-ethyltoluene	-4.5
70	*p*-ethyltoluene	-3.9

Table B-4 BAC-corrected $\Delta_f H^\circ$ data calculated at the level for G4 for small nonaromatic radicals (•H, •OH, •OCH_3, •CHO, •$CH{=}CH_2$, •CH_3, •CH_2CH_3).

Mol. #	Molecule Name	$\Delta_f H^\circ_{G4/BAC}$ [kJ mol^{-1}]
1	Hydrogen (•H)	218.0
2	Hydroxy (•OH)	35.2
3	Methoxy(•OCH_3)	16.8
4	Formyl(•CHO)	40.2
5	Vinyl(•$CH{=}CH_2$)	294.5
6	Methyl(•CH_3)	144.7
7	Ethyl(•CH_2CH_3)	118.1

Table B-5 The database of Bond Dissociation Energies (BDEs).

Molecule and Bond Name		BDE [kJ mol^{-1}]
Benzene and Single Substituted MAHs		
1	**C_6H_6 (Benzene)**	
	C_6H_5-**H**	473.3
2	**C_6H_5OH (Phenol)**	
	C_6H_5-**OH**	468.5
	C_6H_5O-**H**	368.1
	C_6H_4OH[*o*-(C_b-**H**)]	476.1
	C_6H_4OH[*m*-(C_b-**H**)]	472.7
	C_6H_4OH[*p*-(C_b-**H**)]	479.0
3	**$C_6H_5OCH_3$ (Anisole)**	
	C_6H_5-**OCH_3**	428.6
	C_6H_5O-**CH_3**	273.1
	$C_6H_5OCH_2$-**H**	402.1
	$C_6H_4OCH_3$[*o*-(C_b-**H**)]	471.4
	$C_6H_4OCH_3$[*m*-(C_b-**H**)]	470.0
	$C_6H_4OCH_3$[*p*-(C_b-**H**)]	476.6
4	**C_6H_5CHO (Benzaldehyde)**	
	C_6H_5-**CHO**	415.3
	C_6H_5CO-**H**	373.6
	C_6H_4[*o*-(C_b-**H**)]	474.9
	C_6H_4[*m*-(C_b-**H**)]	476.2
	C_6H_4[*p*-(C_b-**H**)]	474.9

5	**$C_6H_5CH=CH_2$ (Styrene)**	
	C_6H_5-**$CH=CH_2$**	484.4
	C_6H_5C(-**H**)$=CH_2$	433.3
	$C_6H_5CH=CH$-**H**(trans)	470.2
	$C_6H_5CH=CH$-**H**(cis)	465.8
	$C_6H_4CH=CH_2$[*o*-(C_b-**H**)]	476.0
	$C_6H_4CH=CH_2$[*m*-(C_b-**H**)]	477.1
	$C_6H_4CH=CH_2$[*p*-(C_b-**H**)]	478.3
6	**$C_6H_5CH_3$ (Toluene)**	
	C_6H_5-**CH_3**	433.3
	$C_6H_5CH_2$-**H**	377.0
	$C_6H_4CH_3$[*o*-(C_b-**H**)]	472.2
	$C_6H_4CH_3$[*m*-(C_b-**H**)]	472.3
	$C_6H_4CH_3$[*p*-(C_b-**H**)]	474.5
7	**$C_6H_5CH_2CH_3$ (Ethyl Benzene)**	
	C_6H_5-**CH_2CH_3**	427.6
	C_6H_5(-**H**)-CH_3	364.6
	$C_6H_5CH_2$-**CH_3**	324.7
	$C_6H_4CH_3$[*o*-(Cb-**H**)]	470.7
	$C_6H_4CH_3$[*m*-(Cb-**H**)]	470.9
	$C_6H_4CH_3$[*p*-(Cb-**H**)]	473.1
Double Substituted Benzenes		
8	***o*-dihydroxybenzene (catechol)**	
	[(*o*-OH)]C_6H_4-**OH**	473.8
	[(*o*-OH)]C_6H_4O-**H**	330.8
9	***m*-dihydroxybenzene (resorcinol)**	
	[(*m*-OH)]C_6H_4-**OH**	467.9
	[(*m*-OH)]C_6H_4O-**H**	365.0
10	***p*-dihydroxybenzene (hydroquinone)**	
	[(*p*-OH)]C_6H_4-**OH**	466.4
	[(*p*-OH)]C_6H_4O-**H**	347.1
11	**o-hydroxymethoxybenzene (*o*-guaiacol)**	
	[(*o*-OCH_3)]C_6H_4-**OH**	470.3
	[(*o*-OCH_3)]C_6H_4O-**H**	362.8
	[(*o*-OH)]C_6H_4-**OCH_3**	435.2
	[(*o*-OH)]C_6H_4O-**CH_3**	237.6
	[(*o*-OH)]$C_6H_4OCH_2$-**H**	404.5
12	***m*-hydroxymethoxybenzene (*m*-guaiacol)**	
	[(*m*-OCH_3)]C_6H_4-**OH**	465.7
	[(*m*-OCH_3)]C_6H_4O-**H**	359.1

	[(*m*-OH)]C_6H_5-**OCH_3**	428.0
	[(*m*-OH)]C_6H_4O-**CH_3**	270.5
	[(*m*-OH)]$C_6H_4OCH_2$-**H**	401.1
13	***p*-hydroxymethoxybenzene (*p*-guaiacol)**	
	[(*p*-OCH_3)]C_6H_4-**OH**	464.5
	[(*p*-OCH_3)]C_6H_4O-**H**	343.9
	[(*p*-OH)]C_6H_4-**OCH_3**	426.5
	[(*p*-OH)]C_6H_4O-**CH_3**	252.6
	[(*p*-OH)]$C_6H_4OCH_2$-**H**	402.6
14	***o*-hydroxyformylbenzene**	
	[(*o*-CHO)]C_6H_4-**OH**	502.1
	[(*o*-CHO)]C_6H_4O-**H**	401.9
	[(*o*-OH)]C_6H_4-**CHO**	447.0
	[(*o*-OH)]C_6H_4CO-**H**	387.2
15	***m*-hydroxyformylbenzene**	
	[(*m*-CHO)]C_6H_4-**OH**	471.5
	[(*m*-CHO)]C_6H_4O-**H**	372.8
	[(*m*-OH)]C_6H_4-**CHO**	414.3
	[(*m*-OH)]C_6H_4CO-**H**	373.5
16	***p*-hydroxyformylbenzene**	
	[(*p*-CHO)]C_6H_4-**OH**	473.8
	[(*p*-CHO)]C_6H_4O-**H**	372.3
	[(*p*-OH)]C_6H_4-**CHO**	424.2
	[(*p*-OH)]C_6H_4CO-**H**	370.0
17	***o*-hydroxyvinylbenzene**	
	[(*o*-$CH=CH_2$)]C_6H_4-**OH**	469.0
	[(*o*-$CH=CH_2$)]C_6H_4O-**H**	357.2
	[(*o*-OH)]C_6H_4-**$CH=CH_2$**	485.1
	[(*o*-OH)]C_6H_4C(-**H**)=CH_2	420.2
	[(*o*-OH)]$C_6H_4CH=CH$-**H**(trans)	466.6
	[(*o*-OH)]$C_6H_4CH=CH$-**H**(cis)	448.3
18	***m*-hydroxyvinylbenzene**	
	[(*m*-$CH=CH_2$)]C_6H_4-**OH**	472.2
	[(*m*-$CH=CH_2$)]C_6H_4O-**H**	368.3
	[(*m*-OH)]C_6H_4-**$CH=CH_2$**	483.2
	[(*m*-OH)]C_6H_4C(-**H**)=CH_2	430.4
	[(*m*-OH)]$C_6H_4CH=CH$-**H**(trans)	469.5
	[(*m*-OH)]$C_6H_4CH=CH$-**H**(cis)	465.0
19	***p*-hydroxyvinylbenzene**	
	[(*p*-$CH=CH_2$)]C_6H_4-**OH**	473.2

	[(*p*-CH=CH_2)]C_6H_4O-**H**	351.9
	[(*p*-OH)]C_6H_4-**CH=CH_2**	489.3
	[(*p*-OH)]C_6H_4C(-**H**)=CH_2	431.6
	[(*p*-OH)]C_6H_4CH=CH-**H**(trans)	470.0
	[(*p*-OH)]C_6H_4CH=CH-**H**(cis)	465.1
20	***o*-hydroxymethylbenzene (o-Cresol)**	
	[(*o*-CH_3)]C_6H_4-**OH**	468.4
	[(*o*-CH_3)]C_6H_4O-**H**	358.6
	[(*o*-OH)]C_6H_4-**CH_3**	437.2
	[(*o*-OH)]$C_6H_4CH_2$-**H**	376.1
21	***m*-hydroxymethylbenzene (m-Cresol)**	
	[(*m*-CH_3)]C_6H_4-**OH**	468.0
	[(*m*-CH_3)]C_6H_4O-**H**	365.3
	[(*m*-OH)]C_6H_4-**CH_3**	432.7
	[(*m*-OH)]$C_6H_4CH_2$-**H**	377.1
22	***p*-hydroxymethylbenzene (p-Cresol)**	
	[(*p*-CH_3)]C_6H_4-**OH**	467.8
	[(*p*-CH_3)]C_6H_4O-**H**	359.3
	[(*p*-OH)]C_6H_4-**CH_3**	436.6
	[(*p*-OH)]$C_6H_4CH_2$-**H**	374.4
23	***o*-hydroxyethylbenzene**	
	[(*o*-CH_2CH_3)]C_6H_4-**OH**	466.8
	[(*o*-CH_2CH_3)]C_6H_4O-**H**	357.8
	[(*o*-OH)]C_6H_4-**CH_2CH_3**	431.4
	[(*o*-OH)]C_6H_4CH(-**H**)CH_3	364.5
	[(*o*-OH)]$C_6H_4CH_2$-**CH_3**	323.7
24	***m*-hydroxyethylbenzene**	
	[(*m*-CH_2CH_3)]C_6H_4-**OH**	466.7
	[(*m*-CH_2CH_3)]C_6H_4O-**H**	364.2
	[(*m*-OH)]C_6H_4-**CH_2CH_3**	427.1
	[(*m*-OH)]C_6H_4CH(-**H**)CH_3	363.9
	[(*m*-OH)]$C_6H_4CH_2$-**CH_3**	324.9
25	***p*-hydroxyethylbenzene**	
	[(*p*-CH_2CH_3)]C_6H_5-**OH**	466.6
	[(*p*-CH_2CH_3)]C_6H_5O-**H**	358.6
	[(*p*-OH)]C_6H_4-**CH_2CH_3**	431.1
	[(*p*-OH)]C_6H_4CH(-**H**)CH_3	363.0
	[(*p*-OH)]$C_6H_4CH_2$-**CH_3**	322.3
26	***o*-dimethoxybenzene**	
	[(*o*-OCH_3)]C_6H_4-**OCH_3**	411.2
	[(*o*-OCH_3)]C_6H_4O-**CH_3**	249.1

	[(*o*-OCH_3)]$C_6H_4OCH_2$-**H**	398.6
27	***m*-dimethoxybenzene**	
	[(*m*-OCH_3)]C_6H_4-**OCH_3**	425.5
	[(*m*-OCH_3)]C_6H_4O-**CH_3**	264.3
	[(*m*-OCH_3)]$C_6H_4OCH_2$-**H**	398.2
28	***p*-dimethoxybenzene**	
	[(*p*-OCH_3)]C_6H_4-**OCH_3**	424.5
	[(*p*-OCH_3)]C_6H_4O-**CH_3**	249.3
	[(*p*-OCH_3)]$C_6H_4OCH_2$-**H**	399.9
29	***o*-methoxyformylbenzene**	
	[(*o*-CHO)]C_6H_4-**OCH_3**	428.9
	[(*o*-CHO)]C_6H_4O-**CH_3**	274.1
	[(*o*-CHO)]$C_6H_4OCH_2$-**H**	405.4
	[(*o*-OCH_3)]C_6H_4-**CHO**	408.9
	[(*o*-OCH_3)]C_6H_4CO-**H**	373.8
30	***m*-methoxyformylbenzene**	
	[(*m*-CHO)]C_6H_4-**OCH_3**	433.0
	[(*m*-CHO)]C_6H_4O-**CH_3**	279.7
	[(*m*-CHO)]$C_6H_4OCH_2$-**H**	405.9
	[(*m*-OCH_3)]C_6H_4-**CHO**	413.5
	[(*m*-OCH_3)]C_6H_4CO-**H**	372.1
31	***p*-methoxyformylbenzene**	
	[(*p*-CHO)]C_6H_4-**OCH_3**	434.8
	[(*p*-CHO)]C_6H_4O-**CH_3**	278.7
	[(*p*-CHO)]$C_6H_4OCH_2$-**H**	404.0
	[(*p*-OCH_3)]C_6H_4-**CHO**	423.2
	[(*p*-OCH_3)]C_6H_4CO-**H**	370.6
32	***o*-methoxyvinylbenzene**	
	[(*o*-$CH=CH_2$)]C_6H_4-**OCH_3**	428.5
	[(*o*-$CH=CH_2$)]C_6H_4O-**CH_3**	262.1
	[(*o*-$CH=CH_2$)]$C_6H_4OCH_2$-**H**	405.1
	[(*o*-OCH_3)]C_6H_4-**$CH=CH_2$**	479.7
	[(*o*-OCH_3)]C_6H_4C(-**H**)$=CH_2$	425.0
	[(*o*-OCH_3)]$C_6H_4CH=CH$-**H**(trans)	464.2
	[(*o*-OCH_3)]$C_6H_4CH=CH$-**H**(cis)	463.3
33	***m*-methoxyvinylbenzene**	
	[(*m*-$CH=CH_2$)]C_6H_4-**OCH_3**	432.3
	[(*m*-$CH=CH_2$)]C_6H_4O-**CH_3**	273.8
	[(*m*-$CH=CH_2$)]$C_6H_4OCH_2$-**H**	405.4
	[(*m*-OCH_3)]C_6H_4-**$CH=CH_2$**	481.0
	[(*m*-OCH_3)]C_6H_4C(-**H**)$=CH_2$	427.4

	[(*m*-OCH_3)]C_6H_4CH=CH-**H**(trans)	467.1
	[(*m*-OCH_3)]C_6H_4CH=CH-**H**(cis)	462.5
34	***p*-methoxyvinylbenzene**	
	[(*p*-$CH=CH_2$)]C_6H_4-**OCH_3**	433.2
	[(*p*-$CH=CH_2$)]C_6H_4O-**CH_3**	257.3
	[(*p*-$CH=CH_2$)]$C_6H_4OCH_2$-**H**	405.7
	[(*p*-OCH_3)]C_6H_4-**$CH=CH_2$**	487.3
	[(*p*-OCH_3)]C_6H_4C(-**H**)=CH_2	429.0
	[(*p*-OCH_3)]C_6H_4CH=CH-**H**(trans)	467.6
	[(*p*-OCH_3)]C_6H_4CH=CH-**H**(cis)	462.7
35	***o*-methoxymethylbenzene**	
	[(*o*-CH_3)]C_6H_4-**OCH_3**	432.5
	[(*o*-CH_3)]C_6H_4O-**CH_3**	264.2
	[(*o*-CH_3)]$C_6H_4OCH_2$-**H**	401.3
	[(*o*-OCH_3)]C_6H_4-**CH_3**	432.5
	[(*o*-OCH_3)]$C_6H_4CH_2$-**H**	373.2
36	***m*-methoxymethylbenzene**	
	[(*m*-CH_3)]C_6H_4-**OCH_3**	427.4
	[(*m*-CH_3)]C_6H_4O-**CH_3**	270.1
	[(*m*-CH_3)]$C_6H_4OCH_2$-**H**	400.4
	[(*m*-OCH_3)]C_6H_4-**CH_3**	429.8
	[(*m*-OCH_3)]$C_6H_4CH_2$-**H**	374.3
37	***p*-methoxymethylbenzene**	
	[(*p*-CH_3)]C_6H_4-**OCH_3**	427.7
	[(*p*-CH_3)]C_6H_4O-**CH_3**	264.6
	[(*p*-CH_3)]$C_6H_4OCH_2$-**H**	401.8
	[(*p*-OCH_3)]C_6H_4-**CH_3**	434.5
	[(*p*-OCH_3)]$C_6H_4CH_2$-**H**	372.4
38	***o*-methoxyethylbenzene**	
	[(*o*-CH_2CH_3)]C_6H_4-**OCH_3**	427.1
	[(*o*-CH_2CH_3)]C_6H_4O-**CH_3**	263.5
	[(*o*-CH_2CH_3)]$C_6H_4OCH_2$-**H**	399.5
	[(*o*-OCH_3)]C_6H_4-**CH_2CH_3**	426.8
	[(*o*-OCH_3)]C_6H_4CH(-**H**)CH_3	361.5
	[(*o*-OCH_3)]$C_6H_4CH_2$-**CH_3**	320.9
39	***m*-methoxyethylbenzene**	
	[(*m*-CH_2CH_3)]C_6H_4-**OCH_3**	426.1
	[(*m*-CH_2CH_3)]C_6H_4O-**CH_3**	269.0
	[(*m*-CH_2CH_3)]$C_6H_4OCH_2$-**H**	399.4
	[(*m*-OCH_3)]C_6H_4-**CH_2CH_3**	424.2
	[(*m*-OCH_3)]C_6H_4CH(-**H**)CH_3	362.2

	[(*m*-OCH_3)]$C_6H_4CH_2$-**CH_3**	322.1
40	***p*-methoxyethylbenzene**	
	[(*p*-CH_2CH_3)]C_6H_4-**OCH_3**	426.4
	[(*p*-CH_2CH_3)]C_6H_4O-**CH_3**	263.8
	[(*p*-CH_2CH_3)]$C_6H_4OCH_2$-**H**	400.5
	[(*p*-OCH_3)]C_6H_4-**CH_2CH_3**	428.9
	[(*p*-OCH_3)]C_6H_4CH(-**H**)CH_3	361.1
	[(*p*-OCH_3)]$C_6H_4CH_2$-**CH_3**	320.2
41	***o*-diformylbenzene**	
	[(*o*-CHO)]C_6H_4-**CHO**	399.3
	[(*o*-CHO)]C_6H_4CO-**H**	267.2
42	***m*-diformylbenzene**	
	[(*m*-CHO)]C_6H_4-**CHO**	413.4
	[(*m*-CHO)]C_6H_4CO-**H**	372.1
43	***p*-diformylbenzene**	
	[(*p*-CHO)]C_6H_4-**CHO**	411.0
	[(*p*-CHO)]C_6H_4CO-**H**	372.0
44	***o*-formylvinylbenzene**	
	[(*o*-$CH=CH_2$)]C_6H_4-**CHO**	406.6
	[(*o*-$CH=CH_2$)]C_6H_4CO-**H**	368.8
	[(*o*-CHO)]C_6H_4-**$CH=CH_2$**	477.8
	[(*o*-CHO)]C_6H_4C(-**H**)$=CH_2$	416.4
	[(*o*-CHO)]$C_6H_4CH=CH$-**H**(trans)	472.5
	[(*o*-CHO)]$C_6H_4CH=CH$-**H**(cis)	465.0
45	***m*-formylvinylbenzene**	
	[(*m*-$CH=CH_2$)]C_6H_4-**CHO**	418.3
	[(*m*-$CH=CH_2$)]C_6H_4CO-**H**	371.2
	[(*m*-CHO)]C_6H_4-**$CH=CH_2$**	486.5
	[(*m*-CHO)]C_6H_4C(-**H**)$=CH_2$	427.6
	[(*m*-CHO)]$C_6H_4CH=CH$-**H**(trans)	470.7
	[(*m*-CHO)]$C_6H_4CH=CH$-**H**(cis)	466.5
46	***p*-formylvinylbenzene**	
	[(*p*-$CH=CH_2$)]C_6H_4-**CHO**	420.3
	[(*p*-$CH=CH_2$)]C_6H_4CO-**H**	378.5
	[(*p*-CHO)]C_6H_4-**$CH=CH_2$**	486.0
	[(*p*-CHO)]C_6H_4C(-**H**)$=CH_2$	417.8
	[(*p*-CHO)]$C_6H_4CH=CH$-**H**(trans)	471.4
	[(*p*-CHO)]$C_6H_4CH=CH$-**H**(cis)	466.6
47	***o*-formylmethylbenzene**	
	[(*o*-CH_3)]C_6H_4-**CHO**	408.7
	[(*o*-CH_3)]C_6H_4CO-**H**	368.3

	[(*o*-CHO)]C_6H_4-**CH_3**	432.6
	[(*o*-CHO)]$C_6H_4CH_2$-**H**	374.1
48	***m*-formylmethylbenzene**	
	[(*m*-CH_3)]C_6H_4-**CHO**	415.0
	[(*m*-CH_3)]C_6H_4CO-**H**	372.2
	[(*m*-CHO)]C_6H_4-**CH_3**	436.9
	[(*m*-CHO)]$C_6H_4CH_2$-**H**	378.0
49	***p*-formylmethylbenzene**	
	[(*p*-CH_3)]C_6H_4-**CHO**	418.0
	[(*p*-CH_3)]C_6H_4CO-**H**	371.9
	[(*p*-CHO)]C_6H_4-**CH_3**	436.4
	[(*p*-CHO)]$C_6H_4CH_2$-**H**	372.9
50	***o*-formylethylbenzene**	
	[(*o*-CH_2CH_3)]C_6H_4-**CHO**	407.0
	[(*o*-CH_2CH_3)]C_6H_4CO-**H**	365.7
	[(*o*-CHO)]C_6H_4-**CH_2CH_3**	426.7
	[(*o*-CHO)]C_6H_4CH(-**H**)CH_3	362.8
	[(*o*-CHO)]$C_6H_4CH_2$-**CH_3**	321.6
51	***m*-formylethylbenzene**	
	[(*m*-CH_2CH_3)]C_6H_4-**CHO**	413.5
	[(*m*-CH_2CH_3)]C_6H_4CO-**H**	370.6
	[(*m*-CHO)]C_6H_4-**CH_2CH_3**	431.1
	[(*m*-CHO)]C_6H_4CH(-**H**)CH_3	364.4
	[(*m*-CHO)]$C_6H_4CH_2$-**CH_3**	325.6
52	***p*-formylethylbenzene**	
	[(*p*-CH_2CH_3)]C_6H_4-**CHO**	416.4
	[(*p*-CH_2CH_3)]C_6H_4CO-**H**	370.3
	[(*p*-CHO)]C_6H_4-**CH_2CH_3**	430.5
	[(*p*-CHO)]C_6H_4CH(-**H**)CH_3	365.0
	[(*p*-CHO)]$C_6H_4CH_2$-**CH_3**	320.4
53	***o*-divinylbenzene**	
	[(*o*-$CH=CH_2$)]C_6H_4-**$CH=CH_2$**	478.3
	[(*o*-$CH=CH_2$)]C_6H_4C(-**H**)=CH_2	417.3
	[(*o*-$CH=CH_2$)]$C_6H_4CH=CH$-**H**(trans)	468.8
	[(*o*-$CH=CH_2$)]$C_6H_4CH=CH$-**H**(cis)	464.3
54	***m*-divinylbenzene**	
	[(*m*-$CH=CH_2$)]C_6H_4-**$CH=CH_2$**	487.7
	[(*m*-$CH=CH_2$)]C_6H_4C(-**H**)=CH_2	426.6
	[(*m*-$CH=CH_2$)]$C_6H_4CH=CH$-**H**(trans)	473.1
	[(*m*-$CH=CH_2$)]$C_6H_4CH=CH$-**H**(cis)	468.8
55	***p*-divinylbenzene**	

	[(*p*-CH=CH_2)]C_6H_4-**CH=CH_2**	489.6
	[(*p*-CH=CH_2)]C_6H_4C(-**H**)=CH_2	418.6
	[(*p*-CH=CH_2)]C_6H_4CH=CH-**H**(trans)	473.9
	[(*p*-CH=CH_2)]C_6H_4CH=CH-**H**(cis)	469.5
56	***o*-vinylmethylbenzene**	
	[(*o*-CH_3)]C_6H_4-**CH=CH_2**	477.8
	[(*o*-CH_3)]C_6H_4C(-**H**)=CH_2	416.9
	[(*o*-CH_3)]C_6H_4CH=CH-**H**(trans)	469.0
	[(*o*-CH_3)]C_6H_4CH=CH-**H**(cis)	463.0
	[(*o*-CH=CH_2)]C_6H_4-**CH_3**	430.5
	[(*o*-CH=CH_2)]$C_6H_4CH_2$-**H**	375.8
57	***m*-vinylmethylbenzene**	
	[(*m*-CH_3)]C_6H_4-**CH=CH_2**	483.2
	[(*m*-CH_3)]C_6H_4C(-**H**)=CH_2	425.8
	[(*m*-CH_3)]C_6H_4CH=CH-**H**(trans)	468.3
	[(*m*-CH_3)]C_6H_4CH=CH-**H**(cis)	464.7
	[(*m*-CH=CH_2)]C_6H_4-**CH_3**	436.9
	[(*m*-CH=CH_2)]$C_6H_4CH_2$-**H**	378.0
58	***p*-vinylmethylbenzene**	
	[(*p*-CH_3)]C_6H_4-**CH=CH_2**	485.4
	[(*p*-CH_3)]C_6H_4C(-**H**)=CH_2	425.2
	[(*p*-CH_3)]C_6H_4CH=CH-**H**(cis)	469.5
	[(*p*-CH_3)]C_6H_4CH=CH-**H**(trans)	465.0
	[(*p*-CH=CH_2)]C_6H_4-**CH_3**	438.1
	[(*p*-CH=CH_2)]$C_6H_4CH_2$-**H**	370.9
59	***o*-vinylethylbenzene**	
	[(*o*-CH_2CH_3)]C_6H_4-**CH=CH_2**	476.6
	[(*o*-CH_2CH_3)]C_6H_4C(-**H**)=CH_2	415.9
	[(*o*-CH_2CH_3)]C_6H_4CH=CH-**H**(trans)	466.2
	[(*o*-CH_2CH_3)]C_6H_4CH=CH-**H**(cis)	462.3
	[(*o*-CH=CH_2)]C_6H_4-**CH_2CH_3**	425.1
	[(*o*-CH=CH_2)]C_6H_4CH(-**H**)CH_3	365.4
	[(*o*-CH=CH_2)]$C_6H_4CH_2$-**CH_3**	323.8
60	***m*-vinylethylbenzene**	
	[(*m*-CH_2CH_3)]C_6H_4-**CH=CH_2**	481.9
	[(*m*-CH_2CH_3)]C_6H_4C(-**H**)=CH_2	423.7
	[(*m*-CH_2CH_3)]C_6H_4CH=CH-**H**(trans)	467.9
	[(*m*-CH_2CH_3)]C_6H_4CH=CH-**H**(cis)	462.3
	[(*m*-CH=CH_2)]C_6H_4-**CH_2CH_3**	431.3
	[(*m*-CH=CH_2)]C_6H_4CH(-**H**)CH_3	365.4
	[(*m*-CH=CH_2)]$C_6H_4CH_2$-**CH_3**	325.8

61	***p*-vinylethylbenzene**	
	[(*p*-CH_2CH_3)]C_6H_4-**CH=CH_2**	484.0
	[(*p*-CH_2CH_3)]C_6H_4C(-**H**)=CH_2	423.8
	[(*p*-CH_2CH_3)]C_6H_4CH=CH-**H**(trans)	468.1
	[(*p*-CH_2CH_3)]C_6H_4CH=CH-**H**(cis)	463.5
	[(*p*-CH=CH_2)]C_6H_4-**CH_2CH_3**	432.4
	[(*p*-CH=CH_2)]C_6H_4CH(-**H**)CH_3	358.8
	[(*p*-CH=CH_2)]$C_6H_4CH_2$-**CH_3**	318.6
62	***o*-dimethylbenzene (o-Xylene)**	
	[(*o*-CH_3)]C_6H_4-**CH_3**	429.3
	[(*o*-CH_3)]$C_6H_4CH_2$-**H**	374.5
63	***m*-dimethylbenzene (m-Xylene)**	
	[(*m*-CH_3)]C_6H_4-**CH_3**	431.7
	[(*m*-CH_3)]$C_6H_4CH_2$-**H**	375.0
64	***p*-dimethylbenzene (p-Xylene)**	
	[(*p*-CH_3)]C_6H_4-**CH_3**	433.3
	[(*p*-CH_3)]$C_6H_4CH_2$-**H**	374.9
65	***o*-methylethylbenzene**	
	[(*o*-CH_2CH_3)]C_6H_4-**CH_3**	426.7
	[(*o*-CH_2CH_3)]$C_6H_4CH_2$-**H**	373.5
	[(*o*-CH_3)]C_6H_4-**CH_2CH_3**	422.5
	[(*o*-CH_3)]C_6H_4CH(-**H**)CH_3	362.6
	[(*o*-CH_3)]$C_6H_4CH_2$-**CH_3**	321.0
66	***m*-methylethylbenzene**	
	[(*m*-CH_2CH_3)]C_6H_4-**CH_3**	430.4
	[(*m*-CH_2CH_3)]$C_6H_4CH_2$-**H**	374.4
	[(*m*-CH_3)]C_6H_4-**CH_2CH_3**	426.1
	[(*m*-CH_3)]C_6H_4CH(-**H**)CH_3	362.9
	[(*m*-CH_3)]$C_6H_4CH_2$-**CH_3**	322.8
67	***p*-methylethylbenzene**	
	[(*p*-CH_2CH_3)]C_6H_4-**CH_3**	432.0
	[(*p*-CH_2CH_3)]$C_6H_4CH_2$-**H**	373.7
	[(*p*-CH_3)]C_6H_4-**CH_2CH_3**	427.7
	[(*p*-CH_3)]C_6H_4CH(-**H**)CH_3	345.1
	[(*p*-CH_3)]$C_6H_4CH_2$-**CH_3**	322.7
68	***o*-diethylbenzene**	
	[(*o*-CH_2CH_3)]C_6H_4-**CH_2CH_3**	419.5
	[(*o*-CH_2CH_3)]C_6H_4CH(-**H**)CH_3	361.6
	[(*o*-CH_2CH_3)]$C_6H_4CH_2$-**CH_3**	319.7
69	***m*-diethylbenzene**	
	[(*m*-CH_2CH_3)]C_6H_4-**CH_2CH_3**	424.9

	[(*m*-CH_2CH_3)]C_6H_4CH(-**H**)CH_3	362.5
	[(*m*-CH_2CH_3)]$C_6H_4CH_2$-**CH_3**	322.3
70	***p*-diethylbenzene**	
	[(*p*-CH_2CH_3)]C_6H_4-**CH_2CH_3**	426.4
	[(*p*-CH_2CH_3)]C_6H_4CH(-**H**)CH_3	361.7
	[(*p*-CH_2CH_3)]$C_6H_4CH_2$-**CH_3**	321.5

B.5 Experimental Validation of G4/BAC Data

Experimental validation of the G4/BAC data is made through the comparison of the BDE values calculated with G4/BAC method with the available experimental data. All the reported experimental BDE data in Luo's handbook and the cited literature [2-29] are plotted against the G4/BAC data in **Figure B-15**. In **Figure B-16**, the deviations of the G4/BAC data from the literature values are plotted against G4/BAC data for bond strengths.

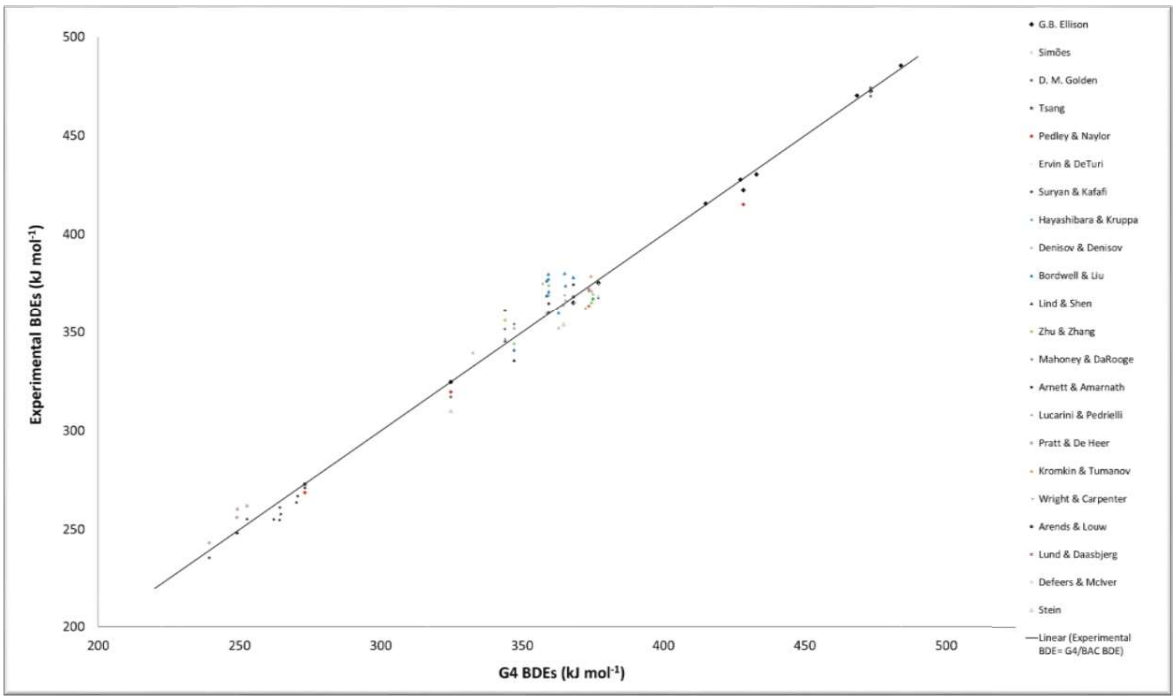

Figure B-15 Reported experimental BDE data in the literature plotted against G4/BAC data in the present study. Color code (shown on the right) is used to depict the references for the studies from where the data is taken [2-29].

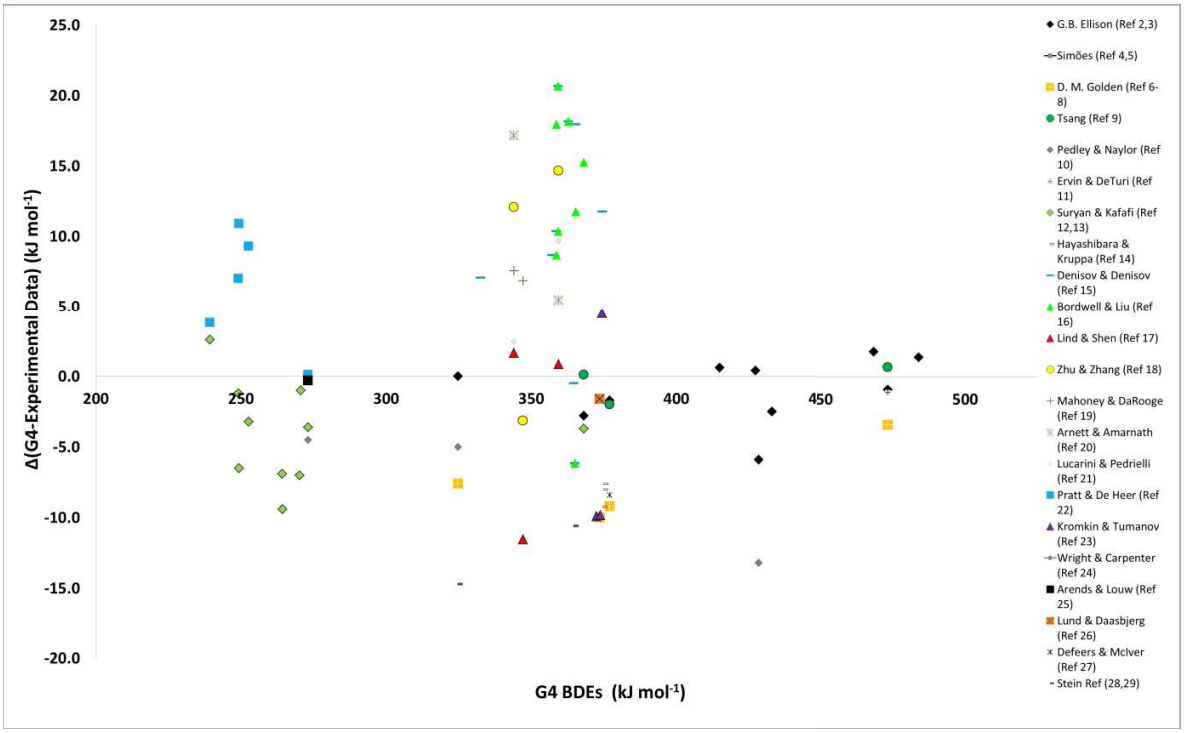

Figure B-16 Plot of the deviation of the G4/BAC data from the reported experimental values for the BDEs of the bonds in monocyclic aromatic hydrocarbons (MAHs) against G4/BAC data [2-29].

B.6 The BDE Analysis: Bond Dissociation Energy Plots

The objective of BDE Analysis is to identify substituent interactions in monocyclic aromatic radicals. This analysis uses the change of BDEs upon addition of a substituent group (ΔBDE). With the following relation, one uses the BDE analysis to identify the substituent effects in the MARs, i.e. $NNI_{Radical}$:

$\Delta BDE = NNI_{Parent} - NNI_{Radical}$ (See **Chapter 4** for the derivation of this relation)

Here, the ΔBDEs are calculated in the present study and the NNI_{Parent} values are taken from Chapter 3 [1]. The ΔBDE plots which are not shown in the manuscript are presented in this subsection in **Figure B-17**, **Figure B-24** and **Figure B-26**. In **Figure B-18 – Figure B-22**, **Figure B-27** and **Figure B-28**, the BDEs of various bonds are plotted for varying substituent groups.

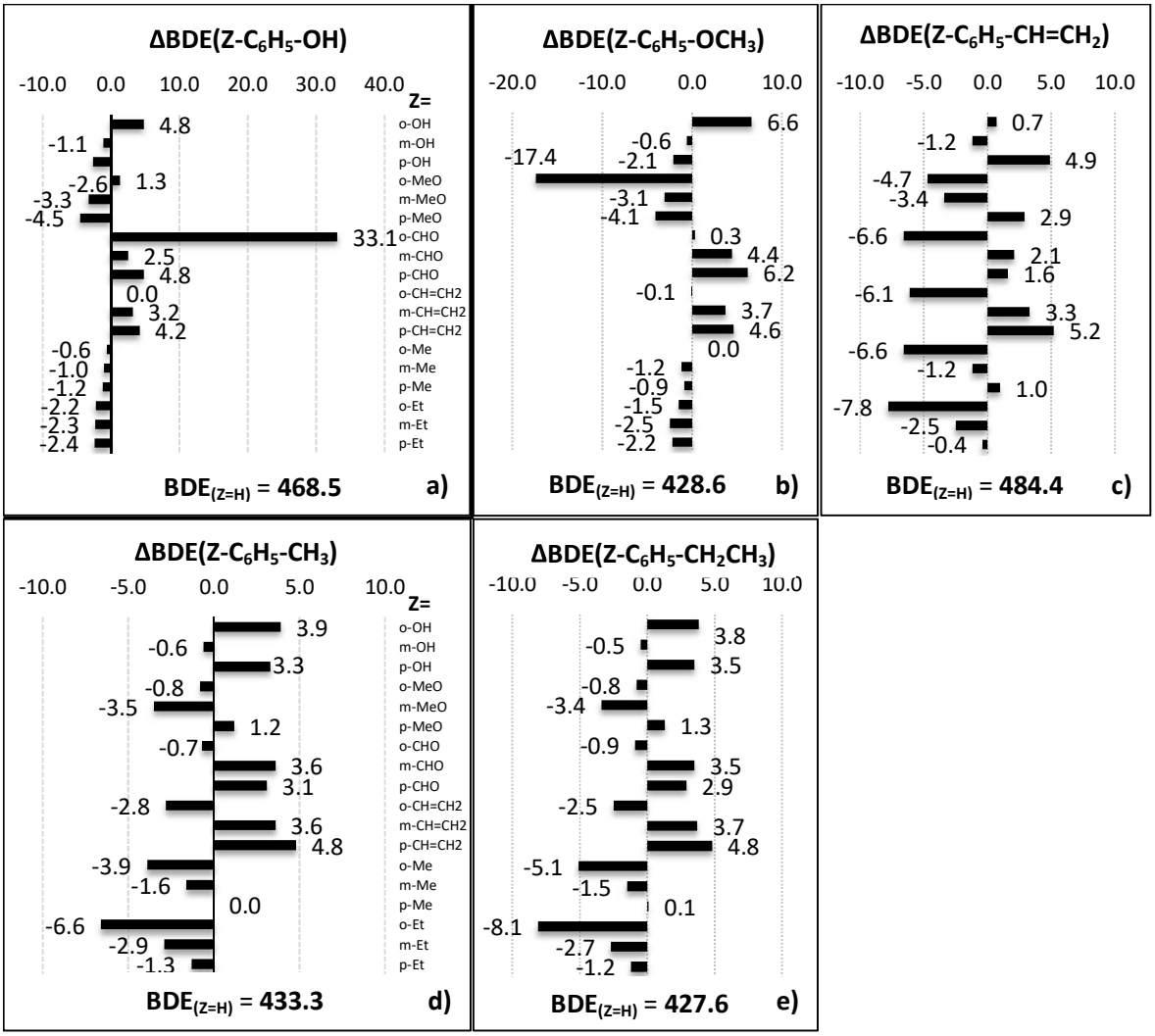

Figure B-17 ΔBDE (= BDE_Z – BDE_H) for the bonds in substituted C_6H_4-X molecules, where: X= **a)** -OH, **b)** -OCH_3, **c)** -$CH{=}CH_2$, **d)** -CH_3 and **e)** -CH_2CH_3 for various Z groups. Below each plot, the BDEs of the bonds in unsubstituted MAHs ($BDE_{(Z=H)}$) are given. See text for the details regarding the definition of ΔBDEs. Note that the scale of the x-axis differs for the different bonds. All units are kJ mol^{-1}.

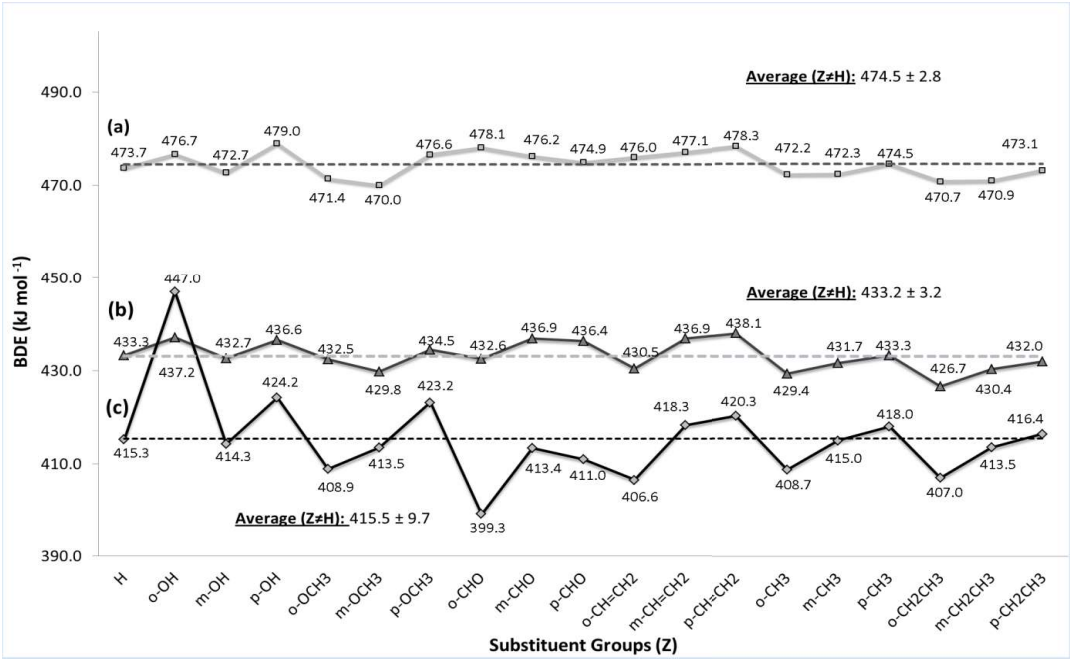

Figure B-18 BDEs for the bonds in substituted Z-C_6H_4-X molecules with X= -H **(a)**, -CH_3 **(b)**, and -CHO **(c)**. The average values do not include the unsubstituted case (Z = H). Units are in kJ mol^{-1}.

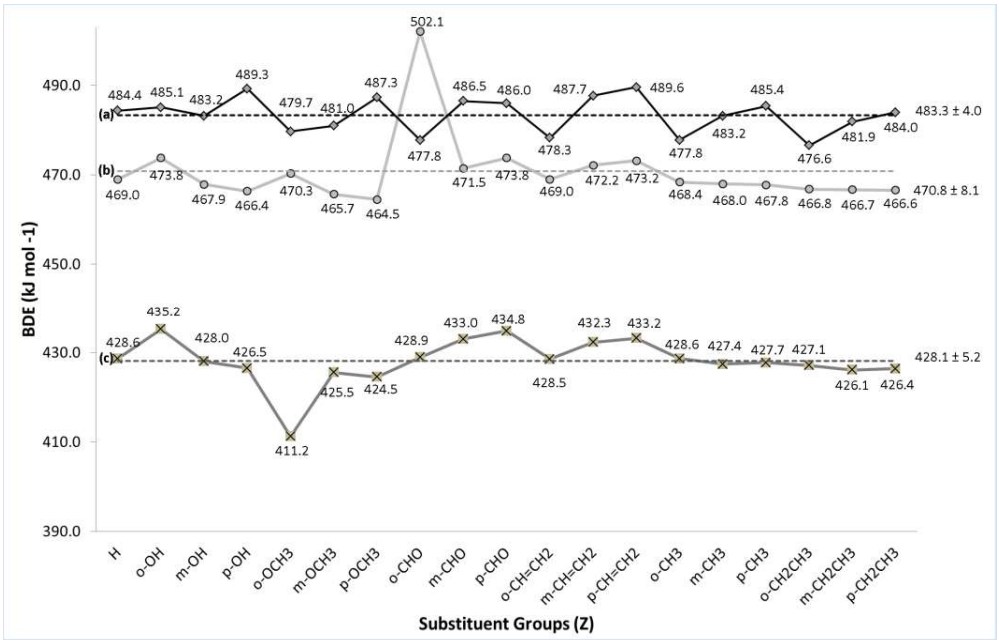

Figure B-19 BDEs of substituted Z-C_6H_4-X molecules with X= $CH=CH_2$ **(a)**, OH **(b)**, and OCH_3 **(c)**. The average values do not include the unsubstituted case (Z = H). Units are in kJ mol^{-1}.

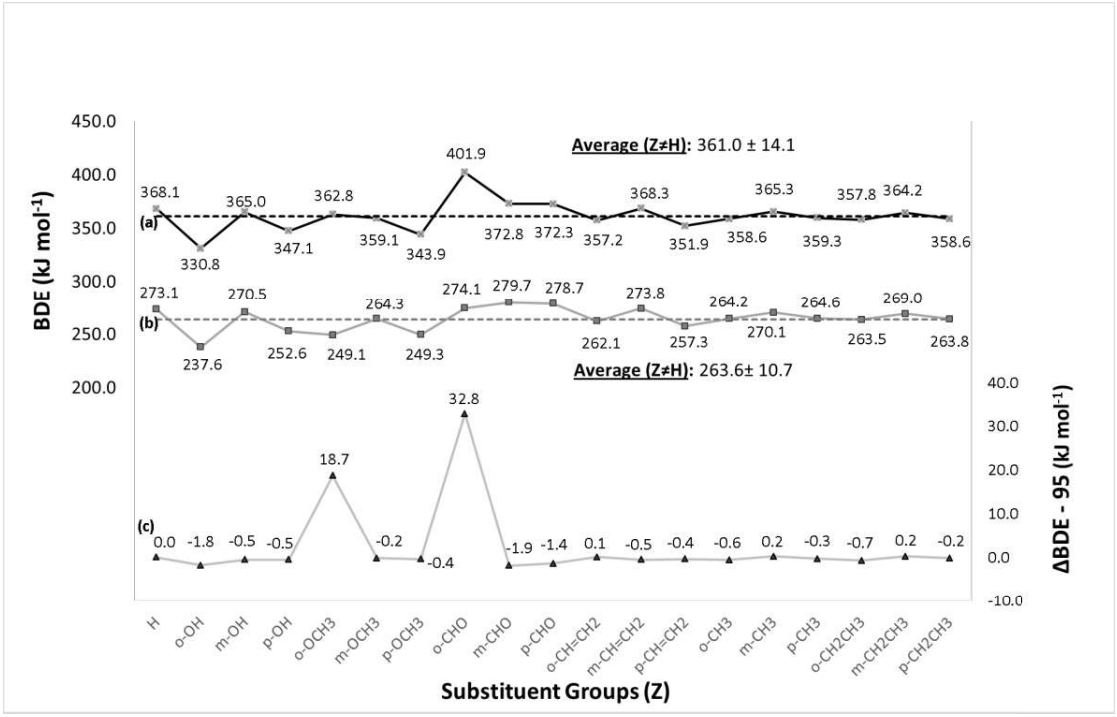

Figure B-20 BDEs for the Z-C_6H_4O-H (trace **(a)**) and Z-C_6H_4O-CH_3 (trace **(b)**) bonds in unsubstituted and substituted phenols and anisoles. Trace **(c)** presents the difference between two traces **a)** and **b)** corrected by 95 kJ mol^{-1} (the difference between the Z = H cases). The average values do not include the unsubstituted case (Z = H). Units are in kJ mol^{-1}.

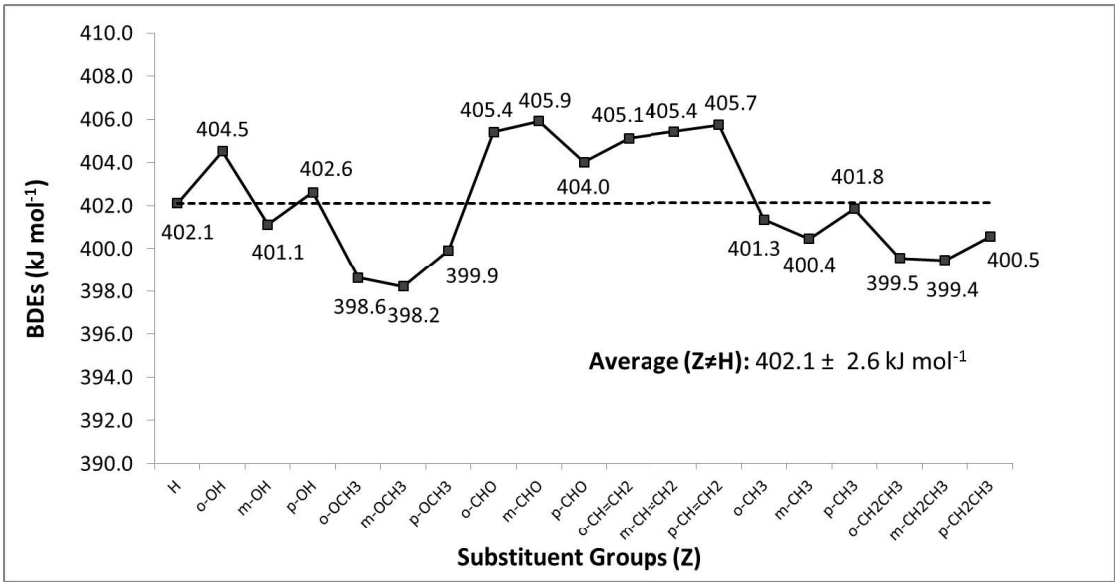

Figure B-21 BDE changes for Z-$C_6H_4OCH_2$-H bonds in substituted anisoles with respect to varying Z groups. The average value does not include the unsubstituted case (Z = H). Units are in kJ mol^{-1}.

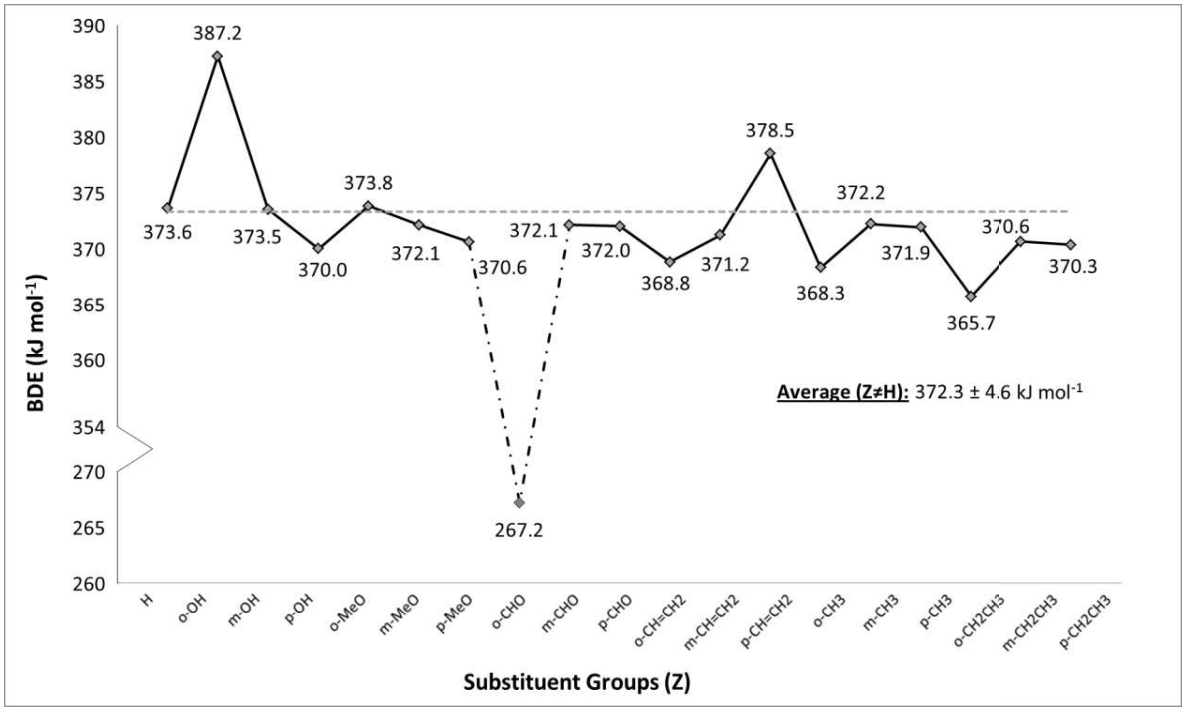

Figure B-22 BDE changes for Z-$C_6H_4C(=O)$-H bonds in substituted benzaldehydes with respect to varying Z substituents. The average value does not include the unsubstituted (Z = H) and the outlier case (Z = *o*-CHO). Units are in kJ mol^{-1}.

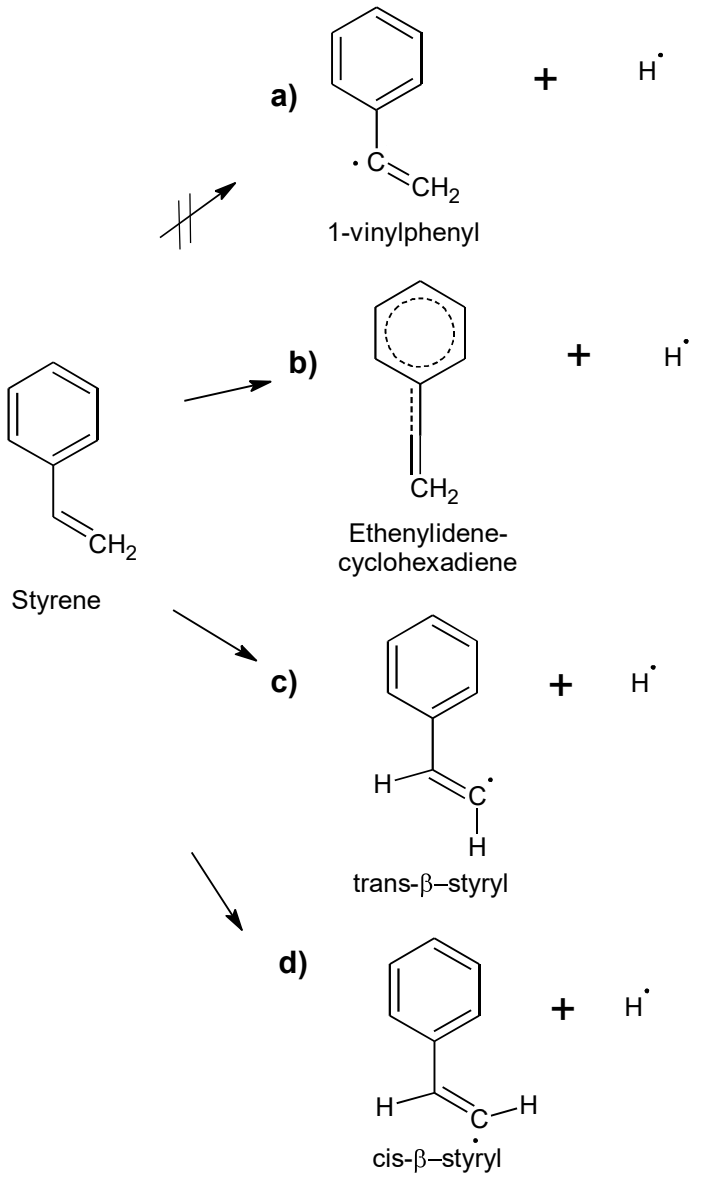

Figure B-23 Prototypical reactions that yield **a)** α-styryl ($C_5H_5C\bullet{=}CH_2$), **b)** ethenylidene-cyclohexadiene, **c)** trans-β-styryl (t-β-styryl) and **d)** cis-β-styryl (c-β-styryl) radicals.

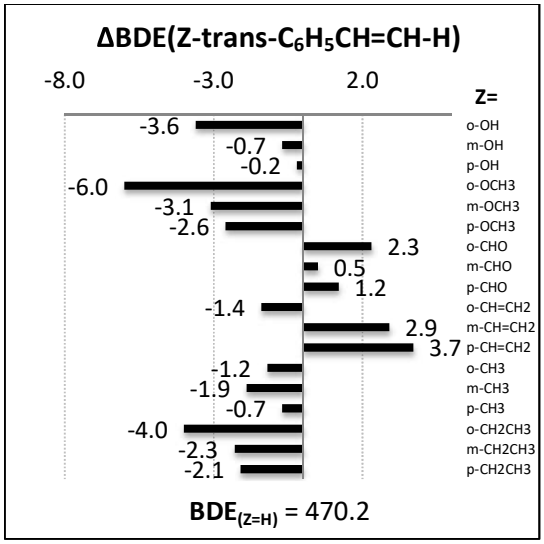

Figure B-24 ΔBDEs (= BDE_Z – BDE_H) for Z-trans-C_6H_4CH=CH-H for 18 different Z groups. Below the plot, the BDE of the bond in unsubstituted styrene ($BDE_{(Z=H)}$) is given. See text for the details regarding the definition of ΔBDEs. Note that the scale of the x-axis differs for the different bonds. All units are kJ mol^{-1}.

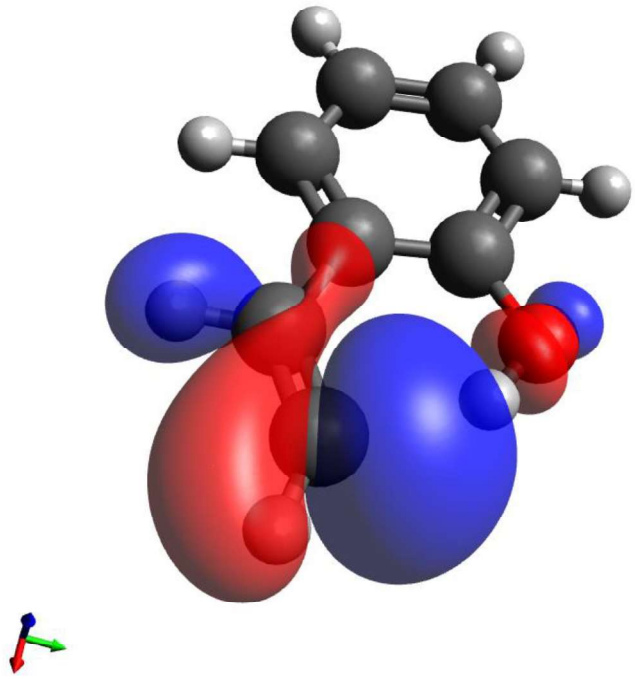

Figure B-25 3D molecular orbital representation of the substituent interaction in *o*-OH substituted trans-*β*-styryl radical.

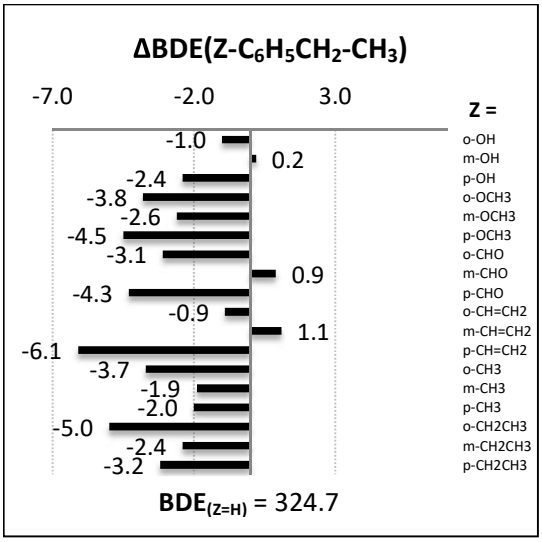

Figure B-26 ΔBDEs (= $BDE_Z - BDE_H$) for Z-$C_6H_4CH_2$-CH_3 for 18 different Z groups. Below the plot, the BDE of the bond in unsubstituted ethyl benzene ($BDE_{(Z=H)}$) is given. See text for the details regarding the definition of ΔBDEs. Note that the scale of the x-axis differs for the different bonds. All units are kJ mol^{-1}.

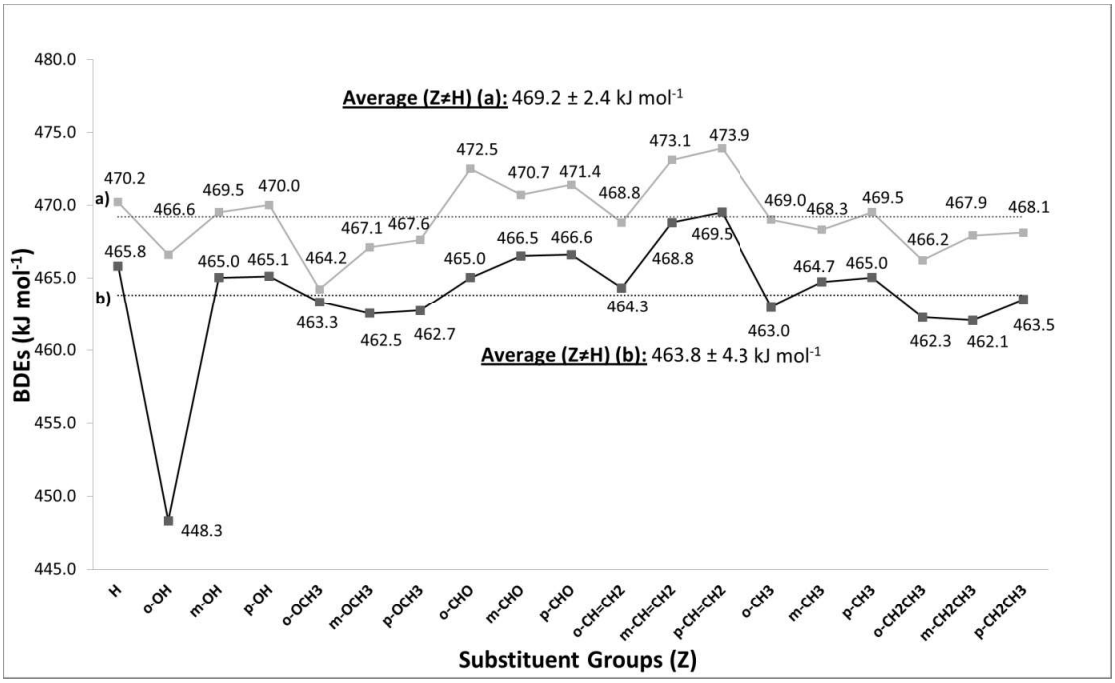

Figure B-27 The variation of BDEs with respect to varying Z groups in cases where **a)** Z-cis-$C_6H_4CH{=}CH\bullet$ (dissociation of the trans C-H bond in styrene) and **b)** Z-trans-$C_6H_4CH{=}CH\bullet$ (dissociation of the cis C-H bond in styrene) is formed. The average values do not include the unsubstituted case (Z = H).

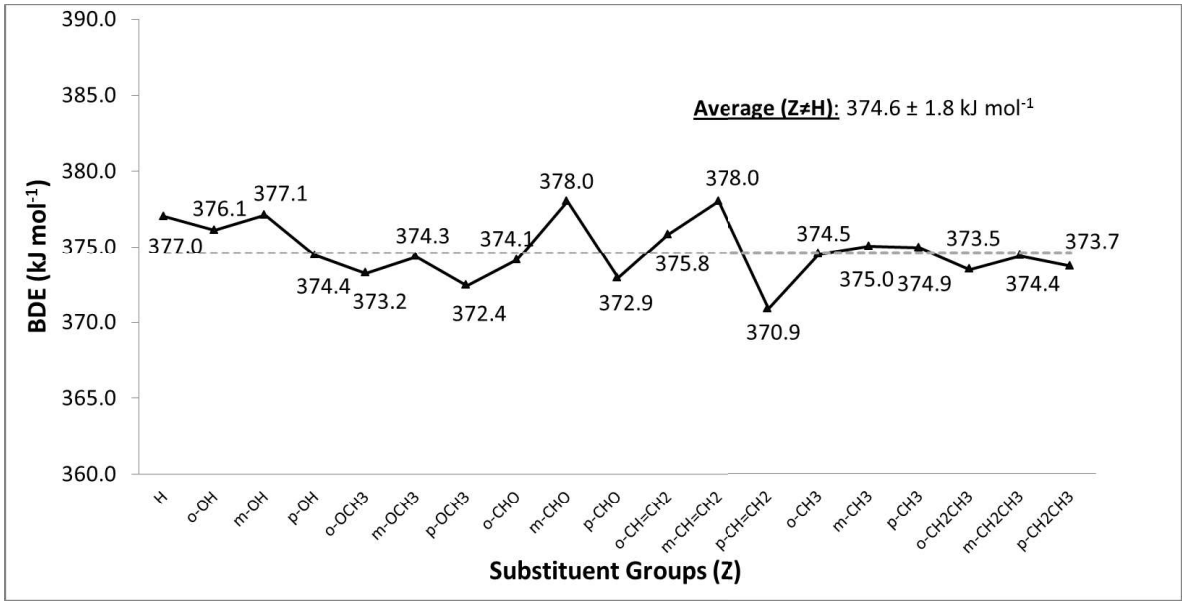

Figure B-28 BDE changes for Z-$C_6H_4CH_2$-H bonds in substituted toluenes with respect to varying Z groups. The average values do not include the unsubstituted case (Z = H).

B.7 Definition and Physical Origins of the Non-Nearest Neighbor Interactions

The physical origins of the substituent effects in MARs and the definition of these NNIs are given in **Table B-6**.

Table B-6 Definitions of NNIs for the prediction of thermodynamic properties in MARs and an explanation of the cause of the interaction.

NNI #	Interaction	Contributing Physical Effects
Anisyl Radicals ($C_6H_4OCH_2$•) + Substituent		
NNI1	$C_6H_4OCH_2$• — *p*-OH/OCH_3	* destabilizing mesomeric effects +M (OCH_2•) with +M (OH)
NNI2	$C_6H_4OCH_2$• — *o*-CHO	* destabilizing neighboring electron withdrawing groups (-I effects)
NNI3	$C_6H_4OCH_2$• — *o*-OCH_3	* destabilizing anomeric effect (Lone Pair Repulsion)
Phenoxyl Radicals (C_6H_4O•) + Substituent		
NNI4	C_6H_4O• — *o*-OH	* Hydrogen bond * stabilizing mesomeric effects +M (OH) with -M (C_6H_5O•)
NNI5	C_6H_4O• — *o*-OCH_3	* stabilizing mesomeric effects +M (OCH_3) with -M (C_6H_5O•) * steric interaction
NNI6	C_6H_4O• — *m*-OCH_3	* likely a combination of inductive and electrostatic effects because the orientation of the OCH_3 group is crucial
NNI7	C_6H_4O• — *p*-OH/OCH_3	* stabilizing mesomeric effects +M (OH/OCH_3) with -M (C_6H_5O•)
NNI8	C_6H_4O• — *o*-CHO	* steric interaction * destabilizing mesomeric effects -M (CHO) with -M (C_6H_5O•)
NNI9	C_6H_5O• — *m*-CHO	* destabilizing inductive effects -I (OCH_3) with -I (C_6H_5O•)
NNI10	C_6H_4O• — *o*-CH=CH_2	* destabilizing steric interaction * stabilizing mesomeric effects +M (CH=CH_2) with -M (C_6H_5O•)
NNI11	C_6H_4O• — *p*-CH=CH_2	* stabilizing mesomeric effects +M (CH=CH_2) with -M (C_6H_5O•)
NNI12	C_6H_4O• — *o*-CH_3/CH_2CH_3	* hyperconjugation
NNI13	C_6H_4O• — *p*-CH_3/CH_2CH_3	* hyperconjugation
Benzoyl Radicals (C_6H_4C•=O) + Substituent		
NNI14	C_6H_4C•=O — *o*-OH	* stabilizing mesomeric effects +M (OH) with -M (C•=O) * H-bond

NNI15	$C_6H_4C•=O$ — *p*-OH/OCH_3	* stabilizing mesomeric effects +M (OH) with -M (C•=O)
NNI16	$C_6H_4C•=O$ — *o*-OCH_3	* destabilizing anomeric effect (Repulsion between lone pair and single electron on (C•=O))
NNI17	$C_6H_4C•=O$ — *m*-CHO	* destabilizing inductive effects -I (CHO) with -I (C•=O) similar to m-CHO—CHO[1]
NNI18	$C_6H_4C•=O$ — *p*-CHO	* destabilizing inductive effects -I (CHO) with -I (C•=O) * destabilizing mesomeric effects -M (CHO) with -M (C•=O)
NNI19	$C_6H_4C•=O$ — *o*-$CH=CH_2$	* weak steric interaction * destabilizing mesomeric effects -M ($CH=CH_2$) with -M (C•=O)
Styryl Radicals ($C_6H_4CH=CH•$) + Substituent		
NNI20	trans-$C_6H_4CH=CH•$ — *o*-OH	* 3-center, 3-electron bond (O-H---C•)
NNI21	trans/cis-$C_6H_4CH=CH•$ — *o*-CHO	* steric interaction
NNI22	trans/cis-$C_6H_4CH=CH•$) — *o*-$CH=CH_2$	* steric interaction
NNI23	trans/cis-$C_6H_4CH=CH•$) — *o*-CH_3/CH_2CH_3	* steric interaction
NNI24	cis-$C_6H_4CH=CH•$	* cis correction
Benzyl ($C_6H_4CH=CH•$)/ 1-Phenylethyl Radicals ($C_6H_4C•HCH_3$) + Substituent		
NNI25	$C_6H_4CH_2•$/$C_6H_5C•HCH_3$ — *p*-$CH=CH_2$	* stabilizing mesomeric effects -M ($CH=CH_2$) with +M ($C_6H_5C•$)
NNI26	$C_6H_4CH_2•$/$C_6H_5C•HCH_3$ — *o*-$CH=CH_2$	* steric interaction preventing resonance
NNI27	$C_6H_4CH_2•$/$C_6H_5C•HCH_3$ — *p*-CHO	* stabilizing mesomeric effects -M (CHO) with +M ($C_6H_5C•$)
NNI28	$C_6H_4CH_2•$/$C_6H_5C•HCH_3$ — *o*-CHO	* steric interaction
NNI29	*o*-$C_6H_4CH_2•$—CH_3/CH_2CH_3 *o*-$C_6H_4CH•CH_3$— CH_3/CH_2CH_3	* steric interaction restricting internal rotation * hyperconjugation

B.8 Initial Determination of GAV and NNI Parameters

As described in the paper, the GAV and the NNI parameters are determined simultaneously based on a least squares linear regression minimization procedure of the differences between Group Additivity calculations and the first principles data for the reference thermochemical database that possess 316 MARs. The NNIs that account for the substituent interactions between nonradical substituents are defined in **Chapter 3**. These NNIs are provided below in **Table B-7**.

The GAVs and the NNIs that are obtained from the linear regression are tabulated in **Table B-8** and **Table B-9**, respectively. The statistics of the linear regression is given in **Table B-10**.

Table B-7 NNIs taken from **Chapter 3** that are required for the NNIs in substituted MAHs [1].

NNIs of Nonradical Substituent Interactions	$\Delta_f H^\circ$ [kJ mol^{-1}]	S° [J mol^{-1} K^{-1}]	C_p [J mol^{-1} K^{-1}]						
			300 K	400 K	500 K	600 K	800 K	1000 K	1500 K
o-OH+ OH/OCH_3	-3.0	-5.6	-2.7	-1.5	0.2	2.0	4.2	4.8	3.7
o-OH+ CHO	-27.4	-21.3	-10.4	-9.0	-7.4	-6.0	-3.4	-1.4	1.8
o-CHO+ CHO	21.1	6.4	1.7	1.7	1.6	1.4	0.4	-0.8	-2.5
o-Anomeric Effect (OH+OH or OCH_3+OCH_3)	14.7	7.8	0.0	-3.4	-4.7	-5.0	-4.4	-3.7	-2.2
o-OCH_3+CHO	7.9	-1.7	-2.6	0.3	2.6	3.9	4.1	3.3	1.3
o-CH_3/CH_2CH_3+ CH_3/CH_2CH_3	4.2	-6.6	3.3	2.9	2.6	2.5	2.3	2.0	1.5
o-CH_3/CH_2CH_3+ CHO	8.1	-2.4	4.0	3.0	2.0	1.1	0.0	-0.6	-0.9
o-CH=CH_2+ OH/OCH_3	2.6	-3.3	2.5	2.7	2.6	2.5	2.1	1.8	1.2
o-CH=CH_2+ CHO	11.9	-2.6	1.3	1.6	2.1	2.5	2.4	1.8	0.3
o-CH=CH_2+ CH=CH_2	8.1	-2.3	4.6	3.2	2.1	1.3	0.2	-0.2	-0.5
o-CH=CH_2+ CH_3/CH_2CH_3	4.6	-5.7	-5.7	5.6	4.9	4.2	2.9	2.1	1.0
m-CHO+ CHO	4.8	0.1	1.7	1.0	0.5	0.1	-0.4	-0.7	-0.8
p-CHO+ CHO	9.9	-0.8	1.8	1.4	1.0	0.7	0.1	-0.3	-0.9
p-OH/OCH_3+ OH/OCH_3	7.3	4.0	1.7	0.4	-0.8	-1.7	-2.3	-2.3	-1.7
p-CHO+ OH/OCH_3	-4.6	-0.8	-1.6	-1.0	-0.3	0.2	0.9	1.2	1.5

Table B-8 GAVs for standard enthalpy of formation ($\Delta_f H^\circ$) and entropy (S°) at 298 K, and heat capacity (C_p) at various temperatures for the MARs derived from the reference database, given with 97.5% confidence intervals.

GAVs	$\Delta_f H^\circ$	S°	C_p [J mol^{-1} K^{-1}]						
	[kJ mol^{-1}]	[J mol^{-1} K^{-1}]	300 K	400 K	500 K	600 K	800 K	1000 K	1500 K
Ċ$_b$	270.4 ± 1.1	52.6 ± 0.9	12.2 ± 0.8	14.9	16.7	18.0	19.6	20.6	21.3
C$_b$-(Ȯ)	-16.3 ± 1.4	73.6 ± 1.2	28 ± 1	32.8	36.4	39.0	42.2	44.1	45.5
O-(C$_b$)(Ċ)	-130.2 ± 1.1	28.5 ± 1	15.7 ± 0.8	20.0	21.1	21.4	20.9	20.8	20.3
C$_b$-(CȮ)	48.4 ± 1.3	102.7 ± 1.1	42.7 ± 0.9	48.5	53.2	56.5	60.8	63.3	65.5
Ċ-(C$_b$)(H)$_2$	112.9 ± 0.9	111.6 ± 0.8	27.2 ± 0.7	33.7	38.8	42.6	48.0	52.2	58.6
Ċ-(C$_b$)(C)(H)	124.8 ± 1.2	32.5 ± 1.1	21.7 ± 0.9	26.0	30.1	32.9	36.9	40.1	44.0

Table B-9 The NNIs that are determined from the simultaneous linear regression (along with GAVs) from the training dataset.[a]

NNIs	$\Delta_f H^\circ$	S°	C_p [J mol^{-1} K^{-1}]						
	[kJ mol^{-1}]	[J mol^{-1} K^{-1}]	300 K	400 K	500 K	600 K	800 K	1000 K	1500 K
NNI1	6.1 ± 2.3	3.7 ± 2.0	0.1 ± 1.7	-1.0	-2.0	-2.5	-2.7	-2.4	-1.4
NNI2	8 ± 3.1	-4.2 ± 2.7	2 ± 2.2	4.9	6.0	6.0	4.6	3.1	0.8
NNI3	11 ± 2.3	1.1 ± 2.0	4.7 ± 1.7	1.8	-0.2	-0.8	-0.8	-0.7	-0.3
NNI4	-36.9 ± 1.6	-10.9 ± 1.4	-8.2 ± 1.2	-7.3	-6.3	-5.0	-2.9	-1.3	1.4
NNI5	-7.2 ± 1.6	-0.1 ± 1.3	-2.5 ± 1.1	-2.7	-2.3	-1.5	-0.3	0.2	0.6
NNI6	-8.3 ± 2.3	-4.8 ± 2.0	0.7 ± 1.7	2.7	3.7	3.6	3.0	2.1	1.0
NNI7	-15.4 ± 2.0	-3 ± 1.7	-2.7 ± 1.4	-2.2	-1.5	-1.0	0.2	0.8	1.8
NNI8	6.2 ± 1.6	-0.4 ± 1.3	-1 ± 1.1	-0.3	0.6	1.6	2.7	2.8	1.7
NNI9	4.6 ± 2.0	2.8 ± 1.7	2.2 ± 1.5	2.3	2.1	1.9	1.4	0.9	0.6
NNI10	-8 ± 2.8	-4.3 ± 2.4	0.4 ± 2.0	0.2	0.3	0.5	1.2	1.6	1.8
NNI11	-12.9 ± 3.1	-3.1 ± 2.6	0.2 ± 2.2	0.1	0.1	0.4	0.9	1.2	1.3
NNI12	-8.4 ± 1.7	0.4 ± 1.4	-0.2 ± 1.2	-0.3	-0.2	-0.1	0.0	0.0	0.1
NNI13	-5.8 ± 2.5	0.1 ± 2.1	-0.7 ± 1.8	-0.6	-0.5	-0.5	-0.3	-0.2	-0.1
NNI14	-16.5 ± 2.3	-19.6 ± 2.0	-5.9 ± 1.7	-3.6	-1.6	0.7	4.5	6.8	8.2
NNI15	-8.1 ± 2.1	-3.7 ± 1.8	-2.8 ± 1.5	-1.9	-0.9	0.2	1.7	2.4	2.7
NNI16	6.7 ± 2.4	2.4 ± 2.0	3.1 ± 1.7	1.7	0.5	0.0	-0.5	-0.8	-0.5
NNI17	5.4 ± 3.1	4.4 ± 2.6	0.5 ± 2.2	0.6	0.4	0.1	-0.5	-0.6	0.4
NNI18	5.3 ± 3.2	13.4 ± 2.7	-0.7 ± 2.3	-2.1	-3.1	-3.6	-4.0	-3.7	-2.7
NNI19	3.7 ± 2.8	-8.4 ± 2.4	4.1 ± 2.0	4.5	4.4	4.1	3.1	2.2	1.1
NNI20	-14.7 ± 1.9	-17.7 ± 1.7	-5.5 ± 1.4	-2.9	0.5	4.4	10.1	12.1	9.7
NNI21	13.5 ± 1.8	-5.3 ± 1.6	1.9 ± 1.3	3.2	3.5	3.2	2.4	1.9	1.3
NNI22	7.2 ± 2.0	-5.3 ± 1.7	1.8 ± 1.4	2.8	2.4	2.0	1.2	0.8	0.4
NNI23	3.7 ± 1.4	-4 ± 1.2	3 ± 1.0	2.9	2.3	1.7	0.8	0.5	0.1
NNI24	-3.9 ± 1.0	-3.7 ± 0.9	1.5 ± 0.7	1.6	2.1	2.3	2.2	2.1	1.6
NNI25	-6.2 ± 2.4	-4.8 ± 2.0	0.3 ± 1.7	0.8	1.2	1.5	1.9	1.8	1.4
NNI26	6.4 ± 2.4	-1.1 ± 2.0	2.3 ± 1.7	2.1	1.5	1.0	0.4	-0.1	-0.3
NNI27	-5.1 ± 2.4	0.8 ± 2.0	-1.6 ± 1.7	-1.2	-0.8	-0.6	-0.4	-0.2	0.2
NNI28	5.5 ± 1.7	2.1 ± 1.5	1.8 ± 1.2	2.1	1.8	1.2	0.3	-0.2	-0.6
NNI29	2.9 ± 1.5	-3.8 ± 1.3	3.8 ± 1.1	2.9	2.1	1.4	0.7	0.4	0.1

[a] The interactions pertaining to the NNIs given here can be found in **Table 4-3**.

Table B-10 Statistical analysis for the linear regression analysis of the GAVs and NNIs for the standard enthalpies of formation ($\Delta_f H^\circ$) and entropies (S°) at 298 K and heat capacities (C_p) at various temperatures for MARs.[a]

	$\Delta_f H^\circ$	S°	C_p [J mol^{-1} K^{-1}]						
	[kJ mol^{-1}]	[J mol^{-1} K^{-1}]	300 K	400 K	500 K	600 K	800 K	1000 K	1500 K
MAD	1.92	1.66	1.26	1.09	1.02	1.01	1.01	0.93	0.74
RMS	2.39	2.03	1.71	1.48	1.39	1.39	1.45	1.32	1.05
MAX	6.66	4.91	5.85	5.03	5.17	5.54	5.96	5.74	4.60
F	14924	9340	1599	2999	4236	4986	5544	7434	13420

[a] **F:** Significance; **MAD:** mean average deviation; **RMS:** root mean square ; **MAX:** maximum deviation.

B.9 Thermochemical Data of The Validation Set

The transferability of the preliminary GAV/NNI parameters (See **Table B-7** and **Table B-8**) to the MARs outside the training set are tested on a set of 53 triple and quadruple substituted MARs (See **Figure B-8 - Figure B-13**). The thermochemical data for the validation set is given in **Table B-11.**

The NNI parameters defined for the MARs bring a significant improvement to the GA based predictions which can be seen in **Table B-12**. In this table, GA predictions with and without $NNI_{Radical}$ parameters are given. Below the table, there is a statistical comparison of these two cases where the sharp decrease in deviations upon the addition of NNIs can be seen.

Table B-11 Thermochemical database used as the validation set for the preliminary Group Additive Values (GAVs) and non-nearest neighbor interactions (NNIs). The units of standard enthalpy of formation ($\Delta_f H^\circ$) data is given in kJ mol^{-1} whereas the units of entropies (S°) and heat capacities (C_p) are given in J mol^{-1} K^{-1}.

Validation Set														
#	**Radicals**	$\Delta_f H^\circ$ (298 K)		S° (298 K)				C_p						
		$\Delta_f H^\circ_{G4}$	$\Delta_f H^\circ_{G4/BAC}$	S°	S°_{int}	$\sigma_{tot^\circ sym}$	n_{opt}	300 K	400 K	500 K	600 K	800 K	1000 K	1500 K
V-1/1	1-C•-2-CHO-5-OH-6-OCH_3	-116.2	-121.5	428.0	437.1	3	1	168.9	207.8	242.0	270.5	312.2	339.8	376.8
V-1/2	1-C•-2-OH-3-OCH_3-5-CHO	-116	-121.3	424.3	433.4	3	1	170.3	210.9	244.8	272.2	311.7	338.1	375.0
V-2/1	1-OCH_2•-2,3-OH	-236.5	-250.0	409.5	415.2	2	1	164.3	203.8	236.6	262.3	297.5	319.3	349.3
V-2/2	1-OCH_2•-2-OH-4-CH=CH_2	7.6	-0.9	443.0	448.7	2	1	183.1	229.3	267.7	298.2	341.1	369.4	410.0
V-2/3	1-OCH_2•-2-OCH_3-3-CH_3	-57.3	-65.0	459.2	483.3	18	1	187.3	230.6	269.5	302.2	352.0	387.4	440.3
V-2/4	1-OCH_2•-2-CHO-5-CH_3	-37	-39.9	437.5	452.4	6	1	177.0	223.2	261.4	291.8	335.9	366.0	409.6

V-2/5	1-OCH_2•-2,3,4-CH_3	21.6	19.7	465.3	492.7	27	1	194.3	243.5	286.8	323.0	378.4	418.3	478.8
V-3/1	1-O•-2,3,4-OH	-519.7	-536.2	377.2	377.2	1	1	147.7	184.2	214.0	237.8	271.1	292.1	318.7
V-3/2	1-O•-2-OH-4-OCH_3-6-CHO	-443.1	-453.2	440.3	449.4	3	1	178.8	221.5	258.4	288.7	332.9	362.0	400.7
V-3/3	1-O•-2-OH-3-CH=CH_2	-88.9	-96.7	387.4	387.4	1	1	146.2	187.1	221.2	248.3	287.5	314.0	352.4
V-3/4	1-O•-2-OH-3-CH_3	-192.6	-200.4	368.3	377.4	3	1	132.1	168.7	199.9	225.3	262.9	289.0	327.2
V-3/5	1-O•-2,3-OCH_3	-243.3	-254.6	444.2	462.5	9	1	183.2	224.4	260.6	290.3	333.6	363.1	406.5
V-3/6	1-O•-2-OCH_3-6-CH=CH_2	-39.4	-46.4	434.8	443.9	3	1	172.6	217.2	255.7	287.1	333.2	364.8	410.5
V-3/7	1-O•-2-CHO-4-OCH_3	-232.8	-239.3	419.1	428.2	3	1	167.5	207.0	241.3	269.9	312.4	340.9	378.7
V-3/8	1-O•-2,3-CHO	-158.8	-160.5	413.7	419.5	2	1	158.9	196.4	228.2	254.0	291.1	314.5	343.5
V-3/9	1-O•-2-CHO-6-CH=CH_2	0	-2.2	416.4	416.4	1	1	161.6	204.2	240.8	270.7	314.3	342.9	380.8
V-3/10	1-O•-2-CH=CH_2-4-CH_3	74.8	72.0	406.3	415.5	3	1	154.3	197.8	235.2	265.9	311.5	343.2	389.3
V-3/11	1-O•-2-CH_3-3-CHO	-92.5	-94.7	407.2	416.4	3	1	146.5	184.6	217.5	244.6	284.6	312.0	350.9
V-3/12	1-O•-2,6-CH_2CH_3	-70.5	-75.5	461.8	485.8	18	1	189.6	240.8	286.2	323.9	381.0	421.7	482.6
V-4/1	1-C•=O-2,4-OH	-256.7	-265.4	379.3	379.3	1	1	143.6	179.1	207.9	230.6	262.7	283.8	313.7
V-4/2	1-C•=O-2-OH-4-OCH_3	-239.5	-247.4	409.0	418.1	3	1	165.6	206.2	240.3	267.6	307.1	333.9	372.6
V-4/3	1-C•=O-2-OH-5-CHO	-198.1	-201.2	403.4	403.4	1	1	151.4	188.5	219.3	244.2	280.3	304.6	338.9
V-4/4	1-C•=O-2-OH-6-CH=CH_2	-0.5	-4.1	409.5	409.5	1	1	167.0	210.3	245.1	272.5	311.9	338.6	376.8
V-4/5	1-C•=O-2-OH-3-CH_3	-107.6	-111.2	389.6	398.7	3	1	151.9	190.4	222.8	249.4	289.5	317.8	357.2
V-4/6	1-C•=O-2-OCH_3-3-CHO	-135.5	-137.8	456.8	466.0	3	1	182.8	226.7	263.6	292.8	333.7	360.2	396.4
V-4/7	1-C•=O-3-CHO-4-CH_3	-30.7	-28.8	428.0	437.1	3	1	167.0	205.3	238.3	265.5	305.9	333.5	372.4
V-4/8	1-C•=O-2-CH=CH_2-3-CH_3	154.4	155.8	432.5	441.6	3	1	177.1	221.2	258.1	287.7	331.3	361.8	407.6
V-4/9	1-C•=O-3-CH_3-4-OH	-98.7	-102.3	404.2	413.4	3	1	154.7	191.8	223.4	249.0	286.3	311.4	347.5
V-5/1	1-(t-CH=CH•)-2,5-OH	44.4	35.2	394.5	394.5	1	1	161.1	202.9	237.6	265.1	302.8	325.7	355.2
V-5/2	1-(t-CH=CH•)-2-OH-5-CH_2CH_3	154.8	149.5	439.4	448.5	3	1	185.3	236.2	280.7	317.5	371.5	406.9	454.4
V-5/3	1-(t-CH=CH•)-3,4-CHO	176.2	178.2	451.4	451.4	1	1	181.6	225.1	262.1	292.3	336.0	364.3	401.6
V-5/4	1-(t-CH=CH•)-2-CHO-5-CH=CH_2	353.1	354.5	450.8	450.8	1	1	189.2	240.1	281.9	315.0	362.6	394.5	439.3
V-5/5	1-(t-CH=CH•)-2-CH=CH_2-3-CH_3	440.5	441.4	439.3	448.5	3	1	186.6	234.9	276.0	309.5	359.6	394.9	447.8
V-5/6	1-(t-CH=CH•)-2-CH=CH_2-5-CH_3	433.7	434.6	440.5	449.6	3	1	180.5	231.0	274.1	309.0	360.3	395.9	448.5
V-5/7	1-(t-CH=CH•)-2-CH_2CH_3-4-CH_3	308.5	308.3	461.3	479.6	9	1	195.4	246.7	291.2	327.9	383.7	423.6	483.7
V-5/8	1-(c-CH=CH•)-2,3-OH	49.3	40.1	403.8	403.8	1	1	162.4	202.0	234.0	259.3	294.8	317.9	350.2
V-5/9	1-(c-CH=CH•)-2-CHO-4-CH=CH_2	361.6	363.0	452.7	452.7	1	1	190.4	238.8	279.1	311.4	358.6	390.7	436.7
V-5/10	1-(c-CH=CH•)-2-CHO-6-CH_3	267.9	269.3	434.9	444.0	3	1	177.0	220.7	257.6	287.7	332.8	364.3	410.3
V-5/11	1-(c-CH=CH•)-3-CHO-4-CH_3	251.4	252.8	435.8	444.9	3	1	174.6	218.3	255.9	286.8	332.8	364.8	411.1
V-5/12	1-(c-CH=CH•)-2,4-CH=CH_2	540.5	541.4	463.5	463.5	1	1	197.4	250.9	295.4	330.9	382.7	418.6	471.9
V-5/13	1-(c-CH=CH•)-2-CH=CH_2-4-CH_3	437.8	438.7	443.7	452.9	3	1	180.9	231.0	273.6	308.0	358.7	394.2	447.2
V-5/14	1-(c-CH=CH•)-2-CH_3-4-CH=CH_2	438.6	439.5	441.8	450.9	3	1	180.4	230.8	273.2	307.5	358.5	394.2	447.5
V-5/15	1-(c-CH=CH•)-2,3- CH_3	342.9	343.8	419.6	437.9	9	1	164.4	210.2	249.8	282.6	332.4	368.0	421.7
V-6/1	1-CH_2•-2,4-CH=CH_2	335.9	336.8	433.2	433.2	1	1	182.8	234.5	277.6	312.3	363.2	398.8	451.8
V-6/2	1-CH_2•-2-CH=CH_2-3-CH_3	251.2	252.1	411.6	420.7	3	1	169.2	215.2	254.9	287.6	337.0	372.2	425.5
V-6/3	1-CH_2•-2,3-CH_3	147.5	148.4	385.7	403.9	9	1	152.7	196.6	234.8	266.5	314.7	349.4	401.9
V-6/4	1-CH_2•-2-CH_3-5-	119.8	119.6	428.4	446.7	9	1	177.7	227.4	270.7	306.6	361.6	401.2	461.5
V-6/5	1-CH_2•-2,5-CH_2CH_3	100.1	98.7	467.3	485.6	9	1	200.9	256.8	305.7	346.4	408.6	453.6	521.8
V-6/6	1-CH_2•-3-CH_3-4-CHO	52.1	53.5	401.8	410.9	3	1	161.7	203.2	239.1	268.8	313.5	345.0	391.1
V-6/7	1-CH_2•-3-CH_3-4-CH=CH_2	239.3	240.2	404.8	419.7	6	1	172.7	220.3	260.4	293.0	341.7	376.2	428.1
V-6/8	1-CH_2•-3,4-CH_3	141.1	142.0	388.3	406.6	9	1	154.8	197.9	235.7	267.1	315.2	349.8	402.2
V-6/9	1-CH_2•-3,6-CH_2CH_3	100.1	98.7	466.9	485.1	9	1	200.7	256.7	305.6	346.3	408.5	453.5	521.6
V-6/10	*p*-$(CH_3)C_6H_5CH$•CH_3	142.8	142.2	395.8	414.0	9	1	146.2	191.1	230.5	263.2	312.9	348.3	401.6

Table B-12 Comparison of the predictive capability (deviations between G4/BAC and GA calculated values) of GA parameters before and after the application of $NNI_{Radical}$ parameters for standard enthalpy of formations ($\Delta_f H^\circ$), entropies (S°) at 298 K and heat capacities (C_p) at 300 K.[a][b]

		$\Delta_f H^\circ$ [kJ mol^{-1}]		S° [J mol^{-1} K^{-1}]		C_p [J mol^{-1} K^{-1}] (300 K)	
#	**MAR Name**[b]	**Before $NNI_{Radical}$**[c]	**After $NNI_{Radical}$**	**Before $NNI_{Radical}$**[c]	**After $NNI_{Radical}$**	**Before $NNI_{Radical}$**[c]	**After $NNI_{Radical}$**
V1/1	1-C•-2-OCH_3-3-OH-5-CHO	-2.2	2.2	-2.9	2.9	3.7	-3.7
V1/2	1-C•-2-OH-3-OCH_3-5-CHO	-2.4	2.4	0.8	-0.8	2.2	-2.2
V2/1	1-OCH_2•-2,3-OH	0.9	-0.9	2.3	-2.3	1.6	-1.6
V2/2	1-OCH_2•-2-OH-4-CH=CH_2	-1.3	1.3	4.6	-4.6	-0.1	0.1
V2/3	1-OCH_2•-2-OCH_3-3-CH_3	-15.3	4.3	-0.5	-0.6	1.4	-6.1

V2/4	1-OCH_2•-2-CHO-5-CH_3	-4.2	-3.8	7.5	-3.3	-2.3	0.3
V2/5	1-OCH_2•-2,3,4-CH_3	-1.1	1.1	-3.2	3.2	1.7	-1.7
V3/1	1-O•-2,3,4-OH	49.0	3.3	0.4	2.6	11.6	-0.7
V3/2	1-O•-2-OH-4-OCH_3-6-CHO	50.4	-4.3	1.3	2.1	13.9	-2.0
V3/3	1-O•-2-OH-3-CH=CH_2	39.8	-2.9	0.6	-0.6	12.1	-3.9
V3/4	1-O•-2-OH-3-CH_3	41.7	-4.8	1.0	-1.0	8.3	-0.1
V3/5	1-O•-2,3-OCH_3	8.1	7.4	2.0	2.8	0.1	1.7
V3/6	1-O•-2-OCH_3-6-CH=CH_2	8.0	7.2	0.6	3.7	4.0	-1.9
V3/7	1-O•-2-CHO-4-OCH_3	14.3	-5.1	5.7	-2.3	1.8	1.9
V3/8	1-O•-2,3-CHO	-7.2	-3.6	-2.1	-0.3	-1.8	0.6
V3/9	1-O•-2-CHO-6-CH=CH_2	0.0	1.8	5.3	-0.6	1.1	-0.5
V3/10	1-O•-2-CH=CH_2-4-CH_3	13.2	0.6	4.0	0.2	0.5	-0.2
V3/11	1-O•-2-CH_3-3-CHO	1.4	2.4	-10.0	6.8	4.9	-6.9
V3/12	1-O•-2,6-CH_2CH_3	20.3	-3.5	-2.2	1.4	0.3	0.1
V4/1	1-C•=O-2,4-OH	26.7	-2.1	21.8	1.5	12.7	-4.0
V4/2	1-C•=O-2-OH-4-OCH_3	29.8	-5.2	25.4	-2.1	11.7	-3.0
V4/3	1-C•=O-2-OH-5-CHO	14.1	-3.0	16.4	-1.2	5.1	0.3
V4/4	1-C•=O-2-OH-6-CH=CH_2	9.3	3.5	21.8	6.2	3.7	-1.9
V4/5	1-C•=O-2-OH-3-CH_3	17.2	-0.7	19.7	-0.1	3.6	2.3
V4/6	1-C•=O-3-OCH_3-4-CH_3	-14.6	2.5	-4.7	-2.1	-1.2	-2.4
V4/7	1-C•=O-3-CHO-4-CH_3	0.2	-5.6	-1.6	-2.8	-0.6	0.1
V4/8	1-C•=O-2-CH=CH_2-3-CH_3	-1.3	-2.4	1.3	-7.1	-1.6	-2.5
V4/9	1-C•=O-3-CH_3-4-OH	8.3	-0.2	5.0	-1.3	0.7	2.1
V5/1	1-(t-CH=CH•)-2,5-OH	15.4	3.2	21.3	0.1	5.0	-0.9
V5/2	1-(t-CH=CH•)-2-OH-5-CH_2CH_3	17.9	0.7	19.1	2.3	3.4	0.7
V5/3	1-(t-CH=CH•)-3,4-CHO	0.8	3.1	5.8	-2.1	-1.5	0.4
V5/4	1-(t-CH=CH•)-2-CHO-5-CH=CH_2	-10.0	0.4	10.7	-1.7	-3.5	0.4
V5/5	1-(t-CH=CH•)-2-CH=CH_2-3-CH_3	-4.9	1.6	5.1	3.9	-3.0	-1.4
V5/6	1-(t-CH=CH•)-2-CH=CH_2-5-CH_3	-2.7	-0.6	9.7	-0.7	-2.6	-1.8
V5/7	1-(t-CH=CH•)-2-CH_2CH_3-4-CH_3	3.8	-3.6	5.3	2.4	-7.6	2.9
V5/8	1-(c-CH=CH•)-2,3-OH	0.2	-0.2	2.4	-2.4	-0.7	0.7
V5/9	1-(c-CH=CH•)-2-CHO-4-CH=CH_2	-18.5	5.0	8.8	-3.5	-4.6	2.6
V5/10	1-(c-CH=CH•)-2-CHO-6-CH_3	-24.0	6.8	4.6	4.7	-6.5	0.9
V5/11	1-(c-CH=CH•)-3-CHO-4-CH_3	0.6	-0.6	1.3	-1.3	-0.1	0.1
V5/12	1-(c-CH=CH•)-2,4-CH=CH_2	-10.3	3.1	8.7	-3.4	-4.2	0.9
V5/13	1-(c-CH=CH•)-2-CH=CH_2-4-CH_3	-6.8	-0.4	6.4	-1.1	-3.0	-0.3
V5/14	1-(c-CH=CH•)-2-CH_3-4-CH=CH_2	-7.6	3.9	8.4	-4.4	-2.5	-1.1
V5/15	1-(c-CH=CH•)-2,3-CH_3	-6.9	3.2	1.9	2.1	1.5	-5.1
V6/1	1-CH_2•-2,4-CH=CH_2	0.3	-0.5	3.6	2.3	-3.2	0.6
V6/2	1-CH_2•-2-CH=CH_2-3-CH_3	-9.6	3.2	-2.5	3.6	0.8	-3.1
V6/3	1-CH_2•-2,3-CH_3	-5.5	2.6	0.5	3.3	-0.4	0.4

V6/4	1-CH_2•-2-CH_3-5-CH_2CH_3	-1.5	-1.4	2.8	1.0	-3.5	3.5
V6/5	1-CH_2•-2,5-CH_2CH_3	-1.2	-1.7	2.4	1.4	-1.5	1.5
V6/6	1-CH_2•-3-CH_3-4-CHO	5.9	-1.3	-0.1	-0.7	-0.8	2.4
V6/7	1-CH_2•-3-CH_3-4-CH=CH_2	2.3	3.9	-1.5	6.3	-2.6	2.3
V6/8	1-CH_2•-3,4-CH_3	-3.3	0.4	4.4	-0.6	-5.8	5.8
V6/9	1-CH_2•-3,6-CH_2CH_3	-1.2	-1.7	2.9	0.9	-1.3	1.3
V6/10	*p*-(CH_3)C_6H_5CH•CH_3	-1.3	1.3	0.0	0.0	0.0	0.0
Statistics		**$\Delta_f H^\circ$ [kJ mol^{-1}]**		**S° [J mol^{-1} K^{-1}]**		**C_p [J mol^{-1} K^{-1}] (300 K)**	
Mean Absolute Deviation (MAD)		10.7	2.7	5.9	2.3	3.5	1.8
Maximum Absolute Deviation (MAX)		50.4	7.4	25.1	7.1	13.9	6.9

[a] The *ab initio* and the GA based thermochemical databases for the validation set is given in **Table B-11** of the Supporting Information.
[b] The full names and the numbering of the MARs in the validation set are described in **Section B.2**. In order to avoid any confusion, the depictions of these MARs are also given in **Figure B-8 - Figure B-13** of the Supporting Information.
[c] This term includes GA predictions based on the GAVs for the closed and open shell groups and the NNIs that describe the interactions between non-radical groups which are defined by **Chapter 3** and excludes the NNIs that are defined in this paper.

B.10 Deviations between GA and *Ab initio* Calculated Datasets

The GAVs and the NNIs for the heat capacities (C_p) at 400 K, 500 K, 600 K, 800 K, 1000 K and 1500 K are given along with their 97.5% confidence intervals in **Table B-13** and **Table B-14**, respectively. In **Table B-15**, the deviations between Group Additivity (GA) and *ab initio* based data for the final thermochemical database is given for the full database (369 MARs). The histograms for the differences between two datasets for $\Delta_f H^\circ$ and S° at 298K and C_p at various temperatures (300 K, 400 K, 500 K, 600 K, 800 K, 1000 K and 1500 K) are given in **Figure B-29**, **Figure B-30** and **Figure B-31**, respectively.

Table B-13 GAVs for heat capacity (C_p) at various temperatures for the MARs of the final database. The standard deviations relate to 97.5% confidence intervals.

GAVs	C_p [J mol^{-1} K^{-1}]					
	400 K	500 K	600 K	800 K	1000 K	1500 K
$\dot{C}_b$	14.7 ± 0.67	16.4 ± 0.64	17.7 ± 0.64	19.4 ± 0.66	20.5 ± 0.61	21.3 ± 0.47
C_b-($\dot{O}$)	32.8 ± 0.89	36.4 ± 0.85	38.9 ± 0.85	42.2 ± 0.88	44.1 ± 0.81	45.5 ± 0.63
O-($\dot{C}$)(C_b)	19.8 ± 0.7	21.1 ± 0.67	21.4 ± 0.67	21 ± 0.69	20.9 ± 0.64	20.3 ± 0.5
C_b-($C\dot{O}$)	48.9 ± 0.81	53.6 ± 0.77	57 ± 0.77	61.4 ± 0.8	63.9 ± 0.73	65.9 ± 0.57
$\dot{C}$-(C_b)(H)$_2$	33.6 ± 0.6	38.7 ± 0.58	42.5 ± 0.58	48 ± 0.59	52.1 ± 0.55	58.5 ± 0.42
$\dot{C}$-(C_b)(C)(H)	26 ± 0.79	30.1 ± 0.76	33 ± 0.76	37 ± 0.78	40.1 ± 0.72	44 ± 0.56

Table B-14 Correction values for non-nearest neighbor interactions (NNIs) derived based on full G4/BAC radical set for the heat capacities (C_p) at various temperatures. [a] The standard deviations relate to 97.5% confidence intervals.

NNI #	Description of Interaction	C_p [J mol^{-1} K^{-1}]					
		400 K	500 K	600 K	800 K	1000 K	1500 K
NNI1	$C_6H_5OCH_2$•— *p*-OH/OCH_3	-0.8 ± 1.51	-1.8 ± 1.44	-2.4 ± 1.44	-2.7 ± 1.48	-2.5 ± 1.36	-1.4 ± 1.06
NNI2	$C_6H_5OCH_2$•— *o*-OCH_3	5.0 ± 1.82	6 ± 1.74	5.8 ± 1.74	4.2 ± 1.79	2.6 ± 1.64	0.6 ± 1.28
NNI3	$C_6H_5OCH_2$•— *o*-CHO	0.9 ± 1.42	-0.9 ± 1.36	-1.5 ± 1.36	-1.4 ± 1.40	-1.2 ± 1.29	-0.6 ± 1.00
NNI4	C_6H_5O• — *o*-OH	-7.7 ± 0.99	-6.7 ± 0.94	-5.3 ± 0.94	-3.1 ± 0.97	-1.4 ± 0.89	1.4 ± 0.69
NNI5	C_6H_5O• — *o*-OCH_3	-2.7 ± 0.97	-2.2 ± 0.92	-1.4 ± 0.92	-0.3 ± 0.95	0.2 ± 0.87	0.6 ± 0.68
NNI6	C_6H_5O• — *m*-OCH_3	3.0 ± 1.42	4.1 ± 1.36	4.1 ± 1.36	3.4 ± 1.40	2.4 ± 1.28	1.0 ± 1.00
NNI7	C_6H_5O•— *p*-OH/OCH_3	-2.4 ± 1.12	-1.8 ± 1.07	-1.3 ± 1.07	0.0 ± 1.10	0.7 ± 1.01	1.8 ± 0.79

NNI8	C_6H_5O•─ *o*-CHO	-0.2 ± 0.94	0.8 ± 0.89	1.8 ± 0.89	2.9 ± 0.92	3.0 ± 0.85	1.8 ± 0.66
NNI9	C_6H_5O•─ *m*-CHO	1.8 ± 1.21	1.8 ± 1.16	1.7 ± 1.16	1.2 ± 1.19	0.8 ± 1.09	0.6 ± 0.85
NNI10	C_6H_5O•─ *o*-$CH=CH_2$	0.0 ± 1.4	0.1 ± 1.33	0.4 ± 1.33	1.1 ± 1.37	1.4 ± 1.26	1.6 ± 0.98
NNI11	C_6H_5O•─ *p*-$CH=CH_2$	0.2 ± 2.05	0.2 ± 1.95	0.5 ± 1.95	1.0 ± 2.01	1.3 ± 1.85	1.3 ± 1.44
NNI12	C_6H_5O•─ *o*-CH_3/CH_2CH_3	-0.5 ± 0.97	-0.4 ± 0.92	-0.2 ± 0.92	-0.1 ± 0.95	-0.1 ± 0.87	-0.1 ± 0.68
NNI13	C_6H_5O•─ *p*-CH_3/CH_2CH_3	-0.6 ± 1.5	-0.4 ± 1.43	-0.4 ± 1.43	-0.3 ± 1.47	-0.2 ± 1.35	-0.1 ± 1.05
NNI14	C_6H_5C•=O─ *o*-OH	-4.5 ± 1.17	-2.9 ± 1.12	-1.0 ± 1.12	2.3 ± 1.15	4.7 ± 1.06	6.9 ± 0.82
NNI15	C_6H_5C•=O─ *p*-OH/OCH_3	-2.7 ± 1.2	-2.0 ± 1.15	-1.0 ± 1.15	0.2 ± 1.18	0.8 ± 1.08	1.5 ± 0.84
NNI16	C_6H_5C•=O─ *o*-OCH_3	1.4 ± 1.45	0.4 ± 1.39	0.0 ± 1.39	-0.6 ± 1.43	-0.8 ± 1.31	-0.7 ± 1.02
NNI17	C_6H_5C•=O─ *m*-CHO	0.7 ± 1.49	0.7 ± 1.42	0.5 ± 1.42	0.0 ± 1.46	-0.3 ± 1.34	0.1 ± 1.05
NNI18	C_6H_5C•=O─ *p*-CHO	-2.4 ± 2.1	-3.5 ± 2.00	-4.1 ± 2.00	-4.5 ± 2.06	-4.3 ± 1.90	-3.2 ± 1.48
NNI19	C_6H_5C•=O─ *o*-$CH=CH_2$	3.5 ± 1.55	3.2 ± 1.48	2.6 ± 1.48	1.5 ± 1.52	0.6 ± 1.40	0.1 ± 1.09
NNI20	trans/cis-$C_6H_5CH=CH$•─ *o*-OH	-2.9 ± 1.18	0.6 ± 1.12	4.6 ± 1.13	10.1 ± 1.16	12.0 ± 1.06	9.4 ± 0.83
NNI21	trans/cis-$C_6H_5CH=CH$•─ *o*-CHO	3.4 ± 1.04	3.6 ± 0.99	3.3 ± 0.99	2.4 ± 1.02	1.8 ± 0.94	1.0 ± 0.73
NNI22	trans/cis-$C_6H_5CH=CH$•─ *o*-$CH=CH_2$	2.5 ± 1.05	2.2 ± 1.00	1.8 ± 1.01	1.1 ± 1.03	0.7 ± 0.95	0.3 ± 0.74
NNI23	trans/cis-$C_6H_5CH=CH$•─ *o*-CH_3/CH_2CH_3	2.7 ± 0.81	2.1 ± 0.78	1.5 ± 0.78	0.6 ± 0.80	0.3 ± 0.74	-0.1 ± 0.57
NNI24	$C_6H_5CH=CH$• Cis Correction	1.6 ± 0.64	2.2 ± 0.61	2.4 ± 0.61	2.4 ± 0.62	2.2 ± 0.57	1.7 ± 0.45
NNI25	$C_6H_5CH_2$• /C_6H_5C•HCH_3─ *p*-$CH=CH_2$	2.1 ± 1.12	1.8 ± 1.07	1.2 ± 1.07	0.4 ± 1.10	-0.2 ± 1.02	-0.5 ± 0.79
NNI26	$C_6H_5CH_2$• /C_6H_5C•HCH_3─ *o*-$CH=CH_2$	1.2 ± 1.37	0.6 ± 1.31	0.1 ± 1.31	-0.5 ± 1.35	-0.7 ± 1.24	-0.7 ± 0.97
NNI27	$C_6H_5CH_2$• /C_6H_5C•HCH_3─ *p*-CHO	1.1 ± 1.34	1.2 ± 1.28	1.4 ± 1.28	1.6 ± 1.32	1.6 ± 1.21	1.3 ± 0.94
NNI28	$C_6H_5CH_2$• /C_6H_5C•HCH_3─ *o*-CHO	-0.9 ± 1.44	-0.6 ± 1.38	-0.4 ± 1.38	-0.3 ± 1.42	-0.1 ± 1.3	0.3 ± 1.02
NNI29	$C_6H_5CH_2$• /C_6H_5C•HCH_3─ *o*-CH_3/CH_2CH_3	2.6 ± 0.91	1.8 ± 0.87	1.2 ± 0.87	0.5 ± 0.9	0.3 ± 0.82	0.0 ± 0.64

Table B-15 Differences between group additively and *ab initio* calculated values for standard enthalpy of formation ($\Delta_f H°$), entropy ($S°$) and heat capacity (C_p) of the final dataset of MARs. Standard enthalpies of formation ($\Delta_f H°$) are given in kJ mol^{-1}, whereas entropies ($S°$) and heat capacities (C_p) are in J mol^{-1} K^{-1}.

Group additivity calculated (GA) – *Ab Initio* calculated values (AI)										
#	**Training and validation set for GAV and NNI**	$\Delta_f H°$	$S°$	C_p						
		298 K	**298 K**	**300 K**	**400 K**	**500 K**	**600 K**	**800 K**	**1000 K**	**1500 K**
T1/1	C_6H_5•	1.4	1.5	-1.6	-1.1	-1.1	-0.9	-0.6	-0.4	-0.1
T1/2	*o*-OHC_6H_4•	-1.4	3.5	-2.1	-2.8	-3.0	-2.9	-2.2	-1.7	-0.8
T1/3	*m*-OHC_6H_4•	2.6	-1.1	0.8	0.7	0.3	0.2	0.1	0.0	0.0
T1/4	*p*-OHC_6H_4•	-3.7	-1.4	0.7	0.8	0.7	0.7	0.5	0.4	0.3
T1/5	*o*-$MeOC_6H_4$•	3.2	1.6	-0.3	-1.4	-2.5	-2.9	-2.4	-1.6	-0.5
T1/6	*m*-$MeOC_6H_4$•	4.6	-0.8	0.5	0.5	0.3	0.4	0.6	0.7	0.7
T1/7	*p*-$MeOC_6H_4$•	-2.0	-1.6	0.6	0.9	1.0	1.1	1.2	1.2	0.9
T1/8	*o*-$CHOC_6H_4$•	-4.1	2.6	-3.1	-3.0	-2.7	-2.1	-1.0	-0.3	0.5
T1/9	*m*-$CHOC_6H_4$•	-2.2	-0.2	0.4	0.5	0.3	0.4	0.6	0.7	0.7
T1/10	*p*-$CHOC_6H_4$•	-0.9	0.0	0.6	0.6	0.4	0.5	0.8	0.8	0.6
T1/11	*o*-$CH{=}CH_2C_6H_4$•	-0.7	2.0	-3.9	-2.6	-2.3	-2.0	-1.6	-1.2	-0.6
T1/12	*m*-$CH{=}CH_2C_6H_4$•	-1.8	0.7	-0.9	-0.7	-0.8	-0.8	-0.6	-0.4	-0.1
T1/13	*p*-$CH{=}CH_2C_6H_4$•	-3.0	0.7	-0.8	-0.5	-0.6	-0.6	-0.4	-0.3	0.0
T1/14	*o*-$CH_3C_6H_4$•	2.6	0.3	-0.5	-0.3	-0.5	-0.5	-0.4	-0.3	0.0
T1/15	*m*-$CH_3C_6H_4$•	2.5	0.7	-0.6	-0.4	-0.7	-0.7	-0.6	-0.5	-0.1
T1/16	*p*-$CH_3C_6H_4$•	0.3	0.8	-0.6	-0.3	-0.6	-0.5	-0.5	-0.4	-0.1
T1/17	*o*-$CH_2CH_3C_6H_4$•	4.4	-1.9	1.5	1.3	0.8	0.7	0.7	0.6	0.7
T1/18	*m*-$CH_2CH_3C_6H_4$•	4.2	-1.0	0.0	0.4	0.1	0.2	0.4	0.4	0.6
T1/19	*p*-$CH_2CH_3C_6H_4$•	2.0	-0.4	-0.4	0.1	-0.1	0.1	0.3	0.3	0.5
T1/20	1-C•-3-OH-4-OCH_3	1.0	-1.5	2.4	3.5	3.1	2.2	0.5	-0.4	-1.2
T1/21	1-C•-3-OH-4-CHO	-6.1	-0.9	0.0	-3.8	0.0	0.0	0.3	0.4	0.2
T1/22	1-C•-2-CH_3-4-OH	-1.5	-2.6	1.7	1.6	1.2	1.0	0.7	0.5	0.3
T1/23	1-C•-2-OCH_3-3-OH-6-CHO	2.4	0.5	1.2	0.4	0.0	-0.5	-1.3	-1.9	-2.5
T2/1	$C_6H_5OCH_2$•	-0.3	-2.2	-0.6	-0.1	0.5	1.0	1.4	1.4	0.9
T2/2	*o*-$OHC_6H_4OCH_2$•	1.1	4.0	-0.1	-0.3	-1.2	-2.5	-3.8	-3.9	-2.7
T2/3	*m*-$OHC_6H_4OCH_2$•	1.3	-3.6	0.8	0.9	1.3	1.5	1.6	1.4	0.8
T2/4	*p*-$OHC_6H_4OCH_2$•	-2.1	-0.5	1.6	1.2	0.8	0.6	0.3	0.1	0.0
T2/5	*o*-$OCH_3C_6H_4OCH_2$•	-0.9	-1.5	-4.6	-3.1	-1.3	0.1	1.7	2.0	1.5
T2/6	*m*-$OCH_3C_6H_4OCH_2$•	3.7	-0.4	1.4	1.2	1.6	1.9	2.3	2.2	1.5
T2/7	*p*-$OCH_3C_6H_4OCH_2$•	0.3	-1.2	1.3	1.1	0.9	0.8	0.7	0.7	0.5
T2/8	*o*-$CHOC_6H_4OCH_2$•	-1.9	-0.7	-1.6	-1.4	-0.9	-0.3	0.4	0.6	0.5
T2/9	*m*-$CHOC_6H_4OCH_2$•	-3.3	-4.0	-1.1	-0.3	0.6	1.3	2.1	2.2	1.5
T2/10	*p*-$CHOC_6H_4OCH_2$•	1.7	-2.9	1.1	1.1	1.3	1.6	2.0	1.9	1.0
T2/11	*o*-$CH{=}CH_2C_6H_4OCH_2$•	-5.5	3.1	-4.1	-4.0	-3.2	-2.5	-1.3	-0.7	-0.3
T2/12	*m*-$CH{=}CH_2C_6H_4OCH_2$•	-3.1	-2.4	-0.5	-0.1	0.6	1.0	1.4	1.3	0.8
T2/13	*p*-$CH{=}CH_2C_6H_4OCH_2$•	-3.7	-0.2	-0.4	-0.1	0.4	0.6	1.0	0.9	0.5
T2/14	*o*-$CH_3C_6H_4OCH_2$•	1.7	3.9	-3.8	-3.8	-3.4	-2.8	-1.8	-1.2	-0.6
T2/15	*m*-$CH_3C_6H_4OCH_2$•	1.3	-2.8	0.1	0.4	0.9	1.2	1.5	1.3	0.8
T2/16	*p*-$CH_3C_6H_4OCH_2$•	-2.0	-1.5	0.7	1.0	1.4	1.7	1.8	1.5	0.9
T2/17	*o*-$CH_2CH_3C_6H_4OCH_2$•	3.8	2.4	-3.2	-3.2	-2.8	-2.3	-1.3	-1.0	-0.4
T2/18	*m*-$CH_2CH_3C_6H_4OCH_2$•	2.7	-1.5	1.6	1.7	2.0	2.3	2.6	2.2	1.7
T2/19	*p*-$CH_2CH_3C_6H_4OCH_2$•	-0.3	-1.4	0.8	1.2	1.7	2.1	2.5	2.2	1.6
T2/20	1-OCH_2•-3,4-OH	-0.6	-2.7	2.5	2.5	2.0	1.5	1.0	1.0	0.7
T2/21	1-OCH_2•-2-OH-6-OCH_3	2.1	0.9	4.9	2.6	0.3	-1.7	-3.7	-3.9	-2.7
T2/22	1-OCH_2•-2-OH-4-CHO	0.3	0.9	0.9	-1.0	-2.3	-3.3	-3.6	-3.1	-1.9

T2/23	1-OCH_2•-2-OH-5-CHO	-4.5	1.4	-0.4	-0.3	-0.8	-1.8	-3.3	-3.7	-3.2
T2/24	1-OCH_2•-2-OH-5-$CH=CH_2$	5.3	3.7	0.4	0.5	-0.4	-2.0	-3.8	-4.2	-3.2
T2/25	1-OCH_2•-2-OCH_3-4-OH	1.0	1.3	-3.2	-3.3	-2.5	-1.6	-0.4	0.0	0.2
T2/26	1-OCH_2•-2-OCH_3-6-OH	2.1	0.9	4.9	2.6	0.3	-1.7	-3.7	-3.9	-2.7
T2/27	1-OCH_2•-2-OCH_3-4-CH_3	-0.2	-0.9	-3.3	-2.1	-0.7	0.4	1.6	1.8	1.3
T2/28	1-OCH_2•-2-OCH_3-5-CH_3	-0.6	-1.0	-4.1	-2.4	-0.8	0.5	1.8	2.0	1.5
T2/29	1-OCH_2•-2-CHO-3-CH_3	1.5	-0.2	1.9	1.6	0.6	-0.5	-1.8	-2.0	-1.3
T2/30	1-OCH_2•-2-CHO-4-CH_3	-2.5	-1.6	0.0	-0.2	-0.1	0.2	0.5	0.5	0.3
T3/31	1-OCH_2•-2-CH_3-4-OH	0.8	2.8	-2.0	-2.0	-2.1	-2.1	-2.1	-1.9	-1.4
T2/32	1-OCH_2•-3-CH_3-4-OH	0.4	0.1	-0.2	0.7	0.9	0.8	0.5	0.3	0.0
T2/33	1-OCH_2•-2,3-CH_3	2.3	1.6	0.0	-0.5	-0.3	0.2	0.9	0.9	0.8
T3/1	C_6H_5O•	-2.1	0.8	-1.1	-0.7	-0.5	-0.3	0.1	0.2	0.2
T3/2	*o*-OHC_6H_4O•	0.0	0.8	-0.3	-0.1	-0.1	-0.1	-0.3	-0.4	-0.4
T3/3	*m*-OHC_6H_4O•	1.0	2.3	-2.3	-2.5	-2.2	-1.8	-1.1	-0.7	-0.4
T3/4	*p*-OHC_6H_4O•	-4.7	-2.8	0.7	0.6	0.4	0.2	0.1	0.2	0.8
T3/5	*o*-$OCH_3C_6H_4O$•	-0.1	1.6	-0.2	-0.5	-0.5	-0.4	-0.2	0.0	0.1
T3/6	*m*-$OCH_3C_6H_4O$•	-0.2	-0.9	-0.5	-0.8	-0.6	-0.4	0.4	0.7	0.6
T3/7	*p*-$OCH_3C_6H_4O$•	-1.7	-2.3	0.8	0.5	0.1	-0.2	0.0	0.5	1.5
T3/8	*o*-$CHOC_6H_4O$•	-2.7	-1.7	-0.7	-0.6	-0.6	-0.5	-0.3	-0.1	0.2
T3/9	*m*-$CHOC_6H_4O$•	-3.3	-1.1	-1.7	-0.6	0.2	0.8	1.4	1.4	1.4
T3/10	*p*-$CHOC_6H_4O$•	-3.9	-4.2	0.8	0.7	0.8	0.9	1.3	1.3	0.8
T3/11	*o*-$CH=CH_2C_6H_4O$•	0.3	0.3	-0.2	-0.2	-0.1	0.0	0.0	0.1	0.0
T3/12	*m*-$CH=CH_2C_6H_4O$•	-2.3	0.4	-1.3	-0.8	-0.5	-0.3	0.1	0.3	0.2
T3/13	*p*-$CH=CH_2C_6H_4O$•	1.0	1.0	-0.3	-0.3	-0.3	-0.3	-0.1	-0.1	-0.2
T3/14	*o*-$CH_3C_6H_4O$•	-0.6	2.1	-0.9	-0.7	-0.5	-0.2	0.0	0.1	0.1
T3/15	*m*-$CH_3C_6H_4O$•	0.8	0.3	-0.6	-0.4	-0.3	-0.2	0.0	0.1	0.1
T3/16	*p*-$CH_3C_6H_4O$•	-1.4	-0.1	-0.5	-0.5	-0.3	-0.2	0.0	0.0	0.0
T3/17	*o*-$CH_2CH_3C_6H_4O$•	0.4	2.5	-0.2	-0.3	-0.4	-0.2	0.0	0.1	0.3
T3/18	*m*-$CH_2CH_3C_6H_4O$•	2.3	-1.4	0.7	0.8	0.8	0.9	1.2	1.1	1.0
T3/19	*p*-$CH_2CH_3C_6H_4O$•	-0.2	-2.0	0.5	0.7	0.9	0.9	1.2	1.1	0.9
T3/20	1-O•-2,3-OH	-4.0	-1.6	-1.4	-2.4	-2.6	-2.0	-0.6	0.6	1.1
T3/21	1-O•-3,4-OH	2.6	1.7	1.2	0.6	0.0	-0.7	-1.9	-2.3	-1.6
T3/22	1-O•-2-OH-4-OCH_3	2.1	-0.1	-2.4	-2.1	-2.0	-2.1	-1.5	-0.9	0.6
T3/23	1-O•-2-OH-6-OCH_3	-6.3	-2.8	1.3	1.1	1.0	0.9	0.8	0.7	0.5
T3/24	1-O•-2-OH-3-CHO	-2.4	3.2	1.0	-0.3	-1.1	-1.5	-1.5	-1.3	-0.3
T3/25	1-O•-2-OH-4-CHO	4.1	-2.4	-0.9	0.2	1.4	2.4	3.5	3.5	1.8
T3/26	1-O•-2-OH-6-CHO	-2.0	-1.0	-0.3	-0.8	-1.1	-1.1	-0.6	-0.1	0.2
T3/27	1-O•-2-OH-4-$CH=CH_2$	0.2	0.4	0.2	0.1	0.0	-0.2	-0.5	-0.6	-0.5
T3/28	1-O•-2-OH-5-$CH=CH_2$	0.1	1.9	-1.4	-0.7	-0.4	-0.4	-0.6	-0.7	-0.7
T3/29	1-O•-2-OH-6-$CH=CH_2$	-0.4	2.8	0.1	0.1	0.0	-0.2	-0.4	-0.6	-0.4
T3/30	1-O•-2-OH-4-CH_3	0.8	0.4	-0.1	-0.1	-0.1	-0.2	-0.5	-0.7	-0.6
T3/31	1-O•-2-OH-5-CH_3	3.1	0.5	-0.2	0.0	0.0	0.0	-0.4	-0.5	-0.6
T3/32	1-O•-2-OH-6-CH_3	0.6	2.1	-0.8	-0.5	-0.3	-0.3	-0.5	-0.6	-0.6
T3/33	1-O•-2-OCH_3-3-OH	0.5	0.0	4.0	3.9	3.5	2.8	1.2	0.1	-1.3
T3/34	1-O•-3-OCH_3-4-OH	2.8	-2.1	4.7	0.9	-0.1	0.3	4.9	2.3	-1.2
T3/35	1-O•-2,3-OCH_3	-1.1	2.2	-2.1	-2.6	-2.7	-2.6	-1.3	-0.1	1.7
T3/36	1-O•-2,6-OCH_3	6.3	-1.0	-1.3	-1.8	-1.9	-1.5	-0.5	0.1	0.5
T3/37	1-O•-3,4-OCH_3	4.0	3.5	-3.9	-1.0	-1.0	0.0	-4.9	-2.4	0.4
T3/38	1-O•-2-OCH_3-3-CHO	4.3	1.1	0.6	2.0	2.8	3.0	1.8	0.2	-1.1
T3/39	1-O•-2-OCH_3-4-CHO	0.4	-4.4	-1.3	-0.9	-0.4	-0.1	0.3	0.4	0.3
T3/40	1-O•-2-OCH_3-6-CHO	-0.8	1.5	0.2	-0.1	-0.5	-0.6	-0.5	-0.2	0.1
T3/41	1-O•-2-OCH_3-3-$CH=CH_2$	-2.5	3.1	2.5	2.1	1.6	0.8	-0.6	-1.4	-1.9
T3/42	1-O•-2-OCH_3-4-$CH=CH_2$	-1.3	-1.4	0.0	0.3	0.3	0.5	0.6	0.7	0.7
T3/43	1-O•-2-OCH_3-3-CH_3	3.2	-0.2	0.8	1.1	1.0	0.6	-0.9	-2.1	-2.8
T3/44	1-O•-2-OCH_3-4-CH_3	-0.3	1.7	0.1	-0.3	-0.4	-0.4	-0.3	-0.1	0.0

T3/45	1-O•-2-OCH_3-5-CH_3	2.7	2.0	-0.1	-0.5	-0.6	-0.6	-0.5	-0.4	-0.1
T3/46	1-O•-3-OCH_3-4-CHO	1.6	2.3	2.3	3.7	3.6	2.4	0.2	-1.1	-1.8
T3/47	1-O•-3-OCH_3-6-CHO	-1.4	2.5	-0.5	-0.5	0.0	0.1	0.6	0.9	1.1
T3/48	1-O•-2-CHO-4-OH	-1.6	2.2	0.3	0.6	1.0	0.8	0.1	-0.6	-1.0
T3/49	1-O•-2-CHO-5-OH	-1.6	2.3	-2.1	-2.0	-1.4	-1.0	-0.5	-0.2	0.3
T3/50	1-O•-2-CHO-6-OH	-1.9	-1.2	-0.2	-0.6	-0.8	-0.8	-0.4	-0.1	0.1
T3/51	1-O•-2-CHO-5-OCH_3	-1.5	-3.2	-0.7	-0.6	-0.1	0.1	0.6	0.9	1.1
T3/52	1-O•-3-CHO-4-OH	-5.4	-0.1	0.5	0.9	1.6	1.9	2.8	2.9	-0.9
T3/53	1-O•-3-CHO-4-OCH_3	2.0	-0.7	0.5	0.0	-1.3	-2.8	-3.9	-3.3	-0.8
T3/54	1-O•-3-CHO-6-OCH_3	-0.8	2.6	-3.5	-2.3	-0.9	0.1	1.3	1.6	2.0
T3/55	1-O•-2,4-CHO	-2.8	-1.5	0.4	0.1	-0.2	-0.2	-0.2	-0.2	0.1
T3/56	1-O•-2,5-CHO	2.5	-2.2	0.8	1.1	0.9	0.9	0.9	1.0	0.9
T3/57	1-O•-3,4-CHO	2.6	2.1	-3.1	-4.5	-4.9	-4.8	-4.0	-3.1	-1.2
T3/58	1-O•-2-CHO-3-CH=CH_2	-1.7	0.5	2.9	2.1	1.6	1.2	0.2	-0.5	-1.2
T3/59	1-O•-2-CHO-5-CH=CH_2	-2.2	0.3	-0.6	-0.4	-0.4	-0.3	-0.2	-0.2	-0.1
T3/60	1-O•-2-CHO-3-CH_3	2.2	1.5	2.2	1.9	1.5	1.0	-0.1	-1.0	-1.4
T3/61	1-O•-2-CHO-4-CH_3	0.3	-0.3	0.2	0.2	0.0	0.0	-0.2	-0.2	-0.2
T3/62	1-O•-2-CHO-5-CH_3	1.9	0.7	0.3	0.1	-0.1	-0.1	-0.2	-0.2	-0.1
T3/63	1-O•-2-CHO-6-CH_3	-0.4	0.0	-0.5	-0.5	-0.5	-0.5	-0.3	0.0	0.1
T3/64	1-O•-2-CH=CH_2-5-CH_3	4.4	1.1	-0.4	-0.3	-0.2	-0.1	-0.2	-0.2	-0.3
T3/65	1-O•-2-CH=CH_2-6-CH_3	0.6	-2.1	-1.5	-1.2	-1.0	-0.8	-0.6	-0.5	-0.4
T3/66	1-O•-2-CH_3-4-CHO	-0.8	-3.5	0.6	0.6	0.7	0.9	1.1	1.2	0.6
T3/67	1-O•-2,6-CH_3	0.4	3.8	-1.3	-1.0	-0.6	-0.4	-0.1	0.0	-0.1
T3/68	1-O•-2-CH_2CH_3-4-CHO	0.5	-3.6	1.8	1.3	1.1	1.2	1.4	1.4	1.1
T4/1	C_6H_5C•=O	-1.4	-0.2	0.0	0.0	0.1	0.2	0.4	0.4	0.3
T4/2	*o*-OHC_6H_5C•=O	-3.0	-1.2	-3.6	-4.1	-4.7	-5.2	-5.9	-5.5	-2.7
T4/3	*m*-OHC_6H_5C•=O	-1.2	-0.7	0.2	0.3	0.4	0.4	0.4	0.3	0.1
T4/4	*p*-OHC_6H_5C•=O	-2.7	-2.0	0.9	0.5	0.2	0.0	-0.3	-0.5	-0.1
T4/5	*o*-$OCH_3C_6H_5C$•=O	1.2	-2.4	0.4	1.1	1.5	1.8	1.9	1.7	1.0
T4/6	*m*-$OCH_3C_6H_5C$•=O	1.5	-0.8	-1.0	-1.0	-0.7	-0.5	0.1	0.5	0.5
T4/7	*p*-$OCH_3C_6H_5C$•=O	-2.5	-3.2	0.7	0.1	-0.5	-0.7	-0.5	-0.1	0.6
T4/8	*m*-$CHOC_6H_5C$•=O	-0.9	-2.7	0.9	1.4	1.5	1.6	1.4	1.3	1.2
T4/9	*p*-$CHOC_6H_5C$•=O	-1.1	-0.3	-0.9	-0.7	-0.6	-0.5	-0.6	-0.6	-0.5
T4/10	*o*-CH=$CH_2C_6H_5C$•=O	-3.4	1.8	0.8	0.2	-0.5	-1.0	-1.3	-1.3	-0.8
T4/11	*m*-CH=$CH_2C_6H_5C$•=O	0.8	-1.2	0.6	0.4	0.4	0.4	0.5	0.5	0.3
T4/12	*p*-CH=$CH_2C_6H_5C$•=O	-5.7	-0.3	0.6	0.3	0.2	0.2	0.3	0.3	0.1
T4/13	*o*-$CH_3C_6H_5C$•=O	-1.5	3.5	-1.0	-0.7	-0.4	-0.1	0.3	0.4	0.3
T4/14	*m*-$CH_3C_6H_5C$•=O	0.8	-0.9	0.9	0.6	0.5	0.5	0.5	0.4	0.2
T4/15	*p*-$CH_3C_6H_5C$•=O	1.9	0.7	1.1	0.7	0.4	0.3	0.1	0.0	-0.1
T4/16	*o*-$CH_2CH_3C_6H_5C$•=O	1.2	0.8	-0.8	-1.1	-1.0	-0.8	-0.2	0.0	0.4
T4/17	*m*-$CH_2CH_3C_6H_5C$•=O	2.6	-3.2	1.5	1.4	1.3	1.3	1.4	1.3	1.1
T4/18	*p*-$CH_2CH_3C_6H_5C$•=O	3.6	-0.2	1.8	1.6	1.4	1.3	1.2	1.0	0.8
T4/19	1-C•=O-2,3-OH	1.3	0.2	0.6	-0.2	-0.5	-0.4	0.0	0.6	0.7
T4/20	1-C•=O-2,5-OH	-4.2	1.4	0.1	-0.2	-0.6	-1.5	-3.4	-4.9	-5.1
T4/21	1-C•=O-3,4-OH	-2.9	1.5	-1.1	-1.7	-1.8	-1.8	-1.7	-1.5	-0.7
T4/22	1-C•=O-3-OH-4-OCH_3	-1.6	-0.1	0.4	-1.3	-2.3	-2.7	-2.3	-1.5	-0.3
T4/23	1-C•=O-3-OH-6-OCH_3	1.8	-0.8	0.6	1.8	2.2	1.8	1.3	0.8	-0.1
T4/24	1-C•=O-2-OH-3-CHO	-1.9	2.2	0.3	-1.1	-1.9	-2.2	-1.8	-1.0	0.2
T4/25	1-C•=O-3-OH-4-CH=CH_2	1.9	-1.7	5.4	5.4	4.9	4.2	3.0	2.2	1.0
T4/26	1-C•=O-2-OH-4-CH_3	5.5	1.9	3.8	4.1	4.2	4.3	4.4	4.3	2.5
T4/27	1-C•=O-2-OH-5-CH_3	-3.3	-1.8	-2.5	-3.1	-3.8	-4.6	-5.7	-5.4	-2.8
T4/28	1-C•=O-2-OH-6-CH_3	1.7	-1.5	-0.2	0.3	0.8	1.3	2.0	2.2	1.5
T4/29	1-C•=O-2-OCH_3-4-OH	2.4	0.8	-1.4	-1.3	-1.0	-0.7	-0.4	-0.2	0.3
T4/30	1-C•=O-3-OCH_3-4-OH	1.6	0.9	0.6	0.9	1.0	0.6	-0.7	-1.9	-2.7
T4/31	1-C•=O-2-OCH_3-3-CH_3	-3.0	1.1	1.0	-1.2	-3.2	-4.4	-4.9	-4.3	-2.8

T4/32	1-C•=O-2-OCH_3-5-CH_3	1.2	-3.3	1.9	2.3	2.5	2.5	2.2	1.9	0.9
T4/33	1-C•=O-2-OCH_3-6-CH_3	-0.7	3.6	-4.4	-3.2	-1.3	0.2	1.6	1.8	1.2
T4/34	1-C•=O-3-CHO-4-OH	-0.8	-2.7	-1.6	-0.7	0.0	0.2	-0.2	-1.1	-3.4
T4/35	1-C•=O-2-CH=CH_2-4-CH_3	1.1	2.9	1.7	0.7	-0.4	-1.1	-1.7	-1.7	-1.1
T4/36	1-C•=O-2-CH=CH_2-5-CH_3	4.8	1.9	1.1	0.3	-0.6	-1.1	-1.4	-1.4	-0.9
T4/37	1-C•=O-2-CH=CH_2-6-CH_3	-1.7	2.8	-5.7	-3.7	-1.9	-0.6	0.5	0.7	0.5
T4/38	1-C•=O-2-CH_3-4-OH	1.7	2.4	-0.4	-0.4	-0.5	-0.7	-0.8	-0.8	-0.2
T4/39	1-C•=O-2-CH_3-4-CHO	0.8	-1.5	1.7	1.2	0.8	0.4	-0.1	-0.3	-0.4
T4/40	1-C•=O-2-CH_3-4-CH=CH_2	-4.5	4.1	-0.5	-0.5	-0.3	-0.1	0.2	0.3	0.2
T4/41	1-C•=O-2,3-CH_3	0.3	1.8	-0.8	-0.4	-0.1	0.2	0.6	0.8	1.0
T4/42	1-C•=O-3-CH_3-4-CHO	0.7	-0.5	-5.3	-3.6	-2.1	-0.9	0.5	1.0	1.1
T5/1	t-C_6H_5CH=CH•	-1.0	2.2	-0.5	-0.6	-0.5	-0.3	-0.1	-0.1	0.1
T5/2	*o*-(OH)t-C_6H_5CH=CH•	0.2	1.0	-1.5	-1.4	-1.1	-1.0	-0.8	-0.4	0.1
T5/3	*m*-(OH)t-C_6H_5CH=CH•	-0.2	1.2	0.3	0.1	0.2	0.2	0.1	0.0	0.0
T5/4	*p*-(OH)t-C_6H_5CH=CH•	-0.5	0.9	2.1	1.3	0.9	0.6	0.3	0.0	-0.1
T5/5	*o*-(OCH_3)t-C_6H_5CH=CH•	-1.4	3.3	-1.3	-1.4	-1.2	-1.2	-1.3	-1.5	-1.3
T5/6	*m*-(OCH_3)t-C_6H_5CH=CH•	2.1	-0.6	-0.6	-0.6	-0.2	0.0	0.5	0.6	0.6
T5/7	*p*-(OCH_3)t-C_6H_5CH=CH•	1.6	0.1	1.8	0.8	0.6	0.5	0.5	0.5	0.5
T5/8	*o*-(CHO)t-C_6H_5CH=CH•	2.3	1.5	-0.4	-1.4	-1.9	-2.1	-2.0	-1.5	-0.4
T5/9	*m*-(CHO)t-C_6H_5CH=CH•	-3.2	-2.9	-0.2	0.0	0.3	0.6	1.0	1.0	0.8
T5/10	*p*-(CHO)t-C_6H_5CH=CH•	-2.5	-1.6	1.4	1.0	0.9	1.0	1.1	1.0	0.6
T5/11	*o*-(CH=CH_2)t-C_6H_5CH=CH•	-0.1	-2.8	-0.7	0.2	0.1	0.0	-0.2	-0.2	0.0
T5/12	*m*-(CH=CH_2)t-C_6H_5CH=CH•	-3.9	1.9	0.1	-0.3	-0.2	-0.2	0.0	0.0	0.1
T5/13	*p*-(CH=CH_2)t-C_6H_5CH=CH•	-3.9	3.4	0.1	-0.3	-0.4	-0.4	-0.5	-0.5	-0.4
T5/14	*o*-(CH_3)t-C_6H_5CH=CH•	0.6	-1.8	-5.7	-3.5	-2.5	-1.9	-1.1	-0.8	-0.4
T5/15	*m*-(CH_3)t-C_6H_5CH=CH•	0.0	1.7	0.4	-0.1	-0.1	-0.1	-0.1	-0.1	0.0
T5/16	*p*-(CH_3)t-C_6H_5CH=CH•	-0.3	2.3	0.4	0.0	-0.1	-0.1	-0.1	-0.2	0.0
T5/17	*o*-(CH_2CH_3)t-C_6H_5CH=CH•	1.9	0.0	-2.4	-1.3	-0.9	-0.6	-0.2	-0.2	0.0
T5/18	*m*-(CH_2CH_3)t-C_6H_5CH=CH•	3.0	-1.0	1.6	1.4	1.2	1.2	1.1	0.8	0.9
T5/19	*p*-(CH_2CH_3)t-C_6H_5CH=CH•	1.3	-3.4	0.7	0.5	0.5	0.6	0.8	0.6	0.7
T5/20	1-(t-CH=CH•)-2,3-OH	-4.0	-1.2	0.9	1.6	2.7	3.0	2.9	2.6	1.8
T5/21	1-(t-CH=CH•)-2,4-OH	3.7	0.9	1.2	1.4	1.8	1.6	0.5	-0.7	-1.7
T5/22	1-(t-CH=CH•)-3,4-OH	-0.1	4.3	-1.6	-2.4	-2.2	-1.9	-1.2	-0.6	0.1
T5/23	1-(t-CH=CH•)-2-OH-4-CHO	-4.1	1.0	0.1	-0.4	-0.5	-0.5	0.2	0.9	1.4
T5/24	1-(t-CH=CH•)-2-OH-6-CHO	6.3	1.4	2.9	3.1	3.6	3.9	2.7	0.4	-3.5
T5/25	1-(t-CH=CH•)-2-OH-5-CH=CH_2	-3.2	0.9	-1.0	-0.9	-0.8	-0.9	-0.8	-0.7	-0.3
T5/26	1-(t-CH=CH•)-2-OH-5-CH_3	-2.3	0.1	-0.7	-0.7	-0.6	-0.7	-0.6	-0.3	0.2
T5/27	1-(t-CH=CH•)-2-OH-6-CH_3	-4.3	3.8	-4.4	-3.7	-2.9	-2.2	-0.9	-0.2	0.3
T5/28	1-(t-CH=CH•)-2-OH-4-CH_2CH_3	3.6	-2.7	0.1	0.2	0.4	0.4	0.4	0.3	0.6
T5/29	1-(t-CH=CH•)-2-OH-5-CH_2CH_3	3.7	-4.5	2.7	2.7	2.0	1.4	0.7	0.7	0.9
T5/30	1-(t-CH=CH•)-2-CHO-4-OH	0.3	3.3	2.6	0.7	-0.3	-1.0	-1.4	-1.1	-0.2
T5/31	1-(t-CH=CH•)-3-CHO-4-OH	-0.7	-2.2	-0.3	-0.4	-0.1	-0.1	-0.4	-1.5	-4.5
T5/32	1-(t-CH=CH•)-2,4-CHO	3.0	-0.5	2.8	0.7	-0.3	-0.8	-1.0	-0.9	-0.5
T5/33	1-(t-CH=CH•)-2-CH=CH_2-4-CH_3	1.0	1.7	0.6	0.6	0.1	-0.2	-0.5	-0.5	-0.2
T5/34	1-(t-CH=CH•)-2-CH=CH_2-6-CH_3	1.4	-4.1	2.2	3.1	3.1	2.7	1.8	1.1	0.3
T5/35	1-(t-CH=CH•)-2-CH_3-4-CHO	-0.4	-2.7	-0.5	0.2	0.4	0.4	0.6	0.6	0.3
T5/36	1-(t-CH=CH•)-2,3-CH_3	-1.6	-0.6	0.7	1.6	1.9	2.2	2.4	2.3	1.8
T5/37	1-(t-CH=CH•)-2,4-CH_3	1.7	-0.5	-2.6	-1.5	-1.1	-0.9	-0.7	-0.6	-0.4
T5/38	1-(t-CH=CH•)-2-CH_3-4-CH_2CH_3	3.4	0.3	-1.9	-0.7	-0.3	-0.1	0.2	0.2	0.4
T5/39	c-C_6H_5CH=CH•	-1.2	3.3	-1.2	-1.4	-1.7	-1.5	-1.0	-0.9	-0.5
T5/40	*o*-(OH)c-C_6H_5CH=CH•	0.3	1.6	-1.7	-0.8	0.0	0.6	1.0	0.8	0.3
T5/41	*m*-(OH)c-C_6H_5CH=CH•	-0.5	1.0	1.2	0.4	-0.2	-0.4	-0.4	-0.5	-0.5
T5/42	*p*-(OH)c-C_6H_5CH=CH•	-1.2	1.6	1.2	0.3	-0.4	-0.7	-0.8	-0.8	-0.8
T5/43	*o*-(OCH_3)c-C_6H_5CH=CH•	1.9	-1.2	2.5	1.1	-0.4	-1.4	-2.1	-2.3	-2.0
T5/44	*m*-(OCH_3)c-C_6H_5CH=CH•	1.7	0.5	0.9	0.0	-0.5	-0.4	0.0	0.1	0.1

T5/45	*p*-(OCH_3)c-C_6H_5CH=CH•	0.9	1.0	0.9	-0.1	-0.7	-0.8	-0.5	-0.3	-0.2
T5/46	*o*-(CHO)c-C_6H_5CH=CH•	-1.0	-2.6	-2.6	-1.3	-0.7	-0.3	0.2	0.4	0.7
T5/47	*m*-(CHO)c-C_6H_5CH=CH•	-3.2	-3.4	1.4	0.8	0.5	0.9	2.2	2.9	3.1
T5/48	*p*-(CHO)c-C_6H_5CH=CH•	-3.1	3.8	1.0	0.3	-0.2	-0.2	0.1	0.1	0.0
T5/49	*o*-($CH=CH_2$)c-C_6H_5CH=CH•	-0.4	0.6	-2.8	-1.7	-1.4	-1.0	-0.3	-0.1	0.0
T5/50	*m*-($CH=CH_2$)c-C_6H_5CH=CH•	-4.0	2.6	-0.6	-1.0	-1.3	-1.3	-0.9	-0.7	-0.5
T5/51	*p*-($CH=CH_2$)c-C_6H_5CH=CH•	-4.1	3.9	-0.7	-1.2	-1.7	-1.7	-1.5	-1.4	-1.0
T5/52	*o*-(CH_3)c-C_6H_5CH=CH•	-1.2	3.4	0.2	-0.1	-0.6	-0.7	-0.8	-0.8	-0.7
T5/53	*m*-(CH_3)c-C_6H_5CH=CH•	0.6	2.4	-0.1	-0.5	-1.0	-1.0	-0.9	-0.9	-0.7
T5/54	*p*-(CH_3)c-C_6H_5CH=CH•	-0.6	2.9	-0.4	-0.9	-1.3	-1.3	-1.1	-1.0	-0.7
T5/55	*o*-(CH_2CH_3)c-C_6H_5CH=CH•	2.2	2.9	-1.7	-1.1	-1.0	-0.8	-0.7	-0.8	-0.7
T5/56	*m*-(CH_2CH_3)c-C_6H_5CH=CH•	1.4	0.7	0.0	-0.2	-0.6	-0.5	-0.1	-0.1	0.2
T5/57	*p*-(CH_2CH_3)c-C_6H_5CH=CH•	1.1	1.1	0.1	-0.2	-0.6	-0.5	-0.2	-0.2	0.0
T5/58	1-(c-CH=CH•)-2,4-OH	2.4	4.0	-2.0	-1.6	-0.9	-0.6	-0.2	-0.3	-0.6
T5/59	1-(c-CH=CH•)-2,5-OH	-2.2	0.6	0.2	1.1	1.7	1.7	1.4	0.8	-0.2
T5/60	1-(c-CH=CH•)-2-OH-4-OCH_3	5.2	4.9	-2.2	-2.0	-1.3	-0.8	0.0	0.3	0.1
T5/61	1-(c-CH=CH•)-2-OH-5-OCH_3	-2.2	-0.7	-0.1	1.3	2.2	2.3	2.0	1.5	0.3
T5/62	1-(c-CH=CH•)-2-OH-4-$CH=CH_2$	-2.1	2.9	-1.5	-0.8	-0.1	0.4	0.7	0.6	0.0
T5/63	1-(c-CH=CH•)-3-OH-5-$CH=CH_2$	1.3	3.4	0.5	-0.5	-1.2	-1.7	-1.8	-1.8	-1.5
T5/64	1-(c-CH=CH•)-2-OH-3-CH_3	2.0	3.7	-5.4	-2.9	-1.2	-0.2	0.6	0.6	0.2
T5/65	1-(c-CH=CH•)-2-OH-4-CH_3	1.7	2.2	-0.9	-0.4	0.1	0.5	0.8	0.6	0.1
T5/66	1-(c-CH=CH•)-2-OH-5-CH_3	-1.8	0.9	-1.4	-0.3	0.5	1.0	1.3	1.0	0.3
T5/67	1-(c-CH=CH•)-3-OH-5-CH_3	5.8	4.3	0.0	-0.8	-1.5	-2.0	-2.2	-2.2	-1.8
T5/68	1-(c-CH=CH•)-2-OH-3-CH_2CH_3	3.5	4.0	-5.4	-3.1	-1.6	-0.5	0.5	0.4	0.4
T5/69	1-(c-CH=CH•)-3-CHO-4-OH	-1.6	2.1	-0.5	-0.8	-0.9	-0.9	-0.3	-0.1	-0.3
T5/70	1-(c-CH=CH•)-2,4-CHO	-0.8	-0.2	0.9	1.0	0.9	0.9	0.9	0.8	0.5
T5/71	1-(c-CH=CH•)-2-CHO-5-$CH=CH_2$	-1.5	-1.0	-1.4	-0.5	-0.1	0.1	0.4	0.6	0.6
T5/72	1-(c-CH=CH•)-2-CHO-4-CH_3	-0.1	-2.4	-2.0	-0.8	-0.3	0.0	0.3	0.5	0.7
T5/73	1-(c-CH=CH•)-2-$CH=CH_2$-4-OH	-0.1	0.4	0.8	1.2	0.8	0.4	0.1	-0.1	-0.3
T5/74	1-(c-CH=CH•)-2-$CH=CH_2$-5-CH_3	0.2	1.8	-1.3	-0.2	-0.2	-0.2	-0.1	-0.1	-0.1
T5/75	1-(c-CH=CH•)-2-$CH=CH_2$-6-CH_3	1.1	1.5	2.3	-5.4	-4.0	-2.9	-1.7	-1.1	-0.6
T5/76	1-(c-CH=CH•)-2-CH_3-4-OH	0.2	2.6	2.7	1.6	0.6	-0.1	-0.7	-0.9	-1.0
T5/77	1-(c-CH=CH•)-2-CH_3-4-CHO	-2.1	-0.2	1.9	1.1	0.4	0.2	0.2	0.2	-0.2
T5/78	1-(c-CH=CH•)-2-CH_3-4-$CH=CH_2$	-3.6	3.6	0.1	0.3	-0.2	-0.5	-0.8	-0.8	-0.9
T5/79	1-(c-CH=CH•)-3-CH_3-4-$CH=CH_2$	-2.0	1.5	0.4	0.8	0.7	0.8	0.8	0.7	0.2
T5/80	1-(c-CH=CH•)-2,4-CH_3	-0.2	3.7	1.0	0.4	-0.3	-0.6	-0.9	-0.9	-0.9
T6/1	$C_6H_5CH_2$•	-3.2	0.8	-2.3	-1.7	-1.2	-0.6	-0.1	0.0	0.2
T6/2	*o*-(OH)$C_6H_5CH_2$•	-1.2	-0.3	-1.5	-0.5	0.2	0.6	1.0	0.8	0.5
T6/3	*m*-(OH)$C_6H_5CH_2$•	-2.7	-1.3	-0.3	-0.1	0.1	0.3	0.5	0.4	0.2
T6/4	*p*-(OH)$C_6H_5CH_2$•	-2.4	-1.6	0.4	0.4	0.5	0.5	0.5	0.2	0.1
T6/5	*o*-(OCH_3)$C_6H_5CH_2$•	1.6	4.9	0.3	-1.3	-2.3	-2.7	-2.6	-2.3	-1.4
T6/6	*m*-(OCH_3) $C_6H_5CH_2$•	-0.8	-2.3	-1.8	-1.2	-0.5	0.0	0.8	0.9	0.8
T6/7	*p*-(OCH_3)$C_6H_5CH_2$•	-0.8	-1.8	0.3	0.2	0.3	0.5	0.9	0.9	0.7
T6/8	*o*-(CHO)$C_6H_5CH_2$•	-1.0	2.9	-1.3	-1.2	-1.0	-0.6	-0.3	-0.1	0.0
T6/9	*m*-(CHO)$C_6H_5CH_2$•	-4.2	-0.1	-0.4	-0.2	0.2	0.6	1.2	1.2	1.0
T6/10	*p*-(CHO)$C_6H_5CH_2$•	-3.5	-2.4	-0.7	-0.3	0.3	0.8	1.3	1.3	1.0
T6/11	*o*-($CH=CH_2$)$C_6H_5CH_2$•	-0.2	0.9	-1.9	-1.7	-1.3	-0.9	-0.3	-0.2	0.0
T6/12	*m*-($CH=CH_2$)$C_6H_5CH_2$•	-3.8	0.4	-2.1	-1.6	-1.1	-0.7	-0.1	0.0	0.1
T6/13	*p*-($CH=CH_2$)$C_6H_5CH_2$•	-2.5	-0.6	-0.6	-0.2	0.0	0.4	0.5	0.4	0.4
T6/14	*o*-(CH_3)$C_6H_5CH_2$•	-0.7	1.2	-1.4	-1.2	-1.0	-0.9	-0.6	-0.4	-0.2
T6/15	*m*-(CH_3)$C_6H_5CH_2$•	-1.7	0.2	-1.4	-1.1	-0.8	-0.5	-0.1	0.0	0.1
T6/16	*p*-(CH_3)$C_6H_5CH_2$•	-2.2	-0.2	-1.3	-0.9	-0.6	-0.3	0.0	0.0	0.1
T6/17	*o*-(CH_2CH_3)$C_6H_5CH_2$•	-0.6	0.9	0.5	0.3	0.1	0.0	-0.2	-0.4	-0.4
T6/18	*m*-(CH_2CH_3)$C_6H_5CH_2$•	-0.7	-0.9	-1.1	-0.5	-0.1	0.3	0.9	0.8	0.9
T6/19	*p*-(CH_2CH_3)$C_6H_5CH_2$•	-0.6	-1.5	-0.7	-0.2	0.1	0.5	1.0	0.8	0.8

T6/20	1-CH_2•-2,3-OH	0.0	-0.1	-0.5	-0.6	-0.3	-0.2	0.0	0.2	0.5
T6/21	1-CH_2•-2,4-OH	0.7	-2.5	3.5	3.1	3.0	2.5	1.8	1.2	0.7
T6/22	1-CH_2•-2,5-OH	-0.6	-0.2	0.8	1.3	1.6	1.2	0.8	0.3	-0.3
T6/23	1-CH_2•-2,6-OH	1.6	-1.4	2.2	2.7	3.1	3.0	2.6	1.9	0.9
T6/24	1-CH_2•-2-OH-3-OCH_3	2.0	-0.6	2.8	4.1	4.2	3.4	1.5	0.1	-1.2
T6/25	1-CH_2•-2-OH-4-OCH_3	0.8	-2.0	0.8	1.4	2.0	2.1	2.2	1.9	1.2
T6/26	1-CH_2•-2-OCH_3-4-OH	3.0	2.9	1.3	-0.3	-1.5	-2.3	-2.7	-2.5	-1.8
T6/27	1-CH_2•-2,4-OCH_3	4.8	4.3	1.7	-0.2	-1.3	-2.0	-2.0	-1.7	-1.1
T6/28	1-CH_2•-2-OCH_3-4-CHO	5.9	2.8	1.3	0.4	-0.8	-1.9	-2.9	-3.0	-2.4
T6/29	1-CH_2•-2-OCH_3-4-CH=CH_2	4.1	3.8	2.2	0.3	-1.2	-2.0	-2.5	-2.4	-1.6
T6/30	1-CH_2•-2-OCH_3-4-CH_3	3.0	3.7	0.9	-1.0	-2.1	-2.7	-2.7	-2.4	-1.5
T6/31	1-CH_2•-2-OCH_3-4-CH_2CH_3	4.2	4.1	1.7	-0.1	-1.2	-1.7	-1.6	-1.4	-0.6
T6/32	1-CH_2•-2,4-CHO	0.4	-1.3	1.7	1.0	0.7	0.6	0.5	0.3	0.1
T6/33	1-CH_2•-2,5-CHO	4.2	-3.0	1.4	0.7	0.4	0.4	0.3	0.3	-0.1
T6/34	1-CH_2•-2,6-CHO	-3.0	-1.4	0.1	1.2	1.6	1.4	1.0	0.6	0.5
T6/35	1-CH_2•-2-CHO-4-CH=CH_2	0.2	2.0	0.1	0.2	0.3	0.4	0.4	0.4	0.2
T6/36	1-CH_2•-2-CH=CH_2-3-OH	5.9	-1.4	0.2	-2.7	-4.1	-4.6	-4.3	-3.5	-1.9
T6/37	1-CH_2•-2-CH=CH_2-3-OCH_3	-4.8	-0.1	2.5	3.4	3.8	3.7	3.2	2.6	1.7
T6/38	1-CH_2•-2,3-CH=CH_2	0.5	2.4	-1.7	-2.3	-2.5	-2.6	-2.4	-2.0	-1.3
T6/39	1-CH_2•-2-CH_3-3-OH	-2.3	-1.8	0.6	1.3	1.9	1.9	1.8	1.5	0.8
T6/40	1-CH_2•-2-CH_3-4-OH	1.3	-0.7	1.1	0.6	0.5	0.1	-0.2	-0.3	-0.4
T6/41	1-CH_2•-2-CH_3-5-OH	-2.2	-1.3	0.4	0.4	0.6	0.4	0.3	0.2	0.0
T6/42	1-CH_2•-2-CH_3-6-OH	1.6	0.8	-1.5	-0.8	-0.1	0.0	0.2	0.3	0.1
T6/43	1-CH_2•-2-CH_3-4-CHO	0.3	-2.3	-0.1	0.0	0.2	0.5	0.7	0.9	0.6
T6/44	1-CH_2•-2-CH_3-6-CHO	0.7	0.8	-1.9	-2.3	-2.3	-2.1	-1.7	-1.1	-0.6
T6/45	1-CH_2•-2-CH_3-4-CH=CH_2	0.9	0.1	0.1	0.1	0.1	0.0	-0.1	-0.1	-0.1
T6/46	1-CH_2•-2-CH_3-5-CH=CH_2	-0.9	1.0	-1.3	-1.1	-0.9	-0.9	-0.6	-0.4	-0.3
T6/47	1-CH_2•-2,4-CH_3	0.6	0.5	-0.5	-0.5	-0.5	-0.5	-0.5	-0.4	-0.3
T6/48	1-CH_2•-2,5-CH_3	0.2	0.5	-0.6	-0.6	-0.5	-0.6	-0.5	-0.4	-0.3
T6/49	1-CH_2•-3-CH_3-4-OH	-0.2	0.4	-2.2	-1.2	-0.4	-0.1	0.2	0.1	0.0
T6/50	1-CH_2•-3-CH_3-4-OCH_3	1.9	1.8	-1.8	-2.5	-3.3	-3.7	-3.6	-3.0	-1.8
T6/51	1-CH_2•-3,5-CH_3	-0.4	-0.3	-0.6	-0.6	-0.5	-0.3	-0.1	-0.1	0.0
T6/52	1-CH_2•-3,6-CH_3	-0.1	0.5	-0.5	-0.5	-0.5	-0.6	-0.5	-0.4	-0.3
T6/53	C_6H_5CH•CH_3	-1.0	0.7	-0.9	-0.7	-0.6	-0.4	-0.3	-0.3	-0.1
T6/54	*o*-(OH)C_6H_5CH•CH_3	0.1	0.2	-1.6	-0.5	0.3	0.7	0.8	0.7	0.3
T6/55	*m*-(OH)C_6H_5CH•CH_3	0.4	-1.6	1.4	1.0	0.8	0.5	0.2	0.1	-0.1
T6/56	*p*-(OH)C_6H_5CH•CH_3	-1.0	-1.9	1.6	1.2	1.0	0.7	0.3	0.0	-0.2
T6/57	*o*-(OCH_3)C_6H_5CH•CH_3	3.1	0.8	0.6	-0.8	-1.6	-2.0	-2.2	-2.1	-1.7
T6/58	*m*-(OCH_3)C_6H_5CH•CH_3	1.2	-1.3	-1.8	-0.5	0.5	1.0	1.4	1.4	1.0
T6/59	*p*-(OCH_3)C_6H_5CH•CH_3	0.4	-1.3	1.4	1.1	1.0	0.9	0.8	0.8	0.5
T6/60	*o*-(CHO)C_6H_5CH•CH_3	1.5	1.5	-0.1	-0.9	-1.4	-1.4	-1.2	-0.9	-0.4
T6/61	*m*-(CHO)C_6H_5CH•CH_3	-0.9	-3.1	0.7	0.6	0.6	0.7	0.8	0.8	0.6
T6/62	*p*-(CHO)C_6H_5CH•CH_3	-3.8	2.6	-0.3	-0.1	0.1	0.4	0.7	0.8	0.9
T6/63	*o*-(CH=CH_2)C_6H_5CH•CH_3	0.3	1.6	-1.4	-1.1	-0.8	-0.6	-0.3	-0.3	-0.1
T6/64	*m*-(CH=CH_2)C_6H_5CH•CH_3	-1.3	0.7	-0.9	-0.7	-0.6	-0.5	-0.4	-0.3	-0.2
T6/65	*p*-(CH=CH_2)C_6H_5CH•CH_3	-0.6	0.2	0.6	0.6	0.6	0.4	0.2	0.2	0.1
T6/66	*o*-(CH_3)C_6H_5CH•CH_3	-0.1	2.0	-0.8	-1.0	-1.1	-1.2	-1.1	-0.9	-0.6
T6/67	*m*-(CH_3)C_6H_5CH•CH_3	0.3	0.1	-0.1	-0.2	-0.3	-0.3	-0.4	-0.4	-0.2
T6/68	*o*-(CH_2CH_3)C_6H_5CH•CH_3	-0.2	2.0	0.9	0.5	0.1	-0.2	-0.5	-0.8	-0.7
T6/69	*m*-(CH_2CH_3)C_6H_5CH•CH_3	1.3	-1.5	0.1	0.3	0.3	0.5	0.6	0.5	0.6
T6/70	*p*-(CH_2CH_3)C_6H_5CH•CH_3	1.4	-1.9	0.5	0.6	0.6	0.6	0.6	0.5	0.5
V1/1	1-C•-2-OH-3-CHO-5-OCH_3	-2.0	-2.8	3.5	4.8	4.8	4.0	2.6	1.4	-0.4
V1/2	1-C•-2-CHO-5-OH-6-OCH_3	-2.2	0.9	2.1	1.7	2.0	2.3	3.1	3.1	1.4
V2/1	1-OCH_2•-2,3-OH	1.0	2.1	1.4	1.2	0.6	-0.3	-1.2	-1.1	-0.8
V2/2	1-OCH_2•-2-OH-4-CH=CH_2	-1.2	4.4	-0.3	-1.0	-1.9	-3.2	-4.2	-4.1	-2.9

V2/3	1-OCH_2•-2-OCH_3-3-CH_3	-3.7	0.5	5.1	5.5	4.7	4.0	3.0	2.2	1.0
V2/4	1-OCH_2•-2-CHO-5-CH_3	2.9	2.5	-0.2	-0.1	0.3	0.7	1.0	1.0	0.5
V2/5	1-OCH_2•-2,3,4-CH_3	-1.0	-3.4	1.4	1.4	1.8	2.4	3.1	3.0	2.4
V3/1	1-O•-2,3,4-OH	-4.1	-2.4	0.3	1.0	2.2	2.7	2.7	1.8	0.6
V3/2	1-O•-2-OH-4-OCH_3-6-CHO	3.0	-1.9	1.8	1.4	0.7	0.0	-0.7	-0.8	-0.3
V3/3	1-O•-2-OH-3-CH=CH_2	2.5	0.6	3.5	3.5	3.0	2.6	1.5	1.0	0.3
V3/4	1-O•-2-OH-3-CH_3	4.4	1.0	-0.2	0.1	0.1	0.1	-0.3	-0.5	-0.5
V3/5	1-O•-2,4-OCH_3	-5.3	-2.1	-1.4	-1.7	-1.9	-2.4	-2.0	-1.3	-0.3
V3/6	1-O•-2-OCH_3-6-CH=CH_2	-5.0	-3.0	1.7	1.7	1.5	1.4	1.5	1.5	1.3
V3/7	1-O•-2-CHO-4-OCH_3	4.0	2.2	-1.8	-0.9	-0.3	-0.3	-0.4	-0.6	-0.6
V3/8	1-O•-2,3-CHO	3.0	0.7	-1.1	-1.4	-1.4	-1.1	-1.1	-1.3	-1.4
V3/9	1-O•-2-CHO-6-CH=CH_2	-0.9	0.8	0.3	0.1	-0.1	-0.1	-0.2	-0.2	-0.1
V3/10	1-O•-2-CH=CH_2-4-CH_3	0.8	0.2	-0.1	-0.1	-0.1	-0.1	-0.1	-0.2	-0.1
V3/11	1-O•-2-CH_3-3-CHO	-2.7	-5.7	6.0	5.1	4.2	3.3	2.4	1.7	1.2
V3/12	1-O•-2,6-CH_2CH_3	2.9	-0.3	-0.8	-0.7	-0.6	-0.5	0.0	0.0	0.4
V4/1	1-C•=O-2,4-OH	1.2	-1.2	2.9	3.5	3.9	4.1	4.3	4.2	3.0
V4/2	1-C•=O-2-OH-4-OCH_3	4.3	2.4	1.9	2.4	2.5	2.8	3.7	4.2	3.6
V4/3	1-C•=O-2-OH-5-CHO	1.8	0.5	-1.0	0.0	1.2	2.1	3.2	3.5	3.0
V4/4	1-C•=O-2-OH-6-CH=CH_2	-3.6	-3.3	0.5	0.3	0.6	0.9	1.2	1.2	0.8
V4/5	1-C•=O-2-OH-3-CH_3	0.3	0.4	-3.0	-2.4	-1.9	-1.7	-2.2	-3.3	-4.5
V4/6	1-C•=O-3-OCH_3-4-CH_3	-2.7	0.9	1.8	0.5	-0.6	-1.3	-1.8	-1.7	-0.8
V4/7	1-C•=O-3-CHO-4-CH_3	4.7	1.6	-0.3	-0.1	-0.2	-0.5	-0.9	-1.0	-0.3
V4/8	1-C•=O-2-CH=CH_2-3-CH_3	2.6	-6.2	1.6	2.3	2.6	2.9	2.9	2.6	1.5
V4/9	1-C•=O-3-CH_3-4-OH	-0.4	1.1	-2.6	-1.9	-1.5	-1.3	-1.1	-0.9	-0.3
V5/1	1-(t-CH=CH•)-2,5-OH	-3.0	0.1	1.1	-0.3	-1.3	-2.0	-1.4	-0.3	0.8
V5/2	1-(t-CH=CH•)-2-OH-5-CH_2CH_3	-0.5	-2.1	-0.5	-0.3	-0.2	-0.1	0.2	0.4	1.0
V5/3	1-(t-CH=CH•)-3,4-CHO	-3.4	2.2	0.1	-0.5	-0.8	-1.2	-1.8	-2.0	-1.4
V5/4	1-(t-CH=CH•)-2-CHO-5-CH=CH_2	0.4	1.6	0.5	-0.9	-1.5	-1.8	-1.8	-1.4	-0.5
V5/5	1-(t-CH=CH•)-2-CH=CH_2-3-CH_3	-1.5	-4.0	0.7	2.8	3.5	3.8	3.3	2.7	1.6
V5/6	1-(t-CH=CH•)-2-CH=CH_2-5-CH_3	0.7	0.6	1.1	1.1	0.5	0.1	-0.3	-0.4	-0.1
V5/7	1-(t-CH=CH•)-2-CH_2CH_3-4-CH_3	3.8	-2.1	-3.1	-2.4	-2.0	-1.6	-1.0	-0.8	-0.3
V5/8	1-(c-CH=CH•)-2,3-OH	0.2	2.4	-0.5	0.0	0.5	0.6	0.6	0.4	0.1
V5/9	1-(c-CH=CH•)-2-CHO-4-CH=CH_2	-3.9	3.4	-2.2	-1.2	-0.8	-0.5	-0.1	0.2	0.4
V5/10	1-(c-CH=CH•)-2-CHO-6-CH_3	-5.2	-4.6	-1.2	0.5	1.2	1.6	1.9	2.1	1.9
V5/11	1-(c-CH=CH•)-3-CHO-4-CH_3	0.6	1.3	0.1	-0.2	-0.8	-1.1	-1.0	-1.0	-0.7
V5/12	1-(c-CH=CH•)-2,4-CH=CH_2	-2.7	3.2	-2.0	-1.3	-1.3	-1.2	-0.8	-0.6	-0.4
V5/13	1-(c-CH=CH•)-2-CH=CH_2-4-CH_3	0.8	0.9	-0.8	-0.5	-1.1	-1.3	-1.1	-0.9	-0.5
V5/14	1-(c-CH=CH•)-2-CH_3-4-CH=CH_2	-3.4	4.6	0.6	-0.1	-0.8	-1.1	-1.4	-1.3	-1.2
V5/15	1-(c-CH=CH•)-2,3-CH_3	-2.7	-1.9	4.6	4.3	3.6	3.3	2.7	2.2	1.3
V6/1	1-CH_2•-2,4-CH=CH_2	1.3	-0.5	-0.5	-0.2	0.1	0.2	0.5	0.4	0.3
V6/2	1-CH_2•-2-CH=CH_2-3-CH_3	-2.8	-2.9	2.6	4.5	4.9	4.7	3.7	2.8	1.5
V6/3	1-CH_2•-2,3-CH_3	-2.7	-3.0	3.0	2.7	2.4	2.2	2.1	1.8	1.4
V6/4	1-CH_2•-2-CH_3-5-CH_2CH_3	1.3	-0.7	-0.1	0.0	0.1	0.2	0.4	0.4	0.5
V6/5	1-CH_2•-2,5-CH_2CH_3	1.6	-1.1	1.9	1.6	1.3	1.0	0.9	0.4	0.4
V6/6	1-CH_2•-3-CH_3-4-CHO	0.8	0.6	-2.0	-1.1	-0.6	-0.4	-0.2	-0.3	-0.2
V6/7	1-CH_2•-3-CH_3-4-CH=CH_2	-3.4	-5.1	-1.8	-0.7	0.0	0.7	1.1	1.1	0.8
V6/8	1-CH_2•-3,4-CH_3	-0.5	0.9	-2.4	-1.5	-1.1	-0.9	-0.7	-0.6	-0.4
V6/9	1-CH_2•-3,6-CH_2CH_3	1.6	-0.6	2.1	1.7	1.4	1.1	1.0	0.5	0.6
V6/10	*p*-(CH_3)C_6H_5CH•CH_3	-1.4	-0.1	0.0	0.0	-0.1	-0.1	-0.3	-0.3	-0.2

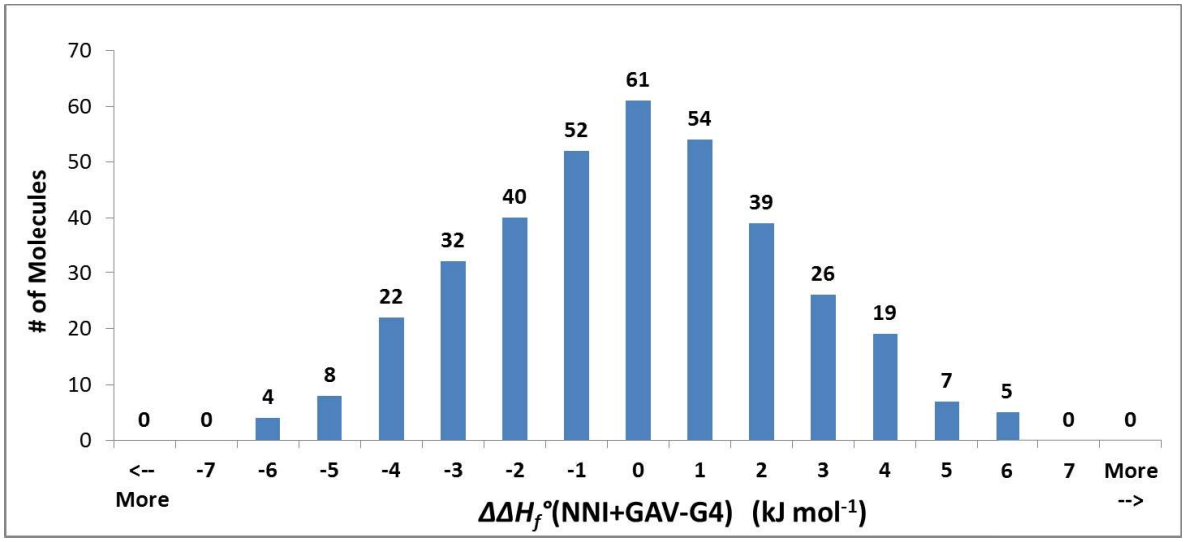

Figure B-29 Distribution of the differences between the final thermochemical data calculated with GA parameters and G4/BAC method for $\Delta_f H^\circ$ values of the MARs in the final set, $\Delta\Delta_f H°$((NNI+GAV)-G4).

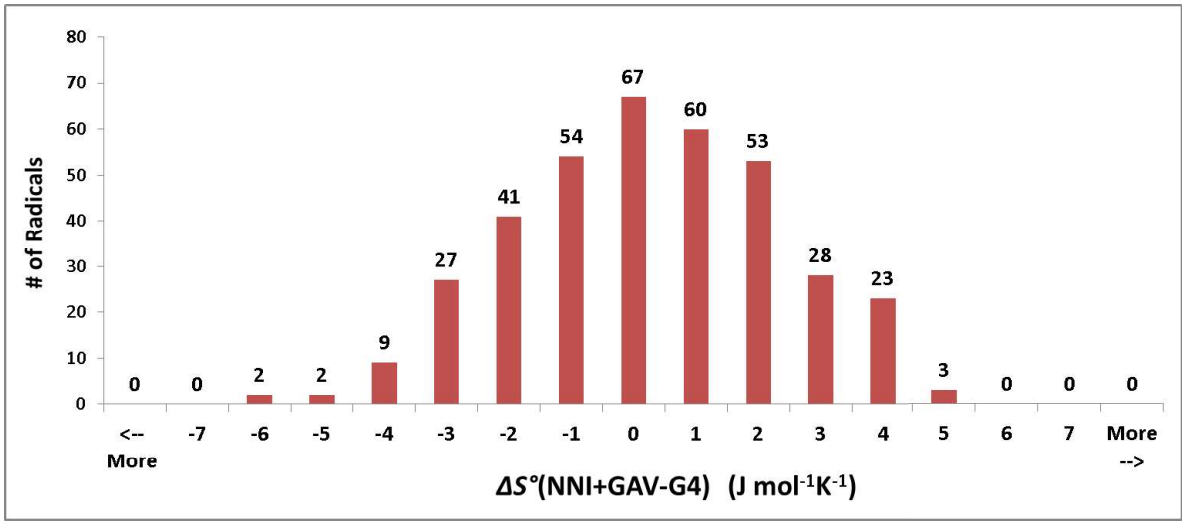

Figure B-30 Distribution of the differences between the final thermochemical data calculated with GA parameters and G4/BAC method for S° values of the MARs in the final set, $\Delta S°$((NNI+GAV)-G4).

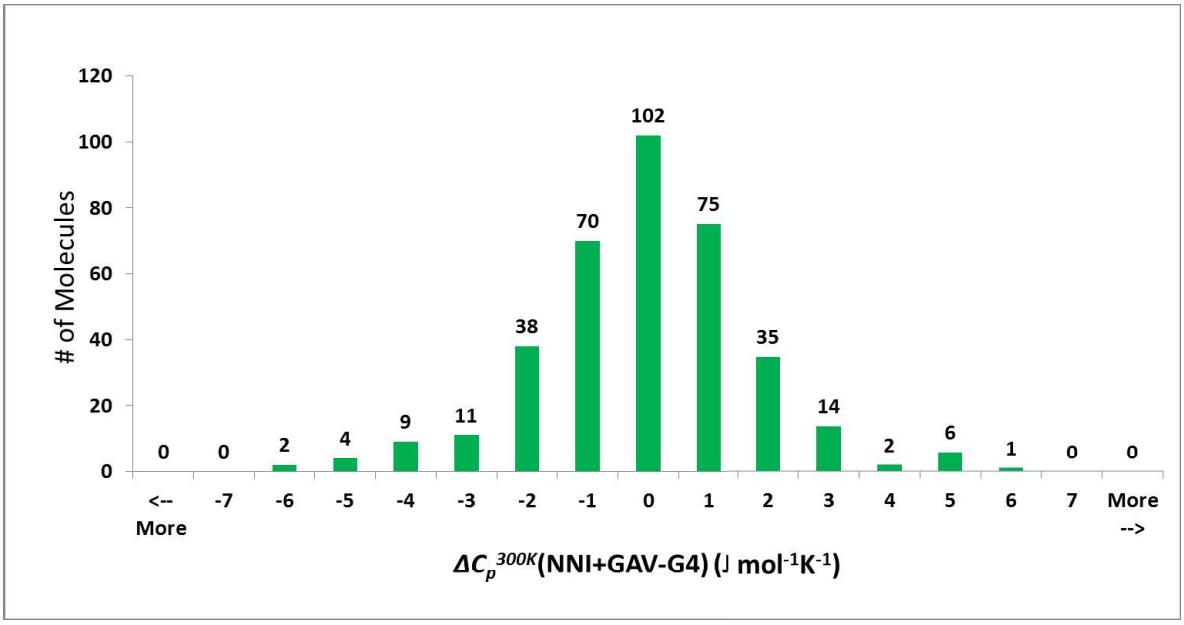

Figure B-31 Distribution of the differences between the final thermochemical data calculated with GA parameters and G4/BAC method for C_p^{300K} values of the MARs in the final set, ΔC_p^{300K} ((NNI+GAV)-G4).

B.11 References

[1] Ince A, Carstensen H-H, Reyniers M-F, Marin GB. First-principles based group additivity values for thermochemical properties of substituted aromatic compounds. *AIChE Journal.* 2015;61(11):3858-3870.

[2] Blanksby SJ, Ellison GB. Bond Dissociation Energies of Organic Molecules. *Accounts of Chemical Research.* 2003;36(4):255-263.

[3] Scheer AM, Mukarakate C, Robichaud DJ, Nimlos MR, Carstensen HH, Ellison GB. Unimolecular thermal decomposition of phenol and d(5)-phenol: Direct observation of cyclopentadiene formation via cyclohexadienone. *Journal of Chemical Physics.* 2012;136(4).

[4] Simões RG, Agapito F, Diogo HP, da Piedade MEM. Enthalpy of Formation of Anisole: Implications for the Controversy on the O–H Bond Dissociation Enthalpy in Phenol. *The Journal of Physical Chemistry A.* 2014;118(46):11026-11032.

[5] Simões JAM, Griller D. Enthalpy of formation of the benzoyl radical by photoacoustic calorimetry. *Chemical Physics Letters.* 1989;158(1–2):175-177.

[6] Rodgers AS, Golden DM, Benson SW. Kinetics of the reaction of iodobenzene and hydrogen iodide. Heat of formation of the phenyl radical and its implications on the reactivity of benzene. *Journal of the American Chemical Society.* 1967;89(18):4578-4583.

[7] Rossi M, Golden DM. Absolute rate constants for metathesis reactions of allyl and benzyl radicals with hydriodic acid (hydriodic acid-d). Heat of formation of allyl and benzyl radicals. *Journal of the American Chemical Society.* 1979;101(5):1230-1235.

[8] McMillen DF, Golden DM. Hydrocarbon Bond Dissociation Energies. *Annual Review of Physical Chemistry.* 1982;33(1):493-532.

[9] Tsang W. Heats of Formation of Organic Free Radicals by Kinetic Methods. In: Martinho Simões J, Greenberg A, Liebman J, eds. *Energetics of Organic Free Radicals.* Vol 4: Springer Netherlands; 1996:22-58.

[10] Pedley JB. *Thermochemical data of organic compounds*. 2nd ed. London: Chapman and Hall; 1986.

[11] Ervin KM, DeTuri VF. Anchoring the Gas-Phase Acidity Scale†. *The Journal of Physical Chemistry A.* 2002;106(42):9947-9956.

[12] Suryan MM, Kafafi SA, Stein SE. The thermal decomposition of hydroxy- and methoxy-substituted anisoles. *Journal of the American Chemical Society.* 1989;111(4):1423-1429.

[13] Suryan MM, Kafafi SA, Stein SE. Dissociation of substituted anisoles: substituent effects on bond strengths. *Journal of the American Chemical Society.* 1989;111(13):4594-4600.

[14] Hayashibara K, Kruppa GH, Beauchamp JL. Photoelectron spectroscopy of the o-, m-, and p-methylbenzyl radicals. Implications for the thermochemistry of the radicals and ions. *Journal of the American Chemical Society.* 1986;108(18):5441-5443.

[15] Denisov ET, Denisova T. *Handbook of antioxidants: bond dissociation energies, rate constants, activation energies, and enthalpies of reactions.* Vol 100: CRC press; 1999.

[16] Bordwell FG, Liu W-Z. Solvent Effects on Homolytic Bond Dissociation Energies of Hydroxylic Acids. *Journal of the American Chemical Society.* 1996;118(44):10819-10823.

[17] Lind J, Shen X, Eriksen TE, Merenyi G. The one-electron reduction potential of 4-substituted phenoxyl radicals in water. *Journal of the American Chemical Society.* 1990;112(2):479-482.

[18] Zhu Q, Zhang X-M, Fry AJ. Bond dissociation energies of antioxidants. *Polymer Degradation and Stability.* 1997;57(1):43-50.

[19] Mahoney LR, DaRooge MA. Kinetic behavior and thermochemical properties of phenoxy radicals. *Journal of the American Chemical Society.* 1975;97(16):4722-4731.

[20] Arnett EM, Amarnath K, Harvey NG, Cheng J. Determination and interrelation of bond heterolysis and homolysis energies in solution. *Journal of the American Chemical Society.* 1990;112(1):344-355.

[21] Lucarini M, Pedrielli P, Pedulli GF, Cabiddu S, Fattuoni C. Bond Dissociation Energies of O−H Bonds in Substituted Phenols from Equilibration Studies. *The Journal of Organic Chemistry.* 1996;61(26):9259-9263.

[22] Pratt DA, de Heer MI, Mulder P, Ingold KU. Oxygen−Carbon Bond Dissociation Enthalpies of Benzyl Phenyl Ethers and Anisoles. An Example of Temperature

Dependent Substituent Effects. *Journal of the American Chemical Society.* 2001;123(23):5518-5526.

[23] Tumanov VE, Kromkin EA, Denisov ET. Estimation of dissociation energies of C—H bonds in oxygen-containing compounds from kinetic data for radical abstraction reactions. *Russian Chemical Bulletin.* 2002;51(9):1641-1650.

[24] Wright JS, Carpenter DJ, McKay DJ, Ingold KU. Theoretical Calculation of Substituent Effects on the O−H Bond Strength of Phenolic Antioxidants Related to Vitamin E. *Journal of the American Chemical Society.* 1997;119(18):4245-4252.

[25] Arends IWCE, Louw R, Mulder P. Kinetic study of the thermolysis of anisole in a hydrogen atmosphere. *The Journal of Physical Chemistry.* 1993;97(30):7914-7925.

[26] Lund H, Daasbjerg K, Lund T, Pedersen SU. ChemInform Abstract: Electron Transfer in Aliphatic Nucleophilic Substitution. *ChemInform.* 1995;26(44):no-no.

[27] DeFrees DJ, McIver RT, Hehre WJ. Heats of formation of gaseous free radicals via ion cyclotron double resonance spectroscopy. *Journal of the American Chemical Society.* 1980;102(10):3334-3338.

[28] Barton BD, Stein SE. Pyrolysis of ethylpyridines. Relative stability of isomeric picolinyl radicals. *Journal of the Chemical Society, Faraday Transactions 1: Physical Chemistry in Condensed Phases.* 1981;77(8):1755-1762.

[29] Robaugh DA, Stein SE. Very-low-pressure pyrolysis of ethylbenzene, isopropylbenzene, and tert-butylbenzene. *International Journal of Chemical Kinetics.* 1981;13(5):445-462.

Appendix C

Supporting Information for Chapter 5

Contents

C.1 The Linear Regression Procedure and the Statistical Analysis

The Linear Regression and the calculation of $\overline{GAV/NNI}$ vector

As described in the text, a thermochemical property (y) of a species is calculated through additivity of the values of GAV and NNI parameters based on how many times they occur in that species. This leads to the following equation:

$$\sum_{i=1}^{n} X_i \beta_i = y \qquad \text{(C-1)}$$

where X_i is the number of occurence of the parameter *i* in the species and β_i is the value of the i^{th} parameter, which is calculated through the linear regression procedure. For each molecule/radical *j*, $\sum_{i=1}^{n} X_{ij}\beta_i$ is equal to $\hat{y}_j$, which is the group additively calculated thermochemical data of the molecule/radical whereas y_j represents the CBS-QB3/BAC based thermochemical data for *j*.

Once Eq. (C-1) is written for all the *m* number of species, an overdetermined system of linear equations is obtained:

$$\sum_{j=1}^{m} X_{ij}\beta_i = y_j \qquad (i=1,2,\ldots\ldots n) \qquad \text{(C-2)}$$

Here, X_{ij} is the occurrence matrix which carries the information on how many times each of the parameters occur in each of the species and it has the dimensions of m x n.

Least-squares linear regression is carried out to solve this system of equations and obtain β_i vector, which contains the GAV/NNI parameters.

The difference between y_j and $\hat{y}_j$ can be called as "residual", as given in Eq. (C-3).

$$r_j = y_j - \sum_{i=1}^{n} X_i \beta_i \tag{C-3}$$

and the sum of the square of these residuals (SSQ) are given in Eq. (C-4).

$$SSQ = \sum_{j=1}^{m} (y_j - \hat{y}_j)^2 \tag{C-4}$$

The objective function SSQ, i.e. the square root of the difference between *ab initio* data and the GA predictions with respect to the GAV/NNI parameters, β is minimized (argmin (SSQ)).

$$\frac{\partial SSQ}{\partial \beta} = 0 \tag{C-5}$$

This minimization yields the following equation:

$$(X^T X)\bar{\beta} = X^T \bar{y} \tag{C-6}$$

The expression in Eq. (C-6) can be rearranged to the following equation that yields $\bar{\beta}$, which is the $\overline{GAV/NNI}$ vector given in the text:

$$\overline{GAV/NNI} = (X^T X)^{-1} X^T \bar{y} \tag{C-7}$$

Since, the occurrence matrix and the $\bar{y}$ vector, which contains the CBS-QB3/BAC calculated thermochemical data are available, $\overline{GAV/NNI}$ vector can easily be calculated from Eq. (C-7) above. The $(X^T X)^{-1}$ matrix is separately calculated since it is needed for the calculation of confidence intervals, as explained below.

Calculation of Uncertainty of Parameters

First, mean squared errors (MSE) are calculated using SSQ and the degrees of freedom:

$$MSE = \frac{SSQ}{n_{molecules} - n_{parameters}} \quad \text{(C-8)}$$

MSE includes the variance of the residuals and the errors due to bias, i.e. systematic errors.

$$MSE = \sigma^2 + Bias^2 \quad \text{(C-9)}$$

These confidence intervals represent uncertainties only due to statistical errors. Several systematic sources of error exists, as explained in the text, they are not taken into consideration in this study and hence, the MSE is assumed to be equal to only σ^2.

Then, the variance-covariance matrix of parameters is calculated from the following equation:

$$\sum_{ij} Cov(X_i, X_j) = (X^T X)^{-1} * \sigma^2 \quad \text{(C-10)}$$

The diagonal of the covariance-variance matrix ($Cov(X_i, X_j)$) contains variances of the parameters, whereas the covariances of the parameters are obtained from the off-diagonals of this matrix.

The square root of the diagonal elements of the covariance-variance matrix, i.e. the standard deviations on the parameters, are used to calculate the confidence interval (CI_i) at 97.5% confidence level ($t_{97.5}$) of the i^{th} parameter.

$$CI_i = t_{97.5,i} * \sqrt{Cov(X_i, X_i)} \quad \text{(C-11)}$$

The final GAV and NNI parameters are reported with their uncertainties ($\beta_i \pm CI_i$) in **Table 5-3** and **Table 5-4**, respectively for the toluene derivatives and in **Table 5-7** and **Table 5-8** for the benzylic radicals, respectively.

C.2 List of Species

In this section of the Supporting Information, all the 336 species that appear in various sections of the article are listed.

- 168 of these species are toluene derivatives (abbreviated as "**TD**") and the remaning 168 are benzylic radicals (abbreviated as "**BR**").
- Two separate thermochemical databases are formed for the toluene derivatives and the benzylic radicals.
- Each of these databases are split into two: training set (abbreviated as "**T**") and validation set (abbreviated as "**V**").
- Training sets from both databases include 114 species, which are used for the initial simultaneous determination of GAVs and NNIs. The training sets encompass the unsubstituted and the singly substituted forms of species where all the *ortho(-o)*, *meta(-m)* and *para(-p)* substitution of hydroxy (-OH), methoxy (-OCH_3), formyl (-CHO), vinyl (-$CH{=}CH_2$), methyl (-CH_3) and ethyl (-CH_2CH_3) groups are considered. Therefore, 19 species (1 unsubstituted + 18 substituted) are studied per subset, which sums up to a total number of 114 species (19 x 6 subsets = 114) in each of the training sets.
- The predictive capability of these GAV/NNI parameters are tested on the validation sets of 54 species. These sets consist of doubly substituted **TD** or **BR** species.
- Finally, two sets are combined and the GAV/NNI parameter set is reoptimized based on these final databases of 168 species.

In the database of toluene derivatives(**TD**), there are six subsets, which are given in the following order:

1- Unsubstituted and substituted Isopropylbenzenes

2- Unsubstituted and substituted Allylbenzenes

3- Unsubstituted and substituted α-methyl allylbenzenes

4- Unsubstituted and substituted α-vinyl allylbenzenes

5- Unsubstituted and substituted Diphenylmethanes

6- Unsubstituted and substituted 1,1-diphenylethanes

In the database of benzylic radicals (**BR**), there are six subsets, which are given in the following order:

1- Unsubstituted and substituted 2-phenyl-2-propyl radicals

2- Unsubstituted and substituted 3-phenyl-1-propen-3-yl radicals

3- Unsubstituted and substituted 3-phenyl-1-buten-3-yl radicals

4- Unsubstituted and substituted 3-phenyl-1,4-pentadien-3-yl radicals

5- Unsubstituted and substituted Diphenylmethyl radicals

6- Unsubstituted and substituted 1,1-diphenylethyl radicals

The code given for any species that appear in this manuscript is "**XXYm/n**" where

- **XX** can be either TD or BR
- **Y** can be either T or V
- **m** can be a number from 1 to 6, representing the number corresponding to one of the six subsets given above.
- **n** represents the number of the species within the subset.

For example, the code that corresponds to the n^{th} toluene derivative in m^{th} subset in the training set of the toluene derivatives is given as "**TDTm/n**". For example, consider the code "**TDT4/17"**. The first two capital letters "**TD**" indicates that the species is a toluene derivative. The third capital letter indicates that this is a toluene derivative from the training set. The number "4/17" shows that this is the 17^{th} species in the 4^{th} subset, which is o-$(CH_2CH_3)C_6H_5CH(CH{=}CH_2)_2$.

Then, the transferability of the GAV/NNI parameters obtained from the training sets is tested on validation sets that encompasses 54 doubly substituted **TD**s or **BR**s.

The structures of the species are given in **Figure C-1** - **Figure C-24**, as described below in detail.

For the toluene derivatives,

- Training set is given in **Figure C-1** to **Figure C-6**.
- Validation set is given in **Figure C-7** to **Figure C-12**.

For the benzylic radicals,

- Training set is given in **Figure C-13** to **Figure C-18**.
- Validation set is given in **Figure C-19** to **Figure C-24**.

Each figure represents the set of structures for a different subset.

C.2.1 List of Toluene Derivatives

I. *Training Set*

I.1 Isopropylbenzene Subset

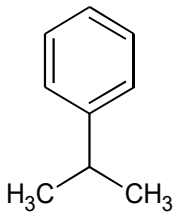

TDT1/1-$C_6H_5CH(CH_3)_2$

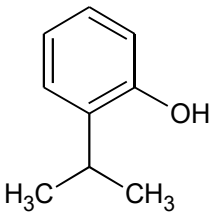

TDT1/2-o-$(OH)C_6H_5CH(CH_3)_2$

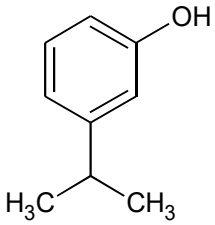

TDT1/3-m-$(OH)C_6H_5CH(CH_3)_2$

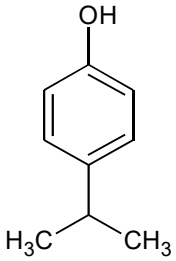

TDT1/4-p-$(OH)C_6H_5CH(CH_3)_2$

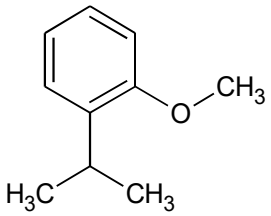

TDT1/5-o-$(OCH_3)C_6H_5CH(CH_3)_2$

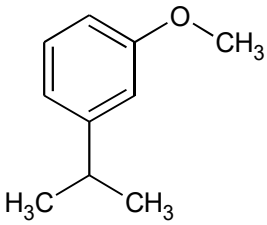

TDT1/6-m-$(OCH_3)C_6H_5CH(CH_3)_2$

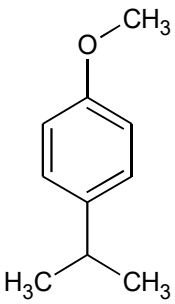

TDT1/7-p-$(OCH_3)C_6H_5CH(CH_3)_2$

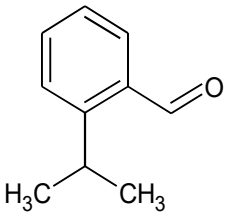

TDT1/8-o-$(CHO)C_6H_5CH(CH_3)_2$

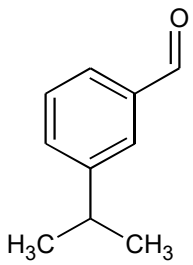

TDT1/9-m-$(CHO)C_6H_5CH(CH_3)_2$

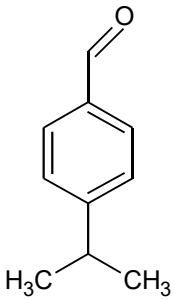

TDT1/10-p-$(CHO)C_6H_5CH(CH_3)_2$

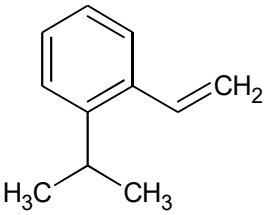

TDT1/11-o-$(CH{=}CH_2)C_6H_5CH(CH_3)_2$

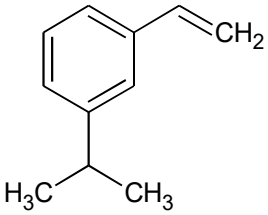

TDT1/12-m-$(CH{=}CH_2)C_6H_5CH(CH_3)_2$

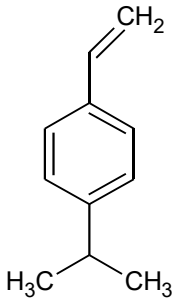

TDT1/13-p-(CH=CH$_2$)C$_6$H$_5$CH(CH$_3$)$_2$

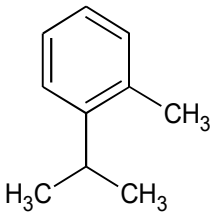

TDT1/14-o-(CH$_3$)C$_6$H$_5$CH(CH$_3$)$_2$

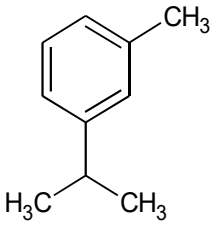

TDT1/15-m-(CH$_3$)C$_6$H$_5$CH(CH$_3$)$_2$

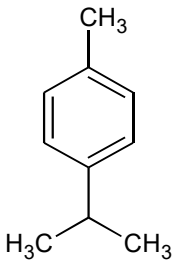

TDT1/16-p-(CH$_3$)C$_6$H$_5$CH(CH$_3$)$_2$

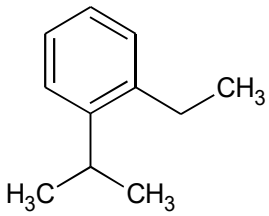

TDT1/17-o-(CH$_2$CH$_3$)C$_6$H$_5$CH(CH$_3$)$_2$

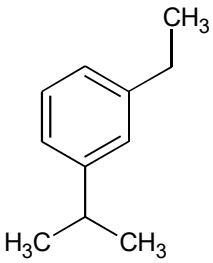

TDT1/18-m-(CH$_2$CH$_3$)C$_6$H$_5$CH(CH$_3$)$_2$

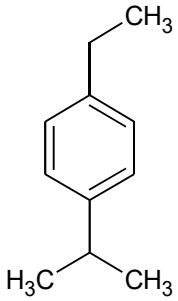

TDT1/19-p-(CH$_2$CH$_3$)C$_6$H$_5$CH(CH$_3$)$_2$

Figure C-1 List of toluene derivatives in isopropylbenzene subset of the training set.

I.2 AllylBenzene Subset

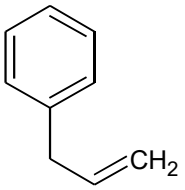

TDT2/1-C$_6$H$_5$CH$_2$CH=CH$_2$

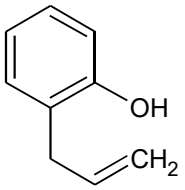

TDT2/2-o-(OH)C$_6$H$_5$CH$_2$CH=CH$_2$

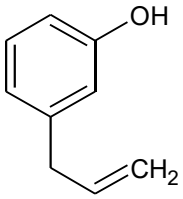

TDT2/3-m-(OH)C$_6$H$_5$CH$_2$CH=CH$_2$

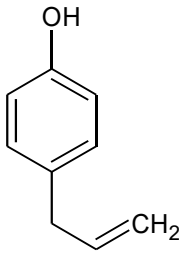

TDT2/4-p-(OH)C$_6$H$_5$CH$_2$CH=CH$_2$

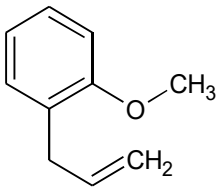

TDT2/5-o-(OCH$_3$)C$_6$H$_5$CH$_2$CH=CH$_2$

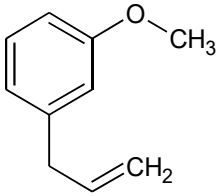

TDT2/6-m-(OCH$_3$)C$_6$H$_5$CH$_2$CH=CH$_2$

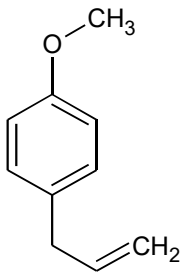

TDT2/7-p-(OCH$_3$)C$_6$H$_5$CH$_2$CH=CH$_2$

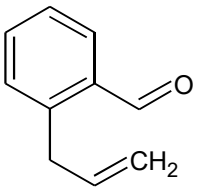

TDT2/8-o-(CHO)C$_6$H$_5$CH$_2$CH=CH$_2$

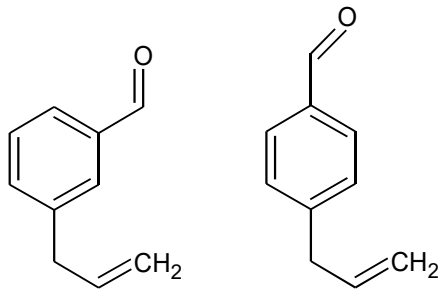

TDT2/9-m-(CHO)$C_6H_5CH_2CH=CH_2$ **TDT2/10**-p-(CHO)$C_6H_5CH_2CH=CH_2$ **TDT2/11**-o-(CH=CH_2)$C_6H_5CH_2CH=CH_2$ **TDT2/12**-m-(CH=CH_2)$C_6H_5CH_2CH=CH_2$

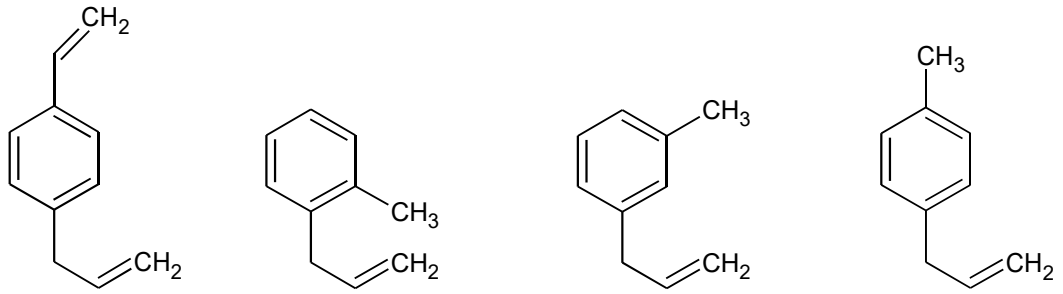

TDT2/13-p-(CH=CH_2)$C_6H_5CH_2CH=CH_2$ **TDT2/14**-o-(CH_3)$C_6H_5CH_2CH=CH_2$ **TDT2/15**-m-(CH_3)$C_6H_5CH_2CH=CH_2$ **TDT2/16**-p-(CH_3)$C_6H_5CH_2CH=CH_2$

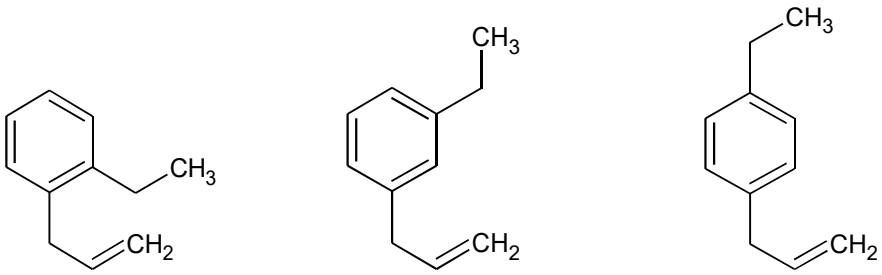

TDT2/17-o-(CH_2CH_3)$C_6H_5CH_2CH=CH_2$ **TDT2/18**-m-(CH_2CH_3)$C_6H_5CH_2CH=CH_2$ **TDT2/19**-p-(CH_2CH_3)$C_6H_5CH_2CH=CH_2$

Figure C-2 List of toluene derivatives in allylbenzene subset of the training set.

I.3 α-Methyl AllylBenzene Subset

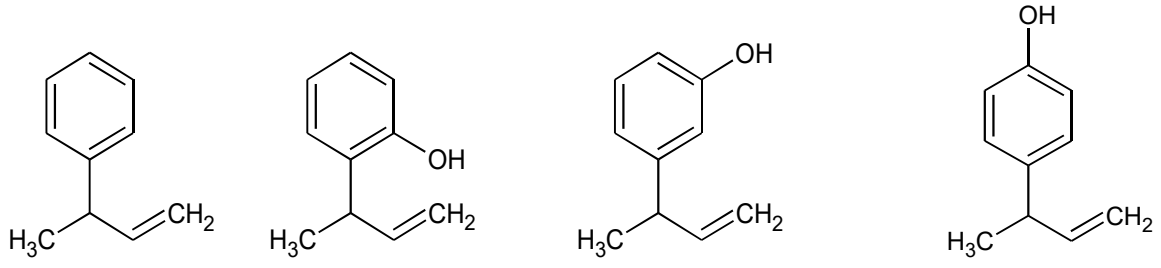

TDT3/1-$C_6H_5C(CH_3)HCH=CH_2$ **TDT3/2**-o-(OH)$C_6H_5C(CH_3)HCH=CH_2$ **TDT3/3**-m-(OH)$C_6H_5C(CH_3)HCH=CH_2$ **TDT3/4**-p-(OH)$C_6H_5C(CH_3)HCH=CH_2$

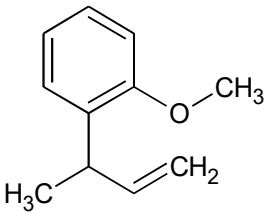

TDT3/5-o-$(OCH_3)C_6H_5C(CH_3)HCH=CH_2$

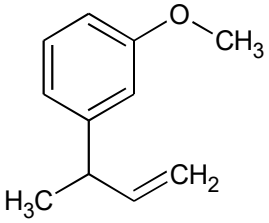

TDT3/6-m-$(OCH_3)C_6H_5C(CH_3)HCH=CH_2$

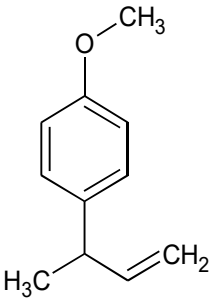

TDT3/7-p-$(OCH_3)C_6H_5C(CH_3)HCH=CH_2$

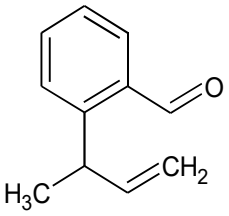

TDT3/8-o-$(CHO)C_6H_5C(CH_3)HCH=CH_2$

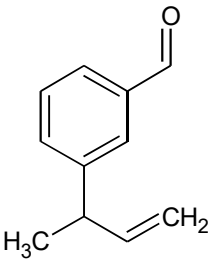

TDT3/9-m-$(CHO)C_6H_5C(CH_3)HCH=CH_2$

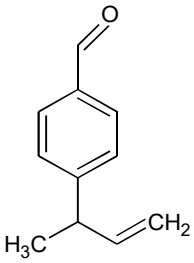

TDT3/10-p-$(CHO)C_6H_5C(CH_3)HCH=CH_2$

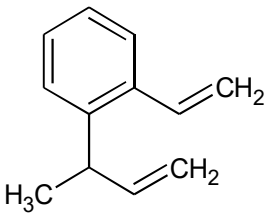

TDT3/11-o-$(CH=CH_2)C_6H_5C(CH_3)HCH=CH_2$

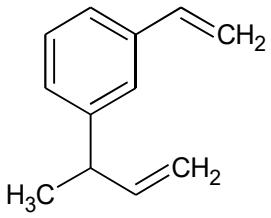

TDT3/12-m-$(CH=CH_2)C_6H_5C(CH_3)HCH=CH_2$

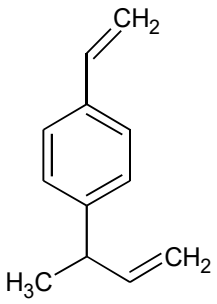

TDT3/13-p-$(CH=CH_2)C_6H_5C(CH_3)HCH=CH_2$

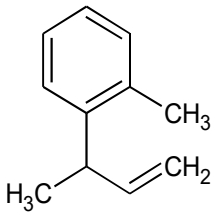

TDT3/14-o-$(CH_3)C_6H_5C(CH_3)HCH=CH_2$

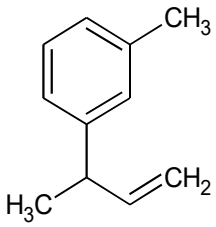

TDT3/15-m-$(CH_3)C_6H_5C(CH_3)HCH=CH_2$

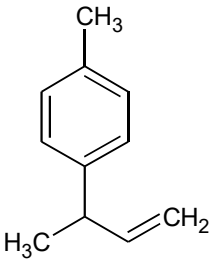

TDT3/16-p-$(CH_3)C_6H_5C(CH_3)HCH=CH_2$

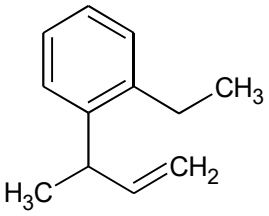

TDT3/17-o-$(CH_2CH_3)C_6H_5C(CH_3)HCH=CH_2$

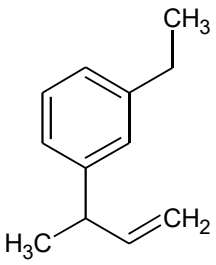

TDT3/18-m-$(CH_2CH_3)C_6H_5C(CH_3)HCH=CH_2$

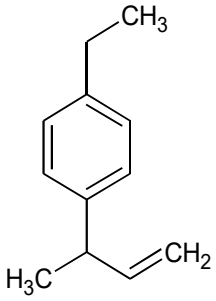

TDT3/19-p-$(CH_2CH_3)C_6H_5C(CH_3)HCH=CH_2$

Figure C-3 List of toluene derivatives in α-methyl allylbenzene subset of the training set.

I.4 α-Vinyl AllylBenzene Subset

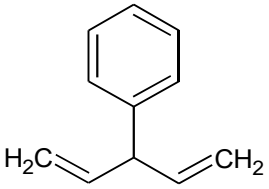

TDT4/1-$C_6H_5CH(CH=CH_2)_2$

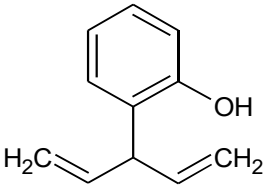

TDT4/2-o-$(OH)C_6H_5CH(CH=CH_2)_2$

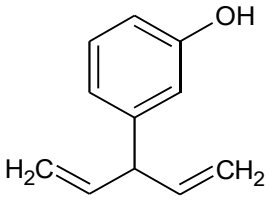

TDT4/3-m-$(OH)C_6H_5CH(CH=CH_2)_2$

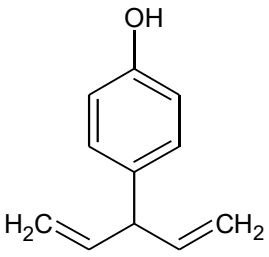

TDT4/4-p-$(OH)C_6H_5CH(CH=CH_2)_2$

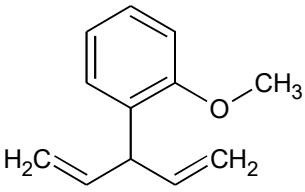

TDT4/5-o-$(OCH_3)C_6H_5CH(CH=CH_2)_2$

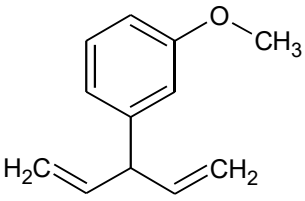

TDT4/6-m-$(OCH_3)C_6H_5CH(CH=CH_2)_2$

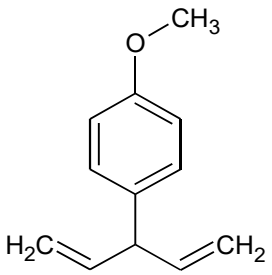

TDT4/7-p-$(OCH_3)C_6H_5CH(CH=CH_2)_2$

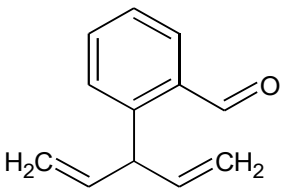

TDT4/8-o-$(CHO)C_6H_5CH(CH=CH_2)_2$

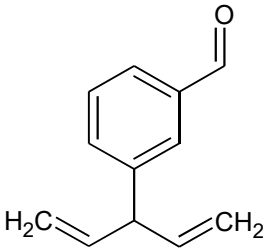

TDT4/9-m-$(CHO)C_6H_5CH(CH=CH_2)_2$

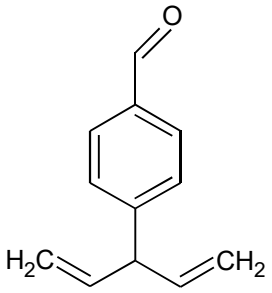

TDT4/10-p-$(CHO)C_6H_5CH(CH=CH_2)_2$

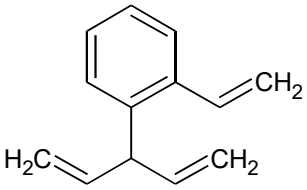

TDT4/11-o-$(CH=CH_2)C_6H_5CH(CH=CH_2)_2$

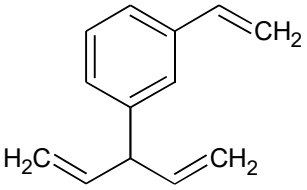

TDT4/12-m-$(CH=CH_2)C_6H_5CH(CH=CH_2)_2$

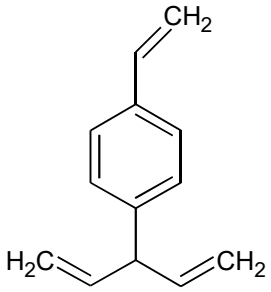

TDT4/13-p-$(CH=CH_2)C_6H_5CH(CH=CH_2)_2$

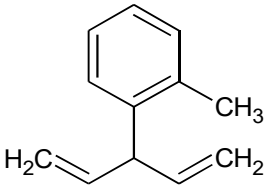

TDT4/14-o-$(CH_3)C_6H_5CH(CH=CH_2)_2$

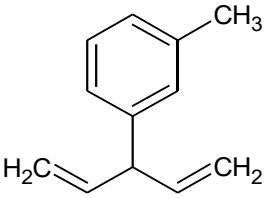

TDT4/15-m-$(CH_3)C_6H_5CH(CH=CH_2)_2$

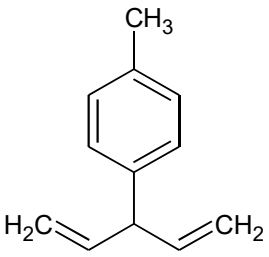

TDT4/16-p-$(CH_3)C_6H_5CH(CH=CH_2)_2$

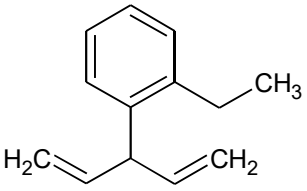

TDT4/17-o-$(CH_2CH_3)C_6H_5CH(CH=CH_2)_2$

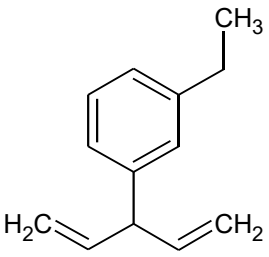

TDT4/18-m-$(CH_2CH_3)C_6H_5CH(CH=CH_2)_2$

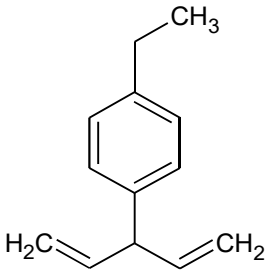

TDT4/19-p-$(CH_2CH_3)C_6H_5CH(CH=CH_2)_2$

Figure C-4 List of toluene derivatives in α-vinyl allylbenzene subset of the training set.

I.5 Diphenylmethane Subset

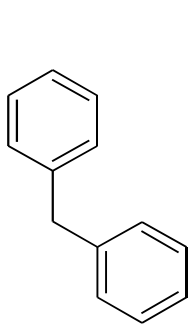

TDT5/1-$(C_6H_5)_2CH_2$

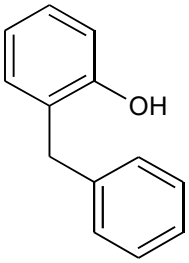

TDT5/2-o-$(OH)(C_6H_5)_2CH_2$

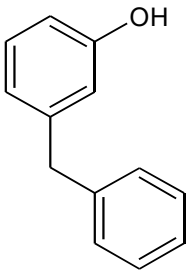

TDT5/3-m-$(OH)(C_6H_5)_2CH_2$

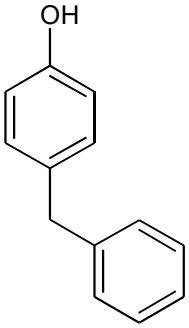

TDT5/4-p-$(OH)(C_6H_5)_2CH_2$

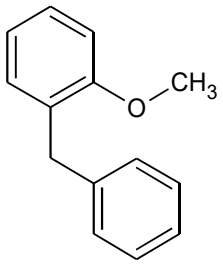

TDT5/5-o-$(OCH_3)(C_6H_5)_2CH_2$

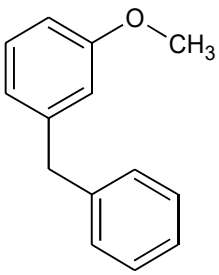

TDT5/6-m-$(OCH_3)(C_6H_5)_2CH_2$

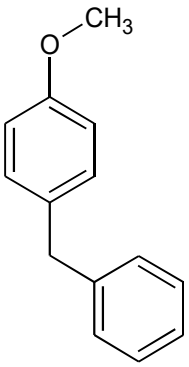

TDT5/7-p-$(OCH_3)(C_6H_5)_2CH_2$

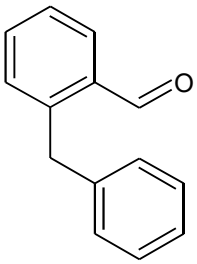

TDT5/8-o-$(CHO)(C_6H_5)_2CH_2$

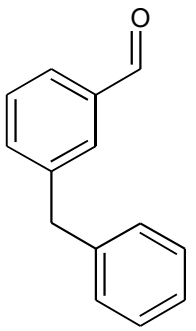

TDT5/9-m-(CHO)$(C_6H_5)_2CH_2$

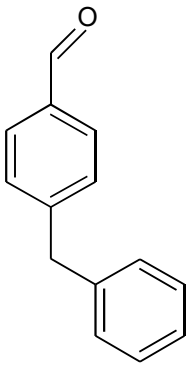

TDT5/10-p-(CHO)$(C_6H_5)_2CH_2$

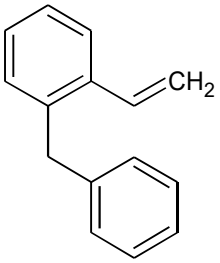

TDT5/11-o-(CH=CH_2)$(C_6H_5)_2CH_2$

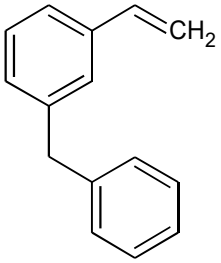

TDT5/12-m-(CH=CH_2)$(C_6H_5)_2CH_2$

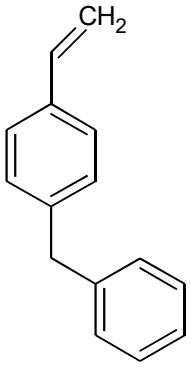

TDT5/13-p-(CH=CH_2)$(C_6H_5)_2CH_2$

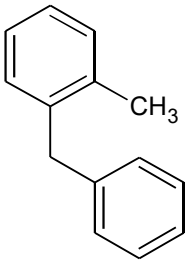

TDT5/14-o-$(CH_3)(C_6H_5)_2CH_2$

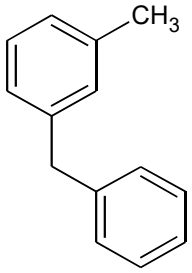

TDT5/15-m-$(CH_3)(C_6H_5)_2CH_2$

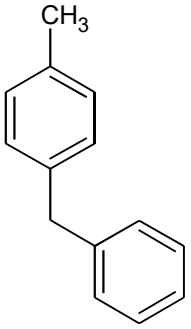

TDT5/16-p-$(CH_3)(C_6H_5)_2CH_2$

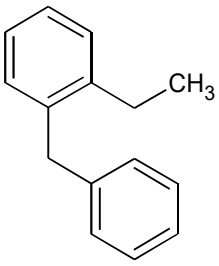

TDT5/17-o-$(CH_2CH_3)(C_6H_5)_2CH_2$

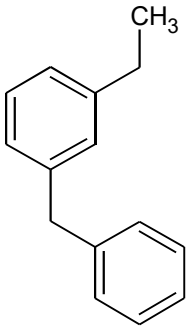

TDT5/18-m-$(CH_2CH_3)(C_6H_5)_2CH_2$

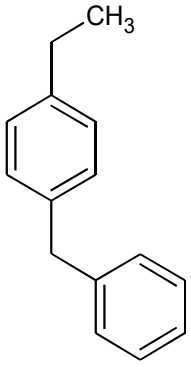

TDT5/19-p-$(CH_2CH_3)(C_6H_5)_2CH_2$

Figure C-5 List of toluene derivatives in diphenylmethane subset of the training set

I.6 1,1-Diphenylethane Subset

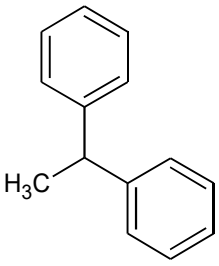

TDT6/1-$C(C_6H_5)_2HCH_3$

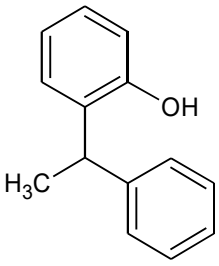

TDT6/2-o-$(OH)C(C_6H_5)_2HCH_3$

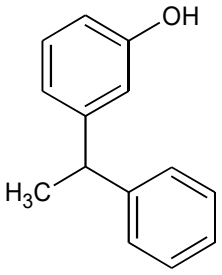

TDT6/3-m-$(OH)C(C_6H_5)_2HCH_3$

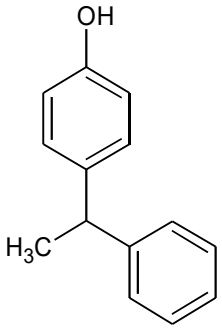

TDT6/4-p-$(OH)C(C_6H_5)_2HCH_3$

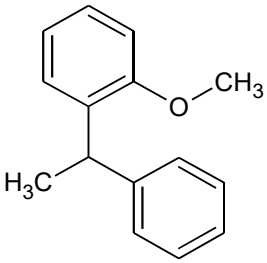

TDT6/5-o-$(OCH_3)C(C_6H_5)_2HCH_3$

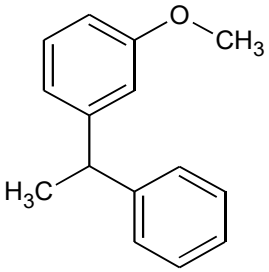

TDT6/6-m-$(OCH_3)C(C_6H_5)_2HCH_3$

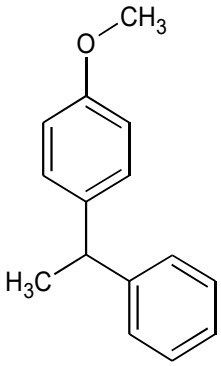

TDT6/7-p-(OCH_3) $C(C_6H_5)_2HCH_3$

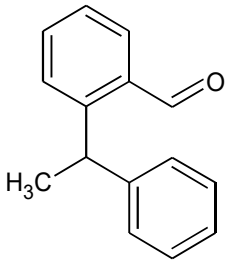

TDT6/8-o-(CHO) $C(C_6H_5)_2HCH_3$

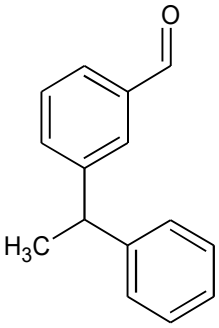

TDT6/9-m-$(CHO)C_6H_5CH(CH_3)_2$

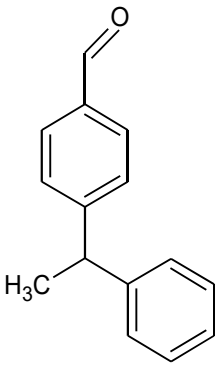

TDT6/10-p-$(CHO)C_6H_5CH(CH_3)_2$

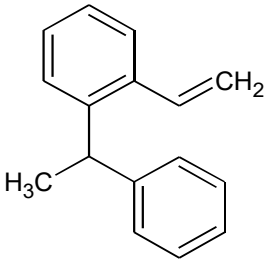

TDT6/11-o-$(CH{=}CH_2)$ $C(C_6H_5)_2HCH_3$

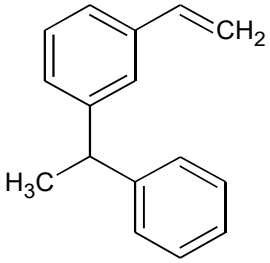

TDT6/12-m-$(CH{=}CH_2)C_6H_5CH(CH_3)_2$

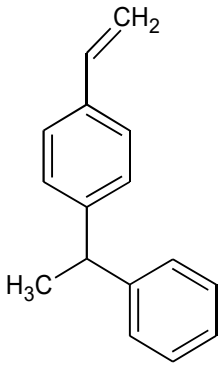

TDT6/13-p-(CH=CH$_2$)C(C$_6$H$_5$)$_2$HCH$_3$

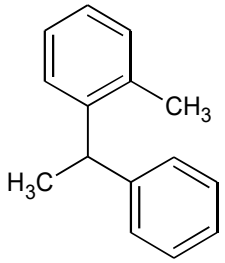

TDT6/14-o-(CH$_3$)C(C$_6$H$_5$)$_2$HCH$_3$

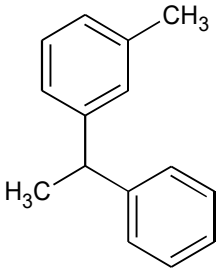

TDT6/15-m-(CH$_3$)C(C$_6$H$_5$)$_2$HCH$_3$

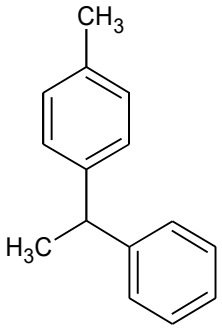

TDT6/16-p-(CH$_3$)C(C$_6$H$_5$)$_2$HCH$_3$

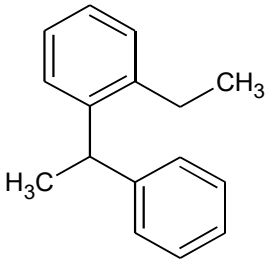

TDT6/17-o-(CH$_2$CH$_3$)C(C$_6$H$_5$)$_2$HCH$_3$

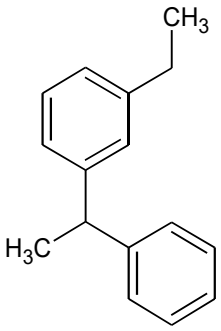

TDT6/18-m-(CH$_2$CH$_3$)C(C$_6$H$_5$)$_2$HCH$_3$

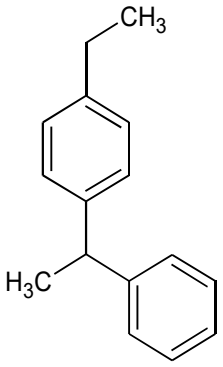

TDT6/19-p-(CH$_2$CH$_3$)C(C$_6$H$_5$)$_2$HCH$_3$

Figure C-6 List of toluene derivatives in 1,1-diphenylethane subset of the training set.

II. ***Validation Set***

II.1 Doubly Substituted Isopropylbenzene Subset

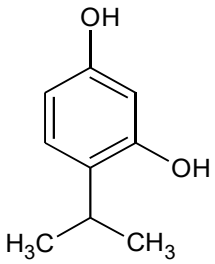

TDV1/1-2-OH-4-OH-C$_6$H$_5$CH(CH$_3$)$_2$

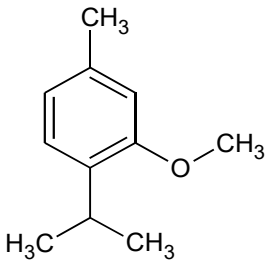

TDV1/2-2-OCH$_3$-4-CH$_3$-C$_6$H$_5$CH(CH$_3$)$_2$

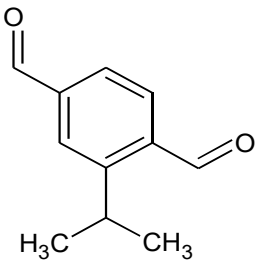

TDV1/3-2-CHO-5-CHO-C$_6$H$_5$CH(CH$_3$)$_2$

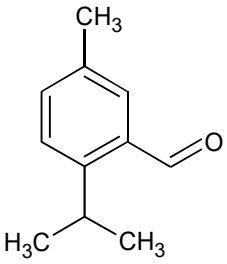

TDV1/4-2-CHO-4-CH_3-$C_6H_5CH(CH_3)_2$

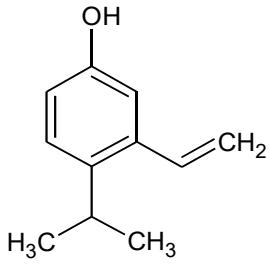

TDV1/5-2-CH=CH2-4-OH-$C_6H_5CH(CH_3)_2$

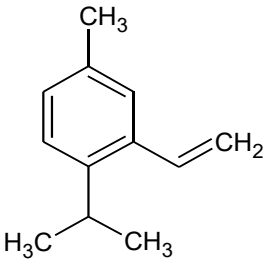

TDV1/6-2-CH=CH_2-4-CH3-$C_6H_5CH(CH_3)_2$

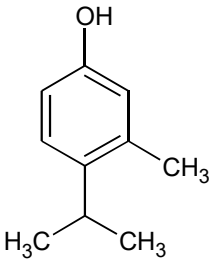

TDV1/7-2-CH_3-4-OH-$C_6H_5CH(CH_3)_2$

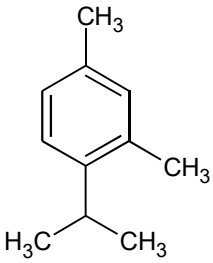

TDV1/8-2-CH_3-4-CH_3-$C_6H_5CH(CH_3)_2$

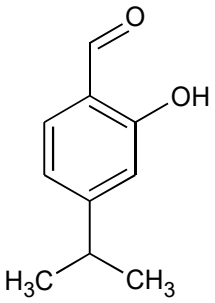

TDV1/9-3-OH-4-CHO-$C_6H_5CH(CH_3)_2$

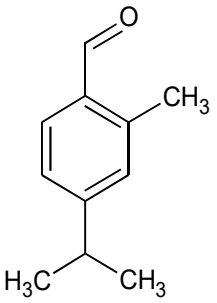

TDV1/10-3-CH_3-4-CHO-$C_6H_5CH(CH_3)_2$

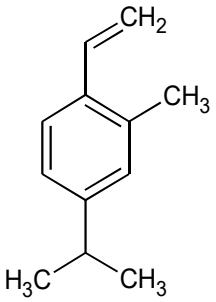

TDV1/11-3-CH_3-4-CH=CH_2-$C_6H_5CH(CH_3)_2$

Figure C-7 List of toluene derivatives in isopropylbenzene subset of the test set.

II.2 Doubly Substituted Allylbenzene Subset

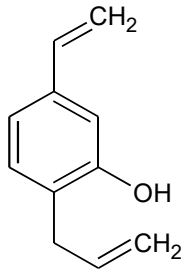

TDV2/1-2-OH-4-CH=CH$_2$-C$_6$H$_5$CH$_2$CH=CH$_2$

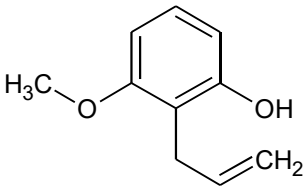

TDV2/2-2-OH-6-OCH$_3$-C$_6$H$_5$CH$_2$CH=CH$_2$

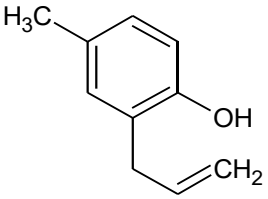

TDV2/3-2-OH-5-CH$_3$-C$_6$H$_5$CH$_2$CH=CH$_2$

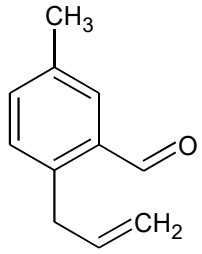

TDV2/4-2-CHO-4-CH$_3$-C$_6$H$_5$CH$_2$CH=CH$_2$

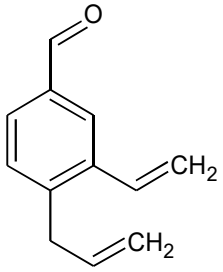

TDV2/5-2-CH=CH$_2$-4-CHO-C$_6$H$_5$CH$_2$CH=CH$_2$

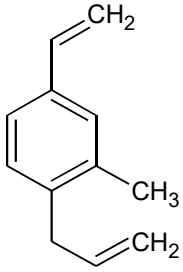

TDV2/6-2-CH$_3$-4-CH=CH$_2$-C$_6$H$_5$CH$_2$CH=CH$_2$

Figure C-8 List of toluene derivatives in allylbenzene subset of the test set.

II.3 Doubly Substituted α-Methyl Allylbenzene Subset

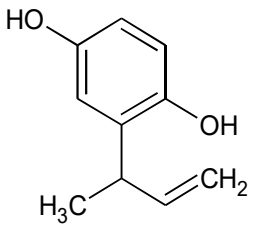

TDV3/1-2-OH-5-OH-C$_6$H$_5$C(CH$_3$)HCH=CH$_2$

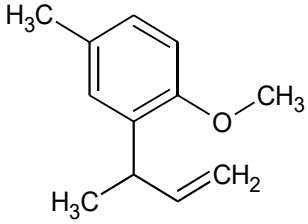

TDV3/2-2-OCH$_3$-5-CH$_3$-C$_6$H$_5$C(CH$_3$)HCH=CH$_2$

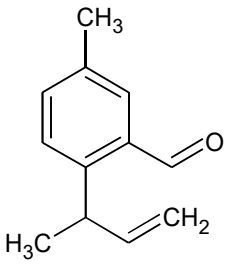

TDV3/3-2-CHO-4-CH$_3$-C$_6$H$_5$C(CH$_3$)HCH=CH

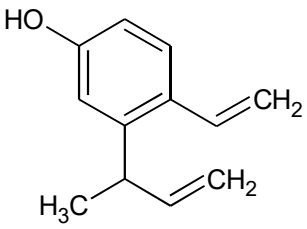

TDV3/4-2-CH=CH$_2$-5-OH-C$_6$H$_5$C(CH$_3$)HCH=CH$_2$

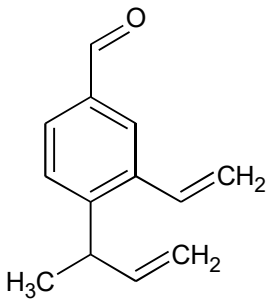

TDV3/5-2-CH=CH$_2$-4-CHO-C$_6$H$_5$C(CH$_3$)HCH=CH$_2$

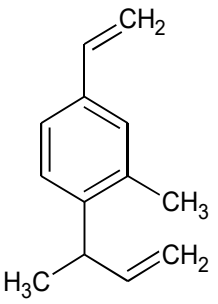

TDV3/6-2-CH$_3$-4-CH=CH$_2$-C$_6$H$_5$C(CH$_3$)HCH=CH$_2$

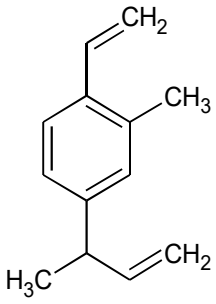

TDV3/7-3-CH$_3$-4-CH=CH$_2$-C$_6$H$_5$C(CH$_3$)HCH=CH$_2$

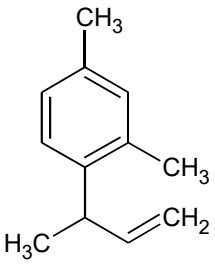

TDV3/8-2-CH$_3$-4-CH$_3$-C$_6$H$_5$C(CH$_3$)HCH=CH$_2$

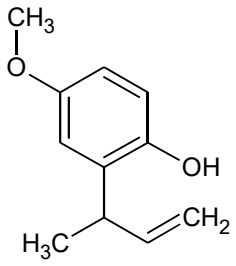

TDV3/9-2-OH-5-OCH$_3$-C$_6$H$_5$C(CH$_3$)HCH=CH$_2$

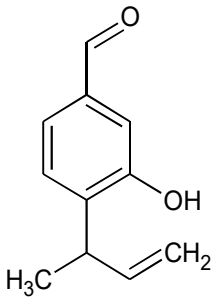

TDV3/10-2-OH-4-CHO-C$_6$H$_5$C(CH$_3$)HCH=CH$_2$

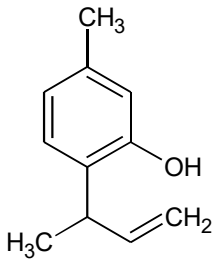

TDV3/11-2-OH-4-CH$_3$-C$_6$H$_5$C(CH$_3$)HCH=CH$_2$

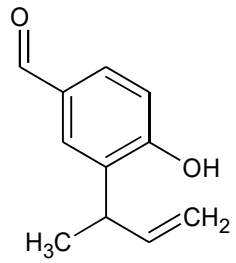

TDV3/12-2-OH-5-CHO-C$_6$H$_5$C(CH$_3$)HCH=CH$_2$

Figure C-9 List of toluene derivatives in α-methylallylbenzene subset of the test set.

II.4 Doubly Substituted α-Vinyl Allylbenzene Subset

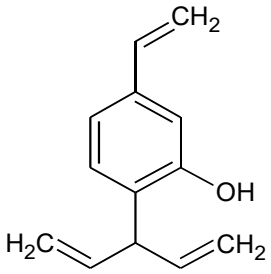

TDV4/1-2-OH-4-CH=CH$_2$-C$_6$H$_5$CH(CH=CH$_2$)$_2$

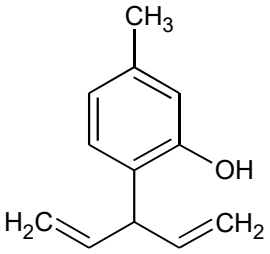

TDV4/2-2-OH-4-CH$_3$-C$_6$H$_5$CH(CH=CH$_2$)$_2$

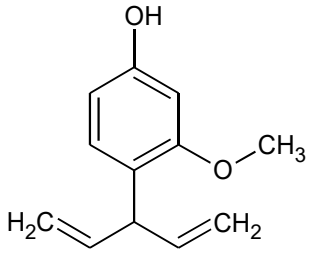

TDV4/3-2-OCH$_3$-4-OH-C$_6$H$_5$CH(CH=CH$_2$)$_2$

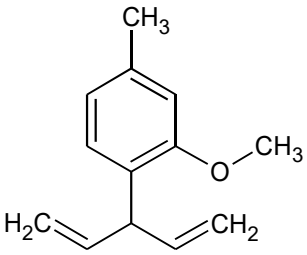

TDV4/4-2-OCH$_3$-4-CH$_3$-C$_6$H$_5$CH(CH=CH$_2$)$_2$

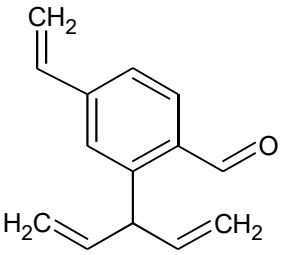

TDV4/5-2-CHO-5-CH=CH$_2$-C$_6$H$_5$CH(CH=CH$_2$)$_2$

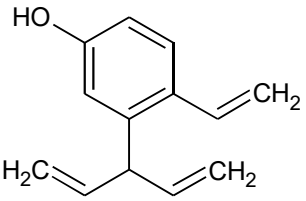

TDV4/6-2-CH=CH$_2$-5-OH-C$_6$H$_5$CH(CH=CH$_2$)$_2$

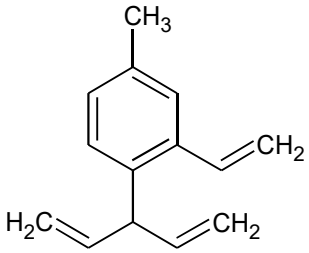

TDV4/7-2-CH=CH$_2$-4-CH$_3$-C$_6$H$_5$CH(CH=CH$_2$)$_2$

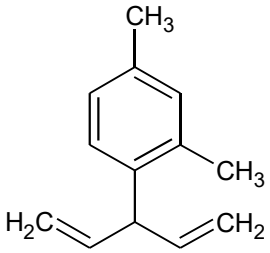

TDV4/8-2-CH$_3$-4-CH$_3$-C$_6$H$_5$CH(CH=CH$_2$)$_2$

Figure C-10 List of toluene derivatives in α-vinylallylbenzene subset of the test set.

II.5 Doubly Substituted Diphenylmethane Subset

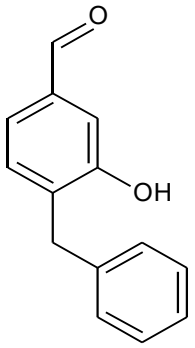

TDV5/1-2-OH-4-CHO-$(C_6H_5)_2CH_2$

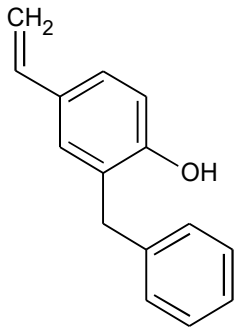

TDV5/2-2-OH-5-CH=CH_2-$(C_6H_5)_2CH_2$

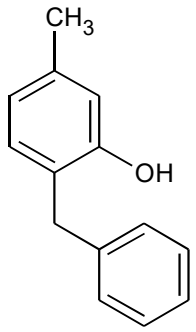

TDV5/3-2-OH-4-CH_3-$(C_6H_5)_2CH_2$

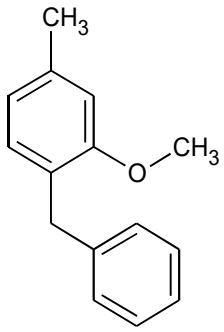

TDV5/4-2-OCH_3-4-CH_3-$(C_6H_5)_2CH_2$

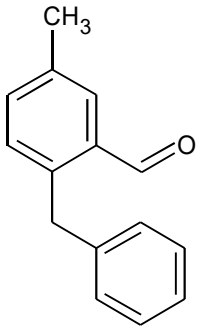

TDV5/5-2-CHO-4-CH_3-$(C_6H_5)_2CH_2$

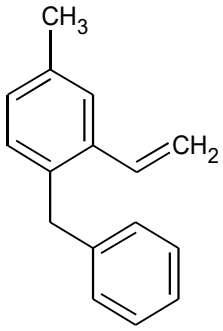

TDV5/6-2-CH=CH_2-4-CH_3-$(C_6H_5)_2CH_2$

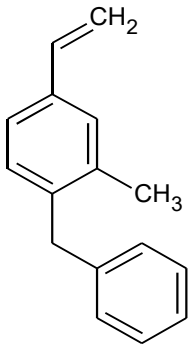

TDV5/7-2-CH_3-4-CH=CH_2-$(C_6H_5)_2CH_2$

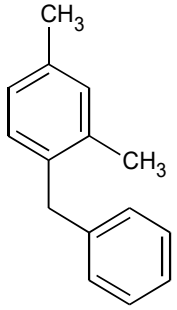

TDV5/8-2-CH_3-4-CH_3-$(C_6H_5)_2CH_2$

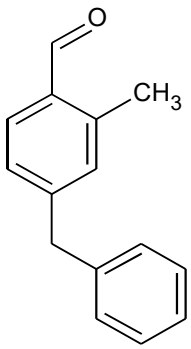

TDV5/9-3-CH_3-4-CHO-$(C_6H_5)_2CH_2$

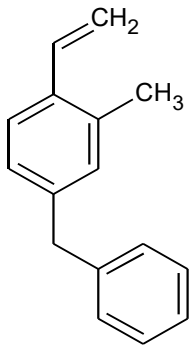

TDV5/10-3-CH_3-4-CH=CH_2-$(C_6H_5)_2CH_2$

Figure C-11 List of toluene derivatives in diphenylmethane subset of the test set.

II.6 Doubly Substituted 1,1-Diphenylethane Subset

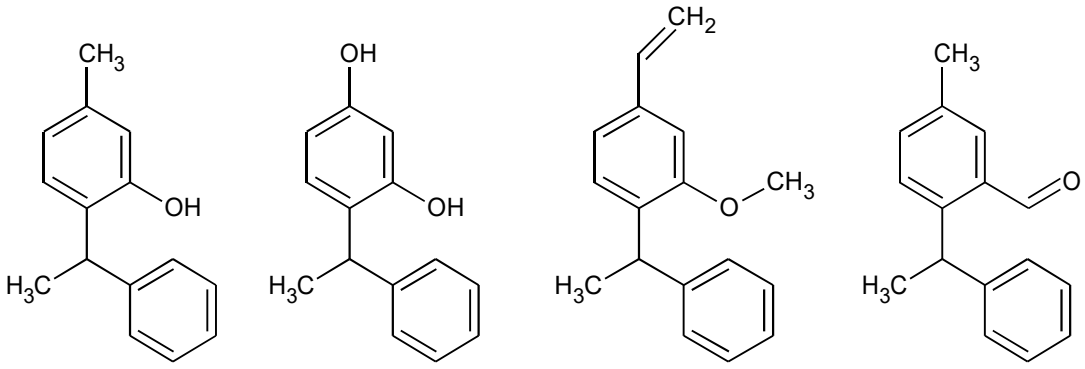

TDV6/1-2-OH-4-CH_3-C(C_6H_5)$_2$HCH_3 **TDV6/2**-2-OH-4-OH-C(C_6H_5)$_2$HCH_3 **TDV6/3**-2-OCH_3-4-CH=CH_2-C(C_6H_5)$_2$HCH_3 **TDV6/4**-2-CHO-4-CH_3-C(C_6H_5)$_2$HCH_3

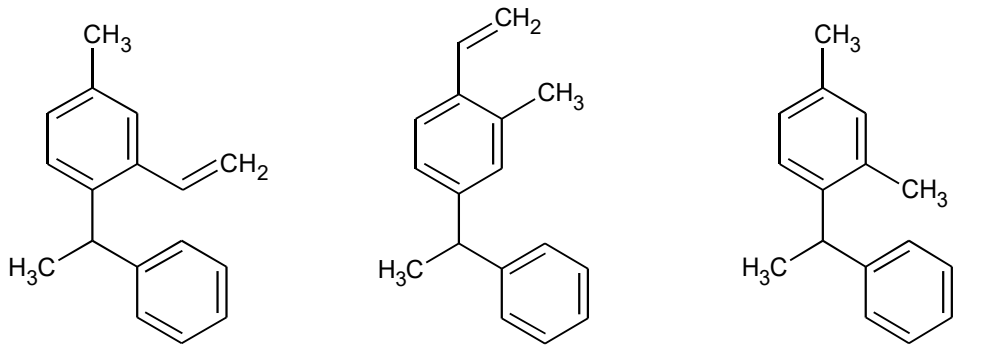

TDV6/5-2-CH=CH_2-4-CH_3-C(C_6H_5)$_2$HCH_3 **TDV6/6**-3-CH_3-4-CH=CH_2-C(C_6H_5)$_2$HCH_3 **TDV6/7**-2-CH_3-4-CH_3-C(C_6H_5)$_2$HCH_3

Figure C-12 List of toluene derivatives in 1,1-diphenylethane subset of the test set.

C.2.2 List of Benzylic Radicals

I. *Training Set*

I.1 Benzylic Radicals from Isopropyl Benzenes

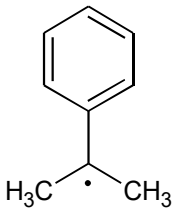

BRT1/1-$C_6H_5C\bullet(CH_3)_2$

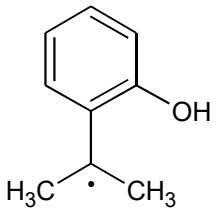

BRT1/2-o-$(OH)C_6H_5C\bullet(CH_3)_2$

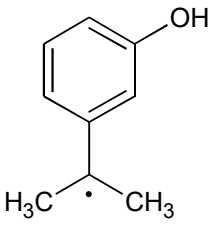

BRT1/3-m-$(OH)C_6H_5C\bullet(CH_3)_2$

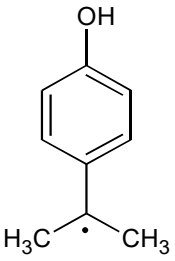

BRT1/4-p-$(OH)C_6H_5C\bullet(CH_3)_2$

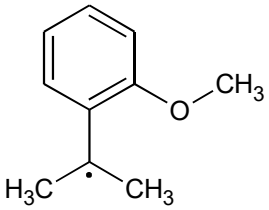

BRT1/5-o-$(OCH_3)C_6H_5C\bullet(CH_3)_2$

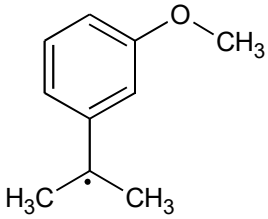

BRT1/6-m-$(OCH_3)C_6H_5C\bullet(CH_3)_2$

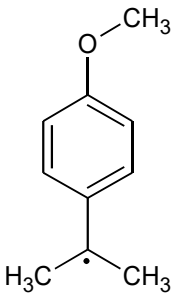

BRT1/7-p-$(OCH_3)C_6H_5C\bullet(CH_3)_2$

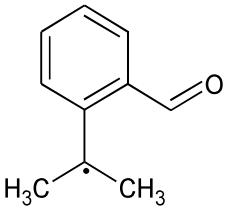

BRT1/8-o-$(CHO)C_6H_5C\bullet(CH_3)_2$

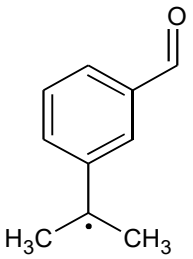

BRT1/9-m-$(CHO)C_6H_5C\bullet(CH_3)_2$

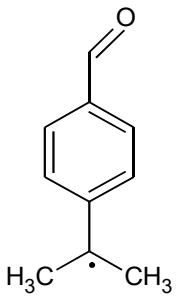

BRT1/10-p-$(CHO)C_6H_5C\bullet(CH_3)_2$

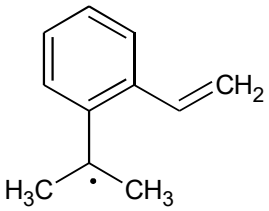

BRT1/11-o-$(CH{=}CH_2)C_6H_5C\bullet(CH_3)_2$

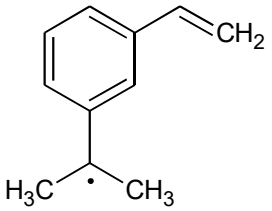

BRT1/12-m-$(CH{=}CH_2)C_6H_5C\bullet(CH_3)_2$

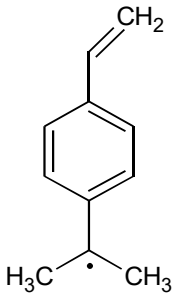

BRT1/13-p-(CH=CH$_2$)C$_6$H$_5$CH(CH$_3$)$_2$

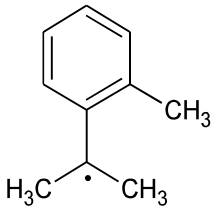

BRT1/14-o-(CH$_3$)C$_6$H$_5$CH(CH$_3$)$_2$

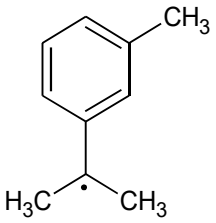

BRT1/15-m-(CH$_3$)C$_6$H$_5$CH(CH$_3$)$_2$

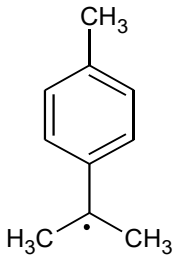

BRT1/16-p-(CH$_3$)C$_6$H$_5$CH(CH$_3$)$_2$

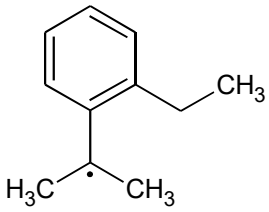

BRT1/17-o-(CH$_2$CH$_3$)C$_6$H$_5$C•(CH$_3$)$_2$

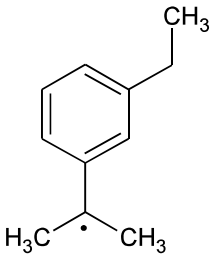

BRT1/18-m-(CH$_2$CH$_3$)C$_6$H$_5$C•(CH$_3$)$_2$

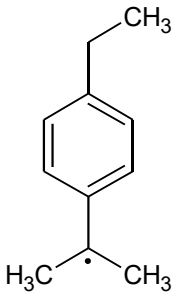

BRT1/19-p-(CH$_2$CH$_3$)C$_6$H$_5$C•(CH$_3$)$_2$

Figure C-13 List of benzylic radicals in "radicals from isopropylbenzenes (2-phenyl-2-propyl)" subset of the training set.

I.2 Benzylic Radicals from AllylBenzenes

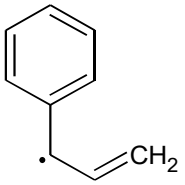

BRT2/1-C$_6$H$_5$C•HCH=CH$_2$

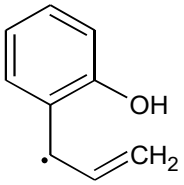

BRT2/2-o-(OH)C$_6$H$_5$C•HCH=CH$_2$

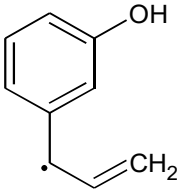

BRT2/3-m-(OH)C$_6$H$_5$C•HCH=CH$_2$

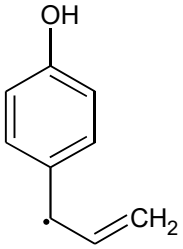

BRT2/4-p-(OH)C$_6$H$_5$C•HCH=CH$_2$

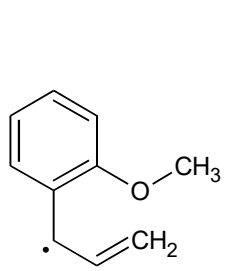

BRT2/5-o-$(OCH_3)C_6H_5C•HCH=CH_2$

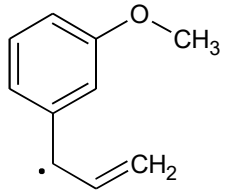

BRT2/6-m-$(OCH_3)C_6H_5C•HCH=CH_2$

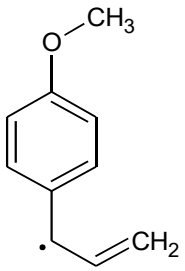

BRT2/7-p-$(OCH_3)C_6H_5C•HCH=CH_2$

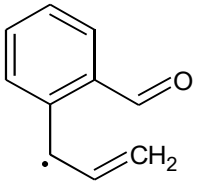

BRT2/8-o-$(CHO)C_6H_5C•HCH=CH_2$

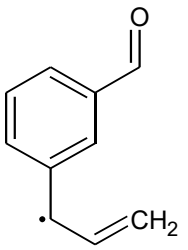

BRT2/9-m-$(CHO)C_6H_5C•HCH=CH_2$

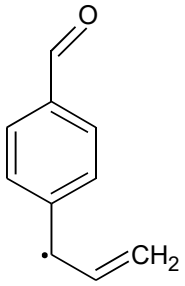

BRT2/10-p-$(CHO)C_6H_5C•HCH=CH_2$

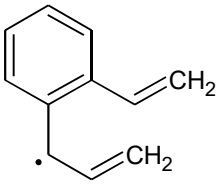

BRT2/11-o-$(CH=CH_2)C_6H_5C•HCH=CH_2$

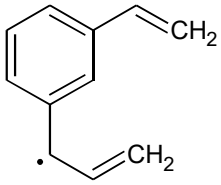

BRT2/12-m-$(CH=CH_2)C_6H_5C•HCH=CH_2$

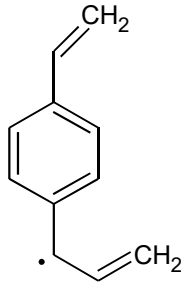

BRT2/13-p-$(CH=CH_2)C_6H_5C•HCH=CH_2$

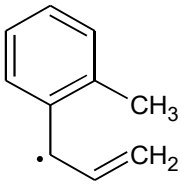

BRT2/14-o-$(CH_3)C_6H_5C•HCH=CH_2$

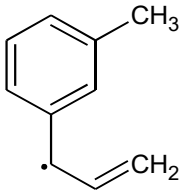

BRT2/15-m-$(CH_3)C_6H_5C•HCH=CH_2$

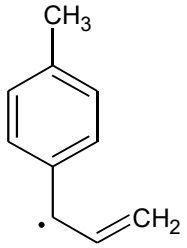

BRT2/16-p-$(CH_3)C_6H_5C•HCH=CH_2$

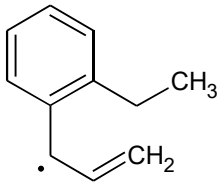

BRT2/17-o-$(CH_2CH_3)C_6H_5C•HCH=CH_2$

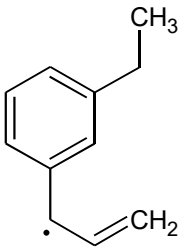

BRT2/18-m-$(CH_2CH_3)C_6H_5C•HCH=CH_2$

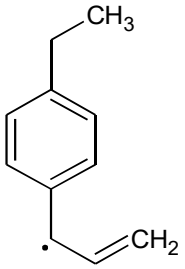

BRT2/19-p-$(CH_2CH_3)C_6H_5C•HCH=CH_2$

Figure C-14 List of benzylic radicals in "radicals from allylbenzenes (3-phenyl-1-propen-3-yl)" subset of the training set.

I.3 Benzylic Radicals from α-Methyl AllylBenzenes

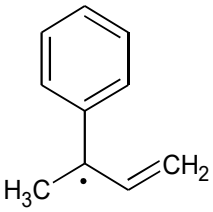

BRT3/1-$C_6H_5C\bullet(CH_3)CH=CH_2$

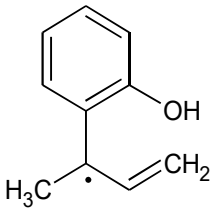

BRT3/2-o-$(OH)C_6H_5C\bullet(CH_3)CH=CH_2$

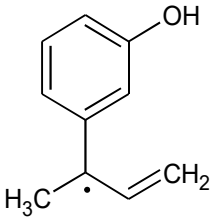

BRT3/3-m-$(OH)C_6H_5C\bullet(CH_3)CH=CH_2$

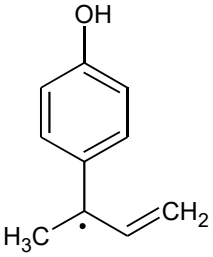

BRT3/4-p-$(OH)C_6H_5C\bullet(CH_3)CH=CH_2$

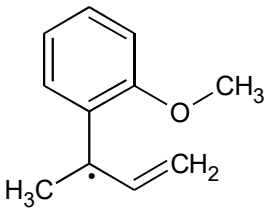

BRT3/5-o-$(OCH_3)C_6H_5C\bullet(CH_3)CH=CH_2$

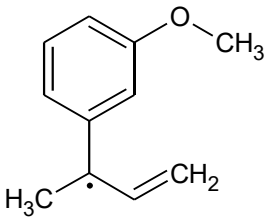

BRT3/6-m-$(OCH_3)C_6H_5C\bullet(CH_3)CH=CH_2$

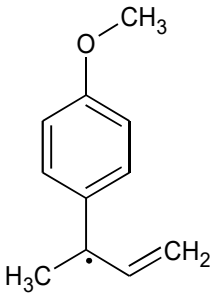

BRT3/7-p-$(OCH_3)C_6H_5C\bullet(CH_3)CH=CH_2$

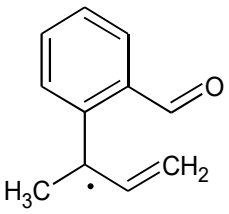

BRT3/8-o-$(CHO)C_6H_5C\bullet(CH_3)CH=CH_2$

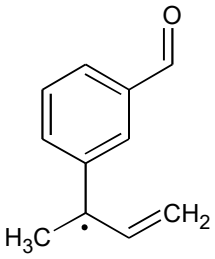

BRT3/9-m-$(CHO)C_6H_5C\bullet(CH_3)CH=CH_2$

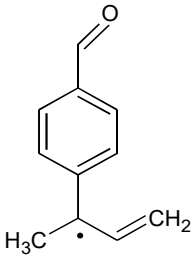

BRT3/10-p-$(CHO)C_6H_5C\bullet(CH_3)CH=CH_2$

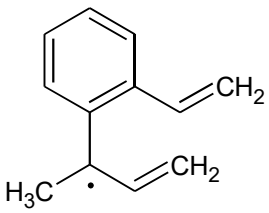

BRT3/11-o-$(CH=CH_2)C_6H_5C\bullet(CH_3)CH=CH_2$

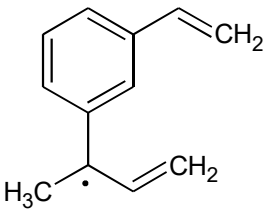

BRT3/12-m-$(CH=CH_2)C_6H_5C\bullet(CH_3)CH=CH_2$

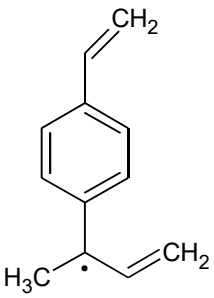

BRT3/13-p-$(CH=CH_2)C_6H_5C\bullet(CH_3)CH=CH_2$

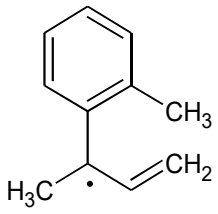

BRT3/14-o-$(CH_3)C_6H_5C\bullet(CH_3)CH=CH_2$

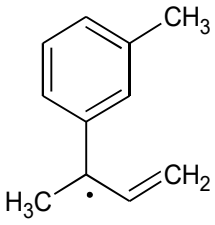

BRT3/15-m-$(CH_3)C_6H_5C\bullet(CH_3)CH=CH_2$

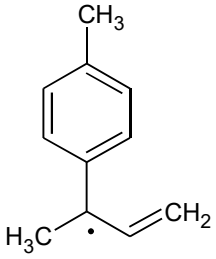

BRT3/16-p-$(CH_3)C_6H_5C\bullet(CH_3)CH=CH_2$

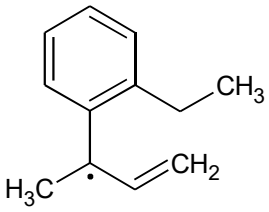

BRT3/17-o-$(CH_2CH_3)C_6H_5C\bullet(CH_3)CH=CH_2$

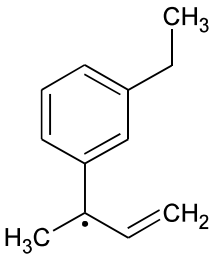

BRT3/18-m-$(CH_2CH_3)C_6H_5C\bullet(CH_3)CH=CH_2$

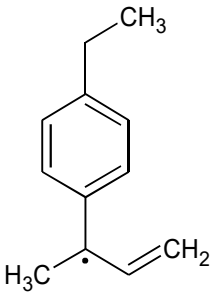

BRT3/19-p-$(CH_2CH_3)C_6H_5C\bullet(CH_3)CH=CH_2$

Figure C-15 List of benzylic radicals in "radicals from α-methylallylbenzene (3-phenyl-1-buten-3-yl)" subset of the training set.

I.4 Benzylic Radicals from α-Vinyl AllylBenzenes

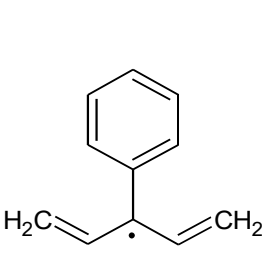

BRT4/1-$C_6H_5C\bullet(CH{=}CH_2)_2$

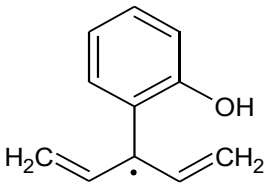

BRT4/2-o-$(OH)C_6H_5C\bullet(CH{=}CH_2)_2$

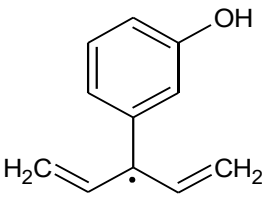

BRT4/3-m-$(OH)C_6H_5C\bullet(CH{=}CH_2)_2$

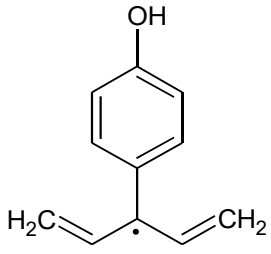

BRT4/4-p-$(OH)C_6H_5C\bullet(CH{=}CH_2)_2$

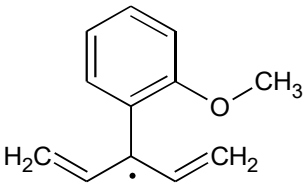

BRT4/5-o-$(OCH_3)C_6H_5C\bullet(CH{=}CH_2)_2$

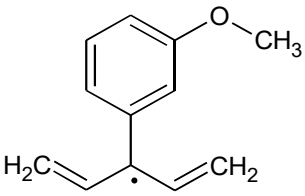

BRT4/6-m-$(OCH_3)C_6H_5C\bullet(CH{=}CH_2)_2$

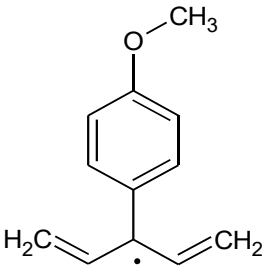

BRT4/7-p-$(OCH_3)C_6H_5C\bullet(CH{=}CH_2)_2$

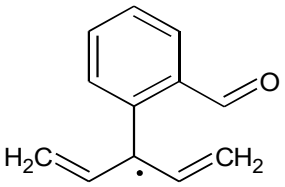

BRT4/8-o-$(CHO)C_6H_5C\bullet(CH{=}CH_2)_2$

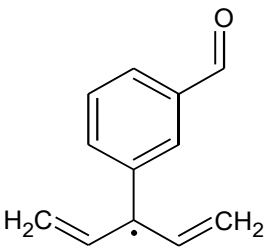

BRT4/9-m-$(CHO)C_6H_5C\bullet(CH{=}CH_2)_2$

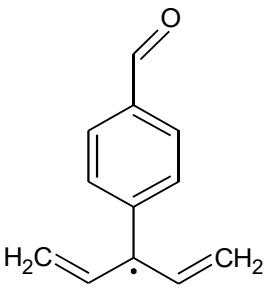

BRT4/10-p-$(CHO)C_6H_5C\bullet(CH{=}CH_2)_2$

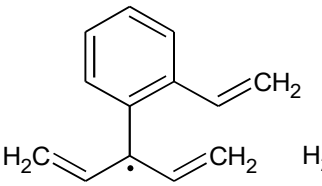

BRT4/11-o-$(CH{=}CH_2)C_6H_5C\bullet(CH{=}CH_2)_2$

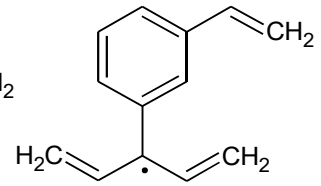

BRT4/12-m-$(CH{=}CH_2)C_6H_5C\bullet(CH{=}CH_2)_2$

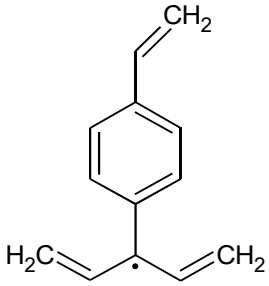

BRT4/13-p-$(CH{=}CH_2)C_6H_5C\bullet(CH{=}CH_2)_2$

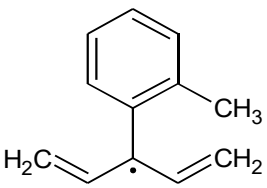

BRT4/14-o-$(CH_3)C_6H_5C\bullet(CH{=}CH_2)_2$

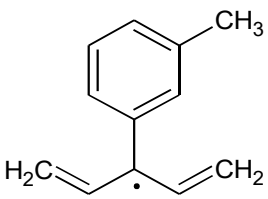

BRT4/15-m-$(CH_3)C_6H_5C\bullet(CH{=}CH_2)_2$

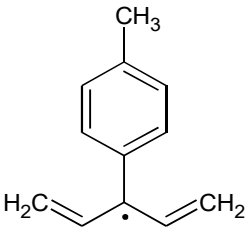

BRT4/16-p-$(CH_3)C_6H_5C\bullet(CH{=}CH_2)_2$

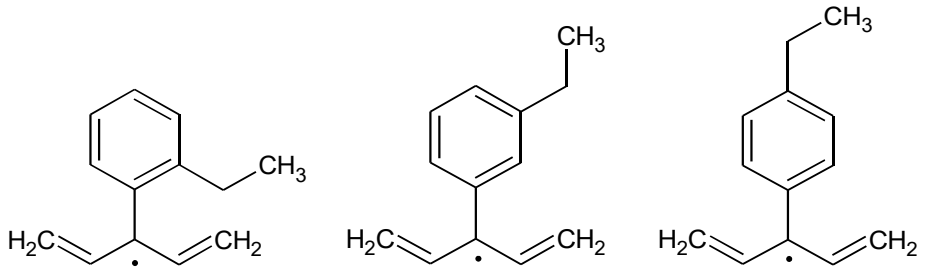

BRT4/17-o-$(CH_2CH_3)C_6H_5C\bullet(CH=CH_2)_2$ **BRT4/18**-m-$(CH_2CH_3)C_6H_5C\bullet(CH=CH_2)_2$ **BRT4/19**-p-$(CH_2CH_3)C_6H_5C\bullet(CH=CH_2)_2$

Figure C-16 List of benzylic radicals in "radicals from α-vinylallylbenzene (3-phenyl-1,4-pentadien-3-yl)" subset of the training set.

I.5 Benzylic Radicals from Diphenylmethanes

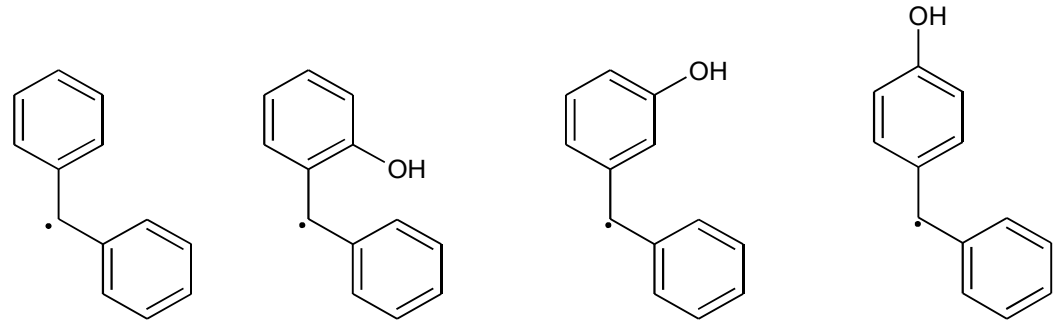

BRT5/1-$(C_6H_5)_2CH\bullet$ **BRT5/2**-o-$(OH)(C_6H_5)_2CH\bullet$ **BRT5/3**-m-$(OH)(C_6H_5)_2CH\bullet$ **BRT5/4**-p-$(OH)(C_6H_5)_2CH\bullet$

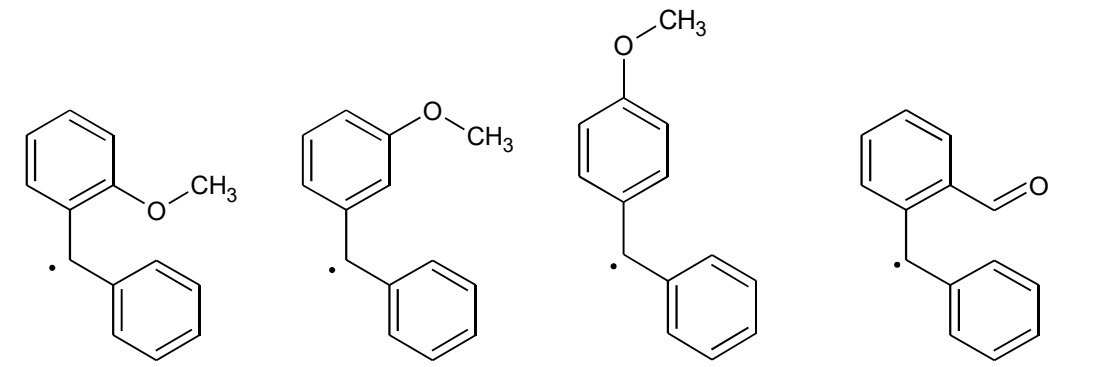

BRT5/5-o-$(OCH_3)(C_6H_5)_2CH\bullet$ **BRT5/6**-m-$(OCH_3)(C_6H_5)_2CH\bullet$ **BRT5/7**-p-$(OCH_3)(C_6H_5)_2CH\bullet$ **BRT5/8**-o-$(CHO)(C_6H_5)_2CH\bullet$

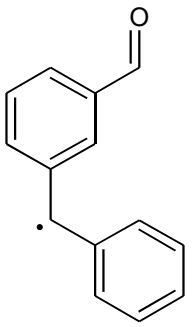

BRT5/9-m-(CHO)(C_6H_5)$_2$CH•

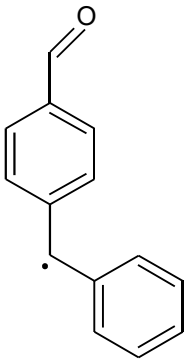

BRT5/10-p-(CHO)(C_6H_5)$_2$CH•

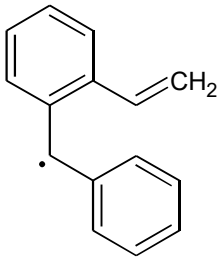

BRT5/11-o-(CH=CH_2)(C_6H_5)$_2$CH•

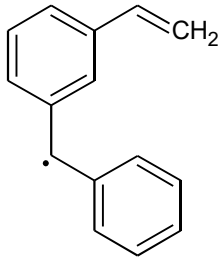

BRT5/12-m-(CH=CH_2)(C_6H_5)$_2$CH•

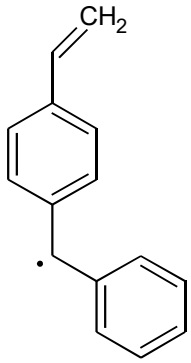

BRT5/13-p-(CH=CH_2)(C_6H_5)$_2$CH•

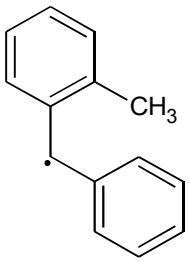

BRT5/14-o-(CH_3)(C_6H_5)$_2$CH•

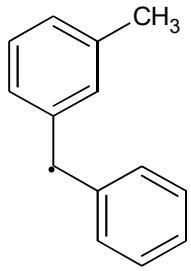

BRT5/15-m-(CH_3)(C_6H_5)$_2$CH•

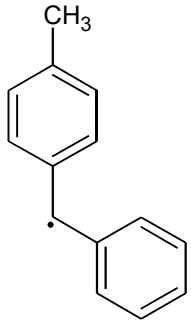

BRT5/16-p-(CH_3)(C_6H_5)$_2$CH•

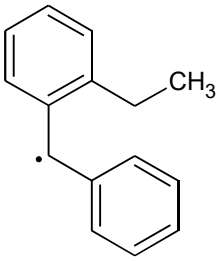

BRT5/17-o-(CH_2CH_3)(C_6H_5)$_2$CH•

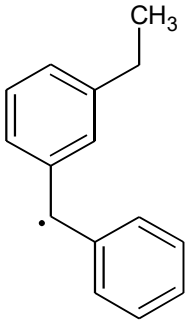

BRT5/18-m-(CH_2CH_3)(C_6H_5)$_2$CH•

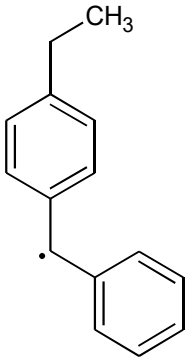

BRT5/19-p-(CH_2CH_3)(C_6H_5)$_2$CH•

Figure C-17 List of benzylic radicals in "radicals from diphenylmethane (diphenylmethyl)" subset of the training set.

I.6 Benzylic Radicals from 1,1-Diphenylethanes

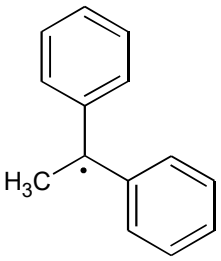

BRT6/1- C•$(C_6H_5)_2CH_3$

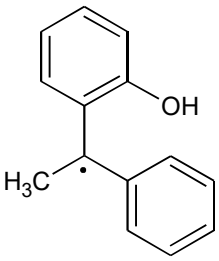

BRT6/2-o-(OH)C•$(C_6H_5)_2CH_3$

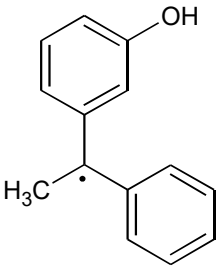

BRT6/3-m-(OH)C•$(C_6H_5)_2CH_3$

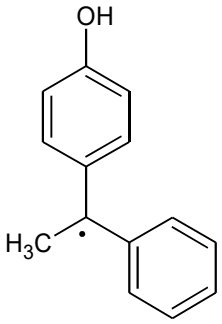

BRT6/4-p-(OH)C•$(C_6H_5)_2CH_3$

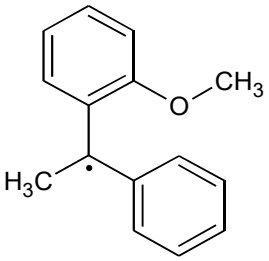

BRT6/5-o-(OCH_3)C•$(C_6H_5)_2CH_3$

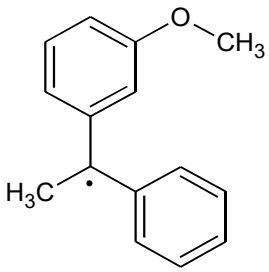

BRT6/6-m-(OCH_3)C•$(C_6H_5)_2CH_3$

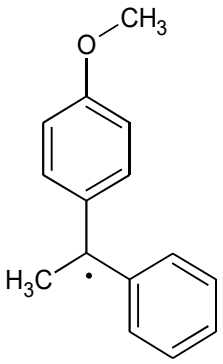

BRT6/7-p-(OCH_3)C•$(C_6H_5)_2CH_3$

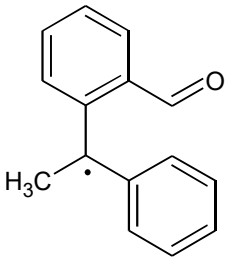

BRT6/8-o-(CHO)C•$(C_6H_5)_2CH_3$

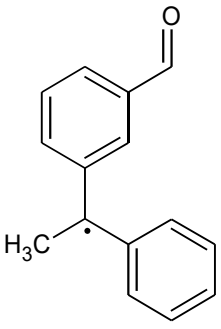

BRT6/9-m-(CHO)C•$(C_6H_5)_2CH_3$

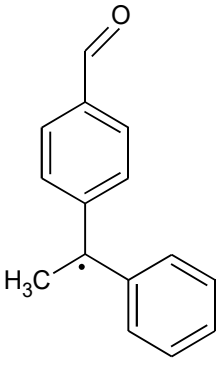

BRT6/10-p-(CHO)C•$(C_6H_5)_2CH_3$

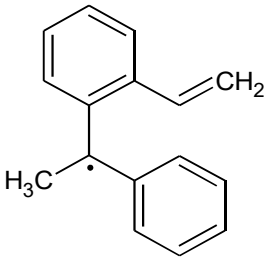

BRT6/11-o-$(CH{=}CH_2)$C•$(C_6H_5)_2CH_3$

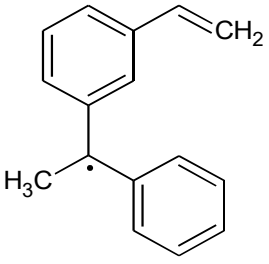

BRT6/12-m-$(CH{=}CH_2)$C•$(C_6H_5)_2CH_3$

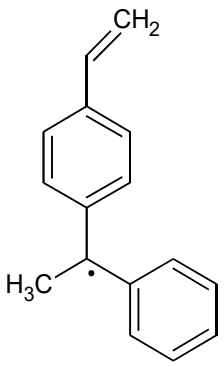

BRT6/13-p-(CH=CH$_2$)C•(C$_6$H$_5$)$_2$CH$_3$

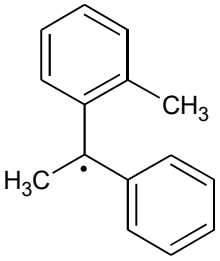

BRT6/14-o-(CH$_3$)C•(C$_6$H$_5$)$_2$CH$_3$

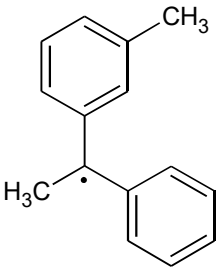

BRT6/15-m-(CH$_3$)C•(C$_6$H$_5$)$_2$CH$_3$

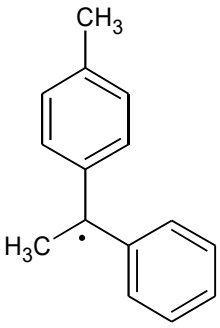

BRT6/16-p-(CH$_3$)C•(C$_6$H$_5$)$_2$CH$_3$

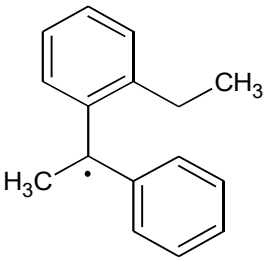

BRT6/17-o-(CH$_2$CH$_3$)C•(C$_6$H$_5$)$_2$CH$_3$

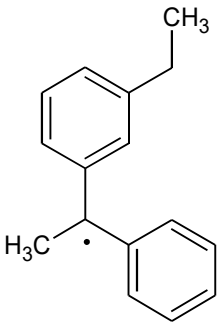

BRT6/18-m-(CH$_2$CH$_3$)C•(C$_6$H$_5$)$_2$CH$_3$

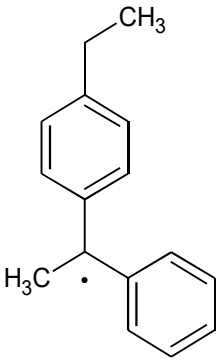

BRT6/19-p-(CH$_2$CH$_3$)C•(C$_6$H$_5$)$_2$CH$_3$

Figure C-18 List of benzylic radicals in "radicals from 1,1-diphenylethane (1,1-diphenylethyl)" subset of the training set.

II. *Validation Set*

II.1 Benzylic radicals from Doubly substituted Isopropylbenzenes

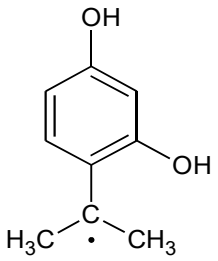

BRV1/1-2-OH-4-OH-C$_6$H$_5$C•(CH$_3$)$_2$

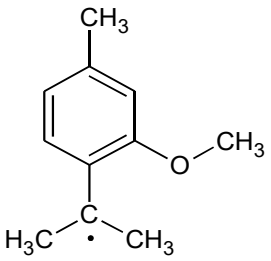

BRV1/2-2-OCH$_3$-4-CH$_3$-C$_6$H$_5$C•(CH$_3$)$_2$

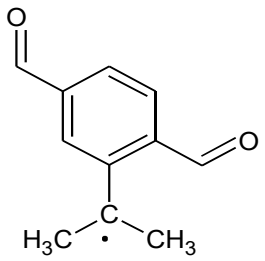

BRV1/3-2-CHO-5-CHO-C$_6$H$_5$C•(CH$_3$)$_2$

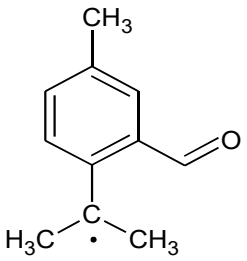

BRV1/4-2-CHO-4-CH$_3$-C$_6$H$_5$C•(CH$_3$)$_2$

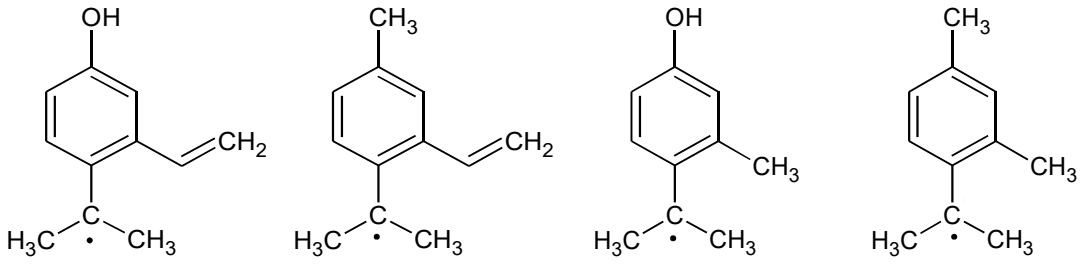

BRV1/5-2-CH=CH$_2$-4-OH-C$_6$H$_5$C•(CH$_3$)$_2$ **BRV1/6**-2-CH=CH$_2$-4-CH$_3$-C$_6$H$_5$C•(CH$_3$)$_2$ **BRV1/7**-2-CH$_3$-5-OH-C$_6$H$_5$C•(CH$_3$)$_2$ **BRV1/8**-2-CH$_3$-4-CH$_3$-C$_6$H$_5$C•(CH$_3$)$_2$

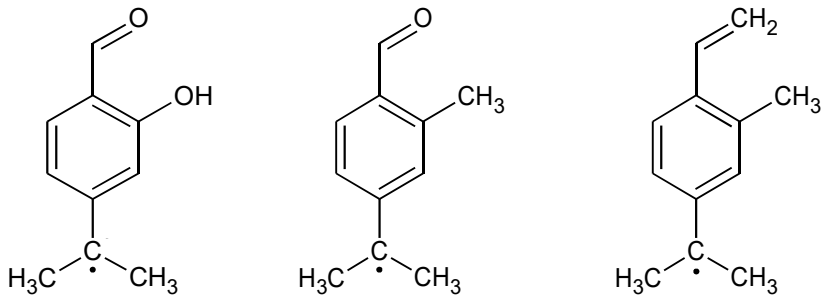

BRV1/9-3-OH-4-CHO-C$_6$H$_5$C•(CH$_3$)$_2$ **BRV1/10**-3-CH$_3$-4-CHO-C$_6$H$_5$C•(CH$_3$)$_2$ **BRV1/11**-3-CH$_3$-4-CH=CH$_2$-C$_6$H$_5$C•(CH$_3$)$_2$

Figure C-19 List of benzylic radicals in "radicals from isopropylbenzenes (2-phenyl-2-propyl)" subset of the test set.

II.2 Benzylic radicals from Doubly substituted Allylbenzenes

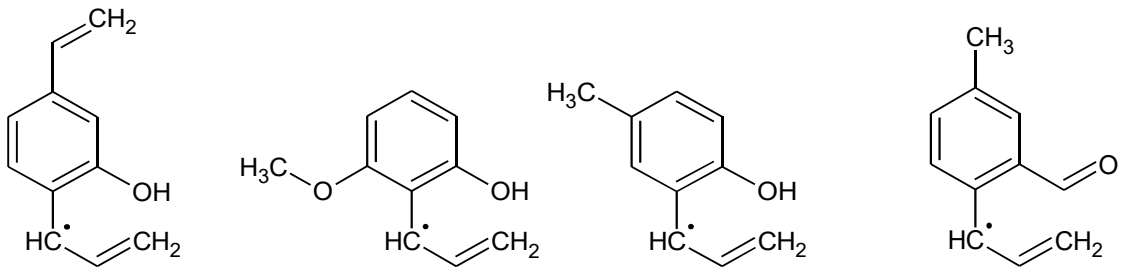

BRV2/1-2-OH-4-CH=CH$_2$-C$_6$H$_5$C•CH=CH$_2$ **BRV2/2**-2-OH-6-OCH$_3$-C$_6$H$_5$C•(CH$_3$)$_2$ **BRV2/3**-2-OH-5-CH$_3$-C$_6$H$_5$C•(CH$_3$)$_2$ **BRV2/4**-2-CHO-4-CH$_3$-C$_6$H$_5$C•(CH$_3$)$_2$

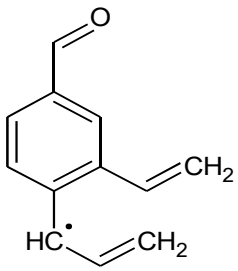

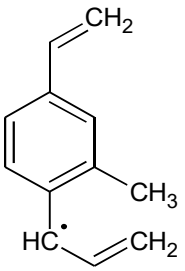

BRV2/5-2-CH=CH_2-4-CHO-C_6H_5C•CH=CH_2 **BRV2/6**-2-CH_3-4-CH=CH_2-C_6H_5C•$(CH_3)_2$

Figure C-20 List of benzylic radicals in "radicals from allylbenzenes (3-phenyl-1-propen-3-yl)" subset of the test set.

II.3 Benzylic radicals from Doubly substituted α-Methyl Allylbenzenes

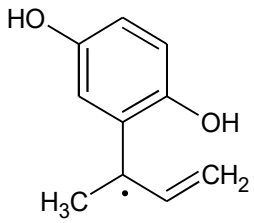

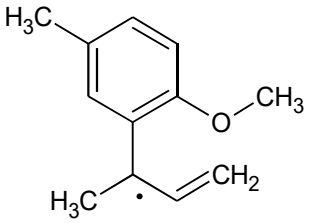

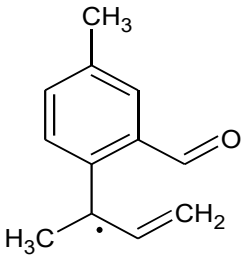

BRV3/1-2-OH-5-OH-C_6H_5C•(CH_3)CH=CH_2 **BRV3/2**-2-OCH_3-5-OH-C_6H_5C•(CH_3)CH=CH_2 **BRV3/3**-2-CHO-4-CH_3-C_6H_5C•(CH_3)CH=CH_2

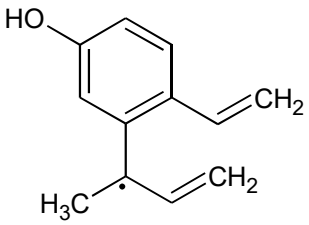

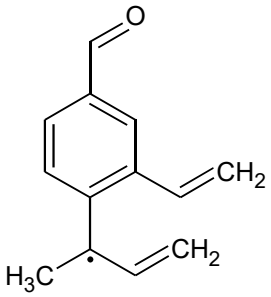

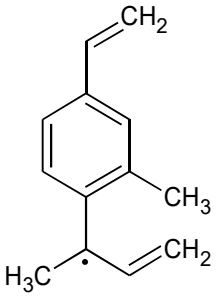

BRV3/4-2-CH=CH_2-5-OH-C_6H_5C•(CH_3)CH=CH_2 **BRV3/5**-2-CH=CH_2-4-CHO-C_6H_5C•(CH_3)CH=CH_2 **BRV3/6**-2-CH_3-4-CH=CH_2-C_6H_5C•(CH_3)CH=CH_2

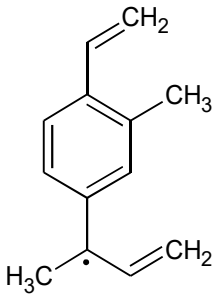

BRV3/7-3-CH_3-4-$CH=CH_2$-C_6H_5C•$(CH_3)CH=CH_2$

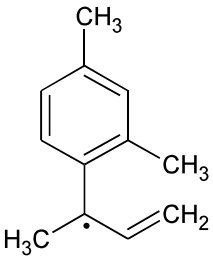

BRV3/8-2-CH_3-4-CH_3-C_6H_5C•$(CH_3)CH=CH_2$

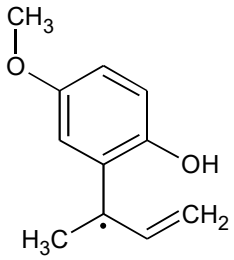

BRV3/9-2-OH-4-OCH_3-C_6H_5C•$(CH_3)CH=CH_2$

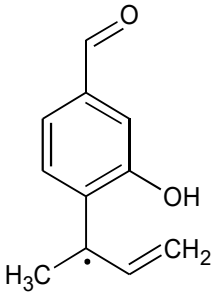

BRV3/10-2-OH-4-CHO-C_6H_5C•$(CH_3)CH=CH_2$

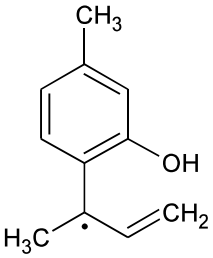

BRV3/11-2-OH-4-CH_3-C_6H_5C•$(CH_3)CH=CH_2$

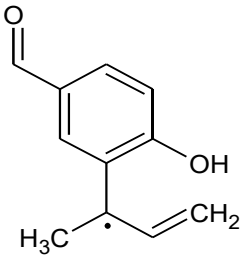

BRV3/12-2-OH-5-CHO-C_6H_5C•$(CH_3)CH=CH_2$

Figure C-21 List of benzylic radicals in "radicals from α-methylallylbenzene (3-phenyl-1-buten-3-yl)" subset of the test set.

II.4 Benzylic radicals from Doubly substituted α-Vinyl Allylbenzenes

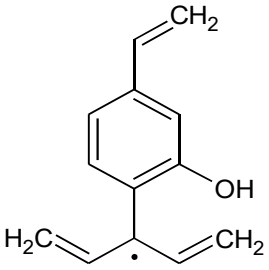

BRV4/1-2-OH-4-CH=CH$_2$-C$_6$H$_5$C•(CH=CH$_2$)$_2$

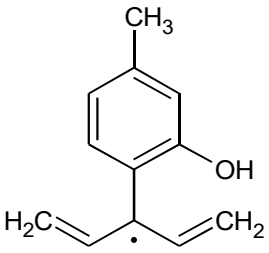

BRV4/2-2-OH-4-CH$_3$-C$_6$H$_5$C•(CH=CH$_2$)$_2$

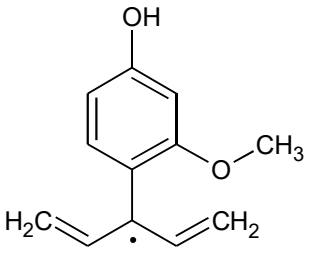

BRV4/3-2-OCH$_3$-4-OH-C$_6$H$_5$C•(CH=CH$_2$)$_2$

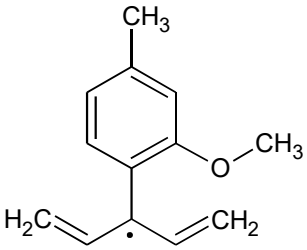

BRV4/4-2-OCH$_3$-4-CH$_3$-C$_6$H$_5$C•(CH=CH$_2$)$_2$

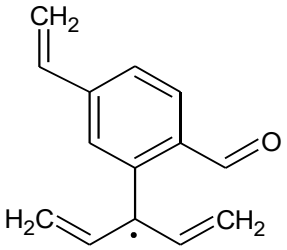

BRV4/5-2-CHO-5-CH=CH$_2$-C$_6$H$_5$C•(CH=CH$_2$)$_2$

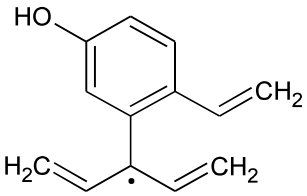

BRV4/6-2-CH=CH$_2$-5-OH-C$_6$H$_5$C•(CH=CH$_2$)$_2$

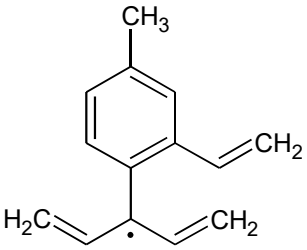

BRV4/7-2-CH=CH$_2$-4-CH$_3$-C$_6$H$_5$C•(CH=CH$_2$)$_2$

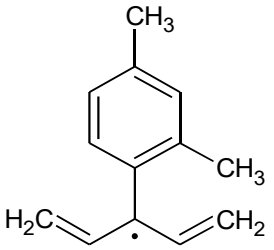

BRV4/8-2-CH$_3$-4-CH$_3$-C$_6$H$_5$C•(CH=CH$_2$)$_2$

Figure C-22 List of benzylic radicals in "radicals from α-vinylallylbenzene (3-phenyl-1,4-pentadien-3-yl)" subset of the test set.

II.5 Benzylic radicals from Doubly substituted Diphenylmethanes

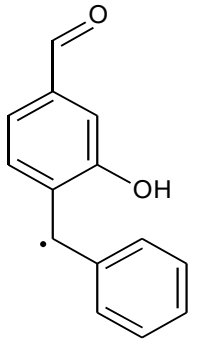

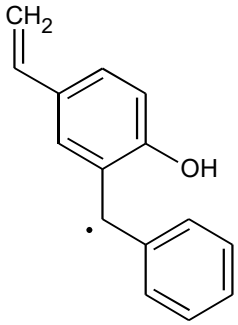

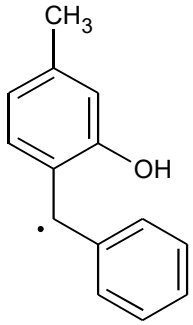

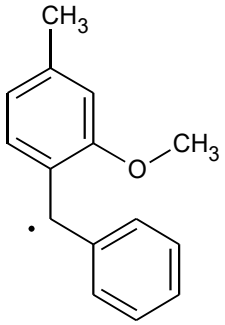

BRV5/1-2-OH-4-CHO-$(C_6H_5)_2CH$• **BRV5/2**-2-OH-5-$CH=CH_2$-$(C_6H_5)_2CH$• **BRV5/3**-2-OH-4-CH_3-$(C_6H_5)_2CH$• **BRV5/4**-2-OCH_3-4-CH_3-$(C_6H_5)_2CH$•

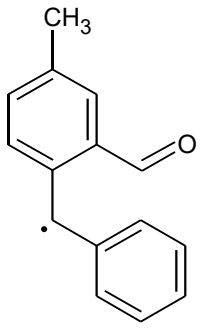

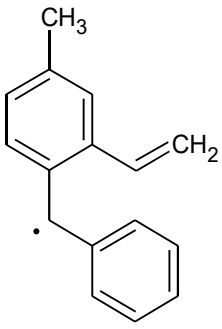

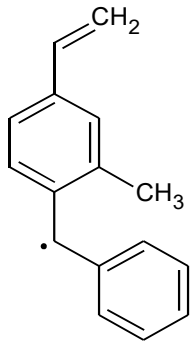

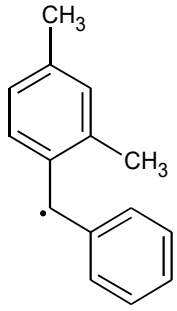

BRV5/5-2-CHO-4-CH_3-$(C_6H_5)_2CH$• **BRV5/6**-2-$CH=CH_2$-4-CH_3-$(C_6H_5)_2CH$• **BRV5/7**-2-CH_3-4-$CH=CH_2$-$(C_6H_5)_2CH$• **BRV5/8**-2-CH_3-4-CH_3-$(C_6H_5)_2CH$•

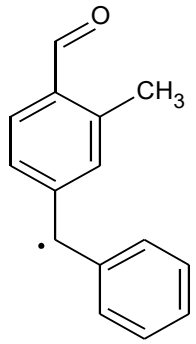

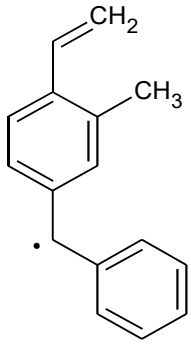

BRV5/9-3-CH_3-4-CHO-$(C_6H_5)_2CH$• **BRV5/10**-3-CH_3-4-$CH=CH_2$-$(C_6H_5)_2CH$•

Figure C-23 List of benzylic radicals in "radicals from diphenylmethane (diphenylmethyl)" subset of the test set.

II.6 Benzylic radicals from Doubly substituted 1,1-Diphenylethane*s*

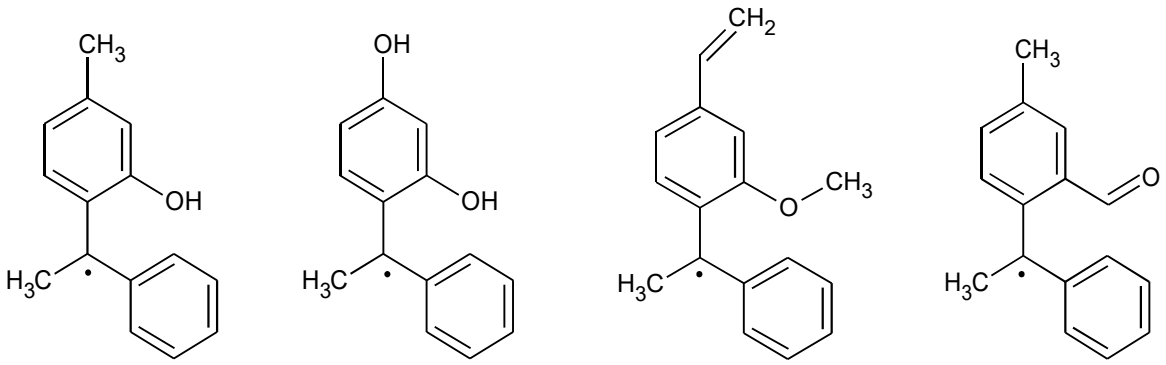

BRV6/1-2-OH-4-CH_3-C•$(C_6H_5)_2CH_3$ **BRV6/2**-2-OH-4-OH-C•$(C_6H_5)_2CH_3$ **BRV6/3**-2-OCH_3-4-CH=CH_2-C•$(C_6H_5)_2CH_3$ **BRV6/4**-2-CHO-4-CH_3-C•$(C_6H_5)_2CH_3$

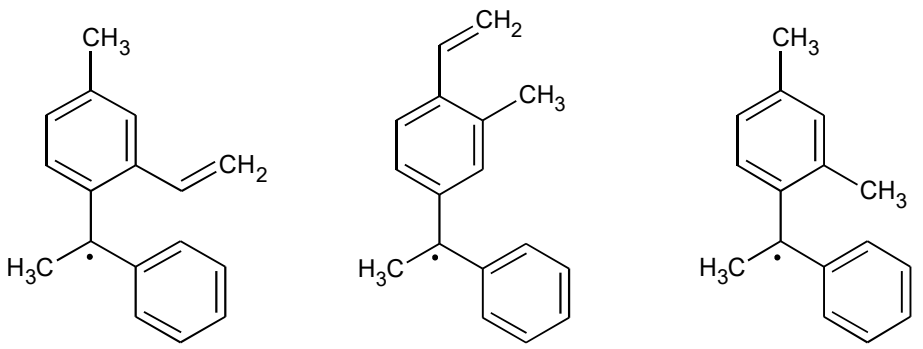

BRV6/5-2-CH=CH_2-4-CH_3-C•$(C_6H_5)_2CH_3$ **BRV6/6**-3-CH_3-4-CH=CH_2-C•$(C_6H_5)_2CH_3$ **BRV6/7**-2-CH_3-4-CH_3-C•$(C_6H_5)_2CH_3$

Figure C-24 List of benzylic radicals in "radicals from 1,1-diphenylethane (1,1-diphenylethyl)" subset of the test set.

C.3 Thermochemical Database

This section of the Supporting Information contains four tables consisting of thermochemical databases for the species in this study.

Table C-1: Training Set of Toluene Derivatives

Table C-2: Validation Set of Toluene Derivatives

Table C-3: Training Set of Toluene Derivatives

Table C-4: Validation Set of Toluene Derivatives

C.3.1 Toluene Derivatives

I. *Training Set*

Table C-1 Thermochemical database used as the training set for development of Group Additive Values (GAVs) and non-nearest neighbor interactions (NNIs) for toluene derivatives. The units of standard enthalpy of formation ($\Delta_f H^\circ$) data is given in kJ mol^{-1} whereas the units of entropies (S°) and heat capacities (C_p) are given in J mol^{-1} K^{-1}.

Molecules		$\Delta_f H^\circ$ (298 K)		S° (298 K)				C_p [J mol^{-1} K^{-1}]						
		$\Delta_f H^\circ_{CBSQB3}$	$\Delta_f H^\circ_{CBS-QB3+SOC+BAC}$	S°	S°_{int}	$\sigma_{tot^\circ sym}$	n_{opt}	300 K	400 K	500 K	600 K	800 K	1000 K	1500 K
Subset 1: Isopropylbenzenes														
TDT1/1	H	16.0	3.4	388.4	412.5	18	1	153.4	200.7	241.7	275.5	326.6	363.2	418.7
TDT1/2	*o*-OH	-165.8	-177.7	421.9	440.2	9	1	177.2	224.9	265.7	299.1	349	384.5	438.2
TDT1/3	*m*-OH	-164.4	-176.3	423.4	441.7	9	1	174.4	223.7	265.4	299.2	349.5	385.3	439.6
TDT1/4	*p*-OH	-163.0	-174.9	423.5	441.8	9	1	174.4	223.6	265.2	299	349.4	385.2	439.6
TDT1/5	*o*-OCH_3	-144.6	-153.3	455.3	482.7	27	1	195.9	251	299.1	338.5	397.8	439.7	501.8
TDT1/6	*m*-OCH_3	-143.8	-152.5	451.1	484.3	54	1	195.8	250	296.5	334.7	392.8	434.7	498.5
TDT1/7	*p*-OCH_3	-142.5	-151.2	457.7	485.1	27	1	195.9	249.9	296.3	334.6	392.7	434.6	498.5
TDT1/8	*o*-CHO	-101.5	-109.4	438.4	456.6	9	1	184.7	232.4	277.4	314.5	370.5	409.9	467.8
TDT1/9	*m*-CHO	-110.5	-118.4	439.6	457.8	9	1	181.9	232.4	276.4	312.8	368	407.2	465.9
TDT1/10	*p*-CHO	-110.9	-118.8	440.0	458.2	9	1	181.8	232.4	276.4	312.8	367.9	407.2	465.8
TDT1/11	*o*-$CH{=}CH_2$	89.9	74.5	445.0	463.2	9	1	192.2	247.7	297.3	338	399.1	442.3	506.3
TDT1/12	*m*-$CH{=}CH_2$	82.8	67.4	453.5	471.8	9	1	191.3	247.3	295.7	335.5	395.9	439.2	504.7
TDT1/13	*p*-$CH{=}CH_2$	82.8	67.4	454.1	472.4	9	1	191.7	247.4	295.7	335.5	395.9	439.1	504.7
TDT1/14	*o*-CH_3	-14.9	-27.2	419.4	446.8	27	1	177.6	230.4	277.1	315.9	375.1	417.4	480.7
TDT1/15	*m*-CH_3	-18.6	-30.9	429.9	457.3	27	1	174.7	227.3	273.4	311.8	370.4	412.6	476.3
TDT1/16	*p*-CH_3	-18.4	-30.7	431.3	458.8	27	1	175.1	227.5	273.5	311.8	370.5	412.8	476.7
TDT1/17	*o*-CH_2CH_3	-31.8	-46.2	459.0	486.4	27	1	205.1	263.2	314.6	357.7	423.5	470.6	540.5
TDT1/18	*m*-CH_2CH_3	-37.0	-51.4	470.7	498.1	27	1	200.0	257.9	309	351.7	417.1	464.5	536.6
TDT1/19	*p*-CH_2CH_3	-36.8	-51.2	471.1	498.5	27	1	199.6	257.6	308.8	351.5	417	464.5	536.8
Subset 2: Allylbenzenes														
TDT2/1	H	148.1	134.5	388.4	394.1	2	1	142.0	185.6	223.2	254.1	300.3	333	381.9

TDT2/2	*o*-OH	-39.4	-52.3	398.4	398.4	1	1	172.6	216.6	257	287.1	332.6	362.9	407.3
TDT2/3	*m*-OH	-33.5	-46.4	426.3	426.3	1	1	164.7	209.7	247.7	278.3	323.5	355	402
TDT2/4	*p*-OH	-30.4	-43.3	423.4	423.4	1	1	163.8	209.1	247.2	278	323.4	355.2	402.9
TDT2/5	*o*-OCH_3	-11.8	-21.5	451.6	460.8	3	1	184.9	236.1	280.3	316.4	370.4	408.2	463.9
TDT2/6	*m*-OCH_3	-10.1	-19.8	458.5	467.6	3	1	185.9	235.9	278.8	313.9	366.9	404.7	461.5
TDT2/7	*p*-OCH_3	-9.2	-18.9	458.0	467.1	3	1	184.8	235.2	278.2	313.5	366.6	404.6	461.5
TDT2/8	*o*-CHO	29.8	20.9	439.5	439.5	1	1	176.7	222.5	262.4	295.4	345.1	379.7	429.6
TDT2/9	*m*-CHO	24.3	15.4	447.9	447.9	1	1	171.8	218.1	258.6	292	342.4	377.6	428.6
TDT2/10	*p*-CHO	23.3	14.4	447.5	447.5	1	1	170.9	217.7	258.3	291.9	342.4	377.8	429.2
TDT2/11	*o*-$CH=CH_2$	219.0	202.6	448.1	448.1	1	1	186.8	238.1	282	317.8	371	408.4	464.4
TDT2/12	*m*-$CH=CH_2$	216.0	199.6	452.2	452.2	1	1	179.5	231.9	276.9	313.7	368.7	407.4	465.1
TDT2/13	*p*-$CH=CH_2$	215.8	199.4	452.4	452.4	1	1	179.4	231.8	276.8	313.7	368.7	407.4	465.1
TDT2/14	*o*-CH_3	118.0	104.7	424.3	433.5	3	1	167.2	214.9	257.3	292.6	346.1	384.3	441.2
TDT2/15	*m*-CH_3	115.1	101.8	430.4	439.6	3	1	163.6	212.3	255	290.4	344.2	382.5	440
TDT2/16	*p*-CH_3	115.4	102.1	430.4	439.5	3	1	163.5	212.1	254.8	290.2	344.1	382.6	440.4
TDT2/17	*o*-CH_2CH_3	100.6	85.2	463.6	472.8	3	1	189.5	243.8	292	332.2	393.2	436.7	501.3
TDT2/18	*m*-CH_2CH_3	96.5	81.1	470.1	479.3	3	1	188.3	242.6	290.4	330.1	390.7	434.2	499.7
TDT2/19	*p*-CH_2CH_3	97.0	81.6	470.2	479.3	3	1	188.2	242.5	290.3	330.1	390.6	434.1	499.5
Subset 3: α-Methyl Allylbenzenes														
TDT3/1	H	123.3	107.6	412.5	421.6	6	2	167.4	217.8	261.3	296.8	349.6	386.8	442.1
TDT3/2	*o*-OH	-56.1	-71.1	439.1	442.4	3	2	197.0	246.9	289.4	323.9	375.2	411.2	464.5
TDT3/3	*m*-OH	-55.6	-70.6	448.6	452.0	3	2	188.7	240.9	284.9	320.3	372.2	408.2	462.1
TDT3/4	*p*-OH	-54.5	-69.5	448.0	451.3	3	2	188.9	241	285.1	320.5	372.5	408.8	463
TDT3/5	*o*-OCH_3	-36.3	-48.1	470.1	482.6	9	2	214.6	271.2	320.3	360.6	421.1	463.6	526
TDT3/6	*m*-OCH_3	-35.2	-47.0	481.6	494.1	9	2	209.8	267	315.9	355.7	415.2	457.3	520.6
TDT3/7	*p*-OCH_3	-34.3	-46.1	484.2	496.7	9	2	209.6	266.9	315.9	355.8	415.6	458	521.5
TDT3/8	*o*-CHO	5.9	-5.1	458.2	461.6	3	2	205.4	257.5	302.8	340.4	396.9	436.1	492.5
TDT3/9	*m*-CHO	-1.2	-12.2	472.2	475.6	3	2	197.4	250.4	296.6	334.5	391.1	430.5	488.1
TDT3/10	*p*-CHO	-2.0	-13.0	470.0	473.4	3	2	195.6	249.5	296.1	334.4	391.5	431.4	489.3
TDT3/11	*o*-$CH=CH_2$	197.9	179.4	469.7	473.1	3	2	211.2	268.8	318.2	358.6	419.4	462.4	526.4
TDT3/12	*m*-$CH=CH_2$	191.0	172.5	477.0	480.4	3	2	204.7	264	314.8	356.1	417.3	460.2	524.2
TDT3/13	*p*-$CH=CH_2$	191.0	172.5	482.3	485.7	3	2	204.9	264	314.9	356.3	417.9	461.1	525.4
TDT3/14	*o*-CH_3	94.4	79.0	445.4	457.9	9	2	192.8	247.9	296.3	336.5	397	439.7	502.9
TDT3/15	*m*-CH_3	90.3	74.9	454.3	466.8	9	2	189.6	244.8	293.2	333.2	393.4	436.1	500
TDT3/16	*p*-CH_3	89.9	74.5	454.5	467.0	9	2	189.0	244.4	292.9	333	393.4	436.3	500.6
TDT3/17	*o*-CH_2CH_3	75.8	58.3	482.2	494.7	9	2	216.8	279	333.2	377.9	445.1	492.7	563.4
TDT3/18	*m*-CH_2CH_3	71.9	54.4	494.9	507.4	9	2	213.7	274.8	328.3	372.6	439.4	487	558.7
TDT3/19	*p*-CH_2CH_3	72.0	54.5	495.8	508.3	9	2	213.6	274.6	328.3	372.7	439.8	487.7	559.8
Subset 4: α-Vinyl Allylbenzenes														
TDT4/1	H	233.8	215.2	441.1	446.9	2	1	186.7	237.6	281.1	316.7	369.8	407.4	463.9
TDT4/2	*o*-OH	51.8	33.9	459.6	459.6	1	1	206.8	271.9	321.3	359.4	412	446.8	497.9
TDT4/3	*m*-OH	54.7	36.8	475.6	475.6	1	1	209.3	261.9	305.6	340.8	392.6	429	484.1
TDT4/4	*p*-OH	55.8	37.9	475.9	475.9	1	1	207.9	260.8	305	340.5	392.9	429.6	484.9
TDT4/5	*o*-OCH_3	74.6	59.9	499.1	508.3	3	1	234.1	291.3	340.3	380.5	440.7	483.3	546.7
TDT4/6	*m*-OCH_3	74.4	59.7	509.7	518.8	3	1	230.1	287.8	336.4	376	435.3	477.8	542.5
TDT4/7	*p*-OCH_3	73.9	59.2	511.6	520.8	3	1	226.3	283.8	333	373.3	434	477.3	542.7
TDT4/8	*o*-CHO	116.2	102.3	478.1	483.9	2	1	225.5	279.2	324.7	362.1	418.1	457.1	513.7
TDT4/9	*m*-CHO	109.1	95.2	497.7	497.7	1	1	213.1	264.8	311.6	350.1	408	448.8	508.9
TDT4/10	*p*-CHO	109.2	95.3	499.3	499.3	1	1	215.5	269.5	316.1	354.3	411.7	452	511.1
TDT4/11	*o*-$CH=CH_2$	306.5	285.1	497.0	497.0	1	1	234.0	294.8	343.9	383.6	443.1	485.2	548.7
TDT4/12	*m*-$CH=CH_2$	298.4	277.0	505.5	505.5	1	1	223.9	283.7	334.4	375.6	437	480.5	546
TDT4/13	*p*-$CH=CH_2$	301.7	280.3	498.6	504.3	2	1	223.9	283.7	334.7	376.2	438.1	481.7	547.2
TDT4/14	*o*-CH_3	201.4	183.1	470.2	479.4	3	1	212.8	269.8	318.6	358.7	418.9	461.4	524.9
TDT4/15	*m*-CH_3	200.8	182.5	482.9	492.1	3	1	208.6	264.5	312.9	352.9	413.2	456.3	521.6
TDT4/16	*p*-CH_3	201.1	182.8	482.6	491.7	3	1	208.1	264.1	312.7	352.9	413.6	457	522.4
TDT4/17	*o*-CH_2CH_3	185.2	164.8	511.2	520.4	3	1	235.0	296.5	351.9	397.3	465.3	513.2	584.5
TDT4/18	*m*-CH_2CH_3	182.1	161.7	523.1	532.2	3	1	233.3	294.7	348.2	392.3	459.3	507.4	580.7
TDT4/19	*p*-CH_2CH_3	182.4	162.0	525.8	535.0	3	1	232.8	294.4	348.1	392.6	459.9	508.3	581.4
Subset 5: Diphenylmethanes														
TDT5/1	H	177.5	162.0	447.2	458.7	4	1	177.6	240.8	295	338.7	402.5	446.1	509
TDT5/2	*o*-OH	-3.0	-18.6	477.8	483.5	2	1	203.4	267.1	321	364.4	427.6	470.9	534.4
TDT5/3	*m*-OH	-1.9	-17.5	483.0	488.8	2	1	198.4	263.6	318.2	361.7	424.4	466.9	528.7
TDT5/4	*p*-OH	-0.6	-16.2	483.1	488.9	2	1	198.6	263.8	318.5	362.1	425.1	467.9	529.6
TDT5/5	*o*-OCH_3	16.4	3.9	508.2	523.1	6	1	222.6	293.2	353.2	401.8	473.6	523.2	595.6
TDT5/6	*m*-OCH_3	19.4	6.9	516.8	531.7	6	1	220.4	290	349.2	396.9	467.1	515.8	587.2
TDT5/7	*p*-OCH_3	20.1	7.6	518.2	533.1	6	1	220.1	290.1	349.6	397.6	468.2	516.9	588.1
TDT5/8	*o*-CHO	58.6	46.9	495.1	500.9	2	1	216.7	281.9	337.6	383	449.9	495.9	561.7

TDT5/9	*m*-CHO	52.1	40.4	507.3	513.0	2	1	206.8	272.8	329.5	375.6	443.1	489.2	554.8
TDT5/10	*p*-CHO	52.0	40.3	505.2	511.0	2	1	206.2	272.9	330.1	376.4	444.2	490.4	555.8
TDT5/11	*o*-CH=CH_2	248.9	229.7	501.3	507.1	2	1	225.4	295	354.4	402.2	472.2	520.4	591.3
TDT5/12	*m*-CH=CH_2	245.2	226.0	511.7	517.5	2	1	214.7	286.5	347.7	397	469.1	518.6	590.8
TDT5/13	*p*-CH=CH_2	245.7	226.5	510.4	516.2	2	1	214.9	287	348.5	398.1	470.5	520	591.9
TDT5/14	*o*-CH_3	142.2	128.0	482.1	497.0	6	1	204.7	271.1	329.1	376.5	446.8	495.6	566.9
TDT5/15	*m*-CH_3	144.7	128.6	489.8	504.7	6	1	199.2	267.4	326.3	374.3	445.2	494.4	566.3
TDT5/16	*p*-CH_3	144.6	128.5	489.5	504.4	6	1	199.0	267.4	326.5	374.8	446.1	495.4	567.2
TDT5/17	*o*-CH_2CH_3	128.1	109.9	516.8	531.7	6	1	226.8	299.9	363.6	415.7	493.3	547.4	626.7
TDT5/18	*m*-CH_2CH_3	125.4	107.2	529.7	544.6	6	1	223.9	297.5	361.4	413.6	491.2	545.3	625
TDT5/19	*p*-CH_2CH_3	126.1	107.9	530.1	545.0	6	1	223.8	297.7	361.9	414.4	492.3	546.5	626.1
Subset 6: 1,1-Diphenylethanes														
TDT6/1	H	153.5	135.1	472.0	492.6	12	1	205.6	274.2	333	380.6	450.3	498.3	568.5
TDT6/2	*o*-OH	-26.9	-44.6	496.2	505.3	6	2	236.7	306.2	364.1	410.1	476.8	522.6	590.1
TDT6/3	*m*-OH	-26.9	-44.6	509.7	518.8	6	2	224.7	294.9	354.3	402	471.2	518.7	588.3
TDT6/4	*p*-OH	-24.3	-42.0	508.1	517.2	6	2	226.4	296.9	356.4	404.1	473.1	520.3	589.3
TDT6/5	*o*-OCH_3	-8.9	-23.5	527.4	545.6	18	2	253.3	329.6	394.2	446.1	522.2	574.7	651.6
TDT6/6	*m*-OCH_3	-4.6	-19.2	550.3	559.4	6	2	248.4	323.4	387.2	438.9	515.2	568.4	647.1
TDT6/7	*p*-OCH_3	-4.0	-18.6	544.0	562.3	18	2	247.3	322.7	387	439	515.7	569	647.6
TDT6/8	*o*-CHO	35.3	21.5	513.9	523.1	6	2	244.5	317.1	378.7	428.3	500.3	549	618.3
TDT6/9	*m*-CHO	28.1	14.3	526.3	535.4	6	2	233.6	305.1	366.7	416.8	490.6	541.3	614.5
TDT6/10	*p*-CHO	28.3	14.5	528.5	537.6	6	2	234.0	306.1	368	418.3	492.2	542.8	615.5
TDT6/11	*o*-CH=CH_2	222.3	201.0	529.4	538.5	6	2	246.5	323.8	389.4	442.2	519.2	572.5	651.1
TDT6/12	*m*-CH=CH_2	221.1	199.8	537.2	546.3	6	2	242.1	319.2	385	438.3	516.6	570.7	650.4
TDT6/13	*p*-CH=CH_2	221.7	200.4	536.6	545.7	6	2	242.3	319.4	385.5	439	517.6	571.8	651.3
TDT6/14	*o*-CH_3	119.2	101.0	505.9	524.2	18	2	233.1	304.7	367.4	418.8	495.2	548.4	626.9
TDT6/15	*m*-CH_3	119.9	101.7	516.2	534.4	18	2	225.4	299.1	362.9	415	492.3	546.3	625.8
TDT6/16	*p*-CH_3	118.7	100.5	517.9	536.2	18	2	225.8	298.5	362	414.2	491.9	546.2	626
TDT6/17	*o*-CH_2CH_3	106.3	86.0	538.7	557.0	18	2	256.8	336.5	405.6	462	545.5	603.5	688.7
TDT6/18	*m*-CH_2CH_3	101.4	81.1	554.4	572.6	18	2	251.6	330.5	399	455.2	538.9	597.7	684.7
TDT6/19	*p*-CH_2CH_3	102.2	81.9	555.4	573.7	18	2	251.5	330.7	399.6	456	539.9	598.7	685.7

II. *Validation Set*

Table C-2 Thermochemical database used as the validation set for testing the Group Additive Values (GAVs) and non-nearest neighbor interactions (NNIs) for toluene derivatives. The units of standard enthalpy of formation ($\Delta_f H^\circ$) data is given in kJ mol^{-1} whereas the units of entropies (S°) and heat capacities (C_p) are given in J mol^{-1} K^{-1}.

Molecules		$\Delta_f H°$ (298 K)		$S°$ (298 K)				C_p [J mol^{-1} K^{-1}]						
		$\Delta_f H^\circ_{CBSQB3}$	$\Delta_f H^\circ_{CBS-QB3+SOC+BAC}$	S°	S°_{int}	$\sigma_{tot°sym}$	n_{opt}	**300 K**	**400 K**	**500 K**	**600 K**	**800 K**	**1000 K**	**1500 K**
Subset 1: Isopropylbenzenes														
TDV1/1	2-OH-4-OH	-342.1	-353.3	446.7	465.0	9	1	199.6	250.1	292.2	325.9	375.3	409.8	461.5
TDV1/2	2-OCH_3-4-CH_3	-177.8	-186.3	489.1	525.7	81	1	216.7	276.2	328.4	372	438.8	486.8	558.8
TDV1/3	2-CHO-5-CHO	-222.8	-226.1	483.6	501.9	9	1	218.0	267.7	315.5	355.2	414.7	455.9	514.2
TDV1/4	2-CHO-4-CH_3	-135.1	-142.8	472.2	499.6	27	1	204.9	260.7	310	351.3	414.4	459.2	525
TDV1/5	2-CH=CH_2-4-OH	-89.6	-104.4	475.4	493.6	9	1	215.4	272.2	321.9	361.9	421.1	460	524.3
TDV1/6	2-CH=CH_2-4-CH_3	53.5	38.3	484.4	511.8	27	1	213.5	274.5	327.8	372.1	439.6	487.9	560.4
TDV1/7	2-CH_3-4-OH	-191.0	-202.7	451.2	478.6	27	1	198.4	253.1	300.4	339.2	397.6	439.1	501.5
TDV1/8	2-CH_3-4-CH_3	-45.0	-57.1	456.9	493.4	81	1	199.6	257.5	309	352.3	418.7	464	538
TDV1/9	3-OH-4-CHO	-318.3	-325.5	444.2	468.2	18	1	195.5	248.9	294.8	332.5	389.1	428.9	488
TDV1/10	3-CH_3-4-CHO	-139.6	-147.3	478.8	506.2	27	1	210.4	264.3	312.1	352.4	414.2	458.6	524.8
TDV1/11	3-CH_3-4-CH=CH_2	54.1	38.9	484.5	511.9	27	1	217.7	277.5	329.6	373	439.3	487.3	560.4
Subset 2: Allylbenzenes														
TDV2/1	2-OH-4-CH=CH_2	33.0	17.3	455.9	455.9	1	1	211.6	263	308	347	404.3	440	490.1
TDV2/2	2-OH-6-OCH_3	-195.2	-204.3	452.4	461.6	3	1	215.1	271.4	316.9	352.5	403.5	438.4	489.7
TDV2/3	2-OH-5-CH_3	-68.6	-81.3	434.1	443.2	3	1	195.2	244.4	290	327	379	413.3	464.9
TDV2/4	2-CHO-4-CH_3	-3.9	-12.6	469.4	478.5	3	1	197.9	249.2	294	331.5	388.8	429.2	488.1

TDV2/5	2-CH=CH_2-4-CHO	94.8	83.0	496.0	496.0	1	1	214.0	267.6	315.7	355	413.4	454	512.9
TDV2/6	2-CH_3-4-CH=CH_2	185.5	169.3	481.9	491.0	3	1	204.3	261	310.8	352.1	414.4	458.5	524.3
Subset 3: α-Methyl Allylbenzenes														
TDV3/1	2-OH-5-OH	-230.6	-244.9	469.4	472.8	3	2	221.6	271.6	313.1	346.8	396.8	431.9	484.4
TDV3/2	2-OCH_3-5-CH_3	-70.8	-82.4	510.9	532.5	27	2	233.2	293.4	347.3	397	461.4	508.8	583
TDV3/3	2-CHO-4-CH_3	-28.5	-39.3	497.6	510.1	9	2	225.5	282.5	332.7	374.7	438.7	484.2	551.6
TDV3/4	2-CH=CH_2-5-OH	20.1	2.3	494.6	498.0	3	2	236.8	295.7	345	384.8	443.9	485.5	547.7
TDV3/5	2-CH=CH_2-4-CHO	72.4	58.5	516.1	519.4	3	2	241.2	302	354.3	397.2	461.9	507.3	573.6
TDV3/6	2-CH_3-4-CH=CH_2	161.3	143.0	503.3	515.8	9	2	230.4	294.8	350.4	396.2	465.1	513.8	586.2
TDV3/7	3-CH_3-4-CH=CH_2	162.8	144.5	508.4	520.9	9	2	231.4	294.3	348.9	393.9	461.8	508	582.8
TDV3/8	2-CH_3-4-CH_3	61.2	46.0	481.7	503.3	27	2	214.2	275	328.4	372.9	440.7	489.1	561.4
TDV3/9	2-OH-5-OCH_3	-230.6	-244.9	469.4	472.8	3	2	221.6	271.6	313.1	346.8	396.8	431.9	484.4
TDV3/10	2-OH-4-CHO	-184.4	-194.7	487.5	490.9	3	2	228.4	283.1	329	365.9	420.4	458.1	512.8
TDV3/11	2-OH-4-CH_3	-88.6	-103.4	475.6	488.1	9	2	218.5	273.4	320.9	360	419	460.7	522.9
Subset 4: α-Vinyl Allylbenzenes														
TDV4/1	2-OH-4-CH=CH_2	119.4	98.6	516.1	516.1	1	1	242.3	318	374	414	477	519	580
TDV4/2	2-OH-4-CH_3	19.5	1.8	493.7	502.9	3	1	228.7	299	352	392	452	497	554
TDV4/3	2-OCH_3-4-OH	-101.9	-116.0	529.6	538.7	3	1	257.1	316.2	365.8	405.9	465.1	506.5	568.3
TDV4/4	2-OCH_3-4-CH_3	42.3	27.8	533.9	552.2	9	1	257.1	318.1	371.4	415.8	483.4	531.6	604.3
TDV4/5	2-CHO-5-CH=CH_2	181.5	164.7	543.7	543.7	1	1	260.0	322.8	375.9	419.4	485	531.4	599.9
TDV4/6	2-CH=CH_2-5-OH	129.7	108.9	527.0	527.0	1	1	257.4	310	368.7	408.2	466	509	572
TDV4/7	2-CH=CH_2-4-CH_3	271.7	250.5	534.8	544.0	3	1	250.4	316.4	371.7	416.7	484.2	532.5	605.7
TDV4/8	2-CH_3-4-CH_3	170.0	151.9	506.1	524.4	9	1	237.3	298.9	352.2	396.4	463.5	511.4	583.4
Subset 5: Diphenylmethanes														
TDV5/1	2-OH-4-CHO	-131.0	-142.0	522.2	528.0	2	1	237.8	305.4	361.9	409	473.2	518.3	583
TDV5/2	2-OH-5-CH=CH_2	64.1	45.6	535.5	541.3	2	1	241.8	314.1	375.4	424.7	496.6	546	618.1
TDV5/3	2-OH-4-CH_3	-35.7	-51.1	519.7	528.8	3	1	225.0	293.7	352.7	400.6	474	520.6	593
TDV5/4	2-OCH_3-4-CH_3	-16.1	-28.4	544.8	568.8	18	1	244.5	320.3	385.5	438.7	517.9	573.2	654.2
TDV5/5	2-CHO-4-CH_3	24.8	13.4	531.6	546.5	6	1	238.4	308.4	369.2	419.1	493.6	545.2	619.9
TDV5/6	2-CH=CH_2-4-CH_3	215.3	196.3	544.8	559.7	6	1	248.0	322.3	386.4	438.6	515.9	569.8	649.7
TDV5/7	2-CH_3-4-CH=CH_2	211.9	192.9	540.0	554.9	6	1	242.6	317.5	382.6	435.9	514.7	569.5	649.9
TDV5/8	2-CH_3-4-CH_3	110.6	94.7	517.9	541.9	18	1	227.9	298.4	361	412.8	490.5	544.9	625.2
TDV5/9	3-CH_3-4-CHO	23.0	11.6	535.7	550.6	6	1	234.2	304.1	364.8	414.7	488.8	539.9	611
TDV5/10	3-CH_3-4-CH=CH_2	217.4	198.4	539.1	559.8	12	1	244.0	318.1	382.3	434.9	513.2	568	648.8
Subset 6: 1,1-Diphenylethanes														
TDV6/1	2-OH-4-CH_3	-56.5	-74.0	531.8	550.1	18	2	258.6	332.7	395.5	446.1	520.5	572.2	648.6
TDV6/2	2-OH-4-OH	-205.7	-222.7	521.6	530.7	6	2	259.0	332	390	435	503	549	616.3
TDV6/3	2-OCH_3-4-CH=CH_2	64.8	47.3	590.2	602.7	9	2	291.2	376.4	448.4	506.2	590.9	649.3	735.1
TDV6/4	2-CHO-4-CH_3	1.6	-12.0	549.2	567.5	18	2	266.9	344.4	410.9	465	544	598.8	676.9
TDV6/5	2-CH=CH_2-4-CH_3	192.7	171.6	566.2	584.5	18	2	276.4	357.3	426.8	483.3	566.8	624.9	714
TDV6/6	3-CH_3-4-CH=CH_2	192.8	171.7	570.1	588.4	18	2	269.3	350.1	419.7	476.5	561.2	620.6	708.8
TDV6/7	2-CH_3-4-CH_3	89.5	71.5	541.8	569.2	54	2	252.2	338.8	405.4	460.5	543.1	601.1	687.1

C.3.2 Benzylic Radicals

I. *Training Set*

Table C-3 Thermochemical database used as the training set for development of Group Additive Values (GAVs) and non-nearest neighbor interactions (NNIs) for benzylic radicals. The units of standard enthalpy of formation ($\Delta_f H^\circ$) data is given in kJ mol^{-1} whereas the units of entropies (S°) and heat capacities (C_p) are given in J mol^{-1} K^{-1}.

Radicals		$\Delta_f H°$ (298 K)		$S°$ (298 K)				C_p [J mol^{-1} K^{-1}]						
		$\Delta_f H^\circ_{CBSQB3}$	$\Delta_f H^\circ_{CBS-QB3+SOC+BAC}$	S°	S°_{int}	$\sigma_{tot^\circ sym}$	n_{opt}	300 K	400 K	500 K	600 K	800 K	1000 K	1500 K
Subset 1: 2-phenyl-2-propyls (Radicals from Isopropylbenzenes)														
BRT1/1	H	161.0	148.6	392.1	421.9	36	1	144.4	189.7	229.5	262.5	312.6	348.2	401.1
BRT1/2	*o*-OH	-7.8	-19.5	427.6	451.6	18	1	165.2	211.6	251.7	284.6	334.0	368.7	419.9
BRT1/3	*m*-OH	-20.0	-31.7	428.8	452.9	18	1	164.4	211.7	252.2	285.4	335.0	369.8	421.3
BRT1/4	*p*-OH	-17.8	-29.5	428.5	452.5	18	1	165.4	212.5	252.9	286.0	335.5	370.3	422.2
BRT1/5	*o*-OCH_3	12.7	4.2	459.6	492.7	54	1	189.7	235.0	280.7	319.0	377.1	418.3	479.1
BRT1/6	*m*-OCH_3	1.7	-6.9	461.3	494.5	54	1	187.1	239.0	284.2	321.6	378.7	419.7	481.0
BRT1/7	*p*-OCH_3	2.5	-6.1	460.1	493.3	54	1	186.5	238.8	284.1	321.8	379.0	419.9	481.1
BRT1/8	*o*-CHO	56.7	49.0	446.5	470.5	18	1	184.7	229.5	269.6	303.4	354.9	391.2	444.3
BRT1/9	*m*-CHO	35.5	27.8	446.0	470.1	18	1	172.5	221.4	264.5	300.4	354.8	393.1	448.6
BRT1/10	*p*-CHO	27.6	19.9	445.2	469.3	18	1	171.9	220.9	263.9	299.8	354.2	392.7	448.6
BRT1/11	*o*-$CH=CH_2$	249.4	234.2	456.8	480.9	18	1	197.4	248.6	293.1	329.7	384.8	424.1	482.9
BRT1/12	*m*-$CH=CH_2$	227.5	212.3	456.1	480.1	18	1	182.3	236.0	283.0	321.9	380.7	422.3	483.7
BRT1/13	*p*-$CH=CH_2$	219.7	204.5	452.2	476.2	18	1	181.7	236.1	283.5	322.7	381.9	423.7	485.3
BRT1/14	*o*-CH_3	152.3	140.2	430.6	463.8	54	1	172.9	221.3	264.6	301.1	357.0	397.2	457.3
BRT1/15	*m*-CH_3	127.9	115.8	433.8	466.9	54	1	166.0	216.4	261.2	298.8	356.4	397.8	459.7
BRT1/16	*p*-CH_3	127.9	115.8	435.8	469.0	54	1	164.8	215.2	260.1	297.9	355.8	397.5	459.6
BRT1/17	*o*-CH_2CH_3	135.1	120.9	472.2	505.4	54	1	194.0	249.2	298.2	339.4	402.4	447.7	515.7
BRT1/18	*m*-CH_2CH_3	109.5	95.3	474.8	507.9	54	1	189.5	245.5	295.5	337.6	402.2	448.6	517.8
BRT1/19	*p*-CH_2CH_3	109.2	95.0	476.8	510.0	54	1	189.5	245.5	295.6	337.7	402.4	449.1	519.1
Subset 2: 3-phenyl-1-propen-3-yls (Radicals from Allylbenzenes)														
BRT2/1	H	259.8	246.4	376.5	376.5	1	1	139.7	183.7	220.8	250.8	294.9	325.5	370.3
BRT2/2	*o*-OH	81.4	68.7	404.0	404.0	1	1	166.8	210.1	246.1	275.1	317.6	347.1	390.8
BRT2/3	*m*-OH	76.1	63.4	406.4	406.4	1	1	162.1	206.9	244.6	274.6	317.9	347.6	391.2
BRT2/4	*p*-OH	79.9	67.2	405.2	405.2	1	1	160.6	206.4	244.3	274.4	317.9	347.7	391.4
BRT2/5	*o*-OCH_3	100.8	91.3	433.4	442.6	3	1	186.2	232.5	275.4	310.2	362.0	398.2	451.4
BRT2/6	*m*-OCH_3	96.8	87.3	441.8	450.9	3	1	181.3	231.6	274.1	308.7	360.1	396.2	449.7
BRT2/7	*p*-OCH_3	99.7	90.2	440.0	449.2	3	1	181.9	232.8	275.6	310.2	361.4	397.3	450.4
BRT2/8	*o*-CHO	142.7	134.0	416.2	416.2	1	1	172.1	218.7	260.6	295.0	343.0	375.7	419.9
BRT2/9	*m*-CHO	135.5	126.8	429.4	429.4	1	1	169.7	216.0	256.2	288.9	337.3	370.4	417.6
BRT2/10	*p*-CHO	131.4	122.7	425.5	425.5	1	1	168.6	217.4	259.3	293.1	342.3	375.4	421.0
BRT2/11	*o*-$CH=CH_2$	335.6	319.4	431.9	431.9	1	1	184.7	236.1	278.9	313.2	363.8	399.3	452.1
BRT2/12	*m*-$CH=CH_2$	326.9	310.7	435.4	435.4	1	1	177.3	230.0	274.5	310.4	363.2	399.8	453.6
BRT2/13	*p*-$CH=CH_2$	321.2	305.0	435.2	435.2	1	1	177.2	230.0	274.7	310.8	364.0	400.8	454.7
BRT2/14	*o*-CH_3	230.8	217.7	405.0	414.2	3	1	168.2	217.6	259.1	292.7	342.5	377.4	429.2
BRT2/15	*m*-CH_3	225.4	212.3	412.7	421.8	3	1	162.1	210.6	252.5	286.9	338.5	375.0	428.8
BRT2/16	*p*-CH_3	226.3	213.2	411.7	420.8	3	1	161.2	210.2	252.4	287.0	338.7	375.1	428.9
BRT2/17	*o*-CH_2CH_3	212.8	197.6	442.9	452.1	3	1	190.4	246.4	294.3	333.1	390.5	430.6	489.8
BRT2/18	*m*-CH_2CH_3	208.0	192.8	452.4	461.5	3	1	186.1	240.7	288.0	326.8	385.3	426.7	488.2
BRT2/19	*p*-CH_2CH_3	207.7	192.5	450.5	459.7	3	1	186.8	240.5	287.8	326.7	385.2	426.7	488.4
Subset 3: 3-phenyl-1-buten-3-yls (Radicals from α-Methyl allylbenzenes)														
BRT3/1	H	234.2	218.7	410.4	425.3	6	1	162.5	212.8	255.2	289.4	339.8	375.0	426.5
BRT3/2	*o*-OH	57.7	42.9	441.7	450.9	3	1	190.0	240.5	282.0	315.0	363.2	396.8	446.9
BRT3/3	*m*-OH	54.6	39.8	445.7	454.8	3	1	183.4	236.1	279.4	313.6	363.3	397.4	447.1
BRT3/4	*p*-OH	54.5	39.7	444.0	453.2	3	1	182.6	235.3	278.6	313.1	363.2	397.6	447.9
BRT3/5	*o*-OCH_3	85.9	74.3	477.1	495.4	9	1	211.1	266.2	313.0	351.2	408.2	448.1	506.7
BRT3/6	*m*-OCH_3	73.3	61.7	479.6	497.9	9	1	204.5	262.1	310.2	348.9	406.3	446.5	505.7
BRT3/7	*p*-OCH_3	74.1	62.5	481.5	499.8	9	1	205.4	262.6	310.5	349.2	406.7	447.0	506.6

BRT3/8	*o*-CHO	125.8	115.0	462.8	472.0	3	1	199.6	252.8	297.3	333.0	385.6	421.8	473.9
BRT3/9	*m*-CHO	108.9	98.1	469.5	478.6	3	1	190.9	245.0	290.7	327.8	382.4	419.9	473.2
BRT3/10	*p*-CHO	105.9	95.1	469.9	479.0	3	1	189.4	244.1	290.4	327.8	383.0	420.9	474.6
BRT3/11	*o*-CH=CH_2	313.9	295.6	472.6	481.7	3	1	204.0	263.1	312.1	351.0	408.0	447.7	507.2
BRT3/12	*m*-CH=CH_2	302.9	284.6	474.1	489.0	6	1	199.3	259.6	309.5	349.5	408.5	449.3	509.1
BRT3/13	*p*-CH=CH_2	296.5	278.2	475.2	484.4	3	1	198.7	258.7	309.4	350.1	410.0	451.3	511.2
BRT3/14	*o*-CH_3	217.5	202.3	448.6	466.9	9	1	187.5	239.7	285.3	323.2	380.7	421.6	483.1
BRT3/15	*m*-CH_3	200.6	185.4	457.8	476.1	9	1	184.9	239.9	287.2	325.8	383.7	424.4	484.4
BRT3/16	*p*-CH_3	201.2	186.0	458.1	476.3	9	1	184.2	239.7	287.3	326.2	384.3	425.3	485.5
BRT3/17	*o*-CH_2CH_3	198.2	180.9	488.8	507.1	9	1	212.2	269.4	320.3	362.8	427.4	473.6	542.8
BRT3/18	*m*-CH_2CH_3	182.3	165.0	492.3	510.5	9	1	209.6	270.3	322.6	365.6	430.1	475.8	543.4
BRT3/19	*p*-CH_2CH_3	182.8	165.5	494.9	513.1	9	1	207.8	269.4	322.3	365.6	430.7	476.6	544.7
Subset 4: 3-phenyl-1,4-pentadien-3yls (Radicals from α-Vinyl allylbenzenes)														
BRT4/1	H	318.5	299.9	439.1	444.9	2	1	181.4	232.0	275.6	311.3	364.2	400.9	453.4
BRT4/2	*o*-OH	126.0	108.1	450.8	456.6	2	1	208.3	256.5	302.0	338.0	389.3	424.0	474.4
BRT4/3	*m*-OH	137.2	119.3	467.1	472.9	2	1	202.4	254.9	299.2	334.7	386.6	422.1	473.3
BRT4/4	*p*-OH	139.9	122.0	463.3	469.1	2	1	201.7	254.3	298.8	334.6	387.1	423.0	474.3
BRT4/5	*o*-OCH_3	159.8	145.1	493.2	508.1	6	1	229.8	282.5	331.5	371.1	430.4	472.6	536.3
BRT4/6	*m*-OCH_3	156.5	141.8	497.5	512.4	6	1	222.7	280.6	329.7	369.6	429.0	470.7	531.5
BRT4/7	*p*-OCH_3	157.2	142.5	501.5	516.3	6	1	223.2	280.8	330.2	370.4	430.5	472.3	532.9
BRT4/8	*o*-CHO	189.4	175.5	471.8	471.8	1	1	206.5	264.6	312.9	351.6	408.3	447.3	504.0
BRT4/9	*m*-CHO	194.0	180.1	486.9	492.6	2	1	209.1	263.4	310.1	348.4	405.1	444.0	498.9
BRT4/10	*p*-CHO	195.7	181.8	487.8	493.6	2	1	207.3	261.9	309.2	348.1	405.7	445.2	500.0
BRT4/11	*o*-CH=CH_2	378.4	357.0	478.6	484.3	2	1	215.6	278.6	330.8	372.4	433.5	476.2	540.1
BRT4/12	*m*-CH=CH_2	387.7	366.3	496.3	502.0	2	1	218.4	278.0	329.0	370.4	431.6	474.0	535.5
BRT4/13	*p*-CH=CH_2	387.2	365.8	492.0	497.7	2	1	216.4	276.4	328.0	370.1	432.2	475.0	536.2
BRT4/14	*o*-CH_3	278.3	260.0	456.7	465.8	3	1	198.0	259.5	308.3	348.2	407.5	449.1	512.0
BRT4/15	*m*-CH_3	286.6	268.3	474.3	489.2	6	1	202.7	258.5	307.1	347.2	407.3	449.5	510.8
BRT4/16	*p*-CH_3	286.9	268.6	473.8	488.7	6	1	202.7	258.4	307.0	347.3	407.9	450.4	511.8
BRT4/17	*o*-CH_2CH_3	264.0	243.6	495.2	504.3	3	1	228.7	286.6	342.2	387.6	455.6	503.7	575.5
BRT4/18	*m*-CH_2CH_3	268.0	247.6	509.6	524.5	6	1	226.9	288.5	342.2	386.5	453.3	500.5	569.8
BRT4/19	*p*-CH_2CH_3	268.2	247.8	509.5	524.4	6	1	227.6	288.7	342.4	386.9	454.2	501.6	570.7
Subset 5: Diphenylmethyls (Radicals from diphenylmethane)														
BRT5/1	H	316.7	300.6	434.8	446.3	4	1	180.0	242.8	295.6	337.7	398.3	438.8	495.6
BRT5/2	*o*-OH	131.6	116.2	470.9	476.7	2	1	202.8	270.2	322.0	362.8	420.7	459.3	514.4
BRT5/3	*m*-OH	137.0	121.6	475.3	475.3	1	1	204.0	267.6	320.3	361.9	420.9	460.0	515.1
BRT5/4	*p*-OH	136.6	121.2	469.2	475.0	2	1	201.0	265.5	318.9	361.2	421.2	460.9	516.5
BRT5/5	*o*-OCH_3	156.4	144.1	493.7	508.6	6	1	227.8	298.5	357.5	404.3	470.6	514.6	576.8
BRT5/6	*m*-OCH_3	154.5	142.2	507.2	522.1	6	1	220.8	290.1	348.6	395.5	463.5	509.4	574.6
BRT5/7	*p*-OCH_3	154.6	142.3	513.0	522.1	3	1	220.8	290.1	348.6	395.5	463.5	509.4	574.5
BRT5/8	*o*-CHO	198.6	187.1	487.0	492.8	2	1	216.3	284.1	338.5	382.4	446.0	487.9	544.8
BRT5/9	*m*-CHO	191.8	180.3	491.2	497.0	2	1	208.6	274.8	330.6	375.4	439.8	482.4	541.2
BRT5/10	*p*-CHO	187.7	176.2	490.5	496.2	2	1	208.3	274.3	330.1	375.0	439.9	483.1	542.7
BRT5/11	*o*-CH=CH_2	391.2	372.2	497.9	503.6	2	1	226.6	295.3	353.4	400.1	469.8	513.9	577.2
BRT5/12	*m*-CH=CH_2	383.0	364.0	503.4	509.1	2	1	217.8	289.1	349.2	397.0	465.8	511.9	577.2
BRT5/13	*p*-CH=CH_2	378.3	359.3	501.4	507.2	2	1	218.0	289.2	349.4	397.6	467.1	513.6	579.1
BRT5/14	*o*-CH_3	287.1	271.2	479.6	494.5	6	1	211.7	274.7	330.7	376.3	442.9	488.2	553.0
BRT5/15	*m*-CH_3	283.3	267.4	481.6	496.5	6	1	201.9	269.5	327.2	373.8	441.6	487.4	552.7
BRT5/16	*p*-CH_3	283.3	267.4	481.0	495.9	6	1	201.8	269.4	327.1	373.8	441.9	488.2	553.8
BRT5/17	*o*-CH_2CH_3	267.0	249.0	511.2	526.1	6	1	234.5	305.2	366.3	416.1	489.3	539.5	611.9
BRT5/18	*m*-CH_2CH_3	264.8	246.8	518.5	533.4	6	1	226.6	299.8	362.6	413.4	487.6	538.3	611.1
BRT5/19	*p*-CH_2CH_3	265.0	247.0	520.0	534.8	6	1	226.5	299.7	362.5	413.5	488.2	539.2	612.5
Subset 6: 1,1-diphenylethyls (Radicals from diphenylethane)														
BRT6/1	H	292.4	273.8	473.0	493.6	12	1	206.9	272.5	328.4	373.5	439.3	484.4	549.9
BRT6/2	*o*-OH	107.0	89.1	500.6	515.5	6	1	228.4	293.2	352.6	399.8	466.7	510.9	573.7
BRT6/3	*m*-OH	111.7	93.8	508.7	523.6	6	1	229.2	296.5	352.7	397.3	461.7	505.6	569.9
BRT6/4	*p*-OH	111.3	93.4	509.6	524.5	6	1	223.2	292.5	350.3	396.3	462.2	506.7	571.2
BRT6/5	*o*-OCH_3	136.2	121.5	530.5	554.6	18	1	261.2	328.2	388.7	437.1	508.1	557.4	630.1
BRT6/6	*m*-OCH_3	130.4	115.7	541.2	565.2	18	1	250.2	322.3	383.0	431.9	503.8	553.9	627.9
BRT6/7	*p*-OCH_3	131.0	116.3	539.7	563.7	18	1	247.3	320.9	383.0	432.9	505.8	556.1	629.7
BRT6/8	*o*-CHO	178.2	164.3	527.8	542.7	6	1	238.4	306.4	364.8	412.4	482.4	530.0	597.5
BRT6/9	*m*-CHO	166.2	152.3	531.4	546.2	6	1	237.2	305.9	364.5	411.7	480.9	528.2	596.1
BRT6/10	*p*-CHO	162.3	148.4	528.2	543.0	6	1	237.2	306.4	365.2	412.7	482.2	529.6	597.5
BRT6/11	*o*-CH=CH_2	365.1	343.7	533.8	548.7	6	1	247.6	320.4	382.8	433.3	507.6	558.7	633.1
BRT6/12	*m*-CH=CH_2	357.9	336.5	536.5	551.4	6	1	246.1	319.4	381.8	432.2	505.9	556.9	631.8
BRT6/13	*p*-CH=CH_2	354.0	332.6	537.1	552.0	6	1	246.8	320.9	383.9	434.8	509.0	559.8	633.9
BRT6/14	*o*-CH_3	266.9	248.6	511.0	535.1	18	1	229.2	298.1	359.2	409.2	483.1	534.2	608.7

BRT6/15	*m*-CH_3	258.1	239.8	515.3	539.3	18	1	228.8	299.4	360.2	409.5	482.4	532.9	607.4
BRT6/16	*p*-CH_3	258.9	240.6	513.7	537.7	18	1	228.9	299.5	360.5	410.2	483.6	534.3	608.6
BRT6/17	*o*-CH_2CH_3	245.8	225.4	549.2	573.2	18	1	252.9	330.0	397.0	451.6	532.4	588.3	669.5
BRT6/18	*m*-CH_2CH_3	240.8	220.4	553.9	577.9	18	1	253.7	328.0	393.9	447.7	527.5	583.3	665.8
BRT6/19	*p*-CH_2CH_3	239.7	219.3	552.8	576.9	18	1	253.3	329.7	395.8	449.7	529.6	585.2	667.5

II. *Validation Set*

Table C-4 Thermochemical database used as the validation set for development of Group Additive Values (GAVs) and non-nearest neighbor interactions (NNIs) for benzylic radicals. The units of standard enthalpy of formation ($\Delta_f H^\circ$) data is given in kJ mol^{-1} whereas the units of entropies (S°) and heat capacities (C_p) are given in J mol^{-1} K^{-1}.

Radicals		$\Delta_f H°$ (298 K)		$S°$ (298 K)				C_p [J mol^{-1} K^{-1}]						
		$\Delta_f H^\circ_{CBSQB3}$	$\Delta_f H^\circ_{CBS-QB3+SOC+BAC}$	S°	S°_{int}	$\sigma_{tot^\circ sym}$	n_{opt}	**300 K**	**400 K**	**500 K**	**600 K**	**800 K**	**1000 K**	**1500 K**
Subset 1: Double Substituted 2-phenyl-2-propyls (Radicals from Isopropylbenzenes)														
BRV1/1	2-OH-4-OH	-185.8	-196.8	455.4	479.4	18	1	188.1	235.5	275.8	308.5	357.0	390.8	440.8
BRV1/2	2-OCH_3-4-CH_3	-19.8	-28.1	496.2	538.5	162	1	213.4	268.8	317.5	358.6	422.5	468.6	537.5
BRV1/3	2-CHO-5-CHO	-63.9	-67.0	489.3	513.4	18	1	212.8	262.2	305.7	342.3	397.8	436.6	491.7
BRV1/4	2-CHO-4-CH_3	22.6	15.1	478.5	511.7	54	1	203.3	255.2	301.2	339.9	399.2	441.3	503.2
BRV1/5	2-CH=CH_2-4-OH	67.3	52.7	481.8	505.8	18	1	216.9	270.5	316.0	352.9	407.8	446.5	504.2
BRV1/6	2-CH=CH_2-4-CH_3	213.6	198.6	489.5	522.7	54	1	217.8	274.6	324.3	365.7	428.7	473.8	541.6
BRV1/7	2-CH_3-4-OH	-27.4	-38.9	461.1	494.3	54	1	193.1	243.4	287.6	324.2	379.7	419.1	478.2
BRV1/8	2-CH_3-4-CH_3	118.8	106.9	466.6	508.9	162	1	194.1	247.6	296.0	337.1	400.8	446.8	515.9
BRV1/9	3-OH-4-CHO	-180.2	-187.2	452.4	476.5	18	1	185.9	237.5	282.2	319.3	375.0	414.1	471.1
BRV1/10	3-CH_3-4-CHO	-0.7	-8.2	482.4	515.5	54	1	202.9	253.1	299.1	338.3	399.0	442.5	506.3
BRV1/11	3-CH_3-4-CH=CH_2	190.9	175.9	486.3	519.5	54	1	208.1	266.4	317.7	360.5	426.1	473.0	543.0
Subset 2: Double Substituted 3-phenyl-1-propen-3-yls (Radicals from Allylbenzenes)														
BRV2/1	2-OH-4-CH=CH_2	142.3	126.7	460.8	460.8	1	1	206.4	260.1	305.0	340.9	392.5	427.5	477.8
BRV2/2	2-OH-6-OCH_3	-75.1	-84.0	465.2	474.3	3	1	205.6	257.0	299.5	333.4	384.2	419.2	469.1
BRV2/3	2-OH-5-CH_3	50.0	37.5	442.0	451.1	3	1	188.4	236.4	277.4	310.9	361.1	396.5	449.3
BRV2/4	2-CHO-4-CH_3	106.8	98.3	449.5	458.7	3	1	193.5	245.2	293.4	332.1	384.5	424.0	481.5
BRV2/5	2-CH=CH_2-4-CHO	203.9	192.3	475.2	475.2	1	1	213.2	269.9	317.7	356.1	412.0	449.7	502.9
BRV2/6	2-CH_3-4-CH=CH_2	291.3	275.3	458.2	467.4	3	1	206.6	263.4	314.4	354.7	414.6	458.1	516.5
Subset 3: Double Substituted 3-phenyl-1-buten-3-yls (Radicals from α-Methyl allylbenzenes)														
BRV3/1	2-OH-5-OH	-111.9	-126.0	480.1	489.2	3	1	215.1	265.5	306.3	338.6	385.8	418.6	467.2
BRV3/2	2-OCH_3-5-CH_3	52.0	40.6	512.2	539.6	27	1	230.7	291.9	344.6	387.8	452.4	497.8	565.0
BRV3/3	2-CHO-4-CH_3	91.9	81.3	496.7	515.0	9	1	215.8	274.2	324.5	365.7	426.9	469.3	531.1
BRV3/4	2-CH=CH_2-5-OH	135.1	117.4	501.1	510.2	3	1	231.3	289.1	336.9	375.0	431.1	470.4	529.5
BRV3/5	2-CH=CH_2-4-CHO	185.2	171.5	519.0	528.2	3	1	236.5	295.0	348.0	390.0	452.0	495.0	559.2
BRV3/6	2-CH_3-4-CH=CH_2	282.5	264.4	506.7	525.0	9	1	231.0	291.2	343.4	386.6	452.0	498.5	567.6
BRV3/7	3-CH_3-4-CH=CH_2	268.4	250.3	508.9	527.2	9	1	227.2	290.8	344.9	389.0	454.7	500.7	568.6
BRV3/8	2-CH_3-4-CH_3	184.1	169.1	484.7	512.1	27	1	209.3	266.5	317.1	359.5	424.5	471.2	541.6
BRV3/9	2-OH-5-OCH_3	-93.3	-104.3	507.3	525.6	9	1	236.0	291.6	337.5	374.5	429.6	468.4	526.2
BRV3/10	2-OH-4-CHO	-72.7	-82.8	488.9	498.1	3	1	219.5	272.9	317.5	353.5	406.4	442.8	494.6
BRV3/11	2-OH-4-CH_3	26.2	11.6	481.7	500.0	9	1	213.2	268.3	315.5	352.9	408.2	449.3	509.4
BRV3/12	2-OH-5-CHO	-69.4	-79.5	489.9	499.1	3	1	218.9	272.9	317.7	353.9	407.3	443.9	495.9
Subset 4: Double Substituted 3-phenyl-1,4-pentadien-3yls (Radicals from α-Vinyl allylbenzenes)														
BRV4/1	2-OH-4-CH=CH_2	198.4	177.6	510.8	516.5	2	1	242.3	301.3	354.3	396.6	456.8	498.8	558.3
BRV4/2	2-OH-4-CH_3	97.7	80.0	489.7	504.6	6	1	228.0	281.2	332.7	373.9	433.3	474.7	533.7
BRV4/3	2-OCH_3-4-OH	-22.3	-36.4	520.3	535.2	6	1	250.5	304.7	354.6	394.2	452.5	493.7	556.4
BRV4/4	2-OCH_3-4-CH_3	126.8	112.3	531.2	549.5	9	1	252.7	310.6	364.0	407.8	474.8	523.4	596.3
BRV4/5	2-CHO-5-CH=CH_2	255.9	239.1	528.1	528.1	1	1	243.5	310.2	366.1	411.0	476.8	522.0	587.7
BRV4/6	2-CH=CH_2-5-OH	199.8	179.0	508.2	508.2	1	1	237.4	302.0	354.8	396.5	456.8	498.7	561.4
BRV4/7	2-CH=CH_2-4-CH_3	354.2	333.0	515.1	524.2	3	1	237.3	305.3	362.4	408.6	477.3	525.7	598.6
BRV4/8	2-CH_3-4-CH_3	242.7	224.6	495.0	513.3	9	1	219.3	283.5	338.4	383.4	450.9	499.0	570.9
Subset 5: Double Substituted Diphenylmethyls (Radicals from diphenylmethane)														

BRV5/1	2-OH-4-CHO	2.9	-7.9	516.8	522.6	2	1	239.2	305.0	361.0	405.0	468.6	509.4	564.6
BRV5/2	2-OH-5-CH=CH_2	197.4	179.1	529.0	534.7	2	1	242.0	313.0	375.0	423.0	494.3	537.6	599.3
BRV5/3	2-OH-4-CH_3	102.3	87.1	504.7	519.6	6	1	228.6	295.9	352.7	398.2	464.0	508.5	572.7
BRV5/4	2-OCH_3-4-CH_3	122.2	110.1	529.5	553.5	18	1	249.8	325.3	389.2	440.5	514.4	564.1	635.1
BRV5/5	2-CHO-4-CH_3	163.1	151.8	524.5	539.4	6	1	236.8	306.9	366.6	415.1	486.1	534.6	603.5
BRV5/6	2-CH=CH_2-4-CH_3	357.2	338.4	534.5	549.4	6	1	244.3	323.0	386.0	437.0	513.4	563.0	635.3
BRV5/7	2-CH_3-4-CH=CH_2	347.9	329.1	533.7	548.6	6	1	249.1	323.0	387.0	439.0	515.0	566.9	635.4
BRV5/8	2-CH_3-4-CH_3	253.5	237.8	507.6	531.7	18	1	232.0	303.5	365.7	416.5	490.4	540.5	612.4
BRV5/9	3-CH_3-4-CHO	158.8	147.5	521.6	536.5	6	1	235.7	305.4	365.0	413.5	484.7	532.8	600.3
BRV5/10	3-CH_3-4-CH=CH_2	349.4	330.6	530.2	545.1	6	1	245.6	321.1	385.0	436.5	511.5	562.6	636.1
Subset 6: Double Substituted 1,1-diphenylethyls (Radicals from diphenylethane)														
BRV6/1	2-OH-4-CH_3	74.5	57.2	537.7	561.8	18	1	253.0	327.3	388.3	437.8	508.0	561.2	632.8
BRV6/2	2-OH-4-OH	-72.9	-89.7	523.3	547.3	18	1	255.0	324.6	382.2	427.7	492.2	534.8	595.6
BRV6/3	2-OCH_3-4-CH=CH_2	197.7	180.4	591.9	615.9	18	1	293.8	373.2	441.0	494.8	575.4	630.9	711.8
BRV6/4	2-CHO-4-CH_3	142.2	128.8	560.9	584.9	18	1	265.9	337.8	400.1	451.3	527.4	580.0	655.9
BRV6/5	2-CH=CH_2-4-CH_3	333.0	312.1	567.2	591.2	18	1	273.0	352.0	420.7	475.3	556.6	611.8	693.2
BRV6/6	3-CH_3-4-CH=CH_2	324.1	303.2	566.9	590.9	18	1	271.3	350.7	418.0	472.4	552.7	608.5	691.2
BRV6/7	2-CH_3-4-CH_3	235.4	217.6	549.6	582.7	54	1	255.9	330.4	395.5	449.2	529.4	585.4	667.9

C.4 Group Additive Based Parameter Development for Toluene Derivatives

C.4.1 Preliminary GAVs and Identification of NNIs

Table C-5 Preliminary GAVs assignments for specific groups used in the description of different toluene derivative classes. Note that the uncertainties are the same for all groups, as each of these GAVs are derived from the same number of molecules.

GAVs	$\Delta_f H^\circ$ [kJ mol^{-1}]	S° [J mol^{-1}K^{-1}]	C_p [J mol^{-1} K^{-1}]						
			300 K	400 K	500 K	600 K	800 K	1000 K	1500 K
C-(C$_b$)(C)$_2$(H)	-2.5 ± 1.19	-52.0 ± 2.62	24.9 ± 1.46	31.0 ± 1.41	35.4 ± 1.42	38.4 ± 1.42	42.5 ± 1.37	45.2 ± 1.25	48.1 ± 0.98
C-(C$_b$)(C$_d$)(H)$_2$	-19.0 ± 1.19	35.3 ± 2.62	26.1 ± 1.46	32.9 ± 1.41	38.2 ± 1.42	42.3 ± 1.42	48.6 ± 1.37	53.3 ± 1.25	59.4 ± 0.98
C-(C$_b$)(C$_d$)(C)(H)	-2.2 ± 1.19	-64.2 ± 2.62	26.4 ± 1.46	33.4 ± 1.41	37.9 ± 1.42	40.9 ± 1.42	44.5 ± 1.37	46.4 ± 1.25	47.5 ± 0.98
C-(C$_b$)(C$_d$)$_2$(H)	-0.5 ± 1.19	-62.1 ± 2.62	31.5 ± 1.46	37.9 ± 1.41	41.0 ± 1.42	42.8 ± 1.42	44.6 ± 1.37	45.7 ± 1.25	46.2 ± 0.98
C-(C$_b$)$_2$(H)$_2$	-22.2 ± 1.19	39.4 ± 2.62	23.5 ± 1.46	29.8 ± 1.41	35.2 ± 1.42	39.3 ± 1.42	45.4 ± 1.37	50.1 ± 1.25	55.5 ± 0.98
C-(C$_b$)$_2$(C)(H)	-5.7 ± 1.19	-60.0 ± 2.62	25.9 ± 1.46	31.3 ± 1.41	35.2 ± 1.42	37.6 ± 1.42	40.2 ± 1.37	41.9 ± 1.25	42.4 ± 0.98

Table C-6 Deviations between data obtained from group additivity and *ab initio* calculations, where group additive data is calculated based on the preliminary GAVs given in **Table C-5**.[a]

Molecule #		$\Delta_f H^\circ$ [kJ mol^{-1}]			S° [J mol^{-1} K^{-1}]			C_p [J mol^{-1} K^{-1}]		
		Reference Data	GA	GA-Reference Data[a]	Reference Data	GA	GA-Reference Data[a]	Reference Data	GA	GA-Reference Data[a]
1	TDT1/1	3.4	3.7	0.3	412.5	411.5	-1.0	153.4	152.8	-0.6
2	TDT1/2	-177.7	-174.1	3.6	440.2	439.2	-1.0	177.2	176.2	-1.0
3	TDT1/3	-176.3	-174.1	2.2	441.7	439.3	-2.4	174.4	176.2	1.8
4	TDT1/4	-174.9	-174.1	0.8	441.8	439.2	-2.6	174.4	176.2	1.8
5	TDT1/5	-153.3	-153.1	0.3	482.7	481.7	-1.0	195.9	197.2	1.3
6	TDT1/6	-152.5	-153.1	-0.5	484.3	481.7	-2.6	195.9	197.2	1.3
7	TDT1/7	-151.2	-153.1	-1.8	485.1	481.6	-3.4	195.9	197.2	1.3
8	TDT1/8	-109.4	-116.9	-7.4	456.6	458.8	2.2	184.7	183.3	-1.5
9	TDT1/9	-118.4	-116.9	1.6	457.8	458.8	1.0	181.9	183.2	1.3
10	TDT1/10	-118.8	-116.9	2.0	458.2	458.8	0.6	181.8	183.2	1.4
11	TDT1/11	74.5	69.7	-4.7	463.2	469.5	6.3	192.2	190.7	-1.6
12	TDT1/12	67.4	69.7	2.4	471.8	469.5	-2.3	191.3	190.6	-0.7
13	TDT1/13	67.4	69.7	2.4	472.4	469.5	-2.9	191.7	190.6	-1.1
14	TDT1/14	-27.2	-29.5	-2.2	446.8	456.6	9.8	177.6	175.3	-2.3
15	TDT1/15	-30.9	-29.5	1.5	457.3	456.6	-0.7	174.7	175.4	0.6
16	TDT1/16	-30.7	-29.5	1.3	458.8	456.5	-2.2	175.1	175.3	0.2

17	**TDT1/17**	-46.2	-50.1	-3.8	486.4	495.1	8.7	205.1	200.6	-4.6
18	**TDT1/18**	-51.4	-50.1	1.4	498.1	495.1	-3.0	200.0	200.5	0.5
19	**TDT1/19**	-51.2	-50.1	1.2	498.5	495.1	-3.4	199.6	200.6	0.9
20	**TDT2/1**	134.5	135.2	0.7	394.1	393.5	-0.7	142.0	142.4	0.4
21	**TDT2/2**	-52.3	-42.6	9.7	398.4	421.1	22.7	172.6	165.8	-6.8
22	**TDT2/3**	-46.4	-42.6	3.8	426.3	421.1	-5.2	164.7	165.8	1.1
23	**TDT2/4**	-43.3	-42.6	0.7	423.4	421.2	-2.3	163.8	165.8	2.0
24	**TDT2/5**	-21.5	-21.6	0.0	460.8	463.5	2.7	184.9	186.8	1.9
25	**TDT2/6**	-19.8	-21.6	-1.7	467.6	463.6	-4.1	185.9	186.8	0.9
26	**TDT2/7**	-18.9	-21.6	-2.6	467.1	463.5	-3.6	184.8	186.8	2.0
27	**TDT2/8**	20.9	14.6	-6.2	439.5	440.6	1.1	176.7	172.8	-3.9
28	**TDT2/9**	15.4	14.6	-0.7	447.9	440.6	-7.3	171.8	172.8	1.0
29	**TDT2/10**	14.4	14.6	0.3	447.5	440.6	-6.9	170.9	172.8	1.9
30	**TDT2/11**	202.6	201.2	-1.3	448.1	451.3	3.2	186.8	180.2	-6.6
31	**TDT2/12**	199.6	201.2	1.7	452.2	451.3	-0.9	179.5	180.2	0.7
32	**TDT2/13**	199.4	201.2	1.9	452.4	451.4	-1.1	179.4	180.2	0.8
33	**TDT2/14**	104.7	102.0	-2.6	433.5	438.4	4.9	167.2	164.9	-2.3
34	**TDT2/15**	101.8	102.0	0.3	439.6	438.4	-1.2	163.6	164.9	1.3
35	**TDT2/16**	102.1	102.0	0.0	439.5	438.4	-1.1	163.5	164.8	1.4
36	**TDT2/17**	85.2	81.4	-3.7	472.8	476.9	4.1	189.5	190.1	0.6
37	**TDT2/18**	81.1	81.4	0.4	479.3	476.9	-2.4	188.3	190.1	1.8
38	**TDT2/19**	81.6	81.4	-0.1	479.3	476.9	-2.4	188.2	190.1	1.9
39	**TDT3/1**	107.6	109.1	1.5	421.6	421.0	-0.6	167.4	168.0	0.6
40	**TDT3/2**	-71.1	-68.7	2.4	442.4	448.7	6.3	197.0	191.4	-5.6
41	**TDT3/3**	-70.6	-68.7	1.9	452.0	448.6	-3.3	188.7	191.4	2.7
42	**TDT3/4**	-69.5	-68.7	0.8	451.3	448.7	-2.6	188.9	191.4	2.5
43	**TDT3/5**	-48.1	-47.7	0.5	482.6	491.1	8.5	214.6	212.4	-2.2
44	**TDT3/6**	-47.0	-47.7	-0.6	494.1	491.0	-3.0	209.8	212.4	2.6
45	**TDT3/7**	-46.1	-47.7	-1.5	496.7	491.1	-5.6	209.6	212.4	2.8
46	**TDT3/8**	-5.1	-11.5	-6.3	461.6	468.1	6.6	205.4	198.4	-7.0
47	**TDT3/9**	-12.2	-11.5	0.8	475.6	468.2	-7.4	197.4	198.4	1.0
48	**TDT3/10**	-13.0	-11.5	1.6	473.4	468.1	-5.2	195.6	198.4	2.8
49	**TDT3/11**	179.4	175.1	-4.2	473.1	478.8	5.8	211.2	205.8	-5.4
50	**TDT3/12**	172.5	175.1	2.7	480.4	478.9	-1.5	204.7	205.8	1.1
51	**TDT3/13**	172.5	175.1	2.7	485.7	478.8	-6.8	204.9	205.8	0.9
52	**TDT3/14**	79.0	75.9	-3.0	457.9	466.0	8.1	192.8	190.5	-2.3
53	**TDT3/15**	74.9	75.9	1.1	466.8	466.0	-0.8	189.6	190.5	0.9
54	**TDT3/16**	74.5	75.9	1.5	467.0	465.9	-1.0	189.0	190.5	1.5
55	**TDT3/17**	58.3	55.3	-2.9	494.7	504.5	9.8	216.8	215.7	-1.1
56	**TDT3/18**	54.4	55.3	1.0	507.4	504.5	-2.9	213.7	215.8	2.0
57	**TDT3/19**	54.5	55.3	0.9	508.3	504.4	-3.8	213.6	215.7	2.1

58	**TDT4/1**	215.2	215.9	0.7	446.9	444.8	-2.2	186.7	186.8	0.1
59	**TDT4/2**	33.9	38.1	4.2	459.6	472.5	12.8	206.8	210.2	3.4
60	**TDT4/3**	36.8	38.1	1.3	475.6	472.4	-3.2	209.3	210.2	0.9
61	**TDT4/4**	37.9	38.1	0.2	475.9	472.4	-3.5	207.9	210.2	2.3
62	**TDT4/5**	59.9	59.1	-0.7	508.3	514.8	6.5	234.1	231.2	-2.9
63	**TDT4/6**	59.7	59.1	-0.5	518.8	514.9	-4.0	230.1	231.2	1.1
64	**TDT4/7**	59.2	59.1	0.0	520.8	514.8	-6.0	226.3	231.2	4.9
65	**TDT4/8**	102.3	95.4	-6.9	483.9	491.9	8.0	225.5	217.2	-8.3
66	**TDT4/9**	95.2	95.4	0.2	497.7	492.0	-5.8	213.1	217.2	4.1
67	**TDT4/10**	95.3	95.4	0.1	499.3	491.9	-7.4	215.5	217.2	1.7
68	**TDT4/11**	285.1	281.9	-3.1	497.0	502.6	5.6	234.0	224.6	-9.4
69	**TDT4/12**	277.0	281.9	5.0	505.5	502.6	-2.9	223.9	224.6	0.7
70	**TDT4/13**	280.3	281.9	1.7	504.3	502.7	-1.7	223.9	224.6	0.7
71	**TDT4/14**	183.1	182.7	-0.3	479.4	489.7	10.3	212.8	209.3	-3.5
72	**TDT4/15**	182.5	182.7	0.3	492.1	489.7	-2.4	208.6	209.3	0.7
73	**TDT4/16**	182.8	182.7	0.0	491.7	489.8	-2.0	208.1	209.3	1.2
74	**TDT4/17**	164.8	162.1	-2.6	520.4	528.2	7.8	235.0	234.5	-0.5
75	**TDT4/18**	161.7	162.1	0.5	532.2	528.2	-4.0	233.3	234.5	1.2
76	**TDT4/19**	162.0	162.1	0.2	535.0	528.2	-6.8	232.8	234.5	1.7
77	**TDT5/1**	162.0	161.8	-0.2	458.7	458.2	-0.5	177.6	178.1	0.5
78	**TDT5/2**	-18.6	-16.0	2.6	483.5	486.0	2.4	203.4	201.5	-1.9
79	**TDT5/3**	-17.5	-16.0	1.5	488.8	485.9	-2.9	198.4	201.6	3.1
80	**TDT5/4**	-16.2	-16.0	0.2	488.9	485.9	-3.0	198.6	201.6	2.9
81	**TDT5/5**	3.9	5.2	1.2	523.1	528.3	5.2	222.6	222.5	-0.1
82	**TDT5/6**	6.9	5.2	-1.8	531.7	528.4	-3.4	220.4	222.5	2.1
83	**TDT5/7**	7.6	5.2	-2.5	533.1	528.3	-4.8	220.1	222.5	2.4
84	**TDT5/8**	46.9	41.4	-5.6	500.9	505.4	4.5	216.7	208.5	-8.2
85	**TDT5/9**	40.4	41.4	0.9	513.0	505.5	-7.6	206.8	208.5	1.7
86	**TDT5/10**	40.3	41.4	1.0	511.0	505.4	-5.6	206.2	208.6	2.3
87	**TDT5/11**	229.7	228.0	-1.8	507.1	516.1	9.0	225.4	215.9	-9.5
88	**TDT5/12**	226.0	228.0	1.9	517.5	516.1	-1.4	214.7	216.0	1.2
89	**TDT5/13**	226.5	228.0	1.4	516.2	516.1	-0.1	214.9	215.9	1.0
90	**TDT5/14**	128.0	128.7	0.7	497.0	503.3	6.2	204.7	200.7	-4.1
91	**TDT5/15**	128.6	128.8	0.1	504.7	503.3	-1.5	199.2	200.6	1.4
92	**TDT5/16**	128.5	128.8	0.2	504.4	503.2	-1.2	199.0	200.7	1.6
93	**TDT5/17**	109.9	108.2	-1.8	531.7	541.7	10.0	226.8	225.9	-1.0
94	**TDT5/18**	107.2	108.2	0.9	544.6	541.8	-2.9	223.9	225.8	1.9
95	**TDT5/19**	107.9	108.2	0.2	545.0	541.7	-3.3	223.8	225.8	2.0
96	**TDT6/1**	135.1	135.4	0.3	492.6	485.9	-6.7	205.6	205.8	0.2
97	**TDT6/2**	-44.6	-42.4	2.2	505.3	513.6	8.3	236.7	229.2	-7.5
98	**TDT6/3**	-44.6	-42.4	2.2	518.8	513.6	-5.2	224.7	229.2	4.5

99	**TDT6/4**	-42.0	-42.4	-0.4	517.2	513.6	-3.6	226.4	229.3	2.8
100	**TDT6/5**	-23.5	-21.2	2.2	545.6	556.0	10.4	253.3	250.2	-3.1
101	**TDT6/6**	-19.2	-21.2	-2.1	559.4	556.0	-3.4	248.4	250.3	1.8
102	**TDT6/7**	-18.6	-21.2	-2.7	562.3	556.0	-6.3	247.3	250.3	2.9
103	**TDT6/8**	21.5	15.0	-6.6	523.1	533.0	10.0	244.5	236.2	-8.3
104	**TDT6/9**	14.3	15.0	0.6	535.4	533.1	-2.3	233.6	236.2	2.6
105	**TDT6/10**	14.5	15.0	0.4	537.6	533.1	-4.5	234.0	236.2	2.2
106	**TDT6/11**	201.0	201.6	0.5	538.5	543.8	5.3	246.5	243.6	-2.9
107	**TDT6/12**	199.8	201.6	1.7	546.3	543.8	-2.5	242.1	243.7	1.5
108	**TDT6/13**	200.4	201.6	1.1	545.7	543.8	-1.9	242.3	243.7	1.3
109	**TDT6/14**	101.0	102.4	1.3	524.2	530.9	6.7	233.1	228.3	-4.8
110	**TDT6/15**	101.7	102.4	0.6	534.4	530.9	-3.5	225.4	228.3	2.9
111	**TDT6/16**	100.5	102.4	1.8	536.2	530.9	-5.3	225.8	228.3	2.5
112	**TDT6/17**	86.0	81.8	-4.3	557.0	569.3	12.4	256.8	253.6	-3.3
113	**TDT6/18**	81.1	81.8	0.6	572.6	569.4	-3.2	251.6	253.6	1.9
114	**TDT6/19**	81.9	81.8	-0.2	573.7	569.3	-4.3	251.5	253.5	2.0

[a]**GA- Reference Data**: If the absolute value of this difference is significantly high regardless of its sign, it points out to the need of a NNI correction. A positive difference shows that the *ab initio* data for that specific molecule is lower than the group additively calculated data, which means that a negative correction is needed and vice versa.

C.4.2 Initial simultaneous optimization of GAVs and NNIs

Table C-7 Comparison of the differences between the reference dataset and the group additively calculated data for unsubstituted and substituted isopropylbenzenes with the previously reported NNIs for toluenes/ethylbenzenes.

Substituents on isopropylbenzene	$\Delta_f H^\circ$ [kJ mol^{-1}]		S° [J mol^{-1} K^{-1}]	
	CBS-GAV[a]	NNI[b]	CBS-GAV[a]	NNI[b]
***o*-CHO**	7.4	8.1	-2.2	-2.4
***o*-CH=CH$_2$**	4.7	4.6	-6.3	-5.7
***o*-CH$_3$**	2.2	4.4	-9.8	-6.6
***o*-CH$_2$CH$_3$**	3.8	4.4	-8.7	-6.6

[a]**Reference Data-GA**: The differences are given in the form of "**–(GA-Reference Data)**" to be able to compare these differences with the reported non-nearest neighbor interaction corrections.
[b]The NNIs are taken from **Chapter 3**.

Table C-8 NNI parameters used to correct for the interactions between two substituent groups, taken from **Chapter 3**.

Interaction[a]	$\Delta_f H^\circ$ [kJ mol^{-1}]	S° [J mol^{-1} K^{-1}]	C_p [J mol^{-1} K^{-1}]						
			300 K	400 K	500 K	600 K	800 K	1000 K	1500 K
o-CH$_3$/CH$_2$CH$_3$ + CHO	8.1	-2.4	4.0	3.0	2.0	1.1	0.0	-0.6	-0.9
o-CH$_3$/CH$_2$CH$_3$ + CH=CH$_2$	4.6	-5.7	5.7	5.6	4.9	4.2	2.9	2.1	1.0
o-CH$_3$/CH$_2$CH$_3$ + CH$_3$/CH$_2$CH$_3$	4.2	-6.6	3.3	2.9	2.6	2.5	2.3	2	1.5
o-OH + CHO	-27.4	-21.3	-10.4	-9.0	-7.4	-6.0	-3.4	-1.4	1.8
o-CHO + CHO	4.0	-2.4	4.0	3.0	2.0	1.1	0.0	-0.9	-0.9
p-CHO + CHO	9.9	-0.8	1.8	1.4	1.0	0.7	0.1	-0.3	-0.9
p-OH/OCH$_3$ + OH/OCH$_3$	7.3	4.0	1.7	0.4	-0.8	-1.7	-2.3	-2.3	-1.7
p-OH/OCH$_3$ + CHO	-4.6	-0.8	-1.6	-1.0	-0.3	0.2	0.9	1.2	1.5

[a]The interactions between two substituents are given in the following format: **a-X + Y** where **a-** reflects the relative positioning of the two substituents, which can be *ortho* (*o*-), *meta* (*m*-) or *para* (*p*-), **X** and **Y** are the two substituent groups separated by a plus sign (+).

Table C-9 GAVs obtained from the simultaneous optimization of GAVs and NNIs using the training set of toluene derivative classes.

GAVs	$\Delta_f H^\circ$ [kJ mol^{-1}]	S° [J mol^{-1}K^{-1}]	C_p [J mol^{-1}K^{-1}]						
			300 K	400 K	500 K	600 K	800 K	1000 K	1500 K
C-(C$_b$)(C)$_2$(H)	-3.6 ± 0.74	-50.9 ± 1.03	24.1 ± 0.79	30.3 ± 0.71	34.7 ± 0.62	37.8 ± 0.58	42.1 ± 0.55	44.9 ± 0.57	48 ± 0.54
C-(C$_b$)(C$_d$)(H)$_2$	-19.3 ± 0.79	39.5 ± 1.09	24.1 ± 0.85	31.1 ± 0.76	36.3 ± 0.66	40.6 ± 0.61	47 ± 0.59	51.9 ± 0.60	58.5 ± 0.57
C-(C$_b$)(C$_d$)(C)(H)	-2.9 ± 0.78	-61 ± 1.08	24.5 ± 0.83	31.8 ± 0.75	36.4 ± 0.65	39.5 ± 0.60	43.2 ± 0.58	45.3 ± 0.59	46.7 ± 0.56
C-(C$_b$)(C$_d$)$_2$(H)	-1.1 ± 0.79	-58.5 ± 1.09	30 ± 0.85	36.1 ± 0.76	39 ± 0.66	40.7 ± 0.61	42.6 ± 0.59	43.9 ± 0.6	44.9 ± 0.57
C-(C$_b$)$_2$(H)$_2$	-22.8 ± 0.78	42.6 ± 1.08	21.7 ± 0.83	28.1 ± 0.75	33.7 ± 0.65	37.9 ± 0.60	44.1 ± 0.58	49 ± 0.59	54.7 ± 0.56
C-(C$_b$)$_2$(C)(H)	-6.3 ± 0.78	-56.8 ± 1.08	24.1 ± 0.83	29.5 ± 0.75	33.5 ± 0.65	36 ± 0.60	38.7 ± 0.58	40.7 ± 0.59	41.4 ± 0.56

Table C-10 NNIs values obtained from the simultaneous optimization of GAVs and NNIs using the training set of toluene derivative classes.

NNIs	$\Delta_f H^\circ$ [kJ mol^{-1}]	S° [J mol^{-1}K^{-1}]	C_p [J mol^{-1}K^{-1}]						
			300 K	400 K	500 K	600 K	800 K	1000 K	1500 K
NNITD1	-9.4 ± 3.32	-26.9 ± 4.61	8.8 ± 3.56	7.7 ± 3.19	10.1 ± 2.76	9.5 ± 2.58	9.8 ± 2.49	8.4 ± 2.54	5.4 ± 2.41
NNITD2	-1.8 ± 1.93	-8.9 ± 2.67	6.8 ± 2.07	5.8 ± 1.85	4.8 ± 1.60	4.2 ± 1.50	3.7 ± 1.44	3.5 ± 1.47	3.2 ± 1.4
NNITD3	-3.6 ± 3.32	-16.4 ± 4.61	-2.0 ± 3.56	10.5 ± 3.19	15.9 ± 2.76	18.8 ± 2.58	19.5 ± 2.49	17.8 ± 2.54	13.8 ± 2.41
NNITD4	-0.1 ± 1.51	-10.1 ± 2.08	3.1 ± 1.61	3.6 ± 1.44	4.2 ± 1.25	4.6 ± 1.16	5.0 ± 1.12	5.0 ± 1.14	4.2 ± 1.09
NNITD5	3.6 ± 0.83	-10.5 ± 1.14	6.4 ± 0.89	5.6 ± 0.79	5.1 ± 0.69	4.7 ± 0.64	3.8 ± 0.62	3.3 ± 0.63	1.9 ± 0.6

Table C-11 Deviations between the training set data obtained from group additivity and *ab initio* calculations before and after the inclusion of newly derived NNI parameters, where group additive data is calculated based on the simultaneously optimized GAVs and NNIs given in **Table C-9** and **Table C-10**, respectively.

Molecule #		$\Delta_f H^\circ$ [kJ mol^{-1}]					S° [J mol^{-1}K^{-1}]					C_p [J mol^{-1}K^{-1}]				
		CBS[a]	Bef. new NNIs[b]	Af. new NNIs[c]	Δ(Bef. new NNIs)[d]	Δ(Af. new NNIs)[e]	CBS[a]	Bef. new NNIs[b]	Af. new NNIs[c]	Δ(Bef. new NNIs)[d]	Δ(Af. new NNIs)[e]	CBS[a]	Bef. new NNIs[b]	Af. new NNIs[c]	Δ(Bef. new NNIs)[d]	Δ(Af. new NNIs)[e]
1	**TDT1/1**	3.4	2.5	2.5	0.3	-0.8	412.5	412.7	412.7	-0.9	0.2	153.4	152.0	152.0	-0.6	-1.4
2	**TDT1/2**	-177.7	-175.3	-175.3	3.6	2.5	440.2	440.4	440.4	-0.9	0.2	177.2	175.4	175.4	-1.0	-1.8
3	**TDT1/3**	-176.3	-175.3	-175.3	2.2	1.1	441.7	440.4	440.4	-2.4	-1.3	174.4	175.4	175.4	1.8	1.0
4	**TDT1/4**	-174.9	-175.3	-175.3	0.8	-0.3	441.8	440.4	440.4	-2.5	-1.4	174.4	175.4	175.4	1.8	1.0
5	**TDT1/5**	-153.3	-154.2	-154.2	0.3	-0.8	482.7	482.8	482.8	-1.0	0.1	195.9	196.4	196.4	1.3	0.5
6	**TDT1/6**	-152.5	-154.2	-154.2	-0.5	-1.6	484.3	482.8	482.8	-2.6	-1.5	195.8	196.4	196.4	1.4	0.6
7	**TDT1/7**	-151.2	-154.2	-154.2	-1.8	-2.9	485.1	482.8	482.8	-3.4	-2.3	195.9	196.4	196.4	1.3	0.5
8	**TDT1/8**	-109.4	-118.0	-109.9	-7.4	-0.4	456.6	459.9	457.5	2.2	0.9	184.7	182.4	186.4	-1.5	1.7
9	**TDT1/9**	-118.4	-118.0	-118.0	1.6	0.5	457.8	459.9	459.9	1.0	2.1	181.9	182.4	182.4	1.3	0.5
10	**TDT1/10**	-118.8	-118.0	-118.0	2.0	0.9	458.2	459.9	459.9	0.6	1.7	181.8	182.4	182.4	1.4	0.6
11	**TDT1/11**	74.5	68.6	73.2	-4.7	-1.2	463.2	470.6	464.9	6.3	1.7	192.2	189.8	195.5	-1.6	3.3
12	**TDT1/12**	67.4	68.6	68.6	2.4	1.3	471.8	470.6	470.6	-2.3	-1.2	191.3	189.8	189.8	-0.7	-1.5
13	**TDT1/13**	67.4	68.6	68.6	2.4	1.3	472.4	470.6	470.6	-2.9	-1.8	191.7	189.8	189.8	-1.1	-1.9
14	**TDT1/14**	-27.2	-30.5	-26.3	-2.2	0.9	446.8	457.7	451.1	9.8	4.3	177.6	174.5	177.8	-2.3	0.2
15	**TDT1/15**	-30.9	-30.5	-30.5	1.5	0.4	457.3	457.7	457.7	-0.7	0.4	174.7	174.5	174.5	0.6	-0.2
16	**TDT1/16**	-30.7	-30.5	-30.5	1.3	0.2	458.8	457.7	457.7	-2.2	-1.1	175.1	174.5	174.5	0.2	-0.6
17	**TDT1/17**	-46.2	-51.1	-46.9	-3.8	-0.7	486.4	496.2	489.6	8.7	3.2	205.1	199.7	203.0	-4.6	-2.1
18	**TDT1/18**	-51.4	-51.1	-51.1	1.4	0.3	498.1	496.2	496.2	-3.0	-1.9	200.0	199.7	199.7	0.5	-0.3
19	**TDT1/19**	-51.2	-51.1	-51.1	1.2	0.1	498.5	496.2	496.2	-3.4	-2.3	199.6	199.7	199.7	0.9	0.1
20	**TDT2/1**	134.5	134.9	134.9	0.7	0.4	394.1	397.6	397.6	-0.7	3.5	142.0	140.4	140.4	0.4	-1.6
21	**TDT2/2**	-52.3	-42.9	-52.3	9.7	0.0	398.4	425.3	398.4	22.7	0.0	172.6	163.8	172.6	-6.8	0.0
22	**TDT2/3**	-46.4	-42.9	-42.9	3.8	3.5	426.3	425.3	425.3	-5.2	-1.0	164.7	163.8	163.8	1.1	-0.9
23	**TDT2/4**	-43.3	-42.9	-42.9	0.7	0.4	423.4	425.3	425.3	-2.3	1.9	163.8	163.8	163.8	2.0	0.0

24	**TDT2/5**	-21.5	-21.8	-21.9	0.0	-0.4	460.8	467.7	457.5	2.7	-3.3	184.9	184.8	187.9	1.9	3.0
25	**TDT2/6**	-19.8	-21.8	-21.8	-1.7	-2.0	467.6	467.7	467.7	-4.1	0.1	185.9	184.8	184.8	0.9	-1.1
26	**TDT2/7**	-18.9	-21.8	-21.8	-2.6	-2.9	467.1	467.7	467.7	-3.6	0.6	184.8	184.8	184.8	2.0	0.0
27	**TDT2/8**	20.9	14.4	17.9	-6.2	-2.9	439.5	444.8	434.3	1.1	-5.2	176.7	170.8	177.2	-3.9	0.5
28	**TDT2/9**	15.4	14.4	14.4	-0.7	-1.0	447.9	444.8	444.8	-7.3	-3.1	171.8	170.8	170.8	1.0	-1.0
29	**TDT2/10**	14.4	14.4	14.4	0.3	0.0	447.5	444.8	444.8	-6.9	-2.7	170.9	170.8	170.8	1.9	-0.1
30	**TDT2/11**	202.6	201.0	204.6	-1.3	2.0	448.1	455.4	445.0	3.2	-3.1	186.8	178.2	184.6	-6.6	-2.2
31	**TDT2/12**	199.6	201.0	201.0	1.7	1.4	452.2	455.4	455.4	-0.9	3.3	179.5	178.2	178.2	0.7	-1.3
32	**TDT2/13**	199.4	201.0	201.0	1.9	1.6	452.4	455.4	455.4	-1.1	3.1	179.4	178.2	178.2	0.8	-1.2
33	**TDT2/14**	104.7	101.8	105.4	-2.6	0.7	433.5	442.6	432.1	4.9	-1.4	167.2	162.9	169.3	-2.3	2.1
34	**TDT2/15**	101.8	101.8	101.8	0.3	0.0	439.6	442.6	442.6	-1.2	3.0	163.6	162.9	162.9	1.3	-0.7
35	**TDT2/16**	102.1	101.8	101.8	0.0	-0.3	439.5	442.6	442.6	-1.1	3.1	163.5	162.9	162.9	1.4	-0.6
36	**TDT2/17**	85.2	81.2	84.8	-3.7	-0.4	472.8	481.1	470.6	4.1	-2.2	189.5	188.1	194.5	0.6	5.0
37	**TDT2/18**	81.1	81.2	81.2	0.4	0.1	479.3	481.1	481.1	-2.4	1.8	188.3	188.1	188.1	1.8	-0.2
38	**TDT2/19**	81.6	81.2	81.2	-0.1	-0.4	479.3	481.1	481.1	-2.4	1.8	188.2	188.1	188.1	1.9	-0.1
39	**TDT3/1**	107.6	108.4	108.4	1.5	0.8	421.6	424.2	424.2	-0.6	2.6	167.4	166.1	166.1	0.6	-1.3
40	**TDT3/2**	-71.1	-69.4	-71.2	2.4	-0.1	442.4	451.9	443.0	6.3	0.6	197.0	189.5	196.3	-5.6	-0.6
41	**TDT3/3**	-70.6	-69.4	-69.4	1.9	1.2	452.0	451.9	451.9	-3.3	-0.1	188.7	189.5	189.5	2.7	0.8
42	**TDT3/4**	-69.5	-69.4	-69.4	0.8	0.1	451.3	451.9	451.9	-2.6	0.6	188.9	189.5	189.5	2.5	0.6
43	**TDT3/5**	-48.1	-48.4	-48.4	0.5	-0.3	482.6	494.3	484.1	8.5	1.5	214.6	210.5	213.6	-2.2	-1.0
44	**TDT3/6**	-47.0	-48.4	-48.4	-0.6	-1.3	494.1	494.3	494.3	-3.0	0.2	209.8	210.5	210.5	2.6	0.7
45	**TDT3/7**	-46.1	-48.4	-48.4	-1.5	-2.2	496.7	494.3	494.3	-5.6	-2.4	209.6	210.5	210.5	2.8	0.9
46	**TDT3/8**	-5.1	-12.2	-8.6	-6.3	-3.4	461.6	471.4	460.9	6.6	-0.7	205.4	196.5	202.9	-7.0	-2.5
47	**TDT3/9**	-12.2	-12.2	-12.2	0.8	0.1	475.6	471.4	471.4	-7.4	-4.2	197.4	196.5	196.5	1.0	-0.9
48	**TDT3/10**	-13.0	-12.2	-12.2	1.6	0.9	473.4	471.4	471.4	-5.2	-2.0	195.6	196.5	196.5	2.8	0.9
49	**TDT3/11**	179.4	174.5	178.1	-4.2	-1.3	473.1	482.0	471.6	5.8	-1.5	211.2	203.9	210.3	-5.4	-0.9
50	**TDT3/12**	172.5	174.5	174.5	2.7	2.0	480.4	482.0	482.0	-1.5	1.7	204.7	203.9	203.9	1.1	-0.8
51	**TDT3/13**	172.5	174.5	174.5	2.7	2.0	485.7	482.0	482.0	-6.8	-3.6	204.9	203.9	203.9	0.9	-1.0
52	**TDT3/14**	79.0	75.3	78.9	-3.0	-0.1	457.9	469.2	458.7	8.1	0.8	192.8	188.6	195.0	-2.3	2.2
53	**TDT3/15**	74.9	75.3	75.3	1.1	0.4	466.8	469.2	469.2	-0.8	2.4	189.6	188.6	188.6	0.9	-1.0
54	**TDT3/16**	74.5	75.3	75.3	1.5	0.8	467.0	469.2	469.2	-1.0	2.2	189.0	188.6	188.6	1.5	-0.4
55	**TDT3/17**	58.3	54.7	58.3	-2.9	0.0	494.7	507.7	497.2	9.8	2.5	216.8	213.8	220.2	-1.1	3.4
56	**TDT3/18**	54.4	54.7	54.7	1.0	0.3	507.4	507.7	507.7	-2.9	0.3	213.7	213.8	213.8	2.0	0.1
57	**TDT3/19**	54.5	54.7	54.7	0.9	0.2	508.3	507.7	507.7	-3.8	-0.6	213.6	213.8	213.8	2.1	0.2
58	**TDT4/1**	215.2	215.3	215.3	0.7	0.1	446.9	448.4	448.4	-2.2	1.4	186.7	185.4	185.4	0.1	-1.3
59	**TDT4/2**	33.9	37.5	33.9	4.2	0.0	459.6	476.0	459.6	12.8	0.0	206.8	208.8	206.8	3.4	0.0
60	**TDT4/3**	36.8	37.5	37.5	1.3	0.7	475.6	476.0	476.0	-3.2	0.4	209.3	208.8	208.8	0.9	-0.5
61	**TDT4/4**	37.9	37.5	37.5	0.2	-0.4	475.9	476.0	476.0	-3.5	0.1	207.9	208.8	208.8	2.3	0.9
62	**TDT4/5**	59.9	58.6	58.5	-0.7	-1.4	508.3	518.4	508.3	6.5	0.0	234.1	229.8	232.8	-2.9	-1.2
63	**TDT4/6**	59.7	58.6	58.6	-0.5	-1.1	518.8	518.4	518.4	-4.0	-0.4	230.1	229.8	229.8	1.1	-0.3
64	**TDT4/7**	59.2	58.6	58.6	0.0	-0.6	520.8	518.4	518.4	-6.0	-2.4	226.3	229.8	229.8	4.9	3.5

65	**TDT4/8**	102.3	94.8	98.3	-6.9	-3.9	483.9	495.5	485.1	8.0	1.2	225.5	215.8	222.2	-8.3	-3.3
66	**TDT4/9**	95.2	94.8	94.8	0.2	-0.4	497.7	495.5	495.5	-5.8	-2.2	213.1	215.8	215.8	4.1	2.7
67	**TDT4/10**	95.3	94.8	94.8	0.1	-0.5	499.3	495.5	495.5	-7.4	-3.8	215.5	215.8	215.8	1.7	0.3
68	**TDT4/11**	285.1	281.4	285.0	-3.1	-0.1	497.0	506.2	495.7	5.6	-1.2	234.0	223.2	229.6	-9.4	-4.4
69	**TDT4/12**	277.0	281.4	281.4	5.0	4.4	505.5	506.2	506.2	-2.9	0.7	223.9	223.2	223.2	0.7	-0.7
70	**TDT4/13**	280.3	281.4	281.4	1.7	1.1	504.3	506.2	506.2	-1.7	1.9	223.9	223.2	223.2	0.7	-0.7
71	**TDT4/14**	183.1	182.2	185.8	-0.3	2.7	479.4	493.3	482.9	10.3	3.5	212.8	207.9	214.3	-3.5	1.5
72	**TDT4/15**	182.5	182.2	182.2	0.3	-0.3	492.1	493.3	493.3	-2.4	1.2	208.6	207.9	207.9	0.7	-0.7
73	**TDT4/16**	182.8	182.2	182.2	0.0	-0.6	491.7	493.3	493.3	-2.0	1.6	208.1	207.9	207.9	1.2	-0.2
74	**TDT4/17**	164.8	161.6	165.2	-2.6	0.4	520.4	531.8	521.4	7.8	1.0	235.0	233.1	239.5	-0.5	4.5
75	**TDT4/18**	161.7	161.6	161.6	0.5	-0.1	532.2	531.8	531.8	-4.0	-0.4	233.3	233.1	233.1	1.2	-0.2
76	**TDT4/19**	162.0	161.6	161.6	0.2	-0.4	535.0	531.8	531.8	-6.8	-3.2	232.8	233.1	233.1	1.7	0.3
77	**TDT5/1**	162.0	161.2	161.2	-0.2	-0.8	458.7	461.5	461.5	-0.5	2.7	177.6	176.3	176.3	0.5	-1.3
78	**TDT5/2**	-18.6	-16.6	-18.4	2.6	0.2	483.5	489.2	480.3	2.4	-3.2	203.4	199.7	206.5	-1.9	3.1
79	**TDT5/3**	-17.5	-16.6	-16.6	1.5	0.9	488.8	489.2	489.2	-2.9	0.3	198.4	199.7	199.7	3.1	1.3
80	**TDT5/4**	-16.2	-16.6	-16.6	0.2	-0.4	488.9	489.2	489.2	-3.0	0.2	198.6	199.7	199.7	2.9	1.1
81	**TDT5/5**	3.9	4.5	4.4	1.2	0.5	523.1	531.6	521.4	5.2	-1.7	222.6	220.7	223.7	-0.1	1.1
82	**TDT5/6**	6.9	4.5	4.5	-1.8	-2.4	531.7	531.6	531.6	-3.4	-0.2	220.4	220.7	220.7	2.1	0.3
83	**TDT5/7**	7.6	4.5	4.5	-2.5	-3.1	533.1	531.6	531.6	-4.8	-1.6	220.1	220.7	220.7	2.4	0.6
84	**TDT5/8**	46.9	40.7	44.3	-5.6	-2.6	500.9	508.7	498.2	4.5	-2.7	216.7	206.7	213.0	-8.2	-3.7
85	**TDT5/9**	40.4	40.7	40.7	0.9	0.3	513.0	508.7	508.7	-7.6	-4.4	206.8	206.7	206.7	1.7	-0.1
86	**TDT5/10**	40.3	40.7	40.7	1.0	0.4	511.0	508.7	508.7	-5.6	-2.4	206.2	206.7	206.7	2.3	0.5
87	**TDT5/11**	229.7	227.3	230.9	-1.8	1.2	507.1	519.3	508.9	9.0	1.8	225.4	214.1	220.4	-9.5	-5.0
88	**TDT5/12**	226.0	227.3	227.3	1.9	1.3	517.5	519.3	519.3	-1.4	1.8	214.7	214.1	214.1	1.2	-0.6
89	**TDT5/13**	226.5	227.3	227.3	1.4	0.8	516.2	519.3	519.3	-0.1	3.1	214.9	214.1	214.1	1.0	-0.8
90	**TDT5/14**	128.0	128.1	131.7	0.7	3.7	497.0	506.5	496.0	6.2	-1.0	204.7	198.8	205.1	-4.1	0.4
91	**TDT5/15**	128.6	128.1	128.1	0.1	-0.5	504.7	506.5	506.5	-1.5	1.7	199.2	198.8	198.8	1.4	-0.4
92	**TDT5/16**	128.5	128.1	128.1	0.2	-0.4	504.4	506.5	506.5	-1.2	2.0	199.0	198.8	198.8	1.6	-0.2
93	**TDT5/17**	109.9	107.5	111.1	-1.8	1.2	531.7	545.0	534.5	10.0	2.8	226.8	224.0	230.3	-1.0	3.5
94	**TDT5/18**	107.2	107.5	107.5	0.9	0.3	544.6	545.0	545.0	-2.9	0.3	223.9	224.0	224.0	1.9	0.1
95	**TDT5/19**	107.9	107.5	107.5	0.2	-0.4	545.0	545.0	545.0	-3.3	-0.1	223.8	224.0	224.0	2.0	0.2
96	**TDT6/1**	135.1	134.8	134.8	0.3	-0.3	492.6	489.1	489.1	-6.7	-3.5	205.6	204.0	204.0	0.2	-1.6
97	**TDT6/2**	-44.6	-43.0	-44.8	2.2	-0.2	505.3	516.8	507.9	8.3	2.6	236.7	227.4	234.2	-7.5	-2.5
98	**TDT6/3**	-44.6	-43.0	-43.0	2.2	1.6	518.8	516.8	516.8	-5.2	-2.0	224.7	227.4	227.4	4.5	2.7
99	**TDT6/4**	-42.0	-43.0	-43.0	-0.4	-1.0	517.2	516.8	516.8	-3.6	-0.4	226.4	227.4	227.4	2.8	1.0
100	**TDT6/5**	-23.5	-21.9	-22.0	2.2	1.5	545.6	559.2	549.0	10.4	3.4	253.3	248.4	251.4	-3.1	-1.9
101	**TDT6/6**	-19.2	-21.9	-21.9	-2.1	-2.7	559.4	559.2	559.2	-3.4	-0.2	248.4	248.4	248.4	1.8	0.0
102	**TDT6/7**	-18.6	-21.9	-21.9	-2.7	-3.3	562.3	559.2	559.2	-6.3	-3.1	247.3	248.4	248.4	2.9	1.1
103	**TDT6/8**	21.5	14.3	17.8	-6.6	-3.6	523.1	536.3	525.8	10.0	2.7	244.5	234.4	240.7	-8.3	-3.8
104	**TDT6/9**	14.3	14.3	14.3	0.6	0.0	535.4	536.3	536.3	-2.3	0.9	233.6	234.4	234.4	2.6	0.8
105	**TDT6/10**	14.5	14.3	14.3	0.4	-0.2	537.6	536.3	536.3	-4.5	-1.3	234.0	234.4	234.4	2.2	0.4

106	**TDT6/11**	201.0	200.9	204.5	0.5	3.5	538.5	547.0	536.5	5.3	-2.0	246.5	241.8	248.1	-2.9	1.6
107	**TDT6/12**	199.8	200.9	200.9	1.7	1.1	546.3	547.0	547.0	-2.5	0.7	242.1	241.8	241.8	1.5	-0.3
108	**TDT6/13**	200.4	200.9	200.9	1.1	0.5	545.7	547.0	547.0	-1.9	1.3	242.3	241.8	241.8	1.3	-0.5
109	**TDT6/14**	101.0	101.7	105.3	1.3	4.3	524.2	534.1	523.6	6.7	-0.6	233.1	226.5	232.8	-4.8	-0.3
110	**TDT6/15**	101.7	101.7	101.7	0.6	0.0	534.4	534.1	534.1	-3.5	-0.3	225.4	226.5	226.5	2.9	1.1
111	**TDT6/16**	100.5	101.7	101.7	1.8	1.2	536.2	534.1	534.1	-5.3	-2.1	225.8	226.5	226.5	2.5	0.7
112	**TDT6/17**	86.0	81.1	84.7	-4.3	-1.3	557.0	572.6	562.1	12.4	5.1	256.8	251.7	258.0	-3.3	1.2
113	**TDT6/18**	81.1	81.1	81.1	0.6	0.0	572.6	572.6	572.6	-3.2	0.0	251.6	251.7	251.7	1.9	0.1
114	**TDT6/19**	81.9	81.1	81.1	-0.2	-0.8	573.7	572.6	572.6	-4.3	-1.1	251.5	251.7	251.7	2.0	0.2

Statistics	$\Delta_f H^\circ$ [kJ mol^{-1}]		S° [J mol^{-1} K^{-1}]		C_p [J mol^{-1} K^{-1}] (300 K)	
Mean Absolute Deviation (MAD)	1.8	1.1	4.5	1.7	2.4	1.2
Maximum Absolute Deviation (MAX)	9.7	4.4	22.7	5.2	9.5	5.0

[a]**CBS:** Reference dataset of CBS-QB3 results with spin orbit and bond additive corrections (SOCs and BACs).
[b]**Bef. new NNIs:** Group additively calculated data based on GAVs and previously defined NNIs given in **Table C-8**, excluding the NNIs for isopropylbenzene and the new NNIs in **Table C-10**, which are defined in this paper.
[c]**Af. new NNIs:** Group additively calculated data based on GAVs and all the NNIs given in **Table C-9** and **Table C-10**, respectively.
[d]Δ(**Bef. new NNIs):** The difference between CBS and "**Bef. new NNIs**".
[e]Δ(**Af. new NNIs):** Deviation of GA calculated data from CBS-QB3.

C.4.3 Optimized structures of some toluene derivatives that are used for the explanation of physical contributions to NNIs

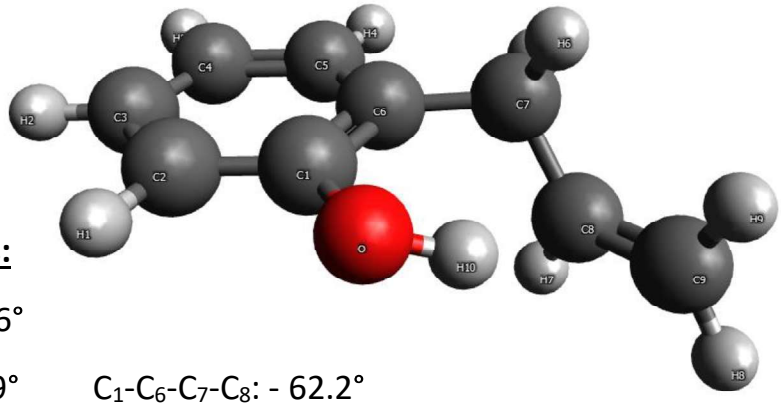

Dihedral Angles:

C_6-C_1-O-H_{10}: 21.6°

C_1-C_6-C_7-H_6: 60.9° C_1-C_6-C_7-C_8: - 62.2°

Figure C-25 Three-dimensional optimized structure of *o*-OH substituted allylbenzene (molecule **TDT2/2**). (**Dark grey:** Carbon, **Light grey:** Hydrogen, **Red:** Oxygen). Three of the dihedral angles that are crucial for the substituent interactions are also provided in the figure.

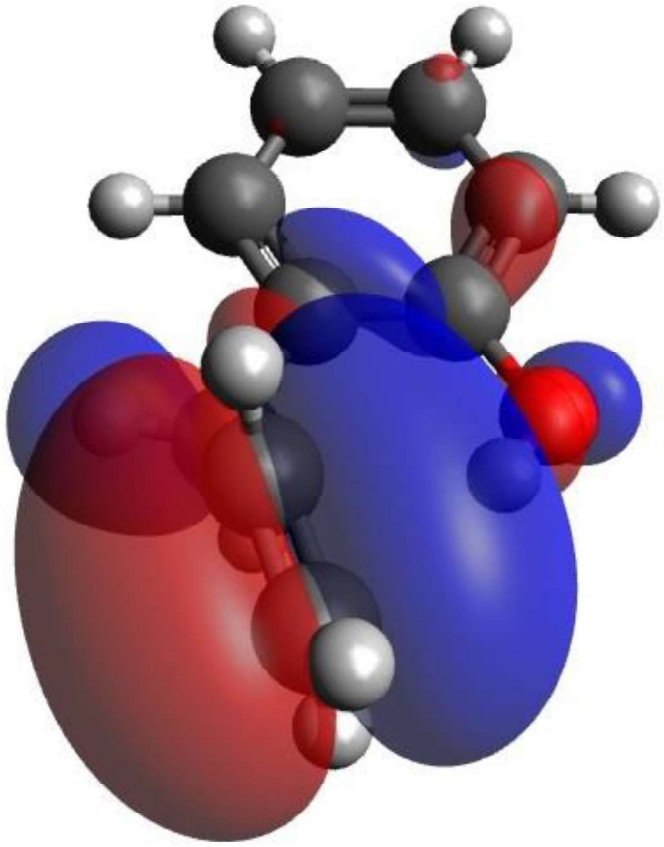

Figure C-26 3D molecular orbital representation of the substituent interaction in *o*-OH substituted allylbenzene (molecule **TDT2/2**).

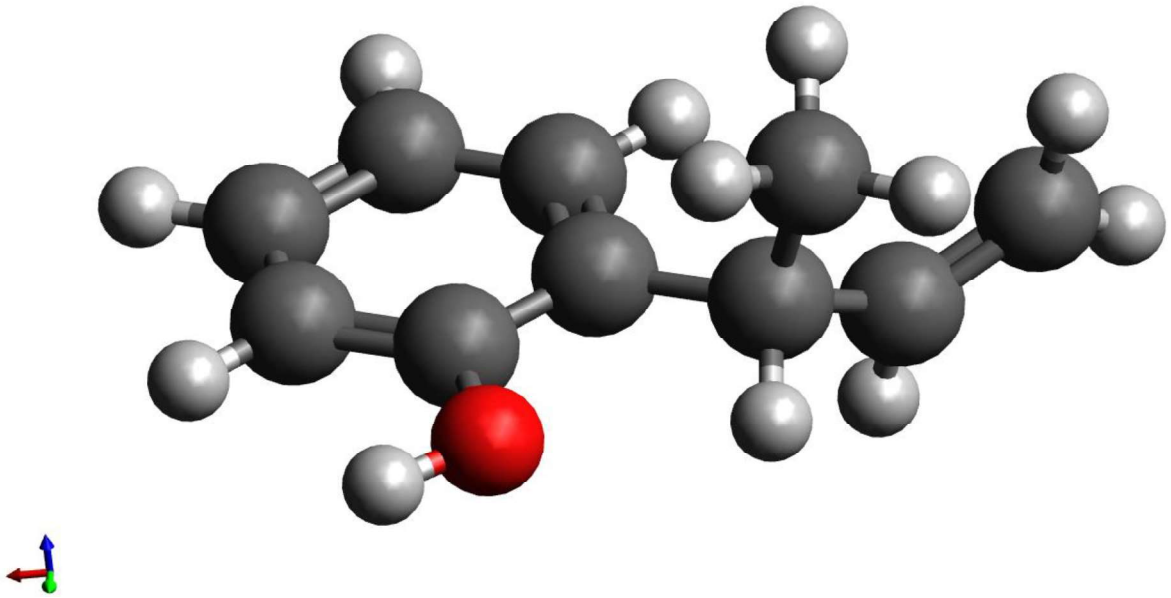

Figure C-27 Three dimensional optimized structure of *o*-OH substituted α-methyl allylbenzene (molecule **TDT3/2**). (**Dark grey:** Carbon, **Light grey:** Hydrogen, **Red:** Oxygen)

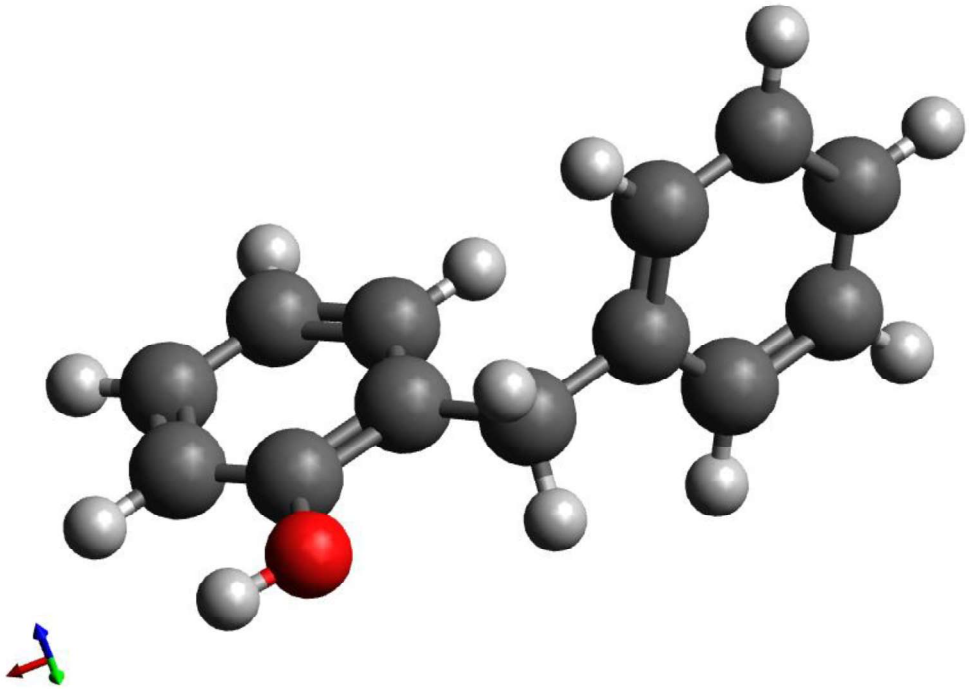

Figure C-28 Three dimensional optimized structure of *o*-OH substituted diphenylmethane (molecule **TDT5/2**). (**Dark grey:** Carbon, **Light grey:** Hydrogen, **Red:** Oxygen)

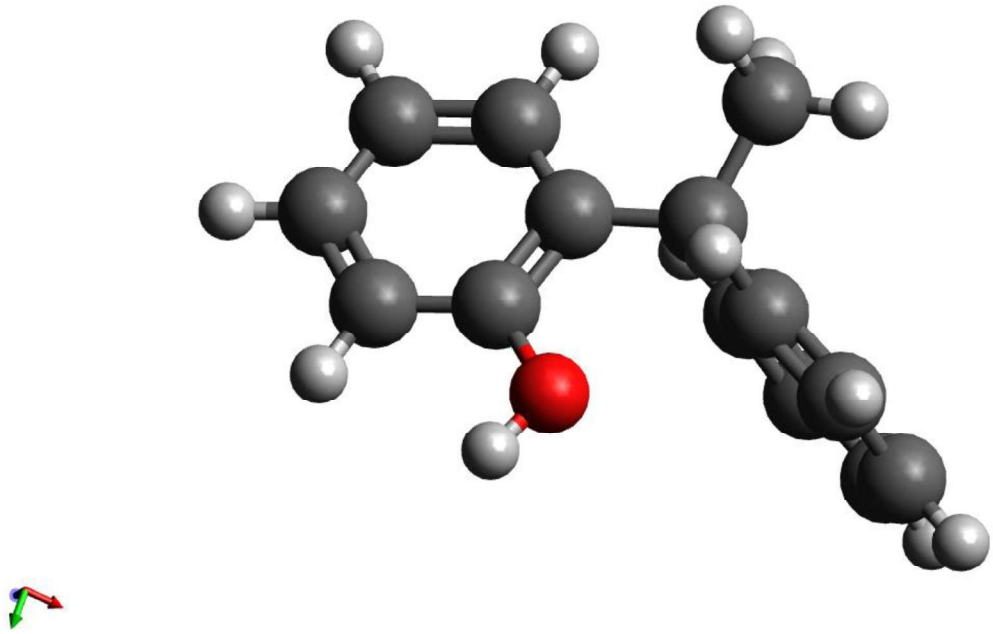

Figure C-29 Three dimensional optimized structure of *o*-OH substituted diphenylethane (molecule **TDT6/2**). (**Dark grey:** Carbon, **Light grey:** Hydrogen, **Red:** Oxygen)

Dihedral Angles:

C_1-C_2-O-H_9: 20°

C_2-C_1-C_7-C_8: 72° C_2-C_1-C_7-C_{10}: - 55.3°

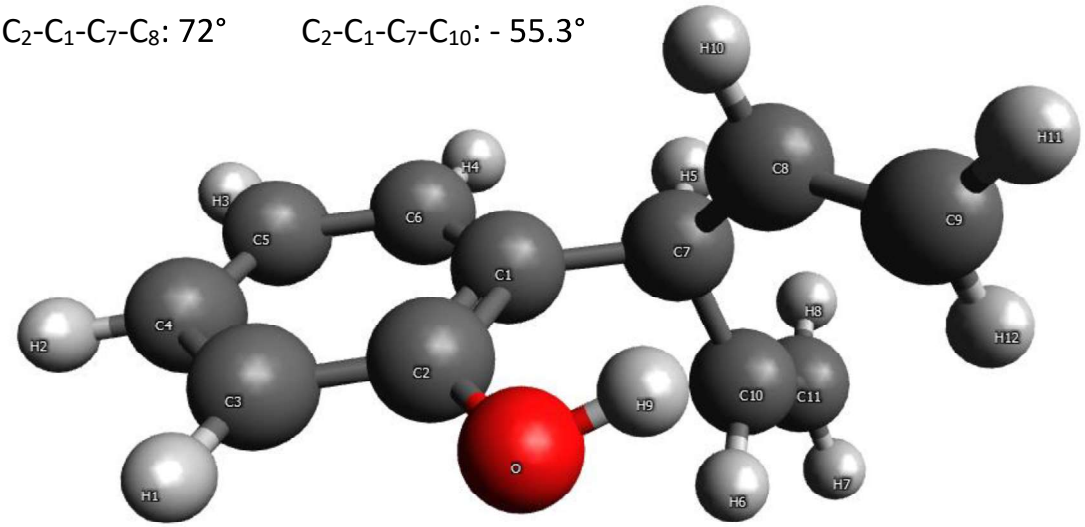

Figure C-30 Three dimensional optimized structure of *o*-OH substituted α-vinyl allylbenzene (molecule **TDT4/2**). (**Dark grey:** Carbon, **Light grey:** Hydrogen, **Red:** Oxygen). Three of the dihedral angles that are crucial for the substituent interactions are also provided in the figure.

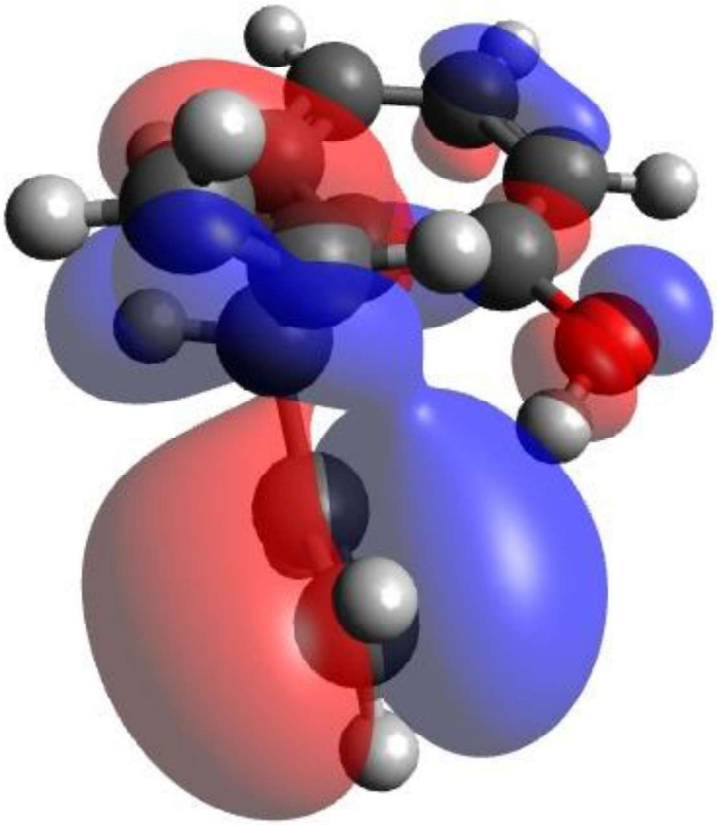

Figure C-31 3D molecular orbital representation of the substituent interaction in *o*-OH substituted allylbenzene (molecule **TDT4/2**).

C.4.4 Testing GAV/NNI Parameters: The Validation Set

Table C-12 Deviations between the validation set data obtained from group additivity and *ab initio* calculations before and after the inclusion of newly derived NNI parameters, where group additive data is calculated based on the simultaneously optimized GAVs and NNIs given in **Table C-9** and **Table C-10**, respectively.

Molecule #		$\Delta_f H^\circ$ [kJ mol^{-1}]					S° [J mol^{-1} K^{-1}]					C_p [J mol^{-1} K^{-1}]				
		CBS[a]	Bef. new NNIs[b]	Af. new NNIs[c]	Δ(Bef. new NNIs)[d]	Δ(Af. new NNIs)[e]	CBS[a]	Bef. new NNIs[b]	Af. new NNIs[c]	Δ(Bef. new NNIs)[d]	Δ(Af. new NNIs)[e]	CBS[a]	Bef. new NNIs[b]	Af. new NNIs[c]	Δ(Bef. new NNIs)[d]	Δ(Af. new NNIs)[e]
1	**TDV1/1**	-353.3	-353.0	-353.0	0.3	0.3	465.0	468.1	468.1	3.1	3.1	199.6	198.8	198.8	-0.8	-0.8
2	**TDV1/2**	-186.3	-187.2	-187.2	-0.9	-0.9	525.7	527.8	527.8	2.1	2.1	216.7	218.9	218.9	2.2	2.2
3	**TDV1/3**	-226.1	-228.5	-220.4	-2.4	5.7	501.9	506.3	503.9	4.4	2.0	218.0	214.6	218.6	-3.4	0.6
4	**TDV1/4**	-142.8	-151.0	-142.9	-8.2	-0.1	499.6	504.9	502.5	5.3	2.9	204.9	204.9	208.9	0.0	4.0
5	**TDV1/5**	-104.4	-109.1	-104.5	-4.7	-0.1	493.6	498.3	492.6	4.7	-1.0	215.4	213.2	218.9	-2.2	3.5
6	**TDV1/6**	38.3	35.6	40.2	-2.7	1.9	511.8	515.6	509.9	3.8	-1.9	213.5	212.3	218.0	-1.2	4.5
7	**TDV1/7**	-202.7	-208.3	-204.1	-5.6	-1.4	478.6	485.4	478.8	6.8	0.2	198.4	197.9	201.2	-0.5	2.8
8	**TDV1/8**	-57.1	-63.6	-59.4	-6.5	-2.3	493.4	502.7	496.1	9.3	2.7	199.6	197.0	200.3	-2.6	0.7
9	**TDV1/9**	-325.5	-323.1	-323.1	2.4	2.4	468.2	466.3	466.3	-1.9	-1.9	195.5	195.4	195.4	-0.1	-0.1
10	**TDV1/10**	-147.3	-142.9	-142.9	4.4	4.4	506.2	502.5	502.5	-3.7	-3.7	210.4	208.9	208.9	-1.5	-1.5
11	**TDV1/11**	38.9	40.2	40.2	1.3	1.3	511.9	509.9	509.9	-2.0	-2.0	217.7	218.0	218.0	0.3	0.3
12	**TDV2/1**	17.3	23.2	13.8	5.9	-3.5	455.9	483.2	456.3	27.3	0.4	211.6	201.6	210.4	-10.0	-1.2
13	**TDV2/2**	-204.3	-199.6	-209.1	4.7	-4.8	461.6	495.4	458.4	33.8	-3.2	215.1	208.2	220.1	-6.9	5.0
14	**TDV2/3**	-81.3	-76.0	-85.4	5.3	-4.1	443.2	470.3	443.4	27.1	0.2	195.2	186.3	195.1	-8.9	-0.1
15	**TDV2/4**	-12.6	-18.7	-15.1	-6.1	-2.5	478.5	489.8	479.3	11.3	0.8	197.9	193.3	199.7	-4.6	1.8
16	**TDV2/5**	83.0	80.5	84.1	-2.5	1.1	496.0	502.7	492.2	6.7	-3.8	214.0	208.6	215.0	-5.4	1.0
17	**TDV2/6**	169.3	167.9	171.5	-1.4	2.2	491.0	500.5	490.0	9.5	-1.0	204.3	200.7	207.1	-3.6	2.8
18	**TDV3/1**	-244.9	-239.9	-241.7	5.0	3.2	472.8	483.6	474.7	10.8	1.9	221.6	214.6	221.4	-7.0	-0.2
19	**TDV3/2**	-82.4	-81.4	-81.5	1.0	0.9	532.5	539.3	529.2	6.8	-3.3	233.2	233.0	236.1	-0.2	2.9
20	**TDV3/3**	-39.3	-45.2	-41.6	-5.9	-2.3	510.1	516.4	505.9	6.3	-4.2	225.5	219.0	225.4	-6.5	-0.1
21	**TDV3/4**	2.3	-3.3	0.3	-5.6	-2.0	498.0	509.8	499.3	11.8	1.3	236.8	227.3	233.7	-9.5	-3.1
22	**TDV3/5**	58.5	54.0	57.6	-4.5	-0.9	519.4	529.3	518.8	9.9	-0.6	241.2	234.3	240.7	-6.9	-0.5
23	**TDV3/6**	143.0	141.4	145.0	-1.6	2.0	515.8	527.1	516.6	11.3	0.8	230.4	226.4	232.8	-4.0	2.4
24	**TDV3/7**	144.5	146.0	146.0	1.5	1.5	520.9	521.4	521.4	0.5	0.5	231.4	232.1	232.1	0.7	0.7
25	**TDV3/8**	46.0	42.2	45.8	-3.8	-0.2	503.3	514.2	503.7	10.9	0.4	214.2	211.1	217.5	-3.1	3.3
26	**TDV3/9**	-244.9	-239.9	-241.7	5.0	3.2	472.8	483.6	474.7	10.8	1.9	221.6	214.6	221.4	-7.0	-0.2
27	**TDV3/10**	-194.7	-189.9	-191.7	4.8	3.0	490.9	499.1	490.2	8.2	-0.7	228.4	219.9	226.7	-8.5	-1.7
28	**TDV3/11**	-103.4	-102.5	-104.3	0.9	-0.9	488.1	496.9	488.0	8.8	-0.1	218.5	212.0	218.8	-6.5	0.3
29	**TDV3/12**	-204.3	-194.5	-203.9	9.8	0.4	473.4	498.3	471.4	24.9	-2.0	225.3	218.3	227.1	-7.0	1.8

30	**TDV4/1**	98.6	103.6	100.0	5.0	1.4	516.1	533.9	517.5	17.8	1.4	242.3	246.6	244.6	4.3	2.3
31	**TDV4/2**	1.8	4.4	0.8	2.6	-1.0	502.9	521.0	504.6	18.1	1.7	228.7	231.3	229.3	2.6	0.6
32	**TDV4/3**	-116.0	-119.2	-119.3	-3.2	-3.3	538.7	546.1	536.0	7.4	-2.7	257.1	253.2	256.3	-3.9	-0.8
33	**TDV4/4**	27.8	25.5	25.4	-2.3	-2.4	552.2	563.4	553.3	11.2	1.1	257.1	252.3	255.4	-4.8	-1.7
34	**TDV4/5**	164.7	160.9	164.5	-3.8	-0.2	543.7	553.4	542.9	9.7	-0.8	260.0	253.6	260.0	-6.4	0.0
35	**TDV4/6**	108.9	103.6	107.2	-5.3	-1.7	527.0	533.9	523.4	6.9	-3.6	257.4	246.6	253.0	-10.8	-4.4
36	**TDV4/7**	250.5	248.3	251.9	-2.2	1.4	544.0	551.2	540.7	7.2	-3.3	250.4	245.7	252.1	-4.7	1.7
37	**TDV4/8**	151.9	149.1	152.7	-2.8	0.8	524.4	538.3	527.8	13.9	3.4	237.3	230.4	236.8	-6.9	-0.5
38	**TDV5/1**	-142.0	-137.1	-138.9	4.9	3.1	528.0	536.3	527.4	8.3	-0.6	237.8	230.1	236.9	-7.7	-0.9
39	**TDV5/2**	45.6	49.5	47.7	3.9	2.1	541.3	547.0	538.1	5.7	-3.2	241.8	237.5	244.3	-4.3	2.5
40	**TDV5/3**	-51.1	-49.7	-51.5	1.4	-0.4	528.8	534.1	525.2	5.3	-3.6	225.0	222.2	229.0	-2.8	4.0
41	**TDV5/4**	-28.4	-28.6	-28.7	-0.2	-0.3	568.8	576.5	566.4	7.7	-2.4	244.5	243.2	246.3	-1.3	1.8
42	**TDV5/5**	13.4	7.6	11.2	-5.8	-2.2	546.5	553.6	543.1	7.1	-3.4	238.4	229.2	235.6	-9.2	-2.8
43	**TDV5/6**	196.3	194.2	197.8	-2.1	1.5	559.7	564.3	553.8	4.6	-5.9	248.0	236.6	243.0	-11.4	-5.0
44	**TDV5/7**	192.9	194.2	197.8	1.3	4.9	554.9	564.3	553.8	9.4	-1.1	242.6	236.6	243.0	-6.0	0.4
45	**TDV5/8**	94.7	95.0	98.6	0.3	3.9	541.9	551.4	540.9	9.5	-1.0	227.9	221.3	227.7	-6.6	-0.2
46	**TDV5/9**	11.6	15.7	15.7	4.1	4.1	550.6	551.2	551.2	0.6	0.6	234.2	233.2	233.2	-1.0	-1.0
47	**TDV5/10**	198.4	198.8	198.8	0.4	0.4	559.8	558.6	558.6	-1.2	-1.2	244.0	242.3	242.3	-1.7	-1.7
48	**TDV6/1**	-74.0	-76.1	-77.9	-2.1	-3.9	550.1	561.8	552.9	11.7	2.8	258.6	249.9	256.7	-8.7	-1.9
49	**TDV6/2**	-222.7	-220.8	-222.6	1.9	0.1	530.7	544.5	535.6	13.8	4.9	259.0	250.8	257.6	-8.2	-1.4
50	**TDV6/3**	47.3	44.2	44.1	-3.1	-3.2	602.7	617.1	607.0	14.4	4.3	291.2	286.2	289.3	-5.0	-1.9
51	**TDV6/4**	-12.0	-18.8	-15.2	-6.8	-3.2	567.5	581.3	570.8	13.8	3.3	266.9	256.9	263.3	-10.0	-3.6
52	**TDV6/5**	171.6	167.8	171.4	-3.8	-0.2	584.5	592.0	581.5	7.5	-3.0	276.4	264.3	270.7	-12.1	-5.7
53	**TDV6/6**	171.7	172.4	172.4	0.7	0.7	588.4	586.3	586.3	-2.1	-2.1	269.3	270.0	270.0	0.7	0.7
54	**TDV6/7**	71.5	68.6	72.2	-2.9	0.7	569.2	579.1	568.6	9.9	-0.6	252.2	249.0	255.4	-3.2	3.2

Statistics	$\Delta_f H^\circ$ [kJ mol^{-1}]		S° [J mol^{-1} K^{-1}]		C_p [J mol^{-1} K^{-1}] (300 K)	
Mean Absolute Deviation (MAD)	3.5	2.0	9.5	2.1	4.9	1.9
Maximum Absolute Deviation (MAX)	9.8	5.7	33.8	5.9	12.1	5.7

[a]**CBS:** Reference dataset of CBS-QB3 results with spin orbit and bond additive corrections (SOCs and BACs).
[b]**Bef. new NNIs:** Group additively calculated data based on GAVs and previously defined NNIs given in **Table C-8**, excluding the NNIs for isopropylbenzene and the new NNIs in **Table C-10**, which are defined in this paper.
[c]**Af. new NNIs:** Group additively calculated data based on GAVs and all the NNIs given in **Table C-9** and **Table C-10**, respectively.
[d]Δ(**Bef. new NNIs):** The difference between CBS and "**Bef. new NNIs**".
[e]Δ(**Af. new NNIs):** Deviation of GA calculated data from CBS-QB3.

C.4.5 Final Optimization of GA Parameters

Table C-13 Deviations between the final set data (training set + validation set) obtained from group additivity and *ab initio* calculations, where group additive data is calculated based on the final GAVs and NNIs given in **Table 5-3** and **Table 5-4** in the text, respectively.

Molecules		$\Delta_f H^\circ$ [kJ mol^{-1}]	S° [J mol^{-1} K^{-1}]	C_p [J mol^{-1} K^{-1}]						
				300 K	400 K	500 K	600 K	800 K	1000 K	1500 K
1	TDT1/1	-1.200	0.117	-1.947	-1.510	-0.870	-0.287	0.343	0.420	0.530
2	TDT1/2	2.100	0.117	-2.347	-1.210	-0.070	0.513	1.243	1.420	1.930
3	TDT1/3	0.700	-1.383	0.453	-0.010	0.230	0.413	0.743	0.620	0.530
4	TDT1/4	-0.700	-1.483	0.453	0.090	0.430	0.613	0.843	0.720	0.530
5	TDT1/5	-1.200	0.017	-0.047	-1.310	-2.470	-3.187	-3.757	-3.680	-2.170
6	TDT1/6	-2.000	-1.583	0.053	-0.310	0.130	0.613	1.243	1.320	1.130
7	TDT1/7	-3.300	-2.383	-0.047	-0.210	0.330	0.713	1.343	1.420	1.130
8	TDT1/8	-0.800	0.817	1.153	3.190	1.830	0.913	-0.157	-0.880	-1.370
9	TDT1/9	0.100	2.017	-0.047	0.190	0.830	1.513	2.343	2.420	1.430
10	TDT1/10	0.500	1.617	0.053	0.190	0.830	1.513	2.443	2.420	1.530
11	TDT1/11	-1.600	1.617	2.753	3.390	2.030	0.813	-1.157	-2.380	-2.870
12	TDT1/12	0.900	-1.283	-2.047	-1.810	-1.270	-0.887	-0.857	-1.380	-2.270
13	TDT1/13	0.900	-1.883	-2.447	-1.910	-1.270	-0.887	-0.857	-1.280	-2.270
14	TDT1/14	0.500	4.217	-0.347	-1.110	-1.670	-1.787	-2.057	-2.280	-1.570
15	TDT1/15	0.000	0.317	-0.747	-0.910	-0.570	-0.187	0.343	0.520	1.330
16	TDT1/16	-0.200	-1.183	-1.147	-1.110	-0.670	-0.187	0.243	0.320	0.930
17	TDT1/17	-1.100	3.117	-2.647	-3.210	-3.170	-3.187	-3.157	-3.180	-1.370
18	TDT1/18	-0.100	-1.983	-0.847	-0.810	-0.170	0.313	0.943	0.920	1.030
19	TDT1/19	-0.300	-2.383	-0.447	-0.510	0.030	0.513	1.043	0.920	0.830
20	TDT2/1	0.415	3.405	-1.832	-1.663	-1.394	-1.145	-0.887	-1.005	-1.141
21	TDT2/2	2.252	0.820	-1.018	0.610	-0.715	0.285	0.486	0.350	-0.713
22	TDT2/3	3.515	-1.095	-1.132	-1.263	-1.094	-0.945	-0.787	-0.705	-0.341
23	TDT2/4	0.415	1.805	-0.232	-0.663	-0.594	-0.645	-0.687	-0.905	-1.241
24	TDT2/5	0.701	-2.834	2.250	1.831	1.318	1.552	0.878	0.712	1.308
25	TDT2/6	-1.985	0.005	-1.332	-1.463	-1.194	-0.845	-0.387	-0.305	-0.341
26	TDT2/7	-2.885	0.505	-0.232	-0.763	-0.594	-0.445	-0.087	-0.205	-0.341
27	TDT2/8	-2.840	-4.710	0.422	0.822	1.394	1.684	1.721	1.719	1.547
28	TDT2/9	-0.985	-3.195	-1.232	-0.763	-0.394	0.055	0.413	0.395	0.259
29	TDT2/10	0.015	-2.795	-0.332	-0.363	-0.094	0.155	0.413	0.195	-0.341
30	TDT2/11	2.060	-2.610	-2.278	-1.878	-1.006	-0.416	0.521	1.219	1.847
31	TDT2/12	1.415	3.205	-1.532	-1.663	-1.494	-1.345	-1.187	-1.205	-1.141
32	TDT2/13	1.615	3.005	-1.432	-1.563	-1.394	-1.345	-1.187	-1.205	-1.141
33	TDT2/14	0.760	-0.910	2.022	2.222	2.094	1.784	1.121	0.619	0.247
34	TDT2/15	0.015	2.905	-0.932	-1.163	-1.194	-1.045	-0.987	-1.005	-0.841

35	**TDT2/16**	-0.285	3.005	-0.832	-0.963	-0.994	-0.845	-0.887	-1.105	-1.241
36	**TDT2/17**	-0.340	-1.710	4.922	4.022	3.394	2.584	1.321	0.519	0.147
37	**TDT2/18**	0.115	1.705	-0.432	-0.763	-0.594	-0.345	-0.187	-0.405	-0.541
38	**TDT2/19**	-0.385	1.705	-0.332	-0.663	-0.494	-0.345	-0.087	-0.305	-0.341
39	**TDT3/1**	0.470	2.543	-1.427	-1.307	-1.530	-1.367	-1.281	-1.270	-0.925
40	**TDT3/2**	-0.946	0.219	-0.936	0.191	0.497	0.873	1.126	0.984	1.567
41	**TDT3/3**	0.870	-0.157	0.673	0.093	-0.330	-0.467	-0.581	-0.370	-0.025
42	**TDT3/4**	-0.230	0.543	0.473	-0.007	-0.530	-0.667	-0.881	-0.970	-0.925
43	**TDT3/5**	0.456	2.003	-1.645	-0.713	-0.718	-0.170	-0.916	-1.153	-0.376
44	**TDT3/6**	-1.630	0.143	0.573	-0.007	-0.330	-0.167	0.219	0.630	0.975
45	**TDT3/7**	-2.530	-2.457	0.773	0.093	-0.330	-0.267	-0.181	-0.070	0.075
46	**TDT3/8**	-3.685	-0.173	-2.472	-1.622	-1.042	-0.838	-1.172	-1.146	-0.937
47	**TDT3/9**	-0.230	-4.257	-1.027	-0.507	-0.430	0.033	0.619	1.030	1.175
48	**TDT3/10**	0.570	-2.057	0.773	0.393	0.070	0.133	0.219	0.130	-0.025
49	**TDT3/11**	-1.585	-0.973	-0.872	-0.022	0.758	1.262	1.028	0.754	0.263
50	**TDT3/12**	1.670	1.643	-0.927	-1.207	-1.430	-1.267	-0.881	-0.470	0.175
51	**TDT3/13**	1.670	-3.657	-1.127	-1.207	-1.530	-1.467	-1.481	-1.370	-1.025
52	**TDT3/14**	-0.385	1.327	2.228	1.778	1.058	0.362	-0.872	-1.246	-1.037
53	**TDT3/15**	0.070	2.343	-1.127	-1.107	-1.430	-1.367	-1.281	-1.070	-0.425
54	**TDT3/16**	0.470	2.143	-0.527	-0.707	-1.130	-1.167	-1.281	-1.270	-1.025
55	**TDT3/17**	-0.285	3.027	3.428	1.378	0.158	-0.638	-1.672	-1.946	-1.537
56	**TDT3/18**	-0.030	0.243	-0.027	-0.407	-0.530	-0.367	0.019	0.330	0.875
57	**TDT3/19**	-0.130	-0.657	0.073	-0.207	-0.530	-0.467	-0.381	-0.370	-0.225
58	**TDT4/1**	0.191	1.435	-1.058	-0.828	-0.360	-0.459	-0.511	-0.589	-0.627
59	**TDT4/2**	-0.133	-1.033	-0.967	-0.100	-0.733	-2.867	-2.300	-0.433	-1.133
60	**TDT4/3**	0.791	0.435	-0.258	-0.628	-0.060	-0.159	-0.011	0.111	0.073
61	**TDT4/4**	-0.309	0.135	1.142	0.472	0.540	0.141	-0.311	-0.489	-0.727
62	**TDT4/5**	-0.223	0.496	-1.476	-0.534	0.252	0.738	0.454	0.428	1.022
63	**TDT4/6**	-1.009	-0.365	-0.058	-0.528	0.140	0.341	1.089	1.411	1.173
64	**TDT4/7**	-0.509	-2.365	3.742	3.472	3.540	3.041	2.389	1.911	0.973
65	**TDT4/8**	-3.764	1.720	-2.903	-3.042	-1.972	-1.730	-1.402	-0.865	-0.039
66	**TDT4/9**	-0.309	-2.165	2.942	2.372	2.540	3.241	3.289	3.011	1.773
67	**TDT4/10**	-0.409	-3.765	0.542	0.672	1.040	1.041	0.989	0.811	0.273
68	**TDT4/11**	0.036	-0.680	-4.003	-4.342	-3.972	-2.930	-1.702	-0.765	0.061
69	**TDT4/12**	4.491	0.735	-0.458	-0.628	-0.060	0.041	0.389	0.511	0.473
70	**TDT4/13**	1.191	1.935	-0.458	-0.628	-0.360	-0.559	-0.711	-0.689	-0.727
71	**TDT4/14**	2.836	4.020	1.897	0.158	-0.272	-1.030	-1.802	-1.665	-0.939
72	**TDT4/15**	-0.209	1.235	-0.458	-0.528	-0.160	-0.259	-0.111	0.011	0.073
73	**TDT4/16**	-0.509	1.635	0.042	-0.128	0.040	-0.259	-0.511	-0.689	-0.727
74	**TDT4/17**	0.536	1.520	4.897	4.158	2.428	0.770	-0.902	-1.165	-0.539
75	**TDT4/18**	-0.009	-0.365	0.042	-0.028	0.540	0.741	1.089	1.211	0.973

76	TDT4/19	-0.309	-3.165	0.542	0.272	0.640	0.441	0.489	0.311	0.273
77	TDT5/1	-1.413	3.341	-1.212	-1.264	-1.601	-1.655	-1.698	-1.663	-0.951
78	TDT5/2	-0.929	-2.982	3.078	3.033	2.526	1.986	1.209	0.191	-1.458
79	TDT5/3	0.287	0.941	1.388	0.436	-0.001	-0.255	-0.298	-0.163	0.249
80	TDT5/4	-1.013	0.841	1.188	0.236	-0.301	-0.655	-0.998	-1.163	-0.651
81	TDT5/5	0.974	-0.598	0.769	0.330	0.011	0.242	-0.932	-1.846	-3.102
82	TDT5/6	-3.013	0.441	0.388	0.036	-0.001	0.245	0.802	1.037	1.249
83	TDT5/7	-3.713	-0.959	0.688	-0.064	-0.401	-0.455	-0.298	-0.063	0.349
84	TDT5/8	-3.168	-1.574	-3.358	-2.979	-2.213	-1.826	-1.689	-2.040	-3.263
85	TDT5/9	-0.313	-3.759	-0.012	0.136	0.299	0.545	1.102	1.237	1.349
86	TDT5/10	-0.213	-1.759	0.588	0.036	-0.301	-0.255	0.002	0.037	0.349
87	TDT5/11	0.632	2.926	-4.658	-3.179	-1.813	-0.726	0.711	1.660	2.237
88	TDT5/12	0.687	2.441	-0.512	-0.664	-0.701	-0.555	-0.198	0.037	0.449
89	TDT5/13	0.187	3.741	-0.712	-1.164	-1.501	-1.655	-1.598	-1.363	-0.651
90	TDT5/14	3.132	0.126	0.742	1.621	1.887	1.974	1.811	1.760	1.837
91	TDT5/15	-1.113	2.341	-0.312	-0.664	-0.901	-0.855	-0.598	-0.463	0.149
92	TDT5/16	-1.013	2.641	-0.112	-0.664	-1.101	-1.355	-1.498	-1.463	-0.751
93	TDT5/17	0.632	3.926	3.842	3.521	3.387	3.174	2.611	2.260	2.037
94	TDT5/18	-0.313	0.941	0.188	-0.064	-0.001	0.245	0.702	0.937	1.449
95	TDT5/19	-1.013	0.541	0.288	-0.264	-0.501	-0.555	-0.398	-0.263	0.349
96	TDT6/1	-0.001	-4.032	-1.201	-0.526	-0.689	-0.843	-1.162	-1.249	-1.226
97	TDT6/2	-0.418	1.744	-2.210	-1.929	-1.662	-1.003	0.345	1.106	2.066
98	TDT6/3	1.899	-2.532	3.099	3.274	2.811	2.157	1.238	0.651	-0.126
99	TDT6/4	-0.701	-0.932	1.399	1.274	0.711	0.057	-0.662	-0.949	-1.126
100	TDT6/5	2.885	3.428	-1.919	-1.932	-2.077	-1.346	-1.197	-0.732	0.123
101	TDT6/6	-2.401	-0.732	0.399	0.774	0.911	0.957	1.038	1.051	0.574
102	TDT6/7	-3.001	-3.632	1.499	1.474	1.111	0.857	0.538	0.451	0.074
103	TDT6/8	-3.257	2.752	-3.146	-0.941	-1.001	-2.214	0.347	-0.725	1.961
104	TDT6/9	0.299	0.368	1.199	1.974	2.011	2.057	1.938	1.751	0.874
105	TDT6/10	0.099	-1.832	0.799	0.974	0.711	0.557	0.338	0.251	-0.126
106	TDT6/11	3.843	-1.948	2.254	2.159	2.099	1.986	2.047	2.175	1.661
107	TDT6/12	1.399	0.168	0.099	0.774	0.911	0.857	0.638	0.551	0.074
108	TDT6/13	0.799	0.768	-0.101	0.574	0.411	0.157	-0.362	-0.549	-0.826
109	TDT6/14	4.643	-0.548	0.354	2.159	2.499	2.386	1.747	1.575	1.061
110	TDT6/15	0.299	-0.832	1.499	1.774	1.411	1.157	0.638	0.251	-0.126
111	TDT6/16	1.499	-2.632	1.099	2.374	2.311	1.957	1.038	0.351	-0.326
112	TDT6/17	-0.957	5.152	1.854	1.059	0.299	-0.414	-1.253	-1.225	-0.739
113	TDT6/18	0.299	-0.532	0.499	1.074	1.311	1.357	1.338	1.151	0.974
114	TDT6/19	-0.501	-1.632	0.599	0.874	0.711	0.557	0.338	0.151	-0.026
115	TDV1/1	-0.100	3.017	-1.347	-1.910	-1.770	-1.887	-1.757	-1.580	-0.470
116	TDV1/2	-1.300	2.017	1.653	0.690	0.230	-0.287	-0.957	-1.280	-0.770

117	**TDV1/3**	5.300	1.917	0.053	2.690	1.130	0.013	-0.857	-1.180	-0.570
118	**TDV1/4**	-0.500	2.817	3.453	2.090	1.230	0.513	-0.257	-0.680	-0.170
119	**TDV1/5**	-0.500	-1.083	2.953	3.390	2.230	1.313	0.143	2.220	0.030
120	**TDV1/6**	1.500	-1.983	3.953	3.790	3.530	3.113	2.143	1.520	1.430
121	**TDV1/7**	-1.800	0.117	2.253	0.690	-0.170	-0.687	-1.257	-1.680	-1.470
122	**TDV1/8**	-2.700	2.617	0.153	-1.010	-1.570	-1.787	-1.857	0.620	-0.470
123	**TDV1/9**	2.000	-1.983	-0.647	-0.810	-0.170	0.213	1.143	1.620	2.030
124	**TDV1/10**	4.000	-3.783	-2.047	-1.510	-0.870	-0.587	-0.057	-0.080	0.030
125	**TDV1/11**	0.900	-2.083	-0.247	0.790	1.730	2.213	2.443	2.120	1.430
126	**TDV2/1**	-1.248	1.220	-2.218	0.510	1.885	-0.215	-3.114	-2.550	-0.313
127	**TDV2/2**	-1.462	-1.919	3.464	-0.196	-0.803	-0.118	1.451	1.767	1.336
128	**TDV2/3**	-1.848	1.020	-1.118	0.010	-1.715	-3.215	-2.114	-0.550	0.087
129	**TDV2/4**	-2.440	1.290	1.722	1.322	1.794	1.984	1.821	1.719	1.447
130	**TDV2/5**	1.160	-3.310	0.922	2.022	1.694	1.484	1.521	1.619	1.447
131	**TDV2/6**	2.260	-0.510	2.722	2.422	2.194	1.684	0.921	0.619	0.347
132	**TDV3/1**	2.354	1.519	-0.436	0.390	0.797	0.673	0.526	0.284	0.867
133	**TDV3/2**	1.656	-2.897	2.255	4.287	4.282	-0.170	2.584	3.147	1.024
134	**TDV3/3**	-2.585	-3.673	-0.072	0.578	1.058	1.262	0.828	0.254	-1.637
135	**TDV3/4**	-2.285	1.827	-3.072	-2.422	-1.242	-0.538	-0.172	-0.046	-0.137
136	**TDV3/5**	-1.185	-0.073	-0.472	0.178	1.058	1.762	1.928	1.854	1.163
137	**TDV3/6**	1.715	1.327	2.428	1.178	0.558	0.062	-0.872	-1.146	-1.137
138	**TDV3/7**	1.170	0.443	0.573	1.293	1.370	1.533	1.319	3.330	0.975
139	**TDV3/8**	-0.485	0.927	3.328	1.878	0.958	0.362	-0.772	-1.146	-1.137
140	**TDV3/9**	2.354	1.519	-0.436	0.390	0.797	0.673	0.526	0.284	0.867
141	**TDV3/10**	2.154	-1.081	-1.936	-2.610	-2.703	-2.027	-0.674	0.084	1.367
142	**TDV3/11**	-1.746	-0.481	0.064	0.890	0.997	1.173	1.126	0.984	1.567
143	**TDV3/12**	2.307	-1.142	0.888	-0.934	1.349	3.262	3.292	0.984	-0.397
144	**TDV4/1**	1.267	0.367	1.333	0.100	0.167	1.933	0.800	1.567	-0.033
145	**TDV4/2**	-1.133	0.667	-0.367	0.000	0.567	0.933	1.500	-1.133	1.167
146	**TDV4/3**	-2.123	-2.204	-1.076	-0.934	-0.448	-0.262	-0.646	-0.472	0.322
147	**TDV4/4**	-1.223	1.596	-1.976	-0.134	1.152	1.838	1.554	1.628	1.822
148	**TDV4/5**	-0.064	-0.180	0.397	-0.342	0.428	0.370	-0.202	-0.965	-3.039
149	**TDV4/6**	-1.564	-2.980	-4.003	3.558	-3.972	-3.130	-1.302	-2.265	-2.339
150	**TDV4/7**	1.536	-2.680	2.097	-0.142	0.228	0.370	0.998	1.435	1.461
151	**TDV4/8**	0.936	4.020	-0.103	-1.742	-1.872	-2.330	-2.602	-2.165	-1.039
152	**TDV5/1**	1.971	-0.282	-0.922	-1.867	-1.974	-3.514	-0.991	-1.209	-1.958
153	**TDV5/2**	0.971	-2.882	2.478	2.333	1.726	1.086	0.309	-0.709	-1.958
154	**TDV5/3**	-1.529	-3.282	3.978	3.633	2.826	2.186	-1.391	-0.009	-1.658
155	**TDV5/4**	0.174	-1.298	1.369	0.430	-0.289	-0.258	-1.432	-2.346	-3.302
156	**TDV5/5**	-2.768	-2.174	-2.558	-2.279	-1.813	-1.526	-1.589	-1.840	-3.063
157	**TDV5/6**	0.932	-4.674	-4.758	-3.279	-1.813	-0.726	0.811	1.760	2.237

158	**TDV5/7**	4.332	0.126	0.642	1.521	1.987	1.974	2.011	2.060	2.037
159	**TDV5/8**	3.332	0.226	0.042	1.521	1.987	2.074	1.911	1.960	1.937
160	**TDV5/9**	3.487	1.241	-0.912	-0.964	-1.001	-1.055	-0.798	-0.563	2.649
161	**TDV5/10**	-0.213	-0.559	-1.612	0.536	1.599	2.145	2.402	2.237	1.849
162	**TDV6/1**	-4.118	1.944	-1.610	-1.229	-1.062	-0.603	0.445	1.006	1.966
163	**TDV6/2**	-0.118	4.044	-1.110	-3.229	-2.762	-1.503	-2.555	-2.994	-3.234
164	**TDV6/3**	-1.815	4.228	-2.019	-2.432	-2.677	-2.046	-1.797	-1.132	-0.177
165	**TDV6/4**	-2.857	3.352	-3.046	-4.141	-4.601	-4.714	-3.653	-2.825	-0.839
166	**TDV6/5**	0.143	-2.948	-5.146	-4.141	-3.301	-2.714	-1.753	-0.725	-2.839
167	**TDV6/6**	0.999	-2.632	1.099	2.674	3.111	3.257	2.738	2.251	1.074
168	**TDV6/7**	1.043	-0.548	3.754	-4.741	-3.501	-2.914	-2.353	-1.625	-0.739

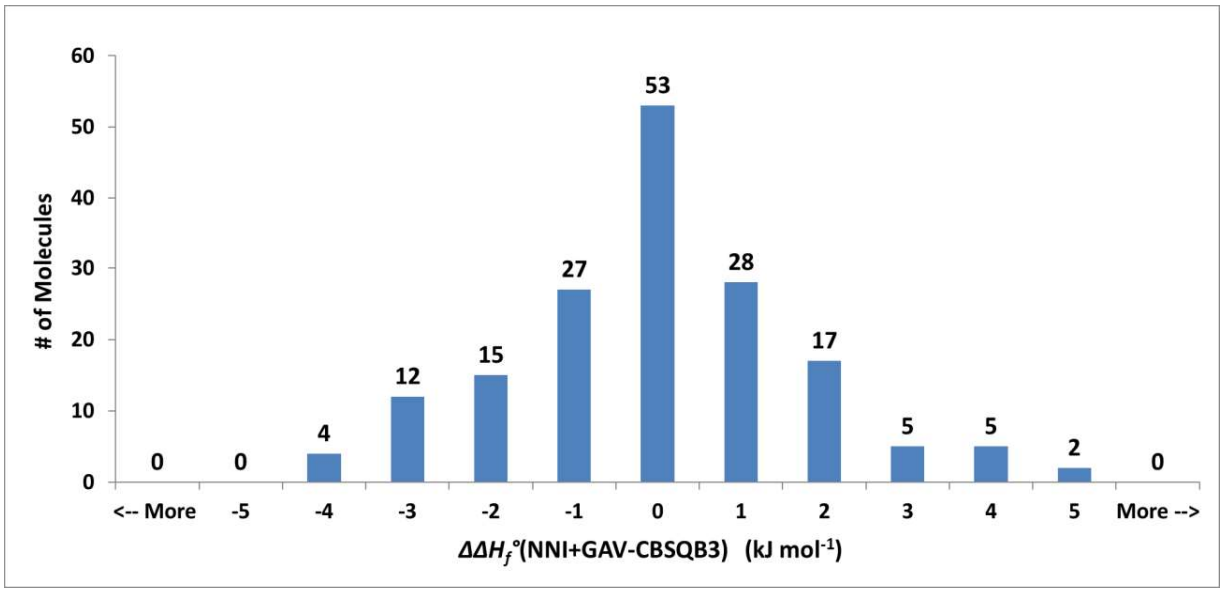

Figure C-32 Distribution of the differences between the final thermochemical data calculated with GA parameters and the *ab initio* reference dataset (CBSQB3) for the $\Delta_f H^\circ$ values of the toluene derivatives in the final set, $\Delta\Delta_f H°$((NNI+GAV)-CBSQB3).

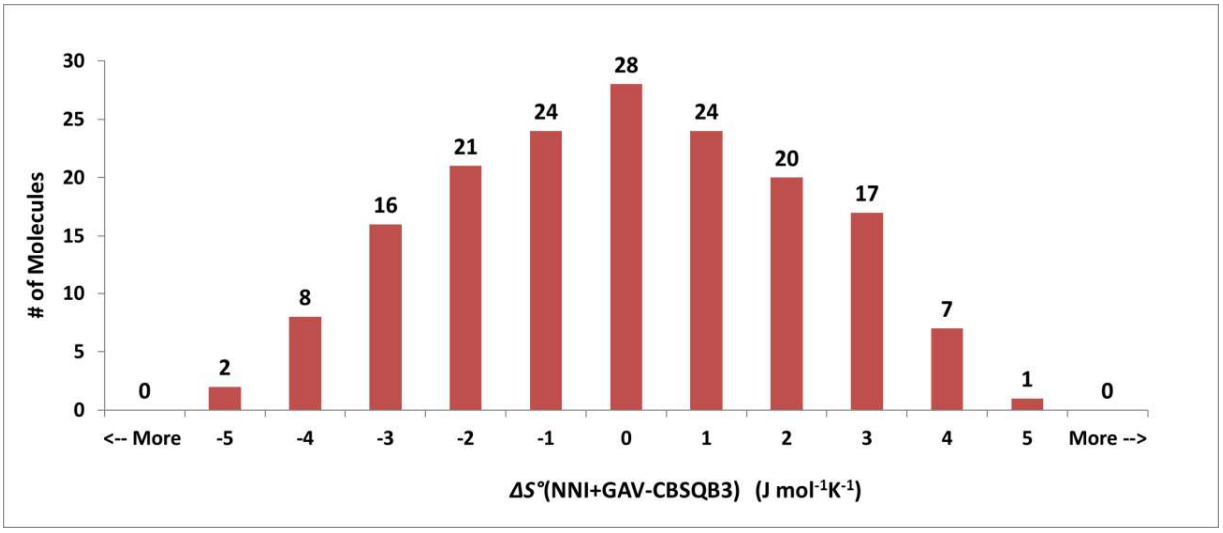

Figure C-33 Distribution of the differences between the final thermochemical data calculated with GA parameters and the *ab initio* reference dataset (CBSQB3) for the S° values of the toluene derivatives in the final set, $\Delta S°$((NNI+GAV)-CBSQB3).

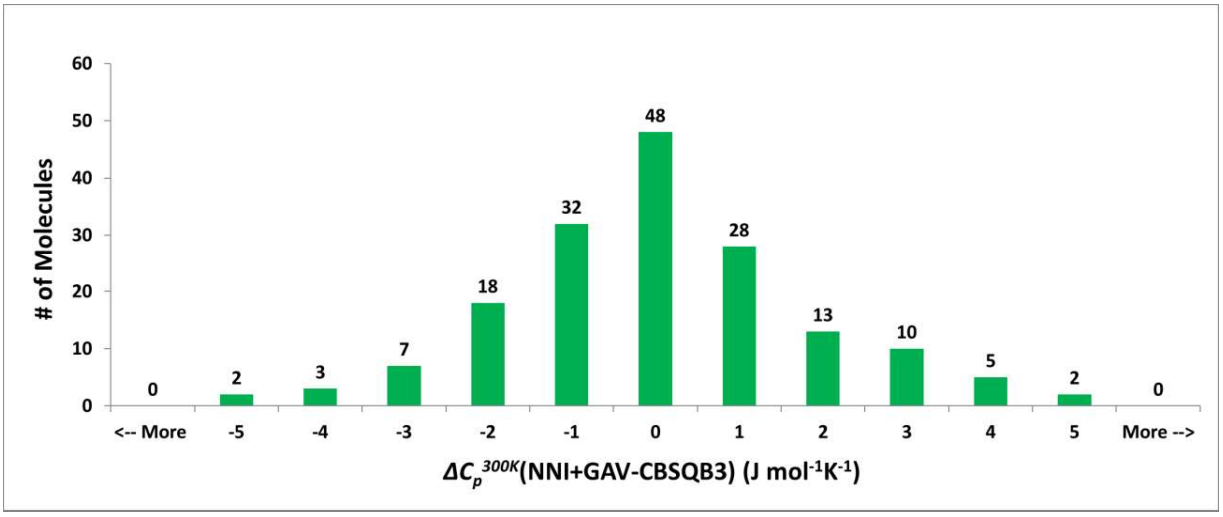

Figure C-34 Distribution of the differences between the final thermochemical data calculated with GA parameters and the *ab initio* reference dataset (CBSQB3) for the $C_p^{\mathbf{300K}}$ values of the toluene derivatives in the final set, ΔC_p^{300K}((NNI+GAV)-CBSQB3).

C.5 Group Additive Based Parameter Development for Benzylic Radicals

C.5.1 Preliminary GAVs and Identification of NNIs

Table C-14 Preliminary GAVs assignments for specific groups used in the description of different benzylic radical classes. Note that the uncertainties are the same for all groups, as each of these GAVs are derived from the same number of molecules.

GAVs	$\Delta_f H^\circ$ [kJ mol^{-1}]	S° [J mol^{-1} K^{-1}]	C_p [J mol^{-1} K^{-1}]						
			300 K	400 K	500 K	600 K	800 K	1000 K	1500 K
Ċ-(C$_b$)(C)$_2$	147.0 ± 2.9	-40.0 ± 2.24	16.3 ± 1.52	19.9 ± 1.3	22.5 ± 1.1	24.5 ± 0.95	27.2 ± 0.76	28.6 ± 0.66	28.7 ± 0.6
Ċ-(C$_b$)(C$_d$)(H)	93.0 ± 2.9	18.4 ± 2.24	23.8 ± 1.52	30.9 ± 1.3	35.7 ± 1.1	39.0 ± 0.95	43.1 ± 0.76	45.7 ± 0.66	48 ± 0.6
Ċ-(C$_b$)(C$_d$)(C)	110.8 ± 2.9	-58 ± 2.24	21.0 ± 1.52	28.0 ± 1.3	31.4 ± 1.1	33.0 ± 0.95	34.1 ± 0.76	33.8 ± 0.66	31.1 ± 0.6
Ċ-(C$_b$)(C$_d$)$_2$	81.4 ± 2.9	-69.2 ± 2.24	24.0 ± 1.52	30.1 ± 1.3	33.4 ± 1.1	35.4 ± 0.95	37.1 ± 0.76	37.4 ± 0.66	35.1 ± 0.6
Ċ-(C$_b$)$_2$(H)	116.0 ± 2.9	29.0 ± 2.24	26.1 ± 1.52	32.4 ± 1.3	36.5 ± 1.1	39.0 ± 0.95	41.1 ± 0.76	41.7 ± 0.66	41.2 ± 0.6
Ċ-(C$_b$)$_2$(C)	132.6 ± 2.9	-52.3 ± 2.24	26.7 ± 1.52	28.8 ± 1.3	30.1 ± 1.1	30.2 ± 0.95	29.2 ± 0.76	28.0 ± 0.66	23.9 ± 0.6

Table C-15 Deviations between the thermochemical data obtained from group additivity and *ab initio* calculations for the trainings set of benzylic radicals, where group additive data is calculated based on the preliminary GAVs given in **Table C-14**.

Molecule #		$\Delta_f H^\circ$ [kJ mol^{-1}]			S° [J mol^{-1} K^{-1}]			C_p [J mol^{-1} K^{-1}]		
		Reference Data	GA	GA-Reference Data[a]	Reference Data	GA	GA-Reference Data[a]	Reference Data	GA	GA-Reference Data[a]
1	BRT1/1	148.6	150.0	1.4	421.9	423.1	1.2	144.4	144.7	0.3
2	BRT1/2	-19.5	-27.7	-8.2	451.6	450.8	-0.8	165.2	168.1	2.9
3	BRT1/3	-31.7	-27.7	4.0	452.9	450.7	-2.1	164.4	168.2	3.7
4	BRT1/4	-29.5	-27.7	1.8	452.5	450.8	-1.7	165.4	168.1	2.7
5	BRT1/5	4.2	-6.7	-10.8	492.7	493.2	0.5	189.7	189.1	-0.6
6	BRT1/6	-6.9	-6.7	0.2	494.5	493.1	-1.3	187.1	189.1	2.0
7	BRT1/7	-6.1	-6.7	-0.6	493.3	493.2	-0.1	186.5	189.1	2.6
8	BRT1/8	49.0	35.2	-13.8	466.9	470.2	3.4	184.2	175.1	-9.1
9	BRT1/9	27.8	29.6	1.8	470.1	470.2	0.2	172.5	175.1	2.6
10	BRT1/10	19.9	24.6	4.7	469.3	470.2	1.0	171.9	175.2	3.2
11	BRT1/11	234.2	222.7	-11.5	480.9	480.9	0.1	197.4	182.5	-14.9
12	BRT1/12	212.3	216.2	3.9	480.1	480.9	0.9	182.3	182.6	0.2

13	**BRT1/13**	204.5	210.1	5.6	482.4	480.9	-1.4	181.9	182.5	0.6
14	**BRT1/14**	140.2	119.9	-20.3	463.8	467.9	4.2	172.9	167.5	-5.4
15	**BRT1/15**	115.8	117.1	1.3	466.9	468.0	1.1	166.0	167.5	1.5
16	**BRT1/16**	115.8	117.1	1.3	469.0	468.0	-1.0	164.8	167.5	2.7
17	**BRT1/17**	120.9	99.3	-21.6	505.4	506.5	1.2	194.0	192.5	-1.6
18	**BRT1/18**	95.3	96.4	1.1	507.9	506.6	-1.3	189.5	192.5	2.9
19	**BRT1/19**	95.0	96.4	1.4	510.0	506.5	-3.4	189.5	192.4	2.9
20	**BRT2/1**	246.4	246.7	0.2	376.5	376.4	-0.1	139.7	140.0	0.3
21	**BRT2/2**	68.9	68.9	-0.1	404.0	404.1	0.1	166.8	163.4	-3.4
22	**BRT2/3**	63.4	68.9	5.4	406.7	404.1	-2.6	161.2	163.4	2.2
23	**BRT2/4**	67.2	68.9	1.6	405.2	404.1	-1.1	160.6	163.5	2.8
24	**BRT2/5**	91.3	89.9	-1.4	442.6	446.4	3.9	186.2	184.5	-1.8
25	**BRT2/6**	87.3	89.9	2.6	450.9	446.5	-4.4	181.3	184.4	3.1
26	**BRT2/7**	90.2	89.9	-0.3	449.2	446.4	-2.7	181.9	184.4	2.5
27	**BRT2/8**	134.0	126.1	-7.9	416.2	423.6	7.4	172.1	170.4	-1.7
28	**BRT2/9**	126.8	126.1	-0.7	429.4	423.5	-5.8	168.8	170.4	1.6
29	**BRT2/10**	122.6	126.1	3.5	425.5	423.5	-1.9	168.6	170.4	1.8
30	**BRT2/11**	319.4	312.7	-6.7	431.9	434.3	2.4	184.7	177.9	-6.9
31	**BRT2/12**	310.7	312.7	2.0	435.4	434.3	-1.1	177.3	177.8	0.5
32	**BRT2/13**	305.0	312.7	7.7	435.2	434.2	-0.9	177.2	177.9	0.6
33	**BRT2/14**	217.7	213.5	-4.2	414.2	421.2	7.1	168.2	162.9	-5.4
34	**BRT2/15**	212.3	213.5	1.2	421.8	421.3	-0.5	162.1	162.9	0.7
35	**BRT2/16**	213.2	213.5	0.3	420.8	421.3	0.5	161.2	162.9	1.6
36	**BRT2/17**	197.6	192.9	-4.7	452.1	459.8	7.8	190.4	187.7	-2.7
37	**BRT2/18**	192.8	192.9	0.1	461.5	459.9	-1.6	186.1	187.8	1.6
38	**BRT2/19**	192.4	192.9	0.5	465.8	459.9	-5.9	186.0	187.7	1.7
39	**BRT3/1**	218.7	222.1	3.4	425.3	427.2	1.9	162.5	162.5	0.1
40	**BRT3/2**	42.9	44.3	1.4	450.9	454.9	4.0	190.0	186.0	-4.0
41	**BRT3/3**	39.8	44.3	4.5	454.8	455.0	0.1	183.4	186.0	2.6
42	**BRT3/4**	39.7	44.3	4.6	453.2	454.9	1.7	182.6	186.0	3.4
43	**BRT3/5**	74.3	65.3	-8.9	495.4	497.3	1.9	211.1	206.9	-4.1
44	**BRT3/6**	61.7	65.3	3.7	497.9	497.3	-0.6	204.5	207.0	2.5
45	**BRT3/7**	62.5	65.3	2.9	499.8	497.3	-2.5	205.4	206.9	1.6
46	**BRT3/8**	115.0	101.5	-13.4	472.0	474.4	2.4	199.6	193.0	-6.6
47	**BRT3/9**	98.1	101.5	3.5	478.6	474.5	-4.2	190.9	193.0	2.1
48	**BRT3/10**	95.1	101.5	6.5	479.0	474.5	-4.6	189.4	193.0	3.6
49	**BRT3/11**	295.6	288.1	-7.4	481.7	485.1	3.4	204.0	200.4	-3.6
50	**BRT3/12**	285.3	288.1	2.9	488.4	485.1	-3.3	200.3	200.4	0.1
51	**BRT3/13**	278.2	288.1	10.0	484.4	485.1	0.7	198.7	200.4	1.7
52	**BRT3/14**	202.3	188.9	-13.3	466.9	472.1	5.2	187.5	185.4	-2.1
53	**BRT3/15**	185.4	188.9	3.6	476.1	472.1	-4.0	184.9	185.3	0.5

54	BRT3/16	186.0	188.9	3.0	476.3	472.2	-4.2	184.2	185.3	1.2
55	BRT3/17	180.9	168.3	-12.5	507.1	510.7	3.6	212.2	210.3	-1.9
56	BRT3/18	165.0	168.3	3.4	510.5	510.8	0.2	209.6	210.3	0.7
57	BRT3/19	165.5	168.3	2.9	513.1	510.8	-2.4	207.8	210.3	2.5
58	BRT4/1	299.9	297.9	-2.1	444.9	437.6	-7.3	181.4	179.3	-2.1
59	BRT4/2	107.7	120.0	12.3	458.3	465.3	7.0	201.9	202.8	0.8
60	BRT4/3	119.3	120.0	0.7	472.9	465.3	-7.6	202.4	202.7	0.3
61	BRT4/4	122.0	120.0	-2.0	469.1	465.3	-3.8	201.7	202.8	1.0
62	BRT4/5	145.1	141.1	-4.0	499.7	507.7	8.0	229.3	223.8	-5.6
63	BRT4/6	141.8	141.1	-0.7	512.4	507.7	-4.7	222.7	223.8	1.0
64	BRT4/7	142.5	141.1	-1.4	516.3	507.7	-8.6	223.2	223.8	0.5
65	BRT4/8	168.3	177.3	9.0	471.8	484.8	13.0	206.5	209.8	3.2
66	BRT4/9	180.1	177.3	-2.8	492.6	484.8	-7.8	209.1	209.7	0.6
67	BRT4/10	181.8	177.3	-4.5	493.6	484.8	-8.8	207.3	209.7	2.4
68	BRT4/11	357.0	363.9	6.9	478.6	495.5	16.9	215.6	217.1	1.5
69	BRT4/12	366.3	363.9	-2.4	502.0	495.5	-6.5	218.4	217.1	-1.3
70	BRT4/13	365.8	363.9	-1.9	497.7	495.5	-2.2	216.4	217.2	0.7
71	BRT4/14	259.2	264.7	5.5	467.3	482.5	15.2	202.5	202.1	-0.4
72	BRT4/15	268.3	264.7	-3.6	489.2	482.5	-6.7	202.7	202.1	-0.6
73	BRT4/16	268.6	264.7	-3.9	488.7	482.5	-6.2	202.7	202.1	-0.6
74	BRT4/17	243.6	244.1	0.5	504.3	521.1	16.8	228.7	227.0	-1.7
75	BRT4/18	247.6	244.1	-3.5	524.5	521.1	-3.4	226.9	227.0	0.1
76	BRT4/19	246.6	244.1	-2.5	524.4	521.1	-3.3	227.6	227.1	-0.6
77	BRT5/1	300.6	300.0	-0.6	446.3	447.9	1.6	180.0	180.7	0.7
78	BRT5/2	116.2	122.2	6.0	474.2	475.6	1.4	207.6	204.1	-3.5
79	BRT5/3	121.6	122.2	0.6	475.3	475.5	0.3	204.0	204.1	0.1
80	BRT5/4	121.2	122.2	1.0	475.0	475.6	0.6	201.0	204.1	3.1
81	BRT5/5	144.1	143.3	-0.8	508.6	518.0	9.4	227.8	225.1	-2.7
82	BRT5/6	142.2	143.3	1.1	522.1	518.0	-4.1	220.8	225.1	4.3
83	BRT5/7	142.3	143.3	1.0	522.1	518.0	-4.1	220.8	225.1	4.3
84	BRT5/8	185.6	179.5	-6.1	492.8	495.1	2.3	216.3	211.1	-5.2
85	BRT5/9	180.3	179.5	-0.8	497.0	495.1	-1.9	208.6	211.1	2.5
86	BRT5/10	176.2	179.5	3.3	496.2	495.1	-1.1	208.3	211.1	2.8
87	BRT5/11	372.2	366.1	-6.1	503.6	505.8	2.2	220.4	218.5	-1.9
88	BRT5/12	364.0	366.1	2.1	509.1	505.8	-3.3	217.8	218.5	0.7
89	BRT5/13	359.3	366.1	6.8	507.2	505.7	-1.4	218.0	218.5	0.5
90	BRT5/14	269.4	266.9	-2.5	487.1	492.8	5.7	210.1	203.5	-6.6
91	BRT5/15	267.4	266.9	-0.5	496.5	492.8	-3.7	201.9	203.5	1.6
92	BRT5/16	267.4	266.9	-0.5	495.9	492.8	-3.1	201.8	203.5	1.7
93	BRT5/17	249.0	246.3	-2.7	526.1	531.4	5.3	234.5	228.4	-6.1
94	BRT5/18	246.8	246.3	-0.5	533.4	531.3	-2.0	226.6	228.4	1.8

95	**BRT5/19**	247.0	246.3	-0.7	534.8	531.4	-3.4	226.5	228.4	1.9
96	**BRT6/1**	273.8	273.7	-0.2	493.6	493.7	0.0	206.9	206.6	-0.3
97	**BRT6/2**	86.8	95.9	9.0	518.8	521.4	2.5	228.2	229.9	1.8
98	**BRT6/3**	93.8	95.9	2.0	523.6	521.3	-2.3	229.2	230.0	0.8
99	**BRT6/4**	93.4	95.9	2.4	524.5	521.3	-3.2	223.2	229.9	6.8
100	**BRT6/5**	121.5	116.9	-4.6	554.6	563.7	9.1	261.2	250.9	-10.2
101	**BRT6/6**	115.7	116.9	1.2	565.2	563.7	-1.5	250.2	251.0	0.8
102	**BRT6/7**	116.3	116.9	0.6	563.7	563.7	0.0	247.3	251.0	3.7
103	**BRT6/8**	164.3	153.1	-11.2	542.7	540.8	-1.9	238.4	236.9	-1.4
104	**BRT6/9**	152.3	153.1	0.8	546.2	540.9	-5.4	237.2	237.0	-0.2
105	**BRT6/10**	148.4	153.1	4.7	543.0	540.9	-2.2	237.2	236.9	-0.2
106	**BRT6/11**	343.7	339.7	-4.0	548.7	551.6	2.8	247.6	244.4	-3.2
107	**BRT6/12**	336.5	339.7	3.2	551.4	551.5	0.1	246.1	244.4	-1.7
108	**BRT6/13**	332.6	339.7	7.1	552.0	551.6	-0.5	246.8	244.3	-2.4
109	**BRT6/14**	247.4	240.5	-6.9	538.2	538.5	0.3	229.2	229.4	0.2
110	**BRT6/15**	239.8	240.5	0.7	539.3	538.5	-0.8	228.8	229.3	0.6
111	**BRT6/16**	240.6	240.5	-0.1	537.7	538.5	0.8	228.9	229.4	0.5
112	**BRT6/17**	225.4	219.9	-5.5	573.2	577.2	3.9	252.9	254.2	1.4
113	**BRT6/18**	219.8	219.9	0.1	579.9	577.1	-2.8	251.5	254.3	2.8
114	**BRT6/19**	219.9	219.9	0.0	576.7	577.2	0.4	253.4	254.3	0.9

[a] **GA- Reference Data**: If the absolute value of this difference is significantly high regardless of its sign, it points out to the need of a NNI correction. A positive difference shows that the *ab initio* data for that specific molecule is lower than the group additively calculated data, which means that a negative correction is needed and vice versa.

C.5.2 Initial simultaneous optimization of GAVs and NNIs

Table C-16 NNI parameters used to correct for the interactions between two substituent groups, taken from **Chapter 4**.

Interaction[a]	$\Delta_f H^\circ$ [kJ mol^{-1}]	S° [J mol^{-1} K^{-1}]	C_p [J mol^{-1} K^{-1}]						
			300 K	400 K	500 K	600 K	800 K	1000 K	1500 K
o-CH_2•/ C•HCH_3+ CHO	5.6	2.1	1.8	2.1	1.8	1.2	0.4	-0.2	-0.5
o-CH_2•/ C•HCH_3+ $CH=CH_2$	6.5	-1.0	2.3	1.2	0.6	0.1	-0.5	-0.7	-0.7
o-CH_2•/ C•HCH_3+ CH_3/CH_2CH_3	2.9	-3.8	3.8	2.6	1.8	1.2	0.5	0.3	0.0
p-CH_2•/ C•HCH_3+ $CH=CH_2$	-5.0	0.8	-1.8	-0.9	-0.6	-0.4	-0.3	-0.1	0.3
p-CH_2•/ C•HCH_3+ CH_3/CH_2CH_3	-6.2	-4.7	0.3	1.1	1.2	1.4	1.6	1.6	1.3

[a] The interactions between two substituents are given in the following format: **a-X + Y** where **a-** reflects the relative positioning of the two substituents, which can be *ortho (o-), meta (m-)* or *para (p-)*, **X** and **Y** are the two substituent groups separated by a plus sign (+).

Table C-17 Comparison of the differences between the reference dataset and the group additively calculated data for unsubstituted and substituted isopropylbenzenes with the previously reported NNIs for toluenes/ethylbenzenes.

Substituents on 2-phenyl-2-propyl	$\Delta_f H^\circ$ [kJ mol^{-1}]		S° [J mol^{-1} K^{-1}]	
	CBS-GAV[a]	NNI[b]	CBS-GAV[a]	NNI[b]
***o*-OH**	8.2	-	0.8	-
***o*-OCH_3**	10.8	-	-0.5	-
***o*-CHO**	13.8	5.5	-3.4	1.9
***o*-$CH=CH_2$**	11.5	6.7	-0.1	-0.5
***o*-CH_3**	20.3	2.7	-4.2	-3.6
***o*-CH_2CH_3**	21.6	2.7	-1.2	-3.6
***p*-CHO**	-4.7	-5.2	-1.0	0.6
***p*-$CH=CH_2$**	-5.6	-5.8	-1.4	-3.7

[a] **Reference Data-GA**: The differences are given in the form of "**–(GA-Reference Data)**" to be able to compare these differences with the reported non-nearest neighbor interaction corrections.
[b] The NNIs are taken from **Chapter 4**.

Table C-18 GAVs obtained from the simultaneous optimization of GAVs and NNIs using the training set of benzylic radicals.

GAVs	$\Delta_f H^\circ$	S°	C_p [J mol^{-1} K^{-1}]						
	[kJ mol^{-1}]	[J mol^{-1} K^{-1}]	300 K	400 K	500 K	600 K	800 K	1000 K	1500 K
Ċ-(C_b)(C)$_2$	141.7 ± 0.98	-40.1 ± 1.16	14.8 ± 1.09	19.4 ± 0.95	22.0 ± 0.81	24.1 ± 0.73	27.1 ± 0.71	28.8 ± 0.67	29.4 ± 0.52
Ċ-(C_b)(C_d)(H)	91.5 ± 0.95	20.1 ± 1.12	22.7 ± 1.05	30.1 ± 0.92	34.5 ± 0.78	37.9 ± 0.70	42.3 ± 0.68	45.1 ± 0.64	47.8 ± 0.50
Ċ-(C_b)(C_d)(C)	107.3 ± 1.01	-56.3 ± 1.19	19.1 ± 1.12	27.4 ± 0.98	31.1 ± 0.83	32.6 ± 0.75	34.1 ± 0.73	34 ± 0.69	35.3 ± 0.54
Ċ-(C_b)(C_d)$_2$	83.8 ± 0.98	-63.3 ± 1.16	23.9 ± 1.09	30.8 ± 0.95	33.1 ± 0.81	34.8 ± 0.73	36.6 ± 0.71	37 ± 0.67	37.1 ± 0.52
Ċ-(C_b)$_2$(H)	115.4 ± 0.93	31.0 ± 1.1	24.7 ± 1.03	31.9 ± 0.9	36.2 ± 0.77	38.6 ± 0.69	41.1 ± 0.67	41.6 ± 0.63	41.9 ± 0.49
Ċ-(C_b)$_2$(C)	131.9 ± 0.93	-51.4 ± 1.1	25.2 ± 1.03	29.3 ± 0.9	30.9 ± 0.77	31.1 ± 0.69	30.6 ± 0.67	31.7 ± 0.63	31.8 ± 0.49

Table C-19 NNIs values obtained from the simultaneous optimization of GAVs and NNIs using the training set of benzylic radicals.

NNIs	$\Delta_f H^\circ$	S°	C_p [J mol^{-1} K^{-1}]						
	[kJ mol^{-1}]	[J mol^{-1} K^{-1}]	300 K	400 K	500 K	600 K	800 K	1000 K	1500 K
NNIBR1	11.7 ± 2.69	-0.2 ± 3.17	1.0 ± 2.97	-2.5 ± 2.6	-2.4 ± 2.21	-2.0 ± 2.00	-1.5 ± 1.94	-1.4 ± 1.83	-1.8 ± 1.42
NNIBR2	21.6 ± 3.67	-0.2 ± 4.34	11.7± 4.06	7.7 ± 3.56	4.8 ± 3.02	2.7 ± 2.73	-0.4 ± 2.65	-2.4 ± 2.51	-4.5 ± 1.95
NNIBR3	20.2 ± 3.67	-0.5 ± 4.34	17.0 ± 4.06	13.9 ± 3.56	11.1 ± 3.02	8.7 ± 2.73	4.8 ± 2.65	2.3 ± 2.50	-1.0 ± 1.95
NNIBR4	26.0 ± 2.69	-3.1 ± 3.17	5.6 ± 2.97	4.3 ± 2.6	3.0 ± 2.21	2.0 ± 2.01	0.3 ± 1.94	-0.8 ± 1.83	-2.6 ± 1.42
NNIBR5	5.9 ± 1.84	-7.5 ± 2.18	4.8 ± 2.04	4.2 ± 1.79	4.2 ± 1.52	4.0 ± 1.37	3.0 ± 1.33	2.1 ± 1.25	0.5 ± 0.98
NNIBR6	2.1 ± 3.68	-5.7 ± 4.35	5.9 ± 4.07	4 ± 3.56	2.5 ± 3.03	1.5 ± 2.74	0.1 ± 2.65	-0.3 ± 2.50	-0.1 ± 1.95
NNIBR7	14.6 ± 1.88	-5 ± 2.22	5.6 ± 2.08	3.3 ± 1.82	1.8 ± 1.54	0.8 ± 1.4	-0.4 ± 1.35	-1.0 ± 1.28	-1.0 ± 1.01
NNIBR8	-4.8 ± 1.57	-0.1 ± 1.85	0.6 ± 1.74	0.6 ± 1.52	0.8 ± 1.29	0.8 ± 1.17	1.0 ± 1.13	1.1 ± 1.07	1.1 ± 0.83
NNIBR9	-14.3 ± 3.67	-14.6 ± 4.34	5.7 ± 4.06	1.4 ± 3.56	2.8 ± 3.02	3.3 ± 2.73	2.8 ± 2.65	1.9 ± 2.50	1.1 ± 1.95
NNIBR10	1.6 ± 3.67	-5.5 ± 4.34	6.2 ± 4.06	1.7 ± 3.56	1.5 ± 3.02	0.9 ± 2.73	0.3 ± 2.65	0.5 ± 2.50	3.7 ± 1.95
NNIBR11	-5.9 ± 2.02	-20.3 ± 2.39	-1.7 ± 2.24	0.6 ± 1.96	1.6 ± 1.66	1.8 ± 1.51	1.4 ± 1.46	1.4 ± 1.38	3.5 ± 1.07
NNIBR12	-5.8 ± 2.61	-4 ± 3.08	0 ± 2.88	0.5 ± 2.53	1.4 ± 2.14	2.1 ± 1.94	2.6 ± 1.88	2.4 ± 1.77	1.5 ± 1.38
NNIBR13	3.3 ± 2.61	-10.9 ± 3.08	7.9 ± 2.88	6.4 ± 2.53	6.4 ± 2.14	6 ± 1.94	4.6 ± 1.88	3.3 ± 1.77	1.6 ± 1.38
NNIBR14	6.8 ± 1.45	-3.6 ± 1.71	5.3 ± 1.6	3.8 ± 1.41	3 ± 1.19	2.5 ± 1.08	2.3 ± 1.05	1.8 ± 0.99	0.8 ± 0.77

Table C-20 Deviations between data obtained from group additivity and *ab initio* calculations before and after the inclusion of newly derived NNI parameters, where group additive data is calculated based on the simultaneously optimized GAVs and NNIs given in **Table C-18** and **Table C-19**, respectively.

Radical #		$\Delta_f H^\circ$ [kJ mol^{-1}]					S° [J mol^{-1} K^{-1}]					C_p [J mol^{-1} K^{-1}]				
		CBS[a]	Bef. new NNIs[b]	Af. new NNIs[c]	Δ(Bef. new NNIs)[d]	Δ(Af. new NNIs)[e]	CBS[a]	Bef. new NNIs[b]	Af. new NNIs[c]	Δ(Bef. new NNIs)[d]	Δ(Af. new NNIs)[e]	CBS[a]	Bef. new NNIs[b]	Af. new NNIs[c]	Δ(Bef. new NNIs)[d]	Δ(Af. new NNIs)[e]
1	**BRT1/1**	148.6	147.9	147.9	-0.7	-0.7	421.9	423.7	423.7	1.8	1.8	144.4	142.6	142.6	-1.8	-1.8
2	**BRT1/2**	-19.5	-29.9	-18.2	-10.4	1.3	451.6	451.5	451.3	-0.1	-0.3	165.2	166.0	167.0	0.8	1.8
3	**BRT1/3**	-31.7	-29.9	-29.9	1.8	1.8	452.9	451.5	451.5	-1.3	-1.3	164.4	166.0	166.0	1.5	1.5
4	**BRT1/4**	-29.5	-29.9	-29.9	-0.4	-0.4	452.5	451.5	451.5	-1.0	-1.0	165.4	166.0	166.0	0.6	0.6
5	**BRT1/5**	4.2	-8.8	2.9	-13.0	-1.3	492.7	494.0	493.8	1.3	1.0	189.7	187.0	188.0	-2.7	-1.7
6	**BRT1/6**	-6.9	-8.8	-8.8	-2.0	-2.0	494.5	494.0	494.0	-0.5	-0.5	187.1	187.0	187.0	-0.1	-0.1
7	**BRT1/7**	-6.1	-8.8	-8.8	-2.8	-2.8	493.3	494.0	494.0	0.7	0.7	186.5	187.0	187.0	0.5	0.5
8	**BRT1/8**	49.0	27.4	49.0	-21.6	0.0	470.5	470.7	470.5	0.2	0.0	184.7	173.0	184.7	-11.7	0.0
9	**BRT1/9**	27.8	27.4	27.4	-0.4	-0.4	470.1	470.7	470.7	0.6	0.6	172.5	173.0	173.0	0.5	0.5
10	**BRT1/10**	19.9	27.4	22.2	7.5	2.3	469.3	470.7	471.3	1.5	2.1	171.9	173.0	171.4	1.0	-0.6
11	**BRT1/11**	234.2	214.0	234.2	-20.1	0.0	480.9	481.9	481.4	1.1	0.6	197.4	180.4	197.9	-17.0	0.5
12	**BRT1/12**	212.3	214.0	214.0	1.8	1.8	480.1	481.9	481.9	1.8	1.8	182.3	180.4	180.4	-1.9	-1.9
13	**BRT1/13**	204.5	214.0	208.2	9.6	3.8	476.2	481.9	478.2	5.7	2.0	181.7	180.4	180.7	-1.4	-1.1
14	**BRT1/14**	140.2	114.9	140.9	-25.3	0.7	463.8	468.7	465.7	5.0	1.9	172.9	165.1	171.1	-7.8	-1.8
15	**BRT1/15**	115.8	114.9	114.9	-0.9	-0.9	466.9	468.7	468.7	1.8	1.8	166.0	165.1	165.1	-0.9	-0.9
16	**BRT1/16**	115.8	114.9	114.9	-0.9	-0.9	469.0	468.7	468.7	-0.3	-0.3	164.8	165.1	165.1	0.3	0.3
17	**BRT1/17**	120.9	94.2	120.2	-26.6	-0.6	505.4	507.1	504.1	1.8	-1.3	194.0	190.3	196.3	-3.8	2.3
18	**BRT1/18**	95.3	94.2	94.2	-1.0	-1.0	507.9	507.1	507.1	-0.8	-0.8	189.5	190.3	190.3	0.8	0.8
19	**BRT1/19**	95.0	94.2	94.2	-0.7	-0.7	510.0	507.1	507.1	-2.8	-2.8	189.5	190.3	190.3	0.8	0.8
20	**BRT2/1**	246.4	245.6	245.6	-0.8	-0.8	376.5	378.2	378.2	1.7	1.7	139.7	139.0	139.0	-0.7	-0.7
21	**BRT2/2**	68.7	67.9	67.9	-0.9	-0.9	404.0	406.0	406.0	2.0	2.0	166.8	162.4	162.4	-4.4	-4.4
22	**BRT2/3**	63.4	67.9	67.9	4.4	4.4	406.4	406.0	406.0	-0.4	-0.4	162.1	162.4	162.4	0.2	0.2
23	**BRT2/4**	67.2	67.9	67.9	0.6	0.6	405.2	406.0	406.0	0.8	0.8	160.6	162.4	162.4	1.8	1.8
24	**BRT2/5**	91.3	88.9	94.8	-2.3	3.6	442.6	448.4	441.0	5.9	-1.6	186.2	183.4	188.1	-2.8	1.9
25	**BRT2/6**	87.3	88.9	88.9	1.7	1.7	450.9	448.4	448.4	-2.5	-2.5	181.3	183.4	183.4	2.1	2.1
26	**BRT2/7**	90.2	88.9	88.9	-1.2	-1.2	449.2	448.4	448.4	-0.7	-0.7	181.9	183.4	183.4	1.5	1.5
27	**BRT2/8**	134.0	125.1	131.0	-8.8	-2.9	416.2	425.2	417.7	9.0	1.5	172.1	169.4	174.1	-2.7	2.1
28	**BRT2/9**	126.8	125.1	125.1	-1.6	-1.6	429.4	425.2	425.2	-4.2	-4.2	169.7	169.4	169.4	-0.3	-0.3
29	**BRT2/10**	122.7	125.1	119.9	2.5	-2.7	425.5	425.2	425.8	-0.3	0.3	168.6	169.4	167.8	0.8	-0.8
30	**BRT2/11**	319.4	311.8	317.7	-7.6	-1.7	431.9	436.4	428.9	4.5	-3.0	184.7	176.8	181.5	-7.9	-3.2
31	**BRT2/12**	310.7	311.8	311.8	1.1	1.1	435.4	436.4	436.4	1.0	1.0	177.3	176.8	176.8	-0.5	-0.5
32	**BRT2/13**	305.0	311.8	306.0	6.8	1.0	435.2	436.4	432.7	1.2	-2.5	177.2	176.8	177.1	-0.5	-0.2

33	**BRT2/14**	217.7	212.6	218.5	-5.1	0.9	414.2	423.2	415.7	9.0	1.5	168.2	161.5	166.2	-6.8	-2.0
34	**BRT2/15**	212.3	212.6	212.6	0.3	0.3	421.8	423.2	423.2	1.3	1.3	162.1	161.5	161.5	-0.6	-0.6
35	**BRT2/16**	213.2	212.6	212.6	-0.6	-0.6	420.8	423.2	423.2	2.4	2.4	161.2	161.5	161.5	0.2	0.2
36	**BRT2/17**	197.6	192.0	197.9	-5.6	0.3	452.1	461.6	454.1	9.5	2.1	190.4	186.7	191.4	-3.7	1.1
37	**BRT2/18**	192.8	192.0	192.0	-0.8	-0.8	461.5	461.6	461.6	0.1	0.1	186.1	186.7	186.7	0.6	0.6
38	**BRT2/19**	192.5	192.0	192.0	-0.5	-0.5	459.7	461.6	461.6	1.9	1.9	186.8	186.7	186.7	-0.1	-0.1
39	**BRT3/1**	218.7	218.5	218.5	-0.2	-0.2	425.3	429.0	429.0	3.7	3.7	162.5	160.7	160.7	-1.7	-1.7
40	**BRT3/2**	42.9	40.7	42.9	-2.2	0.0	450.9	456.8	451.1	5.9	0.2	190.0	184.1	190.0	-5.9	0.0
41	**BRT3/3**	39.8	40.7	40.7	0.9	0.9	454.8	456.8	456.8	2.0	2.0	183.4	184.1	184.1	0.7	0.7
42	**BRT3/4**	39.7	40.7	40.7	1.0	1.0	453.2	456.8	456.8	3.6	3.6	182.6	184.1	184.1	1.5	1.5
43	**BRT3/5**	74.3	61.8	76.5	-12.4	2.2	495.4	499.3	494.3	3.9	-1.1	211.1	205.1	210.7	-5.9	-0.4
44	**BRT3/6**	61.7	61.8	61.8	0.2	0.2	497.9	499.3	499.3	1.4	1.4	204.5	205.1	205.1	0.7	0.7
45	**BRT3/7**	62.5	61.8	61.8	-0.6	-0.6	499.8	499.3	499.3	-0.5	-0.5	205.4	205.1	205.1	-0.2	-0.2
46	**BRT3/8**	115.0	98.0	112.7	-16.9	-2.3	472.0	476.0	471.0	4.1	-0.9	199.6	191.1	196.7	-8.4	-2.9
47	**BRT3/9**	98.1	98.0	98.0	0.0	0.0	478.6	476.0	476.0	-2.6	-2.6	190.9	191.1	191.1	0.2	0.2
48	**BRT3/10**	95.1	98.0	93.2	3.0	-1.9	479.0	476.0	475.9	-3.0	-3.1	189.4	191.1	191.8	1.7	2.3
49	**BRT3/11**	295.6	284.7	299.3	-10.9	3.7	481.7	487.2	482.2	5.5	0.5	204.0	198.5	204.1	-5.5	0.1
50	**BRT3/12**	284.6	284.7	284.7	0.1	0.1	489.0	487.2	487.2	-1.8	-1.8	199.3	198.5	198.5	-0.8	-0.8
51	**BRT3/13**	278.2	284.7	279.8	6.5	1.7	484.4	487.2	487.1	2.9	2.7	198.7	198.5	199.2	-0.1	0.5
52	**BRT3/14**	202.3	185.5	200.1	-16.8	-2.1	466.9	474.0	469.0	7.1	2.1	187.5	183.2	188.8	-4.2	1.3
53	**BRT3/15**	185.4	185.5	185.5	0.1	0.1	476.1	474.0	474.0	-2.1	-2.1	184.9	183.2	183.2	-1.6	-1.6
54	**BRT3/16**	186.0	185.5	185.5	-0.5	-0.5	476.3	474.0	474.0	-2.3	-2.3	184.2	183.2	183.2	-0.9	-0.9
55	**BRT3/17**	180.9	164.9	179.5	-16.0	-1.4	507.1	512.4	507.4	5.4	0.4	212.2	208.4	214.0	-3.8	1.8
56	**BRT3/18**	165.0	164.9	164.9	-0.1	-0.1	510.5	512.4	512.4	1.9	1.9	209.6	208.4	208.4	-1.2	-1.2
57	**BRT3/19**	165.5	164.9	164.9	-0.6	-0.6	513.1	512.4	512.4	-0.7	-0.7	207.8	208.4	208.4	0.7	0.7
58	**BRT4/1**	299.9	300.2	300.2	0.3	0.3	444.9	443.5	443.5	-1.4	-1.4	181.4	179.3	179.3	-2.1	-2.1
59	**BRT4/2**	108.1	122.4	108.1	14.3	0.0	456.6	471.3	456.7	14.7	0.1	208.3	202.7	208.4	-5.6	0.1
60	**BRT4/3**	119.3	122.4	122.4	3.1	3.1	472.9	471.3	471.3	-1.6	-1.6	202.4	202.7	202.7	0.3	0.3
61	**BRT4/4**	122.0	122.4	122.4	0.4	0.4	469.1	471.3	471.3	2.2	2.2	201.7	202.7	202.7	0.9	0.9
62	**BRT4/5**	145.1	143.5	145.1	-1.6	0.0	508.1	513.8	508.3	5.7	0.2	229.8	223.7	229.9	-6.1	0.1
63	**BRT4/6**	141.8	143.5	143.5	1.7	1.7	512.4	513.8	513.8	1.4	1.4	222.7	223.7	223.7	0.9	0.9
64	**BRT4/7**	142.5	143.5	143.5	1.0	1.0	516.3	513.8	513.8	-2.6	-2.6	223.2	223.7	223.7	0.4	0.4
65	**BRT4/8**	175.5	179.7	173.8	4.2	-1.7	471.8	490.5	470.2	18.7	-1.6	206.5	209.7	208.0	3.1	1.5
66	**BRT4/9**	180.1	179.7	179.7	-0.4	-0.4	492.6	490.5	490.5	-2.1	-2.1	209.1	209.7	209.7	0.6	0.6
67	**BRT4/10**	181.8	179.7	179.7	-2.1	-2.1	493.6	490.5	490.5	-3.1	-3.1	207.3	209.7	209.7	2.4	2.4
68	**BRT4/11**	357.0	366.3	360.4	9.4	3.5	484.3	501.7	481.4	17.4	-3.0	215.6	217.1	215.4	1.5	-0.1
69	**BRT4/12**	366.3	366.3	366.3	0.1	0.1	502.0	501.7	501.7	-0.3	-0.3	218.4	217.1	217.1	-1.3	-1.3
70	**BRT4/13**	365.8	366.3	366.3	0.6	0.6	497.7	501.7	501.7	4.0	4.0	216.4	217.1	217.1	0.6	0.6
71	**BRT4/14**	260.0	267.2	261.2	7.2	1.3	465.8	488.5	468.2	22.7	2.3	198.0	201.8	200.1	3.7	2.1
72	**BRT4/15**	268.3	267.2	267.2	-1.1	-1.1	489.2	488.5	488.5	-0.7	-0.7	202.7	201.8	201.8	-0.9	-0.9
73	**BRT4/16**	268.6	267.2	267.2	-1.4	-1.4	488.7	488.5	488.5	-0.2	-0.2	202.7	201.8	201.8	-0.9	-0.9

74	**BRT4/17**	243.6	246.5	240.6	3.0	-2.9	504.3	526.9	506.6	22.6	2.3	228.7	227.0	225.3	-1.7	-3.4
75	**BRT4/18**	247.6	246.5	246.5	-1.0	-1.0	524.5	526.9	526.9	2.4	2.4	226.9	227.0	227.0	0.1	0.1
76	**BRT4/19**	247.8	246.5	246.5	-1.2	-1.2	524.4	526.9	526.9	2.5	2.5	227.6	227.0	227.0	-0.7	-0.7
77	**BRT5/1**	300.6	299.3	299.3	-1.3	-1.3	446.3	450.1	450.1	3.7	3.7	180.0	179.3	179.3	-0.8	-0.8
78	**BRT5/2**	116.2	121.5	115.7	5.3	-0.4	476.7	477.9	473.9	1.2	-2.8	202.8	202.7	202.7	-0.2	-0.1
79	**BRT5/3**	121.6	121.5	121.5	-0.1	-0.1	475.3	477.9	477.9	2.6	2.6	204.0	202.7	202.7	-1.4	-1.4
80	**BRT5/4**	121.2	121.5	121.5	0.3	0.3	475.0	477.9	477.9	2.9	2.9	201.0	202.7	202.7	1.7	1.7
81	**BRT5/5**	144.1	142.6	145.9	-1.5	1.8	508.6	520.3	509.5	11.7	0.9	227.8	223.7	231.6	-4.2	3.8
82	**BRT5/6**	142.2	142.6	142.6	0.4	0.4	522.1	520.3	520.3	-1.8	-1.8	220.8	223.7	223.7	2.9	2.9
83	**BRT5/7**	142.3	142.6	142.6	0.3	0.3	522.1	520.3	520.3	-1.8	-1.8	220.8	223.7	223.7	2.8	2.8
84	**BRT5/8**	187.1	178.8	185.6	-8.4	-1.6	492.8	497.1	493.4	4.3	0.6	216.3	209.7	215.0	-6.6	-1.3
85	**BRT5/9**	180.3	178.8	178.8	-1.6	-1.6	497.0	497.1	497.1	0.1	0.1	208.6	209.7	209.7	1.0	1.0
86	**BRT5/10**	176.2	178.8	173.9	2.5	-2.3	496.2	497.1	496.9	0.8	0.7	208.3	209.7	210.3	1.4	2.0
87	**BRT5/11**	372.2	365.4	372.2	-6.8	0.0	503.6	508.3	504.6	4.6	1.0	226.6	217.1	222.4	-9.5	-4.2
88	**BRT5/12**	364.0	365.4	365.4	1.4	1.4	509.1	508.3	508.3	-0.9	-0.9	217.8	217.1	217.1	-0.7	-0.7
89	**BRT5/13**	359.3	365.4	360.6	6.1	1.3	507.2	508.3	508.1	1.1	1.0	218.0	217.1	217.7	-0.9	-0.3
90	**BRT5/14**	271.2	266.2	273.0	-5.0	1.8	494.5	495.1	491.4	0.5	-3.1	211.7	201.8	207.1	-10.0	-4.7
91	**BRT5/15**	267.4	266.2	266.2	-1.2	-1.2	496.5	495.1	495.1	-1.5	-1.5	201.9	201.8	201.8	-0.1	-0.1
92	**BRT5/16**	267.4	266.2	266.2	-1.2	-1.2	495.9	495.1	495.1	-0.9	-0.9	201.8	201.8	201.8	-0.1	-0.1
93	**BRT5/17**	249.0	245.6	252.4	-3.4	3.4	526.1	533.5	529.8	7.3	3.7	234.5	227.0	232.3	-7.5	-2.2
94	**BRT5/18**	246.8	245.6	245.6	-1.2	-1.2	533.4	533.5	533.5	0.1	0.1	226.6	227.0	227.0	0.4	0.4
95	**BRT5/19**	247.0	245.6	245.6	-1.4	-1.4	534.8	533.5	533.5	-1.4	-1.4	226.5	227.0	227.0	0.4	0.4
96	**BRT6/1**	273.8	272.9	272.9	-0.9	-0.9	493.6	495.0	495.0	1.4	1.4	206.9	205.1	205.1	-1.8	-1.8
97	**BRT6/2**	89.1	95.1	89.4	6.0	0.3	515.5	522.8	518.8	7.3	3.4	228.4	228.5	228.5	0.1	0.2
98	**BRT6/3**	93.8	95.1	95.1	1.3	1.3	523.6	522.8	522.8	-0.8	-0.8	229.2	228.5	228.5	-0.8	-0.8
99	**BRT6/4**	93.4	95.1	95.1	1.7	1.7	524.5	522.8	522.8	-1.7	-1.7	223.2	228.5	228.5	5.3	5.3
100	**BRT6/5**	121.5	116.2	119.5	-5.2	-1.9	554.6	565.2	554.4	10.7	-0.2	261.2	249.5	257.4	-11.7	-3.7
101	**BRT6/6**	115.7	116.2	116.2	0.6	0.6	565.2	565.2	565.2	0.1	0.1	250.2	249.5	249.5	-0.8	-0.8
102	**BRT6/7**	116.3	116.2	116.2	0.0	0.0	563.7	565.2	565.2	1.6	1.6	247.3	249.5	249.5	2.2	2.2
103	**BRT6/8**	164.3	152.4	159.2	-11.8	-5.1	542.7	542.0	538.3	-0.7	-4.4	238.4	235.5	240.8	-2.9	2.4
104	**BRT6/9**	152.3	152.4	152.4	0.2	0.2	546.2	542.0	542.0	-4.3	-4.3	237.2	235.5	235.5	-1.7	-1.7
105	**BRT6/10**	148.4	152.4	147.6	4.1	-0.8	543.0	542.0	541.9	-1.1	-1.2	237.2	235.5	236.1	-1.7	-1.0
106	**BRT6/11**	343.7	339.1	345.8	-4.6	2.2	548.7	553.2	549.5	4.5	0.8	247.6	242.9	248.2	-4.7	0.6
107	**BRT6/12**	336.5	339.1	339.1	2.6	2.6	551.4	553.2	553.2	1.8	1.8	246.1	242.9	242.9	-3.3	-3.3
108	**BRT6/13**	332.6	339.1	334.2	6.5	1.7	552.0	553.2	553.1	1.2	1.0	246.8	242.9	243.5	-3.9	-3.3
109	**BRT6/14**	248.6	239.9	246.7	-8.7	-1.9	535.1	540.0	536.4	4.9	1.3	229.2	227.6	232.9	-1.6	3.7
110	**BRT6/15**	239.8	239.9	239.9	0.1	0.1	539.3	540.0	540.0	0.7	0.7	228.8	227.6	227.6	-1.2	-1.2
111	**BRT6/16**	240.6	239.9	239.9	-0.7	-0.7	537.7	540.0	540.0	2.3	2.3	228.9	227.6	227.6	-1.3	-1.3
112	**BRT6/17**	225.4	219.3	226.0	-6.1	0.7	573.2	578.4	574.8	5.2	1.5	252.9	252.8	258.1	-0.1	5.2
113	**BRT6/18**	220.4	219.3	219.3	-1.1	-1.1	577.9	578.4	578.4	0.5	0.5	253.7	252.8	252.8	-0.9	-0.9
114	**BRT6/19**	219.3	219.3	219.3	0.0	0.0	576.9	578.4	578.4	1.5	1.5	253.3	252.8	252.8	-0.5	-0.5

Statistics	$\Delta_f H^\circ$ [kJ mol^{-1}]		S° [J mol^{-1} K^{-1}]		C_p [J mol^{-1} K^{-1}] (300 K)	
Mean Absolute Deviation (MAD)	4.0	1.2	3.3	1.6	2.4	1.3
Maximum Absolute Deviation (MAX)	26.6	5.1	22.7	4.4	17.0	5.3

[a] **CBS:** Reference dataset of CBS-QB3 results with spin orbit and bond additive corrections (SOCs and BACs).
[b] **Bef. new NNIs:** Group additively calculated data based on GAVs and previously defined NNIs given in **Table C-16**, excluding the NNIs for isopropylbenzene and the new NNIs in **Table C-19**, which are defined in this paper.
[c] **Af. new NNIs:** Group additively calculated data based on GAVs and all the NNIs given in **Table C-18** and **Table C-19**, respectively.
[d] Δ(**Bef. new NNIs):** The difference between CBS and "**Bef. new NNIs**".
[e] Δ(**Af. new NNIs):** Deviation of GA calculated data from CBS-QB3.

C.5.3 Optimized structures of some benzylic radicals that are used for the explanation of physical contributions to NNIs

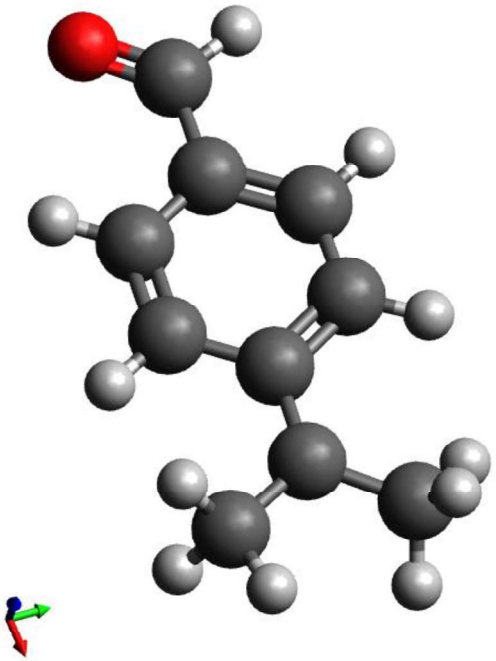

Figure C-35 Three dimensional optimized structure of *p*-CHO substituted 3-phenyl-1-propen-3-yl (molecule **BRT1/10**). (**Dark grey:** Carbon, **Light grey:** Hydrogen, **Red:** Oxygen)

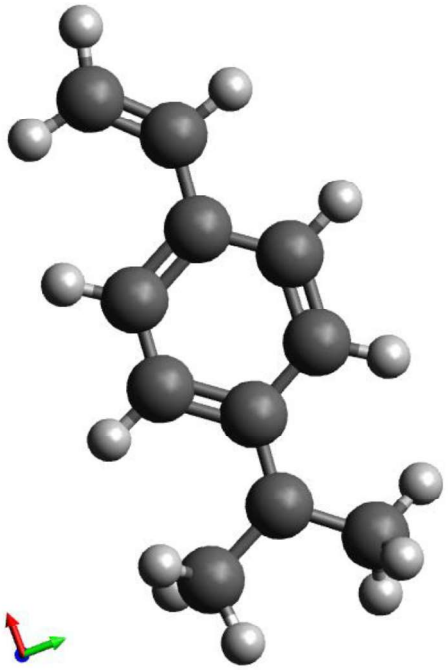

Figure C-36 Three dimensional optimized structure of *p*-CH=CH_2 substituted 3-phenyl-1-propen-3-yl (molecule **BRT1/13**). (**Dark grey:** Carbon, **Light grey:** Hydrogen)

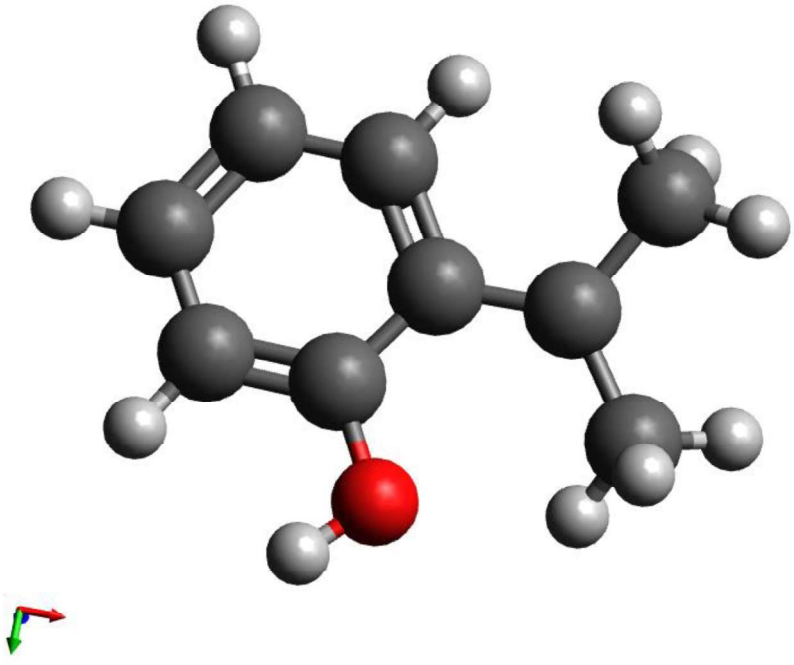

Figure C-37 Three dimensional optimized structure of *o*-OH substituted 3-phenyl-1-propen-3-yl (molecule **BRT1/2**). (**Dark grey:** Carbon, **Light grey:** Hydrogen, **Red:** Oxygen)

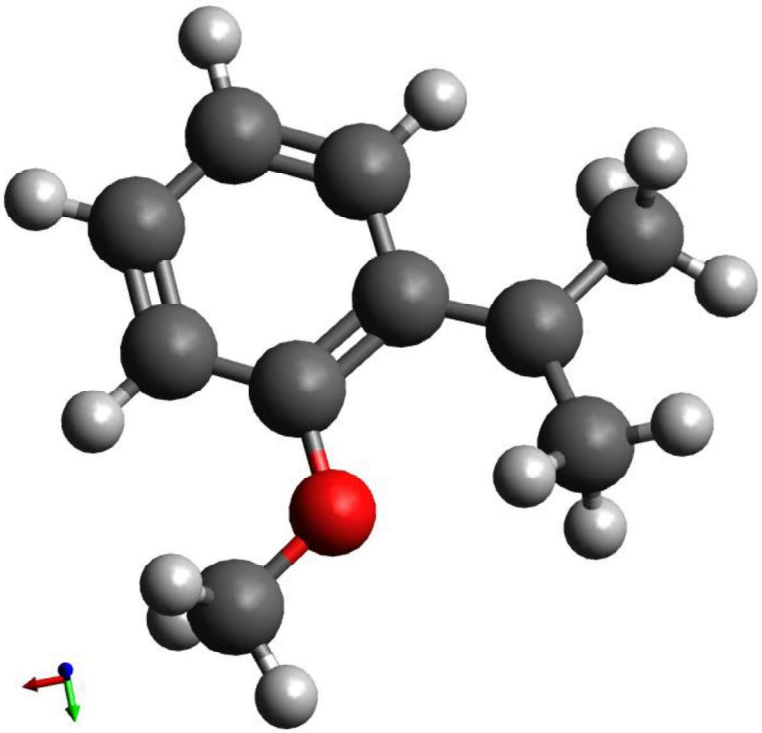

Figure C-38 Three dimensional optimized structure of *o*-OCH_3 substituted 3-phenyl-1-propen-3-yl (molecule **BRT1/5**). (**Dark grey:** Carbon, **Light grey:** Hydrogen, **Red:** Oxygen).

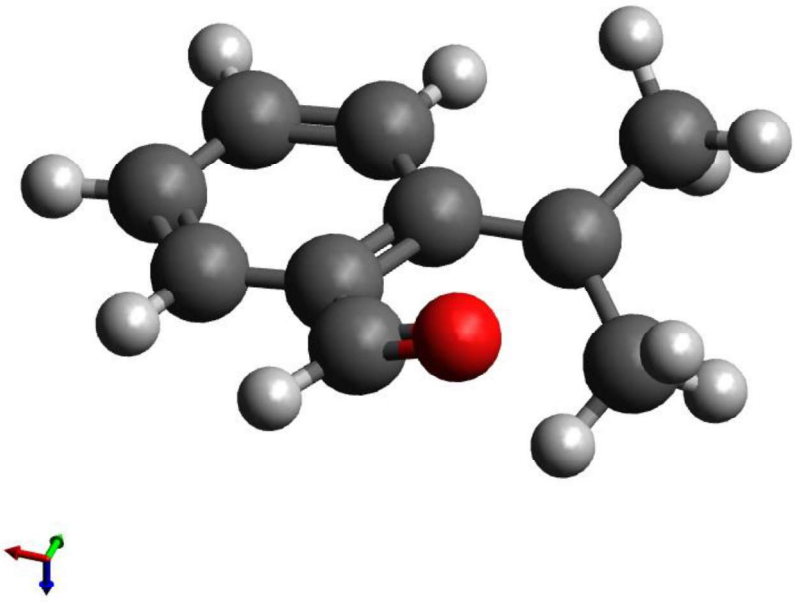

Figure C-39 Three dimensional optimized structure of o-CHO substituted 3-phenyl-1-propen-3-yl (molecule **BRT1/8**). (**Dark grey:** Carbon, **Light grey:** Hydrogen, **Red:** Oxygen

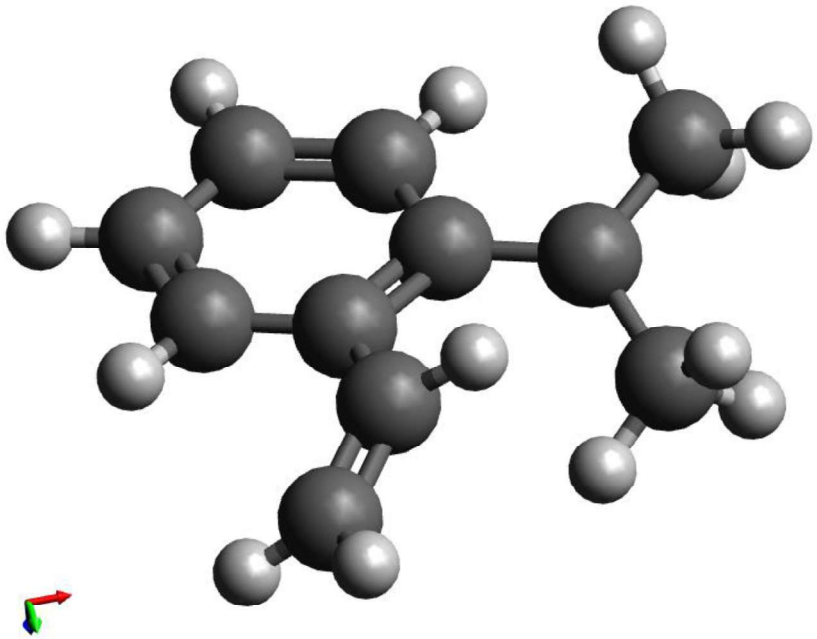

Figure C-40 Three dimensional optimized structure of *o*-CH=CH_2 substituted 3-phenyl-1-propen-3-yl (molecule **BRT1/11**). (**Dark grey:** Carbon, **Light grey:** Hydrogen

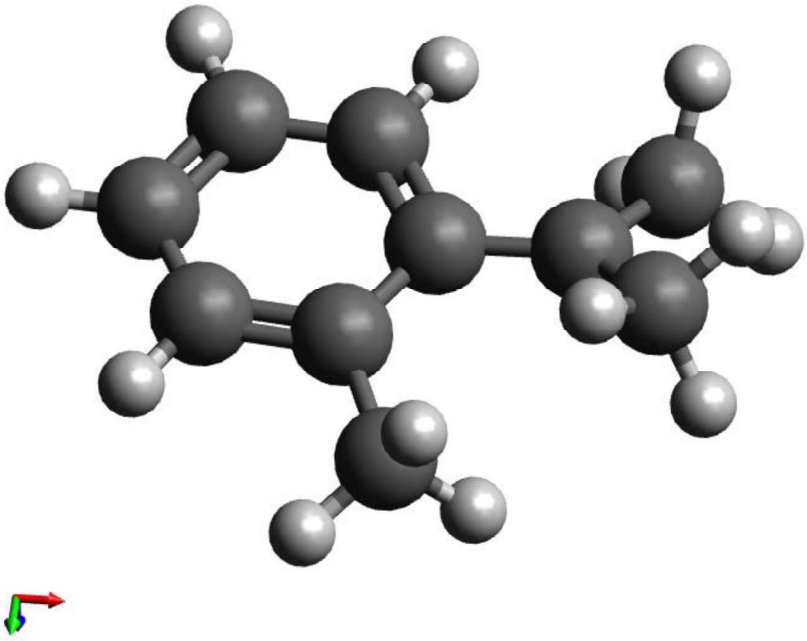

Figure C-41 Three dimensional optimized structure of *o*-CH_3 substituted 3-phenyl-1-propen-3-yl (molecule **BRT1/14**). (**Dark grey:** Carbon, **Light grey:** Hydrogen).

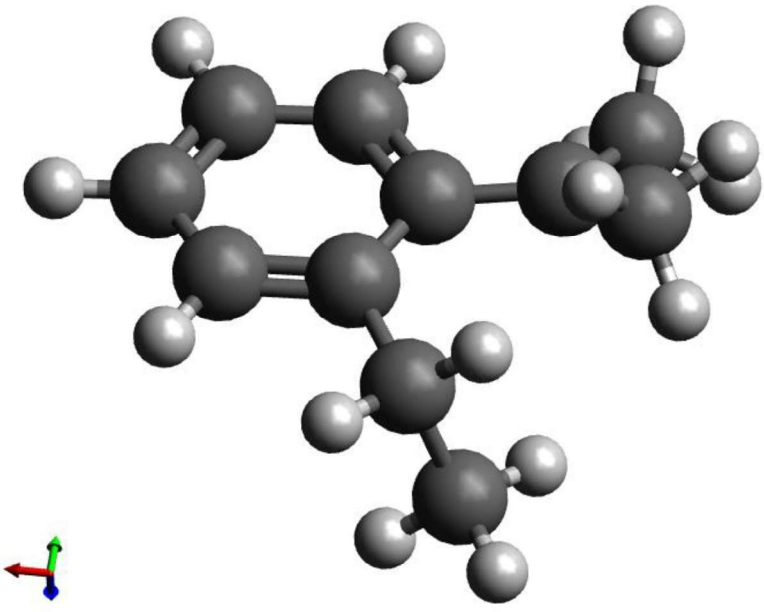

Figure C-42 Three dimensional optimized structure of *o*-CH_2CH_3 substituted 3-phenyl-1-propen-3-yl (molecule **BRT1/17**). (**Dark grey:** Carbon, **Light grey:** Hydrogen)

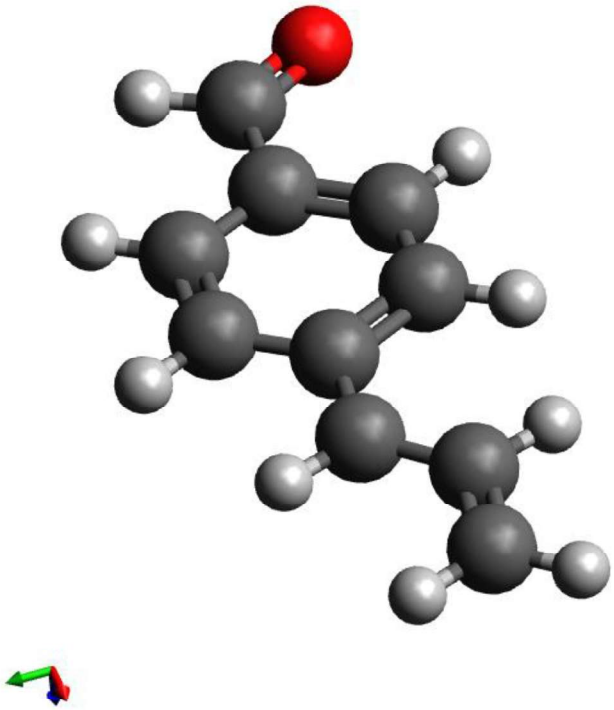

Figure C-43 Three dimensional optimized structure of *p*-CHO substituted 3-phenyl-1-propen-3-yl (molecule **BRT2/10**). (**Dark grey:** Carbon, **Light grey:** Hydrogen, **Red:** Oxygen)

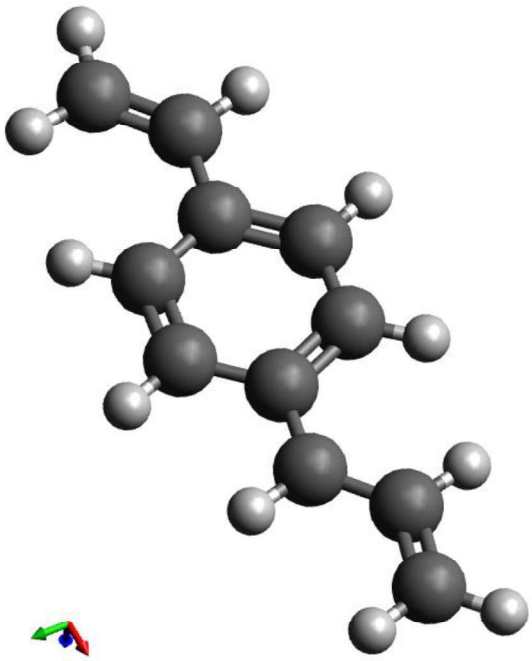

Figure C-44 Three dimensional optimized structure of *p*-CH=CH_2 substituted 3-phenyl-1-propen-3-yl (molecule **BRT2/13**). (**Dark grey:** Carbon, **Light grey:** Hydrogen)

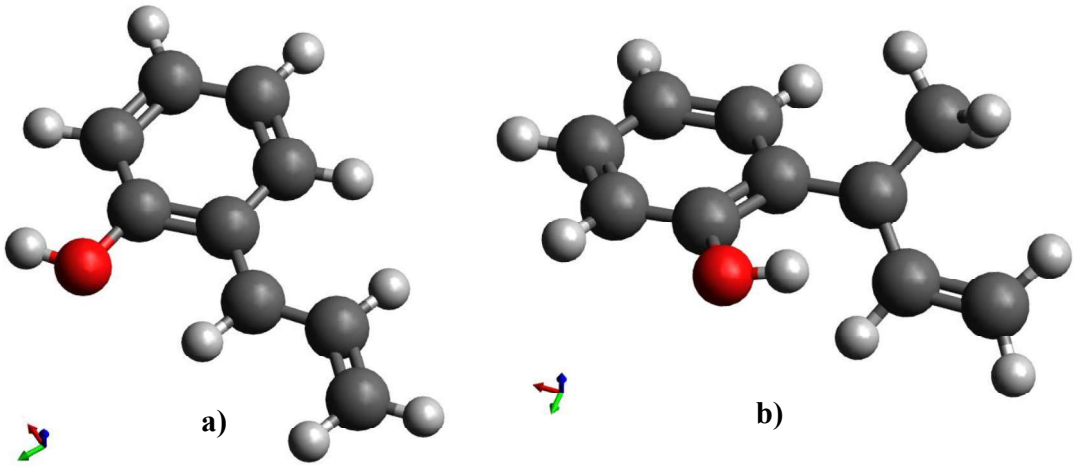

Figure C-45 Comparison of the three dimensional optimized structures of **a)** 3-phenyl-1-propen-3-yl (molecule **BRT2/2**), **b)** *o*-OH substituted 3-phenyl-1-buten-3-yl (molecule **BRT3/1**). (**Dark grey:** Carbon, **Light grey:** Hydrogen, **Red:** Oxygen)

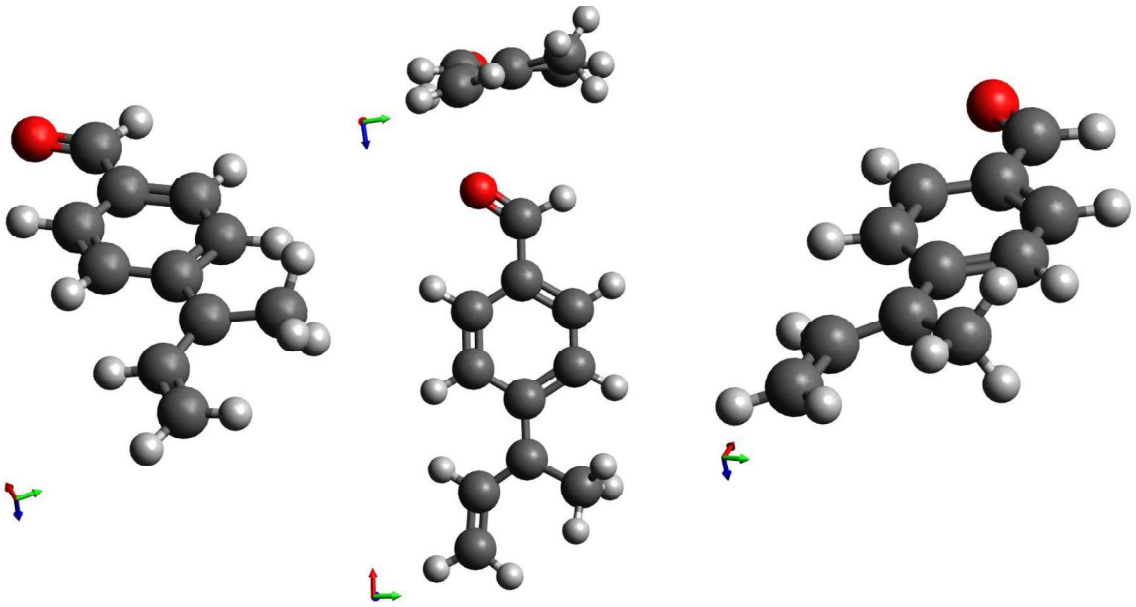

Figure C-46 Three dimensional optimized structure of *p*-CHO substituted 3-phenyl-1-buten-3-yl shown from different perspectives (molecule **BRT3/10**). (**Dark grey:** Carbon, **Light grey:** Hydrogen, **Red:** Oxygen)

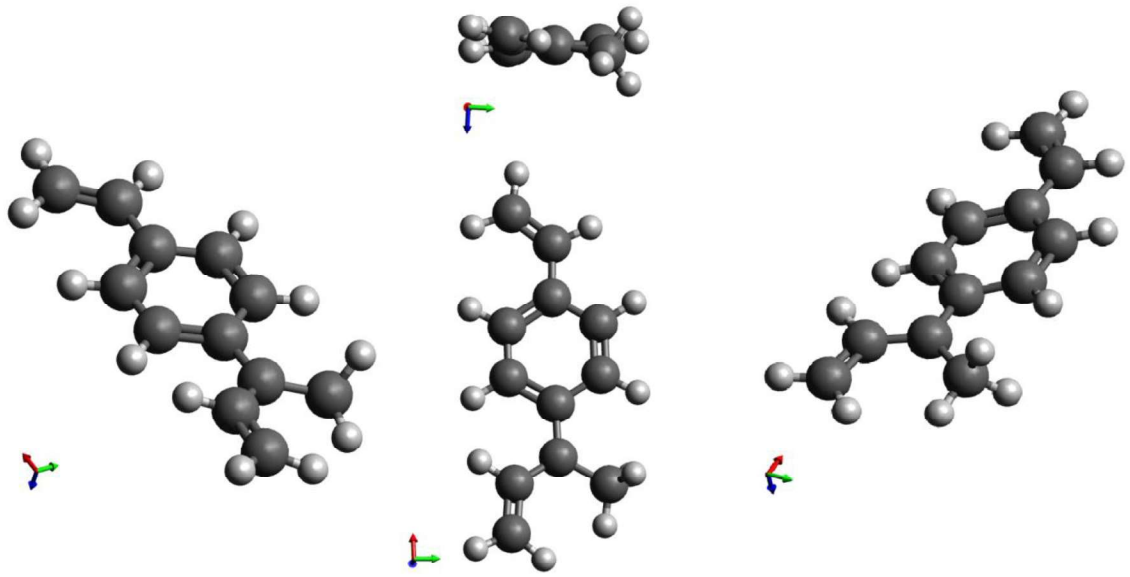

Figure C-47 Three dimensional optimized structure of *p*-CH=CH_2 substituted 3-phenyl-1-buten-3-yl shown from different perspectives (molecule **BRT3/13**). (**Dark grey:** Carbon, **Light grey:** Hydrogen)

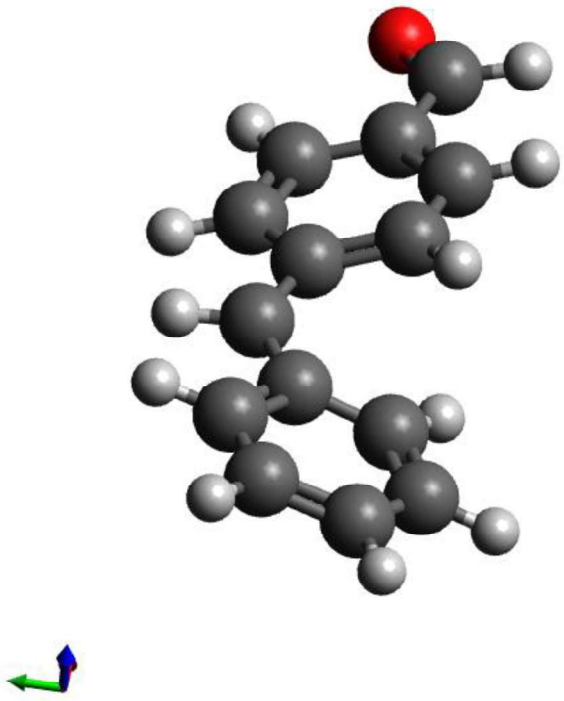

Figure C-48 Three dimensional optimized structure of *p*-CHO substituted diphenylmethyl (molecule **BRT5/10**). (**Dark grey:** Carbon, **Light grey:** Hydrogen, **Red:** Oxygen)

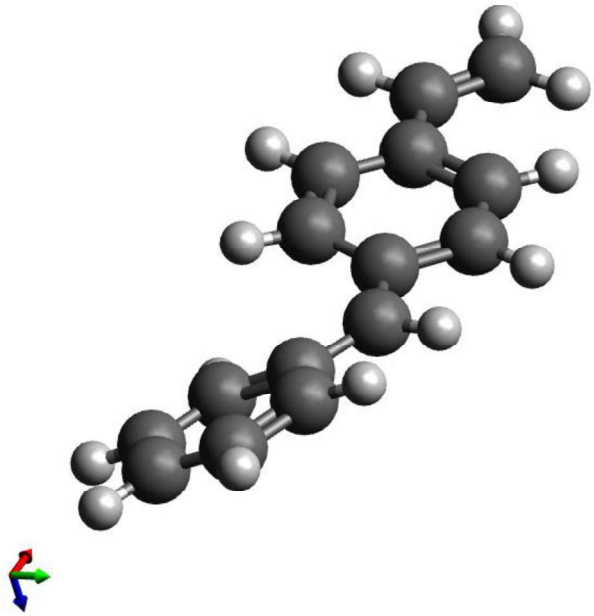

Figure C-49 Three dimensional optimized structure of *p*-CH=CH_2 substituted diphenylmethyl (molecule **BRT5/13**). (**Dark grey:** Carbon, **Light grey:** Hydrogen).

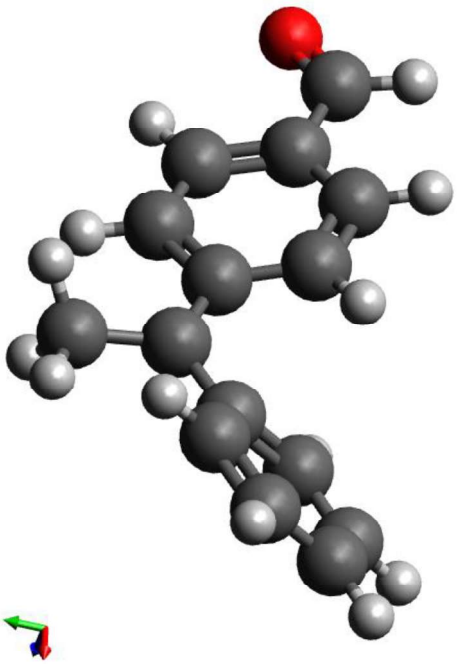

Figure C-50 Three dimensional optimized structure of *p*-CHO substituted diphenylmethyl (molecule **BRT6/10**). (**Dark grey:** Carbon, **Light grey:** Hydrogen, **Red:** Oxygen)

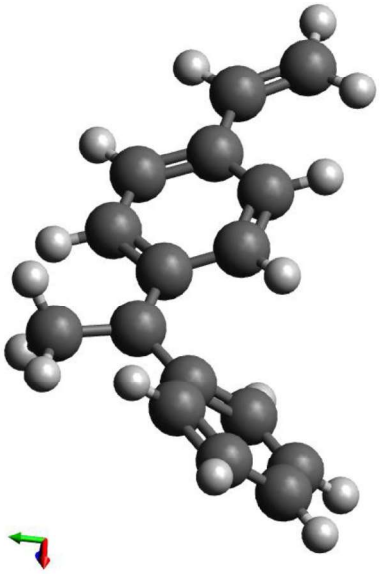

Figure C-51 Three dimensional optimized structure of *p*-CH=CH_2 substituted diphenylmethyl (molecule **BRT6/10**). (**Dark grey:** Carbon, **Light grey:** Hydrogen)

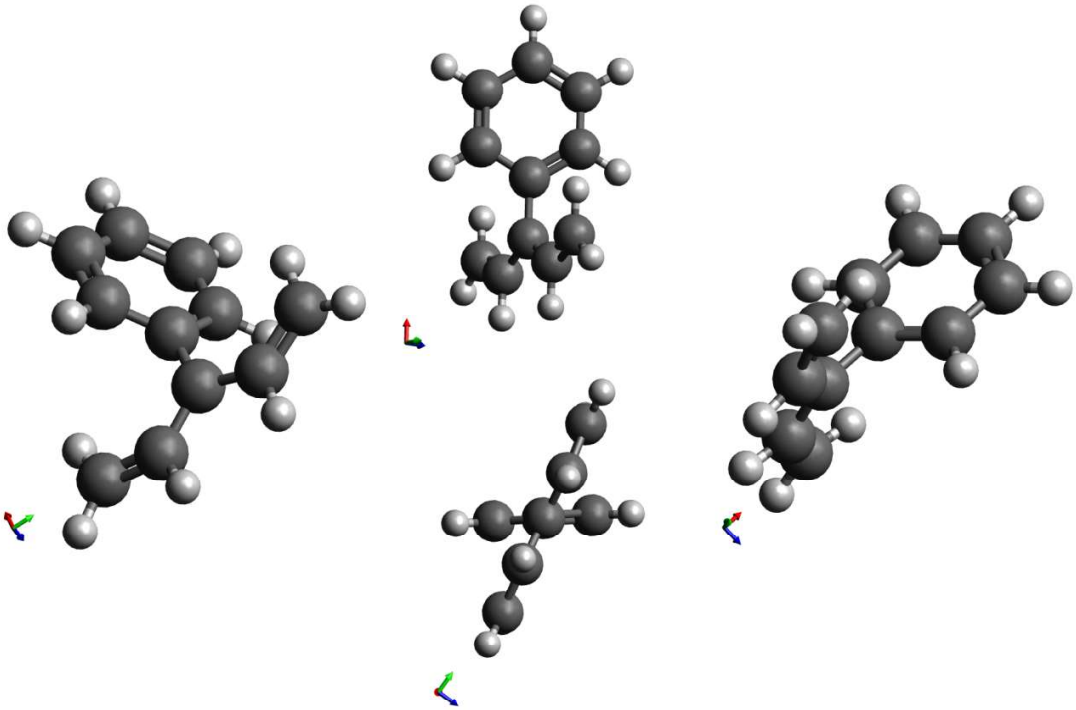

Figure C-52 Three dimensional optimized structure of unsubstituted 3-phenyl-1,4-pentadien-3-yl (molecule **BRT4/1**). (**Dark grey:** Carbon, **Light grey:** Hydrogen)

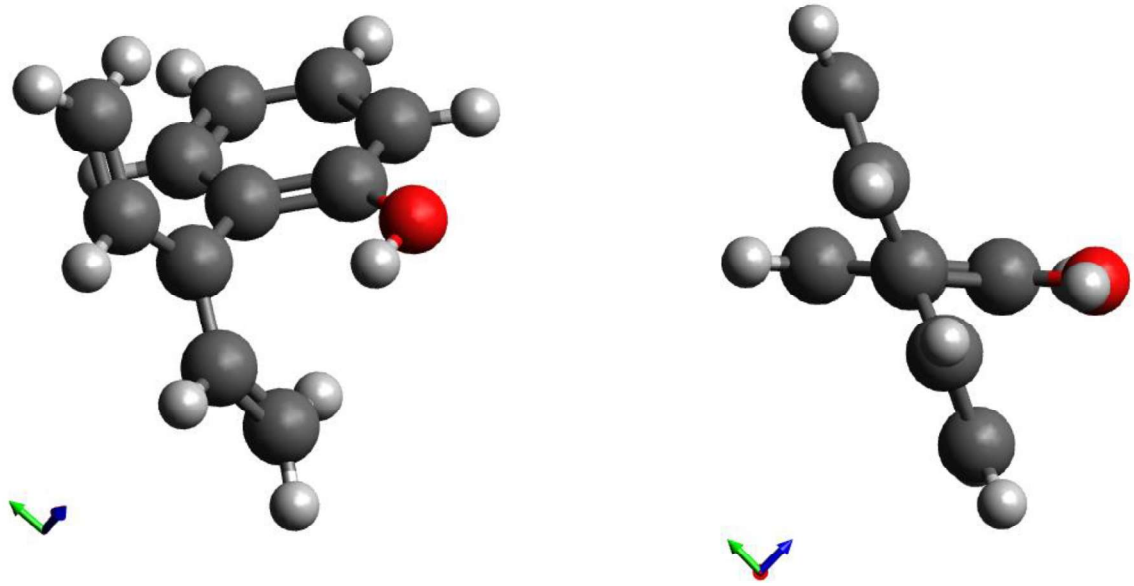

Figure C-53 Three dimensional optimized structure of *o*-OH substituted 3-phenyl-1,4-pentadien-3-yl shown from different perspectives (molecule **BRT4/2**). (**Dark grey:** Carbon, **Light grey:** Hydrogen, **Red:** Oxygen)

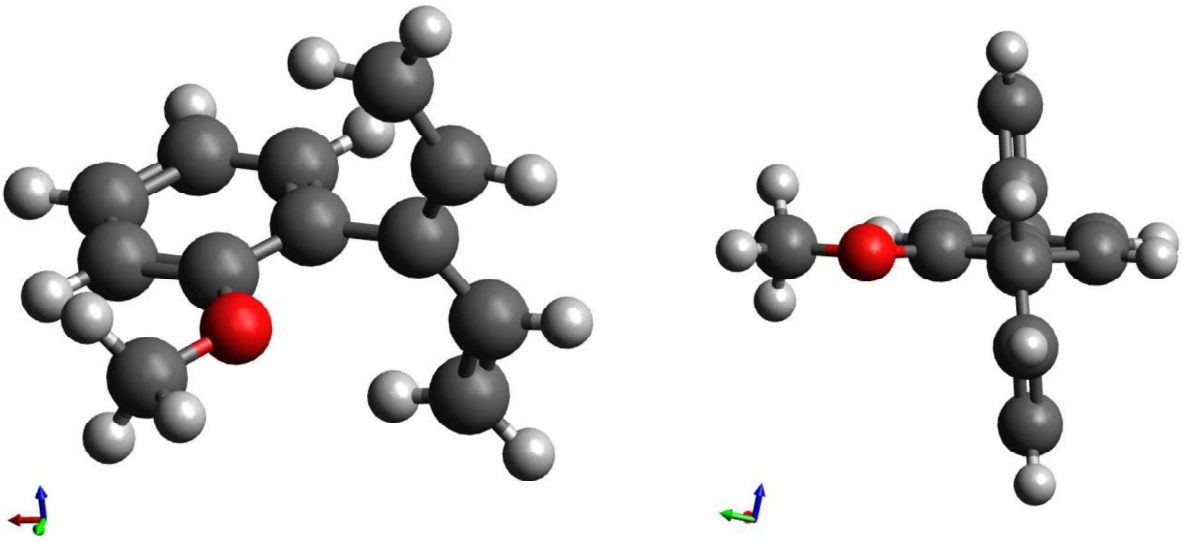

Figure C-54 Three dimensional optimized structure of *o*-OCH_3 substituted 3-phenyl-1,4-pentadien-3-yl shown from different perspectives (molecule **BRT4/5**). (**Dark grey:** Carbon, **Light grey:** Hydrogen, **Red:** Oxygen)

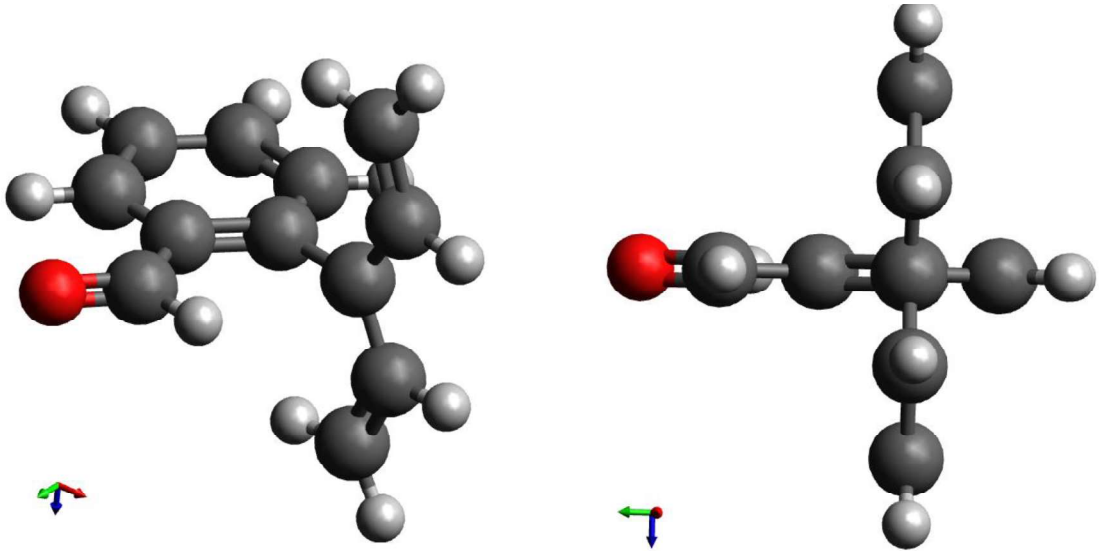

Figure C-55 Three dimensional optimized structure of *o*-CHO substituted 3-phenyl-1,4-pentadien-3-yl shown from different perspectives (molecule **BRT4/8**). (**Dark grey:** Carbon, **Light grey:** Hydrogen, **Red:** Oxygen)

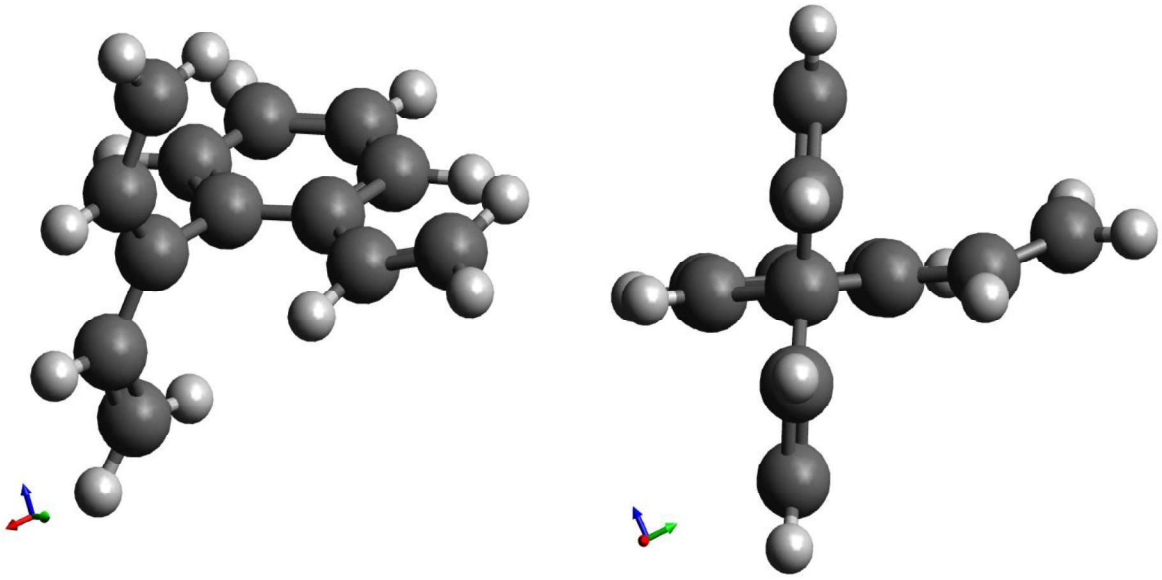

Figure C-56 Three dimensional optimized structure of *o*-CH=CH_2 substituted 3-phenyl-1,4-pentadien-3-yl shown from different perspectives (molecule **BRT4/11**). (**Dark grey:** Carbon, **Light grey:** Hydrogen)

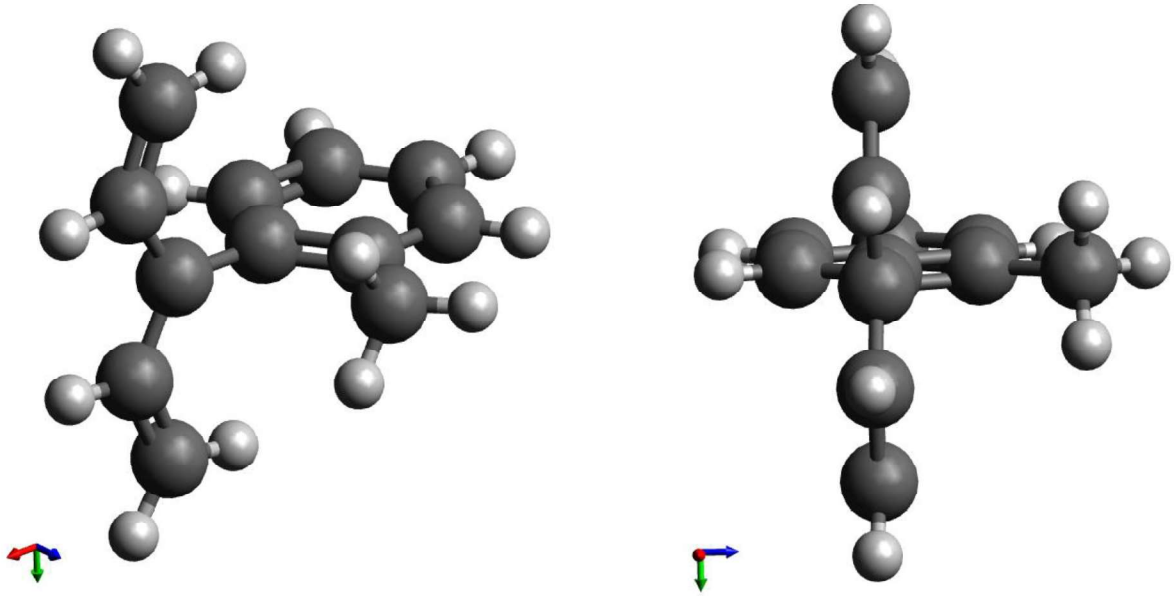

Figure C-57 Three dimensional optimized structure of *o*-CH_3 substituted 3-phenyl-1,4-pentadien-3-yl shown from different perspectives (molecule **BRT4/14**). (**Dark grey:** Carbon, **Light grey:** Hydrogen)

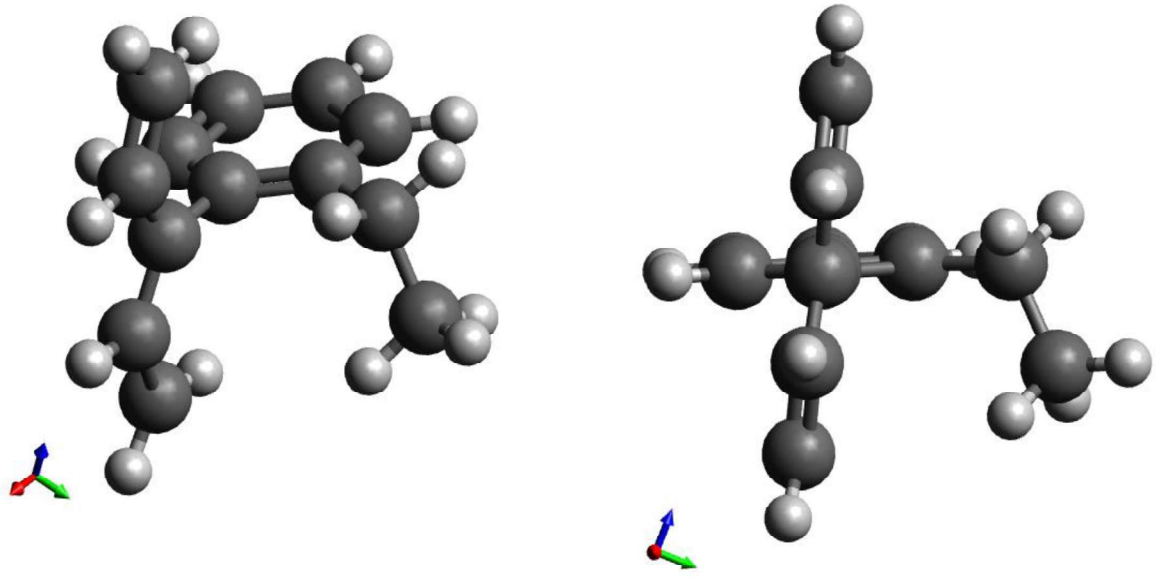

Figure C-58 Three dimensional optimized structure of *o*-CH_2CH_3 substituted 3-phenyl-1,4-pentadien-3-yl shown from different perspectives (molecule **BRT4/17**). (**Dark grey:** Carbon, **Light grey:** Hydrogen)

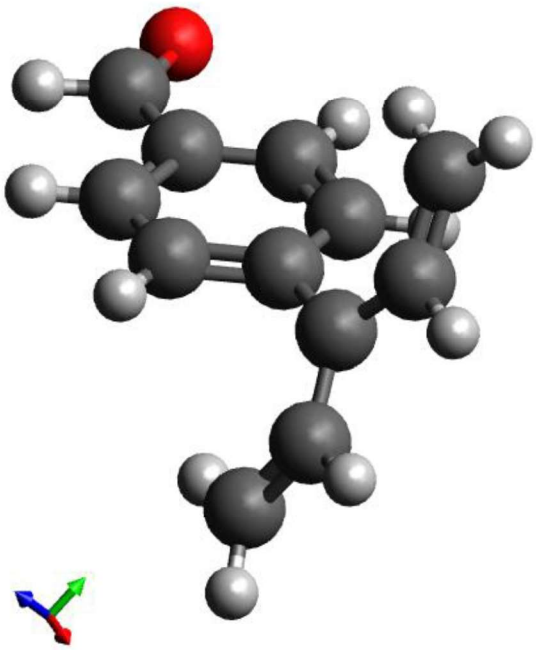

Figure C-59 Three dimensional optimized structure of *p*-CHO substituted 3-phenyl-1,4-pentadien-3-yl (molecule **BRT4/10**). (**Dark grey:** Carbon, **Light grey:** Hydrogen, **Red:** Oxygen)

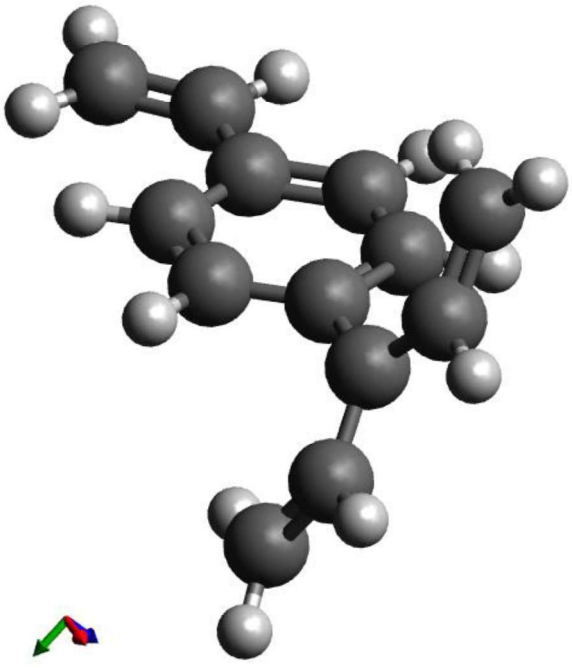

Figure C-60 Three dimensional optimized structure of *p*-CH=CH_2 substituted 3-phenyl-1,4-pentadien-3-yl (molecule **BRT4/13**). (**Dark grey:** Carbon, **Light grey:** Hydrogen)

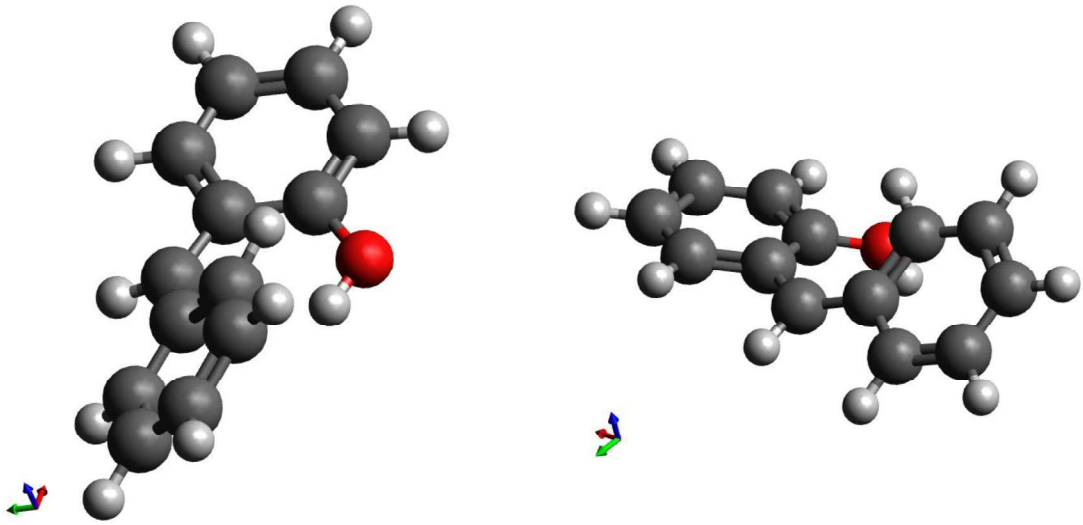

Figure C-61 Three dimensional optimized structure of *o*-OH substituted diphenylmethyl shown from different perspectives (molecule **BRT5/2**). (**Dark grey:** Carbon, **Light grey:** Hydrogen, **Red:** Oxygen)

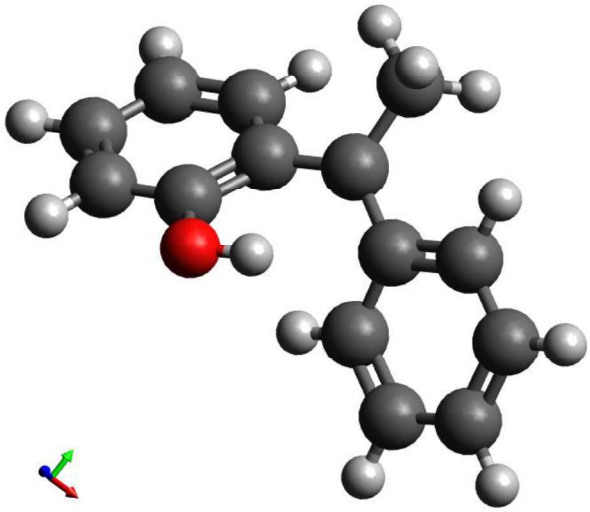

Figure C-62 Three dimensional optimized structure of *o*-OH substituted 1,1-diphenylethyl (molecule **BRT6/2**). (**Dark grey:** Carbon, **Light grey:** Hydrogen, **Red:** Oxygen)

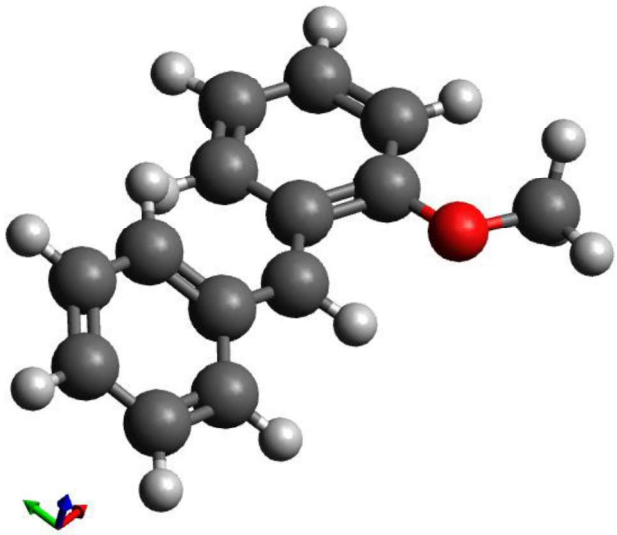

Figure C-63 Three dimensional optimized structure of *o*-OCH_3 substituted diphenylmethyl (molecule **BRT5/5**). (**Dark grey:** Carbon, **Light grey:** Hydrogen, **Red:** Oxygen)

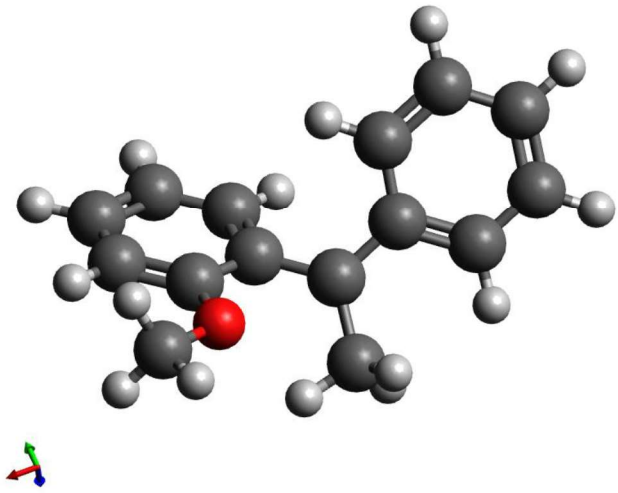

Figure C-64 Three dimensional optimized structure of *o*-OCH_3 substituted 1,1-diphenylethyl (molecule **BRT6/5**). (**Dark grey:** Carbon, **Light grey:** Hydrogen, **Red:** Oxygen)

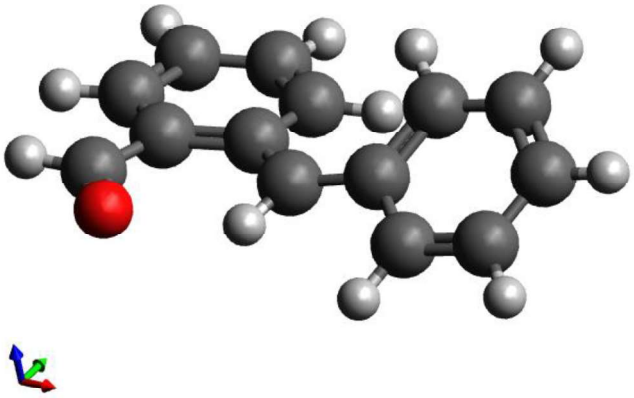

Figure C-65 Three dimensional optimized structure of *o*-CHO substituted diphenylmethyl (molecule **BRT5/8**). (**Dark grey:** Carbon, **Light grey:** Hydrogen, **Red:** Oxygen)

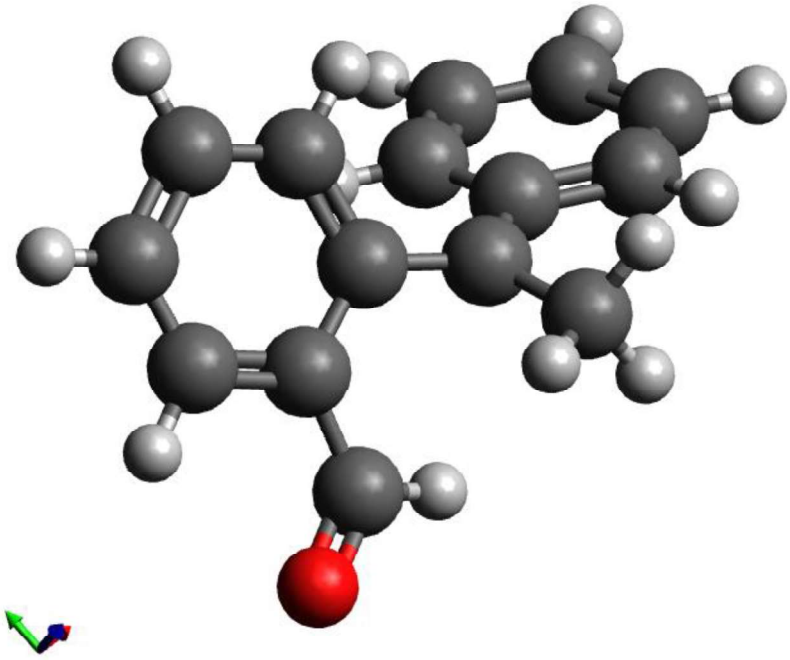

Figure C-66 Three dimensional optimized structure of *o*-CHO substituted 1,1-diphenylethyl (molecule **BRT6/8**). (**Dark grey:** Carbon, **Light grey:** Hydrogen, **Red:** Oxygen)

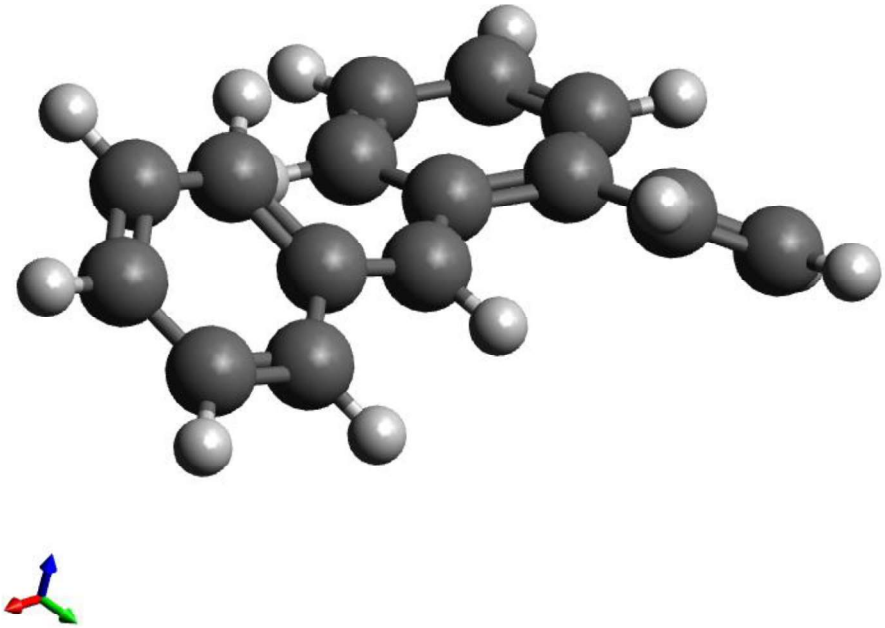

Figure C-67 Three dimensional optimized structure of *o*-CH=CH_2 substituted diphenylmethyl (molecule **BRT5/11**). (**Dark grey:** Carbon, **Light grey:** Hydrogen)

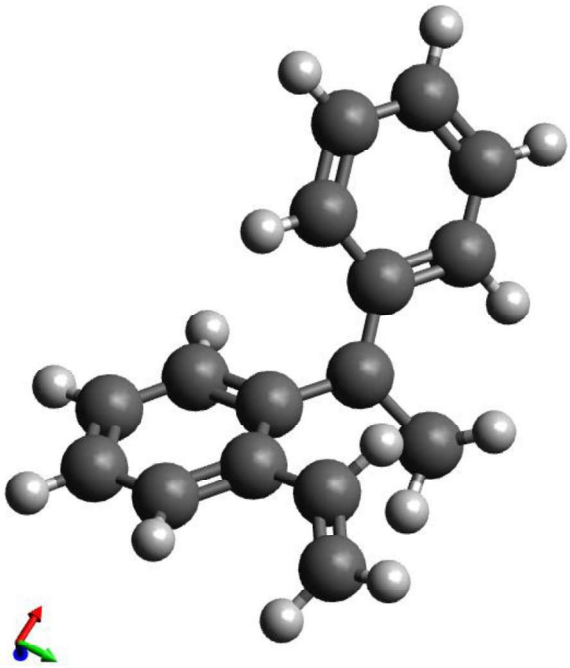

Figure C-68 Three dimensional optimized structure of *o*-CH=CH_2 substituted 1,1-diphenylethyl (molecule **BRT6/11**). (**Dark grey:** Carbon, **Light grey:** Hydrogen)

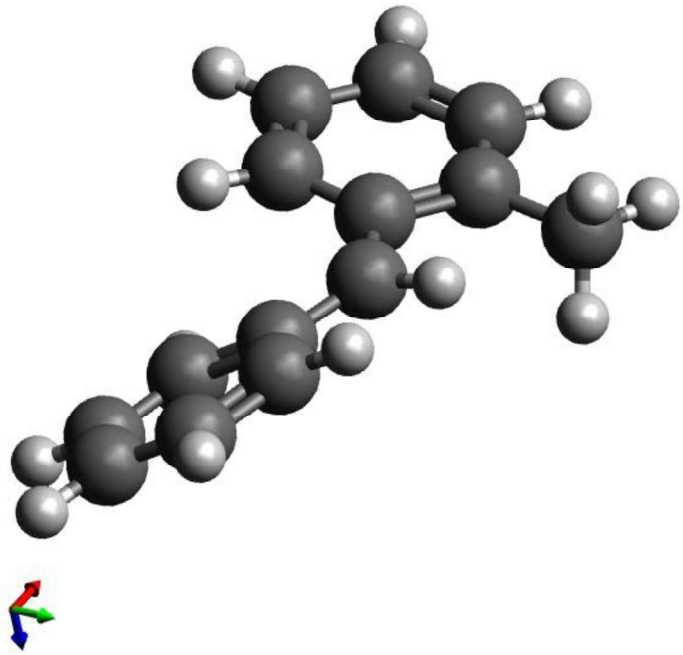

Figure C-69 Three dimensional optimized structure of *o*-CH_3 substituted diphenylmethyl (molecule **BRT5/14**). (**Dark grey:** Carbon, **Light grey:** Hydrogen, **Red:** Oxygen)

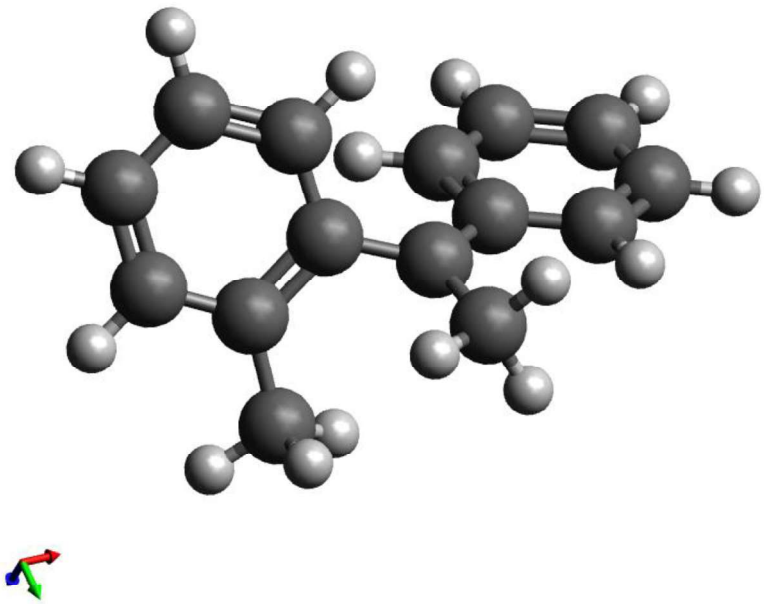

Figure C-70 Three dimensional optimized structure of *o*-CH_3 substituted 1,1-diphenylethyl (molecule **BRT6/14**). (**Dark grey:** Carbon, **Light grey**: Hydrogen)

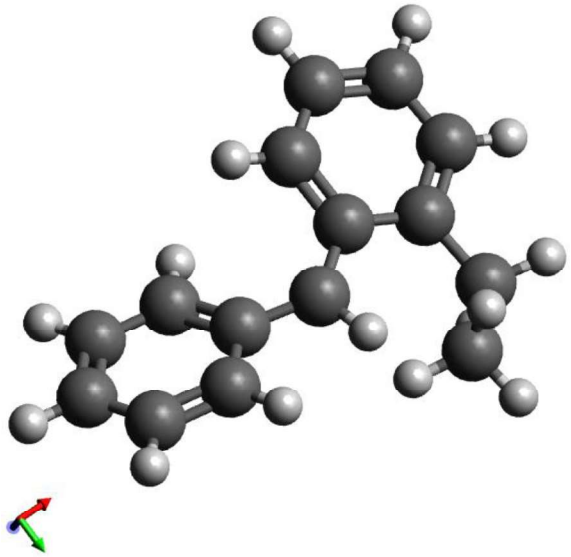

Figure C-71 Three dimensional optimized structure of *o*-CH_2CH_3 substituted diphenylmethyl (molecule **BRT5/17**). (**Dark grey:** Carbon, **Light grey:** Hydrogen)

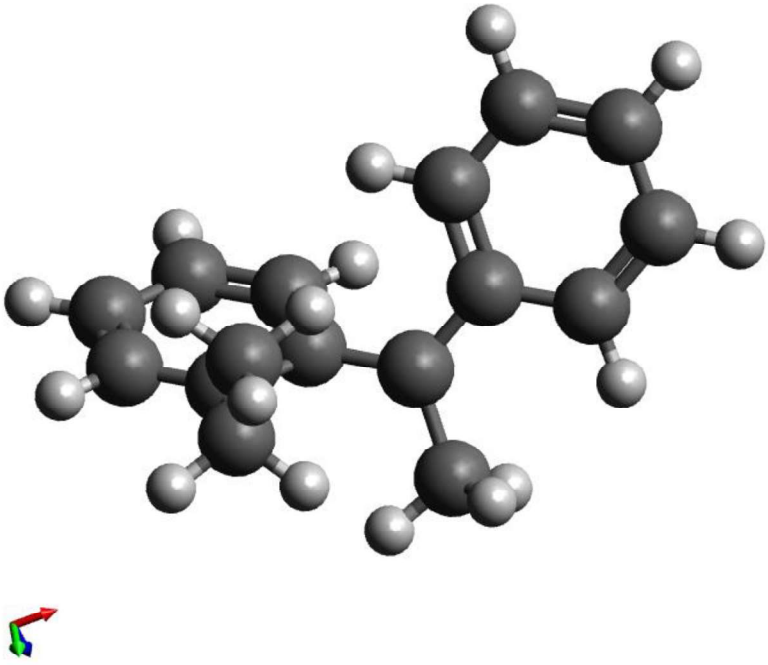

Figure C-72 Three dimensional optimized structure of *o*-CH_2CH_3 substituted 1,1-diphenylethyl (molecule **BRT6/17**). (**Dark grey:** Carbon, **Light grey:** Hydrogen)

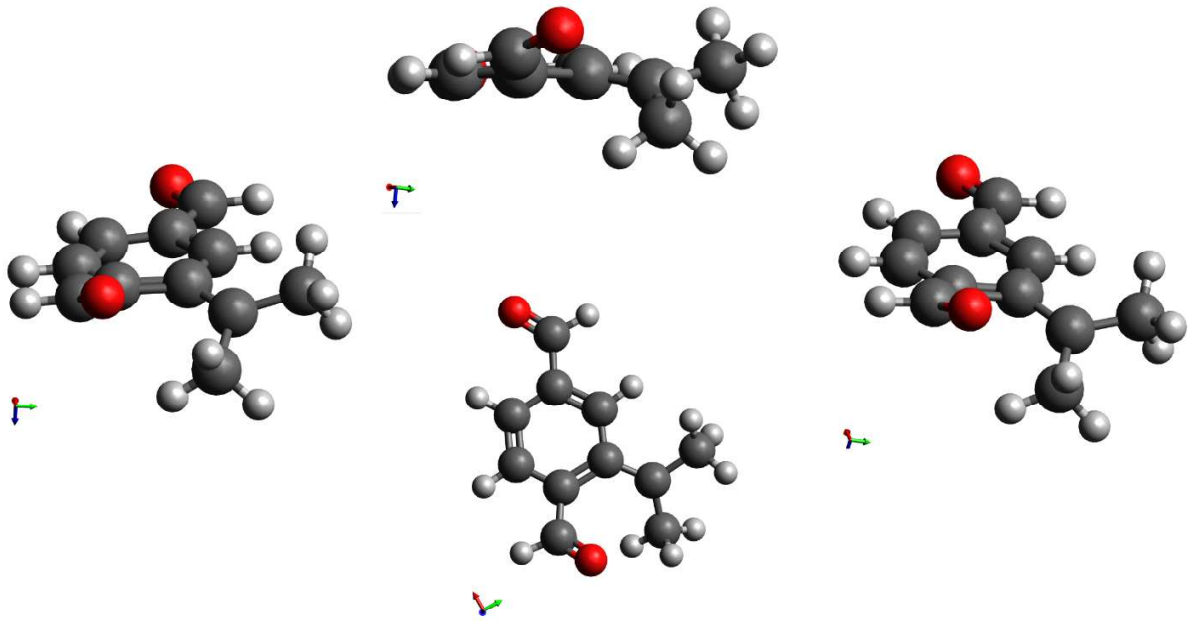

Figure C-73 Three dimensional optimized structure of the doubly substituted 2-phenyl-2-propyl where two formyl (-CHO) substituents are in *o*- position and *m*- position with respect to the extended side chain (molecule **BRV1/3**). (**Dark grey:** Carbon, **Light grey:** Hydrogen, **Red:** Oxygen)

C.5.4 Testing GAV/NNI Parameters: The Validation Set

Table C-21 Deviations between the validation set data obtained from group additivity and *ab initio* calculations before and after the inclusion of newly derived NNI parameters, where group additive data is calculated based on the simultaneously optimized GAVs and NNIs given in **Table C-18** and **Table C-19**, respectively.

Molecule #		$\Delta_f H^\circ$ [kJ mol^{-1}]					S° [J mol^{-1} K^{-1}]					C_p [J mol^{-1} K^{-1}]				
		CBS[a]	Bef. new NNIs[b]	Af. new NNIs[c]	Δ(Bef. new NNIs)[d]	Δ(Af. new NNIs)[e]	CBS[a]	Bef. new NNIs[b]	Af. new NNIs[c]	Δ(Bef. new NNIs)[d]	Δ(Af. new NNIs)[e]	CBS[a]	Bef. new NNIs[b]	Af. new NNIs[c]	Δ(Bef. new NNIs)[d]	Δ(Af. new NNIs)[e]
1	**BRV1/1**	-196.8	-207.7	-196.0	-10.9	0.8	479.4	478.9	478.7	-0.5	-0.7	144.4	145.7	146.7	1.3	2.3
2	**BRV1/2**	-28.1	-41.9	-30.2	-13.8	-2.1	538.5	538.5	538.3	0.0	-0.2	165.2	161.6	162.6	-3.6	-2.6
3	**BRV1/3**	-67.0	-77.7	-61.6	-10.7	5.4	513.4	519.0	516.9	5.6	3.5	164.4	158.6	168.5	-5.8	4.1
4	**BRV1/4**	15.1	-0.2	15.9	-15.3	0.8	511.7	517.5	515.4	5.8	3.7	165.4	159.7	169.6	-5.7	4.2
5	**BRV1/5**	52.7	42.9	56.4	-9.8	3.7	505.8	508.6	508.6	2.8	2.8	189.7	178.4	193.6	-11.3	3.9
6	**BRV1/6**	198.6	187.6	201.1	-11.0	2.5	522.7	525.8	525.8	3.1	3.1	187.1	174.3	189.5	-12.8	2.4
7	**BRV1/7**	-38.9	-60.3	-37.0	-21.4	1.9	494.3	492.5	493.0	-1.8	-1.3	186.5	185.6	187.8	-0.9	1.3
8	**BRV1/8**	106.9	84.4	107.7	-22.5	0.8	508.9	509.7	510.2	0.8	1.3	184.7	182.2	184.4	-2.5	-0.3
9	**BRV1/9**	-187.2	-183.0	-183.0	4.2	4.2	476.5	477.7	477.7	1.2	1.2	172.5	171.4	171.4	-1.1	-1.1
10	**BRV1/10**	-8.2	-2.5	-2.5	5.7	5.7	515.5	513.8	513.8	-1.7	-1.7	171.9	167.6	167.6	-4.3	-4.3
11	**BRV1/11**	175.9	179.7	179.7	3.8	3.8	519.5	516.9	516.9	-2.6	-2.6	197.4	199.1	199.1	1.7	1.7
12	**BRV2/1**	126.7	128.3	129.0	1.6	2.3	460.8	460.2	458.2	-0.6	-2.6	182.3	176.6	181.4	-5.7	-0.9
13	**BRV2/2**	-84.0	-88.7	-88.0	-4.7	-4.0	474.3	476.1	474.1	1.8	-0.2	181.7	182.5	187.3	0.8	5.6
14	**BRV2/3**	37.5	34.9	35.6	-2.6	-1.9	451.1	450.9	448.9	-0.2	-2.2	172.9	169.3	174.1	-3.6	1.2
15	**BRV2/4**	98.3	92.2	98.1	-6.1	-0.2	458.7	470.4	462.8	11.7	4.1	166.0	164.3	169.4	-1.7	3.4
16	**BRV2/5**	192.3	186.2	192.1	-6.1	-0.2	475.2	484.0	476.4	8.8	1.2	164.8	157.2	162.3	-7.6	-2.5
17	**BRV2/6**	275.3	273.0	278.9	-2.3	3.6	467.4	477.4	469.8	10.0	2.4	194.0	187.5	192.6	-6.5	-1.4
18	**BRV3/1**	-126.0	-129.7	-129.0	-3.7	-3.0	489.2	488.3	486.3	-0.9	-2.9	189.5	183.6	188.4	-5.9	-1.1
19	**BRV3/2**	40.6	28.8	43.4	-11.8	2.8	539.6	543.9	538.9	4.3	-0.7	189.5	186.7	192.3	-2.8	2.8
20	**BRV3/3**	81.3	65.0	79.6	-16.3	-1.7	515.0	521.0	516.0	6.0	1.0	139.7	137.8	143.4	-1.9	3.7
21	**BRV3/4**	117.4	106.9	121.5	-10.5	4.1	510.2	514.5	509.5	4.3	-0.7	166.8	157.4	163.0	-9.4	-3.8
22	**BRV3/5**	171.5	164.2	174.0	-7.3	2.5	528.2	534.0	528.9	5.8	0.7	162.1	154.5	160.7	-7.6	-1.4
23	**BRV3/6**	264.4	251.6	261.4	-12.8	-3.0	525.0	531.7	526.6	6.7	1.6	160.6	150.9	157.1	-9.7	-3.5
24	**BRV3/7**	250.3	256.2	251.4	5.9	1.1	527.2	526.0	525.9	-1.2	-1.3	186.2	186.0	186.6	-0.2	0.4
25	**BRV3/8**	169.1	152.4	167.0	-16.7	-2.1	512.1	518.7	513.7	6.6	1.6	181.3	178.3	183.9	-3.0	2.6
26	**BRV3/9**	-104.3	-108.6	-106.5	-4.3	-2.2	525.6	530.7	525.0	5.1	-0.6	181.9	176.1	182.0	-5.8	0.1
27	**BRV3/10**	-82.8	-78.4	-81.1	4.4	1.7	498.1	503.8	498.0	5.7	-0.1	172.1	167.1	173.6	-5.0	1.5
28	**BRV3/11**	11.6	7.7	9.8	-3.9	-1.8	500.0	501.5	495.8	1.5	-4.2	169.7	163.4	169.3	-6.3	-0.4
29	**BRV3/12**	-79.5	-84.3	-82.2	-4.8	-2.7	499.1	503.0	497.3	3.9	-1.8	168.6	162.6	168.5	-6.0	-0.1

30	**BRV4/1**	177.6	188.5	174.2	10.9	-3.4	516.5	529.1	514.5	12.6	-2.0	184.7	182.8	188.5	-1.9	3.8
31	**BRV4/2**	80.0	89.3	75.0	9.3	-5.0	504.6	516.1	501.5	11.5	-3.1	177.3	174.7	180.4	-2.6	3.1
32	**BRV4/3**	-36.4	-34.3	-32.7	2.1	3.7	535.2	541.3	535.8	6.1	0.6	177.2	173.7	179.9	-3.5	2.7
33	**BRV4/4**	112.3	110.4	112.0	-1.9	-0.3	549.5	558.5	553.0	9.0	3.5	168.2	161.9	168.1	-6.3	-0.1
34	**BRV4/5**	239.1	245.8	239.9	6.7	0.8	528.1	548.6	528.3	20.5	0.2	162.1	166.0	164.3	3.9	2.2
35	**BRV4/6**	179.0	188.5	182.6	9.5	3.6	508.2	529.1	508.8	20.9	0.6	161.2	164.2	162.5	3.0	1.3
36	**BRV4/7**	333.0	339.4	333.5	6.4	0.5	524.2	546.3	526.0	22.1	1.8	190.4	192.9	191.2	2.5	0.8
37	**BRV4/8**	224.6	234.0	228.1	9.4	3.5	513.3	533.3	513.0	20.0	-0.3	186.1	191.6	189.9	5.5	3.8
38	**BRV5/1**	-7.9	1.1	-9.5	9.0	-1.6	522.6	524.8	520.7	2.2	-1.9	186.8	180.5	181.1	-6.3	-5.7
39	**BRV5/2**	179.1	187.7	181.9	8.6	2.8	534.7	535.5	531.5	0.8	-3.2	162.5	160.8	160.8	-1.7	-1.7
40	**BRV5/3**	87.1	88.5	82.7	1.4	-4.4	519.6	522.5	518.5	2.9	-1.1	190.0	186.7	186.7	-3.3	-3.3
41	**BRV5/4**	110.1	109.6	112.9	-0.5	2.8	553.5	564.9	554.0	11.4	0.5	183.4	179.9	187.8	-3.5	4.4
42	**BRV5/5**	151.8	145.8	152.6	-6.0	0.8	539.4	542.0	538.4	2.6	-1.0	182.6	178.1	184.0	-4.5	1.4
43	**BRV5/6**	338.4	332.4	339.2	-6.0	0.8	549.4	552.7	549.1	3.3	-0.3	211.1	206.5	212.4	-4.6	1.3
44	**BRV5/7**	329.1	332.4	334.4	3.3	5.3	548.6	552.7	549.0	4.1	0.4	204.5	195.1	201.6	-9.4	-2.9
45	**BRV5/8**	237.8	233.2	240.0	-4.6	2.2	531.7	539.7	536.1	8.0	4.4	205.4	198.1	204.0	-7.3	-1.4
46	**BRV5/9**	147.5	153.9	149.1	6.4	1.6	536.5	539.6	539.5	3.1	3.0	199.6	200.2	200.8	0.6	1.2
47	**BRV5/10**	330.6	337.0	332.2	6.4	1.6	545.1	547.0	546.9	1.9	1.8	190.9	190.7	191.3	-0.2	0.4
48	**BRV6/1**	57.2	62.1	56.3	4.9	-0.9	561.8	567.4	563.4	5.6	1.6	189.4	187.8	187.8	-1.6	-1.6
49	**BRV6/2**	-89.7	-82.6	-88.4	7.1	1.3	547.3	550.2	546.2	2.9	-1.1	204.0	201.0	201.0	-3.0	-3.0
50	**BRV6/3**	180.4	182.4	180.9	2.0	0.5	615.9	622.8	611.8	6.9	-4.1	199.3	192.9	201.4	-6.4	2.1
51	**BRV6/4**	128.8	119.4	126.2	-9.4	-2.6	584.9	586.9	583.3	2.0	-1.6	198.7	191.2	197.1	-7.5	-1.6
52	**BRV6/5**	312.1	306.0	312.8	-6.1	0.7	591.2	597.6	594.0	6.4	2.8	187.5	180.3	186.2	-7.2	-1.3
53	**BRV6/6**	303.2	310.6	305.8	7.4	2.6	590.9	591.9	591.8	1.0	0.9	184.9	185.1	185.7	0.2	0.8
54	**BRV6/7**	217.6	206.8	213.6	-10.8	-4.0	582.7	584.6	581.0	1.9	-1.7	184.2	179.1	185.0	-5.1	0.8

Statistics	$\Delta_f H^\circ$ [kJ mol^{-1}]		S° [J mol^{-1} K^{-1}]		C_p [J mol^{-1} K^{-1}] (300 K)	
Mean Absolute Deviation (MAD)	7.6	2.4	5.6	1.8	4.5	2.2
Maximum Absolute Deviation (MAX)	22.5	5.7	22.1	4.4	12.8	5.7

[a] **CBS:** Reference dataset of CBS-QB3 results with spin orbit and bond additive corrections (SOCs and BACs).
[b] **Bef. new NNIs:** Group additively calculated data based on GAVs and previously defined NNIs given in **Table C-16**, excluding the NNIs for isopropylbenzene and the new NNIs in **Table C-19**, which are defined in this paper.
[c] **Af. new NNIs:** Group additively calculated data based on GAVs and all the NNIs given in **Table C-18** and **Table C-19**, respectively.
[d] Δ(**Bef. new NNIs):** The difference between CBS and "**Bef. new NNIs**".
[e] Δ(**Af. new NNIs):** Deviation of GA calculated data from CBS-QB3.

C.5.5 Final Optimization of GA Parameters

Table C-22 Deviations between the final set data (training set + validation set) obtained from group additivity and *ab initio* calculations, where group additive data is calculated based on the final GAVs and NNIs given in **Table 5-7** and **Table 5-8** in the text, respectively.

Radicals		$\Delta_f H^\circ$ [kJ mol^{-1}]	S° [J mol^{-1} K^{-1}]	C_p [J mol^{-1} K^{-1}]						
				300 K	400 K	500 K	600 K	800 K	1000 K	1500 K
1	BRT1/1	-1.506	1.769	-1.6	-1.225	-1.181	-0.969	-0.819	-0.725	-0.562
2	BRT1/2	1.625	-0.4	1.85	0.35	0.125	0.125	0.075	-0.05	-0.05
3	BRT1/3	0.994	-1.531	1.8	1.275	0.919	0.531	0.081	-0.025	0.137
4	BRT1/4	-1.206	-1.131	0.8	0.475	0.219	-0.069	-0.419	-0.525	-0.762
5	BRT1/5	-0.975	0.9	-1.65	2.65	1.925	1.225	0.575	0.35	0.05
6	BRT1/6	-2.706	-0.731	0.1	-0.325	-0.281	-0.169	-0.019	0.075	-0.262
7	BRT1/7	-3.506	0.469	0.7	-0.125	-0.181	-0.369	-0.319	-0.125	-0.363
8	BRT1/8	-2.067	-2.4	-2.767	-1.2	-0.567	-0.267	-0.033	0.1	0.233
9	BRT1/9	-1.206	0.769	0.7	0.475	0.219	0.231	0.381	0.375	0.038
10	BRT1/10	1.494	2.169	0.1	0.075	0.219	0.431	0.681	0.675	0.338
11	BRT1/11	-2.067	-1.967	-2.1	-1.267	-0.9	-0.533	-0.067	0.1	0.233
12	BRT1/12	0.894	1.469	-1.7	-1.225	-1.081	-0.969	-0.819	-0.625	0.038
13	BRT1/13	2.894	1.669	-0.2	-0.225	-0.381	-0.369	-0.419	-0.425	-0.262
14	BRT1/14	-0.05	1.5	-2.15	-1.525	-1.2	-0.95	-0.625	-0.525	-0.35
15	BRT1/15	-1.806	1.669	-0.4	-0.725	-0.881	-0.869	-0.819	-0.825	-0.762
16	BRT1/16	-1.806	-0.431	0.8	0.475	0.219	0.031	-0.219	-0.525	-0.662
17	BRT1/17	-1.35	-1.5	1.65	1.275	1.2	1.15	1.275	1.275	1.25
18	BRT1/18	-1.906	-0.731	1	0.875	0.819	0.731	0.681	0.675	1.137
19	BRT1/19	-1.606	-2.831	1	0.875	0.719	0.631	0.481	0.175	-0.162
20	BRT2/1	-0.371	1.629	-0.312	-0.265	-0.224	-0.1	0.041	0.029	-0.035
21	BRT2/2	-0.471	1.829	-4.012	-2.165	-0.724	0	0.641	0.729	0.365
22	BRT2/3	4.829	-0.571	0.688	1.035	0.776	0.5	0.341	0.229	-0.035
23	BRT2/4	1.029	0.629	2.188	1.535	1.076	0.7	0.341	0.129	-0.235
24	BRT2/5	3.225	-2.775	1.962	5.3	5.65	5.287	3.362	2.637	0.55
25	BRT2/6	2.029	-2.671	2.488	2.035	2.076	1.9	1.741	1.629	0.765
26	BRT2/7	-0.871	-0.971	1.888	0.835	0.576	0.4	0.441	0.529	0.065
27	BRT2/8	-3.275	0.725	2.062	2.3	1.25	-0.312	-1.138	-1.163	-0.05
28	BRT2/9	-1.271	-4.071	0.088	0.835	0.776	0.9	1.041	1.129	0.765
29	BRT2/10	-2.371	0.429	-0.012	-1.465	-2.924	-3.7	-4.259	-3.971	-2.335
30	BRT2/11	-2.075	-4.275	-3.138	-2.2	0.15	1.787	2.762	3.438	2.85
31	BRT2/12	1.429	0.629	-0.112	-0.265	-0.324	-0.3	-0.159	-0.071	-0.135
32	BRT2/13	1.329	-2.871	0.888	0.835	0.676	0.7	0.641	0.529	0.065
33	BRT2/14	0.425	0.425	-1.638	-2.8	-1.65	-0.713	-0.238	0.637	0.95
34	BRT2/15	0.629	1.229	0.088	0.035	0.076	0.2	0.241	0.029	-0.135

35	**BRT2/16**	-0.271	2.229	0.988	0.435	0.176	0.1	0.041	-0.071	-0.235
36	**BRT2/17**	-0.075	1.125	1.062	-0.9	-0.85	-0.713	-0.938	-0.263	0.35
37	**BRT2/18**	-0.471	0.129	0.988	0.635	0.576	0.7	0.741	0.629	0.465
38	**BRT2/19**	-0.171	1.929	0.288	0.835	0.776	0.8	0.841	0.629	0.265
39	**BRT3/1**	0.197	3.776	-1.539	-0.619	-0.343	-0.074	0.123	-0.03	-0.229
40	**BRT3/2**	1.417	1.376	-0.319	-0.092	0.077	0.28	0.43	0.804	0.744
41	**BRT3/3**	1.297	1.976	0.961	0.581	0.257	0.126	-0.077	-0.13	0.071
42	**BRT3/4**	1.397	3.576	1.761	1.381	1.057	0.626	0.023	-0.33	-0.729
43	**BRT3/5**	2.107	-1.686	-0.545	-0.856	-0.866	-1.237	-1.819	-1.842	-1.033
44	**BRT3/6**	0.497	1.276	0.861	0.281	0.257	0.326	0.523	0.77	0.771
45	**BRT3/7**	-0.303	-0.624	-0.039	-0.219	-0.043	0.026	0.123	0.27	-0.129
46	**BRT3/8**	-2.393	-1.186	-3.045	-4.256	-4.366	-3.837	-2.719	-1.842	-0.333
47	**BRT3/9**	0.297	-2.324	0.461	0.581	0.557	0.626	0.923	1.07	1.171
48	**BRT3/10**	-2.289	-3.002	3.058	2.041	1.37	1.028	0.775	0.553	-0.05
49	**BRT3/11**	3.607	-0.186	-0.045	-1.656	-1.966	-1.537	-0.419	0.458	1.467
50	**BRT3/12**	0.397	-2.024	-0.539	-1.119	-1.043	-0.774	-0.477	-0.13	0.371
51	**BRT3/13**	1.211	2.298	1.158	0.341	-0.43	-0.972	-1.525	-1.647	-1.55
52	**BRT3/14**	-2.293	1.614	1.455	2.644	3.234	3.263	2.581	1.858	0.767
53	**BRT3/15**	0.397	-2.124	-1.139	-0.519	-0.343	-0.074	0.023	0.07	0.271
54	**BRT3/16**	-0.203	-2.324	-0.439	-0.319	-0.443	-0.474	-0.577	-0.83	-0.829
55	**BRT3/17**	-1.493	0.014	1.655	3.644	4.234	4.063	3.181	2.158	1.067
56	**BRT3/18**	0.197	2.076	-0.939	-0.219	0.257	0.526	0.923	0.97	1.271
57	**BRT3/19**	-0.303	-0.524	0.861	0.681	0.557	0.526	0.323	0.17	-0.029
58	**BRT4/1**	0.346	-1.385	-2.208	-1.431	-1.162	-1.031	-1.008	-1.131	-1.038
59	**BRT4/2**	2.8	1.7	-2.3	-1.333	-0.867	-0.433	-0.133	0.6	-2.233
60	**BRT4/3**	3.146	-1.685	0.192	0.169	0.038	-0.031	-0.108	-0.031	-0.038
61	**BRT4/4**	0.446	2.115	0.892	0.769	0.438	0.069	-0.608	-0.931	-1.038
62	**BRT4/5**	-1.133	-1.367	-0.867	-0.467	-0.4	-0.333	-0.2	0.033	-1.8
63	**BRT4/6**	1.746	1.215	0.892	0.169	0.338	0.569	1.092	1.369	1.062
64	**BRT4/7**	1.046	-2.685	0.392	-0.031	-0.162	-0.231	-0.408	-0.231	-0.338
65	**BRT4/8**	-1.962	-1.7	0.4	-0.312	-0.512	-0.413	-0.162	0.05	0.137
66	**BRT4/9**	-0.354	-1.885	0.492	0.569	0.738	0.969	1.492	1.769	1.562
67	**BRT4/10**	-2.054	-2.885	2.292	2.069	1.638	1.269	0.892	0.569	0.462
68	**BRT4/11**	3.138	-3.5	-1.3	-1.413	-1.212	-0.913	-0.662	-0.65	-0.863
69	**BRT4/12**	0.046	-0.585	-1.408	-1.131	-0.962	-0.731	-0.308	-0.031	0.062
70	**BRT4/13**	0.546	3.715	0.592	0.469	0.038	-0.431	-0.908	-1.031	-0.638
71	**BRT4/14**	0.938	2	1.3	-1.413	-0.312	0.288	1.038	1.75	2.438
72	**BRT4/15**	-1.154	-0.785	-0.708	-0.731	-0.662	-0.531	-0.308	-0.231	-0.038
73	**BRT4/16**	-1.454	-0.285	-0.708	-0.631	-0.562	-0.631	-0.908	-1.131	-1.038
74	**BRT4/17**	-3.263	2.1	-4.5	2.188	1.788	1.288	0.238	-0.55	-1.062
75	**BRT4/18**	-1.054	2.515	-0.008	-0.031	0.238	0.569	0.992	1.069	0.962

76	**BRT4/19**	-1.254	2.615	-0.708	-0.231	0.038	0.169	0.092	-0.031	0.062
77	**BRT5/1**	-1.458	3.368	-0.996	-0.492	-0.65	-0.643	-0.904	-1.384	-1.52
78	**BRT5/2**	-0.094	-2.315	1.905	-1.082	0.526	1.758	3.477	3.801	2.459
79	**BRT5/3**	-0.258	2.068	-1.596	-0.792	-0.55	-0.443	-0.204	-0.284	-0.12
80	**BRT5/4**	0.142	2.368	1.404	1.308	0.85	0.257	-0.504	-1.184	-1.52
81	**BRT5/5**	1.015	1.388	1.964	-0.084	-1.063	-1.891	-1.965	-1.898	-1.446
82	**BRT5/6**	0.242	-2.332	2.604	2.408	1.95	1.457	0.796	0.316	-0.32
83	**BRT5/7**	0.142	-2.332	2.604	2.408	1.95	1.457	0.796	0.316	-0.22
84	**BRT5/8**	-1.808	0.416	-0.91	-3.435	-3.013	-2.701	-2.092	-2.081	-1.74
85	**BRT5/9**	-1.658	-0.132	0.804	0.908	0.75	0.757	0.996	1.016	0.98
86	**BRT5/10**	-3.145	0.39	2.201	1.968	1.763	1.558	1.348	0.799	-0.341
87	**BRT5/11**	-0.308	0.316	-3.81	-1.735	-0.713	-0.101	-1.192	0.119	0.96
88	**BRT5/12**	1.242	-1.532	-0.996	-0.492	-0.65	-0.543	-0.304	-0.284	0.08
89	**BRT5/13**	0.355	0.09	-0.099	-0.032	-0.337	-0.742	-1.152	-1.501	-1.641
90	**BRT5/14**	1.492	-3.584	-3.91	-0.235	0.387	0.699	1.408	1.119	0.36
91	**BRT5/15**	-1.358	-1.932	-0.096	0.008	-0.25	-0.343	-0.404	-0.484	-0.22
92	**BRT5/16**	-1.358	-1.332	0.004	0.108	-0.15	-0.343	-0.704	-1.284	-1.32
93	**BRT5/17**	3.093	3.416	-1.81	-0.035	0.787	1.299	2.308	2.119	1.46
94	**BRT5/18**	-1.358	-0.232	0.104	0.408	0.35	0.457	0.896	0.916	1.38
95	**BRT5/19**	-1.558	-1.632	0.204	0.508	0.45	0.357	0.296	0.016	-0.02
96	**BRT6/1**	-0.544	1.13	-1.974	-1.453	-1.181	-1.012	-1.101	-0.98	-0.518
97	**BRT6/2**	1.12	3.947	2.228	4.657	2.195	0.189	-1.72	-1.795	-1.539
98	**BRT6/3**	1.656	-1.17	-0.874	-0.953	-0.681	-0.412	-0.2	0.12	0.382
99	**BRT6/4**	2.056	-2.07	5.126	3.047	1.719	0.588	-0.7	-0.98	-0.918
100	**BRT6/5**	-2.271	0.45	-5.513	-1.045	0.006	0.74	1.339	1.306	0.556
101	**BRT6/6**	0.856	-0.37	-0.874	-1.053	-0.181	0.488	1.3	1.82	1.682
102	**BRT6/7**	0.256	1.13	2.026	0.347	-0.181	-0.512	-0.7	-0.38	-0.118
103	**BRT6/8**	-4.893	-4.422	2.912	3.003	2.956	2.73	2.312	1.823	0.863
104	**BRT6/9**	0.456	-4.27	-1.874	-1.453	-0.881	-0.112	0.7	1.22	1.382
105	**BRT6/10**	-1.231	-1.348	-0.777	-1.394	-1.068	-0.71	-0.149	0.303	0.161
106	**BRT6/11**	2.307	0.278	1.112	1.903	2.156	2.13	1.812	1.323	0.363
107	**BRT6/12**	2.856	1.23	-3.374	-2.053	-0.981	-0.312	0.399	0.72	0.782
108	**BRT6/13**	1.169	0.352	-2.977	-2.994	-2.568	-2.51	-2.249	-1.697	-1.139
109	**BRT6/14**	-1.793	0.878	4.512	5.103	4.156	3.23	2.012	1.123	-0.037
110	**BRT6/15**	0.356	0.33	-1.074	-1.153	-0.981	-0.612	-0.401	0.02	0.382
111	**BRT6/16**	-0.444	1.93	-1.174	-1.253	-1.281	-1.312	-1.601	-1.38	-0.818
112	**BRT6/17**	0.807	1.378	5.712	3.903	2.356	1.23	0.012	-0.677	-0.837
113	**BRT6/18**	-0.844	0.33	-1.074	0.947	1.319	1.588	1.8	1.92	1.982
114	**BRT6/19**	0.256	1.33	-0.674	-0.753	-0.581	-0.412	-0.3	0.02	0.282
115	**BRV1/1**	1.125	-0.5	2.35	0.95	0.825	0.625	0.375	0.15	-0.05
116	**BRV1/2**	-1.775	0	-2.55	-3.95	-2.875	-1.975	-1.025	-0.45	0.05

117	**BRV1/3**	3.333	1.1	1.333	0.9	0.733	0.633	0.567	0.4	0.033
118	**BRV1/4**	-1.267	1.3	1.433	0.3	-0.167	-0.367	-0.533	-0.5	-0.267
119	**BRV1/5**	1.633	0.833	1.8	1.333	1	0.667	0.233	0	-0.167
120	**BRV1/6**	0.433	1.133	0.3	-0.067	-0.1	-0.133	-0.167	-0.1	-0.067
121	**BRV1/7**	1.25	-1.3	1.05	0.875	0.6	0.35	-0.025	-0.125	-0.35
122	**BRV1/8**	0.15	1.3	-0.55	-0.625	-0.6	-0.55	-0.625	-0.625	-0.55
123	**BRV1/9**	3.394	1.369	-0.9	-1.025	-0.681	-0.669	-0.219	0.175	0.538
124	**BRV1/10**	4.594	-1.531	-4.1	-1.925	-0.981	-0.569	-0.319	-0.225	0.137
125	**BRV1/11**	2.994	-2.431	1.9	2.275	2.319	2.431	2.081	1.875	1.438
126	**BRV2/1**	1.829	-0.771	-4.912	-4.765	-4.824	-5	-4.559	-3.871	-2.135
127	**BRV2/2**	-4.471	1.629	1.588	1.135	1.476	1.6	0.941	0.929	2.265
128	**BRV2/3**	-2.371	-0.371	-2.812	-1.265	-0.024	0.6	0.941	0.829	0.265
129	**BRV2/4**	-0.675	3.125	3.462	3	0.45	-1.013	1.163	0.037	-3.25
130	**BRV2/5**	-0.675	0.225	-2.438	-3.5	-2.85	-2.413	-2.337	-1.062	0.45
131	**BRV2/6**	3.125	1.425	-1.338	-1.2	-2.15	-1.913	-2.638	-4.263	-1.85
132	**BRV3/1**	-3.403	-0.724	-5.639	-3.919	-2.643	-2.174	-1.577	-1.33	-0.829
133	**BRV3/2**	2.707	-0.986	2.655	0.644	-0.466	-1.437	-2.219	-2.042	-0.933
134	**BRV3/3**	-1.793	0.714	3.555	1.544	0.434	-0.137	-0.219	0.158	0.867
135	**BRV3/4**	4.007	-0.986	-3.945	-3.156	-1.966	-1.137	-0.219	0.058	0.067
136	**BRV3/5**	1.62	0.236	-1.048	0.403	-0.953	-1.035	-0.567	-0.36	-2.253
137	**BRV3/6**	-3.88	1.136	-3.148	-1.997	-0.753	-0.335	-0.167	-0.36	-0.353
138	**BRV3/7**	0.611	-1.302	1.158	1.041	0.97	0.728	0.475	0.553	0.45
139	**BRV3/8**	-2.193	1.314	2.455	3.044	3.434	3.363	2.581	1.758	0.667
140	**BRV3/9**	-0.783	0.776	-0.219	-0.592	-0.623	-1.02	-1.37	-0.796	-0.056
141	**BRV3/10**	1.031	1.098	1.678	1.467	1.49	1.281	1.082	1.286	1.323
142	**BRV3/11**	-0.383	-2.824	-0.719	-0.692	-1.423	-1.22	-0.77	-2.196	-3.356
143	**BRV3/12**	-1.283	-0.424	-0.419	-0.092	0.477	0.68	0.63	0.904	1.344
144	**BRV4/1**	-0.6	-0.3	1.5	0.167	0.433	0.367	0.467	0	1.167
145	**BRV4/2**	-2.2	-1.4	0.8	1.167	0.433	0.067	-0.333	-0.6	1.067
146	**BRV4/3**	2.567	-0.767	1.833	1.833	1.3	0.967	1	1.233	2.3
147	**BRV4/4**	-1.433	2.133	-0.967	-1.367	-0.9	-0.633	-0.8	-1.267	-0.5
148	**BRV4/5**	0.538	-0.1	1.2	0.387	-0.112	-0.413	-0.562	-0.45	-0.363
149	**BRV4/6**	3.338	0.3	0.3	-0.312	-0.412	-0.613	-0.662	-0.85	-1.263
150	**BRV4/7**	-5.962	1.5	-0.2	-0.913	-0.812	-0.712	-0.662	-0.65	-0.963
151	**BRV4/8**	3.237	-0.6	2.8	1.787	1.588	1.487	1.438	1.35	1.938
152	**BRV5/1**	-2.08	-1.293	-2.998	-1.923	-1.561	-0.941	-0.571	0.183	0.538
153	**BRV5/2**	3.106	-2.415	0.505	2.418	1.126	0.958	-2.023	-0.299	0.759
154	**BRV5/3**	-4.094	-0.315	-1.095	0.418	1.826	2.758	3.977	4.101	2.559
155	**BRV5/4**	1.915	1.388	2.764	0.316	-0.763	-1.691	-1.965	-1.898	-1.346
156	**BRV5/5**	0.392	-1.284	1.39	0.965	0.887	0.999	1.608	0.719	-2.04
157	**BRV5/6**	0.392	-0.584	1.29	-2.235	-1.313	-0.601	-0.992	0.519	1.26

158	**BRV5/7**	4.106	-0.062	-2.413	-1.676	-1.8	-2.2	-2.14	-2.898	1.34
159	**BRV5/8**	1.792	4.116	-1.41	-1.835	-2.613	-3.101	-2.292	-1.681	-0.64
160	**BRV5/9**	0.555	2.59	1.601	1.068	0.863	0.558	0.348	-0.001	-0.441
161	**BRV5/10**	0.555	1.39	0.801	0.868	0.963	0.958	1.148	1.099	0.759
162	**BRV6/1**	-0.08	2.547	0.428	-2.243	-1.505	-1.411	0.78	-2.595	-2.239
163	**BRV6/2**	2.12	-0.153	-0.972	-2.243	-2.605	-3.311	-3.92	-3.395	-2.539
164	**BRV6/3**	-0.658	-3.227	0.784	0.814	1.819	2.842	2.591	2.489	2.236
165	**BRV6/4**	-2.493	-1.722	-1.788	-1.197	-0.344	0.23	1.112	1.323	0.863
166	**BRV6/5**	0.807	2.678	-1.488	-2.497	-3.744	-3.47	-3.388	-2.277	-1.337
167	**BRV6/6**	2.069	0.652	1.023	0.006	0.232	0.49	0.751	1.203	0.961
168	**BRV6/7**	-3.893	-1.822	0.612	0.003	-0.144	-0.37	-0.488	-0.577	-0.837

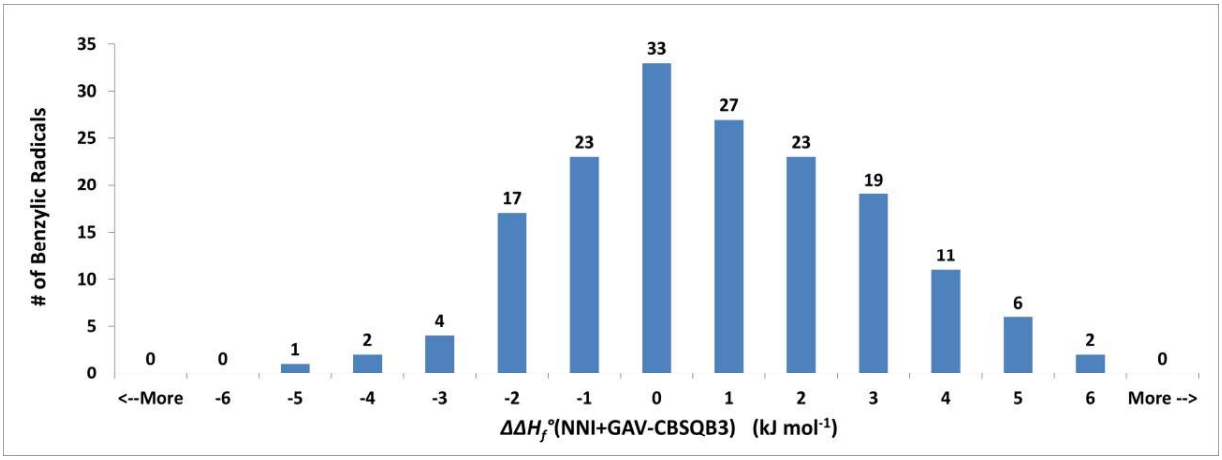

Figure C-74 Distribution of the differences between the final thermochemical data calculated with GA parameters and the *ab initio* reference dataset (CBSQB3) for the $\Delta_f H^\circ$ values of the benzylic radicals in the final set, $\Delta\Delta_f H°$((NNI+GAV)-CBSQB3).

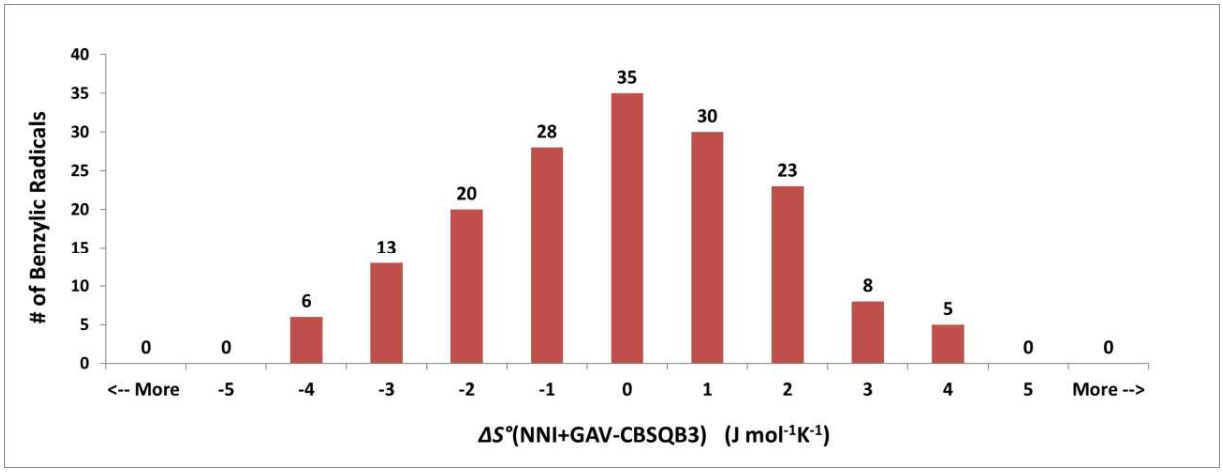

Figure C-75 Distribution of the differences between the final thermochemical data calculated with GA parameters and the *ab initio* reference dataset (CBSQB3) for the S° values of the benzylic radicals in the final set, $\Delta S°$((NNI+GAV)-CBSQB3).

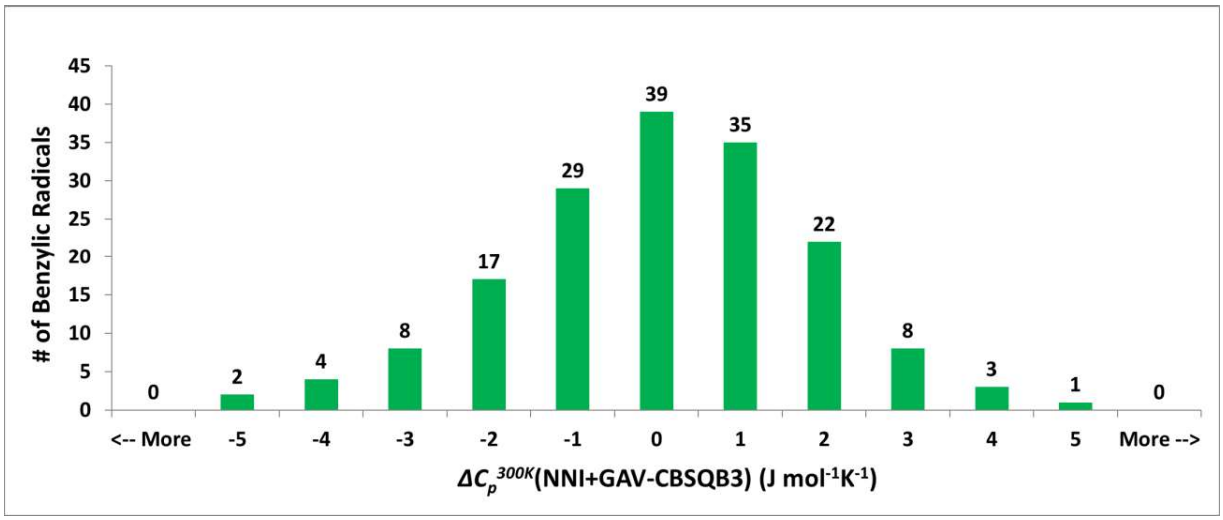

Figure C-76 Distribution of the differences between the final thermochemical data calculated with GA parameters and the *ab initio* reference dataset (CBSQB3) for the $C_p^{\mathbf{300K}}$ values of the benzylic radicals in the final set, ΔC_p^{300K}((NNI+GAV)-CBSQB3).

Appendix D

Supporting Information for Chapter 6

Contents

D.1 The Training Set

D.1.1 List of Reactions

152 hydrogen abstraction reactions (HARs) from unsubstituted and single substituted toluene derivatives (TD) constitute the training set. These reactions are abbreviated with the letter "T".

There are HARs from 8 different toluene derivative classes. These classes are

1. Toluenes

2. Ethylbenzenes

3. Isopropylbenzenes

4. Allylbenzenes (2-phenylpropenes)

5. α-methyl allylbenzenes (3-phenylbutenes)

6. α-vinyl allylbenzenes (3-phenyl-1,4-pentadienes)

7. Diphenylmethanes

8. 1,1-diphenylethanes

The list of HARs from each TD class is given in a figure in the following pages below, from **Figure D-1** to **Figure D-8**.

In the training set, there are 19 reactions from each toluene derivative class. The first reaction in each class represents the unsubstituted case. The following 18 reactions are included single substituted toluene derivatives as reactants where the substituents are -OH, -OCH_3, -CHO, -$CH{=}CH_2$, -CH_3 and -CH_2CH_3 in all *ortho* (*o*-), *meta* (*m*-) and *para* (*p*-) combinations.

A code is given for each of the 152 reactions in the training set. All of them start with "T" to indicate that that reaction is a part of the training set. The first number after "-" represents the class of TDs from which HAR took place. For example, the code "**T-214**" represents 14th HAR in the 2nd class (ethylbenzenes) in the training set. In this reaction, the abstraction is from a substituted ethylbenzene where the substituent is CH_3 that resides in *ortho* position to the hydrocarbon side chain as can be noted from the list above. In another example, "**T-507**" represents 7th HAR from the 5th class (α-methyl allylbenzenes), where the toluene derivatives bears the -OCH_3 group as the substituent that is in *para* position to the extended side chain.

T-101:

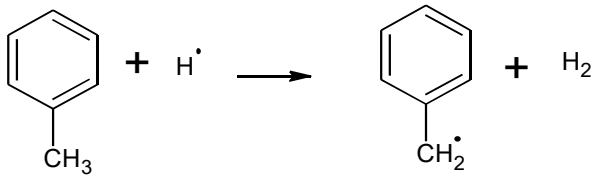

T-102:

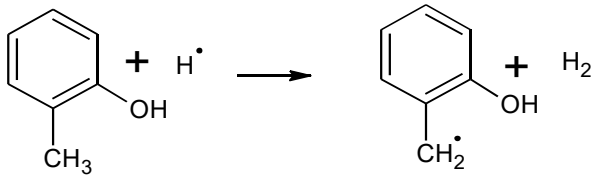

T-103:

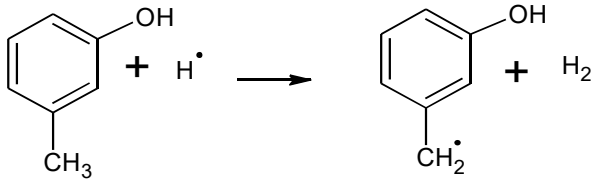

T-104:

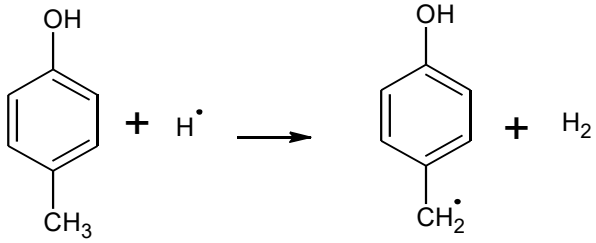

T-105:

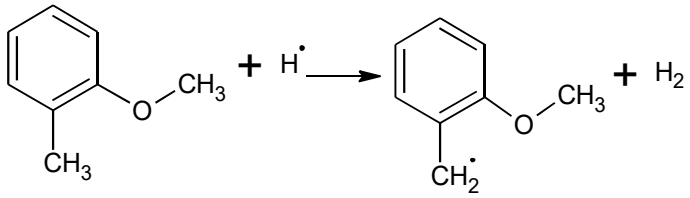

T-106:

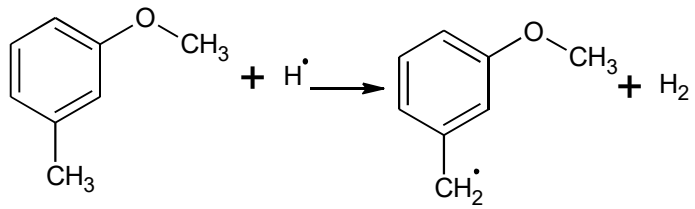

T-107:

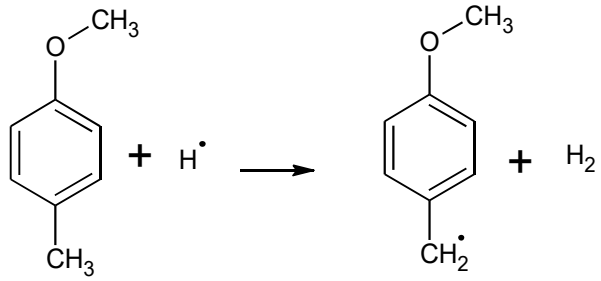

T-108:

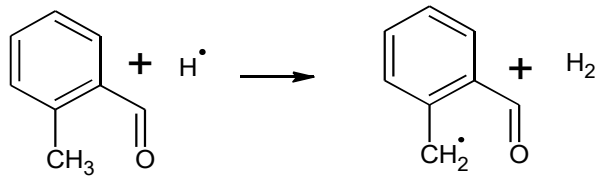

T-109:

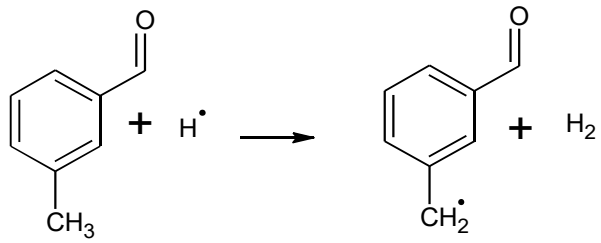

T-110:

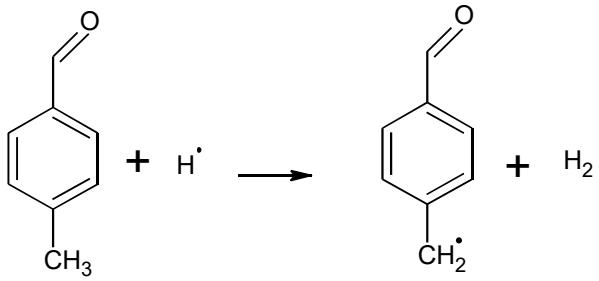

T-111:

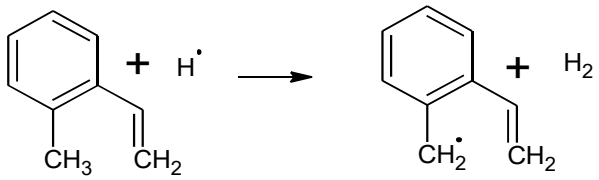

T-112:

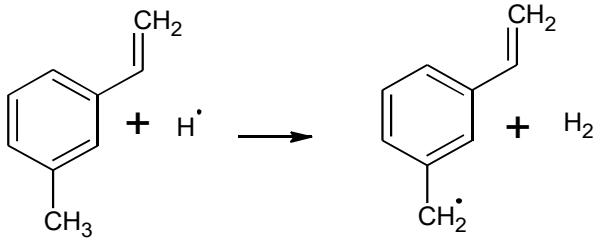

T-113:

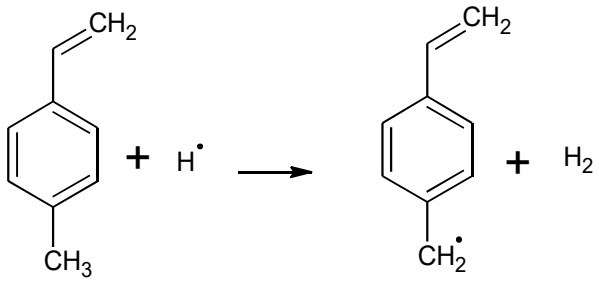

T-114:

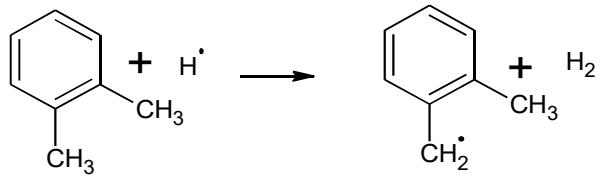

T-115:

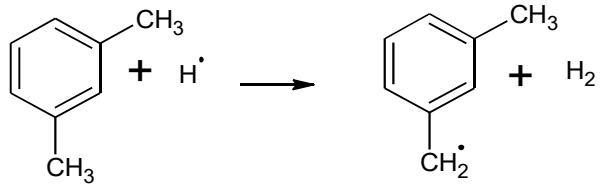

T-116:

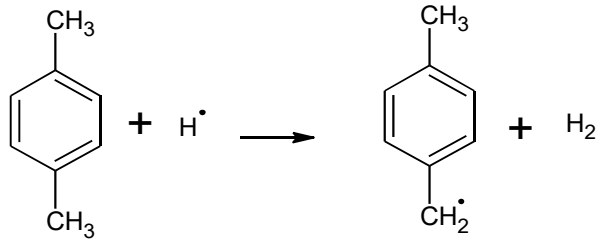

T-117:

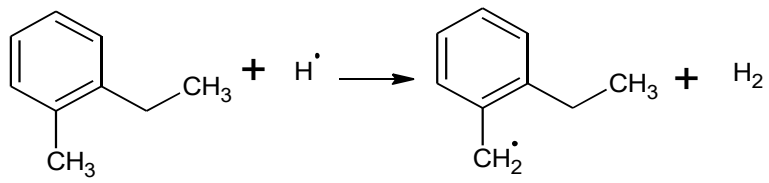

T-118:

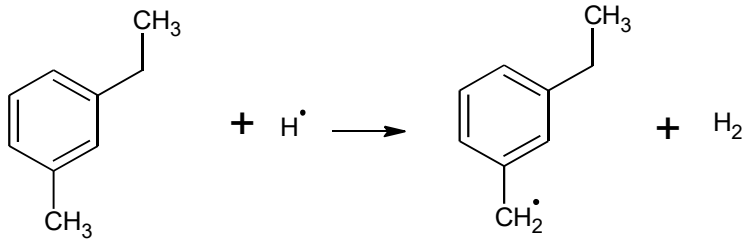

T-119:

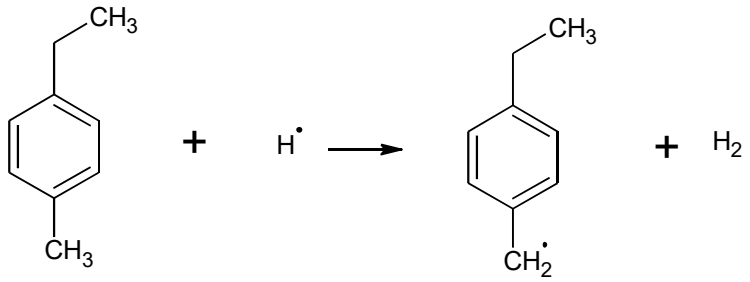

Figure D-1 Hydrogen abstraction reactions from the α-carbon of toluene and singly substituted toluenes.

T-201:

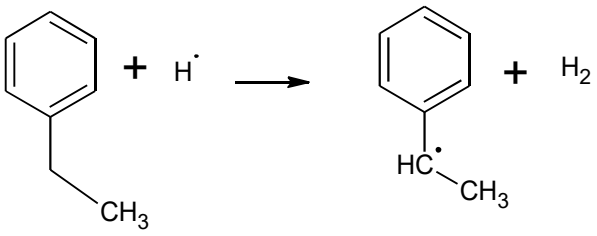

T-202:

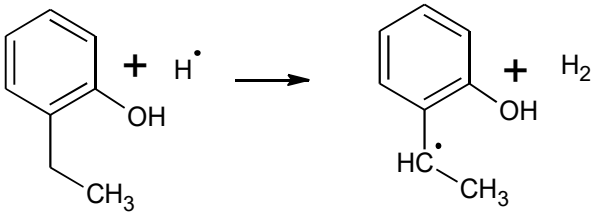

T-203:

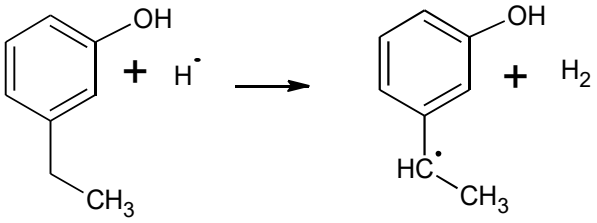

T-204:

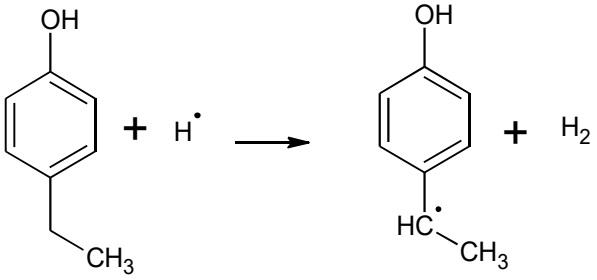

T-205:

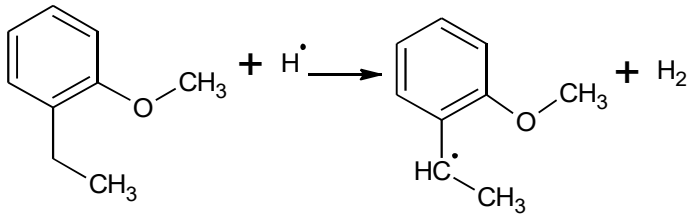

T-206:

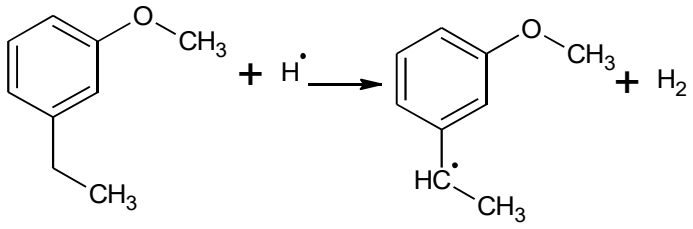

T-207:

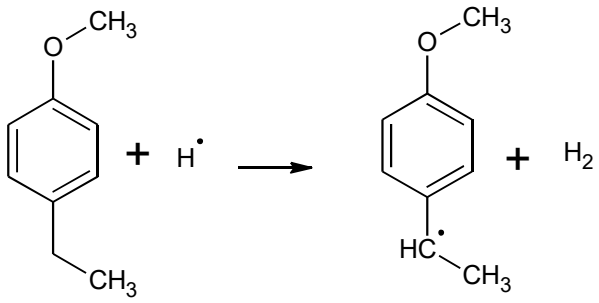

T-208:

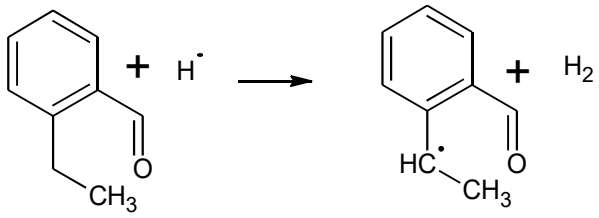

T-209:

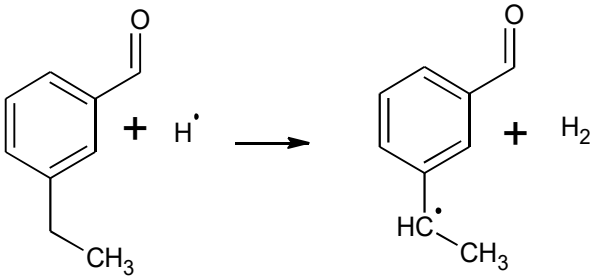

T-210:

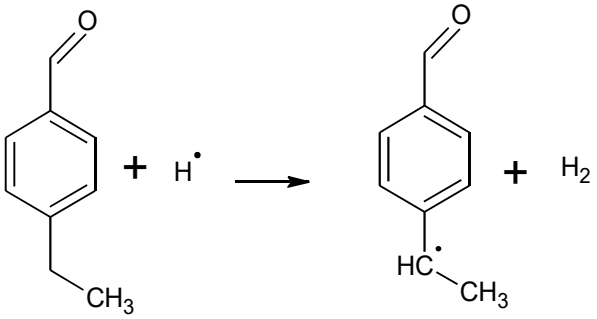

T-211:

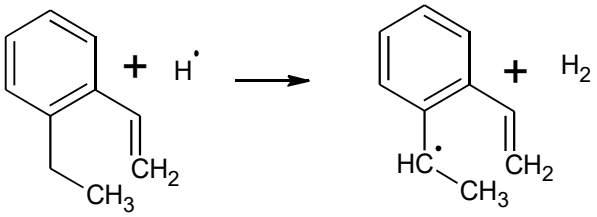

T-212:

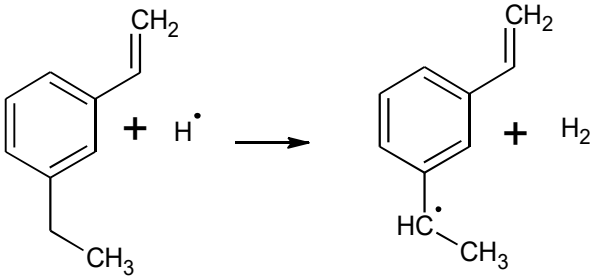

T-213:

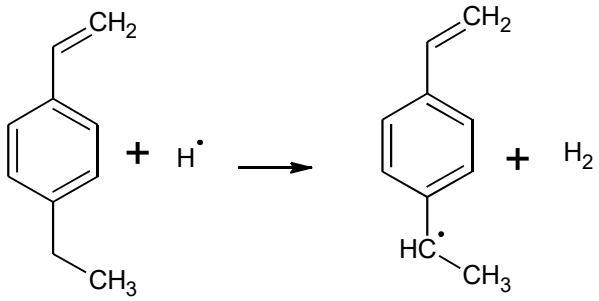

T-214:

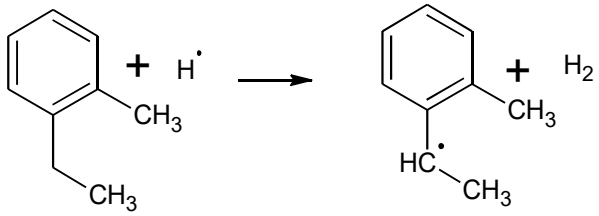

T-215:

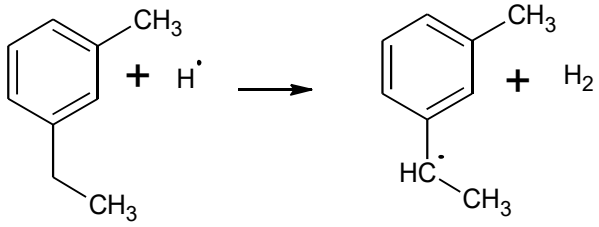

T-216:

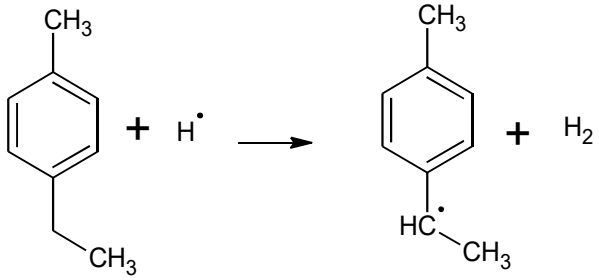

T-217:

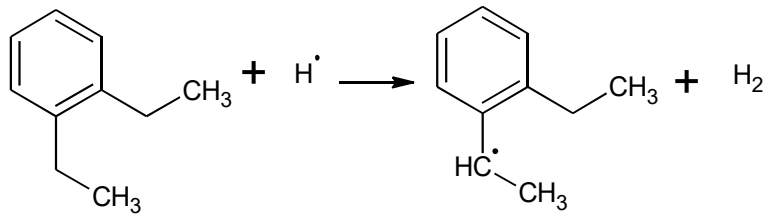

T-218:

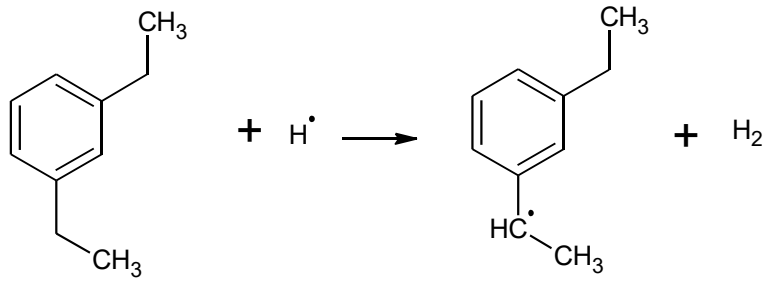

T-219:

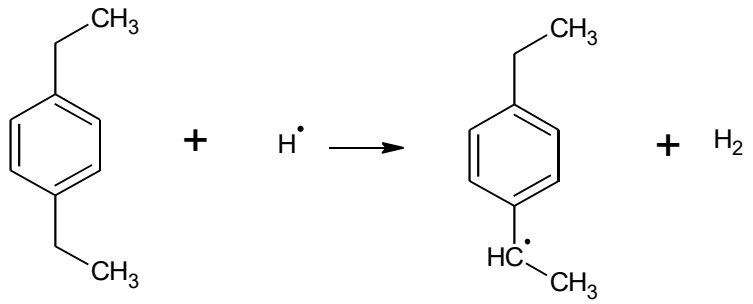

Figure D-2 Hydrogen abstraction reactions from the α-carbon of ethylbenzene and singly substituted ethylbenzene.

T-301:

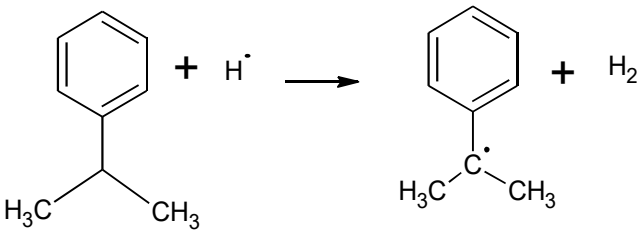

T-302:

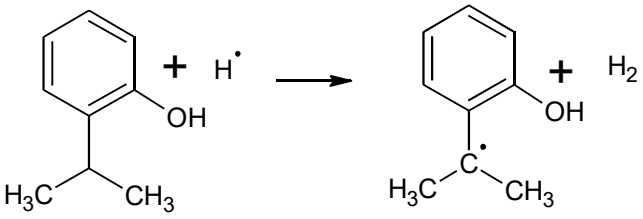

T-303:

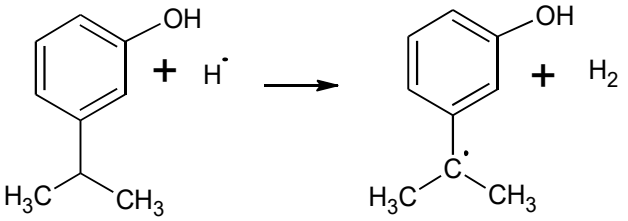

T-304:

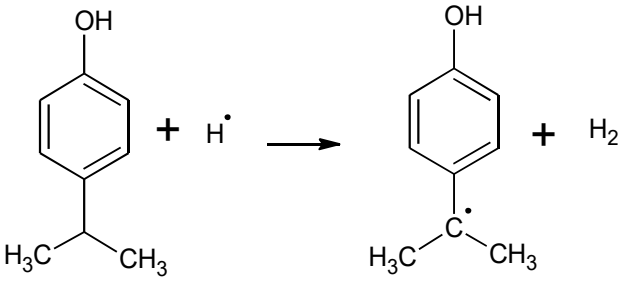

T-305:

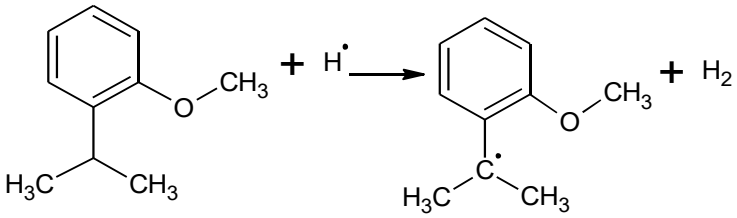

T-306:

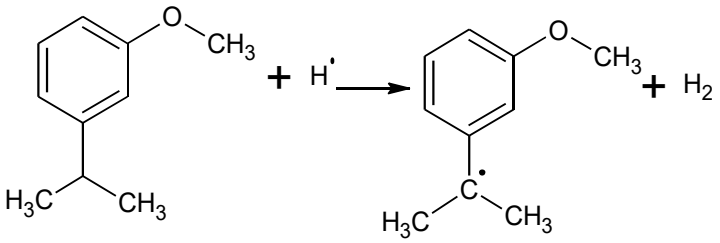

T-307:

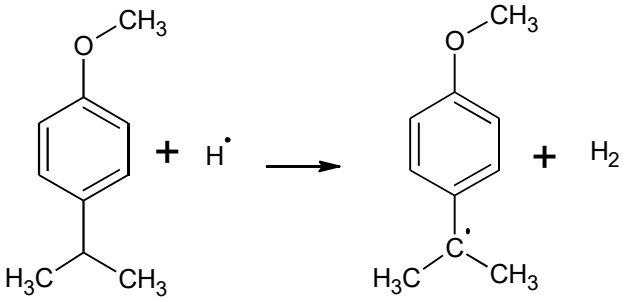

T-308:

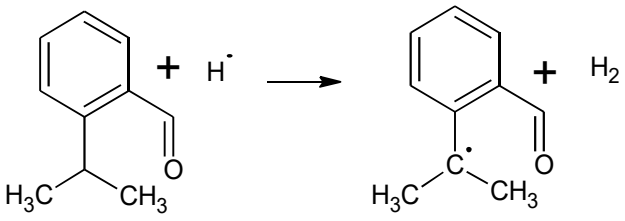

T-309:

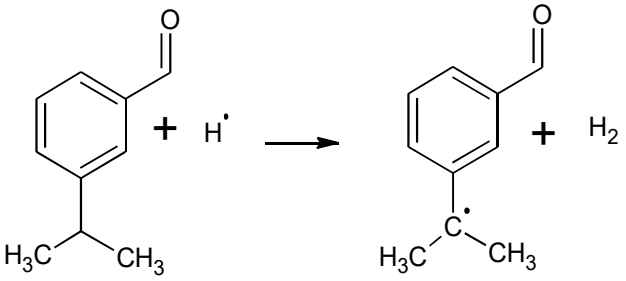

T-310:

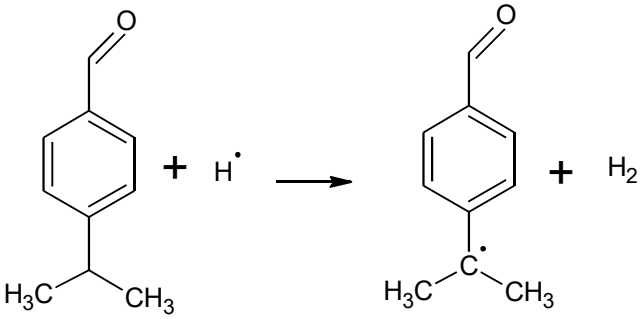

T-311:

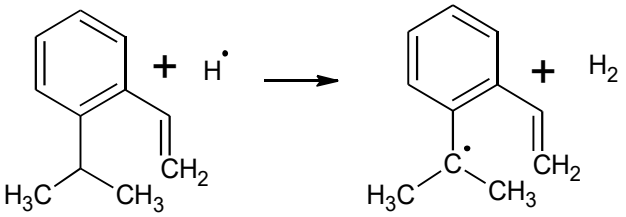

T-312:

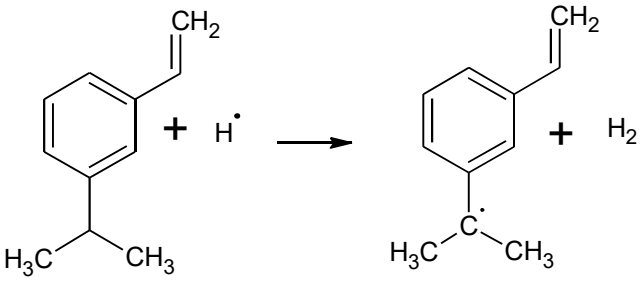

T-313:

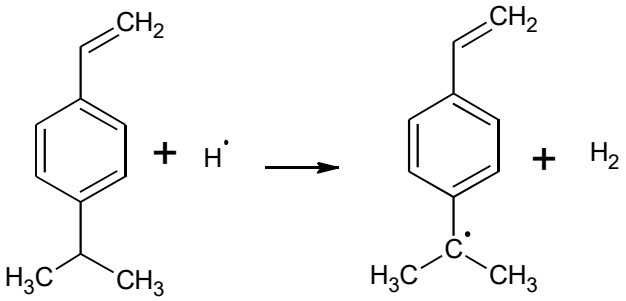

T-314:

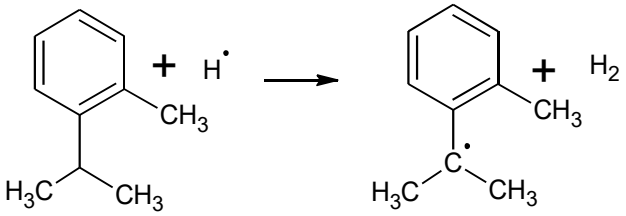

T-315:

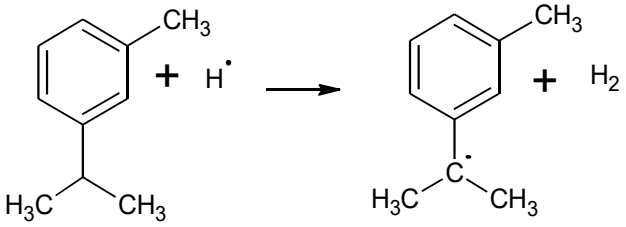

T-316:

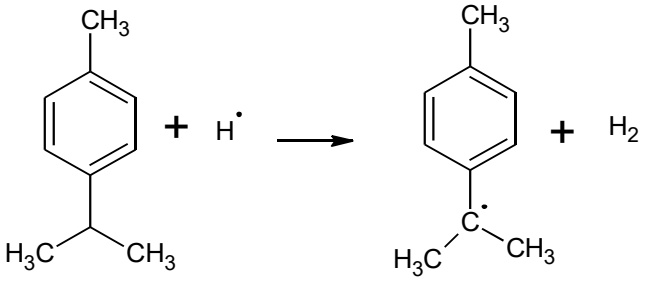

T-317:

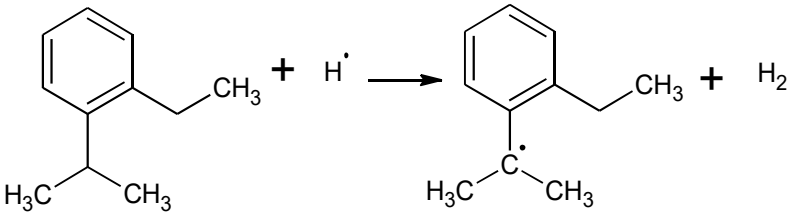

T-318:

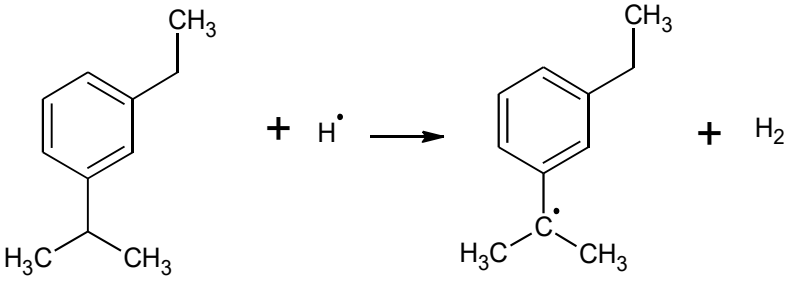

T-319:

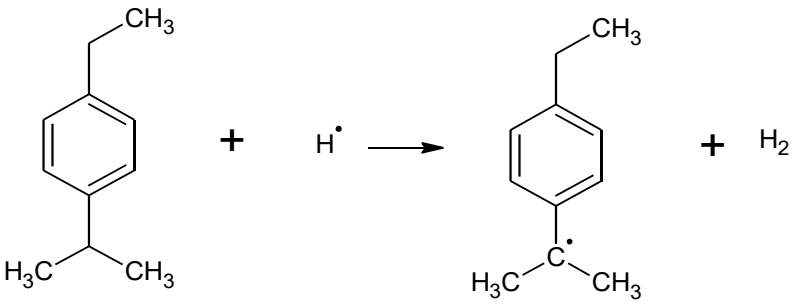

Figure D-3 Hydrogen abstraction reactions from the α-carbon of isopropylbenzene and singly substituted isopropylbenzenes.

T-401:

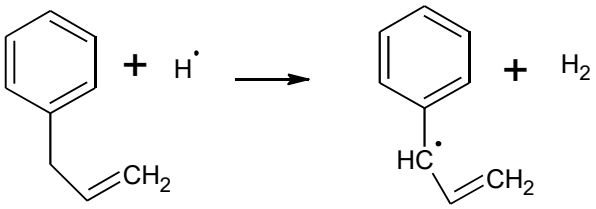

T-402:

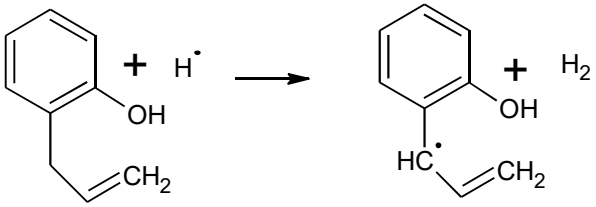

T-403:

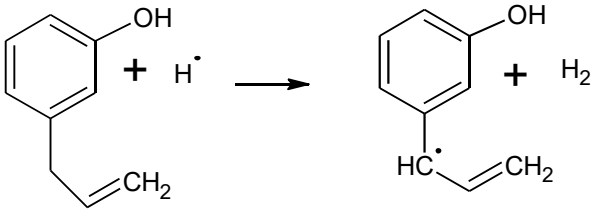

T-404:

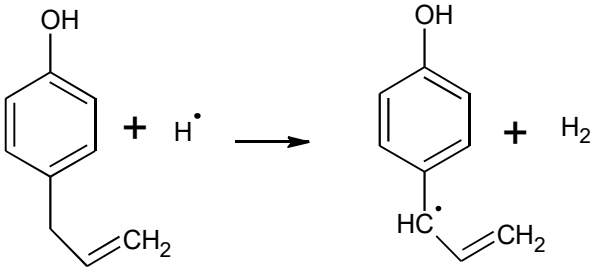

T-405:

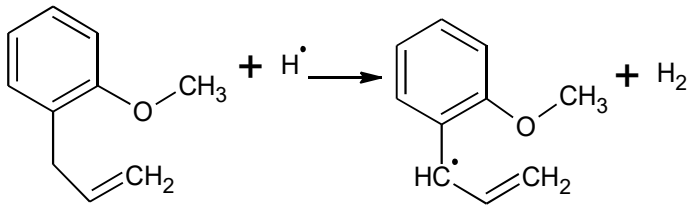

T-406:

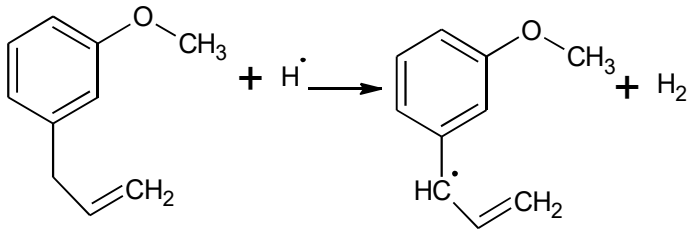

T-407:

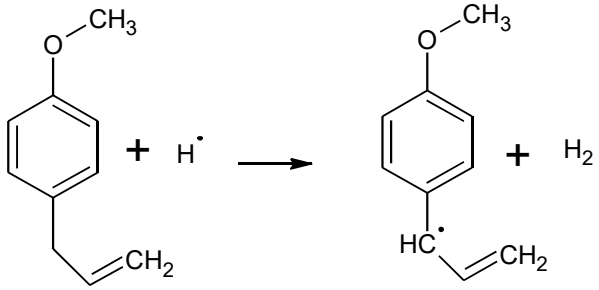

T-408:

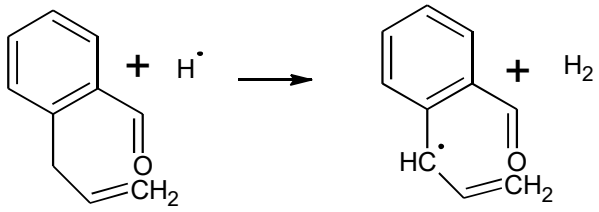

T-409:

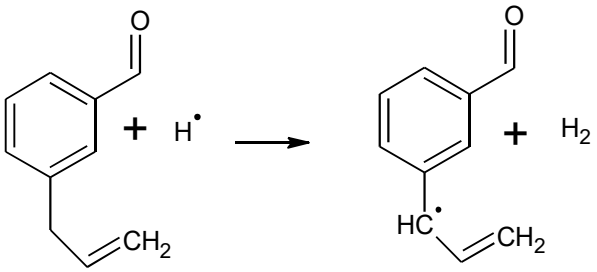

T-410:

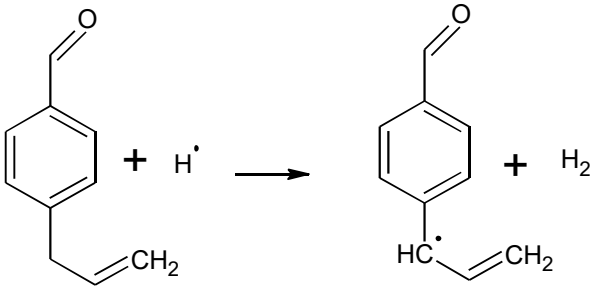

T-411:

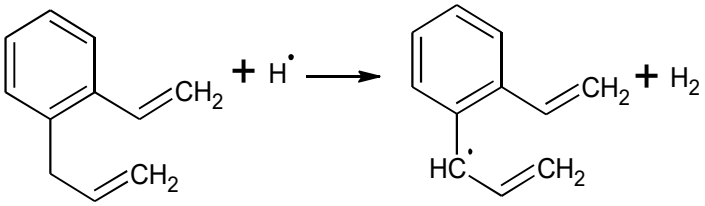

T-412:

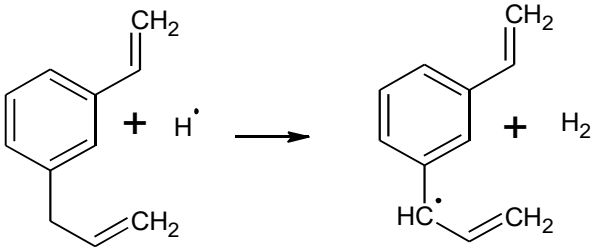

T-413:

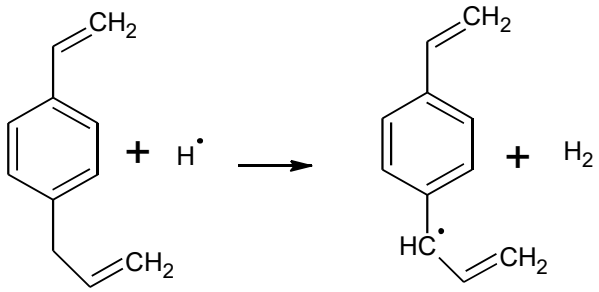

T-414:

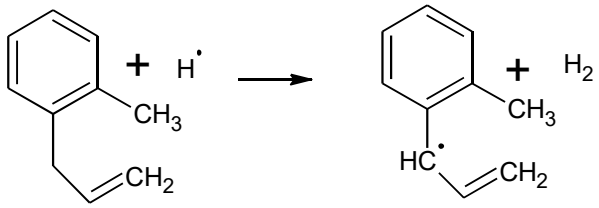

T-415:

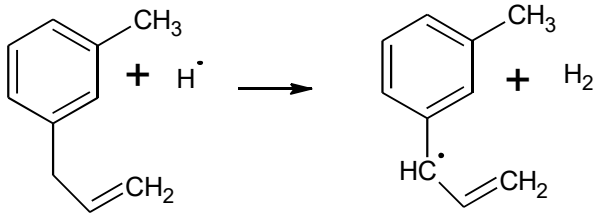

T-416:

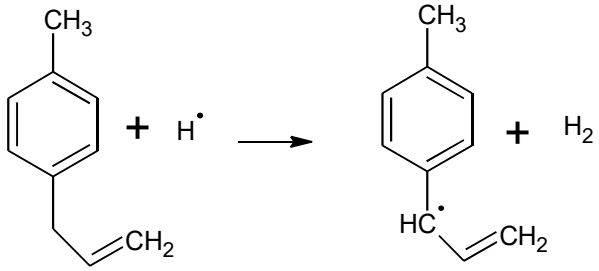

T-417:

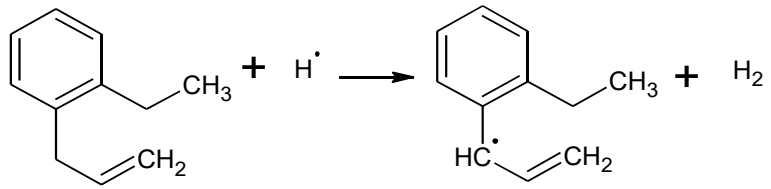

T-418:

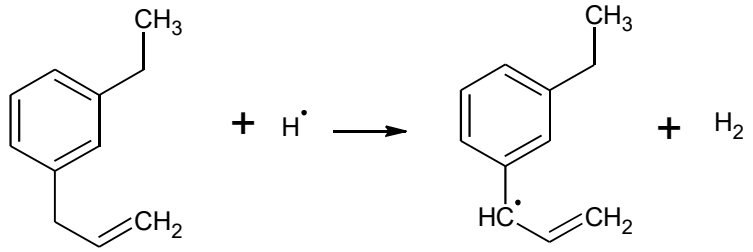

T-419:

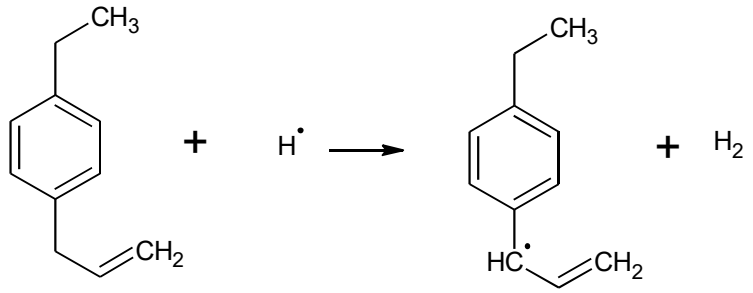

Figure D-4 Hydrogen abstraction reactions from the α-carbon of allylbenzene and singly substituted allylbenzenes.

T-501:

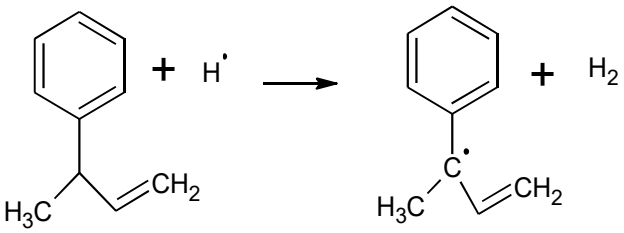

T-502:

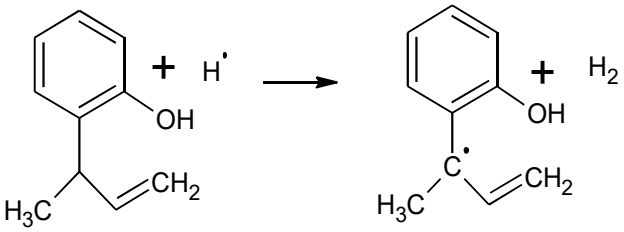

T-503:

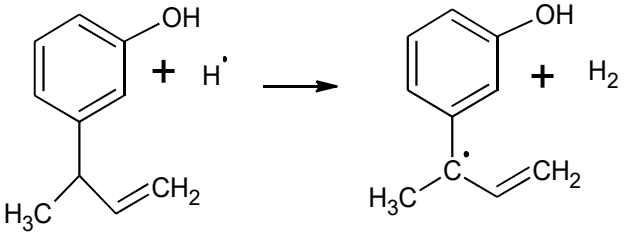

T-504:

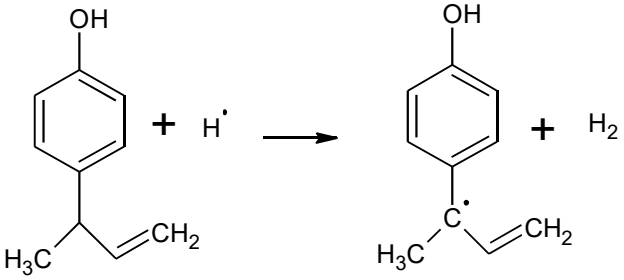

T-505:

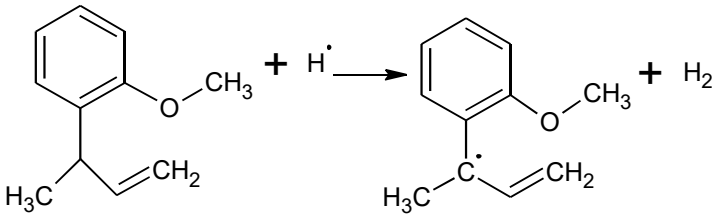

T-506:

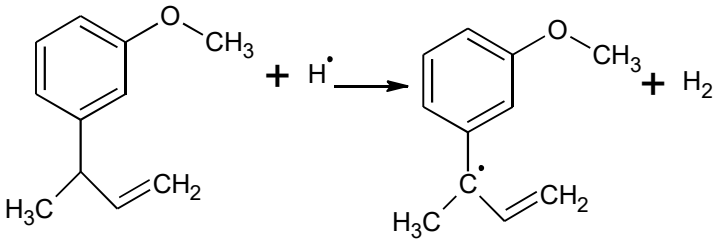

T-507:

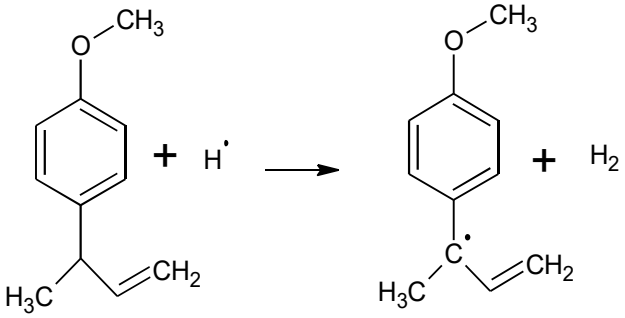

T-508:

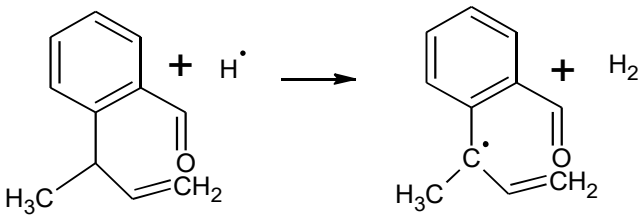

T-509:

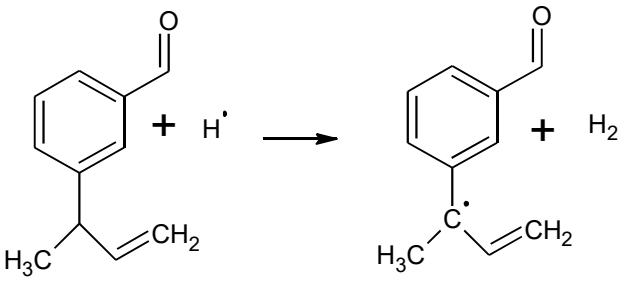

T-510:

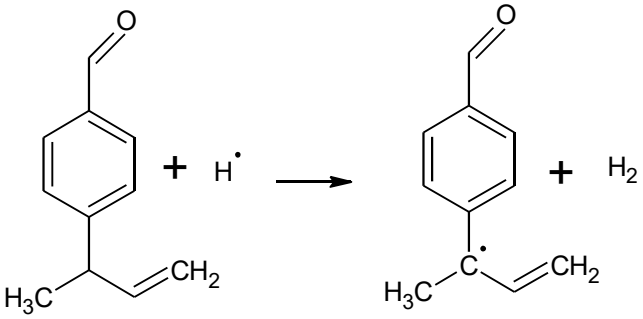

T-511:

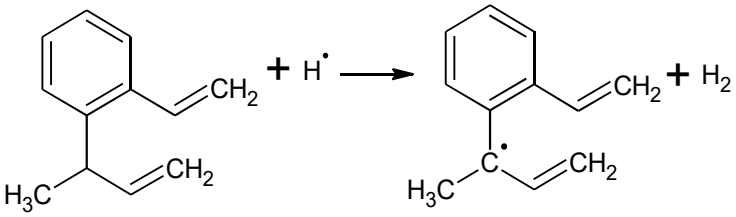

T-512:

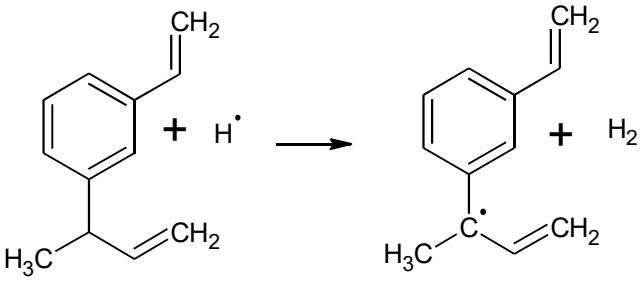

T-513:

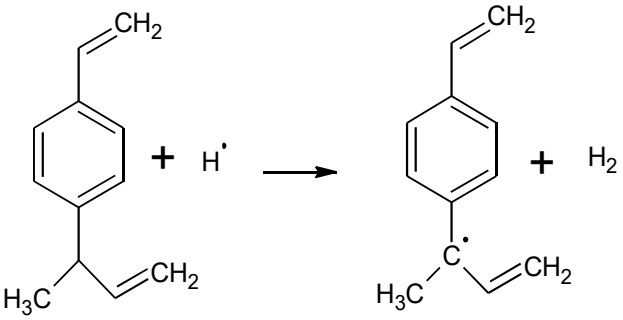

T-514:

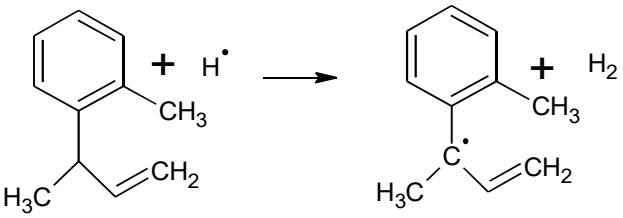

T-515:

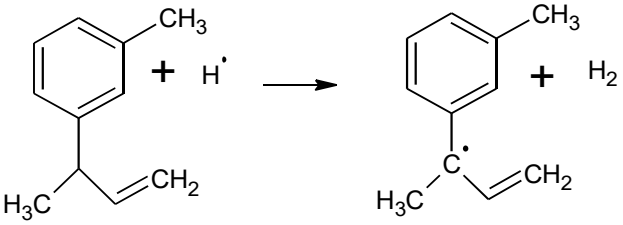

T-516:

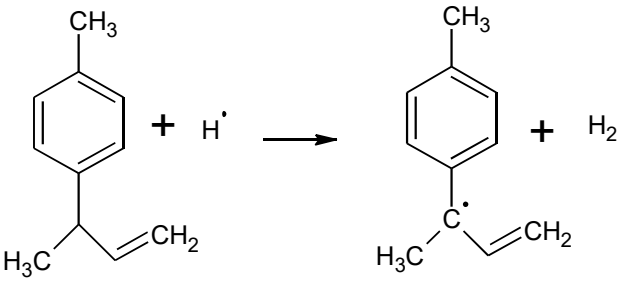

T-517:

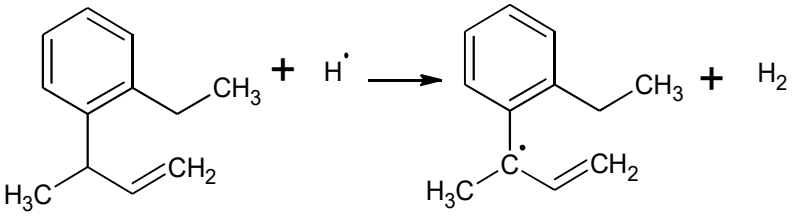

T-518:

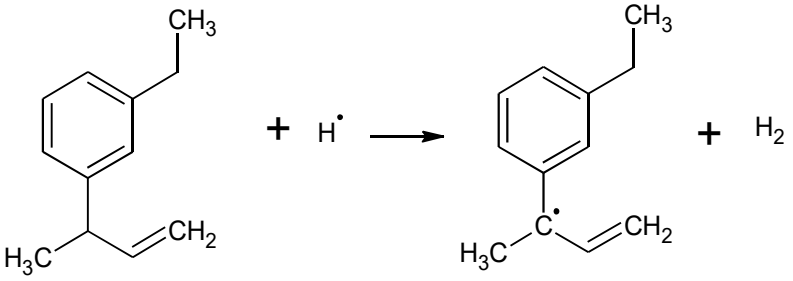

T-519:

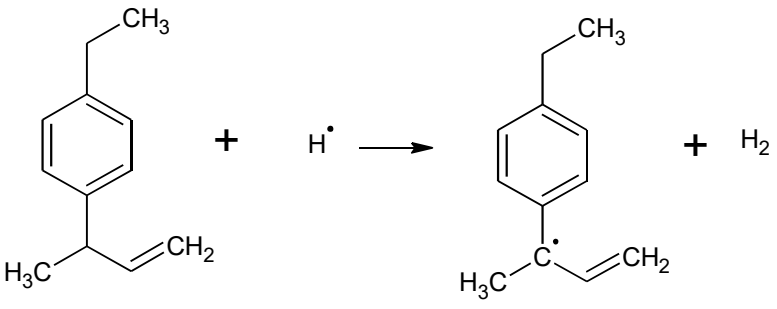

Figure D-5 Hydrogen abstraction reactions from the α-carbon of α-methyl allylbenzene and singly substituted α-methyl allylbenzenes.

T-601:

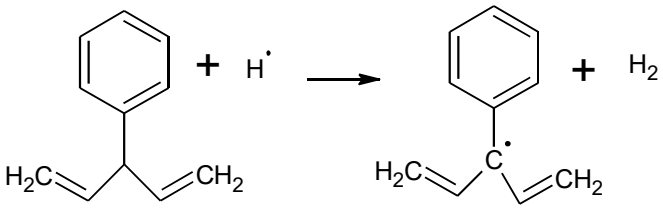

T-602:

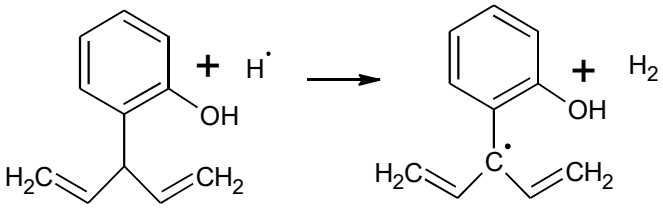

T-603:

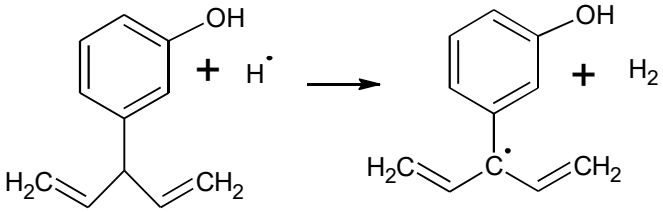

T-604:

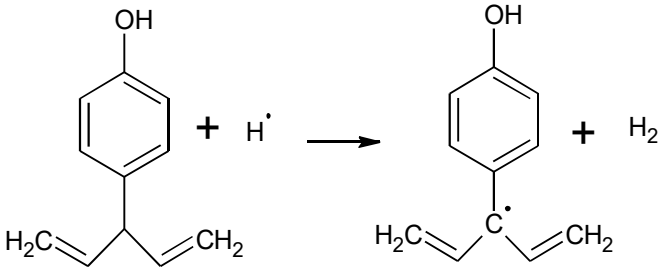

T-605:

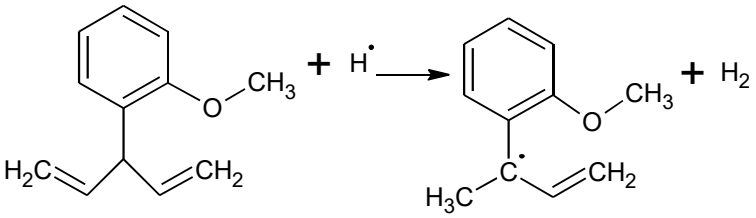

T-606:

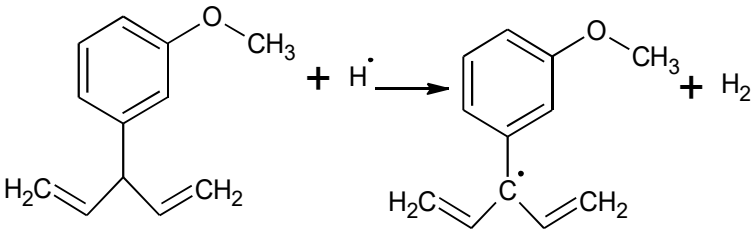

T-607:

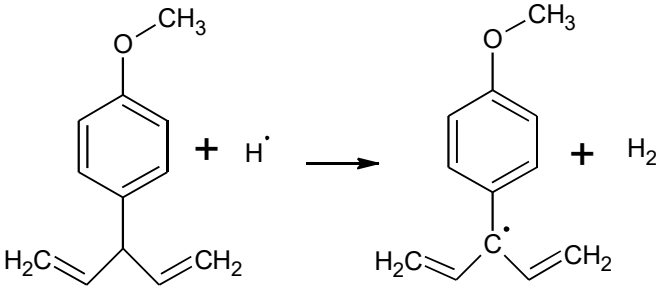

T-608:

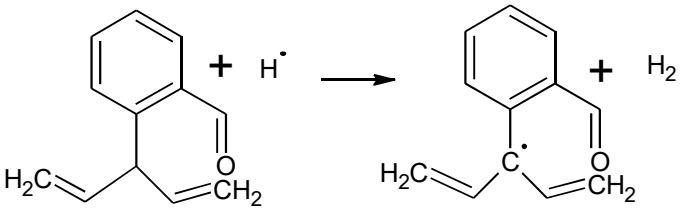

T-609:

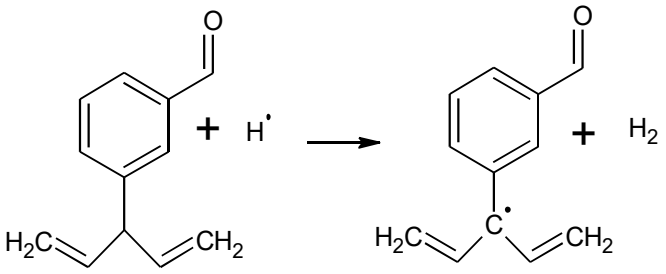

T-610:

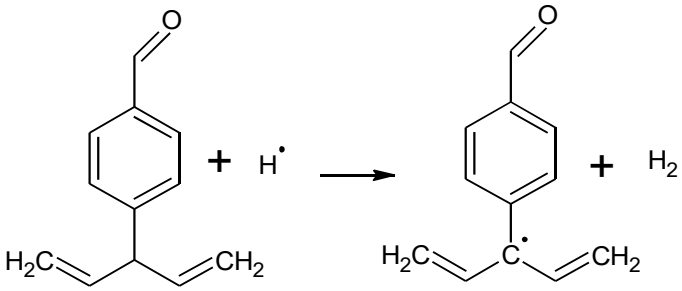

T-611:

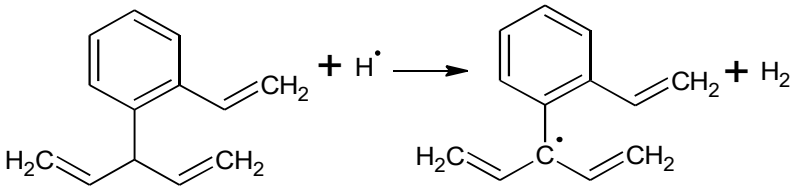

T-612:

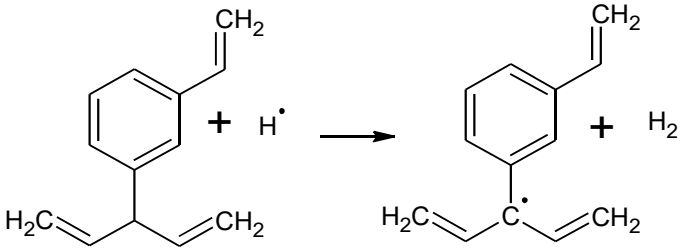

T-613:

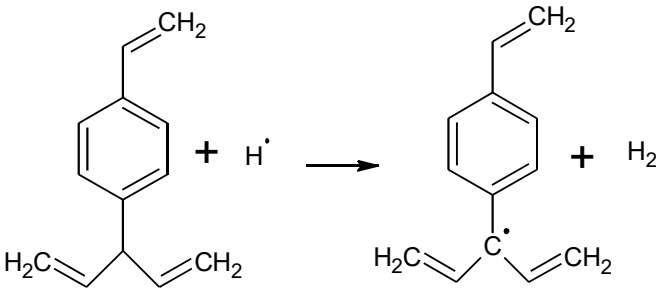

T-614:

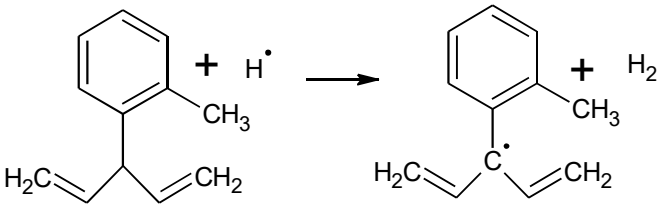

T-615:

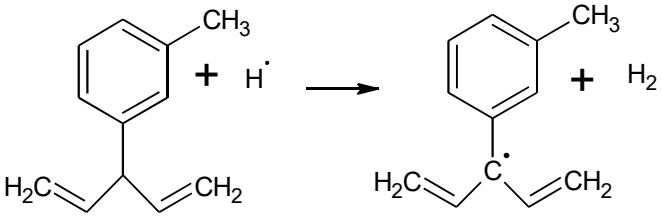

T-616:

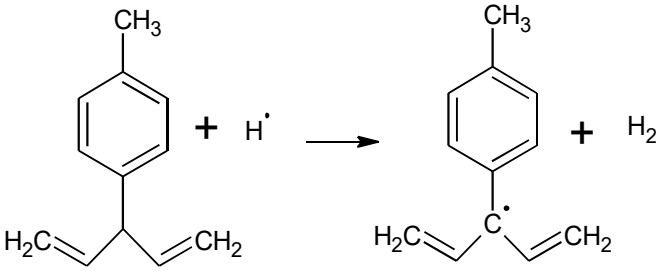

T-617:

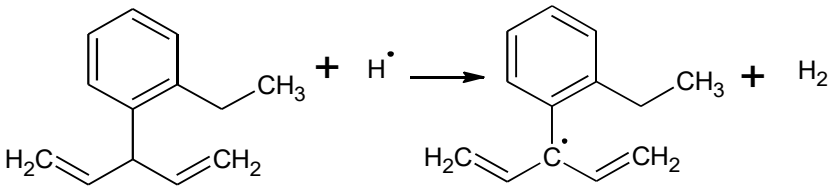

T-618:

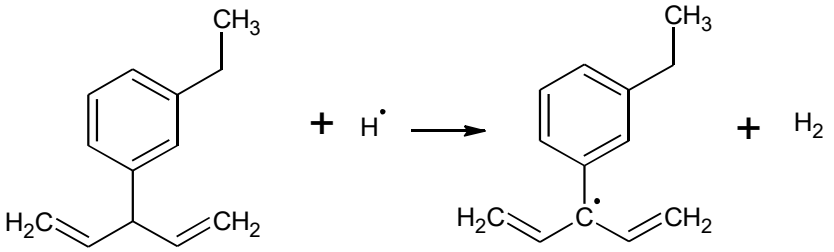

T-619:

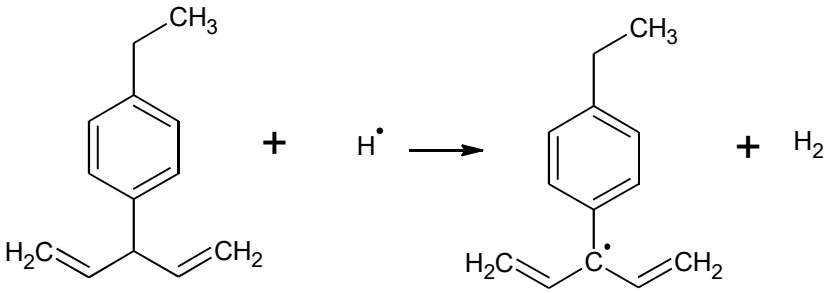

Figure D-6 Hydrogen abstraction reactions from the α-carbon of α-vinyl allylbenzene and singly substituted α-vinyl allylbenzenes.

T-701:

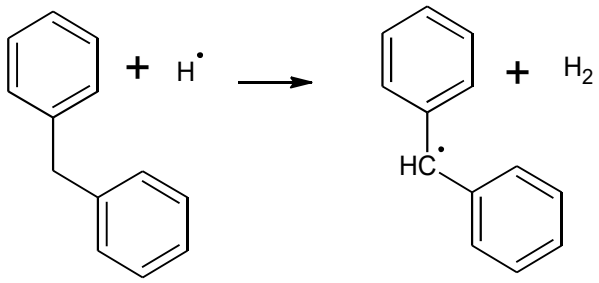

T-702:

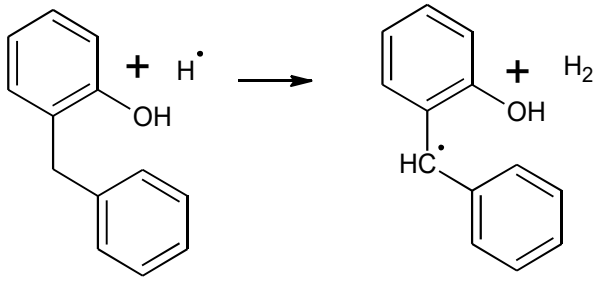

T-703:

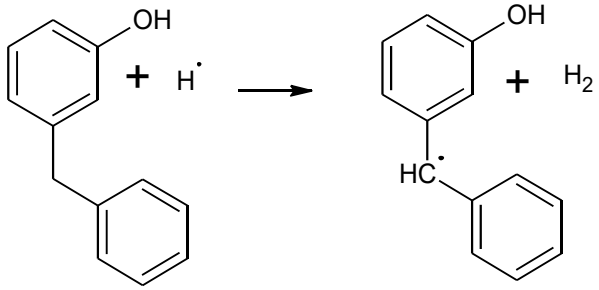

T-704:

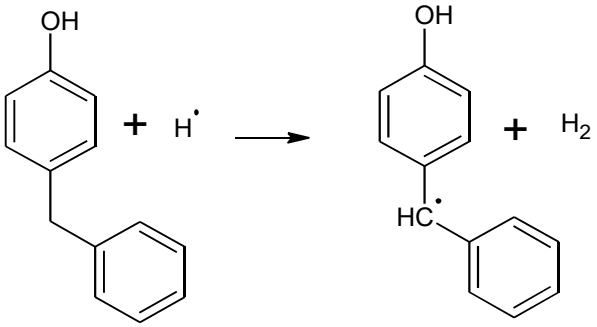

T-705:

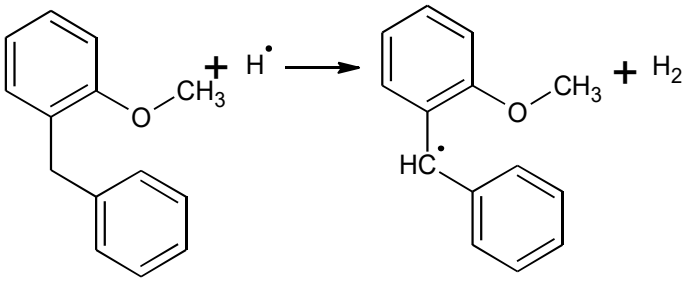

T-706:

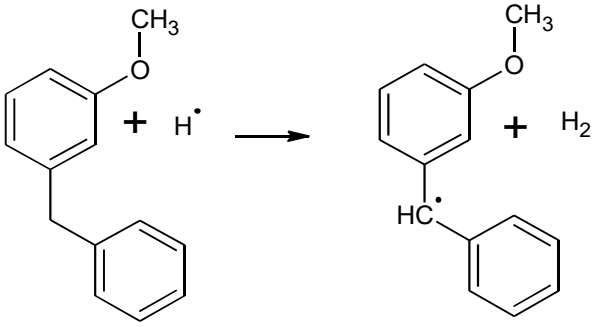

T-707:

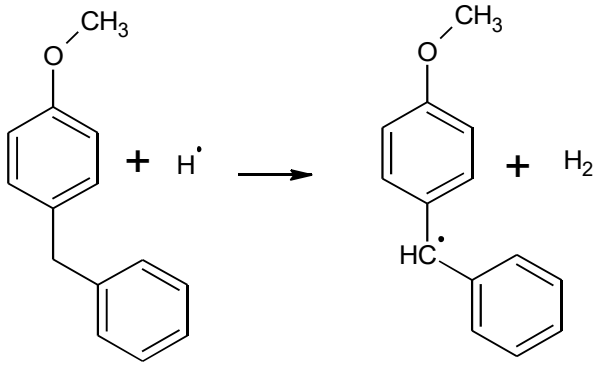

T-708:

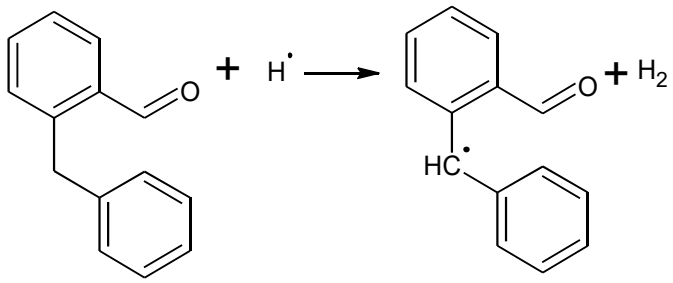

T-709:

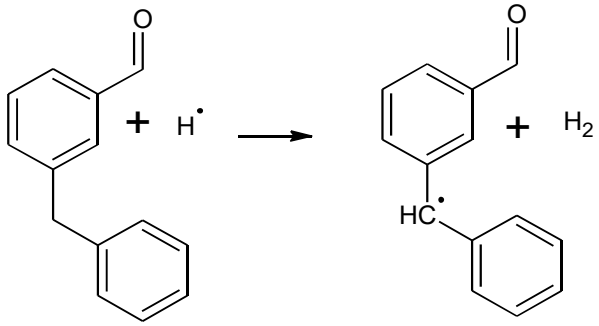

T-710:

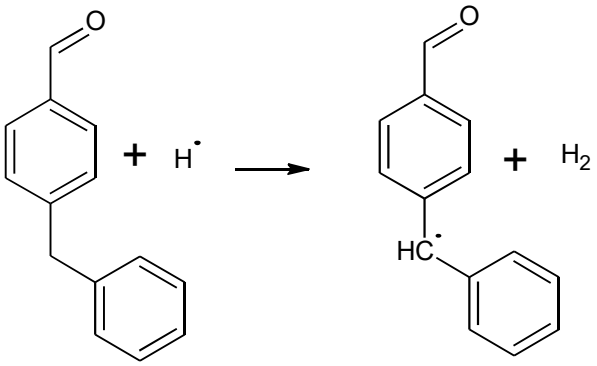

T-711:

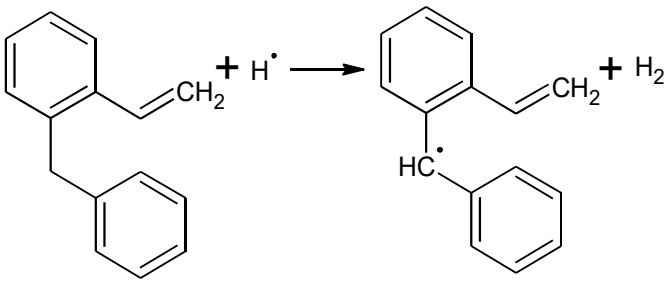

T-712:

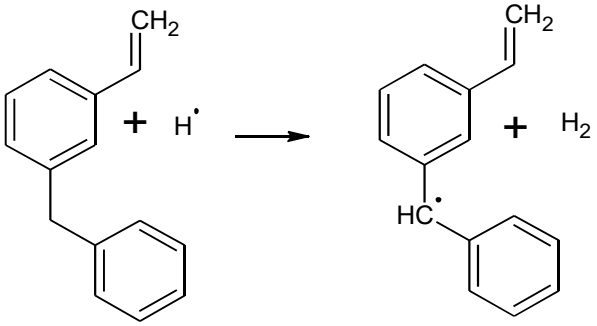

T-713:

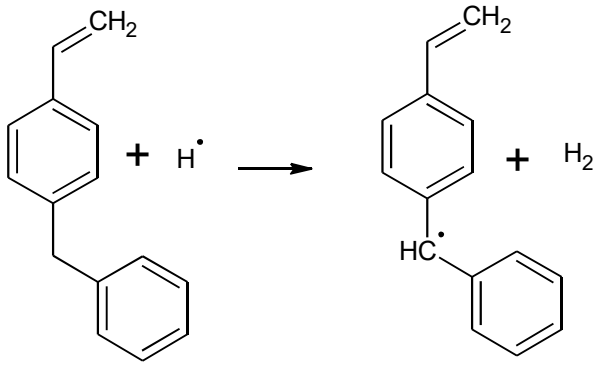

T-714:

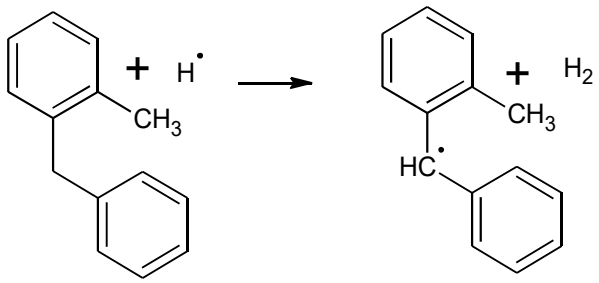

T-715:

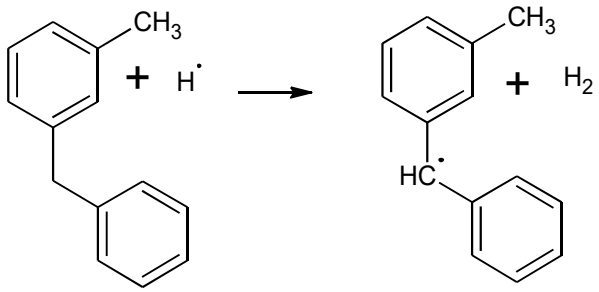

T-716:

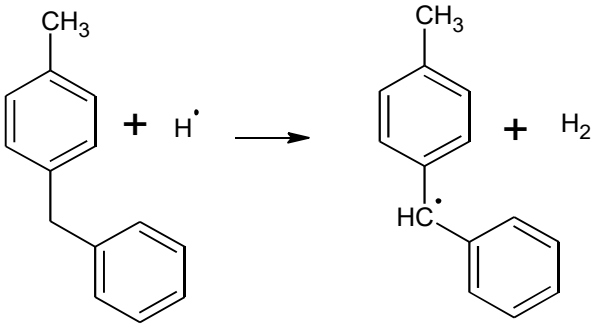

T-717:

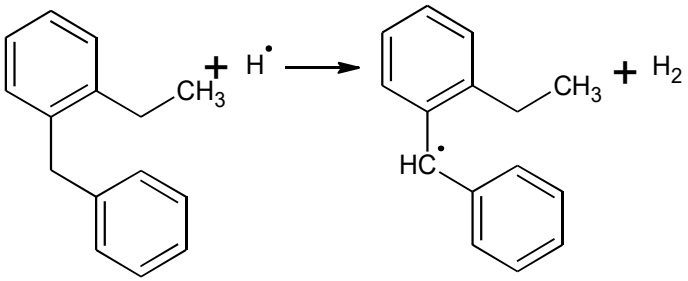

T-718:

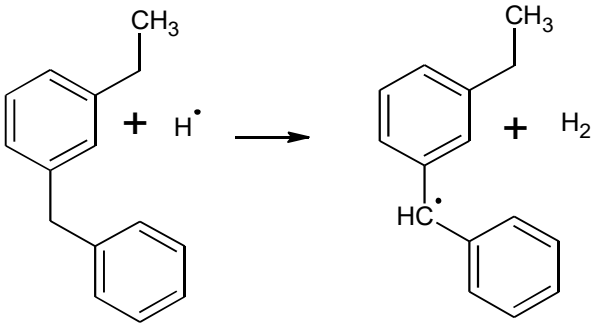

T-719:

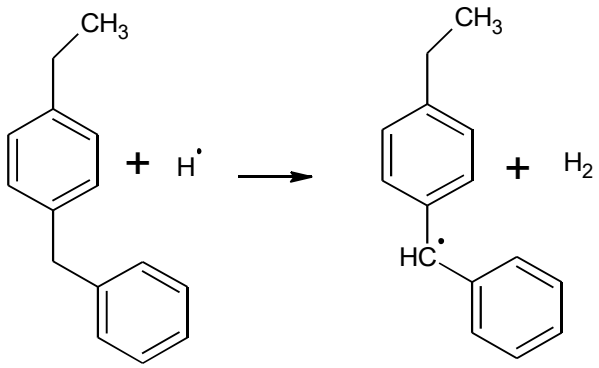

Figure D-7 Hydrogen abstraction reactions from the α-carbon of diphenylmethane and singly substituted diphenylmethanes.

T-801:

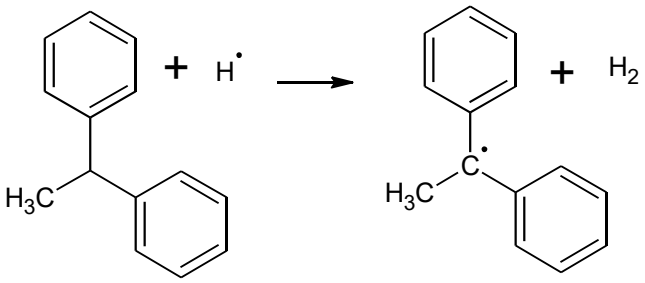

T-802:

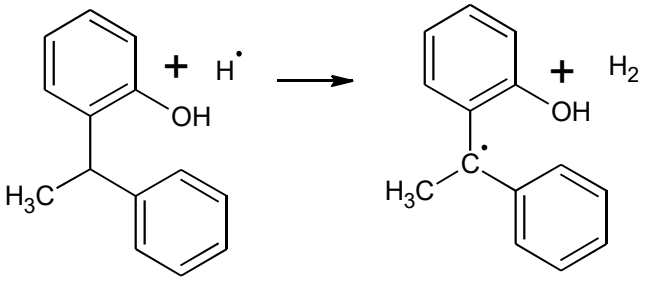

T-803:

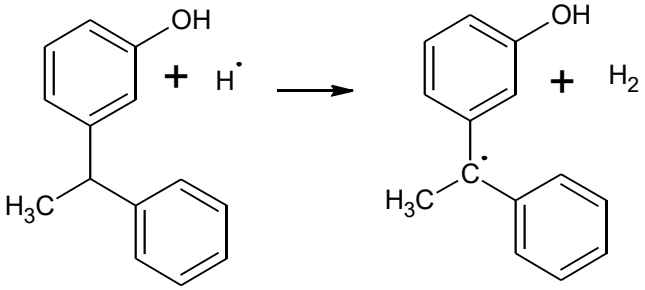

T-804:

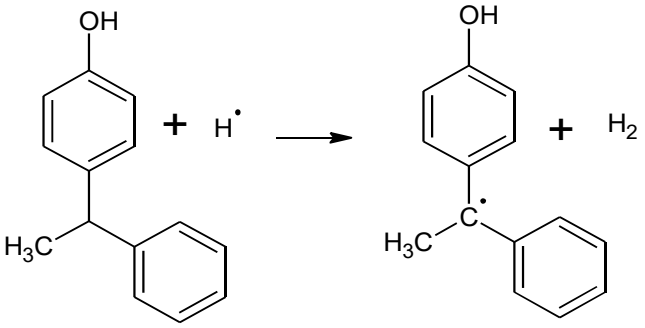

T-805:

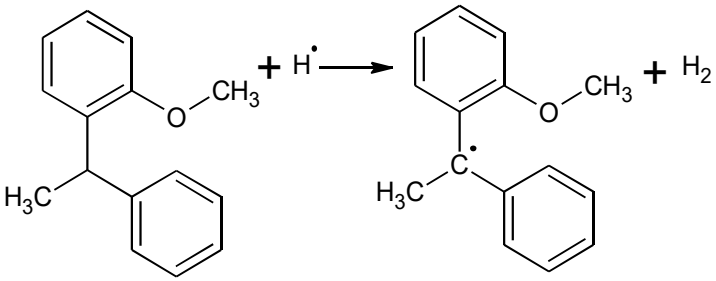

T-806:

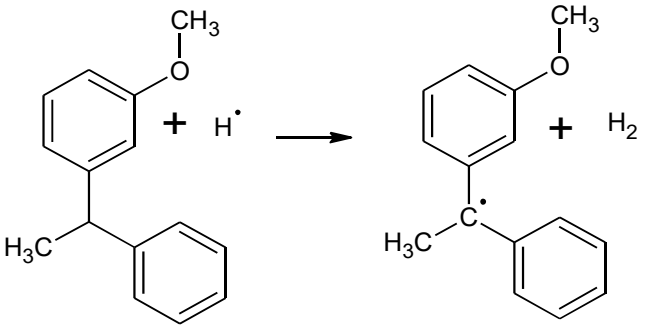

T-807:

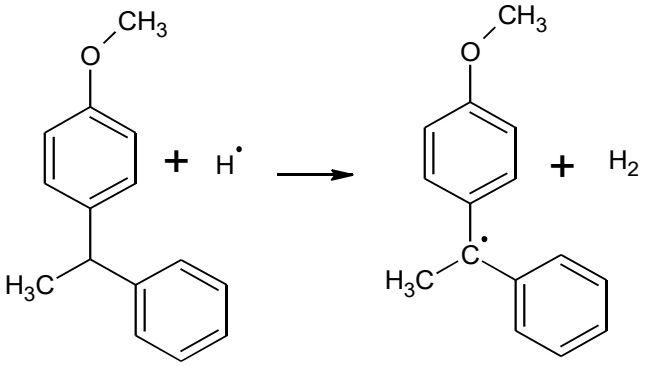

T-808:

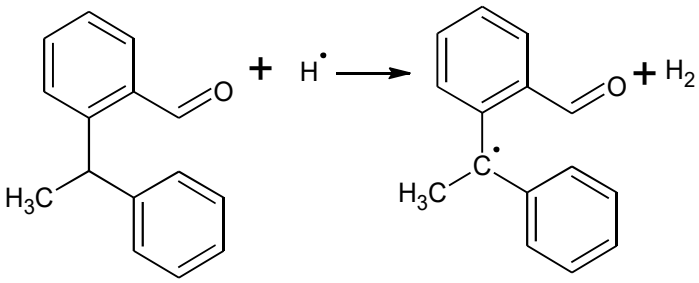

T-809:

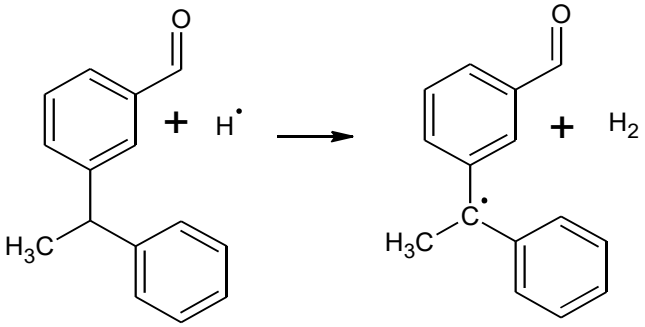

T-810:

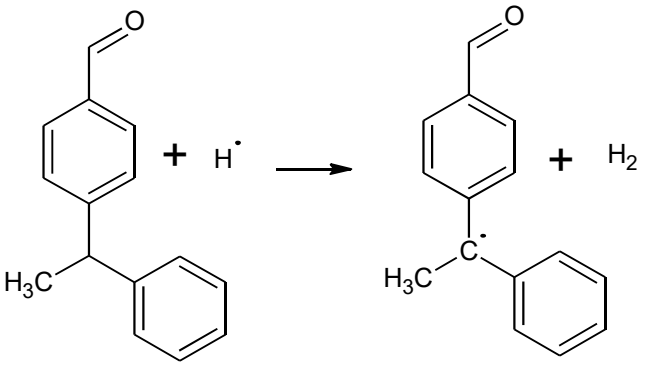

T-811:

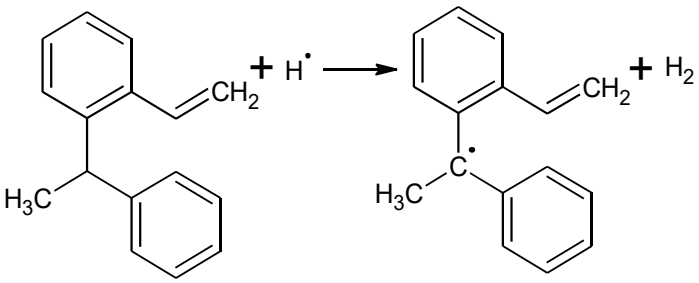

T-812:

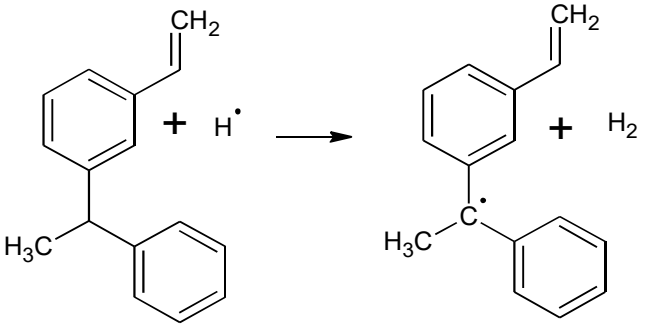

T-813:

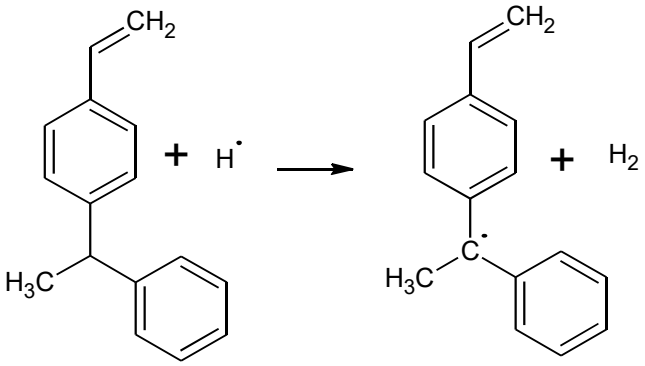

T-814:

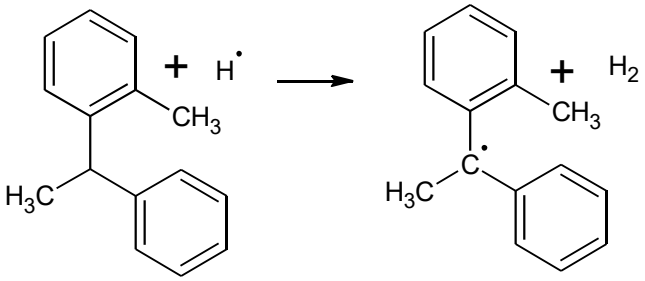

T-815:

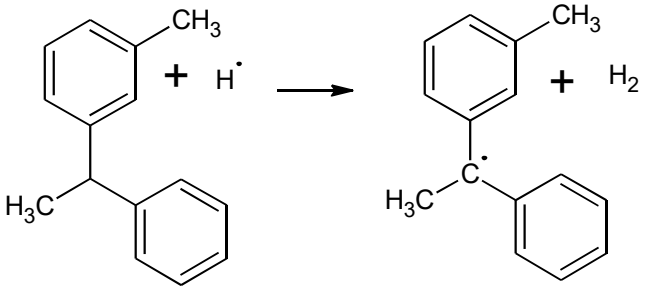

T-816:

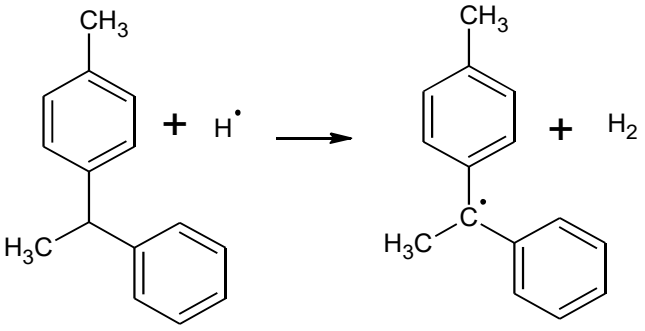

T-817:

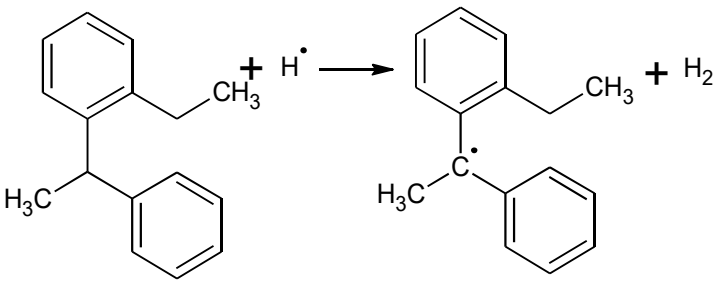

T-818:

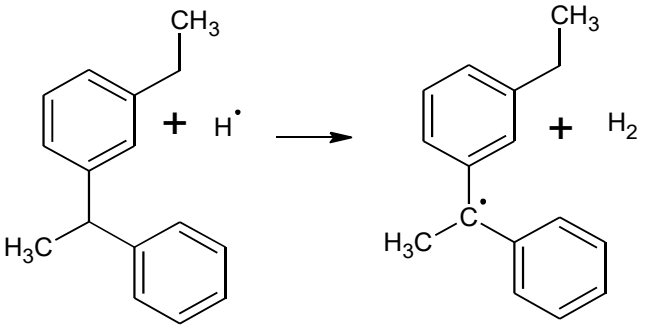

T-819:

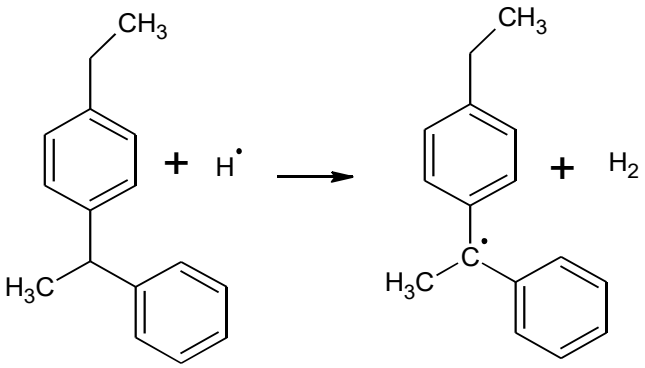

Figure D-8 Hydrogen abstraction reactions from the α-carbon of 1,1-diphenylethane and singly substituted 1,1-diphenylethanes.

D.1.2 **Database of the HARs**

In this subsection, database regarding the HARs in the training set is provided. This database includes

- Activation energy (**E_a**)
- Logarithm of the single event pre-exponential factor (**$\log\tilde{A}$**)
- Tunneling correction factors *(κ)*
- Tunneling correction excluded and included reaction rate coefficients
- Number of single events (n_e)

in both the forward and reverse directions of the HARs in the training set.

This database also consists of

- External symmetry (σ_{ext})
- Internal symmetry (σ_{int})
- The number of optical isomers (n_{opt})

for the reactants, products and the transition state structures that are involved in the HARs in the training set.

Table D-1 Arrhenius parameters (activation energy (Ea) and logarithm of the pre-exponential factor ($\log\widetilde{A}$)) of the reactions in the training set 300 K, given along with reaction rate coefficients and the tunneling correction factor (κ) for forward and reverse reactions.

Reaction #	κ	Forward				Reverse			
		$E_{a,f}$ [a]	$log\widetilde{A}_f$ [b]	k_f [c]	κk_f [d]	$E_{a,r}$ [e]	$log\widetilde{A}_r$ [f]	k_r [g]	κk_r [h]
T-101	4.44	35.8	9.615	6.9E+00	3.0E+01	96.2	8.990	1.7E-11	7.7E-11
T-102	4.24	34.9	9.635	1.0E+01	4.4E+01	96.6	9.271	2.8E-11	1.2E-10
T-103	4.26	35.1	9.134	9.8E+00	4.2E+01	93.5	8.816	3.4E-11	1.5E-10
T-104	3.73	33.7	9.598	1.6E+01	5.9E+01	97.2	9.278	2.2E-11	8.3E-11
T-105	4.00	32.5	9.649	3.6E+01	1.4E+02	94.9	8.802	1.9E-11	7.6E-11
T-106	4.15	34.2	9.629	4.9E+01	2.0E+02	93.3	8.829	3.9E-11	1.6E-10
T-107	3.52	33.8	9.581	1.6E+01	5.7E+01	94.2	8.789	2.5E-11	8.7E-11
T-108	4.55	34.8	9.663	1.1E+01	5.2E+01	97.7	9.273	1.8E-11	8.2E-11
T-109	5.09	35.2	9.625	9.1E+00	4.7E+01	94.7	9.289	6.4E-11	3.3E-10
T-110	4.78	35.3	9.622	8.5E+00	4.1E+01	100.9	9.329	5.7E-12	2.7E-11
T-111	4.48	35.8	10.101	1.3E+01	5.8E+01	99.7	9.249	7.5E-12	3.4E-11
T-112	4.64	35.6	9.639	8.1E+00	3.7E+01	97.5	9.385	2.5E-11	1.2E-10
T-113	3.93	33.2	9.550	1.7E+01	6.6E+01	103.8	9.506	2.7E-12	1.1E-11
T-114	4.43	36.2	9.651	1.3E+01	5.8E+01	97.9	8.834	6.2E-12	2.7E-11
T-115	4.29	34.9	9.993	4.8E+01	2.1E+02	96.3	9.162	2.5E-11	1.1E-10
T-116	4.21	35.4	9.748	1.1E+01	4.6E+01	96.9	8.622	2.8E-12	1.2E-11
T-117	4.29	34.6	9.620	1.1E+01	4.8E+01	96.4	8.783	9.8E-12	4.2E-11
T-118	4.35	35.1	9.623	9.3E+00	4.0E+01	96.2	8.843	1.2E-11	5.3E-11
T-119	4.25	35.3	9.656	9.4E+00	4.0E+01	97.0	9.104	1.7E-11	7.1E-11
T-201	2.10	31.2	9.827	4.8E+01	1.0E+02	101.4	8.435	1.2E-12	2.6E-12
T-202	2.03	27.9	9.737	1.5E+02	3.0E+02	98.2	8.151	2.2E-12	4.5E-12
T-203	2.10	26.9	9.759	2.3E+02	4.8E+02	98.7	8.448	3.7E-12	7.8E-12
T-204	1.75	29.4	9.781	9.0E+01	1.6E+02	101.6	8.433	1.1E-12	2.0E-12
T-205	1.96	26.9	9.720	2.1E+02	4.2E+02	98.3	8.119	2.1E-12	4.0E-12
T-206	2.17	26.6	9.773	2.7E+02	5.8E+02	98.0	8.316	3.6E-12	7.8E-12
T-207	1.69	26.2	9.801	3.3E+02	5.6E+02	98.2	8.430	4.3E-12	7.2E-12
T-208	2.30	33.2	9.803	2.0E+01	4.7E+01	102.8	8.173	3.3E-13	7.6E-13
T-209	2.53	30.0	9.757	6.5E+01	1.7E+02	100.3	8.383	1.6E-12	4.1E-12
T-210	2.16	31.0	9.857	5.6E+01	1.2E+02	107.4	8.279	7.7E-14	1.7E-13
T-211	2.06	30.4	9.640	4.3E+01	8.8E+01	100.0	8.075	9.2E-13	1.9E-12
T-212	2.25	28.6	9.795	1.3E+02	2.9E+02	100.2	8.554	2.5E-12	5.7E-12
T-213	1.83	29.5	9.811	9.3E+01	1.7E+02	109.1	8.490	6.3E-14	1.2E-13
T-214	2.06	27.0	9.525	1.3E+02	2.7E+02	98.7	8.102	1.7E-12	3.5E-12
T-215	2.07	28.0	9.851	1.8E+02	3.8E+02	98.9	8.665	5.5E-12	1.1E-11
T-216	1.94	30.7	9.796	5.4E+01	1.0E+02	101.3	7.939	4.0E-13	7.7E-13
T-217	1.99	31.2	9.957	6.6E+01	1.3E+02	101.4	8.189	6.9E-13	1.4E-12

T-218	2.00	30.6	10.122	1.2E+02	2.4E+02	101.2	8.423	1.3E-12	2.5E-12
T-219	1.94	31.1	9.833	1.0E+02	2.0E+02	102.0	8.407	8.9E-13	1.7E-12
T-301	1.59	23.9	9.790	4.1E+02	6.5E+02	97.0	7.530	1.7E-12	2.8E-12
T-302	2.20	24.3	9.748	3.2E+02	6.9E+02	87.4	7.374	2.8E-11	6.2E-11
T-303	1.61	22.0	9.794	9.0E+02	1.4E+03	96.2	7.444	1.0E-12	1.6E-12
T-304	1.40	22.3	9.781	7.7E+02	1.1E+03	96.7	7.594	1.1E-12	1.6E-12
T-305	2.22	23.0	9.767	5.5E+02	1.2E+03	86.2	7.524	6.5E-11	1.4E-10
T-306	1.53	21.3	9.792	1.2E+03	1.8E+03	95.9	7.536	1.4E-12	2.1E-12
T-307	1.38	21.8	9.819	1.0E+03	1.4E+03	95.9	7.519	1.3E-12	1.8E-12
T-308	2.78	30.2	9.969	5.0E+01	1.4E+02	94.7	8.233	1.1E-11	3.1E-11
T-309	1.71	23.8	9.761	4.0E+02	6.8E+02	97.0	7.057	3.0E-13	5.1E-13
T-310	1.71	26.7	9.786	1.3E+02	2.3E+02	107.0	7.303	9.3E-15	1.6E-14
T-311	1.96	25.6	9.486	1.0E+02	2.0E+02	89.6	7.847	3.5E-11	6.8E-11
T-312	1.62	23.6	9.767	4.5E+02	7.3E+02	98.2	7.612	6.6E-13	1.1E-12
T-313	1.49	25.5	9.757	2.0E+02	3.0E+02	107.6	7.244	6.4E-15	9.6E-15
T-314	2.20	29.9	9.311	1.3E+01	2.8E+01	87.8	7.877	7.8E-11	1.7E-10
T-315	1.56	23.2	9.969	8.1E+02	1.3E+03	96.7	7.904	2.4E-12	3.7E-12
T-316	1.49	23.7	9.894	5.6E+02	8.3E+02	97.2	7.555	8.6E-13	1.3E-12
T-317	2.54	31.3	9.453	1.0E+01	2.5E+01	86.2	7.906	1.6E-10	4.1E-10
T-318	1.55	23.7	9.807	4.7E+02	7.3E+02	96.8	7.532	9.5E-13	1.5E-12
T-319	1.50	24.3	9.835	4.0E+02	5.9E+02	97.6	7.462	5.9E-13	8.8E-13
T-401	1.87	24.6	9.610	4.1E+02	7.6E+02	134.0	8.685	4.4E-18	8.3E-18
T-402	3.61	24.1	10.109	7.8E+02	2.8E+03	128.6	8.715	2.1E-17	7.6E-17
T-403	1.54	26.3	10.178	3.8E+02	5.9E+02	138.0	9.253	1.7E-18	2.6E-18
T-404	1.64	23.0	9.893	7.5E+02	1.2E+03	134.9	8.984	3.1E-18	5.2E-18
T-405	1.74	22.0	9.828	9.5E+02	1.7E+03	131.5	8.787	7.9E-18	1.4E-17
T-406	1.51	22.2	10.160	1.9E+03	2.8E+03	135.3	9.240	4.8E-18	7.3E-18
T-407	1.39	22.9	10.165	1.5E+03	2.0E+03	135.3	9.251	4.9E-18	6.8E-18
T-408	1.90	28.6	10.024	1.1E+02	2.0E+02	136.4	8.925	1.5E-18	2.8E-18
T-409	1.69	25.6	10.141	4.6E+02	7.8E+02	134.5	9.225	6.4E-18	1.1E-17
T-410	1.68	26.5	9.883	1.8E+02	3.0E+02	140.9	9.304	5.9E-19	9.9E-19
T-411	1.61	27.9	9.944	1.2E+02	1.9E+02	132.9	8.709	3.7E-18	5.9E-18
T-412	1.59	24.8	10.238	8.1E+02	1.3E+03	135.4	9.399	6.6E-18	1.0E-17
T-413	1.78	26.5	9.870	1.7E+02	3.1E+02	142.5	9.201	2.5E-19	4.4E-19
T-414	1.56	24.7	9.936	4.2E+02	6.6E+02	132.9	8.814	4.7E-18	7.3E-18
T-415	1.52	24.3	10.329	1.2E+03	1.9E+03	134.2	9.415	1.1E-17	1.7E-17
T-416	1.76	23.3	9.582	3.3E+02	5.8E+02	134.7	9.056	3.9E-18	6.9E-18
T-417	1.53	24.9	10.145	6.3E+02	9.6E+02	133.4	8.994	5.9E-18	9.0E-18
T-418	1.53	24.6	10.164	7.4E+02	1.1E+03	134.4	9.230	6.7E-18	1.0E-17
T-419	1.78	27.0	9.930	1.6E+02	2.9E+02	137.6	8.984	1.1E-18	1.9E-18
T-501	1.42	20.1	9.664	2.8E+03	4.0E+03	128.9	8.039	1.6E-17	2.3E-17

T-502	1.76	20.9	9.685	1.1E+03	1.9E+03	127.6	8.200	1.9E-17	3.3E-17
T-503	1.44	18.2	9.964	6.0E+03	8.6E+03	128.4	8.317	1.8E-17	2.6E-17
T-504	1.41	18.3	9.980	4.9E+03	6.9E+03	125.6	8.308	5.4E-17	7.6E-17
T-505	1.37	19.2	10.082	5.2E+03	7.2E+03	119.3	8.498	1.1E-15	1.5E-15
T-506	1.35	17.8	9.959	7.0E+03	9.5E+03	129.6	8.293	1.1E-17	1.5E-17
T-507	1.32	18.0	9.992	6.8E+03	9.0E+03	129.5	8.262	1.0E-17	1.4E-17
T-508	1.51	21.6	10.092	2.1E+03	3.1E+03	122.0	8.366	2.7E-16	4.0E-16
T-509	1.49	15.9	9.956	1.5E+04	2.3E+04	125.4	8.289	5.6E-17	8.3E-17
T-510	1.49	15.5	9.924	1.6E+04	2.4E+04	130.2	8.285	1.2E-17	1.8E-17
T-511	1.40	16.4	9.761	7.7E+03	1.1E+04	121.1	8.377	3.9E-16	5.4E-16
T-512	1.42	14.9	9.964	2.3E+04	3.2E+04	125.0	7.955	3.0E-17	4.3E-17
T-513	1.39	22.3	9.960	1.2E+03	1.6E+03	137.1	8.430	7.2E-19	1.0E-18
T-514	1.68	20.7	9.792	1.5E+03	2.5E+03	118.7	8.210	7.0E-16	1.2E-15
T-515	1.41	15.0	10.015	2.5E+04	3.5E+04	124.1	8.375	1.2E-16	1.6E-16
T-516	1.38	20.1	9.967	2.9E+03	4.0E+03	129.7	7.997	5.1E-18	7.1E-18
T-517	1.49	21.4	9.816	1.2E+03	1.8E+03	118.8	8.346	9.0E-16	1.3E-15
T-518	1.40	19.6	9.957	3.3E+03	4.7E+03	128.7	8.332	1.7E-17	2.3E-17
T-519	1.37	16.2	9.991	1.4E+04	1.9E+04	125.8	8.295	4.9E-17	6.7E-17
T-601	1.60	19.2	9.566	3.3E+03	5.2E+03	151.6	9.247	7.1E-21	1.1E-20
T-602	1.39	15.3	10.084	2.6E+04	3.6E+04	157.8	8.890	2.6E-22	3.6E-22
T-603	1.30	13.2	9.860	3.6E+04	4.7E+04	153.7	9.101	2.1E-21	2.8E-21
T-604	1.22	14.8	9.854	4.7E+04	5.8E+04	152.3	9.253	1.3E-20	1.6E-20
T-605	1.63	19.9	9.858	1.1E+03	1.8E+03	157.1	8.208	7.2E-23	1.2E-22
T-606	1.48	15.3	9.935	1.8E+04	2.7E+04	154.4	9.203	2.1E-21	3.0E-21
T-607	1.48	18.4	9.896	4.8E+03	7.1E+03	158.5	9.264	4.5E-22	6.7E-22
T-608	1.41	13.9	9.882	2.8E+04	4.0E+04	160.6	8.175	1.6E-23	2.2E-23
T-609	1.78	15.4	9.912	1.7E+04	3.0E+04	153.1	9.212	3.5E-21	6.3E-21
T-610	1.67	16.1	9.925	1.3E+04	2.2E+04	150.8	9.254	9.9E-21	1.7E-20
T-611	1.56	18.3	9.669	3.0E+03	4.7E+03	166.0	8.224	2.1E-24	3.3E-24
T-612	1.61	18.3	9.993	6.3E+03	1.0E+04	151.2	9.228	9.8E-21	1.6E-20
T-613	1.56	20.7	9.867	1.8E+03	2.7E+03	156.5	9.272	1.0E-21	1.6E-21
T-614	1.49	24.4	9.889	4.3E+02	6.4E+02	168.6	8.386	1.1E-24	1.6E-24
T-615	1.56	18.2	9.947	5.9E+03	9.2E+03	155.9	9.229	1.2E-21	1.9E-21
T-616	1.52	14.1	9.912	2.8E+04	4.3E+04	151.7	9.279	7.3E-21	1.1E-20
T-617	1.43	23.6	9.656	3.4E+02	4.9E+02	166.1	8.114	1.6E-24	2.2E-24
T-618	1.53	22.0	10.204	2.5E+03	3.7E+03	156.2	9.467	9.6E-22	1.5E-21
T-619	1.55	21.0	9.938	1.9E+03	2.9E+03	156.4	9.253	1.3E-21	2.0E-21
T-701	2.04	33.5	9.385	7.0E+00	1.4E+01	117.6	9.098	1.7E-14	3.4E-14
T-702	2.25	25.7	9.224	1.1E+02	2.4E+02	110.0	8.698	7.1E-14	1.6E-13
T-703	1.94	28.7	9.481	5.9E+01	1.2E+02	114.1	9.227	4.6E-14	9.0E-14
T-704	1.76	29.1	9.610	6.7E+01	1.2E+02	116.0	9.379	3.0E-14	5.3E-14

T-705	1.98	28.5	9.468	6.2E+01	1.2E+02	111.9	8.789	4.0E-14	8.0E-14
T-706	1.85	27.5	9.657	7.6E+01	1.4E+02	113.8	9.392	7.6E-14	1.4E-13
T-707	1.73	28.4	9.479	6.7E+01	1.2E+02	116.0	9.193	2.0E-14	3.4E-14
T-708	2.37	35.5	9.651	5.7E+00	1.3E+01	117.9	8.856	4.3E-15	1.0E-14
T-709	2.10	32.6	9.421	1.1E+01	2.2E+01	117.2	9.141	1.1E-14	2.2E-14
T-710	2.10	33.1	9.217	5.6E+00	1.2E+01	121.0	9.190	2.6E-15	5.5E-15
T-711	2.66	30.2	9.432	2.9E+01	7.8E+01	115.0	8.702	9.6E-15	2.6E-14
T-712	2.04	29.4	9.514	2.4E+01	4.8E+01	115.7	9.437	2.0E-14	4.0E-14
T-713	2.05	31.2	9.479	2.1E+01	4.4E+01	122.3	9.437	2.8E-15	5.7E-15
T-714	2.01	32.8	9.752	1.1E+01	2.2E+01	112.8	9.015	2.3E-14	4.7E-14
T-715	1.97	32.9	9.734	9.7E+00	1.9E+01	117.8	9.710	1.6E-14	3.1E-14
T-716	1.93	33.3	9.563	5.7E+00	1.1E+01	118.6	9.601	8.8E-15	1.7E-14
T-717	2.41	32.6	9.430	1.1E+01	2.6E+01	113.6	8.665	1.6E-14	3.7E-14
T-718	2.07	33.6	9.577	5.2E+00	1.1E+01	117.7	9.343	7.0E-15	1.5E-14
T-719	1.94	33.6	9.703	7.0E+00	1.4E+01	118.7	9.466	6.2E-15	1.2E-14
T-801	1.49	25.3	9.741	2.1E+02	3.2E+02	108.0	8.864	6.5E-14	9.7E-14
T-802	1.58	22.0	9.232	5.0E+02	7.9E+02	110.8	7.984	1.9E-14	3.1E-14
T-803	1.47	25.1	9.454	2.4E+02	3.5E+02	110.0	8.272	5.3E-14	7.7E-14
T-804	1.37	26.2	9.751	1.5E+02	2.0E+02	111.3	8.595	3.2E-14	4.4E-14
T-805	1.93	25.0	9.624	1.8E+02	3.5E+02	102.8	7.909	4.0E-13	7.8E-13
T-806	1.44	24.5	9.434	2.8E+02	4.1E+02	110.1	8.223	4.5E-14	6.5E-14
T-807	1.36	25.3	9.744	2.1E+02	2.9E+02	111.0	8.561	3.4E-14	4.6E-14
T-808	1.65	28.3	9.738	6.2E+01	1.0E+02	106.6	8.181	8.5E-14	1.4E-13
T-809	1.62	27.7	9.394	7.2E+01	1.2E+02	112.9	8.265	1.6E-14	2.6E-14
T-810	1.61	28.4	9.694	5.4E+01	8.8E+01	116.4	8.621	4.5E-15	7.3E-15
T-811	2.02	28.6	9.376	4.9E+01	9.9E+01	108.6	7.816	3.3E-14	6.6E-14
T-812	1.53	29.0	9.577	4.7E+01	7.2E+01	115.5	8.429	1.5E-14	2.3E-14
T-813	1.44	30.2	9.878	4.1E+01	5.8E+01	120.7	8.949	1.7E-15	2.5E-15
T-814	1.87	27.0	9.395	9.7E+01	1.8E+02	105.6	7.590	1.7E-13	3.1E-13
T-815	1.47	27.1	9.801	1.2E+02	1.7E+02	110.7	8.812	6.8E-14	9.9E-14
T-816	1.43	27.6	9.780	9.0E+01	1.3E+02	111.4	8.601	3.2E-14	4.5E-14
T-817	1.52	30.6	9.560	1.6E+01	2.5E+01	112.4	7.846	3.7E-15	5.6E-15
T-818	1.46	28.1	9.705	6.4E+01	9.4E+01	110.5	8.551	4.1E-14	6.0E-14
T-819	1.43	25.4	9.482	2.2E+02	3.1E+02	109.1	8.299	8.0E-14	1.1E-13

[a] $\mathbf{E_{a,f}}$**:** Activation energy of the forward reaction, given in kJ mol^{-1}.
[b] $\boldsymbol{log\widetilde{A}_f}$**:** Logarithm of the pre-exponential factor of the forward reaction, given in m^3 mol^{-1} s^{-1}.
[c] $\mathbf{k_f}$**:** The reaction rate coefficient for the forward reaction excluding tunneling effects, given in m^3 mol^{-1} s^{-1}.
[d] $\boldsymbol{\kappa k_f}$**:** The reaction rate coefficient for the forward reaction including tunneling effects, given in m^3 mol^{-1} s^{-1}.
[e] $\mathbf{E_{a,r}}$**:** Activation energy of the reverse reaction, given in kJ mol^{-1}.
[f] $\boldsymbol{log\widetilde{A}_r}$**:** Logarithm of the pre-exponential factor of the reverse reaction, given in m^3 mol^{-1} s^{-1}.
[g] $\mathbf{k_r}$**:** The reaction rate coefficient for the reverse reaction excluding tunneling effects, given in m^3 mol^{-1} s^{-1}.
[h] $\boldsymbol{\kappa k_r}$**:** The reaction rate coefficient for the reverse reaction including tunneling effects, given in m^3 mol^{-1} s^{-1}.

Table D-2 Arrhenius parameters (activation energy (**Ea**) and logarithm of the pre-exponential factor ($\log\widetilde{A}$)) of the reactions in the training set 600 K, given along with reaction rate coefficients and the tunneling correction factor (κ) for forward and reverse reactions.

Reaction #	κ	Forward				Reverse			
		$E_{a,f}$ [a]	$\log\widetilde{A}_f$ [b]	k_f [c]	κk_f [d]	$E_{a,r}$ [e]	$\log\widetilde{A}_r$ [f]	k_r [g]	κk_r [h]
T-101	1.41	41.2	10.263	1.39E+04	1.96E+04	98.5	9.252	4.69E-03	6.59E-03
T-102	1.39	39.8	10.214	1.66E+04	2.31E+04	98.9	9.533	8.24E-03	1.15E-02
T-103	1.40	39.8	10.223	9.52E+03	1.33E+04	95.8	9.077	5.38E-03	7.54E-03
T-104	1.36	39.5	10.239	2.06E+04	2.79E+04	99.5	9.538	7.37E-03	1.00E-02
T-105	1.38	39.9	10.209	3.07E+04	4.24E+04	97.2	9.059	3.92E-03	5.41E-03
T-106	1.40	39.4	10.279	3.79E+04	5.29E+04	95.6	9.093	5.83E-03	8.13E-03
T-107	1.35	39.5	10.110	1.18E+04	1.59E+04	96.5	9.050	4.43E-03	5.96E-03
T-108	1.41	40.0	10.279	1.84E+04	2.60E+04	100.8	9.640	7.16E-03	1.01E-02
T-109	1.45	40.6	10.277	1.63E+04	2.36E+04	97.0	9.554	1.27E-02	1.84E-02
T-110	1.43	40.7	10.272	1.57E+04	2.24E+04	103.5	9.623	4.05E-03	5.79E-03
T-111	1.41	40.5	10.344	2.81E+04	3.96E+04	102.3	9.546	4.29E-03	6.04E-03
T-112	1.42	41.0	10.289	1.55E+04	2.21E+04	99.9	9.648	8.87E-03	1.26E-02
T-113	1.37	39.4	10.196	2.02E+04	2.78E+04	106.2	9.782	3.41E-03	4.68E-03
T-114	1.41	40.9	10.213	2.65E+04	3.72E+04	100.2	9.101	2.34E-03	3.30E-03
T-115	1.40	40.3	10.349	8.03E+04	1.12E+05	98.6	9.426	6.81E-03	9.53E-03
T-116	1.39	40.8	9.934	2.04E+04	2.83E+04	99.2	8.887	8.78E-04	1.22E-03
T-117	1.40	39.7	10.227	1.73E+04	2.42E+04	98.9	9.065	2.80E-03	3.92E-03
T-118	1.40	40.5	10.272	1.64E+04	2.29E+04	98.6	9.106	3.32E-03	4.66E-03
T-119	1.40	40.7	10.304	1.71E+04	2.38E+04	99.3	9.371	5.23E-03	7.30E-03
T-201	1.20	35.1	10.291	3.42E+04	4.09E+04	103.2	8.633	8.87E-04	1.06E-03
T-202	1.19	31.7	9.715	5.39E+04	6.41E+04	100.1	8.351	8.65E-04	1.03E-03
T-203	1.20	30.8	9.746	6.92E+04	8.29E+04	100.5	8.647	1.57E-03	1.88E-03
T-204	1.15	33.2	9.757	4.40E+04	5.05E+04	103.3	8.625	8.41E-04	9.66E-04
T-205	1.18	30.7	9.700	6.33E+04	7.47E+04	100.1	8.317	7.98E-04	9.42E-04
T-206	1.21	30.5	9.764	7.63E+04	9.22E+04	99.8	8.518	1.33E-03	1.61E-03
T-207	1.14	30.0	9.779	8.69E+04	9.91E+04	100.0	8.622	1.64E-03	1.87E-03
T-208	1.22	37.1	10.270	2.18E+04	2.66E+04	104.9	8.403	2.19E-04	2.67E-04
T-209	1.25	34.0	10.228	3.69E+04	4.61E+04	102.2	8.587	9.65E-04	1.20E-03
T-210	1.20	34.8	10.321	3.84E+04	4.61E+04	109.4	8.499	1.88E-04	2.27E-04
T-211	1.19	34.2	10.095	2.59E+04	3.08E+04	101.8	8.268	5.05E-04	6.01E-04
T-212	1.22	32.4	10.262	5.41E+04	6.59E+04	102.1	8.754	1.46E-03	1.78E-03
T-213	1.16	33.3	10.269	4.66E+04	5.41E+04	110.9	8.692	2.16E-04	2.51E-04
T-214	1.19	30.7	9.975	3.93E+04	4.70E+04	100.4	8.297	7.06E-04	8.43E-04
T-215	1.19	31.9	10.316	6.85E+04	8.19E+04	100.8	8.745	1.52E-03	1.82E-03
T-216	1.17	34.6	10.259	3.49E+04	4.09E+04	103.2	8.140	2.86E-04	3.36E-04
T-217	1.18	35.0	10.111	4.62E+04	5.45E+04	103.2	8.387	4.99E-04	5.89E-04

T-218	1.18	34.4	10.285	7.65E+04	9.04E+04	103.0	8.621	8.87E-04	1.05E-03
T-219	1.17	35.0	10.297	7.08E+04	8.31E+04	103.8	8.608	7.32E-04	8.60E-04
T-301	1.12	27.7	10.247	6.71E+04	7.54E+04	99.0	7.749	5.32E-04	5.97E-04
T-302	1.21	28.2	10.216	5.67E+04	6.89E+04	89.6	7.609	1.28E-03	1.56E-03
T-303	1.13	25.8	10.254	1.00E+05	1.13E+05	98.1	7.658	2.58E-04	2.91E-04
T-304	1.09	26.0	10.228	9.11E+04	9.93E+04	98.7	7.808	3.27E-04	3.56E-04
T-305	1.22	27.0	10.238	7.67E+04	9.35E+04	88.4	7.763	2.32E-03	2.83E-03
T-306	1.11	25.1	10.248	1.15E+05	1.28E+05	97.9	7.756	3.41E-04	3.79E-04
T-307	1.09	25.5	10.268	1.09E+05	1.19E+05	97.9	7.733	3.25E-04	3.53E-04
T-308	1.28	34.1	10.436	2.91E+04	3.71E+04	96.9	8.481	2.18E-03	2.78E-03
T-309	1.14	27.7	10.220	6.40E+04	7.32E+04	99.0	7.273	9.01E-05	1.03E-04
T-310	1.14	30.5	10.244	3.84E+04	4.39E+04	109.1	7.535	2.14E-05	2.45E-05
T-311	1.18	29.3	9.930	2.36E+04	2.79E+04	91.7	8.070	2.43E-03	2.87E-03
T-312	1.13	27.4	10.224	6.86E+04	7.74E+04	100.2	7.832	2.56E-04	2.89E-04
T-313	1.11	29.2	10.209	4.54E+04	5.02E+04	109.5	7.454	1.64E-05	1.81E-05
T-314	1.21	33.6	9.759	6.74E+03	8.16E+03	89.9	8.109	3.80E-03	4.59E-03
T-315	1.12	27.0	10.426	1.17E+05	1.30E+05	98.7	8.125	6.77E-04	7.57E-04
T-316	1.11	27.5	10.348	8.86E+04	9.80E+04	99.2	7.776	2.74E-04	3.03E-04
T-317	1.25	35.0	9.905	7.07E+03	8.84E+03	88.3	8.143	5.62E-03	7.03E-03
T-318	1.12	27.5	10.263	7.37E+04	8.23E+04	98.8	7.752	2.79E-04	3.12E-04
T-319	1.11	28.0	10.290	6.97E+04	7.71E+04	99.6	7.682	2.03E-04	2.24E-04
T-401	1.17	28.4	10.060	7.68E+04	8.95E+04	136.1	8.912	2.30E-06	2.69E-06
T-402	1.37	28.1	10.586	1.36E+05	1.85E+05	130.5	8.925	3.60E-06	4.91E-06
T-403	1.11	30.1	10.638	1.03E+05	1.14E+05	140.1	9.485	1.94E-06	2.16E-06
T-404	1.13	26.7	10.337	1.02E+05	1.15E+05	136.9	9.210	1.94E-06	2.19E-06
T-405	1.15	25.8	10.284	1.08E+05	1.23E+05	133.6	9.027	2.47E-06	2.83E-06
T-406	1.11	26.0	10.620	2.23E+05	2.47E+05	137.4	9.475	3.26E-06	3.61E-06
T-407	1.09	26.7	10.622	1.97E+05	2.14E+05	137.4	9.486	3.33E-06	3.62E-06
T-408	1.17	32.4	10.484	4.55E+04	5.32E+04	138.7	9.189	1.29E-06	1.51E-06
T-409	1.14	29.4	10.602	1.08E+05	1.23E+05	136.6	9.463	3.67E-06	4.18E-06
T-410	1.14	30.3	10.342	5.00E+04	5.68E+04	143.1	9.560	1.25E-06	1.42E-06
T-411	1.13	31.6	10.394	4.34E+04	4.88E+04	134.9	8.936	1.53E-06	1.72E-06
T-412	1.12	28.6	10.699	1.60E+05	1.80E+05	137.5	9.635	4.56E-06	5.12E-06
T-413	1.15	30.2	10.318	4.79E+04	5.52E+04	144.5	9.431	6.98E-07	8.05E-07
T-414	1.12	28.4	10.379	8.04E+04	8.98E+04	134.9	9.039	1.94E-06	2.17E-06
T-415	1.11	28.1	10.790	2.18E+05	2.42E+05	136.3	9.651	6.01E-06	6.67E-06
T-416	1.15	27.0	10.029	4.73E+04	5.44E+04	136.8	9.285	2.36E-06	2.71E-06
T-417	1.11	28.6	10.596	1.25E+05	1.39E+05	135.4	9.228	2.71E-06	3.01E-06
T-418	1.11	28.4	10.623	1.40E+05	1.56E+05	136.5	9.465	3.78E-06	4.21E-06
T-419	1.15	30.7	10.379	4.98E+04	5.73E+04	139.6	9.212	1.13E-06	1.30E-06
T-501	1.09	23.9	10.116	2.17E+05	2.37E+05	130.9	8.271	2.95E-06	3.23E-06

T-502	1.15	24.6	10.137	9.76E+04	1.12E+05	130.1	8.477	2.82E-06	3.25E-06
T-503	1.10	22.0	10.417	3.15E+05	3.45E+05	130.5	8.543	3.04E-06	3.33E-06
T-504	1.07	22.3	10.731	2.17E+05	2.33E+05	127.7	8.540	5.23E-06	5.61E-06
T-505	1.08	23.1	10.546	3.41E+05	3.70E+05	121.4	8.741	2.92E-05	3.16E-05
T-506	1.08	21.5	10.409	3.39E+05	3.66E+05	131.6	8.520	2.30E-06	2.48E-06
T-507	1.07	21.8	10.266	3.48E+05	3.73E+05	131.5	8.491	2.17E-06	2.33E-06
T-508	1.11	25.4	10.552	2.16E+05	2.39E+05	124.1	8.607	1.26E-05	1.39E-05
T-509	1.11	19.6	10.410	4.97E+05	5.50E+05	127.5	8.518	5.20E-06	5.75E-06
T-510	1.11	19.3	10.378	4.95E+05	5.48E+05	132.7	8.530	3.11E-06	3.44E-06
T-511	1.09	20.2	10.210	2.82E+05	3.08E+05	123.2	8.611	1.53E-05	1.66E-05
T-512	1.09	18.7	10.416	6.12E+05	6.69E+05	127.1	8.184	2.61E-06	2.85E-06
T-513	1.09	26.0	10.411	1.39E+05	1.51E+05	139.2	8.663	6.98E-07	7.58E-07
T-514	1.14	24.4	10.235	1.28E+05	1.46E+05	120.7	8.429	1.66E-05	1.89E-05
T-515	1.09	18.7	10.467	6.82E+05	7.44E+05	126.2	8.606	8.30E-06	9.06E-06
T-516	1.08	23.8	10.420	2.19E+05	2.37E+05	131.8	8.231	1.13E-06	1.22E-06
T-517	1.11	25.2	10.275	1.19E+05	1.32E+05	120.9	8.574	2.23E-05	2.46E-05
T-518	1.09	23.4	10.409	2.34E+05	2.54E+05	130.8	8.564	2.98E-06	3.24E-06
T-519	1.08	20.0	10.444	5.00E+05	5.41E+05	127.9	8.528	4.91E-06	5.32E-06
T-601	1.12	22.9	10.008	2.06E+05	2.31E+05	154.0	9.518	1.28E-07	1.44E-07
T-602	1.09	19.0	10.529	7.49E+05	8.13E+05	159.8	9.115	1.58E-08	1.72E-08
T-603	1.07	16.7	10.286	6.73E+05	7.19E+05	155.9	9.350	5.92E-08	6.33E-08
T-604	1.05	17.6	10.278	7.67E+05	8.07E+05	155.2	9.514	3.03E-07	3.18E-07
T-605	1.25	23.7	10.319	1.20E+05	1.50E+05	159.4	8.471	3.89E-09	4.87E-09
T-606	1.10	19.0	10.380	5.29E+05	5.83E+05	156.8	9.469	6.57E-08	7.25E-08
T-607	1.10	22.1	10.341	2.60E+05	2.87E+05	160.9	9.534	3.33E-08	3.67E-08
T-608	1.09	17.5	10.317	6.14E+05	6.69E+05	162.7	8.401	1.72E-09	1.88E-09
T-609	1.16	19.1	10.360	4.92E+05	5.69E+05	155.5	9.481	8.71E-08	1.01E-07
T-610	1.14	19.8	10.374	4.42E+05	5.03E+05	153.2	9.525	1.54E-07	1.75E-07
T-611	1.12	21.8	10.096	1.55E+05	1.74E+05	168.0	8.445	6.57E-10	7.34E-10
T-612	1.13	22.0	10.442	3.33E+05	3.75E+05	153.4	9.498	2.61E-07	2.94E-07
T-613	1.12	24.4	10.312	1.52E+05	1.69E+05	158.9	9.543	5.09E-08	5.68E-08
T-614	1.21	28.1	10.331	7.63E+04	9.22E+04	170.7	8.625	5.70E-10	6.89E-10
T-615	1.12	21.9	10.389	3.03E+05	3.39E+05	158.2	9.496	5.19E-08	5.80E-08
T-616	1.11	17.7	10.354	6.38E+05	7.10E+05	154.0	9.549	1.36E-07	1.51E-07
T-617	1.09	27.1	10.083	5.20E+04	5.68E+04	168.0	8.326	4.99E-10	5.45E-10
T-618	1.07	24.5	10.657	1.66E+05	1.78E+05	158.1	9.741	4.24E-08	4.53E-08
T-619	1.12	24.7	10.385	1.71E+05	1.90E+05	158.8	9.522	4.97E-08	5.54E-08
T-701	1.19	37.2	9.837	7.78E+03	9.23E+03	119.8	9.346	3.25E-04	3.85E-04
T-702	1.22	29.3	9.655	2.50E+04	3.05E+04	112.1	8.932	2.97E-04	3.62E-04
T-703	1.18	32.4	9.928	2.52E+04	2.97E+04	116.2	9.471	4.44E-04	5.22E-04
T-704	1.15	32.9	10.056	3.10E+04	3.56E+04	118.2	9.630	4.29E-04	4.93E-04

T-705	1.18	32.2	9.917	2.54E+04	3.01E+04	114.1	9.040	2.51E-04	2.97E-04
T-706	1.17	31.2	10.108	4.86E+04	5.71E+04	116.1	9.648	6.94E-04	8.14E-04
T-707	1.15	32.1	9.927	2.68E+04	3.07E+04	118.2	9.441	2.80E-04	3.21E-04
T-708	1.23	39.3	10.101	9.52E+03	1.17E+04	120.3	9.130	9.04E-05	1.11E-04
T-709	1.19	36.4	9.875	1.00E+04	1.20E+04	119.4	9.389	1.93E-04	2.31E-04
T-710	1.19	36.9	9.673	5.73E+03	6.85E+03	123.4	9.458	1.03E-04	1.23E-04
T-711	1.26	34.0	9.886	1.68E+04	2.12E+04	117.2	8.955	1.11E-04	1.40E-04
T-712	1.19	33.2	9.966	1.17E+04	1.39E+04	117.9	9.683	2.62E-04	3.11E-04
T-713	1.19	35.0	9.934	1.52E+04	1.80E+04	124.6	9.695	1.40E-04	1.66E-04
T-714	1.18	36.5	10.198	1.04E+04	1.23E+04	115.0	9.258	1.74E-04	2.06E-04
T-715	1.18	36.7	10.186	9.68E+03	1.14E+04	120.0	9.957	3.20E-04	3.77E-04
T-716	1.17	37.0	10.015	6.11E+03	7.16E+03	120.9	9.853	2.12E-04	2.49E-04
T-717	1.23	36.4	9.879	1.02E+04	1.26E+04	115.8	8.909	1.34E-04	1.65E-04
T-718	1.19	37.4	10.029	5.91E+03	7.04E+03	119.9	9.589	1.40E-04	1.67E-04
T-719	1.17	37.3	10.154	7.92E+03	9.29E+03	120.9	9.717	1.53E-04	1.79E-04
T-801	1.10	29.0	10.189	4.58E+04	5.06E+04	110.1	9.104	1.25E-04	1.38E-04
T-802	1.12	25.4	9.647	5.37E+04	6.02E+04	112.9	8.217	9.63E-05	1.08E-04
T-803	1.10	28.8	9.896	4.88E+04	5.38E+04	112.1	8.509	2.21E-04	2.44E-04
T-804	1.08	29.9	10.192	3.83E+04	4.14E+04	113.5	8.834	1.78E-04	1.93E-04
T-805	1.18	28.9	10.084	3.69E+04	4.34E+04	105.0	8.156	4.06E-04	4.77E-04
T-806	1.10	28.2	9.880	5.23E+04	5.72E+04	112.2	8.460	1.94E-04	2.12E-04
T-807	1.08	29.0	10.186	4.58E+04	4.94E+04	113.1	8.800	1.76E-04	1.90E-04
T-808	1.13	32.0	10.185	2.46E+04	2.79E+04	108.7	8.414	1.78E-04	2.02E-04
T-809	1.13	31.5	9.845	2.52E+04	2.84E+04	115.1	8.508	1.23E-04	1.38E-04
T-810	1.13	32.2	10.145	2.19E+04	2.47E+04	118.7	8.879	6.99E-05	7.87E-05
T-811	1.19	32.4	9.832	2.05E+04	2.43E+04	110.7	8.049	1.03E-04	1.22E-04
T-812	1.11	34.9	10.027	1.92E+04	2.12E+04	117.7	8.670	1.05E-04	1.16E-04
T-813	1.09	33.9	10.325	2.34E+04	2.55E+04	122.9	9.192	6.19E-05	6.76E-05
T-814	1.17	30.7	9.839	2.91E+04	3.39E+04	107.8	7.802	1.76E-04	2.05E-04
T-815	1.10	30.8	10.251	3.63E+04	4.00E+04	112.9	9.053	3.32E-04	3.65E-04
T-816	1.09	31.3	10.227	3.12E+04	3.41E+04	113.6	8.844	1.78E-04	1.95E-04
T-817	1.11	34.3	10.006	1.03E+04	1.14E+04	114.4	8.067	2.52E-05	2.79E-05
T-818	1.10	31.8	10.153	2.41E+04	2.65E+04	112.6	8.790	1.92E-04	2.11E-04
T-819	1.09	29.2	9.929	4.85E+04	5.31E+04	111.3	8.541	2.83E-04	3.09E-04

[a] $\mathbf{E_{a,f}}$**:** Activation energy of the forward reaction, given in kJ mol^{-1}.
[b] $\boldsymbol{log\widetilde{A}_f}$**:** Logarithm of the pre-exponential factor of the forward reaction, given in m^3 mol^{-1} s^{-1}.
[c] $\mathbf{k_f}$**:** The reaction rate coefficient for the forward reaction excluding tunneling effects, given in m^3 mol^{-1} s^{-1}.
[d] $\boldsymbol{\kappa k_f}$**:** The reaction rate coefficient for the forward reaction including tunneling effects, given in m^3 mol^{-1} s^{-1}.
[e] $\mathbf{E_{a,r}}$**:** Activation energy of the reverse reaction, given in kJ mol^{-1}.
[f] $\boldsymbol{log\widetilde{A}_r}$**:** Logarithm of the pre-exponential factor of the reverse reaction, given in m^3 mol^{-1} s^{-1}.
[g] $\mathbf{k_r}$**:** The reaction rate coefficient for the reverse reaction excluding tunneling effects, given in m^3 mol^{-1} s^{-1}.
[h] $\boldsymbol{\kappa k_r}$**:** The reaction rate coefficient for the reverse reaction including tunneling effects, given in m^3 mol^{-1} s^{-1}.

Table D-3 Arrhenius parameters (activation energy (**Ea**) and logarithm of the pre-exponential factor ($\log\widetilde{A}$)) of the reactions in the training set 1000 K, given along with reaction rate coefficients and the tunneling correction factor (κ) for forward and reverse reactions.

Reaction #	κ	Forward				Reverse			
		$E_{a,f}$ [a]	$\log\widetilde{A}_f$ [b]	k_f [c]	κk_f [d]	$E_{a,r}$ [e]	$\log\widetilde{A}_r$ [f]	k_r [g]	κk_r [h]
T-101	1.14	49.8	10.837	5.14E+05	5.84E+05	105.8	9.734	1.60E+01	1.82E+01
T-102	1.13	48.3	10.784	5.43E+05	6.14E+05	106.4	10.029	2.92E+01	3.31E+01
T-103	1.13	49.1	10.738	2.62E+05	2.97E+05	103.1	9.558	1.48E+01	1.68E+01
T-104	1.12	48.4	10.812	6.35E+05	7.11E+05	106.9	10.023	2.73E+01	3.06E+01
T-105	1.13	48.7	10.775	7.81E+05	8.81E+05	104.7	9.553	1.21E+01	1.36E+01
T-106	1.13	48.2	10.855	9.53E+05	1.08E+06	102.9	9.576	1.58E+01	1.79E+01
T-107	1.12	48.7	10.322	2.89E+05	3.24E+05	103.8	9.536	1.29E+01	1.44E+01
T-108	1.14	48.6	10.856	6.17E+05	7.01E+05	108.8	10.163	3.02E+01	3.43E+01
T-109	1.15	49.2	10.852	5.72E+05	6.57E+05	104.3	10.036	3.85E+01	4.42E+01
T-110	1.14	49.3	10.848	5.57E+05	6.36E+05	111.0	10.116	2.07E+01	2.37E+01
T-111	1.14	48.4	10.976	9.22E+05	1.05E+06	109.8	10.035	2.00E+01	2.27E+01
T-112	1.14	49.5	10.863	5.62E+05	6.40E+05	107.2	10.129	3.37E+01	3.85E+01
T-113	1.13	47.9	10.771	6.05E+05	6.81E+05	113.6	10.268	2.16E+01	2.43E+01
T-114	1.13	49.3	10.772	9.43E+05	1.07E+06	107.7	9.592	9.22E+00	1.05E+01
T-115	1.13	48.9	11.219	2.76E+06	3.13E+06	106.0	9.908	2.35E+01	2.66E+01
T-116	1.13	49.4	10.343	7.29E+05	8.24E+05	106.5	9.371	3.17E+00	3.59E+00
T-117	1.13	48.3	10.803	5.66E+05	6.41E+05	106.5	9.563	9.97E+00	1.13E+01
T-118	1.13	49.1	10.846	5.71E+05	6.48E+05	105.9	9.588	1.14E+01	1.29E+01
T-119	1.13	49.2	10.879	6.04E+05	6.84E+05	106.7	9.855	1.91E+01	2.16E+01
T-201	1.07	41.5	10.718	7.11E+05	7.60E+05	110.1	9.087	4.32E+00	4.62E+00
T-202	1.07	38.0	10.615	8.50E+05	9.07E+05	107.0	8.805	3.28E+00	3.50E+00
T-203	1.07	37.2	10.650	1.02E+06	1.09E+06	107.4	9.102	6.16E+00	6.60E+00
T-204	1.05	39.4	10.653	7.81E+05	8.22E+05	110.2	9.073	4.14E+00	4.36E+00
T-205	1.06	37.0	10.601	9.24E+05	9.83E+05	107.0	8.770	3.03E+00	3.22E+00
T-206	1.07	36.9	10.672	1.10E+06	1.18E+06	106.8	8.975	4.96E+00	5.32E+00
T-207	1.05	36.3	10.674	1.20E+06	1.26E+06	106.8	9.070	6.17E+00	6.48E+00
T-208	1.08	43.4	10.696	5.31E+05	5.72E+05	112.0	8.865	1.52E+00	1.63E+00
T-209	1.09	40.4	10.661	7.04E+05	7.65E+05	109.2	9.046	4.37E+00	4.75E+00
T-210	1.07	41.2	10.744	7.81E+05	8.37E+05	116.3	8.957	1.51E+00	1.62E+00
T-211	1.07	40.5	10.519	5.01E+05	5.35E+05	108.7	8.720	2.20E+00	2.35E+00
T-212	1.08	38.9	10.692	9.12E+05	9.82E+05	109.0	9.210	6.53E+00	7.03E+00
T-213	1.06	39.5	10.688	8.34E+05	8.82E+05	117.7	9.138	1.95E+00	2.06E+00
T-214	1.07	37.1	10.398	5.76E+05	6.16E+05	107.4	8.751	2.76E+00	2.95E+00
T-215	1.07	38.3	10.744	1.10E+06	1.18E+06	107.7	9.123	5.23E+00	5.60E+00
T-216	1.06	41.0	10.683	6.97E+05	7.41E+05	110.0	8.593	1.39E+00	1.48E+00
T-217	1.06	41.3	10.833	9.48E+05	1.01E+06	110.1	8.840	2.44E+00	2.60E+00

T-218	1.07	40.8	11.012	1.51E+06	1.61E+06	109.9	9.073	4.27E+00	4.55E+00
T-219	1.06	41.3	10.722	1.46E+06	1.55E+06	110.7	9.062	3.76E+00	4.00E+00
T-301	1.04	34.0	10.666	7.71E+05	8.06E+05	106.1	8.215	1.87E+00	1.96E+00
T-302	1.08	34.7	10.649	6.83E+05	7.35E+05	96.8	8.086	2.13E+00	2.29E+00
T-303	1.05	32.1	10.675	9.90E+05	1.04E+06	105.2	8.125	8.46E-01	8.85E-01
T-304	1.03	32.1	10.637	9.06E+05	9.36E+05	105.6	8.267	1.11E+00	1.15E+00
T-305	1.08	33.5	10.672	8.36E+05	9.01E+05	95.6	8.242	3.50E+00	3.77E+00
T-306	1.04	31.4	10.668	1.07E+06	1.11E+06	104.9	8.221	1.09E+00	1.14E+00
T-307	1.03	31.7	10.678	1.05E+06	1.08E+06	104.8	8.192	1.04E+00	1.07E+00
T-308	1.10	40.6	10.870	5.60E+05	6.14E+05	104.2	8.960	6.53E+00	7.16E+00
T-309	1.05	34.0	10.643	7.33E+05	7.71E+05	106.1	7.741	3.16E-01	3.32E-01
T-310	1.05	36.8	10.664	5.51E+05	5.79E+05	116.3	8.006	1.70E-01	1.79E-01
T-311	1.06	35.6	10.353	3.09E+05	3.29E+05	98.8	8.539	4.75E+00	5.06E+00
T-312	1.05	33.7	10.645	7.66E+05	8.02E+05	107.3	8.298	9.86E-01	1.03E+00
T-313	1.04	35.4	10.622	5.88E+05	6.10E+05	116.5	7.911	1.33E-01	1.38E-01
T-314	1.07	40.0	10.187	1.25E+05	1.34E+05	97.1	8.585	6.46E+00	6.95E+00
T-315	1.04	33.3	10.845	1.27E+06	1.32E+06	105.8	8.591	2.32E+00	2.42E+00
T-316	1.04	33.7	10.763	9.98E+05	1.04E+06	106.2	8.240	9.75E-01	1.01E+00
T-317	1.09	41.5	10.336	1.47E+05	1.60E+05	95.6	8.623	8.46E+00	9.21E+00
T-318	1.04	33.7	10.681	8.28E+05	8.63E+05	105.9	8.217	9.66E-01	1.01E+00
T-319	1.04	34.3	10.706	8.19E+05	8.51E+05	106.7	8.146	7.47E-01	7.76E-01
T-401	1.06	34.6	10.476	9.28E+05	9.82E+05	143.0	9.370	1.57E-01	1.67E-01
T-402	1.12	34.7	11.025	1.63E+06	1.83E+06	137.7	9.395	1.59E-01	1.78E-01
T-403	1.04	36.2	11.046	1.42E+06	1.48E+06	146.9	9.934	1.81E-01	1.89E-01
T-404	1.05	32.8	10.747	1.07E+06	1.12E+06	143.8	9.664	1.41E-01	1.48E-01
T-405	1.05	32.0	10.700	1.06E+06	1.11E+06	140.6	9.487	1.38E-01	1.46E-01
T-406	1.04	32.1	11.027	2.22E+06	2.31E+06	144.2	9.923	2.46E-01	2.55E-01
T-407	1.03	32.7	11.022	2.06E+06	2.13E+06	144.1	9.931	2.51E-01	2.58E-01
T-408	1.06	38.6	10.897	7.57E+05	8.02E+05	145.8	9.655	1.09E-01	1.16E-01
T-409	1.05	35.6	11.014	1.42E+06	1.49E+06	143.5	9.917	2.62E-01	2.75E-01
T-410	1.05	36.4	10.751	7.03E+05	7.36E+05	150.1	10.017	1.50E-01	1.57E-01
T-411	1.04	37.7	10.802	6.76E+05	7.06E+05	141.8	9.386	9.47E-02	9.90E-02
T-412	1.04	34.7	11.109	1.96E+06	2.05E+06	144.4	10.086	3.48E-01	3.64E-01
T-413	1.05	36.4	10.730	6.70E+05	7.06E+05	151.4	9.886	9.39E-02	9.89E-02
T-414	1.04	34.4	10.783	9.63E+05	1.00E+06	141.8	9.487	1.20E-01	1.25E-01
T-415	1.04	34.2	11.197	2.56E+06	2.66E+06	143.1	10.100	4.17E-01	4.33E-01
T-416	1.05	33.2	10.443	5.10E+05	5.37E+05	143.7	9.741	1.70E-01	1.79E-01
T-417	1.04	34.7	11.002	1.54E+06	1.60E+06	142.3	9.677	1.75E-01	1.82E-01
T-418	1.04	34.5	11.030	1.69E+06	1.76E+06	143.3	9.914	2.66E-01	2.77E-01
T-419	1.05	36.9	10.793	7.26E+05	7.65E+05	146.6	9.668	1.02E-01	1.08E-01
T-501	1.03	29.9	10.520	1.81E+06	1.87E+06	137.9	8.727	1.33E-01	1.38E-01

T-502	1.05	30.8	10.551	8.71E+05	9.17E+05	137.2	8.950	1.20E-01	1.27E-01
T-503	1.03	28.1	10.822	2.26E+06	2.34E+06	137.4	8.999	1.32E-01	1.37E-01
T-504	1.03	28.5	10.828	1.42E+06	1.46E+06	134.6	8.993	1.82E-01	1.87E-01
T-505	1.03	29.1	10.952	2.68E+06	2.76E+06	128.3	9.194	6.16E-01	6.34E-01
T-506	1.03	27.5	10.809	2.35E+06	2.41E+06	138.4	8.971	1.09E-01	1.12E-01
T-507	1.03	27.7	10.839	2.45E+06	2.52E+06	138.4	8.942	1.03E-01	1.05E-01
T-508	1.04	31.5	10.958	2.05E+06	2.13E+06	131.0	9.059	3.28E-01	3.41E-01
T-509	1.04	25.7	10.817	2.96E+06	3.08E+06	134.4	8.975	1.78E-01	1.85E-01
T-510	1.04	25.4	10.785	2.87E+06	2.98E+06	140.4	8.993	1.33E-01	1.38E-01
T-511	1.03	26.1	10.610	1.75E+06	1.81E+06	130.0	9.058	3.69E-01	3.81E-01
T-512	1.03	24.7	10.820	3.37E+06	3.48E+06	134.0	8.639	8.66E-02	8.95E-02
T-513	1.03	32.0	10.812	1.38E+06	1.42E+06	146.1	9.117	6.10E-02	6.29E-02
T-514	1.05	30.5	10.645	1.12E+06	1.18E+06	127.6	8.886	3.30E-01	3.46E-01
T-515	1.03	24.8	10.871	3.77E+06	3.89E+06	133.1	9.061	2.56E-01	2.64E-01
T-516	1.03	29.8	10.821	1.82E+06	1.88E+06	138.7	8.685	5.47E-02	5.64E-02
T-517	1.04	31.3	10.682	1.11E+06	1.15E+06	127.7	9.025	4.48E-01	4.65E-01
T-518	1.03	29.4	10.812	1.88E+06	1.94E+06	137.7	9.018	1.33E-01	1.37E-01
T-519	1.03	26.0	10.846	3.06E+06	3.15E+06	134.8	8.983	1.74E-01	1.79E-01
T-601	1.04	29.0	10.415	1.59E+06	1.66E+06	161.1	9.988	3.71E-02	3.88E-02
T-602	1.03	24.8	10.921	4.19E+06	4.32E+06	166.5	9.554	7.17E-03	7.39E-03
T-603	1.02	22.4	10.669	3.13E+06	3.21E+06	162.6	9.791	1.97E-02	2.02E-02
T-604	1.02	23.8	10.655	3.35E+06	3.41E+06	163.0	9.956	6.11E-02	6.22E-02
T-605	1.09	30.1	10.749	1.17E+06	1.28E+06	166.6	8.949	1.74E-03	1.90E-03
T-606	1.04	25.0	10.784	2.98E+06	3.09E+06	163.8	9.931	2.37E-02	2.45E-02
T-607	1.04	28.1	10.743	1.88E+06	1.95E+06	167.9	9.996	1.67E-02	1.73E-02
T-608	1.03	23.3	10.707	3.06E+06	3.16E+06	169.3	8.836	9.81E-04	1.01E-03
T-609	1.05	25.3	10.774	2.82E+06	2.98E+06	162.6	9.951	2.84E-02	3.00E-02
T-610	1.05	25.9	10.784	2.68E+06	2.81E+06	160.3	9.993	4.16E-02	4.36E-02
T-611	1.04	27.7	10.491	1.10E+06	1.14E+06	174.7	8.888	5.75E-04	5.99E-04
T-612	1.05	28.1	10.852	2.40E+06	2.51E+06	160.2	9.969	5.58E-02	5.83E-02
T-613	1.04	30.5	10.718	1.33E+06	1.38E+06	165.9	10.008	2.18E-02	2.27E-02
T-614	1.07	34.3	10.750	9.00E+05	9.65E+05	177.9	9.093	6.31E-04	6.77E-04
T-615	1.04	27.9	10.796	2.16E+06	2.25E+06	165.3	9.960	2.11E-02	2.19E-02
T-616	1.04	23.8	10.759	3.26E+06	3.39E+06	161.1	10.014	3.94E-02	4.10E-02
T-617	1.03	33.0	10.472	5.60E+05	5.78E+05	174.6	8.763	4.35E-04	4.50E-04
T-618	1.02	30.0	11.047	1.91E+06	1.96E+06	164.9	10.189	2.32E-02	2.38E-02
T-619	1.04	30.8	10.792	1.52E+06	1.59E+06	165.8	9.987	2.10E-02	2.19E-02
T-701	1.07	43.5	10.256	1.91E+05	2.04E+05	127.0	9.818	6.07E+00	6.47E+00
T-702	1.08	35.6	10.072	3.26E+05	3.51E+05	119.2	9.402	2.98E+00	3.20E+00
T-703	1.06	38.6	10.344	4.21E+05	4.47E+05	123.4	9.941	6.23E+00	6.61E+00
T-704	1.05	39.0	10.468	5.35E+05	5.64E+05	125.4	10.099	7.06E+00	7.43E+00

T-705	1.06	38.5	10.335	4.19E+05	4.46E+05	121.3	9.513	2.98E+00	3.17E+00
T-706	1.06	37.5	10.526	7.38E+05	7.83E+05	123.3	10.125	9.62E+00	1.02E+01
T-707	1.05	38.3	10.340	4.36E+05	4.59E+05	125.3	9.911	4.60E+00	4.83E+00
T-708	1.08	45.5	10.519	2.76E+05	2.97E+05	127.6	9.610	1.76E+00	1.90E+00
T-709	1.07	42.7	10.294	2.31E+05	2.46E+05	126.6	9.860	3.51E+00	3.75E+00
T-710	1.07	43.2	10.092	1.37E+05	1.46E+05	130.7	9.937	2.58E+00	2.75E+00
T-711	1.09	40.3	10.313	3.20E+05	3.49E+05	124.5	9.433	1.69E+00	1.85E+00
T-712	1.07	39.5	10.385	2.09E+05	2.23E+05	125.0	10.155	4.19E+00	4.46E+00
T-713	1.07	41.3	10.355	3.13E+05	3.34E+05	131.8	10.170	3.84E+00	4.10E+00
T-714	1.06	42.8	10.617	2.40E+05	2.56E+05	122.2	9.731	2.21E+00	2.36E+00
T-715	1.06	43.0	10.604	2.28E+05	2.42E+05	127.1	10.428	6.07E+00	6.45E+00
T-716	1.06	43.3	10.433	1.48E+05	1.57E+05	128.0	10.326	4.32E+00	4.58E+00
T-717	1.08	42.7	10.304	2.35E+05	2.54E+05	123.0	9.386	1.82E+00	1.96E+00
T-718	1.07	43.6	10.448	1.47E+05	1.57E+05	127.1	10.062	2.64E+00	2.82E+00
T-719	1.06	43.6	10.572	1.96E+05	2.08E+05	128.1	10.189	3.12E+00	3.31E+00
T-801	1.04	35.1	10.597	5.78E+05	6.00E+05	117.2	9.570	1.19E+00	1.23E+00
T-802	1.02	31.4	10.049	7.67E+05	7.80E+05	120.0	8.683	1.03E+00	1.05E+00
T-803	1.04	34.8	10.302	6.05E+05	6.27E+05	119.2	8.972	2.22E+00	2.31E+00
T-804	1.03	35.9	10.592	5.18E+05	5.34E+05	120.5	9.295	2.00E+00	2.06E+00
T-805	1.06	35.2	10.509	4.65E+05	4.94E+05	112.3	8.635	2.33E+00	2.48E+00
T-806	1.03	34.3	10.285	6.20E+05	6.42E+05	119.2	8.922	1.96E+00	2.03E+00
T-807	1.03	34.9	10.586	5.74E+05	5.90E+05	120.1	9.261	1.92E+00	1.98E+00
T-808	1.05	38.2	10.595	3.97E+05	4.16E+05	115.7	8.875	1.36E+00	1.42E+00
T-809	1.05	37.7	10.258	3.89E+05	4.07E+05	122.2	8.978	1.56E+00	1.64E+00
T-810	1.05	38.3	10.556	3.57E+05	3.73E+05	125.8	9.352	1.19E+00	1.25E+00
T-811	1.07	38.7	10.255	3.41E+05	3.64E+05	117.8	8.522	9.24E-01	9.85E-01
T-812	1.04	41.0	10.436	3.90E+05	4.05E+05	124.8	9.136	1.65E+00	1.72E+00
T-813	1.03	40.0	10.729	4.37E+05	4.52E+05	129.9	9.654	1.47E+00	1.52E+00
T-814	1.06	37.0	10.258	4.23E+05	4.48E+05	115.1	8.270	1.01E+00	1.07E+00
T-815	1.04	37.0	10.658	5.32E+05	5.52E+05	120.0	9.518	3.55E+00	3.68E+00
T-816	1.03	37.4	10.633	4.75E+05	4.91E+05	120.7	9.308	2.02E+00	2.08E+00
T-817	1.04	40.4	10.410	1.99E+05	2.07E+05	121.3	8.522	3.04E-01	3.16E-01
T-818	1.04	37.9	10.559	3.80E+05	3.94E+05	119.7	9.254	2.01E+00	2.08E+00
T-819	1.03	35.2	10.334	6.21E+05	6.42E+05	118.3	9.006	2.66E+00	2.75E+00

[a] $\mathbf{E_{a,f}}$**:** Activation energy of the forward reaction, given in kJ mol^{-1}.
[b] $\boldsymbol{log\widetilde{A}_f}$**:** Logarithm of the pre-exponential factor of the forward reaction, given in m^3 mol^{-1} s^{-1}.
[c] $\mathbf{k_f}$**:** The reaction rate coefficient for the forward reaction excluding tunneling effects, given in m^3 mol^{-1} s^{-1}.
[d] $\boldsymbol{\kappa k_f}$**:** The reaction rate coefficient for the forward reaction including tunneling effects, given in m^3 mol^{-1} s^{-1}.
[e] $\mathbf{E_{a,r}}$**:** Activation energy of the reverse reaction, given in kJ mol^{-1}.
[f] $\boldsymbol{log\widetilde{A}_r}$**:** Logarithm of the pre-exponential factor of the reverse reaction, given in m^3 mol^{-1} s^{-1}.
[g] **kr:** The reaction rate coefficient for the reverse reaction excluding tunneling effects, given in m^3 mol^{-1} s^{-1}.
[h] $\boldsymbol{\kappa}$**kr**: The reaction rate coefficient for the reverse reaction including tunneling effects, given in m^3 mol^{-1} s^{-1}.

Table D-4 Arrhenius parameters (activation energy (**Ea**) and logarithm of the pre-exponential factor ($\log\widetilde{A}$)) of the reactions in the training set 1500 K, given along with reaction rate coefficients and the tunneling correction factor (κ) for forward and reverse reactions.

Reaction #	κ	Forward				Reverse			
		$E_{a,f}$ [a]	$\log\widetilde{A}_f$ [b]	k_f [c]	κk_f [d]	$E_{a,r}$ [e]	$\log\widetilde{A}_r$ [f]	k_r [g]	κk_r [h]
T-101	1.06	59.4	11.247	4.5E+06	4.8E+06	116.6	10.191	1.3E+03	1.4E+03
T-102	1.06	58.2	11.206	4.5E+06	4.8E+06	117.6	10.503	2.5E+03	2.7E+03
T-103	1.06	57.5	11.211	2.0E+06	2.1E+06	113.9	10.015	1.1E+03	1.2E+03
T-104	1.06	57.3	11.226	5.1E+06	5.4E+06	117.8	10.485	2.4E+03	2.5E+03
T-105	1.06	57.7	11.194	5.7E+06	6.0E+06	115.9	10.027	9.8E+02	1.0E+03
T-106	1.06	56.5	11.267	6.9E+06	7.3E+06	113.7	10.034	1.2E+03	1.3E+03
T-107	1.05	58.9	11.342	2.1E+06	2.2E+06	114.7	9.998	1.0E+03	1.1E+03
T-108	1.06	58.5	11.277	5.2E+06	5.5E+06	120.1	10.644	2.9E+03	3.1E+03
T-109	1.07	58.8	11.261	4.9E+06	5.2E+06	115.1	10.492	3.0E+03	3.3E+03
T-110	1.06	59.0	11.261	4.8E+06	5.1E+06	121.9	10.579	2.2E+03	2.3E+03
T-111	1.06	57.5	11.351	7.3E+06	7.7E+06	120.7	10.499	2.0E+03	2.1E+03
T-112	1.06	59.2	11.273	4.9E+06	5.2E+06	117.9	10.585	3.0E+03	3.2E+03
T-113	1.06	56.9	11.186	4.8E+06	5.1E+06	124.4	10.730	2.5E+03	2.6E+03
T-114	1.06	58.9	11.182	8.1E+06	8.6E+06	118.7	10.058	8.4E+02	8.9E+02
T-115	1.06	58.5	11.630	2.3E+07	2.5E+07	116.7	10.366	2.0E+03	2.1E+03
T-116	1.06	59.1	11.323	6.3E+06	6.7E+06	117.4	9.829	2.8E+02	2.9E+02
T-117	1.06	58.1	11.221	4.7E+06	5.0E+06	117.6	10.034	8.7E+02	9.2E+02
T-118	1.06	58.7	11.257	4.9E+06	5.2E+06	116.7	10.046	9.6E+02	1.0E+03
T-119	1.06	58.9	11.290	5.2E+06	5.5E+06	117.5	10.314	1.7E+03	1.8E+03
T-201	1.03	49.3	11.053	4.3E+06	4.5E+06	121.2	9.557	4.3E+02	4.5E+02
T-202	1.03	45.8	10.472	4.5E+06	4.6E+06	118.1	9.274	2.9E+02	3.0E+02
T-203	1.03	45.1	10.509	5.2E+06	5.4E+06	118.5	9.572	5.5E+02	5.7E+02
T-204	1.02	47.2	10.507	4.4E+06	4.5E+06	121.2	9.540	4.2E+02	4.3E+02
T-205	1.03	44.9	10.457	4.7E+06	4.8E+06	118.1	9.239	2.7E+02	2.8E+02
T-206	1.03	44.8	10.531	5.6E+06	5.8E+06	117.9	9.446	4.4E+02	4.5E+02
T-207	1.02	44.0	10.526	5.9E+06	6.0E+06	117.8	9.536	5.4E+02	5.5E+02
T-208	1.04	51.3	11.030	3.5E+06	3.6E+06	123.5	9.337	1.8E+02	1.9E+02
T-209	1.04	48.4	10.998	4.1E+06	4.3E+06	120.4	9.518	4.2E+02	4.4E+02
T-210	1.03	49.0	11.077	4.7E+06	4.8E+06	127.5	9.428	1.9E+02	2.0E+02
T-211	1.03	48.4	10.852	2.9E+06	3.0E+06	119.7	9.189	2.1E+02	2.1E+02
T-212	1.04	46.8	11.029	5.0E+06	5.2E+06	120.1	9.681	6.3E+02	6.5E+02
T-213	1.03	47.3	11.019	4.7E+06	4.8E+06	128.7	9.604	2.6E+02	2.7E+02
T-214	1.03	44.9	10.732	2.9E+06	3.0E+06	118.5	9.221	2.5E+02	2.6E+02
T-215	1.03	46.2	11.079	5.9E+06	6.1E+06	118.8	9.534	4.2E+02	4.4E+02
T-216	1.03	48.8	11.017	4.1E+06	4.3E+06	121.1	9.062	1.4E+02	1.4E+02
T-217	1.03	49.1	10.865	5.7E+06	5.9E+06	121.2	9.309	2.4E+02	2.5E+02

T-218	1.48	48.7	11.045	6.2E+06	9.2E+06	121.0	9.542	4.2E+02	6.3E+02
T-219	1.03	49.2	11.055	8.8E+06	9.1E+06	121.8	9.531	3.9E+02	4.0E+02
T-301	1.02	41.8	10.997	3.5E+06	3.5E+06	117.2	8.686	1.6E+02	1.6E+02
T-302	1.04	42.6	10.987	3.2E+06	3.3E+06	108.1	8.563	1.3E+02	1.3E+02
T-303	1.02	39.9	11.007	4.1E+06	4.2E+06	116.3	8.596	7.0E+01	7.1E+01
T-304	1.02	39.8	10.964	3.8E+06	3.8E+06	116.7	8.734	9.3E+01	9.5E+01
T-305	1.04	41.4	11.011	3.7E+06	3.8E+06	106.9	8.718	2.0E+02	2.0E+02
T-306	1.02	39.1	10.999	4.3E+06	4.4E+06	116.1	8.691	8.9E+01	9.1E+01
T-307	1.01	39.3	11.003	4.3E+06	4.4E+06	115.8	8.659	8.4E+01	8.5E+01
T-308	1.04	48.5	11.209	3.3E+06	3.4E+06	115.5	9.436	5.2E+02	5.4E+02
T-309	1.02	41.8	10.976	3.3E+06	3.4E+06	117.2	8.214	2.7E+01	2.8E+01
T-310	1.02	44.6	10.995	2.8E+06	2.8E+06	127.5	8.480	2.2E+01	2.2E+01
T-311	1.03	43.5	10.687	1.5E+06	1.5E+06	109.9	9.010	3.0E+02	3.1E+02
T-312	1.02	41.5	10.976	3.4E+06	3.5E+06	118.4	8.769	8.8E+01	9.0E+01
T-313	1.02	43.2	10.950	2.8E+06	2.8E+06	127.5	8.379	1.7E+01	1.8E+01
T-314	1.03	47.9	10.523	7.1E+05	7.4E+05	108.3	9.059	3.9E+02	4.0E+02
T-315	1.02	41.1	11.175	5.5E+06	5.7E+06	116.9	9.062	2.0E+02	2.0E+02
T-316	1.02	41.5	11.092	4.4E+06	4.5E+06	117.3	8.709	8.4E+01	8.5E+01
T-317	1.04	49.4	10.673	8.9E+05	9.3E+05	106.9	9.100	4.8E+02	5.0E+02
T-318	1.02	41.5	11.012	3.7E+06	3.8E+06	117.0	8.688	8.2E+01	8.3E+01
T-319	1.02	42.0	11.035	3.7E+06	3.8E+06	117.7	8.615	6.5E+01	6.6E+01
T-401	1.03	42.4	10.805	4.3E+06	4.4E+06	154.2	9.842	5.9E+01	6.1E+01
T-402	1.06	42.7	11.366	7.6E+06	8.0E+06	149.1	9.877	4.8E+01	5.1E+01
T-403	1.02	43.8	11.370	7.0E+06	7.1E+06	157.9	10.400	7.9E+01	8.1E+01
T-404	1.02	40.5	11.073	4.6E+06	4.7E+06	154.9	10.134	5.5E+01	5.6E+01
T-405	1.02	39.8	11.029	4.4E+06	4.5E+06	151.8	9.959	4.7E+01	4.8E+01
T-406	1.02	39.7	11.350	9.2E+06	9.4E+06	155.2	10.389	9.6E+01	9.8E+01
T-407	1.01	40.2	11.341	8.7E+06	8.9E+06	155.1	10.395	9.8E+01	1.0E+02
T-408	1.03	46.3	11.225	4.1E+06	4.2E+06	157.0	10.129	4.6E+01	4.7E+01
T-409	1.02	43.3	11.341	6.8E+06	6.9E+06	154.6	10.386	1.0E+02	1.0E+02
T-410	1.02	44.1	11.076	3.5E+06	3.5E+06	161.2	10.487	7.5E+01	7.6E+01
T-411	1.02	45.4	11.126	3.5E+06	3.6E+06	152.9	9.854	3.4E+01	3.5E+01
T-412	1.02	42.4	11.434	9.1E+06	9.3E+06	155.4	10.554	1.4E+02	1.4E+02
T-413	1.02	44.1	11.057	3.3E+06	3.4E+06	162.6	10.356	4.9E+01	5.1E+01
T-414	1.02	42.0	11.107	4.4E+06	4.5E+06	152.8	9.956	4.3E+01	4.4E+01
T-415	1.02	41.8	11.520	1.2E+07	1.2E+07	154.2	10.566	1.6E+02	1.6E+02
T-416	1.02	40.9	10.771	2.2E+06	2.3E+06	154.9	10.212	6.6E+01	6.7E+01
T-417	1.02	42.3	11.326	7.1E+06	7.2E+06	153.3	10.144	6.4E+01	6.5E+01
T-418	1.02	42.1	11.353	7.7E+06	7.9E+06	154.4	10.381	1.0E+02	1.0E+02
T-419	1.02	44.7	11.120	3.7E+06	3.8E+06	157.7	10.140	4.4E+01	4.5E+01
T-501	1.02	37.5	10.842	6.9E+06	7.0E+06	149.0	9.196	4.1E+01	4.1E+01

T-502	1.02	38.5	10.879	3.4E+06	3.5E+06	148.5	9.425	3.6E+01	3.7E+01
T-503	1.02	35.7	11.145	8.0E+06	8.1E+06	148.5	9.468	4.0E+01	4.0E+01
T-504	1.01	35.3	11.449	4.6E+06	4.6E+06	145.6	9.460	4.9E+01	4.9E+01
T-505	1.01	36.7	11.275	9.9E+06	1.0E+07	139.3	9.659	1.3E+02	1.3E+02
T-506	1.01	35.1	11.130	8.1E+06	8.2E+06	149.5	9.438	3.4E+01	3.4E+01
T-507	1.01	35.2	10.981	8.5E+06	8.6E+06	149.4	9.408	3.2E+01	3.2E+01
T-508	1.02	39.1	11.280	8.3E+06	8.4E+06	142.0	9.524	7.6E+01	7.7E+01
T-509	1.02	33.3	11.141	9.5E+06	9.7E+06	145.6	9.446	4.7E+01	4.8E+01
T-510	1.02	33.0	11.108	9.1E+06	9.3E+06	151.9	9.465	4.0E+01	4.0E+01
T-511	1.01	33.7	10.931	5.7E+06	5.8E+06	140.9	9.520	8.2E+01	8.3E+01
T-512	1.02	32.3	11.143	1.0E+07	1.1E+07	145.1	9.108	2.3E+01	2.3E+01
T-513	1.01	39.5	11.133	5.7E+06	5.8E+06	157.1	9.584	2.6E+01	2.6E+01
T-514	1.02	38.2	10.971	4.4E+06	4.5E+06	138.7	9.354	6.7E+01	6.8E+01
T-515	1.02	32.3	11.193	1.2E+07	1.2E+07	144.2	9.530	6.4E+01	6.5E+01
T-516	1.01	37.4	11.142	6.9E+06	7.0E+06	149.8	9.153	1.7E+01	1.8E+01
T-517	1.02	38.9	11.005	4.5E+06	4.5E+06	138.7	9.489	9.1E+01	9.2E+01
T-518	1.01	37.0	11.133	7.0E+06	7.1E+06	148.8	9.487	4.0E+01	4.1E+01
T-519	1.01	33.6	11.167	9.9E+06	1.0E+07	145.9	9.451	4.7E+01	4.8E+01
T-601	1.02	36.6	10.740	5.8E+06	5.9E+06	172.4	10.464	2.9E+01	2.9E+01
T-602	1.01	32.2	11.235	1.3E+07	1.3E+07	177.4	10.014	6.9E+00	7.0E+00
T-603	1.01	29.8	10.980	8.8E+06	8.9E+06	173.5	10.250	1.6E+01	1.6E+01
T-604	1.01	31.4	10.961	9.1E+06	9.1E+06	174.4	10.415	3.9E+01	3.9E+01
T-605	1.04	36.9	11.085	4.9E+06	5.1E+06	178.0	9.428	1.7E+00	1.8E+00
T-606	1.02	32.6	11.107	9.3E+06	9.5E+06	174.9	10.402	2.0E+01	2.1E+01
T-607	1.02	35.7	11.065	6.6E+06	6.8E+06	179.0	10.466	1.7E+01	1.7E+01
T-608	1.01	30.7	11.020	8.9E+06	9.0E+06	180.1	9.292	1.0E+00	1.1E+00
T-609	1.02	33.0	11.103	8.9E+06	9.2E+06	173.9	10.426	2.3E+01	2.4E+01
T-610	1.02	33.6	11.111	8.7E+06	8.9E+06	171.5	10.467	3.1E+01	3.2E+01
T-611	1.02	35.2	10.809	3.8E+06	3.9E+06	185.6	9.349	7.7E-01	7.8E-01
T-612	1.02	35.8	11.178	8.5E+06	8.7E+06	170.9	10.445	3.7E+01	3.8E+01
T-613	1.02	38.1	11.042	5.2E+06	5.3E+06	177.1	10.480	2.0E+01	2.1E+01
T-614	1.03	42.1	11.081	4.1E+06	4.2E+06	189.1	9.568	9.6E-01	9.9E-01
T-615	1.02	35.6	11.120	7.6E+06	7.7E+06	176.5	10.433	1.9E+01	2.0E+01
T-616	1.02	31.4	11.083	9.7E+06	9.9E+06	172.3	10.486	3.1E+01	3.1E+01
T-617	1.01	40.4	10.786	2.4E+06	2.4E+06	185.5	9.221	5.8E-01	5.9E-01
T-618	1.01	38.4	11.360	8.4E+06	8.5E+06	175.2	10.649	2.4E+01	2.5E+01
T-619	1.02	38.4	11.116	6.0E+06	6.1E+06	177.0	10.459	2.0E+01	2.0E+01
T-701	1.03	51.3	10.587	1.3E+06	1.3E+06	138.3	10.298	1.2E+03	1.2E+03
T-702	1.04	43.4	10.403	1.6E+06	1.6E+06	130.5	9.880	4.3E+02	4.5E+02
T-703	1.03	46.4	10.674	2.3E+06	2.3E+06	134.7	10.420	1.1E+03	1.1E+03
T-704	1.02	46.7	10.796	2.9E+06	3.0E+06	136.7	10.577	1.3E+03	1.3E+03

T-705	1.03	46.3	10.665	2.3E+06	2.3E+06	132.7	9.994	4.7E+02	4.8E+02
T-706	1.03	45.2	10.856	3.8E+06	3.9E+06	134.7	10.606	1.6E+03	1.7E+03
T-707	1.02	46.0	10.668	2.3E+06	2.4E+06	136.6	10.389	8.5E+02	8.7E+02
T-708	1.04	53.3	10.848	2.0E+06	2.0E+06	138.9	10.092	3.6E+02	3.7E+02
T-709	1.03	50.5	10.625	1.5E+06	1.5E+06	137.9	10.339	6.8E+02	7.1E+02
T-710	1.03	50.9	10.423	8.9E+05	9.2E+05	142.0	10.419	5.9E+02	6.1E+02
T-711	1.04	48.2	10.647	1.9E+06	1.9E+06	135.9	9.915	3.0E+02	3.2E+02
T-712	1.03	47.3	10.716	1.2E+06	1.2E+06	136.4	10.634	7.7E+02	7.9E+02
T-713	1.03	49.1	10.686	1.9E+06	1.9E+06	143.1	10.650	9.2E+02	9.5E+02
T-714	1.03	50.6	10.948	1.5E+06	1.6E+06	133.5	10.211	3.6E+02	3.7E+02
T-715	1.03	50.7	10.934	1.5E+06	1.5E+06	138.5	10.906	1.2E+03	1.2E+03
T-716	1.03	51.0	10.763	9.6E+05	9.9E+05	139.4	10.805	8.9E+02	9.2E+02
T-717	1.04	50.6	10.638	1.5E+06	1.6E+06	134.4	9.868	3.1E+02	3.2E+02
T-718	1.03	51.4	10.780	9.7E+05	1.0E+06	138.4	10.541	5.2E+02	5.4E+02
T-719	1.03	51.3	10.902	1.3E+06	1.3E+06	139.4	10.668	6.5E+02	6.7E+02
T-801	1.02	42.7	10.922	2.7E+06	2.8E+06	128.4	10.042	1.5E+02	1.5E+02
T-802	1.01	39.1	10.374	3.8E+06	3.8E+06	131.2	9.155	1.5E+02	1.6E+02
T-803	1.02	42.5	10.626	2.8E+06	2.9E+06	130.3	9.444	3.2E+02	3.3E+02
T-804	1.01	43.4	10.912	2.5E+06	2.5E+06	131.6	9.765	3.0E+02	3.1E+02
T-805	1.03	43.1	10.843	2.2E+06	2.3E+06	123.7	9.114	2.6E+02	2.6E+02
T-806	1.02	41.9	10.609	2.8E+06	2.9E+06	130.4	9.393	2.8E+02	2.9E+02
T-807	1.01	42.5	10.906	2.7E+06	2.7E+06	131.2	9.730	2.9E+02	2.9E+02
T-808	1.02	45.8	10.920	2.1E+06	2.2E+06	126.7	9.343	1.7E+02	1.7E+02
T-809	1.02	45.4	10.586	2.0E+06	2.1E+06	133.4	9.453	2.6E+02	2.6E+02
T-810	1.02	46.0	10.883	1.9E+06	1.9E+06	137.1	9.828	2.3E+02	2.3E+02
T-811	1.03	46.5	10.587	1.9E+06	1.9E+06	129.1	8.997	1.3E+02	1.3E+02
T-812	1.02	48.7	10.761	2.3E+06	2.4E+06	136.0	9.609	3.0E+02	3.0E+02
T-813	1.02	47.6	11.052	2.5E+06	2.5E+06	141.0	10.124	3.3E+02	3.3E+02
T-814	1.03	44.8	10.589	2.1E+06	2.2E+06	126.5	8.744	1.1E+02	1.1E+02
T-815	1.02	44.6	10.983	2.7E+06	2.7E+06	131.1	9.990	5.3E+02	5.4E+02
T-816	1.02	45.0	10.956	2.4E+06	2.5E+06	131.8	9.779	3.1E+02	3.1E+02
T-817	1.02	48.0	10.733	1.2E+06	1.2E+06	132.3	8.987	4.8E+01	4.9E+01
T-818	1.02	45.5	10.883	2.0E+06	2.0E+06	130.8	9.726	3.0E+02	3.0E+02
T-819	1.02	42.8	10.658	2.9E+06	3.0E+06	129.5	9.477	3.7E+02	3.8E+02

[a] $\mathbf{E_{a,f}}$**:** Activation energy of the forward reaction, given in kJ mol^{-1}.

[b] $\boldsymbol{log\widetilde{A}_f}$**:** Logarithm of the pre-exponential factor of the forward reaction, given in m^3 mol^{-1} s^{-1}.

[c] $\mathbf{k_f}$**:** The reaction rate coefficient for the forward reaction excluding tunneling effects, given in m^3 mol^{-1} s^{-1}.

[d] $\boldsymbol{\kappa k_f}$**:** The reaction rate coefficient for the forward reaction including tunneling effects, given in m^3 mol^{-1} s^{-1}.

[e] $\mathbf{E_{a,r}}$**:** Activation energy of the reverse reaction, given in kJ mol^{-1}.

[f] $\boldsymbol{log\widetilde{A}_r}$**:** Logarithm of the pre-exponential factor of the reverse reaction, given in m^3 mol^{-1} s^{-1}.

[g] $\mathbf{k_r}$**:** The reaction rate coefficient for the reverse reaction excluding tunneling effects, given in m^3 mol^{-1} s^{-1}.

[h] $\boldsymbol{\kappa k_r}$**:** The reaction rate coefficient for the reverse reaction including tunneling effects, given in m^3 mol^{-1} s^{-1}.

Table D-5 Arrhenius parameters (activation energy (**Ea**) and logarithm of the pre-exponential factor ($\log\widetilde{A}$)) of the reactions in the training set 2000 K, given along with reaction rate coefficients and the tunneling correction factor (κ) for forward and reverse reactions.

Reaction #	κ	Forward				Reverse			
		$E_{a,f}$ [a]	$\log\widetilde{A}_f$ [b]	k_f [c]	κk_f [d]	$E_{a,r}$ [e]	$\log\widetilde{A}_r$ [f]	k_r [g]	κk_r [h]
T-101	1.04	67.8	11.502	1.6E+07	1.7E+07	127.2	10.510	1.5E+04	1.6E+04
T-102	1.03	66.9	11.468	1.6E+07	1.6E+07	128.5	10.831	3.0E+04	3.1E+04
T-103	1.04	65.9	10.983	6.6E+06	6.8E+06	124.4	10.333	1.2E+04	1.3E+04
T-104	1.03	65.7	11.482	1.7E+07	1.8E+07	128.4	10.806	2.8E+04	2.9E+04
T-105	1.03	65.5	11.455	1.9E+07	1.9E+07	126.8	10.355	1.1E+04	1.1E+04
T-106	1.04	65.6	11.522	2.2E+07	2.3E+07	124.3	10.352	1.3E+04	1.3E+04
T-107	1.03	67.4	11.468	6.7E+06	6.9E+06	125.4	10.319	1.1E+04	1.1E+04
T-108	1.04	67.3	11.541	1.8E+07	1.9E+07	131.1	10.976	3.6E+04	3.7E+04
T-109	1.04	67.2	11.515	1.7E+07	1.8E+07	125.6	10.810	3.4E+04	3.5E+04
T-110	1.04	67.5	11.517	1.7E+07	1.8E+07	132.5	10.900	2.7E+04	2.8E+04
T-111	1.04	66.4	11.594	2.4E+07	2.5E+07	131.4	10.821	2.4E+04	2.5E+04
T-112	1.04	67.6	11.527	1.7E+07	1.8E+07	128.5	10.903	3.5E+04	3.7E+04
T-113	1.03	65.4	11.442	1.6E+07	1.7E+07	135.1	11.051	3.3E+04	3.4E+04
T-114	1.04	68.1	11.565	2.9E+07	3.0E+07	129.4	10.382	1.0E+04	1.0E+04
T-115	1.04	68.3	11.345	8.2E+07	8.5E+07	127.3	10.684	2.3E+04	2.4E+04
T-116	1.03	68.3	11.364	2.2E+07	2.3E+07	127.9	10.148	4.6E+03	4.7E+03
T-117	1.04	66.7	11.481	1.6E+07	1.7E+07	128.4	10.360	1.0E+04	1.0E+04
T-118	1.04	67.1	11.511	1.7E+07	1.8E+07	127.2	10.364	1.1E+04	1.1E+04
T-119	1.04	67.3	11.544	1.8E+07	1.9E+07	128.1	10.633	1.9E+04	2.0E+04
T-201	1.02	56.7	11.275	1.2E+07	1.3E+07	132.7	9.904	5.5E+03	5.6E+03
T-202	1.02	53.2	10.693	1.2E+07	1.2E+07	129.6	9.622	3.4E+03	3.5E+03
T-203	1.02	52.4	10.731	1.4E+07	1.4E+07	130.1	9.919	6.6E+03	6.8E+03
T-204	1.01	54.5	10.727	1.2E+07	1.2E+07	132.7	9.886	5.3E+03	5.3E+03
T-205	1.02	52.2	10.678	1.2E+07	1.3E+07	129.6	9.586	3.2E+03	3.2E+03
T-206	1.02	52.2	10.754	1.5E+07	1.5E+07	129.5	9.794	5.2E+03	5.3E+03
T-207	1.01	51.3	10.746	1.5E+07	1.5E+07	129.3	9.882	6.4E+03	6.5E+03
T-208	1.02	58.7	11.252	1.0E+07	1.1E+07	135.2	9.686	2.5E+03	2.6E+03
T-209	1.02	55.8	11.222	1.2E+07	1.2E+07	131.9	9.866	5.3E+03	5.4E+03
T-210	1.02	56.3	11.298	1.3E+07	1.4E+07	139.0	9.776	2.8E+03	2.8E+03
T-211	1.02	55.7	11.074	8.3E+06	8.4E+06	131.3	9.536	2.6E+03	2.6E+03
T-212	1.02	54.2	11.252	1.4E+07	1.4E+07	131.7	10.029	7.8E+03	7.9E+03
T-213	1.02	54.6	11.239	1.3E+07	1.3E+07	140.2	9.949	3.9E+03	3.9E+03
T-214	1.02	52.3	10.954	7.7E+06	7.9E+06	130.0	9.569	3.0E+03	3.0E+03
T-215	1.02	53.5	11.301	1.6E+07	1.6E+07	130.4	10.137	4.8E+03	4.9E+03
T-216	1.02	56.2	11.239	1.2E+07	1.2E+07	132.6	9.408	1.8E+03	1.8E+03
T-217	1.02	56.4	11.086	1.6E+07	1.7E+07	132.7	9.656	3.1E+03	3.1E+03

T-218	1.43	56.0	11.267	1.8E+07	2.6E+07	132.5	9.889	5.3E+03	7.6E+03
T-219	1.02	56.5	11.277	2.5E+07	2.6E+07	133.4	9.877	5.0E+03	5.0E+03
T-301	1.01	49.1	11.217	8.6E+06	8.7E+06	128.7	9.032	1.9E+03	1.9E+03
T-302	1.02	50.1	11.211	8.0E+06	8.2E+06	119.7	8.911	1.2E+03	1.2E+03
T-303	1.01	47.3	11.228	9.8E+06	1.0E+07	127.9	8.943	8.0E+02	8.1E+02
T-304	1.01	47.1	11.182	9.0E+06	9.0E+06	128.1	9.078	1.1E+03	1.1E+03
T-305	1.02	48.9	11.235	9.1E+06	9.3E+06	118.5	9.067	1.9E+03	1.9E+03
T-306	1.01	46.5	11.219	1.0E+07	1.0E+07	127.6	9.037	1.0E+03	1.0E+03
T-307	1.01	46.6	11.221	1.0E+07	1.0E+07	127.3	9.003	9.5E+02	9.6E+02
T-308	1.03	56.0	11.433	9.3E+06	9.6E+06	127.0	9.785	5.8E+03	6.0E+03
T-309	1.01	49.2	11.197	8.2E+06	8.3E+06	128.8	8.562	3.1E+02	3.2E+02
T-310	1.01	51.9	11.216	7.2E+06	7.3E+06	139.1	8.829	3.1E+02	3.2E+02
T-311	1.02	50.9	10.909	3.8E+06	3.9E+06	121.4	9.356	3.1E+03	3.1E+03
T-312	1.01	48.8	11.197	8.4E+06	8.5E+06	129.9	9.116	1.1E+03	1.1E+03
T-313	1.01	50.4	11.169	7.1E+06	7.2E+06	139.0	8.724	2.5E+02	2.5E+02
T-314	1.02	55.3	10.745	2.0E+06	2.0E+06	119.9	9.407	3.8E+03	3.8E+03
T-315	1.01	48.4	11.396	1.4E+07	1.4E+07	128.4	9.408	2.3E+03	2.3E+03
T-316	1.01	48.8	11.312	1.1E+07	1.1E+07	128.8	9.054	9.8E+02	9.9E+02
T-317	1.02	56.8	10.896	2.6E+06	2.6E+06	118.5	9.448	4.5E+03	4.6E+03
T-318	1.01	48.8	11.232	9.1E+06	9.2E+06	128.5	9.034	9.5E+02	9.6E+02
T-319	1.01	49.3	11.254	9.3E+06	9.4E+06	129.2	8.961	7.7E+02	7.8E+02
T-401	1.02	49.6	11.025	1.1E+07	1.1E+07	165.8	10.191	1.4E+03	1.5E+03
T-402	1.03	50.1	11.590	1.9E+07	2.0E+07	160.8	10.231	1.1E+03	1.1E+03
T-403	1.01	51.1	11.587	1.8E+07	1.8E+07	169.5	10.747	2.1E+03	2.1E+03
T-404	1.01	47.8	11.291	1.1E+07	1.1E+07	166.5	10.483	1.4E+03	1.4E+03
T-405	1.01	47.1	11.249	1.0E+07	1.1E+07	163.4	10.309	1.1E+03	1.1E+03
T-406	1.01	46.9	11.567	2.2E+07	2.2E+07	166.7	10.736	2.4E+03	2.4E+03
T-407	1.01	47.3	11.557	2.1E+07	2.1E+07	166.6	10.741	2.4E+03	2.5E+03
T-408	1.02	53.6	11.444	1.1E+07	1.1E+07	168.6	10.479	1.2E+03	1.2E+03
T-409	1.01	50.5	11.559	1.7E+07	1.8E+07	166.2	10.734	2.5E+03	2.5E+03
T-410	1.01	51.3	11.294	9.0E+06	9.1E+06	172.7	10.835	2.1E+03	2.1E+03
T-411	1.01	52.6	11.344	9.3E+06	9.5E+06	164.4	10.201	8.1E+02	8.2E+02
T-412	1.01	49.6	11.651	2.3E+07	2.3E+07	167.0	10.901	3.5E+03	3.5E+03
T-413	1.01	51.4	11.276	8.6E+06	8.7E+06	174.2	10.705	1.4E+03	1.5E+03
T-414	1.01	49.3	11.325	1.1E+07	1.1E+07	164.4	10.304	1.0E+03	1.0E+03
T-415	1.01	49.0	11.737	2.9E+07	2.9E+07	165.7	10.913	3.8E+03	3.9E+03
T-416	1.01	48.2	10.991	5.4E+06	5.5E+06	166.5	10.561	1.6E+03	1.7E+03
T-417	1.01	49.5	11.543	1.8E+07	1.8E+07	164.9	10.492	1.5E+03	1.5E+03
T-418	1.01	49.3	11.570	1.9E+07	1.9E+07	165.9	10.728	2.5E+03	2.5E+03
T-419	1.01	51.9	11.339	9.6E+06	9.7E+06	169.3	10.489	1.2E+03	1.2E+03
T-501	1.01	44.7	11.059	1.6E+07	1.6E+07	160.5	9.544	9.0E+02	9.1E+02

T-502	1.01	45.8	11.098	8.0E+06	8.1E+06	160.0	9.773	7.8E+02	7.9E+02
T-503	1.01	42.9	11.363	1.7E+07	1.8E+07	160.0	9.816	8.6E+02	8.7E+02
T-504	1.01	42.3	11.664	9.0E+06	9.1E+06	157.2	9.807	1.0E+03	1.0E+03
T-505	1.01	44.0	11.492	2.2E+07	2.2E+07	150.8	10.004	2.3E+03	2.3E+03
T-506	1.01	42.2	11.345	1.7E+07	1.8E+07	161.0	9.784	7.6E+02	7.6E+02
T-507	1.01	42.3	11.196	1.8E+07	1.9E+07	160.9	9.753	7.1E+02	7.2E+02
T-508	1.01	46.3	11.496	1.9E+07	2.0E+07	153.4	9.868	1.5E+03	1.5E+03
T-509	1.01	40.6	11.359	2.0E+07	2.0E+07	157.1	9.793	9.8E+02	9.9E+02
T-510	1.01	40.2	11.326	1.9E+07	1.9E+07	163.9	9.814	8.6E+02	8.7E+02
T-511	1.01	40.9	11.147	1.2E+07	1.2E+07	152.3	9.863	1.5E+03	1.5E+03
T-512	1.01	39.5	11.360	2.1E+07	2.1E+07	156.6	9.455	4.6E+02	4.7E+02
T-513	1.01	46.7	11.349	1.3E+07	1.4E+07	168.7	9.931	6.7E+02	6.8E+02
T-514	1.01	45.4	11.190	1.0E+07	1.0E+07	150.2	9.700	1.2E+03	1.2E+03
T-515	1.01	39.5	11.410	2.4E+07	2.4E+07	155.7	9.877	1.3E+03	1.3E+03
T-516	1.01	44.6	11.358	1.6E+07	1.6E+07	161.3	9.500	3.9E+02	3.9E+02
T-517	1.01	46.1	11.222	1.0E+07	1.1E+07	150.2	9.833	1.6E+03	1.6E+03
T-518	1.01	44.2	11.350	1.6E+07	1.6E+07	160.3	9.834	8.9E+02	8.9E+02
T-519	1.01	40.7	11.383	2.1E+07	2.1E+07	157.4	9.798	9.7E+02	9.8E+02
T-601	1.01	43.9	10.958	1.3E+07	1.3E+07	184.0	10.814	1.0E+03	1.0E+03
T-602	1.01	39.3	11.449	2.6E+07	2.7E+07	188.8	10.357	2.7E+02	2.7E+02
T-603	1.01	41.1	11.192	1.7E+07	1.7E+07	184.9	10.592	5.8E+02	5.8E+02
T-604	1.00	38.5	11.171	1.7E+07	1.7E+07	186.9	10.757	1.2E+03	1.2E+03
T-605	1.02	43.6	11.309	1.2E+07	1.2E+07	189.6	9.779	6.7E+01	6.8E+01
T-606	1.01	39.8	11.324	1.9E+07	1.9E+07	186.5	10.750	7.6E+02	7.6E+02
T-607	1.01	42.9	11.282	1.5E+07	1.5E+07	190.6	10.814	6.8E+02	6.9E+02
T-608	1.01	37.8	11.232	1.8E+07	1.8E+07	191.4	9.633	4.3E+01	4.3E+01
T-609	1.01	40.3	11.323	1.9E+07	1.9E+07	185.5	10.776	8.5E+02	8.6E+02
T-610	1.01	40.9	11.329	1.8E+07	1.8E+07	183.1	10.816	1.1E+03	1.1E+03
T-611	1.01	42.4	11.025	8.3E+06	8.4E+06	197.1	9.693	3.5E+01	3.6E+01
T-612	1.01	43.1	11.396	1.9E+07	1.9E+07	182.3	10.796	1.2E+03	1.2E+03
T-613	1.01	45.3	11.259	1.2E+07	1.2E+07	188.7	10.828	7.9E+02	8.0E+02
T-614	1.02	49.5	11.302	1.0E+07	1.0E+07	200.7	9.917	4.7E+01	4.8E+01
T-615	1.01	42.8	11.338	1.7E+07	1.7E+07	188.0	10.781	7.4E+02	7.5E+02
T-616	1.01	38.7	11.301	2.0E+07	2.0E+07	183.9	10.834	1.1E+03	1.1E+03
T-617	1.01	47.5	11.000	5.8E+06	5.8E+06	196.8	9.563	2.6E+01	2.7E+01
T-618	1.01	46.0	11.572	2.1E+07	2.1E+07	186.2	10.992	1.0E+03	1.0E+03
T-619	1.01	45.6	11.334	1.4E+07	1.4E+07	188.6	10.808	7.6E+02	7.7E+02
T-701	1.02	58.6	10.807	3.8E+06	3.8E+06	150.1	10.650	2.1E+04	2.2E+04
T-702	1.02	50.7	10.624	4.0E+06	4.1E+06	142.2	10.232	6.6E+03	6.7E+03
T-703	1.02	53.7	10.894	6.2E+06	6.3E+06	146.4	10.771	1.8E+04	1.8E+04
T-704	1.01	54.0	11.015	8.0E+06	8.2E+06	148.4	10.929	2.3E+04	2.3E+04

T-705	1.02	53.6	10.886	6.1E+06	6.2E+06	144.4	10.346	7.5E+03	7.6E+03
T-706	1.02	52.6	11.077	1.0E+07	1.0E+07	146.4	10.959	2.7E+04	2.8E+04
T-707	1.01	53.3	10.888	6.3E+06	6.3E+06	148.3	10.741	1.5E+04	1.5E+04
T-708	1.02	60.5	11.067	6.1E+06	6.2E+06	150.7	10.445	6.5E+03	6.6E+03
T-709	1.02	57.8	10.846	4.3E+06	4.4E+06	149.6	10.691	1.2E+04	1.2E+04
T-710	1.02	58.3	10.643	2.6E+06	2.7E+06	153.8	10.772	1.1E+04	1.2E+04
T-711	1.02	55.6	10.869	5.2E+06	5.4E+06	147.6	10.268	5.2E+03	5.3E+03
T-712	1.02	54.6	10.937	3.2E+06	3.3E+06	148.1	10.987	1.3E+04	1.3E+04
T-713	1.02	56.4	10.906	5.4E+06	5.5E+06	154.8	11.002	1.8E+04	1.8E+04
T-714	1.02	57.9	11.169	4.5E+06	4.6E+06	145.3	10.564	5.9E+03	6.0E+03
T-715	1.02	58.0	11.154	4.3E+06	4.4E+06	150.2	11.258	2.2E+04	2.2E+04
T-716	1.02	58.4	10.983	2.9E+06	2.9E+06	151.1	11.157	1.6E+04	1.7E+04
T-717	1.02	57.9	10.860	4.4E+06	4.5E+06	146.1	10.221	5.1E+03	5.2E+03
T-718	1.02	58.8	11.000	2.9E+06	3.0E+06	150.1	10.894	9.4E+03	9.5E+03
T-719	1.02	58.7	11.122	3.9E+06	3.9E+06	151.2	11.020	1.2E+04	1.2E+04
T-801	1.01	50.0	11.140	6.8E+06	6.9E+06	139.9	10.390	2.0E+03	2.0E+03
T-802	1.01	46.3	10.592	9.6E+06	9.7E+06	142.7	9.503	2.4E+03	2.4E+03
T-803	1.01	49.7	10.844	7.0E+06	7.1E+06	141.9	9.792	4.9E+03	4.9E+03
T-804	1.01	50.6	11.129	6.4E+06	6.4E+06	143.1	10.111	4.7E+03	4.8E+03
T-805	1.02	50.5	11.065	5.6E+06	5.7E+06	135.3	9.465	3.4E+03	3.5E+03
T-806	1.01	49.1	10.826	7.0E+06	7.0E+06	141.9	9.740	4.3E+03	4.4E+03
T-807	1.01	49.7	11.123	6.7E+06	6.7E+06	142.8	10.077	4.4E+03	4.5E+03
T-808	1.01	53.1	11.138	5.6E+06	5.7E+06	138.2	9.689	2.4E+03	2.4E+03
T-809	1.01	52.6	10.805	5.4E+06	5.4E+06	145.0	9.802	4.1E+03	4.2E+03
T-810	1.01	53.3	11.102	5.1E+06	5.2E+06	148.7	10.177	3.9E+03	4.0E+03
T-811	1.02	53.8	10.808	5.0E+06	5.1E+06	140.7	9.345	1.9E+03	1.9E+03
T-812	1.01	56.0	10.980	6.6E+06	6.7E+06	147.5	9.957	5.1E+03	5.1E+03
T-813	1.01	54.8	11.270	6.9E+06	7.0E+06	152.5	10.471	6.1E+03	6.2E+03
T-814	1.02	52.1	10.810	5.6E+06	5.7E+06	138.5	9.093	1.5E+03	1.5E+03
T-815	1.01	51.8	11.201	7.0E+06	7.1E+06	142.7	10.338	8.2E+03	8.2E+03
T-816	1.01	52.3	11.174	6.4E+06	6.5E+06	143.3	10.127	4.8E+03	4.9E+03
T-817	1.01	55.2	10.950	3.2E+06	3.3E+06	143.8	9.332	7.5E+02	7.6E+02
T-818	1.01	52.7	11.101	5.3E+06	5.3E+06	142.4	10.074	4.5E+03	4.6E+03
T-819	1.01	50.1	10.875	7.4E+06	7.4E+06	141.0	9.825	5.5E+03	5.6E+03

[a] $\mathbf{E_{a,f}}$**:** Activation energy of the forward reaction, given in kJ mol^{-1}.
[b] $\boldsymbol{log\tilde{A}_f}$**:** Logarithm of the pre-exponential factor of the forward reaction, given in m^3 mol^{-1} s^{-1}.
[c] $\mathbf{k_f}$**:** The reaction rate coefficient for the forward reaction excluding tunneling effects, given in m^3 mol^{-1} s^{-1}.
[d] $\boldsymbol{\kappa k_f}$**:** The reaction rate coefficient for the forward reaction including tunneling effects, given in m^3 mol^{-1} s^{-1}.
[e] $\mathbf{E_{a,r}}$**:** Activation energy of the reverse reaction, given in kJ mol^{-1}.
[f] $\boldsymbol{log\tilde{A}_r}$**:** Logarithm of the pre-exponential factor of the reverse reaction, given in m^3 mol^{-1} s^{-1}.
[g] $\mathbf{k_r}$**:** The reaction rate coefficient for the reverse reaction excluding tunneling effects, given in m^3 mol^{-1} s^{-1}.
[h] $\boldsymbol{\kappa k_r}$**:** The reaction rate coefficient for the reverse reaction including tunneling effects, given in m^3 mol^{-1} s^{-1}.

Table D-6 External symmetry (σ_{ext}), internal symmetry (σ_{int}) and the number of optical isomers (n_{opt}) for the reactants, products and the transition state of the hydrogen abstraction reactions in the training set, given along with the number of single events for the forward and reverse directions.

Reaction #	Forward						Reverse						Transition State			n_e[d]	
	Reactant 1			Reactant 2			Reactant 1			Reactant 2						$n_{e,f}$[e]	$n_{e,r}$[f]
	σ_{ext}[a]	σ_{int}[b]	n_{opt}[c]	σ_{ext}	σ_{int}	n_{opt}	σ_{ext}	σ_{int}	n_{opt}	σ_{ext}	σ_{int}	n_{opt}	σ_{ext}	σ_{int}	n_{opt}		
T-101	1	6	1	1	1	1	2	1	1	1	1	1	1	2	1	3	1
T-102	1	3	1	1	1	1	1	1	1	1	1	1	1	1	1	3	1
T-103	1	3	1	1	1	1	1	1	1	1	1	1	1	1	1	3	1
T-104	1	3	1	1	1	1	1	1	1	1	1	1	1	1	1	3	1
T-105	1	9	1	1	1	1	1	3	1	1	1	1	1	3	1	3	1
T-106	1	9	1	1	1	1	1	3	1	1	1	1	1	3	1	3	1
T-107	1	9	1	1	1	1	1	3	1	1	1	1	1	3	1	3	1
T-108	1	3	1	1	1	1	1	1	1	1	1	1	1	1	1	3	1
T-109	1	3	1	1	1	1	1	1	1	1	1	1	1	1	1	3	1
T-110	1	3	1	1	1	1	1	1	1	1	1	1	1	1	1	3	1
T-111	1	3	1	1	1	1	1	1	1	1	1	1	1	1	1	3	1
T-112	1	3	1	1	1	1	1	1	1	1	1	1	1	1	1	3	1
T-113	1	3	1	1	1	1	1	1	1	1	1	1	1	1	1	3	1
T-114	2	9	1	1	1	1	1	3	1	1	1	1	1	3	1	6	1
T-115	2	9	1	1	1	1	1	3	1	1	1	1	1	3	1	6	1
T-116	4	9	1	1	1	1	1	3	1	1	1	1	2	3	1	6	0.5
T-117	1	9	1	1	1	1	1	3	1	1	1	1	1	3	1	3	1
T-118	1	9	1	1	1	1	1	3	1	1	1	1	1	3	1	3	1
T-119	1	9	1	1	1	1	1	3	1	1	1	1	1	3	1	3	1
T-201	1	6	1	1	1	1	1	6	1	1	1	1	1	6	2	2	2
T-202	1	3	1	1	1	1	1	3	1	1	1	1	1	3	2	2	2
T-203	1	3	1	1	1	1	1	3	1	1	1	1	1	3	2	2	2
T-204	1	3	1	1	1	1	1	3	1	1	1	1	1	3	2	2	2
T-205	1	9	1	1	1	1	1	9	1	1	1	1	1	9	2	2	2
T-206	1	9	1	1	1	1	1	9	1	1	1	1	1	9	2	2	2
T-207	1	9	1	1	1	1	1	9	1	1	1	1	1	9	2	2	2
T-208	1	3	1	1	1	1	1	3	1	1	1	1	1	3	2	2	2
T-209	1	3	1	1	1	1	1	3	1	1	1	1	1	3	2	2	2
T-210	1	3	1	1	1	1	1	3	1	1	1	1	1	3	2	2	2
T-211	1	3	1	1	1	1	1	3	1	1	1	1	1	3	2	2	2
T-212	1	3	1	1	1	1	1	3	1	1	1	1	1	3	2	2	2
T-213	1	3	1	1	1	1	1	3	1	1	1	1	1	3	2	2	2
T-214	1	9	1	1	1	1	1	9	1	1	1	1	1	9	2	2	2
T-215	1	9	1	1	1	1	1	9	1	1	1	1	1	9	2	2	2

T-216	1	9	1	1	1	1	1	9	1	1	1	1	1	9	2	2	2
T-217	1	9	1	1	1	1	1	9	1	1	1	1	1	9	2	2	2
T-218	1	9	1	1	1	1	1	9	1	1	1	1	1	9	2	2	2
T-219	2	9	1	1	1	1	1	9	1	1	1	1	1	9	2	4	2
T-301	1	18	1	1	1	1	2	36	1	1	1	1	1	18	1	1	4
T-302	1	9	1	1	1	1	1	18	1	1	1	1	1	9	1	1	2
T-303	1	9	1	1	1	1	1	18	1	1	1	1	1	9	1	1	2
T-304	1	9	1	1	1	1	1	18	1	1	1	1	1	9	1	1	2
T-305	1	27	1	1	1	1	1	54	1	1	1	1	1	27	1	1	2
T-306	1	27	1	1	1	1	1	54	1	1	1	1	1	27	1	1	2
T-307	1	27	1	1	1	1	1	54	1	1	1	1	1	27	1	1	2
T-308	1	9	1	1	1	1	1	18	1	1	1	1	1	9	1	1	2
T-309	1	9	1	1	1	1	1	18	1	1	1	1	1	9	1	1	2
T-310	1	9	1	1	1	1	1	18	1	1	1	1	1	9	1	1	2
T-311	1	9	1	1	1	1	1	18	1	1	1	1	1	9	1	1	2
T-312	1	9	1	1	1	1	1	18	1	1	1	1	1	9	1	1	2
T-313	1	9	1	1	1	1	1	18	1	1	1	1	1	9	1	1	2
T-314	1	27	1	1	1	1	1	54	1	1	1	1	1	27	1	1	2
T-315	1	27	1	1	1	1	1	54	1	1	1	1	1	27	1	1	2
T-316	1	27	1	1	1	1	1	54	1	1	1	1	1	27	1	1	2
T-317	1	27	1	1	1	1	1	54	1	1	1	1	1	27	1	1	2
T-318	1	27	1	1	1	1	1	54	1	1	1	1	1	27	1	1	2
T-319	1	27	1	1	1	1	1	54	1	1	1	1	1	27	1	1	2
T-401	1	2	1	1	1	1	1	2	1	1	1	1	1	1	1	2	2
T-402	1	1	1	1	1	1	1	1	1	1	1	1	1	1	1	1	1
T-403	1	1	1	1	1	1	1	1	1	1	1	1	1	1	1	1	1
T-404	1	1	1	1	1	1	1	1	1	1	1	1	1	1	1	1	1
T-405	1	3	1	1	1	1	1	3	1	1	1	1	1	3	1	1	1
T-406	1	3	1	1	1	1	1	3	1	1	1	1	1	3	1	1	1
T-407	1	3	1	1	1	1	1	3	1	1	1	1	1	3	1	1	1
T-408	1	1	1	1	1	1	1	1	1	1	1	1	1	1	1	1	1
T-409	1	1	1	1	1	1	1	1	1	1	1	1	1	1	1	1	1
T-410	1	1	1	1	1	1	1	1	1	1	1	1	1	1	1	1	1
T-411	1	1	1	1	1	1	1	1	1	1	1	1	1	1	1	1	1
T-412	1	1	1	1	1	1	1	1	1	1	1	1	1	1	1	1	1
T-413	1	1	1	1	1	1	1	1	1	1	1	1	1	1	1	1	1
T-414	1	3	1	1	1	1	1	3	1	1	1	1	1	3	1	1	1
T-415	1	3	1	1	1	1	1	3	1	1	1	1	1	3	1	1	1
T-416	1	3	1	1	1	1	1	3	1	1	1	1	1	3	1	1	1
T-417	1	3	1	1	1	1	1	3	1	1	1	1	1	3	1	1	1
T-418	1	3	1	1	1	1	1	3	1	1	1	1	1	3	1	1	1

T-419	1	3	1	1	1	1	1	3	1	1	1	1	1	3	1	1	1
T-501	1	6	2	1	1	1	1	6	1	1	1	1	1	3	2	2	4
T-502	1	3	2	1	1	1	1	3	1	1	1	1	1	3	2	1	2
T-503	1	3	2	1	1	1	1	3	1	1	1	1	1	3	2	1	2
T-504	1	3	2	1	1	1	1	3	1	1	1	1	1	3	2	1	2
T-505	1	9	2	1	1	1	1	9	1	1	1	1	1	9	2	1	2
T-506	1	9	2	1	1	1	1	9	1	1	1	1	1	9	2	1	2
T-507	1	9	2	1	1	1	1	9	1	1	1	1	1	9	2	1	2
T-508	1	3	2	1	1	1	1	3	1	1	1	1	1	3	2	1	2
T-509	1	3	2	1	1	1	1	3	1	1	1	1	1	3	2	1	2
T-510	1	3	2	1	1	1	1	3	1	1	1	1	1	3	2	1	2
T-511	1	3	2	1	1	1	1	3	1	1	1	1	1	3	2	1	2
T-512	1	3	2	1	1	1	1	3	1	1	1	1	1	3	2	1	2
T-513	1	3	2	1	1	1	1	3	1	1	1	1	1	3	2	1	2
T-514	1	9	2	1	1	1	1	9	1	1	1	1	1	9	2	1	2
T-515	1	9	2	1	1	1	1	9	1	1	1	1	1	9	2	1	2
T-516	1	9	2	1	1	1	1	9	1	1	1	1	1	9	2	1	2
T-517	1	9	2	1	1	1	1	9	1	1	1	1	1	9	2	1	2
T-518	1	9	2	1	1	1	1	9	1	1	1	1	1	9	2	1	2
T-519	1	9	2	1	1	1	1	9	1	1	1	1	1	9	2	1	2
T-601	1	2	1	1	1	1	1	1	1	1	1	1	1	1	1	2	1
T-602	1	1	1	1	1	1	1	1	1	1	1	1	1	1	1	1	1
T-603	1	1	1	1	1	1	1	1	1	1	1	1	1	1	1	1	1
T-604	1	1	1	1	1	1	1	1	1	1	1	1	1	1	1	1	1
T-605	1	3	1	1	1	1	1	3	1	1	1	1	1	3	1	1	1
T-606	1	3	1	1	1	1	1	3	1	1	1	1	1	3	1	1	1
T-607	1	3	1	1	1	1	1	3	1	1	1	1	1	3	1	1	1
T-608	1	1	1	1	1	1	1	1	1	1	1	1	1	1	1	1	1
T-609	1	1	1	1	1	1	1	1	1	1	1	1	1	1	1	1	1
T-610	1	1	1	1	1	1	1	1	1	1	1	1	1	1	1	1	1
T-611	1	1	1	1	1	1	1	1	1	1	1	1	1	1	1	1	1
T-612	1	1	1	1	1	1	1	1	1	1	1	1	1	1	1	1	1
T-613	1	1	1	1	1	1	1	1	1	1	1	1	1	1	1	1	1
T-614	1	3	1	1	1	1	1	3	1	1	1	1	1	3	1	1	1
T-615	1	3	1	1	1	1	1	3	1	1	1	1	1	3	1	1	1
T-616	1	3	1	1	1	1	1	3	1	1	1	1	1	3	1	1	1
T-617	1	3	1	1	1	1	1	3	1	1	1	1	1	3	1	1	1
T-618	1	3	1	1	1	1	1	3	1	1	1	1	1	3	1	1	1
T-619	1	3	1	1	1	1	1	3	1	1	1	1	1	3	1	1	1
T-701	1	4	1	1	1	1	2	4	1	1	1	1	1	2	1	2	4
T-702	1	2	1	1	1	1	1	2	1	1	1	1	1	1	1	2	2

T-703	1	2	1	1	1	1	1	2	1	1	1	1	1	1	1	2	2
T-704	1	2	1	1	1	1	1	2	1	1	1	1	1	1	1	2	2
T-705	1	6	1	1	1	1	1	6	1	1	1	1	1	3	1	2	2
T-706	1	6	1	1	1	1	1	6	1	1	1	1	1	3	1	2	2
T-707	1	6	1	1	1	1	1	6	1	1	1	1	1	3	1	2	2
T-708	1	2	1	1	1	1	1	2	1	1	1	1	1	1	1	2	2
T-709	1	2	1	1	1	1	1	2	1	1	1	1	1	1	1	2	2
T-710	1	2	1	1	1	1	1	2	1	1	1	1	1	1	1	2	2
T-711	1	2	1	1	1	1	1	2	1	1	1	1	1	1	1	2	2
T-712	1	2	1	1	1	1	1	2	1	1	1	1	1	2	1	1	1
T-713	1	2	1	1	1	1	1	2	1	1	1	1	1	1	1	2	2
T-714	1	6	1	1	1	1	1	6	1	1	1	1	1	6	1	1	1
T-715	1	6	1	1	1	1	1	6	1	1	1	1	1	6	1	1	1
T-716	1	6	1	1	1	1	1	6	1	1	1	1	1	6	1	1	1
T-717	1	6	1	1	1	1	1	6	1	1	1	1	1	3	1	2	2
T-718	1	6	1	1	1	1	1	6	1	1	1	1	1	6	1	1	1
T-719	1	6	1	1	1	1	1	6	1	1	1	1	1	6	1	1	1
T-801	1	12	1	1	1	1	1	12	1	1	1	1	1	12	1	1	1
T-802	1	6	2	1	1	1	1	6	1	1	1	1	1	3	2	2	4
T-803	1	6	2	1	1	1	1	6	1	1	1	1	1	3	2	2	4
T-804	1	6	2	1	1	1	1	6	1	1	1	1	1	6	2	1	2
T-805	1	9	2	1	1	1	1	18	1	1	1	1	1	9	2	1	4
T-806	1	18	2	1	1	1	1	18	1	1	1	1	1	9	2	2	4
T-807	1	18	2	1	1	1	1	18	1	1	1	1	1	18	2	1	2
T-808	1	6	2	1	1	1	1	6	1	1	1	1	1	6	2	1	2
T-809	1	6	2	1	1	1	1	6	1	1	1	1	1	3	2	2	4
T-810	1	6	2	1	1	1	1	6	1	1	1	1	1	6	2	1	2
T-811	1	6	2	1	1	1	1	6	1	1	1	1	1	3	2	2	4
T-812	1	6	2	1	1	1	1	6	1	1	1	1	1	3	2	2	4
T-813	1	6	2	1	1	1	1	6	1	1	1	1	1	6	2	1	2
T-814	1	18	2	1	1	1	1	18	1	1	1	1	1	9	2	2	4
T-815	1	18	2	1	1	1	1	18	1	1	1	1	1	18	2	1	2
T-816	1	18	2	1	1	1	1	18	1	1	1	1	1	18	2	1	2
T-817	1	18	2	1	1	1	1	18	1	1	1	1	1	18	2	1	2
T-818	1	18	2	1	1	1	1	18	1	1	1	1	1	18	2	1	2
T-819	1	18	2	1	1	1	1	18	1	1	1	1	1	9	2	2	4

[a] $\boldsymbol{\sigma_{ext}}$**:** External symmetry
[b] $\boldsymbol{\sigma_{int}}$**:** Internal symmetry
[c] $\boldsymbol{n_{opt}}$**:** Number of optical isomers
[d] $\boldsymbol{n_{e,f}}$**:** number of single events for the forward reaction
[e] $\boldsymbol{n_{e,r}}$**:** number of single events for the reverse reaction

D.2 Substitutent effects on the HARs

D.2.1 Identification of ΔNNI°s

Any significant difference between the substituent effects (interactions between substituent groups and extended side chains) encountered in the reactants and transition states of the HARs from toluene derivatives by hydrogen atom creates the necessity to define ΔNNI°s to improve the agreement between the *ab initio* and the group additively calculated reaction rate coefficients.

Table D-7 Preliminary values for 8 ΔGAV°s parameters for the forward and reverse directions.

ΔGAV°s	Forward									
	$E_{a,f}$[a]					$\log\widetilde{A}_f$[b]				
	300 K	600 K	1000 K	1500 K	2000 K	300 K	600 K	1000 K	1500 K	2000 K
C_2-(C_b)(H)$_2$	-1.0	-1.1	-1.0	-1.1	-0.9	0.032	-0.016	-0.002	0.027	-0.014
C_2-(C_b)(C)(H)	-6.5	-8.1	-10.3	-12.1	-13.1	0.182	-0.188	-0.337	-0.413	-0.446
C_2-(C_b)(C)$_2$	-11.1	-12.7	-15.0	-16.8	-17.8	0.137	-0.056	-0.208	-0.286	-0.319
C_2-(C_b)(C_d)(H)	-10.9	-12.5	-14.9	-16.9	-18.1	0.392	0.199	0.036	-0.048	-0.084
C_2-(C_b)(C_d)(C)	-17.3	-18.9	-21.4	-23.5	-24.7	0.308	0.118	-0.052	-0.140	-0.177
C_2-(C_b)(C_d)$_2$	-17.8	-19.7	-22.2	-24.2	-25.3	0.272	0.065	-0.107	-0.196	-0.234
C_2-(C_b)$_2$(H)	-4.7	-6.3	-8.6	-10.4	-11.6	-0.100	-0.299	-0.454	-0.534	-0.568
C_2-(C_b)$_2$(C)	-8.9	-10.5	-12.9	-14.9	-16.1	-0.017	-0.219	-0.385	-0.469	-0.505
ΔGAV°s	Reverse									
	$E_{a,r}$[c]					$\log\widetilde{A}_r$[d]				
	300 K	600 K	1000 K	1500 K	2000 K	300 K	600 K	1000 K	1500 K	2000 K
C_2-(C_b)(H)$_2$	0.7	0.8	0.9	1.0	1.1	0.071	0.082	0.089	0.095	0.097
C_2-(C_b)(C)(H)	4.7	4.3	3.9	4.2	5.2	-0.674	-0.741	-0.773	-0.763	-0.722
C_2-(C_b)(C)$_2$	-0.8	-1.1	-1.3	-0.9	0.0	-1.408	-1.446	-1.460	-1.445	-1.417
C_2-(C_b)(C_d)(H)	38.9	38.7	38.3	38.6	39.6	0.072	0.043	0.015	0.028	0.058
C_2-(C_b)(C_d)(C)	29.9	29.7	29.3	29.6	30.6	-0.718	-0.745	-0.772	-0.761	-0.733
C_2-(C_b)(C_d)$_2$	60.6	60.5	60.2	60.5	61.4	-0.029	-0.035	-0.059	-0.048	-0.020
C_2-(C_b)$_2$(H)	20.0	19.9	19.8	20.4	21.5	0.186	0.174	0.166	0.189	0.222

C_2-(C_b)$_2$(C)	14.6	14.4	14.2	14.6	15.6	-0.655	-0.679	-0.695	-0.680	-0.651

[a] **$E_{a,f}$**: Activation energy of the forward reaction, given in kJ mol^{-1}.
[b] **$\log\widetilde{A}_f$:** Logarithm of the pre-exponential factor of the forward reaction, given in m^3 mol^{-1} s^{-1}.
[c] **$E_{a,r}$:** Activation energy of the reverse reaction, given in kJ mol^{-1}.
[d] **$\log\widetilde{A}_r$:** Logarithm of the pre-exponential factor of the reverse reaction, given in m^3 mol^{-1} s^{-1}.

Table D-8 The deviations between the CBS-QB3 data and the GA-based data calculated with 8 preliminary ΔGAV°s parameters given in **Table D-7** for the forward reactions, with respect to the reference reaction.

Reaction #	$E_{a,f}$[a]					$\log\widetilde{A}_f$ [b]				
	300 K	600 K	1000 K	1500 K	2000 K	300 K	600 K	1000 K	1500 K	2000 K
T-101	-1.0	-1.1	-1.0	-1.1	-0.9	0.032	-0.016	-0.002	0.027	-0.014
T-102	-0.1	0.3	0.5	0.1	0.0	0.011	0.033	0.051	0.068	0.020
T-103	-0.3	0.7	-0.3	0.8	1.0	0.113	0.024	0.092	0.063	0.024
T-104	1.2	1.1	0.4	1.1	1.2	0.048	0.009	0.023	0.049	0.006
T-105	2.3	0.2	0.1	0.6	1.4	-0.002	0.038	0.061	0.080	0.033
T-106	0.6	1.3	0.6	1.8	1.3	0.018	-0.032	-0.020	0.007	0.010
T-107	1.0	0.6	0.1	-0.6	-0.5	0.066	0.127	-0.008	-0.068	0.019
T-108	0.0	0.1	0.2	-0.2	-0.3	-0.016	-0.031	-0.020	-0.003	-0.053
T-109	-0.3	-0.5	-0.4	-0.5	-0.2	0.022	-0.030	-0.017	0.013	-0.027
T-110	-0.5	-0.6	-0.5	-0.7	-0.6	0.025	-0.025	-0.013	0.013	-0.029
T-111	-1.0	-0.4	1.2	0.8	0.5	-0.226	-0.097	-0.141	-0.077	-0.106
T-112	-0.7	-0.8	-0.7	-0.8	-0.6	0.008	-0.041	-0.027	0.002	-0.039
T-113	1.6	1.5	1.6	1.4	1.5	0.097	0.051	0.064	0.089	0.045
T-114	-1.3	-0.8	-0.5	-0.6	-1.2	-0.005	0.034	0.064	0.092	-0.077
T-115	-0.1	-0.2	-0.1	-0.2	-1.4	-0.136	-0.102	-0.099	-0.355	0.143
T-116	-0.6	-0.7	-0.6	-0.7	-1.4	-0.102	0.124	0.005	-0.049	0.124
T-117	0.2	0.4	0.5	0.2	0.2	0.027	0.020	0.033	0.053	0.007
T-118	-0.3	-0.4	-0.3	-0.4	-0.2	0.023	-0.025	-0.011	0.018	-0.023
T-119	-0.4	-0.5	-0.5	-0.6	-0.4	-0.009	-0.057	-0.043	-0.015	-0.057
T-201	-1.9	-1.9	-2.0	-2.0	-2.0	-0.031	-0.216	-0.218	-0.218	-0.219
T-202	1.4	1.5	1.5	1.5	1.5	0.060	0.360	0.362	0.363	0.362
T-203	2.4	2.4	2.3	2.2	2.3	0.037	0.330	0.327	0.326	0.324
T-204	-0.1	0.0	0.1	0.1	0.2	0.016	0.318	0.324	0.328	0.328
T-205	2.4	2.4	2.5	2.4	2.5	0.077	0.375	0.377	0.378	0.377
T-206	2.7	2.6	2.6	2.5	2.5	0.024	0.311	0.305	0.303	0.302
T-207	3.1	3.1	3.2	3.3	3.4	-0.004	0.296	0.304	0.308	0.309
T-208	-3.9	-3.9	-4.0	-4.0	-3.9	-0.007	-0.195	-0.195	-0.196	-0.196
T-209	-0.7	-0.8	-0.9	-1.1	-1.1	0.040	-0.152	-0.160	-0.164	-0.166
T-210	-1.7	-1.7	-1.7	-1.7	-1.6	-0.060	-0.245	-0.243	-0.242	-0.242
T-211	-1.1	-1.1	-1.0	-1.1	-1.0	0.157	-0.020	-0.018	-0.018	-0.018
T-212	0.8	0.7	0.6	0.5	0.5	0.002	-0.187	-0.192	-0.195	-0.196

T-213	-0.1	-0.1	-0.1	0.0	0.1	-0.014	-0.194	-0.188	-0.184	-0.183
T-214	2.3	2.4	2.4	2.4	2.4	0.272	0.101	0.102	0.102	0.102
T-215	1.3	1.2	1.2	1.1	1.2	-0.054	-0.241	-0.243	-0.244	-0.245
T-216	-1.4	-1.5	-1.5	-1.5	-1.4	0.001	-0.183	-0.183	-0.183	-0.183
T-217	-1.8	-1.8	-1.8	-1.8	-1.7	-0.160	-0.035	-0.032	-0.031	-0.030
T-218	-1.3	-1.3	-1.3	-1.4	-1.3	-0.326	-0.210	-0.210	-0.210	-0.211
T-219	-1.8	-1.8	-1.8	-1.9	-1.8	-0.037	-0.221	-0.221	-0.221	-0.221
T-301	0.8	0.8	0.8	0.8	0.9	-0.039	-0.039	-0.036	-0.035	-0.034
T-302	0.4	0.3	0.1	0.0	0.0	0.004	-0.009	-0.019	-0.025	-0.028
T-303	2.7	2.7	2.7	2.7	2.8	-0.043	-0.046	-0.046	-0.046	-0.046
T-304	2.4	2.5	2.7	2.8	3.0	-0.030	-0.020	-0.008	-0.002	0.001
T-305	1.7	1.6	1.3	1.2	1.2	-0.015	-0.031	-0.043	-0.050	-0.052
T-306	3.4	3.5	3.4	3.5	3.6	-0.041	-0.041	-0.038	-0.037	-0.037
T-307	2.9	3.0	3.1	3.3	3.5	-0.067	-0.061	-0.048	-0.042	-0.039
T-308	-5.5	-5.5	-5.8	-5.9	-6.0	-0.218	-0.228	-0.240	-0.247	-0.251
T-309	0.9	0.9	0.8	0.8	0.9	-0.009	-0.012	-0.013	-0.014	-0.014
T-310	-2.0	-1.9	-2.0	-2.0	-1.9	-0.034	-0.036	-0.034	-0.034	-0.033
T-311	-0.9	-0.8	-0.8	-0.9	-0.8	0.265	0.277	0.276	0.275	0.274
T-312	1.2	1.2	1.1	1.1	1.3	-0.015	-0.017	-0.015	-0.015	-0.014
T-313	-0.8	-0.7	-0.6	-0.5	-0.4	-0.005	-0.001	0.007	0.011	0.013
T-314	-5.1	-5.1	-5.2	-5.3	-5.2	0.440	0.448	0.442	0.438	0.437
T-315	1.5	1.5	1.5	1.5	1.6	-0.217	-0.218	-0.215	-0.214	-0.213
T-316	1.0	1.0	1.1	1.1	1.3	-0.143	-0.140	-0.134	-0.131	-0.129
T-317	-6.5	-6.5	-6.7	-6.8	-6.8	0.299	0.303	0.294	0.288	0.287
T-318	1.1	1.1	1.1	1.1	1.2	-0.055	-0.055	-0.052	-0.051	-0.050
T-319	0.5	0.5	0.5	0.6	0.7	-0.084	-0.082	-0.076	-0.073	-0.072
T-401	0.3	0.3	0.3	0.2	0.1	0.397	0.402	0.397	0.394	0.393
T-402	0.8	0.6	0.2	-0.2	-0.4	-0.102	-0.123	-0.152	-0.166	-0.172
T-403	-1.4	-1.4	-1.3	-1.3	-1.3	-0.171	-0.176	-0.173	-0.171	-0.170
T-404	1.9	2.0	2.1	2.0	2.0	0.114	0.125	0.126	0.127	0.127
T-405	2.9	2.9	2.8	2.7	2.7	0.179	0.178	0.173	0.170	0.169
T-406	2.7	2.7	2.8	2.8	2.8	-0.153	-0.157	-0.153	-0.150	-0.149
T-407	2.0	2.1	2.2	2.3	2.4	-0.158	-0.159	-0.149	-0.142	-0.139
T-408	-3.7	-3.7	-3.7	-3.8	-3.8	-0.018	-0.021	-0.023	-0.025	-0.026
T-409	-0.7	-0.7	-0.7	-0.8	-0.8	-0.134	-0.140	-0.141	-0.141	-0.141
T-410	-1.6	-1.6	-1.5	-1.6	-1.6	0.123	0.121	0.122	0.123	0.124
T-411	-3.0	-2.9	-2.8	-2.8	-2.8	0.063	0.069	0.071	0.073	0.074
T-412	0.2	0.1	0.2	0.1	0.2	-0.231	-0.237	-0.236	-0.234	-0.234
T-413	-1.6	-1.5	-1.5	-1.6	-1.6	0.136	0.144	0.143	0.142	0.142
T-414	0.2	0.4	0.5	0.5	0.5	0.070	0.084	0.090	0.092	0.092
T-415	0.6	0.6	0.7	0.7	0.7	-0.322	-0.327	-0.324	-0.321	-0.320

T-416	1.7	1.8	1.7	1.6	1.6	0.425	0.434	0.430	0.428	0.427
T-417	0.0	0.1	0.2	0.2	0.2	-0.138	-0.134	-0.129	-0.126	-0.125
T-418	0.3	0.4	0.4	0.4	0.5	-0.157	-0.161	-0.157	-0.154	-0.153
T-419	-2.1	-2.0	-2.1	-2.1	-2.2	0.077	0.083	0.081	0.079	0.078
T-501	-1.6	-1.5	-1.5	-1.6	-1.5	0.259	0.265	0.265	0.265	0.266
T-502	-2.3	-2.3	-2.4	-2.6	-2.7	0.237	0.244	0.235	0.229	0.227
T-503	0.3	0.3	0.3	0.2	0.3	-0.041	-0.036	-0.037	-0.038	-0.038
T-504	0.2	0.0	-0.1	0.6	0.8	-0.057	-0.350	-0.344	-0.341	-0.339
T-505	-0.7	-0.7	-0.8	-0.8	-0.8	-0.159	-0.165	-0.167	-0.168	-0.168
T-506	0.7	0.8	0.9	0.9	0.9	-0.036	-0.027	-0.024	-0.022	-0.021
T-507	0.5	0.6	0.7	0.7	0.8	-0.069	0.115	0.123	0.127	0.129
T-508	-3.1	-3.1	-3.1	-3.2	-3.1	-0.170	-0.171	-0.173	-0.173	-0.172
T-509	2.7	2.7	2.7	2.6	2.6	-0.034	-0.029	-0.032	-0.034	-0.034
T-510	3.0	3.0	3.0	2.9	2.9	-0.002	0.003	0.001	-0.001	-0.001
T-511	2.1	2.2	2.2	2.2	2.3	0.162	0.171	0.175	0.176	0.178
T-512	3.6	3.7	3.7	3.6	3.6	-0.042	-0.035	-0.035	-0.035	-0.035
T-513	-3.7	-3.7	-3.6	-3.6	-3.6	-0.037	-0.030	-0.027	-0.025	-0.024
T-514	-2.2	-2.0	-2.1	-2.3	-2.3	0.130	0.147	0.140	0.136	0.135
T-515	3.6	3.6	3.6	3.6	3.6	-0.092	-0.086	-0.086	-0.086	-0.085
T-516	-1.6	-1.5	-1.5	-1.5	-1.4	-0.044	-0.038	-0.036	-0.035	-0.034
T-517	-2.9	-2.9	-2.9	-3.0	-2.9	0.106	0.106	0.104	0.103	0.103
T-518	-1.1	-1.0	-1.0	-1.1	-1.0	-0.034	-0.027	-0.026	-0.026	-0.025
T-519	2.3	2.3	2.4	2.3	2.4	-0.069	-0.062	-0.061	-0.060	-0.058
T-601	-1.2	-1.3	-1.4	-1.4	-1.3	0.321	0.321	0.316	0.312	0.310
T-602	2.7	2.6	2.8	3.0	3.2	-0.198	-0.201	-0.190	-0.184	-0.181
T-603	4.9	4.8	5.2	5.4	1.4	0.027	0.042	0.061	0.071	0.075
T-604	3.2	3.9	3.8	3.8	4.0	0.033	0.050	0.076	0.090	0.097
T-605	-1.9	-2.2	-2.5	-1.7	-1.1	0.029	0.009	-0.018	-0.034	-0.041
T-606	2.7	2.6	2.6	2.6	2.7	-0.048	-0.052	-0.054	-0.056	-0.057
T-607	-0.4	-0.5	-0.5	-0.5	-0.3	-0.010	-0.013	-0.013	-0.014	-0.014
T-608	4.1	4.0	4.2	4.5	4.8	0.004	0.011	0.024	0.031	0.035
T-609	2.7	2.4	2.3	2.2	2.2	-0.025	-0.032	-0.044	-0.051	-0.055
T-610	2.0	1.7	1.7	1.6	1.7	-0.038	-0.046	-0.054	-0.059	-0.062
T-611	-0.3	-0.3	-0.2	0.0	0.2	0.218	0.232	0.239	0.242	0.243
T-612	-0.2	-0.5	-0.5	-0.6	-0.5	-0.106	-0.114	-0.121	-0.126	-0.128
T-613	-2.7	-2.9	-2.9	-2.9	-2.8	0.020	0.016	0.012	0.010	0.009
T-614	-6.4	-6.5	-6.7	-6.9	-6.9	-0.002	-0.002	-0.019	-0.030	-0.034
T-615	-0.2	-0.3	-0.3	-0.4	-0.3	-0.060	-0.061	-0.065	-0.069	-0.070
T-616	4.0	3.8	3.8	3.8	3.9	-0.025	-0.025	-0.029	-0.032	-0.033
T-617	-5.6	-5.6	-5.4	-5.2	-4.9	0.230	0.246	0.259	0.265	0.268
T-618	-4.0	-3.0	-2.4	-3.2	-3.5	-0.318	-0.328	-0.316	-0.308	-0.305

T-619	-2.9	-3.1	-3.2	-3.2	-3.1	-0.052	-0.057	-0.061	-0.065	-0.066
T-701	-2.3	-2.3	-2.3	-2.3	-2.4	0.130	0.128	0.128	0.127	0.126
T-702	5.4	5.6	5.6	5.6	5.5	0.291	0.310	0.312	0.310	0.309
T-703	2.4	2.5	2.5	2.6	2.5	0.034	0.037	0.039	0.039	0.039
T-704	2.0	2.1	2.2	2.3	2.2	-0.095	-0.091	-0.085	-0.083	-0.082
T-705	2.6	2.7	2.7	2.7	2.6	0.047	0.048	0.048	0.048	0.048
T-706	3.7	3.7	3.7	3.8	3.7	-0.143	-0.144	-0.143	-0.143	-0.143
T-707	2.8	2.8	2.9	3.0	3.0	0.036	0.037	0.043	0.045	0.046
T-708	-4.4	-4.3	-4.3	-4.3	-4.3	-0.136	-0.137	-0.135	-0.134	-0.134
T-709	-1.5	-1.5	-1.5	-1.5	-1.6	0.094	0.090	0.089	0.088	0.088
T-710	-2.0	-1.9	-2.0	-1.9	-2.0	0.297	0.292	0.291	0.290	0.290
T-711	1.0	1.0	0.8	0.8	0.7	0.083	0.078	0.070	0.066	0.065
T-712	1.7	1.7	1.7	1.7	1.7	0.000	-0.001	-0.002	-0.003	-0.003
T-713	-0.1	-0.1	-0.1	-0.1	-0.2	0.036	0.030	0.029	0.028	0.027
T-714	-1.7	-1.6	-1.6	-1.6	-1.7	-0.237	-0.234	-0.234	-0.235	-0.236
T-715	-1.8	-1.8	-1.8	-1.7	-1.8	-0.220	-0.221	-0.220	-0.220	-0.220
T-716	-2.1	-2.1	-2.1	-2.0	-2.1	-0.048	-0.050	-0.049	-0.049	-0.049
T-717	-1.5	-1.4	-1.5	-1.6	-1.7	0.084	0.085	0.079	0.075	0.074
T-718	-2.5	-2.4	-2.4	-2.4	-2.5	-0.062	-0.064	-0.065	-0.066	-0.066
T-719	-2.5	-2.4	-2.4	-2.3	-2.4	-0.188	-0.190	-0.188	-0.188	-0.188
T-801	1.7	1.7	1.8	1.8	1.8	-0.144	-0.145	-0.144	-0.143	-0.143
T-802	5.0	5.3	5.4	5.4	5.4	0.366	0.397	0.403	0.405	0.404
T-803	1.8	2.0	2.1	2.0	2.0	0.143	0.148	0.150	0.152	0.152
T-804	0.7	0.8	1.0	1.1	1.1	-0.154	-0.147	-0.139	-0.134	-0.132
T-805	1.9	1.9	1.7	1.4	1.3	-0.026	-0.039	-0.056	-0.065	-0.069
T-806	2.4	2.5	2.6	2.6	2.6	0.164	0.164	0.167	0.169	0.170
T-807	1.6	1.8	1.9	2.0	2.1	-0.146	-0.142	-0.134	-0.128	-0.126
T-808	-1.4	-1.3	-1.3	-1.3	-1.3	-0.140	-0.141	-0.143	-0.142	-0.141
T-809	-0.8	-0.7	-0.8	-0.9	-0.9	0.204	0.199	0.194	0.193	0.192
T-810	-1.5	-1.4	-1.4	-1.5	-1.5	-0.096	-0.101	-0.104	-0.105	-0.105
T-811	-1.6	-1.6	-1.8	-2.0	-2.1	0.221	0.212	0.198	0.191	0.189
T-812	-2.1	-4.2	-4.2	-4.2	-4.2	0.021	0.018	0.017	0.017	0.017
T-813	-3.3	-3.2	-3.1	-3.0	-3.0	-0.280	-0.281	-0.277	-0.274	-0.273
T-814	-0.1	0.1	-0.1	-0.2	-0.3	0.203	0.206	0.194	0.189	0.187
T-815	-0.2	-0.1	-0.1	-0.1	-0.1	-0.204	-0.206	-0.206	-0.205	-0.204
T-816	-0.7	-0.6	-0.5	-0.5	-0.5	-0.182	-0.183	-0.180	-0.178	-0.177
T-817	-3.7	-3.6	-3.5	-3.5	-3.5	0.037	0.039	0.043	0.046	0.047
T-818	-1.1	-1.0	-1.0	-1.0	-1.0	-0.108	-0.108	-0.107	-0.105	-0.105
T-819	1.5	1.6	1.7	1.7	1.7	0.116	0.116	0.118	0.121	0.122

[a] $\mathbf{E_{a,f}}$**:** Activation energy of the forward reaction, given in kJ mol^{-1}.

[b] $\mathbf{log}\tilde{A}_\mathbf{f}$**:** Logarithm of the pre-exponential factor of the forward reaction, given in m^3 mol^{-1} s^{-1}.

Table D-9 The deviations between the CBS-QB3 data and the GA-based data calculated with 8 preliminary ΔGAV°s parameters given in **Table D-7** for the reverse reactions, with respect to the reference reaction.

Reaction #	$E_{a,f}$[a]					$\log\widetilde{A}_f$ [b]				
	300 K	600 K	1000 K	1500 K	2000 K	300 K	600 K	1000 K	1500 K	2000 K
T-101	0.7	0.8	0.9	1.0	1.1	0.071	0.082	0.089	0.095	0.097
T-102	0.3	0.4	0.3	0.0	-0.2	-0.210	-0.199	-0.206	-0.217	-0.224
T-103	3.4	3.5	3.6	3.7	3.8	0.245	0.257	0.265	0.271	0.274
T-104	-0.3	-0.2	-0.2	-0.2	-0.2	-0.217	-0.204	-0.200	-0.199	-0.199
T-105	2.0	2.1	2.0	1.7	1.5	0.259	0.275	0.270	0.259	0.252
T-106	3.6	3.7	3.8	3.9	4.0	0.232	0.241	0.247	0.252	0.254
T-107	2.7	2.8	2.9	2.9	2.9	0.272	0.284	0.287	0.288	0.288
T-108	-0.8	-1.5	-2.0	-2.5	-2.8	-0.212	-0.305	-0.340	-0.358	-0.369
T-109	2.2	2.3	2.4	2.5	2.7	-0.228	-0.220	-0.213	-0.206	-0.203
T-110	-4.0	-4.2	-4.3	-4.3	-4.3	-0.268	-0.288	-0.293	-0.293	-0.293
T-111	-2.9	-3.0	-3.0	-3.1	-3.1	-0.188	-0.212	-0.212	-0.213	-0.214
T-112	-0.7	-0.6	-0.4	-0.3	-0.2	-0.324	-0.313	-0.306	-0.299	-0.297
T-113	-6.9	-6.9	-6.8	-6.9	-6.8	-0.445	-0.448	-0.445	-0.444	-0.444
T-114	-1.0	-0.9	-1.0	-1.1	-1.1	0.227	0.233	0.231	0.228	0.225
T-115	0.6	0.7	0.8	0.8	1.0	-0.101	-0.092	-0.085	-0.080	-0.078
T-116	0.0	0.1	0.2	0.2	0.3	0.439	0.447	0.452	0.457	0.459
T-117	0.4	0.4	0.2	0.0	-0.1	0.278	0.269	0.260	0.252	0.247
T-118	0.7	0.8	0.9	0.9	1.0	0.218	0.228	0.235	0.240	0.242
T-119	-0.1	0.0	0.1	0.1	0.2	-0.043	-0.037	-0.032	-0.028	-0.026
T-201	-0.5	-0.4	-0.4	-0.4	-0.3	-0.119	-0.122	-0.126	-0.129	-0.116
T-202	2.7	2.8	2.8	2.7	2.8	0.165	0.160	0.156	0.154	0.166
T-203	2.2	2.3	2.3	2.3	2.3	-0.132	-0.136	-0.141	-0.144	-0.132
T-204	-0.7	-0.5	-0.5	-0.4	-0.3	-0.117	-0.114	-0.112	-0.112	-0.098
T-205	2.6	2.7	2.8	2.7	2.8	0.197	0.194	0.191	0.189	0.201
T-206	2.9	3.0	2.9	2.9	2.9	0.000	-0.007	-0.014	-0.018	-0.006
T-207	2.7	2.8	2.9	3.0	3.1	-0.114	-0.111	-0.109	-0.108	-0.094
T-208	-1.9	-2.1	-2.3	-2.7	-2.8	0.143	0.108	0.096	0.090	0.102
T-209	0.5	0.6	0.5	0.4	0.4	-0.067	-0.076	-0.085	-0.090	-0.079
T-210	-6.5	-6.5	-6.6	-6.7	-6.6	0.037	0.012	0.003	0.000	0.012
T-211	0.9	1.0	1.1	1.0	1.1	0.241	0.243	0.241	0.239	0.252
T-212	0.7	0.8	0.7	0.7	0.7	-0.238	-0.243	-0.249	-0.254	-0.242
T-213	-8.2	-8.1	-8.0	-7.9	-7.8	-0.174	-0.181	-0.177	-0.176	-0.162
T-214	2.2	2.4	2.4	2.3	2.3	0.214	0.215	0.210	0.207	0.219
T-215	1.9	2.0	2.0	2.0	2.0	-0.349	-0.234	-0.162	-0.106	-0.349
T-216	-0.4	-0.3	-0.3	-0.3	-0.3	0.377	0.371	0.368	0.366	0.379
T-217	-0.5	-0.4	-0.4	-0.4	-0.4	0.127	0.124	0.121	0.119	0.132

T-218	-0.3	-0.2	-0.2	-0.2	-0.2	-0.107	-0.110	-0.113	-0.115	-0.102
T-219	-1.1	-1.0	-1.0	-1.0	-1.0	-0.091	-0.097	-0.101	-0.103	-0.090
T-301	-1.6	-1.6	-1.6	-1.5	-1.6	0.052	0.057	0.059	0.060	0.060
T-302	8.0	7.9	7.7	7.6	7.5	0.208	0.197	0.188	0.183	0.181
T-303	-0.8	-0.7	-0.7	-0.7	-0.7	0.138	0.148	0.149	0.150	0.150
T-304	-1.3	-1.3	-1.1	-1.0	-1.0	-0.012	-0.002	0.007	0.012	0.014
T-305	9.2	9.0	8.9	8.8	8.7	0.058	0.043	0.032	0.028	0.026
T-306	-0.5	-0.4	-0.4	-0.4	-0.4	0.046	0.050	0.053	0.054	0.055
T-307	-0.5	-0.4	-0.3	-0.2	-0.1	0.063	0.073	0.081	0.087	0.090
T-308	0.7	0.5	0.3	0.2	0.1	-0.651	-0.675	-0.686	-0.691	-0.692
T-309	-1.6	-1.5	-1.5	-1.5	-1.6	0.525	0.533	0.533	0.532	0.531
T-310	-11.6	-11.7	-11.8	-11.8	-11.9	0.279	0.271	0.268	0.266	0.264
T-311	5.7	5.7	5.7	5.8	5.7	-0.265	-0.264	-0.265	-0.264	-0.263
T-312	-2.8	-2.8	-2.7	-2.7	-2.7	-0.030	-0.026	-0.024	-0.023	-0.023
T-313	-12.2	-12.1	-12.0	-11.8	-11.8	0.338	0.352	0.363	0.367	0.369
T-314	7.6	7.5	7.4	7.4	7.3	-0.295	-0.302	-0.311	-0.314	-0.314
T-315	-1.3	-1.3	-1.2	-1.2	-1.2	-0.322	-0.319	-0.317	-0.316	-0.315
T-316	-1.8	-1.8	-1.7	-1.6	-1.6	0.027	0.030	0.034	0.037	0.039
T-317	9.2	9.1	8.9	8.8	8.7	-0.324	-0.337	-0.350	-0.354	-0.356
T-318	-1.4	-1.4	-1.4	-1.3	-1.3	0.050	0.054	0.057	0.058	0.059
T-319	-2.2	-2.2	-2.1	-2.1	-2.1	0.120	0.124	0.128	0.131	0.132
T-401	1.0	1.1	1.1	1.0	1.0	0.377	0.383	0.379	0.377	0.376
T-402	6.5	6.7	6.4	6.1	5.9	0.347	0.370	0.354	0.342	0.337
T-403	-2.9	-2.9	-2.8	-2.7	-2.7	-0.191	-0.190	-0.185	-0.181	-0.179
T-404	0.2	0.3	0.3	0.3	0.3	0.078	0.085	0.085	0.085	0.085
T-405	3.6	3.6	3.5	3.4	3.4	0.275	0.268	0.262	0.259	0.259
T-406	-0.2	-0.1	-0.1	0.0	0.1	-0.178	-0.180	-0.174	-0.170	-0.168
T-407	-0.2	-0.2	0.0	0.1	0.2	-0.189	-0.191	-0.182	-0.176	-0.173
T-408	-1.3	-1.5	-1.7	-1.8	-1.8	0.137	0.106	0.094	0.090	0.088
T-409	0.6	0.6	0.6	0.6	0.6	-0.163	-0.168	-0.168	-0.167	-0.166
T-410	-5.8	-5.9	-6.0	-6.0	-6.0	-0.242	-0.265	-0.268	-0.268	-0.268
T-411	2.2	2.3	2.3	2.3	2.4	0.353	0.360	0.363	0.365	0.366
T-412	-0.3	-0.3	-0.3	-0.2	-0.2	-0.337	-0.340	-0.337	-0.335	-0.333
T-413	-7.4	-7.3	-7.3	-7.4	-7.4	-0.139	-0.136	-0.137	-0.137	-0.137
T-414	2.2	2.3	2.4	2.4	2.4	0.248	0.256	0.262	0.263	0.264
T-415	0.9	0.9	1.0	1.0	1.1	-0.353	-0.356	-0.351	-0.348	-0.345
T-416	0.3	0.4	0.4	0.3	0.3	0.006	0.011	0.008	0.007	0.007
T-417	1.7	1.8	1.8	1.9	1.9	0.068	0.067	0.072	0.075	0.076
T-418	0.7	0.7	0.8	0.8	0.9	-0.168	-0.170	-0.165	-0.162	-0.160
T-419	-2.5	-2.4	-2.4	-2.5	-2.5	0.078	0.083	0.081	0.079	0.079
T-501	-2.8	-2.7	-2.7	-2.8	-2.7	0.233	0.236	0.235	0.233	0.233

T-502	-1.5	-1.8	-2.1	-2.3	-2.3	0.072	0.031	0.012	0.005	0.004
T-503	-2.3	-2.2	-2.3	-2.3	-2.3	-0.045	-0.036	-0.037	-0.038	-0.039
T-504	0.4	0.5	0.5	0.5	0.6	-0.036	-0.033	-0.031	-0.030	-0.030
T-505	6.8	6.8	6.8	6.9	7.0	-0.226	-0.234	-0.232	-0.229	-0.228
T-506	-3.5	-3.4	-3.3	-3.3	-3.2	-0.021	-0.013	-0.009	-0.008	-0.008
T-507	-3.4	-3.3	-3.3	-3.2	-3.1	0.010	0.016	0.020	0.022	0.023
T-508	4.1	4.1	4.1	4.2	4.4	-0.094	-0.100	-0.097	-0.094	-0.092
T-509	0.7	0.7	0.7	0.6	0.7	-0.016	-0.011	-0.013	-0.016	-0.017
T-510	-4.1	-4.5	-5.3	-5.7	-6.1	-0.013	-0.023	-0.031	-0.036	-0.038
T-511	5.0	5.0	5.1	5.3	5.4	-0.105	-0.104	-0.096	-0.090	-0.087
T-512	1.0	1.1	1.1	1.1	1.1	0.317	0.323	0.323	0.322	0.322
T-513	-11.0	-11.0	-11.0	-10.9	-10.9	-0.158	-0.156	-0.155	-0.155	-0.155
T-514	7.4	7.6	7.5	7.5	7.6	0.062	0.078	0.076	0.076	0.076
T-515	2.0	2.0	2.0	2.0	2.1	-0.103	-0.099	-0.099	-0.100	-0.101
T-516	-3.6	-3.6	-3.6	-3.6	-3.5	0.275	0.276	0.277	0.276	0.276
T-517	7.2	7.3	7.4	7.5	7.6	-0.074	-0.067	-0.063	-0.059	-0.056
T-518	-2.6	-2.6	-2.6	-2.6	-2.5	-0.060	-0.056	-0.056	-0.057	-0.058
T-519	0.3	0.3	0.3	0.3	0.4	-0.023	-0.021	-0.021	-0.022	-0.022
T-601	5.2	5.0	4.9	4.7	4.6	-0.286	-0.300	-0.313	-0.321	-0.324
T-602	-1.0	-0.8	-0.5	-0.3	-0.2	0.071	0.102	0.121	0.129	0.133
T-603	3.1	3.1	3.4	3.6	3.7	-0.140	-0.133	-0.116	-0.107	-0.102
T-604	4.5	3.8	3.0	2.7	1.7	-0.292	-0.297	-0.281	-0.272	-0.267
T-605	-0.3	-0.4	-0.6	-0.9	-1.1	0.753	0.746	0.726	0.715	0.711
T-606	2.4	2.3	2.2	2.2	2.1	-0.242	-0.252	-0.256	-0.259	-0.260
T-607	-1.8	-1.9	-1.9	-1.9	-2.0	-0.303	-0.317	-0.321	-0.324	-0.325
T-608	-3.9	-3.6	-3.3	-3.0	-2.8	0.786	0.816	0.839	0.851	0.856
T-609	3.7	3.5	3.4	3.2	3.1	-0.251	-0.263	-0.276	-0.284	-0.287
T-610	6.0	5.9	5.7	5.6	5.5	-0.293	-0.308	-0.318	-0.324	-0.326
T-611	-9.2	-9.0	-8.7	-8.5	-8.5	0.737	0.772	0.787	0.793	0.796
T-612	5.6	5.6	5.8	6.2	6.3	-0.267	-0.281	-0.294	-0.302	-0.306
T-613	0.3	0.1	0.1	0.0	-0.1	-0.311	-0.326	-0.333	-0.337	-0.338
T-614	-11.8	-11.7	-11.8	-12.0	-12.1	0.575	0.592	0.582	0.575	0.572
T-615	0.9	0.8	0.7	0.6	0.5	-0.268	-0.279	-0.285	-0.290	-0.291
T-616	5.1	5.0	4.9	4.8	4.7	-0.318	-0.332	-0.339	-0.343	-0.344
T-617	-9.3	-9.0	-8.6	-8.4	-8.3	0.847	0.891	0.912	0.922	0.927
T-618	0.6	0.9	1.1	1.9	2.4	-0.506	-0.524	-0.514	-0.506	-0.503
T-619	0.4	0.2	0.2	0.1	0.0	-0.292	-0.305	-0.312	-0.317	-0.318
T-701	-1.4	-1.4	-1.4	-1.4	-1.4	0.078	0.081	0.082	0.082	0.081
T-702	6.2	6.3	6.4	6.5	6.5	0.478	0.494	0.498	0.500	0.500
T-703	2.1	2.2	2.2	2.3	2.3	-0.051	-0.045	-0.041	-0.040	-0.040
T-704	0.2	0.2	0.2	0.3	0.3	-0.203	-0.204	-0.199	-0.197	-0.197

T-705	4.3	4.3	4.3	4.3	4.3	0.387	0.387	0.387	0.386	0.385
T-706	2.4	2.4	2.3	2.3	2.3	-0.216	-0.222	-0.225	-0.226	-0.227
T-707	0.2	0.2	0.3	0.3	0.3	-0.017	-0.015	-0.011	-0.009	-0.009
T-708	-1.7	-1.8	-1.9	-2.0	-2.0	0.320	0.297	0.289	0.288	0.287
T-709	-1.1	-1.0	-1.0	-0.9	-1.0	0.035	0.038	0.040	0.041	0.041
T-710	-4.8	-5.0	-5.0	-5.0	-5.1	-0.014	-0.032	-0.037	-0.039	-0.040
T-711	1.2	1.2	1.1	1.1	1.1	0.474	0.471	0.467	0.465	0.463
T-712	0.5	0.6	0.6	0.6	0.6	-0.261	-0.257	-0.255	-0.255	-0.255
T-713	-6.1	-6.2	-6.2	-6.1	-6.2	-0.261	-0.269	-0.270	-0.270	-0.270
T-714	3.3	3.4	3.4	3.4	3.4	0.161	0.168	0.169	0.169	0.168
T-715	-1.6	-1.6	-1.5	-1.5	-1.5	-0.534	-0.531	-0.528	-0.527	-0.527
T-716	-2.4	-2.4	-2.4	-2.4	-2.4	-0.425	-0.427	-0.426	-0.425	-0.425
T-717	2.6	2.7	2.6	2.6	2.6	0.511	0.517	0.514	0.512	0.511
T-718	-1.5	-1.5	-1.5	-1.4	-1.5	-0.166	-0.163	-0.162	-0.162	-0.162
T-719	-2.5	-2.5	-2.5	-2.5	-2.5	-0.289	-0.291	-0.289	-0.289	-0.289
T-801	2.8	2.8	2.8	2.8	2.8	-0.529	-0.531	-0.531	-0.531	-0.531
T-802	0.0	0.0	0.0	0.0	0.1	0.351	0.356	0.356	0.356	0.356
T-803	0.8	0.8	0.9	0.9	0.9	0.063	0.064	0.067	0.067	0.067
T-804	-0.6	-0.6	-0.5	-0.4	-0.3	-0.260	-0.261	-0.256	-0.254	-0.253
T-805	8.0	7.9	7.7	7.5	7.5	0.426	0.418	0.404	0.396	0.393
T-806	0.7	0.7	0.8	0.8	0.9	0.112	0.113	0.117	0.118	0.118
T-807	-0.2	-0.2	-0.1	-0.1	0.0	-0.226	-0.227	-0.222	-0.219	-0.218
T-808	4.2	4.3	4.4	4.5	4.6	0.154	0.159	0.164	0.168	0.170
T-809	-2.1	-2.2	-2.2	-2.2	-2.3	0.070	0.065	0.061	0.058	0.057
T-810	-5.6	-5.7	-5.8	-5.9	-5.9	-0.286	-0.306	-0.313	-0.317	-0.318
T-811	2.2	2.2	2.2	2.1	2.1	0.519	0.524	0.517	0.514	0.513
T-812	-4.8	-4.8	-4.8	-4.8	-4.8	-0.094	-0.097	-0.097	-0.098	-0.098
T-813	-9.9	-10.0	-9.9	-9.8	-9.8	-0.614	-0.619	-0.615	-0.613	-0.612
T-814	5.2	5.1	4.9	4.7	4.3	0.745	0.771	0.769	0.766	0.766
T-815	0.0	0.0	0.1	0.1	0.1	-0.477	-0.479	-0.479	-0.479	-0.479
T-816	-0.6	-0.7	-0.6	-0.6	-0.6	-0.266	-0.271	-0.269	-0.269	-0.268
T-817	-1.7	-1.5	-1.3	-1.2	-1.0	0.489	0.506	0.517	0.524	0.527
T-818	0.3	0.3	0.4	0.4	0.4	-0.216	-0.217	-0.215	-0.215	-0.215
T-819	1.7	1.6	1.7	1.7	1.7	0.036	0.032	0.033	0.034	0.034

[a] $\mathbf{E_{a,r}}$**:** Activation energy of the reverse reaction, given in kJ mol^{-1}.
[b] $\mathbf{log}\widetilde{\boldsymbol{A}}_{\mathbf{r}}$**:** Logarithm of the pre-exponential factor of the reverse reaction, given in m^3 mol^{-1} s^{-1}.

D.2.2 Optimized geometries of the reactions from which ΔNNI°s are identified

In the following figures (**Figure D-9 - Figure D-50**) the optimized structures of the species that participate in the corresponding HARs are shown.

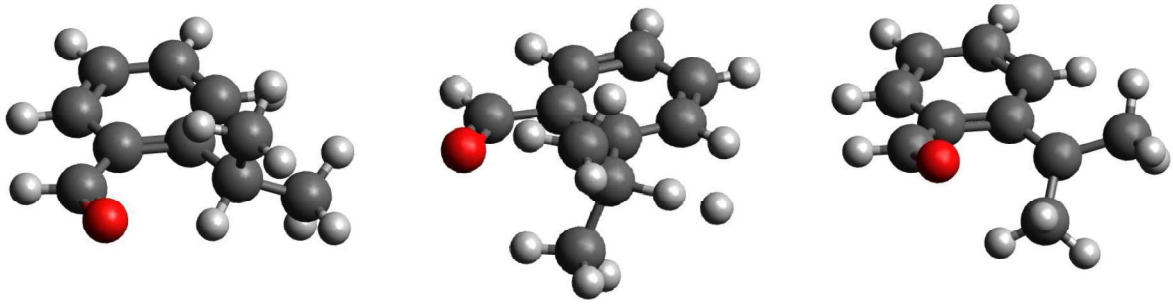

a) ***b)*** ***c)***

Figure D-9 The optimized geometries of the **a)** reactant, **b)** transition state and **c)** product in the hydrogen abstraction reaction from the α-carbon of *o*-CHO substituted isopropylbenzene.

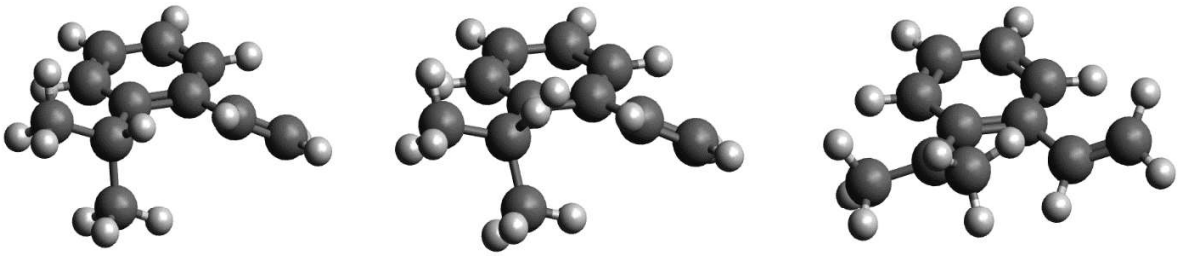

a) ***b)*** ***c)***

Figure D-10 The optimized geometries of the **a)** reactant, **b)** transition state and **c)** product in the hydrogen abstraction reaction from the α-carbon of *o*-$CH{=}CH_2$ substituted isopropylbenzene.

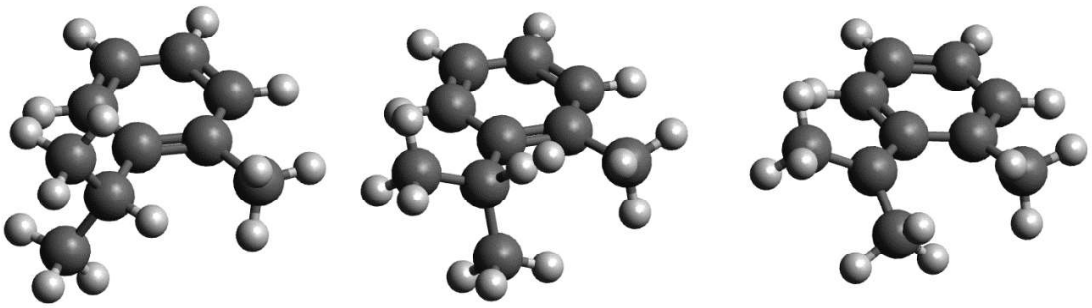

a) ***b)*** ***c)***

Figure D-11 The optimized geometries of the **a)** reactant, **b)** transition state and **c)** product in the hydrogen abstraction reaction from the α-carbon of *o*-CH_3 substituted isopropylbenzene.

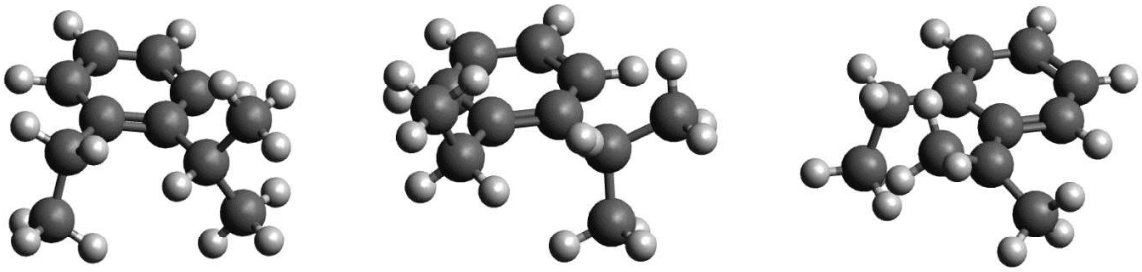

a) ***b)*** ***c)***

Figure D-12 The optimized geometries of the **a)** reactant, **b)** transition state and **c)** product in the hydrogen abstraction reaction from the α-carbon of *o*-CH_2CH_3 substituted isopropylbenzene.

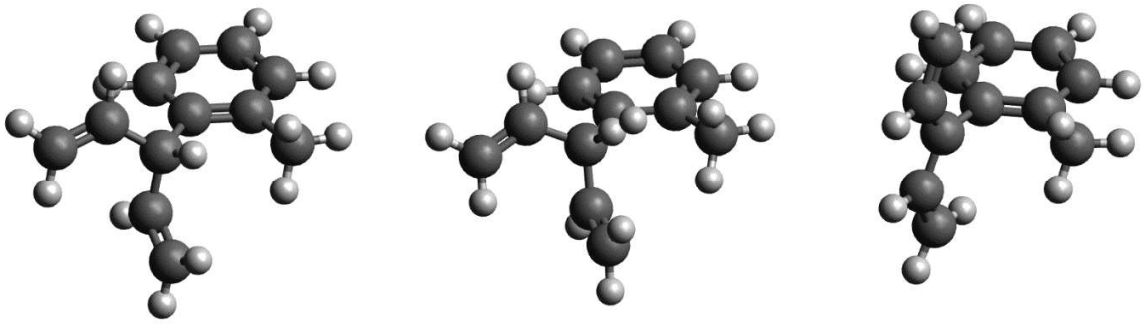

a) ***b)*** ***c)***

Figure D-13 The optimized geometries of the **a)** reactant, **b)** transition state and **c)** product in the hydrogen abstraction reaction from the α-carbon of *o*-CH_3 substituted α-vinylallylbenzene.

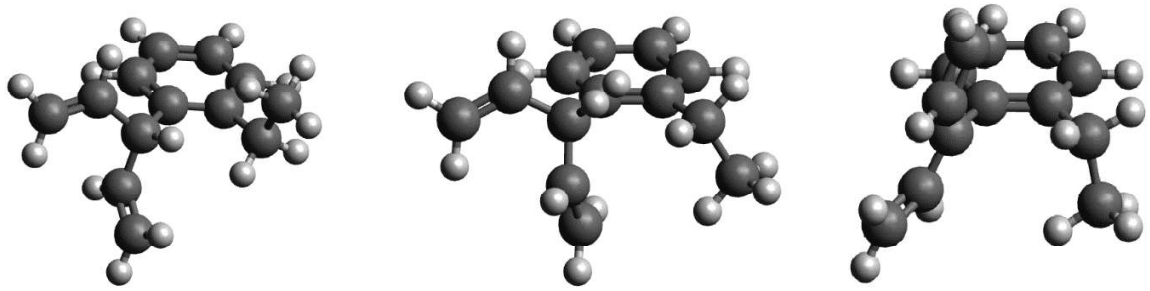

a) ***b)*** ***c)***

Figure D-14 The optimized geometries of the **a)** reactant, **b)** transition state and **c)** product in the hydrogen abstraction reaction from the α-carbon of *o*-CH_2CH_3 substituted α-vinylallylbenzene.

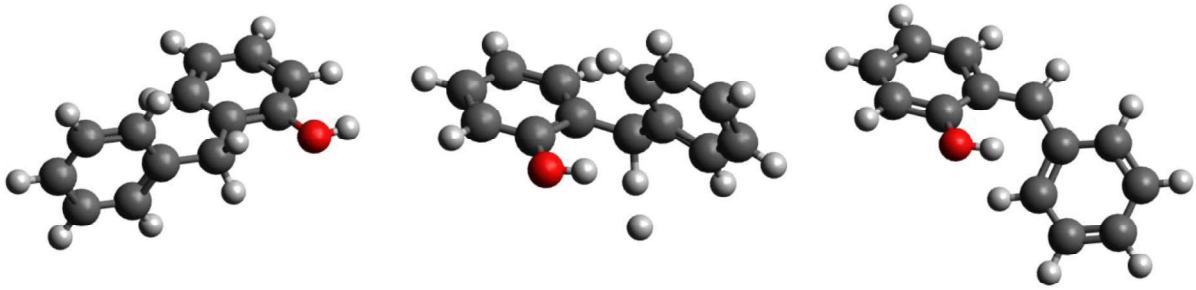

a) ***b)*** ***c)***

Figure D-15 The optimized geometries of the **a)** reactant, **b)** transition state and **c)** product in the hydrogen abstraction reaction from the α-carbon of *o*-OH substituted diphenylmethane.

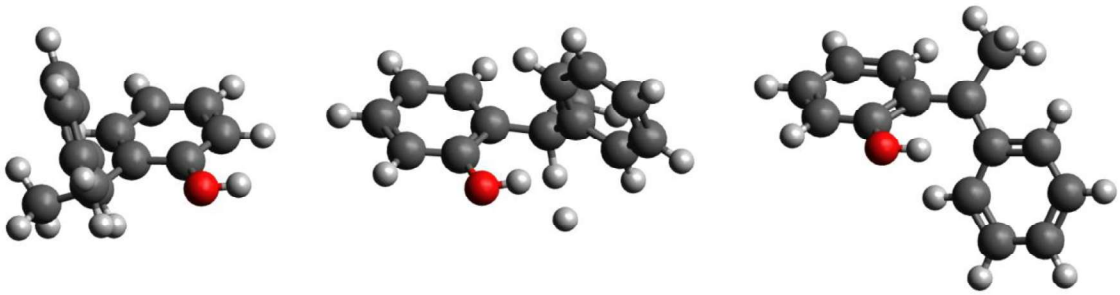

a) ***b)*** ***c)***

Figure D-16 The optimized geometries of the **a)** reactant, **b)** transition state and **c)** product in the hydrogen abstraction reaction from the α-carbon of *o*-OH substituted 1,1-diphenylethane.

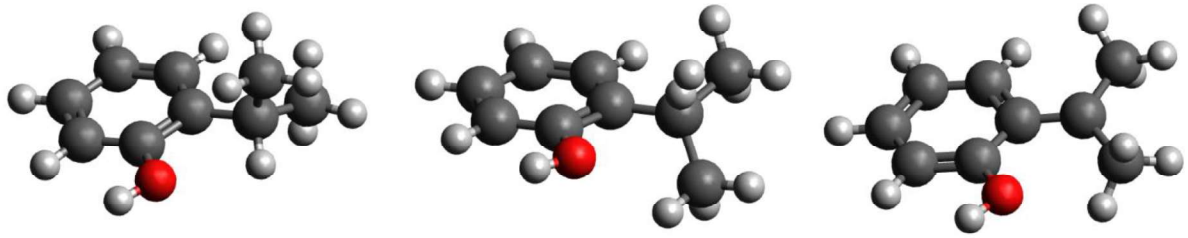

a) *b)* *c)*

Figure D-17 The optimized geometries of the **a)** reactant, **b)** transition state and **c)** product in the hydrogen abstraction reaction from the α-carbon of *o*-OH substituted isopropylbenzene.

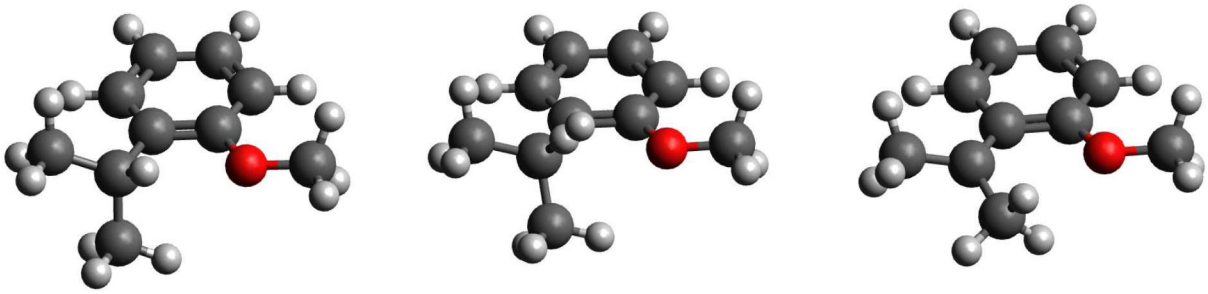

a) *b)* *c)*

Figure D-18 The optimized geometries of **a)** reactant, **b)** transition state and **c)** product in the hydrogen abstraction reaction from the α-carbon of *o*-OCH_3 substituted isopropylbenzene.

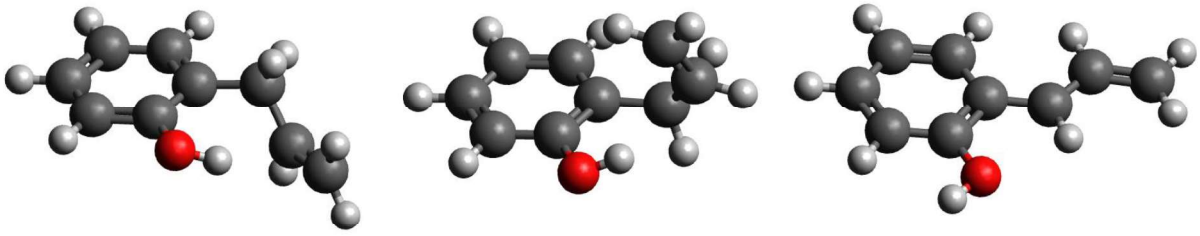

a) *b)* *c)*

Figure D-19 The optimized geometries of **a)** reactant, **b)** transition state and **c)** product in the hydrogen abstraction reaction from the α-carbon of *o*-OH substituted allylbenzene.

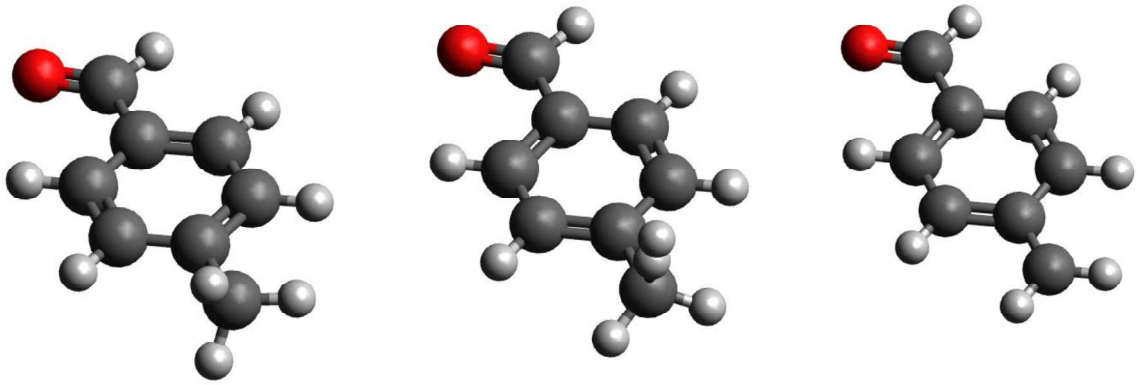

a) ***b)*** ***c)***

Figure D-20 The optimized geometries of **a)** reactant, **b)** transition state and **c)** product in the hydrogen abstraction reaction from the α-carbon of *p*-CHO substituted toluene.

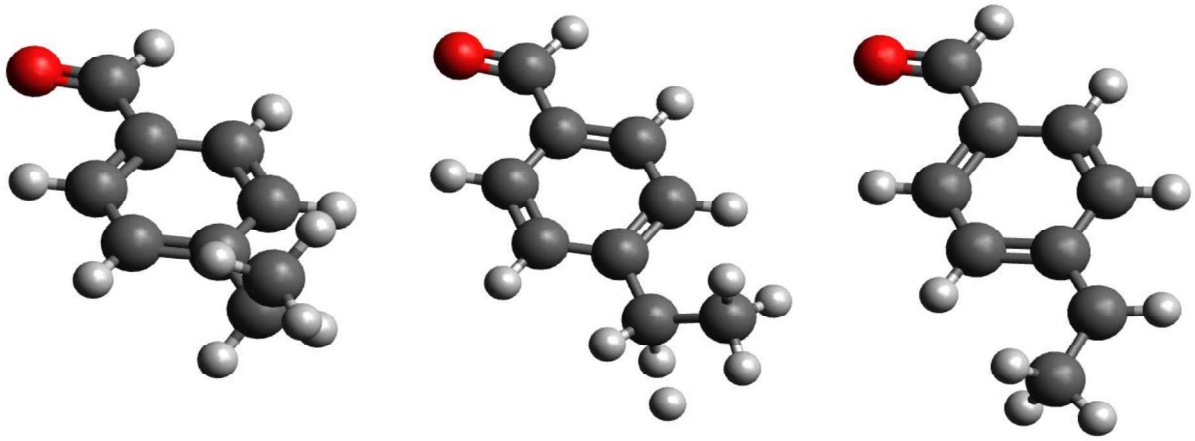

a) ***b)*** ***c)***

Figure D-21 The optimized geometries of **a)** reactant, **b)** transition state and **c)** product in the hydrogen abstraction reaction from the α-carbon of *p*-CHO substituted ethylbenzene.

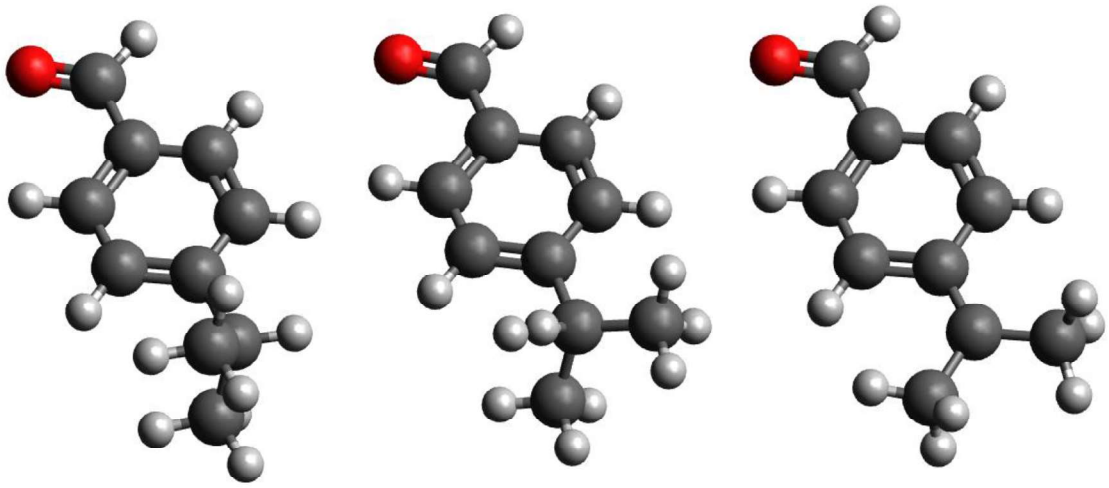

a) *b)* *c)*

Figure D-22 The optimized geometries of **a)** reactant, **b)** transition state and **c)** product in the hydrogen abstraction reaction from the α-carbon of *p*-CHO substituted isopropylbenzene.

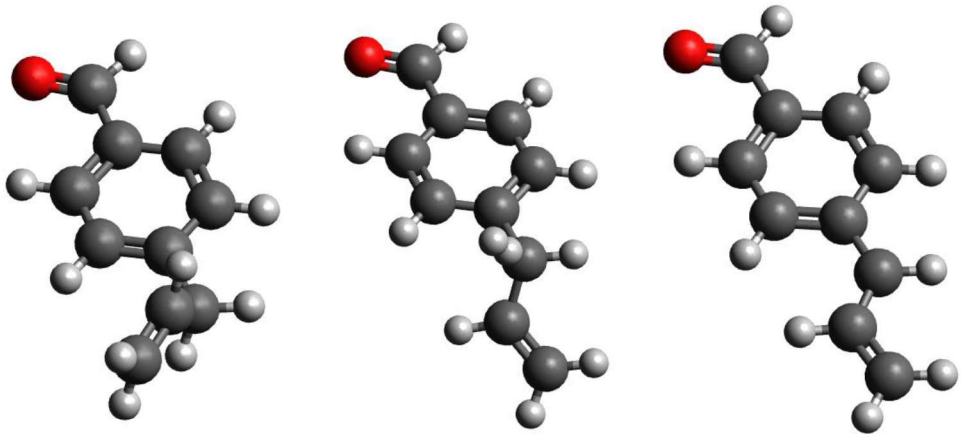

a) *b)* *c)*

Figure D-23 The optimized geometries of **a)** reactant, **b)** transition state and **c)** product in the hydrogen abstraction reaction from the α-carbon of *p*-CHO substituted allylbenzene.

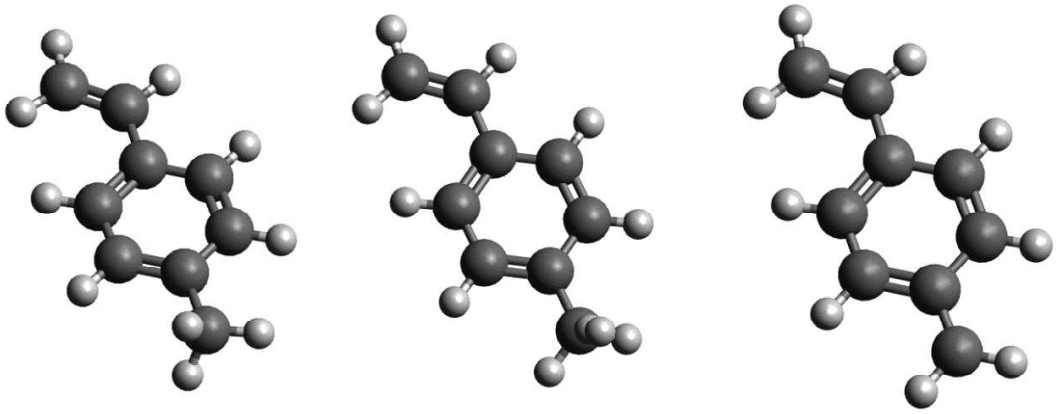

a) ***b)*** ***c)***

Figure D-24 The optimized geometries of **a)** reactant, **b)** transition state and **c)** product in the hydrogen abstraction reaction from the α-carbon of *p*-CH=CH_2 substituted toluene.

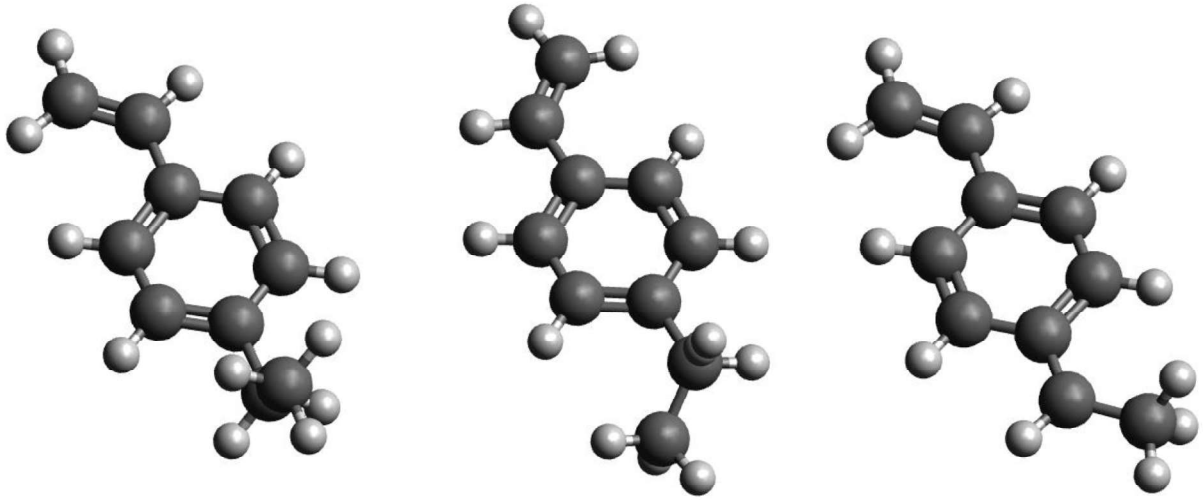

a) ***b)*** ***c)***

Figure D-25 The optimized geometries of **a)** reactant, **b)** transition state and **c)** product in the hydrogen abstraction reaction from the α-carbon of *p*-CH=CH_2 substituted ethylbenzene.

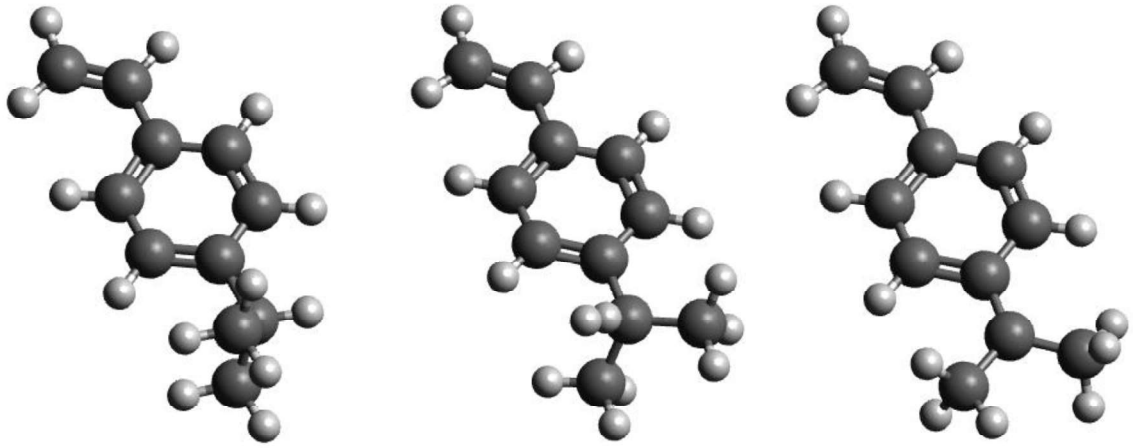

a) *b)* *c)*

Figure D-26 The optimized geometries of **a)** reactant, **b)** transition state and **c)** product in the hydrogen abstraction reaction from the α-carbon of p-CH=CH_2 substituted isopropylbenzene.

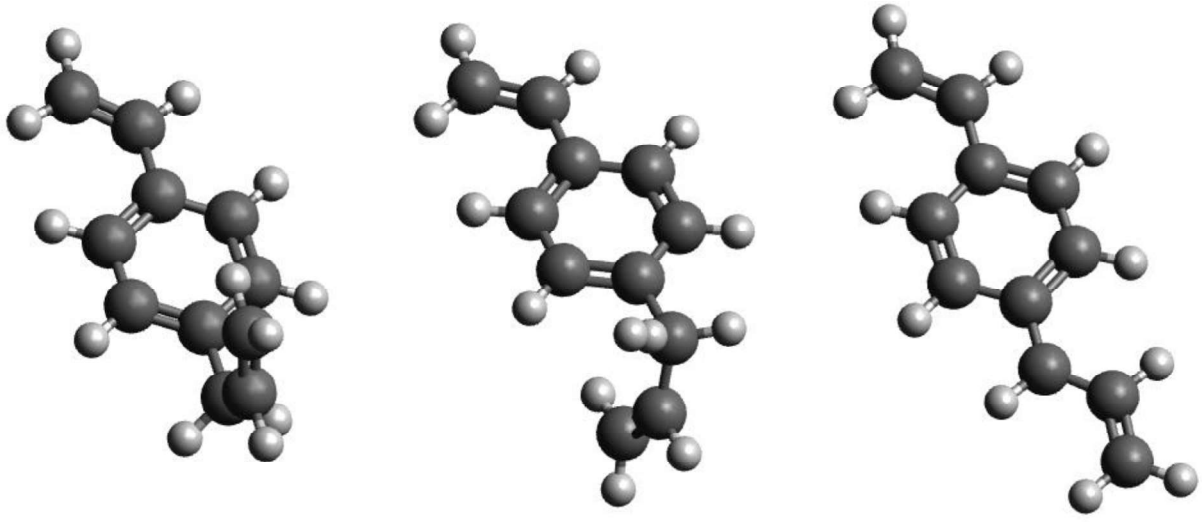

a) *b)* *c)*

Figure D-27 The optimized geometries of **a)** reactant, **b)** transition state and **c)** product in the hydrogen abstraction reaction from the α-carbon of *p*-CH=CH_2 substituted allylbenzene.

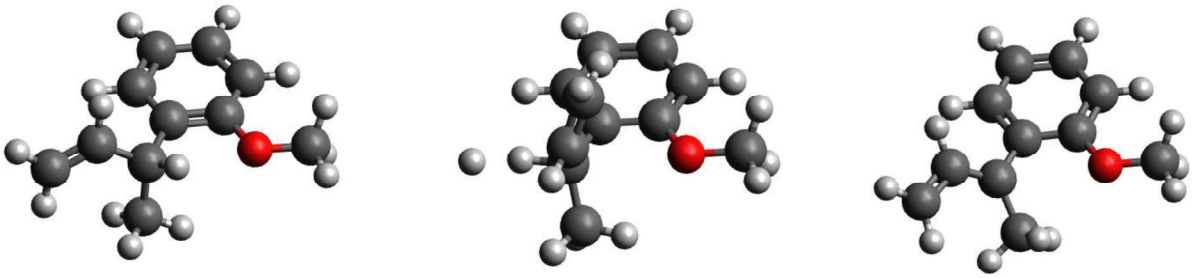

a) ***b)*** ***c)***

Figure D-28 The optimized geometries of **a)** reactant, **b)** transition state and **c)** product in the hydrogen abstraction reaction from the α-carbon of *o*-OCH_3 substituted α-methyl allylbenzene.

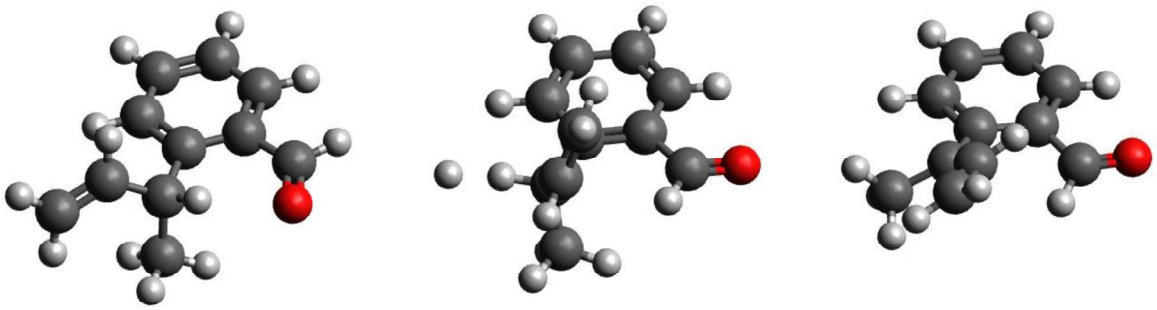

a) ***b)*** ***c)***

Figure D-29 The optimized geometries of a) reactant, b) transition state and c) product in the hydrogen abstraction reaction from the α-carbon of *o*-CHO substituted α-methyl allylbenzene.

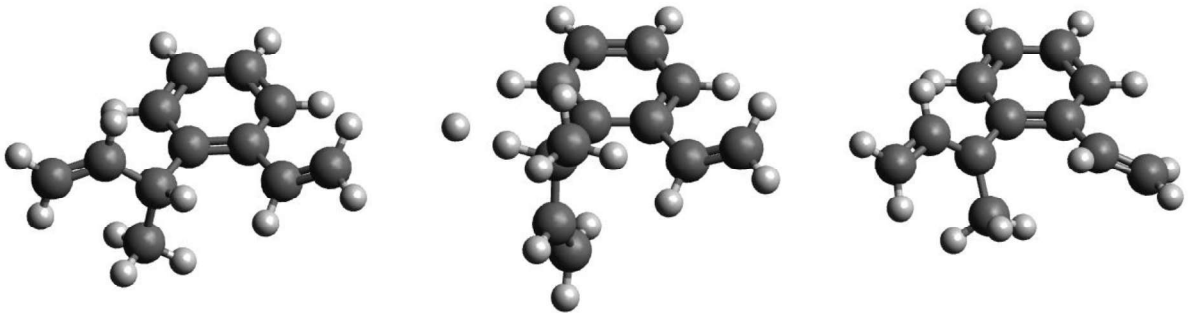

a) ***b)*** ***c)***

Figure D-30 The optimized geometries of **a)** reactant, **b)** transition state and **c)** product in the hydrogen abstraction reaction from the α-carbon of *o*-$CH{=}CH_2$ substituted α-methyl allylbenzene.

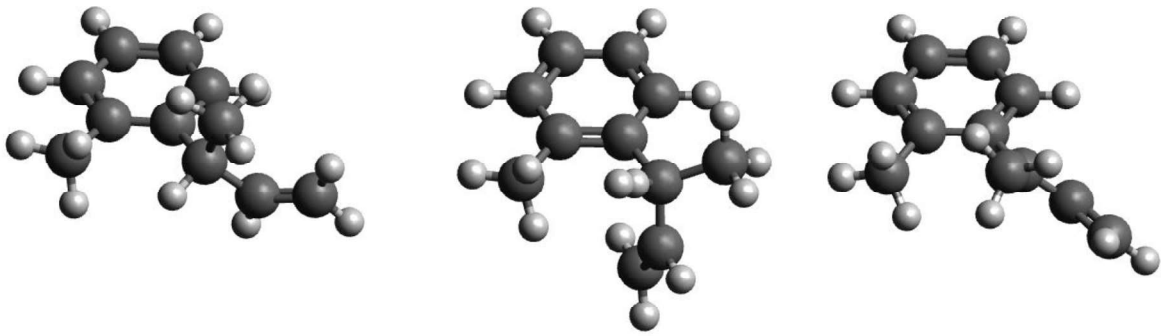

a) *b)* *c)*

Figure D-31 The optimized geometries of **a)** reactant, **b)** transition state and **c)** product in the hydrogen abstraction reaction from the α-carbon of *o*-CH_3 substituted α-methyl allylbenzene.

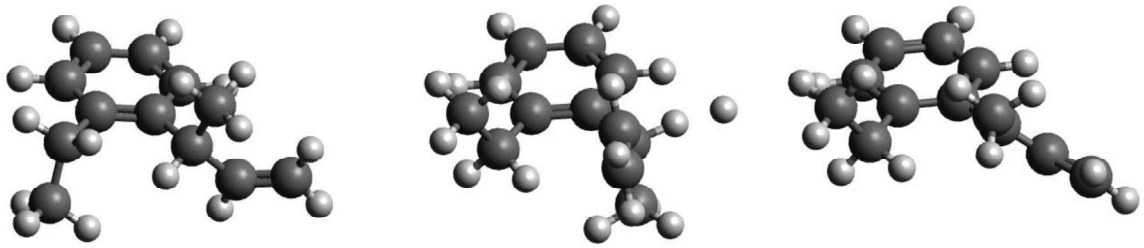

a) *b)* *c)*

Figure D-32 The optimized geometries of **a)** reactant, **b)** transition state and **c)** product in the hydrogen abstraction reaction from the α-carbon of *o*-CH_2CH_3 substituted α-methyl allylbenzene.

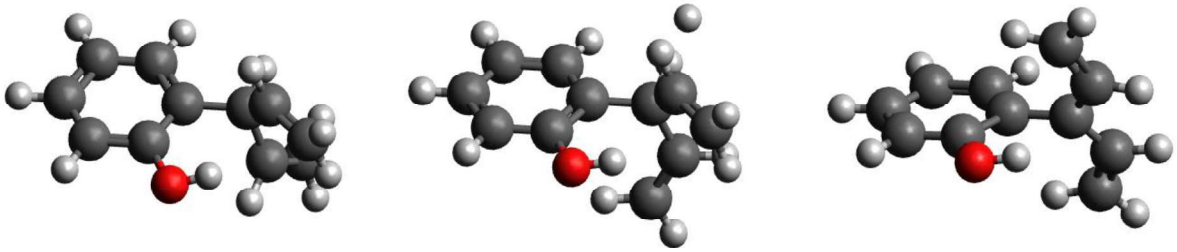

a) *b)* *c)*

Figure D-33 The optimized geometries of **a)** reactant, **b)** transition state and **c)** product in the hydrogen abstraction reaction from the α-carbon of *o*-OH substituted α-vinyl allylbenzene.

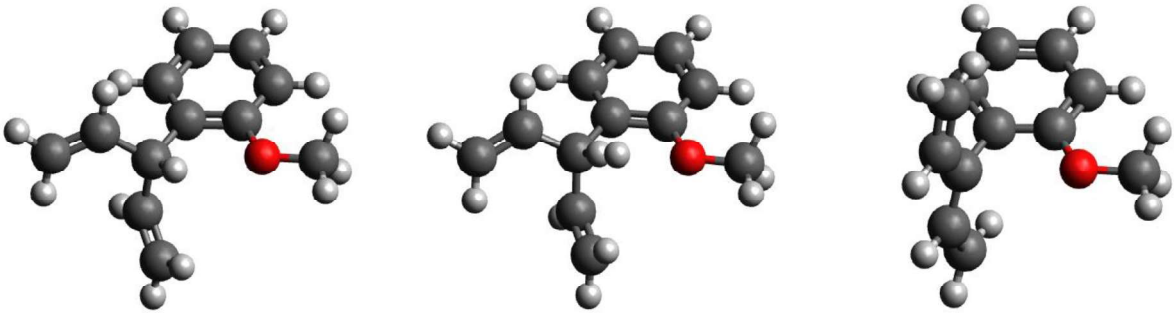

a) ***b)*** ***c)***

Figure D-34 The optimized geometries of **a)** reactant, **b)** transition state and **c)** product in the hydrogen abstraction reaction from the α-carbon of *o*-OCH_3 substituted α-vinyl allylbenzene.

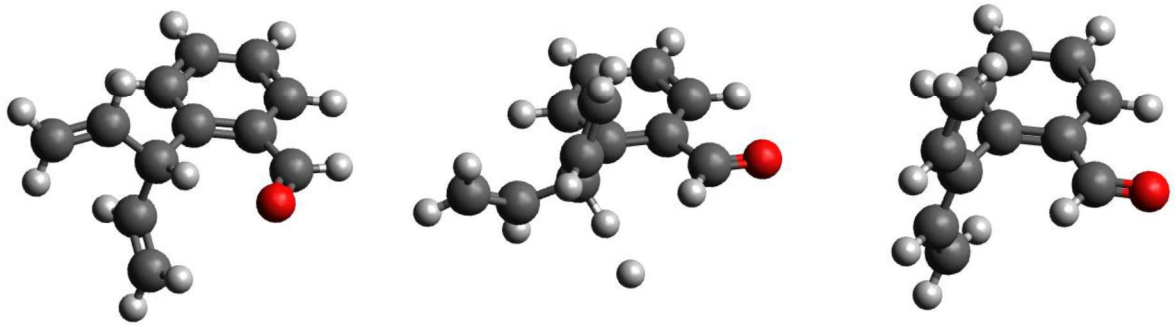

a) ***b)*** ***c)***

Figure D-35 The optimized geometries of **a)** reactant, **b)** transition state and **c)** product in the hydrogen abstraction reaction from the α-carbon of *o*-CHO substituted α-vinyl allylbenzene.

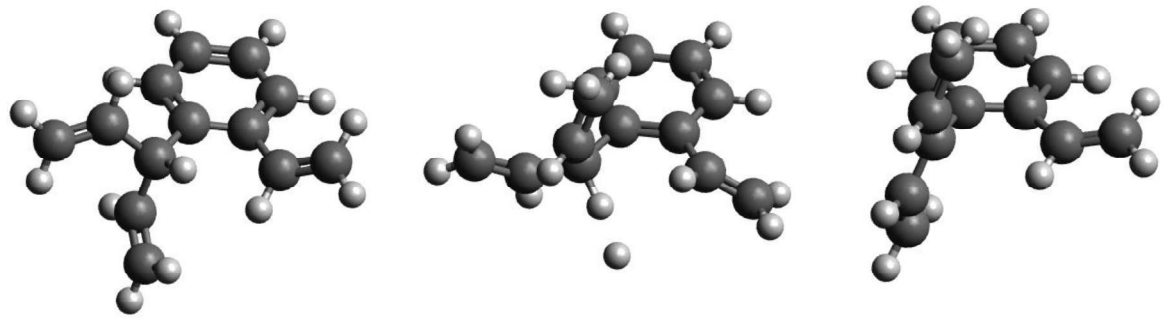

a) *b)* *c)*

Figure D-36 The optimized geometries of **a)** reactant, **b)** transition state and **c)** product in the hydrogen abstraction reaction from the α-carbon of *o*-CH=CH2 substituted α-vinyl allylbenzene.

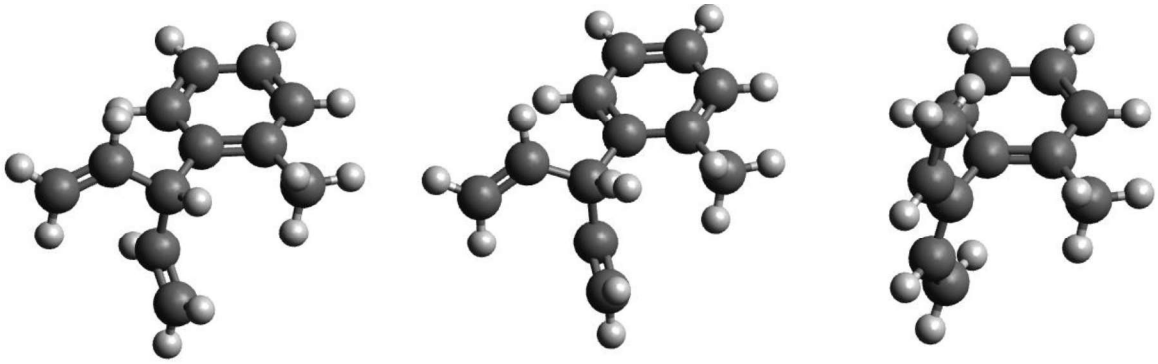

a) *b)* *c)*

Figure D-37 The optimized geometries of **a)** reactant, **b)** transition state and **c)** product in the hydrogen abstraction reaction from the α-carbon of *o*-CH_3 substituted α-vinyl allylbenzene.

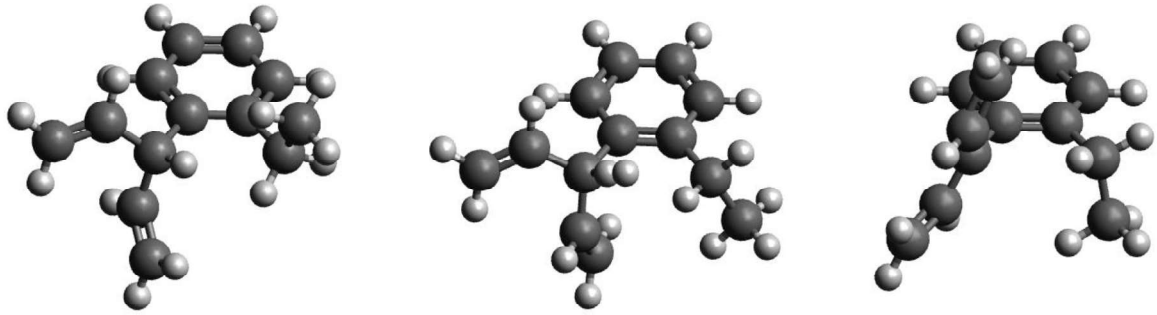

a) ***b)*** ***c)***

Figure D-38 The optimized geometries of **a)** reactant, **b)** transition state and **c)** product in the hydrogen abstraction reaction from the α-carbon of *o*-CH_2CH_3 substituted α-vinyl allylbenzene.

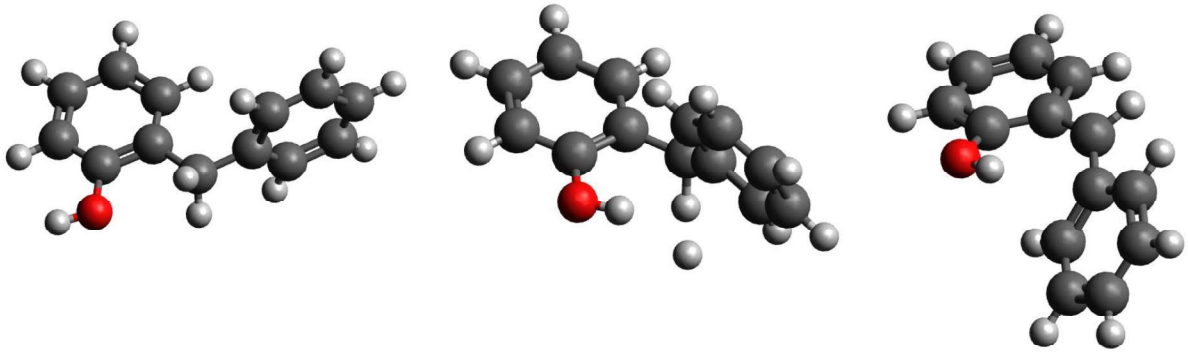

a) ***b)*** ***c)***

Figure D-39 The optimized geometries of **a)** reactant, **b)** transition state and **c)** product in the hydrogen abstraction reaction from the α-carbon of *o*-OH substituted diphenylmethane.

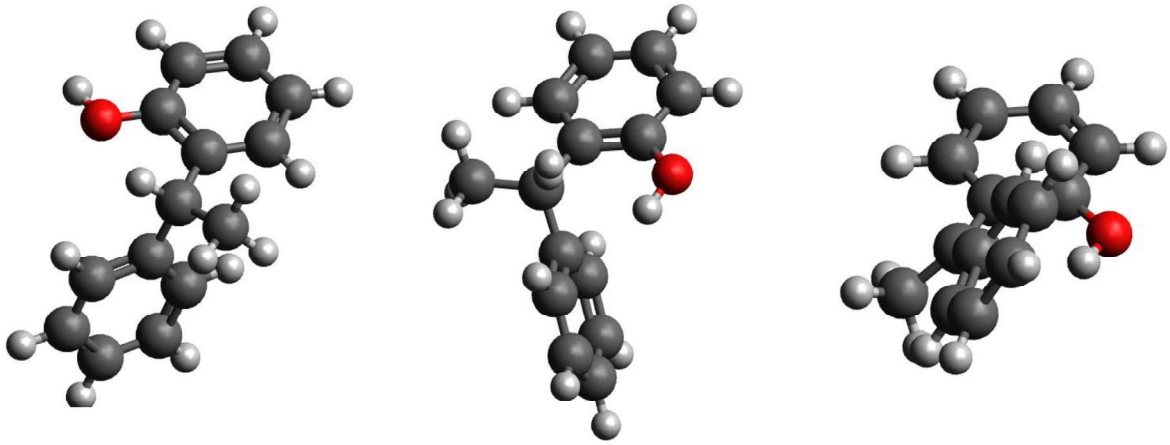

a) ***b)*** ***c)***

Figure D-40 The optimized geometries of **a)** reactant, **b)** transition state and **c)** product in the hydrogen abstraction reaction from the α-carbon of *o*-OH substituted 1,1-diphenylethane.

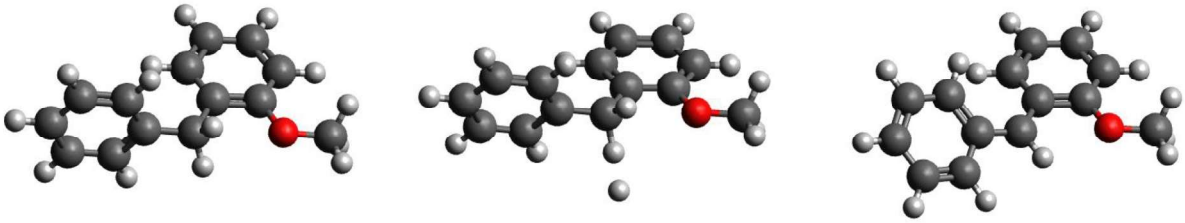

a) ***b)*** ***c)***

Figure D-41 The optimized geometries of **a)** reactant, **b)** transition state and **c)** product in the hydrogen abstraction reaction from the α-carbon of *o*-OCH_3 substituted diphenylmethane.

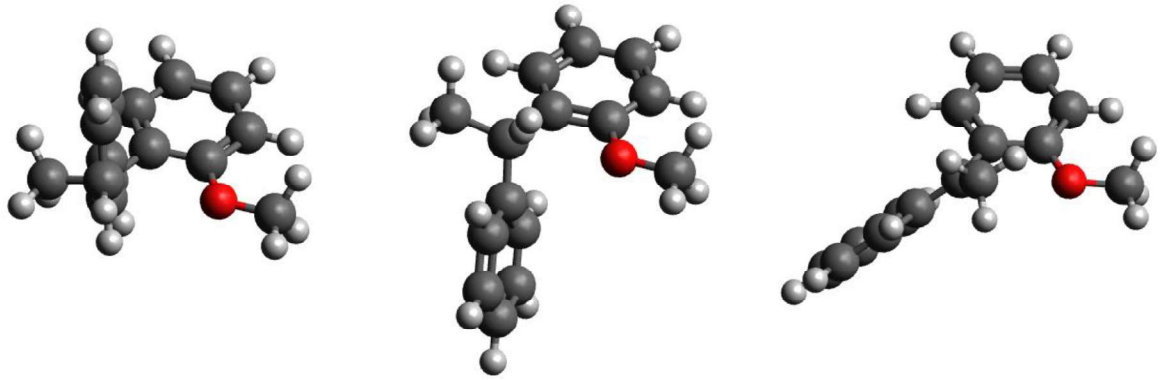

a) ***b)*** ***c)***

Figure D-42 The optimized geometries of **a)** reactant, **b)** transition state and **c)** product in the hydrogen abstraction reaction from the α-carbon of *o*-OCH_3 substituted 1,1-diphenylethane.

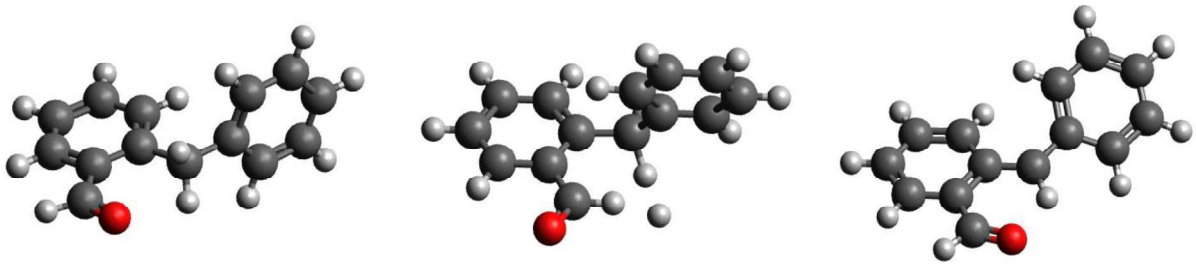

a) ***b)*** ***c)***

Figure D-43 The optimized geometries of **a)** reactant, **b)** transition state and **c)** product in the hydrogen abstraction reaction from the α-carbon of *o*-CHO substituted diphenylmethane.

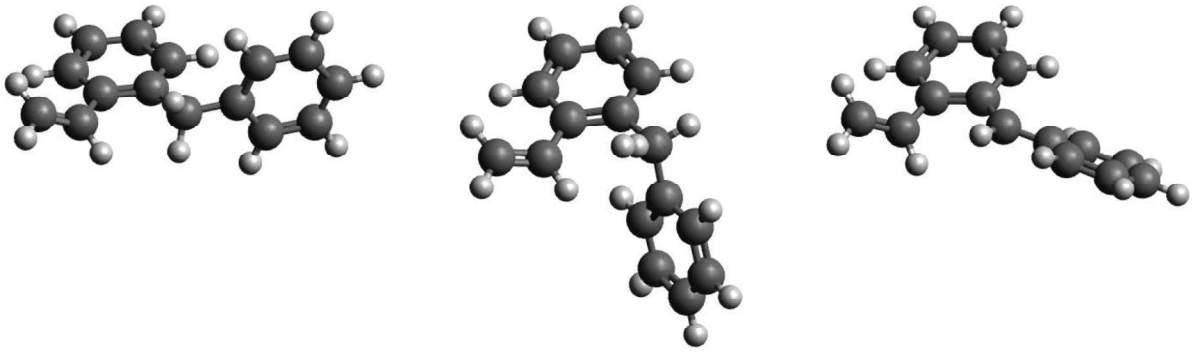

a) ***b)*** ***c)***

Figure D-44 The optimized geometries of **a)** reactant, **b)** transition state and **c)** product in the hydrogen abstraction reaction from the α-carbon of *o*-$CH{=}CH_2$ substituted diphenylmethane.

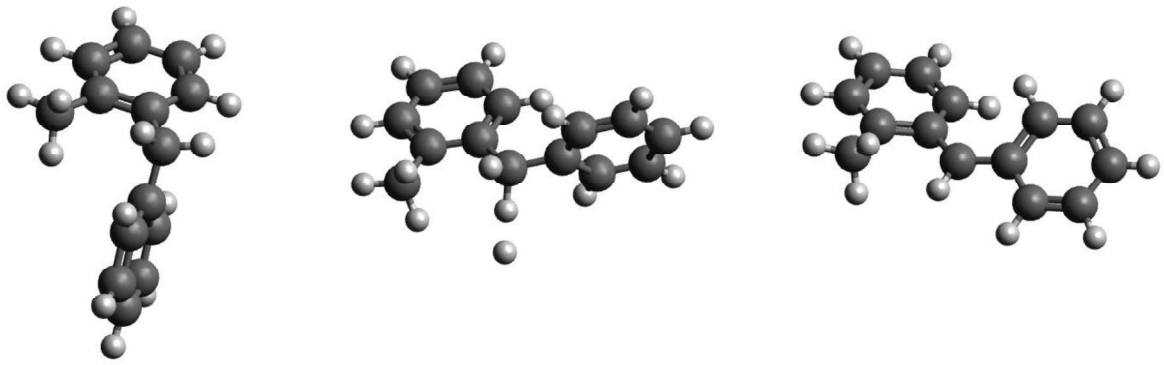

a) *b)* *c)*

Figure D-45 The optimized geometries of **a)** reactant, **b)** transition state and **c)** product in the hydrogen abstraction reaction from the α-carbon of *o*-CH_3 substituted diphenylmethane.

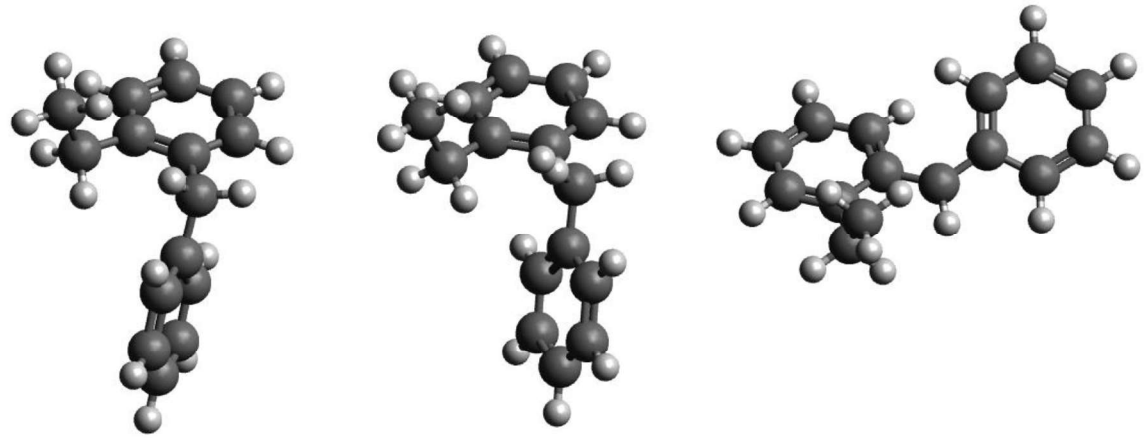

a) *b)* *c)*

Figure D-46 The optimized geometries of **a)** reactant, **b)** transition state and **c)** product in the hydrogen abstraction reaction from the α-carbon of *o*-CH_2CH_3 substituted diphenylmethane.

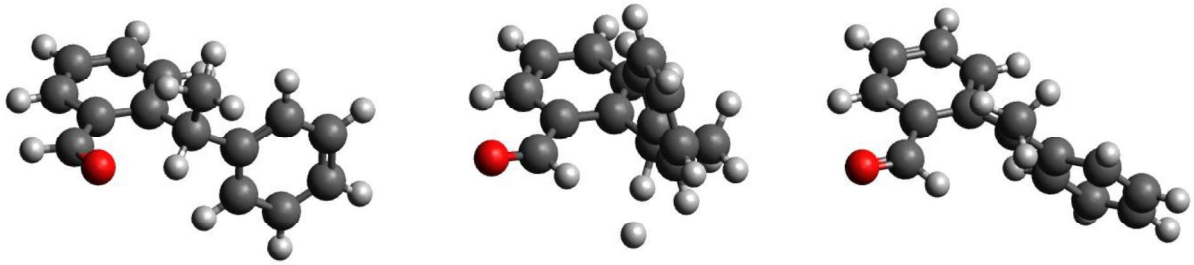

a) *b)* *c)*

Figure D-47 The optimized geometries of **a)** reactant, **b)** transition state and **c)** product in the hydrogen abstraction reaction from the α-carbon of *o*-CHO substituted 1,1-diphenylethane.

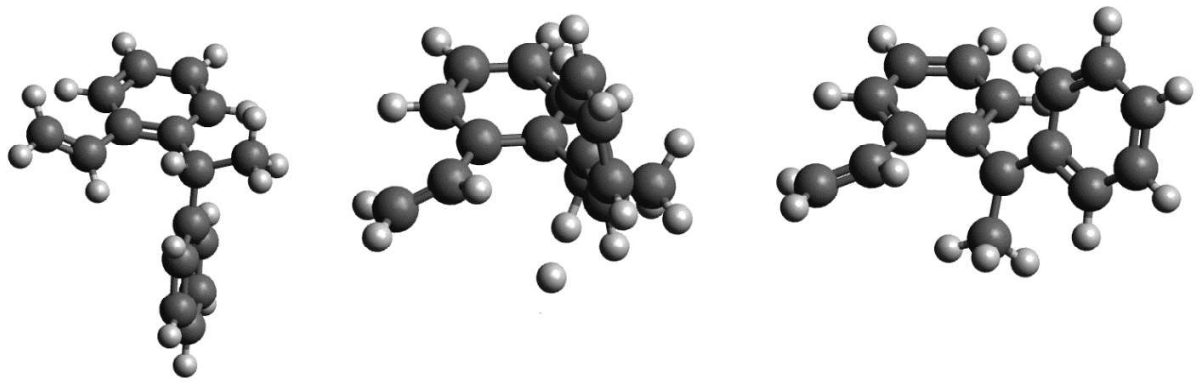

a) ***b)*** ***c)***

Figure D-48 The optimized geometries of **a)** reactant, **b)** transition state and **c)** product in the hydrogen abstraction reaction from the α-carbon of *o*-$CH{=}CH_2$ substituted 1,1-diphenylethane.

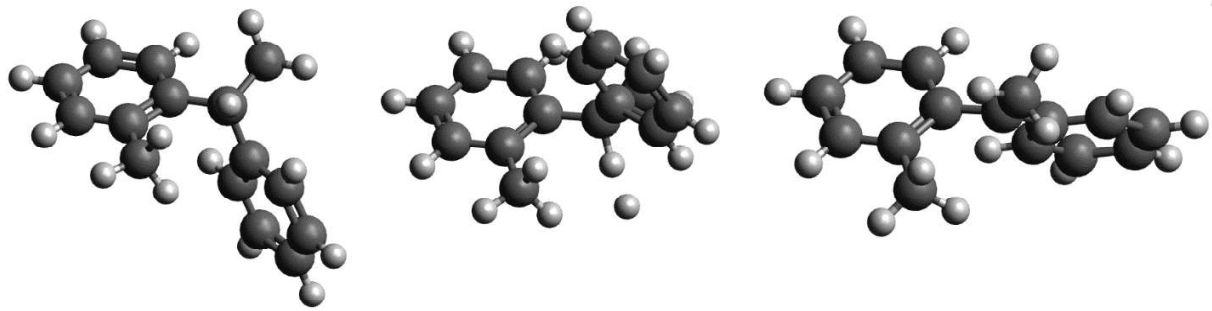

a) ***b)*** ***c)***

Figure D-49 The optimized geometries of **a)** reactant, **b)** transition state and **c)** product in the hydrogen abstraction reaction from the α-carbon of *o*-CH_3 substituted 1,1-diphenylethane.

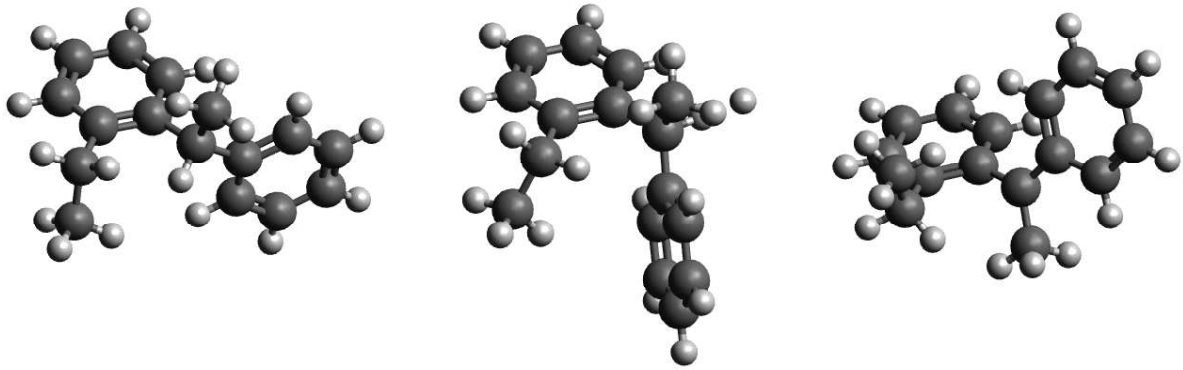

a) ***b)*** ***c)***

Figure D-50 The optimized geometries of **a)** reactant, **b)** transition state and **c)** product in the hydrogen abstraction reaction from the α-carbon of *o*-CH_2CH_3 substituted 1,1-diphenylethane.

D.3 Simultaneous optimization of ΔGAV°s and ΔNNI°s

Table D-10 ΔGAV°s obtained upon simultaneous optimization based on the training set for the forward and reverse directions.

ΔGAV°s	**Forward**									
	$E_{a,f}$[a]					$\log\widetilde{A}_f$[b]				
	300 K	**600 K**	**1000 K**	**1500 K**	**2000 K**	**300 K**	**600 K**	**1000 K**	**1500 K**	**2000 K**
C_2-(C_b)(H)$_2$	-1.0	-1.1	-1.0	-1.1	-0.9	0.032	-0.016	-0.002	0.027	-0.014
C_2-(C_b)(C)(H)	-6.5	-8.1	-10.3	-12.1	-13.1	0.182	-0.188	-0.337	-0.413	-0.446
C_2-(C_b)(C)$_2$	-12.2	-13.8	-16.1	-17.9	-19.0	0.170	-0.023	-0.177	-0.256	-0.289
C_2-(C_b)(C_d)(H)	-10.9	-12.5	-14.9	-16.9	-18.1	0.392	0.199	0.036	-0.048	-0.084
C_2-(C_b)(C_d)(C)	-17.3	-18.9	-21.4	-23.5	-24.7	0.308	0.118	-0.052	-0.140	-0.177
C_2-(C_b)(C_d)$_2$	-18.5	-20.4	-22.9	-25.0	-26.0	0.285	0.080	-0.093	-0.182	-0.220
C_2-(C_b)$_2$(H)	-4.4	-6.0	-8.3	-10.1	-11.3	-0.082	-0.280	-0.435	-0.514	-0.548
C_2-(C_b)$_2$(C)	-8.6	-10.2	-12.6	-14.6	-15.8	0.002	-0.200	-0.365	-0.449	-0.485
ΔGAV°s	**Reverse**									
	$E_{a,r}$[c]					$\log\widetilde{A}_r$[d]				
	300 K	**600 K**	**1000 K**	**1500 K**	**2000 K**	**300 K**	**600 K**	**1000 K**	**1500 K**	**2000 K**
C_2-(C_b)(H)$_2$	-0.1	-0.1	0.0	0.2	0.3	0.059	0.069	0.076	0.082	0.085
C_2-(C_b)(C)(H)	3.9	3.4	3.0	3.4	4.3	-0.685	-0.753	-0.786	-0.776	-0.734
C_2-(C_b)(C)$_2$	1.0	0.7	0.4	0.8	1.7	-1.523	-1.568	-1.586	-1.573	-1.545
C_2-(C_b)(C_d)(H)	38.4	38.2	37.8	38.1	39.0	0.079	0.051	0.021	0.033	0.063
C_2-(C_b)(C_d)(C)	31.2	31.0	30.6	31.0	31.9	-0.767	-0.795	-0.821	-0.809	-0.781
C_2-(C_b)(C_d)$_2$	57.8	57.9	57.6	57.9	58.9	0.261	0.266	0.245	0.259	0.287
C_2-(C_b)$_2$(H)	20.3	20.2	20.1	20.6	21.7	0.359	0.348	0.339	0.361	0.394
C_2-(C_b)$_2$(C)	14.9	14.7	14.4	14.8	15.8	-0.481	-0.505	-0.523	-0.508	-0.479

[a]$E_{a,f}$: Activation energy of the forward reaction, given in kJ mol^{-1}.
[b]$\log\widetilde{A}_f$: Logarithm of the pre-exponential factor of the forward reaction, given in m^3 mol^{-1} s^{-1}.
[c]$E_{a,r}$: Activation energy of the reverse reaction, given in kJ mol^{-1}.
[d]$\log\widetilde{A}_r$: Logarithm of the pre-exponential factor of the reverse reaction, given in m^3 mol^{-1} s^{-1}.

Table D-11 ΔNNI°s obtained upon simultaneous optimization based on the training set for the forward and reverse directions.

$\Delta NNI°$ #	E_a[a]					$\log\tilde{A}$[b]				
	300 K	**600 K**	**1000 K**	**1500 K**	**2000 K**	**300 K**	**600 K**	**1000 K**	**1500 K**	**2000 K**
Forward Reactions ($\Delta NNI_f°$s)										
$\Delta NNI_f°1$	6.8	6.8	7.0	7.1	7.2	-0.207	-0.208	-0.196	-0.190	-0.187
$\Delta NNI_f°2$	6.7	6.7	6.8	6.8	6.6	-0.127	-0.137	-0.134	-0.132	-0.131
$\Delta NNI_f°3$	-5.5	-5.7	-5.8	-5.8	-5.8	-0.347	-0.373	-0.377	-0.377	-0.376
Reverse Reactions ($\Delta NNI_r°$s)										
$\Delta NNI_r°1$	-10.4	-10.2	-10.0	-9.9	-9.8	-0.018	0.002	0.016	0.022	0.024
$\Delta NNI_r°2$	-5.0	-4.9	-4.7	-4.7	-4.6	0.573	0.591	0.601	0.605	0.605
$\Delta NNI_r°3$	-10.2	-10.1	-9.9	-9.8	-9.7	0.424	0.441	0.456	0.462	0.463
$\Delta NNI_r°4$	-6.0	-6.2	-5.9	-5.6	-5.3	-0.354	-0.378	-0.36	-0.347	-0.342
$\Delta NNI_r°5$	7.9	8.0	8.0	8.0	8.0	0.11	0.12	0.122	0.123	0.119
$\Delta NNI_r°6$	-7.4	-7.4	-7.5	-7.6	-7.7	0.136	0.136	0.132	0.127	0.125
$\Delta NNI_r°7$	3.8	3.4	3.1	2.9	2.7	-0.361	-0.403	-0.425	-0.436	-0.44
$\Delta NNI_r°8$	3.1	3.0	3.2	3.5	3.6	-1.043	-1.047	-1.03	-1.022	-1.018
$\Delta NNI_r°9$	6.7	6.2	5.9	5.6	5.3	-1.076	-1.117	-1.143	-1.158	-1.163
$\Delta NNI_r°10$	12.9	12.5	12.3	12.2	12.1	-1.01	-1.053	-1.065	-1.07	-1.072
$\Delta NNI_r°11$	-3.4	-3.5	-3.5	-3.5	-3.5	-0.588	-0.599	-0.6	-0.6	-0.6
$\Delta NNI_r°12$	-6.5	-6.4	-6.3	-6.1	-6.1	-0.58	-0.577	-0.568	-0.563	-0.561
$\Delta NNI_r°13$	-2.2	-2.3	-2.2	-2.1	-2.1	-0.595	-0.601	-0.598	-0.598	-0.598
$\Delta NNI_r°14$	6.3	6.4	6.6	6.6	6.8	0.125	0.135	0.138	0.14	0.14

[a]**E_a:** Activation energy of the reaction, given in kJ mol^{-1}.
[b]**$\log\tilde{A}$:** Logarithm of the pre-exponential factor of the reaction, given in m^3 mol^{-1} s^{-1}.

Table D-12 The deviations between the CBS-QB3 data and the GA-based data calculated with the ΔGAV°s and ΔNNI° parameters for the forward direction with respect to the reference reaction, given in **Table D-10** and **Table D-11**, respectively.

Reaction #	$E_{a,f}$[a]					$\log\widetilde{A}_f$ [b]				
	300 K	600 K	1000 K	1500 K	2000 K	300 K	600 K	1000 K	1500 K	2000 K
T-101	-1.0	-1.1	-1.0	-1.1	-0.9	0.032	-0.016	-0.002	0.027	-0.014
T-102	-0.1	0.3	0.5	0.1	0.0	0.011	0.033	0.051	0.068	0.020
T-103	-0.3	0.7	-0.3	0.8	1.0	0.113	0.024	0.092	0.063	0.024
T-104	1.2	1.1	0.4	1.1	1.2	0.048	0.009	0.023	0.049	0.006
T-105	2.3	0.2	0.1	0.6	1.4	-0.002	0.038	0.061	0.080	0.033
T-106	0.6	1.3	0.6	1.8	1.3	0.018	-0.032	-0.020	0.007	0.010
T-107	1.0	0.6	0.1	-0.6	-0.5	0.066	0.127	-0.008	-0.068	0.019
T-108	0.0	0.1	0.2	-0.2	-0.3	-0.016	-0.031	-0.020	-0.003	-0.053
T-109	-0.3	-0.5	-0.4	-0.5	-0.2	0.022	-0.030	-0.017	0.013	-0.027
T-110	-0.5	-0.6	-0.5	-0.7	-0.6	0.025	-0.025	-0.013	0.013	-0.029
T-111	-1.0	-0.4	1.2	0.8	0.5	-0.226	-0.097	-0.141	-0.077	-0.106
T-112	-0.7	-0.8	-0.7	-0.8	-0.6	0.008	-0.041	-0.027	0.002	-0.039
T-113	1.6	1.5	1.6	1.4	1.5	0.097	0.051	0.064	0.089	0.045
T-114	-1.3	-0.8	-0.5	-0.6	-1.2	-0.005	0.034	0.064	0.092	-0.077
T-115	-0.1	-0.2	-0.1	-0.2	-1.4	-0.136	-0.102	-0.099	-0.355	0.143
T-116	-0.6	-0.7	-0.6	-0.7	-1.4	-0.102	0.124	0.005	-0.049	0.124
T-117	0.2	0.4	0.5	0.2	0.2	0.027	0.020	0.033	0.053	0.007
T-118	-0.3	-0.4	-0.3	-0.4	-0.2	0.023	-0.025	-0.011	0.018	-0.023
T-119	-0.4	-0.5	-0.5	-0.6	-0.4	-0.009	-0.057	-0.043	-0.015	-0.057
T-201	-1.9	-1.9	-2.0	-2.0	-2.0	-0.031	-0.216	-0.218	-0.218	-0.219
T-202	1.4	1.5	1.5	1.5	1.5	0.060	0.360	0.362	0.363	0.362
T-203	2.4	2.4	2.3	2.2	2.3	0.037	0.330	0.327	0.326	0.324
T-204	-0.1	0.0	0.1	0.1	0.2	0.016	0.318	0.324	0.328	0.328
T-205	2.4	2.4	2.5	2.4	2.5	0.077	0.375	0.377	0.378	0.377
T-206	2.7	2.6	2.6	2.5	2.5	0.024	0.311	0.305	0.303	0.302
T-207	3.1	3.1	3.2	3.3	3.4	-0.004	0.296	0.304	0.308	0.309
T-208	-3.9	-3.9	-4.0	-4.0	-3.9	-0.007	-0.195	-0.195	-0.196	-0.196
T-209	-0.7	-0.8	-0.9	-1.1	-1.1	0.040	-0.152	-0.160	-0.164	-0.166
T-210	-1.7	-1.7	-1.7	-1.7	-1.6	-0.060	-0.245	-0.243	-0.242	-0.242
T-211	-1.1	-1.1	-1.0	-1.1	-1.0	0.157	-0.020	-0.018	-0.018	-0.018
T-212	0.8	0.7	0.6	0.5	0.5	0.002	-0.187	-0.192	-0.195	-0.196
T-213	-0.1	-0.1	-0.1	0.0	0.1	-0.014	-0.194	-0.188	-0.184	-0.183
T-214	2.3	2.4	2.4	2.4	2.4	0.272	0.101	0.102	0.102	0.102
T-215	1.3	1.2	1.2	1.1	1.2	-0.054	-0.241	-0.243	-0.244	-0.245
T-216	-1.4	-1.5	-1.5	-1.5	-1.4	0.001	-0.183	-0.183	-0.183	-0.183
T-217	-1.8	-1.8	-1.8	-1.8	-1.7	-0.160	-0.035	-0.032	-0.031	-0.030

T-218	-1.3	-1.3	-1.3	-1.4	-1.3	-0.326	-0.210	-0.210	-0.210	-0.211
T-219	-1.8	-1.8	-1.8	-1.9	-1.8	-0.037	-0.221	-0.221	-0.221	-0.221
T-301	-0.3	-0.3	-0.3	-0.3	-0.3	-0.006	-0.006	-0.005	-0.005	-0.004
T-302	-0.7	-0.8	-1.0	-1.1	-1.2	0.037	0.024	0.012	0.005	0.002
T-303	1.7	1.6	1.7	1.6	1.6	-0.010	-0.013	-0.015	-0.016	-0.016
T-304	1.4	1.4	1.7	1.7	1.8	0.003	0.013	0.023	0.028	0.031
T-305	0.7	0.5	0.3	0.1	0.0	0.018	0.002	-0.012	-0.020	-0.022
T-306	2.4	2.4	2.4	2.4	2.4	-0.008	-0.008	-0.007	-0.007	-0.007
T-307	1.9	1.9	2.1	2.2	2.3	-0.034	-0.028	-0.017	-0.012	-0.009
T-308	0.2	0.2	0.1	0.1	0.0	-0.392	-0.402	-0.405	-0.407	-0.409
T-309	-0.2	-0.2	-0.3	-0.3	-0.3	0.024	0.021	0.018	0.016	0.016
T-310	-3.1	-3.0	-3.1	-3.1	-3.1	-0.001	-0.003	-0.003	-0.004	-0.003
T-311	-2.0	-1.9	-1.9	-2.0	-2.0	0.298	0.310	0.307	0.305	0.304
T-312	0.2	0.1	0.1	0.0	0.1	0.018	0.016	0.016	0.015	0.016
T-313	-1.9	-1.8	-1.7	-1.6	-1.6	0.028	0.032	0.038	0.041	0.043
T-314	0.6	0.6	0.7	0.7	0.8	0.266	0.274	0.277	0.278	0.279
T-315	0.5	0.4	0.5	0.4	0.4	-0.184	-0.185	-0.184	-0.184	-0.183
T-316	-0.1	-0.1	0.1	0.0	0.1	-0.110	-0.107	-0.103	-0.101	-0.099
T-317	-0.8	-0.8	-0.8	-0.8	-0.8	0.125	0.129	0.129	0.128	0.129
T-318	0.1	0.0	0.1	0.0	0.0	-0.022	-0.022	-0.021	-0.021	-0.020
T-319	-0.6	-0.6	-0.6	-0.5	-0.5	-0.051	-0.049	-0.045	-0.043	-0.042
T-401	0.3	0.3	0.3	0.2	0.1	0.397	0.402	0.397	0.394	0.393
T-402	0.8	0.6	0.2	-0.2	-0.4	-0.102	-0.123	-0.152	-0.166	-0.172
T-403	-1.4	-1.4	-1.3	-1.3	-1.3	-0.171	-0.176	-0.173	-0.171	-0.170
T-404	1.9	2.0	2.1	2.0	2.0	0.114	0.125	0.126	0.127	0.127
T-405	2.9	2.9	2.8	2.7	2.7	0.179	0.178	0.173	0.170	0.169
T-406	2.7	2.7	2.8	2.8	2.8	-0.153	-0.157	-0.153	-0.150	-0.149
T-407	2.0	2.1	2.2	2.3	2.4	-0.158	-0.159	-0.149	-0.142	-0.139
T-408	-3.7	-3.7	-3.7	-3.8	-3.8	-0.018	-0.021	-0.023	-0.025	-0.026
T-409	-0.7	-0.7	-0.7	-0.8	-0.8	-0.134	-0.140	-0.141	-0.141	-0.141
T-410	-1.6	-1.6	-1.5	-1.6	-1.6	0.123	0.121	0.122	0.123	0.124
T-411	-3.0	-2.9	-2.8	-2.8	-2.8	0.063	0.069	0.071	0.073	0.074
T-412	0.2	0.1	0.2	0.1	0.2	-0.231	-0.237	-0.236	-0.234	-0.234
T-413	-1.6	-1.5	-1.5	-1.6	-1.6	0.136	0.144	0.143	0.142	0.142
T-414	0.2	0.4	0.5	0.5	0.5	0.070	0.084	0.090	0.092	0.092
T-415	0.6	0.6	0.7	0.7	0.7	-0.322	-0.327	-0.324	-0.321	-0.320
T-416	1.7	1.8	1.7	1.6	1.6	0.425	0.434	0.430	0.428	0.427
T-417	0.0	0.1	0.2	0.2	0.2	-0.138	-0.134	-0.129	-0.126	-0.125
T-418	0.3	0.4	0.4	0.4	0.5	-0.157	-0.161	-0.157	-0.154	-0.153
T-419	-2.1	-2.0	-2.1	-2.1	-2.2	0.077	0.083	0.081	0.079	0.078
T-501	-1.6	-1.5	-1.5	-1.6	-1.5	0.259	0.265	0.265	0.265	0.266

T-502	-2.3	-2.3	-2.4	-2.6	-2.7	0.237	0.244	0.235	0.229	0.227
T-503	0.3	0.3	0.3	0.2	0.3	-0.041	-0.036	-0.037	-0.038	-0.038
T-504	0.2	0.0	-0.1	0.6	0.8	-0.057	-0.350	-0.344	-0.341	-0.339
T-505	-0.7	-0.7	-0.8	-0.8	-0.8	-0.159	-0.165	-0.167	-0.168	-0.168
T-506	0.7	0.8	0.9	0.9	0.9	-0.036	-0.027	-0.024	-0.022	-0.021
T-507	0.5	0.6	0.7	0.7	0.8	-0.069	0.115	0.123	0.127	0.129
T-508	-3.1	-3.1	-3.1	-3.2	-3.1	-0.170	-0.171	-0.173	-0.173	-0.172
T-509	2.7	2.7	2.7	2.6	2.6	-0.034	-0.029	-0.032	-0.034	-0.034
T-510	3.0	3.0	3.0	2.9	2.9	-0.002	0.003	0.001	-0.001	-0.001
T-511	2.1	2.2	2.2	2.2	2.3	0.162	0.171	0.175	0.176	0.178
T-512	3.6	3.7	3.7	3.6	3.6	-0.042	-0.035	-0.035	-0.035	-0.035
T-513	-3.7	-3.7	-3.6	-3.6	-3.6	-0.037	-0.030	-0.027	-0.025	-0.024
T-514	-2.2	-2.0	-2.1	-2.3	-2.3	0.130	0.147	0.140	0.136	0.135
T-515	3.6	3.6	3.6	3.6	3.6	-0.092	-0.086	-0.086	-0.086	-0.085
T-516	-1.6	-1.5	-1.5	-1.5	-1.4	-0.044	-0.038	-0.036	-0.035	-0.034
T-517	-2.9	-2.9	-2.9	-3.0	-2.9	0.106	0.106	0.104	0.103	0.103
T-518	-1.1	-1.0	-1.0	-1.1	-1.0	-0.034	-0.027	-0.026	-0.026	-0.025
T-519	2.3	2.3	2.4	2.3	2.4	-0.069	-0.062	-0.061	-0.060	-0.058
T-601	-1.9	-2.0	-2.1	-2.2	-2.0	0.334	0.336	0.330	0.326	0.324
T-602	2.0	1.9	2.1	2.2	2.5	-0.185	-0.186	-0.176	-0.170	-0.167
T-603	4.2	4.1	4.5	4.6	0.7	0.040	0.057	0.075	0.085	0.089
T-604	2.5	3.2	3.1	3.0	3.3	0.046	0.065	0.090	0.104	0.111
T-605	-2.6	-2.9	-3.2	-2.5	-1.8	0.042	0.024	-0.004	-0.020	-0.027
T-606	2.0	1.9	1.9	1.8	2.0	-0.035	-0.037	-0.040	-0.042	-0.043
T-607	-1.1	-1.2	-1.2	-1.3	-1.0	0.003	0.002	0.001	0.000	0.000
T-608	3.4	3.3	3.5	3.7	4.1	0.017	0.026	0.038	0.045	0.049
T-609	2.0	1.7	1.6	1.4	1.5	-0.012	-0.017	-0.030	-0.037	-0.041
T-610	1.3	1.0	1.0	0.8	1.0	-0.025	-0.031	-0.040	-0.045	-0.048
T-611	-1.0	-1.0	-0.9	-0.8	-0.5	0.231	0.247	0.253	0.256	0.257
T-612	-0.9	-1.2	-1.2	-1.4	-1.2	-0.093	-0.099	-0.107	-0.112	-0.114
T-613	-3.4	-3.6	-3.6	-3.7	-3.5	0.033	0.031	0.026	0.024	0.023
T-614	-0.4	-0.5	-0.7	-0.9	-1.0	-0.116	-0.124	-0.139	-0.147	-0.151
T-615	-0.9	-1.0	-1.0	-1.2	-1.0	-0.047	-0.046	-0.051	-0.055	-0.056
T-616	3.3	3.1	3.1	3.0	3.2	-0.012	-0.010	-0.015	-0.018	-0.019
T-617	0.4	0.5	0.7	0.9	1.0	0.116	0.124	0.139	0.148	0.151
T-618	-4.7	-3.7	-3.1	-4.0	-4.2	-0.305	-0.313	-0.302	-0.294	-0.291
T-619	-3.6	-3.8	-3.9	-4.0	-3.8	-0.039	-0.042	-0.047	-0.051	-0.052
T-701	-2.0	-2.0	-2.0	-2.0	-2.1	0.148	0.147	0.147	0.147	0.146
T-702	0.2	0.1	0.1	0.1	0.1	-0.038	-0.043	-0.046	-0.047	-0.047
T-703	2.7	2.8	2.8	2.9	2.8	0.052	0.056	0.058	0.059	0.059
T-704	2.3	2.4	2.5	2.6	2.5	-0.077	-0.072	-0.066	-0.063	-0.062

T-705	2.9	3.0	3.0	3.0	2.9	0.065	0.067	0.067	0.068	0.068
T-706	4.0	4.0	4.0	4.1	4.0	-0.125	-0.125	-0.124	-0.123	-0.123
T-707	3.1	3.1	3.2	3.3	3.3	0.054	0.056	0.062	0.065	0.066
T-708	-4.1	-4.0	-4.0	-4.0	-4.0	-0.118	-0.118	-0.116	-0.114	-0.114
T-709	-1.2	-1.2	-1.2	-1.2	-1.3	0.112	0.109	0.108	0.108	0.108
T-710	-1.7	-1.6	-1.7	-1.6	-1.7	0.315	0.311	0.310	0.310	0.310
T-711	1.3	1.3	1.1	1.1	1.0	0.101	0.097	0.089	0.086	0.085
T-712	2.0	2.0	2.0	2.0	2.0	0.018	0.018	0.017	0.017	0.017
T-713	0.2	0.2	0.2	0.2	0.1	0.054	0.049	0.048	0.048	0.047
T-714	-1.4	-1.3	-1.3	-1.3	-1.4	-0.219	-0.215	-0.215	-0.215	-0.216
T-715	-1.5	-1.5	-1.5	-1.4	-1.5	-0.202	-0.202	-0.201	-0.200	-0.200
T-716	-1.8	-1.8	-1.8	-1.7	-1.8	-0.030	-0.031	-0.030	-0.029	-0.029
T-717	-1.2	-1.1	-1.2	-1.3	-1.4	0.102	0.104	0.098	0.095	0.094
T-718	-2.2	-2.1	-2.1	-2.1	-2.2	-0.044	-0.045	-0.046	-0.046	-0.046
T-719	-2.2	-2.1	-2.1	-2.0	-2.1	-0.170	-0.171	-0.169	-0.168	-0.168
T-801	2.0	2.0	2.1	2.1	2.1	-0.125	-0.126	-0.124	-0.123	-0.123
T-802	-0.2	-0.1	-0.1	-0.1	-0.1	0.038	0.043	0.046	0.047	0.047
T-803	2.1	2.3	2.4	2.3	2.3	0.162	0.167	0.170	0.172	0.172
T-804	1.0	1.1	1.3	1.4	1.4	-0.135	-0.128	-0.119	-0.114	-0.112
T-805	2.2	2.2	2.0	1.7	1.6	-0.007	-0.020	-0.036	-0.045	-0.049
T-806	2.7	2.8	2.9	2.9	2.9	0.183	0.183	0.187	0.189	0.190
T-807	1.9	2.1	2.2	2.3	2.4	-0.127	-0.123	-0.114	-0.108	-0.106
T-808	-1.1	-1.0	-1.0	-1.0	-1.0	-0.121	-0.122	-0.123	-0.122	-0.121
T-809	-0.5	-0.4	-0.5	-0.6	-0.6	0.223	0.218	0.214	0.213	0.212
T-810	-1.2	-1.1	-1.1	-1.2	-1.2	-0.077	-0.082	-0.084	-0.085	-0.085
T-811	-1.3	-1.3	-1.5	-1.7	-1.8	0.240	0.231	0.218	0.211	0.209
T-812	-1.8	-3.9	-3.9	-3.9	-3.9	0.040	0.037	0.037	0.037	0.037
T-813	-3.0	-2.9	-2.8	-2.7	-2.7	-0.261	-0.262	-0.257	-0.254	-0.253
T-814	0.2	0.4	0.2	0.1	0.0	0.222	0.225	0.214	0.209	0.207
T-815	0.1	0.2	0.2	0.2	0.2	-0.185	-0.187	-0.186	-0.185	-0.184
T-816	-0.4	-0.3	-0.2	-0.2	-0.2	-0.163	-0.164	-0.160	-0.158	-0.157
T-817	-3.4	-3.3	-3.2	-3.2	-3.2	0.056	0.058	0.063	0.066	0.067
T-818	-0.8	-0.7	-0.7	-0.7	-0.7	-0.089	-0.089	-0.087	-0.085	-0.085
T-819	1.8	1.9	2.0	2.0	2.0	0.135	0.135	0.138	0.141	0.142

[a] $\mathbf{E_{a,f}}$**:** Activation energy of the forward reaction, given in kJ mol^{-1}.

[b] $\mathbf{log\widetilde{A}_f}$**:** Logarithm of the pre-exponential factor of the forward reaction, given in m^3 mol^{-1} s^{-1}.

Table D-13 The deviations between the CBS-QB3 data and the GA-based data calculated with the ΔGAV°s and ΔNNI° parameters for the reverse direction with respect to the reference reaction, given in **Table D-10** and **Table D-11**, respectively.

Reaction #	$E_{a,r}$[a]					$\log\widetilde{A}_r$ [b]				
	300 K	600 K	1000 K	1500 K	2000 K	300 K	600 K	1000 K	1500 K	2000 K
T-101	0.1	0.1	0.0	0.2	0.3	0.059	0.069	0.076	0.082	0.085
T-102	0.5	0.5	0.6	0.8	1.0	0.222	0.212	0.219	0.230	0.236
T-103	2.6	2.6	2.7	2.9	3.0	0.233	0.244	0.252	0.258	0.262
T-104	1.1	1.1	1.1	1.0	1.0	0.229	0.217	0.213	0.212	0.211
T-105	1.2	1.2	1.1	0.9	0.7	0.247	0.262	0.257	0.246	0.240
T-106	2.8	2.8	2.9	3.1	3.2	0.220	0.228	0.234	0.239	0.242
T-107	1.9	1.9	2.0	2.1	2.1	0.260	0.271	0.274	0.275	0.276
T-108	1.6	2.4	2.9	3.3	3.6	0.224	0.318	0.353	0.371	0.381
T-109	1.4	1.4	1.5	1.7	1.9	0.240	0.233	0.226	0.219	0.215
T-110	3.1	2.9	2.8	2.9	2.8	0.170	0.180	0.184	0.183	0.186
T-111	3.7	3.9	3.9	3.9	3.9	0.200	0.225	0.225	0.226	0.226
T-112	1.5	1.5	1.3	1.1	1.0	0.336	0.326	0.319	0.312	0.309
T-113	0.2	0.2	0.3	0.3	0.3	0.347	0.340	0.336	0.334	0.337
T-114	1.8	1.8	1.9	1.9	1.9	0.215	0.220	0.218	0.215	0.213
T-115	0.2	0.2	0.1	0.0	0.2	0.113	0.105	0.098	0.093	0.090
T-116	0.8	0.8	0.7	0.6	0.5	0.427	0.434	0.439	0.444	0.447
T-117	0.4	0.5	0.7	0.8	0.9	0.266	0.256	0.247	0.239	0.235
T-118	0.1	0.1	0.0	0.1	0.2	0.206	0.215	0.222	0.227	0.230
T-119	0.9	0.9	0.8	0.7	0.6	0.055	0.050	0.045	0.041	0.038
T-201	1.3	1.3	1.3	1.2	1.2	0.130	0.134	0.139	0.142	0.128
T-202	1.9	1.9	1.9	1.9	1.9	0.154	0.148	0.143	0.141	0.154
T-203	1.4	1.4	1.4	1.5	1.4	0.143	0.148	0.154	0.157	0.144
T-204	1.5	1.4	1.4	1.2	1.2	0.128	0.126	0.125	0.125	0.110
T-205	1.8	1.8	1.9	1.9	1.9	0.186	0.182	0.178	0.176	0.189
T-206	2.1	2.1	2.0	2.1	2.0	0.011	0.019	0.027	0.031	0.018
T-207	1.9	1.9	2.0	2.2	2.2	0.125	0.123	0.122	0.121	0.106
T-208	2.7	3.0	3.2	3.5	3.7	0.132	0.096	0.083	0.077	0.090
T-209	0.3	0.3	0.4	0.4	0.5	0.078	0.088	0.098	0.103	0.091
T-210	0.6	0.6	0.5	0.4	0.5	0.135	0.120	0.112	0.109	0.119
T-211	0.1	0.1	0.2	0.2	0.2	0.230	0.231	0.228	0.226	0.240
T-212	0.1	0.1	0.2	0.1	0.2	0.249	0.255	0.262	0.267	0.254
T-213	1.1	1.0	0.9	0.8	0.7	0.076	0.073	0.068	0.067	0.055
T-214	1.4	1.5	1.5	1.5	1.4	0.203	0.203	0.197	0.194	0.207
T-215	1.1	1.1	1.1	1.2	1.1	0.360	0.246	0.175	0.119	0.361
T-216	1.2	1.2	1.2	1.1	1.2	0.366	0.359	0.355	0.353	0.367
T-217	1.3	1.3	1.3	1.2	1.3	0.116	0.112	0.108	0.106	0.120

T-218	1.1	1.1	1.1	1.0	1.1	0.118	0.122	0.126	0.128	0.114
T-219	1.9	1.9	1.9	1.8	1.9	0.102	0.109	0.114	0.116	0.102
T-301	0.2	0.2	0.1	0.2	0.1	0.063	0.065	0.067	0.068	0.068
T-302	0.6	0.6	0.6	0.6	0.6	0.075	0.077	0.078	0.077	0.078
T-303	1.0	1.1	1.0	1.0	1.0	0.023	0.026	0.023	0.022	0.022
T-304	0.5	0.5	0.6	0.7	0.7	0.127	0.124	0.119	0.116	0.114
T-305	0.6	0.6	0.6	0.6	0.6	0.075	0.077	0.078	0.077	0.077
T-306	1.3	1.4	1.3	1.3	1.3	0.069	0.072	0.073	0.074	0.073
T-307	1.3	1.4	1.4	1.5	1.6	0.052	0.049	0.045	0.041	0.038
T-308	2.5	2.6	2.7	2.8	2.8	0.193	0.206	0.211	0.214	0.215
T-309	0.2	0.3	0.2	0.2	0.1	0.410	0.411	0.407	0.404	0.403
T-310	1.9	2.0	2.1	2.1	2.2	0.274	0.269	0.264	0.261	0.255
T-311	2.5	2.6	2.7	2.8	2.8	0.193	0.205	0.211	0.214	0.214
T-312	1.0	1.0	1.0	1.0	1.0	0.145	0.148	0.150	0.151	0.151
T-313	2.5	2.4	2.3	2.1	2.1	0.333	0.350	0.359	0.362	0.360
T-314	0.8	0.8	0.8	0.7	0.7	0.014	0.017	0.020	0.020	0.021
T-315	0.5	0.5	0.5	0.5	0.5	0.437	0.441	0.443	0.444	0.443
T-316	0.0	0.0	0.0	0.1	0.1	0.088	0.092	0.092	0.091	0.089
T-317	0.8	0.8	0.8	0.7	0.7	0.014	0.018	0.019	0.020	0.021
T-318	0.4	0.4	0.3	0.4	0.4	0.065	0.068	0.069	0.070	0.069
T-319	0.4	0.4	0.4	0.4	0.4	0.005	0.002	0.002	0.003	0.004
T-401	0.5	0.6	0.6	0.5	0.4	0.384	0.391	0.385	0.382	0.381
T-402	0.0	0.0	0.0	0.0	0.0	0.000	0.000	0.000	0.000	0.000
T-403	3.4	3.4	3.3	3.2	3.3	0.184	0.182	0.179	0.176	0.174
T-404	0.3	0.2	0.2	0.2	0.3	0.085	0.093	0.091	0.090	0.090
T-405	3.1	3.1	3.0	2.9	2.8	0.282	0.276	0.268	0.264	0.264
T-406	0.7	0.6	0.6	0.5	0.5	0.171	0.172	0.168	0.165	0.163
T-407	0.7	0.7	0.5	0.4	0.4	0.182	0.183	0.176	0.171	0.168
T-408	1.8	2.0	2.2	2.3	2.4	0.144	0.114	0.100	0.095	0.093
T-409	0.1	0.1	0.1	0.1	0.0	0.156	0.160	0.162	0.162	0.161
T-410	1.6	1.5	1.5	1.4	1.4	0.126	0.137	0.139	0.140	0.144
T-411	1.7	1.8	1.8	1.8	1.8	0.360	0.368	0.369	0.370	0.371
T-412	0.8	0.8	0.8	0.7	0.8	0.330	0.332	0.331	0.330	0.328
T-413	0.0	0.1	0.2	0.0	0.0	0.023	0.008	0.008	0.009	0.013
T-414	1.7	1.8	1.9	1.9	1.8	0.255	0.264	0.268	0.268	0.269
T-415	0.4	0.4	0.5	0.5	0.5	0.346	0.348	0.345	0.343	0.340
T-416	0.2	0.1	0.1	0.2	0.3	0.013	0.019	0.014	0.012	0.012
T-417	1.2	1.3	1.3	1.4	1.3	0.075	0.075	0.078	0.080	0.081
T-418	0.2	0.2	0.3	0.3	0.3	0.161	0.162	0.159	0.157	0.155
T-419	3.0	2.9	2.9	3.0	3.1	0.085	0.091	0.087	0.084	0.084
T-501	1.5	1.4	1.4	1.4	1.4	0.184	0.186	0.186	0.185	0.185

T-502	0.2	0.5	0.8	0.9	1.0	0.023	0.019	0.037	0.043	0.044
T-503	1.0	0.9	1.0	0.9	1.0	0.094	0.086	0.086	0.086	0.087
T-504	1.7	1.8	1.8	1.9	1.9	0.085	0.083	0.080	0.078	0.078
T-505	0.7	0.6	0.6	0.6	0.6	0.139	0.149	0.150	0.150	0.151
T-506	2.2	2.1	2.0	1.9	1.9	0.070	0.063	0.058	0.056	0.056
T-507	2.1	2.0	2.0	1.8	1.8	0.039	0.034	0.029	0.026	0.025
T-508	2.0	2.1	2.1	2.1	2.0	0.007	0.015	0.015	0.015	0.015
T-509	2.0	2.0	2.0	2.0	2.0	0.065	0.061	0.062	0.064	0.065
T-510	3.5	3.2	2.6	2.3	2.0	0.063	0.061	0.058	0.055	0.054
T-511	1.1	1.2	1.1	1.0	1.0	0.018	0.019	0.014	0.011	0.010
T-512	2.3	2.4	2.4	2.5	2.4	0.268	0.273	0.274	0.274	0.274
T-513	3.4	3.3	3.1	2.9	2.8	0.082	0.072	0.066	0.064	0.063
T-514	1.3	1.4	1.3	1.2	1.2	0.149	0.163	0.158	0.155	0.153
T-515	3.3	3.3	3.3	3.4	3.4	0.152	0.149	0.148	0.148	0.149
T-516	2.3	2.3	2.3	2.2	2.2	0.226	0.226	0.228	0.228	0.228
T-517	1.1	1.1	1.2	1.2	1.2	0.013	0.018	0.019	0.020	0.021
T-518	1.3	1.3	1.3	1.2	1.2	0.109	0.106	0.105	0.105	0.106
T-519	1.6	1.6	1.6	1.7	1.7	0.072	0.071	0.070	0.070	0.070
T-601	2.4	2.4	2.3	2.1	2.1	0.004	0.001	0.009	0.014	0.017
T-602	0.0	0.0	0.0	0.0	0.0	0.000	0.000	0.000	0.000	0.000
T-603	0.3	0.5	0.8	1.0	1.2	0.150	0.168	0.188	0.200	0.205
T-604	1.7	1.2	0.4	0.1	0.8	0.002	0.004	0.023	0.035	0.040
T-605	0.0	0.0	0.0	0.0	0.0	0.000	0.000	0.000	0.000	0.000
T-606	0.4	0.3	0.4	0.4	0.4	0.048	0.049	0.048	0.048	0.047
T-607	4.6	4.5	4.5	4.5	4.5	0.013	0.016	0.017	0.017	0.018
T-608	0.0	0.0	0.0	0.0	0.0	0.000	0.000	0.000	0.000	0.000
T-609	0.9	0.9	0.8	0.6	0.6	0.039	0.038	0.028	0.023	0.020
T-610	3.2	3.3	3.1	3.0	3.0	0.003	0.007	0.014	0.017	0.019
T-611	0.9	0.9	1.0	1.1	1.1	0.017	0.020	0.027	0.030	0.031
T-612	2.8	3.0	3.2	3.6	3.8	0.023	0.020	0.010	0.005	0.001
T-613	2.5	2.5	2.5	2.6	2.6	0.021	0.025	0.029	0.030	0.031
T-614	1.7	1.8	2.1	2.4	2.5	0.145	0.160	0.178	0.188	0.193
T-615	1.9	1.8	1.9	2.0	2.0	0.022	0.022	0.019	0.017	0.016
T-616	2.3	2.4	2.3	2.2	2.2	0.028	0.031	0.035	0.036	0.037
T-617	0.8	0.9	1.1	1.2	1.3	0.127	0.139	0.152	0.159	0.162
T-618	2.2	1.7	1.5	0.7	0.1	0.216	0.223	0.210	0.199	0.196
T-619	2.4	2.4	2.4	2.5	2.5	0.002	0.004	0.008	0.010	0.011
T-701	1.1	1.1	1.1	1.2	1.2	0.251	0.255	0.255	0.254	0.253
T-702	3.1	3.1	3.2	3.3	3.2	0.063	0.069	0.071	0.072	0.072
T-703	2.4	2.5	2.5	2.5	2.5	0.122	0.129	0.132	0.132	0.132
T-704	0.5	0.5	0.5	0.5	0.5	0.030	0.030	0.026	0.025	0.025

T-705	1.8	1.8	1.7	1.6	1.6	0.020	0.015	0.008	0.005	0.004
T-706	2.7	2.7	2.6	2.5	2.5	0.043	0.048	0.052	0.054	0.055
T-707	0.5	0.5	0.6	0.5	0.5	0.156	0.159	0.162	0.163	0.163
T-708	3.6	3.8	3.8	3.9	3.9	0.102	0.130	0.137	0.138	0.138
T-709	0.8	0.7	0.7	0.7	0.8	0.208	0.212	0.213	0.213	0.213
T-710	1.8	1.8	1.9	1.9	1.9	0.284	0.277	0.274	0.273	0.273
T-711	0.7	0.8	0.8	0.8	0.8	0.052	0.044	0.041	0.039	0.038
T-712	0.8	0.9	0.9	0.8	0.8	0.088	0.083	0.082	0.083	0.083
T-713	0.5	0.6	0.7	0.8	0.8	0.037	0.040	0.041	0.042	0.043
T-714	1.4	1.4	1.5	1.5	1.5	0.261	0.259	0.257	0.257	0.257
T-715	1.3	1.3	1.2	1.3	1.3	0.361	0.357	0.355	0.355	0.355
T-716	2.1	2.1	2.1	2.2	2.2	0.252	0.253	0.253	0.253	0.253
T-717	0.7	0.7	0.7	0.7	0.7	0.089	0.090	0.088	0.086	0.086
T-718	1.2	1.2	1.2	1.2	1.3	0.007	0.011	0.011	0.010	0.010
T-719	2.2	2.2	2.2	2.3	2.3	0.116	0.117	0.116	0.117	0.117
T-801	3.1	3.1	3.0	3.0	3.0	0.355	0.357	0.359	0.359	0.359
T-802	3.1	3.1	3.2	3.3	3.2	0.063	0.069	0.071	0.072	0.072
T-803	1.1	1.1	1.1	1.1	1.1	0.237	0.238	0.239	0.239	0.239
T-804	0.3	0.3	0.3	0.2	0.1	0.086	0.087	0.084	0.082	0.081
T-805	1.8	1.8	1.7	1.6	1.6	0.020	0.015	0.008	0.005	0.004
T-806	1.0	1.0	1.0	1.0	1.1	0.286	0.287	0.289	0.290	0.290
T-807	0.1	0.1	0.1	0.1	0.2	0.052	0.053	0.050	0.047	0.046
T-808	2.3	2.4	2.5	2.6	2.7	0.267	0.268	0.262	0.258	0.256
T-809	1.8	1.9	2.0	2.0	2.1	0.244	0.239	0.233	0.230	0.229
T-810	1.0	1.1	1.0	1.0	1.1	0.013	0.003	0.002	0.005	0.006
T-811	0.3	0.3	0.3	0.2	0.2	0.098	0.097	0.091	0.088	0.087
T-812	4.5	4.5	4.6	4.6	4.6	0.080	0.077	0.075	0.074	0.074
T-813	3.3	3.2	3.1	2.9	2.8	0.315	0.310	0.304	0.301	0.300
T-814	3.3	3.2	3.0	2.8	2.4	0.324	0.344	0.343	0.340	0.340
T-815	0.3	0.3	0.3	0.3	0.3	0.303	0.305	0.307	0.307	0.307
T-816	0.3	0.4	0.4	0.4	0.4	0.092	0.097	0.097	0.097	0.096
T-817	3.6	3.4	3.2	3.1	2.9	0.068	0.079	0.091	0.098	0.101
T-818	0.6	0.6	0.6	0.6	0.6	0.042	0.043	0.043	0.043	0.043
T-819	2.0	1.9	1.9	1.9	1.9	0.210	0.206	0.205	0.206	0.206

[a] $\mathbf{E_{a,r}}$**:** Activation energy of the reverse reaction, given in kJ mol^{-1}.

[b] $\mathbf{log}\widetilde{\boldsymbol{A}}_{\mathbf{r}}$**:** Logarithm of the pre-exponential factor of the reverse reaction, given in m^3 mol^{-1} s^{-1}.

Table D-14 Factor of deviations (ρ) between the reaction rate coefficients calculated by CBS-QB3 and the set of ΔGAV°/ΔNNI° parameters reported in **Table D-10** and **Table D-11** for the training set.[a]

Reaction #	Factor of deviation									
	Forward					Reverse				
	300 K	600 K	1000 K	1500 K	2000 K	300 K	600 K	1000 K	1500 K	2000 K
T-101	1.63	1.17	1.04	1.00	1.03	1.25	1.10	1.08	1.09	1.26
T-102	1.07	1.02	1.01	1.01	1.01	1.30	1.60	1.69	1.74	1.53
T-103	1.14	1.71	2.05	2.27	2.38	1.58	1.05	1.17	1.31	1.61
T-104	1.41	1.26	1.18	1.14	1.12	1.02	1.43	1.58	1.65	1.45
T-105	3.20	1.89	1.46	1.27	1.19	1.15	1.31	1.43	1.49	1.75
T-106	4.41	2.33	1.78	1.54	1.44	1.79	1.13	1.10	1.24	1.52
T-107	1.44	1.38	1.85	2.17	2.33	1.14	1.16	1.35	1.46	1.76
T-108	1.02	1.13	1.15	1.16	1.17	1.20	1.39	1.74	1.97	1.83
T-109	1.22	1.00	1.07	1.09	1.11	2.95	2.47	2.22	2.08	1.74
T-110	1.31	1.04	1.04	1.07	1.09	4.76	3.16	2.52	2.23	1.72
T-111	1.16	1.73	1.72	1.62	1.56	2.88	1.20	1.15	1.35	1.26
T-112	1.38	1.05	1.05	1.09	1.11	1.15	1.72	1.95	2.05	1.81
T-113	1.51	1.24	1.13	1.07	1.04	2.30	2.66	2.62	2.57	2.09
T-114	1.70	1.23	1.14	1.11	1.09	3.51	2.19	1.87	1.74	1.93
T-115	2.14	2.47	2.57	2.60	1.03	1.14	1.32	1.36	1.36	1.18
T-116	2.06	1.60	1.47	1.42	1.15	3.82	2.93	2.72	2.66	2.13
T-117	1.01	1.06	1.06	1.05	1.05	2.23	1.83	1.73	1.69	1.91
T-118	1.20	1.01	1.06	1.09	1.10	1.78	1.55	1.52	1.52	1.77
T-119	1.19	1.05	1.13	1.15	1.17	1.31	1.02	1.10	1.14	1.00
T-201	2.08	1.10	1.18	1.41	1.46	1.45	1.28	1.36	1.49	1.18
T-202	1.48	1.73	1.02	1.46	1.42	1.26	1.25	1.03	1.00	1.34
T-203	2.30	2.22	1.22	1.70	1.62	2.09	2.26	1.94	1.91	1.44
T-204	1.12	1.41	1.07	1.42	1.42	1.59	1.21	1.30	1.43	1.14
T-205	2.12	2.03	1.11	1.53	1.46	1.16	1.15	1.05	1.08	1.46
T-206	2.69	2.45	1.32	1.82	1.73	2.03	1.92	1.56	1.50	1.11
T-207	3.32	2.79	1.43	1.92	1.80	2.41	2.37	1.94	1.86	1.38
T-208	4.90	1.43	1.57	1.14	1.23	5.39	3.17	2.10	1.60	1.84
T-209	1.53	1.18	1.19	1.34	1.37	1.09	1.39	1.37	1.46	1.14
T-210	1.78	1.23	1.07	1.53	1.58	1.27	1.09	1.00	1.02	1.36
T-211	2.33	1.20	1.67	1.05	1.02	1.93	1.37	1.44	1.40	1.81
T-212	1.29	1.73	1.09	1.63	1.61	1.43	2.11	2.06	2.16	1.68
T-213	1.08	1.49	1.00	1.53	1.53	1.54	1.25	1.29	1.38	1.02
T-214	1.30	1.26	1.45	1.05	1.10	1.05	1.02	1.15	1.17	1.56
T-215	1.82	2.20	1.32	1.92	1.88	3.09	2.20	1.65	1.46	1.05
T-216	1.86	1.12	1.20	1.35	1.39	4.46	2.42	2.28	2.09	2.64
T-217	1.52	1.48	1.13	1.86	1.93	2.59	1.39	1.30	1.19	1.50

T-218	1.22	2.45	1.81	2.03	2.14	1.41	1.28	1.34	1.46	1.16
T-219	1.97	1.14	1.15	1.43	1.49	2.00	1.06	1.18	1.33	1.07
T-301	1.13	1.05	1.02	1.01	1.00	1.05	1.02	1.04	1.01	1.09
T-302	1.46	1.25	1.16	1.11	1.08	1.80	1.57	1.57	1.49	1.34
T-303	1.95	1.42	1.25	1.18	1.14	1.22	1.01	1.15	1.16	1.07
T-304	1.68	1.29	1.15	1.08	1.04	1.38	1.26	1.14	1.15	1.25
T-305	1.20	1.08	1.06	1.05	1.05	1.28	1.15	1.05	1.06	1.14
T-306	2.57	1.62	1.35	1.23	1.17	1.70	1.31	1.12	1.10	1.18
T-307	2.21	1.55	1.33	1.22	1.17	1.61	1.25	1.06	1.04	1.11
T-308	2.63	2.58	2.57	2.56	2.56	2.11	1.23	1.04	1.10	1.28
T-309	1.16	1.10	1.08	1.06	1.06	2.78	2.89	3.09	3.00	2.73
T-310	3.43	1.84	1.43	1.27	1.19	4.86	3.02	2.73	2.44	2.24
T-311	4.43	2.99	2.56	2.36	2.27	1.49	1.11	1.44	1.55	1.50
T-312	1.03	1.03	1.03	1.03	1.03	1.25	1.02	1.01	1.09	1.23
T-313	2.28	1.56	1.34	1.25	1.21	7.06	3.96	3.48	3.09	2.84
T-314	1.51	1.67	1.75	1.80	1.82	1.74	1.42	1.40	1.32	1.19
T-315	1.76	1.65	1.60	1.58	1.57	2.87	2.60	2.38	2.42	2.64
T-316	1.21	1.25	1.26	1.27	1.26	1.05	1.05	1.00	1.04	1.14
T-317	1.91	1.60	1.49	1.44	1.41	1.17	1.04	1.07	1.07	1.01
T-318	1.02	1.04	1.05	1.05	1.05	1.15	1.07	1.01	1.01	1.11
T-319	1.17	1.01	1.04	1.06	1.07	1.40	1.29	1.30	1.24	1.12
T-401	2.28	2.39	2.43	2.45	2.45	2.20	2.60	2.79	2.66	2.44
T-402	1.69	1.48	1.44	1.45	1.45	4.31	1.20	1.38	1.63	1.65
T-403	1.20	1.12	1.26	1.33	1.37	2.92	1.55	1.21	1.01	1.18
T-404	1.62	1.11	1.05	1.14	1.19	1.55	1.55	1.56	1.44	1.30
T-405	2.06	1.17	1.07	1.19	1.25	1.62	1.21	1.59	1.67	1.61
T-406	4.09	2.43	1.97	1.77	1.67	1.00	1.09	1.12	1.22	1.36
T-407	3.16	2.15	1.83	1.67	1.59	1.01	1.11	1.14	1.25	1.38
T-408	4.29	2.01	1.49	1.28	1.18	3.24	2.33	2.01	1.72	1.49
T-409	1.00	1.18	1.26	1.30	1.32	1.31	1.23	1.19	1.27	1.40
T-410	2.56	1.83	1.60	1.50	1.46	2.22	1.67	1.44	1.44	1.45
T-411	3.87	2.11	1.67	1.49	1.40	1.33	1.97	2.32	2.32	2.19
T-412	1.76	1.75	1.74	1.74	1.73	1.35	1.52	1.59	1.75	1.96
T-413	2.66	1.91	1.68	1.58	1.53	1.08	1.07	1.11	1.05	1.01
T-414	1.09	1.14	1.17	1.19	1.20	1.05	1.55	1.83	1.83	1.73
T-415	2.64	2.38	2.27	2.22	2.19	2.26	2.00	1.90	2.00	2.17
T-416	1.40	1.94	2.21	2.36	2.43	1.24	1.27	1.29	1.20	1.08
T-417	1.36	1.37	1.37	1.36	1.35	1.21	1.11	1.25	1.24	1.15
T-418	1.61	1.53	1.50	1.48	1.46	1.37	1.26	1.21	1.28	1.40
T-419	2.83	1.84	1.55	1.42	1.36	4.56	2.65	2.14	1.77	1.52
T-501	3.52	2.54	2.19	2.10	2.03	3.39	2.40	2.23	2.03	1.81

T-502	4.51	2.82	2.28	2.09	1.98	1.43	1.25	1.24	1.15	1.04
T-503	1.20	1.14	1.14	1.11	1.11	1.50	1.17	1.13	1.05	1.06
T-504	1.02	1.27	1.39	1.57	1.75	1.99	1.48	1.22	1.18	1.24
T-505	1.06	1.24	1.35	1.37	1.40	1.48	1.36	1.24	1.25	1.35
T-506	1.42	1.23	1.18	1.12	1.10	2.50	1.54	1.37	1.22	1.07
T-507	1.38	1.26	1.24	1.18	1.17	2.61	1.63	1.45	1.30	1.14
T-508	2.40	1.28	1.03	1.15	1.23	2.68	1.70	1.52	1.35	1.19
T-509	3.06	1.80	1.49	1.32	1.26	2.07	1.47	1.20	1.15	1.20
T-510	3.25	1.80	1.45	1.26	1.19	4.84	2.33	1.43	1.18	1.16
T-511	1.55	1.02	1.13	1.26	1.32	1.84	1.40	1.35	1.25	1.12
T-512	4.55	2.22	1.70	1.44	1.34	1.12	1.36	1.72	1.83	1.76
T-513	4.21	1.98	1.44	1.27	1.18	3.36	1.91	1.52	1.30	1.11
T-514	3.28	2.14	1.77	1.65	1.57	1.02	1.29	1.51	1.54	1.44
T-515	5.02	2.47	1.90	1.62	1.51	4.31	2.34	1.72	1.56	1.59
T-516	1.74	1.26	1.09	1.04	1.01	5.28	3.14	2.72	2.40	2.10
T-517	4.16	2.31	1.79	1.61	1.52	1.26	1.04	1.11	1.13	1.06
T-518	1.48	1.18	1.06	1.03	1.01	1.63	1.19	1.12	1.03	1.09
T-519	2.84	1.81	1.54	1.38	1.32	1.81	1.39	1.17	1.13	1.20
T-601	4.79	3.29	2.76	2.53	2.38	2.18	1.38	1.10	1.04	1.09
T-602	3.31	2.22	1.91	1.76	1.71	1.20	1.17	1.22	1.18	1.08
T-603	4.61	1.99	1.43	1.19	1.10	1.51	1.57	1.71	1.73	1.61
T-604	6.07	2.27	1.53	1.23	1.12	3.94	3.26	1.81	1.40	1.32
T-605	7.03	2.82	1.87	1.50	1.31	1.20	1.17	1.23	1.18	1.09
T-606	2.34	1.56	1.36	1.27	1.24	1.58	1.41	1.43	1.37	1.24
T-607	1.61	1.30	1.17	1.11	1.06	7.14	2.79	2.02	1.64	1.37
T-608	3.61	1.82	1.39	1.21	1.14	1.20	1.17	1.22	1.18	1.08
T-609	2.15	1.46	1.29	1.22	1.20	1.09	1.07	1.19	1.19	1.10
T-610	1.67	1.31	1.22	1.18	1.18	3.06	1.65	1.23	1.12	1.16
T-611	2.61	2.18	2.00	1.93	1.87	1.14	1.02	1.15	1.16	1.09
T-612	1.24	1.02	1.09	1.16	1.21	3.04	2.81	1.65	1.34	1.31
T-613	4.43	2.23	1.65	1.42	1.30	3.10	1.82	1.55	1.36	1.18
T-614	1.09	1.20	1.26	1.31	1.33	1.71	1.17	1.05	1.08	1.24
T-615	1.32	1.11	1.02	1.03	1.07	2.69	1.79	1.60	1.44	1.26
T-616	3.63	1.89	1.49	1.32	1.27	2.26	1.46	1.17	1.10	1.15
T-617	1.15	1.23	1.27	1.31	1.33	1.16	1.34	1.52	1.54	1.45
T-618	3.18	2.03	1.15	1.15	1.33	3.39	2.19	1.46	1.14	1.07
T-619	4.14	1.98	1.44	1.23	1.11	2.51	1.87	1.61	1.41	1.23
T-701	3.25	2.13	1.80	1.65	1.59	3.32	2.61	2.52	2.33	2.08
T-702	1.17	1.12	1.12	1.12	1.12	2.54	1.38	1.02	1.08	1.06
T-703	2.61	1.52	1.22	1.09	1.03	1.68	1.05	1.23	1.31	1.27
T-704	2.93	1.87	1.56	1.41	1.34	1.09	1.01	1.08	1.07	1.01

T-705	2.73	1.54	1.22	1.08	1.02	2.39	1.61	1.47	1.33	1.18
T-706	3.34	2.94	2.14	1.83	1.69	2.76	1.64	1.26	1.17	1.22
T-707	2.96	1.62	1.27	1.12	1.05	1.39	1.51	1.66	1.65	1.53
T-708	3.99	1.74	1.25	1.06	1.02	4.01	1.85	1.42	1.18	1.01
T-709	2.14	1.65	1.49	1.42	1.38	2.59	2.19	2.18	2.05	1.85
T-710	4.10	2.89	2.51	2.34	2.26	1.06	1.55	1.85	1.92	1.81
T-711	1.29	1.02	1.08	1.12	1.15	1.80	1.50	1.48	1.38	1.24
T-712	2.08	1.42	1.22	1.13	1.08	1.44	1.24	1.09	1.09	1.17
T-713	1.07	1.09	1.10	1.10	1.11	1.13	1.14	1.24	1.23	1.14
T-714	1.06	1.25	1.40	1.48	1.52	2.68	2.08	1.77	1.72	1.83
T-715	1.18	1.17	1.32	1.41	1.45	1.14	1.51	1.59	1.73	1.93
T-716	1.99	1.36	1.16	1.08	1.04	1.56	1.00	1.13	1.27	1.45
T-717	2.07	1.62	1.46	1.39	1.35	1.11	1.24	1.38	1.37	1.27
T-718	2.19	1.40	1.17	1.07	1.03	1.95	1.51	1.45	1.34	1.19
T-719	1.63	1.05	1.14	1.24	1.30	2.21	1.39	1.22	1.08	1.05
T-801	2.82	2.00	1.70	1.57	1.51	3.76	1.39	1.15	1.01	1.06
T-802	1.24	1.15	1.13	1.12	1.12	3.61	1.88	1.53	1.30	1.12
T-803	1.56	1.06	1.12	1.23	1.29	1.32	1.62	1.86	1.88	1.76
T-804	1.94	1.67	1.53	1.45	1.41	1.07	1.00	1.04	1.00	1.10
T-805	2.37	1.61	1.37	1.27	1.23	1.68	1.18	1.02	1.05	1.00
T-806	1.87	1.14	1.10	1.23	1.30	1.54	1.85	2.11	2.13	1.99
T-807	2.81	1.99	1.69	1.55	1.47	1.02	1.02	1.08	1.05	1.04
T-808	1.22	1.07	1.17	1.22	1.25	3.90	2.53	2.00	1.88	1.95
T-809	2.12	1.82	1.75	1.71	1.69	4.27	2.93	2.65	2.36	2.08
T-810	1.40	1.05	1.05	1.10	1.13	1.46	1.04	1.08	1.08	1.00
T-811	3.08	2.25	1.99	1.86	1.80	1.33	1.37	1.47	1.43	1.31
T-812	3.21	2.39	1.74	1.49	1.38	4.56	3.42	2.51	2.02	1.69
T-813	1.87	1.02	1.29	1.44	1.52	1.82	1.09	1.14	1.33	1.56
T-814	1.56	1.58	1.61	1.61	1.61	3.86	1.25	1.34	1.63	1.67
T-815	1.54	1.58	1.57	1.56	1.55	1.95	1.85	1.72	1.75	1.90
T-816	1.19	1.36	1.40	1.41	1.42	1.10	1.01	1.03	1.02	1.13
T-817	4.64	2.24	1.71	1.50	1.41	5.85	2.80	2.23	1.90	1.63
T-818	1.18	1.05	1.12	1.15	1.17	1.20	1.07	1.03	1.02	1.06
T-819	1.44	1.06	1.09	1.18	1.23	1.15	1.27	1.56	1.63	1.55

[a]Factor of deviation (ρ): If $k_{AI} > k_{GA}$, then $\rho = \frac{k_{AI}}{k_{GA}}$, if $k_{GA} > k_{AI}$ then $\rho = \frac{k_{GA}}{k_{AI}}$ where k_{AI} denotes reaction rate coefficients calculated with *ab initio* methods and k_{GA} denotes reaction rate coefficients calculated with group additive parameters reported in this study, namely the ΔGAV°/ΔNNI° parameters reported in **Table D-10** and **Table D-11**.

Table D-15 Statistics demonstrating performance of the simultaneously optimized GA parameters.

		Forward					Reverse				
		300 K	**600 K**	**1000 K**	**1500 K**	**2000 K**	**300 K**	**600 K**	**1000 K**	**1500 K**	**2000 K**
E_a[a]	**MAD**[c]	1.7	1.7	1.7	1.7	1.7	1.4	1.5	1.5	1.5	1.5
	MAX[d]	4.7	4.1	4.5	4.6	4.2	4.6	4.5	4.6	4.6	4.6
$\log\tilde{A}$[b]	**MAD**	0.106	0.120	0.127	0.131	0.135	0.143	0.144	0.144	0.143	0.145
	MAX	0.514	0.462	0.455	0.470	0.482	0.437	0.441	0.443	0.444	0.447
k	$\langle\rho\rangle$[e]	1.99	1.55	1.42	1.37	1.35	1.90	1.53	1.45	1.43	1.39
	ρ_{max} [f]	7.03	3.31	2.76	2.91	3.00	7.19	4.00	3.37	3.09	3.04

[a]**E_a:** Statistics for the activation energy, given in kJ mol^{-1}.
[b]**$\log\tilde{A}$:** Statistics for the logarithm of the pre-exponential factor, given in m^3 mol^{-1} s^{-1}.
[c]**MAD:** Mean absolute deviation of the activation energies between the CBS-QB3 based E_as and the E_as calculated by reported GA parameters, given in kJ mol^{-1}.
[d]**MAX:** Maximum absolute deviation between the CBS-QB3 based E_as and the E_as calculated by reported GA parameters among the training set of activation energies, given in m^3 mol^{-1} s^{-1}.
[e]**$\langle\rho\rangle$:** The geometric average of the factor of deviations between the reaction rate coefficients calculated by CBS-QB3 and the GA parameters reported in this study.
[f]**ρ_{max}:** The maximum factor of deviations between the reaction rate coefficients calculated by CBS-QB3 and the GA parameters reported in this study.

D.4 Performance of the Tunneling Correction Function

Table D-16 Comparison of the Eckart tunneling coefficients (κ_{Eckart}) with the ones obtained from the tunneling model (κ_{TCF}) at 300 K, 600 K and 1000 K over the training set.

Reaction #		300 K			600 K			1000 K		
		κ_{Eckart}	κ_{TCF}	ρ	κ_{Eckart}	κ_{TCF}	ρ	κ_{Eckart}	κ_{TCF}	ρ
1	**T-101**	4.4	2.8	1.6	1.4	1.6	1.1	1.1	1.3	1.2
2	**T-102**	4.2	2.7	1.6	1.4	1.5	1.1	1.1	1.3	1.1
3	**T-103**	4.3	2.7	1.6	1.4	1.6	1.1	1.1	1.3	1.1
4	**T-104**	3.7	2.6	1.4	1.4	1.5	1.1	1.1	1.3	1.2
5	**T-105**	4.0	2.5	1.6	1.4	1.6	1.1	1.1	1.3	1.1
6	**T-106**	4.2	2.6	1.6	1.4	1.5	1.1	1.1	1.3	1.1
7	**T-107**	3.5	2.6	1.4	1.3	1.5	1.1	1.1	1.3	1.2
8	**T-108**	4.6	2.7	1.7	1.4	1.6	1.1	1.1	1.3	1.1
9	**T-109**	4.5	2.7	1.6	1.5	1.6	1.1	1.1	1.3	1.1
10	**T-110**	4.8	2.7	1.7	1.4	1.6	1.1	1.1	1.3	1.1
11	**T-111**	4.5	2.8	1.6	1.4	1.6	1.1	1.1	1.3	1.1
12	**T-112**	4.6	2.8	1.7	1.4	1.6	1.1	1.1	1.3	1.1
13	**T-113**	3.9	2.7	1.5	1.4	1.5	1.1	1.1	1.3	1.1
14	**T-114**	4.4	2.8	1.6	1.4	1.6	1.1	1.1	1.3	1.1
15	**T-115**	4.3	2.7	1.6	1.4	1.6	1.1	1.1	1.3	1.1
16	**T-116**	4.2	2.7	1.5	1.4	1.6	1.1	1.1	1.3	1.2
17	**T-117**	4.3	2.7	1.6	1.4	1.5	1.1	1.1	1.3	1.1
18	**T-118**	4.4	2.7	1.6	1.4	1.6	1.1	1.1	1.3	1.1
19	**T-119**	4.3	2.7	1.6	1.4	1.6	1.1	1.1	1.3	1.2
20	**T-201**	2.1	2.4	1.1	1.2	1.4	1.2	1.1	1.2	1.1
21	**T-202**	2.0	2.1	1.0	1.2	1.3	1.1	1.1	1.2	1.1
22	**T-203**	2.1	2.0	1.0	1.2	1.3	1.1	1.1	1.2	1.1
23	**T-204**	1.7	2.2	1.3	1.1	1.4	1.2	1.1	1.2	1.1
24	**T-205**	2.0	2.0	1.0	1.2	1.3	1.1	1.1	1.2	1.1
25	**T-206**	2.2	2.0	1.1	1.2	1.3	1.1	1.1	1.2	1.1
26	**T-207**	1.7	2.0	1.2	1.1	1.3	1.2	1.1	1.2	1.1
27	**T-208**	2.3	2.5	1.1	1.2	1.5	1.2	1.1	1.2	1.1
28	**T-209**	2.5	2.3	1.1	1.2	1.4	1.1	1.1	1.2	1.1
29	**T-210**	2.2	2.3	1.1	1.2	1.4	1.2	1.1	1.2	1.1
30	**T-211**	2.1	2.3	1.1	1.2	1.4	1.2	1.1	1.2	1.1
31	**T-212**	2.3	2.1	1.1	1.2	1.4	1.1	1.1	1.2	1.1
32	**T-213**	1.8	2.2	1.2	1.2	1.4	1.2	1.1	1.2	1.1
33	**T-214**	2.1	2.0	1.0	1.2	1.3	1.1	1.1	1.2	1.1

34	**T-215**	2.1	2.1	1.0	1.2	1.4	1.1	1.1	1.2	1.1
35	**T-216**	1.9	2.3	1.2	1.2	1.4	1.2	1.1	1.2	1.1
36	**T-217**	2.0	2.3	1.2	1.2	1.4	1.2	1.1	1.2	1.1
37	**T-218**	2.0	2.3	1.1	1.2	1.4	1.2	1.1	1.2	1.1
38	**T-219**	1.9	2.3	1.2	1.2	1.4	1.2	1.1	1.2	1.1
39	**T-301**	1.6	1.8	1.1	1.1	1.3	1.1	1.0	1.1	1.1
40	**T-302**	2.2	1.8	1.2	1.2	1.3	1.1	1.1	1.2	1.1
41	**T-303**	1.6	1.7	1.0	1.1	1.2	1.1	1.0	1.1	1.1
42	**T-304**	1.4	1.7	1.2	1.1	1.2	1.1	1.0	1.1	1.1
43	**T-305**	2.2	1.7	1.3	1.2	1.3	1.0	1.1	1.1	1.1
44	**T-306**	1.5	1.6	1.1	1.1	1.2	1.1	1.0	1.1	1.1
45	**T-307**	1.4	1.7	1.2	1.1	1.2	1.1	1.0	1.1	1.1
46	**T-308**	2.8	2.3	1.2	1.3	1.4	1.1	1.1	1.2	1.1
47	**T-309**	1.7	1.8	1.0	1.1	1.3	1.1	1.1	1.1	1.1
48	**T-310**	1.7	2.0	1.2	1.1	1.3	1.2	1.1	1.2	1.1
49	**T-311**	2.0	1.9	1.0	1.2	1.3	1.1	1.1	1.2	1.1
50	**T-312**	1.6	1.8	1.1	1.1	1.3	1.1	1.0	1.1	1.1
51	**T-313**	1.5	1.9	1.3	1.1	1.3	1.2	1.0	1.2	1.1
52	**T-314**	2.2	2.2	1.0	1.2	1.4	1.2	1.1	1.2	1.1
53	**T-315**	1.6	1.7	1.1	1.1	1.3	1.1	1.0	1.1	1.1
54	**T-316**	1.5	1.8	1.2	1.1	1.3	1.1	1.0	1.1	1.1
55	**T-317**	2.5	2.4	1.1	1.3	1.4	1.1	1.1	1.2	1.1
56	**T-318**	1.6	1.8	1.1	1.1	1.3	1.1	1.0	1.1	1.1
57	**T-319**	1.5	1.8	1.2	1.1	1.3	1.2	1.0	1.1	1.1
58	**T-401**	1.9	1.8	1.0	1.2	1.3	1.1	1.1	1.1	1.1
59	**T-402**	3.6	1.8	2.0	1.4	1.3	1.1	1.1	1.2	1.0
60	**T-403**	1.5	2.0	1.3	1.1	1.3	1.2	1.0	1.2	1.1
61	**T-404**	1.6	1.7	1.1	1.1	1.2	1.1	1.0	1.1	1.1
62	**T-405**	1.7	1.7	1.0	1.1	1.2	1.1	1.1	1.1	1.1
63	**T-406**	1.5	1.7	1.1	1.1	1.2	1.1	1.0	1.1	1.1
64	**T-407**	1.4	1.7	1.2	1.1	1.2	1.1	1.0	1.1	1.1
65	**T-408**	1.9	2.1	1.1	1.2	1.4	1.2	1.1	1.2	1.1
66	**T-409**	1.7	1.9	1.1	1.1	1.3	1.1	1.0	1.2	1.1
67	**T-410**	1.7	2.0	1.2	1.1	1.3	1.2	1.0	1.2	1.1
68	**T-411**	1.6	2.1	1.3	1.1	1.3	1.2	1.0	1.2	1.1
69	**T-412**	1.6	1.9	1.2	1.1	1.3	1.1	1.0	1.2	1.1
70	**T-413**	1.8	2.0	1.1	1.2	1.3	1.1	1.1	1.2	1.1
71	**T-414**	1.6	1.8	1.2	1.1	1.3	1.1	1.0	1.1	1.1
72	**T-415**	1.5	1.8	1.2	1.1	1.3	1.1	1.0	1.1	1.1
73	**T-416**	1.8	1.8	1.0	1.2	1.3	1.1	1.1	1.1	1.1
74	**T-417**	1.5	1.9	1.2	1.1	1.3	1.2	1.0	1.2	1.1

75	**T-418**	1.5	1.8	1.2	1.1	1.3	1.2	1.0	1.1	1.1
76	**T-419**	1.8	2.0	1.1	1.2	1.3	1.2	1.1	1.2	1.1
77	**T-501**	1.4	1.6	1.1	1.1	1.2	1.1	1.0	1.1	1.1
78	**T-502**	1.8	1.6	1.1	1.2	1.2	1.1	1.1	1.1	1.1
79	**T-503**	1.4	1.5	1.0	1.1	1.2	1.1	1.0	1.1	1.1
80	**T-504**	1.4	1.5	1.0	1.1	1.2	1.1	1.0	1.1	1.1
81	**T-505**	1.4	1.5	1.1	1.1	1.2	1.1	1.0	1.1	1.1
82	**T-506**	1.4	1.4	1.1	1.1	1.2	1.1	1.0	1.1	1.1
83	**T-507**	1.3	1.5	1.1	1.1	1.2	1.1	1.0	1.1	1.1
84	**T-508**	1.5	1.6	1.1	1.1	1.2	1.1	1.0	1.1	1.1
85	**T-509**	1.5	1.3	1.1	1.1	1.1	1.0	1.0	1.1	1.0
86	**T-510**	1.5	1.3	1.1	1.1	1.1	1.0	1.0	1.1	1.0
87	**T-511**	1.4	1.4	1.0	1.1	1.1	1.0	1.0	1.1	1.1
88	**T-512**	1.4	1.3	1.1	1.1	1.1	1.0	1.0	1.1	1.0
89	**T-513**	1.4	1.7	1.2	1.1	1.2	1.1	1.0	1.1	1.1
90	**T-514**	1.7	1.6	1.1	1.1	1.2	1.1	1.0	1.1	1.1
91	**T-515**	1.4	1.3	1.1	1.1	1.1	1.0	1.0	1.1	1.0
92	**T-516**	1.4	1.6	1.1	1.1	1.2	1.1	1.0	1.1	1.1
93	**T-517**	1.5	1.6	1.1	1.1	1.2	1.1	1.0	1.1	1.1
94	**T-518**	1.4	1.5	1.1	1.1	1.2	1.1	1.0	1.1	1.1
95	**T-519**	1.4	1.4	1.0	1.1	1.1	1.1	1.0	1.1	1.1
96	**T-601**	1.6	1.5	1.1	1.1	1.2	1.1	1.0	1.1	1.1
97	**T-602**	1.4	1.3	1.0	1.1	1.1	1.0	1.0	1.1	1.0
98	**T-603**	1.3	1.2	1.0	1.1	1.1	1.0	1.0	1.1	1.0
99	**T-604**	1.2	1.3	1.1	1.1	1.1	1.1	1.0	1.1	1.1
100	**T-605**	1.6	1.6	1.0	1.3	1.2	1.0	1.1	1.1	1.0
101	**T-606**	1.5	1.3	1.1	1.1	1.1	1.0	1.0	1.1	1.0
102	**T-607**	1.5	1.5	1.0	1.1	1.2	1.1	1.0	1.1	1.1
103	**T-608**	1.4	1.3	1.1	1.1	1.1	1.0	1.0	1.1	1.0
104	**T-609**	1.8	1.3	1.3	1.2	1.1	1.0	1.1	1.1	1.0
105	**T-610**	1.7	1.4	1.2	1.1	1.1	1.0	1.0	1.1	1.0
106	**T-611**	1.6	1.5	1.1	1.1	1.2	1.0	1.0	1.1	1.1
107	**T-612**	1.6	1.5	1.1	1.1	1.2	1.0	1.0	1.1	1.1
108	**T-613**	1.6	1.6	1.0	1.1	1.2	1.1	1.0	1.1	1.1
109	**T-614**	1.5	1.8	1.2	1.2	1.3	1.1	1.1	1.1	1.1
110	**T-615**	1.6	1.5	1.1	1.1	1.2	1.0	1.0	1.1	1.1
111	**T-616**	1.5	1.3	1.2	1.1	1.1	1.0	1.0	1.1	1.0
112	**T-617**	1.4	1.8	1.2	1.1	1.3	1.1	1.0	1.1	1.1
113	**T-618**	1.5	1.7	1.1	1.1	1.2	1.1	1.0	1.1	1.1
114	**T-619**	1.6	1.6	1.0	1.1	1.2	1.1	1.0	1.1	1.1
115	**T-701**	2.0	2.6	1.3	1.2	1.5	1.2	1.1	1.2	1.2

116	**T-702**	2.3	1.9	1.2	1.2	1.3	1.1	1.1	1.2	1.1
117	**T-703**	1.9	2.1	1.1	1.2	1.4	1.2	1.1	1.2	1.1
118	**T-704**	1.8	2.2	1.2	1.1	1.4	1.2	1.1	1.2	1.1
119	**T-705**	2.0	2.1	1.1	1.2	1.4	1.2	1.1	1.2	1.1
120	**T-706**	1.8	2.0	1.1	1.2	1.3	1.1	1.1	1.2	1.1
121	**T-707**	1.7	2.1	1.2	1.1	1.4	1.2	1.1	1.2	1.1
122	**T-708**	2.4	2.8	1.2	1.2	1.5	1.3	1.1	1.3	1.2
123	**T-709**	2.1	2.5	1.2	1.2	1.5	1.2	1.1	1.2	1.1
124	**T-710**	2.1	2.5	1.2	1.2	1.5	1.2	1.1	1.2	1.2
125	**T-711**	2.7	2.3	1.2	1.3	1.4	1.1	1.1	1.2	1.1
126	**T-712**	2.0	2.2	1.1	1.2	1.4	1.2	1.1	1.2	1.1
127	**T-713**	2.0	2.4	1.1	1.2	1.4	1.2	1.1	1.2	1.1
128	**T-714**	2.0	2.5	1.2	1.2	1.5	1.2	1.1	1.2	1.2
129	**T-715**	2.0	2.5	1.3	1.2	1.5	1.2	1.1	1.2	1.2
130	**T-716**	1.9	2.5	1.3	1.2	1.5	1.3	1.1	1.2	1.2
131	**T-717**	2.4	2.5	1.0	1.2	1.5	1.2	1.1	1.2	1.1
132	**T-718**	2.1	2.6	1.2	1.2	1.5	1.2	1.1	1.2	1.2
133	**T-719**	1.9	2.6	1.3	1.2	1.5	1.3	1.1	1.2	1.2
134	**T-801**	1.5	1.9	1.3	1.1	1.3	1.2	1.0	1.2	1.1
135	**T-802**	1.6	1.7	1.1	1.1	1.2	1.1	1.0	1.1	1.1
136	**T-803**	1.5	1.9	1.3	1.1	1.3	1.2	1.0	1.2	1.1
137	**T-804**	1.4	2.0	1.4	1.1	1.3	1.2	1.0	1.2	1.1
138	**T-805**	1.9	1.9	1.0	1.2	1.3	1.1	1.1	1.2	1.1
139	**T-806**	1.4	1.8	1.3	1.1	1.3	1.2	1.0	1.1	1.1
140	**T-807**	1.4	1.9	1.4	1.1	1.3	1.2	1.0	1.2	1.1
141	**T-808**	1.7	2.1	1.3	1.1	1.4	1.2	1.0	1.2	1.1
142	**T-809**	1.6	2.1	1.3	1.1	1.3	1.2	1.0	1.2	1.1
143	**T-810**	1.6	2.1	1.3	1.1	1.4	1.2	1.0	1.2	1.1
144	**T-811**	2.0	2.1	1.1	1.2	1.4	1.1	1.1	1.2	1.1
145	**T-812**	1.5	2.2	1.4	1.1	1.4	1.3	1.0	1.2	1.2
146	**T-813**	1.4	2.3	1.6	1.1	1.4	1.3	1.0	1.2	1.2
147	**T-814**	1.9	2.0	1.1	1.2	1.3	1.1	1.1	1.2	1.1
148	**T-815**	1.5	2.0	1.4	1.1	1.3	1.2	1.0	1.2	1.1
149	**T-816**	1.4	2.1	1.4	1.1	1.3	1.2	1.0	1.2	1.1
150	**T-817**	1.5	2.3	1.5	1.1	1.4	1.3	1.0	1.2	1.2
151	**T-818**	1.5	2.1	1.4	1.1	1.4	1.2	1.0	1.2	1.1
152	**T-819**	1.4	1.9	1.3	1.1	1.3	1.2	1.0	1.2	1.1

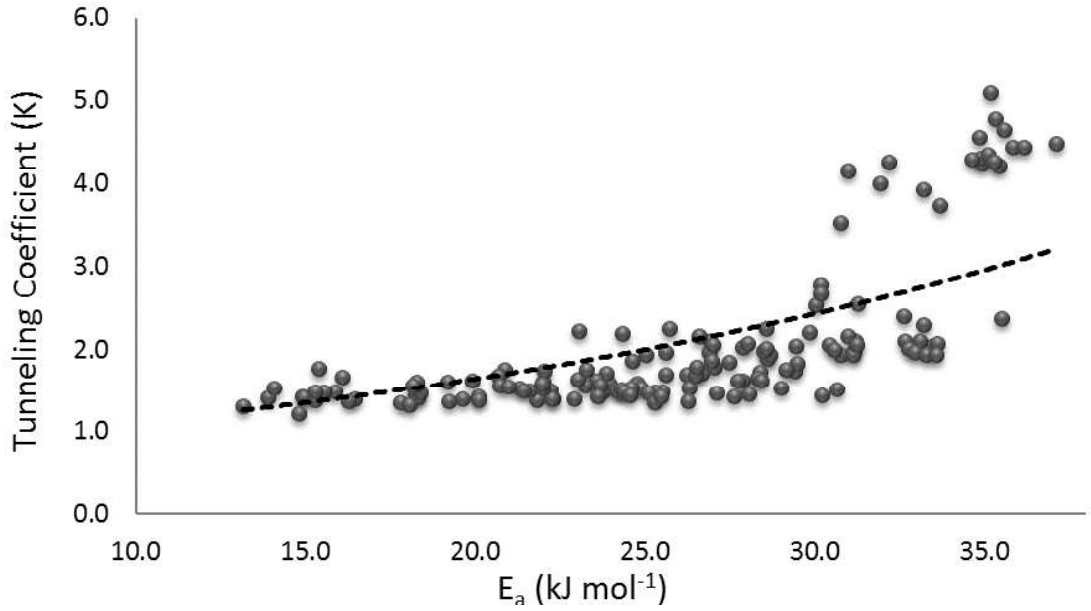

Figure D-51 Tunneling correction function (dashed line) and the Eckart tunneling coefficients (dots) at 300 K.

D.5 Validation of the GA parameters: Validation Set

D.5.1 List of the reactions

In the validation set, the applicability of group additively developed parameters is tested on a set of HARs from α-carbons of doubly substituted toluene derivatives. The main objective in utilizing this validation set is to test the transferability of the ΔNNI°s from singly substituted toluene derivatives to doubly substituted toluene derivatives. The HARs in the validation set are abbreviated with the letter "V". In the validation set, there are different number of reactions for each of the 8 classes mentioned in the training set. The list of HARs from each TD class is given in a figure in the following pages below, from **Figure D-52** to **Figure D-59**.

A code is given for each of the 59 reactions in the training set. All of them start with "V" to indicate that that reaction is a part of the validation set. The first number after "-" represents the class of TDs from which HAR took place. For example, the code "**V-402**" represents 2nd HAR in the 4th class (allylbenzenes) in the validation set.

V-101:

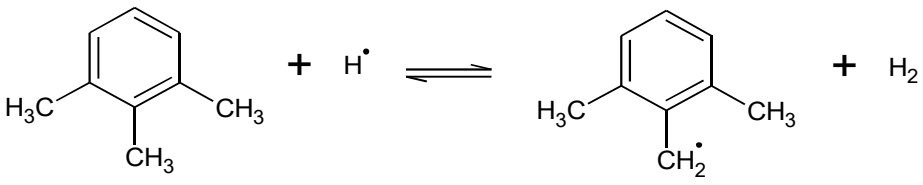

V-102:

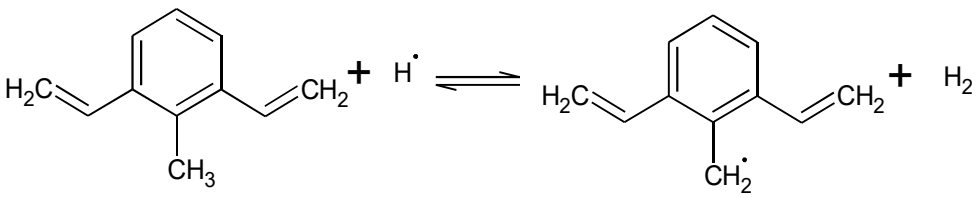

V-103:

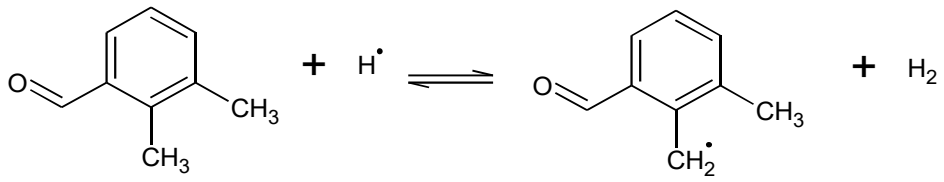

V-104:

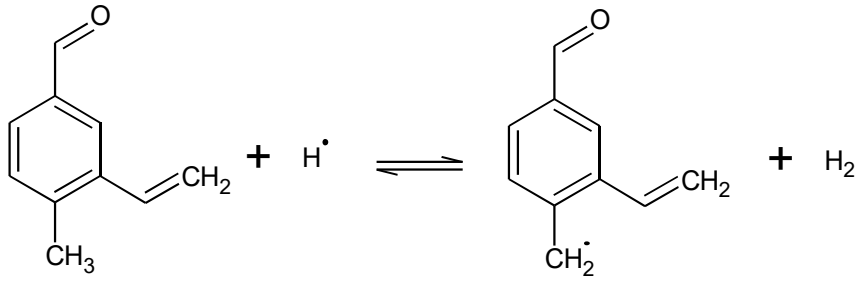

V-105:

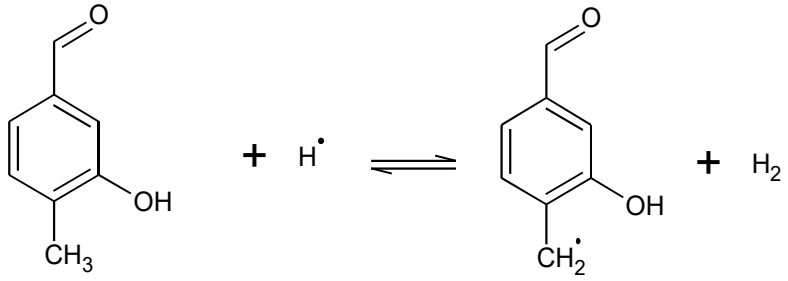

Figure D-52 Hydrogen abstraction reactions from the α-carbon of doubly substituted toluenes.

V-201:

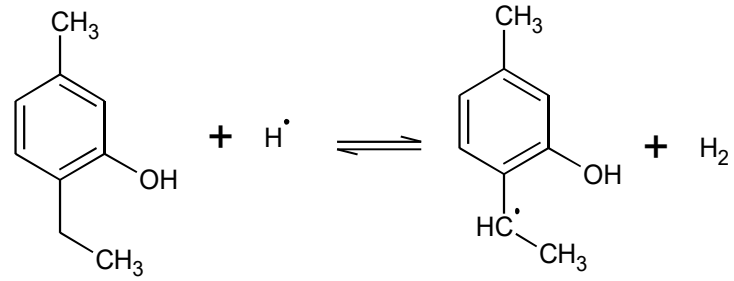

V-202:

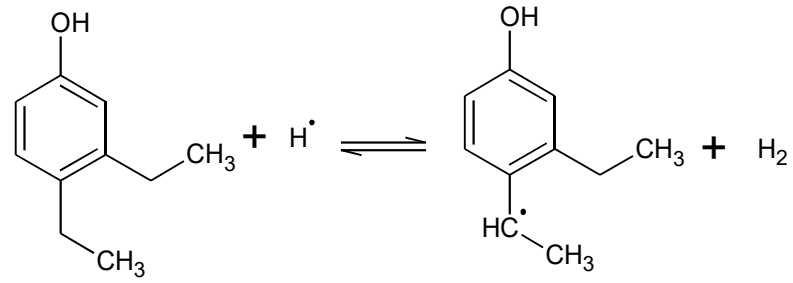

V-203:

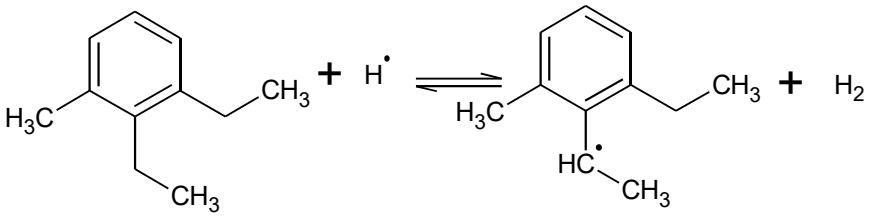

V-204:

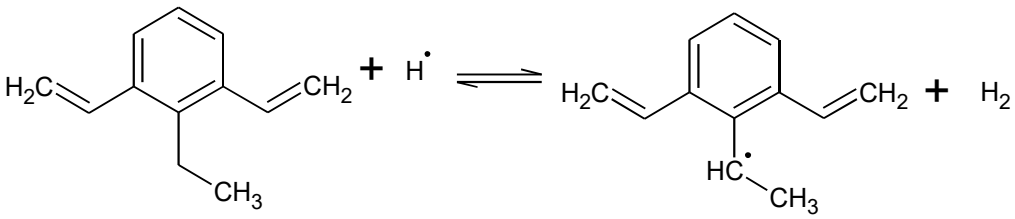

V-205:

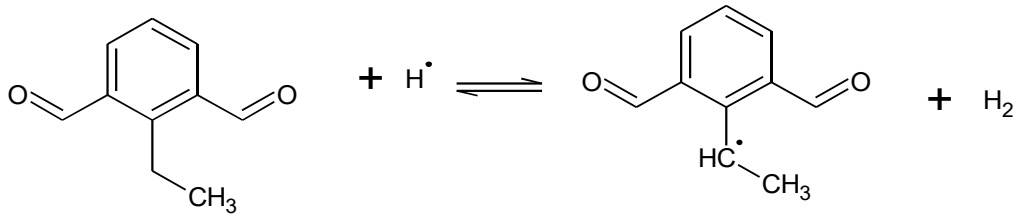

V-206:

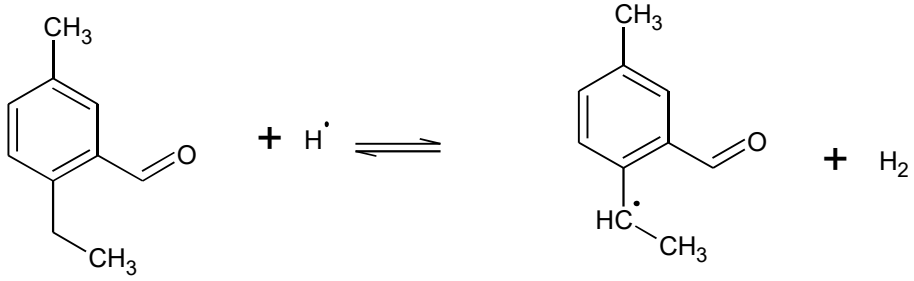

V-207:

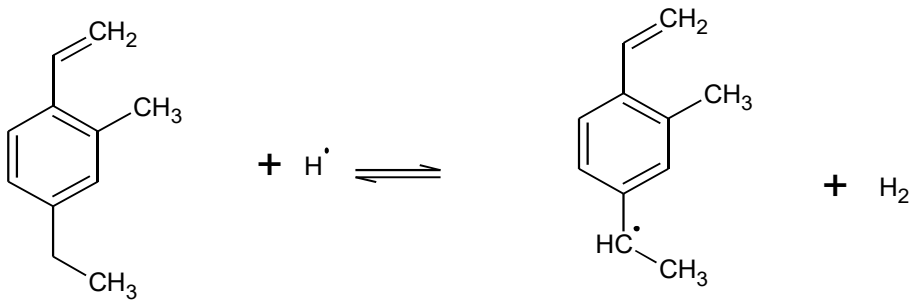

V-208:

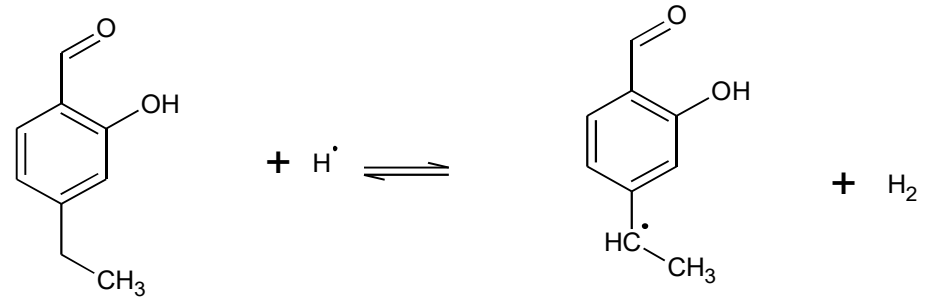

V-209:

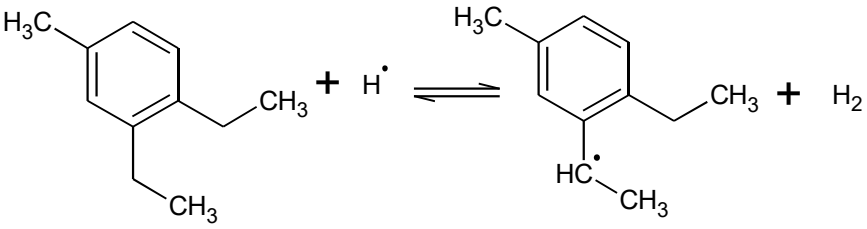

V-210:

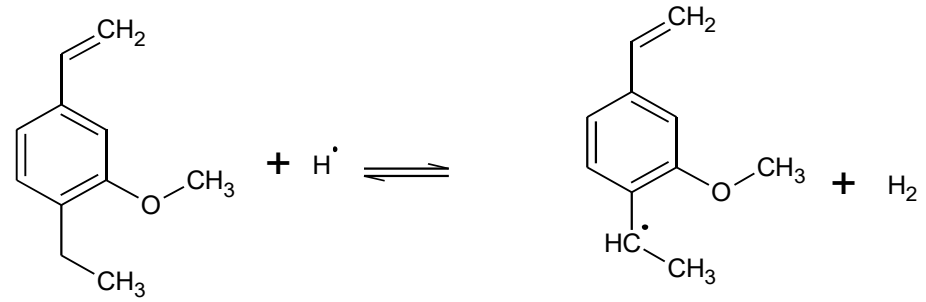

Figure D-53 Hydrogen abstraction reactions from the α-carbon of doubly substituted ethylbenzenes.

V-301:

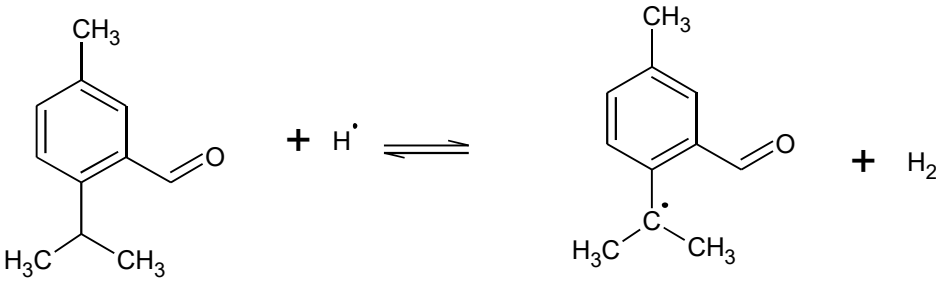

V-302:

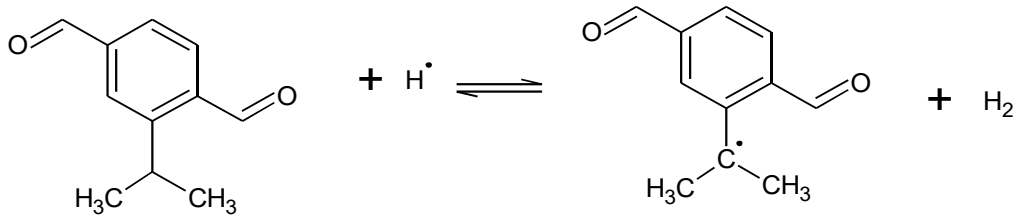

V-303:

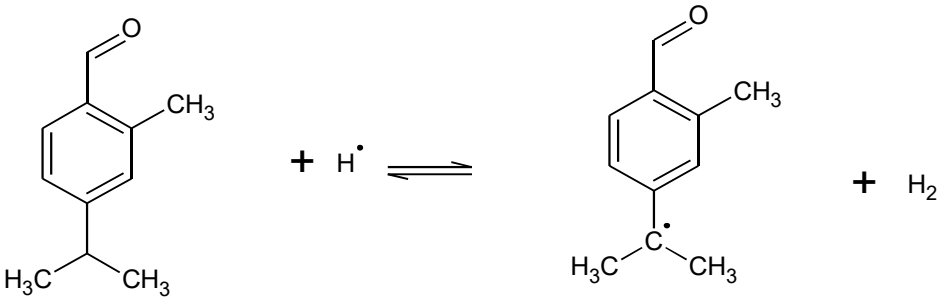

V-304:

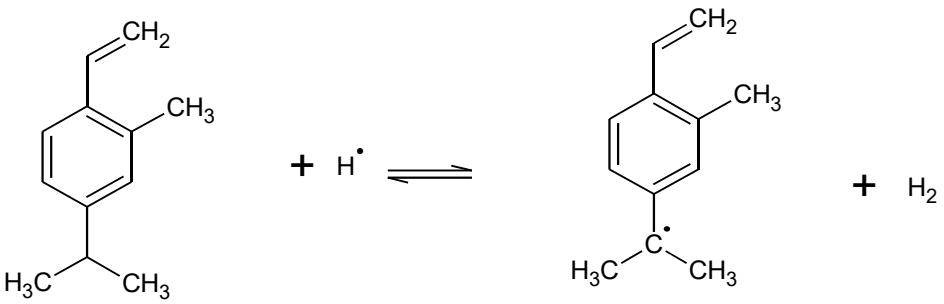

V-305:

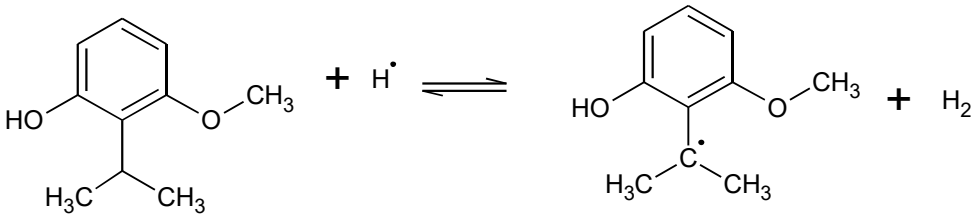

V-306:

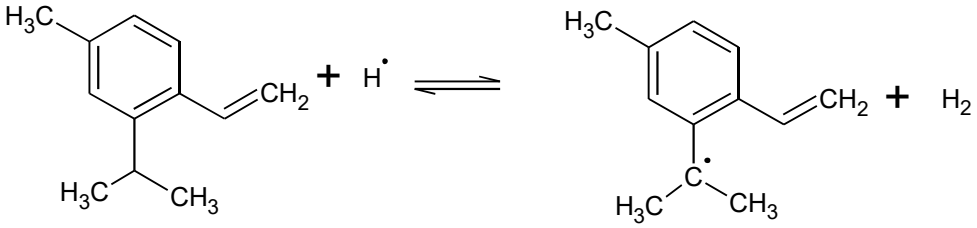

V-307:

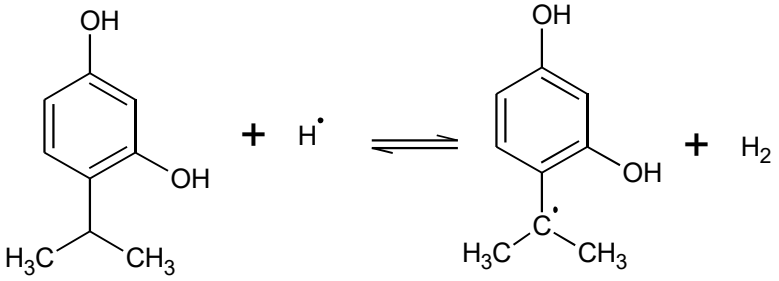

V-308:

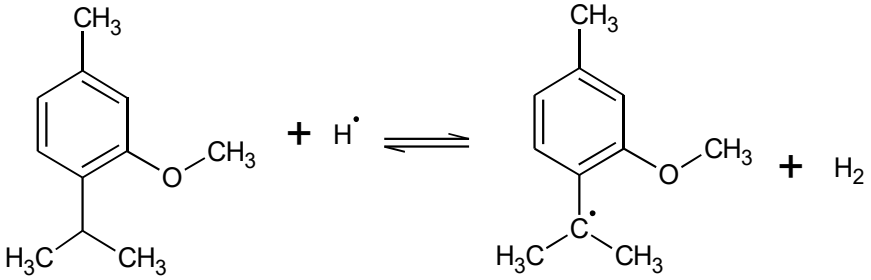

V-309:

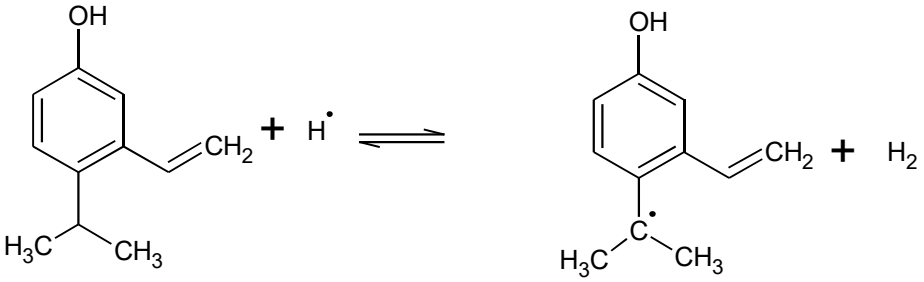

V-310:

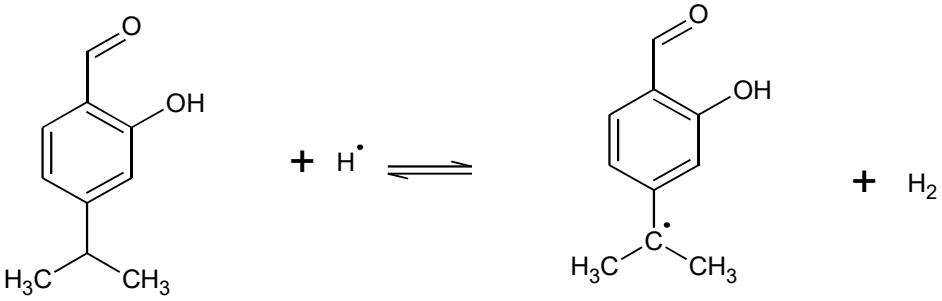

V-311:

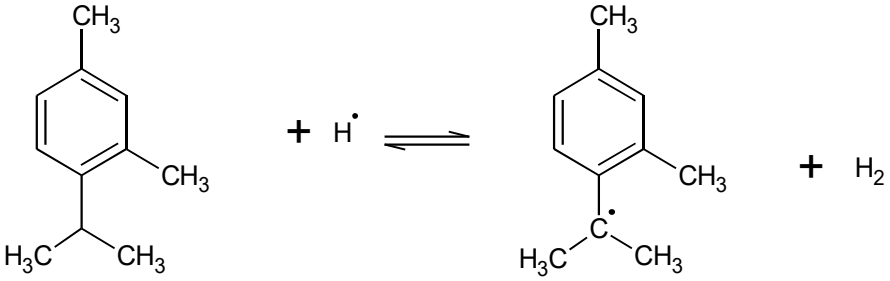

V-312:

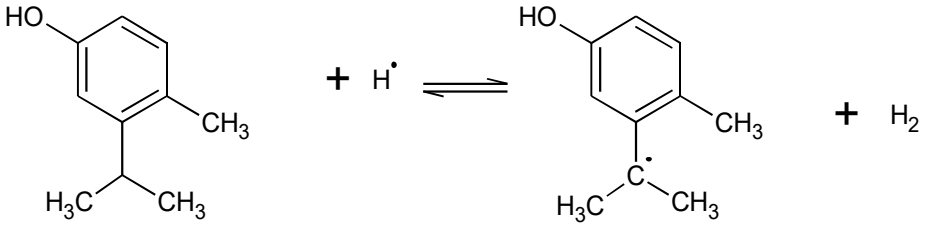

Figure D-54 Hydrogen abstraction reactions from the α-carbon of doubly substituted isopropylbenzenes.

V-401:

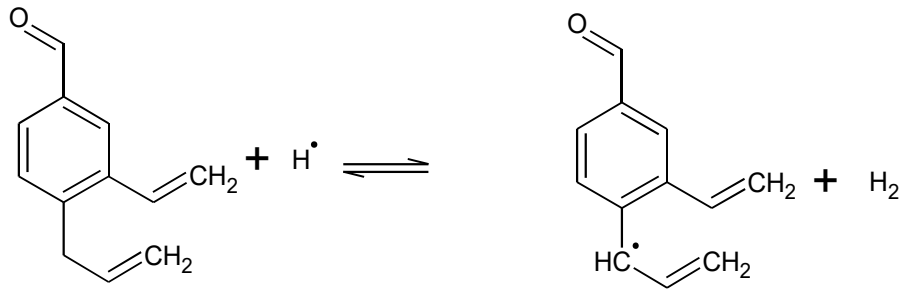

V-402:

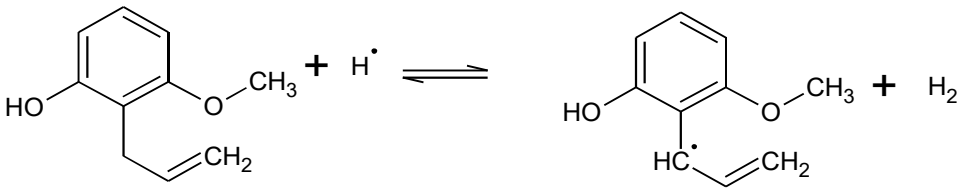

V-403:

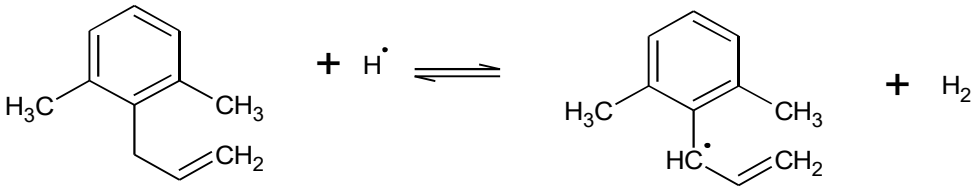

V-404:

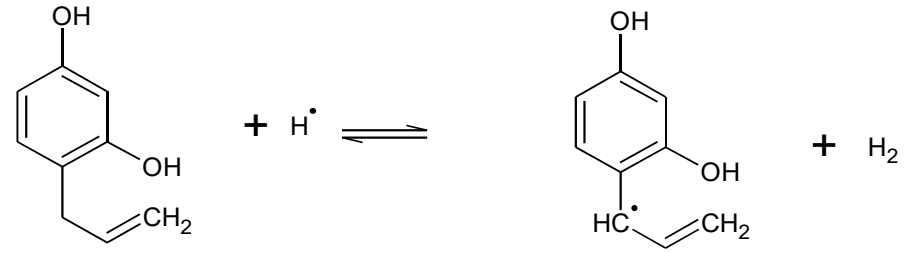

V-405:

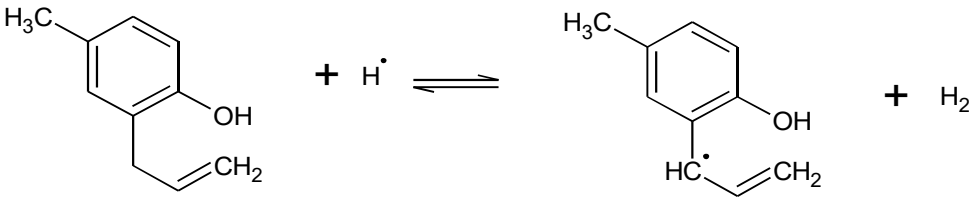

V-406:

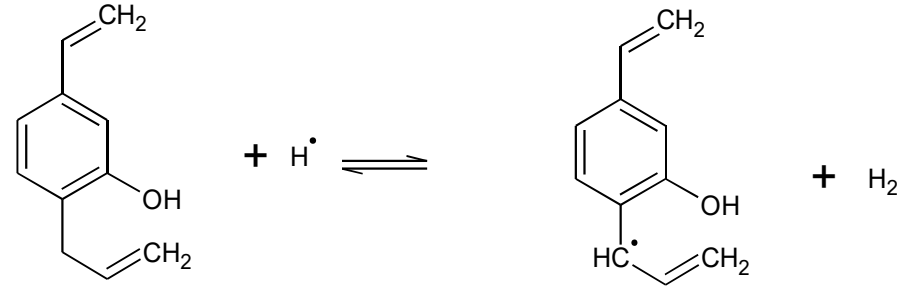

Figure D-55 Hydrogen abstraction reactions from the α-carbon of doubly substituted allylbenzenes.

V-501:

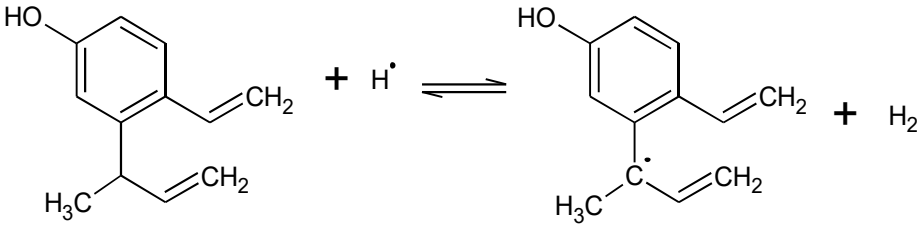

V-502:

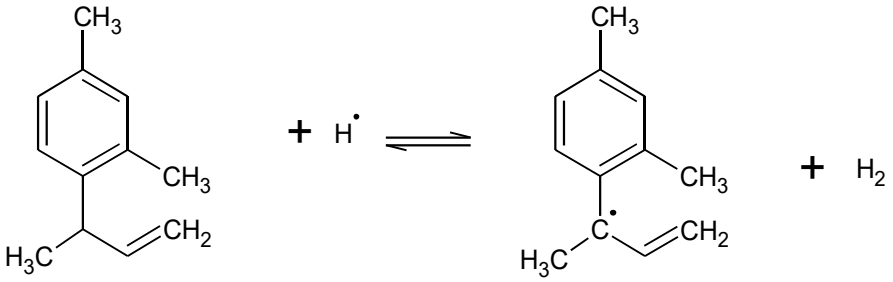

V-503:

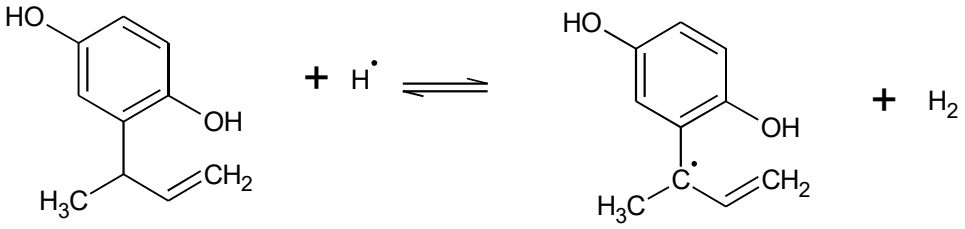

V-504:

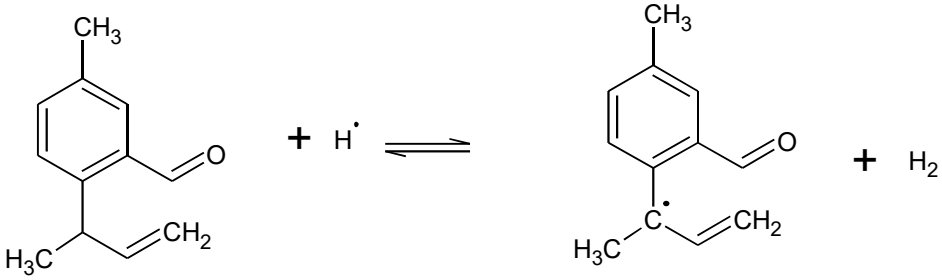

V-505:

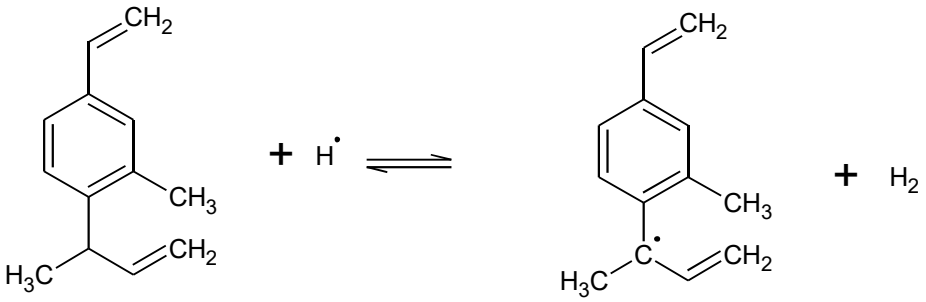

V-506:

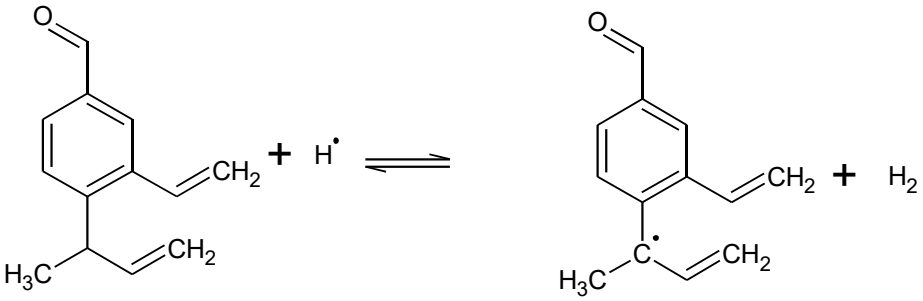

Figure D-56 Hydrogen abstraction reactions from the α-carbon of doubly substituted α-methyl allylbenzenes.

V-601:

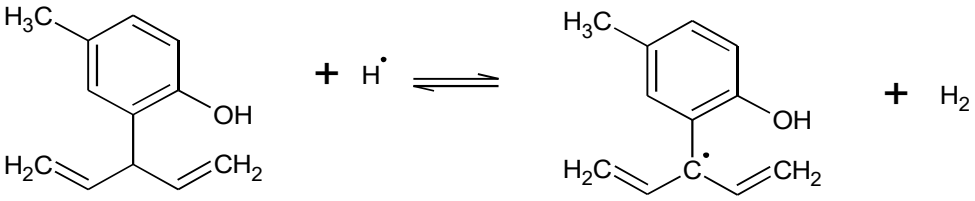

V-602:

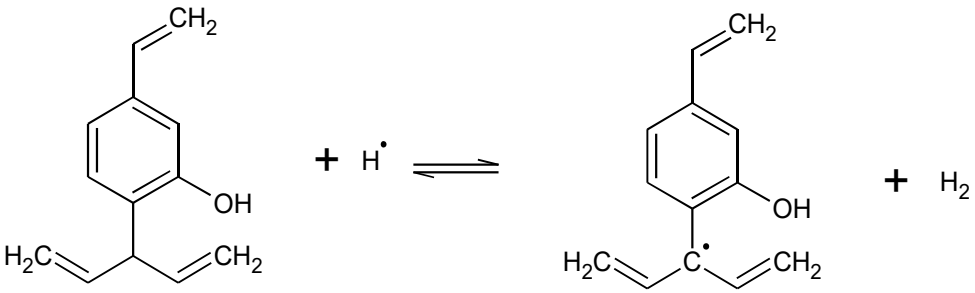

V-603:

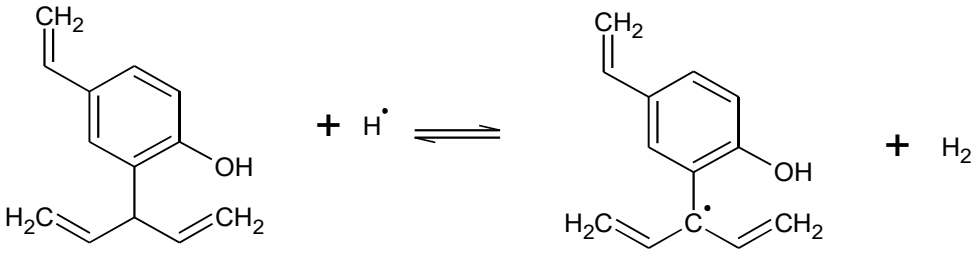

V-604:

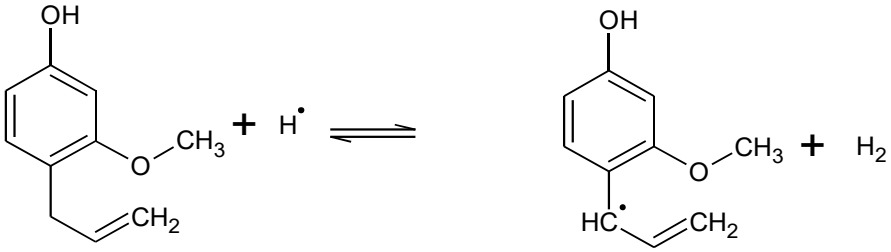

V-605:

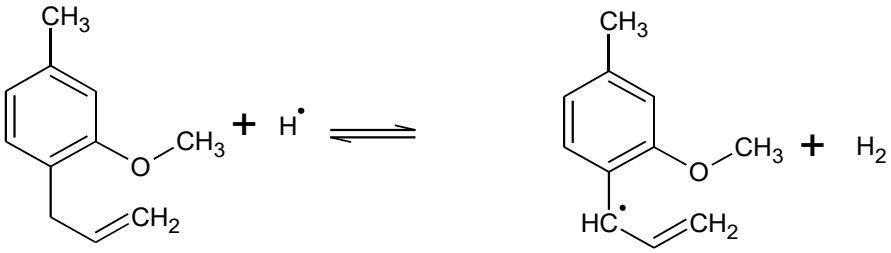

V-606:

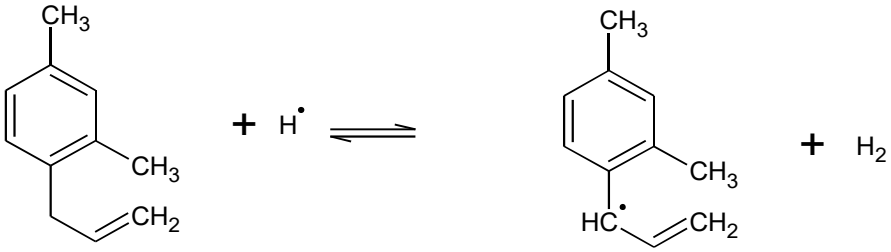

V-607:

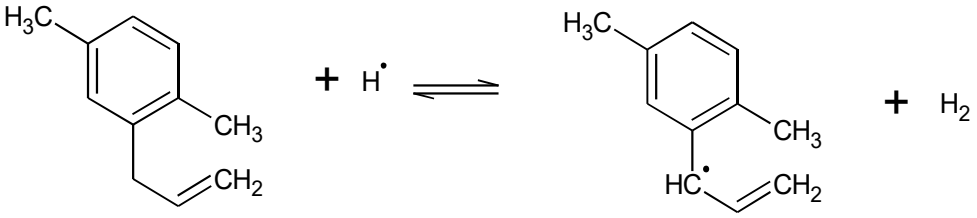

V-608:

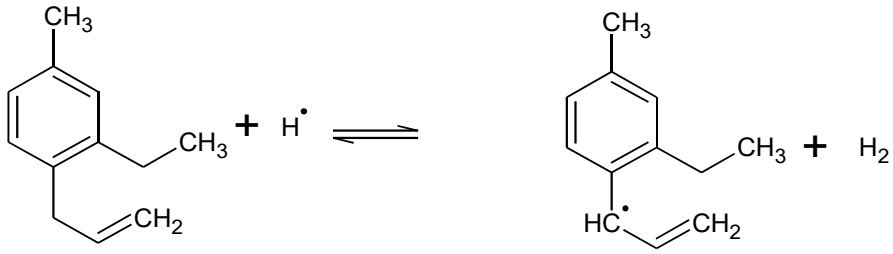

V-609:

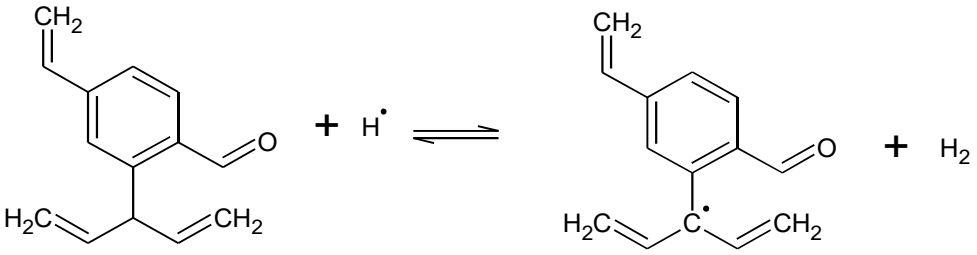

V-610:

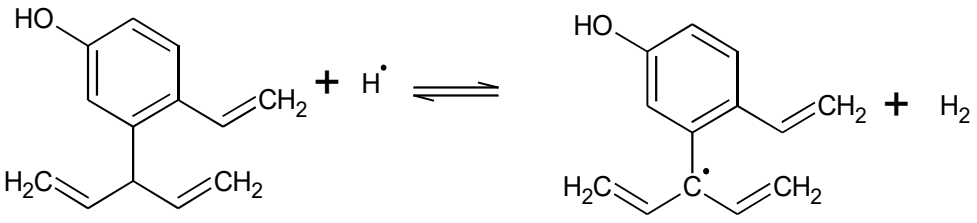

Figure D-57 Hydrogen abstraction reactions from the α-carbon of doubly substituted α-vinyl allylbenzenes.

V-701:

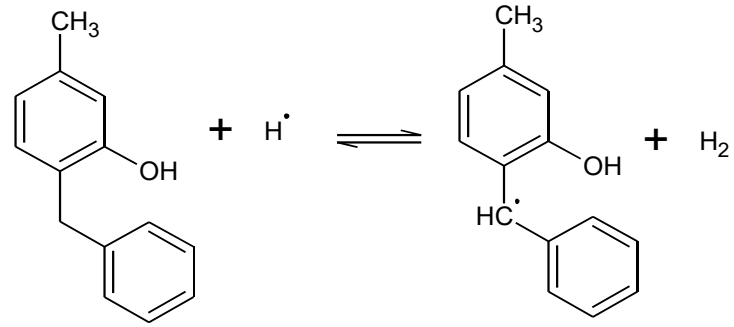

V-702:

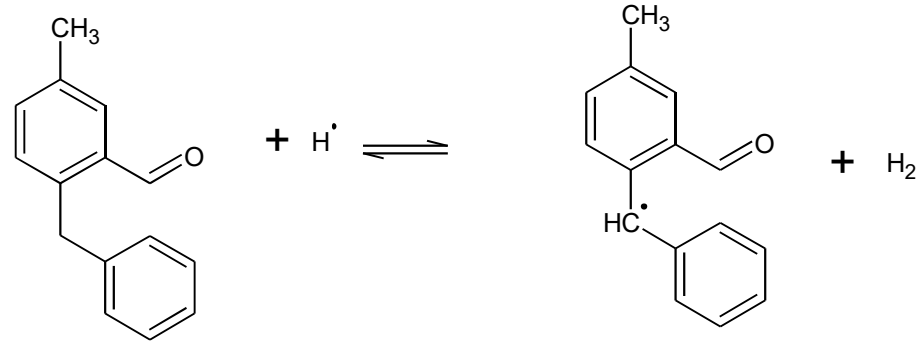

V-703:

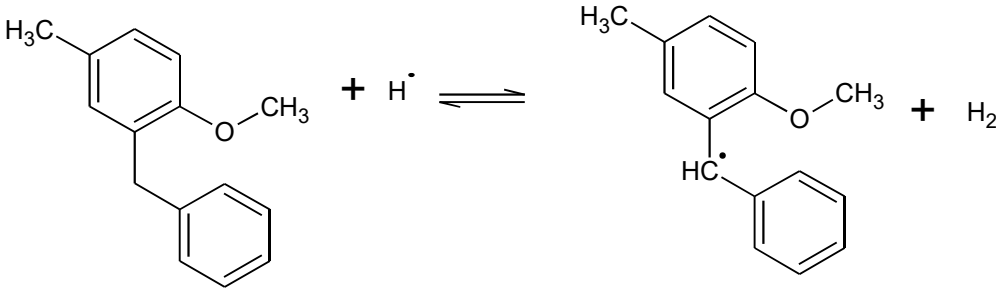

V-704:

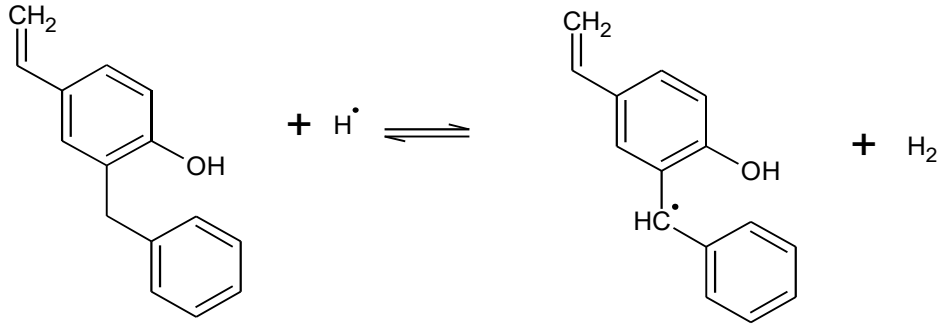

V-705:

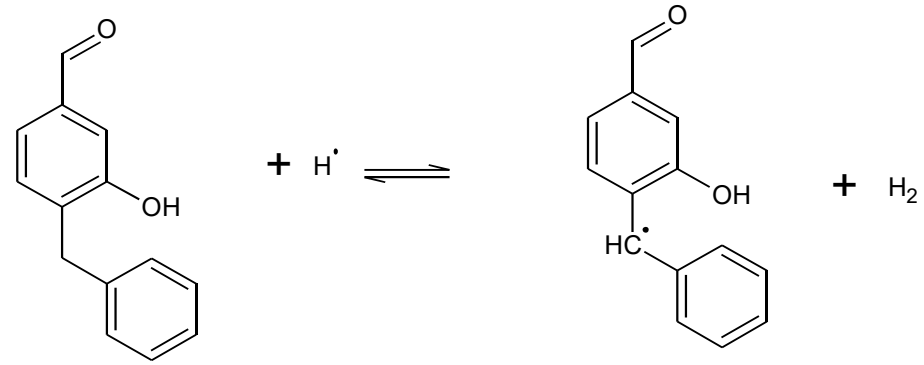

V-706:

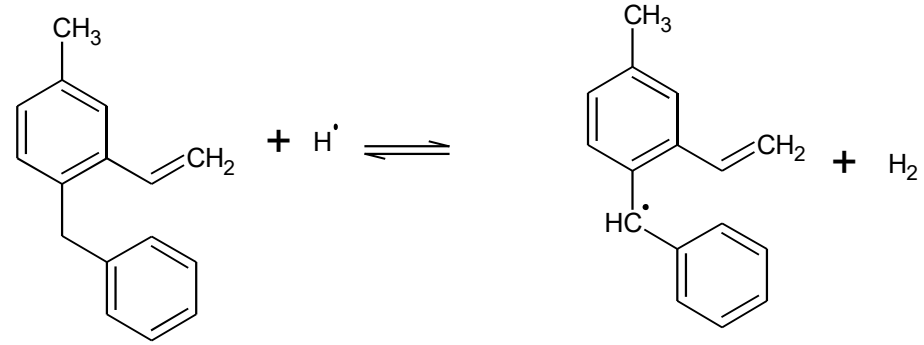

Figure D-58 Hydrogen abstraction reactions from the α-carbon of doubly substituted diphenylmethanes.

V-801:

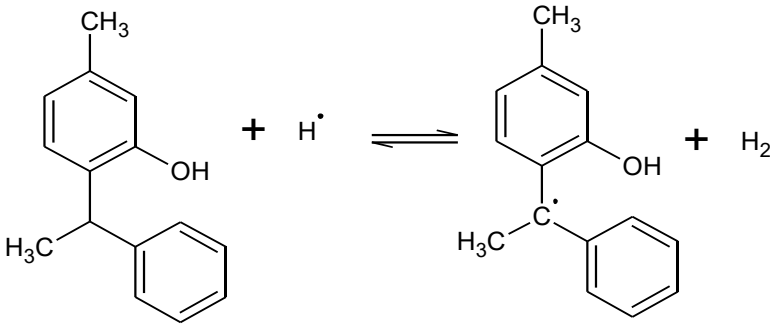

V-802:

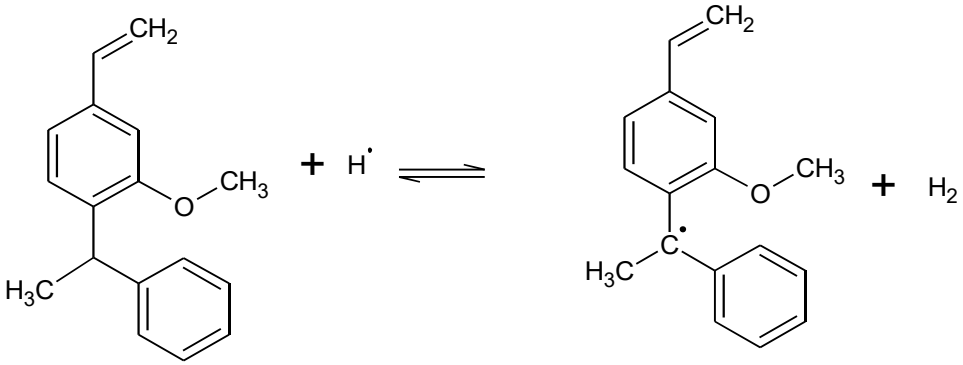

V-803:

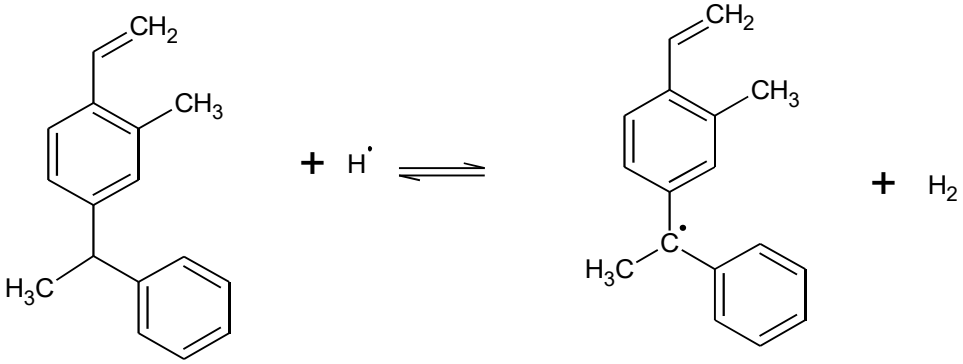

V-804:

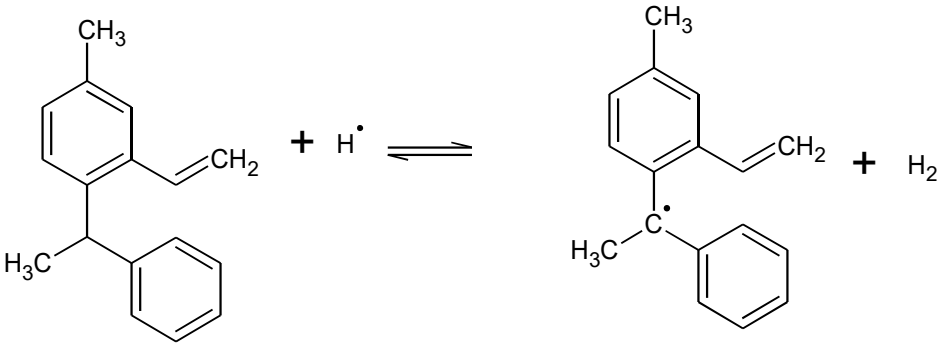

Figure D-59 Hydrogen abstraction reactions from the α-carbon of doubly substituted 1,1-diphenylethanes.

D.5.2 Database of the HARs in the Validation Set

Table D-17 Arrhenius parameters (activation energy (**Ea**) and logarithm of the pre-exponential factor ($\log\widetilde{A}$)) of the HARs in the validation set 300 K, given along with reaction rate coefficients and the Eckart tunneling correction factor (κ) for forward and reverse reactions.

Reaction #	κ	Forward				Reverse			
		$E_{a,f}$ [a]	$log\widetilde{A}_f$ [b]	k_f [c]	κk_f [d]	$E_{a,r}$ [e]	$log\widetilde{A}_r$ [f]	k_r [g]	κk_r [h]
V-101	3.74	33.6	8.981	4.1E+00	1.5E+01	99.6	8.532	3.6E-12	1.3E-11
V-102	4.00	33.3	9.501	1.5E+01	6.1E+01	102.1	9.369	4.0E-12	1.6E-11
V-103	3.72	32.8	9.288	1.1E+01	4.2E+01	99.5	9.127	6.4E-12	2.4E-11
V-104	4.71	35.2	9.252	7.9E+00	3.7E+01	103.3	8.976	2.0E-12	9.3E-12
V-105	4.17	36.3	9.325	6.0E+00	2.5E+01	108.1	9.247	5.3E-13	2.2E-12
V-201	1.87	26.7	9.666	2.1E+02	3.9E+02	97.6	8.224	3.3E-12	6.3E-12
V-202	1.74	26.8	9.483	1.3E+02	2.3E+02	100.0	8.071	9.1E-13	1.6E-12
V-203	1.80	31.8	9.576	2.2E+01	3.9E+01	102.1	7.831	2.3E-13	4.1E-13
V-204	1.70	33.2	9.435	2.2E+01	3.7E+01	98.8	8.290	2.5E-12	4.2E-12
V-205	2.34	34.2	9.755	1.3E+01	2.9E+01	98.1	8.617	6.9E-12	1.6E-11
V-206	2.16	33.4	9.954	2.8E+01	5.9E+01	106.4	8.745	3.4E-13	7.3E-13
V-207	1.86	29.1	9.798	1.1E+02	2.0E+02	112.5	8.521	1.7E-14	3.2E-14
V-208	2.14	26.4	9.734	2.8E+02	5.9E+02	102.3	7.773	1.8E-13	3.9E-13
V-209	2.02	26.3	9.562	1.9E+02	3.9E+02	98.9	8.322	2.6E-12	5.2E-12
V-210	1.82	28.2	9.711	1.3E+02	2.3E+02	109.2	8.193	3.0E-14	5.4E-14
V-301	2.82	29.7	9.645	3.0E+01	8.4E+01	94.6	8.343	1.5E-11	4.2E-11
V-302	2.86	31.3	10.018	3.6E+01	1.0E+02	95.7	8.323	9.0E-12	2.6E-11
V-303	2.56	25.6	9.798	2.1E+02	5.5E+02	107.1	7.657	2.1E-14	5.3E-14
V-304	1.70	26.1	9.754	1.6E+02	2.8E+02	106.7	7.321	1.1E-14	1.9E-14
V-305	1.79	22.4	9.868	9.3E+02	1.7E+03	79.4	7.972	2.8E-09	5.0E-09
V-306	1.92	25.1	9.503	1.4E+02	2.6E+02	92.4	8.151	2.3E-11	4.5E-11
V-307	1.09	19.5	9.717	2.1E+03	2.3E+03	83.2	7.198	1.0E-10	1.1E-10
V-308	2.07	21.9	9.815	1.0E+03	2.1E+03	84.8	7.464	9.8E-11	2.0E-10
V-309	1.71	30.4	9.473	3.0E+01	5.2E+01	92.0	7.844	2.7E-11	4.6E-11
V-310	1.74	21.4	9.506	1.2E+03	2.1E+03	103.4	6.931	1.7E-14	2.9E-14
V-311	2.56	32.1	9.345	1.1E+01	2.9E+01	87.1	7.844	1.9E-10	4.9E-10
V-312	2.78	31.8	9.362	1.3E+01	3.7E+01	87.2	7.543	9.2E-11	2.5E-10
V-401	2.42	28.1	9.932	2.2E+02	5.2E+02	142.7	9.060	3.3E-19	7.9E-19
V-402	1.73	19.6	9.574	2.9E+03	5.1E+03	121.4	8.318	3.0E-16	5.3E-16
V-403	2.83	22.5	9.814	7.9E+02	2.2E+03	133.4	8.793	3.7E-18	1.0E-17
V-404	1.56	23.9	10.136	9.5E+02	1.5E+03	130.6	8.730	9.8E-18	1.5E-17
V-405	2.83	22.1	10.076	1.7E+03	4.8E+03	129.1	8.691	1.6E-17	4.6E-17
V-406	2.30	24.0	10.109	8.5E+02	2.0E+03	135.6	8.904	2.0E-18	4.5E-18
V-501	1.47	20.8	9.989	2.4E+03	3.5E+03	124.4	8.848	3.1E-16	4.5E-16

V-502	1.52	18.5	9.979	5.7E+03	8.7E+03	124.5	8.470	1.2E-16	1.9E-16
V-503	1.76	18.4	9.715	3.2E+03	5.6E+03	123.0	8.261	1.4E-16	2.5E-16
V-504	1.48	21.4	10.151	2.7E+03	4.0E+03	122.3	8.652	4.5E-16	6.6E-16
V-505	1.60	23.9	9.929	5.9E+02	9.4E+02	125.0	8.518	1.1E-16	1.8E-16
V-506	1.54	22.2	10.291	2.6E+03	4.1E+03	130.2	9.042	4.8E-17	7.4E-17
V-601	1.56	18.2	10.234	1.2E+04	1.8E+04	160.2	8.865	1.8E-22	2.9E-22
V-602	1.12	16.4	10.121	1.8E+04	2.1E+04	161.4	9.055	1.8E-22	2.0E-22
V-603	1.41	17.9	10.106	9.8E+03	1.4E+04	160.4	8.603	9.5E-23	1.3E-22
V-604	1.12	20.1	9.780	1.9E+03	2.1E+03	154.2	8.379	6.8E-22	7.6E-22
V-605	1.93	21.5	9.705	9.1E+02	1.8E+03	162.0	7.935	1.1E-23	2.1E-23
V-606	1.54	29.6	10.325	1.5E+02	2.3E+02	171.5	8.569	1.0E-24	1.6E-24
V-607	2.12	20.7	9.871	1.9E+03	4.0E+03	165.6	8.016	3.0E-24	6.4E-24
V-608	1.39	23.0	9.727	5.3E+02	7.4E+02	160.1	7.908	2.2E-23	3.0E-23
V-609	1.43	14.1	9.899	2.8E+04	3.9E+04	160.4	8.245	4.2E-23	6.0E-23
V-610	1.55	10.6	9.701	4.2E+04	6.4E+04	158.9	7.869	3.2E-23	4.9E-23
V-701	2.12	24.7	9.490	3.1E+02	6.6E+02	110.1	8.646	5.9E-14	1.2E-13
V-702	2.19	29.1	9.217	2.8E+01	6.2E+01	119.7	9.178	4.3E-15	9.4E-15
V-703	1.88	25.1	9.414	2.2E+02	4.2E+02	104.5	8.318	2.7E-13	5.0E-13
V-704	2.36	29.4	9.288	2.9E+01	6.9E+01	114.2	8.706	1.4E-14	3.2E-14
V-705	2.61	31.5	9.336	1.4E+01	3.7E+01	117.5	8.704	3.5E-15	9.1E-15
V-706	2.57	34.0	9.665	1.1E+01	2.8E+01	115.9	8.843	9.4E-15	2.4E-14
V-801	1.51	23.1	9.031	2.0E+02	3.0E+02	113.9	8.221	1.5E-14	2.3E-14
V-802	1.88	25.1	9.715	2.2E+02	4.2E+02	104.5	8.318	2.7E-13	5.0E-13
V-803	2.31	27.3	9.612	7.2E+01	1.7E+02	117.6	8.701	3.4E-15	7.8E-15
V-804	1.92	28.6	9.631	4.5E+01	8.7E+01	108.8	8.084	2.8E-14	5.4E-14

[a] $\mathbf{E_{a,f}}$**:** Activation energy of the forward reaction, given in kJ mol^{-1}.
[b] $\boldsymbol{log\widetilde{A}_f}$**:** Logarithm of the pre-exponential factor of the forward reaction, given in m^3 mol^{-1} s^{-1}.
[c] $\mathbf{k_f}$**:** The reaction rate coefficient for the forward reaction excluding tunneling effects, given in m^3 mol^{-1} s^{-1}.
[d] $\boldsymbol{\kappa k_f}$**:** The reaction rate coefficient for the forward reaction including tunneling effects, given in m^3 mol^{-1} s^{-1}.
[e] $\mathbf{E_{a,r}}$**:** Activation energy of the reverse reaction, given in kJ mol^{-1}.
[f] $\boldsymbol{log\widetilde{A}_r}$**:** Logarithm of the pre-exponential factor of the reverse reaction, given in m^3 mol^{-1} s^{-1}.
[g] $\mathbf{k_r}$**:** The reaction rate coefficient for the reverse reaction excluding tunneling effects, given in m^3 mol^{-1} s^{-1}.
[h] $\boldsymbol{\kappa k_r}$**:** The reaction rate coefficient for the reverse reaction including tunneling effects, given in m^3 mol^{-1} s^{-1}.

Table D-18 Arrhenius parameters (activation energy (**Ea**) and logarithm of the pre-exponential factor ($\log\widetilde{A}$)) of the HARs in the validation set 600 K, given along with reaction rate coefficients and the Eckart tunneling correction factor (κ) for forward and reverse reactions.

Reaction #	κ	**Forward**				**Reverse**			
		$\mathbf{E_{a,f}}$ [a]	$\boldsymbol{log\widetilde{A}_f}$ [b]	$\mathbf{k_f}$ [c]	$\boldsymbol{\kappa k_f}$ [d]	$\mathbf{E_{a,r}}$ [e]	$\boldsymbol{log\widetilde{A}_r}$ [f]	$\mathbf{k_r}$ [g]	$\boldsymbol{\kappa k_r}$ [h]
V-101	1.36	37.5	9.558	9.90E+03	1.35E+04	101.5	8.624	2.6E-03	3.6E-03
V-102	1.38	38.4	9.645	9.98E+03	1.38E+04	104.4	9.324	2.3E-03	3.2E-03
V-103	1.36	37.7	9.546	8.51E+03	1.16E+04	101.8	9.124	1.8E-03	2.5E-03

V-104	1.43	40.9	9.941	1.43E+04	2.05E+04	106.2	9.318	2.4E-03	3.4E-03
V-105	1.39	41.9	9.989	1.33E+04	1.84E+04	111.2	9.612	1.7E-03	2.4E-03
V-201	1.17	30.5	10.119	5.88E+04	6.86E+04	99.5	8.429	1.2E-03	1.4E-03
V-202	1.15	30.5	9.922	3.71E+04	4.25E+04	101.8	8.263	5.1E-04	5.8E-04
V-203	1.36	35.5	10.035	1.76E+04	2.39E+04	103.1	8.066	2.5E-04	3.4E-04
V-204	1.35	36.4	9.898	1.07E+04	1.44E+04	100.9	8.526	1.1E-03	1.5E-03
V-205	1.39	37.8	10.222	1.71E+04	2.37E+04	100.5	8.889	2.8E-03	3.8E-03
V-206	1.20	37.3	10.420	3.00E+04	3.60E+04	108.4	8.813	4.7E-04	5.7E-04
V-207	1.16	33.0	10.258	4.89E+04	5.69E+04	114.4	8.730	1.2E-04	1.4E-04
V-208	1.23	30.3	10.123	6.14E+04	7.57E+04	104.3	7.995	1.6E-04	2.0E-04
V-209	1.19	30.1	10.013	4.98E+04	5.92E+04	100.7	8.518	1.1E-03	1.4E-03
V-210	1.16	32.0	10.167	4.85E+04	5.62E+04	111.1	8.401	1.1E-04	1.2E-04
V-301	1.26	33.6	10.056	1.36E+04	1.71E+04	96.9	8.456	2.1E-03	2.7E-03
V-302	1.28	35.2	10.486	2.62E+04	3.36E+04	98.0	8.578	2.2E-03	2.8E-03
V-303	1.11	29.4	10.252	4.90E+04	5.42E+04	109.0	7.734	3.5E-05	3.9E-05
V-304	1.14	29.9	10.212	4.08E+04	4.66E+04	108.8	7.554	2.4E-05	2.8E-05
V-305	1.16	25.9	10.277	1.06E+05	1.23E+05	81.2	8.162	2.5E-02	2.9E-02
V-306	1.18	28.8	9.949	2.76E+04	3.24E+04	94.4	8.377	2.9E-03	3.4E-03
V-307	1.02	22.8	10.123	1.36E+05	1.39E+05	84.8	7.372	2.0E-03	2.0E-03
V-308	1.20	25.8	10.284	1.09E+05	1.31E+05	87.0	7.706	2.7E-03	3.2E-03
V-309	1.14	34.4	9.912	1.65E+04	1.89E+04	94.0	8.067	3.0E-03	3.5E-03
V-310	1.15	25.2	9.967	1.18E+05	1.36E+05	105.5	7.156	1.9E-05	2.2E-05
V-311	1.40	35.5	9.756	9.26E+03	1.30E+04	90.2	8.067	6.6E-03	9.2E-03
V-312	1.23	35.5	9.785	9.90E+03	1.22E+04	90.3	7.766	3.2E-03	3.9E-03
V-401	1.14	31.9	10.452	9.55E+04	1.09E+05	144.9	9.239	8.5E-07	9.6E-07
V-402	1.15	23.4	10.037	2.00E+05	2.29E+05	123.1	8.518	1.3E-05	1.5E-05
V-403	1.23	26.6	10.265	8.89E+04	1.09E+05	135.3	9.059	1.9E-06	2.3E-06
V-404	1.34	27.9	10.622	1.55E+05	2.07E+05	132.6	8.948	2.5E-06	3.4E-06
V-405	1.37	26.5	10.552	1.76E+05	2.41E+05	129.8	8.898	4.0E-06	5.4E-06
V-406	1.36	28.0	10.585	1.41E+05	1.93E+05	137.6	9.121	1.4E-06	1.9E-06
V-501	1.10	24.6	10.455	2.05E+05	2.25E+05	126.6	9.094	2.4E-05	2.6E-05
V-502	1.11	22.3	10.432	3.09E+05	3.43E+05	126.6	8.702	9.6E-06	1.1E-05
V-503	1.15	22.3	10.177	1.73E+05	1.99E+05	125.5	8.547	8.4E-06	9.7E-06
V-504	1.10	25.2	10.610	2.62E+05	2.89E+05	124.5	8.895	2.3E-05	2.5E-05
V-505	1.12	27.6	10.372	9.36E+04	1.05E+05	127.0	8.746	9.7E-06	1.1E-05
V-506	1.11	26.9	10.671	2.14E+05	2.39E+05	134.2	9.234	7.1E-06	7.9E-06
V-601	1.12	22.5	10.750	6.24E+05	6.98E+05	162.8	9.161	1.9E-08	2.2E-08
V-602	1.03	20.8	10.434	4.20E+05	4.32E+05	163.6	9.333	2.5E-08	2.5E-08
V-603	1.36	22.3	10.586	4.42E+05	6.02E+05	162.6	8.820	9.2E-09	1.3E-08
V-604	1.10	23.8	10.224	1.41E+05	1.55E+05	155.3	8.618	2.5E-08	2.8E-08
V-605	1.11	25.2	10.152	9.06E+04	1.00E+05	164.0	8.184	1.6E-09	1.8E-09

V-606	1.11	33.3	10.767	7.36E+04	8.19E+04	173.6	8.798	9.7E-10	1.1E-09
V-607	1.20	24.4	10.315	1.56E+05	1.87E+05	167.8	8.257	8.9E-10	1.1E-09
V-608	1.08	26.5	10.156	7.02E+04	7.62E+04	160.2	8.123	3.0E-09	3.3E-09
V-609	1.09	17.7	10.335	6.19E+05	6.77E+05	162.4	8.472	4.3E-09	4.7E-09
V-610	1.12	14.4	10.137	7.64E+05	8.53E+05	160.9	8.089	2.4E-09	2.7E-09
V-701	1.20	28.3	9.923	5.75E+04	6.92E+04	112.4	8.904	2.6E-04	3.1E-04
V-702	1.21	32.9	9.665	1.28E+04	1.54E+04	122.2	9.455	1.3E-04	1.6E-04
V-703	1.17	28.9	9.875	4.54E+04	5.30E+04	106.6	8.557	3.8E-04	4.4E-04
V-704	1.23	33.0	9.720	1.40E+04	1.72E+04	116.4	8.959	1.3E-04	1.6E-04
V-705	1.25	35.2	9.780	1.04E+04	1.30E+04	119.9	8.974	6.8E-05	8.6E-05
V-706	1.25	37.9	10.126	1.35E+04	1.68E+04	118.1	9.100	1.3E-04	1.6E-04
V-801	1.11	26.6	9.450	2.68E+04	2.97E+04	116.0	8.453	4.5E-08	5.0E-08
V-802	1.17	28.9	10.176	4.54E+04	5.30E+04	106.6	8.557	3.8E-04	4.4E-04
V-803	1.17	31.3	10.098	2.36E+04	2.76E+04	119.9	8.967	6.8E-05	7.9E-05
V-804	1.17	32.4	10.085	1.85E+04	2.17E+04	110.9	8.317	9.2E-05	1.1E-04

[a] $\mathbf{E_{a,f}}$**:** Activation energy of the forward reaction, given in kJ mol^{-1}.
[b] $\boldsymbol{log\widetilde{A}_f}$**:** Logarithm of the pre-exponential factor of the forward reaction, given in m^3 mol^{-1} s^{-1}.
[c] $\mathbf{k_f}$**:** The reaction rate coefficient for the forward reaction excluding tunneling effects, given in m^3 mol^{-1} s^{-1}.
[d] $\boldsymbol{\kappa k_f}$**:** The reaction rate coefficient for the forward reaction including tunneling effects, given in m^3 mol^{-1} s^{-1}.
[e] $\mathbf{E_{a,r}}$**:** Activation energy of the reverse reaction, given in kJ mol^{-1}.
[f] $\boldsymbol{log\widetilde{A}_r}$**:** Logarithm of the pre-exponential factor of the reverse reaction, given in m^3 mol^{-1} s^{-1}.
[g] $\mathbf{k_r}$**:** The reaction rate coefficient for the reverse reaction excluding tunneling effects, given in m^3 mol^{-1} s^{-1}.
[h] $\boldsymbol{\kappa k_r}$**:** The reaction rate coefficient for the reverse reaction including tunneling effects, given in m^3 mol^{-1} s^{-1}.

Table D-19 Arrhenius parameters (activation energy (**Ea**) and logarithm of the pre-exponential factor ($\log\widetilde{A}$)) of the HARs in the validation set 1000 K, given along with reaction rate coefficients and the Eckart tunneling correction factor (κ) for forward and reverse reactions.

Reaction #	κ	Forward				Reverse			
		$E_{a,f}$ [a]	$log\widetilde{A}_f$[b]	k_f[c]	κk_f [d]	$E_{a,r}$ [e]	$log\widetilde{A}_r$[f]	k_r[g]	κk_r [h]
V-101	1.12	45.5	10.104	3.00E+05	3.37E+05	108.6	9.234	7.7E+00	8.6E+00
V-102	1.13	47.1	10.212	3.09E+05	3.49E+05	112.0	9.834	9.7E+00	1.1E+01
V-103	1.12	44.5	10.069	3.17E+05	3.55E+05	109.0	9.624	8.5E+00	9.6E+00
V-104	1.14	45.4	10.522	8.48E+05	9.69E+05	113.8	9.819	1.5E+01	1.7E+01
V-105	1.13	50.2	10.551	5.07E+05	5.72E+05	118.6	10.102	1.6E+01	1.8E+01
V-201	1.06	36.7	10.540	8.34E+05	8.84E+05	106.4	8.882	4.2E+00	4.5E+00
V-202	1.05	36.7	10.337	5.26E+05	5.54E+05	108.6	8.713	2.2E+00	2.3E+00
V-203	1.12	41.9	10.472	3.84E+05	4.31E+05	109.4	8.545	1.4E+00	1.5E+00
V-204	1.12	42.3	10.338	2.69E+05	3.00E+05	108.1	9.000	4.5E+00	5.0E+00
V-205	1.13	44.1	10.663	4.57E+05	5.16E+05	107.9	9.373	1.1E+01	1.2E+01
V-206	1.07	43.6	10.844	7.36E+05	7.89E+05	115.5	9.324	3.9E+00	4.2E+00
V-207	1.06	39.3	10.679	8.49E+05	8.98E+05	121.3	9.182	1.4E+00	1.5E+00
V-208	1.08	36.7	10.523	8.07E+05	8.73E+05	111.4	8.460	8.8E-01	9.5E-01
V-209	1.07	36.4	10.436	6.86E+05	7.32E+05	107.6	8.972	4.5E+00	4.8E+00
V-210	1.06	38.2	10.585	7.76E+05	8.20E+05	117.9	8.850	9.8E-01	1.0E+00
V-301	1.03	40.1	10.490	2.49E+05	2.56E+05	104.2	8.932	6.2E+00	6.3E+00
V-302	1.04	41.7	10.920	5.49E+05	5.69E+05	105.3	9.057	7.2E+00	7.5E+00
V-303	1.04	35.6	10.667	6.39E+05	6.67E+05	115.9	8.112	2.3E-01	2.4E-01
V-304	1.05	36.2	10.632	5.53E+05	5.81E+05	116.0	8.026	1.9E-01	2.0E-01
V-305	1.06	32.3	10.706	1.04E+06	1.10E+06	88.4	8.632	2.1E+01	2.2E+01
V-306	1.06	35.2	10.372	3.43E+05	3.65E+05	101.6	8.846	7.0E+00	7.4E+00
V-307	1.01	28.6	10.506	1.03E+06	1.04E+06	91.4	7.804	2.2E+00	2.2E+00
V-308	1.07	32.3	10.717	1.07E+06	1.15E+06	94.3	8.186	3.6E+00	3.9E+00
V-309	1.05	40.6	10.330	3.24E+05	3.41E+05	101.1	8.534	7.2E+00	7.5E+00
V-310	1.05	31.5	10.389	1.10E+06	1.16E+06	112.6	7.626	1.1E-01	1.2E-01
V-311	1.11	41.2	10.212	2.30E+05	2.55E+05	96.5	8.534	1.2E+01	1.4E+01
V-312	1.07	40.1	10.289	3.13E+05	3.34E+05	96.2	8.233	6.5E+00	6.9E+00
V-401	1.05	38.0	10.845	1.46E+06	1.53E+06	151.8	9.734	1.3E-01	1.3E-01
V-402	1.05	29.6	10.454	1.61E+06	1.69E+06	130.8	8.966	2.7E-01	2.9E-01
V-403	1.08	32.9	10.687	9.30E+05	1.00E+06	142.1	9.534	1.3E-01	1.4E-01
V-404	1.12	34.6	11.065	1.82E+06	2.03E+06	139.8	9.422	1.3E-01	1.5E-01
V-405	1.12	34.4	10.992	1.57E+06	1.76E+06	137.7	9.366	1.5E-01	1.7E-01
V-406	1.12	34.6	11.025	1.66E+06	1.86E+06	144.7	9.592	1.1E-01	1.2E-01
V-501	1.04	30.7	10.861	1.81E+06	1.87E+06	133.5	9.546	7.5E-01	7.8E-01
V-502	1.04	28.4	10.837	2.26E+06	2.35E+06	133.5	9.155	3.0E-01	3.2E-01
V-503	1.05	28.5	10.594	1.27E+06	1.34E+06	132.7	9.023	2.5E-01	2.6E-01

V-504	1.04	31.2	11.016	2.42E+06	2.51E+06	131.4	9.347	6.1E-01	6.3E-01
V-505	1.04	33.6	10.775	1.05E+06	1.09E+06	133.9	9.197	3.2E-01	3.3E-01
V-506	1.04	33.4	11.008	1.83E+06	1.91E+06	141.2	9.612	3.5E-01	3.6E-01
V-601	1.04	28.8	11.173	4.67E+06	4.87E+06	170.0	9.632	1.1E-02	1.2E-02
V-602	1.01	26.9	10.734	2.13E+06	2.16E+06	170.3	9.767	1.5E-02	1.5E-02
V-603	1.12	28.7	11.028	3.38E+06	3.80E+06	162.2	9.291	1.3E-02	1.5E-02
V-604	1.03	29.8	10.624	1.17E+06	1.21E+06	160.1	9.068	1.0E-02	1.1E-02
V-605	1.04	31.3	10.556	8.37E+05	8.70E+05	171.1	8.637	1.0E-03	1.0E-03
V-606	1.04	39.4	11.171	1.30E+06	1.36E+06	180.5	9.251	1.3E-03	1.4E-03
V-607	1.07	30.7	10.734	1.36E+06	1.45E+06	174.9	8.725	7.8E-04	8.3E-04
V-608	1.03	32.4	10.545	7.16E+05	7.38E+05	171.1	8.559	8.4E-04	8.6E-04
V-609	1.03	23.6	10.726	3.12E+06	3.22E+06	169.0	8.909	2.4E-03	2.5E-03
V-610	1.04	20.4	10.537	2.96E+06	3.08E+06	168.1	8.534	1.1E-03	1.2E-03
V-701	1.07	34.6	10.340	6.86E+05	7.35E+05	119.7	9.381	2.7E+00	2.9E+00
V-702	1.07	39.2	10.087	2.20E+05	2.36E+05	129.5	9.936	3.0E+00	3.2E+00
V-703	1.06	35.3	10.301	5.72E+05	6.06E+05	113.8	9.030	2.4E+00	2.6E+00
V-704	1.08	39.3	10.138	2.44E+05	2.63E+05	123.6	9.436	1.9E+00	2.1E+00
V-705	1.09	41.5	10.202	2.16E+05	2.35E+05	127.3	9.460	1.3E+00	1.4E+00
V-706	1.09	44.3	10.554	3.48E+05	3.78E+05	125.4	9.579	2.1E+00	2.3E+00
V-801	1.04	32.6	9.852	2.79E+05	2.90E+05	123.0	8.916	6.2E-04	6.4E-04
V-802	1.06	35.3	10.602	5.72E+05	6.06E+05	113.8	9.030	2.4E+00	2.6E+00
V-803	1.07	37.7	10.489	3.31E+05	3.54E+05	127.2	9.398	1.1E+00	1.2E+00
V-804	1.06	38.7	10.505	3.06E+05	3.25E+05	118.0	8.789	8.4E-01	8.9E-01

[a] $\mathbf{E_{a,r}}$**:** Activation energy of the forward reaction, given in kJ mol^{-1}.
[b] $\boldsymbol{log\widetilde{A}_f}$**:** Logarithm of the pre-exponential factor of the forward reaction, given in m^3 mol^{-1} s^{-1}.
[c] $\mathbf{k_f}$**:** The reaction rate coefficient for the forward reaction excluding tunneling effects, given in m^3 mol^{-1} s^{-1}.
[d] $\boldsymbol{\kappa k_f}$**:** The reaction rate coefficient for the forward reaction including tunneling effects, given in m^3 mol^{-1} s^{-1}.
[e] $\mathbf{E_{a,r}}$**:** Activation energy of the reverse reaction, given in kJ mol^{-1}.
[f] $\boldsymbol{log\widetilde{A}_r}$**:** Logarithm of the pre-exponential factor of the reverse reaction, given in m^3 mol^{-1} s^{-1}.
[g] $\mathbf{k_r}$**:** The reaction rate coefficient for the reverse reaction excluding tunneling effects, given in m^3 mol^{-1} s^{-1}.
[h] $\boldsymbol{\kappa k_r}$**:** The reaction rate coefficient for the reverse reaction including tunneling effects, given in m^3 mol^{-1} s^{-1}.

Table D-20 Arrhenius parameters (activation energy (**Ea**) and logarithm of the pre-exponential factor ($\log\widetilde{A}$)) of the HARs in the validation set 1500 K, given along with reaction rate coefficients and the Eckart tunneling correction factor (κ) for forward and reverse reactions.

Reaction #	κ	Forward				Reverse			
		$E_{a,f}$ [a]	$log\widetilde{A}_f$ [b]	k_f [c]	κk_f [d]	$E_{a,r}$ [e]	$log\widetilde{A}_r$ [f]	k_r [g]	κk_r [h]
V-101	1.06	54.5	10.519	2.45E+09	2.59E+09	119.6	9.745	5.8E+05	6.1E+05
V-102	1.06	55.3	10.731	2.92E+09	3.08E+09	123.3	10.324	1.1E+06	1.1E+06
V-103	1.06	54.3	10.369	3.60E+09	3.80E+09	120.4	10.124	8.6E+05	9.0E+05
V-104	1.06	54.2	10.939	6.75E+09	7.19E+09	124.8	10.287	1.7E+06	1.9E+06
V-105	1.06	59.6	10.950	4.50E+09	4.76E+09	129.3	10.555	2.3E+06	2.4E+06
V-201	1.03	44.6	10.872	4.18E+09	4.30E+09	117.5	9.350	3.7E+05	3.8E+05
V-202	1.02	44.5	10.667	2.63E+09	2.69E+09	119.7	9.182	3.7E+05	3.8E+05
V-203	1.06	49.7	10.812	2.41E+09	2.55E+09	120.1	9.025	3.7E+05	3.9E+05
V-204	1.05	50.4	10.679	1.68E+09	1.77E+09	119.4	9.478	3.7E+05	3.9E+05
V-205	1.06	51.6	11.005	3.23E+09	3.42E+09	119.2	9.853	3.7E+05	3.9E+05
V-206	1.03	51.5	11.177	4.86E+09	5.02E+09	126.6	9.785	3.7E+05	3.8E+05
V-207	1.03	47.1	11.010	4.70E+09	4.83E+09	132.3	9.650	2.1E+05	2.1E+05
V-208	1.04	44.6	10.760	3.22E+09	3.34E+09	122.6	8.934	2.1E+05	2.2E+05
V-209	1.03	44.2	10.770	3.39E+09	3.49E+09	118.7	9.442	3.7E+05	3.8E+05
V-210	1.03	46.0	10.916	4.12E+09	4.23E+09	129.0	9.317	2.1E+05	2.1E+05
V-301	1.02	48.1	10.853	1.51E+09	1.55E+09	115.5	9.456	4.7E+05	4.8E+05
V-302	1.02	49.7	11.259	3.37E+09	3.45E+09	116.6	9.533	4.7E+05	4.8E+05
V-303	1.02	43.4	10.996	3.06E+09	3.13E+09	127.0	8.569	3.9E+04	4.0E+04
V-304	1.02	44.0	10.964	2.71E+09	2.77E+09	127.2	8.501	3.9E+04	4.0E+04
V-305	1.02	40.3	11.047	4.40E+09	4.50E+09	99.6	9.106	6.8E+05	6.9E+05
V-306	1.02	43.0	10.706	1.62E+09	1.65E+09	112.7	9.318	4.7E+05	4.8E+05
V-307	1.02	36.0	10.821	3.69E+09	3.78E+09	102.1	8.257	2.2E+05	2.2E+05
V-308	1.02	40.2	11.055	4.51E+09	4.62E+09	105.6	8.662	2.2E+05	2.2E+05
V-309	1.02	48.7	10.662	1.85E+09	1.89E+09	112.2	9.004	9.4E+05	9.6E+05
V-310	1.02	39.3	10.721	4.49E+09	4.60E+09	123.8	8.101	3.9E+04	4.0E+04
V-311	1.02	48.9	10.567	1.46E+09	1.50E+09	108.2	9.004	7.0E+05	7.1E+05
V-312	1.02	47.9	10.665	1.99E+09	2.03E+09	108.6	8.703	7.0E+05	7.1E+05
V-401	1.02	45.6	11.250	9.19E+09	9.41E+09	162.9	10.232	8.7E+04	8.9E+04
V-402	1.02	37.4	10.782	6.06E+09	6.20E+09	142.1	9.436	9.3E+04	9.5E+04
V-403	1.04	41.1	11.019	3.87E+09	4.01E+09	154.4	10.013	7.7E+04	8.0E+04
V-404	1.05	42.6	11.406	8.37E+09	8.81E+09	151.2	9.905	7.7E+04	8.1E+04
V-405	1.06	42.3	11.332	7.22E+09	7.62E+09	149.9	9.848	4.6E+04	4.9E+04
V-406	1.05	42.5	11.365	7.65E+09	8.07E+09	156.1	10.073	2.6E+04	2.8E+04
V-501	1.02	38.3	11.184	7.08E+09	7.20E+09	144.4	10.009	1.6E+05	1.6E+05
V-502	1.02	37.7	11.159	7.02E+09	7.15E+09	144.5	9.620	1.6E+05	1.6E+05
V-503	1.02	36.3	10.923	4.57E+09	4.69E+09	143.9	9.499	4.5E+04	4.6E+04

V-504	1.02	38.8	11.337	9.67E+09	9.83E+09	142.3	9.811	1.6E+05	1.6E+05
V-505	1.02	41.2	11.096	4.60E+09	4.69E+09	144.9	9.661	1.4E+05	1.4E+05
V-506	1.02	41.5	11.293	7.06E+09	7.19E+09	150.7	10.123	1.4E+05	1.4E+05
V-601	1.02	36.5	11.500	1.70E+10	1.73E+10	181.1	10.104	1.9E+04	1.9E+04
V-602	1.00	36.6	11.124	7.07E+09	7.11E+09	181.2	10.217	1.9E+04	1.9E+04
V-603	1.05	36.2	11.369	1.28E+10	1.35E+10	177.3	9.772	7.2E+03	7.6E+03
V-604	1.02	37.4	10.944	4.40E+09	4.47E+09	171.2	9.532	7.2E+03	7.4E+03
V-605	1.02	38.8	10.878	3.35E+09	3.41E+09	180.5	9.101	1.4E+03	1.4E+03
V-606	1.02	46.9	11.493	7.22E+09	7.35E+09	191.5	9.718	1.4E+03	1.4E+03
V-607	1.03	38.5	11.066	5.33E+09	5.50E+09	186.1	9.201	1.4E+03	1.4E+03
V-608	1.01	39.8	10.859	2.98E+09	3.03E+09	180.1	9.017	1.3E+03	1.3E+03
V-609	1.01	31.0	11.040	9.14E+09	9.28E+09	179.8	9.365	1.3E+03	1.3E+03
V-610	1.02	28.0	10.857	7.62E+09	7.76E+09	179.4	8.996	1.4E+03	1.4E+03
V-701	1.03	42.3	10.671	3.15E+09	3.25E+09	131.0	9.863	3.8E+05	4.0E+05
V-702	1.03	47.0	10.419	1.21E+09	1.25E+09	140.8	10.417	4.5E+05	4.6E+05
V-703	1.03	43.2	10.636	2.71E+09	2.78E+09	125.1	9.506	6.4E+05	6.6E+05
V-704	1.04	47.1	10.470	1.35E+09	1.40E+09	135.0	9.918	3.8E+05	4.0E+05
V-705	1.04	49.4	10.536	1.31E+09	1.36E+09	138.8	9.946	3.4E+05	3.5E+05
V-706	1.04	52.1	10.888	2.36E+09	2.46E+09	136.8	10.061	4.5E+05	4.6E+05
V-801	1.02	40.3	10.176	1.19E+06	1.21E+06	134.1	9.386	1.0E-01	1.1E-01
V-802	1.03	43.2	10.937	2.71E+09	2.78E+09	125.1	9.506	1.5E+05	1.6E+05
V-803	1.04	45.4	10.812	1.70E+09	1.76E+09	138.3	9.867	2.8E+05	2.9E+05
V-804	1.03	46.5	10.837	1.66E+09	1.70E+09	129.2	9.263	1.1E+05	1.1E+05

[a] $\mathbf{E_{a,r}}$**:** Activation energy of the forward reaction, given in kJ mol^{-1}.
[b] $\boldsymbol{log\widetilde{A}_f}$**:** Logarithm of the pre-exponential factor of the forward reaction, given in m^3 mol^{-1} s^{-1}.
[c] $\mathbf{k_f}$**:** The reaction rate coefficient for the forward reaction excluding tunneling effects, given in m^3 mol^{-1} s^{-1}.
[d] $\boldsymbol{\kappa k_f}$**:** The reaction rate coefficient for the forward reaction including tunneling effects, given in m^3 mol^{-1} s^{-1}.
[e] $\mathbf{E_{a,r}}$**:** Activation energy of the reverse reaction, given in kJ mol^{-1}.
[f] $\boldsymbol{log\widetilde{A}_r}$**:** Logarithm of the pre-exponential factor of the reverse reaction, given in m^3 mol^{-1} s^{-1}.
[g] $\mathbf{k_r}$**:** The reaction rate coefficient for the reverse reaction excluding tunneling effects, given in m^3 mol^{-1} s^{-1}.
[h] $\boldsymbol{\kappa k_r}$**:** The reaction rate coefficient for the reverse reaction including tunneling effects, given in m^3 mol^{-1} s^{-1}.

Table D-21 Arrhenius parameters (activation energy (**Ea**) and logarithm of the pre-exponential factor ($\log\widetilde{A}$)) of the reactions in the validation set 2000 K, given along with reaction rate coefficients and the Eckart tunneling correction factor (κ) for forward and reverse reactions.

Reaction #	κ	Forward				Reverse			
		$E_{a,f}$ [a]	$log\widetilde{A}_f$ [b]	k_f [c]	κk_f [d]	$E_{a,r}$ [e]	$log\widetilde{A}_r$ [f]	k_r [g]	κk_r [h]
V-101	1.03	63.3	10.782	1.20E+07	1.24E+07	130.5	9.745	6.0E+03	6.2E+03
V-102	1.03	65.3	11.056	1.27E+07	1.32E+07	134.3	10.324	1.3E+04	1.4E+04
V-103	1.03	63.2	10.643	1.09E+07	1.13E+07	132.1	10.124	4.7E+03	4.9E+03
V-104	1.04	63.4	11.197	2.08E+07	2.16E+07	135.6	10.287	2.3E+04	2.4E+04
V-105	1.03	67.8	11.199	1.60E+07	1.66E+07	139.8	10.555	3.3E+04	3.4E+04
V-201	1.02	51.9	11.093	1.09E+07	1.11E+07	129.0	9.350	4.3E+03	4.3E+03
V-202	1.01	51.8	10.888	6.86E+06	6.96E+06	131.3	9.182	2.5E+03	2.6E+03
V-203	1.03	56.9	11.037	7.11E+06	7.34E+06	131.4	9.025	1.8E+03	1.8E+03
V-204	1.03	57.9	10.905	4.94E+06	5.09E+06	131.0	9.478	5.1E+03	5.2E+03
V-205	1.03	59.8	11.231	9.34E+06	9.66E+06	130.9	9.853	1.2E+04	1.3E+04
V-206	1.02	58.8	11.399	1.46E+07	1.49E+07	138.2	9.785	6.8E+03	7.0E+03
V-207	1.02	54.4	11.231	1.29E+07	1.31E+07	143.9	9.650	3.5E+03	3.5E+03
V-208	1.02	52.0	10.968	8.14E+06	8.32E+06	134.2	8.934	1.2E+03	1.2E+03
V-209	1.02	51.6	10.992	8.81E+06	8.97E+06	130.2	9.442	4.9E+03	5.0E+03
V-210	1.02	53.3	11.137	1.11E+07	1.13E+07	140.5	9.317	2.0E+03	2.0E+03
V-301	1.02	55.5	11.089	4.36E+06	4.47E+06	127.1	9.456	4.6E+03	4.7E+03
V-302	1.03	57.2	11.483	6.78E+06	6.96E+06	128.1	9.533	6.9E+03	7.0E+03
V-303	1.01	50.7	11.215	7.80E+06	7.88E+06	138.5	8.569	4.1E+02	4.2E+02
V-304	1.01	51.3	11.185	6.99E+06	7.09E+06	138.8	8.501	3.4E+02	3.4E+02
V-305	1.02	47.9	11.274	1.06E+07	1.07E+07	111.2	9.106	7.1E+03	7.2E+03
V-306	1.02	50.4	10.928	4.09E+06	4.16E+06	124.2	9.318	5.3E+03	5.3E+03
V-307	1.00	43.1	11.035	8.11E+06	8.13E+06	113.4	8.257	8.6E+02	8.7E+02
V-308	1.02	47.6	11.278	1.08E+07	1.10E+07	117.1	8.662	1.8E+03	1.8E+03
V-309	1.01	56.0	10.883	5.27E+06	5.34E+06	123.7	9.004	5.3E+03	5.3E+03
V-310	1.01	46.7	10.943	1.06E+07	1.07E+07	135.4	8.101	1.6E+02	1.7E+02
V-311	1.01	56.4	10.834	4.59E+06	4.63E+06	120.6	9.004	6.3E+03	6.4E+03
V-312	1.01	54.9	10.876	5.54E+06	5.59E+06	120.4	8.703	3.2E+03	3.2E+03
V-401	1.01	52.8	11.457	2.39E+07	2.42E+07	174.5	10.232	2.1E+03	2.1E+03
V-402	1.01	44.6	11.001	1.37E+07	1.39E+07	153.9	9.436	1.2E+03	1.2E+03
V-403	1.02	49.8	11.240	8.70E+06	8.88E+06	165.9	10.013	1.1E+03	1.1E+03
V-404	1.03	50.0	11.630	2.11E+07	2.17E+07	163.0	9.905	1.0E+03	1.0E+03
V-405	1.03	49.8	11.555	1.80E+07	1.86E+07	161.6	9.848	9.6E+02	9.9E+02
V-406	1.03	50.0	11.589	1.92E+07	1.98E+07	167.9	10.073	1.1E+03	1.1E+03
V-501	1.01	45.5	11.400	1.63E+07	1.65E+07	155.9	10.009	3.8E+03	3.9E+03
V-502	1.01	45.5	11.376	1.54E+07	1.56E+07	155.9	9.620	1.6E+03	1.6E+03
V-503	1.01	43.6	11.143	1.01E+07	1.03E+07	155.5	9.499	1.2E+03	1.2E+03

V-504	1.01	46.0	11.553	2.25E+07	2.27E+07	153.8	9.811	2.8E+03	2.8E+03
V-505	1.01	48.3	11.312	1.12E+07	1.13E+07	156.3	9.661	1.7E+03	1.7E+03
V-506	1.01	47.8	11.460	1.63E+07	1.65E+07	158.4	10.123	1.9E+03	2.0E+03
V-601	1.01	43.7	11.718	3.77E+07	3.81E+07	192.7	10.104	5.3E+02	5.3E+02
V-602	1.00	43.1	11.334	1.62E+07	1.62E+07	192.6	10.217	6.7E+02	6.7E+02
V-603	1.03	41.9	11.593	3.15E+07	3.25E+07	188.3	9.772	3.2E+02	3.3E+02
V-604	1.01	44.5	11.160	9.94E+06	1.00E+07	183.3	9.532	2.5E+02	2.5E+02
V-605	1.01	46.0	11.095	7.80E+06	7.88E+06	191.0	9.101	5.7E+01	5.8E+01
V-606	1.01	54.1	11.710	1.98E+07	2.00E+07	203.0	9.718	1.2E+02	1.2E+02
V-607	1.02	45.8	11.287	1.23E+07	1.26E+07	197.8	9.201	4.9E+01	4.9E+01
V-608	1.01	46.8	11.072	7.07E+06	7.12E+06	192.1	9.017	4.4E+01	4.4E+01
V-609	1.01	38.0	11.252	1.82E+07	1.83E+07	191.2	9.365	1.0E+02	1.0E+02
V-610	1.01	35.1	11.073	1.43E+07	1.45E+07	190.8	8.996	4.6E+01	4.6E+01
V-701	1.02	49.7	10.892	7.86E+06	8.01E+06	142.8	9.863	6.1E+03	6.2E+03
V-702	1.02	54.3	10.640	3.33E+06	3.39E+06	152.5	10.417	1.2E+04	1.2E+04
V-703	1.02	50.6	10.859	6.90E+06	7.01E+06	136.7	9.506	3.9E+03	3.9E+03
V-704	1.02	54.4	10.691	3.72E+06	3.80E+06	146.8	9.918	5.5E+03	5.6E+03
V-705	1.02	56.7	10.758	3.78E+06	3.86E+06	150.6	9.946	4.7E+03	4.8E+03
V-706	1.02	59.5	11.110	7.19E+06	7.36E+06	148.5	10.061	6.8E+03	7.0E+03
V-801	1.01	47.5	10.395	2.84E+06	2.87E+06	145.7	9.386	1.7E+00	1.7E+00
V-802	1.02	50.6	11.160	6.90E+06	7.01E+06	136.7	9.506	3.9E+03	3.9E+03
V-803	1.02	52.5	11.021	4.47E+06	4.54E+06	149.9	9.867	3.7E+03	3.8E+03
V-804	1.02	53.8	11.057	4.49E+06	4.57E+06	140.8	9.263	1.7E+03	1.7E+03

[a] $\mathbf{E_{a,f}}$**:** Activation energy of the forward reaction, given in kJ mol^{-1}.
[b] $\boldsymbol{log\tilde{A}_f}$**:** Logarithm of the pre-exponential factor of the forward reaction, given in m^3 mol^{-1} s^{-1}.
[c] $\mathbf{k_f}$**:** The reaction rate coefficient for the forward reaction excluding tunneling effects, given in m^3 mol^{-1} s^{-1}.
[d] $\boldsymbol{\kappa k_f}$**:** The reaction rate coefficient for the forward reaction including tunneling effects, given in m^3 mol^{-1} s^{-1}.
[e] $\mathbf{E_{a,r}}$**:** Activation energy of the reverse reaction, given in kJ mol^{-1}.
[f] $\boldsymbol{log\tilde{A}_r}$**:** Logarithm of the pre-exponential factor of the reverse reaction, given in m^3 mol^{-1} s^{-1}.
[g] $\mathbf{k_r}$**:** The reaction rate coefficient for the reverse reaction excluding tunneling effects, given in m^3 mol^{-1} s^{-1}.
[h] $\boldsymbol{\kappa k_r}$**:** The reaction rate coefficient for the reverse reaction including tunneling effects, given in m^3 mol^{-1} s^{-1}.

Table D-22 External symmetry (σ_{ext}), internal symmetry (σ_{int}) and the number of optical isomers (n_{opt}) for the reactants, products and the transition state of the hydrogen abstraction reactions in the training set, given along with the number of single events for the forward and reverse directions.

Reaction #	Forward						Reverse						Transition State			n_e[d]	
	Reactant 1			Reactant 2			Reactant 1			Reactant 2							
	σ_{ext}[a]	σ_{int}[b]	n_{opt}[c]	σ_{ext}	σ_{int}	n_{opt}	σ_{ext}	σ_{int}	n_{opt}	σ_{ext}	σ_{int}	n_{opt}	σ_{ext}	σ_{int}	n_{opt}	$n_{e,f}$[e]	$n_{e,r}$[f]
V-101	2	27	1	1	1	1	2	9	1	1	1	1	2	9	1	3	1
V-102	1	6	1	1	1	1	2	1	1	1	1	1	2	1	1	3	1
V-103	1	9	1	1	1	1	1	3	1	1	1	1	1	3	1	3	1
V-104	1	3	1	1	1	1	1	1	1	1	1	1	1	1	2	6	2
V-105	1	3	1	1	1	1	1	1	1	1	1	1	1	1	2	6	2
V-201	1	9	1	1	1	1	1	9	1	1	1	1	1	9	2	2	2
V-202	1	9	1	1	1	1	1	9	1	1	1	1	1	9	2	2	2
V-203	2	27	1	1	1	1	2	27	1	1	1	1	2	27	2	2	2
V-204	2	3	1	1	1	1	2	3	1	1	1	1	2	3	2	2	2
V-205	2	3	1	1	1	1	2	3	1	1	1	1	2	3	2	2	2
V-206	1	9	1	1	1	1	1	9	1	1	1	1	1	9	2	2	2
V-207	1	3	1	1	1	1	1	3	1	1	1	1	1	3	2	2	2
V-208	1	3	1	1	1	1	1	3	1	1	1	1	1	3	2	2	2
V-209	1	27	1	1	1	1	1	27	1	1	1	1	1	27	2	2	2
V-210	1	9	1	1	1	1	1	9	1	1	1	1	1	9	2	2	2
V-301	1	27	1	1	1	1	1	54	1	1	1	1	1	27	1	1	2
V-302	1	9	1	1	1	1	1	18	1	1	1	1	1	9	1	1	2
V-303	1	27	1	1	1	1	1	54	1	1	1	1	1	27	1	1	2
V-304	1	27	1	1	1	1	1	54	1	1	1	1	1	27	1	1	2
V-305	1	27	1	1	1	1	1	54	1	1	1	1	1	27	1	1	2
V-306	1	27	1	1	1	1	1	54	1	1	1	1	1	27	1	1	2
V-307	1	9	1	1	1	1	1	18	1	1	1	1	1	9	1	1	2
V-308	1	81	1	1	1	1	1	162	1	1	1	1	1	81	1	1	2
V-309	1	9	1	1	1	1	1	18	1	1	1	1	1	9	2	2	4
V-310	1	3	1	1	1	1	1	3	1	1	1	1	1	3	2	2	2
V-311	1	81	1	1	1	1	1	162	1	1	1	1	1	81	2	2	4
V-312	1	27	1	1	1	1	1	54	1	1	1	1	1	27	2	2	4
V-401	1	1	1	1	1	1	1	1	1	1	1	1	1	1	2	2	2
V-402	1	3	1	1	1	1	1	3	1	1	1	1	1	3	2	2	2
V-403	1	18	1	1	1	1	1	18	1	1	1	1	1	18	1	1	1
V-404	1	1	1	1	1	1	1	1	1	1	1	1	1	1	1	1	1
V-405	1	3	1	1	1	1	1	3	1	1	1	1	1	3	1	1	1
V-406	1	18	1	1	1	1	1	18	1	1	1	1	1	18	1	1	1
V-501	1	3	2	1	1	1	1	3	1	1	1	1	1	3	2	1	2

V-502	1	27	2	1	1	1	1	27	1	1	1	1	1	27	2	1	2
V-503	1	3	2	1	1	1	1	3	1	1	1	1	1	3	2	1	2
V-504	1	9	2	1	1	1	1	9	1	1	1	1	1	9	2	1	2
V-505	1	9	2	1	1	1	1	9	1	1	1	1	1	9	2	1	2
V-506	1	3	2	1	1	1	1	3	1	1	1	1	1	3	2	1	2
V-601	1	3	1	1	1	1	1	6	1	1	1	1	1	3	1	1	2
V-602	1	1	1	1	1	1	1	2	1	1	1	1	1	1	1	1	2
V-603	1	3	1	1	1	1	1	6	1	1	1	1	1	3	1	1	2
V-604	1	9	1	1	1	1	1	18	1	1	1	1	1	9	1	1	2
V-605	1	9	1	1	1	1	1	18	1	1	1	1	1	9	1	1	2
V-606	1	9	1	1	1	1	1	18	1	1	1	1	1	9	1	1	2
V-607	1	9	1	1	1	1	1	18	1	1	1	1	1	9	1	1	2
V-608	1	1	1	1	1	1	1	2	1	1	1	1	1	1	1	1	2
V-609	1	3	1	1	1	1	1	6	1	1	1	1	1	3	1	1	2
V-610	1	1	1	1	1	1	1	2	1	1	1	1	1	1	1	1	2
V-701	1	6	1	1	1	1	1	6	1	1	1	1	1	6	2	2	2
V-702	1	6	1	1	1	1	1	6	1	1	1	1	1	6	2	2	2
V-703	1	18	1	1	1	1	1	18	1	1	1	1	1	18	2	2	2
V-704	1	2	1	1	1	1	1	2	1	1	1	1	1	2	2	2	2
V-705	1	2	1	1	1	1	1	2	1	1	1	1	1	2	2	2	2
V-706	1	6	1	1	1	1	1	6	1	1	1	1	1	6	2	2	2
V-801	1	18	2	1	1	1	1	18	1	1	1	1	1	18	2	1	2
V-802	1	9	2	1	1	1	1	9	1	1	1	1	1	9	2	1	2
V-803	1	18	2	1	1	1	1	18	1	1	1	1	1	18	2	1	2
V-804	1	18	2	1	1	1	1	18	1	1	1	1	1	18	2	1	2

[a] $\boldsymbol{\sigma_{ext}}$**:** External symmetry
[b] $\boldsymbol{\sigma_{int}}$**:** Internal symmetry
[c] $\boldsymbol{n_{opt}}$**:** Number of optical isomers
[d] $\boldsymbol{n_{e,f}}$**:** number of single events for the forward reaction
[e] $\boldsymbol{n_{e,r}}$**:** number of single events for the reverse reaction

D.5.3 Tunneling coefficients obtained from the Tunneling Correction Function

Table D-23 Comparison of the Eckart tunneling coefficients (κ_{Eckart}) with the ones obtained from the tunneling model (K_{TCF}) at 300 K, 600 K and 1000 K over the validation set.

Reaction #		300 K			600 K			1000 K		
		κ_{Eckart}	κ_{TCF}	ρ	κ_{Eckart}	κ_{TCF}	ρ	κ_{Eckart}	κ_{TCF}	ρ
1	**V-101**	3.7	2.7	1.4	1.4	1.6	1.1	1.1	1.3	1.1
2	**V-102**	4.0	2.7	1.5	1.4	1.6	1.1	1.1	1.3	1.1
3	**V-103**	3.7	2.7	1.4	1.4	1.6	1.1	1.1	1.3	1.1
4	**V-104**	4.7	2.7	1.8	1.4	1.6	1.1	1.1	1.3	1.1
5	**V-105**	4.2	2.7	1.6	1.4	1.6	1.1	1.1	1.3	1.1
6	**V-201**	1.9	2.2	1.2	1.2	1.4	1.2	1.1	1.2	1.1
7	**V-202**	1.7	2.2	1.3	1.1	1.4	1.2	1.1	1.2	1.1
8	**V-203**	1.8	2.2	1.2	1.4	1.4	1.0	1.1	1.2	1.1
9	**V-204**	1.7	2.2	1.3	1.3	1.4	1.0	1.1	1.2	1.1
10	**V-205**	2.3	2.2	1.1	1.4	1.4	1.0	1.1	1.2	1.1
11	**V-206**	2.2	2.2	1.0	1.2	1.4	1.1	1.1	1.2	1.1
12	**V-207**	1.9	2.2	1.2	1.2	1.4	1.2	1.1	1.2	1.1
13	**V-208**	2.1	2.2	1.0	1.2	1.4	1.1	1.1	1.2	1.1
14	**V-209**	2.0	2.2	1.1	1.2	1.4	1.2	1.1	1.2	1.1
15	**V-210**	1.8	2.2	1.2	1.2	1.4	1.2	1.1	1.2	1.1
16	**V-301**	2.8	2.3	1.2	1.3	1.4	1.1	1.0	1.1	1.1
17	**V-302**	2.9	2.3	1.3	1.3	1.4	1.1	1.0	1.1	1.1
18	**V-303**	2.6	1.8	1.4	1.1	1.3	1.1	1.0	1.1	1.1
19	**V-304**	1.7	1.8	1.0	1.1	1.3	1.1	1.1	1.1	1.1
20	**V-305**	1.8	1.8	1.0	1.2	1.3	1.1	1.1	1.1	1.1
21	**V-306**	1.9	2.3	1.2	1.2	1.4	1.2	1.1	1.2	1.1
22	**V-307**	1.1	1.8	1.6	1.0	1.3	1.2	1.0	1.1	1.1
23	**V-308**	2.1	1.8	1.2	1.2	1.3	1.1	1.1	1.1	1.1
24	**V-309**	1.7	2.3	1.3	1.1	1.4	1.2	1.1	1.2	1.1
25	**V-310**	1.7	1.8	1.0	1.1	1.3	1.1	1.1	1.1	1.1
26	**V-311**	2.6	2.3	1.1	1.4	1.4	1.0	1.1	1.2	1.1
27	**V-312**	2.8	2.3	1.2	1.2	1.4	1.1	1.1	1.2	1.1
28	**V-401**	2.4	1.9	1.3	1.1	1.3	1.1	1.0	1.2	1.1
29	**V-402**	1.7	1.9	1.1	1.1	1.3	1.1	1.1	1.2	1.1
30	**V-403**	2.8	1.9	1.5	1.2	1.3	1.0	1.1	1.2	1.1
31	**V-404**	1.6	1.9	1.2	1.3	1.3	1.0	1.1	1.2	1.0

32	**V-405**	2.8	1.9	1.5	1.4	1.3	1.1	1.1	1.2	1.0
33	**V-406**	2.3	1.9	1.2	1.4	1.3	1.1	1.1	1.2	1.0
34	**V-501**	1.5	1.5	1.0	1.1	1.2	1.1	1.0	1.1	1.1
35	**V-502**	1.5	1.5	1.0	1.1	1.2	1.1	1.0	1.1	1.1
36	**V-503**	1.8	1.5	1.2	1.2	1.2	1.0	1.1	1.1	1.0
37	**V-504**	1.5	1.5	1.0	1.1	1.2	1.1	1.0	1.1	1.1
38	**V-505**	1.6	1.5	1.1	1.1	1.2	1.0	1.0	1.1	1.1
39	**V-506**	1.5	1.5	1.0	1.1	1.2	1.1	1.0	1.1	1.1
40	**V-601**	1.6	1.4	1.1	1.1	1.2	1.0	1.0	1.1	1.0
41	**V-602**	1.1	1.4	1.3	1.0	1.2	1.1	1.0	1.1	1.1
42	**V-603**	1.4	1.4	1.0	1.4	1.2	1.2	1.1	1.1	1.0
43	**V-604**	1.1	1.4	1.3	1.1	1.2	1.0	1.0	1.1	1.1
44	**V-605**	1.9	1.4	1.4	1.1	1.2	1.0	1.0	1.1	1.0
45	**V-606**	1.5	1.8	1.2	1.1	1.3	1.1	1.0	1.1	1.1
46	**V-607**	2.1	1.8	1.2	1.2	1.3	1.1	1.1	1.1	1.1
47	**V-608**	1.4	1.8	1.3	1.1	1.3	1.2	1.0	1.1	1.1
48	**V-609**	1.4	1.4	1.0	1.1	1.2	1.1	1.0	1.1	1.1
49	**V-610**	1.5	1.4	1.1	1.1	1.2	1.0	1.0	1.1	1.0
50	**V-701**	2.1	1.9	1.1	1.2	1.3	1.1	1.1	1.2	1.1
51	**V-702**	2.2	2.4	1.1	1.2	1.4	1.2	1.1	1.2	1.1
52	**V-703**	1.9	2.4	1.3	1.2	1.4	1.2	1.1	1.2	1.1
53	**V-704**	2.4	1.9	1.2	1.2	1.3	1.1	1.1	1.2	1.1
54	**V-705**	2.6	1.9	1.3	1.3	1.3	1.0	1.1	1.2	1.1
55	**V-706**	2.6	2.4	1.1	1.3	1.4	1.1	1.1	1.2	1.1
56	**V-801**	1.5	1.7	1.1	1.1	1.2	1.1	1.0	1.1	1.1
57	**V-802**	1.9	2.0	1.1	1.2	1.3	1.1	1.1	1.2	1.1
58	**V-803**	2.3	2.0	1.1	1.2	1.3	1.1	1.1	1.2	1.1
59	**V-804**	1.9	2.0	1.1	1.2	1.3	1.1	1.1	1.2	1.1

D.5.4 The Performance of the GA parameters in predicting the Arrhenius Parameters and the Reaction Rate Coefficients of interest

Table D-24 The deviations between the CBS-QB3 data and the GA-based data for the HARs in the validation set calculated with the ΔGAV°s and ΔNNI° parameters for the forward direction, given in **Table D-10** and **Table D-11**, respectively.

Reaction #	$E_{a,f}$[a]					$\log\widetilde{A}_f$ [b]				
	300 K	600 K	1000 K	1500 K	2000 K	300 K	600 K	1000 K	1500 K	2000 K
V-101	-0.8	-0.7	-0.4	-0.4	-0.1	0.066	0.021	-0.047	0.025	0.030
V-102	-0.7	-0.8	-0.6	-0.6	-0.4	0.146	0.029	0.000	-0.018	-0.070
V-103	-0.7	-0.8	-0.6	-0.7	-0.3	0.127	0.074	0.076	0.072	0.018
V-104	-0.4	-0.8	-0.6	-0.6	-0.4	0.067	0.014	0.026	0.052	0.008
V-105	-1.5	-1.7	-1.4	-1.3	-0.9	0.053	0.018	0.021	0.028	0.028
V-201	2.6	2.7	2.7	2.7	2.8	0.131	-0.044	-0.039	-0.038	-0.038
V-202	2.5	2.6	2.8	2.8	2.9	0.314	0.153	0.164	0.167	0.167
V-203	-2.5	-2.4	-2.4	-2.4	-2.2	0.221	0.041	0.028	0.022	0.019
V-204	-3.9	-3.3	-2.8	-3.1	-3.2	0.362	0.177	0.163	0.155	0.151
V-205	-4.9	-4.7	-4.6	-4.3	-5.1	0.042	-0.147	-0.162	-0.171	-0.175
V-206	-4.1	-4.1	-4.1	-4.1	-4.1	-0.158	-0.345	-0.344	-0.343	-0.343
V-207	0.2	0.2	0.2	0.2	0.3	-0.001	-0.182	-0.178	-0.176	-0.175
V-208	2.9	2.9	2.8	2.7	2.7	0.063	-0.048	-0.023	0.074	0.088
V-209	3.0	3.1	3.1	3.1	3.1	0.234	0.062	0.064	0.065	0.064
V-210	1.2	1.2	1.3	1.3	1.4	0.086	-0.092	-0.085	-0.082	-0.081
V-301	0.7	0.6	0.6	0.6	0.5	-0.067	-0.024	-0.026	-0.052	-0.063
V-302	-1.0	-1.0	-1.1	-1.1	-1.1	-0.440	-0.454	-0.456	-0.458	-0.458
V-303	-2.0	-2.0	-1.9	-1.9	-1.8	-0.013	-0.012	-0.007	-0.004	-0.002
V-304	-2.4	-2.4	-2.5	-2.5	-2.5	0.031	0.029	0.028	0.028	0.028
V-305	1.2	1.6	1.4	1.2	1.0	-0.083	-0.037	-0.046	-0.056	-0.061
V-306	5.3	5.4	5.5	5.6	5.7	0.075	0.084	0.092	0.096	0.098
V-307	4.2	4.6	5.1	5.5	5.7	0.068	0.118	0.154	0.171	0.178
V-308	1.7	1.6	1.4	1.3	1.2	-0.030	-0.044	-0.057	-0.063	-0.066
V-309	-0.1	-0.2	0.1	-0.1	0.0	0.105	0.121	0.134	0.139	0.143
V-310	2.2	2.2	2.2	2.2	2.1	0.279	0.274	0.271	0.270	0.270
V-311	-1.8	-1.3	-0.6	-0.3	-0.4	0.233	0.276	0.252	0.234	0.192
V-312	-1.5	-1.3	0.6	0.7	1.1	0.216	0.247	0.175	0.136	0.150
V-401	-3.2	-3.1	-3.1	-3.1	-3.1	0.075	0.010	0.028	-0.051	-0.039
V-402	5.4	5.3	5.2	5.1	5.1	0.433	0.425	0.419	0.417	0.416
V-403	2.4	2.1	2.0	1.4	-0.1	0.193	0.198	0.187	0.180	0.178
V-404	1.0	0.8	0.3	-0.1	-0.3	-0.129	-0.159	-0.191	-0.206	-0.212
V-405	2.8	2.2	0.5	0.2	-0.1	-0.069	-0.089	-0.118	-0.132	-0.138

V-406	0.9	0.8	0.3	0.0	-0.2	-0.102	-0.123	-0.152	-0.166	-0.172
V-501	-2.3	-2.3	-2.3	-2.4	-2.3	-0.066	-0.073	-0.076	-0.076	-0.075
V-502	0.0	0.0	0.0	-1.8	-2.4	-0.056	-0.050	-0.051	-0.052	-0.051
V-503	0.1	0.1	-0.1	-0.4	-0.4	0.207	0.205	0.191	0.184	0.181
V-504	-2.9	-2.9	-2.9	-2.9	-2.8	-0.228	-0.229	-0.230	-0.229	-0.228
V-505	-5.4	-5.2	-5.2	-5.3	-5.2	-0.006	0.009	0.010	0.011	0.013
V-506	-3.7	-4.5	-5.0	-5.6	-4.7	-0.368	-0.290	-0.223	-0.186	-0.135
V-601	-0.9	-1.6	-1.9	-2.1	-1.9	-0.334	-0.406	-0.429	-0.435	-0.436
V-602	0.9	0.0	0.0	-2.2	-1.3	-0.222	-0.091	0.010	-0.059	-0.052
V-603	-0.6	-1.5	-1.8	-1.8	-0.1	-0.206	-0.243	-0.284	-0.304	-0.312
V-604	-2.8	-3.0	-2.9	-2.9	-2.7	0.120	0.120	0.120	0.121	0.122
V-605	-4.2	-4.4	-4.4	-4.4	-4.2	0.195	0.192	0.188	0.187	0.187
V-606	-5.6	-5.8	-5.8	-5.7	-5.7	-0.552	-0.561	-0.561	-0.560	-0.559
V-607	3.3	3.3	3.0	2.8	2.6	-0.099	-0.108	-0.124	-0.133	-0.136
V-608	1.1	1.1	1.3	1.6	1.6	0.046	0.050	0.065	0.074	0.078
V-609	3.2	3.1	3.3	3.4	3.8	0.000	0.008	0.018	0.026	0.029
V-610	6.8	6.6	6.6	6.5	6.7	0.199	0.206	0.208	0.208	0.209
V-701	1.2	1.1	1.1	1.2	1.2	-0.304	-0.312	-0.315	-0.315	-0.314
V-702	2.3	2.4	2.3	2.3	2.2	0.316	0.318	0.316	0.314	0.314
V-703	6.3	6.3	6.2	6.1	5.9	0.119	0.108	0.102	0.097	0.095
V-704	-3.5	-3.6	-3.6	-3.6	-3.6	-0.103	-0.110	-0.112	-0.113	-0.114
V-705	-5.6	-5.8	-5.8	-5.9	-5.9	-0.150	-0.170	-0.177	-0.180	-0.180
V-706	-2.6	-2.6	-2.8	-2.8	-3.0	-0.133	-0.143	-0.151	-0.155	-0.157
V-801	-1.4	-1.3	-1.3	-1.3	-1.3	0.238	0.240	0.243	0.245	0.246
V-802	2.1	2.1	1.9	1.6	1.4	-0.098	-0.113	-0.130	-0.139	-0.143
V-803	-0.1	-0.3	-0.5	-0.6	-0.5	0.005	-0.035	-0.017	-0.014	-0.004
V-804	-1.4	-1.3	-1.5	-1.6	-1.7	-0.014	-0.021	-0.033	-0.038	-0.041

[a] $\mathbf{E_{a,f}}$**:** Activation energy of the forward reaction, given in kJ mol^{-1}.
[b] $\mathbf{log\widetilde{A}_f}$**:** Logarithm of the pre-exponential factor of the forward reaction, given in m^3 mol^{-1} s^{-1}.

Table D-25 The deviations between the CBS-QB3 data and the GA-based data for the HARs in the validation set calculated with the ΔGAV°s and ΔNNI° parameters for the reverse direction, given in **Table D-10** and **Table D-11**, respectively.

Reaction #	$E_{a,r}$[a]					$\log\widetilde{A}_r$ [b]				
	300 K	600 K	1000 K	1500 K	2000 K	300 K	600 K	1000 K	1500 K	2000 K
V-101	-3.5	-3.1	-2.7	-2.8	-3	0.517	0.697	0.576	0.528	0.583
V-102	-5	-5	-5.1	-5.5	-5.9	-0.32	-0.003	-0.024	-0.051	-0.039
V-103	-3.4	-3.4	-3.2	-3.6	-4.6	-0.078	0.197	0.186	0.149	0.472
V-104	0.7	0.2	0	-0.1	-0.1	0.183	0.123	0.112	0.109	0.103
V-105	-4.1	-4.8	-4.8	-4.5	-4.3	-0.088	-0.171	-0.171	-0.159	-0.156
V-201	2.4	2.4	2.4	2.5	2.5	0.081	0.07	0.066	0.065	0.079
V-202	0.1	0.1	0.2	0.3	0.2	0.234	0.236	0.235	0.233	0.247
V-203	-2	-1.2	-0.6	-0.1	0.1	0.474	0.433	0.403	0.389	0.398
V-204	1.3	1	0.7	0.6	0.5	0.015	-0.027	-0.052	-0.063	-0.052
V-205	2	1.4	1	0.8	0.6	-0.312	-0.389	-0.425	-0.438	-0.429
V-206	-6.3	-6.5	-6.6	-6.6	-6.7	-0.44	-0.314	-0.376	-0.37	-0.366
V-207	-4.5	-4.5	-4.4	-4.3	-4.4	-0.106	-0.111	-0.112	-0.112	-0.102
V-208	5.7	5.6	5.4	5.4	5.3	0.642	0.624	0.61	0.604	0.612
V-209	1.2	1.2	1.2	1.3	1.2	-0.017	-0.019	-0.024	-0.027	-0.014
V-210	-1.2	-1.2	-1.1	-1	-1	0.222	0.218	0.22	0.221	0.232
V-301	-2.4	-2.6	-2.7	-2.8	-2.8	-0.303	-0.181	-0.183	-0.233	-0.108
V-302	-3.6	-3.7	-3.8	-3.9	-3.9	-0.283	-0.302	-0.308	-0.31	-0.312
V-303	-2	-1.7	-1.7	-1.6	-1.7	-0.08	0.07	0.158	0.172	0.15
V-304	-1.6	-1.6	-1.7	-1.8	-1.9	0.256	0.25	0.243	0.24	0.234
V-305	-3	-2.4	-2.1	-2	-1.9	-0.541	-0.474	-0.452	-0.444	-0.442
V-306	-0.2	-0.1	0	0	0.1	-0.111	-0.102	-0.098	-0.095	-0.094
V-307	3.6	4.2	4.9	5.4	5.7	0.251	0.314	0.36	0.383	0.392
V-308	1.9	2	1.9	1.9	1.9	-0.015	-0.02	-0.022	-0.022	-0.021
V-309	0.2	0.3	0.4	0.5	0.6	0.196	0.208	0.215	0.219	0.22
V-310	1.6	1.7	1.6	1.5	1.4	0.646	0.648	0.644	0.64	0.634
V-311	-0.1	-1.1	-0.2	-0.6	-1.4	0.047	0.058	0.07	0.076	0.078
V-312	-0.2	-1.2	0.1	-1	-1.2	0.348	0.359	0.371	0.377	0.379
V-401	-0.2	-0.2	-0.2	-0.2	-0.3	0.119	0.184	0.143	0.115	0.113
V-402	6.4	6.4	6.2	6.4	6.3	0.397	0.407	0.429	0.441	0.446
V-403	1.2	1.4	1.5	0.3	0.3	0.276	0.244	0.221	0.211	0.208
V-404	4	4.1	3.8	3.5	3.2	0.339	0.355	0.333	0.319	0.313
V-405	-0.5	0.7	0	-0.8	-0.7	0.024	0.028	0.029	0.029	0.029
V-406	0.9	0.9	1	1	1	-0.079	-0.076	-0.075	-0.073	-0.077
V-501	-4.4	-4.5	-4.6	-4.4	-4.5	-0.489	-0.501	-0.501	-0.5	-0.499
V-502	-4.6	-4.5	-4.6	-4.5	-4.6	-0.111	-0.109	-0.11	-0.111	-0.111
V-503	4.4	4.1	3.7	3.7	3.6	0.334	0.383	0.409	0.415	0.412

V-504	-2.4	-2.4	-2.5	-2.3	-2.4	-0.293	-0.302	-0.302	-0.302	-0.301
V-505	1.3	1.5	1.6	1.7	1.9	-0.034	-0.018	-0.014	-0.012	-0.011
V-506	-3.9	-5.7	-5.6	-4.1	-0.2	-0.558	-0.506	-0.429	-0.374	-0.331
V-601	-2.5	-3	-3.4	-3.7	-3.9	0.025	-0.046	-0.078	-0.09	-0.095
V-602	-3.6	-3.8	-3.8	-3.8	-3.8	-0.165	-0.218	-0.213	-0.203	-0.199
V-603	-3.3	-3.2	4.4	0.7	1.4	-0.395	-0.349	-0.342	-0.344	-0.347
V-604	2.9	4.1	6.5	6.8	6.4	-0.171	-0.147	-0.119	-0.104	-0.098
V-605	4.9	4.9	4.6	6.2	7.2	0.306	0.281	0.277	0.279	0.279
V-606	-4.6	-4.7	-4.7	-4.8	-4.8	-0.328	-0.333	-0.337	-0.338	-0.339
V-607	1.3	1.1	0.8	0.6	0.4	0.225	0.209	0.189	0.179	0.174
V-608	0.6	2.4	-1.8	0	-0.7	0.267	0.278	0.277	0.275	0.274
V-609	0.3	0.2	0.3	0.3	0.2	-0.07	-0.071	-0.073	-0.073	-0.073
V-610	8.3	8.2	8.1	8.3	8.1	0.372	0.376	0.38	0.384	0.384
V-701	2.9	2.8	2.7	2.6	2.6	0.115	0.097	0.092	0.089	0.089
V-702	-5.4	-5.8	-5.8	-5.7	-5.8	-0.424	-0.456	-0.461	-0.463	-0.463
V-703	5.5	5.7	5.8	6	6.1	0.451	0.467	0.475	0.483	0.487
V-704	-1.1	-1.2	-1.2	-1.3	-1.4	0.055	0.042	0.037	0.034	0.033
V-705	1.9	1.7	1.7	1.5	1.6	0.182	0.162	0.151	0.146	0.142
V-706	-1.6	-1.7	-1.7	-1.7	-1.7	-0.089	-0.101	-0.104	-0.107	-0.108
V-801	-6.2	-6.3	-6.3	-6.2	-6.2	-0.3	-0.305	-0.305	-0.304	-0.303
V-802	0.1	0.2	0.1	0.2	0.2	-0.389	-0.386	-0.387	-0.386	-0.386
V-803	-0.2	-0.3	-0.4	-0.3	-0.1	-0.067	-0.085	-0.049	-0.044	-0.015
V-804	0.1	0	0	0	0.1	-0.17	-0.171	-0.176	-0.178	-0.178

[a] **$E_{a,r}$:** Activation energy of the reverse reaction, given in kJ mol^{-1}.
[b] **$\log \tilde{A}_r$:** Logarithm of the pre-exponential factor of the reverse reaction, given in m^3 mol^{-1} s^{-1}.

Table D-26 Factor of deviations (ρ) between the reaction rate coefficients calculated by CBS-QB3 and the set of ΔGAV°/ΔNNI° parameters reported in **Table D-10** and **Table D-11** for the validation set.[a]

Reaction #	Factor of deviations *(ρ)*									
	Forward					Reverse				
	300 K	600 K	1000 K	1500 K	2000 K	300 K	600 K	1000 K	1500 K	2000 K
V-101	2.04	1.97	2.21	2.15	1.32	4.23	2.21	1.97	1.56	1.34
V-102	1.97	1.93	2.13	1.81	1.25	2.55	2.14	1.81	1.23	1.11
V-103	1.36	2.30	2.09	1.46	1.45	1.70	2.75	2.06	1.53	1.31
V-104	1.67	2.60	1.54	1.56	1.52	2.59	1.13	1.03	1.12	1.15
V-105	2.50	2.89	2.60	2.34	1.98	1.61	1.26	1.09	1.46	1.62
V-201	1.80	1.59	1.35	1.36	1.31	1.85	1.16	1.01	1.01	1.01
V-202	1.03	1.01	1.18	1.17	1.22	2.13	2.02	1.96	1.74	1.71
V-203	5.55	1.80	1.52	1.27	1.15	8.27	5.10	3.74	3.23	2.56
V-204	5.97	2.98	2.19	1.83	1.66	1.25	1.27	1.12	1.16	1.20
V-205	7.45	1.82	1.27	1.05	1.14	4.77	3.26	3.10	3.33	3.44

V-206	3.67	1.19	1.20	1.58	1.76	4.64	2.07	1.07	1.32	1.59
V-207	1.11	1.32	1.37	1.53	1.55	4.64	1.85	1.27	1.04	1.16
V-208	2.71	1.76	1.33	1.05	1.02	2.60	1.27	2.01	2.29	2.48
V-209	1.78	1.38	1.12	1.10	1.06	1.54	1.15	1.07	1.13	1.13
V-210	1.07	1.31	1.25	1.34	1.33	2.73	2.06	1.84	1.58	1.52
V-301	1.93	1.08	1.03	1.18	1.22	1.06	1.35	1.21	1.07	1.11
V-302	2.38	2.12	2.28	2.62	1.91	1.75	1.26	1.03	1.17	1.36
V-303	1.49	1.65	1.35	1.15	1.10	1.17	1.64	1.66	1.48	1.34
V-304	2.94	1.92	1.55	1.30	1.22	3.29	2.33	2.02	1.75	1.65
V-305	2.02	1.37	1.22	1.25	1.24	1.89	1.13	1.08	1.30	1.42
V-306	5.99	2.04	1.39	1.26	1.14	1.01	1.06	1.10	1.03	1.03
V-307	2.84	1.56	1.15	1.05	1.06	1.01	1.54	2.02	2.15	2.35
V-308	2.55	1.47	1.28	1.29	1.28	1.77	1.05	1.12	1.12	1.12
V-309	1.68	1.68	1.55	1.39	1.37	1.95	2.05	2.15	2.03	1.95
V-310	1.29	1.31	1.55	1.56	1.61	2.14	2.98	3.39	3.23	3.11
V-311	2.99	2.44	2.06	1.76	1.58	1.01	1.16	1.18	1.10	1.11
V-312	2.35	2.61	1.58	1.29	1.31	1.89	2.71	2.37	2.28	2.20
V-401	3.29	2.17	1.70	1.14	1.08	1.14	1.70	1.50	1.28	1.25
V-402	2.97	1.03	1.53	1.72	1.89	2.62	1.06	1.70	1.87	2.02
V-403	2.60	1.08	1.29	1.35	1.48	1.02	1.61	1.71	1.82	1.74
V-404	1.72	1.76	1.56	1.60	1.66	1.49	1.10	1.62	1.81	1.85
V-405	5.57	2.05	1.35	1.38	1.42	2.17	1.42	1.45	1.35	1.21
V-406	2.28	1.63	1.43	1.46	1.51	1.03	1.13	1.18	1.28	1.38
V-501	2.12	1.43	1.18	1.02	1.04	2.44	1.26	1.02	1.22	1.34
V-502	1.19	1.06	1.06	1.02	1.02	5.89	3.10	2.42	2.01	1.84
V-503	1.31	1.62	1.65	1.57	1.54	10.34	4.90	3.61	3.31	3.13
V-504	1.85	1.12	1.13	1.34	1.44	1.66	1.31	1.21	1.09	1.04
V-505	7.82	2.85	1.98	1.56	1.39	1.22	1.33	1.60	1.67	1.70
V-506	1.80	1.35	1.16	1.02	1.04	2.03	1.84	1.48	1.09	1.46
V-601	1.65	1.80	2.03	2.31	2.47	1.20	1.48	1.58	1.52	1.48
V-602	1.88	1.11	1.11	1.04	1.05	1.72	1.27	1.24	1.18	1.17
V-603	1.25	1.55	1.59	1.75	2.11	2.73	1.60	1.37	1.08	1.27
V-604	5.24	2.51	1.99	1.67	1.54	2.09	1.72	1.06	1.01	1.06
V-605	6.22	3.47	2.75	2.19	1.96	2.48	1.14	1.15	1.08	1.10
V-606	3.11	1.01	1.67	2.30	2.60	5.34	1.35	1.19	1.59	1.83
V-607	5.65	2.32	1.79	1.70	1.63	1.31	1.63	1.50	1.35	1.29
V-608	1.06	1.06	1.10	1.05	1.08	1.13	1.09	1.47	1.21	1.21
V-609	3.59	1.74	1.35	1.24	1.19	1.78	1.61	1.96	1.88	1.03
V-610	6.23	2.19	1.29	1.04	1.06	7.51	1.88	1.03	1.25	1.38
V-701	3.65	2.40	2.19	2.26	2.25	3.13	1.44	1.10	1.04	1.00
V-702	1.14	1.53	1.77	1.72	1.76	4.08	1.50	1.05	1.47	1.68

V-703	7.68	2.24	1.45	1.30	1.17	1.22	1.66	2.18	2.26	2.40
V-704	2.60	1.68	1.27	1.03	1.07	1.25	1.33	1.28	1.17	1.11
V-705	4.86	2.21	1.43	1.06	1.08	1.66	1.12	1.31	1.31	1.30
V-706	1.92	1.40	1.10	1.13	1.23	1.59	1.46	1.31	1.12	1.06
V-801	1.73	1.27	1.11	1.03	1.06	1.87	1.82	1.11	1.13	1.29
V-802	2.70	1.73	1.52	1.57	1.54	1.16	1.45	1.61	1.86	1.96
V-803	1.09	1.11	1.12	1.02	1.00	1.21	1.35	1.38	1.23	1.26
V-804	1.77	1.41	1.22	1.04	1.01	1.33	1.09	1.03	1.09	1.11

[a] Factor of deviation (ρ): If $k_{AI} > k_{GA}$, then $\rho = \frac{k_{AI}}{k_{GA}}$, if $k_{GA} > k_{AI}$ then $\rho = \frac{k_{GA}}{k_{AI}}$ where k_{AI} denotes reaction rate coefficients calculated with *ab initio* methods and k_{GA} denotes reaction rate coefficients calculated with group additive parameters reported in this study, namely the ΔGAV°/ΔNNI° parameters reported in **Table 6-3** and **Table 6-4**.

Table D-27 Statistics demonstrating the predictive performance of the GA parameters on the validation set.

		Forward					**Reverse**				
		300 K	**600 K**	**1000 K**	**1500 K**	**2000 K**	**300 K**	**600 K**	**1000 K**	**1500 K**	**2000 K**
E_a[a]	**MAD**[c]	2.5	2.5	2.5	2.5	2.5	2.6	2.7	2.7	2.6	2.6
	MAX[d]	6.7	6.5	6.5	6.4	6.7	8.0	7.9	7.6	7.3	7.4
$\log\widetilde{A}$[b]	**MAD**	0.200	0.204	0.207	0.211	0.213	0.297	0.293	0.300	0.302	0.299
	MAX	0.641	0.645	0.644	0.644	0.644	0.646	0.668	0.649	0.663	0.670
k	$\langle\rho\rangle$[e]	2.5	1.7	1.5	1.4	1.4	2.1	1.6	1.5	1.5	1.5
	ρ_{max}[f]	7.8	3.5	2.8	2.6	2.6	10.3	5.1	3.7	3.4	3.4

[a] **E_a:** Statistics for the activation energy, given in kJ mol^{-1}.
[b] **$\log\widetilde{A}$:** Statistics for the logarithm of the pre-exponential factor, given in m^3 mol^{-1} s^{-1}.
[c] **MAD:** Mean absolute deviation of the activation energies between the CBS-QB3 based E_as and the E_as calculated by reported GA parameters, given in kJ mol^{-1}.
[d] **MAX:** Maximum absolute deviation between the CBS-QB3 based E_as and the E_as calculated by reported GA parameters among the training set of activation energies, given in m^3 mol^{-1} s^{-1}.
[e] **$\langle\rho\rangle$:** The geometric average of the factor of deviations between the reaction rate coefficients calculated by CBS-QB3 and the GA parameters reported in this study.
[f] **ρ_{max}:** The maximum factor of deviations between the reaction rate coefficients calculated by CBS-QB3 and the GA parameters reported in this study.

D.6 Final optimization and the performance of the final GA parameters

Table D-28 The deviations between the CBS-QB3 data and the GA-based data for the HARs in the final set (training + validation sets) calculated with the final ΔGAV°s and ΔNNI° parameters in the forward direction with respect to the reference reaction, given in **Table 6-3** and **Table 6-4**, respectively.

Reaction #	$E_{a,f}$[a]					$\log\widetilde{A}_f$[b]				
	300 K	600 K	1000 K	1500 K	2000 K	300 K	600 K	1000 K	1500 K	2000 K
T-101	-1.1	-0.8	-0.8	-1.0	-0.8	0.005	-0.035	-0.041	0.017	-0.034
T-102	-0.2	0.6	0.7	0.2	0.1	-0.016	0.014	0.012	0.058	0
T-103	-0.4	0.6	-0.1	0.9	1.1	0.097	0.005	0.058	0.053	0.485
T-104	1.1	0.9	0.6	1.2	1.3	0.021	-0.01	-0.016	0.039	-0.014
T-105	2.2	0.5	0.3	0.7	1.5	-0.029	0.019	0.022	0.07	0.013
T-106	0.5	1.0	0.8	1.9	1.4	-0.009	-0.051	-0.059	-0.003	-0.054
T-107	0.9	0.9	0.3	-0.5	-0.4	0.039	0.118	0.474	-0.078	-0.001
T-108	-0.1	0.4	0.4	-0.1	-0.2	-0.043	-0.05	-0.059	-0.013	-0.073
T-109	-0.4	-0.2	-0.2	-0.4	-0.1	-0.005	-0.049	-0.056	0.003	-0.047
T-110	-0.6	-0.3	-0.3	-0.6	-0.5	-0.002	-0.044	-0.052	0.003	-0.049
T-111	-1.1	-0.1	0.6	0.9	0.6	-0.253	-0.116	-0.18	-0.087	-0.126
T-112	-0.8	-0.5	-0.5	-0.7	-0.5	-0.019	-0.06	-0.066	-0.008	-0.059
T-113	-0.2	1.0	1.1	1.5	1.6	0.07	0.032	0.025	0.079	0.025
T-114	-1.4	-0.5	-0.3	-0.5	-1.1	-0.032	0.015	0.025	0.082	-0.097
T-115	-0.2	0.1	0.1	-0.1	-1.3	-0.163	-0.121	-0.422	-0.365	0.123
T-116	-0.7	-0.4	-0.4	-0.6	-1.3	-0.129	0.294	0.454	-0.059	0.104
T-117	0.1	0.7	0.7	0.3	0.3	0	0.001	-0.006	0.043	-0.013
T-118	-0.4	-0.1	-0.1	-0.3	-0.1	-0.004	-0.044	-0.05	0.008	-0.043
T-119	-0.5	-0.2	-0.3	-0.5	-0.3	-0.036	-0.076	-0.082	-0.025	-0.077
T-201	-1.8	-1.9	-2.0	-1.9	-2.0	-0.075	-0.201	-0.084	-0.207	-0.208
T-202	1.5	1.5	1.5	1.6	1.5	0.016	0.375	0.019	0.374	0.373
T-203	2.5	2.4	2.3	2.3	2.3	-0.007	0.345	-0.016	0.337	0.335
T-204	0.0	0.0	0.1	0.2	0.2	-0.028	0.333	-0.019	0.339	0.339
T-205	2.5	2.4	2.5	2.5	2.5	0.033	0.39	0.034	0.389	0.388
T-206	2.8	2.6	2.6	2.6	2.5	-0.02	0.326	-0.038	0.314	0.313
T-207	3.2	3.1	3.2	3.4	3.4	-0.048	0.311	-0.039	0.319	0.32
T-208	-3.8	-3.9	-4.0	-3.9	-3.9	-0.051	-0.18	-0.061	-0.185	-0.185
T-209	-0.6	-0.8	-0.9	-1.0	-1.1	-0.004	-0.137	-0.026	-0.153	-0.155
T-210	-1.6	-1.7	-1.7	-1.6	-1.6	-0.104	-0.23	-0.109	-0.231	-0.231
T-211	-1.0	-1.1	-1.0	-1.0	-1.0	0.113	-0.005	0.116	-0.007	-0.007
T-212	0.9	0.7	0.6	0.6	0.5	-0.042	-0.172	-0.058	-0.184	-0.185
T-213	0.0	-0.1	-0.1	0.1	0.1	-0.058	-0.179	-0.054	-0.173	-0.172

T-214	2.4	2.4	2.4	2.5	2.4	0.228	0.116	0.236	0.113	0.113
T-215	1.4	1.2	1.2	1.2	1.2	-0.098	-0.226	-0.109	-0.233	-0.234
T-216	-1.3	-1.5	-1.5	-1.4	-1.4	-0.043	-0.168	-0.049	-0.172	-0.172
T-217	-1.7	-1.8	-1.8	-1.7	-1.7	-0.204	-0.02	-0.199	-0.02	-0.019
T-218	-1.2	-1.3	-1.3	-1.3	-1.3	-0.37	-0.195	-0.377	-0.199	-0.2
T-219	-1.7	-1.8	-1.8	-1.8	-1.8	-0.081	-0.206	-0.087	-0.21	-0.21
T-301	-0.5	-0.5	-0.5	-0.5	-0.5	-0.017	-0.021	-0.021	-0.021	-0.02
T-302	-0.9	-1.0	-1.2	-1.3	-1.4	0.026	0.009	-0.004	-0.011	-0.014
T-303	1.4	1.4	1.4	1.4	1.4	-0.021	-0.028	-0.031	-0.032	-0.032
T-304	1.1	1.2	1.4	1.5	1.6	-0.008	-0.002	0.007	0.012	0.015
T-305	0.4	0.3	0.0	-0.1	-0.2	0.007	-0.013	-0.028	-0.036	-0.038
T-306	2.1	2.2	2.1	2.2	2.2	-0.019	-0.023	-0.023	-0.023	-0.023
T-307	1.6	1.7	1.8	2.0	2.1	-0.045	-0.043	-0.033	-0.028	-0.025
T-308	0.0	0.0	-0.5	-0.5	-0.6	-0.405	-0.431	-0.424	-0.417	-0.415
T-309	-0.4	-0.4	-0.5	-0.5	-0.5	0.013	0.006	0.002	0	0
T-310	-3.3	-3.2	-3.3	-3.3	-3.3	-0.012	-0.018	-0.019	-0.02	-0.019
T-311	-2.2	-2.1	-2.1	-2.2	-2.2	0.287	0.295	0.291	0.289	0.288
T-312	-0.1	-0.1	-0.2	-0.2	-0.1	0.007	0.001	0	-0.001	0
T-313	-2.1	-2.0	-1.9	-1.8	-1.8	0.017	0.017	0.022	0.025	0.027
T-314	0.4	0.4	0.1	0.1	0.2	0.253	0.245	0.258	0.268	0.273
T-315	0.2	0.2	0.2	0.2	0.2	-0.195	-0.2	-0.2	-0.2	-0.199
T-316	-0.3	-0.3	-0.2	-0.2	-0.1	-0.121	-0.122	-0.119	-0.117	-0.115
T-317	-1.0	-1.0	-1.4	-1.4	-1.4	0.112	0.1	0.11	0.118	0.123
T-318	-0.2	-0.2	-0.2	-0.2	-0.2	-0.033	-0.037	-0.037	-0.037	-0.036
T-319	-0.8	-0.8	-0.8	-0.7	-0.7	-0.062	-0.064	-0.061	-0.059	-0.058
T-401	-0.1	0.0	0.1	0.1	0.1	0.381	0.391	0.39	0.392	0.392
T-402	0.4	0.3	0.0	-0.3	-0.4	-0.118	-0.134	-0.159	-0.168	-0.173
T-403	-1.8	-1.7	-1.5	-1.4	-1.3	-0.187	-0.187	-0.18	-0.173	-0.171
T-404	1.5	1.7	1.9	1.9	2.0	0.098	0.114	0.119	0.125	0.126
T-405	2.5	2.6	2.6	2.6	2.7	0.163	0.167	0.166	0.168	0.168
T-406	2.3	2.4	2.6	2.7	2.8	-0.169	-0.168	-0.16	-0.152	-0.15
T-407	1.6	1.8	2.0	2.2	2.4	-0.174	-0.17	-0.156	-0.144	-0.14
T-408	-4.1	-4.0	-3.9	-3.9	-3.8	-0.034	-0.032	-0.03	-0.027	-0.027
T-409	-1.1	-1.0	-0.9	-0.9	-0.8	-0.15	-0.151	-0.148	-0.143	-0.142
T-410	-2.0	-1.9	-1.7	-1.7	-1.6	0.107	0.11	0.115	0.121	0.123
T-411	-3.4	-3.2	-3.0	-2.9	-2.8	0.047	0.058	0.064	0.071	0.073
T-412	-0.2	-0.2	0.0	0.0	0.2	-0.247	-0.248	-0.243	-0.236	-0.235
T-413	-2.0	-1.8	-1.7	-1.7	-1.6	0.12	0.133	0.136	0.14	0.141
T-414	-0.2	0.1	0.3	0.4	0.5	0.054	0.073	0.083	0.09	0.091
T-415	0.2	0.3	0.5	0.6	0.7	-0.338	-0.338	-0.331	-0.323	-0.321
T-416	1.3	1.5	1.5	1.5	1.6	0.409	0.423	0.423	0.426	0.426

T-417	-0.4	-0.2	0.0	0.1	0.2	-0.154	-0.145	-0.136	-0.128	-0.126
T-418	-0.1	0.1	0.2	0.3	0.5	-0.173	-0.172	-0.164	-0.156	-0.154
T-419	-2.5	-2.3	-2.3	-2.2	-2.2	0.061	0.072	0.074	0.077	0.077
T-501	-1.0	-0.9	-0.9	-0.9	-0.8	0.279	0.282	0.275	0.279	0.278
T-502	-1.7	-1.7	-1.8	-1.9	-2.0	0.257	0.261	0.245	0.243	0.239
T-503	0.9	0.9	0.9	0.9	1.0	-0.021	-0.019	-0.027	-0.024	-0.026
T-504	0.8	0.6	0.5	1.3	1.5	-0.037	-0.333	-0.033	-0.327	-0.327
T-505	-0.1	-0.1	-0.2	-0.1	-0.1	-0.139	-0.148	-0.157	-0.154	-0.156
T-506	1.3	1.4	1.5	1.6	1.6	-0.016	-0.01	-0.014	-0.008	-0.009
T-507	1.1	1.2	1.3	1.4	1.5	-0.049	0.132	-0.043	0.141	0.141
T-508	-2.5	-2.5	-2.5	-2.5	-2.4	-0.15	-0.154	-0.163	-0.159	-0.16
T-509	3.3	3.3	3.3	3.3	3.3	-0.014	-0.012	-0.022	-0.02	-0.022
T-510	3.6	3.6	3.6	3.6	3.6	0.018	0.02	0.011	0.013	0.011
T-511	2.7	2.8	2.8	2.9	3.0	0.182	0.188	0.185	0.19	0.19
T-512	4.2	4.3	4.3	4.3	4.3	-0.022	-0.018	-0.025	-0.021	-0.023
T-513	-3.1	-3.1	-3.0	-2.9	-2.9	-0.017	-0.013	-0.017	-0.011	-0.012
T-514	-1.6	-1.4	-1.5	-1.6	-1.6	0.15	0.164	0.15	0.15	0.147
T-515	4.2	4.2	4.2	4.3	4.3	-0.072	-0.069	-0.076	-0.072	-0.073
T-516	-1.0	-0.9	-0.9	-0.8	-0.7	-0.024	-0.021	-0.026	-0.021	-0.022
T-517	-2.3	-2.3	-2.3	-2.3	-2.2	0.126	0.123	0.114	0.117	0.115
T-518	-0.5	-0.4	-0.4	-0.4	-0.3	-0.014	-0.01	-0.016	-0.012	-0.013
T-519	2.9	2.9	3.0	3.0	3.1	-0.049	-0.045	-0.051	-0.046	-0.046
T-601	-2.0	-2.0	-2.1	-2.0	-2.0	0.345	0.345	0.337	0.337	0.335
T-602	1.9	2.0	2.1	2.4	2.5	-0.174	-0.177	-0.169	-0.159	-0.156
T-603	4.1	4.2	4.5	4.8	0.7	0.051	0.066	0.082	0.096	0.1
T-604	2.4	3.3	3.1	3.2	3.3	0.057	0.074	0.097	0.115	0.122
T-605	-2.7	-2.9	-3.2	-2.3	-1.8	0.053	0.033	0.003	-0.009	-0.016
T-606	1.9	2.0	1.9	2.0	2.0	-0.024	-0.028	-0.033	-0.031	-0.032
T-607	-1.2	-1.2	-1.2	-1.1	-1.0	0.014	0.011	0.008	0.011	0.011
T-608	3.3	3.4	3.5	3.9	4.1	0.028	0.035	0.045	0.056	0.06
T-609	1.9	1.8	1.6	1.6	1.5	-0.001	-0.008	-0.023	-0.026	-0.03
T-610	1.2	1.1	1.0	1.0	1.0	-0.014	-0.022	-0.033	-0.034	-0.037
T-611	-1.1	-1.0	-0.9	-0.6	-0.5	0.242	0.256	0.26	0.267	0.268
T-612	-1.0	-1.2	-1.2	-1.2	-1.2	-0.082	-0.09	-0.1	-0.101	-0.103
T-613	-3.5	-3.6	-3.6	-3.5	-3.5	0.044	0.04	0.033	0.035	0.034
T-614	-0.2	-0.2	-0.3	-0.6	-0.7	0.005	0	-0.015	-0.024	-0.028
T-615	-1.0	-1.0	-1.0	-1.0	-1.0	-0.036	-0.037	-0.044	-0.044	-0.045
T-616	3.2	3.2	3.1	3.2	3.2	-0.001	-0.001	-0.008	-0.007	-0.008
T-617	0.6	0.7	1.0	1.1	1.3	0.237	0.248	0.263	0.271	0.274
T-618	-4.8	-3.7	-3.1	-3.8	-4.2	-0.294	-0.304	-0.295	-0.283	-0.28
T-619	-3.7	-3.8	-3.9	-3.8	-3.8	-0.028	-0.033	-0.04	-0.04	-0.041

T-701	-2.2	-2.2	-2.2	-2.2	-2.2	0.149	0.15	0.151	0.152	0.151
T-702	1.7	1.7	1.7	1.7	1.6	0.019	0.019	0.018	0.017	0.017
T-703	2.5	2.6	2.6	2.7	2.7	0.053	0.059	0.062	0.064	0.064
T-704	2.1	2.2	2.3	2.4	2.4	-0.076	-0.069	-0.062	-0.058	-0.057
T-705	2.7	2.8	2.8	2.8	2.8	0.066	0.07	0.071	0.073	0.073
T-706	3.8	3.8	3.8	3.9	3.9	-0.124	-0.122	-0.12	-0.118	-0.118
T-707	2.9	2.9	3.0	3.1	3.2	0.055	0.059	0.066	0.07	0.071
T-708	-4.3	-4.2	-4.2	-4.2	-4.1	-0.117	-0.115	-0.112	-0.109	-0.109
T-709	-1.4	-1.4	-1.4	-1.4	-1.4	0.113	0.112	0.112	0.113	0.113
T-710	-1.9	-1.8	-1.9	-1.8	-1.8	0.316	0.314	0.314	0.315	0.315
T-711	1.1	1.1	0.9	0.9	0.9	0.102	0.1	0.093	0.091	0.09
T-712	1.8	1.8	1.8	1.8	1.9	0.019	0.021	0.021	0.022	0.022
T-713	0.0	0.0	0.0	0.0	0.0	0.055	0.052	0.052	0.053	0.052
T-714	-1.6	-1.5	-1.5	-1.5	-1.5	-0.218	-0.212	-0.211	-0.21	-0.211
T-715	-1.7	-1.7	-1.7	-1.6	-1.6	-0.201	-0.199	-0.197	-0.195	-0.195
T-716	-2.0	-2.0	-2.0	-1.9	-1.9	-0.029	-0.028	-0.026	-0.024	-0.024
T-717	-1.4	-1.3	-1.4	-1.5	-1.5	0.103	0.107	0.102	0.1	0.099
T-718	-2.4	-2.3	-2.3	-2.3	-2.3	-0.043	-0.042	-0.042	-0.041	-0.041
T-719	-2.4	-2.3	-2.3	-2.2	-2.2	-0.169	-0.168	-0.165	-0.163	-0.163
T-801	1.9	1.9	2.0	2.0	2.1	-0.136	-0.134	-0.132	-0.131	-0.131
T-802	1.4	1.5	1.5	1.6	1.6	0.083	0.094	0.098	0.1	0.1
T-803	2.0	2.2	2.3	2.2	2.3	0.151	0.159	0.162	0.164	0.164
T-804	0.9	1.0	1.2	1.3	1.4	-0.146	-0.136	-0.127	-0.122	-0.12
T-805	2.1	2.1	1.9	1.6	1.6	-0.018	-0.028	-0.044	-0.053	-0.057
T-806	2.6	2.7	2.8	2.8	2.9	0.172	0.175	0.179	0.181	0.182
T-807	1.8	2.0	2.1	2.2	2.4	-0.138	-0.131	-0.122	-0.116	-0.114
T-808	-1.2	-1.1	-1.1	-1.1	-1.0	-0.132	-0.13	-0.131	-0.13	-0.129
T-809	-0.6	-0.5	-0.6	-0.7	-0.6	0.212	0.21	0.206	0.205	0.204
T-810	-1.3	-1.2	-1.2	-1.3	-1.2	-0.088	-0.09	-0.092	-0.093	-0.093
T-811	-1.4	-1.4	-1.6	-1.8	-1.8	0.229	0.223	0.21	0.203	0.201
T-812	-1.9	-4.0	-4.0	-4.0	-3.9	0.029	0.029	0.029	0.029	0.029
T-813	-3.1	-3.0	-2.9	-2.8	-2.7	-0.272	-0.27	-0.265	-0.262	-0.261
T-814	0.1	0.3	0.1	0.0	0.0	0.211	0.217	0.206	0.201	0.199
T-815	0.0	0.1	0.1	0.1	0.2	-0.196	-0.195	-0.194	-0.193	-0.192
T-816	-0.5	-0.4	-0.3	-0.3	-0.2	-0.174	-0.172	-0.168	-0.166	-0.165
T-817	-3.5	-3.4	-3.3	-3.3	-3.2	0.045	0.05	0.055	0.058	0.059
T-818	-0.9	-0.8	-0.8	-0.8	-0.7	-0.1	-0.097	-0.095	-0.093	-0.093
T-819	1.7	1.8	1.9	1.9	2.0	0.124	0.127	0.13	0.133	0.134
V-101	1.1	-0.4	-0.2	-0.3	0.0	0.218	0.088	0.061	0.095	0.023
V-102	1.4	-0.5	-0.4	-0.5	-0.3	0.119	0.01	-0.039	-0.028	-0.09
V-103	1.9	-0.5	-0.4	-0.6	-0.2	0.1	0.055	0.037	0.062	-0.002

V-104	-0.5	-0.5	-0.4	-0.5	-0.3	0.04	-0.005	-0.013	0.042	-0.012
V-105	-1.6	-1.4	-1.2	-1.2	-0.8	0.026	-0.001	-0.018	0.018	0.008
V-201	2.7	2.7	2.7	2.8	2.8	0.087	-0.029	0.095	-0.027	-0.027
V-202	2.6	2.6	2.8	2.9	2.9	0.27	0.168	0.298	0.178	0.178
V-203	-2.4	-2.4	-2.4	-2.3	-2.2	0.177	0.056	0.162	0.033	0.03
V-204	-3.8	-3.3	-2.8	-3.0	-3.2	0.318	0.192	0.297	0.166	0.162
V-205	-4.8	-4.7	-4.6	-4.2	-5.1	-0.002	-0.132	-0.028	-0.16	-0.164
V-206	-4.0	-4.1	-4.1	-4.0	-4.1	-0.202	-0.33	-0.21	-0.332	-0.332
V-207	0.3	0.2	0.2	0.3	0.3	-0.045	-0.167	-0.044	-0.165	-0.164
V-208	3.0	2.9	2.8	2.8	2.7	0.019	-0.033	0.111	0.085	0.099
V-209	3.1	3.1	3.1	3.2	3.1	0.19	0.077	0.198	0.076	0.075
V-210	1.3	1.2	1.3	1.4	1.4	0.042	-0.077	0.049	-0.071	-0.07
V-301	0.5	0.4	0.0	0.0	-0.1	-0.08	-0.052	-0.045	-0.062	-0.07
V-302	-1.1	-1.2	-1.6	-1.7	-1.7	-0.453	-0.482	-0.475	-0.468	-0.465
V-303	-2.2	-2.2	-2.1	-2.1	-2.0	-0.024	-0.027	-0.023	-0.02	-0.018
V-304	-2.6	-2.6	-2.7	-2.7	-2.7	0.02	0.014	0.012	0.012	0.012
V-305	1.0	1.4	1.2	1.0	0.8	-0.094	-0.052	-0.062	-0.072	-0.077
V-306	5.1	5.2	4.9	5.0	5.1	0.062	0.056	0.073	0.086	0.091
V-307	4.0	4.4	4.9	5.3	5.5	0.057	0.103	0.138	0.155	0.162
V-308	1.5	1.4	1.2	1.1	1.0	-0.041	-0.059	-0.073	-0.079	-0.082
V-309	-0.2	-0.4	-0.5	-0.7	-0.6	0.092	0.093	0.115	0.129	0.136
V-310	2.0	2.0	2.0	2.0	1.9	0.268	0.259	0.255	0.254	0.254
V-311	-1.9	-1.5	-1.1	-0.9	-1.0	0.22	0.248	0.233	0.224	0.185
V-312	-1.6	-1.5	0.0	0.1	0.5	0.203	0.219	0.156	0.126	0.143
V-401	-3.6	-3.4	-3.3	-3.2	-3.1	0.059	-0.001	0.021	-0.053	-0.04
V-402	5.0	5.0	5.0	5.0	5.1	0.417	0.414	0.412	0.415	0.415
V-403	2.0	1.8	1.8	1.3	-0.1	0.177	0.187	0.18	0.178	0.177
V-404	0.6	0.5	0.1	-0.2	-0.3	-0.145	-0.17	-0.198	-0.208	-0.213
V-405	2.4	1.9	0.3	0.1	-0.1	-0.085	-0.1	-0.125	-0.134	-0.139
V-406	0.5	0.5	0.1	-0.1	-0.2	-0.118	-0.134	-0.159	-0.168	-0.173
V-501	-1.7	-1.7	-1.7	-1.7	-1.6	-0.046	-0.056	-0.066	-0.062	-0.063
V-502	0.6	0.6	0.6	-1.1	-1.7	-0.036	-0.033	-0.041	-0.038	-0.039
V-503	0.7	0.7	0.5	0.3	0.3	0.227	0.222	0.201	0.198	0.193
V-504	-2.3	-2.3	-2.3	-2.2	-2.1	-0.208	-0.212	-0.22	-0.215	-0.216
V-505	-4.8	-4.6	-4.6	-4.6	-4.5	0.014	0.026	0.02	0.025	0.025
V-506	-3.1	-3.9	-4.4	-4.9	-4.0	-0.348	-0.273	-0.213	-0.172	-0.123
V-601	-1.0	-1.6	-1.9	-1.9	-1.9	-0.323	-0.397	-0.422	-0.424	-0.425
V-602	0.8	0.1	0.0	-2.0	-1.3	-0.211	-0.082	0.017	-0.048	-0.041
V-603	-0.7	-1.5	-1.8	-1.6	-0.1	-0.195	-0.234	-0.277	-0.293	-0.301
V-604	-2.9	-3.0	-2.9	-2.7	-2.7	0.131	0.129	0.127	0.132	0.133
V-605	-4.3	-4.4	-4.4	-4.2	-4.2	0.206	0.201	0.195	0.198	0.198

V-606	-5.4	-5.5	-5.4	-5.4	-5.4	-0.431	-0.437	-0.437	-0.436	-0.436
V-607	3.5	3.5	3.3	3.0	2.9	0.022	0.016	0	-0.009	-0.013
V-608	1.3	1.3	1.6	1.8	1.9	0.167	0.174	0.189	0.198	0.201
V-609	3.1	3.2	3.3	3.6	3.8	0.011	0.017	0.025	0.037	0.04
V-610	6.6	6.5	6.5	6.6	6.7	0.21	0.215	0.215	0.219	0.22
V-701	2.7	2.7	2.7	2.8	2.7	-0.247	-0.249	-0.251	-0.251	-0.25
V-702	2.1	2.2	2.1	2.1	2.1	0.317	0.321	0.32	0.319	0.319
V-703	6.1	6.1	6.0	5.9	5.8	0.12	0.111	0.106	0.102	0.1
V-704	-2.0	-2.0	-2.0	-2.0	-2.1	-0.046	-0.047	-0.048	-0.049	-0.049
V-705	-4.1	-4.2	-4.2	-4.3	-4.4	-0.093	-0.107	-0.113	-0.116	-0.116
V-706	-2.8	-2.8	-3.0	-3.0	-3.1	-0.132	-0.14	-0.147	-0.15	-0.152
V-801	0.2	0.3	0.3	0.4	0.4	0.283	0.291	0.295	0.297	0.297
V-802	2.0	2.0	1.8	1.5	1.4	-0.109	-0.121	-0.138	-0.147	-0.151
V-803	-0.2	-0.4	-0.6	-0.7	-0.5	-0.006	-0.043	-0.025	-0.022	-0.012
V-804	-1.5	-1.4	-1.6	-1.7	-1.7	-0.025	-0.029	-0.041	-0.046	-0.049

[a]**$E_{a,f}$:** Activation energy of the forward reaction, given in kJ mol^{-1}.
[b]**$\log\widetilde{A}_f$:** Logarithm of the pre-exponential factor of the forward reaction, given in m^3 mol^{-1} s^{-1}.

Table D-29 The deviations between the CBS-QB3 data and the GA-based data for the HARs in the final set (training + validation sets) calculated with the final ΔGAV°s and ΔNNI° parameters in the reverse direction with respect to the reference reaction, given in **Table 6-3** and **Table 6-4**, respectively.

Reaction #	**$E_{a,f}$[a]**					**$\log\widetilde{A}_f$ [b]**				
	300 K	**600 K**	**1000 K**	**1500 K**	**2000 K**	**300 K**	**600 K**	**1000 K**	**1500 K**	**2000 K**
T-101	0.5	0.6	0.7	0.9	1.0	0.043	0.057	0.063	0.070	0.086
T-102	0.1	0.2	0.1	-0.1	-0.3	-0.238	-0.224	-0.232	-0.242	-0.235
T-103	3.2	3.3	3.4	3.6	3.7	0.217	0.232	0.239	0.246	0.263
T-104	-0.5	-0.4	-0.4	-0.3	-0.3	-0.245	-0.229	-0.226	-0.224	-0.210
T-105	1.8	1.9	1.8	1.6	1.4	0.231	0.250	0.244	0.234	0.241
T-106	3.4	3.5	3.6	3.8	3.9	0.204	0.216	0.221	0.227	0.243
T-107	2.5	2.6	2.7	2.8	2.8	0.244	0.259	0.261	0.263	0.277
T-108	-1.0	-1.7	-2.2	-2.6	-2.9	-0.240	-0.330	-0.366	-0.383	-0.380
T-109	2.0	2.1	2.2	2.4	2.6	-0.256	-0.245	-0.239	-0.231	-0.214
T-110	4.0	4.0	3.9	3.9	3.9	-0.251	-0.260	-0.265	-0.263	-0.255
T-111	-3.1	-3.2	-3.2	-3.2	-3.2	-0.216	-0.237	-0.238	-0.238	-0.225
T-112	-0.9	-0.8	-0.6	-0.4	-0.3	-0.352	-0.338	-0.332	-0.324	-0.308
T-113	1.1	1.3	1.4	1.3	1.4	-0.428	-0.420	-0.417	-0.414	-0.406
T-114	-1.2	-1.1	-1.2	-1.2	-1.2	0.199	0.208	0.205	0.203	0.214
T-115	0.4	0.5	0.6	0.7	0.9	-0.129	-0.117	-0.111	-0.105	-0.089
T-116	-0.2	-0.1	0.0	0.1	0.2	0.411	0.422	0.426	0.432	0.196
T-117	0.2	0.2	0.0	-0.1	-0.2	0.250	0.244	0.234	0.227	0.236
T-118	0.5	0.6	0.7	0.8	0.9	0.190	0.203	0.209	0.215	0.231

T-119	-0.3	-0.2	-0.1	0.0	0.1	-0.071	-0.062	-0.058	-0.053	-0.037
T-201	-1.3	-1.3	-1.3	-1.3	-1.2	-0.146	-0.148	-0.146	-0.148	-0.137
T-202	1.9	1.9	1.9	1.9	1.9	0.138	0.134	0.136	0.135	0.145
T-203	1.4	1.4	1.4	1.5	1.4	-0.159	-0.162	-0.161	-0.163	-0.153
T-204	-1.5	-1.4	-1.4	-1.3	-1.2	-0.144	-0.140	-0.132	-0.131	-0.119
T-205	1.8	1.8	1.9	1.9	1.9	0.170	0.168	0.171	0.170	0.180
T-206	2.1	2.1	2.0	2.1	2.0	-0.027	-0.033	-0.034	-0.037	-0.027
T-207	1.9	1.9	2.0	2.2	2.2	-0.141	-0.137	-0.129	-0.127	-0.115
T-208	-2.7	-3.0	-3.2	-3.6	-3.7	0.116	0.082	0.076	0.071	0.081
T-209	-0.3	-0.3	-0.4	-0.5	-0.5	-0.094	-0.102	-0.105	-0.109	-0.100
T-210	0.9	1.0	0.9	0.8	0.8	0.054	0.040	0.037	0.036	0.040
T-211	0.1	0.1	0.2	0.2	0.2	0.214	0.217	0.221	0.220	0.231
T-212	-0.1	-0.1	-0.2	-0.2	-0.2	-0.265	-0.269	-0.269	-0.273	-0.263
T-213	-0.8	-0.6	-0.5	-0.4	-0.4	-0.157	-0.153	-0.143	-0.140	-0.134
T-214	1.4	1.5	1.5	1.5	1.4	0.187	0.189	0.190	0.188	0.198
T-215	1.1	1.1	1.1	1.2	1.1	-0.376	-0.260	-0.182	-0.125	-0.370
T-216	-1.2	-1.2	-1.2	-1.2	-1.2	0.350	0.345	0.348	0.347	0.358
T-217	-1.3	-1.3	-1.3	-1.3	-1.3	0.100	0.098	0.101	0.100	0.111
T-218	-1.1	-1.1	-1.1	-1.1	-1.1	-0.134	-0.136	-0.133	-0.134	-0.123
T-219	-1.9	-1.9	-1.9	-1.9	-1.9	-0.118	-0.123	-0.121	-0.122	-0.111
T-301	0.1	0.0	-0.1	0.0	0.0	-0.113	-0.122	-0.128	-0.130	-0.127
T-302	-0.6	-0.7	-1.0	-1.1	-1.1	0.168	0.144	0.133	0.128	0.126
T-303	0.9	0.9	0.8	0.8	0.9	-0.027	-0.031	-0.038	-0.040	-0.037
T-304	0.4	0.3	0.4	0.5	0.6	-0.177	-0.181	-0.180	-0.178	-0.173
T-305	0.6	0.4	0.2	0.1	0.1	0.018	-0.010	-0.023	-0.027	-0.029
T-306	1.2	1.2	1.1	1.1	1.2	-0.119	-0.129	-0.134	-0.136	-0.132
T-307	1.2	1.2	1.2	1.3	1.5	-0.102	-0.106	-0.106	-0.103	-0.097
T-308	-1.5	-1.6	-1.7	-1.8	-1.8	-0.110	-0.143	-0.148	-0.144	-0.166
T-309	0.1	0.1	0.0	0.0	0.0	0.360	0.354	0.346	0.342	0.344
T-310	-1.7	-1.7	-1.9	-1.9	-2.0	0.159	0.145	0.134	0.131	0.125
T-311	3.5	3.6	3.7	3.8	3.8	0.276	0.268	0.273	0.283	0.263
T-312	-1.1	-1.2	-1.2	-1.2	-1.1	-0.195	-0.205	-0.211	-0.213	-0.210
T-313	-2.3	-2.1	-2.1	-1.9	-1.9	0.218	0.226	0.229	0.232	0.230
T-314	-0.7	-0.2	-0.8	-0.3	-0.1	-0.085	-0.087	-0.091	-0.093	-0.093
T-315	0.4	0.3	0.3	0.3	0.4	-0.487	-0.498	-0.504	-0.506	-0.502
T-316	-0.1	-0.2	-0.2	-0.1	0.0	-0.138	-0.149	-0.153	-0.153	-0.148
T-317	0.9	1.4	0.8	1.1	1.4	-0.113	-0.122	-0.130	-0.133	-0.135
T-318	0.3	0.2	0.1	0.2	0.3	-0.115	-0.125	-0.130	-0.132	-0.128
T-319	-0.5	-0.6	-0.6	-0.6	-0.5	-0.045	-0.055	-0.059	-0.059	-0.055
T-401	0.2	0.3	0.3	0.3	0.2	0.358	0.363	0.362	0.361	0.361
T-402	-2.0	-2.3	-2.1	-1.9	-1.9	-0.069	-0.073	-0.079	-0.082	-0.082

T-403	-3.7	-3.7	-3.6	-3.4	-3.5	-0.210	-0.210	-0.202	-0.197	-0.194
T-404	-0.6	-0.5	-0.5	-0.4	-0.5	0.059	0.065	0.068	0.069	0.070
T-405	2.8	2.8	2.7	2.7	2.6	0.256	0.248	0.245	0.243	0.244
T-406	-1.0	-0.9	-0.9	-0.7	-0.7	-0.197	-0.200	-0.191	-0.186	-0.183
T-407	-1.0	-1.0	-0.8	-0.6	-0.6	-0.208	-0.211	-0.199	-0.192	-0.188
T-408	-2.1	-2.3	-2.5	-2.5	-2.6	0.118	0.086	0.077	0.074	0.073
T-409	-0.2	-0.2	-0.2	-0.1	-0.2	-0.182	-0.188	-0.185	-0.183	-0.181
T-410	1.7	1.7	1.6	1.6	1.6	-0.216	-0.232	-0.231	-0.229	-0.234
T-411	1.4	1.5	1.5	1.6	1.6	0.334	0.340	0.346	0.349	0.351
T-412	-1.1	-1.1	-1.1	-0.9	-1.0	-0.356	-0.360	-0.354	-0.351	-0.348
T-413	0.1	0.3	0.3	0.2	0.2	-0.113	-0.103	-0.100	-0.098	-0.103
T-414	1.4	1.5	1.6	1.7	1.6	0.229	0.236	0.245	0.247	0.249
T-415	0.1	0.1	0.2	0.3	0.3	-0.372	-0.376	-0.368	-0.364	-0.360
T-416	-0.5	-0.4	-0.4	-0.4	-0.5	-0.013	-0.009	-0.009	-0.009	-0.008
T-417	0.9	1.0	1.0	1.2	1.1	0.049	0.047	0.055	0.059	0.061
T-418	-0.1	-0.1	0.0	0.1	0.1	-0.187	-0.190	-0.182	-0.178	-0.175
T-419	-3.3	-3.2	-3.2	-3.2	-3.3	0.059	0.063	0.064	0.063	0.064
T-501	-1.8	-1.7	-1.6	-1.7	-1.6	0.184	0.190	0.192	0.191	0.197
T-502	-0.5	-0.8	-1.0	-1.2	-1.2	0.023	-0.015	-0.031	-0.037	-0.032
T-503	-1.3	-1.2	-1.2	-1.2	-1.2	-0.094	-0.082	-0.080	-0.080	-0.075
T-504	1.4	1.5	1.6	1.6	1.7	-0.085	-0.079	-0.074	-0.072	-0.066
T-505	2.1	2.2	2.2	2.1	1.7	0.006	-0.008	-0.015	-0.012	-0.040
T-506	-2.5	-2.4	-2.2	-2.2	-2.1	-0.070	-0.059	-0.052	-0.050	-0.044
T-507	-2.4	-2.3	-2.2	-2.1	-2.0	-0.039	-0.030	-0.023	-0.020	-0.013
T-508	-0.6	-0.5	-0.5	-0.6	-0.9	0.138	0.126	0.120	0.123	0.096
T-509	1.7	1.7	1.8	1.7	1.8	-0.065	-0.057	-0.056	-0.058	-0.053
T-510	3.0	2.9	2.3	1.9	1.2	0.083	0.081	0.069	0.071	0.038
T-511	0.3	0.4	0.5	0.5	0.1	0.127	0.122	0.121	0.127	0.101
T-512	2.0	2.1	2.2	2.2	2.2	0.268	0.277	0.280	0.280	0.286
T-513	-3.9	-3.6	-3.4	-3.3	-3.6	-0.062	-0.052	-0.055	-0.048	-0.079
T-514	2.7	3.0	2.9	2.7	2.3	0.294	0.304	0.293	0.293	0.264
T-515	3.0	3.0	3.1	3.1	3.2	-0.152	-0.145	-0.142	-0.142	-0.137
T-516	-2.6	-2.6	-2.5	-2.5	-2.4	0.226	0.230	0.234	0.234	0.240
T-517	2.5	2.7	2.8	2.7	2.3	0.158	0.159	0.154	0.158	0.132
T-518	-1.6	-1.6	-1.5	-1.5	-1.4	-0.109	-0.102	-0.099	-0.099	-0.094
T-519	1.3	1.3	1.4	1.4	1.5	-0.072	-0.067	-0.064	-0.064	-0.058
T-601	2.4	2.4	2.3	2.1	2.1	0.004	0.001	-0.009	-0.014	-0.017
T-602	2.0	2.3	2.4	2.5	2.6	0.047	0.088	0.097	0.098	0.098
T-603	0.3	0.5	0.8	1.0	1.2	0.150	0.168	0.188	0.200	0.205
T-604	1.7	1.2	0.4	0.1	-0.8	-0.002	0.004	0.023	0.035	0.040
T-605	0.1	-0.3	-3.6	-2.5	-2.6	0.189	0.165	0.154	0.149	0.148

T-606	-0.4	-0.3	-0.4	-0.4	-0.4	0.048	0.049	0.048	0.048	0.047
T-607	-4.6	-4.5	-4.5	-4.5	-4.5	-0.013	-0.016	-0.017	-0.017	-0.018
T-608	-0.3	-0.9	0.5	-0.1	0.2	-0.066	-0.069	-0.068	-0.067	-0.067
T-609	0.9	0.9	0.8	0.6	0.6	0.039	0.038	0.028	0.023	0.020
T-610	3.2	3.3	3.1	3.0	3.0	-0.003	-0.007	-0.014	-0.017	-0.019
T-611	-0.5	-0.4	-0.2	-0.2	-0.3	-0.065	-0.056	-0.046	-0.042	-0.040
T-612	2.8	3.0	3.2	3.6	3.8	0.023	0.020	0.010	0.005	0.001
T-613	-2.5	-2.5	-2.5	-2.6	-2.6	-0.021	-0.025	-0.029	-0.030	-0.031
T-614	-3.1	-3.1	-3.3	-3.7	-3.9	-0.227	-0.236	-0.251	-0.260	-0.264
T-615	-1.9	-1.8	-1.9	-2.0	-2.0	0.022	0.022	0.019	0.017	0.016
T-616	2.3	2.4	2.3	2.2	2.2	-0.028	-0.031	-0.035	-0.036	-0.037
T-617	-0.6	-0.4	-0.1	-0.1	-0.1	0.045	0.063	0.079	0.087	0.091
T-618	-2.2	-1.7	-1.5	-0.7	-0.1	-0.216	-0.223	-0.210	-0.199	-0.196
T-619	-2.4	-2.4	-2.4	-2.5	-2.5	-0.002	-0.004	-0.008	-0.010	-0.011
T-701	-1.2	-1.3	-1.3	-1.3	-1.3	0.222	0.229	0.230	0.228	0.234
T-702	3.4	3.5	3.6	3.7	3.8	0.033	0.050	0.058	0.060	0.067
T-703	2.3	2.3	2.3	2.4	2.4	0.093	0.103	0.107	0.106	0.113
T-704	0.4	0.3	0.3	0.4	0.4	-0.059	-0.056	-0.051	-0.051	-0.044
T-705	-3.5	-3.5	-3.4	-3.4	-3.4	-0.062	-0.062	-0.055	-0.054	-0.053
T-706	2.6	2.5	2.4	2.4	2.4	-0.072	-0.074	-0.077	-0.080	-0.074
T-707	0.4	0.3	0.4	0.4	0.4	0.127	0.133	0.137	0.137	0.144
T-708	-3.2	-3.3	-3.3	-3.4	-3.4	-0.064	-0.087	-0.092	-0.092	-0.092
T-709	-0.9	-0.9	-0.9	-0.8	-0.9	0.179	0.186	0.188	0.187	0.194
T-710	1.4	1.5	1.6	1.5	1.2	0.276	0.266	0.254	0.256	0.226
T-711	-0.3	-0.3	-0.3	-0.3	-0.3	0.090	0.087	0.086	0.085	0.084
T-712	0.7	0.7	0.7	0.7	0.7	-0.117	-0.109	-0.107	-0.109	-0.102
T-713	0.1	0.3	0.4	0.4	0.1	0.029	0.029	0.021	0.025	-0.004
T-714	1.8	1.9	2.0	2.0	2.0	-0.223	-0.216	-0.212	-0.211	-0.211
T-715	-1.4	-1.5	-1.4	-1.4	-1.4	-0.390	-0.383	-0.380	-0.381	-0.374
T-716	-2.2	-2.3	-2.3	-2.3	-2.3	-0.281	-0.279	-0.278	-0.279	-0.272
T-717	1.1	1.2	1.2	1.2	1.2	0.127	0.133	0.133	0.132	0.132
T-718	-1.3	-1.4	-1.4	-1.3	-1.4	-0.022	-0.015	-0.014	-0.016	-0.009
T-719	-2.3	-2.4	-2.4	-2.4	-2.4	-0.145	-0.143	-0.141	-0.143	-0.136
T-801	3.4	3.3	3.3	3.3	3.3	-0.331	-0.332	-0.334	-0.335	-0.330
T-802	-2.4	-2.4	-2.4	-2.4	-2.3	-0.040	-0.037	-0.035	-0.035	-0.029
T-803	1.4	1.3	1.4	1.4	1.4	0.261	0.263	0.264	0.263	0.268
T-804	0.0	-0.1	0.0	0.1	0.2	-0.062	-0.062	-0.059	-0.058	-0.052
T-805	0.6	0.5	0.4	0.3	0.2	0.031	0.021	0.011	0.006	0.003
T-806	1.3	1.2	1.3	1.3	1.4	0.310	0.312	0.314	0.314	0.319
T-807	0.4	0.3	0.4	0.4	0.5	-0.028	-0.028	-0.025	-0.023	-0.017
T-808	3.1	3.2	3.4	3.5	3.6	-0.176	-0.173	-0.167	-0.163	-0.161

T-809	-1.5	-1.7	-1.7	-1.7	-1.8	0.268	0.264	0.258	0.254	0.258
T-810	1.0	1.2	1.2	1.0	0.7	0.057	0.044	0.027	0.027	-0.004
T-811	1.1	1.1	1.2	1.1	1.1	0.189	0.192	0.186	0.183	0.182
T-812	-4.2	-4.3	-4.3	-4.3	-4.3	0.104	0.102	0.100	0.098	0.103
T-813	-3.3	-3.1	-2.9	-2.9	-3.2	-0.271	-0.269	-0.275	-0.269	-0.298
T-814	4.1	4.0	3.9	3.7	3.3	0.415	0.439	0.438	0.435	0.435
T-815	0.6	0.5	0.6	0.6	0.6	-0.279	-0.280	-0.282	-0.283	-0.278
T-816	0.0	-0.2	-0.1	-0.1	-0.1	-0.068	-0.072	-0.072	-0.073	-0.067
T-817	-2.8	-2.6	-2.3	-2.2	-2.0	0.159	0.174	0.186	0.193	0.196
T-818	0.9	0.8	0.9	0.9	0.9	-0.018	-0.018	-0.018	-0.019	-0.014
T-819	2.3	2.1	2.2	2.2	2.2	0.234	0.231	0.230	0.230	0.235
V-101	-2.9	-2.4	-2.0	-2.1	-2.3	0.626	0.685	0.709	0.708	0.713
V-102	-5.4	-5.3	-5.4	-5.8	-6.2	-0.035	-0.025	-0.034	-0.050	-0.048
V-103	-2.8	-2.7	-2.5	-2.9	-3.9	-0.094	-0.082	-0.067	-0.084	-0.102
V-104	1.6	1.3	1.1	0.9	0.9	0.102	0.044	0.031	0.029	0.034
V-105	-3.2	-3.7	-3.7	-3.5	-3.3	-0.169	-0.250	-0.252	-0.239	-0.225
V-201	2.4	2.4	2.4	2.5	2.5	0.065	0.056	0.059	0.059	0.070
V-202	0.1	0.1	0.2	0.3	0.2	0.218	0.222	0.228	0.227	0.238
V-203	-2.0	-1.2	-0.6	-0.2	0.1	0.458	0.419	0.396	0.383	0.389
V-204	1.3	1.0	0.7	0.6	0.5	-0.001	-0.041	-0.059	-0.069	-0.061
V-205	2.0	1.4	1.0	0.8	0.6	-0.328	-0.403	-0.432	-0.444	-0.438
V-206	-6.3	-6.5	-6.6	-6.7	-6.7	-0.456	-0.328	-0.383	-0.376	-0.375
V-207	-4.2	-4.1	-4.0	-4.0	-4.1	-0.188	-0.191	-0.187	-0.186	-0.181
V-208	6.0	6.0	5.8	5.7	5.6	0.560	0.544	0.535	0.530	0.533
V-209	1.2	1.2	1.2	1.3	1.2	-0.033	-0.033	-0.031	-0.033	-0.023
V-210	-0.9	-0.8	-0.7	-0.7	-0.7	0.140	0.138	0.145	0.147	0.153
V-301	-1.4	-1.6	-1.7	-1.8	-1.8	-0.220	-0.118	-0.120	-0.163	-0.059
V-302	-2.6	-2.7	-2.8	-2.9	-2.9	-0.200	-0.239	-0.245	-0.240	-0.263
V-303	-1.8	-1.5	-1.5	-1.4	-1.5	-0.195	-0.054	0.028	0.042	0.020
V-304	-1.4	-1.4	-1.5	-1.6	-1.7	0.141	0.126	0.113	0.110	0.104
V-305	-2.8	-2.7	-2.7	-2.7	-2.8	-0.305	-0.282	-0.280	-0.281	-0.284
V-306	0.8	0.9	1.0	1.0	1.1	-0.028	-0.039	-0.035	-0.025	-0.045
V-307	3.6	4.0	4.5	4.9	5.2	0.344	0.381	0.415	0.434	0.441
V-308	1.9	1.8	1.5	1.4	1.4	0.078	0.047	0.033	0.029	0.028
V-309	1.2	1.3	1.4	1.5	1.6	0.279	0.271	0.277	0.289	0.269
V-310	1.8	1.9	1.8	1.7	1.6	0.531	0.524	0.514	0.510	0.504
V-311	0.0	-0.5	-0.2	-0.2	-0.8	-0.052	-0.046	-0.040	-0.037	-0.036
V-312	-0.1	-0.6	0.2	-0.6	-0.6	0.250	0.255	0.261	0.264	0.265
V-401	-0.1	-0.1	-0.1	-0.1	-0.1	0.028	0.089	0.052	0.026	0.023
V-402	5.2	5.1	4.8	5.1	5.1	0.328	0.334	0.350	0.359	0.364
V-403	0.9	1.1	1.2	0.1	0.1	0.250	0.216	0.198	0.190	0.188

V-404	3.7	3.8	3.5	3.3	3.0	0.313	0.327	0.310	0.298	0.293
V-405	-2.5	-1.6	-2.1	-2.7	-2.6	-0.045	-0.045	-0.050	-0.053	-0.053
V-406	-0.8	-1.1	-0.7	-0.5	-0.6	-0.214	-0.216	-0.222	-0.223	-0.229
V-501	-3.0	-3.0	-3.0	-3.0	-3.4	-0.344	-0.361	-0.367	-0.362	-0.388
V-502	-3.2	-3.0	-3.0	-3.1	-3.5	0.034	0.031	0.024	0.027	0.000
V-503	4.1	3.8	3.5	3.4	3.4	-0.038	-0.085	-0.104	-0.111	-0.107
V-504	-1.0	-0.9	-0.9	-0.9	-1.3	-0.148	-0.162	-0.168	-0.164	-0.190
V-505	2.5	3.0	3.1	2.9	2.3	0.131	0.138	0.125	0.135	0.073
V-506	-2.7	-4.2	-4.1	-2.9	0.2	-0.393	-0.350	-0.290	-0.327	-0.047
V-601	-0.5	-0.7	-1.0	-1.2	-1.3	0.072	0.042	0.019	0.008	0.003
V-602	-1.6	-1.5	-1.4	-1.3	-1.2	-0.118	-0.130	-0.116	-0.105	-0.101
V-603	-3.2	-3.5	0.8	-1.8	-1.2	-0.206	-0.184	-0.188	-0.195	-0.199
V-604	3.0	3.8	2.9	4.3	3.8	0.018	0.018	0.035	0.045	0.050
V-605	3.5	3.6	3.4	4.9	5.8	0.224	0.205	0.205	0.207	0.208
V-606	-6.0	-6.0	-5.9	-6.1	-6.2	-0.410	-0.409	-0.409	-0.410	-0.410
V-607	-0.1	-0.2	-0.4	-0.7	-1.0	0.143	0.133	0.117	0.107	0.103
V-608	0.3	1.5	-1.3	-0.1	-0.5	0.201	0.209	0.209	0.208	0.207
V-609	0.0	-0.7	0.8	0.2	0.4	-0.136	-0.140	-0.141	-0.140	-0.140
V-610	6.6	6.7	6.4	6.0	6.0	0.290	0.300	0.308	0.312	0.313
V-701	3.2	3.2	3.1	3.1	3.2	0.085	0.078	0.079	0.077	0.084
V-702	-5.0	-5.3	-5.3	-5.2	-5.3	-0.386	-0.413	-0.417	-0.417	-0.416
V-703	3.9	4.0	4.1	4.2	4.3	0.409	0.421	0.428	0.434	0.438
V-704	-0.8	-0.8	-0.8	-0.8	-0.8	0.025	0.023	0.024	0.022	0.028
V-705	2.0	2.1	2.0	1.8	1.5	0.173	0.158	0.142	0.142	0.110
V-706	-1.2	-1.2	-1.2	-1.2	-1.2	-0.051	-0.058	-0.060	-0.061	-0.061
V-801	-5.5	-5.5	-5.4	-5.3	-5.3	-0.277	-0.273	-0.268	-0.267	-0.260
V-802	-1.1	-1.1	-1.1	-1.1	-1.2	-0.378	-0.380	-0.384	-0.385	-0.387
V-803	-0.2	-0.1	-0.2	-0.2	-0.5	-0.023	-0.044	-0.019	-0.012	-0.013
V-804	0.9	0.9	1.0	0.9	1.0	-0.079	-0.076	-0.081	-0.083	-0.083

[a] **$E_{a,r}$:** Activation energy of the reverse reaction, given in kJ mol^{-1}.
[b] **$\log \widetilde{A}_r$:** Logarithm of the pre-exponential factor of the reverse reaction, given in m^3 mol^{-1} s^{-1}.

Table D-30 Factor of deviations (ρ) between the reaction rate coefficients of the HARs in the final set calculated by CBS-QB3 and the final set of ΔGAV°/ΔNNI° parameters reported in **Table 6-3** and **Table 6-4**.[a]

Reaction #	Factor of deviation									
	Forward					Reverse				
	300 K	600 K	1000 K	1500 K	2000 K	300 K	600 K	1000 K	1500 K	2000 K
T-101	1.15	1.06	1.11	1.10	1.26	1.73	1.11	1.19	1.03	1.06
T-102	1.67	1.12	1.05	1.10	1.23	2.68	1.57	1.52	1.82	1.82
T-103	1.57	1.55	2.18	2.06	1.95	3.28	1.03	1.29	1.25	1.35
T-104	2.22	1.35	1.10	1.24	1.36	1.86	1.37	1.41	1.72	1.72

T-105	5.40	2.05	1.36	1.39	1.45	1.70	1.35	1.59	1.43	1.48
T-106	7.72	2.55	1.67	1.69	1.75	3.21	1.12	1.21	1.18	1.28
T-107	2.14	1.31	2.00	1.98	1.92	1.96	1.22	1.51	1.40	1.48
T-108	1.96	1.25	1.08	1.27	1.42	1.85	1.39	1.58	2.07	2.18
T-109	1.54	1.14	1.01	1.21	1.35	6.39	2.53	2.04	2.20	2.08
T-110	1.54	1.08	1.02	1.18	1.33	6.12	3.78	2.64	2.66	2.44
T-111	2.18	1.91	1.62	1.78	1.90	1.32	1.21	1.04	1.42	1.50
T-112	1.42	1.06	1.01	1.20	1.35	2.61	1.73	1.77	2.16	2.16
T-113	2.51	1.34	1.05	1.17	1.27	6.13	3.05	2.71	2.68	2.56
T-114	1.10	1.11	1.21	1.01	1.12	1.62	2.21	2.07	1.66	1.63
T-115	3.88	2.71	2.41	2.86	3.19	2.38	1.31	1.23	1.43	1.40
T-116	1.16	1.46	1.57	1.30	1.15	1.86	2.98	3.02	2.53	1.79
T-117	1.83	1.17	1.01	1.15	1.28	1.06	1.86	1.92	1.61	1.61
T-118	1.53	1.11	1.00	1.19	1.34	1.20	1.57	1.68	1.45	1.48
T-119	1.51	1.15	1.05	1.27	1.43	1.58	1.00	1.00	1.19	1.19
T-201	1.88	1.07	1.17	1.40	1.46	1.26	1.07	1.07	1.31	1.30
T-202	1.59	1.46	1.39	1.45	1.42	1.40	1.10	1.24	1.14	1.22
T-203	2.54	1.89	1.67	1.68	1.62	2.41	1.66	1.53	1.68	1.58
T-204	1.21	1.15	1.26	1.40	1.41	1.66	1.18	1.01	1.25	1.24
T-205	2.19	1.70	1.51	1.51	1.45	1.24	1.21	1.34	1.24	1.33
T-206	3.07	2.10	1.81	1.81	1.73	2.41	1.41	1.23	1.32	1.23
T-207	2.96	2.25	1.93	1.89	1.78	2.23	1.65	1.50	1.62	1.51
T-208	4.04	1.66	1.14	1.13	1.23	4.28	4.26	2.65	1.81	1.67
T-209	1.15	1.05	1.17	1.34	1.37	1.27	1.06	1.10	1.29	1.26
T-210	1.56	1.05	1.28	1.52	1.57	1.29	1.05	1.10	1.01	1.04
T-211	2.15	1.43	1.22	1.06	1.03	1.71	1.89	1.84	1.59	1.65
T-212	1.53	1.50	1.51	1.62	1.61	1.77	1.57	1.63	1.90	1.85
T-213	1.11	1.23	1.35	1.51	1.52	1.10	1.05	1.15	1.36	1.33
T-214	1.41	1.07	1.06	1.05	1.10	1.07	1.35	1.46	1.33	1.42
T-215	1.98	1.86	1.81	1.91	1.87	3.50	1.60	1.29	1.28	1.15
T-216	1.82	1.07	1.13	1.34	1.39	4.19	3.38	2.93	2.38	2.40
T-217	1.45	1.24	1.55	1.84	1.92	2.38	1.93	1.67	1.35	1.36
T-218	1.28	2.06	2.46	2.88	2.98	1.28	1.08	1.05	1.84	1.78
T-219	1.93	1.06	1.19	1.42	1.48	1.88	1.32	1.08	1.17	1.17
T-301	1.34	1.20	1.08	1.01	1.03	1.17	1.17	1.22	1.37	1.36
T-302	1.25	1.31	1.18	1.07	1.04	1.51	1.71	1.62	1.41	1.40
T-303	1.66	1.25	1.19	1.20	1.18	1.38	1.14	1.10	1.20	1.17
T-304	1.25	1.10	1.08	1.09	1.07	1.36	1.40	1.43	1.59	1.56
T-305	1.40	1.03	1.04	1.09	1.10	1.54	1.06	1.02	1.11	1.10
T-306	2.08	1.41	1.28	1.25	1.21	1.83	1.49	1.42	1.52	1.48
T-307	1.62	1.31	1.25	1.24	1.20	1.57	1.38	1.33	1.43	1.38

T-308	3.02	2.38	2.36	2.57	2.57	1.18	1.11	1.04	1.26	1.35
T-309	1.29	1.24	1.13	1.04	1.02	2.31	2.47	2.42	2.16	2.18
T-310	3.77	2.06	1.50	1.24	1.15	2.90	2.19	1.86	1.55	1.51
T-311	4.25	3.24	2.64	2.30	2.19	2.41	1.04	1.29	1.38	1.43
T-312	1.20	1.17	1.08	1.01	1.00	1.09	1.13	1.29	1.52	1.54
T-313	2.89	1.80	1.42	1.24	1.18	4.83	2.96	2.40	1.98	1.92
T-314	1.65	1.91	1.94	1.81	1.83	1.14	1.00	1.00	1.24	1.26
T-315	1.46	1.44	1.52	1.61	1.62	3.15	2.97	3.01	2.87	2.45
T-316	1.04	1.08	1.19	1.29	1.30	1.10	1.19	1.26	1.43	1.42
T-317	1.81	1.77	1.63	1.44	1.41	2.07	1.53	1.32	1.54	1.52
T-318	1.19	1.10	1.01	1.07	1.08	1.26	1.22	1.25	1.40	1.38
T-319	1.47	1.17	1.02	1.08	1.11	1.33	1.14	1.03	1.12	1.12
T-401	2.45	2.73	2.58	2.44	2.42	2.17	2.45	2.44	2.17	2.19
T-402	3.03	1.52	1.44	1.49	1.50	8.44	1.49	1.14	1.29	1.46
T-403	1.57	1.07	1.17	1.32	1.38	3.49	1.52	1.08	1.23	1.31
T-404	1.32	1.06	1.13	1.14	1.17	1.73	1.50	1.37	1.18	1.17
T-405	1.79	1.01	1.14	1.19	1.24	1.53	1.16	1.39	1.36	1.44
T-406	3.07	2.02	1.82	1.76	1.69	1.23	1.10	1.26	1.49	1.51
T-407	2.19	1.75	1.68	1.66	1.61	1.31	1.10	1.27	1.51	1.53
T-408	4.54	2.30	1.58	1.27	1.17	3.15	2.18	1.76	1.40	1.33
T-409	1.19	1.01	1.18	1.30	1.34	1.20	1.27	1.35	1.56	1.56
T-410	3.07	2.15	1.72	1.51	1.44	2.82	2.05	1.87	1.99	1.91
T-411	4.81	2.50	1.79	1.49	1.39	1.52	1.91	2.05	1.91	1.97
T-412	1.40	1.47	1.62	1.73	1.75	1.17	1.56	1.79	2.14	2.17
T-413	3.00	2.22	1.79	1.58	1.51	1.24	1.17	1.18	1.32	1.30
T-414	1.41	1.36	1.26	1.20	1.19	1.24	1.52	1.62	1.51	1.56
T-415	2.00	1.98	2.10	2.20	2.21	1.87	2.03	2.13	2.43	2.41
T-416	1.60	2.25	2.36	2.36	2.40	1.30	1.21	1.13	1.02	1.03
T-417	1.03	1.14	1.26	1.35	1.37	1.01	1.09	1.12	1.02	1.04
T-418	1.23	1.28	1.39	1.47	1.48	1.14	1.28	1.36	1.56	1.56
T-419	3.19	2.13	1.66	1.42	1.35	4.72	2.52	1.88	1.45	1.36
T-501	3.17	2.54	2.21	2.04	1.98	3.28	2.39	2.05	1.75	1.72
T-502	3.30	2.67	2.25	2.02	1.93	1.13	1.19	1.12	1.01	1.02
T-503	1.35	1.15	1.13	1.14	1.13	1.44	1.16	1.04	1.11	1.12
T-504	1.08	1.29	1.41	1.54	1.71	2.04	1.45	1.32	1.36	1.30
T-505	1.13	1.23	1.34	1.41	1.43	2.10	1.44	1.24	1.22	1.22
T-506	1.49	1.22	1.17	1.15	1.13	2.55	1.56	1.26	1.05	1.02
T-507	1.42	1.24	1.22	1.21	1.19	2.73	1.65	1.34	1.12	1.09
T-508	2.04	1.25	1.03	1.19	1.26	1.72	1.58	1.50	1.38	1.31
T-509	3.54	1.83	1.49	1.36	1.29	2.23	1.49	1.31	1.33	1.27
T-510	3.78	1.82	1.44	1.30	1.22	3.85	2.27	1.54	1.32	1.25

T-511	1.69	1.02	1.14	1.23	1.29	1.28	1.32	1.34	1.28	1.24
T-512	5.04	2.23	1.69	1.48	1.38	1.16	1.35	1.58	1.58	1.67
T-513	3.89	1.99	1.46	1.23	1.15	4.54	2.00	1.43	1.16	1.03
T-514	2.51	2.05	1.76	1.59	1.53	1.69	1.16	1.47	1.56	1.58
T-515	5.52	2.48	1.88	1.66	1.54	4.41	2.35	1.87	1.81	1.68
T-516	1.61	1.27	1.10	1.02	1.01	5.27	3.15	2.51	2.07	1.99
T-517	3.58	2.28	1.79	1.57	1.48	1.93	1.12	1.10	1.15	1.17
T-518	1.36	1.18	1.07	1.00	1.02	1.61	1.19	1.03	1.13	1.15
T-519	3.04	1.80	1.52	1.42	1.35	1.80	1.38	1.26	1.31	1.26
T-601	4.47	3.41	2.82	2.55	2.41	2.95	1.56	1.28	1.25	1.20
T-602	3.07	2.06	1.85	1.74	1.68	1.98	1.20	1.00	1.01	1.07
T-603	4.01	1.82	1.37	1.17	1.08	1.37	1.47	1.50	1.45	1.47
T-604	4.95	2.05	1.46	1.21	1.09	4.06	3.43	2.05	1.66	1.45
T-605	6.46	2.62	1.83	1.48	1.32	1.25	1.44	2.24	1.66	1.68
T-606	2.32	1.48	1.32	1.25	1.22	1.26	1.28	1.24	1.14	1.12
T-607	1.63	1.37	1.20	1.12	1.08	5.73	2.53	1.75	1.37	1.24
T-608	3.40	1.70	1.35	1.19	1.12	1.04	1.09	1.17	1.17	1.18
T-609	2.55	1.44	1.27	1.21	1.19	1.63	1.08	1.01	1.02	1.01
T-610	1.87	1.28	1.20	1.17	1.17	4.32	1.88	1.44	1.35	1.28
T-611	2.50	2.27	2.05	1.95	1.90	1.06	1.01	1.03	1.10	1.09
T-612	1.15	1.05	1.07	1.15	1.19	4.13	3.17	1.93	1.61	1.44
T-613	4.26	2.33	1.69	1.44	1.32	2.36	1.63	1.34	1.13	1.07
T-614	1.33	1.10	1.05	1.08	1.04	2.49	1.17	1.11	1.39	1.47
T-615	1.27	1.16	1.04	1.02	1.06	2.04	1.60	1.38	1.20	1.14
T-616	3.70	1.80	1.45	1.31	1.25	2.92	1.63	1.35	1.32	1.27
T-617	1.74	1.79	1.75	1.88	1.73	1.77	1.48	1.35	1.21	1.23
T-618	3.11	2.22	1.19	1.13	1.31	2.63	2.05	1.27	1.05	1.17
T-619	3.99	2.07	1.47	1.24	1.13	1.91	1.67	1.38	1.18	1.11
T-701	3.97	2.67	2.04	1.67	1.59	3.23	2.66	2.28	1.83	1.82
T-702	2.06	1.22	1.11	1.04	1.08	4.05	1.64	1.23	1.21	1.09
T-703	2.03	1.20	1.08	1.08	1.03	1.65	1.02	1.12	1.03	1.11
T-704	2.07	1.44	1.35	1.39	1.33	1.03	1.04	1.01	1.18	1.15
T-705	2.18	1.22	1.07	1.07	1.02	4.15	2.11	1.52	1.13	1.07
T-706	2.48	2.31	1.88	1.81	1.68	2.57	1.59	1.38	1.49	1.39
T-707	2.06	1.24	1.10	1.10	1.04	1.59	1.60	1.53	1.30	1.34
T-708	4.20	2.11	1.40	1.06	1.02	3.05	1.86	1.38	1.03	1.03
T-709	2.54	2.07	1.69	1.43	1.38	2.44	2.22	1.97	1.61	1.61
T-710	4.85	3.61	2.84	2.36	2.27	1.21	1.64	1.70	1.56	1.54
T-711	1.38	1.16	1.19	1.12	1.14	1.22	1.47	1.42	1.20	1.21
T-712	1.71	1.13	1.07	1.12	1.08	1.48	1.21	1.21	1.39	1.34
T-713	1.30	1.37	1.25	1.11	1.11	1.17	1.21	1.14	1.00	1.03

T-714	1.30	1.01	1.23	1.46	1.51	3.00	1.99	1.80	1.96	1.87
T-715	1.49	1.08	1.16	1.39	1.45	1.13	1.47	1.75	2.20	2.21
T-716	2.56	1.73	1.33	1.09	1.05	1.60	1.03	1.24	1.62	1.66
T-717	2.14	1.96	1.64	1.39	1.35	1.20	1.25	1.33	1.19	1.24
T-718	2.63	1.75	1.33	1.08	1.03	1.87	1.53	1.31	1.05	1.04
T-719	2.10	1.33	1.00	1.23	1.29	2.26	1.43	1.11	1.17	1.21
T-801	2.06	1.65	1.57	1.59	1.54	3.41	1.31	1.19	1.17	1.01
T-802	1.23	1.04	1.10	1.19	1.13	2.67	1.69	1.36	1.10	1.06
T-803	1.13	1.14	1.22	1.22	1.26	1.47	1.72	1.79	1.62	1.69
T-804	1.31	1.35	1.40	1.46	1.44	1.29	1.09	1.00	1.16	1.15
T-805	2.25	1.41	1.29	1.30	1.27	1.14	1.08	1.09	1.03	1.02
T-806	1.32	1.07	1.19	1.21	1.27	1.76	1.98	2.03	1.84	1.91
T-807	1.88	1.61	1.55	1.56	1.51	1.23	1.10	1.04	1.10	1.08
T-808	1.50	1.10	1.09	1.24	1.28	4.31	2.38	1.94	1.96	1.82
T-809	2.65	2.17	1.88	1.68	1.64	4.32	3.04	2.52	2.03	1.99
T-810	1.76	1.25	1.02	1.12	1.16	1.06	1.05	1.05	1.03	1.07
T-811	3.10	2.53	2.10	1.82	1.74	1.02	1.39	1.48	1.36	1.40
T-812	4.25	2.89	1.89	1.47	1.34	4.89	3.62	2.40	1.74	1.62
T-813	2.63	1.20	1.18	1.46	1.56	2.82	1.22	1.16	1.49	1.66
T-814	1.70	1.81	1.70	1.57	1.56	4.83	1.21	1.36	1.56	1.79
T-815	1.11	1.30	1.44	1.58	1.59	1.75	1.74	1.79	2.03	1.98
T-816	1.19	1.11	1.28	1.43	1.45	1.26	1.08	1.01	1.18	1.17
T-817	6.20	2.70	1.85	1.48	1.37	5.74	3.04	2.32	1.83	1.76
T-818	1.64	1.16	1.03	1.17	1.20	1.07	1.00	1.01	1.13	1.10
T-819	1.01	1.16	1.19	1.17	1.20	1.01	1.36	1.50	1.41	1.49
V-101	1.73	2.56	2.89	3.28	3.18	7.56	3.53	3.01	2.54	2.11
V-102	2.31	2.49	3.40	2.14	1.91	2.81	3.06	1.99	1.30	1.22
V-103	1.59	2.74	2.79	2.98	3.05	1.87	2.91	2.27	1.63	1.12
V-104	1.42	2.00	1.34	1.21	1.23	2.63	1.11	1.05	1.07	1.04
V-105	2.13	2.23	2.27	1.82	1.60	1.58	1.28	1.01	1.38	1.47
V-201	2.08	1.56	1.36	1.35	1.28	1.94	1.20	1.04	1.09	1.01
V-202	1.19	1.03	1.18	1.19	1.25	2.03	1.96	1.87	1.62	1.67
V-203	4.80	1.83	1.51	1.25	1.18	7.90	3.39	2.84	2.32	2.35
V-204	6.23	3.04	2.17	1.80	1.70	1.30	1.31	1.17	1.29	1.22
V-205	6.45	1.85	1.26	1.07	1.11	4.99	3.37	2.87	2.68	2.34
V-206	3.18	1.22	1.21	1.57	1.71	4.43	2.00	1.03	1.37	1.63
V-207	1.04	1.30	1.38	1.51	1.51	3.97	1.73	1.20	1.07	1.19
V-208	3.13	1.73	1.34	1.05	1.04	3.04	1.18	1.88	2.21	2.42
V-209	2.06	1.35	1.12	1.09	1.03	1.61	1.19	1.12	1.10	1.16
V-210	1.23	1.28	1.26	1.32	1.30	2.33	1.93	1.73	1.79	1.48
V-301	1.82	1.09	1.04	1.16	1.20	1.16	1.16	1.03	1.56	1.05

V-302	2.24	2.14	2.30	2.58	2.69	1.42	1.09	1.14	1.74	1.58
V-303	1.59	1.68	1.30	1.12	1.07	1.14	1.37	1.40	1.16	1.15
V-304	3.14	1.95	1.49	1.27	1.19	2.46	1.95	1.70	1.54	1.41
V-305	1.89	1.35	1.27	1.28	1.27	1.52	1.03	1.28	1.55	1.65
V-306	5.63	2.06	1.40	1.24	1.11	1.22	1.09	1.07	1.04	1.20
V-307	2.65	1.53	1.20	1.08	1.04	1.21	1.33	1.71	2.97	2.02
V-308	2.39	1.44	1.33	1.32	1.30	2.16	1.21	1.05	1.23	1.04
V-309	1.79	1.66	1.53	1.41	1.40	1.58	1.77	1.83	2.30	1.67
V-310	1.21	1.34	1.49	1.53	1.58	1.60	2.49	2.84	2.89	2.89
V-311	3.18	2.41	2.04	1.78	1.61	1.23	1.00	1.01	1.20	1.05
V-312	2.50	2.58	1.56	1.31	1.34	1.55	2.34	2.02	1.58	1.89
V-401	3.60	2.26	1.66	1.14	1.08	1.11	1.44	1.25	1.22	1.04
V-402	2.71	1.07	1.49	1.73	1.89	2.81	1.03	1.40	1.61	1.63
V-403	2.37	1.13	1.26	1.33	1.48	1.15	1.42	1.45	1.00	1.47
V-404	1.56	1.69	1.60	1.65	1.65	1.68	1.03	1.38	1.80	1.55
V-405	5.08	1.96	1.39	1.42	1.42	2.02	1.30	1.20	1.40	1.03
V-406	2.08	1.57	1.47	1.51	1.51	1.23	1.27	1.46	1.99	1.71
V-501	1.80	1.32	1.10	1.01	1.06	1.52	1.19	1.53	1.79	2.02
V-502	1.39	1.15	1.14	1.00	1.00	3.66	2.05	1.61	1.33	1.22
V-503	1.11	1.50	1.53	1.52	1.52	6.85	2.54	1.85	2.02	1.59
V-504	1.57	1.03	1.22	1.38	1.46	1.03	1.15	1.25	1.35	1.45
V-505	6.66	2.83	1.88	1.52	1.37	2.19	1.27	1.04	1.00	1.02
V-506	1.54	1.25	1.08	1.01	1.06	1.13	1.09	1.12	1.76	1.15
V-601	1.55	1.77	2.09	2.29	2.41	1.26	1.31	1.24	1.02	1.08
V-602	1.77	1.10	1.08	1.06	1.02	1.81	1.12	1.02	1.10	1.17
V-603	1.18	1.53	1.63	1.79	2.06	2.21	1.11	1.74	1.35	1.45
V-604	5.57	2.55	1.93	1.69	1.58	2.58	1.97	1.24	1.01	1.10
V-605	6.62	4.12	2.68	2.22	2.01	3.35	1.23	1.11	1.25	1.13
V-606	3.75	1.23	1.35	1.60	1.99	5.03	1.48	1.15	1.35	1.78
V-607	4.68	1.85	1.44	1.20	1.25	1.23	1.49	1.46	1.16	1.33
V-608	1.14	1.33	1.36	1.51	1.41	1.84	1.38	2.09	2.11	1.63
V-609	3.38	1.72	1.38	1.23	1.16	1.39	1.16	1.44	1.41	1.42
V-610	9.48	2.17	1.32	1.03	1.09	7.99	1.85	1.02	1.16	1.42
V-701	5.88	2.83	2.36	2.09	2.13	3.35	1.46	1.12	1.18	1.02
V-702	1.08	1.61	1.76	1.73	1.80	3.33	1.30	1.22	1.58	1.94
V-703	7.28	2.14	1.46	1.28	1.15	1.51	1.43	1.87	2.44	2.08
V-704	1.61	1.42	1.18	1.11	1.01	1.17	1.31	1.26	1.08	1.10
V-705	3.02	1.88	1.32	1.14	1.03	1.99	1.01	1.16	1.12	1.15
V-706	2.02	1.47	1.10	1.13	1.21	1.30	1.27	1.13	1.13	1.09
V-801	1.89	2.03	1.96	2.06	1.91	5.21	1.77	1.12	1.10	1.34
V-802	2.69	1.72	1.59	1.61	1.57	1.45	1.70	1.91	2.05	2.31

V-803	1.08	1.12	1.08	1.02	1.02	1.12	1.05	1.07	1.15	1.02
V-804	1.78	1.42	1.17	1.02	1.02	1.65	1.28	1.22	1.24	1.31

[a] Factor of deviation (ρ): If $k_{AI} > k_{GA}$, then $\rho = \frac{k_{AI}}{k_{GA}}$, if $k_{GA} > k_{AI}$ then $\rho = \frac{k_{GA}}{k_{AI}}$ where k_{AI} denotes reaction rate coefficients calculated with *ab initio* methods and k_{GA} denotes reaction rate coefficients calculated with group additive parameters reported in this study, namely the ΔGAV°/ΔNNI° parameters reported in **Table 6-3** and **Table 6-4**.

D.7 Applicability of GA parameters on the set of HARs from toluene derivatives with substituted extended side chains

D.7.1 List of HARs from TDs with substituted extended side chains

In the set of reactions given in **Figure D-60** below, there is no substituent group on the phenyl ring else than the extended side chain, but there are substituents on the extended side chain. This set is utilized to explore the predictability of the ΔGAV°s on HARs from other toluene derivatives than the ones that are present in the training set and the validation set. These 16 reactions are considered as a special set and they are represented with codes from **S-101** to **S-116**.

S-101:

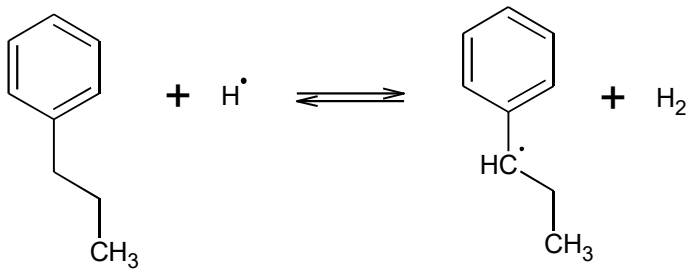

S-102:

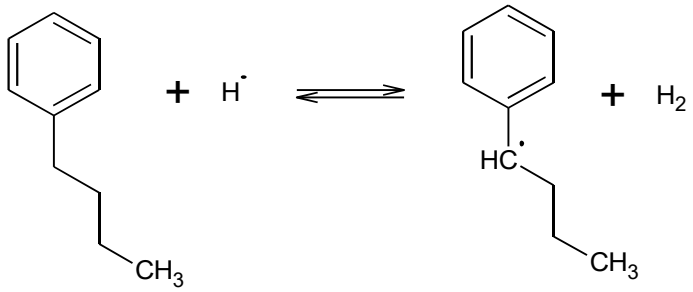

S-103:

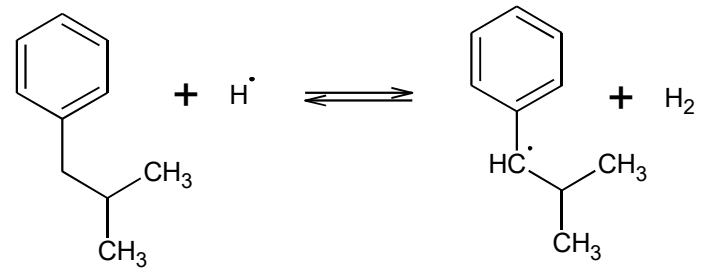

S-104:

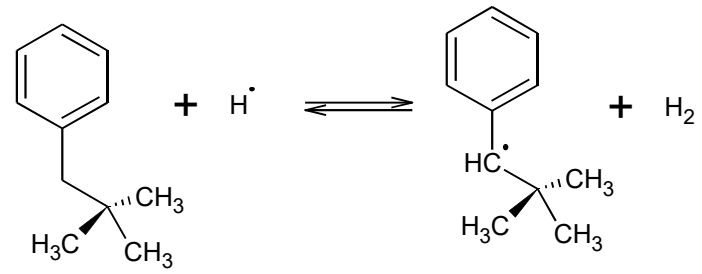

S-105:

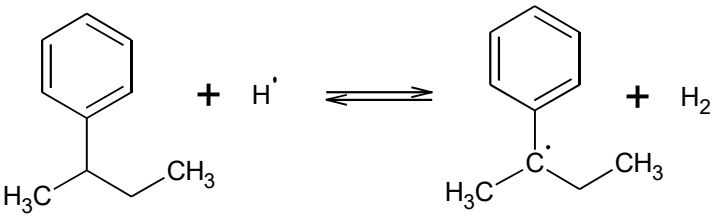

S-106:

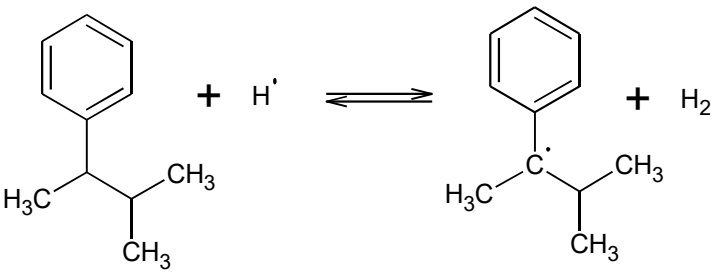

S-107:

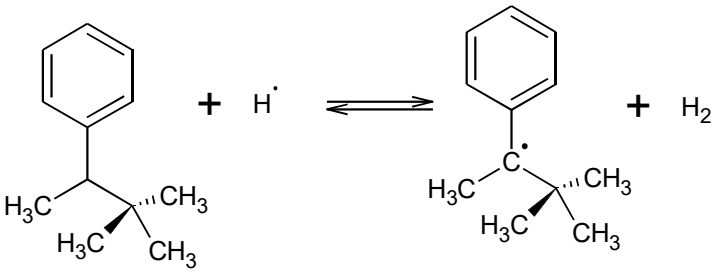

S-108:

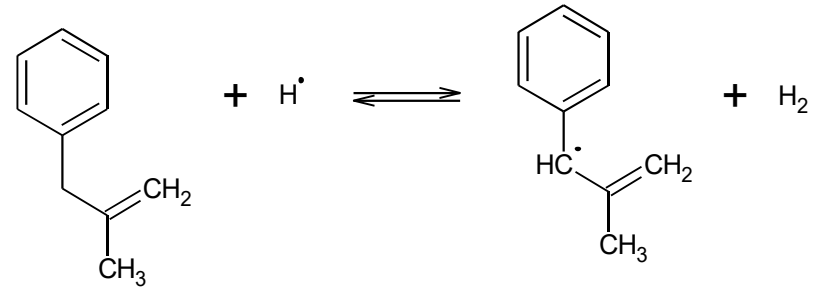

S-109:

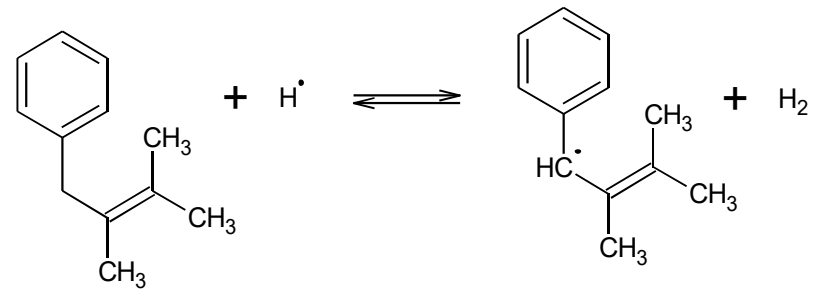

S-110:

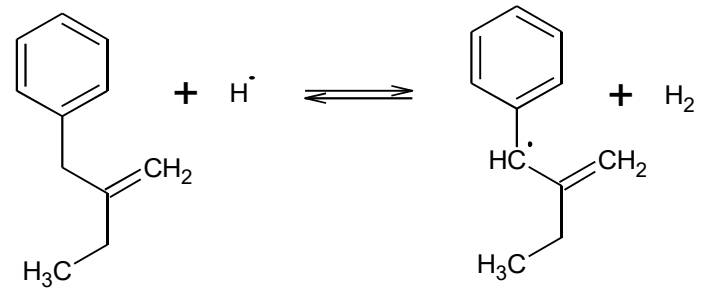

S-111:

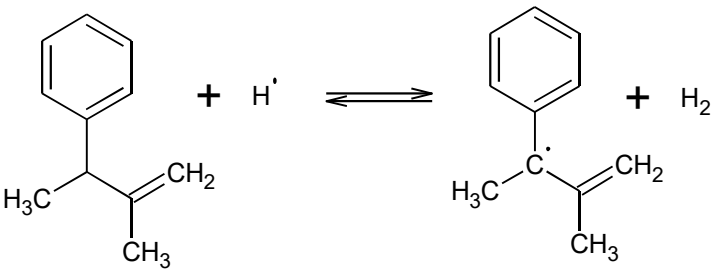

S-112:

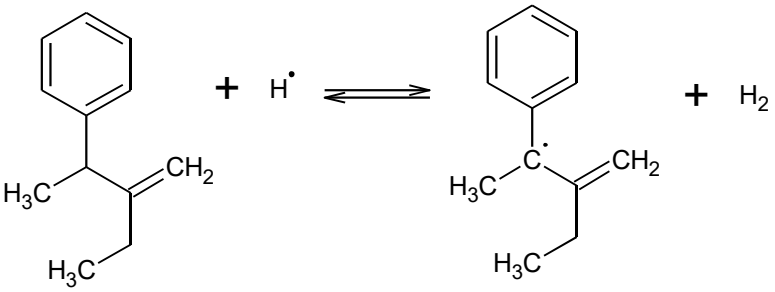

S-113:

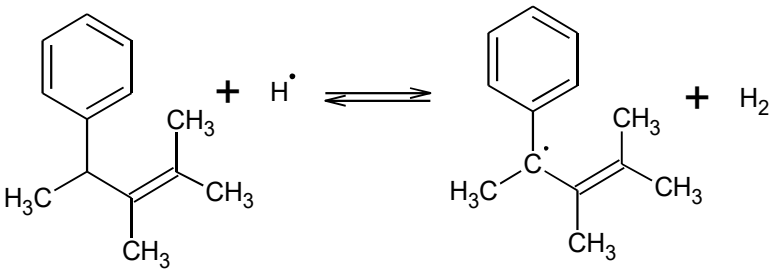

S-114:

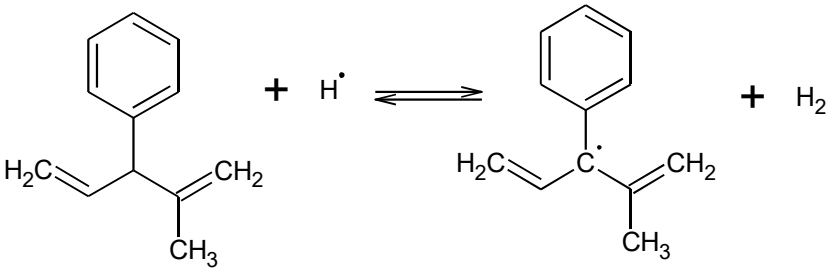

S-115:

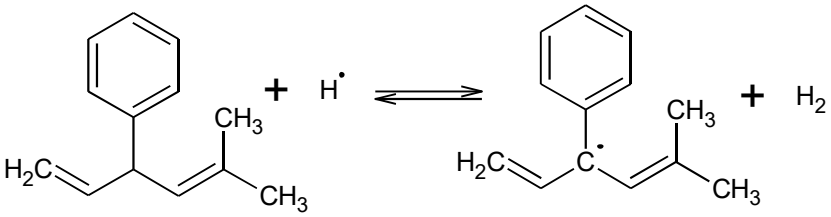

S-116:

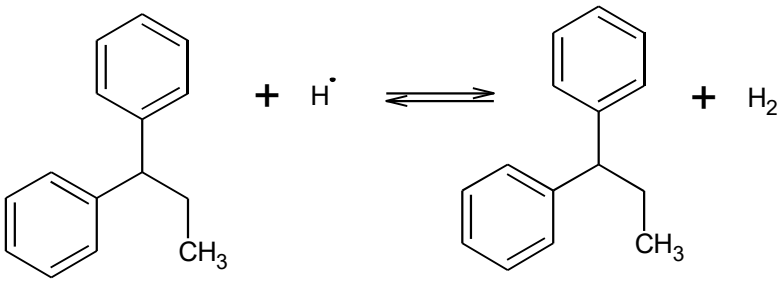

Figure D-60 The list of hydrogen abstraction reactions from the α-carbon of toluenes derivatives with substituted extended side chains.

D.7.2 Reaction data for the set of HARs from TDs with substituted extended side chains

Table D-31 Arrhenius parameters (activation energy ($\mathbf{E_a}$) and logarithm of the pre-exponential factor ($\log\widetilde{A}$)) of the reactions in the set of "HARs from TDs with substituted extended side chains" at 300 K, given along with reaction rate coefficients and the tunneling correction factor (κ) for forward and reverse reactions.

Reaction #	κ	Forward				Reverse			
		$E_{a,f}$ [a]	$log\widetilde{A}_f$ [b]	k_f [c]	κk_f [d]	$E_{a,r}$ [e]	$log\widetilde{A}_r$ [f]	k_r [g]	κk_r [h]
S-101	2.32	33.6	9.648	3.3E+01	7.7E+01	99.6	8.106	2.8E-12	6.52E-12
S-102	2.60	33.3	9.677	2.4E+01	6.2E+01	102.1	9.068	3.3E-13	8.56E-13
S-103	2.62	31.8	9.553	3.9E+01	1.0E+02	99.5	8.826	4.1E-12	1.07E-11
S-104	3.35	32.2	9.729	1.4E+01	4.5E+01	103.3	8.976	1.9E-12	6.48E-12
S-105	1.45	27.5	9.924	1.7E+02	2.5E+02	108.1	9.247	5.2E-13	7.58E-13
S-106	1.66	25.1	9.824	2.7E+02	4.5E+02	93.0	7.211	2.1E-12	3.48E-12
S-107	2.96	26.2	9.595	1.1E+02	3.3E+02	75.4	8.036	1.6E-08	4.73E-08
S-108	1.77	26.5	9.834	2.6E+02	4.5E+02	123.1	8.792	4.6E-16	8.07E-16
S-109	1.28	21.4	9.934	2.0E+03	2.6E+03	136.1	8.750	2.2E-18	2.84E-18
S-110	1.81	23.0	9.739	5.9E+02	1.1E+03	114.1	8.760	1.6E-14	2.82E-14
S-111	1.68	19.7	9.978	1.7E+03	2.8E+03	108.0	8.423	8.4E-14	1.40E-13
S-112	1.85	16.8	9.935	9.8E+03	1.8E+04	104.0	8.220	2.6E-13	4.88E-13
S-113	1.33	20.3	9.131	1.8E+02	2.3E+02	112.9	7.857	3.1E-15	4.16E-15
S-114	1.69	25.1	9.907	8.3E+02	1.4E+03	144.7	8.558	4.7E-20	7.89E-20
S-115	1.52	21.3	9.724	1.1E+03	1.7E+03	149.2	9.280	2.0E-20	3.07E-20
S-116	1.92	26.4	9.694	1.2E+02	2.3E+02	108.8	8.826	7.7E-14	1.48E-13

[a] $\mathbf{E_{a,f}}$: Activation energy of the forward reaction, given in kJ mol^{-1}.
[b] $\boldsymbol{log\widetilde{A}_f}$: Logarithm of the pre-exponential factor of the forward reaction, given in m^3 mol^{-1} s^{-1}.
[c] $\mathbf{k_f}$: The reaction rate coefficient for the forward reaction excluding tunneling effects, given in m^3 mol^{-1} s^{-1}.
[d] $\boldsymbol{\kappa k_f}$: The reaction rate coefficient for the forward reaction including tunneling effects, given in m^3 mol^{-1} s^{-1}.
[e] $\mathbf{E_{a,r}}$: Activation energy of the reverse reaction, given in kJ mol^{-1}.
[f] $\boldsymbol{log\widetilde{A}_r}$: Logarithm of the pre-exponential factor of the reverse reaction, given in m^3 mol^{-1} s^{-1}.
[g] $\mathbf{k_r}$: The reaction rate coefficient for the reverse reaction excluding tunneling effects, given in m^3 mol^{-1} s^{-1}.
[h] $\boldsymbol{\kappa k_r}$: The reaction rate coefficient for the reverse reaction including tunneling effects, given in m^3 mol^{-1} s^{-1}.

Table D-32 Arrhenius parameters (activation energy ($\mathbf{E_a}$) and logarithm of the pre-exponential factor ($\log\widetilde{A}$)) of the reactions in the set of "HARs from TDs with substituted extended side chains" at 600 K, given along with reaction rate coefficients and the tunneling correction factor (κ) for forward and reverse reactions.

Reaction #	κ	Forward				Reverse			
		$E_{a,f}$ [a]	$log\widetilde{A}_f$ [b]	k_f [c]	κk_f [d]	$E_{a,r}$ [e]	$log\widetilde{A}_r$ [f]	k_r [g]	κk_r [h]
S-101	1.22	35.2	9.735	2.56E+04	3.13E+04	101.5	8.323	1.2E-03	1.51E-03
S-102	1.24	36.2	10.293	9.03E+03	1.12E+04	104.4	9.334	3.5E-03	4.29E-03
S-103	1.26	35.5	9.987	2.51E+04	3.15E+04	101.8	9.090	3.3E-03	4.20E-03
S-104	1.40	36.9	10.234	7.30E+03	1.02E+04	106.2	9.318	2.3E-03	3.25E-03
S-105	1.10	32.1	10.452	4.96E+04	5.45E+04	111.2	9.612	1.7E-03	1.85E-03
S-106	1.14	28.9	10.278	5.69E+04	6.47E+04	95.0	7.432	2.9E-04	3.26E-04
S-107	1.30	30.2	10.067	4.00E+04	5.20E+04	77.6	8.278	6.6E-02	8.54E-02
S-108	1.27	30.3	10.234	6.38E+04	8.11E+04	125.4	9.051	2.7E-05	3.43E-05
S-109	1.06	25.2	10.201	2.02E+05	2.14E+05	138.3	8.998	1.8E-06	1.91E-06
S-110	1.16	26.7	10.241	8.08E+04	9.35E+04	116.3	9.004	1.5E-04	1.75E-04
S-111	1.14	23.5	10.119	1.18E+05	1.34E+05	110.0	8.647	2.3E-04	2.65E-04
S-112	1.17	20.6	10.386	3.88E+05	4.53E+05	105.9	8.431	3.2E-04	3.78E-04
S-113	1.07	25.8	9.734	2.04E+04	2.19E+04	114.8	8.065	2.3E-05	2.50E-05
S-114	1.20	24.2	10.359	6.92E+04	8.32E+04	146.9	8.808	2.1E-07	2.49E-07
S-115	1.11	22.3	10.015	6.84E+04	7.61E+04	151.8	9.586	2.3E-07	2.57E-07
S-116	1.17	30.2	10.144	3.23E+04	3.80E+04	111.1	9.088	2.6E-04	3.02E-04

[a]**$E_{a,f}$:** Activation energy of the forward reaction, given in kJ mol^{-1}.
[b]***$log\widetilde{A}_f$*:** Logarithm of the pre-exponential factor of the forward reaction, given in m^3 mol^{-1} s^{-1}.
[c]**kf:** The reaction rate coefficient for the forward reaction excluding tunneling effects, given in m^3 mol^{-1} s^{-1}.
[d]**κkf:** The reaction rate coefficient for the forward reaction including tunneling effects, given in m^3 mol^{-1} s^{-1}.
[e]**$E_{a,r}$:** Activation energy of the reverse reaction, given in kJ mol^{-1}.
[f]**log$\widetilde{A}$r**: Logarithm of the pre-exponential factor of the reverse reaction, given in m^3 mol^{-1} s^{-1}.
[g]**kr**: The reaction rate coefficient for the reverse reaction excluding tunneling effects, given in m^3 mol^{-1} s^{-1}.
[h]**κkr**: The reaction rate coefficient for the reverse reaction including tunneling effects, given in m^3 mol^{-1} s^{-1}.

Table D-33 Arrhenius parameters (activation energy ($\mathbf{E_a}$) and logarithm of the pre-exponential factor ($\mathbf{log\widetilde{A}}$)) of the reactions in the set of "HARs from TDs with substituted extended side chains" at 1000 K, given along with reaction rate coefficients and the tunneling correction factor (**κ**) for forward and reverse reactions.

Reaction #	κ	Forward				Reverse			
		$E_{a,f}$ [a]	$log\widetilde{A}_f$ [b]	k_f [c]	κk_f [d]	$E_{a,r}$ [e]	$log\widetilde{A}_r$ [f]	k_r [g]	κk_r [h]
S-101	1.08	42.2	10.280	5.51E+05	5.94E+05	108.6	8.787	5.0E+00	5.41E+00
S-102	1.08	44.5	10.873	2.72E+05	2.94E+05	112.0	9.831	1.9E+01	2.07E+01
S-103	1.12	41.9	10.421	3.38E+05	3.79E+05	109.0	9.563	1.5E+01	1.65E+01
S-104	1.13	40.0	10.673	2.36E+05	2.67E+05	113.8	9.819	1.5E+01	1.69E+01
S-105	1.04	33.9	10.849	7.03E+05	7.28E+05	118.6	10.102	1.6E+01	1.66E+01
S-106	1.05	35.2	10.696	7.19E+05	7.54E+05	102.2	7.903	7.3E-01	7.69E-01

S-107	1.10	38.3	10.506	6.39E+05	7.06E+05	85.0	8.766	4.2E+01	4.64E+01
S-108	1.14	37.6	10.500	1.07E+06	1.22E+06	132.7	9.534	7.9E-01	9.04E-01
S-109	1.02	31.1	10.594	1.86E+06	1.91E+06	145.1	9.442	1.5E-01	1.49E-01
S-110	1.06	33.0	10.657	8.56E+05	9.04E+05	123.4	9.471	2.1E+00	2.24E+00
S-111	1.05	29.8	10.539	9.61E+05	1.01E+06	117.1	9.113	2.0E+00	2.07E+00
S-112	1.06	26.9	10.811	2.52E+06	2.67E+06	112.9	8.895	2.0E+00	2.09E+00
S-113	1.03	31.7	9.952	1.97E+05	2.03E+05	121.5	8.506	2.9E-01	2.94E-01
S-114	1.07	35.2	10.783	8.73E+05	9.34E+05	154.1	9.283	3.4E-02	3.64E-02
S-115	1.04	31.1	10.630	6.26E+05	6.51E+05	159.1	10.065	5.7E-02	5.89E-02
S-116	1.06	36.5	10.566	4.53E+05	4.81E+05	118.5	9.573	2.4E+00	2.56E+00

[a] $\mathbf{E_{a,f}}$**:** Activation energy of the forward reaction, given in kJ mol^{-1}.
[b] $\boldsymbol{log\widetilde{A}_f}$**:** Logarithm of the pre-exponential factor of the forward reaction, given in m^3 mol^{-1} s^{-1}.
[c] $\mathbf{k_f}$**:** The reaction rate coefficient for the forward reaction excluding tunneling effects, given in m^3 mol^{-1} s^{-1}.
[d] $\boldsymbol{\kappa k_f}$**:** The reaction rate coefficient for the forward reaction including tunneling effects, given in m^3 mol^{-1} s^{-1}.
[e] $\mathbf{E_{a,r}}$**:** Activation energy of the reverse reaction, given in kJ mol^{-1}.
[f] $\boldsymbol{log\widetilde{A}_r}$**:** Logarithm of the pre-exponential factor of the reverse reaction, given in m^3 mol^{-1} s^{-1}.
[g] $\mathbf{k_r}$**:** The reaction rate coefficient for the reverse reaction excluding tunneling effects, given in m^3 mol^{-1} s^{-1}.
[h] $\boldsymbol{\kappa k_r}$**:** The reaction rate coefficient for the reverse reaction including tunneling effects, given in m^3 mol^{-1} s^{-1}.

Table D-34 Arrhenius parameters (activation energy ($\mathbf{E_a}$) and logarithm of the pre-exponential factor ($\boldsymbol{log\widetilde{A}}$)) of the reactions in the set of "HARs from TDs with substituted extended side chains" at 1500 K, given along with reaction rate coefficients and the tunneling correction factor ($\boldsymbol{\kappa}$) for forward and reverse reactions.

Reaction #	κ	Forward				Reverse			
		$E_{a,f}$ [a]	$log\widetilde{A}_f$ [b]	k_f [c]	κk_f [d]	$E_{a,r}$ [e]	$log\widetilde{A}_r$ [f]	k_r [g]	κk_r [h]
S-101	1.04	49.4	10.695	3.41E+06	3.54E+06	119.6	9.252	4.6E+02	4.8E+02
S-102	1.04	50.1	10.934	1.99E+06	2.06E+06	123.3	10.311	2.1E+03	2.2E+03
S-103	1.06	49.9	10.760	2.10E+06	2.22E+06	120.4	10.043	1.4E+03	1.5E+03
S-104	1.06	48.9	10.924	1.80E+06	1.91E+06	124.8	10.287	1.7E+03	1.8E+03
S-105	1.02	42.5	11.120	3.49E+06	3.55E+06	129.3	10.555	2.3E+03	2.3E+03
S-106	1.02	42.9	11.026	3.39E+06	3.47E+06	113.4	8.380	5.4E+01	5.5E+01
S-107	1.05	46.3	10.846	3.42E+06	3.59E+06	96.5	9.251	1.6E+03	1.6E+03
S-108	1.03	44.4	11.340	4.76E+06	4.89E+06	144.3	10.022	2.0E+02	2.0E+02
S-109	1.01	38.5	10.909	7.40E+06	7.47E+06	155.9	9.901	5.9E+01	6.0E+01
S-110	1.03	40.7	10.987	3.69E+06	3.79E+06	134.7	9.950	3.6E+02	3.7E+02
S-111	1.02	37.6	10.872	3.65E+06	3.73E+06	128.3	9.588	2.6E+02	2.7E+02
S-112	1.03	34.8	11.144	8.55E+06	8.79E+06	124.2	9.369	2.2E+02	2.3E+02
S-113	1.01	39.1	10.269	8.04E+05	8.14E+05	132.3	8.963	4.5E+01	4.6E+01
S-114	1.03	37.4	11.117	4.13E+06	4.26E+06	165.5	9.763	2.0E+01	2.1E+01
S-115	1.02	38.7	10.746	2.50E+06	2.54E+06	170.3	10.540	4.1E+01	4.1E+01
S-116	1.03	44.3	10.899	2.26E+06	2.32E+06	129.9	10.057	3.4E+02	3.5E+02

[a] $\mathbf{E_{a,f}}$**:** Activation energy of the forward reaction, given in kJ mol^{-1}.
[b] $\boldsymbol{log\widetilde{A}_f}$**:** Logarithm of the pre-exponential factor of the forward reaction, given in m^3 mol^{-1} s^{-1}.
[c] $\mathbf{k_f}$**:** The reaction rate coefficient for the forward reaction excluding tunneling effects, given in m^3 mol^{-1} s^{-1}.

[d] $\boldsymbol{\kappa k_f}$: The reaction rate coefficient for the forward reaction including tunneling effects, given in $m^3\ mol^{-1}\ s^{-1}$.
[e] $\mathbf{E_{a,r}}$: Activation energy of the reverse reaction, given in kJ mol^{-1}.
[f] $\boldsymbol{log\widetilde{A}_r}$: Logarithm of the pre-exponential factor of the reverse reaction, given in $m^3\ mol^{-1}\ s^{-1}$.
[g] $\mathbf{k_r}$: The reaction rate coefficient for the reverse reaction excluding tunneling effects, given in $m^3\ mol^{-1}\ s^{-1}$.
[h] $\boldsymbol{\kappa k_r}$: The reaction rate coefficient for the reverse reaction including tunneling effects, given in $m^3\ mol^{-1}\ s^{-1}$.

Table D-35 Arrhenius parameters (activation energy ($\mathbf{E_a}$) and logarithm of the pre-exponential factor ($\mathbf{log\widetilde{A}}$)) of the reactions in the set of "HARs from TDs with substituted extended side chains" at 2000 K, given along with reaction rate coefficients and the tunneling correction factor ($\boldsymbol{\kappa}$) for forward and reverse reactions.

Reaction #	κ	Forward				Reverse			
		$E_{a,f}$ [a]	$log\widetilde{A}_f$ [b]	k_f [c]	κk_f [d]	$E_{a,r}$ [e]	$log\widetilde{A}_r$ [f]	k_r [g]	κk_r [h]
S-101	1.02	55.7	10.958	9.93E+06	1.01E+07	130.5	9.581	5.6E+03	5.7E+03
S-102	1.03	56.4	11.124	4.21E+06	4.32E+06	134.3	10.644	2.7E+04	2.8E+04
S-103	1.03	57.4	10.984	6.12E+06	6.32E+06	132.1	10.396	1.8E+04	1.8E+04
S-104	1.04	56.4	11.234	5.81E+06	6.02E+06	135.6	10.611	2.3E+04	2.4E+04
S-105	1.01	49.1	11.672	9.06E+06	9.14E+06	139.8	10.870	3.3E+04	3.4E+04
S-106	1.01	50.2	11.245	8.58E+06	8.69E+06	125.1	8.730	5.8E+02	5.9E+02
S-107	1.03	53.7	11.069	9.28E+06	9.55E+06	108.2	9.605	1.2E+04	1.2E+04
S-108	1.01	52.1	11.060	1.99E+07	2.01E+07	156.1	10.377	4.0E+03	4.1E+03
S-109	1.01	45.6	11.123	1.71E+07	1.72E+07	167.3	10.244	1.5E+03	1.5E+03
S-110	1.02	48.0	11.206	8.95E+06	9.08E+06	146.4	10.303	6.0E+03	6.1E+03
S-111	1.01	44.9	11.093	8.30E+06	8.41E+06	140.0	9.938	3.8E+03	3.9E+03
S-112	1.02	42.1	11.366	1.84E+07	1.87E+07	135.8	9.719	3.0E+03	3.0E+03
S-113	1.01	46.3	10.484	1.88E+06	1.90E+06	143.7	9.303	7.1E+02	7.2E+02
S-114	1.02	43.4	11.339	1.05E+07	1.07E+07	177.2	10.115	6.1E+02	6.3E+02
S-115	1.01	45.9	10.964	5.80E+06	5.86E+06	181.9	10.889	1.4E+03	1.4E+03
S-116	1.02	51.7	11.120	5.88E+06	5.98E+06	141.7	10.411	5.1E+03	5.2E+03

[a] $\mathbf{E_{a,f}}$: Activation energy of the forward reaction, given in kJ mol^{-1}.
[b] $\boldsymbol{log\widetilde{A}_f}$: Logarithm of the pre-exponential factor of the forward reaction, given in $m^3\ mol^{-1}\ s^{-1}$.
[c] $\mathbf{k_f}$: The reaction rate coefficient for the forward reaction excluding tunneling effects, given in $m^3\ mol^{-1}\ s^{-1}$.
[d] $\boldsymbol{\kappa k_f}$: The reaction rate coefficient for the forward reaction including tunneling effects, given in $m^3\ mol^{-1}\ s^{-1}$.
[e] $\mathbf{E_{a,r}}$: Activation energy of the reverse reaction, given in kJ mol^{-1}.
[f] $\boldsymbol{log\widetilde{A}_r}$: Logarithm of the pre-exponential factor of the reverse reaction, given in $m^3\ mol^{-1}\ s^{-1}$.
[g] $\mathbf{k_r}$: The reaction rate coefficient for the reverse reaction excluding tunneling effects, given in $m^3\ mol^{-1}\ s^{-1}$.
[h] $\boldsymbol{\kappa k_r}$: The reaction rate coefficient for the reverse reaction including tunneling effects, given in $m^3\ mol^{-1}\ s^{-1}$.

Table D-36 External symmetry (σ_{ext}), internal symmetry (σ_{int}) and the number of optical isomers (n_{opt}) for the reactants, products and the transition state of the hydrogen abstraction reactions in the set of "HARs from TDs with substituted extended side chains", given along with the number of single events for the forward and reverse directions.

Reaction #	Forward						Reverse						Transition State			n_e[d]	
	Reactant 1			Reactant 2			Reactant 1			Reactant 2							
	σ_{ext}[a]	σ_{int}[b]	n_{opt}[c]	σ_{ext}	σ_{int}	n_{opt}	σ_{ext}	σ_{int}	n_{opt}	σ_{ext}	σ_{int}	n_{opt}	σ_{ext}	σ_{int}	n_{opt}	$n_{e,f}$[e]	$n_{e,r}$[f]
S-101	1	6	1	1	1	1	1	6	1	1	1	1	1	6	2	2	2
S-102	1	6	1	1	1	1	1	6	1	1	1	1	1	6	2	2	2
S-103	1	18	1	1	1	1	1	18	1	1	1	1	1	18	2	2	2
S-104	1	54	1	1	1	1	1	54	1	1	1	1	1	54	2	2	2
S-105	1	18	2	1	1	1	1	18	1	1	1	1	1	18	2	1	2
S-106	1	54	2	1	1	1	1	54	1	1	1	1	1	54	2	1	2
S-107	1	486	1	1	1	1	1	486	1	1	1	1	1	486	2	2	2
S-108	1	6	1	1	1	1	1	6	1	1	1	1	1	6	2	2	2
S-109	1	36	1	1	1	1	1	36	1	1	1	1	1	36	2	2	2
S-110	1	6	2	1	1	1	1	6	1	1	1	1	1	6	2	1	2
S-111	1	18	2	1	1	1	1	18	1	1	1	1	1	18	2	1	2
S-112	1	18	2	1	1	1	1	18	1	1	1	1	1	18	2	1	2
S-113	1	162	2	1	1	1	1	162	1	1	1	1	1	162	2	1	2
S-114	1	6	2	1	1	1	1	6	1	1	1	1	1	6	2	1	2
S-115	1	18	1	1	1	1	1	18	1	1	1	1	1	18	1	1	1
S-116	1	12	1	1	1	1	1	12	1	1	1	1	1	12	1	1	1

[a]**σ_{ext}:** External symmetry
[b]**σ_{int}:** Internal symmetry
[c]**n_{opt}:** Number of optical isomers
[d]**$n_{e,f}$:** number of single events for the forward reaction
[e]**$n_{e,r}$:** number of single events for the reverse reaction

D.7.3 The Performance of the GA parameters in predicting the Arrhenius Parameters and the Reaction Rate Coefficients of interest

Table D-37 The deviations between the CBS-QB3 data and the GA-based data for the HARs in the set of "HARs from TDs with substituted extended side chains" calculated with the ΔGAV°s and ΔNNI° parameters in the forward direction with respect to the reference reaction, given in **Table 6-3** and **Table 6-4**, respectively.

Reaction #	$E_{a,f}$[a]					$\log\widetilde{A}_f$ [b]				
	300 K	600 K	1000 K	1500 K	2000 K	300 K	600 K	1000 K	1500 K	2000 K
S-101	2.9	1.4	1.8	1.4	0.7	-0.074	-0.170	-0.110	-0.070	-0.049
S-102	2.7	2.1	3.3	1.8	1.1	-0.060	0.109	0.186	0.050	0.034
S-103	1.7	1.6	1.6	1.7	1.8	-0.122	-0.044	-0.040	-0.037	-0.036
S-104	1.9	2.5	0.3	1.0	1.1	-0.034	0.079	0.086	0.045	0.089
S-105	2.6	3.1	0.1	0.6	0.2	0.070	0.106	0.094	0.064	0.230
S-106	1.0	1.0	1.0	0.9	0.9	0.020	0.019	0.018	0.017	0.016
S-107	1.7	1.8	3.0	3.2	3.2	-0.095	-0.087	-0.077	-0.073	-0.072
S-108	1.0	1.1	1.8	1.2	1.5	-0.086	-0.114	-0.187	0.070	-0.179
S-109	-2.3	-2.4	-2.5	-2.7	-2.8	-0.036	-0.131	-0.140	-0.145	-0.147
S-110	-1.3	-1.3	-1.3	-1.2	-1.2	-0.134	-0.111	-0.108	-0.106	-0.106
S-111	0.8	0.8	0.9	1.1	1.2	0.028	-0.131	-0.123	-0.118	-0.116
S-112	-1.1	-1.1	-0.9	-0.8	-0.6	0.006	0.002	0.013	0.018	0.020
S-113	1.2	2.3	2.2	2.2	2.1	-0.396	-0.324	-0.417	-0.419	-0.420
S-114	5.2	2.2	5.6	2.0	1.0	0.004	0.008	0.019	0.026	0.028
S-115	2.7	1.0	2.8	2.8	2.7	-0.088	-0.164	-0.057	-0.160	-0.159
S-116	-0.5	-0.6	-0.4	-0.3	-0.2	0.038	0.040	0.047	0.050	0.052

[a] **$E_{a,f}$:** Activation energy of the forward reaction, given in kJ mol^{-1}.
[b] **$\log\widetilde{A}_f$:** Logarithm of the pre-exponential factor of the forward reaction, given in m^3 mol^{-1} s^{-1}.

Table D-38 The deviations between the CBS-QB3 data and the GA-based data for the HARs in the set of "HARs from TDs with substituted extended side chains" calculated with the ΔGAV°s and ΔNNI° parameters in the reverse direction with respect to the reference reaction, given in **Table 6-3** and **Table 6-4**, respectively.

Reaction #	$E_{a,r}$[a]					$\log\widetilde{A}_r$ [b]				
	300 K	600 K	1000 K	1500 K	2000 K	300 K	600 K	1000 K	1500 K	2000 K
S-101	-0.1	-0.3	-0.4	-0.1	0.2	-0.130	-0.177	-0.190	-0.173	-0.160
S-102	1.6	1.7	1.9	2.4	2.8	0.832	0.834	0.854	0.886	0.902
S-103	-0.1	-0.1	-0.1	0.4	1.3	0.590	0.590	0.586	0.618	0.655
S-104	2.4	2.9	3.1	3.4	3.6	0.740	0.818	0.843	0.862	0.869
S-105	7.7	8.1	8.1	8.2	8.2	1.824	1.923	1.931	1.934	1.934
S-106	-2.4	-2.7	-2.8	-2.4	-1.6	-0.212	-0.257	-0.269	-0.241	-0.205
S-107	-14.1	-14.3	-14.3	-13.7	-12.8	0.613	0.589	0.594	0.630	0.669
S-108	-7.2	-7.3	-7.2	-6.7	-5.8	-0.259	-0.287	-0.282	-0.247	-0.207
S-109	1.5	1.3	1.0	1.1	1.7	-0.301	-0.339	-0.375	-0.367	-0.340
S-110	-13.2	-13.4	-13.5	-13.1	-12.2	-0.291	-0.333	-0.346	-0.319	-0.282
S-111	-12.4	-12.8	-12.9	-12.5	-11.8	0.177	0.110	0.093	0.117	0.151
S-112	-15.1	-15.5	-15.7	-15.3	-14.6	-0.026	-0.106	-0.125	-0.101	-0.068
S-113	-9.1	-9.6	-10.0	-9.9	-9.3	-0.389	-0.472	-0.514	-0.508	-0.483
S-114	-5.9	-6.3	-6.4	-5.9	-5.1	-0.703	-0.773	-0.782	-0.752	-0.715
S-115	-3.0	-3.0	-3.1	-2.7	-1.9	0.019	0.005	0.000	0.025	0.060
S-116	-1.4	-1.5	-1.5	-1.0	-0.2	0.288	0.258	0.255	0.285	0.323

[a]**$E_{a,r}$:** Activation energy of the reverse reaction, given in kJ mol^{-1}.
[b]**$\log\widetilde{A}_r$:** Logarithm of the pre-exponential factor of the reverse reaction, given in m^3 mol^{-1} s^{-1}.

Table D-39 Factor of deviations (ρ) between the reaction rate coefficients calculated by CBS-QB3 and the set of ΔGAV°/ΔNNI° parameters reported in **Table 6-3** and **Table 6-4**.[a]

Reaction #	Factor of deviation (ρ)									
	Forward					Reverse				
	300 K	600 K	1000 K	1500 K	2000 K	300 K	600 K	1000 K	1500 K	2000 K
S-101	2.85	1.38	1.10	1.11	1.20	1.93	1.29	1.20	1.44	1.30
S-102	3.50	3.85	2.23	1.54	1.96	3.94	3.66	2.51	1.60	1.49
S-103	2.15	1.36	1.73	1.46	1.34	3.15	3.58	2.28	1.94	1.28
S-104	4.81	4.21	2.45	1.71	1.41	1.92	2.78	2.09	1.78	1.68
S-105	3.23	1.64	1.24	1.00	1.06	1.87	6.27	17.69	32.13	42.27
S-106	1.81	1.38	1.20	1.03	1.01	2.46	1.10	1.22	1.31	1.38
S-107	4.98	3.44	2.56	2.05	1.81	33434.05	289.50	49.44	22.16	15.08
S-108	3.80	2.91	2.14	2.19	1.31	39.38	4.57	1.89	1.26	1.07
S-109	1.49	1.10	1.36	1.41	1.52	7.21	3.93	3.20	2.67	2.55
S-110	1.25	1.26	1.44	1.41	1.44	1373.71	23.33	4.68	2.30	1.59
S-111	2.62	2.41	2.19	1.97	1.88	3024.46	57.78	12.10	5.90	4.14

S-112	2.48	1.41	1.21	1.19	1.18	10541.68	82.50	12.20	4.98	3.22
S-113	31.30	14.74	10.92	8.95	8.34	89.88	5.45	1.72	1.01	1.31
S-114	7.79	4.68	2.56	1.78	1.44	8.43	1.16	1.95	2.79	3.22
S-115	6.50	5.11	3.68	2.94	2.63	6.55	2.39	1.66	1.46	1.37
S-116	1.49	1.24	1.21	1.31	1.32	4.28	2.51	2.14	2.18	2.17

[a]Factor of deviation (ρ): If $k_{AI} > k_{GA}$, then $\rho = \frac{k_{AI}}{k_{GA}}$, if $k_{GA} > k_{AI}$ then $\rho = \frac{k_{GA}}{k_{AI}}$ where kAI denotes reaction rate coefficients calculated with *ab initio* methods and kGA denotes reaction rate coefficients calculated with group additive parameters reported in this study, namely the ΔGAV°/ΔNNI° parameters reported in **Table 6-3** and **Table 6-4**.

Table D-40 Statistics demonstrating the predictive performance of the GA parameters on "HARs from TDs with substituted extended side chains" set in the forward direction.

		Forward				
		300 K	**600 K**	**1000 K**	**1500 K**	**2000 K**
$\mathbf{E_a}$[a]	**MAD**[c]	2.0	1.6	1.8	1.5	1.4
	MAX[d]	5.2	3.1	5.6	3.2	3.2
$\mathbf{log\widetilde{A}}$[b]	**MAD**	0.119	0.175	0.174	0.140	0.178
	MAX	0.268	0.341	0.374	0.320	0.459
k	$\langle\rho\rangle$[e]	2.9	2.2	1.8	1.5	1.5
	ρ_{max}[f]	7.8	5.1	3.7	2.9	2.6

[a]**E_a:** Statistics for the activation energy, given in kJ mol^{-1}.
[b]**$log\widetilde{A}$:** Statistics for the logarithm of the pre-exponential factor, given in m^3 mol^{-1} s^{-1}.
[c]**MAD:** Mean absolute deviation of the activation energies between the CBS-QB3 based E_as and the E_as calculated by reported GA parameters, given in kJ mol^{-1}.
[d]**MAX:** Maximum absolute deviation between the CBS-QB3 based E_as and the E_as calculated by reported GA parameters among the training set of activation energies, given in m^3 mol^{-1} s^{-1}.
[e]**$\langle\rho\rangle$:** The geometric average of the factor of deviations between the reaction rate coefficients calculated by CBS-QB3 and the GA parameters reported in this study.
[f]**ρ_{max}:** The maximum factor of deviations between the reaction rate coefficients calculated by CBS-QB3 and the GA parameters reported in this study.

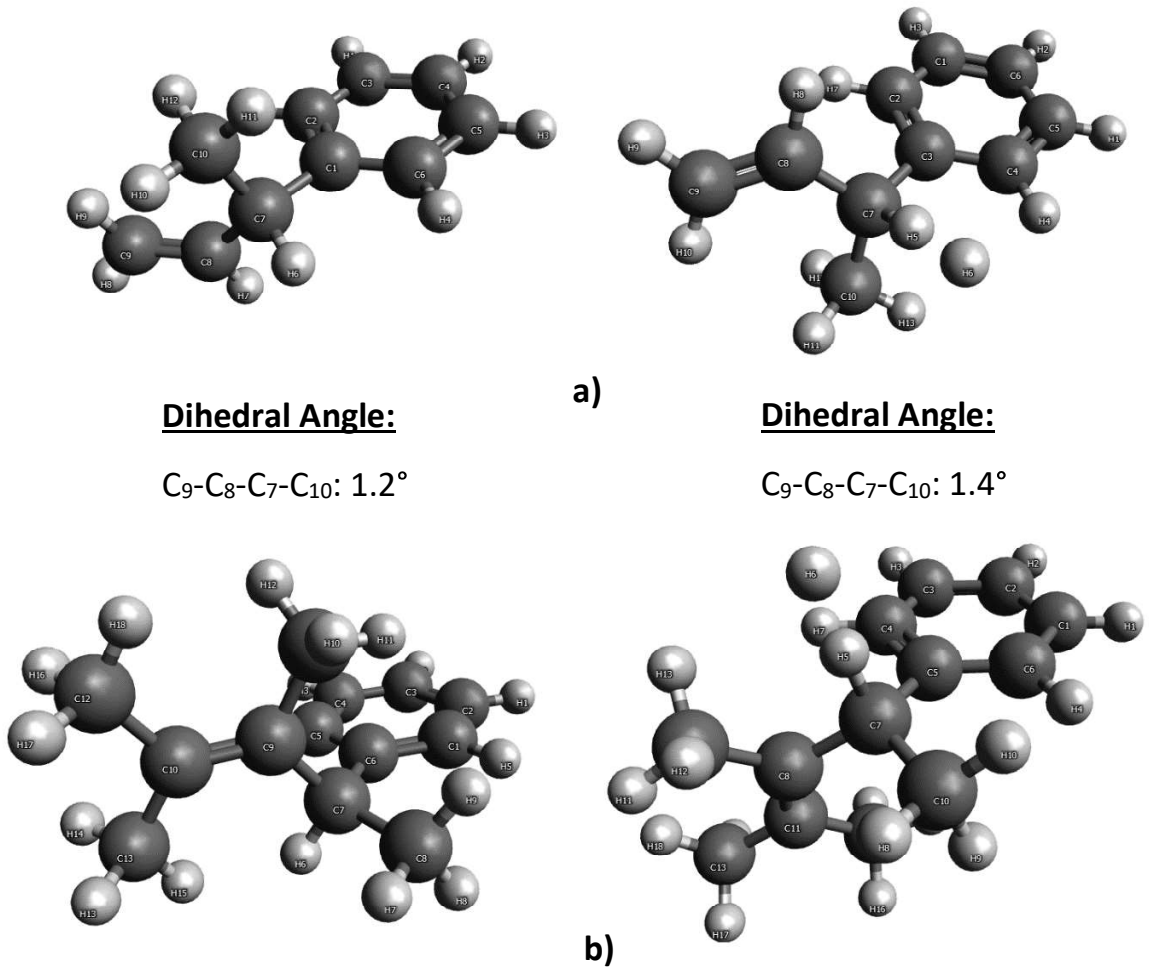

Figure D-61 Comparison of the HARs from **a)** α-methylallylbenzene and **b)** 2,3-dimethyl-4-phenylpent-2-ene in the forward directions. Reactants of the reactions are given on the left whereas on the right, transition state structures are provided. The dihedral angles between the two substituent groups on the α carbon, CH_3 group and the rest of the extended side chain is provided.

Glossary

Ab initio	A Latin word that signifies "from the beginning". *Ab initio* is a term that is utilized to describe calculations that are based on “first-principles” which refer to the fundamental laws of nature at the level of electrons without any additional assumptions, empirical or experimental data. These calculations yield the energy of a system by solving the Schrödinger equation which is the fundamental relationship that describes energies and motion of electrons.
Activation energy	The minimum energy (E_a) that is required to activate the potential reactants so that a chemical reaction is initiated. This is one of the two parameters in the Arrhenius equation $k = A\exp(-E_a/RT)$.

Anomeric Effect	The anomeric effect refers to the conformational preference of a gauche structure over an antistructure for molecules with a C-X-C-Y moiety where X and Y are heteroatoms having nonbonding electron pairs.
Aromaticity	The electron delocalization that is encountered in cyclic compounds, which provides enhanced thermodynamic stability with respect to the other possible geometric or connective arrangements with the same set of atoms.
Arrhenius preexponential factor	The temperature independent pre-exponential factor A in the Arrhenius equation $k = A \exp(-E_a/RT)$.
Basis set	Set of functions combined in a linear fashion to create molecular orbitals in the framework of *ab initio* calculations.
Benson's Group additivity method	This method enables prediction of molecular properties based on the molecular structures. In this method, thermochemical property of a molecule can be written as a sum of contributions arising from its constituent groups.
Bond additive corrections (BACs)	The bond-wise additive terms to minimize systematic errors encountered in *ab initio* calculated standard enthalpies of formations.

Bond dissociation energy	The bond dissociation energy (BDE) of a X-Y bond in a molecule XY is defined as the difference between the sum of $\Delta_f H^\circ$ of the $X^\bullet$ and $Y^\bullet$ radicals, and the $\Delta_f H^\circ$ of the XY parent molecule.
Diffuse function	These are extended Gaussian basis functions with a small exponent, meaning that the electrons are spread far away from the nucleus. The use of diffuse functions are crucial for the description of anions or dipole moments, however they can also be important for cases where there is intra- and/or intermolecular bonding.
Density Functional Theory	A quantum chemical method that describes the properties of the molecule based on determination of the electron density of the molecule.
Electron Correlation	The repulsive interaction between electrons of a quantum system.
Enthalpy	A thermodynamic quantity that presents a measure of the energy of the system. The enthalpy (H) is calculated from the internal energy (U) as $H = U + pV$, with p the pressure and V the volume of the system.
Entropy	The entropy (S) is a thermodynamic property that is relevant to the disorder of the system. As the number of possible configurations of a system increases, the entropy of the system increases as well.

Gibbs free energy	The thermodynamic quantity that represents the maximum reversible work that can be performed by a thermodynamic system at a constant temperature and pressure. This is calculated from the enthalpy (H) and the entropy (S) of a system using the relationship $G = H - TS$
Group contribution method	A Benson-inspired group additivity method to develop predictive kinetic parameters with the aim of obtaining accurate reaction rate coefficients for a wide range of reactions.
Hamiltonian operator	The operator that corresponds to the total energy in quantum mechanics.
Rigid rotor and harmonic oscillator approximation	In this approximation, the rovibrational modes of motion are approximated to harmonic oscillator (HO), i.e. motion of two masses on a spring. This approximation is successful in describing the vibrations, however lacks accuracy while describing low-frequency vibrational motions such as internal rotations since the one dimensional harmonic oscillator potential well can be very different than the real potential curve of a rotation around a single bond.
Hindered rotor treatment	The 1-D hindered rotor treatment involves determination of the potential energy profile for internal rotation and solving the Schrödinger equation for this motion to obtain the energy levels.

Hydrogen bond	The attractive intramolecular/intermolecular force that forms a special type of dipole-dipole interaction which occurs when a hydrogen atom is bonded to a strongly electronegative atom in the proximity of another electronegative atom with a lone pair of electrons.
Hyperconjugation	The interaction of a filled or partially filled orbital, typically a σ orbital with a nearby empty orbital, non-bonding p-orbital, antibonding σ or π orbital, or filled π orbital. This interaction yields an extended molecular orbital and hence, increases the stability of the system.
Inductive effect	The transmission of charge through a chain of atoms in a molecule via σ system, leading to a permanent dipole in a bond. The inductive effect decreases with increasing distance and as a rule of thumb, inductive effect is assumed to be negligible for distances larger than three atoms.
Internal Energy	The internal energy U is the total energy contained by a thermodynamic system which is composed of the kinetic energy and potential energy.
Isodesmic scheme	It is a reaction scheme in which the type of chemical bonds broken in the reactant are the same as the type of bonds formed in the

	reaction product. This hypothetical reaction scheme is used as a means of correcting for systematic errors in *ab initio* calculation.
Level of theory	A level of theory is one of the various approaches to solve the Schrödinger equation. One level of theory is distinguished from another by the level of complexity it brings in its treatment of 1) electron correlation and 2) the basis set.
Lewis structures	Lewis structures are the electron-dot diagrams that indicate the bonding between atoms of a molecule, and the lone pairs of electrons that may exist in the molecule.
Lignocellulosic biomass	The dry plant matter which is the most abundantly available raw material in the world for bio-fuel production. Lignocellulosic biomass is mainly composed of three components: lignin, cellulose and hemicellulose.
Mesomeric effect (+M effect and -M effect)	The effect attributed to a substituent due to overlap of p- or π-orbitals with the p- or π-orbitals of the rest of the molecular entity. If a substituent has electron donating mesomeric effect, this is known as +M effect whereas electron withdrawing mesomeric effect is -M effect.

Natural bond orbital method	A method that is employed to calculate the distribution of electron density within a molecule (in atoms and in bonds between atoms).
Number of single events	The number of energetically equivalent paths that reactants can follow to be converted into products.
Partition function	A function that represents the average number of states accessible at a given temperature. A partition function is composed of different components that correspond to normal modes of motion such as vibrational, rotational or translational partition function.
Polarization function	Polarization is the nonuniform distribution of electric charge due to some intra or intermolecular effects, e.g. electronegativity. The inclusion of polarization function within a basis set enhances the capability of the *ab initio* calculation to take these polarization effects into account.
Pyrolysis	The thermal decomposition of organic components in the absence of molecular oxygen at elevated temperatures.
Scaling factor	Empirical factor that is used to improve the agreement between experimental and calculated vibrational frequencies.

Single-event preexponential factor	The pre-exponential factor excluding the number of single events of the reaction.
Self-Consistent field	The iterative method that is designed to solve the Schrödinger equation. In this method, a proper Hamiltonian operator is selected along with an initial guess wavefunction and then, the Schrödinger equation is solved to obtain more accurate set of orbitals.
Single point calculation	The calculation of the wavefunction and charge density, and hence the energy, of a particular arrangement of nuclei.
Slater determinant	The simplest possible antisymmetric wave function, i.e a wave function that satisfies the Pauli principle that describes a multi electron system.
Spin-orbit coupling	Interaction of a particle spin with its motion.
Spin contamination	A non-systematic source of mathematical error in energy calculations for the open shell structures which is caused by the artificial mixing of states with different electronic spin-states. Spin contamination results from the fact that the alpha and beta orbitals are allowed to differ from each other during unrestricted calculations. Consequently, the wave function is no longer an eigenfunction of the total spin operator $<S^2>$.

Standard enthalpy of formation	The standard enthalpy of formation is the change of enthalpy that accompanies the formation of one mole of a substance in its standard state from its constituent elements in their standard state.
Steam cracking	A petrochemical process in which saturated compounds (hydrocarbons, oxygenates) decompose into small unsaturated compounds in the presence of steam at elevated temperatures.
Transition state structure	The saddle point on the potential energy surface along the minimum energy path.
Transition state theory	The kinetic theory that allows to calculate rate coefficients assuming quasi-equilibrium between the reactant and transition state.
Tunneling coefficient	The coefficient that is employed to incorporate the effect of the tunneling of particles through the reaction barrier into reaction rate coefficients.
Zero-point vibrational energy	The ground state energy of the vibrations at 0 K which is calculated from the harmonic frequencies obtained from a normal mode analysis.

List of publications

Journal Papers

1. Ince A, Carstensen H-H, Reyniers M-F, Marin GB. First-principles based group additivity values for thermochemical properties of substituted aromatic compounds. *AIChE Journal.* **2015**;61(11):3858-3870.

2. Ince A, Carstensen H-H, Sabbe MK, Reyniers M-F, Marin GB. Group additive modeling of substituent effects in monocyclic aromatic hydrocarbon radicals. *AIChE Journal.* As of 08.05.2017, the accepted manuscript is only available online (**DOI:** 10.1002/aic.15588).

Poster Presentations

1. Ince A, Carstensen H-H, Sabbe MK, Reyniers M-F, Marin GB.First-principles based group additivity values for thermochemical properties of substituted aromatic compounds. **2015**, 9th International Conference on Chemical Kinetics (ICCK), Proceedings, 28 June – 2 July, Ghent, Belgium.

Oral Presentations

1. Carstensen H-H, Ince A, Sabbe MK, Reyniers M-F, Marin GB.Towards automated mechanism generation of lignin pyrolysis models: development of Group Additivity parameters for aromatic species, **2015**, 249th ACS National Meeting, 22-26 March, Denver, USA.

Manuscripts Prepared for Publication

1. Ince A, Carstensen H-H, Sabbe MK, Reyniers M-F, Marin GB. Modeling of Thermodynamics of Toluene Derivatives and Benzylic Radicals Via Group Additivity.

2. Ince A, Carstensen H-H, Sabbe MK, Reyniers M-F, Marin GB. Group Additive Kinetic Modeling of Benzylic Hydrogen Abstractions from Toluene Derivatives by Hydrogen Atoms.